PROCEEDINGS OF
THE
WEDNESDAY SLIDE CONFERENCE
2023-2024

JOINT PATHOLOGY CENTER VETERINARY PATHOLOGY SERVICE
SILVER SPRING, MD 20910

On behalf of the Joint Pathology Center, I would like to express our immense gratitude to all the contributors who submitted cases to the 2023-2024 Wednesday Slide Conference. This educational exercise would not be possible without the collective efforts of institutions and individuals around the world who share a commitment to and passion for the advancement of veterinary pathology.

Throughout this conference year, the following veterinary pathologists shared their time and expertise by moderating for Wednesday Slide Conference: Jeremy Bearss, Brittany Beavis, Bruce Williams, Kelsey Fiddes, Alicia Moreau, Katherine Scott, Charles Bradley, Chris Gardiner, Kurt Williams, Elise LaDouceur, Anna Travis, Rachel Neto, Tony Alves, Sherri Daye, Linden Craig, Patricia Pesavento, Andrew Miller, Christopher Schellhase, David Needle, Francisco Uzal, Amy Durham, Paul Stromberg, Don Meuten, Julie Engiles, Neel Aziz, and Susan Bender. Thank you all for making this year a success!

The Joint Pathology Center's military and civilian staff and residents make an undertaking like this possible. I would like to personally thank Dr. Bruce Williams for leading and championing the WSC program and for his mentorship; Ms. Rachel Terry for her help in compiling and distributing conference results; Ms. Kenenya Gathers for accessioning and organizing cases; and Ms. Stacey Tamer for providing special and immunohistochemical stain support.

Finally, I would like to thank Marc and Kacey for their unwavering support throughout this jam-packed year; I could not have done it without you. I would also like to thank my emotional support residents, the second year JPC resident class, for the listening ears and the many kindnesses extended to me over the past year. And a final, very special thanks goes to Kate, who was the best girl, and is the reason that I am fortunate enough to spend my days thinking about animals.

Sam Medlin, DVM

2023-2024 WSC Coordinator

Case	JPC No.	Slide ID No.	Species	Tissue	Lesion/condition	Page
Conference 1 – August 16, 2023						
1	4167690	F20-0035032	Horse	Kidney, lymph node	Purpura hemorrhagica / *Streptococcus equi* subsp. *equi*	8
2	4182639	122	Sheep	Heart	Myocardial mineralization and neocrosis / Nutritional myopathy	13
3	4166753	21-619-2	Sheep	Brain	Granulomatous encephalitis / *Coenurus cerebralis*	17
4	4153148	F18-122528	Alpaca	Brain	Teratoma	21
Conference 2 – August 23, 2023						
1	4179965	1-2002	Dog	Brain	Cerebellar cortical atrophy / Neuronal ceroid lipofuscinosis	27
2	4183330	90	Cat	Brain	Dysplastic gangliocytoma	32
3	4188569	P-1360-22	Dog	Brainstem	Meningioangiomatosis	37
4	4196118	F21-114368	Cat	Spinal cord, spinal nerves	Lymphoma	42
Conference 3 – August 30, 2023						
1	4153013	1800382c	Horse	Haired skin	Cutaneous mast cell tumor	49
2	4181131	P21 350	Cat	Haired skin	Cowpox viral dermatitis	52
3	4167923	P-1360-22	Göttingen minipig	Haired skin	Thrombocytopenia purpura of Göttingen minipigs	61
4	4117644	18RD161	Dog	Periorbital tissue	Canine lobular orbital adenoma	66
Conference 4 – September 13, 2023						
1	4196024	F22-43990	Horse	Liver	Necrosuppurative hepatitis / Tyzzer's disease	72
2	4101303	N16-421	Chicken	Crop, Liver	Proliferative ingluvitis/ Capillariasis	77
3	4181837	22-006	Cow	Heart	Cardiac lymphoma	80
4	4181835	22-0019	Bull	Liver	Granulomatous hepatitis / *Mycobacterium bovis*	87
Conference 5 – September 20, 2023						
1	4165964	20V-3048	Cat	Lung	Idiopathic pulmonary fibrosis	94
2	4183456	NA	Dog	Kidney	Granulomatous interstitial nephritis / *Rasamonsia argillacea*	97
3	4181857	73907	Marmoset	Lung	Metastatic duodenal mucinous adenocarcinoma	101
4	4183332	H22-1044	Calf	Kidney	Renal dysplasia	106
Conference 6 – September 27, 2023						
1	4198440	23-176	Saker Falcon	Aorta	Atherosclerosis	113
2	4152935	18101170-4	Dog	Jejunum	Eosinophilic and granulomatous enteritis / *Pythium insidiosum*	119
3	4186711	A-73/22X	Chicken	Trachea	Fibrinonecrotizing tracheitis / Fowl pox virus and Gallid herpes virus 1 (Infectious laryngotracheitis)	125
4	4198199	23-147	Dog	Skeletal muscle, heart, lung	Rhabdomyosarcoma	130
Conference 7 – October 4, 2023						
1	4134862	SP19-1418	Dog	Haired skin	Lymphoplasmacytic dermatitis and folliculitis / *Pelodera strongyloides*	139

Case	JPC No.	Slide ID No.	Species	Tissue	Lesion/condition	Page
2	4181696	B22-02929	Dog	Haired skin	Epidermal dysplasia with solar elastosis / actinic dermatosis	142
3	4181698	H21-3024	Cat	Haired skin	Thymoma-associated exfoliative dermatitis	147
4	4198646	22-016721	Dog	Claw	Symmetric lupoid onychodystrophy	152
Conference 8 – October 11, 2023						
1	4166463	T21-15865	Horse	Small Intestine	Lymphoplasmacytic and eosinophilic enteritis / *Eimeria leuckarti*	158
2	4181149	20-12730	Pig	Lung	Interstitial pneumonia / *Asccaris suum*	163
3	4198668	21-1210-1-10	Octopus	Digestive gland, esophagus	Chronic cestodiasis	167
4	4066089	N15-19	Colt	Colon	Granulomatous colitis / cyathostomiasis	171
Conference 9 – October 18, 2023						
1	4198546	D23-000602	Dog	Lung	Pulmonary veno-occlusive disease and capillary hemangiomatosis	177
2	4165963	L20 16795	Dog	Lung	Eosinophilic pneumonia / Eosinophilic pulmonary granulomatosis	182
3	4121043	V17-19285	Cow	Lung	Atypical interstitial pneumonia / 2-methylindole toxicity	188
4	4184463	N-133-22	Ram	Lung	Bronchopneumonia / Maedi-visna virus	192
Conference 10 – November 15, 2023						
1	4186705	WSC 22-23 PRF_1	Betta Fish	Kidney	Teratoma, egg binding, and granulomatous and fibrosing gastritis	199
2	4182288	21:4131	Red abalone	Gut, kidney	Epithelial necrosis / Withering syndrome	203
3	4170514	21681	Harbour porpoise	Lung	Broncho- and interstitial verminous pneumonia	207
4	4198544	D18-031756	Bald eagle	Liver	Granulomatous trematodiasis / *Erschioviorchis* sp.	211
Conference 11 – November 29, 2023						
1	4198266	21-26171	Cat	Liver	Hepatocellular necrosis and lipidosis	216
2	4199340	67262	Turtle	Head	Osteonecrosis and epithelial inclusion cysts / *Emydomcyes testavorans*	221
3	4198856	15-016B	Sheep	Liver	Necrotizing hepatitis/*F. tularensis*	225
4	4181840	21-3928-1-1	Zebrafish	Ovary and coelom	Egg associated inflammation	230
Conference 12 – December 6, 2023						
1	4168071	NE19-2218	Cat	Eye	Granulomatous endophthalmitis / *Histoplasma capsulatum*	237
2	4198501	N1022/395030	Bull	Eye	Ocular dysgenesis with retinal dysplasia	241
3	4166756	20-111408	Cow	Eye	Necrotizing vasculitis / Thrombotic meningoencephalitis	248

Case	JPC No.	Slide ID No.	Species	Tissue	Lesion/condition	Page
4	4198645	S23-0025.09	Cat	Eye	Pyogranulomatous keratoconjunctivitis, scleritis, and uveitis / *Mycobacterium lepraemurium*	252
Conference 13 – December 13, 2023						
1	4153538	1235813-010	Cynomolgus macaque	Nasal cavity	Malignant neoplasm	258
2	4201814	MK1805004	Rhesus macaque	Liver, gallbladder, common bile duct	Necrotizing choledochitis and lymphocytic and eosinophilic cholangiohepatitis and cholecystitis/ Cytomegalovirus and *Cryptosporidium* sp.	261
3	4199849	75340-21	Rat	Heart, lung	Suppurative endocarditis, myocarditis, and valvulitis / Group B *Streptococci*	267
4	4117301	16-47	Rat	Kidney	Suppurative pyelonephritis / *Proteus mirabilis*	272
Conference 14 – January 3, 2024						
1	4181848	E9514/18B2	Horse	Haired skin	Granulomatous dermatitis / Cutaneous leishmaniasis	278
2	4136176	N18-166	Horse	Nasal cavity	Granulomatous rhinitis / Phaeohyphomycosis	283
3	4134351	36715.18	Horse	Larynx	Proliferative laryngitis / *Rhinosporidium seeberi*	288
4	4198552	S2303061	Horse	Kidney	Suppurative embolic nephritis / *Actinobacillus equuli*	293
Conference 15 – January 10, 2024						
1	4117908	Case 1	Goat	Jaw	Giant cell tumor of bone	299
2	4175180	UMVP 775-20	Chicken	Vertebra	Necrotizing spondylitis / Kinky back	304
3	4200200	23-024517	Dog	Long bone	Metastatic pilomatricoma	308
4	4182283	N20-1511	Parakeet	Femur	Metastatic Sertoli cell tumor	312
Conference 16 – January 17, 2024						
1	4199659	N23-20/B	Rabbit	Liver, spleen, cecum	Necrotizing typhlitis and splenitis / *Yersinia pseudotuberculosis*	317
2	4168203	1650/20	Parakeet	Liver	Necrotizing hepatitis	323
3	4065132	P15-818	Horse	Liver	Massive hepatocellular necrosis / Theiler's disease	327
4	4167959	21H8353B1	Cat	Liver	Hepatic amyloidosis and portal vein hypoplasia	330
Conference 17 – January 24, 2024						
1	4181062	P22-05552-5	Dog	Mediastinal mass	Ganglioneuroblastoma	337
2	4117531	69236	Rhesus macaque	Cerebrum	Pituitary adenoma	343
3	4198553	NC-23-0000344	Dog	Cerebrum	Eosinophilic meningoencephalitis	350
4	4182282	N22-623	Dog	Spinal cord	Perivascular histiocytosis / Globoid cell leukodystrophy	355
Conference 18 – February 1, 2024						
1	4174101	20N16744	Bison	Lung	Fibrinosuppurative and necrotizing bronchopneumonia /*Mycoplasma bovis*	360

Case	JPC No.	Slide ID No.	Species	Tissue	Lesion/condition	Page
2	4201808	X-1571-23	Skunk	Pancreas, cerebrum	Necrotizing meningoencephalitis and pancreatitis / Influenza A virus	364
3	4182581	S2010162M1	Rabbit	Liver	Necrotizing hepatitis / Rabbit Hemorrhagic Disease Virus 2	369
4	4066665	X-15818-14	Deer	Lung	Granulomatous pneumonia / *Cryptococcus gattii*	374
Conference 19 – February 7, 2024						
1	4198263	AP21-3301	Cornsnake	Stomach, ileum, colon	Necrotizing gastroenterocolitis	381
2	4199030	Case 2	Opossum	Lung	Neutrophilic and histiocytic interstitial pneumonia / *Didelphostrongylus hayesi*	386
3	4179970	S-21-645	Porcupine	Liver	Necrotizing hepatitis / *Toxoplasma gondii*	390
4	4199658	22-2188-7	Visayan hornbill	Ventriculus	Fibrinoid and heterophilic vasculitis with koilin erosion	395
Conference 20 – February 14, 2024						
1	4117871	BC 2018	Dog	Colon	Necrotizing colitis / *Neospora caninum*	402
2	4182588	21H13412	Horse	Colon, lymph node	Pyogranulomatous and necrotizing colitis and lymphadenitis / *Rhodococcus equi*	407
3	4199186	S 220/23	Cow	Small intestine	Segmental mural hemorrhage / Hemorrhagic Bowel Syndrome	411
4	4181693	S21-1623	Pig	Small intestine	Lymphoplasmacytic enteritis / Porcine adenovirus	415
Conference 21 – April 3, 2024						
1	4200196	50812	Dog	Thymus	Thymoma, type A	421
2	4200383	21-952-1	Dog	Oral mucosa	Osteogenic melanoma	431
3	4141990	17 C 1597	Dog	Eye	Lymphoma	437
4	4198261	AP22-4407-4	Dog	Pancreas	Hyalinizing exocrine pancreatic adenocarcinoma	441
Conference 22 – April 10, 2024						
1	4184462	M22-06546	Cow	Lymph node, liver	Bridging fibrosis and biliary hyperplasia / *Fasciola hepatica*	447
2	4180147	3191106034	Horse	Mammary gland, lymph node	Granulomatous and eosinophilic mastitis / *Halicephalobus gingivalis*	452
3	4198864	T23-17829	Dog	Skeletal muscle	Osteosarcoma	457
4	4166550	O347/20	Dog	Urinary bladder	Urothelial cell carcinoma	459
Conference 23 – April 17, 2024						
1	4205634	21 1232-73 B3	Cat	Vertebra	Vertebral angiomatosis	468
2	4183637	21-43601	Sandhill crane	Tibiotarsal joint	Chondromatosis	474
3	4186710	X-2070-21	Hedgehog	Lymph node, jaw	Pyogranulomatous osteomyelitis and lymphadenitis /*Neisseria animaloris*	480
4	4199017	P23-1279	Rat	Tail	Vertebral malformation	485
Conference 24 – April 24, 2024						
1	4200376	21-1552-8	Flamingo	Kidney	Amyloidosis and urate tophi	492

Case	JPC No.	Slide ID No.	Species	Tissue	Lesion/condition	Page
2	4199016	A22-520	Tortoise	Skin	Necrotizing dermatitis / *Austwickia chelonae*	500
3	4199510	14123 A1	Crocodile	Skin	Necrotizing and proliferative dermatitis / Crocodilepox virus	505
4	4159327	Case 2	Koala	Lung	Pyogranulomatous broncho-pneumonia / *Actinomyces* sp.	508
Conference 25 – May 1, 2024						
1	4199774	23020713-2	Goat	Placenta	Lymphohistiocytic placentitis / *Coxiella burnetii*	515
2	4201723	N-588/22	Goat	Mammary gland	Necrotizing and lymphohistio-cytic mastitis / *Mycoplasma aga-lactiae*	520
3	4201720	V23-002999	Rabbit	Uterus	Uterine adenocarcinoma, endo-metrial venous aneurysm, and cystic endometrial hyperplasia	525
4	4182638	119	Ram	Penis	Ulcerative balanitis	530

Joint Pathology Center
Veterinary Pathology Services

WEDNESDAY SLIDE CONFERENCE 2023-2024

Conference #1 16 August 2023

CASE I:

Signalment:
6-year-old, warmblood mare, equine (*Equus caballus*)

History:
The animal presented for treatment following a 24-hour history of lethargy and inappetence. The mare was diagnosed with Strangles three weeks prior and was being medically managed with flunixin meglumine. At presentation, serum creatinine was 4.0 mg/dL, then rose to 10.2 mg/dL despite aggressive diuresis. The animal became anuric and was euthanized due to poor prognosis.

Figure 1-1. Kidney, horse. Dark red to black areas of hemorrhage extend from the cortex into the medulla. (Photo courtesy of: Colorado State University Veterinary Diagnostic Laboratory, http://csu-cvmbs.colostate.edu/vdl/Pa-ges/default.aspx)

Figure 1-2. Intestine, horse. There are confluent areas of hemorrhage on the intestinal serosa and mesentery. (Photo courtesy of: Colorado State University Veterinary Diagnostic Laboratory, http://csu-cvmbs.colostate.edu/-vdl/Pages/default.aspx)

Gross Pathology:
The kidneys were mottled dark red and tan throughout, with dark red to black streaks extending from the cortex into the medulla. Multiple abdominal serosal surfaces contained petechiae and ecchymoses. There was serosanguinous thoracic and pericardial effusion, and generalized intramuscular and ventral subcutaneous edema. The mandibular and retropharyngeal lymph nodes were swollen, edematous and reddened, and at least one lymph node exuded purulent material when incised. One guttural pouch contained a hard nodule of inspissated purulent material adhered to the ventral mucosal surface.

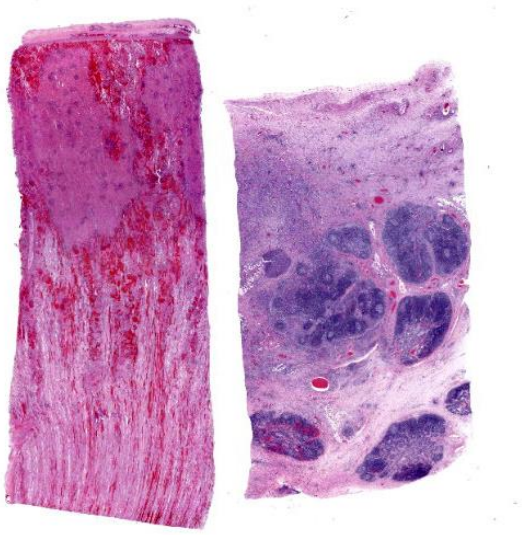

Figure 1-3. Kidney and lymph nodes, horse. There are multifocal to coalescing areas of necrosis within the renal cortex which extend into the medulla. Lymph nodes are separated and surrounded by fibrosis. (HE, 7X)

Laboratory Results:
Aerobic culture from a retropharyngeal lymph node swab yielded moderate mixed growth including *Streptococcus equi* subsp. *equi*, *Streptococcus equi* subsp. *zooepidemicus*, *Sphingobacterium* spp. and *Pseudomonas* spp.

Microscopic Description:
Kidney: Multiple irregular regions of the cortex are composed of coagulative necrosis characterized by partial loss of nuclear and cellular detail, hypereosinophilia, and karyorrhectic debris with maintenance of tissue architecture. Random scattered small to medium caliber blood vessels have segmental to circumferential transmural smudged eosinophilic walls infiltrated by intact and degenerate neutrophils, with some infrequent fragmentation of the tunica intima and media. Diffusely glomeruli in intact regions are segmentally to globally expanded by smudged homogenous eosinophilic matrix, intact and karyorrhectic neutrophils with fewer other mixed leukocytes (fibrinocellular crescents). Bowman's space is frequently filled with erythrocytes. Tubular epithelial cells are multifocally pyknotic and sloughed into the lumen. The interstitium is multifocally expanded by small aggregates of neutrophils. Tubules are multifocally filled with brightly eosinophilic proteinaceous fluid. Adipose tissue on the capsular surface is infiltrated by lymphocytes, plasma cells, and neutrophils within a thin layer of well-vascularized fibrous tissue.

Lymph node: The architecture of the node is nearly effaced by extensive fibrosis admixed with aggregates of neutrophils which are occasionally ringed by epithelioid macrophages. Occasionally small clusters of basophilic 1-3 micron cocci are present within inflammatory foci. Lymphoid follicles are multifocally distributed through the tissue. Occasionally, small caliber blood vessels along the periphery are surrounded or obscured by moderate numbers of lymphocytes, plasma cells, neutrophils, and macrophages.

Contributor's Morphologic Diagnoses:
Kidney: Glomerulonephritis, severe, multifocal, segmental to global, with fibrinocellular crescents.

Kidney: Fibrinonecrotizing and suppurative vasculitis, severe, multifocal subacute-active, with coagulative necrosis (infarction), hemorrhage and edema.

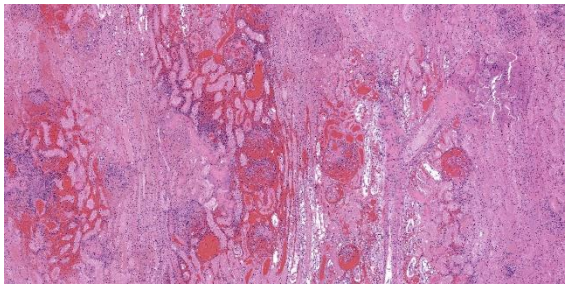

Figure 1-4. Kidney, horse. There is infarction and loss of glomerular and tubular detail within the renal cortex. (HE, 55X)

Lymph node: Pyogranulomatous lymphadenitis, severe, multifocal to coalescing, chronic, with fibrosis and rare cocci.

Contributor's Comment:

Streptococcus equi equi-associated purpura hemorrhagica (PH) is a well-characterized, though uncommon immune complex-driven vasculitis following prolonged infection with *S. equi equi*, otherwise known as Strangles. In the case of *S. equi equi*-associated PH, complexes are formed between Streptococcal M protein (SeM) and IgA which deposit in vessel walls.[4] Immune complex formation and deposition in tissue depends on the amount of antigen, antigen:antibody ratio, and size of the complexes. Type III hypersensitivity reactions occur when there is slightly more antigen than antibody in circulation, forming complexes small enough to remain soluble but large enough to accumulate within tissue and initiate the complement cascade, resulting in the classic leukoclastic vasculitis.[7,9] Other individual immunologic factors may also play a role in defective clearance of immunocomplexes. Free SeM can also activate the NLRP3 inflammasome, inducing IL-1β production, promoting pyroptosis in macrophages, and worsening systemic inflammation.[8]

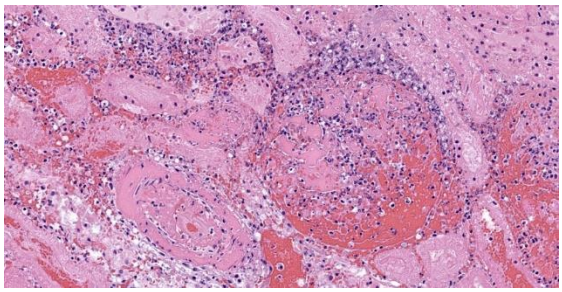

Figure 1-5. Kidney, horse. There is vasculitis and thrombosis of renal vessels and the adjacent glomeruli. There is coagulative necrosis of tubules in this area as well. (HE, 257X)

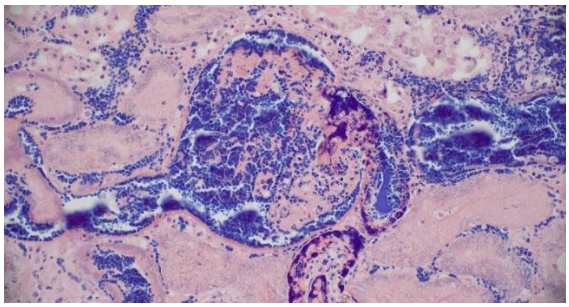

Figure 1-6. Kidney, horse. A PTAH stain demonstrates the presence of polymerized fibrin within glomeruli. Fibrin is a dark navy blue. (PTAH, 400X)

Immune complexes can be detected in the circulation of affected horses.[4] Horses with prior exposure or who are vaccinated are at a slightly higher risk of developing PH with subsequent *S. equi equi* infection, presumably due to preexisting antibody titers priming formation of immunocomplexes.[1] The percent of horses with Strangles that develop PH varies, with two studies of outbreaks reporting 6.5% and 5.4% respectively.[2] Other bacteria, including *Corynebacterium pseudotuberculosis*, and some viruses induce PH, also through a type III hypersensitivity mechanism.[9] The typical clinical presentation of PH is variable but often includes well-demarcated, gravity-dependent edema with petechiae and/or ecchymoses on the mucous membranes and skin.[1,10] This case is unusual in that the primary clinical presentation was acute anuric renal failure, presumably secondary to the numerous and extensive renal infarctions. Infarctive PH resulting from vessel occlusion secondary to vasculitis is described most commonly with infarction of skeletal muscle, leading to stiffness and pain, or in the gastrointestinal tract, leading to colic. While the infarctions were responsible for acute severe renal failure, the non-infarcted glomerular tufts contained abundant inflammation, regions of necrosis, and fibrin thrombi (fibrinocellular crescents).

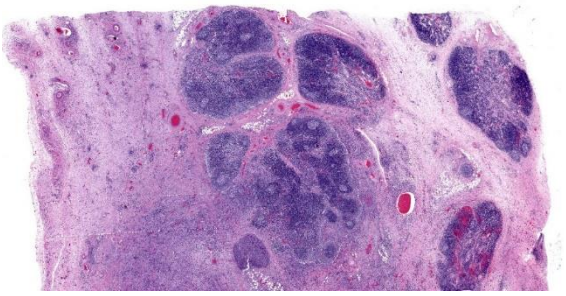

Figure 1-7. Lymph nodes, horse. Lymph nodes are separated and surrounded by fibrosis. (HE, 33X)

Glomeruli are a well-known target for immunocomplex (IC) deposition in a variety of type III diseases such as systemic lupus erythematosus. Demonstration of glomerular IC deposition has not been confirmed in horses with *S. equi equi* associated PH, however glomerulonephritis with basement membrane IC deposition is reported as part of post-streptococcal infection in humans.[6] Henoch-Schonlein syndrome is a human form of IgA IC disease that causes purpura, arthritis, gastrointestinal symptoms, and glomerulonephritis and is thought to be caused by infections including streptococcal organisms, viruses, medication, insect bites and other causes.[5] It is suspected that the glomerulonephritis observed in this case may have been due to local IC deposition; however, the extensive tissue damage and inflammation precludes more careful evaluation of glomerular architecture and basement membrane thickness via electron microscopy. Special stains, including PTAH and PAS, confirmed fibrin deposition in glomeruli, though the mesangial basement membrane was predominantly obscured.

Contributing Institution:
Colorado State University
Veterinary Diagnostic Laboratory
https://vetmedbiosci.colostate.edu/vdl

JPC Diagnosis:
Kidney, vessels and glomeruli: Vasculitis, necrotizing, multifocal to coalescing, severe with thrombosis and extensive cortical and medullary infarction.

Lymph node: Lymphadenitis, suppurative, focally extensive, moderate, with reactive hyperplasia.

JPC Comment:
Purpura hemorrhagica is a prototypical Type III hypersensitivity-mediated disease. As the contributor notes, the classic histologic lesion is leukoclastic vasculitis, with an inflammatory infiltrate composed of neutrophils in which nuclei have disintegrated into fragments termed "nuclear dust" or, less poetically, "leukocytoclasia."[3] The contributor provides a nice discussion of the factors that lead to immune complex deposition within vascular walls and trigger the Type III hypersensitivity reaction.

Type III hypersensitivity reactions can be thought of as "innocent bystander" reactions because the injured tissue is not a direct target of the immune response; rather, once deposited within tissues, the immune complexes themselves activate multiple cellular processes and cascades that result in inflammation and tissue damage.[7] Most critically, immune complexes lead to complement activation when IgG and/or IgM are cross-linked with C1, leading to the formation of the C3 and C5 convertases of the classical complement pathway. Cleavage products of classical pathway, C3a and C5a, cause increased vascular permeability and vasodilation. C5a is also chemotactic for neutrophils and macrophages, luring them to sites of immune complex deposition where their released and elaborated proteolytic enzymes and free radicals damage surrounding tissues. Vascular damage can compromise the intima, leading to exposure

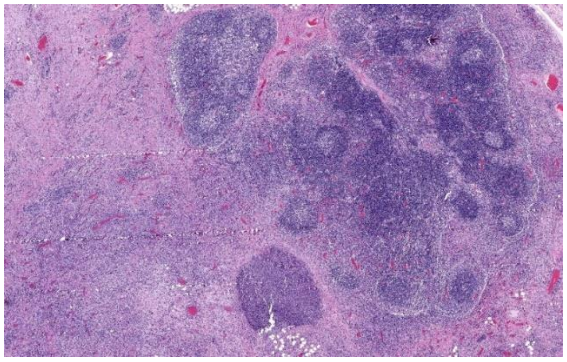

Figure 1-8. Lymph nodes, horse. Inflamed fibrous connective tissue surrounds and infiltrates a lymph node. Germinal centers are hypocellular due to lymphocyte loss.

of subintimal collagen, coagulation cascade and platelet activation, and the production of microthombi with subsequent infarction.

This sequence of Type III hypersensitivity-mediated injury is not unique to Strangles-associated purpura hemorrhagica, but is part of a stereotyped pattern of injury in several immune-mediated diseases of veterinary importance. The contributor mentions systemic lupus erythematosus, where DNA and nuceloproteins serve as antigenic niduses for immune complex formation. Others include equine infectious anemia, equine recurrent infectious uveitis, "blue eye" secondary to canine adenovirus 1 infection, hypersensitivity pneumonitis, rheumatoid arthritis, and acute glomerulonephritis, among others.[7]

The conference moderator, COL Jeremy Bearss, outgoing JPC director, stressed the importance of examining vessels in all tissues. Though easily overlooked among more eye-catching histologic features, the vessels often contain a wealth of diagnostic information as in this case, where the leukoclastic vasculitis is a key histologic feature.

Careful consideration was given to the contributor's description of fibrinocellular crescents; however, no fibrinocellular crescents were noted in the histologic sections examined during the conference.

References:

1. Boyle AG, Timoney JF, Newton JR, Hines MT, Waller AS, Buchanan BR. *Streptococcus equi* infections in horses: guidelines for treatment, control, and prevention of Strangles—revised consensus statement. *J Vet Intern Med*. 2018;32(2):633-647.
2. Duffee LR, Stefanovski D, Boston RC, Boyle AG. Predictor variables for and complications associated with *Streptococcus equi* subsp *equi* infection in horses. *J Am Vet Med Assoc*. 2015;247 (10):1161-1168.
3. Fraticelli P, Benfaremo D, Gabrielli, A. Diagnosis and management of leukocytoclastic vasculitis. *Intern Emerg Med*. 2021;16:831-841.
4. Galan JE, Timoney JF. Immune complexes in purpura hemorrhagica of the horse contain IgA and M antigen of *Streptococcus equi*. *J Immunol*. 1985; 135(5):3134-3137.
5. Lanzkowsky S, Lanzkowsky P, Schoenlein J. Henoch-Schoenlein Purpura. *Pediatr Rev*. 1992;13(4).
6. Rodriguez-Iturbe B, Haas M. Post-Streptococcal Glomerulonephritis. In: Ferretti JJ, Stevens DL, Fischetti VA, eds. *Streptococcus pyogenes: Basic Biology to Clinical Manifestations*. University of Oklahoma Health Sciences Center; 2016.
7. Snyder PW. Diseases of Immunity. In: Zachary JF, ed. *Pathologic Basis of Veterinary Disease*. 6th ed. Elsevier; 2017:242-285, 319-322.
8. Valderrama JA, Riestra AM, Gao NJ, et al. Group A streptococcal M protein activates the NLRP3 inflammasome. *Nat Microbiol*. 2017;2(10):1425-1434.
9. Valentine BA. Skeletal Muscle. In: Zachary JF, ed. *Pathologic Basis of*

Veterinary Disease. 6th ed. Elsevier; 2017:908-953.
10. Whelchel DD, Chaffin MK. Sequelae and complications of *Streptococcus equi* subspecies *equi* infections in the horse. *Equine Vet Educ*. 2009;21(3):135 -141.

CASE II:

Signalment:
1-month-old, male, Rasa Aragonesa sheep (*Ovis aries*)

History:
This animal was one of 400 lambs on a single farm. 250 lambs became lethargic and apathetic and 10 lambs died suddenly.

Gross Pathology:
Approximately 40% of the endocardium and myocardium of both ventricles had well-demarcated, multifocal foci of white, hard, crunchy tissue admixed with areas of mild hemorrhage.

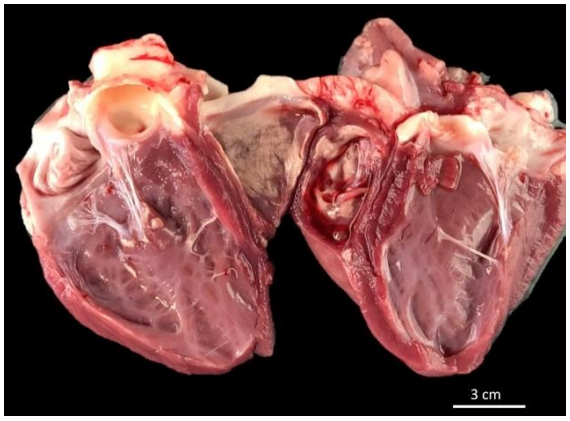

Figure 2-1. Heart, sheep. 40% of the ventricular myocardium, especially in subendocardial regions have foci of fibrosis, mineralization, and hemorrhage. (Photo courtesy of: Universidad de Zaragoza. *Departamento de Patología Animal, https://patologiaanimal.unizar.es)*

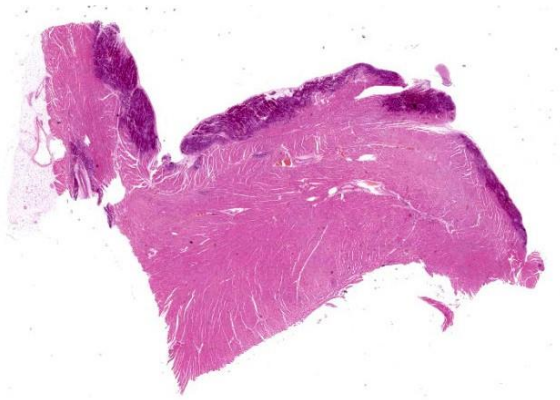

Figure 2-2. Heart, sheep. One section from the ventricular wall and septum is submitted for examination. There is well-demarcated dark discoloration of the subendocardial myocardium. (HE, 6X)

Microscopic Description:
Heart: Diffusely up to 40% of the tissue is affected by a degenerative and necrotizing process. On a focally extensive area of the myocardium close to endocardium, some cardiomyocytes are swollen with moderate amounts of vacuolation and pale eosinophilic cytoplasm (degeneration), others are shrunken and hypereosinophilic, with loss of cross striations and fragmentation of myofibrils, and occasional contraction bands, with pyknosis and karyorrhexis (necrosis). Many degenerate and necrotic myocytes contain abundant amounts of basophilic granular material (mineral). Multifocally, scattered among the tissue are few neutrophils and lymphocytes admixed with moderate edema and mild hemorrhage. Few satellite nuclei surrounding affected fibers are hyperplastic.

Contributor's Morphologic Diagnosis:
Cardiac muscle: Focally extensive necrosis and degeneration with mineralization, polyphasic, subacute, moderate.

Contributor's Comment:
The most common nutritional deficiency leading to nutritional myopathy is selenium deficiency. Nutritional myopathy resulting from vitamin E deficiency in the absence of

selenium deficiency is uncommon in mammals but may be more common in birds and reptiles.[2] Selenium is primarily considered a powerful antioxidant because of its role in the glutathione peroxidase system.[4] Antioxidant systems are believed to have evolved as a means of surviving in an oxygenated atmosphere by dealing with free radicals and the toxic products of their metabolism. Animal antioxidant defense mechanisms are based on the synthesis of numerous biological antioxidants that include the antioxidant enzymes glutathione, thioredoxin, and coenzyme Q. There is also a range of dietary antioxidants which can be provided in feed, which include vitamin E, carotenoids, polyphenolics, and selenium (as a precursor to selenoproteins). Under stress conditions, the internal antioxidant system network alone cannot deal properly with excess reactive oxygen species formation and requires additional help from dietary antioxidant sources provided via feed/water. Vitamin E and selenium are major feed-derived antioxidants.[8]

Nutritional myopathy in sheep is probably more prevalent in more areas of the world than the disease in cattle. The names white muscle disease, rigid lamb disease, and stiff lamb disease were coined to describe the most frequently encountered clinical patterns in 2-4 week-old lambs, which very often are spring lambs, recently turned out onto the first green pasture.[2] Congenital nutritional myopathy does occur in lambs, but not often. The typical disease may occur as an outbreak among lambs from 1 day to 2 months of age or beyond. Mortality at this stage may be very low or may reach 50%. The next peak of incidence occurs at 4-8 months of age as weaned lambs are put onto lush pastures following mowing or into feedlots. Mortality is not usually very high, but the incidence of minimal clinical disease may be moderately high and that of subclinical disease may be higher still.[2]

Lesions and their corresponding clinical signs are as varied as the circumstances under which myopathy occurs. The lesions may be detectable in lamb fetuses at least 2 weeks before parturition. In the congenital disease, tongue and neck muscles used in suckling movements often contain the most severe lesions. When the lesions occur in lambs a few days older, they are likely to be much more extensive and involve primarily the major muscles of the shoulder and thigh but also back, neck, and respiratory (diaphragm and intercostal) muscles.[2] Severe, often fatal myocardial necrosis is typically part of the important vitamin E and selenium-responsive syndromes of nutritional myopathy of lambs, calves, swine, and horses, and in mulberry heart disease of swine. It may also be seen as part of equine rhabdomyolysis and of capture myopathy and other exertional syndromes where vitamin E and selenium depletion produce cardiomyocyte alterations characterized by contraction band necrosis and myofibrillar lysis.[4,7]

Given the potential for a common mechanism of cell injury in both selenium deficiency and selenium toxicity, it is not surprising that the primary lesion in these two diseases is myocardial necrosis. Therefore, in cases of acute myocardial necrosis, it is imperative that tissue selenium levels are quantified before a diagnosis of selenium deficiency is rendered.[1] Polyunsaturated fatty acid levels must also be examined as supplementation with polyunsaturated fatty acids can greatly increase the severity of these changes.[4]

Several mineral deficiencies might be present at the same time in a sheep herd. Cases of poor growth performance in lambs should be investigated taking several mineral deficiencies, particularly cobalt, copper, and selenium into account. Clinical examination can often give only suspected diagnoses, so to access possible mineral deficiencies, a

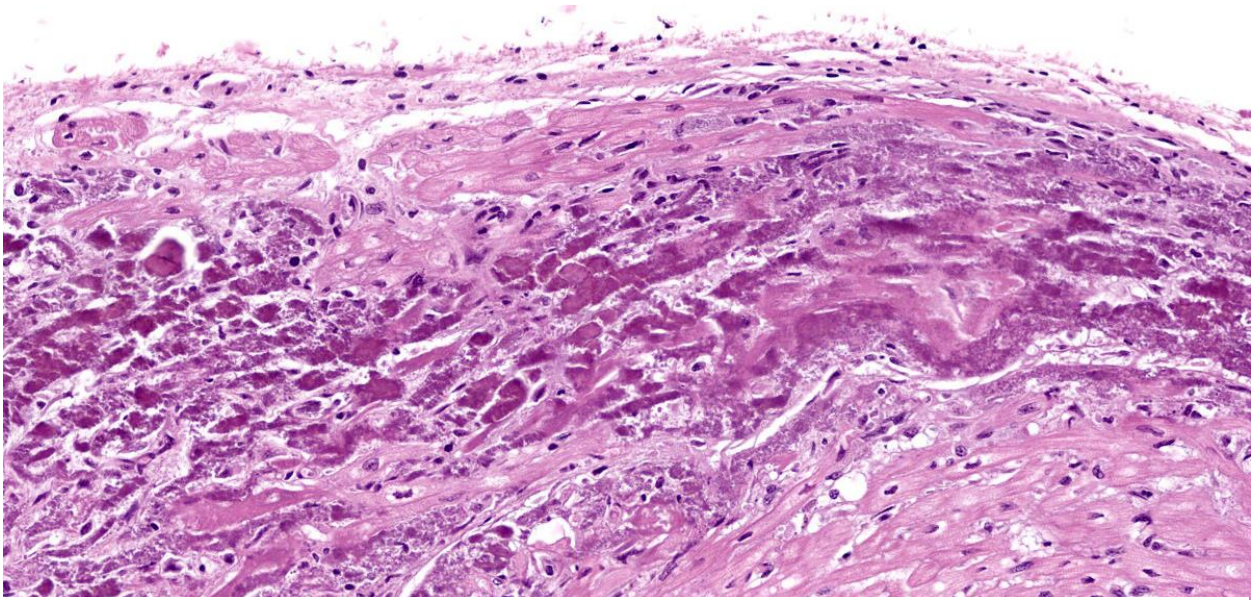

Figure 2-3. Heart, sheep. Higher magnification of an area of myofiber degeneration and necrosis with mineralization of deeper myofibers. (HE, 270X)

nutritional assessment should be performed sampling not only blood, but also liver tissue via biopsy or post-mortem samples.[3]

Contributing Institution:
University of Zaragoza
Departamento de Patología Animal (Área histología)
University of Zaragoza
Zaragoza, Spain

JPC Diagnosis:
Heart, myocardium: Mineralization and necrosis, subendocardial, diffuse, severe, with fibrosis.

JPC Comment:
The striking myocardial mineralization observed grossly and histologically in this case is an excellent example of pathologic calcification. Pathologic calcification is the abnormal deposition of calcium salts, along with smaller amounts of iron, magnesium, and other mineral salts, within soft tissues.[6] Pathologic calcification comes in two forms: dystrophic calcification and metastatic calcification.

Metastatic calcification occurs primarily in normal tissues due to a calcium-phosphate imbalance ("metastatic is metabolic") and is more likely to occur when the serum product of the calcium-phosphorus concentration exceeds 70 mg/dL. Causes for calcium-phosphate imbalance are many and include chronic kidney disease, vitamin D toxicosis, inappropriately elevated parathyroid hormone, or humoral hypercalcemia of malignancy. Metastatic calcification tends to occur in tissues that exist in alkaline environments, primarily the stomach, kidneys, and lungs.
Dystrophic calcification, by contrast, occurs in areas of tissue necrosis ("dystrophic is dead") and typically occurs in patients with normal serum calcium levels. Intracellular calcium overload is an expected consequence of cell death as ischemia leads to the opening of membrane calcium channels and the flooding of the cytosol with calcium normally sequestered in the sarco- or endoplasmic reticulum and mitochondria.[5] Neccrotic myofibers are particularly prone to dystrophic calcification due to the high levels of calcium ions stored in the sarcoplasmic reticulum; thus, selenium or vitamin E deficiency-

driven necrosis may quickly lead to whole myocyte calcification and to the white, gritty lesion for which white muscle disease gets its common name.[5]

Nutritional myopathy, the preferred term for white muscle disease, may present differently in different species. The contributor provides a good summary of the typical disease presentation in young, suckling animals. In affected adult horses, the temporal and masseter muscles are often preferentially affected with swelling and stiffness leading to impaired mastication.[9] The disease in cattle, sheep, goats, and camelids more typically affects the postural muscles and the muscles of locomotion without the profound involvement of the temporalis and masseter muscles seen in horses.[9] Severe disease in all species can lead to necrosis and dystrophic calcification of the myocardium or endocardium, as illustrated in this case.

Lesions may also differ based on chronicity. In animals with severe, acute myopathy leading to death (typically young animals) lesions are characterized by widespread muscle necrosis and dystrophic mineralization with minimal inflammation. In subacute or chronic disease, lesions are polyphasic with active necrosis, macrophage infiltration, and regeneration all present simultaneously.[9]

There was dispirited discussion among conference participants about the phasic nature of the myocardial lesions in this case. Lesions resulting from nutritional myopathy, a chronic process, would be expected to be polyphasic; however, the slides reviewed in conference appeared to the moderator and conference participants to be largely monophasic and characterized solely by necrosis and mineralization. Participants discussed whether the young age of the animal at death precluded full lesion development or if the examined histologic section was unrepresentative. No satisfactory resolution was reached during conference discussion and the final JPC morphologic diagnosis slyly skirts the issue by omitting any reference to phase.

References:

1. Amini K, Simko E, Davies JL. Diagnostic exercise: Sudden death associated with myocardial contraction band necrosis in boer goat kids. *Vet Pathol*. 2011; (48):1212–1215.
2. Cooper BJ, Valentine BA. Muscle and Tendon. In: Maxie MG, ed. *Jubb, Kennedy & Palmer's Pathology of Domestic Animals*. Vol 1. 6th ed. Elsevier; 2016: 164-249.
3. Helmer C, Hannemann R, Humann-Ziehank E, et al. A case of concurrent molybdenosis, secondary copper, cobalt and selenium deficiency in a small sheep herd in Northern Germany. *Animals*. 2021;11(7):1864.
4. Kennedy S, Rice DA. Histopathologic and ultrastructural myocardial alterations in calves deficient in vitamin E and selenium and fed polyunsaturated fatty acids. *Vet Pathol*. 1992 Mar;29(2):129-38.
5. Miller MA, Lyle T, Zachary JF. Mechanisms and Morphology of Cellular Injury, Adaptation, and Death. In: Zachary JF, ed. *Pathologic Basis of Veterinary Disease*. 7th ed. Elsevier; 2022: 47-48.
6. Oakes, SA. Cell Injury, Cell Death, and Adaptations. In: *Robbins & Cotran Pathologic Basis of Disease*. 10th ed. Elsevier; 2022:65-66.
7. Robinson WF, Robinson NA. Cardiovascular System. In: Maxie MG, ed. *Jubb, Kennedy & Palmer's Pathology of Domestic Animals*. Vol 3. 6th ed. Elsevier; 2016: 1-101.
8. Surai PF, Kochish II, Fisinin VI, Juniper DT. Revisiting oxidative stress and the use of organic selenium in dairy cow

nutrition. *Animals (Basel)*. 2019 Jul;9(7): 462.
9. Valentine BA. Skeletal Muscle. In: Zachary JF, ed. *Pathologic Basis of Veterinary Disease*. 7th ed. Elsevier; 2022:1009, 1018, 1025-1027.

CASE III:

Signalment:
4-year-old, female, Southern Pre-alps sheep (*Ovis aries*).

History:
Several animals of a herd showed neurologic symptoms including amaurosis for several weeks. Some animals progressed to death, others were euthanized and submitted for necropsy. This case was referred (alive) to the veterinary hospital for pedagogic purposes. The animal presented depressed, with a left head tilt, circling to the left, and a hypermetric forelimb gait. MRI showed a 4 cm liquid mass in the left cerebral hemisphere compressing the lateral ventricle. The mass was surgically removed; 2 days later the animal was euthanized because of status epilepticus.

Microscopic Description:
Cerebrum: The cerebral parenchyma is characterized by a compressive cystic nodular lesion lined by diffuse, moderate to severe inflammation composed of a large number of lymphocytes and plasma cells surrounding several macrophages, epithelioid cells and multinucleated giant cells with up to 11 nuclei. Multifocally, between the granulomatous inflammation and the cyst wall there is a large amount of amorphous eosinophilic material and cellular debris (liquefactive necrosis). The cyst wall is composed of a thin outer undulating hyaline layer with microtriches (microvilli) and an inner layer of areolar tissue (germinative membrane). Arising from the germinative membrane, multiple larval metazoan parasites are visible

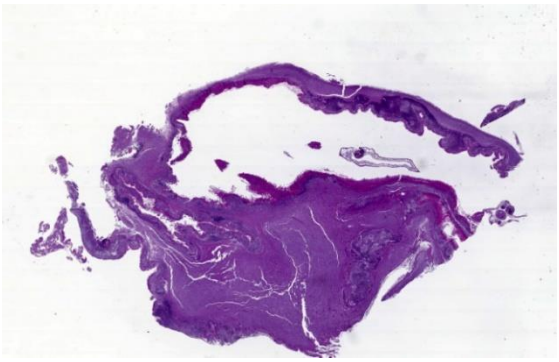

Figure 3-1. Cerebrum, sheep. Within the cerebrum, there is a cystic focus of inflammation containing a coenurus. At this magnification, cross sections of multiple scolices are visible. (6X)

(protoscolices). They are up to 1mm in diameter, lined by an eosinophilic smooth, ridged tegument, which is also visible inside the parasite (inverted tegument). They contain a solid parenchyma with many basophilic to clear oval, up to 15µm basophilic bodies (calcareous corpuscles), an invaginated scolex containing multiple anterior suckers composed of muscular rings comprising radial striations of muscle fibers, and a rostellum with multiple birefringent hooks. Digestive tract, reproductive tract, and pseudocoelom are absent. Lymphocytes and plasma cells are multifocally visible in perivascular areas (lymphocytic cuffs).

Contributor's Morphologic Diagnoses:
Cerebrum: Encephalitis, granulomatous, focally extensive, chronic, moderate with intralesional coenurus protoscolices.

Contributor's Comment:
Coenurus cerebralis is the intermediate stage of *Taenia multiceps*. *C. cerebralis* has a worldwide distribution, affecting primarily sheep and goats, though it has been described in other animals, including cattle, buffalos, yak, horse and pig.[4]

T. multiceps has an indirect life cycle. Canids, including domestic dogs, are

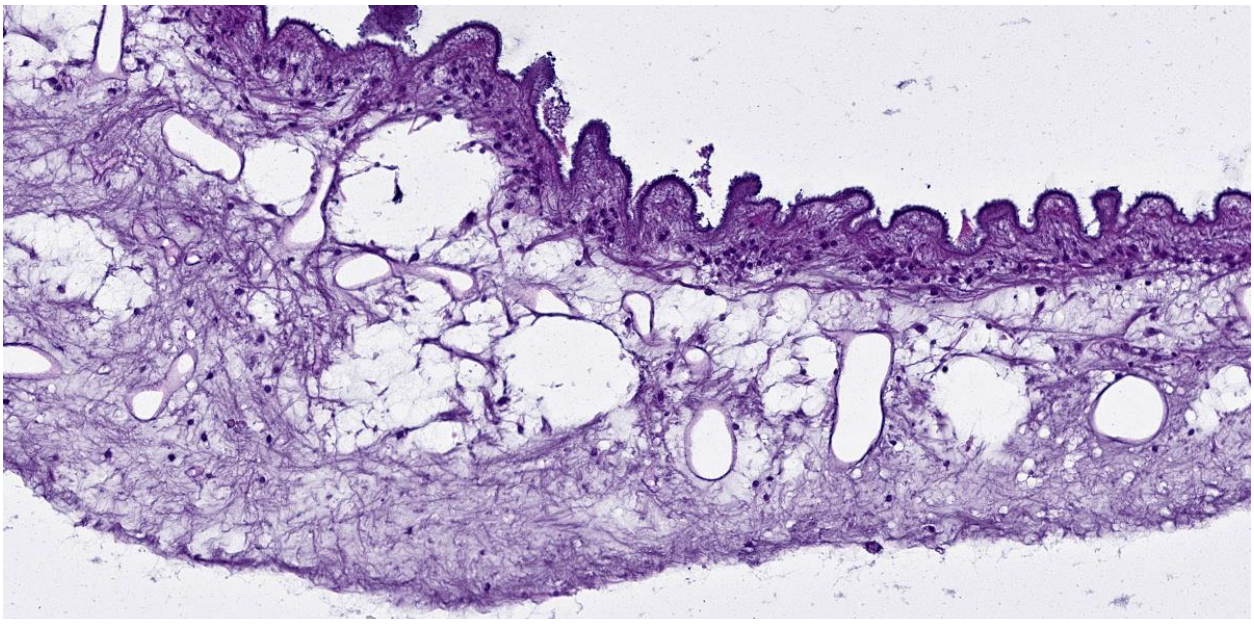

Figure 3-2. Cerebrum, sheep. A fragment of the bladder wall is free-floating within the cystic space. The bladder has a tegument with numerous ridges (top), a spongy parenchyma with numerous somatic cell nuclei subjacent to the tegument, and scattered 10-30um calcareous corpuscles within the spongy parenchyma. (316X)

definitive hosts. Adult worms, up to 100 cm in length, live in the small intestine of definitive hosts, who shed embryonated eggs and gravid proglottids in their faeces, contaminating pasture and water. When eaten by intermediate hosts, eggs release oncospheres (larvae) in the intestine. The oncospheres burrow through the intestinal wall, enter the circulation and migrate to the central nervous system, most often the cerebrum, where they form one or more unilocular bladder cysts.[4] Cerebral coenurosis is caused by *Coenurus cerebralis*, the larval stage of *T. multiceps*. The cysts grow over 6-8 months, eventually causing clinical signs.[4] *T. multiceps* protoscolices develop from the inner cyst wall and can reproduce asexually so
that each coenurus may contain up to 400-500 scolices. The life cycle is completed when a definitive host eats the coenurus, releasing protoscolices, which attach to the intestinal wall and develop into adults in 42 to 60 days. This requires canids to have access to the brain of an infected animal.[4]

The cerebral clinical disease is commonly referred as "sturdy" or "gid." Acute and chronic forms exist. The acute disease is caused by larval migration through the brain. Its severity depends on the number of ingested eggs and migrating parasites. The chronic form is more commonly observed and it occurs in older animals.[4] It is due to cyst development in the brain, and less frequently in the spinal cord, causing parenchymal compression which leads to significant neurological signs and death.[4] Clinical signs of *C. cerebralis* include ataxia, blindness, head pressing and circling towards the affected side of the brain.[4,5,7] Signs progress to coma and death if untreated. Spinal cord lesions cause progressive hind limb paresis/paralysis.[4,5] Diagnosis is made using a combination of clinical signs, neurological examination, ultrasound and necropsy. [4]

Coenurus has been rarely reported in extracerebral locations. These reports are mostly from Asian countries. Non-cerebral coenurus

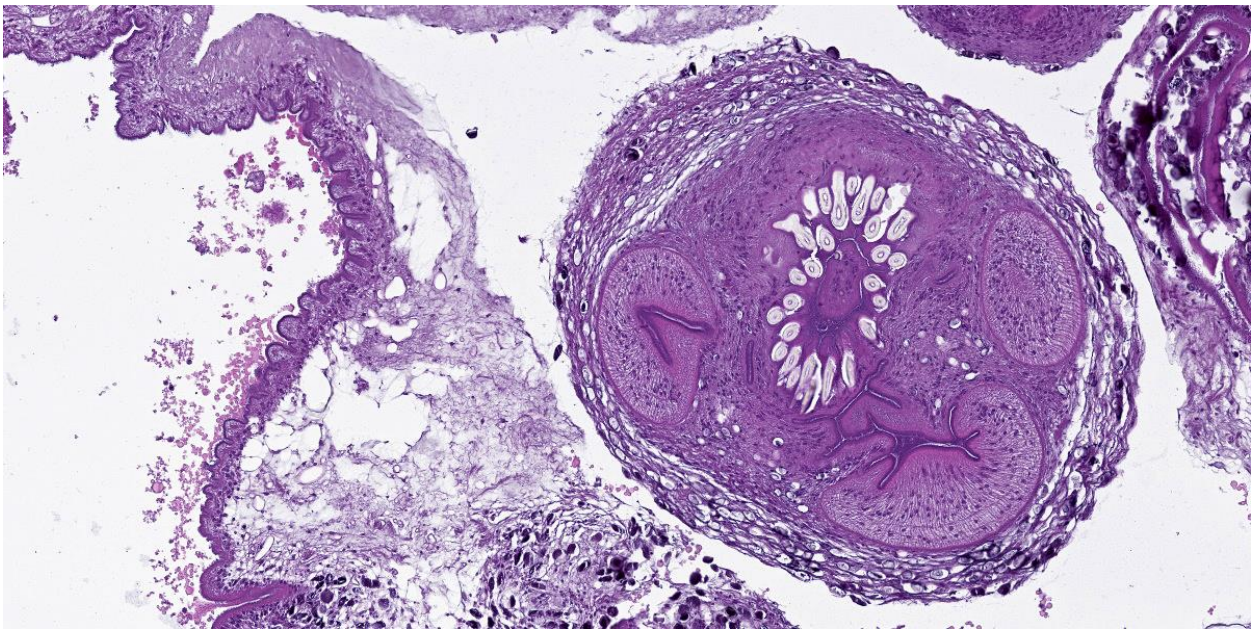

Figure 3-3. Cerebrum, sheep. A cross section of an inverted scolex contains an armed rostellum and several muscular suckers. (93X)

has been described in the skeletal muscle, fascia, adipose tissue, lungs, peritoneum and pelvic cavity of sheep and goats.[1,4] Non-cerebral coenurus is often asymptomatic and only detected at slaughter, but may cause muscle pain.[4]

Grossly, *C. cerebralis* is composed of thin walled, fluid-filled, unilocular cysts up to 7cm in diameter. The cyst walls have multifocal white nodules comprising clusters of protoscolices.[6] Cysts more commonly occur in the cerebrum than in cerebellum or spinal cord. The cysts cause cerebral compression and can be responsible for hydrocephalus and cerebral or cerebellar herniation.[4,7]

Histologically, the cyst wall comprises an external eosinophilic layer with basophilic microtriches (microvilli) and an inner germinative layer made up of areolar tissue.[2] Multiple *T. multiceps* protoscolices arise from invaginations of the cyst wall. Protoscolices have four muscular anterior suckers, a rostellum with up to 34 hooks arranged in 2 rows, and an eosinophilic invaginated tegument.

They also have standard features of cestodes including a parenchyma containing calcareous corpuscles, no pseudocoelom and no digestive or reproductive tract.[6]

Changes to the cerebral/cerebellar parenchyma range from mild to severe liquefactive necrosis and lymphocytic/ granulomatous inflammation with an infiltration of macrophages, lymphocytes, plasma cells and foreign-body multinucleated giant cells. Accompanying changes include neuronal degeneration and necrosis, satellitosis, neuronophagia, demyelination, gliosis and formation of microglial nodules, non-suppurative meningitis and meningeal hyperaemia and oedema.[2,6]

Humans are rarely infected. The main location of intermediate forms in humans is the subcutaneous tissue, but cerebral coenurosis is also described.[4]

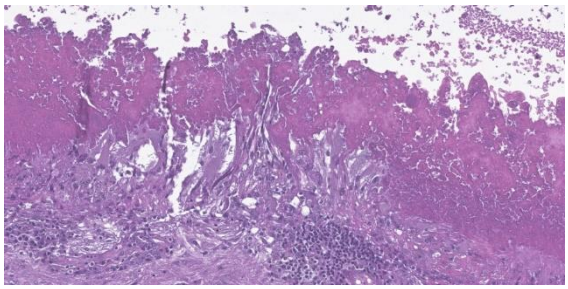

Figure 3-4. Cerebrum, sheep. The coenurus is surrounded by a thick layer of granulomatous inflammation with a peripheral layer of pleomorphic epithelioid macrophages. (306X)

Contributing Institution:
VetAgro Sup
Campus Vétérinaire
Anatomie Pathologique
89 Av. de l'Europe
63370 Lempdes, France
www.vetagro-sup.fr

JPC Diagnosis:
Cerebrum: Encephalitis, granulomatous, focally extensive, severe, with coenurus.

JPC Comment:
Cerebral coenurosis is thought to have been reported for the first time by Hippocrates, who described a condition causing epilepsy in sheep and goats that was characterized by an excess of fluid in the brain.[8] More recently, studies from 1656 and 1724 reported the presence of water-filled sacs or bladders in sheep and cattle, remarking that these bladders were frequent causes of vertigo and death in affected animals.[8] It took until 1853, and feeding cysts taken from infected brains to unsuspecting dogs, to work out the life cycle that the contributor so nicely details.

Today, while coenurosis is reported sporadically in sheep and goats in many European countries (with a relatively high prevalence in Sardinia), the disease is a major endemic disease of small ruminants in the Middle East, particularly in Turkey, Egypt, Iraq, and Jordan.[8] In this group, prevalence rates range from 2.9% of Jordanian sheep to 22.8-23.68% of Iraqi sheep and goats.[8] A wide range of prevalence is reported in Africa, from a low of 4-8% prevalence in Ethiopian sheep and goats to 42.1% in Tanzanian sheep and goats.[8] The disease burden borne by animals and farmers in these regions is significant, and transmission is difficult to control given that wild canids and herding dogs have the ability to travel and spread eggs and proglottids widely.

Infection prevention in endemic areas focuses heavily on educating farmers about proper sanitation and carcass disposal. In Sardinia, Italy, a recent novel preventive measure featured controlled feeding stations, accessible only to birds, where carrion and offal were fed to vultures.[8] Though not yet currently commercially available, vaccination against coenurosis is under development, with the first successful field test of a vaccine based on an oncosphere secretory antigen conducted in Sardinia in 2009.[9] Once neurologic signs of coenurosis are manifest, treatment options include antihelminthic treatments such as praziquantel, and surgical removal, which is frequently successful though uncommonly performed.

As the contributor notes, cerebral coenurosis is zoonotic and humans may become infected by ingesting eggs present in the feces of definitive hosts.[3] Once ingested, oncospheres hatch from the eggs, penetrate the intestinal wall, and travel via the circulation to target organs, including the brain, eyes, and muscle tissue.[3] Luckily, such transmission are rare, with only approximately 40 reported human cases; nevertheless, for those unlucky few, treatment requires invasive treatments with results as generally unsatisfactory as in other species.[3]

Conference discussion focused on the general approach to histologic evaluation of

parasites. The moderator emphasized that the ability to recognize the broad category of parasite, such as cestode, trematode, or nematode, was often sufficient to get to a diagnosis when coupled with host species and anatomic location.

References:

1. Amrabadi O, Oryan A, Moazeni M, Shari-Fiyazdi H, Akbari M. Histopathological and molecular evaluation of the experimentally infected goats by the larval forms of *Taenia multiceps*. *Iran J Parasitol*. 2019 Mar;14:95–105.
2. El-Neweshy MS, Khalafalla RE, Ahmed MMS, Al Mawly JH, El-Manakhly E-SM. First report of an outbreak of cerebral coenurosis in Dhofari goats in Oman. *Braz J Vet Parasitol*. 2019 Aug 1;28(3):479–488.
3. Labuschagne J, Frean J, Parbhoo K, et al. Disseminated human subarachnoid coenurosis. *Trop Med Infect Dis*. 2022;7 (12):405.
4. Oryan A, Akbari M, Moazeni M, Amrabadi OR. Cerebral and non-cerebral coenurosis in small ruminants. *Trop Biomed*. 2014 Mar;31:1–16.
5. Ozmen O, Sahinduran S, Haligur M, Sezer K. Clinicopathologic observations on *Coenurus cerebralis* in naturally infected sheep. *Schweiz Arch Tierheilkd*. 2005 Mar;147:129–134.
6. Rahsan Y, Nihat Y, Bestami Y, Adnan A, Nuran A. Histopathological, immunohistochemical, and parasitological studies on pathogenesis of *Coenurus cerebralis* in sheep. *J Vet Res*. 2018 Mar; 62:35-41.
7. Scott PR. Diagnosis and treatment of coenurosis in sheep. *Vet Parasitol*. 2012 Sep 30;189:75-78.
8. Varcasia A, Tamponi C, Ahmed F, et al. *Taenia multiceps* coenurosis: a review. *Parasites & Vectors*. 2022;15:84.
9. Varcasia A, Tosciri G, Sanna, Coccone GN, et al. Preliminary field trial of a vaccine against coenurosis caused by *Taenia multiceps*. *Vet Parasitol*. 2009 Jun 10;162:285-289.

CASE IV:

Signalment:
8 year-old female alpaca (*Vicugna pacos*)

History:
The animal presented with a one-week history of lethargy, self-isolation from the herd, and progressive neurologic signs.

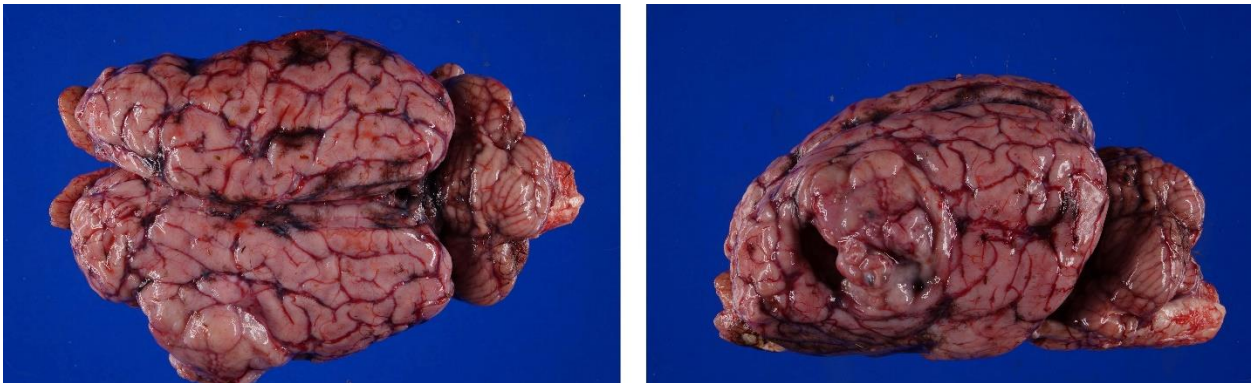

Figure 4-1. Cerebrum, alpaca. A 4.5cm mass is firmly adherent to the left dorsolateral hemisphere. (Photo courtesy of: Colorado State University College of Veterinary Medicine, http://csu-cvmbs.colostate.edu/vdl/Pages/default.aspx)

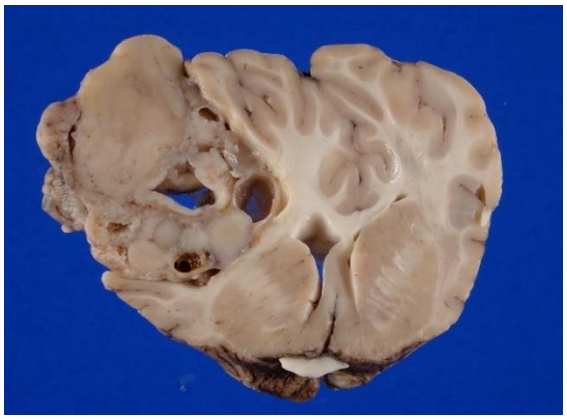

Figure 4-2. Cerebrum, alpaca. The mass in cut section infiltrates the underlying temporal lobe. (Photo courtesy of: Colorado State University College of Veterinary Medicine, http://csu-cvmbs.colostate.edu/vdl/Pages-/default.aspx)

Gross Pathology:
Firmly adhered to the dura and compressing the left dorsolateral cerebrum, including the frontal, parietal and temporal lobes and causing rightward deviation of midline, is a 4.5 cm diameter, multilobulated, well demarcated, firm mass. On cut section the mass varies from pale to dark tan with multifocal regions of cavitation filled with clear, straw colored, viscous fluid. Additionally, there is moderate cerebellar herniation through the foramen magnum.

Imaging Results:
On postmortem MRI, there is a large, broad-based mass in the mid aspect of the dorsal left calvarium causing marked rightward deviation and compression of the falx, left lateral ventricle, left frontal, parietal, and temporal lobes. The mass also causes moderate dorsal compression of the left mesencephalon.

Microscopic Description:
Compressing the cerebrum is a well demarcated, densely cellular, multilobular neoplasm composed of several populations of primitive cells as well as tissue representing all three primordial germ cell lines. Primitive neuroectodermal cells are arranged in dense sheets, as well as pseudorosettes and occasionally rosettes. These primitive cells are often elongate with indistinct cell borders, a moderate amount of eosinophilic cytoplasm and ovoid to elongate nuclei. Anisocytosis and anisokaryosis in this population varies from mild to moderate and mitoses vary based of region. In more mitotically active regions, there are up to 15 mitoses in a single 400x field. Ectodermal components are comprised of well differentiated neurons associated with glial cells and neuropil. Additionally there are numerous cysts filled with lamellated keratin and keratin debris and lined by orderly stratified squamous epithelium. In a single keratin cyst, numerous cross sections of hair shafts are present (not available in all sections provided). Endodermal components are comprised of multifocal regions where neoplastic tissue forms variably sized cysts lined by a single layer of cuboidal to pseudostratified columnar epithelium. The apical surface of this epithelium occasionally has variably distinct, irregular cilia-like projections (respiratory epithelium). Mesodermal elements are comprised of nodules of mesenchymal cells (fibroblasts), as well as bands of smooth muscle adherent to the basal surface of both squamous and respiratory epithelial

Figure 4-3. Cerebrum, alpaca. A heterogenous, multilobular, infiltrative and cystic mass effaces the neuroparenchyma. (HE, 5X)

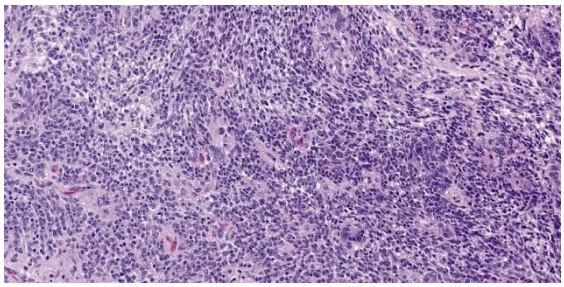

Figure 4-4. Cerebrum, alpaca. The predominant cell in the neoplasm is a poorly differentiated neuroectodermal cell which is arranged in nests and packets, sheets, streams, and occasional rosettes and pseudorosettes. (HE, 5X)

lined cysts. There is a single focus of well-differentiated cartilage (not present in all sections), as well as infrequent foci where there are individualized to small aggregates of adipocytes. The mitotic rate is low across all well-differentiated cell types. Adjacent normal neuropil is not present in all sections.

Immunohistochemistry for synaptophysin reveals primitive neuroectodermal cells that multifocally exhibit punctate to diffuse cytoplasmic immunoreactivity for synaptophysin. Neoplastic neurons and neuropil also exhibit strong cytoplasmic labeling for synaptophysin. Blood vessels, bands of smooth muscle dissecting between large nodules of primitive neuroectodermal cells, and smooth muscle adherent to the basal surface of epithelial lined cysts exhibits strong staining for smooth muscle actin. Several large nodules of primitive neuroectodermal neoplastic cells exhibit irregular, punctate cytoplasmic labeling with cytokeratin. Additionally, epithelium lining cysts exhibit strong cytoplasmic staining for cytokeratin. All neoplastic structures, except epithelial structures that are cytokeratin positive, have strong cytoplasmic staining for vimentin.

Contributor's Morphologic Diagnosis:
Cerebrum: Teratoma

Contributor's Comment:
In human literature, classification of teratomas histologically is divided into three categories: mature, immature, and malignant.[6] Mature teratomas are characterized by several types of mature, well-differentiated tissues, and immature teratomas are comprised of poorly differentiated, primitive tissues.[6] Both types are classically comprised of tissues from all three germ layers. Histopathology of teratomas is widely varied but distinct in complexity. Diagnosis is made when tissue types from two or more of the germinal layers are present. The three germinal layers and tissues representing each of them are as follows:[3,6]

- Mesoderm: notochord, musculoskeletal system (including bone and cartilage), muscular layer of stomach and intestine, circulatory and lymphatic systems, reproductive system (excluding germ cells), dermis of skin, adrenal cortex;
- Endoderm: epithelial linings (digestive tract, respiratory system, urinary system), liver, pancreas, epithelial component of the thymus, thyroid and parathyroid; and

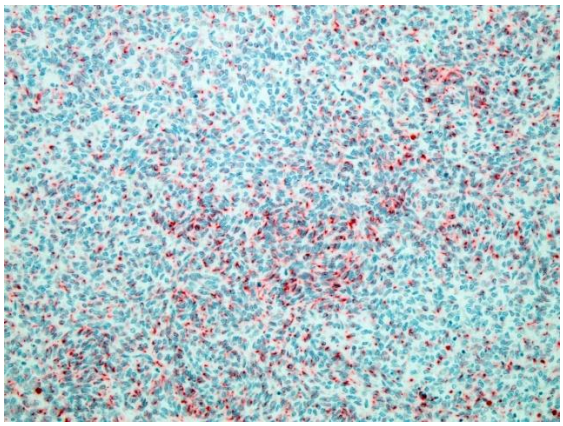

Figure 4-5. Cerebrum, alpaca: The predominant and primitive cell type is positive for cytokeratin. (anti-AE1/AE3, 200X) (Photo courtesy of: Colorado State University College of Veterinary Medicine, http://csu-cvmbs.colostate.-edu/vdl/Pages/default.aspx)

- Ectoderm: epidermis of skin, sweat glands, hair follicles, epithelial lining of mouth and anus, cornea and lens, nervous system, adrenal medulla, tooth enamel, epithelium of pineal and pituitary glands.

Teratocarcinomas (malignant variants) are, in both human and veterinary literature, very rare. These tumors contain somatic-type neoplastic components and, in people, the most commonly seen are rhabdomyosarcomas and undifferentiated sarcomas.[6] Ultimately, a diagnosis of immature teratoma was given based on the high proportion of primitive neuroectodermal components.

In general, teratomas are benign tumors that most often arise in the gonads. In rare circumstances, however, they arise in extragonadal locations, including within the calvarium, and cause significant clinical disease secondary to local mass effect. A handful of reports exist documenting teratomas within the cranium in a variety of veterinary species including a rabbit, kitten, rat, dog, kestrel and an alpaca.[1,2,4,5,11] Other reports of nongonadal sites include adrenal teratomas in ferrets, a renal teratoma in a llama and retrobulbar teratomas in a cat, kestrel and great blue heron.[5,9,12,13,14]

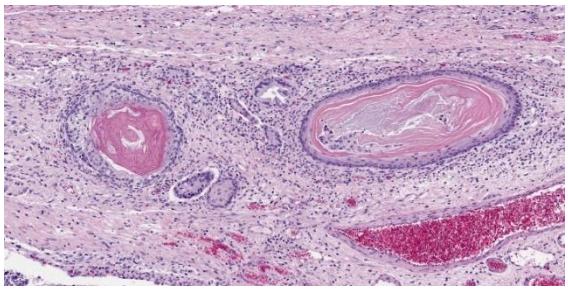

Figure 4-6. Cerebrum, alpaca. Ectodermal structures recapitulating hair follicles are scattered throughout the mass. (HE, 147X)

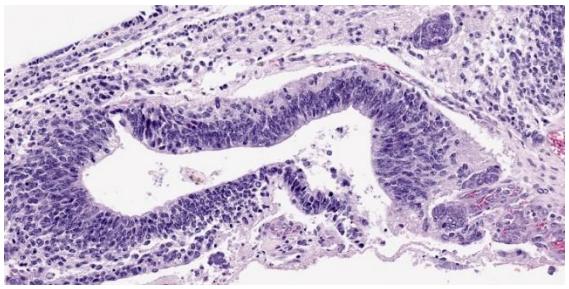

Figure 4-7. Cerebrum, alpaca. Pseudostratified epithelium recapitulates endodermal elements of gut or respiratory epithelium. (HE, 260X)

Contributing Institution:
Colorado State University
College of Veterinary Medicine
https://vetmedbiosci.colostate.edu/vdl/

JPC Diagnosis:
Cerebrum: Teratoma.

JPC Comment:
With a name derived from the Greek words "teras," meaning monster, and "onkoma" meaning swelling, teratomas have been objects of fascination and speculation for centuries, likely due to their startling propensity to produce a disorganized jumble of anatomic structures such as hair, teeth, and eyes.[10] Historically, teratomas have often been interpreted as evidence of Satanic possession or all manner of salacious activities, and all of this attention had an unexpected benefit: research surrounding this fascinating entity led fairly directly to the discovery of embryonic stem cells in the late twentieth century.[7]

As the contributor details, teratomas are distinguished from other tumors by the presence of tissue from multiple embryonic germ layers. This developmental plasticity is shared with embryonic stem cells which are defined by their pluripotency and capacity for self-renewal. In the last thirty years, tremendous strides have been made in developing pluripotent and induced pluripotent human stem cell lines which hold the tantalizing

possibility of revolutionizing regenerative and transplant medicine.

A definitional concern when developing stem cell lines is how to test for pluripotency. This can be done by a variety of in vitro and in vivo measures; however, the gold standard method to confirm developmental pluripotency is the in vivo "teratoma assay."[8] The assay involves injecting presumptively pluripotent stem cells into immunodeficient mice, where, if truly pluripotent, they develop teratomas. These tumors are allowed to grow and are then removed and analyzed histologically to ensure that the tumor produced cell populations from all three developmental layers.[8] The teratoma assay also allows pathologists to assess whether the resulting mass contains malignant elements which may increase the incidence of stem cell-induced malignancies, a current roadblock to more widespread implementation of clinical trials for stem cell therapies.[8] While ethical and humane questions surround the assay and alternatives to its use are being actively sought, the once- maligned teratoma has, for now, found new work as a cornerstone of the embryonic stem cell revolution.

References:

1. Bishop L. Intracranial teratoma in a domestic rabbit. *Vet Pathol*. 1978; 15(4): 525-530.
2. Chénier S, Quesnel A, Girard C. Intracranial teratoma and dermoid cyst in a kitten. *Jour Vet Diag Invest*. 1998;10(4): 381-384.
3. Higgins RJ, Bollen AW, Dickinson PJ, Sisó-Llonch S. Tumors of the Nervous System. In Meuten DJ, ed. *Tumors in domestic animals*. 5th ed. Wiley Blackwell; 2017: 834-891.
4. Hill FI, Mirams CH. Intracranial teratoma in an alpaca (*Vicugna pacos*) in New Zealand. *Vet Rec*. 2008;162(6):188-189.
5. López RM, Múrcia DB. First description of malignant retrobulbar and intracranial teratoma in a lesser kestrel (*Falco naumanni*). *Avian Pathol*. 2008;37(4): 413-414.
6. Louis DN, Ohaki H, Wiestler OD, et al. Germ Cell Tumors. In *WHO classification of tumors of the central nervous system*. 4th ed. International Agency for Research on Cancer; 2016:285-291.
7. Maehle AH. Ambiguous cells: the emergence of the stem cell concept in the nineteenth and twentieth centuries. Notes Rec R Soc Lond. 2011 Dec 20;65 (4):359-78.
8. Montilla-Rojo J, Bialecka M, Wever KE, et al. Teratoma assay for testing pluripotency and malignancy of stem cells: insufficient reporting and uptake of animal-free models-a systematic review. *Int J Mol Sci*. 2023;24(4): 3879.
9. Patel JH, Kosheluk C, Nation PN. Renal teratoma in a llama. *Can Vet J*. 2004; 45(11):938-940.
10. Raup. C. "Teratomas." Embryo Project Encylopedia. https://embryo.asu.edu/handle /10776/1919.
11. Reindel J, Bobrowski W, Gough A, Anderson J. Malignant intracranial teratoma in a juvenile Wistar rat. *Vet Pathol*. 1996;33(4):462-465.
12. Schelling, SH. Retrobulbar teratoma in a great blue heron (*Ardea Herodias*). *Jour Vet Diag Invest*. 1994;6(4):514–516.
13. Williams BH, Yantis LD, Craig SL, Geske RS, Li X, Nye R. Adrenal teratoma in four domestic ferrets (*Mustela putorius furo*). *Vet Pathol*. 2001;38(3): 328–331.
14. Wray JD, Doust RT, McConnell F, Dennis RT, Blunden AS. Retrobulbar teratoma causing exophthalmos in a cat. *J Feline Med Surg*. 2008;10(2):175-180.

WSC 2023-2024
Conference 1 Self-Assessment

1. The vasculitis seen in purpura hemorrhagica is the result of which type of hypersensitivity?
    a. Type I
    b. Type II
    c. Type III
    d. Type IV

2. While most commonly seen in association with *Streptococcus equi* var. *equi*, purpura hemorrhagic may also be seen in association with which of the following bacteria in the horse?
    a. Corynebacterium pseudotuberculosis
    b. Salmonella typhimurium
    c. Actinobacillus suis
    d. E. coli

3. In birds and reptiles, nutritional myopathy is the result of
    a. Vit E deficiency in the absence of selenium deficiency
    b. Vit E deficiency with normal selenium levels
    c. Selenium deficiency in the absence of Vit E deficiency
    d. Selenium deficiency with normal Vit E levels.

4. Mammary gland Which of the following is not present in *Taenia multiceps*?
    a. Armed rostellum
    b. Muscular suckers
    c. Calcareous corpuscles
    d. Paired internal ceca

5. Nervous tissue is derived from which of the following.?
    a. Ectoderm
    b. Mesoderm
    c. Endoderm

Joint Pathology Center
Veterinary Pathology Services

WEDNESDAY SLIDE CONFERENCE 2023-2024

Conference #2 **23 August 2023**

CASE I:

Signalment:
2-year-old, female spayed Australian cattle dog, canine (*Canis lupus familiaris*)

History:
Unspecified clinical signs began at 11-12 months of age. An MRI performed at 21 months of age revealed brain atrophy. Clinical signs progressed to ataxia, anxiety, blindness, and aggression and the animal was euthanized at 23 months of age.

Gross Pathology:
The cerebral gyri are uniformly narrow and widely separated by deep, prominent sulci. The cerebellar folia in all lobes are more deeply incised than expected for a normal brain. There are no other significant findings.

Microscopic Description:
Cerebellar atrophy is manifest as slender folia that retain an anatomically normal branching pattern. This change is quantitatively similar throughout the cerebellum. At higher magnification, the molecular layer is narrow, and the internal granule layer is also thin and depleted of cell nuclei. Interestingly, the Purkinje cell layer is variably altered and the distance between cells is sometimes less than normal, possibly due to shrinkage in other layers. Neuronal cell bodies are multifocally swollen by variable amounts of cytoplasmic, granular to globoid, lightly eosinophilic to brown pigment which occasionally peripheralizes the Nissl substance or nucleus. Rare individual neurons are brightly eosinophilic and shrunken with pyknotic nuclei. Sections stained with Luxol Fast Blue-PAS highlighted cytoplasmic inclusion bodies consistent with lipofuscin.

Figure 1-1. Cerebellum, dog. View of the dorsal cerebrum with the calvarium removed. The gyri are pinched and narrow, while the sulci are prominent. (Photo courtesy of: Veterinary Medical Diagnostic Lab, University of Missouri, https://vmdl.missouri.edu/)

Contributor's Morphologic Diagnosis:
Brain: Cerebellar cortical atrophy with intracytoplasmic neuronal storage material consistent with lipofuscin.

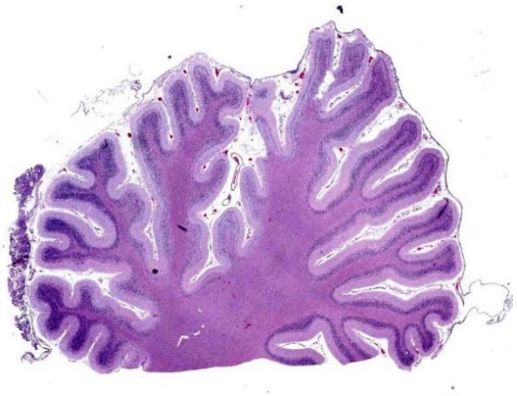

Figure 1-2. Cerebellum, dog. The cerebellar cortex is diffusely thinned across the entire section. (HE, 5X)

Contributor's Comment:

The neuronal ceroid lipofuscinoses (NCLs) are a group of inherited neurodegenerative diseases characterized by progressive decline following normal development. Characteristic of the group is accumulation of auto fluorescent pigment contained in lysosomes of neurons and other cell types.[11]

Dogs are useful models of pathogenesis for this group of diseases and can be used to test the efficacy of therapies for humans.[4] There are 13 canine sequence variants in 8 canine NCL orthologs of human NCLs that produce pathology similar to human diseases and various NCLs have been discovered in 20 different dog breeds.[4] The various subtypes of NCLs are referred to by the name of the particular mutated gene: "CLN," meaning ceroid lipofuscinosis, neuronal, followed by a number.

CLN types 1-4 are diseases of late infantile or juvenile onset, compared to CLNs 5-8 that have infantile onset.[11] There are 27 different mutations known in humans.[11] In CLN5 disease, affected dogs start showing clinical signs at around a year of age. Similar to this dog, the pathology in other breeds and humans consists of severe, generalized, progressive cerebral and cerebellar atrophy. The defective gene product is a soluble glycoprotein that is cleaved in the endoplasmic reticulum and is transported to lysosomes and cleaved by mannose-6-phosphate.[6,11] Intraneuronal storage of the subunit c of mitochondrial ATP synthase and Saponins A and D follows.[11] For all forms of CLN the end product is highly fluorescent and examination of unstained sections by fluorescence microscopy is the most sensitive form of detection.[4] Electron-dense ultrastructural deposits are similar but not identical between the different types of lipofuscinosis.[11]

This patient was an Australian cattle dog that began showing neurological signs at 11-12 months of age. MRI imaging detected diffuse brain atrophy at 21 mos and the dog was euthanized at 23 mos. CLN5 in this breed of dog is the result of a homozygous C->T transition at position 30,574,637 on chromosome 22, reflected in the transcript (CLN5:c:619C>T). This change coverts a glutamine to a termination codon (p.Gln207TER).[5] An identical

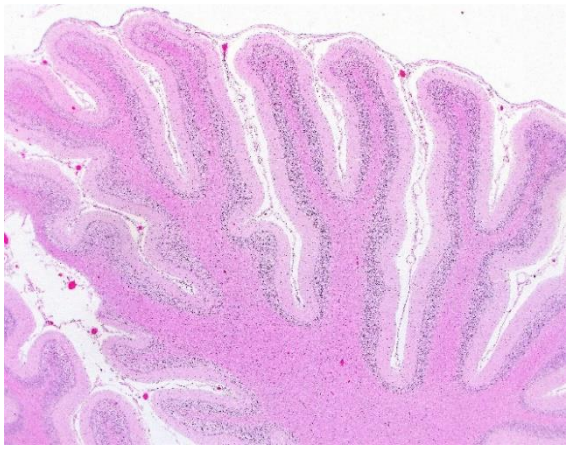

Figure 1-3. Cerebellum, dog. The midline cerebellar cortex demonstrates preservation of the architecture of the folia that are of diminished thickness. (HE, 40X) (Photo courtesy of: Veterinary Medical Diagnostic Lab, University of Missouri, https://vmdl.missouri.edu/)

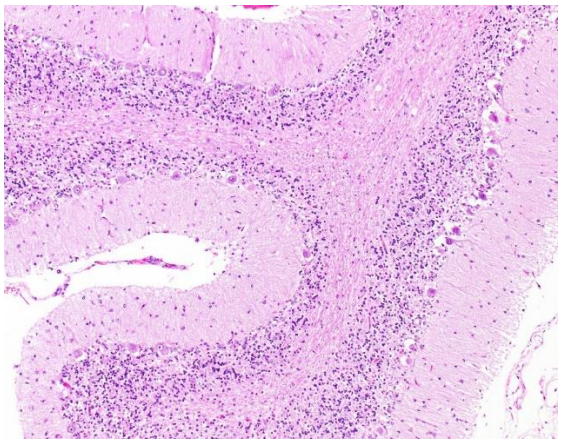

Figure 1-4. Cerebellum, dog. Higher magnification of the cortex shows relative preservation of Purkinje cells and reduced density of the internal granular layer. (HE, 100X) (Photo courtesy of: Veterinary Medical Diagnostic Lab, University of Missouri, https://vmdl.mis-souri.edu/)

mutation has been found in border collies and Laborador-Beagle mix dogs.[7,8,10] A second autosomal recessive mutation in the CLN5 gene (c.934_935delAG) causes disease in Golden Retrievers.[2] Purebred dogs often concentrate homozygous animals, leading to affected offspring. For instance, a high mutant allele frequency (34.8%) has been found in kennels of border collie dogs in Japan, with an allele carrier frequency of 8.1%.[7,8] Popular breeds may also develop more than one CLN mutation (e.g., CLN8 in Australian shepherd dogs and CLN12 in Australian cattle dogs).[3,9]

Increasingly, inborn errors of metabolism are being identified in mixed breed dogs in which neither parent is clinically affected. That several breeds may have a high incidence of heterozygosity and produce affected offspring may suggest that some locations are genetic hotspots in dogs. Finding a CLN5 affected Laborador-Beagle dog is presumably an example to this occurrence.[10] Recent studies of large populations of dogs suggest that some recessive mutations may occur at moderate frequencies in a number of different breeds so that inborn errors of metabolism are increasingly likely in mixed breed dogs.[1,12]

Contributing Institution:
University of Missouri
Veterinary Medical Diagnostic Lab
https://vmdl.missouri.edu/

JPC Diagnosis:
Cerebellum: Cortical atrophy, diffuse, with neuronal ceroidosis.

JPC Comment:
The storage diseases that collectively comprise the neuronal ceroid lipofuscinoses are rather poorly named, as the storage material is neither exclusively ceroid nor lipofuscin. Instead, as the contributor notes, compounds such as subunit c of mitochondrial ATP synthase and sphingolipid activator proteins A and D may constitute the bulk of the retained material.[2]

Inherited neuronal ceroid lipofuscinoses have been described in a variety of cat, sheep, dog, and cattle breeds and are a heterogenous group of diseases. The various disease presentations reflect the diversity of genetic mutations that underly the disease entities, with most mutations occurring primarily in genes that code for lysosomal enzymes (ARSG, ATP13A2, CLN5, CTSD, PPT1, TPP1), endoplasmic reticulum proteins

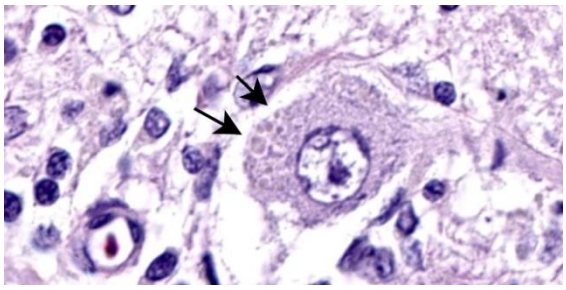

Figure 1-5. Cerebellum, dog. Purkinje cells contain large cytoplasmic vacuoles containing lipofuscin-like pigment. (HE, 1600X)

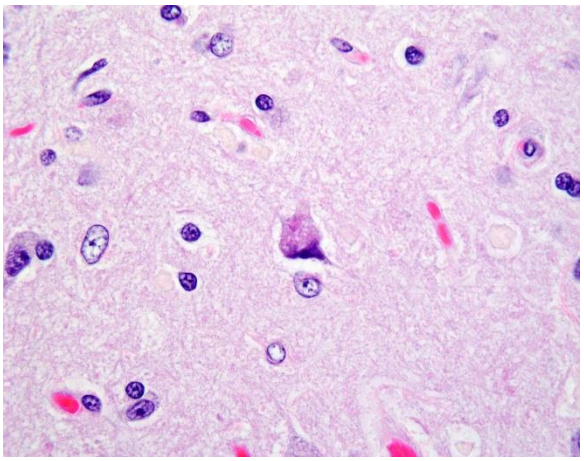

Figure 1-6. Cerebellum, dog. Occasional necrotic neurons with abundant lipofuscin-like pigment are encountered in the brainstem (as well as other sites). (HE, 100X)(Photo courtesy of: Veterinary Medical Diagnostic Lab, University of Missouri, https://vmdl.missouri.edu/)

(CLN6), and endoplasmic reticulum-Golgi complex intermediate compartments (CLN8).[3] All mutations result in the inappropriate storage of proteins and lipofuscin-like lipopigments in multiple organs, but the most clinically significant damage occurs in the cerebral cortex, retina, and cerebellar Purkinje cells.[2] Lesions in these regions result in extensive cellular loss and atrophy with the concomitant clinical signs of dementia, blindness, and ataxia.[2]

Disease presentation, even among species with the same gene mutation, can be subtly different. For instance, the disease presentation in Border Collies and a few other related dogs breeds are due, as the contributor discusses above, to mutation in the CLN5 gene. In these animals, there are gait and visual deficits with increasing aggression and dementia by 18-24 months of age, a case presentation that mirrors the clinical history in this case.[2] The resulting blindness is central in nature as retinal lesions are usually mild. The CLN5 gene deletion typically concentrates neuronal loss in the Purkinje cell layer and the limbic system, resulting in the ataxia and behavior changes that characterize this particular NCL.[2] By contrast, the mutated bovine CLN5 in Devon cattle causes blindness by 14 months of age due to severe retinal atrophy but with only mild neuronal loss within the cerebrum and cerebellum.[2]

While the underlying pathogeneses of the NCLs are still largely unknown, diagnosis is relatively straightforward. NCL-associated storage granules are characteristically autofluorescent under ultraviolet light, have characteristic ultrastructural lamellar profiles, are PAS and Luxol Fast Blue positive, and are weakly acid fast.[2,12]

Conference discussion led by this week's moderator, MAJ Brittany Beavis, Chief of Molecular Pathology at the United States Army Medical Research Institute of Infectious Diseases, centered on the Purkinje cell layer, which appeared atrophic in some sections and relatively normal in others. Conference participants discussed how Purkinje cells can be subject to neurogenic atrophy due to loss of granule cells in addition to the direct damage caused by inappropriate retention of storage material. The variable ratio of these damaging inputs within the affected tissue could be one reason for the heterogeneity

Breed	Mutated Gene
Devon cattle	CLN5
English Setter	CLN8
Border Collie	CLN5
Australian Shepherd	CLN6
American Bulldog	CTSD
Staffordshire Terrier	ARSG
Tibetan Terrier	ATP13A2
Dachshund	PPT1
Miniature Dachshund	TPP1
Borderdale sheep	CLN5
South Hampshire sheep	CLN6

Table 1-1. Selected breeds with associated NCL-related mutations.

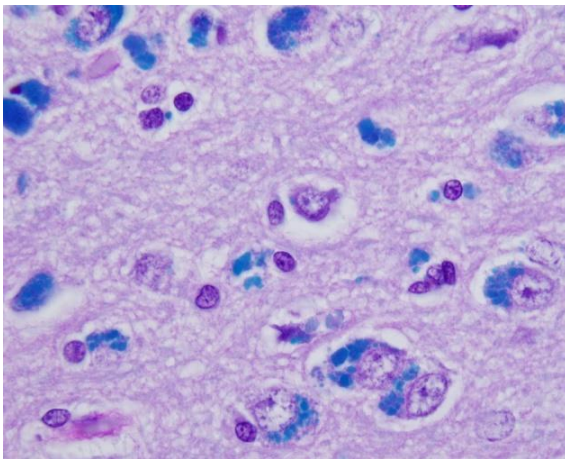

Figure 1-7. A combination Luxol Fast Blue/Periodic Acid-Schiff stain demonstrates numerous lipofuscin-like granules in neurons. (LFB/PAS, 400X) (Photo courtesy of: Veterinary Medical Diagnostic Lab, University of Missouri, https://vmdl.missouri.edu/)

observed within the Purkinje cell layer and is illustrative of the interconnectivity among the cerebellar layers and among neural structures more generally.

References:

1. Donner J, Anderson H, Davison S, et al. Frequency and distribution of 152 genetic disease variants in over 100,000 mixed breed and purebred dogs. *PLoS Genet*. 2018;14(4):e1007361.
2. Cantile C, Youssef S. Nervous System. In: Maxie MG, ed. *Jubb, Kennedy and Palmer's Pathology of Domestic Animals*. Vol 1. 6th ed. Elsevier; 2016: 290-291.
3. Chalkley MD, Armien AG, Gilliam DH, et al. Characterization of neuronal ceroid-lipofuscinosis in 3 cats. *Vet Pathol*. 2014;51(4):796-804.
4. Gilliam D, Kolicheski A, Johnson GS, et al. Golden Retriever dogs with neuronal ceroid lipofuscinosis have a two-base-pair deletion and frameshift in CLN5. *Mol Genet Metab*. 2015;115(2-3):101-9.
5. Guo J, Johnson GS, Brown HA, et al. A CLN8 nonsense mutation in the whole genome sequence of a mixed breed dog with neuronal ceroid lipofuscinosis and Australian Shepherd ancestry. *Mol Genet Metab*. 2014;112(4):302-9.
6. Katz ML, Rustad E, Robinson GO, et al. Canine neuronal ceroid lipofuscinoses: Promising models for preclinical testing of therapeutic interventions. *Neurobiol Dis*. 2017;108:277-287.
7. Kolicheski A, Johnson GS, O'Brien DP, et al. Australian cattle dogs with neuronal ceroid lipofuscinosis are homozygous for a CLN5 nonsense mutation previously identified in border collies. *J Vet Intern Med*. 2016;30(4):1149-58.
8. Mamo A, Jules F, Dumaresq-Doiron K, et al. The role of ceroid lipofuscinosis neuronal protein 5 (CLN5) in endosomal sorting. *Molec Cell Biol*. 2012;32:1855-1866.
9. Mizukami K, Chang HS, Yabuki A, et al. Neuronal ceroid lipofuscinosis in border collie dogs in Japan: clinical and molecular epidemiological study (2000-2011). *ScientificWorldJournal*. 2012; 2012:383174.
10. Mizukami K, Chang HS, Yabuki A, et al. Novel rapid genotyping assays for neuronal ceroid lipofuscinosis in border collie dogs and high frequency of the mutant allele in Japan. *J Vet Diagn Invest.* 2011;23(6):1131-1139.
11. Schmutz I, Jagannathan V, Bartenschlager F, et al. ATP13A2 missense variant in Australian cattle dogs with late onset neuronal ceroid lipofuscinosis. *Mol Genet Metab*. 2019;127(1):95-106.
12. Vandevelde RJH, Oevermann A. *Veterinary Neuropathology: Essentials of Theory and Practice*. 1st ed. John Wiley & Sons, Ltd;2012:181.
13. Villani NA, Bullock G, Michaels JR, et al. A mixed breed dog with neuronal ceroid lipofuscinosis is homozygous for a CLN5 nonsense mutation previously identified in border collies and Australian

cattle dogs. *Mol Genet Metab*. 2019; 127(1):107-115.
14. Wakley SU, Suzuki K, Suzuki, K. Chapter 6: Lysosomal Storage Diseases. In: Love S, Budka H, Ironside JW, eds. *Greenfield's Neuropathology*. CRC Press;2015:495-507.
15. Zierath S, Hughes AM, Fretwell N, et al. Frequency of five disease-causing genetic mutations in a large mixed-breed dog population (2011-2012). PLoS One. 2017;12(11): e0188543.

CASE II:

Signalment:
3-year-old, male neutered domestic short hair cat, feline (*Felis catus*)

History:
This animal was referred to University hospital with a 5-month history of progressive ataxia and a 5-day history of lethargy. Neurological abnormalities included obtundation and profound cerebellovestibular ataxia of all limbs. Proprioceptive positioning was diffusely delayed, hopping was markedly reduced to absent, and extensor postural thrust was absent. There was also positional vertical nystagmus. MRI scan revealed abnormal areas of hyperintensity in the cerebellum along with cerebellar herniation.

Gross Pathology:
The cerebellum is enlarged with 'coning' of the vermis. The cerebral gyri are flattened and widened. On sectioning, the cerebellar white matter was markedly expanded. Thoracic, abdominal, and pelvic organs are unremarkable.

Laboratory Results:
Serology for *Toxoplasma gondii* was negative.

Figure 2-1. Brain, cat. The cerebellum is mildly enlarged, folia are flattened, and there is coning of the vermis. (Photo courtesy of: School of Veterinary Medicine, University College Dublin, Belfield, Dublin 4, Ireland, http://www.ucd.ie/vetmed/)

Microscopic Description:
Numerous large dysplastic neurons up to approximately 60 μm in diameter populate the cerebellar Purkinje cell layer and extend into the molecular and granular layers. These pleomorphic cells are characterised by scant to abundant pale to brightly eosinophilic cytoplasm. Their nuclei are occasionally eccentrically located and up to approximately 30 μm in size varying from round to oval to reniform in shape with vesicular chromatin and a prominent nucleolus. In affected areas, the Purkinje cells are shrunken or lost and there is variable marked depletion of neurons in the granular layer. The neuropil is frequently rarefied or finely vacuolated (oedema) and contains numerous, variably-sized swollen axons (spheroids). These severe changes frequently alternate with sharply defined areas where the normal cerebellar architecture is maintained. The white matter is extensively rarefied and contains large numbers of gemistocytes. Examination with a luxol fast blue stain confirmed marked loss of myelin in affected areas while no change in myelination was found in the cerebellar molecular layer. The meninges and perivascular spaces were multifocally infiltrated by low numbers of lymphocytes. Affected regions of cerebellum were immunohistochemically labeled for

Figure 2-2. Cerebellum, cat. 80% of cerebellar folia are thickened with thinning of the granular cell layer and diminished staining of the granular cell layer within the affected region. There is coning of the posterior vermis. (HE, 6X)

GFAP (astrocytes), NeuN (neuronal nuclei), NF clone 52 (axonal neurofilament H; heavy), and NF clone 312 (axonal pan-neurofilament). Immunohistochemical labeling of PTEN was also carried out to investigate the possibility of loss of PTEN protein expression as a result of PTEN gene mutation. There was consistent cell-specific labeling with each of these five antibodies. While immunolabeling with GFAP or NeuN was not found in dysplastic cells, axonal immunolabeling of NF52 and NF312 was maintained in their axons. Dysplastic neurons presented a heterogenous labeling pattern for PTEN, with the vast majority showing the absence of nuclear and reduced cytoplasmic immunolabeling. There were no abnormal findings in other brain regions.

Contributor's Morphologic Diagnosis:

Brain: Dysplastic cerebellar gangliocytoma.

Contributor's Comment:

This is the first report of dysplastic gangliocytoma of the cerebellum in a cat that had presented with neurological deficits indicating cerebello-vestibular system disease. Dysplastic gangliocytoma of the cerebellum, commonly known as Lhermitte-Duclos disease, is an infrequent benign tumour described in human patients.[9] The neoplasm usually presents as a single unilateral discrete mass in the cerebellum, and bilateral involvement is very rare.[3,4,10,17] There is debate as to whether dysplastic gangliocytoma of the cerebellum represents a true neoplasm or a hamartoma.[14] Hamartomas are disorganised masses of normal to dysplastic cells which arise at sites where these cells are normally present.[8] The fact that these lesions frequently originate from clonal chromosomal aberrations makes their differentiation from benign tumours challenging and perhaps arbitrary. The World Health Organization (WHO) central nervous system conference has graded dysplastic gangliocytoma of the cerebellum as a grade 1 neoplasia.[13] The classic macroscopic lesion is a unilateral enlargement of the cerebellum with maintenance of the folia.[3,10,17] Microscopic findings are variable and include replacement of the cerebellar granular layer by large, well-differentiated, dysplastic ganglion cells.[4] Dysplastic gangliocytoma of the cerebellum can occur sporadically, but has also been associated with Cowden syndrome, an autosomal dominant genetic disorder characterised by multiple hamartomas that leads to an increased risk of developing benign and malig-

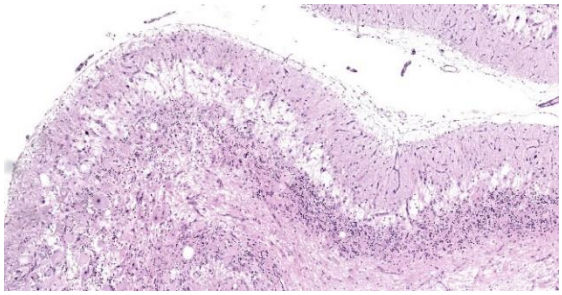

Figure 2-3. Cerebellum, cat. There is marked vacuolation of the molecular layer, loss of Purkinje cells, and marked hypocellularity of the granular cell layer. There is spongiosis of the folial white matter. (HE, 81X)

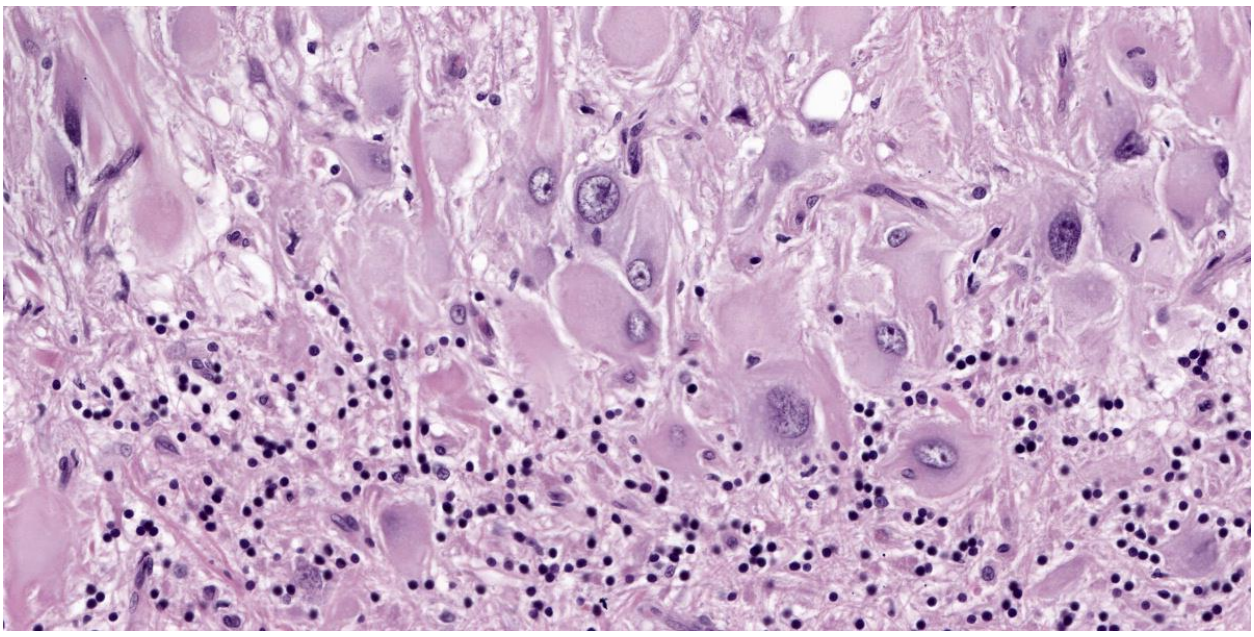

Figure 2-4. Cerebellum, cat. Affected regions of the cerebellar cortex are populated by pleomorphic ganglion cells. Cells range up to 30µm and have pleomorphic nuclei and occasionally prominent cytoplasmic vacuoles. (HE, 315X)

nant tumours. Cowden syndrome is associated with germline mutations of the phosphatase and tensin homolog (PTEN) gene, a tumour suppressor gene that leads to activation of the PI3K/AKT signaling pathway and uncontrolled cell proliferation.[8]

In human patients the lesion is defined by the following components: (1) variable replacement of the cerebellar internal granular layer by dysplastic ganglion cells, (2) abnormal myelinisation of the molecular layer, (3) reduced number of Purkinje cells, (4) large, bizarre neurons, and (5) vacuolisation of cerebellar white matter.[4] Each of these criteria were met in the current case except for abnormal myelinisation of the molecular layer. Interestingly, the current case posed a bilateral presentation, which is rarely described in human patients.[3,10,17] The mild inflammation, not considered to be of clinical significance, most likely occurred secondary to decreased cerebrospinal flow as a result of cerebellar enlargement and herniation.[5] Immunohistochemical labeling confirmed that the dysplastic cells were of neuronal origin; axonal neurofilament immunolabeling was present, although NeuN immunolabeling was absent. Similar results have been reported in gangliocytomas in human patients.[15]

Cowden syndrome is a multiple hamartoma syndrome associated with PTEN mutation in 80% of cases of dysplastic gangliocytoma of the cerebellum in human patients, and clinical diagnosis is made by the presence of a combination of characteristic criteria including mucocutaneous lesions and a wide variety of benign and malignant tumors.[4] Major and minor diagnostic criteria for Cowden syndrome in humans include adult onset of dysplastic gangliocytoma of the cerebellum and benign lipomas.[6,10] A single case of Cowden-like syndrome has been described in the veterinary literature involving a Great Dane puppy that had colorectal hamartomatous polyposis, ganglioneuromatosis, and an associated PTEN mutation.[2] PTEN mutation resulting in downregulation/dysfunction has been reported and is suspected to contribute

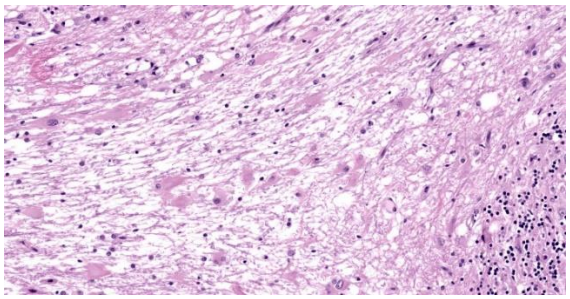

Figure 2-5. Cerebellum, cat. There is marked spongiosis of the cerebellar white matter and numerous gemistocytic astrocytes. (HE, 400X)

to tumorigenesis in cats and dogs.[12,16] In the current case, on IHC for PTEN mutations, the majority of dysplastic neurons showed loss of nuclear PTEN immunolabeling and reduced cytoplasmic immunolabeling. This may suggest that a PTEN mutation contributed to tumourigenesis in this case similar to what has been reported in Cowden syndrome. Although the 'gold standard' diagnosis of germline mutations like PTEN has been Sanger sequencing, studies have suggested the possibility of IHC detection of PTEN mutations as a superior approach as this technique also addresses potential epigenetic elements contributing to the loss of PTEN function.[7]

Contributing Institution:
University College Dublin
School of Veterinary Medicine
Belfield, Dublin 4, Ireland
http://www.ucd.ie/vetmed/

JPC Diagnosis:
Cerebellum: Dysplastic gangliocytoma.

JPC Comment:
The uncontrolled growth that characterizes cancer is effected through two broad mechanisms: gain of function mutations in normal proteins that promote cell growth, or loss of function mutations that diminish the efficacy of cell growth inhibitors. The former mutations turn normal genes into oncogenes that drive cell proliferation via the production of constitutively active oncoproteins.[11] Mutations of the latter type occur in tumor suppressor genes, leading to failure of growth inhibition, a fundamental hallmark of carcinogenesis.[11]

PTEN mutation, highlighted by the contributor as a critical factor in the development of many dysplastic gangliocytomas, is an example of a loss of function mutation in a tumor suppressor. PTEN is a participant in a canonical cell growth pathway that begins with a receptor tyrosine kinase (RTK). RTKs are transmembrane proteins with an extracellular growth factor binding domain and a cytoplasmic tyrosine kinase domain. In normal signal transduction, an extracellular growth factor binds the RTK's extracellular binding domain, transiently activating the RTK and causing it to dimerize and autophosphorylate tyrosine residues on its cytoplasmic tail. These phosphorylated tyrosine residues serve as binding and activation sites for cytoplasmic signaling molecules, most notably RAS.[11] In the activated state, RAS stimulates two downstream signaling cascades: the MAPK cascade and the PI3K/AKT pathway. The common end point of both pathways is the activation or production of transcription factors that move to the nucleus and increase production of proteins that drive progression through the cell cycle. Many proteins within these pathways are encoded by proto-oncogenes; in fact, gain of function point mutations in RAS that cause constant activation of downstream, pro-growth pathways are the most common proto-oncogene abnormalities in human tumors.[11]

In this exuberant signaling milieu, PTEN's function is to inhibit PI3K, the first of a series of serine/threonine kinases in the PI3K/AKT pro-growth pathway. Regulation at this stage is critical as AKT, the next kinase in the signaling cascade, phosphorylates more than

150 proteins involved in regulating protein synthesis and apoptosis.[11] If PTEN acquires a loss of function mutation, as is the case in up to 80% of dysplastic cerebellar gangliocytomas, this cellular brake is lost, leading to unchecked, pro-growth downstream signaling and a predisposition to tumor development.[9]

The contributor alludes to the debate over the classification of this entity. A hamartoma, as stated above, is a non-neoplastic growth characterized by an abnormal growth of cells in their normal anatomic location. Some sources distinguish hamartomas from neoplasia by pathogenesis; hamartoma is usually the result of a systemic genetic abnormality while neoplasia tends to be monoclonal since it originates from a single transformed cell.[1] In this case, the eye-catching dysplastic neurons are in their native location and possibly arise from a germline mutation in PTEN, making classification as a hamartoma seem appropriate. As noted above, however, the human lesion is described by the WHO as a grade 1 neoplasm, and the literature includes a variety of terminology, including the term "hamartomatous neoplasm," which provides little clarity.

Conference participants engaged this debate without reaching general consensus, though most participants felt this entity more likely represented a hamartoma. No matter the terminology, the biological behavior of this entity is benign, though significant morbidity can accompany its growth within the confines of the skull.

References:

1. Batsakis JG. Nomenclature of developmental tumors. *Ann Otol Rhino Laryngol.* 1984;93(1):98-99.
2. Bemelmans I, Küry S, Albaric O, et al. Colorectal hamartomatous polyposis and ganglioneuromatosis in a dog. *Vet Pathol*. 2011;48(5):1012–1015.
3. Borni M, Kammoun B, Kolsi F, et al. The Lhermitte-Duclos disease: a rarebilateral cerebellar location of a rare pathology. *Pan Afr Med J*. 2019;33:118.
4. Brat DJ, Perry A. *Pattern Recognition Series: Practical Surgical Neuropathology: A Diagnostic Approach*. 2nd ed. Elsevier; 2018.
5. Deren KE, Packer M, Forsyth J, et al. Reactive astrocytosis, microgliosis and inflammation in rats with neonatal hydrocephalus. *Exp Neurol*. 2010;226(1): 110–119.
6. Derrey S, Proust F, Debono B, et al. Association between Cowden syndrome and Lhermitte-Duclos disease. *Surg Neurol*. 2004;61(5):447–454.
7. Djordjevic B, Hennessy BT, Li J, et al. Clinical assessment of PTEN loss in endometrial carcinoma: immunohistochemistry outperforms gene sequencing. *Mod Pathol*. 2012;25(5):699–708.
8. Hargis AM, Myers S. The Integument. In: Zachary JF, ed. *Pathologic Basis of Veterinary Disease*. 6th ed. Elsevier; 2017:1009.
9. Joo G, Doumanian J. Radiographic findings of dysplastic cerebellar gangliocytoma (Lhermitte-Duclos Disease) in a woman with Cowden syndrome: a case study and literature review. *J Radiol Case Rep*. 2020;14(3):1-6.
10. Khandpur U, Huntoon K, Smith-Cohn M, et al. Bilateral recurrent dysplastic cerebellar gangliocytoma (Lhermitte-Duclos disease) in Cowden syndrome: a case report and literature review. *World Neurosurg*. 2019;127:319-325.
11. Kumar V, Abbas AK, Aster JC. Neoplasia. In: *Pathologic Basis of Veterinary Disease*. 10th ed. Elsevier; 2022: 286-292.
12. Levine RA, Forest T, Smith C. Tumor suppressor PTEN is mutated in canine osteosarcoma cell lines and tumors. *Vet Pathol*. 2002;39(3):372–378.

13. Louis DN, Perry A, Reifenberger G, et al. The 2016 World Health Organization classification of tumors of the central nervous system: a summary. *Acta Neuropathol*. 2016;131(6):803-820.
14. Nowak DA, Trost HA. Lhermitte-Duclos disease (dysplastic cerebellar gan-gliocytoma): a malformation, hamartoma or neoplasm? *Acta Neurol Scand*. 2002; 105(3):137–145.
15. Rainov NG, Holzhausen H-J, Burkert W. Dysplastic gangliocytoma of the cerebellum (Lhermitte-Duclos disease). *Clin Neurol Neurosurg*. 1995; 97(2):175 -180.
16. Ressel L, Millanta F, Caleri E, et al. Reduced PTEN protein expression and its prognostic implications in canine and feline mammary tumors. *Vet Pathol*. 2009;46(5):860–868.
17. Zak M, Ledbetter M, Maertens P. Infantile Lhermitte-Duclos disease treated successfully with rapamycin. *J Child Neurol*. 2017;32(3):322–326.

CASE III:

Signalment:
11-month-old, female spayed Labrador Retriever dog, canine (*Canis lupus familiaris*)

History:
The dog submitted to the CHUV (Centre Hospitalier Universitaire Vétérinaire), Faculté de Médecine Vétérinaire, University of Montreal, because of recurring respiratory difficulties (panting with its mouth closed) along with a head tilt and turning to the right. Clinical signs had been ongoing for over 9 months. Clinical signs were still present after therapeutic trials with different immunosuppressive drugs. Humane euthanasia was performed at home by the family veterinarian due to the guarded prognosis.

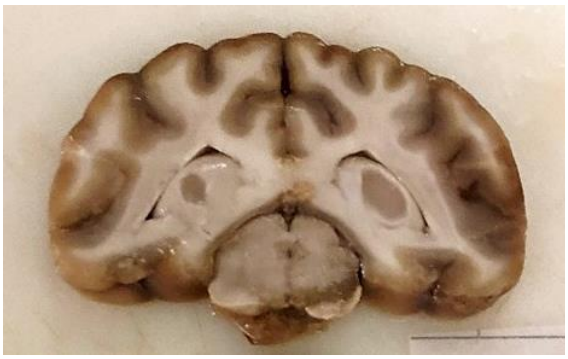

Figure 3-1. Brainstem, dog. There is an area of grey discoloration in the right portion of brain stem which extends slightly to the left of the midline. (Photo courtesy of: Centre de Diagnostic Vétérinaire de l'Université de Montréal, Faculté de Médecine Vétérinaire, Université de Montréal

Gross Pathology:
This 24.5 kg Labrador Retriever dog is submitted frozen for necropsy examination and is in a suboptimal state of conservation following thawing. The animal has adequate muscle mass and body fat stores. The right portion of the cerebral trunk displays a 3x1x1cm area of greyish discoloration which extends slightly to the left of the midline. The overlying leptomeninges have a dark discoloration. The spinal cord is unremarkable grossly. The heart weighs 221 g (0.9% of BW, within normal limits). All other internal organs are normal grossly.

Microscopic Description:
Brain: The observed gross changes in the area of the brain stem correspond to a poorly cellular and poorly delineated process that is continuous with the leptomeninges and multifocally infiltrates the neuroparenchyma. These changes are characterized by anastomosing fronds of spindle to stellate cells surrounded by a mostly loosely arranged fibrous stroma of variable density. This stroma is usually centered around numerous blood vessels, mostly small arterioles. The fusiform cells have a pale acidophilic cytoplasm that is finely fibrillar and moderately well

delineated. The nucleus varies from elongated with rounded ends to round with a finely granular chromatin with no apparent nucleolus. Anisocytosis and anisokaryosis are minimal, atypia is unremarkable and no mitoses are observed. These spindle cells do not stain with GFAP immunohistochemistry staining. The lining of blood vessels located within that stroma is positive for Factor VIII. The leptomeninges overlying these proliferative changes are mildly to moderately thickened multifocally in some areas by similar proliferating spindle cells and contain multifocal and superficially numerous melanin-laden cells (melanocytes). In the adjacent neuroparenchyma, few neurons displaying chromatolysis and rare spheroids are observed.

Contributor's Morphologic Diagnosis:
Brain stem: Cerebral meningioangiomatosis

Contributor's Comment:
Meningioangiomatosis (MA) is, in animals at least, a rare benign lesion, best regarded as a malformation or hamartoma producing circumscribed plaques on the surface of the brain stem and cervical spinal cord.[3] Hamartomas are mass lesions characterized by disorderly overgrowth of tissue elements. MA is seen most commonly in young dogs. Blood vessels appear in excess in these lesions and are cuffed by proliferating cells considered meningothelial in origin. The lesion usually does not extend into the underlying neural substance, which shows mixed degeneration and reactive changes, but can occasionally grow deeper along perivascular spaces.[3,19]

In veterinary medicine, this unique lesion has been described in a few dogs, one cat, one horse with associated mushroom toxicity, one cow that was part of a neuropathology BSE survey in Scotland, and in a CD-1 mouse. [1,2,4,10,15,17,21,22,25] This lesion described by Corbett et al in a 13-y-old cat was located in the leptomeninges and outer neuroparenchyma of the right pyriform and temporal telencephalic lobes, with extensive hemorrhage.[4]

Human MA has been described as coexisting with meningiomas, arteriovenous malformations, oligodendrogliomas, meningeal hemangiopericytomas and orbital erosions.[7] An association with another nervous lesion has also been described in a 3-month-old German shepherd dog with a thalamic astrocytic hamartoma with tectal meningioangiomatosis, and in a 4-y-old Labrador retriever dog with a fibrous meningioma.[11,23]

MA typically occurs in the brain stem and cervical spinal cord of young dogs. An imaging study documented thoracolumbar spinal cord involvement in two dogs (4-y-old male Boxer and 5-month-old female Labrador), an unusual site for this condition.[12] In a 5-year-old dog, a focus of MA located in the caudal thoracolumbar spinal cord and associated with abnormal hind limb gait was successfully excised and resulted in improvement of clinical signs with a good long-term prognosis.[6] This benign lesion could then be curable with surgical resection depending on accessibility of the location, as in humans.[9]

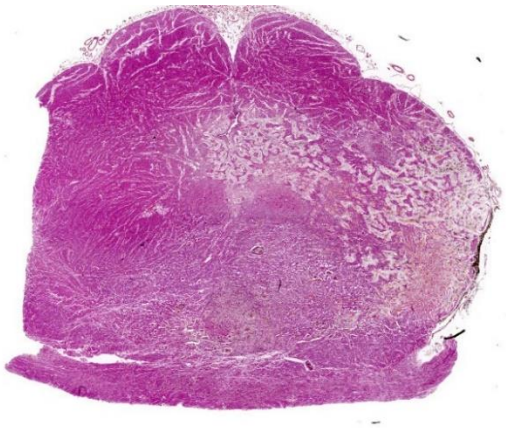

Figure 3-2. Brainstem, dog. A network of haphazardly arranged fibrovascular bundles infiltrates the brainstem. (HE, 6X)

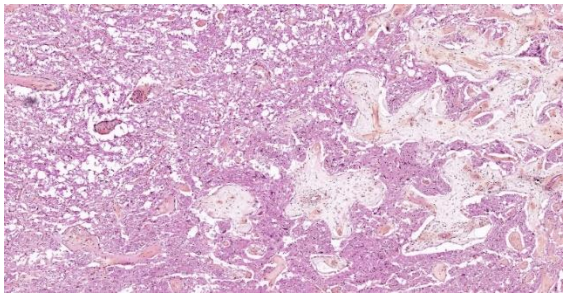

Figure 3-3. Brainstem, dog. The ingrowing bands of fibrous connective tissue contain entrapped thick-walled arterioles. (HE, 52X)

In humans, the sporadic form of MA often results in headache and epilepsy. Focal cortical dysplasia has been described adjacent to foci of such lesions following surgical resection in cases of the sporadic form.[13] MA lesions can demonstrate variable degrees of calcification, cystic degeneration, tumor-like appearance and/or enhancement, making radiologic diagnosis a challenge. Multicystic MA is also recognized as a rare variant of the condition, in which the cysts may have resulted from the gradual accumulation of cerebrospinal fluid in the perivascular spaces of arachnoid/vascular tissue trapped in the cortical parenchyma.[16] Diagnosis of MA lesions can prove difficult but if done timely, prognosis with adequate surgical resection is typically good for seizure control in humans.[9,18,26]

The other form of MA is, in humans, associated with neurofibromatosis type 2 (NF2). NF2-associated lesions are usually asymptomatic. The autosomal dominant mutation in NF2 in humans is located on chromosome 22q12 and encodes for the protein merlin, which is widely expressed and important for cell growth regulation. Individuals with this mutation have a predisposition to develop tumors, particularly vestibular schwannomas and meningiomas, amongst others.[5,26] MA and associated meningioma tissues were evaluated in a case series of 5 human patients using a next generation sequencing assay targeting 1425 cancer-related genes. Of the two MA cases associated with meningioma, one had deletions in the NF2 gene in both the MA and the meningioma, whereas the other had a NF2 deletion in only the MA component. Additional mutations were identified in the MA components of these cases, suggesting that the MA arises from the meningioma rather than the opposite.[8]

In another small case series involving six human patients with MA, neurofibrillary tangles were observed in neurons present both within the MA plaques and in the surrounding cortex. Neither senile plaques nor granulovacuolar degeneration were noted. The factors stimulating the production of neurofibrillary tangles in these cases remains unknown.[14]

Contributing Institution:
Centre de Diagnostic Vétérinaire de l'Université de Montréal (CDVUM)
Faculté de Médecine Vétérinaire
Université de Montréal
Saint-Hyacinthe, Qc, Canada
cdvum@umontreal.ca

JPC Diagnosis:
Brainstem: Meningioangiomatosis.

JPC Comment:
The contributor provides an excellent overview of meningioangiomatosis (MA), a rare entity in both human and veterinary medicine. Being our second hamartomatous entity of the week, it also provides an opportunity to compare and contrast the pathogeneses of NF2-associated MA and the dysplastic cerebellar gangliocytoma examined in the previous case.

Both entities are caused by loss of function mutations in tumor suppressor genes: PTEN in the case of dysplastic cerebellar gangliocytoma, and NF2 in certain cases of MA. NF2 encodes the protein product merlin, which is expressed primarily in neural tissue

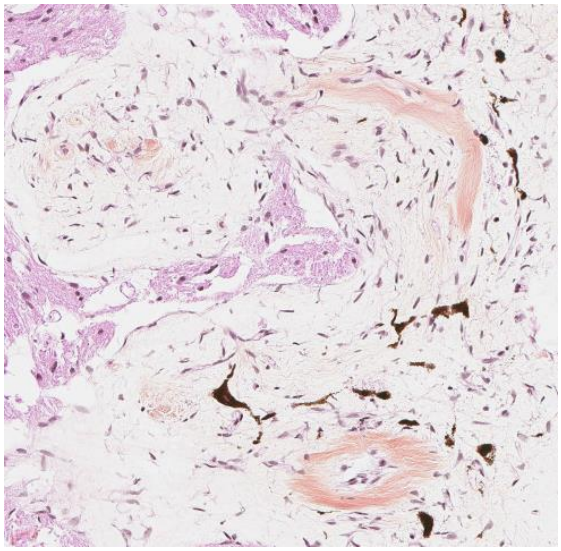

Figure 3-4. Brainstem, dog. Vessels within the fibrous bands are highlighted by a Factor VIII stain. (anti FVIIIa, 200X)

and mediates contact inhibition of cell growth via signals received from the extracellular matrix.[20] Merlin acts as a cell proliferation/arrest toggle, signaling cell proliferation pathways when phosphorylated and cell growth arrest pathways when hypo-phosphorylated. At high cell density, merlin becomes hypo-phosphorylated in response to hyaluronate (HA), a component of extracellular matrix that surrounds cells, thus preventing proliferation when the cellular neighborhood becomes too crowded. Merlin's progrowth activity is mediated by a cytoplasmic interaction with CD44, a transmembrane HA receptor; when cell density is low, merlin is phosphorylated, complexed with CD44, and growth permissive.[20]

Similar to PTEN in the previous case, merlin operates in a complex signaling environment. When not complexed with CD44, merlin is active and inhibits receptor tyrosine kinases (RTKs) and their downstream targets, including the previously discussed PI3K/AKT progrowth pathway. In this way, active merlin functions similarly to PTEN, but at an upstream point in the signaling cascade.[24] In this state, merlin also simultaneously signals pro-apoptotic pathways and inhibits survival and growth pathways. Once complexed with CD44, however, merlin is phosphorylated, inactivated, and no longer able to inhibit RTKs, leading to the reverse effects described above: the PI3K/AKT pathway is activated, apoptotic pathways are inhibited, and survival and proliferative pathways are activated.[24] In cases of NF2-associated MA, the mutation in NF2 leads to a dysfunctional merlin, which is unable to function as a brake on the RTK, PI3K/AKT cell growth pathway, leading to a variety of neuroproliferative conditions, including MA.

Signaling pathways are complex webs, with redundant, competing inhibitory and proliferative signals. This delicate balance is perturbed when any player in the process is dysfunctional. This week, cases II and III provide examples of this complexity by illustrating the effects of two tumor suppressors that are activated by different stimuli, inhibit different steps of the same canonical signaling pathway, and lead to neuroproliferative disorders when mutated.

Comparisons to the previous case brought a reprise of the hamartoma vs. neoplasia debate during the conference. Conference participants were particularly curious about the ingrowth of the abnormal tissue from a focal area of pigmented leptomeninges at the right brainstem. Participants discussed the invasive nature of this lesion and wondered if this entity might be best considered a low grade neoplasm. With no consensus reached, the debate rages on.

References:

1. Balne E, Roth DR, Perentes E. Cerebral meningioangiomatosis in a CD-1 mouse: A case report and comparison with humans and dogs. *Exp Toxicol Pathol*. 2008;60: 247-251.

2. Bishop TM, Morrison J, Summers BA, et al. Meningioangiomatosis in young dogs: a case series and literature review. *J Vet Intern Med*. 2014;18: 522-528.
3. Cantile C, Youssef S. Nervous System. In: Maxie MG, ed. *Jubb, Kennedy and Palmer's Pathology of Domestic Animals*. Vol 1. 6th ed. Elsevier; 2016: 404.
4. Corbett MP, Kopec BL, Kent M, et al. Encephalic meningioangiomatosis in a cat. *J Vet Diagn Invest*. 2022;34(5):889-893.
5. Coy S, Rashid R, Stemmer-Rachamimov A, et al. An update on the CNS manifestations of neurofibromatosis type 2. *Acta Neuropathol*. 2020;139: 643-665.
6. Dantio MC, Dennis AJ, Bergman RL, et al. Surgical treatment of suspected meningioangiomatosis in the thoracolumbar spinal cord. *J Am Anim Hosp Assoc*. 2020;56(4): e564-01.
7. Deb P, Gupta A, Sharma M, et al. Meningioangiomatosis with meningioma: an uncommon association of a rare entity-report of a case and review of the literature. *Childs Nerv Syst*. 2006;22: 78-83.
8. Dono A, Pothiawala AZ, Lewis CT, et al. Molecular alterations in meningioangiomatosis causing epilepsy. *J Neuropathol Exp Neurol*. 2021;80: 1043-1051.
9. Feng R, Hu J, Che X, et al. Diagnosis and surgical treatment of sporadic meningioangiomatosis. *Clin Neurol Neurosurg*. 2013;115: 1407-1414.
10. Frazier K, Liggett A, Hines M 2nd, et al. Mushroom toxicity in a horse with meningioangiomatosis. *Vet Hum Toxicol*. 2000;42(3): 166-167.
11. Ginal PJ, Blanco B, Perez J, et al. Meningioangiomatosis associated with fibrous meningioma in a dog. *Vet Rec*. 2009;164: 756-758.
12. Gonçalves R, Johnston P, Wessmann A, et al. Imaging diagnosis: canine meningioangiomatosis. *Vet Radiol Ultrasound*. 2010;51(2): 148-151.
13. Grabowski MM, Prayson RA. Focal cortical dysplasia in meningioangiomatosis. *Clin Neuropathol*. 2015;34: 76-82.
14. Halper J, Scheithauer BW, Okazaki H, et al. Meningioangiomatosis: a report of six cases with special reference to the occurrence of neurofibrillary tangles. *J Neuropathol Exp Neurol*. 1986;45(4):426-446.
15. Jeffrey M. A neuropathological survey of brains submitted under the Bovine Spongiform Encephalopathy Orders in Scotland. *Vet Rec*. 1992;131(15): 332-337.
16. Li P, Cui G, Wang Y, et al. Multicystic meningioangiomatosis. *BMC Neurology*. 2014;14:32.
17. Lorenzo V, Pumarola M, Munoz A. Meningioangiomatosis in a dog: magnetic resonance imaging and neuropathological studies. *J Small Animal Practice*. 1998;39: 486-489.
18. Makary MS, Kobalka P, Giglio P, et al. Meningioangiomatosis: clinical, imaging and histopathologic characteristics. *J Clin Imaging Sci*. 2020;10(36): 1-4.
19. Marr J, Miranda IC, Miller AD, et al. A review of proliferative vascular disorders of the central nervous system of animals. *Vet Pathol*. 2021;58 (5): 864-880.
20. Morrison H, Sherman LS, Legg J, et al. The NF2 tumor suppressor gene product, merlin, mediates contact inhibition of growth through interactions with CD44. *Genes Dev*. 2001;15(8):968-980.
21. Pumarola M, Martin de las Mulas J, Vilafranca M, et al. Meningioangiomatosis in the brain stem of a dog. *J Comp Pathol*. 1996;115: 197-201.
22. Ribas JL, Carpenter J, Hena H. Comparison of meningioangiomatosis in a man and a dog. *Vet Pathol.* 1990;27:369-371.
23. Sebastianelli M, Mandara MT, Pavone S, et al. Thalamic astrocytic hamartoma and associated meningioangiomatosis in a German shepherd dog. *Res Vet Sci*. 2013;94: 644-647.

24. Stamenkovic I, Yu Q. Merlin, a "magic" linker between extracellular cues and intracellular signaling pathways that regulate cell motility, proliferation, and survival. *Curr Protein Pept Sci*. 2010;11(6): 471-484.
25. Stebbins KE, McGrath JT. Meningio-angiomatosis in a dog. *Vet Pathol*. 1988; 25: 167-168.
26. Tomkinson C, Lu JQ. Meningioangiomatosis: A review of the variable manifestations and complex pathophysiology. *J Neurol Sci*. 2018;392: 130-136.

CASE IV:

Signalment:
13-year-old, male castrated Ragdoll cat, feline (*Felis catus*)

History:
The animal presented with acute (2-3 week) onset of progressive non-painful bilateral hindlimb paraparesis that showed no improvement on corticosteroids. The lesion was localized to the L4 segment by neurology consult, but advanced imaging was declined due to cost. The animal had known chronic kidney disease that was otherwise well-managed and stable. The patient was euthanized due to poor prognosis.

Laboratory Results:
FIV/FELV testing was negative.
PARR on FFPE spinal cord tissue revealed a clonally rearranged T cell receptor gene.

Gross Pathology:
No significant gross lesions are observed in the central nervous tissues or lymphoid organs. Other findings include: (1) marked cardiomegaly (32.68 g) and left ventricular wall thickening; (2) gross bilateral enlargement of the parathyroid glands; and (3) bilateral irregular kidney contours.

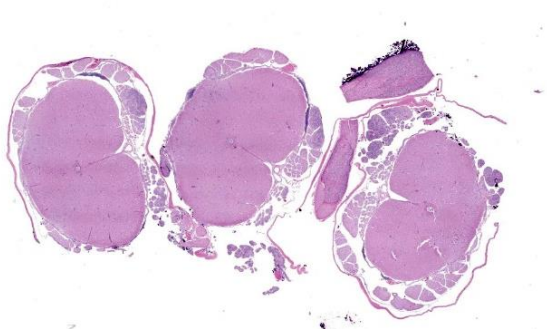

Figure 4-1. Spinal cord, cat. Multiple sections of spinal cord and spinal nerves are submitted for examination. There is scattered hypercellularity of the meninges seen at this magnification. (HE, 5X)

Microscopic Description:
Spinal cord (L1-L5): Neoplastic intermediate to large (nuclei = 1.5 to 2 x RBC) round cells arranged in sheets expand the leptomeninges, infiltrate into the spinal nerve roots, and surround vessels (up to 6 cell layers thick) within the neuropil. Neoplastic cells have distinct cell borders and a small amount of amphophilic, granular cytoplasm. Nuclei are irregularly round with peripheralized chromatin and 1 variably distinct, basophilic nucleolus. There is moderate anisocytosis and anisokaryosis. There are 6 mitotic figures in 0.237 mm^2 (equivalent to 1 high power field). Separating neoplastic cells are a moderate number of small lymphocytes, histiocytes, rare plasma cells, and neutrophils. Throughout the neuropil there is increased cellularity due to neoplastic round cells and reactive glial cells. White matter myelin sheathes are occasionally dilated and contain a swollen axon (spheroid) or foamy macrophages (digestion chambers). Within the neuropil are frequent homogenous, basophilic staining, round, cytoplasmic inclusions (Lafora bodies). Occasionally neurons have peripheralized Nissl substance and yellow brown cytoplasmic pigment , interpreted as lipofuscin.

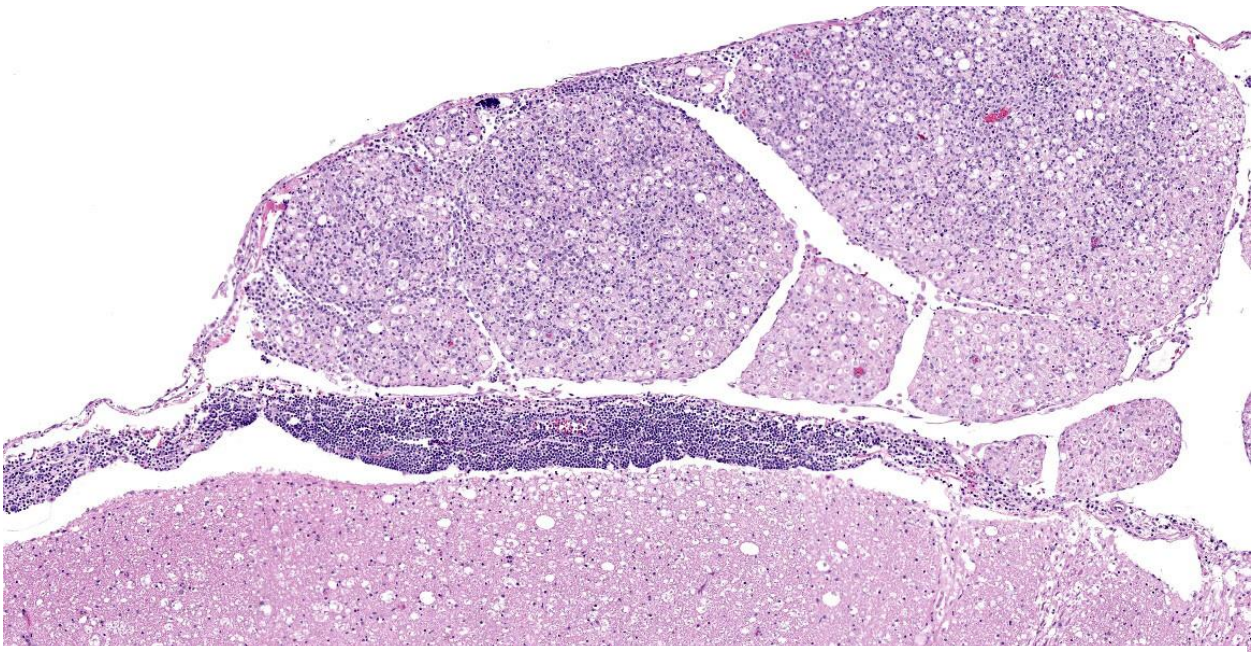

Figure 4-2. Spinal cord, cat. Neoplastic lymphocytes infiltrate and expand the meninges (center) and the adjacent spinal nerve (top). There are numerous dilated sheaths and damaged axons within the spinal nerve and underlying spinal cord. (HE, 77X)

Contributor's Morphologic Diagnosis:
Spinal cord, L1-L5: Lymphoma (neurolymphomatosis), T-cell, with mild/moderate white and grey matter degeneration with multifocal Lafora bodies (incidental).

Contributor's Comment:
The acute neurologic presentation in this case was associated with lymphoma of the spinal cord, spinal nerve roots, and leptomeninges. Infiltrates of neoplastic lymphocytes with a mixed inflammatory response extended into the leptomeninges of the cerebrum, cerebellum, and brainstem (tissues not provided).
Because some areas had more mixed inflammatory infiltrates, immunohistochemistry for FIP antigen was performed to rule out Feline Infectious Peritonitis and no immunoreactivity was noted. Immunohistochemistry for CD3 demonstrates strong immunoreactivity in the neoplastic cells infiltrating or expanding neural tissue, consistent with a T cell lymphoma. Small aggregates of CD20 expressing cells (B-cells) are attributed to secondary inflammation which does not infiltrate into neural tissue. Formalin-fixed paraffin embedded (FFPE) tissue was submitted for PARR, which identified a clonally rearranged T cell receptor gene, further supporting the diagnosis of T cell lymphoma in this case. A complete postmortem examination was performed with histologic review of select samples of all major organ systems, and no involvement of any other organ systems was noted in this case (tissues not provided).

While lymphomas in cats are common and nervous system involvement may be part of a multicentric process, primary lymphomas of the nervous system are considered rare.[6] Primary lymphomas of the nervous system include both neuroinvasive and intravascular lymphomas. Our case is an example of the neuroinvasive subtype. Intravascular lymphoma is a rare subtype in which there is preferential accumulation of neoplastic lymphocytes within small blood vessels in the central nervous system (CNS) and

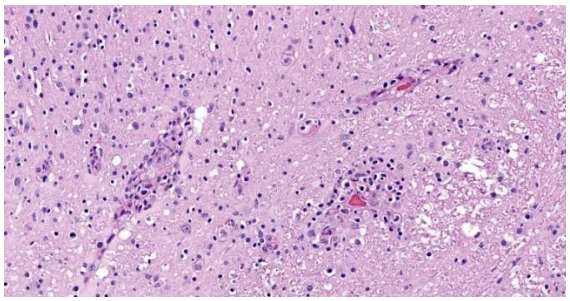

Figure 4-3. Spinal cord, cat. Neoplastic lymphocytes extend from the infiltrated meninges along Virchow-Robin spaces. (HE, 306X)

extraneurally in some organs. This usually occurs without leukemia or systemic mass lesions. Complete vessel occlusion by neoplastic cells can lead to infarction in these cases.[6]

When there is diffuse infiltration of malignant lymphoid cells into peripheral nerves, the term neurolymphomatosis is used.[5,8] This is most common in humans due to non-Hodgkin's lymphoma and may encompass cases with or without CNS involvement. In humans, it is almost exclusively B cell origin, though rare reports of T cell associated lymphomas have been reported.[4] Though a distinct mechanism for neurotropism has not been identified in either human or veterinary literature, CD56 (NCAM, neural cell adhesion molecule) has been implicated.[7,9]

There have been scattered case reports of neurotropic lymphoma or neurolymphomatosis of cats in the veterinary literature.[3,5,7,10-14,16,18,19] An older case series and more recent studies have also described primary central nervous system feline lymphoma with variable gross and clinical presentations and immunophenotypes.[1,11,14,15,19] There is roughly equal distribution of both T and B cell lineages reported in both case reports and case series, which contrasts to the majority B cell immunophenotype reported in humans.[4] The most common location for primary CNS lymphoma in cats is the spinal cord. Similarly, peripheral nervous system (PNS) involvement can occur exclusively in the PNS or simultaneously with CNS lymphoma.

The clinical (antemortem) diagnosis of primary nervous system lymphoma may be challenging. Advanced imaging combined with cerebrospinal fluid (CSF) analysis may offer the best chance at antemortem diagnosis, but often results can vary and be nonspecific.[1] CSF analysis was not performed in this case. Gross findings may be minimal, as neoplastic infiltrates may not create grossly visible enlargement or a discrete mass effect. Histologic examination and immunohistochemistry remain the gold standard in both human and veterinary medicine.[17] Important clinical differential diagnoses for hindlimb paresis/paralysis include thromboembolic disease (such as saddle thrombus or fibrocartilaginous embolism), demyelinating diseases (i.e. peripheral neuropathies), other neoplasms of the spinal cord or spinal canal, infectious meningomyelitis/neuritis (e.g., Feline Infectious Peritonitis, toxoplasmosis, rabies), trauma, degenerative disk disease, neurotoxins (i.e. bromethalin), or metabolic abnormalities (such as hypoglycemia or electrolyte disturbances).

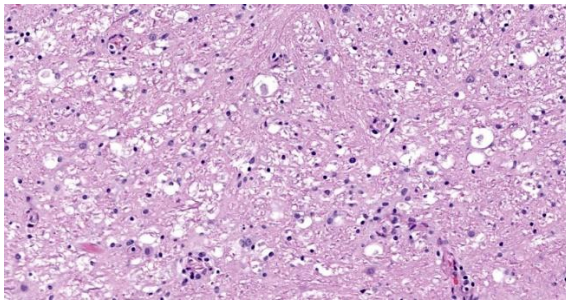

Figure 4-4. Spinal cord, cat. Adjacent to the neoplasm, white matter contains numerous dilated myelin sheaths and swollen axons. (HE, 255X)

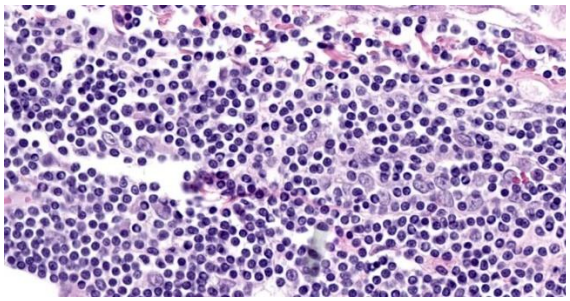

Figure 4-5. Spinal cord, cat. High magnification of lymphocytes within the meninges. (HE, 731X)

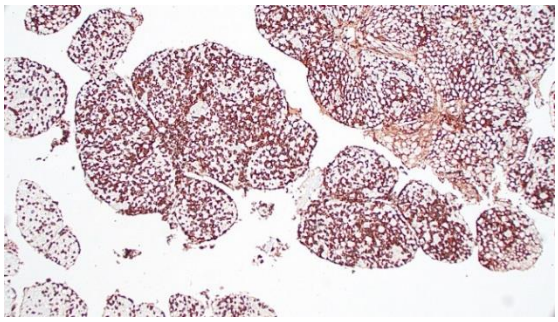

Figure 4-6. Spinal cord, cat. Neoplastic cells demonstrate strong cytomembranous staining for CD3. (anti-CD3, 100X)

JPC Diagnosis:
Spinal cord and spinal nerves: Lymphoma.

JPC Comment:
The contributor provides an excellent review of neurolymphomatosis and correctly notes that this entity presents a particular diagnostic challenge.

In addition to cats, neurolymphomatosis has been reported in a smattering of dogs and horses, often with minimal perivascular cuffing of clonal lymphocytes throughout the CNS.[6] Clinical signs in affected animals are variable, typically non-specific, and stem from Wallerian degeneration of axons due to heavy lymphocytic infiltration of the peripheral nerves. The most common presenting complaints are single or multi-limb lameness, muscle weakness, monoparesis or plegia, and cauda equine syndrome, depending on the particular nerves affected.[2]

Antemortem diagnosis in humans is typically made on the basis of enlargement or enhancement of nerves and nerve roots on MRI and PET/CT images and the examination of peripheral nerve biopsy speciments.[2] Even so, in one case study series, 45% of cases were diagnosed as neurolymphomatosis only at autopsy.[17] In veterinary medicine, MRI exam is typically cannot provide definitive diagnosis due to the lack of historically consistent MRI findings among histologically confirmed cases of neurolymphomatosis.[6]

Postmortem gross findings can include bilateral asymmetrical or symmetrical thickening of the spinal or cranial nerves, though it is more common to find no gross lesions, as illustrated in this case. Definitive diagnosis requires histologic evidence of infiltration of nerve fascicles of B- or T-cell lymphocytes in rows between peripheral nerve axons and within intraneural and epineural spaces.[6]

Conference participants discussed two histologic features of this case that do not strictly fit the case definition of neurolymphomatosis: the abundant mixed inflammatory infiltrate composed of B lymphocytes and plasma cells within the leptomeninges and the presence of abundant neoplastic T lymphocytes within the spinal cord parenchyma.

Prior to reviewing IHC results, conference participants assumed meningeal lymphocytes were an extension of the neoplastic process; however, IHC results convincingly indicate that the meningeal lymphocytes are B lymphocytes admixed with fewer plasma cells and few histiocytes, indicating that these aggregates most likely represent chronic inflammation. Conference participants felt the chronic inflammation could be plausibly explained by the presence of long-standing neoplastic infiltration of the spinal nerves, though this feature has not been consistently described in this entity. More confounding

was the presence of neoplastic lymphocytes within the spinal cord. Neurolymphomatosis is, by definition, neoplastic infiltration of the peripheral nervous system without infiltration of other organs. The presence of lymphocytes within the spinal cord parenchyma, along with the inability to conclusively rule out other lymphomatous foci elsewhere in the animal, led to a conservative JPC diagnosis of lymphoma.

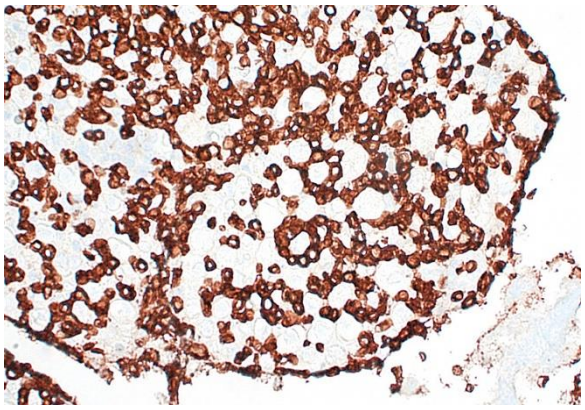

Figure 4-7. Spinal cord, cat. Neoplastic cells demonstrate strong cytomembranous staining for CD3. (anti-CD3, 400X)

References:

1. Durand A, Keenihan E, Schweizer D, et al. Clinical and magnetic resonance imaging features of lymphoma involving the nervous system in cats. *J Vet Intern Med*. 2022;36(2):679-693.
2. Fantaconi N, Walker JJA, Ives EJ. What is your neurologic diagnosis? *JAVMA.* 2020;257(10):1013-1016.
3. Fondevila D, Vilafranca M, Pumarola M. Primary central nervous system T-cell lymphoma in a cat. *Vet Pathol*. 1998;35(6):550-553.
4. Gan HK, Azad A, Cher L, Mitchell PL. Neurolymphomatosis: diagnosis, management, and outcomes in patients treated with rituximab. *Neuro Oncol*. 2010; 12(2):212-215.
5. Higgins MA, Rossmeisl JH Jr, Saunders GK, Hayes S, Kiupel M. B-cell lymphoma in the peripheral nerves of a cat. *Vet Pathol.* 2008;45(1):54-57.
6. Higgins RJ, Bollen AW, Dickinson PJ, Siso-Llonch S. Tumors of the Nervous System. In: Meuten DJ, ed. *Tumors in Domestic Species*. 5th ed. Wiley Blackwell; 2020:872-877.
7. Hsueh CS, Tsai CY, Lee JC, et al. $CD56^{+}$ B-cell neurolymphomatosis in a cat. *J Comp Pathol*. 2019;169:25-29.
8. Kelly JJ, Karcher DS. Lymphoma and peripheral neuropathy: a clinical review. *Muscle Nerve*. 2005;31(3):301-313.
9. Kern WF, Spier CM, Hanneman EH, Miller TP, Matzner M, Grogan TM. Neural cell adhesion molecule-positive peripheral T-cell lymphoma: a rare variant with a propensity for unusual sites of involvement. *Blood*. 1992;79(9):2432-2437.
10. Linzmann H, Brunnberg L, Gruber AD, Klopfleisch R. A neurotropic lymphoma in the brachial plexus of a cat. *J Feline Med Surg.* 2009;11(6):522-524.
11. Mandara MT, Domini A, Giglia G. Feline lymphoma of the nervous system: immunophenotype and anatomical patterns in 24 cases. *Front Vet Sci*. 2022; 9:959466.
12. Mandrioli L, Morini M, Biserni R, Gentilini F, Turba ME. A case of feline neurolymphomatosis: pathological and molecular investigations. *J Vet Diagn Invest*. 2012;24(6):1083-1086.
13. Mellanby RJ, Jeffery ND, Baines EA, Woodger N, Herrtage ME. Magnetic resonance imaging in the diagnosis of lymphoma involving the brachial plexus in a cat. *Vet Radiol Ultrasound*. 2003;44 (5):522-525.
14. Mello LS, Leite-Filho RV, Panziera W, et al. Feline lymphoma in the nervous system: pathological, immunohistochemical, and etiological aspects in 16

cats. *Pesq Vet Bras.* 2019;39(06):393-401.
15. Rissi DR, McHale BJ, Miller AD. Primary nervous system lymphoma in cats. *J Vet Diagn Invest*. 2022;34(4):712-717.
16. Sakurai M, Azuma K, Nagai A, et al. Neurolymphomatosis in a cat. *J Vet Med Sci*. 2016;78(6):1063-1066.
17. Shree R, Goyal MK, Modi M, et al. The diagnostic dilemma of neurolymphomatosis. *J Clin Neurol*. 2016;12(3):274-281.
18. van Koulil Q, Santifort KM, Beukers M, Ioannidis M, Van Soens I. Neurolymphomatosis in a cat with diffuse neuromuscular signs including cranial nerve involvement. *Vet Rec Case* Rep. 2022; 10:e482.
19. Zaki FA, Hurvitz AI. Spontaneous neoplasms of the central nervous system of the cat. *J Small Anim Pract*. 1976;17 (12):773-782.

WSC 2023-2024
Conference 2 Self-Assessment

1. Lipofuscin granules demonstrate autofluorescence in unstained slides.
    a. True
    b. False

2. Only homozygous dogs manifest clinical signs of ceroid lipofuscinosis.
    a. True
    b. False

3. In which of the following is dysplastic cerebellar glangliocytoma more commonly identified?
    a. Ox
    b. Humans
    c. Cats
    d. Rodents

4. What is the most common location for meningioangiomatosis in young dogs?
    a. Cerebrum
    b. Cerebellum
    c. Brainstem
    d. Optic nerve

5. True or false. Neurolymphomatosis in humans are most commonly of B-cell origin.?
    a. True
    b. False

Joint Pathology Center
Veterinary Pathology Services

WEDNESDAY SLIDE CONFERENCE 2023-2024

Conference #3 **30 August 2023**

CASE I:

Signalment:
14-year-old, American Paint gelding, horse (*Equus caballus*)

History:
The horse presented to its primary care veterinarian for an approximately 3 cm in diameter mass on the right facial crest that had been present for about two months. The mass began increasing in size two weeks prior to presentation. An in-house fine needle aspiration (FNA) cytology revealed 'macrophages and bacteria'. On ultrasonography the mass was noted to have a soft tissue echogenicity, lobulated appearance and several small fluid-filled pockets throughout.

Gross Pathology:
The mass was excised and submitted for histologic examination. The mass was transected prior to submission into two, approximately 5.0 x 2.0 cm, triangle-shaped sections of haired skin. On cut section there were multiple, variably sized and shaped foci that contained a yellow granular material.

Microscopic Description:
Haired skin, right facial crest: On histologic examination there is a poorly demarcated, nonencapsulated, non-compressive mass in the hypodermis. The mass extends to the lateral and deep surgical borders. The mass comprises islands and sheets of individualized round cells, supported by a dense collagenous stroma. The round cells have distinct cell borders and a moderate to high nuclear to cytoplasmic ratio. The cytoplasm is scant to moderate, grey blue and coarsely granular. The intracytoplasmic granules stained positively with toluidine blue stain (mast cell granules). The nucleus was centric, round to oval with a finely reticular chromatin pattern and a small to inconspicuous nucleolus. Mitotic figures are not present in the sections examined. Comprising approximately 30-40% of the area of the neoplasm are multiple, variably-sized (100-700µm), irregularly shaped,

Figure 1-1. Haired skin, horse. Two sections of skin with a hypodermal mass with yellow foci scattered throughout were submitted to the contributor. (Photo courtesy of: Department of Veterinary Pathology and Prairie Diagnostic Services, Western College of Veterinary Medicine, University of Saskatchewan)

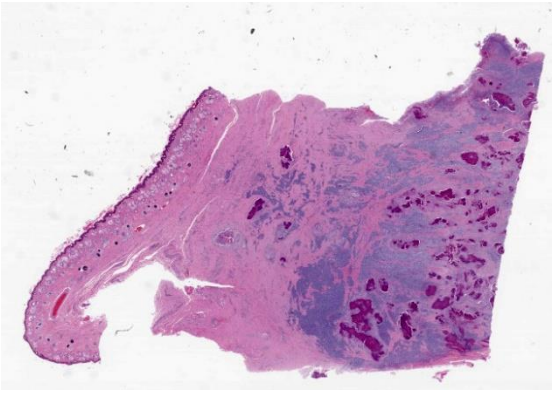

Figure 1-2. Haired skin, horse. A moderately cellular area with scattered foci of eosinophilic debris effaces the deep dermis and subcutis. (HE, 5X)

bright pink foci of necrosis with a central core of disintegrating inflammatory cells (eosinophils) and karyorrhectic debris, a peripheralized layer of multinucleated giant cells, foamy macrophages and a few layers of fibroblasts. Neoplastic mast cells, admixed with moderate numbers of eosinophils and a few lymphocytes, surround these foci.

Contributor's Morphologic Diagnosis:
Cutaneous mast cell tumor.

Contributor's Comment:
Mast cell tumors are relatively uncommon in horses. They are usually benign tumors, with only a few reports where they show aggressive behaviour. Equine cutaneous MCTs are reported to commonly affect head, neck, trunk and limb.[1,2] They are rarely reported to affect other areas such as upper respiratory tract, oral cavity and eye.[2] There is a predilection in males, and no apparent breed predilection. The majority of these tumors are non-pruritic and non-painful.[3] They show slow, progressive growth or become static, even over a course of two years.[2] Rarely a lesion may show sudden rapid growth.[1] Equine mast cell tumors are also called mastocytosis or mastocytoma due to their clinical features and benign behaviour. There is some discussion in the literature regarding their representation as a true neoplastic process.[1,2,3]

Histologically, they manifest as well demarcated masses in the dermis or subcutis, comprised of sheets of well-differentiated mast cells admixed with a few eosinophils and prominent areas of necrosis, fibrosis and dystrophic mineralization and rare mitotic figures.[2,3] The mast cell granules are often numerous but difficult to visualize with routine hematoxylin and eosin staining.[2] Histochemical stains to highlight the mast cell granules were performed in this case (toluidine blue and Luna stains) and confirm the diagnosis. Histological grading schemes do not exist for equine cutaneous MCTs. Prognosis is usually good and complete surgical excision is curative. Recurrence after surgical excision is uncommon. Spontaneous regression has been reported in cases with incomplete surgical excision.

Contributing Institution:
Department of Veterinary Pathology and
Prairie Diagnostic Services
Western College of Veterinary Medicine,
University of Saskatchewan
52 Campus Drive
Saskatoon, Saskatchewan
S7N 5B4 Canada

JPC Diagnosis:
Haired skin: Mast cell tumor.

JPC Comment:
Equine mast cell tumors (MCTs) may present a diagnostic challenge when first encountered due to a few unique histologic features. As in other species, equine MCTs contain round cells with pale eosinophilic cytoplasm often separated by collagen fibers and accompanied by eosinophils. Unlike in other species, equine MCTs may contain large lakes of eosinophilic debris surrounded by fibrosis.

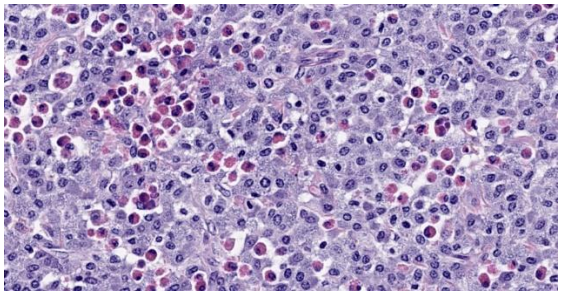

Figure 1-3. Haired skin, horse. The neoplasm is composed of sheets of moderately granulated mast cells with numerous scattered eosinophils. (HE, 571X)

Mast cells may be fewer than in MCTs from other species and cytoplasmic granules may be inapparent until revealed by toluidine blue or Giemsa staining. Tumors may also mineralize extensively with chronicity, leading to radiologically visible calcification.[2]

The development and proliferation of mast cells is regulated by stem cell factor (SCF), the ligand for the *c-kit* gene product KIT, a tyrosine kinase receptor also known as CD117.[4] In many canine MCTs, *c-kit* mutations cause activation of KIT in the absence of SCF, resulting in aberrant stimulation of pro-growth signaling pathways. Studies suggest that *c-kit* mutations may play a substantial role in the neoplastic transformation of mast cells in dogs and that differing KIT expression patterns can be used to assess grade, prognosis, and risk of recurrence.[4]

KIT expression, assessed with IHC staining using anti-KIT antibodies, is classified into three patterns, denoted by the numerals I-III. KIT staining pattern I consists of a membranous staining pattern, the expected localization for a transmembrane receptor tyrosine kinase; pattern II consists of focal to stippled cytoplasmic staining; and pattern III is characterized by diffuse cytoplasmic staining.[5] In well-differentiated canine MCTs, KIT expression is generally in a type I pattern, while high grade tumors have predominantly type II and III labelling; thus, translocation of KIT from the plasma membrane to the cytoplasm is associated with tumor recurrence and shorter overall survival times.[5]

In contrast to canine MCTs, in which grading and prognostic indices are well established, only two studies have assessed how morphologic features, proliferative activity, or KIT expression patterns can be used to predict biologic behavior in equine MCTs.[1,4] These two studies reached contradictory conclusions. The first found that KIT staining patterns and histologic features were not associated with poor clinical outcome or abnormal tumor behavior.[1] By contrast, the most recent study found that most equine MCTs were composed of mast cells with mild anisokaryosis, a low proliferative rate, and a dominance of KIT pattern I staining, representing well-differentiated MCTs and benign behavior.[4] Approximately one-third of cases in this study were comprised of mast cells exhibiting more infiltrative growth, moderate to marked anisokaryosis, a higher degree of proliferation, and KIT staining patterns II and III, representing poorly-differentiated MCTs associated with more potentially aggressive behavior.[4] These results indicate that it may be possible, as in canine MCTs, to make hay out of differential KIT staining to identify the small subset of potentially more aggressive equine MCTs. More research is needed to define the associations among biological behavior, morphology, proliferative indices, and KIT expression patterns in equine MCTs.[4]

This week's moderator, JPC's very own Dr. Bruce Williams, discussed this entity as one in which diagnosis is typically made on H&E evaluation alone. Toluidine blue and Giemsa stains can be used to visualize initially inapparent mast cell granules, and equine MCTs do show expected positive immunoreactivity to CD25, CD117, and tryptase, but the unique histologic appearance of equine MCTs

usually obviates the need to pony up the time and money for histochemical and immunohistochemical stains.

The primary differential diagnosis for equine MCTs is equine collagenolytic granulomas, which contain, as the name implies, large numbers of eosinophils; however, collagenolytic granulomas often contain flame figures and do not contain the lakes of eosinophilic debris and sheets of mast cells characteristic of equine MCTs.

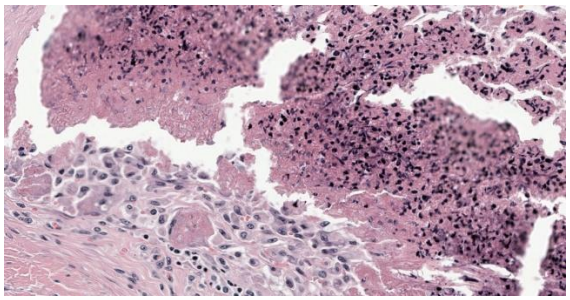

Figure 1-4. Haired skin, horse. Lakes of eosinophilic cellular debris are surrounded by epithelioid macrophages and rare multinucleated cells. (HE, 530X)

References:

1. Clarke L, Simon A, Ehrhart EJ, et al. Histologic characteristics and KIT staining patterns of equine cutaneous mast cell tumors. *Vet Pathol*. 2014;51(3):560-562.
2. Mair TS, Krudewig C. Mast cell tumors (mastocytosis) in the horse: a review of the literature and report of 11 cases. *Equine Vet Educ*. 2008;20(4):177-182.
3. Millward LM, Hamberg A, Mathews J, et al. Multicentric mast cell tumors in a horse. *Vet Clin Pathol*. 2010;39(3):365-370.
4. Ressel L, Ward S, Kipar A. Equine cutaneous mast cell tumours exhibit variable differentiation, proliferation activity and KIT expression. *J Comp Pathol*. 2015;153(4):236-243.
5. Webster JD, Yuzbasiyan-Gurkan V, Kaneene JB, Miller RA, Resau JH, Kiupel M. The role of *c-KIT* in tumorigenesis: evaluation in canine cutaneous mast cell tumors. *Neoplasia*. 2006;8(2):104-111.

CASE II:

Signalment:
6-year-old, male neutered domestic short hair, cat (*Felis catus*)

History:
Presented to referring vets for acute onset swelling and lameness of right forelimb with subsequent development of generalised subcutaneous oedema on the right side of the body including the right hindlimb. The cat

Figure 2-1. Presentation, cat. The cat has generalized subcutaneous edema of the right side of the body. (Photo courtesy of: Department of Veterinary Medicine, The Queen's Veterinary School Hospital, University of Cambridge, Cambridge CB3 0ES, UK, https://www.vet.cam.ac.uk)

Figure 2-2. Right forelimb and neck, cat. Incision of the skin demonstrates the extent of the subcutaneous edema. (Photo courtesy of: Department of Veterinary Medicine, The Queen's Veterinary School Hospital, University of Cambridge, Cambridge CB3 0ES, UK)

has outdoor access and no travel history (from the UK). The case was referred for medical investigation following further deterioration. Initial haematology and biochemistry revealed marked leukocytosis, neutrophila and basophilia, and a marked hypoalbuminaemia. Platelet count was normal but with a prolonged PT and aPTT and elevated D-dimers. Full body CT scan demonstrated marked multifocal subcutaneous and intramuscular oedema. Hepatic, splenic and peripheral lymph node cytology demonstrated neutrophilic inflammation and reactive lymphoid tissue. Culture of oedema fluid revealed a moderate growth of alpha-haemolytic colonies resistant to amoxicillin/clavulanate, cephalexin, penicillin G, TMPS and erythromycin, and sensitive to doxycycline, gentamicin and oxytetracycline. Further clinical destabilisation and an uncertain prognosis prompted elective euthanasia.

Gross Pathology:
Extensive subcutaneous oedema, multifocal small dermal papules, erosions and ulcers, areas of fascial haemorrhage overlying antebrachial muscles, thoracic effusion and right prescapular lymphadenomegaly.

Laboratory Results:
Feline poxvirus qPCR: detected, 19.08 Ct units. (the higher the Ct, the lower amount of DNA present in the sample; Ct values typically range from 15 to 40; 40 indicates much lower DNA levels than 15).

Microscopic Description:
Haired skin and subcutaneous adipose tissue: Affecting 100% of the tissue, the epidermis has lost normal structure. Multifocally there is extensive epidermal necrosis, characterised by keratinocytes with karyorrhectic and karyolytic nuclei, loss of cellular detail, and replacement by eosinophilic debris (necrotic debris and fibrin), nuclear debris and haemorrhage. In areas with viable keratinocytes, keratinocytes demonstrate hypereosinophilia and ballooning (ballooning degeneration), with cytoplasm often expanded by eosinophilic inclusion bodies (type A inclusion bodies). Keratinocytes are also disassociated, with keratinocyte necrosis and loss resulting

Figure 2-3. Haired skin, cat: One section of infarcted skin and subcutis are submitted for examination. There is diffuse severe edema visible at this low magnification. (HE, 6X)

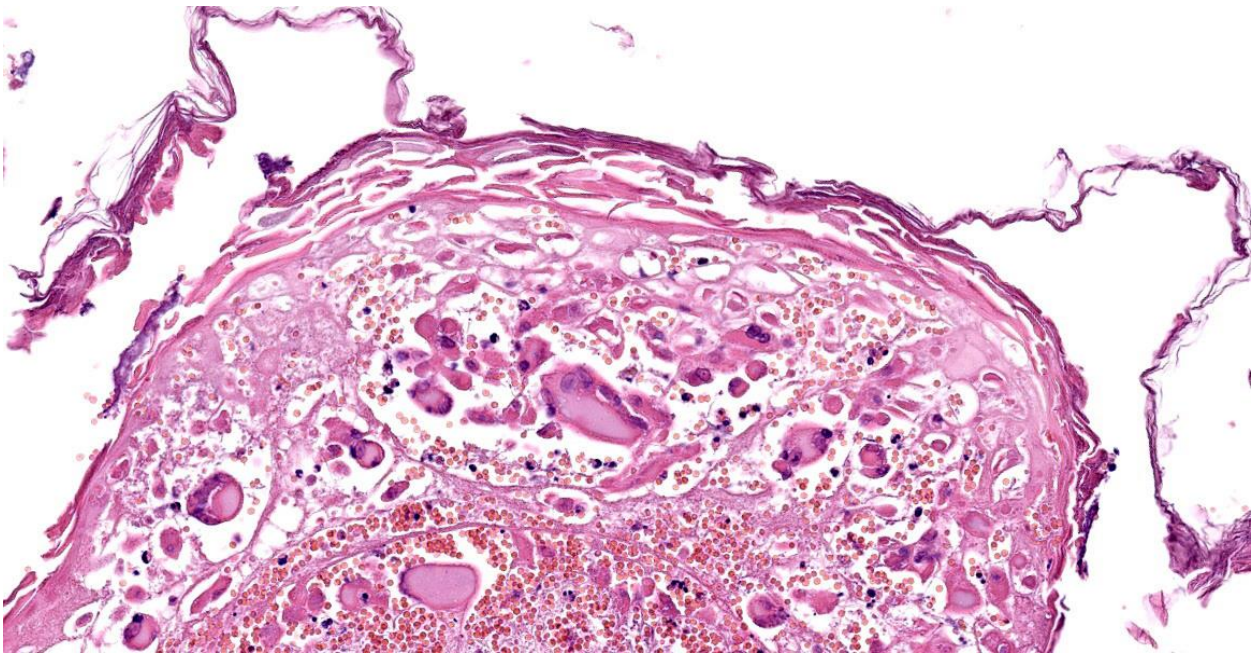

Figure 2-4. Haired skin, cat. There is diffuse necrosis of the epidermis. There are numerous viral syncytia in the epidermis. (HE, 302X)

in reticular degeneration. There are frequent viral syncytia, and these often have nuclei peripheralized by intracytoplasmic eosinophilic inclusion bodies. The epidermis and dermis are expanded by haemorrhage, fibrin and wispy eosinophilic material (oedema).

The same epidermal changes, including the necrosis, extend into hair follicles, affecting all levels of the follicular epithelium. At the lower levels of the hair follicles, where there are more viable cells, follicular epithelial cells demonstrate cytoplasmic ballooning that is often accompanied by eosinophilic intracytoplasmic inclusion bodies, and viral syncytial cells. Small sebaceous glands are almost completely effaced by necrosis of the sebocytes. Diffusely throughout the dermis and epidermis, there are low to moderate numbers of neutrophils and lymphocytes, with fewer eosinophils and macrophages, and scattered leukocytoclastic debris. Throughout the dermis, multifocally veins and to a lesser extent arteries have mural-associated neutrophils, and/or walls replaced by smudgy eosinophilic debris (fibrinoid necrosis), with intramural and perivascular leukocytoclastic debris. Perivascular spindle-cells and occasionally endothelial cells contain eosinophilic cytoplasmic inclusion bodies. Within the subcutis there are similar vascular changes to those described in the dermis, although frequently larger vessels are affected, resulting in marked expansion of the subcutaneous adipose tissue by haemorrhage, fibrin, and wispy eosinophilic material (oedema).

Contributor's Morphologic Diagnosis:
Haired skin and subcutis, ventrum: Dermatitis, folliculitis and cellulitis, necrotising, severe, diffuse, with leukocytoclastic vasculitis, keratinocyte intracytoplasmic eosinophilic inclusion bodies, keratinocyte viral syncytia, and epithelial ballooning degeneration.

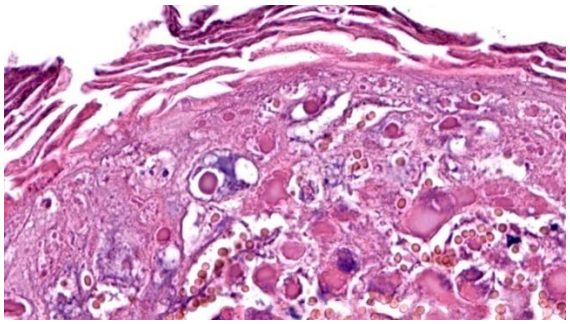

Figure 2-5. Haired skin, cat. Epithelial cells contain large eosinophilic viral inclusions. (HE, 887X)

Contributor's Comment:
This case demonstrates a systemic form of pox virus infection in cats, resulting in a clinical presentation of progressive marked cellulitis and necrotising dermatitis. This case lacked an observed primary cutaneous lesion or respiratory clinical changes, and prior to post-mortem examination, whilst a vasculitis was suspected, pox-viral related vasculitis was not a considered differential. On microscopic examination of the dermal and subcutaneous lesions, the frequent intracytoplasmic inclusion bodies were noted prompting qPCR for feline pox virus on stored frozen tissues. Feline poxvirus qPCR reveals moderately high levels of feline pox virus within the tissues, therefore pox viral infection is considered the cause of the necrotising process that has resulted in the clinical and histological features described in this case. Immunohistochemistry for pox virus demonstrated specific immunoreactivity within epithelial cells in affected areas. This cat had an extended post-mortem interval in cool storage, which is likely to have contributed to the poor preservation of some inflammatory cells.

Cow pox/cat pox virus is a large, enveloped, double-stranded DNA, cytocidal virus that is part of the Orthopoxviridae genus, within the Poxviridae family. The orthopox genus also includes ectromelia virus, monkeypox virus, smallpox virus (variola), vaccinia virus, and rabbitpox virus. Cowpox is endemic in Europe and Northern and Central Asia with a wide host range that includes people.[7,17,32] Cowpox infection in most species results in localised dermal lesions or systemic disease that may be fatal. Wild rodents, especially bank voles (*Clethrionmys glareolus)*, serve as the viral reservoir and infection of rodents, and subsequently secondary species such as humans and cats, varies seasonally with a peak in autumn and subsequently secondary transmission to cats.[1,4]

Cow pox is the most common poxviral infection of cats, with the common presentation involving the skin, often initially with a single primary lesion, which is assumed to be secondary to intradermal inoculation via a rodent bite.[26] Systemic infections can occur following the viraemic phase, and include pyrexia and lethargy, and occasionally pneumonia.[20,26] Feline cowpox infection is occasionally concurrent with other feline viruses, including viruses expected to cause immune dysfunction. At this stage the relationship between the clinical progression and severity of feline cowpox infection in cats co-infected with other viruses is not clear.[8] FIV has been suggested to exacerbate feline cowpox infection, with larger and more persistent primary lesions, however up to 30% of cats infected with cowpox are also seropositive to FIV with no change in disease course.[1] Feline herpesvirus and feline

cowpox co-infection resulted in a necrotising pneumonia involving both viruses and a pox-viral dermatitis, however the cat successfully recovered with supportive treatment and antimicrobials.[14] A case of a cat with cowpox and feline parvovirus infection resulting in a dermatitis, panniculitis and enteritis was not associated with more severe poxvirus-associated disease.[24]

The FIV/FeLV status of the cat in this case was not defined. Special stains did not highlight bacteria within the subcutis, however a secondary bacterial infection, as indicated by the positive culture of the oedema fluid, is considered likely. Rare areas of ulcerated skin were associated with mats of superficial fungal hyphae, and deeper invasion was not observed. For both secondary infections, a systemic role for either the agents or elaborated toxins is considered a possible co-factor in the severe presentation in this case.

A systemic form of feline cowpox, primarily presenting with severe dermal oedema is unusual. This presentation has been previously reported in a 4 year old male neutered domestic short haired cat that exhibited known hunting behaviours, and ultimately resulted in pox-viral associated neurological lesions and euthanasia of the cat.[2] More localised dermal oedema was described in a series of five cats that presented with dermal plaques, oedema and hyperaemia affecting the hindlimbs,[16] and two cases of localised forelimb oedema in a four-cat feline cowpox case series from the UK.[9] Of the five-cat case series, all cats were geographically and temporarily grouped and in four of the cases, the cowpox viruses had an identical haemagglutinin gene sequence suggesting a common source of infection.[16]

*Pathogenesis***.** Epidermal lesions are the result of viral replication in keratinocytes resulting in cellular dysfunction and eventual lysis either due to host-cell related mechanisms or to the actions of immune cells such as NK cells.[3,30] Viral proteins involved in viral entry to cells also induce host cell fusion, resulting in syncytia formation.[28] Cowpox, similar to other pox viruses, contains an epidermal growth factor homologue that is able to influence cellular differentiation and proliferation of keratinocytes.[27] The virus can infect and damage endothelial cells and in some experimental models produces a consumptive coagulopathy, resulting in more widespread dermal or submucosal necrotising lesions as a consequence of vascular damage, thrombosis and tissue infarction.[5,15,23] Cowpox virus has a range of immunomodulatory proteins that include IFN-gamma receptor and TNF-alpha receptor homologues, IL-1beta binding proteins, and anti-inflammatory Serpins.[27]

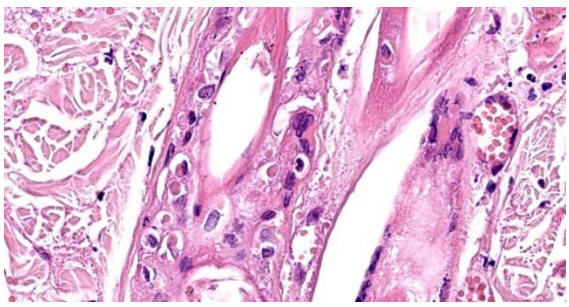

Figure 2-6. Haired skin, cat. Viral inclusions, syncytia, and epithelial changes extend into the follicles. (HE, 757X)

*Typical and atypical clinical findings***.** Cats often present with a single primary skin lesion on the head, neck, forelimb or paws.[1] Secondary bacterial infection of the lesion may induce confounding clinical signs. A viremia with pyrexia, lethargy and inappetence may follow 1-3 weeks following the initial infection.[26] Widespread skin lesions may follow the viremia with papules and nodules that ulcerate and crust, but skin healing is ultimately expected.[1] The mucocutaneous junction and oral cavity may be affected, forming ulcerative foci.[9] Pneumonias in the absence of skin lesions has also been reported rarely with both cases resulting in a fatal pneumonia that was caused by a genetically similar but not identical viral strain.[11,25] Exotic felids, especially cheetahs, can be infected with cowpox virus.[18] The clinical signs range from dermal and oral lesions to a necrotising pneumonia, of which two out of nine cases (22%) of cheetah infections were fatal.[31]

Typical gross findings. The typical macroscopic epidermal changes include erythematous macules developing into papules and then pustules that rupture and crust.[1] In this case, and in other reported atypical feline cowpox presentations, there was marked dermal and subcuticular oedema due to, in this case at least, widespread pox-viral associated vasculitis/vascular dysfunction. Marked subcutaneous oedema is a clinical feature more associated with Mousepox (ectromelia) virus infection.[22]

Typical microscopic findings. The typical microscopic findings in cases of feline cowpox are well defined. Epidermal lesions start with keratinocyte cytoplasmic swelling and vacuolation (intracellular oedema and ballooning degeneration), and progress through cell rupture to multiloculated vesicles (reticular degeneration) and epidermal necrosis.[1,12] Epidermal hyperplasia is often present and may be marked. Accompanying dermal changes include oedema, mononuclear cell infiltrate and a variable neutrophilic infiltrate. With time, the neutrophilic infiltrate extends into the epidermis creating pustules. Cox pox, like other pox viruses, creates intracytoplasmic inclusion bodies that vary in number and size. Large brightly eosinophilic inclusions are identified as A-type inclusions, and are predominantly composed of viral protein in which mature virions are embedded.[6] A-type inclusions are thought to protect infectious particles after release into the environment, and increase in size throughout the infection by coalescence of multiple smaller bodies.[13] B-Type pox inclusions are smaller, more basophilic, and are the sites of viral replication (viral factories).

Ultrastructure. On electron microscopy Poxviral particles are enveloped and are brick shaped. Single virions have multiple protruding surface spicules.[11]

Additional diagnostic tests. Confirmation of the diagnosis can be made using electron microscopy, immunofluorescence, virus isolation, and PCR on tissues, which also includes skin scabs and pulmonary or thoracic aspirates.[21,26]

Treatment. Treatment focuses on controlling/preventing secondary bacterial infections and immunomodulation with recombinant feline interferon omega.[2,20]

Genus	Representative Viruses
Orthopoxvirus	• Cowpox virus • Vaccinia virus (buffalopox virus, rabbitpox virus) • Horsepox virus • Camelpox virus • Ectromelia virus (mousepox virus) • Monkeypox virus
Parapoxvirus	• Orf virus (contagious pustular dermatitis virus, contagious ecthyma virus) • Pseudocowpox virus (milker's nodule virus) • Bovine papular stomatitis virus • Parapox virus of red deer
Avipoxvirus	• Fowlpox virus • Pigeonpox virus
Capripoxvirus	• Sheeppox virus • Goatpox virus • Lumpy skin disease virus
Leporipoxvirus	• Myxoma virus • Rabbit fibroma virus
Suipoxvirus	• Swinepox virus
Molluscipoxvirus	• Molluscum contagiosum virus
Yatapoxvirus	• Tanapox virus • Yaba monkey tumor virus

Table 2-1. Selected Poxviridae genera and representative members.

Contributing Institution:
Department of Veterinary Medicine
The Queen's Veterinary School Hospital
University of Cambridge.
Cambridge CB3 0ES, UK.
https://www.vet.cam.ac.uk

JPC Diagnosis:
Haired skin and subcutis: Vasculitis, necrotizing, diffuse, severe, with cutaneous infarction, epithelial ballooning degeneration, numerous epithelial viral syncytia and intracytoplasmic inclusions.

JPC Comment:
The contributor provides an excellent, thorough overview of cowpox infection in cats. While the cat is the most commonly recognized incidental host, cowpox also infects dogs, rats, mice, humans, horses, and various exotic mammals.[10] Perhaps surprising given its name, cowpox infection is rare in cattle.

The *Poxviridae* is a large family of enveloped DNA viruses that are highly epitheliotropic and cause cutaneous and systemic disease.[19] Poxviruses encode their own replication machinery, including an RNA polymerase, which enables their characteristic cytoplasmic replication. Animal poxviruses exist within the subfamily *Chordopoxvirinae*, which is further subdivided into 22 different genera (see Table 2-1 for a sampling of genera and representative members).

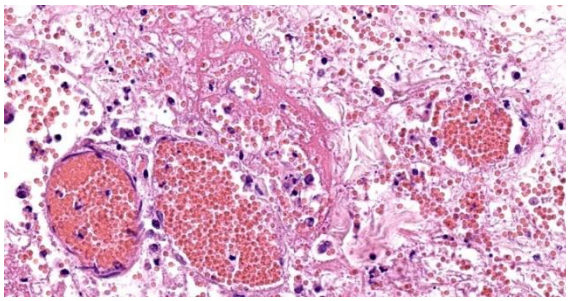

Figure 2-7. Haired skin, cat. Within the dermis and subcutis, widespread vasculitis gives rise to marked hemorrhage and edema within these areas. (HE, 360X)

The orthopoxviruses, including cowpox, are notable for their wide host spectrum and are among the most important and well-characterized poxviruses due to their impact on human and animal health. Their most notable and feared member, the *Variola* virus, is the causative agent of smallpox.[29]

Poxviruses damage cells in multiple ways. Degenerative changes are caused by direct cytotoxic damage due to poxviral replication and subsequent rupturing of the host cell membrane, leading to typical vesicular lesions.[19] As in this case, the dermis and submucosa may be subject to ischemia due to vascular damage caused by viral replication within endothelial cells.[19] Poxviruses also induce proliferative lesions due, in some poxviruses, to a viral gene that encodes a mitogenic protein with significant similarity to epidermal growth factor.

Pox lesions tend to develop in a particular sequence, with erythematous macules becoming papular, and then vesicular.[19] The vesicles become "pocks," pustules with a depressed center and raised border which then rupture, forming crusts.[19] Histologically, poxvirus lesions are characterized by marked epithelial hyperplasia with serocellular crusts and intracytoplasmic inclusion bodies. Both the gross and histologic lesions are characteristic, facilitating easy diagnosis in most cases.

In conference, participants discussed the remarkable coagulative necrosis present in the epithelium and dermis in this case. The moderator emphasized that this indicator of infarction, when present, should precipitate a close evaluation of deep vessels. While we noted the contributor's description of cytoplasmic inclusion bodies within affected endothelium, no convincing endothelial cytoplasmic inclusions were found in the sections we received in this submission. The unrewarding hunt for endothelial inclusions did not dampen the participants' enthusiasm for the robust, multifocal vasculitis, believed by the moderator to be the main driver of the striking pathology in this case; thus, the JPC morphologic diagnosis leads with vasculitis to reflect the centrality of this histologic finding.

References:

1. Bennett M, Gaskell CJ, Baxby D, Gaskell RM, Kelly DF, Naidoo J. Feline cowpox virus infection. 1990. *J Small Anim Pract*. 1990;31:167-173.
2. Breheny CR, Fox V, Tamborini A, et al. Novel characteristics identified in two cases of feline cowpox virus infection. *JFMS Open Rep*. 2017;3(2):205511-6917717191.
3. Burshtyn DN. NK cells and poxvirus infection. *Front Immunol*. 2013;4:7.
4. Chantrey J, Meyer H, Baxby D, et al. Cowpox: reservoir hosts and geographic range. *Epidemiol Infect*. 1999;122(3): 455-60.
5. Chapman JL, Nichols DK, Martinez MJ, Raymond JW. Animal models of orthopoxvirus infection. *Vet Pathol*. 2010;47(5):852-70.
6. Condit RC, Moussatche N, Traktman P. In a nutshell: structure and assembly of

the vaccinia virion. *Adv Virus Res*. 2006;66:31-124.
7. Essbauer S, Pfeffer M, Meyer H. Zoonotic poxviruses. *Vet Microbiol*. 2010; 140(3-4):229-36.
8. Foster AP. Immunomodulation and immunodeficiency. *Vet Dermatol*. 2004; 15(2):115-26.
9. Godfrey DR, Blundell CJ, Essbauer S, et al. Unusual presentations of cowpox infection in cats. *J Small Anim Pract*. 2004;45(4):202-5.
10. Greene CE. Poxvirus infections. In: Greene CE, ed. *Infectious Diseases of the Dog and Cat*. 4th ed. Elsevier; 2012:166-169.
11. Hinrichs U, van de Poel H, van den Ingh TSGAM. Necrotizing Pneumonia in a Cat Caused by an Orthopox Virus. *J Comp Path*.1999;121(2):191-196.
12. Hnilica K. Viral, Rickettsial, and Protozoal Skin Diseases. *Small Animal Dermatology: A color atlas and therapeutic guide (Third Edition)*, W.B. Saunders; 2011:159-174.
13. Howard AR, Moss B. Formation of orthopoxvirus cytoplasmic A-type inclusion bodies and embedding of virions are dynamic processes requiring microtubules. *J Virol*. 2012;86(10):5905-14.
14. Johnson MS, Martin M, Stone B, Hetzel U, Kipar A. Survival of a cat with pneumonia due to cowpox virus and feline herpesvirus infection. *J Small Anim Pract*. 2009;50(9):498-502.
15. Johnson RF, Yellayi S, Cann JA, et al. Cowpox virus infection of cynomolgus macaques as a model of hemorrhagic smallpox. *Virology*. 2011;418(2):102-12.
16. Jungwirth N, Puff C, Köster K, et al. Atypical cowpox virus infection in a series of cats. *J Comp Pathol*. 2018; 158:71-76.
17. Kaysser P, von Bomhard W, Dobrzykowski L, Meyer H. Genetic diversity of feline cowpox virus, Germany 2000-2008. *Vet Microbiol*. 2010;141(3-4):282-8.
18. Marennikova SS, Maltseva NN, Korneeva VI, Garanina N. Outbreak of pox disease among carnivora (felidae) and edentata. *J Infect Dis*. 1977;135 (3):358-66.
19. Mauldin EA, Peters-Kennedy J. Integumentary System. In: Maxie MG, ed. *Pathology of Domestic Animals*. Vol 1. 6th ed. Elsevier; 2016:616, 619-620.
20. McInerney J, Papasouliotis K, Simpson K, et al. Pulmonary cowpox in cats: five cases. *J Feline Med Surg*. 2016;18(6): 518-25.
21. Möstl K, Addie D, Belák S, et al. Cowpox virus infection in cats: ABCD guidelines on prevention and management. *J Feline Med Surg*. 2013;15(7):557-9.
22. Nicklas W, Bleich A, Mähler M. Viral Infections of Laboratory Mice. In: Hedrich HJ, Bullock G, eds. *The Laboratory Mouse.* Elsevier;2012:427-480.
23. Roth SJ, Klopfleisch R, Osterrieder N, Tischer BK. Cowpox virus serpin CrmA is necessary but not sufficient for the red pock phenotype on chicken chorioallantoic membranes. *Virus Res*. 2012;163(1): 254-61.
24. Schaudien D, Meyer H, Grunwald D, Janssen H, Wohlsein P. Concurrent infection of a cat with cowpox virus and feline parvovirus. *J Comp Pathol*. 2007;137**(**2-3):151-4.
25. Schöniger S, Chan DL, Hollinshead M, Humm K, Smith GL, Beard PM. Cowpox virus pneumonia in a domestic cat in Great Britain. *Vet Rec*. 2007;160(15): 522-3.

26. Scott DW, Miller WH Jr., Griffin CE. Viral, Rickettsial, and Protozoal Skin Diseases. In: Miller W, Griffin C, Campbell K, eds. *Muller & Kirk's Small Animal Dermatology*. Elsevier;2001:517-542.
27. Seet BT, Johnston JB, Brunetti CR, et al. Poxviruses and immune evasion. *Annu Rev Immunol*. 2003;21:377-423.
28. Senkevich TG, Ojeda S, Townsley A, Nelson GE, Moss B. Poxvirus multiprotein entry-fusion complex. *Proc Natl Acad Sci*. 2005;102(51):18572-7.
29. Silva NIO, Silva de Oliveira J, Kroon EG, Trinidade G, Betania PD. Here, there, and everywhere: the wide host range and geographic distribution of zoonotic orthopoxviruses. *Viruses*. 2021;13(1):43.
30. Smith GL, Law M. The exit of vaccinia virus from infected cells. *Virus Res*. 2004;106(2):189-97.
31. Stagegaard J, Kurth A, Stern D, et al. Seasonal recurrence of cowpox virus outbreaks in captive cheetahs (Acinonyx jubatus). *PLoS One*. 2017;12(11): e0187089.
32. Vorou RM, Papavassiliou VG, Pierroutsakos IN. Cowpox virus infection: an emerging health threat. *Curr Opin Infect Dis*. 2008;21(2):153-6.

CASE III:

Signalment:
6-month-old, intact male Göttingen minipig (*Sus scrofa*)

History:
A 6-month-old, intact male, single-housed, 12 kg, Göttingen minipig presented with bilateral ear erythema at the apical margins 4 hours post repetitive auricular venipuncture. The pig had open cage bar communication

Figure 3-1. Presentation, Göttingen minipig. There are petechiae and ecchymoses on the face, nose, and skin of the head and neck. There is bilateral infarction of the ear tips. (Photo courtesy of: Comparative Pathology Department, Research Support Division, USAMRICD, Aberdeen Proving Ground, MD, https://usamricd.amedd.army.mil/)

with conspecifics. The pig had a jugular venous access port (VAP) and telemetry implanted 2 months prior to presentation. The pig was enrolled in a pharmacokinetics study 1 month prior and received 2 intramuscular doses of scopolamine. On exam, the pig was bright, alert, and responsive (BAR) with 10 needle punctures per ear and extensive bruising. At the 24 hour recheck, the pig was BAR but the erythema expanded the entire pinnae with ulceration, crusting, epidermal thickening, and apical margin necrosis. Aerobic culture revealed Staphylococcus aureus and povidone-iodine scrub with silver sulfadiazine therapy was initiated. Primary differentials included research/conspecific-induced trauma, bacterial, and/or viral systemic disease. At the 48 hour recheck, the pig presented with depression, inappetance, dyspnea, cold extremities, petechiation on snout, lips, rectum, and prepuce, and red-purple discoloration on all limbs distal to hock/elbow. Blood was taken for clinical pathology and was still watery 20 minutes later. The pig was euthanized due to poor study candidacy and disease severity.

Figure 3-2. Ear pinna, Göttingen minipig. Higher magnification of the infarcted ear tip. (Photo courtesy of: Comparative Pathology Department, Research Support Division, USAMRICD, Aberdeen Proving Ground, MD)

Gross Pathology:
This 12 kg, male, Göttingen minipig is in lean body condition with adequate subcutaneous and visceral fat, 2.5/5 body condition score, and well-hydrated. There are multifocally extensive petechiae, purpura, and ecchymoses on the nose, ears, lips, lower limbs, ventrum, prepuce, anus, and tail. Bilaterally, the ear tips are dark & necrotic. The right pinna has a hole in the middle from an ear tag. There is a subcutaneous VAP port on the right lateral neck and a subcutaneous telemetry device on the right side of the ventral neck. Both have no significant gross lesions. The gums and conjunctiva are pale and there are multifocal petechiae on the palate. There is abundant hemorrhagic foam in the trachea. The lungs are noncollapsed and extensively dark with multifocal petechiae and purpura. There are multifocal petechiae on the heart ventricles and there is a small amount of serosanguinous fluid in the pericardial sac. The liver, spleen, and kidneys are dark and enlarged (post-euthanasia congestion). The liver, kidneys, and intestinal serosa have multifocally extensive petechiae. The gallbladder contains a small amount of hemorrhagic bile. The stomach contains a moderate amount of normal ingesta and gas and there are multifocal petechiae and erosions/ulcers on the fundic mucosa. The small intestine contains a moderate amount of bile-stained digesta and gas. The cecum contains a moderate amount of dark hemorrhagic contents. The colon contains a small amount of normal feces. The urinary bladder is empty. No significant gross lesions were observed in any other organs.

Laboratory Results:
Clinical pathology revealed a regenerative anemia, low hemoglobin, marked thrombocytopenia, and elevated ALT, AST, GGT, and albumin. A differential count supported thrombocytopenia with schistocytosis, nucleated RBCs, acanthocytes, and target cells.

Microscopic Description:
Ear pinna: There is focally extensive full-thickness coagulative necrosis affecting the distal end. Multifocally there are vascular thrombi present and various arteriosclerotic changes to the arterioles and small muscular arteries (endothelial cell hypertrophy, myointimal proliferation, smooth muscle cell vacuolation, medial thickening, concentric laminar wall thickening ("onion-skinning"), luminal stenosis, and/or periarteritis). Inflammation is scattered and primarily composed

Figure 3-3. Hindlimb, Göttingen minipig. There are petechiae and ecchymoses on the skin of the hindlimbs. (Photo courtesy of: Comparative Pathology Department, Research Support Division, USAMRICD, Aberdeen Proving Ground, MD

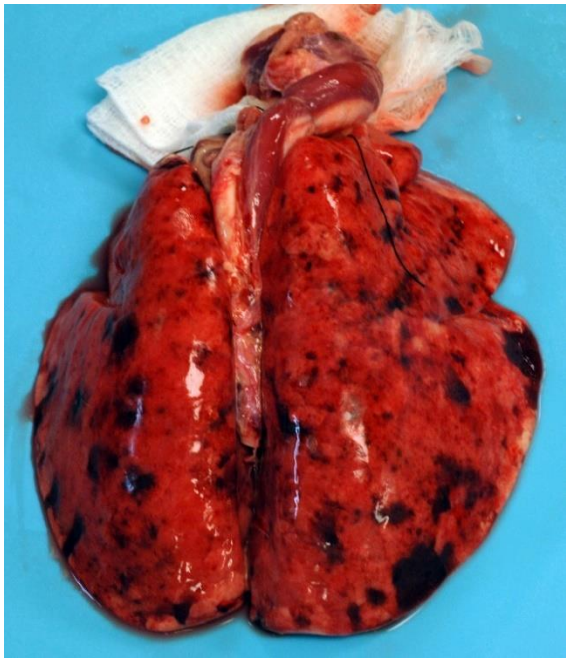

Figure 3-4. Lungs, Göttingen minipig. There are hemorrhages throughout the lungs. (Photo courtesy of: Comparative Pathology Department, Research Support Division, USAMRICD, Aberdeen Proving Ground, MD)

of macrophages, lymphocytes, eosinophils, and neutrophils. There is also multifocal areas of periarticular hemorrhage and occasional hemosiderin-laden macrophages.

Changes in other organs (not submitted):
Heart: Multifocal severe myocardial fiber degeneration, necrosis, and loss with hemorrhage, vascular thrombi, and various arteriosclerotic changes to the arterioles and small muscular arteries.

Kidney, bilateral: Diffuse severe membranoproliferative glomerulonephritis with tubular degeneration, necrosis, and proteinosis, hemorrhage, vascular thrombi, and various arteriosclerotic changes to the arterioles and small muscular arteries.

Lung: Severe multifocally extensive intraairway and interstitial hemorrhage, fibrin, and edema with vascular thrombi and various arteriosclerotic changes to the arterioles and small muscular arteries.

Liver: Moderate to severe multifocal centrilobular to midzonal hepatocellular degeneration and necrosis with hemorrhage and vascular thrombi.

Stomach, fundus: Severe focally extensive mucosal necrosis with submucosal inflammation, edema, hemorrhage, vascular thrombi, and various arteriosclerotic changes to the arterioles and small muscular arteries.

Pancreas: Multifocal moderate acinar degeneration and necrosis with hemorrhage, vascular thrombi, and various arteriosclerotic changes to the arterioles and small muscular arteries.

Diaphragm: Multifocal moderate myofiber degeneration and necrosis with hemorrhage, vascular thrombi, and various arteriosclerotic changes to the arterioles and small muscular arteries.

Spleen: Diffuse moderate extramedullary hematopoiesis (EMH) with vascular thrombi and various arteriosclerotic changes to the arterioles and small muscular arteries.
Bone marrow: Diffuse moderate megakaryocytic hyperplasia.

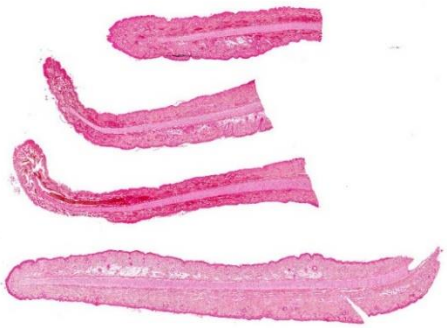

Figure 3-5. Ear pinnae, Göttingen minipig. Four sections of ear tip are submitted for examination. (HE 6X)

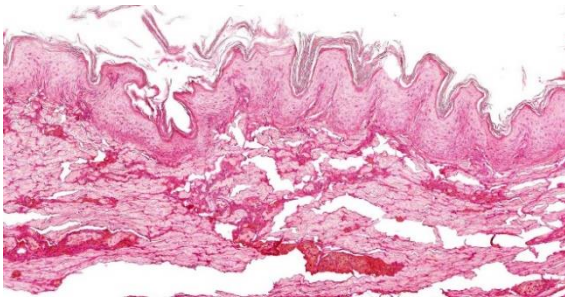

Figure 3-6. Ear pinna, Göttingen minipig. There is diffuse coagulative necrosis (infarction) with lack of stain affinitiy of the ear tip. (HE, 123X)

Adrenal gland, bilateral: Multifocal moderate hemorrhage.

Gallbladder: Multifocal moderate submucosal hemorrhage and edema.

Ileum: Diffuse moderate GALT lymphocytolysis with vascular thrombi and various arteriosclerotic changes to the arterioles and small muscular arteries.

Duodenum: Multifocal vascular thrombi and various arteriosclerotic changes to the arterioles and small muscular arteries.

Lymph node, various: Multifocal moderate draining hemorrhage and lymphocytolysis with histiocytosis, erythrophagocytosis, hemosiderin-laden macrophages, vascular thrombi, and various arteriosclerotic changes to the arterioles and small muscular arteries.

Contributor's Morphologic Diagnosis:
Ear pinna: Necrosis, full-thickness, focally extensive, severe, with vascular thrombi and various arteriosclerotic changes to the arterioles and small muscular arteries.

Contributor's Comment:
Severe thrombocytopenia and anemia are consistent clinical findings with thrombocytopenia purpura syndrome of Göttingen minipigs, along with extensive hemorrhages in subcutaneous tissues and various other organs.[1,6] This syndrome is a spontaneous degenerative vasculopathy that rarely occurs in European and North American herds of Göttingen minipigs.[1,6] It primarily affects sexually mature males and females but has been seen in animals as young as 7 weeks of age.[6] Histologically, there are distinctive features of arteriosclerosis in various tissues, primarily in small- to medium-sized arteries and arterioles. These features include endothelial cell hypertrophy, myointimal proliferation, smooth muscle cell vacuolation, medial thickening typically by myxoid deposits, concentric laminar wall thickening ("onion-skinning"), luminal stenosis, and/or periarteritis.[6-8] Unlike spontaneous atherosclerosis of aged swine, lipid accumulation is not a feature.[6] Membranoproliferative glomerulonephritis and myocardial infarcts also feature prominently in this disease.[6,7] The pathogenesis is unknown at this time but it is proposed to be due to a type III hypersensitivity causing the widespread degenerative vasculopathy.[1,6,7]

Other rule-outs for cutaneous hemorrhages in pigs, although less likely in research bred animals, include: (1) neonatal thrombocytopenic purpura – hypersensitivity due to incompatible colostral antibodies; (2) vitamin K deficiency/anticoagulant rodenticide poisoning;

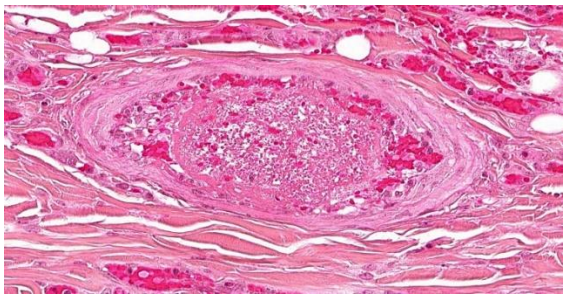

Figure 3-7. Ear pinna, Göttingen minipig. Dermal arterioles demonstrate mural thickening as a result of intimal hyperplasia and adventitial fibrosis and often contain non-occlusive fibrin thrombi. (HE, 387X)

and (3) viral infections, such as porcine circovirus, classical swine fever, and African swine fever.

Contributing Institution:
Comparative Pathology Department, Research Support Division
USAMRICD
8350 Ricketts Point Rd.
Aberdeen Proving Ground, MD 21010-5400
https://usamricd.amedd.army.mil/

JPC Diagnosis:
Haired skin, ear tip: Arteriolosclerosis, multifocal, moderate, with thrombosis, occasional arteritis and periarteritis, and focally extensive cutaneous infarction.

JPC Comment:
The syndrome nicely described by the contributor and illustrated by this case is a rare syndrome with an uncertain pathogenesis that is specific to Göttingen minipigs. As the contributor notes, one of the major differential diagnoses for this condition in swine is neonatal thrombocytopenia purpura, an immune-mediated condition in suckling pigs that has been described in veterinary literature for 50 years.[5] The case presentation is similar to the syndrome in Göttingen minipigs, but with a much younger age of onset and a different pathogenesis.

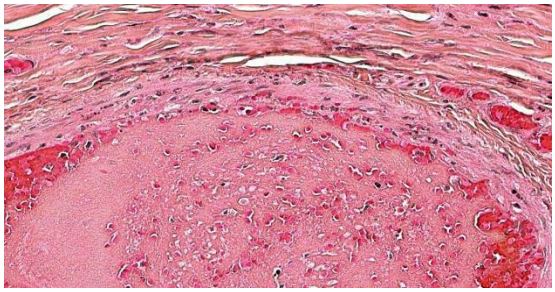

Figure 3-8. Ear pinna, Göttingen minipig. Occasionally, arteriolar walls contain exuded protein, necrotic smooth muscle, mural and adventitial necrotic neutrophils, and cellular debris. (HE, 508X)

In neonatal thrombocytopenic purpura, suckling pigs typically become symptomatic around 3 days of age, recover, and then experience a re-emergence of symptoms around day 14 which quickly leads to death.[5] Piglets are pale and inactive and post-mortem exam reveals severe hemorrhage and edema in the lungs, heart, kidneys, subcutis, joints, gastrointestinal and respiratory tracts, and skeletal muscle. Histologic findings include hemorrhages in various tissues and depletion of megakaryocytes in the bone marrow and spleen.[5]

Thrombocytopenia develops due to isoimmune antibodies developed by the sow during gestation against boar thrombocyte antigens present in the piglets' blood. Piglets ingest these isoantibodies with colostrum which render existing platelets useless and have a cytotoxic effect on bone marrow megakaryocytes.[5] Matings between Landrace and Large White pigs increase the risk that the resulting piglets will develop neonatal thrombocytopenia purpura.

Due to the need for prior sensitization, neonatal thrombocytopenia purpura occurs only on subsequent matings of a sow to the same boar. Because of this, the disease fell out of fashion with the advent of modern artificial insemination and the concomitant reduction in multiple identical matings.[5] However, in a case of good intentions gone awry, the disease is being seen more frequently now that animal welfare preferences have catalyzed changes in livestock rearing practices. Of particular salience here is the use of natural mating as part of a larger push to allow animals to exhibit natural behaviors in all aspects of their lives.[2] A recent outbreak occurred on a Swiss organic farm that practiced natural mating of pigs using one of only three boars kept on the property, increasing the chances of repeat matings.[5] Thirteen piglets from two separate litters died of neonatal

thrombocytopenia purpura before management practices, including exchanging boars periodically, documenting and managing matings, and switching all boars to the Duroc breed, were implemented.

The syndrome is similar to neonatal isoerythrolysis in foals in which anemia and subsequent organ failure result when foals inherit a blood type from the stallion against which the mare has previously developed antibodies. Similar to the syndrome described above, foals ingest the isoantibodies with colostrum which end up in the bloodstream and attach to the foal's erythrocytes, causing their immune destruction.

Conference discussion centered on the pathogenesis of thrombocytopenia purpura of the Göttingen minipig. As the contributor notes, the current literature suggests that the degenerative vasculopathy characteristic of this disease is caused by a type III hypersensitivity reaction; however, causality has not been established and the moderator remains skeptical that the condition is solely immune-mediated. This case also provided a second opportunity to discuss the importance of a conscientious examination of vasculature, which here was multifocally thrombosed due presumably to intimal damage and the resulting exposure of collagen and tissue factor. The widespread thrombosis described by the contributor in various tissues likely resulted in a consumptive coagulopathy that explains the systemic, widespread hemorrhage seen in this animal. Due again to the centrality of the vasculature to the histologic presentation, the JPC morphologic diagnosis once again leads with the vascular changes.

References:

1. Carrasco L, Madsen W, Salguero F, Núñez, Sánchez-Cordón P, Bollen P. Immune complex-associated thrombocytopenic purpura syndrome in sexually mature Göttingen minipigs. *J Comp Path*. 2003;128:25-32.
2. Dawkins MS. Natural behavior is not enough: farm animal welfare needs modern answers to Tinberg's four questions. *Animals (Basel)*. 2023;13(6):988.
3. Grand N. Diseases of minipigs. In: McAnulty P, ed. *The Minipig in Biomedical Research*. 1st ed. CRC Press; 2012.
4. Helke K, Nelson K, Sargeant A, et al. Background pathological changes in minipigs: a comparison of the incidence and nature among different breeds and populations of minipigs. *Tox Path*. 2015; 44(3):325-337.
5. Joller S, Hafliger IM, Drogemuller C, Richard OK, Grahofer A. Thrombocytopenic purpura on an organic farm with pen mating: a case report on the re-emergence of an old disease. *Porc Health Manag*. 2020;6(18).
6. Maratea K, Snyder P, Stevenson G. Vascular lesions in nine Göttingen minipigs with thrombocytopenic purpura syndrome. *Vet Pathol*. 2006;43:447-454.
7. McInnes E, McKeag S. A brief review of infrequent spontaneous findings, peculiar anatomical microscopic features, and potential artifacts in Göttingen minipigs. *Tox Path*. 2016;44(3):338-345.
8. Swindle M, Makin A, Herron A, Clubb Jr F, Frazier K. Swine as models in biomedical research and toxicology testing. *Vet Pathol*. 2012;49(2):344-356.

CASE IV:

Signalment:

11-year-old, spayed female bassett hound, dog (*canis familiaris*)

History:

The patient was observed over a period of several months to develop a fluctuant soft tissue swelling associated with the upper eyelid, which was indicated to be subconjunctival/

Figure 4-1. Periocular tissue, dog. A friable 3.5 x 1.8 x 1.0 cm mass of interconnected lobules of tan tissue was submitted to the contributor. (Photo courtesy of: University of Wisconsin, School of Veterinary Medicine, Madison WI. https://www.vetmed.wisc.-edu/departments/pathobiological-sciences/)

subcutaneous with extension posteriorly towards the orbit. Interpretation of a fine needle aspirate was consistent with a neoplasm of epithelial origin. The entire submitted tissue was expressible through a small conjunctival incision over the mass at surgery, and the submitting veterinarian described a tissue with the gross appearance of fat.

Gross Pathology:
The submitted specimen consisted of multiple well demarcated and interconnected lobules of tan tissue and measured 3.5 x 1.8 x 1.0 cm. The consistency of the tissue was friable, with lobules falling away from the main mass during manipulation.

Laboratory Results:
Fine needle aspirate suggested an epithelial neoplasm.

Microscopic Description:
The tissue is mainly composed of an unencapsulated, poorly-delineated, densely cellular and multilobular neoplastic mass infiltrating and expanding the adjacent connective tissue. The mass is composed of cuboidal epithelial neoplastic cells, arranged into acini, cords and trabeculae supported by a delicate fibrovascular stroma. The neoplastic cells present moderate amounts of granular, lightly basophilic cytoplasm with indistinct cell borders, and round to oval nuclei with homogenous to condensed chromatin and 1-3 variably distinct nucleoli. Anisocytosis and anisokaryosis are mild, and no mitotic figures are seen. A homogenous basophilic secretory material is distributed between the trabeculae of neoplastic cells and sometimes throughout the extracellular space. There is a focal accumulation of foamy macrophages expanding the connective tissue adjacent to the mass. The neoplastic cells extend beyond the surgical margins.

Contributor's Morphologic Diagnosis:
Orbital connective tissue: Canine lobular orbital adenoma.

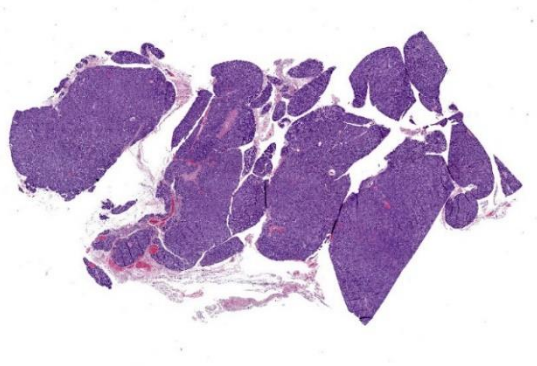

Figure 4-2. Periocular tissue, dog. A multilobular neoplasm is present. (HE 6X)

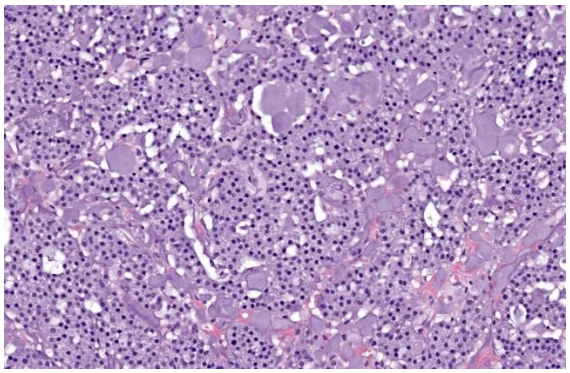

Figure 4-3. Periocular tissue, dog. Neoplastic epithelial cells are present in nests and packets and surround clear spaces that are often filled with a basophilic proteinaceous fluid. (HE 6X)

Contributor's Comment:
The gross and morphologic features of this mass are consistent with the diagnosis of canine lobular orbital adenoma. The key features attributed to this neoplasm include a well-differentiated glandular morphology, distinctive multi-lobular growth pattern, and a lack of glandular ducts and ductular differentiation of the neoplastic cells.[2] These neoplasms are frequently described clinically and/or grossly as being remarkably friable, which is attributed to the scant amounts of connective tissue supporting the dense glandular lobular units. This neoplasm is associated with a high rate of local recurrence, which is attributed to its friable nature and tendency to disperse within the orbit, causing difficulties in achieving clean surgical margins.[2] In the original case series describing this neoplasm, 10 out of 13 cases with available follow-up information experienced local recurrence (4 with multiple episodes of recurrence, with an average time after removal to recurrence of 395 days) with one case of recurrence associated with enucleation/exenteration, and the remaining 3 cases without recurrence being euthanized for reasons unrelated to this tumor.[2] The origin of this neoplasm is unknown. Empirical data from the Comparative Ocular Pathology Laboratory of Wisconsin (COPLOW) suggests that accessory lacrimal glands observed throughout the subconjunctival and orbital connective tissue are the most likely tissue of origin; however, lacrimal, third eyelid, or zygomatic salivary glands are other possibilities.[2] Supporting evidence for a tissue of origin include location of the tumor within the orbit if it is relatively localized (e.g. supero-temporal suggesting lacrimal gland) and the morphologic and histochemical features of any adjacent non-neoplastic glandular tissue (e.g. primarily serous units suggesting lacrimal gland).[1,2,6] The dorsal localization of this case's neoplasm suggests it may be lacrimal in origin; however, this feature does not serve as definitive evidence.

The examined tissues in this case did not include any non-neoplastic glandular tissue to support a specific tissue of origin.

Orbital neoplasia has been cited as the most commonly described disease of the orbit in dogs, with many of these neoplasms representing primary disease.[2] However, metastatic tumors, neoplasia that extends into the orbit from nearby locations such as the oral and nasal cavities, and non-neoplastic orbital diseases such as orbital abscess also occur and must be differentiated.[3]

Contributing Institution:
University of Wisconsin
School of Veterinary Medicine
Madison, WI
https://www.vetmed.wisc.edu/departments/pathobiological-sciences/

JPC Diagnosis:
Periocular tissue: Canine orbital lobular adenoma.

JPC Comment:
Canine lobular orbital adenoma (CLOA) is a rather descriptive name for an enigmatic

tumor. First formally described in a University of Wisconsin case series in 2004, little progress has been made in positively identifying the tissue of origin and descriptions of the entity often focus on distinguishing it from more well-known entities such as lacrimal or salivary gland tumors.[2]

Pathogenesis likewise remains mysterious. One recent study investigating the pathogenesis of this entity found no association between canine papillomavirus and the development of canine lobular orbital adenoma.[4] Another recent study performed metagenomic analysis on 31 confirmed CLOAs looking for associations with an expanded group of DNA viruses in the neoplastic and normal conjunctival tissues and similarly found no associations.[5]

CLOAs occur in middle age to older dogs without breed predilection. The typical clinical presentation is a mass in the eyelid or subconjunctiva or, less commonly, in the retrobulbar tissues. Approximately 13% of cases are bilateral.[5] Grossly, the neoplastic tissue appears nodular, translucent, and friable.

The histologic appearance of the tumor in this case is characteristic of CLOAs; there are abundant acini composed of epithelial cells filled with PAS-positive granules without accompanying ductal differentiation. Tissue samples submitted for histopathologic evaluation typically consist, as in this case, of neoplastic tissue without any surrounding orbital structures or contextual tissues, perhaps due to the neoplasm's friable nature.[2] When surrounding tissues are present for evaluation, the lobular growth characteristic of this neoplasm extends into the connective tissues of the orbit.[2] The published immunohistochemical profile of CLOAs include positive immunoreactivity for CK 19 and AE1/AE3 and negative immunoreactivity for SMA, CK14,

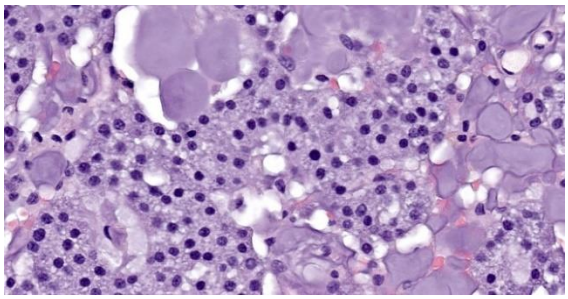

Figure 4-4. Periocular tissue, dog. High magnification of neoplastic cells with moderate amounts of granular cytoplasm. (HE, 520X)

CALP, and p63, though this combination is not specific to this entity.[6]

Conference discussion focused mainly on the difficulty of tissue identification and histologic diagnosis. Conference participants offered a variety of differential diagnoses, including metastatic glandular tumors of the thyroid, lacrimal, sebaceous, and salivary glands, but even though diagnostically incorrect, all participants felt honored to be present for this novel tumor's Wednesday Slide Conference debut.

References:

1. Giudice C, Marco R, Mirko R, Luca M, Giorgio C. Zygomatic gland adenoma in a dog: histochemical and immunohistochemical evaluation. *Vet Ophthalmol.* 2005;8(1): 13-16.
2. Headrick JF, Bentley E, Dubielzig RR. Canine lobular orbital adenoma: a report of 15 cases with distinctive features. *Vet Ophthalmol.* 2004;7(1):47-51.
3. Hendrix DVH, Gelatt KN. Diagnosis, treatment and outcome of orbital neoplasia in dogs: a retrospective study of 44 cases. *J Small Anim Pract.* 2000;41(3):105-108.
4. Schaefer EAF, Chu S, Pearce JW, Bryan JN, Flesner BK. Papillomavirus DNA not detected in canine lobular orbital adenoma and normal conjunctival tissue. *BMC Vet Res*. 2019;15:226.

5. Schaefer EAF, Chu S, Wylie KM, et al. Metagenomic analysis of DNA viruses with targeted sequence capture of canine lobular orbital adenomas and normal conjunctiva. *Microorganisms*. 2023;11(5):1163.
6. Wang F, Ting CT, Liu Y. Orbital adenocarcinoma of lacrimal gland origin in a dog. *J Vet Diagn Invest.* 2001;13(2):159-161.

WSC 2023-2024
Conference 3 Self-Assessment

1. Equine mast cell tumors are usually associated with widespread metastatic disease.
    a. True
    b. False

2. Which of the following is the reservoir host for the cowpox virus?
    a. Cows
    b. Cats
    c. Sheep
    d. Rodents

3. Which of the following is the most common systemic manifestation of cowpox in cats?
    a. Encephalitis
    b. Panophthalmitis
    c. Myocarditis
    d. Pneumonia

4. Thrombocytopenic purpura is most commonly seen in what breed of minipig?
    a. Gottingen
    b. Yucatan
    c. Sinclair
    d. Kunekune

5. True or false. Canine lobular orbital adenoma has a high rate of recurrence.
    a. True
    b. False

WEDNESDAY SLIDE CONFERENCE 2023-2024

Conference #4 **13 September 2023**

CASE I:

Signalment:
1-month-old, Quarter Horse colt, horse (*Equus caballus*)

History:
This foal presented to the Equine Emergency Service acutely ill with a fever, tachypnea, diarrhea, and seizures. Laboratory data revealed elevated liver enzymes and bile acids, left shift neutropenia, elevated fibrinogen, hypoglycemia, hyperlactatemia, and electrolyte abnormalities (see details below under laboratory results). Abdominal ultrasound identified hepatomegaly. The foal was humanely euthanized due to poor prognosis.

Gross Pathology:
On postmortem examination, the foal was in good body condition. The sclera and mucous membranes were mildly yellow (icterus). The liver was diffusely enlarged, mottled pale red to dark purple with disseminated pinpoint to ~1 mm diameter pale tan foci scattered throughout all lobes. The wall of the right dorsal colon was moderately thickened by edema, and the mucosa was diffusely dark purple. The right dorsal colon contained a moderate amount of opaque, homogeneous, bright yellow, watery digesta. The small colon contained small, soft, partially formed fecal balls. The skeletal muscle was diffusely pale tan to red. The lungs were slightly wet, heavy and mottled pale pink to dark red. On section, they oozed a small amount of serous fluid. A complete postmortem was performed, and no other significant gross lesions were identified.

Laboratory Results:

CBC	
Neutrophils	100 cells/µl (3,000-7,000)
Bands	400 cells/µl (0-100)
Fibrinogen	800 mg/dL (100-400)
Chemistry	
AST	1593 IU/L (185-375)
T-bilirubin	3.3 mg/dL (0.4-1.8)
SDH	223 IU/L (0-10)
GGT	54 IU/L (10-25)
Glucose	62 mmol/L (70-135)
Sodium	123 mEQ/L (132-142)
Chloride	84.4 mEQ/L (97-104)
Bicarb	20 mEQ/L (26-33)
Anion gap	22 mmol/L (8-15)
Icterus	6 mg/dL (1-3)
Lactate	7.2 mmol/L (1.11-1.78)
Bile acids	12 µmol/L (0-8.0)

PCR testing performed on fresh liver tissue at the University of Kentucky for *Clostridium piliforme* was positive.

PCR testing on fresh feces performed at University of California Davis was negative for the following: *Clostridium difficile* toxin A and B, *Lawsonia intracellularis*, *Salmonella* spp., *Cryptosporidium* spp., *Rhodococcus*

Figure 1-1. Liver, foal. The liver is diffusely enlarged and mottled pale red to dark purple. (Photo courtesy of: National Institutes of Health Comparative Biomedical Scientist Training Program (CBSTP) in collaboration with Colorado State University Veterinary Diagnostic Laboratory, https://nih-cbstp.nci.nih.gov/; https://vet medbiosci.colostate.edu/vdl).

equi, *Clostridium perfringens* antigen, *C. perfringens* alpha toxin, *C. perfringens* beta toxin, *C. perfringens* beta2 toxin, *C. perfringens* cytotoxin netF, and *C. perfringens* enterotoxin. PCR testing for *C. piliforme* was not performed on the feces.

Microscopic Description:
Liver: Multifocally and randomly affecting approximately 80% of the hepatic parenchyma are numerous 150-300 micron diameter foci of lytic necrosis characterized by fibrin, cellular debris, and high numbers of degenerate neutrophils. Necrotic foci are often coalescent, forming larger discrete sites (up to ~1 mm) of necrosis. There are hypereosinophilic and shrunken necrotic hepatocytes with pyknotic or karyorrhectic nuclei at the interface between necrotic and viable tissue. Peripheral to regions of necrosis, less affected hepatocytes occasionally contain numerous intracytoplasmic, stacked, pale, basophilic, filamentous bacilli. The portal interstitium is expanded by edema and variable numbers of lymphocytes and plasma cells. Few neutrophils and lymphocytes infiltrate through the hepatic capsule, which is also mildly edematous. The mesothelium is mildly reactive. Steiner's stain reveals numerous, stacked, argyrophilic elongate bacilli within hepatocytes at the periphery of necrotic foci.

Contributor's Morphologic Diagnosis:
Liver: Severe acute multifocal random necrosuppurative hepatitis with intrahepatocellular argyrophilic filamentous bacilli, etiology consistent with *Clostridium piliforme*.

Contributor's Comment:
Tyzzer's disease is a bacterial infection caused by *Clostridium piliforme*, an anaerobic, generally gram-negative, argyrophilic, pleomorphic, obligate intracellular bacillus. It can cause clinical disease in a variety of animals, including rodents, foals, calves, dogs, nonhuman primates, and cats.[5] One case of Tyzzer's disease has also been reported in an

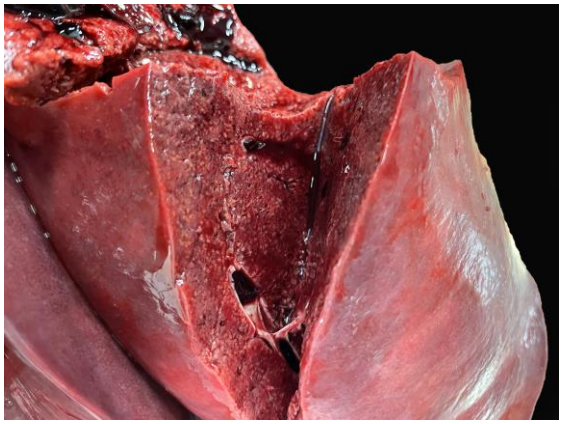

Figure 1-2. Liver, foal. The liver is diffusely enlarged, mottled pale red to dark purple with disseminated pinpoint to ~1 mm diameter pale tan foci scattered throughout the parenchyma of all lobes. (Photo courtesy of: National Institutes of Health Comparative Biomedical Scientist Training Program (CBSTP) in collaboration with Colorado State University Veterinary Diagnostic Laboratory).

Figure 1-3. Colon, foal. The wall of the right dorsal colon is moderately thickened by edema, and the mucosa is diffusely dark purple. The right dorsal colon contains a moderate amount of opaque, homogeneous, bright yellow, watery digesta. (Photo courtesy of: National Institutes of Health Comparative Biomedical Scientist Training Program (CBSTP) in collaboration with Colorado State University Veterinary Diagnostic Laboratory).

HIV-1 infected human.[7] Clinical disease generally occurs in young or immunocompromised animals and can cause lethargy, fever, anorexia, icterus, seizures, coma and death.[8] Foals generally succumb to fatal disease between 2 and 4 weeks of age.[8]

The pathogenesis of Tyzzer's disease is not fully elucidated. However, it is postulated that fecal-oral transmission of spores leads to gastrointestinal infection of mucosal enterocytes in the ileum, cecum and colon. Following necrotizing enteritis/typhlocolitis, portal circulation of bacteria leads to hepatic and systemic involvement.[6] Adult horses are generally resistant to disease but can harbor and shed *C. piliforme* in their feces. Foals commonly consume the dam's feces within the first few weeks of life, and it is likely that in many cases contaminated feces from the dam is a primary source of infection.[8] However, spores of *C. piliforme* can also persist in the environment for at least 5 years, so long-term environmental contamination can also be problematic.[1]

Tyzzer's disease classically causes a triad of hepatitis, colitis and myocarditis. The prevalence of each of these lesions varies between species. In foals, the most common finding is multifocal necrotizing hepatitis that is occasionally accompanied by necrotizing lymphohistiocytic colitis and less frequently a multifocal necrotizing myocarditis. In a recent case series of 25 cases, all foals had hepatitis, 10/25 had colitis, and only 8/25 had myocarditis.[3] The triad of concurrent lesions is more commonly observed in rodents and lagomorphs.[6] In this case, there was necrotizing hepatitis, a mild to moderate necrotizing lymphohistiocytic colitis and mild patchy gray matter edema with proliferation of Alzheimer type II astrocytes. There were no remarkable microscopic findings in the myocardium. The changes in the brain are compatible with hepatic encephalopathy. Hepatic encephalopathy in cases of Tyzzer's disease results from hyperammonemia secondary to acute liver failure. Horses, in contrast to carnivores and ruminants, do not exhibit spongy vacuolation of myelin (status spongiosis) with hyperammonemia.[4]

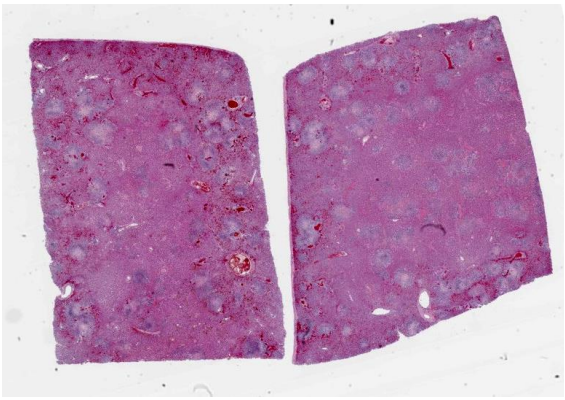

Figure 1-4. Liver, foal. Two sections of liver are 50% effaced by areas of lytic necrosis. (HE, 5X)

The diagnosis of Tyzzer's disease can be made with gross and histologic findings with the presence of intracellular filamentous bacteria within hepatocytes. The bacteria can be faintly visualized on H&E and highlighted by silver stains (such as Steiner's or Warthin-Starry), Giemsa, and periodic acid-Schiff stains.[6] PCR amplification of the 16S rRNA gene of *C. piliforme* can be performed to further support Tyzzer's disease. Considering the close phylogenetic proximity to other nonpathogenic clostridia, such as *C. colinum*, the PCR results should be interpreted with the gross and histologic findings. *C. piliforme* is very difficult to culture but can be isolated by inoculation of embryonated chicken eggs or specific primary cell lines.[1]

Other differentials that may be considered with multifocal necrosuppurative hepatitis without distinct intracellular filamentous bacteria in a foal include EHV-1 or bacteria that lead to septicemia (e.g. *Salmonella* spp., *Actinobacillus equuli*, *Listeria monocytogenes*). Other causes of foal diarrhea include equine rotavirus, equine coronavirus, *Rhodococcus equi*, *Clostridium perfringens*, *Clostridium difficile*, *Lawsonia intracellularis*, and *Cryptosporidium* spp.

Contributing Institution:
National Institutes of Health Comparative Biomedical Scientist Training Program (CBSTP) in collaboration with
Colorado State University Veterinary Diagnostic Laboratory
https://nih-cbstp.nci.nih.gov/
https://vetmedbiosci.colostate.edu/vdl/

JPC Diagnosis:
Liver: Hepatitis, necrotizing, multifocal to coalescing, random, with occasional intracytoplasmic bacilli.

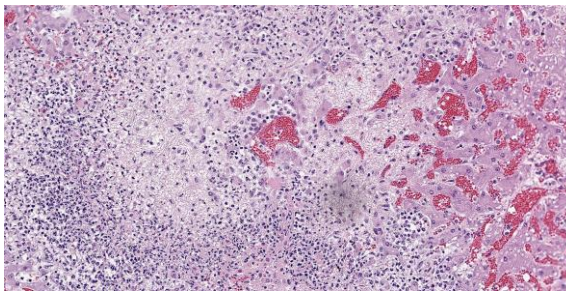

Figure 1-5. Liver, foal. Higher magnification of areas of lytic necrosis. There is loss of hepatocytes and infiltration of large numbers of necrotic and viable neutrophils and fewer macrophages admixed with abundant cellular debris. (HE, 5X)

JPC Comment:
The contributor provides an excellent, thorough review of Tyzzer disease, a well-known and well-described clostridial disease of wide veterinary importance. Less well-known, sadly, is the fascinating biography of Dr. Ernest Edward Tyzzer, the scientific Renaissance man for whom Tyzzer disease is named.

Dr. Tyzzer was born in a suburb of Boston in 1875 and paid his way through college and Harvard Medical School by trapping muskrat, fox, mink, skunk, and weasels.[10] His pathology and parasitology-steeped career began in his second year of medical school when, during one of his trapping trips, he discovered parasites in a fox carcass and brought the carcass to class, endearing himself to the pathology faculty (though perhaps less so to his fellow students).

His curiosity about the natural world led to a broad study of infectious agents in a variety of species. Immediately after graduating from medical school, Tyzzer began studying the histologic lesions of varicella virus and determined that the intranuclear inclusions generated in the disease were likely viral in nature and not morphologic stages of an unknown protozoal parasite, the accepted

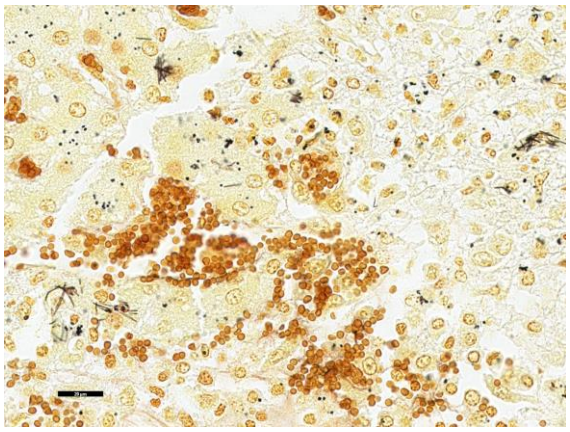

Figure 1-6. Liver, foal. A silver stain demonstrates haphazardly arranged stacks of filamentous bacilli consistent with Clostridium piliforme. (Steiners, 400X) (Photo courtesy of: National Institutes of Health Comparative Biomedical Scientist Training Program (CBSTP) in collaboration with Colorado State University Veterinary Diagnostic Laboratory).

theory at the time.[10] Tyzzer spent the next eleven years as the Director of Research for the Harvard Cancer Commission, where he investigated the occurrence of spontaneous murine tumors, host responses to transplantable tumors, and the biology of metastasis. During this time, three mice supplied by Tyzzer to one of his research collaborators became the founding members of the DBA inbred strain of mice now commonly used in medical research.[10]

Dr. Tyzzer also discovered and described the first *Cryptosporidium* species, *C. muris*, in the gastric glands of laboratory mice in 1907. Two follow-on publications in 1910 and 1912 contained further descriptions, gleaned solely from light microscope observations, about the life cycle and biology of *C. parvum* and *C. muris* that are still largely accepted today.[9]

Tyzzer was also responsible for correctly classifying the causative agent of blackhead in turkeys, naming it *Histomonas meleagridis*, and identifying that ingestion of contaminated nematode eggs was the connection between *Histomonas meleagridis* and *Heterakis* spp.[10] Having worked out the pathogenesis of the disease, Tyzzer then set up an experimental turkey farm where he worked out effective management practices to produce healthy turkeys and outlined these practices in pamphlets distributed to farmers by the Massachusetts Department of Agriculture. Tyzzer received a citation from the Governor of Massachusetts for this work, crediting him for saving the Massachusetts turkey industry.[10]

Dr. Tyzzer was involved in the discovery and elucidation of many other conditions not described above, including Tyzzer's disease, the causative agent of which he first described in a colony of Japanese waltzing mice in 1917. Tyzzer was also known for his humor, which was on display after he published a case report on his very own bleeding rectal polyp and accompanying *Entamoeba coli* infection. Though never identifying the patient, his manuscript stated that no systematic follow up study could be arranged "owing to the non-cooperative attitude of the patient".[10]

This week's slide conference, moderated by MAJ Kelsey Fiddes, Chief of Resident Training at the Joint Pathology Center, kicked off with this classic presentation of Dr. Tyzzer's eponymous disease. As is typical of this disease, the characteristic filamentous bacilli are covertly stacked within the cytoplasm of hepatocytes near the outside edge of necrotic lesions and require some imagination to appreciate with H&E staining alone. Silver stains such as Steiner's and Warthin-Starry allowed visualization of these bacteria and their classic "haystack" appearance.

Conference discussion focused mainly on differences in clinical presentations among various species. The classic "heart, intestine, liver" triad of lesions repeated breathlessly

by countless pathology residents is seen mainly in laboratory animals, while horses manifest their Tyzzer mainly through necrotizing hepatitis, as in our case. *Clostridium piliforme* infection in rats is associated with megaloileitis and with encephalitis in gerbils. Finally, a 2023 retrospective study found that the most common manifestation of Tyzzer disease in kittens is ulcerative colitis, followed by hepatitis and perianal dermatitis.[2]

References:

1. Barthold SW, Griffey SM, Percy DH. Mouse. Pathology of laboratory rodents and rabbits. 4th ed. Wiley;2016:1–118.
2. Fingerhood S, Mendonca FS, Uzal FA. Tyzzer disease in 19 preweaned orphaned kittens. *J Vet Diagn Invest*. 2023;35(2): 212-216.
3. García JA, Navarro MA, Fresneda K, Uzal FA. Clostridium piliforme infection (Tyzzer disease) in horses: retrospective study of 25 cases and literature review. *J Vet Diagn Invest*. 2022;34(3):421–428.
4. Hasel KM, Summers BA, De Lahunta A. Encephalopathy with idiopathic hyperammonaemia and Alzheimer type II astrocytes in Equidae. *Equine Vet J*. 1999; 31(6):478–482.
5. Jubb KVF, Kennedy PC, Palmer N. Pathology of domestic animals. Academic press; 2012.
6. Navarro MA, Uzal FA. Pathobiology and diagnosis of clostridial hepatitis in animals. *J Vet Diagn Invest*. 2020;32(2): 192–202.
7. Smith KJ, Skelton HG, Hilyard EJ, et al. Bacillus piliformis infection (Tyzzer's disease) in a patient infected with HIV-1:
8. confirmation with 16S ribosomal RNA sequence analysis. *J Am Acad Dermatol*. 1996;34(2):343–348.
9. Swerczek TW. Tyzzer's disease in foals: retrospective studies from 1969 to 2010. *Can Vet J*. 2013;54(9):876.
10. Tzipori S, Widmer G. A hundred-year retrospective on cryptosporidiosis. *Trends Parasitol*. 2008;24(4):184-189.
11. Weller TH. *Ernest Edward Tyzzer 1875-1965*. National Academy of Sciences; 1978.

CASE II:

Signalment:
3-month-old, female Speckled Sussex, avian (*Gallus gallus*)

History:
Four birds from a backyard flock were losing weight and anorexic. This bird died suddenly.

Gross Pathology:
Necropsy was performed on a 3-month-old intact female chicken. It was dark brown with light speckling. The keel bone was prominent and pectoral muscles were atrophied. The eyes were sunken in the orbits. Loose white to green fecal material was present around the cloaca and ventral tail feathers. Diffusely the skin was bright red.

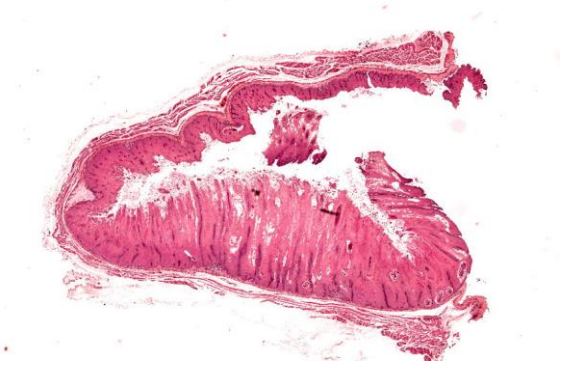

Figure 2-1. Crop, chicken. There is segmental and marked hyperplasia of the squamous mucosa of the crop (center bottom). (HE, 5X)

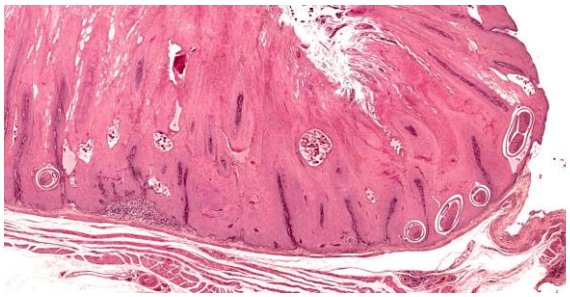

Figure 2-2. Crop, chicken. There are few cross and tangential sections of nematodes and eggs in tunnels within the hyperplastic mucosa. (HE, 37X)

Laboratory Results:
Fecal examination revealed few eggs (0-3/10X) of *Capillaria* sp., *Ascaridia* sp. and *Heterakis gallinarum*.

Microscopic Description:
Crop: Numerous cross-sections of nematodes are embedded within the markedly thickened mucosa. The parasites are 160-350 micrometers in diameter and contain an approximately 6 micrometer smooth cuticle, coelmyarian musculature, hypodermal bacillary bands, a body cavity, a multinucleated intestine and ovaries. There are bioperculated, oval embryonated eggs (*Capillaria* sp.) within the space occupied by the nematode, or in spaces by themselves within the mucosal epithelium.

Contributor's Morphologic Diagnosis:
Crop: Ingluvitis, proliferative, multifocal, moderate with intralesional nematode parasites, *Capillaria* sp.

Contributor's Comment:
The crop and esophageal mucosa is markedly thickened and contain numerous cross sections of parasites and eggs. The cuticle, digestive tract and body cavity qualifies these as nematode parasites. The bioperculated, oval embryonated eggs present in the parasite, within and on the surface of the mucosa are consistent with *Capillaria* sp. Similar nematode parasites and eggs were also present in the small intestine and double operculated eggs (*Capillaria* sp.) and eggs consistent with *Ascaridia* and *Heterakis gallinae* infections are present on fecal flotation. Although chickens can harbor many species of *Capillaria*, only *Capillaria annulatus* and *contortus* are present in both the crop and small intestine. As nematode parasites were not recovered during necropsy, definitive identification was not possible.

This chicken had a severely thickened crop mucosa and was malnourished as evidenced by the prominent keel bone and pectoral muscle atrophy. The loose fecal material around the cloaca and ventral tail feathers are consistent with diarrhea, which is often associated with heavy intestinal *Capillaria* infections. *Capillaria* infections are usually of little consequence in most chickens; however, when there are heavy infections in the crop

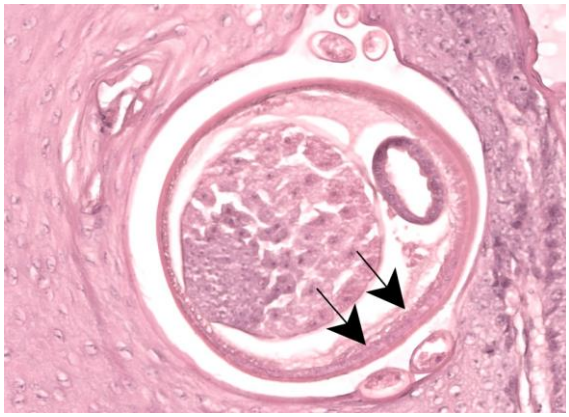

Figure 2-3. Crop, chicken. Cross section of an adult female aphasmid nematode with a smooth cuticle, pseudocoelom, bacillary band (arrows), a small intestine lined by uninucleate cells, and a cross section of an ovary. There are few eggs in the space surrounding the nematode. (HE, 382X)

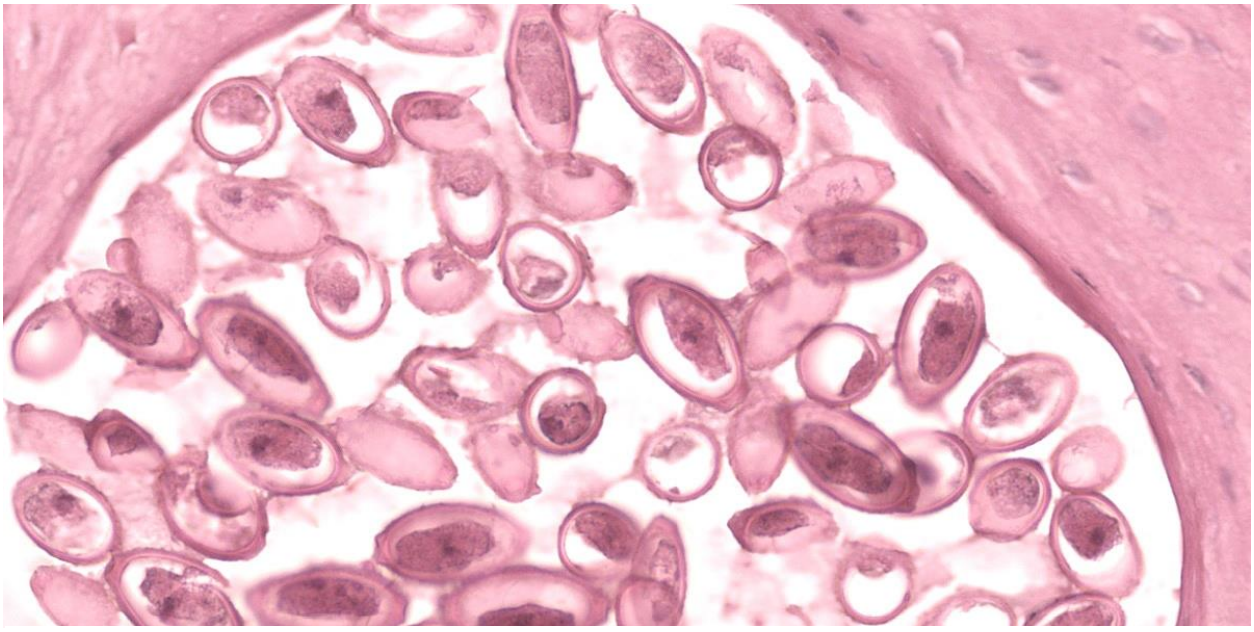

Figure 2-4. Crop, chicken. Numerous asymmetrically bioperculated eggs are present within tunnels in the hyperplastic mucosa. (HE, 680X)

and esophagus by *C. annulatus* or *contortus* (the most pathogenic *Capillaria* species) the-mucosa can become so thickened that swallowing can be difficult to impossible. This can result in high mortality as was present in this case. All 4 chickens in this backyard flock died and had lesions similar to those in this chicken. As both *C. annulatus* and *contortus* are transmitted by earthworms, backyard flocks in humid environments are extremely susceptible. Death of this chicken was subsequent to heavy Capillaria infections of the crop, esophagus and small intestine.

Contributing Institution:
Tuskegee University
Pathobiology Department
https://www.tuskegee.edu/programs-courses/colleges-schools/cvm

JPC Diagnosis:
Crop, mucosa: Hyperplasia, segmental, marked, with few adult female aphasmid nematodes and numerous eggs.

JPC Comment:
Capillariasis is a common disease of free-range chickens. Some species within the *Capillaria* genus infect the upper digestive system, particularly the crop and esophagus, while others cause intestinal or cecal disease.[1] The adult worms are thin and filamentous, giving them the monikers "thread worms" or "hairworms," and produce characteristic bi-operculate eggs. These worms burrow into their preferred mucosal lining, typically without causing clinical signs, but with increasing numbers, severe inflammation, diarrhea, wasting, and death may occur.

The life cycles vary among the *Capillaria* species; some have a direct life cycle, while other require an intermediate host, most commonly an invertebrate such as an earthworm.[1] The most common *Capillaria* species that cause disease in chickens are *C. contorta*, *C. annulata*, *C. anatis*, *C. bursata*, *C. caudinflata*, and *C. obsignata*. As the contributor notes, of these, *C. annulata* and *C. contorta* are found in the crop and esophagus, *C. anatis* occurs in the ceca, and the balance inhabit

the small intestine. Depending on the species and life cycle, chickens are infected by ingesting litter containing worm eggs or by ingesting an infected intermediate host.

As in this case, the typical histologic lesion of crop capillariosis is thickening and inflammation of the mucosa, while intestinal and cecal-focused *Capillaria* species may cause inflammation, hemorrhage, and erosion of the gastrointestinal linings.

Conference discussion centered around histologic differences between the avian crop and esophagus and the difficulty in differentiating between the two locations. While differences appear to be species-specific, in general the crop has no or few glands compared to the esophagus, where glands are typically more numerous. Conference participants felt it was quite difficult to determine if examined section was esophagus or crop, and many participants felt they would have had to wing it were it not for the contributor's gross necropsy findings.

Conference participants also noted the very mild nature of the inflammatory infiltrate and postulated that this might be because larvae are typically restricted to the mucosa in crop capillariasis. Participants felt that the striking hyperplasia was the more important histologic finding and deserved pride of place in the JPC morphologic diagnosis.

References:

1. Swayne DE, Glisson JR, McDougald LR, et.al. *Diseases of Poultry*. 13th ed. Blackwell Publishing Ltd;2008:1162-1164.

CASE III:

Signalment:
4-year-old Holstein cow, bovine (*Bos taurus*)

History:
The cow developed progressive weight loss, recumbency, weakness, depression, and mild hyperthermia. Despite treatment with an antibiotic (ceftiofur), a non-steroidal anti-inflammatory drug (flunixin), a corticosteroid (dexamethasone), and a parenteral solution containing vitamins, glucose and amino acids, her clinical condition deteriorated over a few weeks, necessitating euthanasia due to poor prognosis. The cow was pregnant at approximately 5 months of gestation.

Gross Pathology:
Multifocally infiltrating/expanding the myocardium and extending into the adjacent endocardium and epicardium in the atria, interventricular septum and the left ventricular free wall, there were multiple, yellowish/tan, irregular mass-like foci of approximately 1 to 8 cm, with poorly defined borders. In the myocardium, some of the larger foci exhibited a central 1–2 cm area of necrosis, demarcated by an incomplete thin (1–2 mm) red rim/halo (hemorrhage). The mesenteric lymph nodes were markedly enlarged, measuring up to 15 x 8 cm.

Laboratory Results:
In 2019, the cow had tested positive for serum antibodies against bovine leukemia virus (BLV) by ELISA and for BLV by qPCR on a sample of whole blood (6.45 x 104 BLV genome copies/µL), and a complete blood count revealed leukocytosis (white blood cells: 14.7 x 109/L; reference range: 5.8–12.6 x 109/L) with lymphocytosis (10.07 x 109/L; reference range: 1.7–5.6 x 109/L). A sample of heart obtained during the autopsy also tested positive for BLV by qPCR (1 x 106 genome copies/mg).

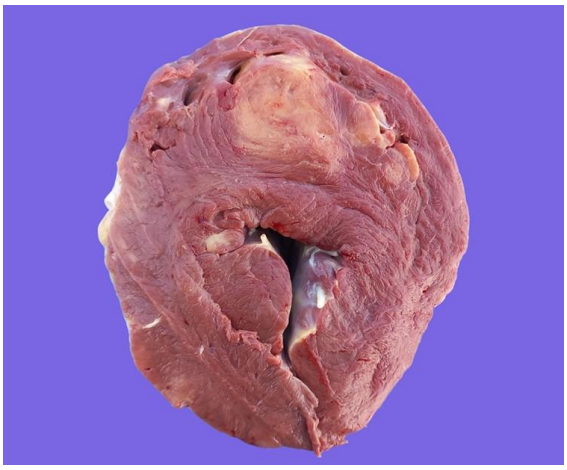

Figure 3-1. Heart, ox. Multiple, yellowish/tan, irregularly shaped, foci with indistinct borders ranging from 1 to 8 cm infiltrate the myocardium. The larger focus (upper center) involve the right aspect of the interventricular septum. (Photo courtesy of: Plataforma de Investigación en Salud Animal, Instituto Nacional de Investigación Agropecuaria (INIA), La Estanzuela, Uruguay).

Microscopic Description:
Two sections of heart are examined. Extensively infiltrating the myocardial interstitium including the endomysium, separating myocardial fibers, and multifocally infiltrating the endocardium and the conduction system, is an unencapsulated, densely cellular neoplasm composed of round cells arranged in sheets. Neoplastic cells are round to oval, with distinct borders, scarce cytoplasm, and high nuclear-to-cytoplasmic ratio. Nuclei are large, round, oval or reniform (moderate anisokaryosis), with coarse or clumped chromatin and 1 to 3 magenta nucleoli. The mitotic count is up to 8 per 400x field. Additionally, in one of the sections there is a fairly well-demarcated central area of necrosis that involves both the cardiomyocytes and the entrapped infiltrating neoplastic cells. In this area cardiomyocytes have hypereosinophilic and coagulated sarcoplasm, with loss of transverse striations (necrosis), neoplastic cells exhibit karyolysis, and there are occasional foci of erythrocyte extravasation (hemorrhages). Occasional intact, thick-walled, oval, basophilic, protozoal cysts morphologically resembling *Sarcocystis* spp. cysts are present within the sarcoplasm of cardiomyocytes.

Contributor's Morphologic Diagnosis:
Heart: Lymphoma, holstein, bovine.

Contributor's Comment:
The diagnosis of Enzootic Bovine Leukosis (EBL) in this cow was based on gross, microscopic, molecular (qPCR), and serological (ELISA) findings. The seroprevalence of BLV was high in the herd.

EBL is caused by BLV, genus *Deltaretrovirus*, family *Retroviridae*, which is closely related to primate T-lymphotropic viruses including human T-cell lymphotropic virus 1 and 2 and simian T-cell lymphotropic virus.[14,16] EBL is a contagious lymphoproliferative condition, and the most frequent neoplastic disease of cattle.[14] The disease has been reported in almost every cattle raising country during the last century.[12,14,16] However, to date, BLV has been successfully eradicated from over 20 countries, including several European countries, New Zealand, and Australia.[6,14,20] Thus, it is mainly present in eastern Europe, the Americas, and some Asian and middle eastern countries.[6,14] Most of these countries have reported continuous increases in BLV prevalence in beef and dairy cattle herds, although prevalence is usually higher in dairy farms.[1,14,16] While BLV has been linked to breast cancer in women, the eventual causal relationship between this virus and breast cancer is still a matter of debate in the scientific community.[2,5,8]

BLV is harbored in circulating lymphocytes of infected cattle and can be transmitted horizontally and vertically; the former being the main form of transmission.[6,13,14,20] As fresh blood, semen, saliva, milk, and nasal secretions are known sources of BLV proviral DNA, direct contact, iatrogenic procedures, blood-sucking insects, and natural breeding are potential transmission routes.[6,14,20] Vertical transmission via transplacental infection or ingestion of colostrum/milk is thought to account for a small proportion of BLV infections.[13,14] Intrauterine transmission has been reported to occur in 4–8% of calves born to BLV seropositive dams.[6] Transmission through the ingestion of colostrum or milk from BLV-infected cows is possible since they both can contain provirus or free viral particles. However, colostrum and milk can also contain high titers of protective antibodies that could prevent infection in calves.[12,13] Quantification of the risk of this transmission route is currently lacking.[13]

BLV is capable of infecting different immune cells, with a predilection for B-lymphocytes.[16] Viral infection occurs after destabilization of the cell membrane by a transmembrane glycoprotein. Afterwards, the virus integrates into the host cell genome, interfering with gene expression and altering proliferative and apoptotic processes.[14] These mechanisms are responsible for the different clinical features of the disease in cattle. On one hand, animals suffering from benign persistent lymphocytosis develop a massive proliferation of B-lymphocytes as a consequence of a blockage of their apoptosis along with an increase of proliferation.[11] In contrast, neoplastic transformation is associated with

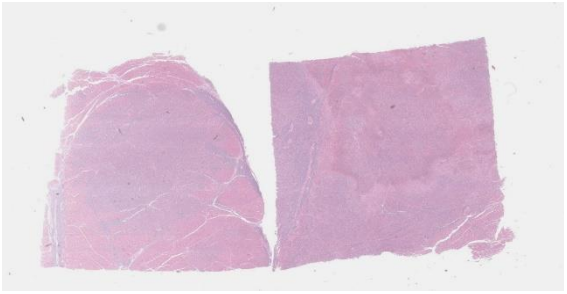

Figure 3-2. Heart, ox. Two sections of myocardium are submitted for examination.

inactivation of the tumor suppressor gene p53.[14]

Exposure to BLV may lead to four different outcomes: a) failure in establishing an infection, probably due to genetic resistance of the host and/or other factors; b) asymptomatic infection, which is characterized by detectable antibodies and no clinical or hematological abnormalities; c) persistent lymphocytosis with detectable antibody titers; and d) development of malignant lymphocytic neoplasia (lymphoma) in seropositive individuals.[6,12,14] In the case described herein, the cow had evidence of persistent lymphocytosis in 2019, and while she was asymptomatic at that time, whether she concurrently had subclinical lymphoma was not determined. It is believed that the outcome of the infection may be influenced by the genetic constitution of the individual, its immune status, and the infective dose.[6] The majority of infected cattle (70%) remain asymptomatic, while approximately 30% develop a benign lymphocytosis that persists for years, and it is not associated with the tumoral disease.[6,14,17] The development of lymphoma occurs in 1–5% of BLV-infected individuals usually after a latency period of 1–8 years, regardless of the development of persistent lymphocytosis, and is considered the only symptomatic form of EBL.[6,12,17]

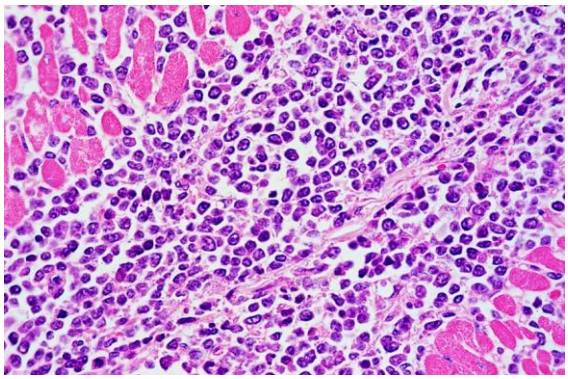

Figure 3-3. Heart, ox. Infiltrating the myocardial interstitium and separating individual cardiomyocytes is a densely cellular neoplasm of neoplastic lymphocytes arranged in sheets. (Photo courtesy of: Plataforma de Investigación en Salud Animal, Instituto Nacional de Investigación Agropecuaria (INIA), La Estanzuela, Uruguay). (HE, 200X)

While lymphoma occurs regardless of the development of persistent lymphocytosis, it is estimated that approximately two thirds of the cows that develop BLV-induced lymphoma previously undergo persistent lymphocytosis.[11]

BLV-induced lymphoma may be located in any organ, but the abomasum, kidney, heart, spinal cord, uterus, and lymph nodes are the most commonly affected ones.[4,6] Therefore, the clinical presentation may vary depending on the organ or tissue involved.[4,6] Overall, the most frequent clinical findings consist of inappetence, weight loss, drop in milk production, pallor, weakness, recumbency, etc.[6,15] In the case presented here, although the heart was extensively affected, no signs or lesions compatible with congestive heart failure were detected, suggesting that extensive cardiac involvement may have occurred somewhat recently prior to clinical disease, or without significantly affecting cardiac function until a few weeks before euthanasia, when the cow became symptomatic. Additionally, because there was histologic evidence of neoplastic infiltration in the conduction system of the heart, as well as evidence of acute myocardial necrosis, we speculate that either one or both pathological findings could have precipitated the clinical deterioration in this case. Besides the heart and mesenteric lymph nodes, no other tissues were affected in this cow.

Macroscopically, lymphomas are yellowish, white to tan, bulging masses with a homogeneous aspect. Neoplastic tissue is usually firmer than normal lymphoid tissue, and it can be found surrounding bright yellow necrotic foci.[3,6] In the heart, two gross presentations, consisting of nodular and diffuse forms, have been described.[3] In the former, bulging lesions are located in the atrium and blend into the epicardial fat, thus making them hard to differentiate. Diffuse cardiac lesions are usually disseminated in the ventricular myocardium. Interestingly, our findings include both patterns since nodular lesions were present in the right atrium but there were also extensive lesions in the myocardium of the interventricular septum and left ventricular free wall.

Histological findings typically include dense cellular masses or diffusely infiltrative neoplasms composed of sheets of neoplastic round cells (B cells) that infiltrate, disrupt and/or replace the parenchyma of the affected organs.[10] Neoplastic cells exhibit scarce cytoplasm and distinct cell borders, and large, irregularly round nuclei. The mitotic index is usually high.[6]

Clinically, differential diagnoses for the cardiac presentation include various conditions including bacterial infections (*Histophilus somni*, abscess, and bacterial endocarditis), parasitic diseases (i.e. sarcocystiosis, cysticercosis), traumatic reticulopericarditis, and primary cardiac tumors (rhabdomyoma, rhabdomyosarcoma, peripheral nerve sheath tumors [neurofibroma, schwannoma, neurinoma, neurofibroma], hemangioma, hemangiosarcoma, fibroma, fibrosarcoma, angiolipoma, angioleiomyoma, leiomyoma, leiomyosarcoma, adenomatoid tumor, hamartoma, mesothelioma, and myxoma).[6,19] Enlargement of lymph nodes can be found in many other conditions, such as tuberculosis, paratuberculosis, caseous lymphadenitis, actinobacillosis, sporadic bovine leukosis (which is not caused by BLV), zygomycotic lymphadenitis, theileriosis, brucellosis, etc.[6] Histologically, lymphoma is readily distinguishable from all these conditions, except for sporadic bovine leukosis, which usually occurs in young calves instead of adult cattle.

Antemortem diagnosis of BLV exposure and infection can be accomplished by serologic (ELISA, agar gel immunodiffusion) and molecular methods (PCR, qPCR). Lymphoma can be diagnosed by cytology and/or histopathology coupled with viral detection by PCR in postmortem specimens.[6,14,20]

Contributing Institution:
Plataforma de Investigación en Salud Animal
Instituto Nacional de Investigación Agropecuaria (INIA)
La Estanzuela, Uruguay
www.inia.uy

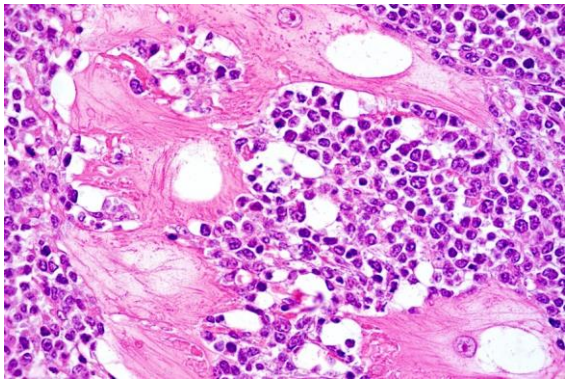

Figure 3-4. Heart, ox. Neoplastic cells infiltrate the cardiac conduction system, surrounding and separating Purkinje fibers. (Photo courtesy of: Plataforma de Investigación en Salud Animal, Instituto Nacional de Investigación Agropecuaria (INIA), La Estanzuela, Uruguay). (HE, 400X)

JPC Diagnoses:
1. Myocardium: Lymphoma.
2. Myocardium: Sarcocysts, few.

JPC Comment:
As the contributor details, aggressive efforts have led to the eradication of EBL in many countries; however, this fact belies the difficulty of eradication, largely due to the limited ability to identify "aleukemic" animals who are infected but subclinical.[7] To that end, much of the current research surrounding EBL is focused on developing effective diagnostics that can be used to identify and remove asymptomatic animals from herds.

Among these new diagnostics are droplet digital PCR (ddPCR) assays that can be used to identify and quantify BLV provirus (viral DNA that has been integrated into the host genome) in animals with recent infection or low proviral load.[7,15] ddPCR is a relatively recent nucleic acid quantification modality that has several benefits over PCR and quantitative PCR, including 1) the ability to provide quantitative counts without the need for a reference curve, and 2) the ability to provide reproducible quantitative data in

unpurified samples that contain minute amounts of target DNA.[7] Recent research shows that ddPCR can detect proviral DNA as early as 2 days post-infection, much earlier than the 13 days post infection with traditional PCR-based methods.[7] ddPCR is also able to detect and quantify provirus in individual and bulk tank milk, an important diagnostic advantage allowing testing of easily accessible samples that have far lower levels of provirus and far higher levels of contaminates than required or allowed with legacy PCR techniques.[7]

The key innovation of the ddPCR technique is the fractioning of DNA samples into tens of thousands of individual droplets using an oil and water technique. Once the sample is fractionated, the PCR reaction is carried out in each individual droplet. Once the PCR reaction has terminated, the fluorescent properties of each individual droplet are analyzed in a method similar to flow cytometry, and the number of droplets that contain sample is used to quantify the original amount of proviral DNA.[9]

It is hoped that ddPCR quantification of proviral DNA levels in whole blood or milk may be a good indicator of disease and disease progression in the field.[18] The quantification of proviral DNA can also inform herd management decisions as animals with low proviral loads are less effective virus transmitters and thus can be segregated, but need not necessarily be culled, to prevent disease transmission to naïve animals.[7]

The most recent research into BLV diagnostics has innovated on the ddPCR proviral assay. Previous research has identified an association between the bovine MHC-DRB3 gene and proviral load in certain species of cattle, with one allele associated with a high proviral load (a BLV susceptibility gene) and another allele associated with a low proviral load (a BLV resistant gene). This year, researchers developed a single-well assay that combines the ddPCR proviral quantitative assay with allele typing, including identification of homo- and heterozygotes, to provide a more holistic view of which animals are at risk of spreading disease.[15] These diagnostic innovations could soon provide a pathway for economically viable eradication efforts that minimize culling, even in areas of high disease prevalence.

This case presents a classic demographic, clinical, gross, and histologic case of BLV-induced lymphoma. In a heart with this gross appearance, lymphoma should be at the top of the differential list, though neurofibroma and granulomatous disease can't be definitely ruled out prior to histologic evaluation. Conference participants discussed the curious subgross appearance of the examined tissue section, which contains a large confluent, well-demarcated area of pallor reminiscent of an infarct; however, histologically, while neoplastic cells in this area are often necrotic, the cardiomyocytes appear viable. No conclusions were reached as to the origin of this unique appearance.

The scattered sarcocysts are a common, incidental finding in cattle and are most commonly tissue cysts of *Sarcocystis cruzi*.

References:

1. Bartlett PC, Ruggiero VJ, Hutchinson HC, et al. Current developments in the epidemiology and control of Enzootic Bovine Leukosis as caused by bovine leukemia virus. *Pathogens*. 2020;9(12): 1058.
2. Buehring GC, Shen HM, Schwartz DA, Lawson JS. Bovine leukemia virus linked to breast cancer in Australian women and identified before breast

cancer development. *PLoS One*. 2017;12(6): e0179367.
3. Buergelt C, Clark E, del Piero F. *Bovine Pathology: A Text and Color Atlas*. CABI International;2018:285.
4. Burton A, Nydam D, Long E, Divers T. Signalment and clinical complaints initiating hospital admission, methods of diagnosis, and pathological findings associated with bovine lymphoma (112 cases). *J Vet Intern Med*. 2010; 24:960-964.
5. Ceriani MC, Lendez PA, Martinez Cuesta L, et al. Bovine Leukemia Virus Presence in Breast Tissue of Argentinian Females and Its Association With Cell Proliferation and Prognosis Markers. *Multidiscip Cancer Investig*. 2018; 2(4):16–24.
6. Constable P, Hinchcliff K, Done S, Grünberg W. *Veterinary medicine: a textbook of the diseases of cattle, horses, sheep, pigs and goats*. 11th ed. Saunders Elsevier; 2017:785–794.
7. DeBrun ML, Cosme B, Petersen M, et al. Development of a droplet digital PCR assay for quantification of the proviral load of bovine leukemia virus. *J Vet Diagn Invest*. 2022;34(3):439-447.
8. Delarmelina E, Buzelin MA, de Souza BS, et al. High positivity values for bovine leukemia virus in human breast cancer cases from Minas Gerais, Brazil. *PLoS One*. 2020;15(10):e0239745.
9. Hindson BJ, Ness KD, Masquelier DA, et al. High-throughput droplet digital PCR system for absolute quantification of DNA copy number. *Anal Chem*. 2011;83(22):8604-8610.
10. Hishamnuri WNAD, Nakagun S, Maezawa M, et al. Disseminated thymic B-cell lymphoma in a Holstein heifer. *J Vet Diagn Invest*. 2019;31(6):852–855.
11. Juliarena MA, Gutierrez SE, Ceriani C. Determination of proviral load in bovine leukemia virus–infected cattle with and without lymphocytosis. *Am J Vet Res*. 2007;68(11):1220–1225.
12. Juliarena MA, Barrios CN, Lützelschwab CM, Esteban EN, Gutiérrez SE. Bovine leukemia virus: Current perspectives. *Virus Adapt Treat*. 2017;9:13–26.
13. Kuczewski A, Orsel K, Barkema HW, Mason S, Erskine R, van der Meer F. Invited review: Bovine leukemia virus—Transmission, control, and eradication. *J Dairy Sci*. 2021;104(6):6358–6375.
14. Marawan MA, Alouffi A, El Tokhy S, et al. Bovine leukaemia virus: Current epidemiological circumstance and future prospective. *Viruses*. 2021;13(11):1–24.
15. Notsu K, El Daous H, Mitoma S, Wu X, Norimine J, Sekiguchi S. Identifying pathogen and allele type simultaneously in a single well using droplet digital PCR. *mSphere*. 2023;8(1):e0049322.
16. Polat M, Takeshima SN, Aida Y. Epidemiology and genetic diversity of bovine leukemia virus. *Virol J*. 2017;14(1):1–16.
17. Schwartz I, Lévy D. Pathobiology of bovine leukemia virus. *Vet Res*. 1994; 25(6):521–536.
18. Smith B, Van Metre D, Pusterla N. Large Animal Internal Medicine. Elsevier Mosby; 2020:1874.
19. Une Y, Shirota K, Nomura Y. Cardiac angioleiomyoma in 44 cattle in japan (1982-2009). *Vet Pathol*. 2010;47(5): 923–930.
20. World Organisation for Animal Health (OIE). Enootic Bovine Leukosis. In: *OIE Terrestrial manual*. 8th ed. OIE;2018:1-12.

CASE IV:

Signalment:
3-year-old, Holstein bull (*Bos taurus*)

History:
A Holstein bull with a history of chronic weight loss and wasting was slaughtered on-farm for human consumption. Since multiple lesions were found in the liver, lung, bronchial and hepatic lymph nodes, the practitioner decided to submit these samples for diagnostic workup.

Gross Pathology:
The liver, lungs, and hepatic and bronchial lymph nodes had multiple granulomas. In the liver, these granulomas were multifocal to coalescing, roughly round, nodular, firm, and were readily visible protruding from the diaphragmatic surface of the capsule. The granulomas ranged from 0.5 to 5 cm in diameter and were frequently surrounded by a pearly white capsule of connective tissue (fibrosis). On cut surface, the granulomas frequently contained a yellowish central area of caseous material (necrosis) and crepitated when sliced with the blade of the knife, suggesting mineralization.

Laboratory Results:
Mycobacterium bovis was isolated from fresh samples of lung and bronchial lymph node inoculated in egg yolk agar. *Mycobacterium bovis* DNA was amplified by qPCR from frozen samples of hepatic and bronchiolar lymph nodes.

Microscopic Description:
Liver: approximately 50% of the parenchyma is replaced by multiple granulomas. The granulomas are composed of a pale eosinophilic center with cellular debris (necrosis) and scattered deposits of coarse basophilic or amphophilic amorphous to crystalline material (mineralization). These necrotic and

Figure 4-1. Liver, ox. Multiple coalescing, irregularly round, 0.5 to 5 cm granulomas protrude from beneath the hepatic capsule. (Photo courtesy of: Nacional de Investigación Agropecuaria (INIA), Route 50, Kilometer 11, La Estanzuela, Colonia 70006, Uruguay).

mineralized centers are surrounded and infiltrated by inflammatory cells, notably epithelioid macrophages, occasionally forming multinucleated giant cells with peripherally located nuclei (Langhans type), and fewer lymphocytes and plasma cells. The granulomas are frequently surrounded by a thick capsule of collagenous fibrous connective tissue. The hepatic parenchyma in adjacent areas is displaced and partially compressed by the granulomas. In these regions there is distortion/disruption of the hepatic cord histoarchitecture, hepatocytes are atrophic, the sinusoids are expanded by connective tissue (fibrosis), with variable degrees of portal, bridging, dissecting and perivenular fibrosis. In these areas there are also scattered infiltrates of lymphocytes, macrophages, and multinucleated giant cells. Portal areas also exhibit moderate bile duct hyperplasia. Intracellular, 2-µm long, acid fast bacilli were detected in multinucleated giant cells in histologic sections of liver stained with Ziehl-Neelsen.

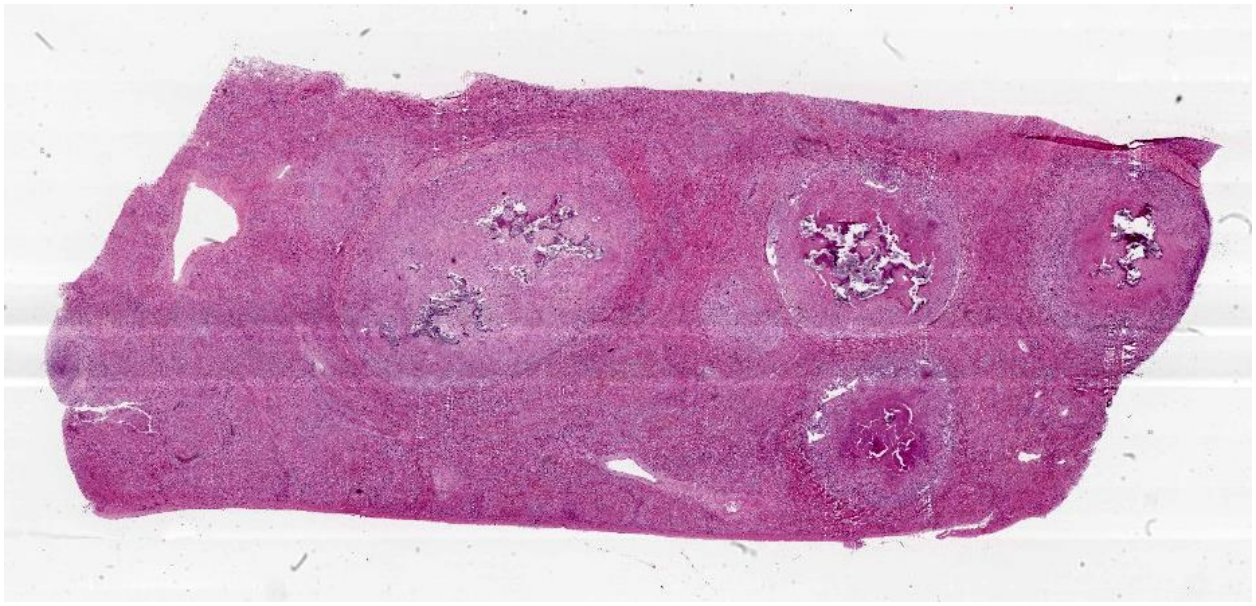

Figure 4-2. Liver, ox. One section of liver is submitted for examination. There are several discrete granulomas effacing approximately 50% of the section. (HE, 5X)

Contributor's Morphologic Diagnosis:
Liver: Hepatitis, granulomatous, multifocal to coalescing, chronic, severe with caseous necrosis and mineralization, multinucleated giant cells, intra-histiocytic acid-fast bacilli, and fibrosis, Holstein bull, bovine.

Contributor's Comment:
The diagnosis of bovine tuberculosis in this case was mainly based on pathological findings coupled with the identification of acid-fast bacilli by Ziehl-Neelsen, and isolation and molecular identification of *Mycobacterium bovis*.

Mycobacteria are facultative intracellular, aerobic, non-motile, pleomorphic bacilli.[8,16] They resist decolorization by acids during staining procedures because of the high content of lipids of their cell walls. Hence, they are considered acid-fast bacteria and can be stained with Ziehl-Neelsen or Fite-Faraco stains, but not with Gram stains.[17] The mycobacteria that cause tuberculosis are grouped within the Mycobacterium tuberculosis complex (MTBC), which includes *M. tuberculosis*, *M. bovis*, *M. caprae*, *M. africanum*, *M. microti*, *M. canettii*, *M. pinnipedii*, *M. orygis*, *M. suricattae*, *M. mungi*, and the Dassie and Chimpanzee bacilli.[3,11] Within this extensive group, only two members are confirmed causes of bovine tuberculosis: *M. bovis* and, to a lesser extent, *M. caprae*.[6,12]

Although bovine tuberculosis has a worldwide distribution, its prevalence has declined significantly in many regions, and approximately 20 countries (mainly from Europe) are considered tuberculosis-free as a result of rigorous eradication programs.[2,5] Similar eradication programs are currently being implemented in other countries, such as the US, Mexico, New Zealand, and Japan.[5] The disease is still widely spread in Africa, Asia, and Central and South America.[2,5]

Mycobacteria are very resistant to environmental conditions, which facilitates indirect infection from contaminated sources.[9] However, direct transmission from infected animals is the main route of infection.[9] Inhalation of aerosols containing mycobacteria is

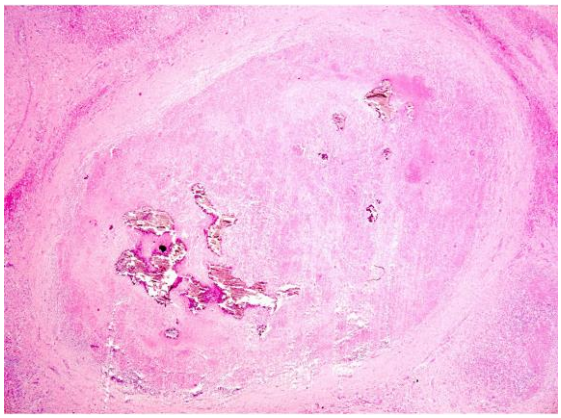

Figure 4-3. Liver, ox. Replacing the hepatic parenchyma is a granuloma with a central area of caseous necrosis and mineralization surrounded by a thick capsule of connective tissue. (Photo courtesy of: Nacional de Investigación Agropecuaria (INIA), Route 50, Kilometer 11, La Estanzuela, Colonia 70006, Uruguay). (HE, 100X)

the primary route of transmission in cattle.[6,9] *Mycobacterium bovis* can also be excreted in feces, urine, and colostrum/milk; hence, contaminated feedstuff and water are potential sources of infection. Oral transmission requires a large infective dose.[6,9] In young calves, infection through ingestion of unpasteurized colostrum/milk from infected cows is possible.[9] Other uncommon infection sources and routes include cutaneous exposure, congenital infection, or transmission through semen, vaginal and uterine discharges, among others.[6]

Bovine tuberculosis spreads throughout the organism in two stages: i) the primary complex and ii) post-primary dissemination. After lodging in the lesion inflicted at the entry site, mycobacteria are transported to the draining lymph node(s) where they establish a secondary infectious focus, generating the primary complex.[7] When both lesions (at the entry point and the local lymph node) are present, the primary complex is classified as complete, and when the lesion at the site of entry is absent (as in most cases occurring after digestive transmission) the primary complex is referred to as incomplete.[7] Depending on the immune status of the host, dissemination from the primary complex (post-primary dissemination) may occur either via lymphatic or hematogenous spread, or through pre-existing anatomical routes in the organs. Each of these forms of spread will determine different post-primary presentations: late generalization or chronic organ tuberculosis.[6,7] Another presentation is called early generalization, which occurs due to the infection's spread during the early stages as a consequence of a poor immune response.[7]

The clinical presentation usually varies with the localization of the infection. Overall, clinical signs are nonspecific (i.e., progressive weight loss, fluctuating fever, weakness, inappetence), thus the diagnosis should not be based on clinical examination alone. It should be considered that cattle with extensive miliary lesions may be clinically normal.[5,6]

The characteristic gross lesion is the tubercle, a circumscribed, often encapsulated, tan to yellow granuloma, often with central caseous necrosis and/or mineralization, which has been referred to as a "caseocalcareous granuloma".[4] There is large variation in the size of the tubercles; they can be small enough to be overlooked during autopsy, or involve a major part of an organ.[18] Tubercles are most frequently seen in bronchial, retropharyngeal, and mediastinal lymph nodes.[4] Other sites commonly affected include the lung, liver, spleen, and the serosal surfaces of body cavities.[18] Other locations, including the brain and meninges, have also been described.[14]

Histologically, small granulomas consist of epithelioid macrophages and few Langhans-type multinucleated giant cells and neutrophils.[4,7,11] As the lesion progresses, a central area of caseous necrosis, consisting of eosinophilic homogeneous material with necrotic cell debris and mineralization develops.[4,7,11]

This necrotic core is surrounded by macrophages, multinucleated giant cells, lymphocytes, and occasional neutrophils.[4,7,11] Over time, a fibrous connective tissue capsule is formed. Acid-fast bacilli may be found extracellularly in the necrotic core or within the cytoplasm of macrophages and giant cells.[7,11] The absence of acid-fast bacilli on histopathological examination does not rule out tuberculosis.[7,18]

Differential diagnoses on clinical or gross pathology grounds include many conditions such as mycobacteriosis associated with the M. avium-intracellulare complex, atypical mycobacteria, bacterial pneumonia and lung abscesses (i.e. *Mycoplasma bovis*, *Pasteurella multocida*, *Trueprella pyogenes*, aspiration pneumonia), actinobacillosis, fungal diseases (zygomycosis, blastomycosis, aspergillosis, histoplasmosis, coccidioidomycosis), foreign body granuloma, traumatic pericarditis, bovine leukemia virus, and cestode cysts.[5,6,10] However, histologically, tuberculoid granulomas are usually easily distinguishable from all these conditions.

Diagnostic assays include direct tests for the identification of the agent, generally in postmortem specimens, such as microscopic examination, culture, immunohistochemistry, and molecular techniques.[6,18] Indirect tests are performed on specimens from live animals to detect infected individuals, and can be based on the cellular (intradermal tuberculin test, gamma-interferon test, and lymphocyte proliferation test) or humoral immunity (ELISA).[6.18]

Contributing Institution:
Plataforma de Investigación en Salud Animal
Instituto Nacional de Investigación Agropecuaria (INIA)
La Estanzuela, Uruguay
www.inia.uy

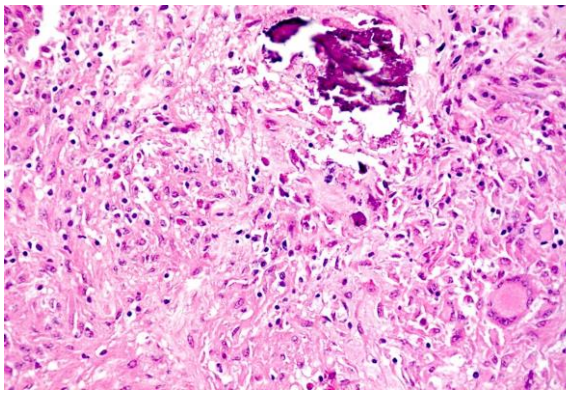

Figure 4-4. Liver, ox. There is infiltration by abundant macrophages that occasionally form multinucleated giant cells with peripherally located nuclei, and fewer lymphocytes, scattered mineralization, and fibrosis (Photo courtesy of: Nacional de Investigación Agropecuaria (INIA), Route 50, Kilometer 11, La Estanzuela, Colonia 70006, Uruguay). (HE, 400X)

JPC Diagnosis:
Liver: Granulomas, multifocal to coalescing, with bridging fibrosis.

JPC Comment:
As noted by the contributor, the classic lesion of tuberculosis is the tubercle, or tuberculous granuloma. Though a seemingly simple structure, the presence of a granuloma is the result of a complex sequence of inflammatory events requiring 1) the presence of an inciting agent with indigestible, poorly degradable, and persistent antigens, 2) a Th1 host immune response, and 3) an interplay between cytokines, chemokines, and other inflammatory mediators within the chronic inflammatory lesion.[1]

Granulomas are classically described as forming via a Type IV, cell-mediated hypersensitivity reaction. Sensitization occurs upon initial exposure to the antigen, which forms antigen-specific T memory lymphocytes. With chronic exposure, here enabled by the virulence factors that allow *Mycobacterium bovis* to live within macrophages

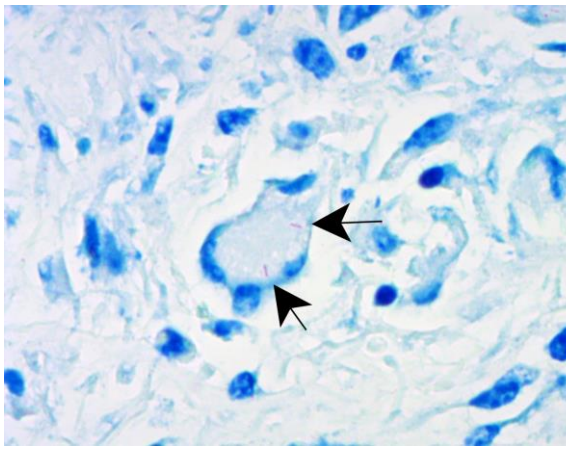

Figure 4-5. Liver, ox. Two ~2-µm long acid-fast bacilli (arrows) compatible with Mycobacterium bovis are present within the cytoplasm of a multinucleated giant cell. (Photo courtesy of: Nacional de Investigación Agropecuaria (INIA), Route 50, Kilometer 11, La Estanzuela, Colonia 70006, Uruguay). (Ziehl-Nielsen, 400X)

indefinitely, memory T lymphocytes recognize these persistent antigens presented in MHC II complexes by macrophages, and initiate a complex inflammatory sequence. Th1 lymphocytes secrete cytokines, such as TNF and IL-17, which recruit monocytes from the circulation to the site of inflammation. Once in the tissue, Th1-lymphocyte derived IFN-ɣ converts the monocytes to activated macrophages. The activated macrophages then secrete cytokines such as IL-12 which facilitate further development of Th1 lymphocytes.[15] Activated macrophages also elaborate IL-1 and TNF-α, both of which act to increase local expression of adhesion molecules on endothelial cells, thus recruiting more leukocytes to the inflammatory party. Meanwhile, Th1 lymphocytes secrete IL-2, which acts in an autocrine fashion to induce Th1 lymphocyte proliferation.[15]

The result of this persistent, Th1 lymphocyte-driven inflammation is the granuloma, which functions to wall off persistent antigenic stimuli from the rest of the body and is typically described as paucibacillary due to the few identifiable acid-fast bacteria. There are only a few conditions that are associated with the formation of granulomas, so their presence provides the astute pathologist with a radically pruned differential list.

In contrast to this nodular granulomatous morphology, certain mycobacterial conditions are associated with diffuse/lepromatous inflammation which is paradigmatically associated with a Th2 lymphocyte-predominant response. Lepromatous responses are poorly delineated, have a widespread distribution, abundant bacteria, relatively fewer lymphocytes, many macrophages, and lack a distinct capsule.[1]

In lepromatous immunological response, Th2 lymphocytes elaborate IL-4, IL-10, and TGF-β which inhibit the Th1 response and inactivate the microbicidal responses of macrophages, most notably iNOS. This facilitates the survival of the bacilli and shuts down the interplay between lymphocytes and macrophages that lead to granuloma formation.[13] The resulting diffuse granulomatous inflammation is seen in *Mycobacterium leprae* infection in humans and *Mycobacterium avium* subsp. *paratuberculosis* infection (Johne's disease) in cattle, sheep, and goats.[1]

This case rounds out this week's tour of classic entities with excellent examples of paradigmatic, Th1-driven tubercle formation. Conference participants felt the tubercles were so paradigmatic that a morphologic diagnosis of "granulomas" encapsulated a host of implied histologic features, including granulomatous inflammation, mineralization, necrosis, and concentric fibrosis. Conference participants discussed the striking bridging fibrosis and thought the consequent ischemia could account for the diffuse hepatocellular atrophy observed in less affected areas of the hepatic parenchyma.

References:

1. Ackermann MR. Inflammation and healing. In: Zachary JF, ed. *Pathologic Basis of Veterinary Disease*. 7th ed. Elsevier;2022:143-145.
2. Awada L, Tizzani P, Erlacher-Vindel E, Forcella S, Caceres P. Bovine tuberculosis: worldwide picture. In: *Bovine tuberculosis*. Wallingford, Oxfordshire, UK: CABI; 2018:1–15.
3. Azé J, Sola C, Zhang J, et al. Genomics and machine learning for taxonomy consensus: the mycobacterium tuberculosis complex paradigm. *PLoS One*. 2015;10 (7):e0130912.
4. Caswell JL, Williams KJ. Respiratory System. In: *Jubb, Kennedy and Palmer's Pathology of Domestic Animals*. 6th ed. Vol 2. Elsevier;2016:465-591.
5. Center for Food Security & Public Health (CFSPH). Zoonotic tuberculosis in mammals, including bovine and caprine tuberculosis. 2019.
6. Constable P, Hinchcliff K, Done S, Grünberg W. *Veterinary medicine: a textbook of the diseases of cattle, horses, sheep, pigs and goats*. 11th ed. Saunders Elsevier;2017:2015–2023.
7. Domingo M, Vidal E, Marco A. Pathology of bovine tuberculosis. *Res Vet Sci*. 2014;97(Supplement):S20–S29.
8. Kanipe C, Palmer MV. Mycobacterium bovis and you: A comprehensive look at the bacteria, its similarities to Mycobacterium tuberculosis, and its relationship with human disease. *Tuberculosis* (Edinb). 2020;125:1–28.
9. Menzies F, Neill S. Cattle-to-cattle transmission of bovine tuberculosis. *Vet J*. 2000;160:92–106.
10. Ortega J, Uzal FA, Walker R, et al. Zygomycotic lymphadenitis in slaughtered feedlot cattle. *Vet Pathol*. 2010;47(1): 108–115.
11. Palmer MV, Kanipe C, Boggiatto PM. The bovine tuberculoid granuloma. *Pathogens*. 2022;11(1).
12. Pesciaroli M, Alvarez J, Boniotti MB, et al. Tuberculosis in domestic animal species. *Res Vet Sci*. 2014;97(S):S78–S85.
13. Rodrigues de Sousa J, Sotto MN, and Quaresma JAS. Leprosy as a complex infection: breakdown of the Th1 and Th2 immune paradigm in the immunopathogenesis of disease. *Front Immunol*. 2017;8:1635.
14. Silveira AM, Nascimento EM, Konradt G, et al. Tuberculosis of the central nervous system in cattle in Paraíba, Brazil. *Pesqui Vet Bras*. 2018;38(11):2099–2108.
15. Snyder P. Diseases of Immunity. In: Zachary JF, ed. *Pathologic Basis of Veterinary Disease*. 7th ed. Elsevier; 2022:322-325.
16. Ünüvar S. Microbial foodborne diseases. *Foodborne Dis*. 2018;15:1–31.
17. Vilchèze C, Kremer L. Acid-fast positive and acid-fast negative mycobacterium tuberculosis: the Koch paradox. *Microbiol Spectr*. 2017;5(2).
18. World Organisation for Animal Health (OIE). Bovine tuberculosis. In: *OIE Terrestrial manual*. 8th ed. OIE;2018;1058-1074.

WSC 2023-2024
Conference 4 Self-Assessment

1. Unlike other clostridia, *Clostridium piliform* are gram-negative.
    a. True
    b. False

2. Which of the following is the most likely to demonstrate the full triad of intestinal, liver, and heart lesions in Tyzzer's disease
    a. Cows
    b. Horses
    c. Cats
    d. Rodents

3. Capillaria contortus can be found simultaneously in the crop and which of the following?
    a. Proventriculus
    b. Ventriculus
    c. Small intestine
    d. Cecum

4. Which is the preferred cell for infection with bovine leukosis virus?
    a. T-lymhocytes
    b. B-lymphocytes
    c. Dendritic cells
    d. M cells

5. The most common method of transmission *Mycobacterium bovis* in cattle is by?
    a. Ingestion
    b. Inhalation
    c. Wound infection
    d. Arthropod bite

Joint Pathology Center
Veterinary Pathology Services

WEDNESDAY SLIDE CONFERENCE 2023-2024

Conference #5 **20 September 2023**

CASE I:

Signalment:
3-year-old, female spayed domestic short hair, feline (*Felis catus*)

History:
This patient had a history of unspecified respiratory problems and presented to the referring veterinarian in an agonal state. Prior to presentation, the cat developed sudden breathing difficulties followed by collapse.

Gross Pathology:
Gross examination reveals a carcass with a body condition score of 4 out of 5, mild dehydration and mild autolysis. The lungs have a moderate, diffuse, cobblestone appearance and are meaty with patchy red to dark red discoloration. On section, a small amount of mucoid, pale yellow material can be expressed from many bronchioles. There is a large amount of this material in the bronchi and distal two thirds of the trachea.

Microscopic Description:
Lung: The pulmonary architecture is disrupted by widespread fibrosis affecting the axial interstitium and many alveolar septa, creating pseudolobulation with frequent multifocal alveolar emphysema ('honeycombing'). Multiple alveolar septa are lined by pleomorphic, commonly low columnar epithelial cells with reactive nuclei (alveolar epithelial metaplasia) and there is type II pneumocyte hyperplasia. There are scattered foci of smooth muscle hyperplasia intermixed with the fibrous connective tissue. Variable cellular infiltrates, consisting mostly of neutrophils and macrophages, are present in alveoli rimming obliterated bronchioles. Bronchioles are filled with mucus and tend to be either denuded or lined by a mix of cuboidal and squamous epithelium.

Contributor's Morphologic Diagnosis:
Lung: Severe, chronic, bronchointerstitial pneumonia with marked alveolar septal and interstitial fibrosis, emphysema, alveolar epithelial columnar metaplasia, type II pneumocyte hyperplasia, and cuboidal to squamous metaplasia of bronchiolar epithelium.

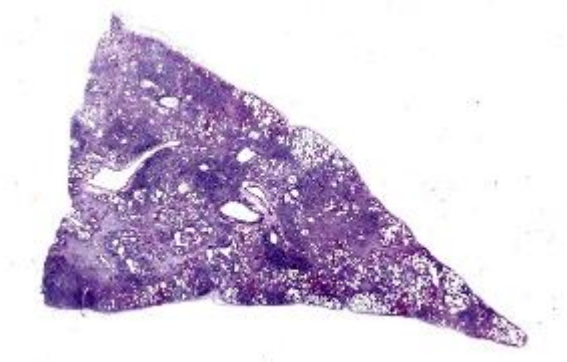

Figure 1-1. Lung, cat. In this section of lung, there is a nodularity to the parenchyma with areas of fibrosis and loss of architecture alternating with areas in which the alveolar septa are expanded and alveoli are variably ectatic ("honeycombing"). (HE, 6X)

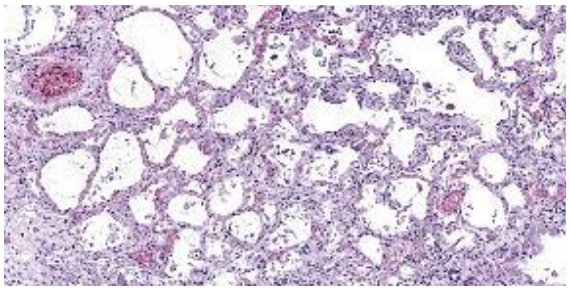

Figure 1-2. Lung, cat. Diffusely throughout the section, alveolar septa are expanded by collagen and fibroblasts, macrophages, and fewer neutrophils, and are often lined by type II pneumocytes. (HE, 121X)

Contributor's Comment:
The histologic appearance of the lung is consistent with feline idiopathic pulmonary fibrosis. Key histologic features of this uncommon condition as seen here include: 1) interstitial fibrosis with foci of fibroblast/myofibroblast proliferation, 2) columnar metaplasia of alveolar epithelium with type II pneumocyte hyperplasia (in some cases, mucous cell metaplasia is also common, but not seen in our case) and 3) smooth muscle hyperplasia/metaplasia.[1-3,5] This is similar to the histologic changes seen in idiopathic pulmonary fibrosis in humans.[5] This condition typically affects middle to older aged cats, although it has also been reported in cats under three years of age.[1-5] Presenting signs are largely respiratory related and include coughing, open mouth breathing, increased respiratory effort and rate, and respiratory distress.[1-5] Prognosis is usually poor and most individuals pass away within a year of presenting with respiratory signs despite treatment with steroids, bronchodilators, antibiotics and diuretics.[1-5] The cause for the condition is unknown, although a defect in type II pneumocyte development and function has been proposed.[1,5]

Contributing Institution:
Oregon State University
Corvallis, OR 97331
https://vetmed.oregonstate.edu/diagnostic

JPC Diagnosis:
Lung: Fibrosis, interstitial, diffuse, severe, with neutrophilic and histiocytic alveolitis, and smooth muscle and type II pneumocyte hyperplasia.

JPC Comment:
Feline idiopathic pulmonary fibrosis (FIPF) is one of several pulmonary diseases of veterinary importance that are characterized by fibrosis of the alveolar septa. Others include pulmonary fibrosis of West Highland Terriers, canine pulmonary fibrosis disease of unknown etiology, and equine multinodular pulmonary fibrosis, a helpfully named disease associated with equine herpesvirus-5.

As the contributor notes, the key histologic findings of FIPF include interstitial fibrosis with foci of fibroblasts or myofibroblasts, honeycombing of alveoli with alveolar epithelial metaplasia, and alveolar interstitial smooth muscle metaplasia.[1] These changes occur without a significant interstitial inflammatory infiltrate. The expansion of alveolar septa by fibrous connective tissue and smooth muscle leads to decreased pulmonary compliance, and the resulting pattern of respiratory distress is typically inspiratory or mixed inspiratory/expiratory. This distinguishes FIPF clinically from the more common bronchial-centered disorders in cats,

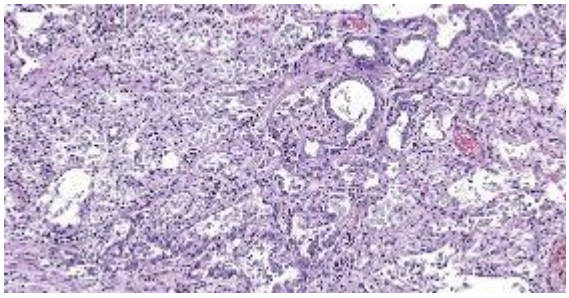

Figure 1-3. Lung, cat. Regionally, alveoli are lined by type II pneumocytes and contain large numbers of alveolar macrophages, fewer neutrophils, and cellular debris. (HE, 145X)

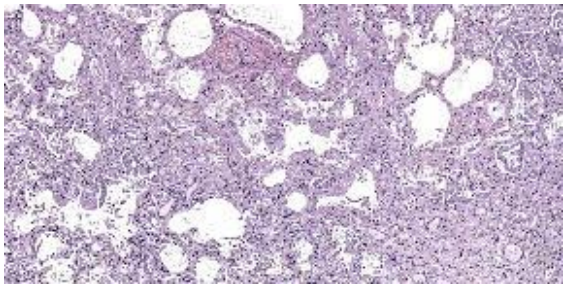

Figure 1-4. Lung, cat. Regionally, the fibrosis effaces alveolar architecture. (HE, 145X)

such as asthma and chronic bronchitis, which are characterized by expiratory distress.[1]

Definitive diagnosis of FIPF requires the demonstration of the previously described architectural and fibrous changes via histopathology. Published cases that include radiographic results report pronounced patchy to diffuse changes on thoracic radiographs, but the described changes are nonspecific and a mix of radiographic patterns has been described.[1-3] Bronchioalveolar lavage and fine needle aspirates can be used to rule out infectious causes for the clinical signs, but are unable to rule in a diagnosis of FIPF.[1]

While ante-mortem pulmonary biopsy can be useful for definitive diagnosis, care should be taken as up to 24% of cats in one study had concomitant pulmonary neoplasia, typically in areas of marked fibrosis.[1,4] This association is also seen in human cases of idiopathic pulmonary fibrosis, and when sampled as part of ante-mortem biopsy, pulmonary malignancy may complicate recognition of the concurrent FIPF which is often the primary cause of respiratory symptoms.[1,4]

Standard empiric therapies for feline respiratory disease, such as corticosteroids, rarely result in clinical improvement of FIPF patients, and a robust understanding of the disease pathogenesis is needed before therapeutic targets can be identified. Future treatments are likely to be focused on pharmacologic modulation of fibroblast-pulmonary parenchymal cell interactions, including TGF-β antagonists, inhibition of collagen-synthesis enzymes, and matrix metalloproteinase activity enhancement.[1]

This week's conference was moderated by MAJ Alicia Moreau, Chief of Education and Training and the Joint Pathology Center. MAJ Moreau discussed the terminology used to describe this condition in the veterinary literature. Of particular interest was the use of the term "alveolar epithelial metaplasia," which is often used as a key histologic feature of this entity. Participants felt this term was inconsistently or rarely defined in the literature, but in practice is often used to mean type II pneumocyte hyperplasia. Similar inconsistencies were noted with the term "honeycombing," which is defined differently depending on the source; however, most definitions contemplate confluent airspaces lined by cuboidal or hyperplastic epithelium and surrounded by fibrosis.

Conference participants felt that the defining histologic characteristic of this condition was the abundant fibrosis. Consequently, the JPC morphologic diagnosis leads with fibrosis while still acknowledging the mild inflammatory infiltrates present within the alveoli.

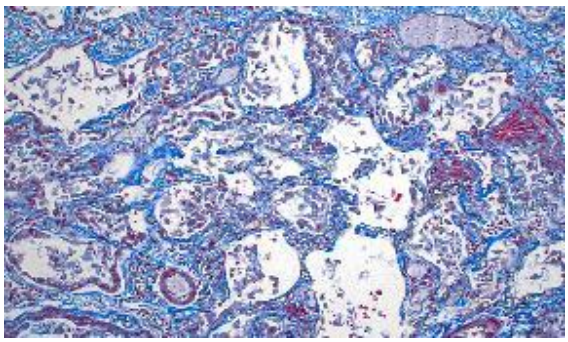

Figure 1-5. Lung, cat. A Masson's trichrome demonstrates the extent of the fibrosis in the section. (HE, 145X)

References:
1. Cohn LA, Norris CR, Hawkins EC, et al. Identification and characterization of an idiopathic pulmonary fibrosis-like condition in cats. *J Vet Intern Med*. 2004; 18(5):632-41.
2. Evola MG, Edmondson EF, Reichle JK, et al. Radiographic and histopathologic characteristics of pulmonary fibrosis in nine cats. *Vet Radiol Ultrasound*. 2014; 55(2):133-140.
3. Le Boedec K, Roady PJ, O'Brien RT. A case of atypical diffuse feline fibrotic lung disease. *J Feline Med Surg*. 2014; 16(10):858-863.
4. Reinero C. Interstitial lung diseases in dogs and cats part I: the idiopathic interstitial pneumonias. *Vet J*. 2019; 243: 48-54.
5. Williams K, Malarkey D, Cohn L, et al. Identification of spontaneous feline idiopathic pulmonary fibrosis: morphology and ultrastructural evidence for a type II pneumocyte defect. *Chest*. 2004; 125(6): 2278-2288.

CASE II:

Signalment:
4-year-old, male neutered Borzoi, canine (*Canis lupus familiaris*)

History:
The patient presented for unlocalized pain and frequent episodes of vocalization and was diagnosed with discospondylitis of the L3-L4 vertebrae. Surgical stabilization was performed and the dog was discharged with pain relief and empirical antibiotics. After initial improvement, the dog started to display pain and developed polyuria. Radiographs revealed a lytic lesion at the C4-C5 region. Azotemia with proteinuria developed, and cytological examination of the urine revealed

Figure 2-1. Kidney, dog. Enlargement of the right kidney with multifocal, 4-6 mm, white plaques on the cortical surface (fungal granulomas), and variably sized areas of hemorrhage. (Photo courtesy of: Massey University School of Veterinary Science, https://www.massey.ac.nz/about/colleges-schools-and-institutes/college-of-sciences/school-of-veterinary-science/)

numerous fungal hyphae. Culture of blood and urine was positive for *Rasamsonia (Geosmithia) argillacea*. Itraconazole therapy was implemented, but the patient declined rapidly and was euthanized.

Gross Pathology:
The patient was in a fresh state of preservation and poor body condition (BCS 2/9; total body weight 19kg), with generalised muscular atrophy and severe dehydration. Gross examination revealed enlargement of the right kidney with multifocal 4-6mm white plaques on the cortical surface interspersed with multifocal, variably sized areas of hemorrhage. There was severe bilateral pyelonephritis, with pyonephrosis of the right kidney. Multiple raised, pale, variably sized nodules were present in the splenic parenchyma and in two mesenteric lymph nodes. There was discospondylitis of the lumbar spine at the L3-L4 junction, and osteomyelitis of the cervical spine at the C4-C5 region. The lungs appeared normal and no other abnormalities were noted.

Figure 2-2. Kidney, dog. Severe bilateral pyelonephritis, with pyonephrosis of the right kidney. (Photo courtesy of: Massey University School of Veterinary Science)

Laboratory Results:
Rasamsonia (Geosmithia) argillacea was cultured from urine and blood.

Microscopic Description:
Kidney: Multifocally throughout the cortex, glomeruli and tubules are surrounded and replaced by numerous fibroblasts and abundant eosinophilic collagen bundles (interstitial fibrosis). Tubular epithelial changes include marked epithelial degeneration and necrosis characterized by swollen, vacuolated epithelial cells and shrunken hypereosinophilic, pyknotic cells, respectively. Deeply basophilic granular material (mineral), or bright eosinophilic homogenous material (protein) is present within the lumen of many tubules. Multifocally within the cortex are large aggregates of macrophages, lymphocytes, and plasma cells which surround large regions of amorphous eosinophilic material (fibrin), cellular debris, and 5-10µm diameter, fine, parallel walled, occasionally branching, septate hyphae and 5-7µm diameter conidia. These frequently appear adjacent to arcuate arteries and veins, with numerous PAS positive hyphae disrupting and invading the endothelium (angioinvasion) with marked endothelial necrosis characterized by shrunken, hypereosinophilic pyknotic cells, and destruction of the adventitia and tunica media. Within the renal pelvis, a large area of amphophilic necrotic debris is admixed with abundant PAS positive fungal hyphae and conidia. Multifocally throughout the cortex and medulla there are interstitial aggregates of lymphocytes and plasma cells.

Similar granulomatous inflammation, with PAS-positive fungal hyphae and conidia, is present within the mesenteric lymph nodes, spleen, and lumbar vertebral segment (not submitted).

Contributor's Morphologic Diagnoses:
1. Kidney: Nephritis, interstitial, granulomatous, chronic, multifocal, severe, with numerous PAS positive fungal hyphae and conidia, angioinvasion and marked interstitial fibrosis with cortical tubular degeneration and necrosis, acute, multifocal, marked.
2. Kidney: Pyelonephritis, chronic, granulomatous, with numerous PAS positive fungal hyphae and conidia.

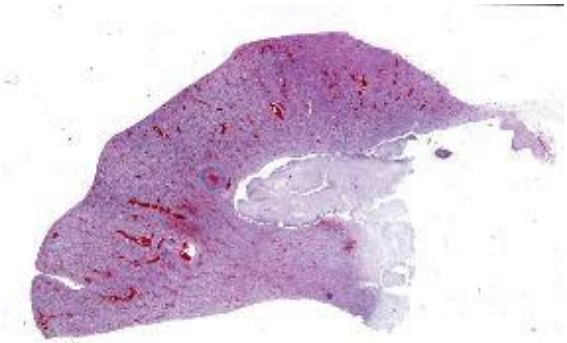

Figure 2-3. Kidney, dog. At subgross magnification, a large mat of fungus expands the renal pelvis, there are multiple chronic infarcts with flattening of the subcapsular surface, and cellular infiltrates around the arcuate arteries. (HE, 5X)

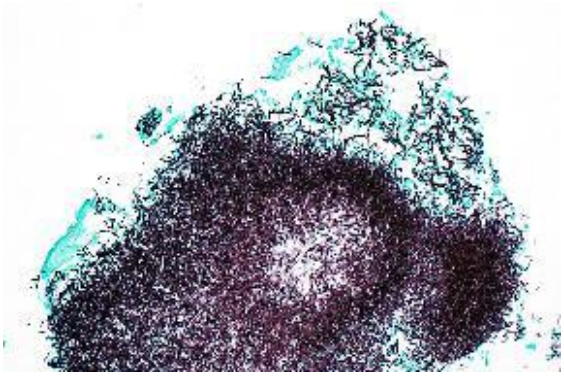

Figure 2-4. Kidney, dog. A GMS stain demonstrates a large mat of fungal hyphae within the renal pelvis. (GMS, 100X)

Contributor's Comment:

Here we present a case of disseminated systemic fungal infection with *Rasamsonia argillacea.* Fungal pyelonephritis with systemic dissemination is an uncommon clinical presentation in dogs, with the most common fungal isolate in canine pyelonephritis being *Aspergillus* spp., with *A. terreus* and *A. reflectus* the most frequently reported species.[2,4,8] *Cryptococcus* spp., *Candida* spp., *Penicillium* spp., *Paecilomyces* spp., *Sagenomella* spp., as well as systemic phaeohyphomycosis, are less commonly reported.[1,5]

In dogs, disseminated mycoses can clinically manifest as weight loss, lethargy, discospondylitis, osteomyelitis, urinary tract infections, polyuria, polydipsia, ophthalmitis, head tilt and gait difficulties.[4]

Rasamsonia is a recently described genus of saprobic thermotolerant fungal organisms of the Trichocomaceae family.[3] These are nonpigmented filamentous fungi and include four species that share phenotypic and genetic similarities: *R. argillacea, R. eburnean, R. piperina,* and *R. aegroticola.*[3] These fungi were previously classified as *Geosmithia* and *Talaromyces,* however recent studies reclassified the fungus as *Rasamsonia* based on genetic sequencing.[6,7]

The first case of disseminated *Rasamsonia* (referred to as *Geosmithia argillacea*) in humans or animals was reported in a German Shepherd.[5] German Shepherds appear overrepresented, perhaps owing to their susceptibility to disseminated fungal disease, particularly with *Aspergillus* spp.[2,9] IgA deficiency has been suggested as a possible predisposing factor for disseminated aspergillosis in this breed.[11,10] Other factors that may contribute to the German Shepherd's susceptibility to systemic fungal mycoses include depressed IgM responses or impaired mitogen-induced lymphocyte transformation.[11] In regard to *R. argillacea* infection, one study reported that five of eight dogs with *R. argillacea* were German Shepherds and six were spayed females.[3]

To our knowledge this is the first report of *Rasamsonia (Geosmithia) argillacea* causing disseminated disease in a dog in New Zealand or Australia. Due to the scant number of reported cases, the pathogenesis of *R. argillacea* infection is not well established. In most cases of systemic fungal mycoses, the portal of entry is usually unknown.[4] The most common portal of entry for fungal infections is the respiratory tract via inhalation, which then allows systemic spread after an initial respiratory infection.[4] Based on studies involving *Aspergillus* spp., the cycle begins with deposition of fungal conidia from the environment in the respiratory system.[4] Fungal species such as *Paecilomyces* spp. have also been reported to produce *in vivo* conidia, and these, along with the secondary spores produced, facilitate hematogenous spread.[4]

The portal of entry could not be identified in this case, which is consistent with the reported literature.[4] The presenting complaint of lumbar spinal pain with discospondylitis was the first indication of any clinical disease in this dog. The dog had a prior bout of suspected kennel cough, but this was over 12

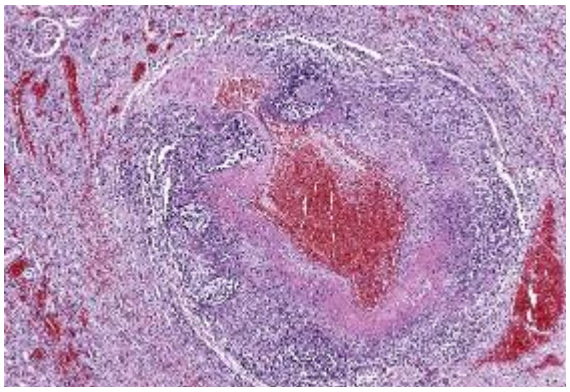

Figure 2-5. Kidney, dog. There is necrotizing arteritis of the arcuate arteries with extrusion of abundant pink proteinaceous material into the media and innumerable necrotic neutrophils in the media and adventitia. (HE, 62X)

months prior to the presentation of lumbar spinal pain, so perhaps this is where the initial infection was acquired. It is also possible that the infection was first acquired via the urinary tract, which then lead to pyelonephritis and systemic spread. Primary fungal pyelonephritis in dogs is only rarely reported.[5] In one case report, unilateral pyelonephritis was reported, with no evidence of systemic spread, indicating a possible ascending infection from the urinary tract.[5] In another case report, a primary fungal granuloma with *Paecilomyces variotii*, with no other evidence of systemic involvement was reported.[10] In both studies the primary route of entry could not be identified. It has also been suggested that immunosuppression due to other pathological conditions or immunosuppressive therapy may play a role.[4]

The gross and histological lesions in this case are astounding, with numerous fungal hyphae, granulomatous inflammation, angioinvasion and multinucleated giant cells within multiple organs. *Rasamsonia argillacea* appears to be an emerging pathogen in both human and animal medicine.[3] With the increasing reports in dogs, more research is needed to help further characterize *Rasamsonia* infections and to optimize diagnosis and treatment to improve overall prognosis.

Contributing Institution:
School of Veterinary Science
Massey University
Palmerston, North New Zealand 4442

JPC Diagnosis:
Kidney: Pyelonephritis, necrotizing and suppurative, focally extensive, severe, with fibrinous and necrotizing arteritis, multiple infarcts, and innumerable fungal hyphae.

JPC Comment:
The contributor provides an excellent overview of *Rasamsonia* infection in dogs. Though case reports are scarce, recent reports suggest that disseminated *Rasamsonia* infections commonly cause lesions in the spinal column, central nervous system, kidneys, spleen, lymph nodes, lungs, and heart.[3] *Rasamsonia* is considered an emerging pathogen, though it is frequently misidentified as *Penicillium* and *Paecilomyces* spp. based on morphologic similarities, and the apparent increase in incidence may be due, in part, to increased use of more accurate molecular speciation techniques in recent years.

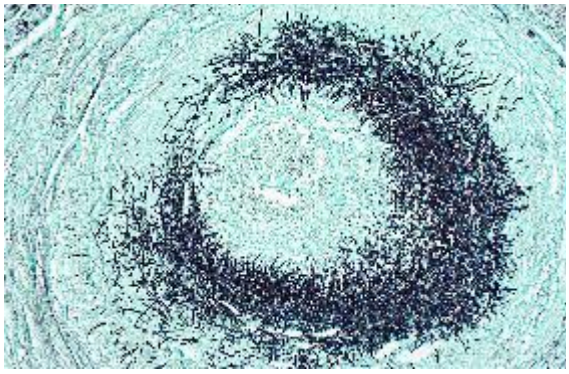

Figure 2-6. Kidney, dog. A GMS stain demonstrates numerous fungal hyphae in the necrotic arcuate arterial wall. (HE, 100X)

This case is typical, in that the presenting complaint is often spinal pain due to *Rasamsonia* discospondylitis. Imaging studies of these patients typically reveal sclerotic and lytic vertebral lesions, most commonly in the thoracic spine.[3] These radiographic findings are similar to those in the relatively more common condition of disseminated aspergillosis, where approximately half of affected dogs show radiographic signs of discospondylitis.[9] Treatment in these cases is generally unsuccessful due to fungal resistance to available antifungal medications and the questionable ability of these medications to penetrate all affected tissues.[5]

In conference, discussion centered on the acute versus chronic nature of the observed histologic lesions. Large confluent areas of coagulative necrosis are present adjacent to the renal pelvis and in wedges extending from the medulla to the cortex. There are also extensive areas of fibrosis which represent more chronic insults arising from the damage to the arcuate arteries. Discussion also focused on the morphology of the dazzling fungal hyphae present in the renal pelvis and in arterial walls. Participants discussed differentials, including *Candida* spp. and *Penicillium* spp., and the need for fungal culture to identify the organism definitively.

References:

1. Day M, Holt P. Unilateral fungal pyelonephritis in a dog. *Vet Pathol*. 1994;31: 250-252.
2. Day M, Penhale W. An immunohistochemical study of canine disseminated aspergillosis. *Aus Vet J*. 1991;68:383-386.
3. Dear JD, Reagan KL, Hulsebosch SE, et al. Disseminated *Rasamsonia argillacea* species complex infections in 8 dogs. *J of Vet Int Med*. 2021;35:2232-2240.
4. Elad D. Disseminated canine mold infections. *Vet J*. 2019;243:82-90.
5. Grant DC, Sutton DA, Sandberg CA, et al. Disseminated *Geosmithia argillacea* infection in a German shepherd dog. *Med Mycol*. 2009;47:221-226.
6. Houbraken J, Giraud S, Meijer M, et al. Taxonomy and antifungal susceptibility of clinically important *Rasamsonia* species. *J of Clin Microbiol*. 2013;51:22-30.
7. Houbraken J, Spierenburg H, Frisvad JC. Rasamsonia, a new genus comprising thermotolerant and thermophilic *Talaromyces* and *Geosmithia* species. *Antonie Van Leeuwenhoek*. 2012;101:403-421.
8. Jang S, Dorr T, Biberstein E, Wong A. *Aspergillus deflectus* infection in four dogs. *J of Med and Vet Mycol*. 1986;24: 95-104.
9. Schultz RM, Johnson EG, Wisner ER, et al. Clinicopathologic and diagnostic imaging characteristics of systemic aspergillosis in 30 dogs. *J of Vet Int Med*. 2008;22:851-859.
10. Tappin S, Ferrandis I, Jakovljevic S, Villiers E, White R. Successful treatment of bilateral paecilomyces pyelonephritis in a German shepherd dog. *J of Small Ani Prac*. 2012;53:657-660.
11. Zhang S, Corapi W, Quist E, Griffin S, Zhang M. Aspergillus versicolor, a new causative agent of canine disseminated aspergillosis. *J of Clin Microbiol*. 2012;50: 187-191.

CASE III:

Signalment:

11-year-old, male intact common marmoset, primate (*Callithrix jacchus*)

History:

This male marmoset's clinical history included significant weight loss, poor body condition, chronic intermittent diarrhea, and progressive reticulocytosis, thrombocytosis, and hypoalbuminemia. Diagnostic evaluation ruled out infection by *Giardia* spp.,

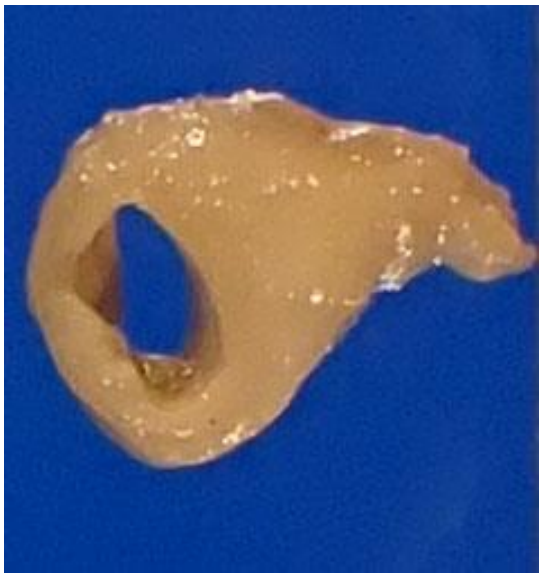

Figure 3-1. Duodenum, common marmoset. The small intestine from the level of the pylorus and extending distally 8cm was pale and thickened, measuring up to 7mm on cross section. (Photo courtesy of: Johns Hopkins University, Department of Molecular and Comparative Pathobiology, https://mcp.bs.jhmi.edu/)

Klebsiella pneumoniae, *Campylobacter coli*, *C. jejuni*, *Salmonella* spp., and *Shigella* spp., and revealed two biotypes of *E. coli* on fecal culture. Late in the disease course, there was radiographic evidence of an expansile lesion of the left patella. Treatment with nutritional support, antimicrobials, and immunomodulatory medications yielded minimal and transient improvement.

Gross Pathology:
Gross postmortem evaluation demonstrated little to no subcutaneous, visceral, or perirenal adipose tissue. Within all lung lobes were innumerable coalescing, firm, tan nodules, measuring up to 4 mm in diameter. The small intestine from the level of the pylorus and extending distally 8 cm was paler than the more normal, aborad, intestine. There was transmural thickening of the proximal duodenum, measuring up to 7 mm on cross section.

Laboratory Results:
Significant clinical pathology values: thrombocytosis (1,042 k/µL) and hypoalbuminemia (2.9 g/dL).

Microscopic Description:
Effacing and replacing approximately 75-80% of the pulmonary parenchyma are multiple neoplastic masses that are moderately well-demarcated, nonencapsulated, moderately cellular, and highly infiltrative. Neoplastic cells are arranged in a lepidic growth pattern along pre-existing alveolar septa and also form disorganized acini and clusters. Alveoli are expanded by lakes of mucin with paucicellular neoplastic cells aligned along remnant alveolar septa. Neoplastic cells are round to polygonal with variably distinct cell borders and frequently exhibit large intracytoplasmic clear vacuoles which marginate the nucleus (signet ring cells).

The nuclei contain one to three variably prominent eccentric nucleoli. The remainder of the cytoplasm is granular and moderately to deeply basophilic. Anisocytosis and anisokaryosis are moderate, and mitoses are rarely observed. Neoplastic cells are frequently clustered around medium sized vessels and

Figure 3-2. Lungs, common marmoset. Numerous nodules are present within all lung lobes, measuring up to 4mm. (Photo courtesy of: Johns Hopkins University, Department of Molecular and Comparative Pathobiology)

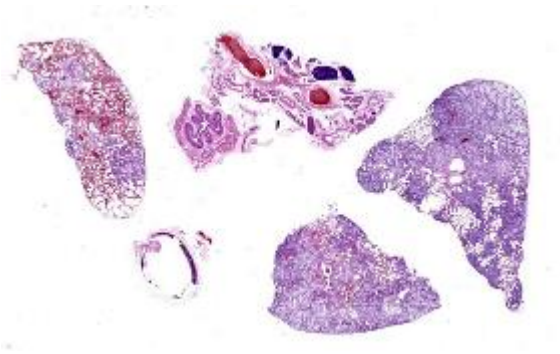

Figure 3-3. Lung, common marmoset. At subgross magnification, coalescing nodules of neoplasia are present within all cross-sections of lung. (Photo courtesy of: Johns Hopkins University, Department of Molecular and Comparative Pathobiology)(HE, 2x)

expand and disrupt the tunica media and adventitia**.** There is moderate infiltration of neoplastic foci and alveoli with large foamy alveolar macrophages containing mucin and fewer lymphocytes. Alveoli frequently contain small amounts of eosinophilic proteinaceous fluid (edema) and fibrin. Alveolar septa are expanded in multiple areas by neoplastic cells, collagen fibers, edema, and inflammatory cells including lymphocytes and macrophages.

Contributor's Morphologic Diagnosis:
Lung: Metastatic duodenal mucinous adenocarcinoma.

Contributor's Comment:
This marmoset was euthanized following chronic clinical decompensation that was unresponsive to medical management. The clinical differential diagnoses in this case included Marmoset Wasting Syndrome (MWS), infectious enteropathies, and enteric neoplasia due to the thin body condition, diarrhea, bony lesions, and progressive hypoalbuminemia. Proximal duodenal mucinous adenocarcinoma with both local invasion and distant metastasis was diagnosed in this case, and wasting was attributable to chronic neoplastic and inflammatory changes of the intestine which likely impaired absorption and resulted in malnourishment.

Reports of small intestinal adenocarcinomas are uncommon in the gastrointestinal tract of aged nonhuman primates despite those of the large intestine being among the most frequently observed.[1,2,8,9] One limited case series and infrequent case reports have documented small intestinal adenocarcinomas in the marmoset.[1,3]
In marmosets, small intestinal adenocarcinomas typically begin as carcinomas *in situ* at the level of the jejunum or ileum before infiltrating the intestinal wall, and histology often demonstrates signet ring morphology and mucinous matrix.[3,4] Local invasion and metastasis to mesenteric lymph nodes were reported in 6/10 cases of marmoset small intestinal adenocarcinoma, but distant metastases were not noted.[3]

The proximal duodenal localization in this case is atypical, as is the extensive metastatic disease. In this case, metastases were noted in the lungs, liver, and parapatellar adipose.[6] Additionally, the primary tumor and all metastases demonstrated absent to attenuated expression of pancytokeratin, indicating active neoplastic epithelial-mesenchymal tran-

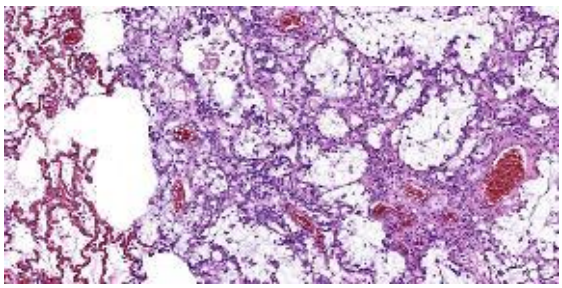

Figure 3-4. Lung, common marmoset. Neoplastic epithelial cells are present in nests and poorly formed glands and line alveolar septa. Alveolar lumina are often filled with mucin. (Photo courtesy of: Johns Hopkins University, Department of Molecular and Comparative Pathobiology) (HE, 131X)

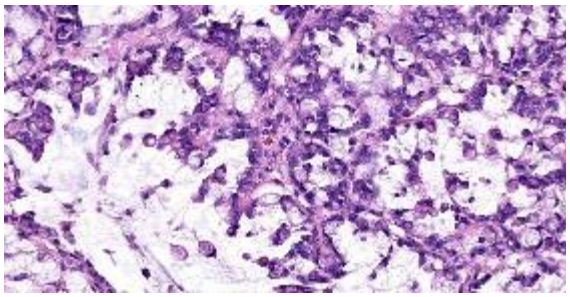

Figure 3-5. Lung, common marmoset. High magnification of neoplastic cells with abundant cytoplasmic mucus. (Photo courtesy of: Johns Hopkins University, Department of Molecular and Comparative Pathobiology) (HE, 131X)

sition and suggesting a poorer prognosis.[6] This case highlights the importance of considering infiltrative adenocarcinoma as a differential in captive marmosets exhibiting refractory weight loss and diarrhea.

Contributing Institution:
Johns Hopkins University
Department of Molecular and Comparative Pathobiology
Baltimore, MD 21230
https://mcp.bs.jhmi.edu/

JPC Diagnosis:
Lung: Mucinous adenocarcinoma, metastatic.

JPC Comment:
Adenocarcinomas arising in the small and large intestines of marmosets are rare and are thought to share a similar pathogenesis: dysregulation of the Wnt/ β-catenin signaling pathway.[4] This pathway is an evolutionarily conserved signaling cascade that regulates myriad cellular processes, including cell proliferation, differentiation, and apoptosis.[7] Under normal homeostatic conditions, β-catenin is subject to constitutive phosphorylation mediated by a complex of proteins, including the tumor suppressor gene product adenomatous poliposis coli (APC). The phosphorylation of β-catenin leads to its ubiquitination and subsequent proteosomal degradation, and prevents its accumulation in the cytosol.[7]

The activation of the canonical Wnt/ β-catenin pathway begins with the binding of the signaling ligand Wnt to Frizzled receptors at the plasma membrane. This binding recruits a variety of intracellular signaling proteins, including Disheveled and the APC complex, to the Frizzled receptor and inhibits the constitutive phosphorylation of β-catenin. Released from inhibition, β-catenin then accumulates in the cytosol, translocates to the nucleus, and activates Wnt-dependent gene expression.[7] In human colorectal cancers, this signaling sequence is most commonly perturbed by loss-of-function mutations in APC, leading to loss of β-catenin phosphorylation and degradation and, consequently, to unchecked cellular proliferation.

β-catenin also exerts influence outside of the Wnt signaling pathway through its interactions with cadherins, transmembrane proteins that mediate cell adhesion by linking the actin cytoskeletons of neighboring cells. β-catenin binds to the cytosolic domains of cadherins and stabilizes these normal cell to cell anchoring interactions. An increase in cytosolic β-catenin upsets this balance and can result in loss of cohesion among cells, a necessary precondition for metastasis.[4]

Though similar oncogenic mechanisms are at work throughout the intestinal tract, adenocarcinomas are far more likely to arise in the large intestine than in the small intestine.

Factors currently thought to account for this disparity include: the faster transit time of digesta through the small intestine which decreases exposure to toxins when compared to the large intestine; the higher levels of IgA and mucosal-associated lymphoid tissue providing immune surveillance in the small

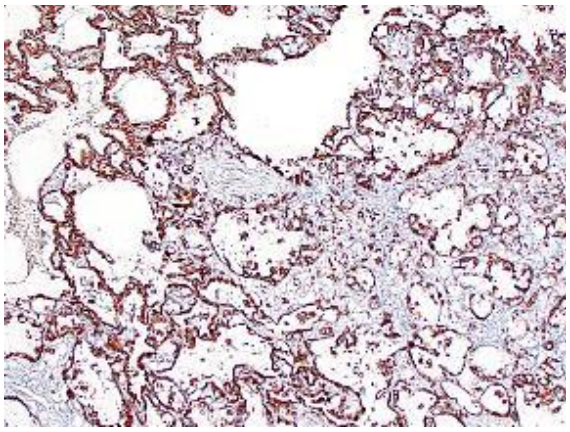

Figure 3-6. Lung, common marmoset. Neoplastic cells demonstrate strong cytoplasmic positivity for cytokeratin. (anti-AE1/AE3, 100X)

intestine; and the increased distance between small intestinal crypt stem cells and the intestinal lumen which decreases exposure to luminal carcinogens.[4]

This case provoked a robust discussion among conference participants, several of whom felt they could not definitively rule out a primary pulmonary origin for this tumor. Immunohistochemical stains for TTF-1 and AE1/AE3 were examined during conference and largely served to confound. Though the contributor reported absent or attenuated pan-cytokeratin immunoreactivity, AE1/AE3 staining performed at the Joint Pathology Center revealed diffuse, strong cytoplasmic reactivity within the neoplastic cell population (Fig 3-6). The neoplastic cells were diffusely negative for TTF-1, a marker of primary pulmonary adenocarcinoma; however, there are case reports of TTF-1 negative primary pulmonary mucinous adenocarcinomas, including one recent case report in a marmoset.[5] Ultimately, the morphology of the tumor and the multifocal distribution in the lungs convinced participants that the tumor represented metastatic disease. Participants also briefly discussed the signet ring cells found through this section. Though interesting, signet ring cell morphology can also be found in melanomas and squamous cell carcinomas, among other tumors, and has no known prognostic significance.

References:

1. Brack M. Gastrointestinal tumors observed in nonhuman primates at the German primate center. *J Med Primatol*. 1998;27:319–324.
2. Johnson LD, Ausman LM, Sehgal PK, King NW. A prospective study of the epidemiology of colitis and colon cancer in cotton-top tamarins (Saguinus oedipus). *Gastroenterology*. 1996;110(1):102–115.
3. Miller AD, Kramer JA, Lin KC, Knight H, Martinot A, Mansfield KG. Small intestinal adenocarcinoma in common marmosets (Callithrix jacchus). *Vet Pathol*. 2010;47(5):969-976.
4. Miller AD. Chapter 18 - Neoplastic Diseases. In: Marini R, Wachtman L, Tardif S, Mansfield K, Fox J, eds. *The Common Marmoset in Captivity and Biomedical Research*. Academic Press 2019:305-309.
5. Mineshige T, Inoue T, Kawai K, et al. Spontaneous pulmonary adenocarcinoma in a common marmoset (*Callithrix jacchus*). *J Med Primatol.* 2021;50:335-338.
6. Peterson C, Plunkard J, Johanson A, Izzi J, Gabrielson K. Immunohistochemical characterization of a duodenal adenocarcinoma with pulmonary, hepatic and parapatellar metastases in a common marmoset (Callithrix jacchus). *J Comp Pathol*. 2021;189:1–7.
7. Silva-Garcia O, Valdez-Alarcón JJ, Baizabal-Aguirre VM. Wnt/β-catenin signaling as a molecular target by pathogenic bacteria. *Front. Immunol*. 2019;10:1-14.
8. Simmons HA, Mattison JA. The incidence of spontaneous neoplasia in two populations of captive rhesus macaques

(Macaca mulatta). *Antioxid Redox Signal*. 2011;14(2):221–227.
9. Valverde CR, Tarara RP, Griffey SM, Roberts JA. Spontaneous intestinal adenocarcinoma in geriatric macaques (Macaca sp.). *Comp Med*. 2000;50(5): 540-544.

CASE IV:

Signalment:
12-day-old, Charolais bull, bovine (*Bos taurus*)

History:
The calf was unwell for 1 week and unable to suck with no response to antibiotic treatment. Only one calf was affected.

Gross Pathology:
The patient weighed 50 kg and was in age-appropriate body condition. Bilaterally the kidneys were tan-grey with an uneven subcapsular surface featuring multifocal pinpoint indentations. The calyces were oedematous.

Laboratory Results:
Urinalysis: Glucose = 14mml/l; Specific Gravity = 1.030; Protein = 2g/l; pH = 6; moderate number of nitrates; no leucocytes, urobilinogen, or RBCs.

Liver selenium: 71.50 umol/kg (normal range =5-20 umol/kg).

Zinc Sulphate Turbidity: Adequate colostral immunity.

Microscopic Description:
Kidney: The cortex is diffusely and markedly disrupted by large numbers of cystic spaces up to 120 um in diameter lined by a monolayer of cuboidal epithelium that is multifocally exfoliated and floating freely within these cystic lumens (autolysis). These cysts are separated by a large amount of fibro-myxoid, oedematous stroma that is composed of collagen bundles and plump fibroblasts. Multifocally, and predominantly within the cortex, are variably sized areas that exhibit pale eosinophilic, glassy, loose stroma with scattered stellate cells (primitive mesenchyme). Multifocally the glomeruli are small and mildly to moderately hypercellular with occasionally mildly thickened Bowman's capsules. Multifocally some glomeruli are irregularly lobulated. Multifocally the cortical tubules exhibit a small amount of luminal radiating achromatic crystalline material that is birefringent under polarized light (calcium oxalate crystals). Multifocally some of the cortical tubular epithelium exhibits a small amount of yellow, globular intracytoplasmic pigment. Multifocally medullary tubules exhibit dark basophilic epithelium that occasionally undergoes 'piling up.' Multifocally lumens within the medulla exhibit a small amount of eosinophilic, homogenous to glassy material (protein casts). Very rarely some of the tubules at the cortico-medullary junction exhibit ciliated epithelium

Figure 4-1. Kidney, calf. Bilaterally the kidneys were tan-grey with an uneven subcapsular surface featuring multifocal pinpoint indentations. The calyces were oedematous. (Photo courtesy of: Veterinary Sciences Centre, School of Veterinary Medicine, University College Dublin, Belfield, Dublin 4, Ireland, http://www .ucd.ie/vetmed/)

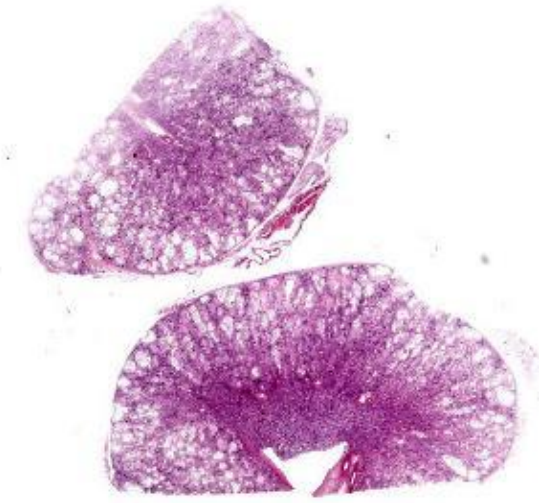

Figure 4-2. Kidney, calf. There is marked loss of tubules and remaining tubules are markedly ectatic. There are linear rays of fibrosis extending downward into the medulla which contain numerous fetal glomeruli and few sclerotic tubules. (HE, 27X)

(persistent mesonephric ducts). Multifocally interstitial blood vessels exhibit mildly thickened tunica media. Multifocally the stroma is infiltrated by small to moderate numbers of lymphocytes and plasma-cells (interstitial nephritis).

Contributor's Morphologic Diagnoses:

1. Kidney: Asynchronous maturation, interstitial fibrosis, with fetal glomeruli, immature tubules, primitive mesenchyme, persistent metanephric ducts, consistent with renal dysplasia.
2. Kidney: Lymphoplasmacytic nephritis, chronic, mild.

Contributor's Comment:

Renal dysplasia is defined as disorganised development of renal parenchyma due to anomalous differentiation and has been described in numerous species including humans, sheep, pigs, cats, horses and, most frequently, dogs.[2,11] The cause(s) of renal dysplasia are not well understood but are likely to be multifactorial and in some cases are considered congenital.[2] Proposed causes include genetic mechanisms, as well as in-utero infections and deficiencies affecting fetal development. Renal dysplasia has been identified in multiple dog breeds including the Golden Retriever, Beagle, Lhasa Apso, Great Dane, Dutch Kooiker dog, Samoyed, Alaskan Malamute, Cavalier King Charles Spaniel and Bulldog.[1,7,11,13] Renal dysplasia with hepatic fibrosis was described in Norwich terriers with INPP5E splice site variant causing lethal ciliopathy.[3] Examples of fetal infections resulting in renal dysplasia include panleukopenia virus in cats, canine herpes virus in dogs and BVDV infection in cattle.[10] In pigs, hypovitaminosis A is considered a cause of renal dysplasia.[2]

The gross presentation of the kidneys of affected animals varies, but affected kidneys are usually small, misshapen, fibrosed, and feature multiple cysts and tortuous ureters. One or both kidneys may be affected in an individual. In some cases, dysplastic kidneys show only minimal gross changes, such as having a slightly irregular contour.[2] The histopathological criteria to achieve a diagnosis of renal dysplasia include:

1. The presence of anomalous or undeveloped structures;
2. The presence of undifferentiated mesenchyme in the cortex or medulla;
3. Groups of immature glomeruli in non-neonatal animals;
4. Lack of glomeruli or tubules in some lobes of the kidneys;
5. Collecting tubules with blind ends within cortical connective tissue;
6. Atypical tubular epithelium;
7. The presence of primitive (metanephric) ducts lined by cuboidal or columnar epithelium; and

8. Dysontogenic (cartilaginous or osseous) metaplasia, mainly seen in humans.[2]

Because ureteral anomalies are often present in cases of renal dysplasia, dysplastic kidneys are also highly susceptible to developing pyelonephritis. Various forms of renal dysplasia and nephropathy have been described in ruminants, including: renal dysplasia in Japanese black cattle;[12] autosomal dominant cystic renal dysplasia in Suffolk sheep;[8] renal dysplasia with hydronephrosis and congenital ureteral strictures of unknown cause in two Holstein-Friesian calves;[15] immune mediated mesangiocapillary glomerulonephritis in Finnish Landrace lambs (cause unknown but thought to represent a recessive, inherited defect of the complement system);[5] nephropathy in Japanese black cattle caused by a claudin 16 gene deletion mutation;[6] and familial glomerulopathy and peripheral neuropathy in Gelbvieh cattle.[9]

The cause of the renal dysplasia in the case presented here remains unknown. Both calf and dam were negative for BVDV and no abnormalities were found in other tissues. The significance of the very high liver selenium concentration remains unclear.

Contributing Institution:
Veterinary Sciences Centre
School of Veterinary Medicine
University College Dublin
Belfield, Dublin 4, Ireland
http://www.ucd.ie/vetmed/

JPC Diagnosis:
Kidney: Asynchronous maturation with fetal glomeruli, tubular loss, marked interstitial fibrosis, and mild lymphoplasmacytic interstitial nephritis.

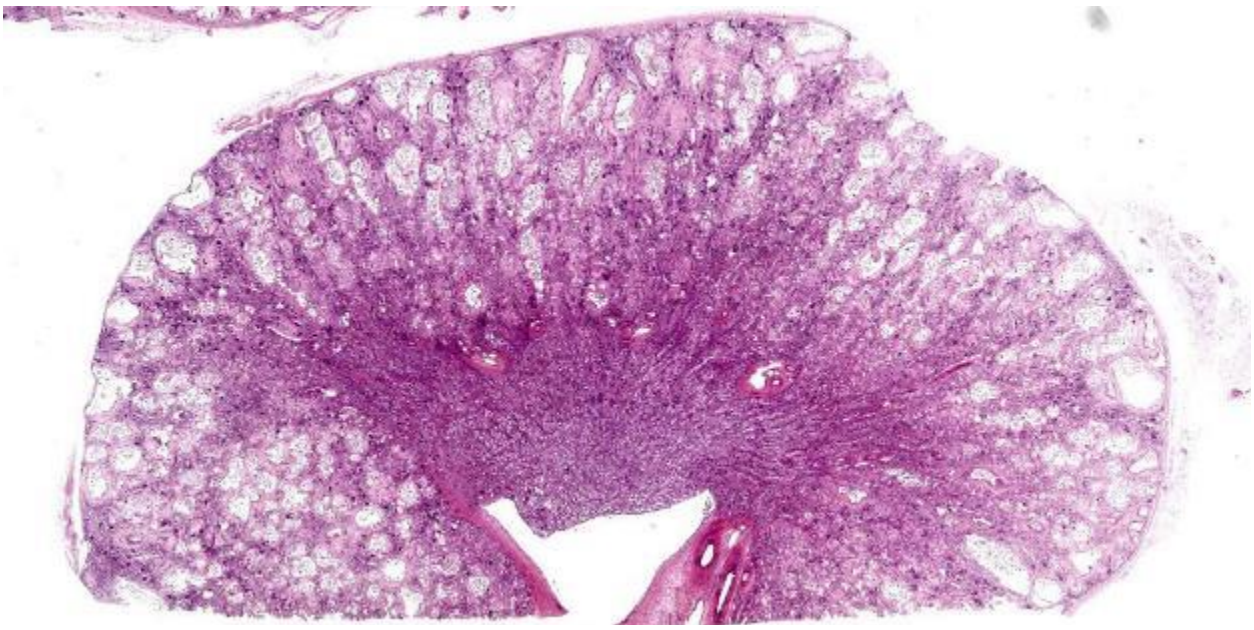

Figure 4-3. Kidney, calf: Normal cortical architecture is replaced by large ectatic tubules separated by areas of fibrosis and fetal glomeruli. The change is largely restricted to the cortex. (HE, 87)

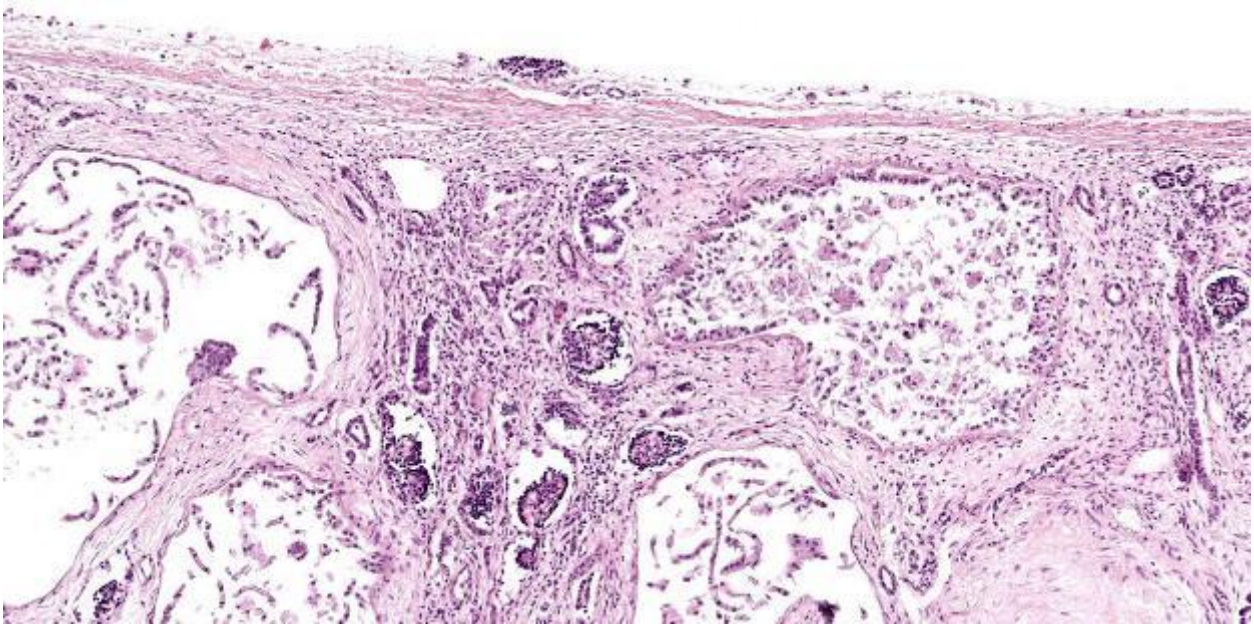

Figure 4-4. Kidney, calf. Segmentally in the cortex, there are rays of fibrous connective tissue extending to the capsule which contain numerous fetal glomeruli and atrophic tubules. (HE, 87)

JPC Comment:
Renal dysplasia is a broad term that encompasses a range of gross and histologic abnormalities caused by development gone rogue.
In mammals, two precursor kidneys are formed prior to the arrival, in the mature animal, of the metanephric kidney. The first is the pronephros, which contains primitive tubules and a pronephric duct, that grows caudally and terminates in the fetal cloaca.[4] The tubules of the pronephros degenerate, but the pronephric duct persists as the mesonephric duct. The mesonephric duct, in turn, induces the formation of the mesonephric kidney, which consists of tubules that terminate in vascular proliferations arising from the dorsal aorta on one end and the mesonephric duct on the other. In amphibians and fish, the mesonephros becomes the functional mature kidney. In reptiles, birds, and mammals, the mesonephros degenerates, setting the stage for the arrival of the metanephros.[4]

The metanephric kidney beings as an evagination from the mesonephric duct, called the ureteric bud.[11] The ureteric bud moves cranially and differentiates into the ureter, renal pelvis, and collecting ducts. The ureteric bud grows into a mass of mesenchymal cells known as the metanephrogenic mass or the metanephric blastema. As the ureteric bud successively divides into collecting ducts, these ducts induce nephrogenic differentiation of the metanephric blastema. These proto-nephrons elongate, canalize and induce the formation of immature glomeruli at one end, and connect with the collecting ducts at the other. Nephrons continue to develop from deep to superficial within the kidney and, in some species, continue to form and mature after birth.

The term renal dysplasia implies disorder of the complex interactions between the ureteric bud and the metanephric blastema, resulting in anomalous metanephric differentiation.[11] The contributor outlines several canonical histologic criteria, at least one of which must be present for a diagnosis of renal dysplasia. Two of these criteria, the presence of

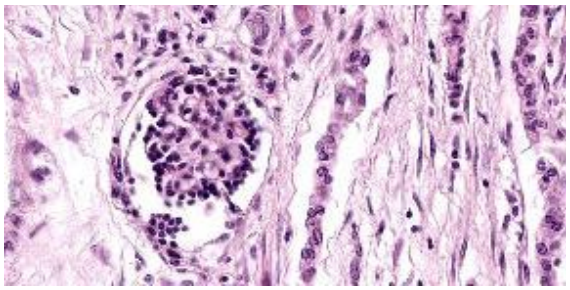

Figure 4-5. Kidney, calf. Fetal glomerulus. (HE, 400X)

metanephric ducts surrounded by primitive mesenchyme and the formation of dysontogenic tissues, both indicate total failure of the initial interaction between the ureteric bud and the metanephric blastema.[11] In contrast, the presence of fetal glomeruli and tubules, the presence of persistent mesenchyme, and the presence of anomalous structures indicate that the induction of the metanephric blastema was initiated but failed to undergo complete differentiation.[11]

As the contributor notes, ureteral anomalies are common in cases of renal dysplasia. This is unsurprising given the close developmental relationship between the kidney and the collecting system. Among the reported ureteral anomalies associated with renal dysplasia are ectopic ureters, ureteral obstruction with accompanying hydronephrosis, hydroureter, and congenital urothelial cell hyperplasia.[10,14,15]

Conference discussion focused on the difficulty of definitively identifying structures, such as persistent metanephric ducts or primitive mesenchyme, amid the histologic noise present in a kidney as dysplastic as the section examined in conference. While fetal glomeruli are more obvious, their presence can be a normal finding in the neonates of some species, such as dogs, in which renal development continues through the first few weeks of life.

Discussion also focused on the term "renal dysplasia," which has fallen somewhat out of favor due to its relatively elastic meaning which has become somewhat overstretched over time due to inconsistent use. The currently proposed term, "renal maldevelopment," is meant to describe the disorganized development of renal parenchyma exemplified by this case. The term "renal dysplasia," while well-ensconced in the veterinary literature, should be thought of as an umbrella term, covering a heterogenous group of renal developmental anomalies.

References:

1. Bruder MC, Shoieb AM, Shirai N, Boucher GG, Brodie TA. Renal dysplasia in Beagle dogs: four cases. *Toxicol Pathol*. 2010;38(7):1051-1057.
2. Cianciolo RE, Mohr FC. Urinary system. In: Maxie MG, ed. *Jubb, Kennedy,and Palmer's Pathology of Domestic Animals*. Vol. 2. 6th ed. Philadelphia, PA: Elsevier; 2016:393.
3. Dillard KJ, Hytönen MK, Fischer D, et al. A splice site variant in INPP5E causes diffuse cystic renal dysplasia and hepatic fibrosis in dogs. *PLoS One*. 2018;13(9):e0204073.
4. Fletcher TF, Weber AF. Veterinary developmental anatomy (veterinary embryology). University of Minnesota College of Veterinary Medicine. 2013. Accessed September 20, 2023. http://vanat.cvm.umn.edu/vanatpdf/EmbryoLectNotes.pdf.
5. Frelier PF, Armstrong DL, Pritchard. Ovine mesangiocapillary glomerulonephritis type I and crescent formation. *Vet. Pathol.* 1990;27(1):26-34.
6. Hirayama H, Kegeyama S, Moriyasu S, et al. Genetic diagnosis of claudin 16 deficiency and sex determination in bovine preimplantation embryos. *J. Reprod. Dev.* 2004; 50:613-618.

7. Kerlin R., Van Winkle TJ. Renal dysplasia in Golden Retrievers. *Vet. Pathol.* 1992; 32:327-329.
8. O'Toole D, Jeffrey M, Jones T, Morgan G, Green R. Pathology of renal dysplasia and bladder aplasia-hypoplasia in a flock of sheep. *J. Vet. Diagn. Invest.* 1993; 5:591-602.
9. Panciera RJ, Washburn KE, Streeter RN, Kirkpatrick JG. A familial peripheral neuropathy and glomerulopathy in Gelbvieh calves. *Vet. Pathol.* 2003;40 (1):63-70.
10. Percy DH, Carmichael LE, Albert DM, King JM, Jonas AM. Lesions in puppies surviving infection with canine herpesvirus. *Vet Pathol.* 1971;8(1):37-53.
11. Picut CA, Lewis RM. Microscopic features of canine renal dysplasia. *Vet Pathol.* 1987;24(2):156-163.
12. Sugiyama A, Ozaki K, Miyazaki, Tanabe Y, Takeuchi T, Narama I. Renal dysplasia unrelated to claudin-16 deficiency in Japanese Black cattle. *J Comp Pathol.* 2007;137(1):71-77.
13. Whiteley MH, Bell JS, Rothman DA. Novel allelic variants in the canine cyclooxgenase-2 (Cox-2) promoter are associated with renal dysplasia in dogs. *PLoS One*. 2011;8;6(2):e16684.
14. Yoon HY, Mann FA, Punke JP, Jeong SW. Bilateral ureteral ectopia with renal dysplasia and urolithiasis in a dog. *J Am Anim Hosp Assoc*. 2010;46(3):209-214.
15. Yoshida K, Takezawa S, Itoh M, Takahashi E, Inokuma H, Watanabe K, et al. Renal dysplasia with hydronephrosis and congenital ureteral stricture in two Holstein-Friesian calves. *J Comp Pathol.* 2022;193:20-24.

WSC 2023-2024
Conference 5 Self-Assessment

1. In cases of feline idiopathic pulmonary fibrosis, aggregates of which of the following cell types is present?
    a. Neuroendocrine cells
    b. Clubb cells
    c. Myofibroblasts
    d. Endothelial cells

2. Which of the following is the most likely to demonstrate the full triad of intestinal, liver, and heart lesions in Tyzzer's disease
    a. Cows
    b. Horses
    c. Cats
    d. Rodents

3. True or false: Small intestinal mucinous adenocarcinomas are one of the most common neoplasms in aged NHPs?
    a. True
    b. False

4. Renal dysplasia is most commonly seen in which of the following species?
    a. Cattle
    b. Cats
    c. Horses
    d. Dog

5. Concurrent abnormalities in which of the following are often seen in animals with renal dysplasia?
    a. Bladder
    b. Ureter
    c. Urethra
    d. Prostate

Joint Pathology Center
Veterinary Pathology Services

WEDNESDAY SLIDE CONFERENCE 2023-2024

Conference #6 **27 September 2023**

CASE I:

Signalment:
9-month-old female Saker Falcon, avian (*Falco cherrua*)

History:
A 9-month-old female Saker Falcon kept in a zoo had been showing signs of fatigue during training and loss of appetite for a few weeks, but her weight was stable. She was mainly fed mice and a change of food to quail and chicks improved her appetite. She died a few hours following her daily training, from which she returned breathless.

Gross Pathology:
The pericardial sac contained 1 to 2 ml of translucent light yellow gelatinous material. The heart and the liver showed slight cardiomegaly and hepatomegaly, respectively. A few epicardial petechiae were present on the ventral aspect of the heart. The peripheral connective tissues were turgid and moist (edema). The spleen was diffusely pale. The wall of the aortic arch was diffusely thickened; the inner surface was irregular, wrinkled, and yellow. Lungs showed several extensive, poorly demarcated dark red patches, interpreted as congestion and/or hemorrhages.

Laboratory Results:
PCR for highly pathogenic avian influenza virus (M gene): Negative.

Figure 1-1. Aorta, falcon. The wall of the aortic arch is diffusely thickened; the inner surface is irregular, wrinkled, and yellow. (Photo courtesy of: Laboratoire d'histopathologie animale, Vetagro Sup, campus vétérinaire, http://www.vetagro-sup.fr/)

Microscopic Description:
Brachiocephalic trunks, aortic arch, caudal aorta: The intima and subintimal media of arterial walls are diffusely and irregularly thickened by the accumulation of numerous large foamy cells, cholesterol clefts, large amorphous non-staining lipid deposits, and dense collagen (fibrosis). Occasionally, there are multifocal deposits of hyperbasophilic coarse granular material (mineralization) and cells located in lacunae within a chondroid matrix (chondroid metaplasia). The arterial lumen is often greatly reduced in diameter or almost absent (sub-occlusion). The adventitia is multifocally infiltrated by a small to moderate number of lymphocytes and plasma cells, and rare macrophages and Mott cells, which are occasionally accompanied by the accumulation of a variable amount of basophilic amorphous material (edema fluid).

Within the aorta, lesions are visible in the vicinity of the heart, at the level of the aortic arch, and also in the abdominal region, near the adrenal glands. These lesions extend to the semi-lunar leaflets of the aortic valve. Early changes are seen in the intima of a pulmonary artery. Myxoid material is occasionally present between the smooth muscle fibers of the media.

Contributor's Morphologic Diagnosis:
Brachiocephalic trunks, aortic arch, caudal aorta: Atherosclerosis, multifocally extensive, severe, chronic, Saker Falcon, avian.

Contributor's Comment:
Although atherosclerosis is infrequent in domestic mammals, it is the most common cardiovascular disease found in birds of prey.[8] It is also common in other avian species, notably psittacine birds, but also chickens, finches, emus, and penguins.[21] It frequently occurs in non-human primates as well.[21] Furthermore, pigeons, Japanese quail, turkeys and chickens have been used as animal models of atherosclerosis for medical research.[6,19]

Atherosclerosis is a chronic inflammatory fibroproliferative disease that occurs in the arterial wall in response to endothelial injury. It results from an imbalance in lipid metabolism and an inappropriate immune response with accumulation of cholesterol-laden macrophages in the arterial wall. Atherosclerosis is one pattern of arteriosclerosis; other patterns include simple arteriosclerosis, Monckeberg sclerosis, and fibromuscular intimal hyperplasia.

In birds of prey, atherosclerosis primarily affects older captive individuals, but is reported in Brahminy kite (*Haliastur indus*) from 55 days of age and in other bird species (psittacine, raptors, waterfowl) from one year of age.[8,13,15] Female raptors and female psittacine birds have a higher risk of developing atherosclerosis than males, which may be due to the lipid metabolism involved in egg production.[3,12]

In humans, physical inactivity, obesity, unhealthy diet, hyperlipidemia, hypertension, and tobacco and high alcohol use are well-known risk factors for atherosclerosis, and the impact of exposure to these risk factors accumulates throughout life.[11] Obesity, lack of exercise, hypercholesterolemia, and a high-fat diet (cholesterol, saturated fatty acids) are also suspected risk factors for this disease in birds; however, captive conditions (nutrition, exercise) are not the determining factors in the development of this disease since atherosclerosis has been observed in wild individuals.[3,22] Genetic factors may also predispose animals to development of the condition, but in general, preventing obesity in captive birds and avoiding sudden weight loss in overweight individuals are recommended preventive measures.[8] A 2017 study also found an association between a diet consisting mainly of 1-day-old chicks and increased plasma cholesterol concentration and atherosclerosis when compared with a rat and mouse diet.[10]

Figure 1-2. Aorta, falcon. A cross and longitudinal section of the aorta is presented for examination. The lumen is compromised and the tunica media is greatly expanded. (HE, 5X)

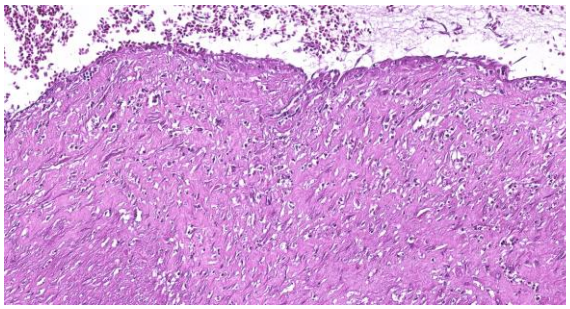

Figure 1-3. Aorta, falcon. There is loss of endothelium and marked intimal hyperplasia with fibrosis, proliferation of fibroblasts, disarray of remnant smooth muscle cells, and infiltration of macrophages. (HE, 195X)

Sudden death is the most frequent clinical manifestation of atherosclerosis in birds. It can also result in dyspnea, weakness, or neurological signs.

Grossly, early lesions are fatty streaks that progress to atheromas; there is loss of elasticity, induration, irregular thickening, and yellow discoloration of the arterial wall with narrowing of the lumen. Erosion/ulceration with thrombosis or intramural hemorrhage may occur, causing a red to brown discoloration. Atherosclerosis most commonly affects large arteries, notably the descending aorta and brachiocephalic trunks, as in the presented case.[22] Hypertrophic cardiomyopathy can also be observed in birds with atherosclerosis; however, this assessment remains subjective in raptors since there are no reference values for the dimensions of a healthy heart.[17] Some birds may show concurrent widespread xanthogranulomatosis or endogenous lipid pneumonia, suggesting a possible correlation or shared etiopathogenesis, such as dyslipidemia, for these conditions.[2,7]

Histopathologically, atherosclerotic plaques have five main components:

1. Increased cellularity of the intima with variable numbers of smooth muscle cells, macrophages, and T lymphocytes (with necrotic debris in the central core);
2. Deposition of extracellular matrix with collagen, elastin, and proteoglycans;
3. Intracellular and extracellular lipids;
4. Neovascularization at the lesion's periphery; and
5. Mineralization (in later stages).

Topographically, a luminal fibrous cap composed of smooth muscle cells and collagen overlies a layer rich in inflammatory and smooth muscle cells which borders a necrotic core containing lipids, foam cells, and cellular debris. Atheromas can be classified as vulnerable (if comprising a thin fibrous cap with large lipid core and dense inflammatory infiltrate) or stable (a thick fibrous cap or fibrous atheroma with little inflammation and lipid deposition). Possible evolution of atheromas include rupture or erosion with thrombosis of the blood vessel, intraplaque hemorrhage, atheroembolism, or aneurysm formation.[17] Several histologic classifications of avian atherosclerotic lesions have been proposed and used in pigeons, quail, chickens, and psittacine birds.[1,4,14,16,18] Some of these classification systems are based on the American Heart Association (AHA) classification of atherosclerotic lesions used in humans.[20]

Myocardial infarction and fibrosis, and medial hyperplasia of vessels of the heart, liver, lung, and kidney are reported in association with atherosclerosis in birds.[3,17] Hepatic steatosis regularly accompanies atherosclerosis, suggesting a disorder of lipid metabolism.[13] In our case, the origin and significance of splenic reticuloendothelial hyperplasia and periportal hepatitis remain unclear. The presence of abundant foamy macrophages suggests a correlation with dysfunctional lipid metabolism that may have caused the atherosclerosis.

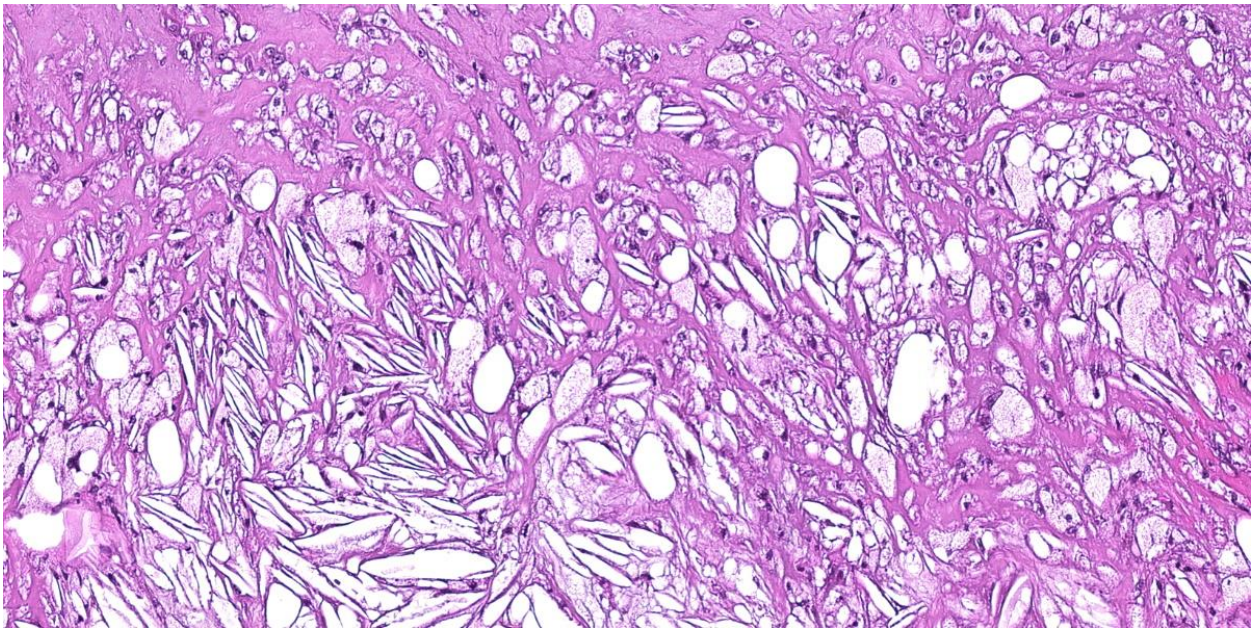

Figure 1-4. Aorta, falcon. The outer half of the tunica media is expanded by large numbers of lipophages with admixed cholesterol clefts and clear space. (HE, 266X)

Atherogenesis has been extensively studied in humans. It is initiated by low-density lipoprotein cholesterol (LDL-C) which, when at blood concentrations in excess of physiological needs, accumulate in the intima.[11] The formation of fibrofatty atheromas (atherosclerotic plaques) includes the following sequence of events: 1) endothelial injury and dysfunction leading to increased vascular permeability, leukocyte adhesion, and thrombosis; 2) continued accumulation of lipoproteins; 3) monocyte and platelet adhesion to the endothelium and emigration of monocytes into the intima, with activation of macrophages; 4) release of factors from activated endothelial cells, macrophages (including interleukin-1, and monocyte chemoattractant protein-1), and platelets (including PDGF), inducing recruitment of smooth muscle cells; 5) smooth muscle cell proliferation, recruitment, and activation of T lymphocytes (with production of interferon gamma), and extracellular matrix deposition (notably collagen); 6) lipid accumulation within the cytoplasm of macrophages and smooth muscle cells (foam cells) and in the extracellular matrix; and 7) calcification.

Known endothelial insults in humans include hemodynamic disturbances, hypertension, hyperlipidemia, toxins (including smoke toxins), inflammation (notably from viral infection and immune reactions), and homocysteine. Atherosclerotic stenosis leads to chronic ischemia while vulnerable plaques can lead to acute and potentially fatal ischemia following rupture, thrombosis, or embolization. Compared with humans, the lymphatic system of birds is underdeveloped and birds such as pigeons lack apolipoproteins E and B-48 and do not synthesize chylomicrons, which limits their use as models for research on the pathogenesis of human atherosclerosis.[19] Also, female birds show major changes in plasma lipoproteins during egg laying.[19]

In domestic animals, pigs, and to a lesser extent rabbits, hamsters, and chickens, are considered atherosensitive; conversely, cats, cattle, goats, and rats are atheroresistant. Although dogs are considered atheroresistant, it

is not uncommon to find atherosclerosis in dogs with hypothyroidism, diabetes, or breed-related hyperlipidemia (e.g., miniature Schnauzer). Arteriolosclerosis is sporadically seen in most animal species and is considered an age-related disease. In cats with renal failure, it is a characteristic of hypertensive encephalopathy which develops because of a prolonged increase in systemic blood pressure.

Contributing Institution:
Laboratoire d'histopathologie animale
Vetagro Sup, campus vétérinaire,
http://www.vetagro-sup.fr/

JPC Diagnoses:
1. Aorta: Atherosclerosis, circumferential, diffuse, severe.
2. Epicardium: Epicarditis, fibrinous, chronic, focally extensive, moderate.

JPC Comment:
Atherosclerosis is a multifactorial disease which is well-studied in humans and often linked to defects in lipid metabolism. Though atherosclerosis is relatively rare in animals, the contributor provides an excellent overview of the clinical, demographic, gross, and histologic manifestations of atherosclerosis across a range of avian species.

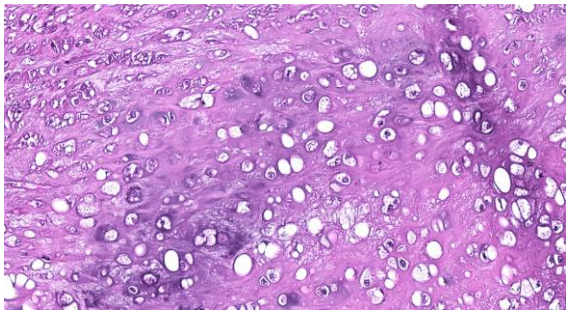

Figure 1-5. Aorta, falcon. The tunica media also contains areas of chondroid metaplasia. (HE, 368X)

In normal lipid metabolism, dietary cholesterol and triglycerides are absorbed by the gastrointestinal tract and incorporated into triglyceride-rich lipoproteins called chylomicrons.[9] These chylomicrons are subject to cleavage by endothelial enzymes and arrive at the liver as cholesterol-rich chylomicron remnants, where the cholesterol is either excreted as bile acids into the biliary tract, excreted as free cholesterol, or packaged into very low density lipoprotein (VLDL) which is then secreted into the blood.[21] VLDL is rich in triglycerides, low in cholesterol, and contains membrane apolipoproteins ApoB, ApoC, and ApoE.[9]

Once in the capillary beds of adipose tissue and muscle, VLDL undergoes lipolysis, and the resulting remnant, now with fewer triglycerides, increased cholesterol, and only containing ApoB and ApoE, is called an intermediate density particle (IDL). IDLs can be either returned to the liver to regenerate VLDLs or can undergo further lipolysis which removes most of the remaining triglycerides and ApoE, yielding a low-density lipoprotein (LDL) which is cholesterol-rich and contains only ApoB.[9]

Most LDL is taken up by the liver via the binding of ApoB to LDL receptors, and is then shuttled to lysosomes where it is metabolized to cholesterol and amino acids. Within hepatocytes, the resulting free cholesterol has an inhibitory effect on both HMG CoA reductase, the rate limiting enzyme in cholesterol synthesis, and the synthesis of new LDL receptors.

Perturbation of any step of this complex pathway can result in hyperlipemia and a corresponding increased risk of atheroma formation. In humans, genetic defects in the LDL receptor are well characterized and cause familial hypercholesterolemia due to the inadequate removal of plasma LDL by the

liver.[9] Similarly, mutations in the gene encoding ApoB, the ligand for LDL receptors, reduces the uptake of LDL particles by the liver, also resulting in hypercholesterolemia.

In veterinary medicine, atherosclerosis can occur naturally in many aged avian species, as detailed by the contributor, and atherosclerosis is the most common vascular lesion in the great vessels of aged psittacines and birds of prey.[8,17] Systemic hypertension is a well-known risk factor for atherosclerosis in humans and it has been suggested that the relatively higher normal blood pressures and serum cholesterol levels in birds may predispose them to atherosclerotic disease.[8]

Rabbits are also susceptible to dietary-induced hypercholesterolemia and atherosclerosis. This predisposition led to the development of Watanabe heritable hyperlipidemic rabbits, which have a genetic defect in the LDL receptor that results in aortic atherosclerosis in 100% of animals by 5 months of age.[22] The resulting disease closely mimics human atherosclerosis and Watanabe rabbits are consequently one of the main animal models used in atherosclerosis research.

Atherosclerosis has also been described in dogs, as noted by the contributor, and in pigs. Pigs do not naturally develop atherosclerosis, but can develop atherosclerotic disease similar to that seen in humans when fed high fat, high cholesterol diets.

This week's conference was moderated by MAJ Katie Scott, Chief of Necropsy at the Walter Reid Army Institute of Research (WRAIR). MAJ Scott reviewed vascular anatomy and stressed the importance of using precise anatomic terminology, particularly in conditions such as atherosclerosis where lesions are typically found in specific histologic layers (e.g., the tunica intima) due to damage to particular structural elements (e.g., the internal elastic lamina).

Several conference participants noted the fibrinous pericarditis and epicarditis present on the examined section. This finding is not typical of avian atherosclerosis and is more commonly highly pathogenic avian influenza, the latter of which was ruled out by the contributor's laboratory testing. Conference participants were suspicious that this unlucky falcon was beset by both atherosclerosis and an unknown infectious agent and chose to provide separate morphologic diagnoses for the two pathogeneses.

References:

1. Beaufrère H, Nevarez JG, Holder K, et al. Characterization and classification of psittacine atherosclerotic lesions by histopathology, digital image analysis, transmission and scanning electron microscopy. *Avian Pathol*. 2011;40(5):531–544.
2. Donovan TA, Garner MM, Phalen D, et al. Disseminated coelomic xanthogranulomatosis in eclectus parrots (*Eclectus roratus*) and budgerigars (*Melopsittacus undulatus*). *Vet Pathol*. 2022;59(1):143–151.
3. Fitzgerald BC, Beaufrère H. Cardiology. In: Speer BL, ed. *Current Therapy in Avian Medicine and Surgery*. Elsevier Health Sciences; 2016.
4. Fricke C, Schmidt V, Cramer K, Krautwald-Junghanns ME, Dorrestein GM. Characterization of atherosclerosis by histochemical and immunohistochemical methods in African grey parrots (*Psittacus erithacus*) and Amazon parrots (*Amazona* spp.). *Avian Dis*. 2009;53: 466–472.
5. Gal A, Castillo-Alcala F. Cardiovascular system, pericardial cavity, and lymphatic vessels. In: Zachary JF, ed. *Pathologic Basis of Veterinary Disease*. 7th ed. Elsevier;2022:681-682,941-942.

6. Gisterå A, Ketelhuth DF, Malin SG, Hansson GK. Animal models of atherosclerosis: supportive notes and tricks of the trade. *Circ Res*. 2022;130(12):1869-1887.
7. Grespan A, Fiedler RT, Guedini BT, Costa LD, Raso TF. Endogenous lipid pneumonia associated with atherosclerosis in a blue-fronted Amazon parrot (*Amazona aestiva*). *J Comp Path.* 2023; 201:130-134.
8. Jones MP. Vascular diseases in birds of prey. *J Exot Pet Med*. 2013;22(4): 348–357.
9. Kumar V, Abbas AK, Aster JC. Genetic disorders. In: Kumar V, Abbas AK, Aster JC, eds. *Pathologic Basis of Disease*. 10th ed. Elsevier;2021:151-154.
10. Legler M, Kummerfeld N, Wohlsein P. Atherosclerosis in birds of prey: a case study and the influence of a one-day-old chicken diet on total plasma cholesterol concentration in different raptor and owl species. *Berl Münch Tierärztl Wochenschr*. 2017;130(7/8):353–363.
11. Libby P, Buring JE, Badimon L., et al. Atherosclerosis. *Nat Rev Dis Primers.* 2019;5(56).
12. Lujan-Vega C, Keel MK, Barker CM, Hawkins MG. Evaluation of atherosclerotic lesions and risk factors of atherosclerosis in raptors in northern California. *J Avian Med Surg*. 2021;35(3):295–304.
13. Nemeth NM, Gonzalez-Astudillo V, Oesterle PT, Howerth EW. A 5-year retrospective review of avian diseases diagnosed at the Department of Pathology, University of Georgia. *J Comp Path.* 2016;155(2-3):105–120.
14. Orita S, Masegi T, Itou K, Kawada M, Yanai T, Ueda K. Spontaneous aortic atherosclerosis in layer chickens. *J Comp Path*. 1994;110:341–347.
15. Potier, R. Lipid blood profile in captive Brahminy kite (*Haliastur indus*) as a possible indication of increased susceptibility to atherosclerosis. *J Zoo Wildl Med*. 2013;44(3):549–554.
16. Santerre RF, Wight TN, Smith SC, Brannigan D. Spontaneous atherosclerosis in pigeons. A model system for studying metabolic parameters associated with atherogenesis. *Am J Path*. 1972;1:1-22.
17. Schmidt RE, Reavill DR, Phalen DN, eds. *Pathology of pet and aviary birds*. Wiley Blackwell; 2015.
18. Shih JC, Pullman EP, Kao KJ. Genetic selection, general characterization, and histology of atherosclerosis-susceptible and-resistant Japanese quail. *Atherosclerosis*. 1983;49(1):41–53.
19. St Clair RW. The contribution of avian models to our understanding of atherosclerosis and their promise for the future. *Lab Anim Sci*. 1998;48(6):565-568.
20. Stary HC. Natural history and histological classification of atherosclerotic lesions: an update. *Arterioscler Thromb Vasc Biol*. 200020(5):1177–1178.
21. Terio KA, McAloose D, Judy SL, eds. *Pathology of Wildlife and Zoo Animals*. Academic Press, Elsevier; 2018.
22. Tristan T. The aging raptor. *Vet Clin North Am Exot Anim Pr*. 2010;13(1):51–84.
23. Watanabe Y. Serial inbreeding of rabbits with hereditary hyperlipidemia (WHHL-rabbit). *Atherosclerosis*. 1980;36(2):261-268.

CASE II:

Signalment:
1-year-old male neutered Boxer, canine (*Canis familiaris*)

History:
The patient presented to the Oklahoma State University Veterinary Teaching Hospital with a four-week history of vomiting and weight loss.

Figure 2-1. Jejunum, dog. A 34 cm section of jejunum is diffusely thickened. (*Photo courtesy of:* Oklahoma State University, Department of Veterinary Pathobiology, https://vetmed.okstate.edu/veterinary-pathobiology/index.html)

Gross Pathology:

A segment of the proximal jejunum, approximately 34 cm long, is severely thickened to 3-4 times the normal size and is diffusely firm. The serosal surface is discolored irregularly dark red to maroon along the length of the affected segment. On cut section, the antimesenteric jejunum wall varies in thickness from 0.3-1 cm, and the wall adjacent to the mesentery is markedly thickened, ranging from 1-4 cm. The transmural thickening, especially involving the submucosa and tunica muscularis, is pale tan and densely taut (fibrous). The lumen is severely narrowed, and toward the mid-portion of the segment, is almost completely obstructed by marked thickening of the intestinal wall. The adjacent mesenteric lymph node is severely enlarged, 8x5x4 cm, and mottled yellow to tan on cut surface.

Laboratory Results:

Fungal 28S sequencing of intestine revealed 94% identity match to *Pythium insidiosum*. Lymph node sequencing was inconclusive.

Microscopic Description:

Small intestine: Three sections of jejunum are examined, each displaying mild to severe inflammation. Severely effacing multifocal and mural regions of the mucosa, submucosa, and tunica muscularis, are extensive numbers of eosinophils, accompanied by moderate to marked numbers of multinucleated giant cells (both Langhans type and foreign body type), epithelioid macrophages, and fewer numbers of lymphocytes, plasma cells, and scattered neutrophils. At the center of these inflammatory lesions, there is a moderate amount of bright, eosinophilic matrix containing karyorrhectic nuclei (necrosis), and occasionally a ghost outline of a non-staining, thin walled, 4-6 µm wide hyphae. In the most affected section, the inflammation and necrosis have distorted the villous architecture and obliterated the muscularis mucosae while dissecting through the submucosa and tunica muscularis. The submucosa is often expanded by marked amounts of fibrous connective tissue and granulation tissue.

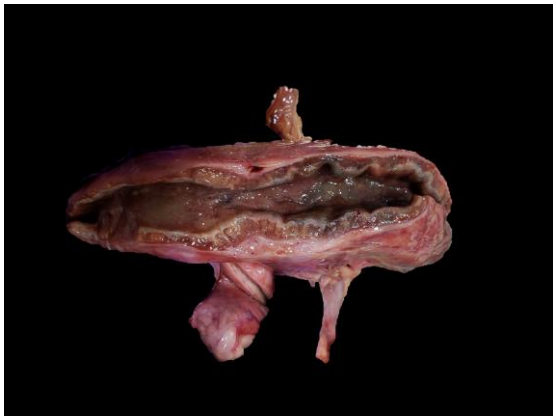

Figure 2-2. Jejunum, dog. An incised section of the thickened segment of jejunum. (*Photo courtesy of:* Oklahoma State University, Department of Veterinary Pathobiology, https://vetmed.okstate.edu/veterinary-pathobiology/index.html)

Figure 2-3. Jejunum, dog. Three sections of the intestinal wall are submitted for examination and the section at bottom right is the most severely affected with marked expansion of the submucosa and muscular tunics. (HE, 5X)

The serosa is either not affected, or markedly expanded by granulation tissue and neovascularization.Within necrotic centers are small numbers of GMS-positive, 5-15 µm wide hyphae, with non-parallel walls, sparse to inapparent septae, and occasional branching.

Contributor's Morphologic Diagnosis:
Jejunum: Severe, segmental, chronic-active, eosinophilic and granulomatous transmural enteritis, with extensive fibrosis, granulation tissue, and small numbers of GMS-positive intralesional hyphae.

Contributor's Comment:
Gross and histologic lesions in this case are consistent with enteric pythiosis. Fungal 28S PCR sequencing revealed 94% identity match to *Pythium insidiosum* and was inconclusive for the submitted mesenteric lymph node.

Pythium insidiosum is a fungus-like, fresh water favoring, aquatic oomycete that is geographically distributed throughout the world, including southeast Asia, Australia, New Zealand, Brazil, Costa Rica, and the Caribbean.[1,5,6,8] Canine pythiosis used to be considered restricted to the states bordering the Gulf Coast in the United States; however, there are several reports in the last two decades indicating the geography of pathogenic *Pythium insidiosum* has expanded, and now includes states within the northeast, southeast, midwest, and as far west as California.[1,4-8,10]

Recent reports have indicated that the zoospores infect mammals via ingestion, or more commonly through cutaneous lesions where the zoospores have marked chemotaxis towards injured skin, and they consequently begin to encyst on the surface of the tissue.[5,6,8] Enteric or colonic pythiosis likely occurs due to a defect within the gastrointestinal tissue allowing the zoospores to adhere and encyst.[6] *Pythium insidiosum* commonly affects horses, less often dogs and cats, and rarely affects cattle, sheep, and a few captive species including bears, camels, a tiger and a jaguar.[5-7] The remainder of this comment will focus on enteric pythiosis in canines.

The classic signalment of this disease in dogs is young, male, large breed dogs (particularly Labradors).[4,6] The median age in most case reports is approximately 2 years old, but has been diagnosed in patients as young as 12

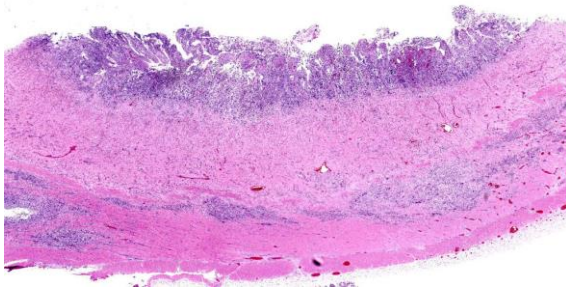

Figure 2-4. Jejunum, dog. There is transmural inflammation. The mucosal lamina propria is expanded by an inflammatory infiltrate, resulting in loss of crypts and villar blunting. The infiltrate is multifocally evident in the submucosa and muscular tunics. (HE, 15X)

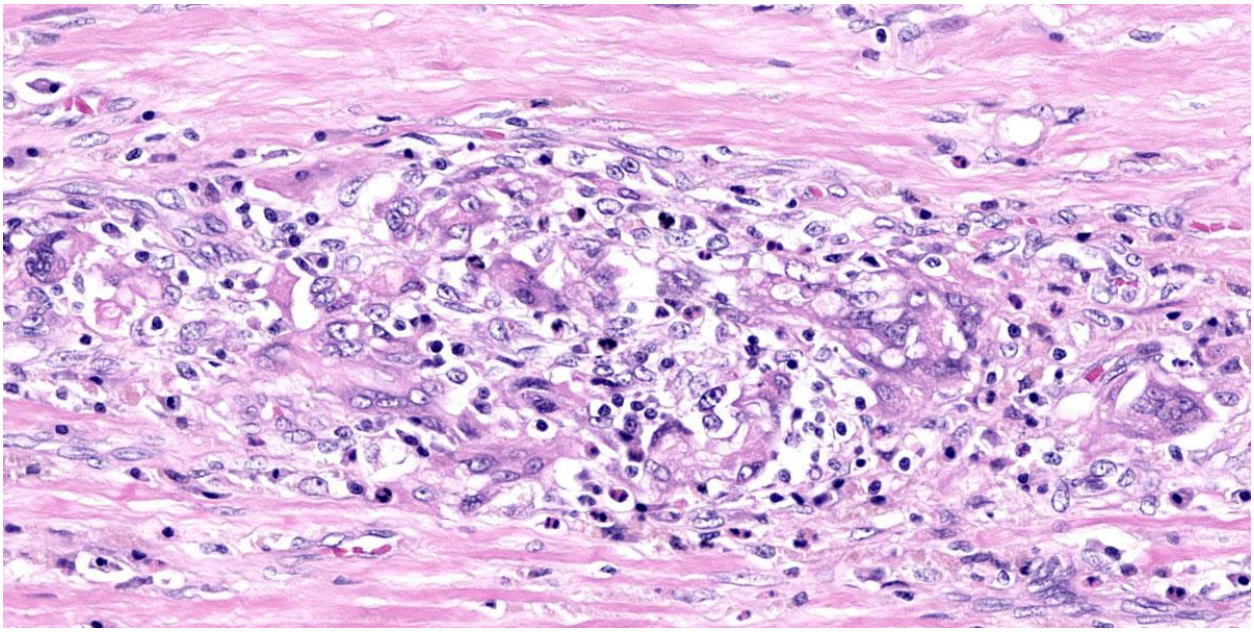

Figure 2-5. Jejunum, dog. In an inflammatory focus in the smooth muscle of the jejunal wall, there are numerous epithelioid and foreign body type macrophages. (HE, 206X)

weeks old and as old as 6 years old.[1,4,8] Gender is evenly distributed between male and female, and large and mixed breed dogs.[1,4] Patients present with chronic, nonspecific gastrointestinal signs such as weight loss, anorexia, vomiting, and/or diarrhea.[1,4-7,10,11] Abdominal masses may be palpated during physical examination.[5,8] Clinical pathology most often reveals eosinophilia, hypoalbuminemia, and hyperglobulinemia, but may also include non-regenerative anemia and calcium irregularities (both hypocalcemia and hypercalcemia have been reported).[1,6,8]

Sites of *Pythium* infection can occur in the esophagus, stomach, small intestines, ileocecal junction, or colon, and tend to spread to adjacent mesentery and mesenteric lymph nodes.[1,4,6,8,10,11] Initial diagnostics include radiographs, ultrasound, or exploratory laparotomy, with cytology or biopsy samples submitted for ancillary testing.[6-8,11] Cytology may reveal eosinophils admixed with granulomatous to pyogranulomatous inflammation, +/- hyphae.[6] Histopathology also reveals similar findings of eosinophilic, granulomatous to pyogranulomatous inflammation with hyphal fragments located within necrotic or inflammatory centers.[4-8,10,11] The inflammation can be transmural or restricted to the submucosa and muscular layers.[6,11]

Gomori's methenamine silver (GMS) is the stain of choice for *Pythium*, as periodic acid-Schiff (PAS) poorly stains hyphae, if at all.[5,6,10] GMS characteristics include rarely septate, occasionally branching hyphae with a diameter of 2-7 µm, but can be greater than 10 µm in diameter, as was described previously in this case.[4-7,11] Care should be taken to differentiate these features from *Lagenidium* or zygomycete infections, as they have similar GMS characteristics and potentially different clinical outcomes in regards to treatment and prognosis.[6] Tests for further differentiation of these three pathogens include, but are not limited to, culture, immunohistochemistry, PCR, and ELISA.[1,5-7,10]

Prognosis is often grave depending on the duration and extent of the lesions.[1,4,6,10,11] If surgical excision is possible, it is

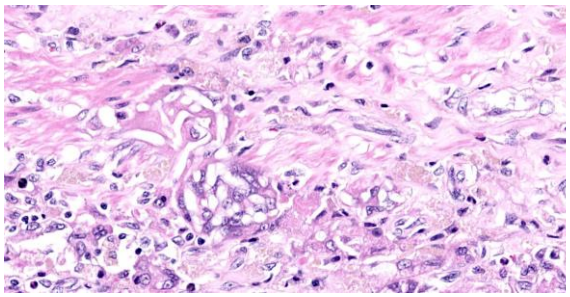

Figure 2-6. Jejunum, dog. Multinucleated foreign body giant cells contain outlines of fungal hyphae in *bas relief*. (HE, 586X)

recommended to have 3-4 cm of surgical margins.[5,6,11] Successful treatment has been reported in a few cases, and in one report of three dogs in California, treatment included the long-term use of anti-inflammatory doses of corticosteroids in conjunction with itraconazole and terbinafine.[10,11]

In conclusion, the submitted case is a classic example of *Pythium insidiosum* enteritis in a dog. The signalment and presenting complaint, in conjunction with necropsy and histologic findings, is a very common presentation of this disease, and serves as a reminder to pathologists and trainees as the distribution of this disease seems to be expanding within the United States.

Contributing Institution:
Oklahoma State University
Department of Veterinary Pathobiology
Stillwater, OK 740784
https://vetmed.okstate.edu/veterinary-pathobiology/index.html

JPC Diagnosis:
Small intestine: Enteritis, transmural, eosinophilic and granulomatous, moderate, with numerous intrahistiocytic and extracellular hyphae.

JPC Comment:
Pythium insidiosum is famously not a fungus, but an oomycete, or "water mold." Although it forms mycelia that are rather fungus-like, its cell walls contain β-glucans and cellulose rather than chitin, its cytoplasmic membrane lacks the ergosterol characteristic of fungi, and importantly, the organism develops biflagellated zoospores in wet environments.[5] In some oomycetes, zoospore formation can occur in minutes on contact with water, considered one of the fastest developmental processes of any organism; however, *P. insidiosum* is rather leisurely about the process, which takes one hour or more in this species.[5]

Once developed, these motile zoospores are chemotactically attracted to defects in mammalian epithelium where they encyst on and adhere to injured tissues via a secreted glycoprotein. *P. insidiosum* grows optimally at mammalian body temperature, which stimulates the zoospores to develop hyphae that secrete proteases to aid their extension through injured tissues, including endothelium.[5]

As hyphae penetrate tissues, they release antigens that are sampled by antigen presenting cells and presented to naïve T lymphocytes. The antigen presenting cells secrete IL-4, which causes the lymphocytes to assume a Th2 phenotype and secrete IL-4, IL-5, and IL-10.[5] These cytokines induce B lymphocytes to secrete IgG, IgM, and IgE antibodies.

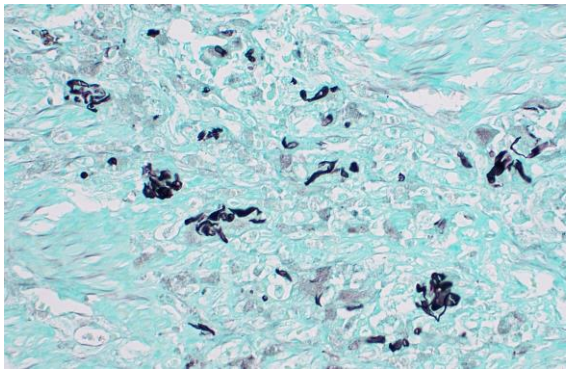

Figure 2-7. Jejunum, dog. A silver stain demonstrates the presence of fungal hyphae within foci of inflammation. (GMS, 400X)

IgE and IL-5 are chemotactic for mast cells and for the eosinophils that characterize *Pythium insidiosum* infection.[5] Summoned by cytokines, mast cells and eosinophils arrive at the scene and degranulate onto the hyphae, causing damage to the organism and to surrounding tissues.

The contributor provides an excellent, thorough review of canine pythiosis. Unlike canine phythiosis, equine pythiosis, also known by the memorable name "swamp cancer," most commonly affects the skin; the intestinal disease seen in dogs is rarely reported in horses.[5] Equine cutaneous lesions occur in skin in contact with water, such as the lower limbs and ventral abdomen, and grossly appear as large, round, granulomatous, ulcerated tissue. On histology, these lesions are granulomatous and characterized by eosinophils and poorly-staining *P. insidiosum* hyphae. The horse uniquely develops multilobulated, irregular cores of necrotic yellow material known as "kunkers," which are formed from degranulated eosinophils and hyphae.[5]

Sheep can develop cutaneous or digestive pythiosis that is substantially similar to the disease in horses and dogs; however, sheep also have their own flavor of pythiosis called ovine rhinofacial pythiosis, or "bull nose."[3] This disease, reported exclusively in Brazil, is an important cause of death and economic loss and is characterized clinically by marked enlargement and deformity of the nasal region, difficulty breathing, and epistaxis.[3] The gross lesion typically extends from the mucocutaneous junction of the nares to the middle nasal cavity and can involve adjacent facial structures, such as the nasal septum and hard palate.[3]

Pythiosis occurs only sporadically in other species. In cats, the disease typically affects the skin and subcutis, but without the ulceration that is common in other species.[3] Cattle in rainy, subtropical climates are sporadically affected, typically on the limbs, by fistulated, ulcerated masses composed of eosinophilic granulomas centered on hyphae.[5] There have been only two reports of pythiosis in birds: ulcerative eosinophilic granulomas in the wings, head, neck, and limbs of a white-faced ibis;[9] and a transmural, necrotic, obstructive esophageal mass filled with heterophils, eosinophils, and hyphae in the esophagus of a red-necked ostrich.[2]

Conference discussion focused on the unique features of this organism, including its dimorphic life cycle, unique cell wall composition, and the inability to differentiate *Pythium* spp. from *Lagenidium* spp. and from the zygomycetes (*Conidiobolus* spp. and *Basidiobolus* spp.) without molecular methods such as PCR.

References:

1. Berryessa, NA, Marks SL, Pesavento PA, et al. Gastrointestinal pythiosis in 10 dogs from California. *J Vet Intern Med*. 2008; 22:1065-1069.
2. de Souto EPF, Kommers GD, Souza AP, et al. A retrospective study of pythiosis in domestic animals in northeast Brazil. *J Comp Pathol*. 2022;195:34-50.
3. do Carmo PMS, Uzal FA, Riet-Correa F. Diseases caused by *Pythium insidiosum* in sheep and goats: a review. *J Vet Diagn Invest*. 2021;33(1):20-24.
4. Fischer, JR, Pace LW, Turk JR, Kreeger JM, Miller MA, Gosser HS. Gastrotinestinal pythiosis in Missouri dogs: eleven cases. *J Vet Diagn Invest.* 1994; 6:380-382.
5. Gaastra W, Lipman LJA, De Cock AWAM, et al. Pythium insidiosum: An overview. *Veterinary Microbiology.* 2010;146:1-16.
6. Grooters, A. Pythiosis, lagenidiosis, and zygomycosis in small animals. *Vet Clin Small Anim.* 2003; 33:695-720.

7. Kepler D, Cole R, Lee-Fowler T, Koehler J, Shrader S, Newton J. Pulmonary pythiosis in a canine patient. *Vet Radiol Ultrasound*. 2019; 60:E20-E23.
8. Liljebjelke KA, Abramson C, Brockus C, Greene CE. Duodenal obstruction caused by infection with Pythium insidiosum in a 12-week-old puppy. *JAVMA*. 2002; 220(8):1188-1191.
9. Pesavento PA, Barr B, Riggs SM, Eigenheer AL, Pamma R, Walker RL. Cutaneous pythiosis in a nestling white faced ibis. *Vet Pathol*. 2008;45:538-541.
10. Reagan KL, Marks SL, Pesavento PA, Maggiore AD, Zhu BY, Grooters AM. Successful management of 3 dogs with colonic pythiosis using itraconazole, terbinafine, and prednisone. *J Vet Intern Med*. 2019; 33:1434-1439.
11. Schmidt CW, Stratton-Phelps M, Torres BT, et al. Treatment of intestinal pythiosis in a dog with a combination of marginal excision, chemotherapy, and immunotherapy. *JAVMA*. 2012; 241 (3):358-363.

CASE III:

Signalment:
27-week-old female laying hen, avian (*Gallus gallus domesticus*)

History:
A laying hen farm with 6 houses and a total of 180,000 animals reared in enriched cages showed an episode of severe respiratory clinical signs in one of the houses with 24-week-old laying hens. The process was diagnosed as an outbreak of infectious laryngotracheitis (ILT) based on compatible severe respiratory signs and consistent gross lesions and was further confirmed by PCR. One month later, the birds continued displaying severe respiratory signs and similar gross lesions at postmortem examinations, but with

Figure 3-1. Trachea, chicken. The tracheal epithelium is diffusely hyperplastic and there is a luminal plug of necrotic epithelium and inflammatory cells. (HE, 5X)

fewer fibrinonecrotic intratracheal casts and proliferative mucosal lesions. Information regarding productive parameters or total flock mortality was not revealed by the producer. Four chickens were submitted for gross postmortem examination, and formalin-fixed samples of the tracheas were submitted for further histopathological evaluation in the diagnostic facilities. The batch had been vaccinated at 8 weeks against *Gallid herpesvirus 1* (GaHV-1) with an eye drop attenuated live vaccine and against fowlpox virus (FWPV) with an attenuated live vaccine by wing web vaccination. Vaccination against other common pathogens was performed following routine vaccination protocol.

Gross Pathology:
All tracheas showed similar changes. The tracheal wall was moderately to markedly thickened, conferring a pipe-stem appearance, which greatly narrowed the tracheal lumen. Tracheal lumina were variably occluded by white dense casts.

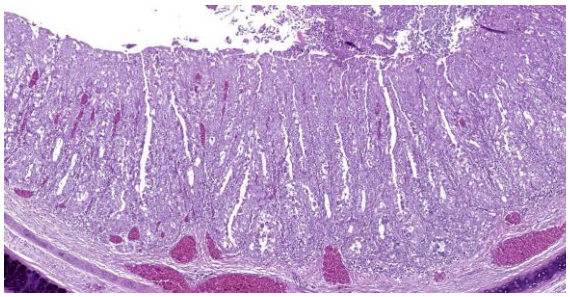

Figure 3-2. Trachea, chicken. The tracheal epithelium thrown into thick villar folds. (HE, 79X)

Laboratory Results:
PCR assays for *Gallid herpesvirus 1* (GaHV-1) and fowlpox virus (FWPV) performed on tracheal samples were positive for both pathogens.

Microscopic Description:
The tracheal lumen is markedly narrowed due to a massive circumferential thickening of the tracheal mucosa, consisting of hyperplastic and hypertrophic epithelial cells. These epithelial cells frequently display cytoplasmic tumefaction and rarefaction (ballooning degeneration). A single 15-50 µm round or ring-shaped eosinophilic inclusion is observed in the cytoplasm of many of the epithelial cells (Bollinger body). In the tracheal lumen large amounts of necrotic debris, degenerated heterophils, abundant bacterial colonies, eosinophilic fibrillar material (fibrin) and mucus are also observed. There are several syncytial cells containing 5-15 nuclei with 3-6 µm eosinophilic intranuclear inclusion bodies that marginate the chromatin and are surrounded by a clear halo. The lamina propria is further expanded by abundant lymphoplasmacytic and, to a lesser extent, heterophilic infiltration.

Contributor's Morphologic Diagnoses:
1. Trachea: Diffuse, circumferential, subacute, severe, hyperplastic, and necrotizing tracheitis with intralesional Bollinger bodies.
2. Trachea: Diffuse, circumferential, subacute, severe, fibrinonecrotizing tracheitis with intralesional syncytial cells and intranuclear inclusion bodies.

Contributor's Comment:
Poultry viral infections are common causes of disease and economic loss and are thus major concerns in poultry production. Infectious laryngotracheitis (ILT) is a respiratory disease of chickens, pheasants, and peafowl which is caused by *Gallid herpesvirus 1* (GaHV-1), an alphaherpesvirus.[8] ILT can cause large economic losses in high density poultry-producing regions; consequently, many efforts are focused on diagnosing and controlling ILT through vaccination, mainly in the form of live attenuated vaccines.[2] These vaccines generally prevent and reduce the severity of the disease and associated mortality, although birds may become latent carriers and shedders of vaccinal viruses. Occasionally, transmission of these vaccinal viruses can occur, enabling viruses to regain virulence and produce mortality, particularly when vaccines are administered in the drinking water or in spray or when Chicken Embryo Origin (CEO) vaccines (as in our case) are used.[6]

Virulence is variable across GaHV-1 strains, which results in ILT having variable degrees of severity. In all cases, virus replicates in epithelial cells across the respiratory tract and conjunctiva, causing severe epithelial damage and accounting for the clinical signs which usually include nasal discharge, conjunctivitis, moist rales, dyspnea, and expectoration of blood-stained mucus. In severe cases, mucoid casts in the trachea obstruct the

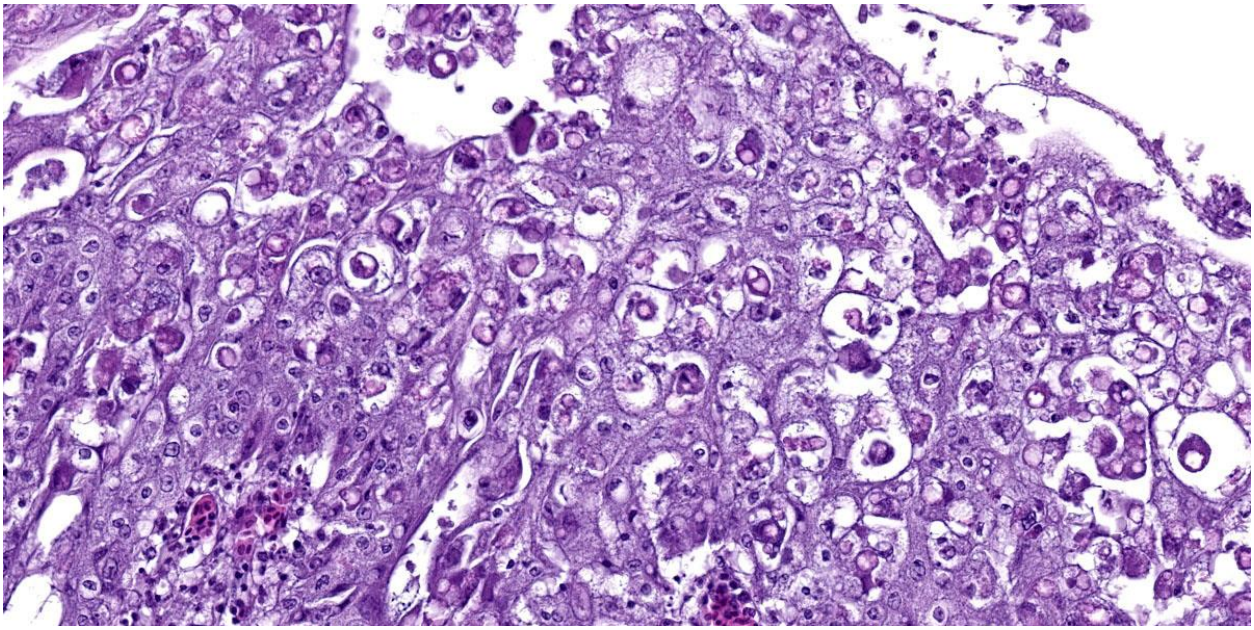

Figure 3-3. Trachea, chicken. The tracheal epithelium exhibits ballooning degeneration with large intracytoplasmic poxviral inclusions ("Bollinger bodies"). (HE, 200X)

airways and lead to asphyxiation.[1]

All these signs correlate with the presence of gross and microscopic findings, which include mucoid to necrotizing tracheitis, frothy ocular secretions, and swelling of infraorbital sinuses caused by epithelial degeneration and necrosis of the previously mentioned tissues. Microscopically, this epithelial damage is often accompanied by lymphocytic and heterophilic inflammation and by syncytial cells with nuclear inclusions, characterized by strong eosinophilic staining surrounded by clear halos. These nuclear inclusions are commonly used as a powerful diagnostic technique as they are pathognomonic for ILT, although they are only present between days 2 and 5 post infection.[11] Birds that survive this acute phase display hyperplastic changes of the epithelium lining the respiratory tract after the first wave of necrosis with absence of syncytial cells and inclusions, which limits histological diagnosis.[1] In the absence of nuclear inclusions, molecular techniques are needed for definitive diagnosis.

Other significant avian pathogens include viruses of the *Poxviridae* family, which includes the genus *Avipox*. Fowlpox virus (FWPV) affects commercial poultry with variable disease manifestations, including cutaneous or diphteric/pharyngeal forms. In the poultry industry, this disease, commonly referred to as fowlpox, is controlled through live modified virus vaccines, which prevent disease manifestations and further production implications.[3] Despite vaccinal efficacy, numerous outbreaks in vaccinated flocks have been reported. Emergence of variant strains of FWPV and enhanced virulence due to the integration of avian reticuloendotheliosis virus (REV) into their genomes are believed to be the main causes of outbreaks in vaccinated animals.[9] Viral genome sequencing was not performed in our case in order to rule out these possibilities. Furthermore, technical vaccine failure cannot be fully ruled out.

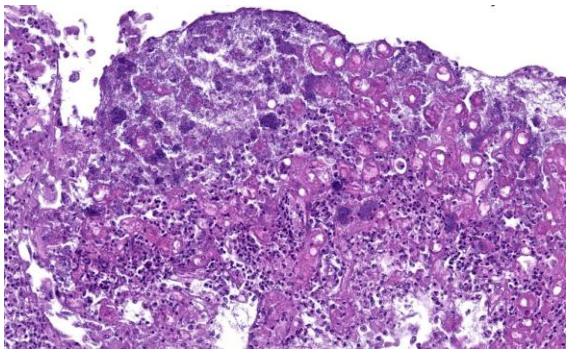

Figure 3-4. Trachea, chicken. The luminal plug is composed of sloughed pox-virus-laden epithelium, infiltrating necrotic and viable neutrophils, abundant cellular debris, and numerous bacterial colonies. (HE, 200X)

Viral replication of FWPV occurs in epithelial cells of the skin and upper alimentary and respiratory tracts, which provoke hyperplastic and proliferative lesions characteristic of poxvirus infections. These lesions are represented grossly by cankers, elevated nodules or patches, and diphteric yellowish lesions in the mucous membranes of the mouth, oesophagus or trachea. These lesions account for the severe respiratory signs commonly exhibited by affected birds. Histologically, affected epithelium is hyperplastic and hypertrophic and undergoes necrosis in the apical region. Infected epithelial cells frequently display large intracytoplasmic inclusion bodies, which are called Bollinger bodies.[11]

Both GaHV-1 and FWPV can result in severe respiratory signs, and significant overlap exists in their clinical signs and gross lesions. To reach definitive diagnosis, samples are usually sent to diagnostic facilities and confirmation is based on histopathological evaluation or molecular diagnostics. Observation of typical viral inclusions of either of the infections is a usual path to definitive diagnosis. Nevertheless, simultaneous dual infections have been described in commercial chickens, and although not common due to generally effective vaccination, the characteristic histological lesions and inclusion bodies of both viruses can appear in the same tracheal section, as in this case.[5,10]

Contributing Institution:
Veterinary Pathology Department
Autonomous University of Barcelona
Barcelona, Spain.
https://www.uab.cat/

JPC Diagnoses:
1. Trachea: Tracheitis, proliferative and necrotizing, circumferential, severe, with ballooning degeneration, and intracytoplasmic viral inclusions.
2. Trachea: Tracheitis, necrotizing, circumferential, with few viral syncytia and intranuclear inclusions.

JPC Comment:
Infectious laryngotracheitis (ILT) has a narrow natural host range when compared with other alphaherpesviruses, and is primarily a disease of chickens. The disease is highly contagious and infected birds shed the virus in their respiratory secretions for 10 days post-infection.[7] GaHV-1 can infect the host via respiratory, ocular, or oral routes, and can be spread by direct transmission from an infected bird or a latent carrier, or through fomites such as litter, feed bags, feathers, dust, footwear, and clothing.[7]

Once inside the animal, replication in the conjunctival, sinus, laryngeal, and tracheal epithelium leads to inflammation, serous or mucoid nasal and ocular discharge, and respiratory distress.[4] The key histologic features used to diagnose ILT are syncytial cells with intranuclear inclusion bodies, most frequently present in the trachea, nasal turbinates and sinuses, conjunctiva, larynx, and primary bronchi.[4] With disease progression, the laryngeal and proximal tracheal epithelium sloughs into the lumen, forming an

exudate that accumulates in the syrinx, and this necrosis and sloughing of the superficial epithelium likely accounts for the loss of identifiable syncytial cells by 5 days post-infection.[4]

The virulence of ILT varies with the infecting strain and is exacerbated by concurrent infection with other respiratory pathogens such as *Mycoplasma gallisepticum, Mycoplasma synoviae*, infectious coryza, and reticuloendotheliosis virus, as well as immunosuppression, including immunosuppression secondary to Marek's disease.[7] If the animal survives, ILT virus may flock to the trigeminal ganglion and, like any good herpesvirus, may establish a life-long latent infection that can be reactivated during periods of stress.

The clinical signs of ILT are similar to those of other viral respiratory diseases of chickens, including Newcastle Disease, Fowl Pox, Infectious Bronchitis, and Avian Influenza.

These diseases can typically be differentiation with histology. In Newcastle disease, surface epithelium is usually still intact, in contrast to the necrosis and sloughing seen with ILT, and multiple organ systems are affected. Fowl pox, as seen in this case, is characterized by large eosinophilic *cytoplasmic* viral inclusions (Bollinger bodies) in contrast to the much smaller, intranuclear viral inclusions of early ILT infection; affected epithelium is proliferative rather than necrotic; and syncytial cells are absent. Finally, infectious bronchitis and avian influenza typically affect a wider range of tissues, most notably the lower respiratory tract.

In conference, the moderator led a discussion of the biology of the two viruses implicated in this case and discussed ways to simplify infectious disease pathology by grouping viruses and bacteria into "boxes" with similar behaviors. The "Pox box" was opened, and

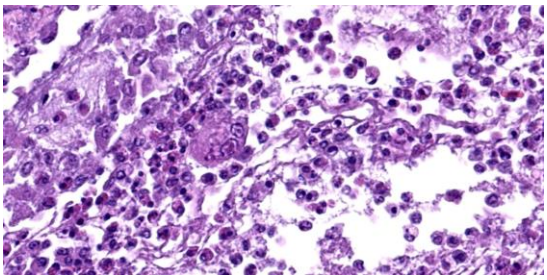

Figure 3-5. Trachea, chicken. Rare multinucleated epithelial cells within the luminal plug contain herpeviral intranuclear inclusions. (HE, 892X)

participants were treated to a review of the some of the more singular poxviruses, including ectromelia, rabbit (Shope) fibroma virus, and myxoma virus.

As the contributor notes, the two concurrent diseases in this case have overlapping histologic features and considerable conference discussion centered on whether it was possible to attribute particular histologic lesions with a specific etiology.

In the end, participants settled on a pair of morphologic diagnoses that, in their redundancy, acknowledge these overlapping clinical and histologic features.

References:

1. Abdul-Aziz T, Fletcher OJ, Barnes HJ. *Avian histopathology*. 4th ed. American Association of Avian Pathologists; 2016.
2. Bagust TJ, Jones RC, Guy JS Avian infectious laryngotracheitis. *Rev. Sci. Tech.* 2000;19(2):483–492.
3. Bolte AL, Meurer J, Kaleta EF. Avian host spectrum of avipoxviruses. *Avian Pathol.* 1999;28(5):415-432.
4. Carnaccini S, Palmieri C, Stoute S, Crispo M, Shivaprasad HL. Infectious laryngotracheitis of chickens: pathologic and immunohistochemistry findings. *Vet Pathol*. 2022;59(1):112-119.
5. Davidson I, Raibstein I, Altory A.

Differential diagnosis of fowlpox and infectious laryngotracheitis viruses in chicken diphtheritic manifestations by mono and duplex real-time polymerase chain reaction. 2014; *Avian Pathol*. 2015;44(1):1-4.
6. García, M. Current and future vaccines and vaccination strategies against infectious laryngotracheitis (ILT) respiratory disease of poultry. *Vet. Microbiol*. 2017;206:157–162.
7. Gowthaman V, Kumar S, Koul M, et al. Infectious laryngotracheitis: etiology, epidemiology, pathobiology, and advances in diagnosis and control: a comprehensive review. *Vet Q*. 2020;40(1):140-161.
8. Menendez KR, García M, Spatz S, Tablante NL. Molecular epidemiology of infectious laryngotracheitis: a review. *Avian Pathol*. 2014;43(2):108-17.
9. Singh P, Kim TJ, Tripathy DN. Re-emerging fowlpox: evaluation of isolates from vaccinated flocks. *Avian Pathol*. 2000;29(5):449-455.
10. Song HS, Kim HS, Kim SH, Kwon YK, Kim HR. Research Note: Simultaneous detection of infectious laryngotracheitis virus, fowlpox virus, and reticuloendotheliosis virus in chicken specimens. *Poult. Sci*. 2021;100(4):100986.
11. Swayne DE, ed. *Diseases of poultry*. 14th ed. Wiley; 2019.

CASE IV:

Signalment:
1-year-old male castrated Boxer, canine (*Canis familiaris*)

History:
The patient presented to the Matthew J. Ryan Veterinary Hospital of the University of Pennsylvania (MJR-VHUP) emergency service with a history of two swellings/masses on the left ventral jaw and adjacent to the left nostril as well as acute vomiting, weight loss, hyporexia, and lethargy. The masses were originally noted by the primary veterinarian who started systemic antibiotics. Over the 14-day course of antibiotics, the masses reduced in size, but subsequently rapidly grew upon completion of the course of antibiotic therapy. Due to the lack of resolution, the primary veterinarian performed a sedated oral exam, skull radiographs, and bloodwork approximately 3 weeks after the patient's initial presentation. The radiographs demonstrated regional soft tissue swelling but no obvious intraoral component. The complete blood count showed a neutrophilic leukocytosis. The patient became progressively lethargic and hyporexic over the following 24 hours and was presented to the emergency service at MJR-VHUP the next day.

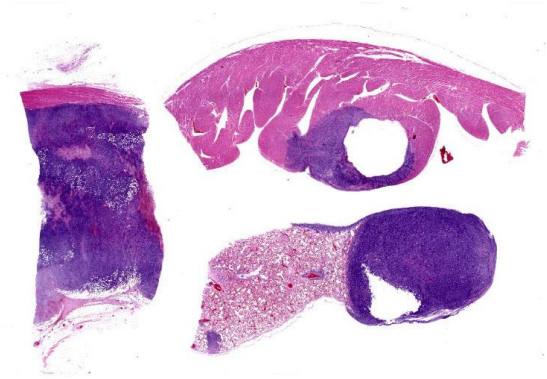

Figure 4-1. Skeletal muscle, heart, lung, dog. A metastatic neoplasm is present in these three submitted tissues. (HE. 5X)

On clinical examination at MJR-VHUP, there was an approximately 10 cm diameter, firm, moveable mass on the left ventrocaudal face at the level of the mandible, which extended to the level of the left maxilla. The mass caused partial occlusion of the left naris and lateral deviation of the nose. The patient was hospitalized and transferred to the Internal Medicine service. Over the course of the patient's 3-day hospitalization, an abdominal ultrasound and thoracic radiographs were performed, which revealed multiple soft tissue nodules throughout the thoracic and

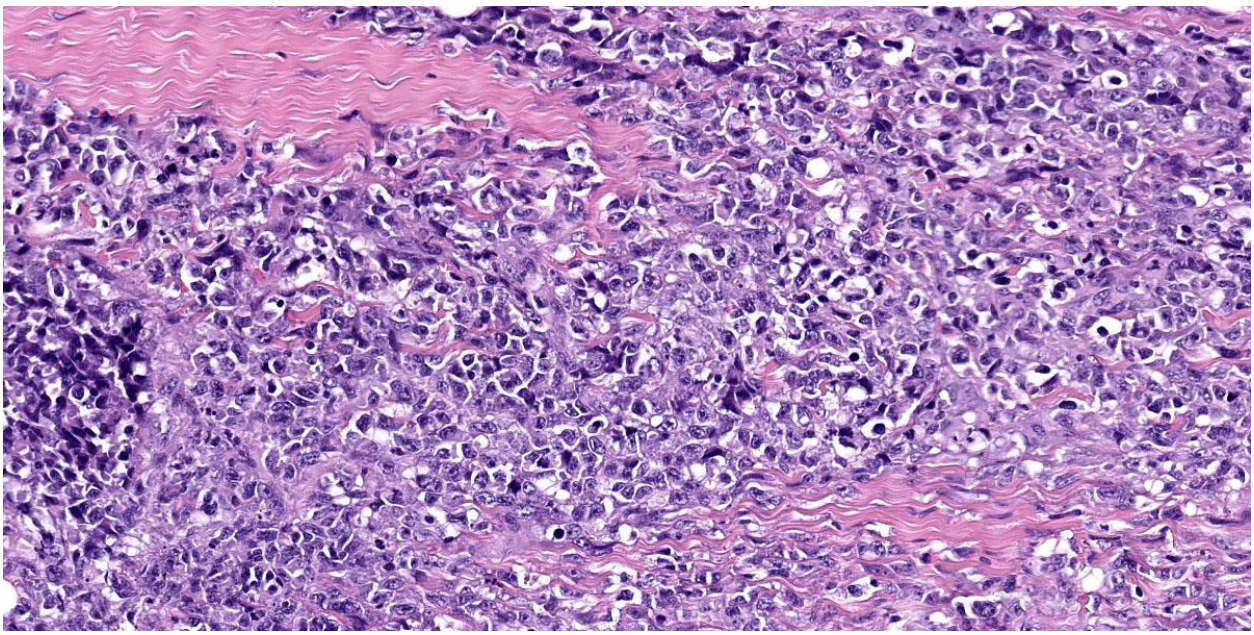

Figure 4-2. Skeletal muscle, dog. The muscle is effaced by sheets of pleomorphic cells. (HE, 319X)

abdominal cavity. Subsequent physical exams revealed additional masses on the left shoulder and within the left and right epaxial muscles. Fine needle aspirates of the left facial/submandibular mass revealed a malignant neoplasm. Due to the rapid, aggressive progression of disease and poor prognosis, euthanasia was performed and a full postmortem examination was completed.

Gross Pathology:
Extending from the rostral muzzle just left of midline to the ventral submandibular region was a 16 x 8 x 6 cm multilobulated, variably firm to hard, white and tan mass that infiltrated through the right nasal bone and rostral hard palate, into the nasal cavity, and expanded the nasal turbinates and displaced the maxillary incisors. On cut surface within the individual neoplastic lobules, the center of the tissue was dark red to brown and variably soft to gelatinous. Similar multilobulated and sometimes cavitated nodules, ranging from 1 cm diameter to 7 x 4 x 2 cm, infiltrated the skeletal muscle of the caudal aspect of the left shoulder, left craniolateral abdominal body wall, left superficial inguinal subcutis, left midabdominal epaxial, and right lumbar epaxial muscles.

Within the thoracic cavity, innumerable nodules expanded the mediastinum, pericardium, pleural surfaces of the thoracic walls, myocardium, and pulmonary parenchyma. Within the abdominal cavity, the omentum, left lobe of the pancreas, and left adrenal gland were expanded by similar nodules. The cavitated nodules often contained a small to moderate amount of dark brown watery to yellow-brown thick opaque fluid. The thoracic cavity contained approximately 1150 mL of watery, light red, opaque fluid.

The left retropharyngeal, left axillary, tracheobronchial, sternal, and mediastinal lymph nodes were enlarged (measuring up to 6 x 1 x 2 cm), had loss of corticomedullary distinction, and were effaced by similar tissue as described above.

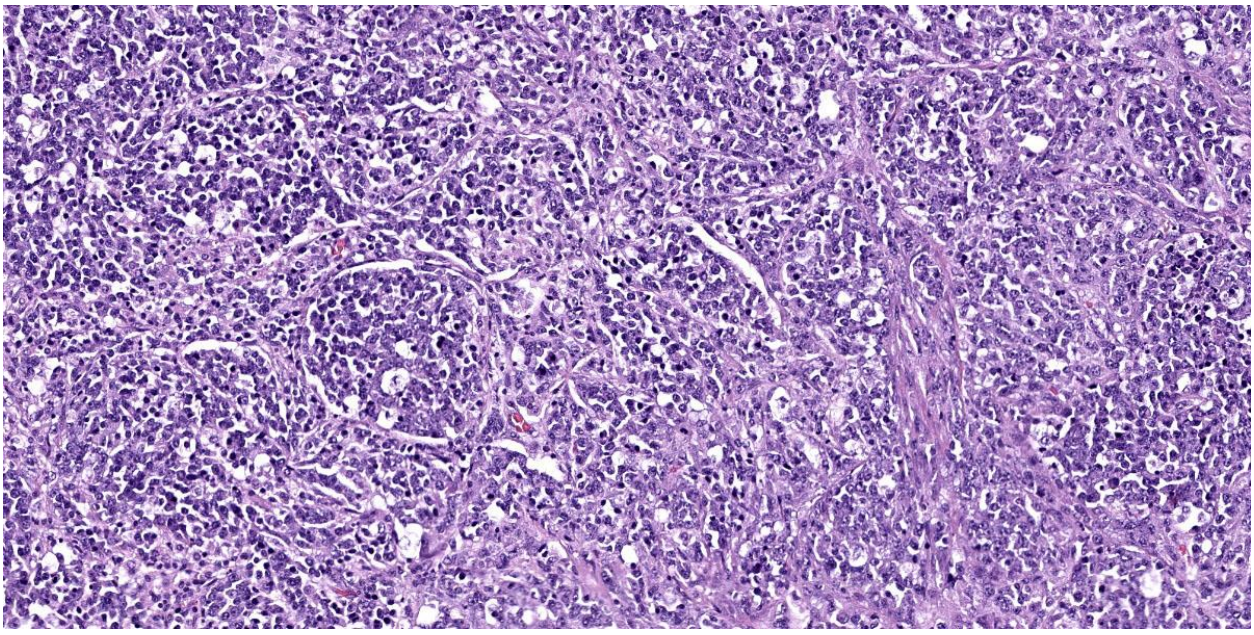

Figure 4-3. Lung, dog. Neoplastic cells expand alveolar septa and fill alveoli. (HE, 87)

Laboratory Results:
Tissue culture from the mass yielded no growth on aerobic or anaerobic cultures.

Antemortem cytology of the left mandibular mass showed neoplastic cells amid a light pink, stippled proteinaceous background. Neoplastic cells were pleomorphic, mainly round when individualized, occasionally spindled, and slightly polygonal when seen in clusters. Nuclei were round to irregularly shaped, with reticular chromatin and occasionally visible light blue irregular nucleoli. There was a scant to moderate amount of deep blue cytoplasm with frequent blebbing, paranuclear clearing, and several distinct vacuoles, rarely containing 1-2 small dark blue/green granules. Mitotic figures were moderately frequent and contained atypical forms.

The cytology sample was diagnosed as a malignant neoplasm, with the primary differential diagnoses including a poorly melanotic/amelanotic melanoma, epithelioid hemangiosarcoma, rhabdomyosarcoma, anaplastic carcinoma, or other embryonal tumor.

Microscopic Description:
Skeletal muscle from the face: One section of skeletal muscle from the face is examined. The tissue architecture is infiltrated to completely effaced by an unencapsulated, densely cellular neoplasm, composed of round to polygonal to spindle-shaped cells arranged in sheets, bundles, streams, and packets separated by a fine fibrovascular stroma. Neoplastic cells have variably distinct cell borders with a scant to moderate amount of eosinophilic to amphophilic cytoplasm and round to ovoid nuclei with open chromatin and a single variably prominent nucleolus. Anisocytosis and anisokaryosis are moderate to marked and there are up to 23 mitotic figures in a single 40x high power field (0.237 mm2). There are multifocal regions of necrosis throughout the neoplastic parenchyma. The skeletal muscle fibers incorporated amongst neoplastic cells exhibit varying degrees of degeneration and necrosis, including hypereosinophilic and swollen to fragmented, amphophilic and granular sarcoplasm.

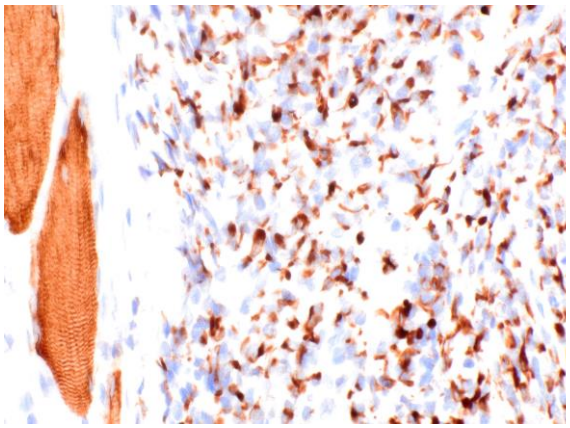

Figure 4-4. Skeletal muscle, dog. Neoplastic cells demonstrate strong cytoplasmic immunoreactivity to desmin. (*Photo courtesy of:* University of Pennsylvania School of Veterinary Medicine, Department of Pathobiology, https://www.vet.upenn.edu/veterinary-hospitals/ryan-veterinary-hospital/services/diagnostic-laboratories). (anti-desmin, 400X)

Heart: One full thickness section of the right ventricular free wall is examined. Within the myocardium and extending through the epicardial surface, there is an infiltrative unencapsulated densely cellular neoplasm comprised of spindle-shaped to polygonal cells arranged in haphazard streams and packets with a scant fibrous stroma. Neoplastic cells are similar to those described in the facial skeletal muscle with large regions of coagulative necrosis scattered throughout the parenchyma. The incorporated myocardial muscle fibers are surrounded by neoplastic cells and demonstrate shrunken angular sarcoplasm (atrophy).

Lung: One section of lung is examined. Within the pulmonary parenchyma, occasionally surrounding large blood vessels, there are multiple variably well-defined to infiltrative, unencapsulated, densely cellular foci of similar round to polygonal neoplastic cells arranged in sheets and packets amongst a fine stroma forming thin fibrous septa. Neoplastic cells infiltrate along the pleural surface and are present within small pulmonary vessels and alveolar capillaries. Adjacent to the neoplastic nodules, there is minimal to mild pulmonary edema with increased numbers of foamy macrophages within the alveolar lumen.

Immunohistochemical staining with PNL2, desmin, CD3, and CD79b were performed on sections of the neoplasm in the skeletal muscle of the face. Neoplastic cells were diffusely negative for PNL2, CD3, and CD79b. Greater than 90% of the neoplastic cells exhibited strong, diffuse, cytoplasmic immunoreactivity with desmin.

Tissues pertinent to the clinical presentation but not included in the submission include the rostral maxillary bone, nasal cavity, and liver. The cortical bone of the rostral maxilla and hard palate was disrupted and effaced by neoplastic cells, which extended into the submucosa of the overlying gingiva and rostral nares. The centrilobular sinusoids within the liver were mildly dilated and filled with blood, interpreted as mild acute passive congestion.

Contributor's Morphologic Diagnoses:
1. Skeletal muscle: Rhadomyosarcoma.
2. Heart and Lung: Metastatic rhadomyosarcoma.

Contributor's Comment:
Based on the clinical history, patient signalment, and cellular morphology on histopathology, differentials for the neoplasm included an amelanotic malignant melanoma, lymphoma, or embryonal tumor, such as a rhabdomyosarcoma of juvenile dogs. The immunohistochemical staining profile is compatible with a rhabdomyosarcoma. The maxillofacial region is favored as the site of origin for this neoplasm, given the clinical history and degree of local invasion; however, with the extensive multi-organ involvement and

overall poor cellular differentiation, a different primary location is not entirely ruled out. Rhabdomyosarcoma (RMS) is a malignant neoplasm of skeletal muscle derived from pluripotent stem cells or mesenchymal progenitor cells capable of myogenic differentiation.[2] This neoplasm is relatively rare in veterinary species and the current literature suggests this neoplasm more commonly arises in dogs younger than 2 years of age.[2,3] In the human medical literature, RMS is considered a common head and neck tumor of children.[7] Immunohistochemistry is commonly utilized to differentiate RMS from other neoplasms because of the variable microscopic appearance, primary locations, and frequent lack of well-differentiated skeletal muscle within RMS. Due to the inconsistent and variable staining properties, as well as lack of specificity of more commonly available skeletal muscle markers (i.e. desmin), a recent publication suggests the use of immunohistochemical markers MyoD1 and myogenin in conjunction with desmin, to improve the accuracy of diagnosing these challenging tumors.[12]

Following the histologic classification criteria outlined in the Caserto 2013 review, the RMS in this case had features consistent with a solid alveolar subtype, characterized by the majority of the neoplastic foci arranged in sheets of round cells closely packed together and divided by thin fibrous septa, reminiscent of a "neuroendocrine pattern." Within the current veterinary literature, this subtype is less frequently diagnosed; however, the true incidence of the different subtypes is unclear given the diagnostic challenge and IHC often needed to make a definitive diagnosis. There is little supporting outcome data in veterinary literature to evaluate prognosis between different subtypes; however, alveolar RMS are considered more locally aggressive with a higher metastatic rate in human patients.[2,10] Case reports of this subtype of canine RMS in the veterinary literature frequently note significant local invasion into the maxilla and an overall, poor clinical progression of disease, similar to what was seen in this case.[4,5,7-9] Other primary locations reported in the human and veterinary literature include the urogenital tract, retroperitoneum, tongue, oral cavity, larynx, skin, heart, and peripheral appendicular and axial skeletal muscle.

Perhaps due to the aggressive disease progression, poor prognosis, and euthanasia at time of initial diagnosis, metastatic rate and sequelae are relatively less frequently discussed in regards to RMS of juvenile dogs; however, a striking feature of this case is the staggering metastatic disease throughout peripheral lymph nodes, skeletal muscle, and thoracic and abdominal cavities. The aggressive nature and pathogenesis of metastasis in human alveolar and embryonal RMS have been attributed to several mutations in transcription factors. A mutation as a result of translocation and fusion of the PAX-FKHR genes has been shown to result in uncontrolled cell growth, progression through the cell cycle, and loss of tumor suppressor function, and is considered a significant factor in the aggressive phenotype seen in alveolar RMS.[2] The transcription factors LMO4 and FOXF1 are involved in tumor migration and are shown to be overexpressed in RMS with distant metastasis.[1] Snail1, a transcription factor associated with epithelial-mesenchymal transition, is shown to be highly expressed in alveolar RMS. It is presumed that this contributes to the downregulation of E-cadherin and increased expression of matrix metalloproteinases (MM2 and MM9), further promoting tumor invasion and metastasis.[1] The IL4 receptor signaling pathway in RMS has also been shown to recruit myoblasts to form mature myotubes, stimulate cell proliferation through the JAK/STAT signaling pathway, and may be involved with lymph node and pulmonary metastasis via CD4+ T

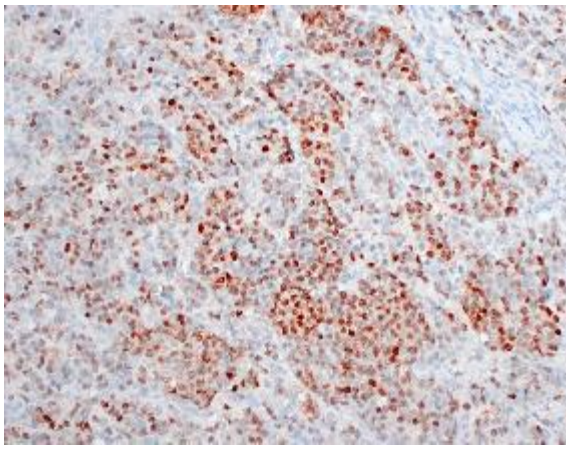

Figure 4-5. Skeletal muscle, dog. Neoplastic cells demonstrate strong nuclear immunoreactivity to myoblast determination protein. (anti-myoD1, 400X)

cell/TH2 cell activation of tumor-associated macrophages.[6] While these specific factors have not been studied in veterinary species, it is possible that a similar tumor pathogenesis contributes to the aggressive behavior of this neoplasm in dogs.

In this case, the patient's clinical decline is attributed to the extensive metastatic disease leading to multi-organ dysfunction. Given the degree of neoplastic infiltrate within the myocardium, it is presumed there was some degree of cardiac dysfunction resulting in early congestive heart failure, demonstrated by the pathologic changes of acute passive congestion in the liver and significant pleural effusion. Furthermore, the local neoplastic invasion into the maxilla combined with extensive multi-organ involvement likely contributed to the patient's hyporexia and ultimately the progression of clinical disease.

Contributing Institution:
University of Pennsylvania
School of Veterinary Medicine
Department of Pathobiology
https://www.vet.upenn.edu/veterinary-hospitals/ryan-veterinary-hospital/services/diagnostic-laboratories

JPC Diagnosis:
Skeletal muscle, heart, lung: Rhabdomyosarcoma, alveolar type.

JPC Comment:
As the contributor notes, rhabdomyosarcoma (RMS) presents a diagnostic challenge due to its variable histomorphology and lack of evident skeletal muscle differentiation on light microscopic evaluation. Skeletal muscle begins its developmental journey as embryonic mesoderm that differentiates into myogenic progenitor cells under the control of transcription factors such as PAX3 and PAX7.[2] These myogenic progenitor cells proliferate and form immature myoblasts under the direction of myoblast determination protein 1 (MyoD1), a transcription factor that acts at hundreds of gene promoters to drive myoblast proliferation.[2] Via an unknown mechanism, myoblasts fuse and elongate and their nuclei line up in rows, forming myotubes with multiple nuclei and shared cytoplasm. Myogenin, a transcription factor in the same family as MyoD1, then directs the myotubes to begin producing actin and myosin-containing sarcomeres that are characteristic of skeletal muscle.[2] Myogenin causes cell cycle arrest, leading to terminally differentiated muscle fibers without replicative capacity; however, satellite cells at the periphery of the myotubes persist as stem cells which are activated when myocytes are damaged.[2] Mature skeletal muscle expresses very little to no MyoD1 or myogenin, but are immunoreactive for desmin, a muscle-specific intermediate filament.[2]

In veterinary medicine, RMSs are typically diagnosed using histologic evaluation supplemented by desmin IHC staining; however, desmin is expressed in many canine neoplasms, including leiomyosarcomas, leiomyomas, and malignant fibrous histiocytomas, and, consequently, positive desmin immunoreactivity has a specificity of around 70% for

RMS.[12] For this reason, when rhabdomyosarcoma is suspected, the current recommendation is to run an IHC panel consisting of desmin, MyoD1, and myogenin, all of which were positive in this tumor.[12]

Canine RMSs are subclassified into three broad categories: embryonal, alveolar, and pleomorphic. Embryonal RMSs are characterized by neoplastic cells that exhibit different stages of development, from myoblastic cells to myotubular cells. Embryonal RMSs are further divided into myotubular (multinucleated and elongated tubular cells), rhabdomyoblastic (large round cells with abundant cytoplasm), and spindle cell (fusiform cells arranged in streams) variants, depending on which embryonal features predominate.[2] Alveolar RMSs are further subclassified into classic alveolar RMS, where fibrous bands divide small round cells into clusters, and solid alveolar RMS, characterized by closely packed round cells with or without thin fibrous septa.[2] Finally, pleomorphic RMSs are characterized by haphazardly arranged spindle cells with marked anisocytosis and anisokaryosis with bizarre mitotic figures.[2] We agree with the contributor that the histologic features of this tumor most closely resembles a solid alveolar RMS. While histologic subtype carries prognostic significance in human RMSs, these associations have not yet been established in veterinary medicine.

Conference discussion focused on the various subtypes of rhabdomyosarcoma and the use of immunohistochemical stains (desmin, MyoD1, myogenin, and PTAH) used to diagnose them. The moderator drew attention to a subtype of embryonal rhabdomyosarcoma, the botryoid rhabdomyosarcoma, which most frequently occurs in the trigone of the urinary bladder in young, large breed dogs. Grossly, this tumor has a polypoid ("botryoid," or "grape-like") appearance that projects into the lumen of the urinary bladder. Histologically, this subtype contains undifferentiated myoblast cells and multinucleated myotube cells in a myxomatous stroma.

References:

1. Armeanu-Ebinger S, Bonin M, Häbig K, et al. Differential expression of invasion promoting genes in childhood rhabdomyosarcoma. *Int J Oncol*. 2011;38(4): 993–1000.
2. Caserto BG. A comparative review of canine and human rhabdomyosarcoma with emphasis on classification and pathogenesis. *Vet Pathol*. 2013;50(5): 806–826.
3. Cooper BJ, Valentine BA. Tumors of muscle. In: Meuten DJ, ed. *Tumors in Domestic Animals*, 5th ed. Ames, Iowa: Iowa State Press; 2017:444-466.
4. Gandi L, Vivekanand S. Maxillofacial rhabdomyosarcoma in the canine maxillofacial area. *Vet World*. 2012 *5*(9): 565-567.
5. Gillem JM, Sullivan L, Sorenmo KU. Diagnosis and multimodal treatment of metastatic maxillofacial juvenile embryonal rhabdomyosarcoma in a young golden retriever. *J Am Anim Hosp Assoc.* 2018:54(5)e545-05.
6. Hosoyama T, Aslam MI, Abraham J, et al. IL-4R drives dedifferentiation, mitogenesis, and metastasis in rhabdomyosarcoma. *Clin Cancer Res*. 2011;17(9): 2757–2766.
7. Kim DY, Hodgin EC, Cho DY, Varnado JE. Juvenile rhabdomyosarcomas in two dogs. *Vet Pathol.* 1996;33(4), 447-450.
8. Murakami M, Sakai H, Iwatani N, et al. Cytologic, histologic, and immunohistochemical features of maxillofacial alveolar rhabdomyosarcoma in a juvenile dog. *Vet Clin Pathol*. 2010;39(1):113–118.
9. Nakaichi M, Itamoto K, Hasegawa K. et al. Maxillofacial rhabdomyosarcoma in the canine maxillofacial area. *J Vet Med Sci.* 2007; 69(1):65-67.

10. Otrocka-Domagala I, Pazdzior-Czapula K, Gesek M, et al. Aggressive, solid variant of alveolar rhabdomyosarcoma with cutaneous involvement in a juvenile Labrador retriever. *J Comp Pathol.* 2015;152(2–3):177–181
11. Püsküllüoglu M, Lukasiewicz E, Miekus K, et al. Differential expression of Snail1 transcription factor and Snail1-related genes in alveolar and embryonal rhabdomyosarcoma subtypes. *Folia Histochem Cytobiol*. 2010;48(4):671–677.
12. Tuohy JL, Byer BJ, Royer S, et al. Evaluation of myogenin and MyoD1 as immunohistochemical markers of canine rhabdomyosarcoma. *Vet Pathol.* 2021; 58(3): 516-526.

WSC 2023-2024
Conference 6 Self-Assessment

1. What is the most common presentation of atherosclerosis in birds?
    a. Limb paresis
    b. Abdominal distention
    c. Head tilt
    d. Sudden death

2. Which of the following has not been described as a cause of atherosclerosis in the dog?
    a. Hypothyroidism
    b. Diabetes mellitus
    c. Breed-related hyperlipidemia
    d. Addison's disease

3. True or false: Small intestinal mucinous adenocarcinomas are one of the most common neoplasms in aged NHPs?
    a. True
    b. False

4. Viral inclusions associated with gallid herpesvirus-1 infection are seen in which of the following periods?
    a. 1-3 dpi
    b. 2-5 dpi
    c. 7-10 dpi
    d. 10-14 dpi

5. Which of the following immunohistochemical markers is least useful inidentifiection of rhabdomyosarcoma in the dog?
    a. Desmin
    b. MyoD1
    c. Muscle-specific actin
    d. Myogenin

WEDNESDAY SLIDE CONFERENCE 2023-2024

Conference #7 **04 October 2023**

CASE I:

Signalment:
9-year-old, male neutered mixed breed dog, canine (*Canis familiaris*)

History:
This patient developed skin nodules primarily affecting the distal forelimbs. The nodules were pruritic, alopecic, and erythematous, with minimal hemorrhagic exudate. Prior treatments included antibiotics, ivermectin, and lime sulfur dips.

The patient is a raccoon hunting dog who lives in an outdoor kennel with a concrete floor and no bedding. The dog has not traveled since the lesions began. Approximately 6 months after the nodules developed, multiple punch biopsies were collected from the right elbow and metacarpus and submitted for examination.

Laboratory Results:
A deep skin scraping revealed suspected larval nematodes as well as inflammatory cells and mixed bacteria.

A bacterial culture of the skin grew *Staphylococcus pseudintermedius*.

Microscopic Description:
Diffusely, follicles are large and distended with keratin and occasional nematode larvae that are 20-30 microns in diameter with double lateral alae and a rhabditiform esophagus.

Figure 1-1. Haired skin, dog. There are pruritic, alopecic, and erythematous nodules within the skin. (*Photo courtesy of:* University of Tennessee, College of Veterinary Medicine, Department of Biomedical and Diagnostic Sciences http://www.vet.utk.edu/departments/path/index.php)

There is hyperplasia of the follicular epithelium. Adnexa are surrounded by plasma cells and fewer lymphocytes. There are multifocal aggregates of macrophages, neutrophils, and eosinophils with fewer multinucleated giant cells which tend to be at the base of follicles. In some sections, this inflammation is associated with follicular rupture with release of free keratin, and presumably nematodes, into the periadnexal dermis. There are varying degrees of hemorrhage and fibrosis around the ruptured follicles. Some follicles also contain bacterial cocci. There is diffuse mild epidermal hyperplasia with ortho-keratotic hyperkeratosis.

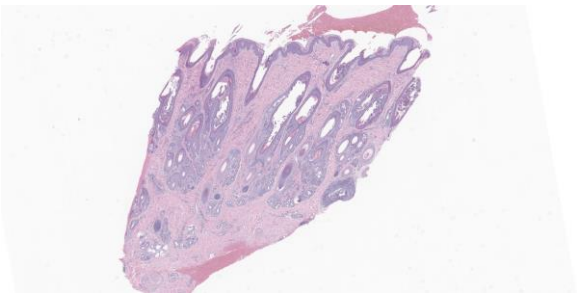

Figure 1-2. Haired skin, dog. A single biopsy of haired skin is submitted for examination. There is diffuse epidermal and follicular epithelial hyperplasia, and hair follicles are dilated. (HE, 5X)

Contributor's Morphologic Diagnosis:
Haired skin: Widespread periadnexal plasmacytic dermatitis with intrafollicular larval nematodes and multifocal follicular rupture with pyogranulomatous dermatitis.

Contributor's Comment:
The clinical, cytologic, and histologic findings are consistent with follicular *Pelodera strongyloides* infection. *P. strongyloides* is a free-living rhabditid nematode that lives in decaying organic matter. Infections are rare, and most infections in the United States have been reported in the Midwestern states.[5] Infections are often associated with dirty environments or the use of damp straw for bedding.[1,5] Cattle, swine, dogs, horses, rodents, sheep, and humans are infected by exposure to infested organic matter.[1,2,5] Lesions occur at sites of contact with contaminated materials, which, in dogs, are primarily the ventrum, paws, distal limbs, perineum, and tail. Short-coated dogs may be more easily parasitized.[5] Removal of the animal from infected bedding may clear the infection, although treatment with anti-parasitics is also warranted.[6] Fittingly, this dog is a short-haired hound dog mix whose lesions were primarily on the distal forelimbs.

Clinically, an erythematous maculopapular rash with variable alopecia is reported. The lesions are extremely pruritic, so there may be associated self-trauma.[5] Histologically, there is epidermal hyperplasia with hyperkeratosis and follicular keratosis. The nematodes can be found in hair follicles and in the superficial keratin.[5] Follicular nematode larvae can penetrate the follicular infundibula, inciting folliculitis that can progress to furunculosis and pyogranulomatous dermatitis.[2] Adnexa are surrounded by mixed inflammatory cells, including eosinophils, lymphocytes, plasma cells, macrophages, and mast cells.[5]

The nematodes are recognized by their small size, double (or paired) lateral alae, rhabditiform esophagus, platymyarian musculature, and intestine lined by uninucleated cells.[3,4] Given the small size of these nematodes, identification of some of these structures on histologic examination is challenging.

Lesions in this dog initially persisted despite appropriate antibiotic therapy, cleaning the environment, and ivermectin treatment. Lesions eventually improved and skin scrapes were negative following treatment with the antibiotic Simplicef (cefpodoxime proxetil) and the broad-spectrum anti-parasitic Advantage Multi (imidacloprid and moxidectin).

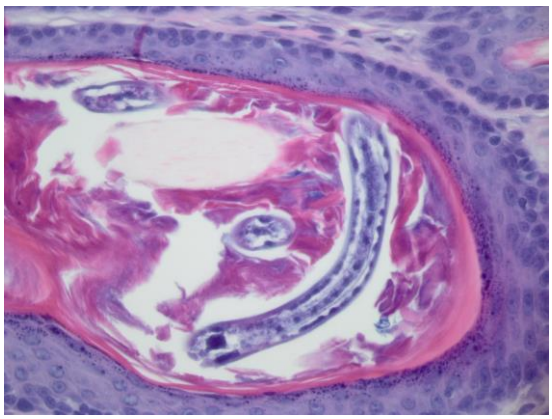

Figure 1-3. Haired skin, dog. Follicles are ectatic and contain keratin debris and numerous nematode larvae. (HE, 400X) (*Photo courtesy of:* University of Tennessee, College of Veterinary Medicine, Department of Biomedical and Diagnostic Sciences)

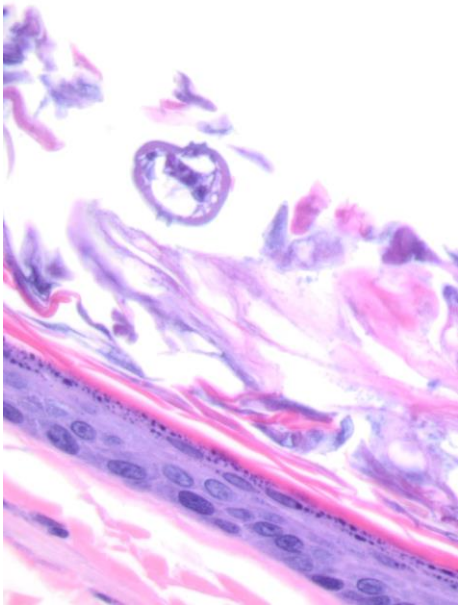

Figure 1-4. Haired skin, dog. Larvae have double lateral alae. (HE, 400X) (*Photo courtesy of:* University of Tennessee, College of Veterinary Medicine, Department of Biomedical and Diagnostic Sciences)

A complete blood count identified consistent leukopenia of unknown cause, so concurrent immunosuppression may have contributed to the infection and delayed response to treatment.

Contributing Institution:
University of Tennessee
College of Veterinary Medicine
Dept. of Biomedical and Biological Sciences
http://www.vet.utk.edu/departments/path/index.php

JPC Diagnosis:
Haired skin: Dermatitis and folliculitis, lymphoplasmacytic, moderate, with furunculosis and numerous intrafollicular nematode larvae and adults.

JPC Comment:
Pelodera is an uncommon cause of canine dermatitis that receives only rare mention in veterinary literature. The contributor provides an excellent summary of this condition.

One of the main differentials for canine *Pelodera* dermatitis is hookworm dermatitis caused by *Ancylostoma caninum*, *Ancylostoma braziliense*, *Ancylostoma ceylanicum*, or *Uncinaria stenocephala*.[7] Similar to *Pelodera* dermatitis, hookworm dermatitis occurs on areas of the body in frequent contact with the ground, including the distal limbs and feet, ventrum, and tail. The third-stage hookworm larvae that invade the skin are generally not host-specific, leading to possible cutaneous larval migrans in many aberrant hosts, such as humans.[7] Clinical signs can include secondary pyoderma and paronychia and epidermal hyperplasia; histologic lesions include eosinophilic, neutrophilic, and histiocytic perivascular dermatitis with degenerate leukocytes lining cutaneous migration paths.[7] In addition to *Pelodera*, *Ancylostoma*, and *Uncinaria*, other helminth genera that can cause cutaneous larval migrans include *Necator*, *Strongyloides*, *Gnathostoma*, and *Bunostoma*.[7]

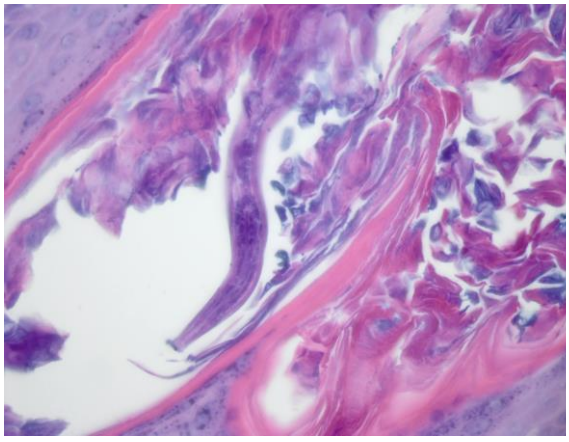

Figure 1-5. Haired skin, dog. Larvae have a rhabditiform esophagus. (HE, 400X) (*Photo courtesy of:* University of Tennessee, College of Veterinary Medicine, Department of Biomedical and Diagnostic Sciences)

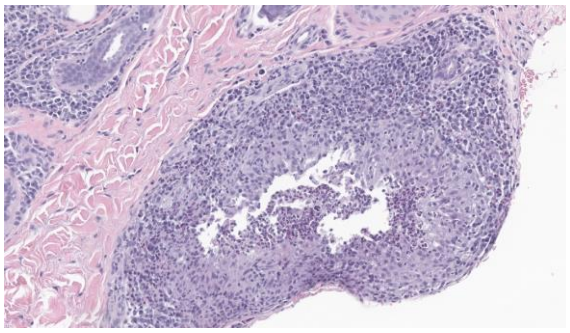

Figure 1-6. Haired skin, dog. There is a ruptured hair follicle which is replaced by pyogranulomous inflammation. (HE, 300X)

The week's conference was moderated by Dr. Charles Bradley, Assistant Professor of Pathobiology at the University of Pennsylvania School of Veterinary Medicine. Dr. Bradley discussed several cutaneous nematodiases in various species. Examples included *Onchocerca cervicalis*, associated with equine bursitis (delightfully named "fistulous withers" and "poll evil," depending on location), and the ventral midline filarial dermatitis caused by *Stephanofilaria stilesi* in cattle. In the cutaneous nematode universe, however, only *Pelodera* invades the hair follicle and causes folliculitis and furunculosis, making for a straight-forward, if uncommon, diagnosis.

Dr. Bradley also discussed carefully curating morphologic diagnoses by including only histologic features essential to the diagnosis; histologic features that are nonspecific, incidental, or not prominent are better left to the description. To that end, the JPC morphologic diagnosis was ruthlessly pruned to highlight the essentials of this condition: the intrafollicular parasites and associated follicular inflammation.

References:

1. Bowman DD. Helminths. In: Bowman DD, ed. *Georgi's Parasitology for Veterinarians*. 10th ed. Elsevier; 2014:191-194.
2. Capitan RGM, Noli C. Trichoscopic diagnosis of cutaneous *Pelodera strongyloides* infestation in a dog. *Vet Dermatol*. 2017;28(4):413-e100.
3. Eberhard ML. Histopathologic Diagnosis. In: Bowman DD, ed. *Georgi's Parasitology for Veterinarians*. 10th ed. Elsevier;2014:418.
4. Gardiner CH, Poynton SL. Morphologic characterization of nematodes in tissue sections. In: *An Atlas of Metazoan Parasites in Animal Tissues*. Armed Forces Institute of Pathology;2006:14-15.
5. Gross TL. Pustular and nodular disease with adnexal destruction. In: *Skin Diseases of the Dog and Cat*. 2nd ed. Blackwell;2005:449-450.
6. Mauldin EA, Peters-Kennedy J. Integumentary System. In: Maxie MG, ed. *Jubb, Kennedy, and Palmer's Pathology of Domestic Animals*. 6th ed. Vol 1. Elsevier; 2016:689.
7. Welle MM, Linder KE. The Integument. In: Zachary JF, ed. *Pathologic Basis of Veterinary Disease*. 7th ed. Elsevier; 2022:1238.

CASE II:

Signalment:
6-year-old, male neutered American pit bull terrier, canine (*Canis familiaris*)

History:
The patient had chronically pruritic, erythematous, and hyperplastic skin with numerous comedones. A prior history of intermittent superficial and deep pyoderma was reported.

Gross Pathology:
Lesions were predominantly on the ventral abdomen, inner thighs, and cranial hind limbs, but were also present over the dorsum and top of the head.

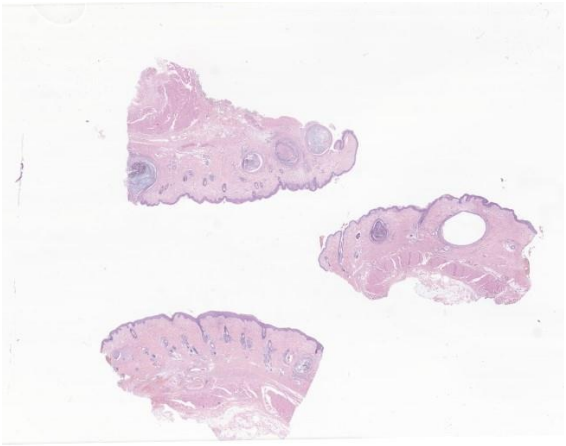

Figure 2-1. Haired skin, dog. Three sections of haired skin are submitted for examination. At low magnification, there are several large comedones within the submitted tissue. (HE, 5X)

Laboratory Results:
Superficial and deep skin scraping was performed and was negative for ectoparasites.

Surface cytology was performed and was reported as pyogranulomatous inflammation with the presence of cocci.

Aerobic culture and sensitivity of the skin surface was performed and *Staphylococcus pseudintermedius* sensitive to most antimicrobials was cultured.

Microscopic Description:
The epidermis is moderately hyperplastic with occasional dysplastic keratinocytes (increased nuclear to cytoplasmic ratio in the stratum spinosum) with suprabasal mitoses, and infrequent hypergranulosis. There are rare suprabasilar apoptotic keratinocytes (sunburn cells). There is multifocal parakeratotic hyperkeratosis. Follicular infundibula are markedly expanded by keratin (comedones) and surrounded by a rim of fibrosis. The superficial dermis has numerous wavy basophilic fibers (solar elastosis) and superficial fibrosis. There is a mild perivascular and perifollicular infiltrate of lymphocytes, plasma cells, and histiocytes with multifocal edema. There is a small focus of free keratin surrounded by macrophages adjacent to one of the comedones. The other sample (not submitted) demonstrated comedone rupture with pyogranulomatous dermatitis.

Contributor's Morphologic Diagnosis:
Haired skin: Epidermal dysplasia with solar elastosis, comedones, and mild dermatitis (actinic dermatosis).

Contributor's Comment:
This case exhibits classic features of actinic dermatosis, also called solar dermatosis or actinic keratosis. Exposure to ultraviolet radiation (most often sunlight) leads to epidermal hyperplasia and dysplasia with scattered suprabasilar mitoses and apoptotic keratinocytes ("sunburn cells"). The stratum corneum often exhibits parakeratotic hyperkeratosis.

In the dermis, elastin fibers are degenerate and appear as thick, wavy, basophilic strands (solar elastosis). Laminar fibrosis occurs in the superficial dermis and extends around follicular infundibula, which dilate to form comedones. There may also be a layer of pale, smudgy collagen fibers in the superficial dermis. There is often a superficial perivascular infiltrate of lymphocytes, plasma cells, and fewer macrophages, neutrophils, and occasionally eosinophils. Comedones may rupture, leading to furunculosis, and lesions can also become secondarily infected. Some cases may exhibit vasculopathy or proliferation of superficial dermal vessels.[2] The epidermis may exhibit hyperpigmentation, though this change is not observed in this patient's nonpigmented skin.[4]

Because exposure to sunlight is the initial step in the pathogenesis of actinic dermatosis, affected dogs are often known sunbathers and may live at low latitudes or high altitudes. Lesions are most common on sparsely haired areas, such as the ventral abdomen, inguinum, axilla, dorsal muzzle, and periorbital regions.

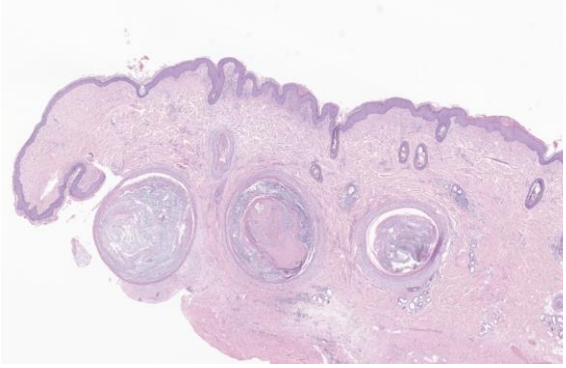

Figure 2-2. Haired skin, dog. There is mild to moderate epidermal hyperplasia and several large comedones. There is mild multifocal perivascular inflammation. (HE, 18X)

Non-pigmented areas are also more commonly affected. Predisposed dog breeds include short-haired dogs such as pit bulls, boxers, whippets, Dalmatians, greyhounds and Italian greyhounds, beagles, and basset hounds.[2]

Actinic dermatosis is also commonly observed in cats, horses, cattle, and humans. In cats, predisposed locations include the face and pinnae. In horses and cattle, lesions are often found on the eyelids (including third eyelid), conjunctiva, and perineum.[7] Grossly, actinic dermatosis appears as patchy erythema, crusts, macules, and papules, progressing to plaques and nodules that may be ulcerated. Comedones may be grossly visible as dark foci or small nodules. Multiple lesions are often present, as solar exposure occurs over a large area of the patient. [2]

Several of the changes described above are protective mechanisms of the epidermis against damage caused by UV radiation. Melanin blocks UV radiation and absorbs free radicals.[1,4] Hyperpigmentation of the epidermis occurs via an immediate redistribution of existing melanin or more chronically via increased melanin synthesis by melanocytes and increased transfer of melanin to keratinocytes, which appears histologically as "hats" over the keratinocyte nuclei.[4] Epidermal hyperplasia and hyperkeratosis, stimulated by epidermal growth factors released after UV exposure, provides an increased physical barrier. [1]

If protective mechanisms fail, the epidermal dysplasia of actinic dermatosis can progress to *in situ* and then frank squamous cell carcinoma (SCC). Dogs with solar-induced SCC may have a longer median survival time than dogs with SCC without evidence of solar damage.[8] UV light causes cross-linking of pyrimidine nucleosides into pyrimidine dimers, which distort the structure of the DNA double helix, leading to DNA replication failure and cell death or transformation. [4] Additionally, investigation into the molecular basis for actinic dermatosis and carcinogenesis in humans demonstrates similar genetic dysregulation between actinic dermatosis and SCC and implicates UV-induced mutations in p53.[5,6] Other solar radiation-induced neoplasms, such as hemangioma/hemangiosarcoma, may occur concurrently in animals with solar exposure.[2,4] Basal cell carcinomas and squamous cell carcinomas in humans are both linked to UV exposure, and p53 mutations are commonly found in these tumors.[3]

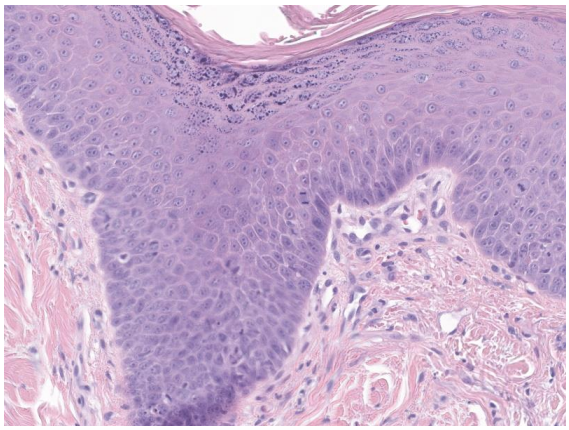

Figure 2-3. Haired skin, dog. There are numerous mitotic figures in the hyperplastic epidermis, and some above the basal layer. (HE, 229X)

Contributing Institution:
University of Pennsylvania
School of Veterinary Medicine
https://www.vet.upenn.edu/veterinary-hospitals/ryan-veterinary-hospital/services/diagnostic-laboratories

JPC Diagnosis:
Haired skin: Epidermal dysplasia, mild to moderate, with keratinocyte apoptosis, solar elastosis, and comedones.

JPC Comment:
As the contributor notes, DNA damage due to sunlight exposure is the inciting cause of actinic dermatosis and the malignant transformation of keratinocytes that may occur with prolonged exposure. Sunlight contains three types of ultraviolet radiation that reach the earth's surface: long wavelength UVA radiation in the 400-315 nm spectrum, UVB radiation (315 to 280 nm), and short-wave UVC radiation (280 to 100 nm).[9] The vast majority of UV radiation that reaches the skin of humans and animals is UVA radiation, as all but approximately 5% of UVB radiation, and all UVC radiation, is absorbed by atmospheric ozone.[1,9] Once UV light reaches the skin, host factors such as amount and type of hair and melanin pigmentation within the skin, as well as environmental factors, ultimately determine the amount of UV exposure received by the skin of a particular animal.[9]

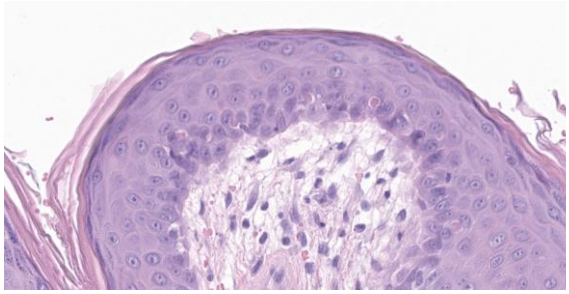

Figure 2-4. Haired skin, dog. There are occasional necrotic keratinocytes scattered throughout the stratum spongiosum ("sunburn cells") (HE, 386X)

UV radiation is considered a "complete carcinogen" in that it is both a mutagen, due to its direct effects on DNA, and a non-specific damaging agent, giving it properties of both a tumor initiator and a tumor promoter.[1] In the skin, UVA penetrates deeply into the dermis and is efficient at generating reactive oxygen species that damage DNA via indirect photosensitizing reactions.[1] In contrast, UVB is almost completely absorbed by the epidermis, where it is directly absorbed by DNA within keratinocytes, leading to molecular rearrangements, such as covalent bonds between adjacent thymine or cytosine bases ("pyrimidine dimers").[1,9] Most pyrimidine dimers are removed by DNA repair mechanism; however, some pyrimidine dimers escape this process and cause cells either to undergo apoptosis, leading to the "sunburn cells" seen in actinic keratosis, or to accumulate DNA mutations during subsequent replication, leading to neoplasia.[1,9]

The lesions of actinic dermatosis described by the contributor and well-illustrated in this case, are a result of chronic exposure to UVB and UVA radiation. At the outset, lesions appear grossly as areas of erythema with scaling and crusting, followed by the appearance of papular or plaque-like foci of thick, lichenified, erythematous crusted patches and plaques.[4,9] Progression to *in situ* carcinoma, squamous cell carcinoma, or basal cell tumors may occur in areas of preneoplastic actinic dermatosis.[9]

Exposure to UV radiation can also damage skin through photosensitization. Photosensitization is skin damage due to the interaction of UV radiation and photodynamic chemicals within the skin.[9] When UV radiation interacts with photodynamic chemicals, the released energy produces a range of reactive oxygen species that damage cell membranes, DNA, proteins, and organelles, causing cell activation, degeneration, and/or death.[9]

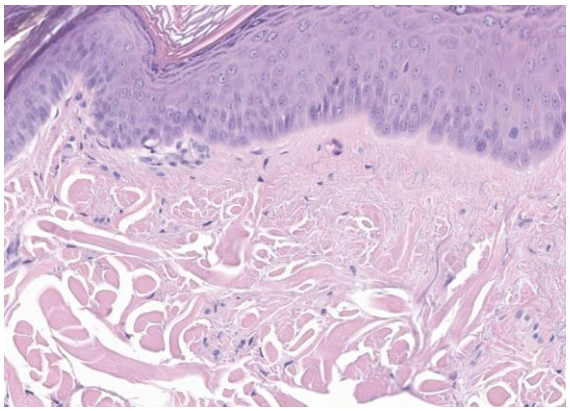

Figure 2-5. Haired skin, dog. There is fibrillation of the superficial dermal elastic fibers (solar elastosis). (HE, 244X)

Photosensitization injury is classified into four types based on the origin of the photodynamic substance. In type I (primary) photosensitization, the photodynamic substance is ingested by the animal, usually in the form of plants or drugs, and then absorbed systemically and deposited into the skin. Type II photosensitization occurs via accumulation of endogenous hematoporphyrins due to the inability to properly metabolize heme pigments. Type III photosensitization occurs when phylloerythrin, a chlorophyll degradation product, accumulates in the skin; this is also known as hepatogenous photosensitization since deposition in the skin is due to the inability of the liver to disposing of phylloerythrin normally. Finally, type IV photosensitization refers to photosensitization for which the pathogenesis is unknown.[4]

A final way that UV radiation can damage skin is through photoallergy. Photoallergy is distinct from photosensitization and occurs when an exogenous photodynamic substance functions as an antigen.[4,9] Gross and histologic pathology is typically due either to an immediate, Type I hypersensitivity reaction or a delayed, Type IV cell-mediated hypersensitivity reaction in which the photoactivated substance acts either as a hapten or an allergen.[9]

Conference participants appreciated the impressive comedones in the examined section. Actinic comedones such as these can be distinguished from regular comedones by their concentric, peripheral fibrosis and the lack of attenuation of the outer root sheath. Inflammation resulting from the rupture of an actinic comedone is sometimes called solar furunculosis.

The moderator also pointed out the substantial dysplastic changes evident within the epithelium, including suprabasilar mitotic activity, irregularly piling up of keratinocytes, and the formation and elongation of rete ridges. In human medicine, these changes might be enough for a diagnosis of *in situ* squamous cell carcinoma; however, veterinary medicine tends to be more cautious of making this leap. The moderator noted that the epithelium appeared to be well on its way to malignant transformation.

Finally, the moderator discussed the importance of differentiating feline actinic dermatosis from Bowenoid in situ carcinoma (BISC), which can exhibit more aggressive and invasive biological behavior. Compared to actinic dermatosis, in BISC, keratinocytes in all layers of the epidermis typically appear more basaloid, rete ridges tend to be more bulbous and extend farther into the dermis, and dysplastic changes extend to the follicular outer root sheath.

References:

1. D'Orazio J, Jarrett S, Amaro-Ortiz A, et al. UV radiation and the skin. *Int J Mol Sci*. 2013;14(6):12222-48.
2. Gross TL, Ihrke PJ, Walder EJ, Affolter VK, eds. *Skin Diseases of the Dog and Cat: Clinical and Histopathologic Diagnosis*. 2nd ed. Blackwell Science Ltd; 2005:136-160.
3. Lacour JP. Carcinogenesis of basal cell carcinomas: genetics and molecular

mechanisms. *Br J Dermatol*. 2002;146 Suppl 61:17-9.
4. Mauldin EA and Peters-Kennedy J. Integumentary System. In: Maxie MG, ed. *Jubb, Kennedy, and Palmer's Pathology of Domestic Animals*. 6th ed. Elsevier; 2016:509-736.
5. Nelson MA, Einspahr JG, Alberts DS, et al. Analysis of the p53 gene in human precancerous actinic keratosis lesions and squamous cell cancers. *Cancer Lett*. 1994: 85(1):23-9.
6. Padilla RS, Sebastian S, Jiang Z, et al. Gene expression patterns of normal human skin, actinic keratosis, and squamous cell carcinoma: a spectrum of disease progression. *Arch Dermatol*. 2010:146 (3):288-93.
7. Valli VE, Bienzle D, Meuten DJ, Linder KE. Epithelial and Melanocytic Tumors of the Skin. In: Meuten DJ, ed. *Tumors in Domestic Animals*. 5th ed. John Wiley & Sons;2017:88-141.
8. Willcox JL, Marks SL, Ueda Y, et al. Clinical features and outcome of dermal squamous cell carcinoma in 193 dogs (1987-2017). *Vet Comp Oncol*. 2019:17 (2):130-138.
9. Welle MM, Linder KE. The Integument. In: Zachary JF, ed. *Pathologic Basis of Veterinary Disease*. 7th ed. Elsevier; 2022:1154-1156.

CASE III:

Signalment:
11-year-old, male neutered domestic short hair, feline (*Felis catus*)

History:
The patient is an outdoor cat with a completed vaccination protocol and no other animals live in the same household. The cat developed skin lesions due to dermatophytosis and was treated with itraconazol. There was partial remission of the skin lesions; however, approximately five months later, the skin lesions progressed despite therapy.

Gross Pathology:
Clinical examination of the skin showed severe diffuse exfoliation and crust formation. In addition, the skin presented with mild to moderate multifocal erythema and follicular casts. The ear canal was filled with dry and brown secretions.

Laboratory Results:
Cytological examination of the skin crusts revealed numerous neutrophils and bacterial cocci. Trichogram examination revealed the presence of follicular casts. A skin scraping was negative for ectoparasites. Wood lamp examination was negative for fungal microorganisms. Blood evaluation revealed mild thrombocytopenia and a mild increase in ALT.

Chest radiographs revealed a mass in the thymic region. Cytologic evaluation of an ultrasound guided fine needle aspirate of the mass was diagnosed as epithelial thymoma.

Figure 3-1. Haired skin, cat. Four sections of haired skin are submitted for examination. At low magnification, a dense layer of hyperkeratosis is evident. (HE, 5X)

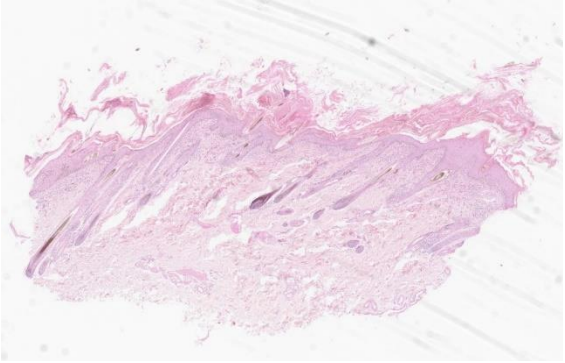

Figure 3-2. Haired skin, cat. A dense layer of hyperkeratosis covers a mildly hyperplastic epidermis. (HE, 16X)

Microscopic Description:
Histological examination of the skin sections revealed a marked, diffuse predominantly orthokeratotic and, to a lesser degree, parakeratotic hyperkeratosis of the epidermis. Multifocally, small aggregates of neutrophils as well as extravasated erythrocytes (haemorrhage) and occasional small bacterial colonies (coccoid bacteria, not seen in all slides) can be seen. The epidermis and hair follicle infundibula are moderately thickened (acanthosis). The following changes are seen in the epidermis and, to a lesser degree, in hair follicles: disruption and vacuolation (interpreted as hydropic degeneration) of the basal keratinocytes; an infiltrate of small lymphocytes within the stratum basale and rarely within upper layers (exocytosis); scattered isolated deeply eosinophilic and rounded cells (apoptotic cells) with loss of cohesion from other keratinocytes in all epidermal layers; increased numbers of intraepidermal melanocytes; and increased numbers of keratinocytes with intracytoplasmic melanin (hyperpigmentation). A moderate band-like mononuclear infiltrate composed mainly of lymphocytes, plasma cells, occasional melanin-laden macrophages (interpreted as melanin incontinence), and mast cells is seen in the superficial dermis and around hair follicles. This infiltrate obscures the dermo-epidermal junction (interpreted as interface dermatitis). Sebaceous glands are absent.

Contributor's Morphologic Diagnosis:
Haired skin: Moderate to severe lymphocytic interface dermatitis with mild transepidermal apoptosis, moderate to severe parakeratotic hyperkeratosis, and severe atrophy of sebaceous glands.

Contributor's Comment:
Thymoma associated exfoliative dermatitis is a rare paraneoplastic syndrome which has been reported in middle-aged to older cats affected by a thymoma.[7,12] This condition has also been reported in rabbits and goats.[1,5] In cats, the exfoliative dermatitis regresses after thymectomy.[2,7,13] Other thymoma associated paraneoplastic syndromes include myasthenia gravis in cats and dogs, erythema multiforme in dogs, and granulocytopenia in cats.[4,13,15,16]

Affected cats present with alopecia, crusting, scaling, desquamation, and erythema usually starting from the head and progressing to the rest of the body.[2,6,12] Keratinaceous debris may build up in interdigital spaces and claw folds. Pruritis is usually absent unless there are dermal lesions, namely alopecia and exfoliation, are reported in goats and rabbits.[1,5]

Typical histopathological lesions in cats include orthokeratotic and parakeratotic hyperkeratosis, extensive desquamation and transepidermal keratinocyte apoptosis, as well as apoptosis of keratinocytes in the follicular infundibula. In addition, there is hydropic degeneration of the basal keratinocytes and cell poor to cell rich CD3+ lymphocytic interface dermatitis. The infiltrative lymphocytes can lead to mural folliculitis with subsequent atrophy of sebaceous glands. Pigmentary incontinence and concurrent *Malasezzia* infections have also been reported.[7,12] Similar histologic lesions have been described in goats and rabbits.[1,5]

In humans, thymomas have been shown to produce autoantigen responsive CD4+ T cells. This has been shown to occur in paraneoplastic myasthenia gravis, erythema multiforme, and graft versus host disease. It is therefore proposed that the same occurs in thymoma associated exfoliative dermatitis in cats due to the occurrence of auto reactive T lymphocytes targeting keratinocytes.[12] Differential diagnoses of thymoma associated exfoliative dermatitis in cats according to histological features of the lesion include non-thymoma associated exfoliative dermatitis, systemic lupus erythematosus, erythema multiforme, and sebaceous adenitis.[7]

Nonthymoma associated exfoliative dermatitis is clinically and histologically indistinguishable from the thymoma associated exfoliative dermatitis.[3,10] The diagnosis is based on the demonstration of the absence of thymic neoplasia and the lesions usually resolve after administration of cyclosporine.[3,10,14]

Erythema multiforme has similar histologic lesions to thymoma-associated exfoliative dermatitis. The lesions in thymoma associated exfoliative dermatitis present with milder transepidermal apoptosis in comparison to erythema multiforme.[6,7,12] In addition, the clinical skin lesions differ and are mainly characterised by erythematous macules, papules or plaques over the dorsum and spreading peripherally.[7,8]

Lupus erythematosus is considered another differential due to histologic similarities. The difference is that in lupus erythematosus, there is usually a more prominent interface dermatitis and mild apoptosis restricted to the basal cells.[7] Gross lesions in lupus erythematosus include erosions and ulcerations on the face, particularly on the nose.[8]

Feline sebaceous adenitis is considered a differential when the sebaceous glands are absent or reduced in number. However, the inflammation will be confined to the follicular isthmus and apoptosis is absent in sebaceous adenitis.[7] A final diagnosis of thymoma-associated exfoliative dermatitis is achieved by evaluation of skin biopsies and demonstration of simultaneously occurring thymic neoplasia.[1]

Contributing Institution:
Institute of Veterinary Pathology
Vetsuisse-Faculty, University Zurich
Winterthurerstrasse 268
8057 Zurich, Switzerland

JPC Diagnosis:
Haired skin: Dermatitis and mural folliculitis, lymphocytic, cytotoxic interface, moderate, with epidermal hyperplasia, parakeratotic hyperkeratosis, and sebaceous gland loss.

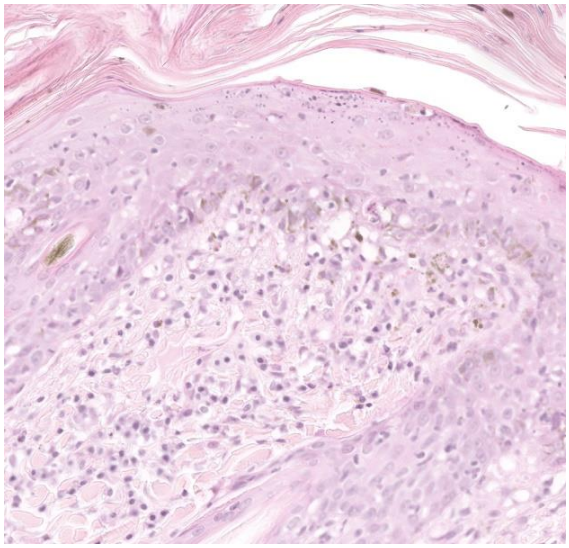

Figure 3-3. Haired skin, cat. A band of low numbers of lymphocytes is present at the dermoepidermal junction and infiltrates the overlying, often vacuolated basal epithelium. (HE, 305X)

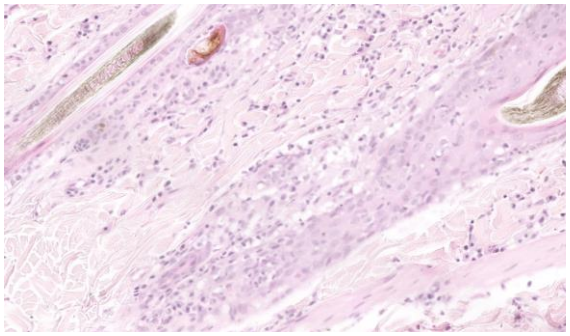

Figure 3-4. Haired skin, cat. There is effacement of sebaceous glands by lymphocytes and macrophages. (HE, 400X)

JPC Comment:
Thymomas are rare in dogs and cats and arise from the epithelium of the thymus. Curiously, thymomas are classified as benign or malignant based on their ability to be resected at surgery, and not based on histopathologic criteria.[13] Regardless of classification, metastasis is uncommon and recurrence after surgical resection is rare.[13]

Patients with thymomas may seek veterinary care due to respiratory symptoms from the primary tumor or for clinical signs referrable to any one of several reported paraneoplastic syndromes. As the contributor notes, the most common thymoma-associated paraneoplastic syndromes include exfoliative dermatitis, erythema multiforme, myasthenia gravis, granulocytopenia, and polymyositis. The association between thymoma and exfoliative dermatitis is poorly understood; however, immune-mediated injury is the current leading theory based on the characteristic presence of a T cell-rich cytotoxic interface dermatitis.[12]

In health, T cells are prevented from attacking self-antigens due to central and peripheral tolerance. Central tolerance begins during T cell development in the thymus, where rearrangement of T cell receptors generates a panoply of epitope receptors sufficient to recognize all possible antigens encountered during the life of the animal. In this generative process, T cell receptors are inadvertently created which have a high affinity for self-peptides. These T cells are screened in the thymic medulla and are either eliminated via apoptosis ("clonal deletion") or differentiated into thymically-derived T regulatory cells ("clonal diversion").[11]

Screening of self-reactive T lymphocytes is achieved through a remarkable process of so-called "promiscuous gene expression" by a subset of thymic epithelial cells called medullary thymic epithelial cells (mTECs).[11] These mTECs present self-antigens to developing T lymphocytes and expose maturing T lymphocytes to a nearly complete representation of the animal's protein coding genome.[11] T lymphocytes that pass this screening (i.e., have low binding affinity for self-peptides) are tolerant for most proteins in the animal's body.[11] A key player in this system is the transcriptional regulator Autoimmune Regulator (AIRE) protein, which is highly expressed in mTECs where it promotes promiscuous gene expression of a wide array of tissue-specific antigens for presentation to the developing T lymphocytes.

The processes of central tolerance work well, but not perfectly; thus, occasionally self-reactive T lymphocytes slip through the thymic cracks and are released into systemic circulation. In addition, though the mTECs present developing T cells with an impressive array of self-peptides, they do present them with all possible self-peptides. The processes of peripheral tolerance, most notably anergy and deletion of self-reacting lymphocytes, acts as a second line of defense against mature lymphocytes that encounter self-peptide for the first time outside the context of the thymus.[11]

Given that the thymus is the key site for establishing immune tolerance, it is not surprising that thymic epithelial cell tumors may

generate syndromes caused by perturbations of this system. In humans, myasthenia gravis is the most studied thymoma-associated neoplastic syndrome. Patients that develop myasthenia gravis have cortical thymomas with active thymopoiesis (i.e., they retain the ability to export mature T lymphocytes).[9] The neoplastic cells express lower levels of MHC Class II and AIRE when compared to normal thymic epithelium; thus, defective negative screening in the thymus, reduced levels of regulatory T cells, and export of autoreactive T lymphocytes are the key features associated with myasthenia gravis in human thymoma patients.[9] As the contributor notes, it is thought that a similar mechanism underlies the apparent auto-immune keratinocyte destruction characteristic of thymoma-associated exfoliative dermatitis in a animals.

Conference discussion focused on distinguishing exfoliative dermatitis from erythema multiforme, as often the histologic lesions can be extremely similar or even identical. The clinical picture in these two conditions is different, however, with erythema multiforme typically causing small multifocal lesions while exfoliative dermatitis tends to be more widespread throughout the body.
Another differential considered, largely due to the loss of sebaceous glands, is sebaceous adenitis; however, involvement of the epidermis in the form of cytotoxic interface dermatitis in this case rules out a diagnosis of sebaceous adenitis, which is characterized by immune destruction of sebaceous units only. The loss of sebaceous units probably does contribute to the exfoliation in this condition, however, as the loss of sebum is a known cause of disordered desquamation. Conference participants discussed several other paraneoplastic syndromes, including paraneoplastic alopecia, nodular dermatofibrosis in German Shepherd dogs, paraneoplastic pemphigus, and superficial necrolytic dermatitis.

There was spirited discussion among conference participants surrounding the term “diffuse” when used to describe distribution in dermatopathologic lesions. The moderator prefers to avoid the term as “nodular to diffuse” dermatitis is one of the eight defined inflammatory reaction patterns in veterinary dermatopathology and its use in a broader-sense may be confusing. In this case, the moderator felt that the terms “dermatitis” and “mural folliculitis” are sufficient to convey the distribution of the lesions examined in conference.

References:

1. Byas AD, Applegate TJ, Stuart A, Byers S, Frank CB. Thymoma-associated exfoliative dermatitis in a goat: case report and brief literature review. *J Vet Diagn Invest*. 2019;31(6):905-908.
2. Cavalcanti JV, Moura MP, Monteiro FO. Thymoma associated exfoliative dermatitis in a cat. *J Feline Med Surg*. 2014; 16(12):1020-1023.
3. Combarros D, Moulin JP, Correge S, Delverdier M, Cadiergues MC. Clinical and histological recovery of non-thymoma-associated exfoliative dermatitis in a cat treated with cyclosporin A. *JFMS Open Rep*. 2020;6(1):205511692-0902 307.
4. Fidel JL, Pargass IS, Dark MJ, Holmes SP. Granulocytopenia associated with thymoma in a domestic shorthaired cat. *J Am Anim Hosp Assoc*. 2008;44(4):210–217.
5. Florizoone K. Thymoma-associated exfoliative dermatitis in a rabbit. *Vet Dermatol*. 2005;16(4), 281–284.
6. Fournier Q, Bavcar S, Philbey AW, Smith S, Varjonen K. A previously undescribed cutaneous paraneoplastic syndrome in a cat with thymoma. *Vet Dermatol*. 2019;30(4):342-e98.
7. Gross TL, Ihrke PJ,Walder EJ, Affolter VK. *Skin Diseases of the Dog and Cat:*

Clinical and Histopathologic Diagnosis. 2nd ed. Wiley-Blackwell;2008:68-79.
8. Hnilica KA. *Small Animal Dermatology: A color atlas and therapeutic guide*. 3rd ed. Elsevier;2011.
9. Lancaster E, Evoli A. Paraneoplastic disorders in thymoma patients. *J Thorac Oncol*. 2014;9(9 Suppl 2):S143-S147.
10. Linek M, Rüfenacht S, Brachelente C, et al. Non-thymoma-associated exfoliative dermatitis in 18 cats. *Vet Dermatol*. 2015; 26(1):40-e13.
11. Proekt I, Miller CN, Lionakis MS, Anderson MS. Insights into immune tolerance from AIRE deficiency. *Curr Opin Immunol*. 2017;49:71-78.
12. Rottenberg S, von Tscharner C, Roosje PJ. Thymoma-associated exfoliative dermatitis in cats. *Vet Pathol*. 2004;41(4): 429-433.
13. Singh A, Boston SE, Poma R. Thymoma-associated exfoliative dermatitis with post-thymectomy myasthenia gravis in a cat. *Can Vet J*. 2010;51(7): 757-760.
14. Szczepanik M, Wilkołek P, Śmiech A, Kalisz G. Non-thymoma-associated exfoliative dermatitis in a European shorthair cat: A case report. *Vet Med Sci*. 2021; 7(6):2108-2112.
15. Tepper LC, Spiegel IB, Davis GJ. Diagnosis of erythema multiforme associated with thymoma in a dog and treated with thymectomy. *J Am Anim Hosp Assoc*. 2011;47(2):e19-e25.
16. Wood SL, Rosenstein DS, Bebchuk T. Myasthenia gravis and thymoma in a dog. *Vet Rec*. 2001;148(18):573-574.

CASE IV:

Signalment:
8-year-old, female spayed boxer, canine (*Canis familiaris*).

History:
The patient was referred to Auburn University Dermatology specialty service for a disease affecting all claws of all four paws with a clinical duration of approximately six months. Affected claws were misshapen, fractured, and ranged from soft to brittle. No systemic abnormalities were reported at the time of admission.

Gross Pathology:
Multiple claws had moderate paronychia characterized by edema, erythema, congestion, and purulent to hemorrhagic exudate at the claw fold with keratinous debris around the claw. All claws had moderate to severe onychodystrophy characterized by onychorrhexis, onychomalacia, onycholysis, onychogryphosis, onychauxis, and onychoschizia. An onychobiopsy without onychectomy employing the technique described by

Mueller and Olivry (1999) was performed and samples were sent for histopathology and fungal culture.

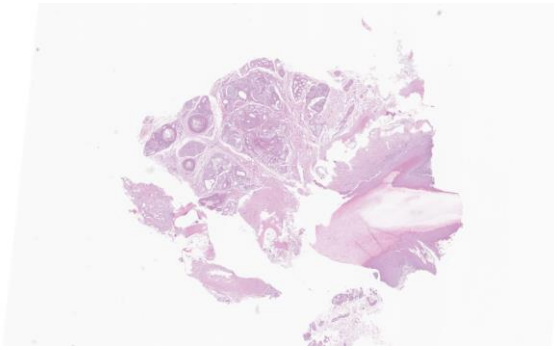

Figure 4-1. Haired skin and claw, dog. A single section of haired skin and fragments of the 3rd phalanx and claw are submitted for examination. (HE, 5X)

Laboratory Results:
Claw tissue submitted for fungal culture was negative for dermatophytes.

Microscopic Description:
Affecting the claw bed, the dermo-epidermal junction is blurred by a band-like infiltrate composed of moderate numbers of lymphocytes, plasma cells, histiocytes, fewer neutrophils, and melanin-laden macrophages (pigmentary incontinence). At these segments and other less inflamed epidermal stretches, the basal epithelium is markedly vacuolated and interspersed with individualized, shrunken hypereosinophilic keratinocytes with pyknotic nuclei (apoptosis). The superficial dermis is minimally replaced by a smudgy collagenous matrix. Eccrine glands are mildly ectatic, filled with amphophilic product, and surrounded by mixtures of similar inflammatory infiltrates within increased concentric bands of fibrous tissue.

Term	Definition
Onychodystrophy	Abnormal claw formation
Paronychia	Inflammation or infection of the claw folds
Onychomalacia	Softening of the claws
Onycholysis	Separation of the claw from the underlying corium but with continuing proximal attachment
Onychogryphosis	Hypertrophy and abnormal curvature of the claws
Onychauxis	Hypertrophy of the claws
Onychoschizia	Splitting or lamination of claws, usually beginning distally
Onychalgia	Claw pain
Onychomadesis	Sloughing of the claws (claw shedding)

Table 4-1. A sampling of claw disorder terminology. Table adapted from Muller and Kirk's *Small Animal Dermatology*. 7th ed. 2012.

Contributor's Morphologic Diagnosis:
Claw to claw base/bed (digit unspecified): Dermatitis, interface and lichenoid, lymphoplasmacytic and histiocytic, moderate, with pigmentary incontinence, basal epithelial vacuolation, and apoptosis (consistent with symmetric lupoid onychodystrophy).

Contributor's Comment:
Symmetric lupoid onychodystrophy (SLO), also known as symmetric lupoid onychitis, is an uncommon primary ungual disease that has been described in dogs.[1,4,6] This condition may occur in dogs of all ages; however, young to middle-aged dogs appear to be more commonly affected.[4] Certain breeds seem to be predisposed, including German Shepherd and Gordon Setter; nevertheless, SLO has been reported in numerous breeds, and sex predisposition has not been described.[1,4,9]

SLO lesions are restricted to the claws and affected dogs are usually otherwise healthy with no systemic involvement.[1] Typically, the first clinical signs observed by owners are licking of the paws and lameness due to onychalgia or onychomadesis.[1,4] Paronychia with onycholysis of multiple claws is observed and, within weeks, several or all claws of all paws are affected.[1,3] After sloughing, regrown claws are commonly misshapen, brittle, dry, and discolored, and secondary bacterial infections are common.[1,4]

The cause and pathogenesis of SLO are controversial and have not been completely elucidated.[4] In a study with Gordon Setters, dog leukocyte antigen (DLA) class II alleles associated with the disease and negatively correlated with the disease were described, suggesting a genetic predisposition.[9] A case series reported the detection of antinuclear antibodies in 3/10 Gordon Setters with SLO, suggesting that SLO may be an auto-immune disease.[2] Nevertheless, some authors believe that the histopathological findings of SLO,

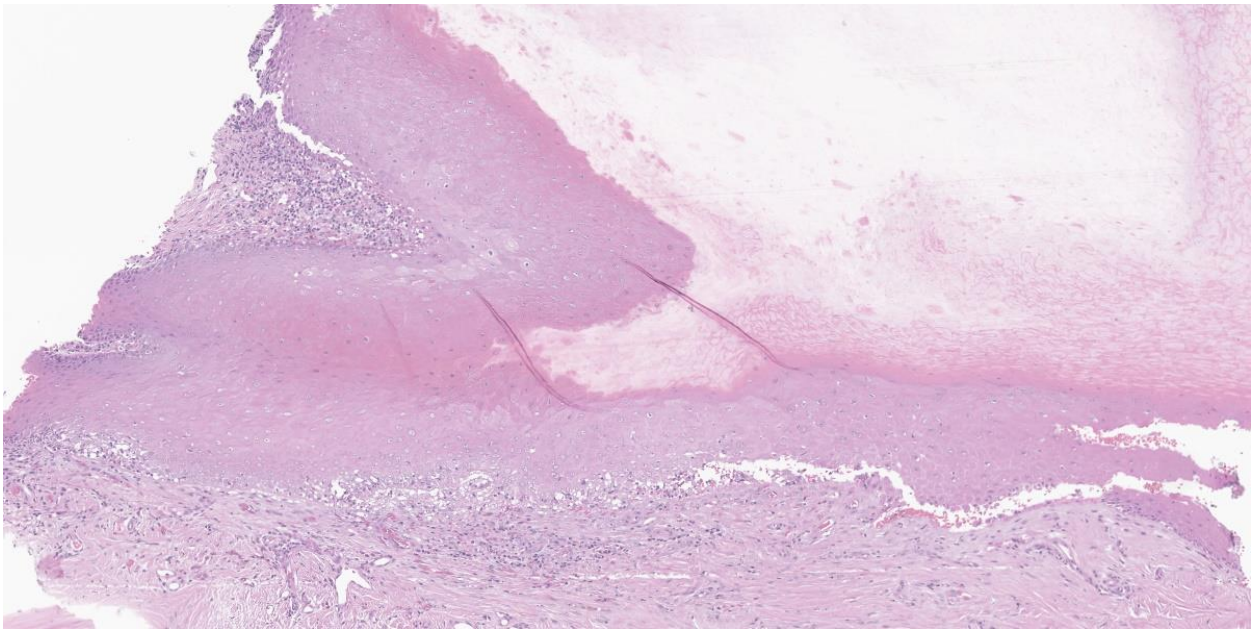

Figure 4-2. Nailbed, dog. There is a linear band of lymphocytes subjacent to the germinative epithelium of the nailbed. (HE, 92X)

characterized by lichenoid-interface dermatitis and basal cell vacuolation/damage affecting the claw represent a tissue response pattern to different conditions and not a separate entity.[4] For instance, lesions affecting the claws with similar histopathological findings to those of SLO have been reported in cases of leishmaniasis, even when amastigotes were not detected in the affected tissue.[3]

The diagnosis of SLO is usually based on the clinical presentation with the disease restricted to the claws/digits and typical histological findings.[4] Distal onychectomy (third phalanx [P3] amputation) has been considered the gold standard method to diagnose SLO. An alternative technique, onychobiopsy without onychectomy, was employed in this case.[5] Through this technique, only a portion of the lateral claw matrix is collected, and no amputation is necessary; however, some downsides include the fact that localized lesions may be missed.[5] Other systemic diseases may affect the claws, including systemic lupus erythematosus, hepatocutaneous syndrome, pemphigus vulgaris, and bullous pemphigoid, leading to potentially overlapping gross or microscopic findings; however, other cutaneous or systemic lesions are expected with these diseases.[4,7]

Several treatments for SLO have been reported with variable success, including supplementation with omega-3 and omega-6 essential fatty acids (EFA), as well as combinations of EFA with other therapies such as topical glucocorticoids, pentoxifylline, and tetracycline/niacinamide.[1,4,6] In this case, the patient showed significant clinical improvement after treatment with pentoxifylline, vitamin E, and omega EFAs.

Contributing Institution:
Auburn University
Department of Veterinary Pathobiology
https://www.vetmed.auburn.edu/academic-departments/dept-of-pathobiology/

JPC Diagnosis:
Nailbed: Onychitis, lymphocytic, cytotoxic interface, marked.

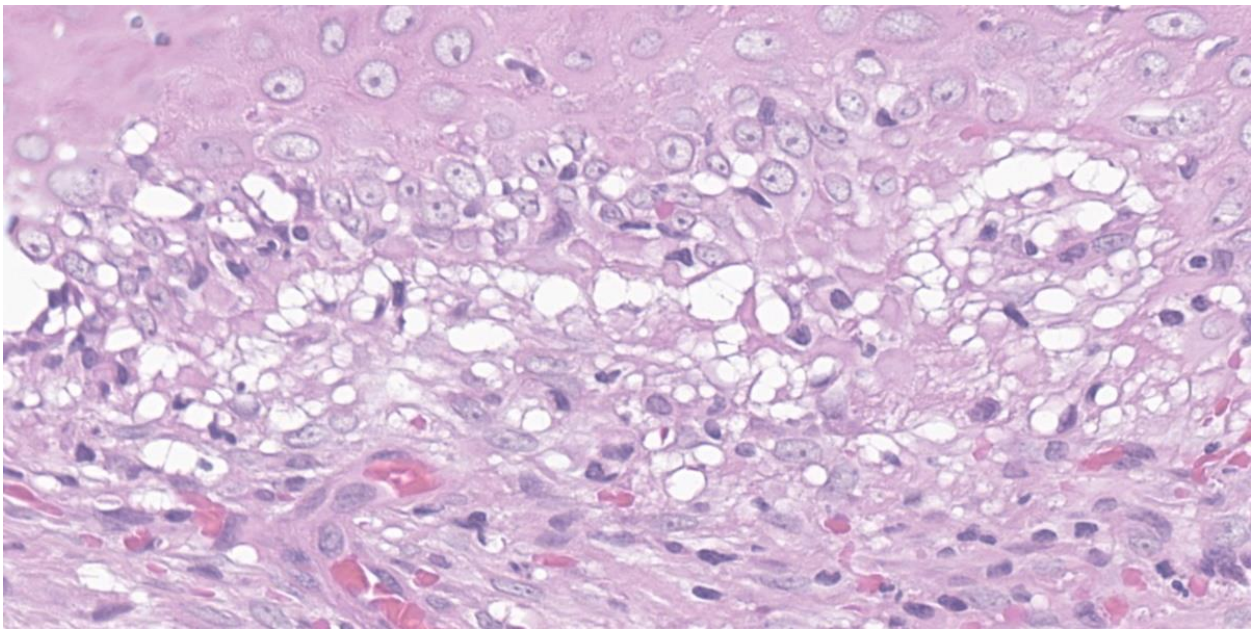

Figure 4-3. Nailbed, dog. There is loss of a discrete dermoepidermal junction and infiltration of the basal layers of the vacuolated germinative epithelium by lymphocytes (cytotoxic interface dermatitis). (HE, 695X)

JPC Comment:
A clinical history of loss of one or more claws on multiple paws within 2 weeks to a few months after initial onset should suggest a diagnosis of SLO.[8] Regrown nails are typically misshapen and friable and will re-slough. The sequence of onychomadesis followed by onychodystrophy is required for an SLO diagnosis and differentiates this condition from idiopathic onychodystrophy of dogs, where there is no onychomadesis preceding onychodystrophy.[8] In addition, SLO lesions are restricted to the claw and no skin or mucosal lesions occur.[8]

The contributor provides an excellent overview of this uncommon condition, and the case presented here is characteristic of the disease. The examined slide exhibits the typical histologic features of SLO - lymphocytic interface dermatitis with basal cell vacuolation, apoptosis, and pigmentary incontinence – though the interface dermatitis can vary widely in severity.[8] Typical histologic findings may also be found in conjunction with superimposed bacterial infections and osteomyelitis.[8] These histologic findings are relatively non-specific and can be found in a variety of diseases of the canine claw, making clinical history paramount in the diagnosis of this condition.

The moderator began by reviewing claw anatomy and the specialized terminology used to describe nail pathology (see Table 4-1). The moderator emphasized that SLO requires lesions in all paws and (almost) all claws; if a patient has the same clinical presentation but with only one affected nail, the moderator would prioritize onychomycosis as a differential diagnosis. The moderator uses a PAS stain to rule in or out onychomycosis as fungal elements are largely impossible to visualize on H&E sections of the claw.

Several participants questioned whether the clefting noted in the examined section is real or artifactual. While clefting can be an artifact caused during tissue collecting and processing, it can also be real and diagnostically

helpful since clefting at the epidermal-dermal junction would be expected to occur in this condition. The moderator believes that the clefting present in this section is real due to the hemorrhage and cellular debris present within the cleft. The moderator also noted that the examined section is an exceptional example of cytotoxic interface dermatitis. The moderator showed more typical examples with less florid inflammatory infiltrates and less affected basilar epithelium.

The JPC morphologic diagnosis was once again whittled down to the essentials. While the original morphologic diagnosis contained many of the same histologic features enumerated in the contributor's diagnosis, conference participants felt that many of the terms, such as basilar cell vacuolation, apoptosis, and pigmentary incontinence, were subsumed within the term "cytotoxic interface onychitis." The resulting morphologic diagnosis is zippy, accurate, and mercilessly brief.

References:

1. Auxilia ST, Hill PB, Thoday KL. Canine symmetrical lupoid onychodystrophy: a retrospective study with particular reference to management. *J Small Anim Pract*. 2001;42:82-87.
2. Bohnhorst JO, Hanssen I, Moen T. Antinuclear antibodies (ANA) in gordon setters with symmetrical lupoid onychodystrophy and black hair follicular dysplasia. *Acta Vet. Scand*. 2001;42(3): 323-329.
3. Koutinas AF, Carlotti DN, Koutinas C, et al. Claw histopathology and parasitic load in natural cases of canine leishmaniosis associated with Leishmania infantum. *Vet. Dermatol*. 2010;21:572-577.
4. Miller WH, Griffin CE, Campbell KL. Diseases of eyelids, claws, anal sacs, and ears. In: Miller WH, Griffin CE, Campbell KL, eds. *Muller and Kirk's Small Animal Dermatology*. 7th ed. Elsevier; 2012:724-773.
5. Mueller RS, Olivry T. Onychobiopsy without onychectomy: description of a new biopsy technique for canine claws. *Vet. Dermatol*. 1999;10:55-59.
6. Mueller RS, Rosychuck RAW, Jonas LD. A retrospective study regarding the treatment of lupoid onychodystrophy in 30 dogs and literature review. *J Am Anim Hosp Assoc*. 2003;39:139-150.
7. Stern AW, Pieper J. Pathology in Practice. *JAVMA*, 2010;246:197-199.
8. Welle MM, Linder KE. The Integument. In: Zachary JF, ed. *Pathologic Basis of Veterinary Disease*. 7th ed. 2022;Elsevier:1244.
9. Wilbe M, Ziener ML, Aronsson A, et al. DLA class II alleles are associated with risk for canine symmetrical lupoid onychodystropy (SLO). *Plos One*. 2010;5: e12332.

WSC 2023-2024
Conference 7 Self-Assessment

1. Which of the following is the most likely source for *Pelodera strongyloides*?
    a. Damp straw
    b. Stagnant water
    c. Bird feces
    d. Crustacean intermediate host

2. True or false: UV light can result in mutations of p53 which may lead to cancer.
    a. True
    b. False

3. True or false: UV light causes damage to DNA by the formation of purine dimers.
    a. True
    b. False

4. Which of the following is NOT a thymoma-associated paraneoplastic syndrome?
    a. Granulocytopenia in cats
    b. Erythema multiforme in dogs
    c. Macrothrombocytosis in dogs
    d. Myasthenia gravis in cats

5. Separation of the claw with continued proximal attachment is called?
    a. Paronychia
    b. Onychogryphosis
    c. Onychoschizia
    d. Onycholysis

Joint Pathology Center
Veterinary Pathology Services

WEDNESDAY SLIDE CONFERENCE 2023-2024

Conference #8 **11 October 2023**

CASE I:

Signalment:
22-year-old, gelding Appaloosa horse (*Equus caballus*)

History:
This horse had a history of chronic left front foot problems that started after a foot abscess caused by a penetrating foreign body. It had chronic recurrent abscesses with 3 hoof wall resection attempts. A CT scan showed evidence of osteomyelitis and radiographs showed laminitis and a distal displacement abscess in the left front foot. The patient also had a history of recurrent squamous cell carcinoma in the penile sheath and a new lesion in the left third eyelid. The patient also had unregulated pituitary pars intermedia dysfunction. The patient started dribbling urine and the clinician was concerned about renal, lower urinary tract, or neurologic disease. Humane euthanasia was elected.

Gross Pathology:
At necropsy, mucosal membranes were congested. The cranial margin of the left third eyelid contained a 3 mm focal raised, pink nodule. The skin at the base of the penis had multifocal to coalescing 4 to 13 cm raised plaques covered by yellow, friable, crusty material. Urine was oozing freely from the urethra. Multiple 1 to 4 cm diameter black nodules were disseminated within the subcutis of the neck and adjacent to the esophagus. One 1 cm diameter round ulcer was present

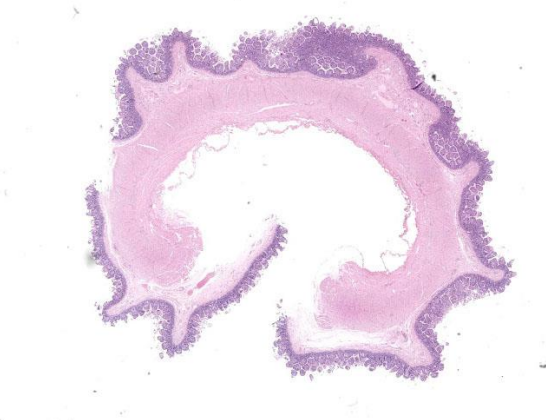

Figure 1-1. Small intestine, horse. One section of small intestine is submitted for examination. There is diffuse villar blunting. (HE, 5X)

at the base of the tongue. Petechiae and ecchymoses were observed on the pericardium. The spleen was enlarged, meaty, and oozed blood. There was a round 3 cm white, soft mass attached to the mesentery, interpreted as lipoma. The liver and kidneys were diffusely congested. The urinary bladder was filled with moderate amounts of opaque yellow urine and the urinary bladder wall was moderately thick and diffusely red. The rest of the urinary tract was unremarkable with no obstructions or uroliths present. Each hoof had variable degrees of fragmentation of the external corneal layer with cracks, with the left front hoof being the most severely affected. On section, the left frontal third phalange had severe deviation of the cranial margin with signs of laminitis and the hoof wall was markedly thickened and contained an air

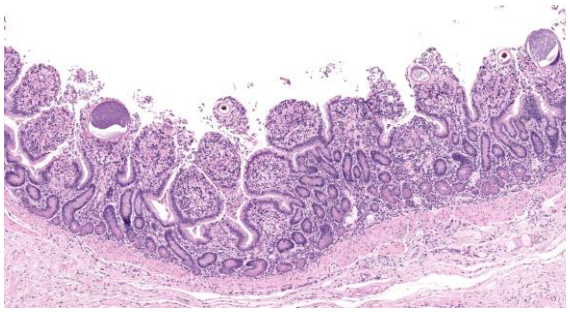

Figure 1-2. Small intestine, horse. There is diffuse villar blunting and scattered intraepithelial macro- and microgametes within the villi. (HE, 66X)

pocket. The pituitary gland was slightly bulged. Representative sections of observed lesions were collected for histopathology.

Microscopic Description:
Small intestine: Most villi are atrophic and blunted. The lamina propria is mildly to moderately expanded by lymphocytes, plasma cells, and eosinophils. A few eosinophils are observed within the submucosa. Within the lamina propria multiple host cells are markedly hypertrophied up to 30-250 µm in diameter with fibrillar cytoplasm and an enlarged peripheral nucleus that forms a crescent along one side of a thick eosinophilic parasitophorous vacuole. The parasitophorous vacuole contains various stages of development of *Eimeria leuckarti*, including microgamonts, macrogamonts, and occasional developing oocysts. Mature microgamonts contain myriad 1-2 µm basophilic microgametes. Intimal bodies are observed in small arteries and arterioles of the submucosa.

Other additional microscopy findings in this horse included pars intermedia pituitary adenoma, squamous cell carcinoma (prepuce and third eyelid), melanomas (neck), osteomyelitis (left front foot), chronic lymphoplasmacytic cystitis, multifocal mineralization of the brain (incidental finding), and eosinophilic preputial dermatitis of unknown etiology (habronemiasis suspected).

Contributor's Morphologic Diagnosis:
Small intestine: Enteritis, eosinophilic and lymphoplasmacytic, mild, subacute with intralesional coccidia (consistent with *Eimeria leuckarti*).

Contributor's Comment:
This horse was in declining health with multiple clinical problems that culminated in humane euthanasia. The intestinal coccidiosis was considered an incidental finding in this horse.

More than a thousand species of *Eimeria* are known to infect domestic and wild animals and birds.[5] *Eimeria leuckarti* is the only species of *Eimeria* consistently reported in horses and it has been consistently found worldwide.[3,10] Infection with *E. leuckarti* is more common in foals but it also affects adult horses.[3,10] Most infections are considered to be of no clinical relevance.[3,10] Clinical enteritis has been reported in very few cases.[3]

E. leuckarti was named after the German scientist Rudolf Leukart and was first recognized as a large-sized protozoan in sections of small intestine of a horse used for teaching anatomy in Switzerland. *E. Leuckarti* has been found in several species of equids including horse, donkey, mule, Asian wild ass, Mountain zebra, and Grant's zebra.[3]

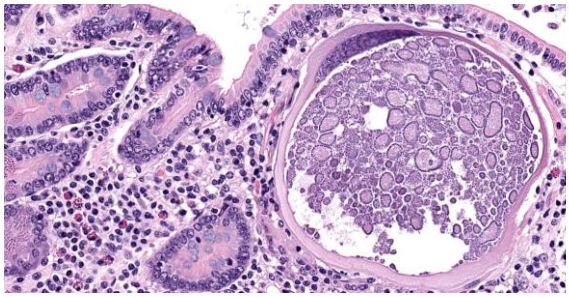

Figure 1-3. Small intestine, horse. Macrogamonts are contained within a hypertrophied enterocyte with a thick hyaline wall and a peripheralized, hypertrophied nucleus. (HE, 350X)

In a study of parasites of horses in farms in Kentucky, *E. leuckarti* infection was common in foals as young as 28 days of age.[7] Prevalence of *E. leuckarti* oocysts in feces of foals in Kentucky from studies in 1986 and 2003 were similar at 41% and 41.6%, respectively, with *E. leuckarti* found in 100% of the farms in the 2003 study and 86% of farms in the 1986 study.[7,8] Foals can acquire the infection on the day of birth, most likely from the contaminated environment rather than from oocysts excreted by their mares.[3] In another study, the prevalence of foals affected by *E. leuckarti* was 59%.[9]

The life cycle for each species of *Eimeria* is host specific and direct.[5] Sexual stages identified as macrogametes (female) are uninucleate and contain peripheral PAS-positive granules. The immature male stage (microgamont, microgametocyte) is multinucleated. When each nucleus becomes incorporated into a sperm-like biflagellate structure (microgamete), the microgamont is considered mature.[5] So far, only gamonts and oocysts of *E. leuckarti* have been found in histological sections of small intestine; asexual stages of *E. leuckarti* have not yet been confirmed.[3]

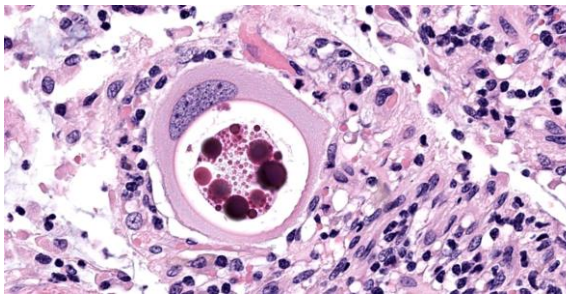

Figure 1-4. Small intestine, horse. A mature macrogamont resides within a hypertrophied epithelial cell. The eosinophilic globules are characteristic and will eventually contribute to the shell of the oocyst. (HE, 667X)

E. leuckarti develop in the cytoplasm of hypertrophied host cells in the lamina propria of the small intestine.[3,5,6] An immunohistochemical study identified these cells as epithelial cells.[6] In this study, the cytoplasm of the host cells was immunopositive for cytokeratin AE1/AE3 and cytokeratin 13. Host cells did not react to vimentin, chromogranin A, neuron-specific enolase, desmin, alpha smooth muscle actin, or factor VIII. It was hypothesized that laminin may regulate the displacement of epithelial host cells parasitized by *E. leuckarti* into the lamina propria.[6] In addition, the expression of CK13 by the host cells implied that the lifespan of the host cells was possibly extended. How the host cells were dislocated to the lamina propria and achieved the extended life span was unclear.[6]

Usually there is no host inflammatory response to *E. leuckarti* and only a mild reaction to degenerate life stages can be seen.[3,10] Parasites are found in the lamina propria towards the luminal part of the villus but some occur throughout villi.[3] In most reports, infections with *E. leuckarti* in equids were considered incidental; however, occasionally it has been considered a cause or contributing factor to enteritis in foals.[3] In many cases, its pathogenicity is attributed to the distinctive large gamonts observed in the lamina propria of horses that died of enteric disease of undetermined cause, however the evidence for *E. leuckarti* causing enteric disease is rarely conclusive.[10]

Detection of *E. leuckarti* oocysts in feces is confirmatory for diagnosis; however, oocysts may be overlooked during routine fecal analysis that uses standard, low specific gravity floatation technique due to the large size and the heavy weight of oocysts.[3,9] The use of a sedimentation technique or floatation method using solution with a specific gravity of 1.3 or higher is recommended because *E. leuckarti* oocysts are large and heavy.[3,9]

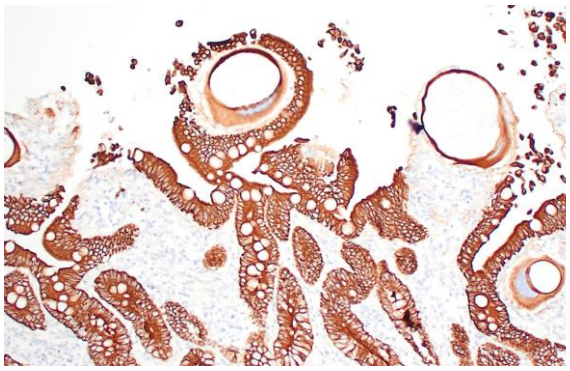

Figure 1-5. Small intestine, horse. A cytokeratin immunohistochemical stain demonstrates that, although the gamonts appear to be in the lamina propria, due to their size, they are actually contained within epithelial cells like other members of the genus *Eimeria*. (anti-AE1/AE3, 200X)

Saturated sodium chloride solution is not recommended.[3] Adding to the difficulty in diagnosing *E. leuckarti* is the short duration of patency and the relatively low oocyst output.[9]

In histological sections, the presence of gamonts and oocysts in the lamina propria of the jejunum and ileum is diagnostic.[3,10] There is a need for case-controlled studies to better understand the pathogenicity of *E. leuckarti* in equids.[3]

Contributing Institution:
Tifton Veterinary Diagnostic and Investigational Laboratory
College of Veterinary Medicine
University of Georgia
43 Brighton Road, Tifton GA 31793.
https://vet.uga.edu/diagnostic-service-labs/veterinary-diagnostic-laboratory/

JPC Diagnosis:
Small intestine: Enteritis, lymphoplasmacytic and eosinophilic, diffuse, mild, with marked villar atrophy and numerous intraepithelial coccidia consistent with *Eimeria leuckarti*.

JPC Comment:
As the contributor notes, *Eimeria leukarti* is a common parasite of the equine gastrointestinal tract; however, despite its ubiquity, it rarely causes significant disease and is most often encountered, as in this case, as an incidental finding at necropsy.

Eimeria spp. are not, however, universally benign. In sheep, *Eimeria gilruthi* forms megaloschizonts in the abomasal mucosa that are visible to the naked eye as multiple white, raised foci, and the clinical disease may include diarrhea, dehydration, anorexia, and weight loss.[1,4] In rabbits, *Eimeria stiedae* develops in the biliary epithelium of bile ducts and can cause significant hepatic changes, visible as large white foci on the surface of the liver, that often culminate in death.[4]

Eimeria spp. are coccidians, which are single-celled obligate intracellular parasites belonging to the phylum Apicomplexa. They keep phylogenetic company with other coccidian genera of veterinary importance, including *Klossiella, Cystoisospora, Hammondia, Besnoitia, Sarcocystis, Neospora,* and *Toxoplasma*, all of which cause disease by destroying their host cells.[2,4] *Eimeria* spp. exhibit the simplest form of the coccidian life cycle, which includes both asexual and sexual stages in the gastrointestinal tract of many vertebrate hosts.[2] Sexual reproduction produces oocysts which are released into the environment by rupture of host gastrointestinal epithelial cells and subsequent passage in the feces. Once in the environment, *Eimeria* oocysts develop eight infective sporozoites through the process of sporulation.[2]

Once the infective sporulated oocyst is ingested by a suitable host, the sporozoites emerge and enter epithelial cells or cells of the lamina propria, where they round up and become trophozoites in a membrane-bound

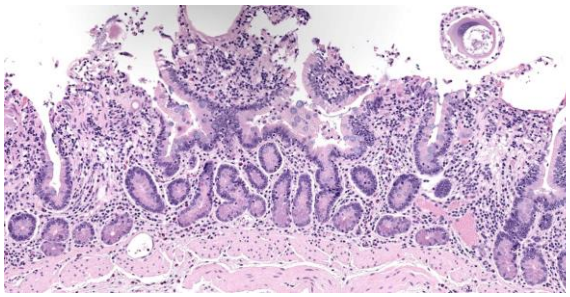

Figure 1-6. Small intestine, horse. There is mild expansion of the lamina propria with mild edema and slightly increased numbers of lymphocytes, plasma cells, and eosinophils. (HE, 144X)

parasitophorous vacuole formed by the host cell membrane.[2] The trophozoites grow larger and multiply asexually within host cells via schizogony (also known as merogony), in which the apical complex is replicated, the nucleus lobulates with portions associated with each apical complex, and the cell membrane contracts and divides to form many individual merozoites encased in a schizont.[4] Depending on the *Eimeria* spp., there may be multiple generations of schizont and merozoite formation; however, the key outcome of schizogony is an exponential increase in the number of zoites and the destruction of host cells in proportion to the degree of infection.[2]

Merozoites produced by the final round of schizogony enter host cells and develop into either microgamonts (male) or macrogamonts (female) through the process of gametogony.[2] Microgamonts undergo repeated nuclear divisions with each nucleus finally incorporated into a flagellated microgamete, which fertilizes the macrogamete to form a zygote.[4] Eosinophilic globular wall-forming bodies present in the macrogamete then coalesce to form a wall around the zygote, forming an oocyst.[2,4] This oocyst is released by rupture of the host cell and the cycle begins anew. This basic life cycle pertains, albeit with increasing complexity and nuance, to the other coccidian genera of veterinary importance.

Our moderator for parasite week was Dr. Chris Gardiner, PhD, self-proclaimed "parasitologist to the stars". Discussion of the parasite in this case focused on identifying the various life stages in tissue section. Several conference participants identified organisms in section as oocysts, though Dr. Gardiner thought they represented trophozoites, the gamont precursor. We noted that the contributor also described oocysts, but none were present in the examined section.

The discussion of pathologic changes centered on the villi, which are substantially blunted, and the degree of inflammation present in the lamina propria. Dr. Bruce Williams noted that intestinal crypts should be closely apposed and should rest on the muscularis mucosae; however, in this case, crypts were widely and irregularly separated and were multifocally elevated off the underlying muscularis mucosae. Though the lamina propria normally hosts a substantial population of inflammatory cells, these crypt changes are important clues that the inflammation (and edema) is more florid than normal, even when, as in this case, the enteritis is considered mild.

References:

1. Ammar SI, Watson AM, Craig LE, et al. *Eimeria gilruthi*-associated abomasitis in a group of ewes. *J Vet Diagn Invest*. 2019;31(1):128-132.
2. Bowman DD. Protozoa. In: Bowman DD, ed. *Georgis' Parasitology for Veterinarians*. 9th ed. Elsevier;2009:92-94.
3. Dubey JP, Bauer C. A review of *Eimeria* infections in horses and other equids. *Vet Parasitol*. 2018;256:58-70.
4. Eberhard, ML. Histopathologic diagnosis. In: Bowman DD, ed. *Georgis'*

Parasitology for Veterinarians. 9th ed. Elsevier;2009:377-380.
5. Gardiner CH, Fayer R, Dubey JP. *An Atlas of Protozoan Parasites in Animal Tissues*. 2nd ed. Armed Forces Institute of Pathology, American Registry of Pathology;1998;20-28.
6. Hirayama K, Okamoto M, Sako T, et al. *Eimeria* organisms develop in the epithelial cells of the equine small intestine. *Vet Pathol*. 2002;39:505-508.
7. Lyons ET, Drudge JH, Tolliver SC. Natural infection with *Eimeria leuckarti*: Prevalence of oocysts in feces of horse foals on several farms in Kentucky during 1986. *Am J Vet Res*. 1988;49:96-98.
8. Lyons ET, Tolliver SC. Prevalence of parasite eggs (*Strongyloides westeri*, *Parascaris equorum*, and strongyles) and oocysts (*Eimeria leuckarti*) in the feces of Thoroughbred foals on 14 farms in central Kentucky in 2003. *Parasitol Res*. 2004;92:400-404.
9. McQueary CA, David EW, Catlin JE. Observations on the life cycle and prevalence of *Eimeria leuckarti* in horses in Montana. *Am J Vet Res.* 1977;38:1673-1674.
10. Uzal FA, Plattner BL, Hostetter JM. Alimentary System. In: Maxie MG, ed. *Jubb, Kennedy, and Palmer's Pathology of Domestic Animals*. 6th ed. Vol 2. Elsevier;2016:233.

CASE II:

Signalment:
6-month-old, female Yorkshire pig (*Sus domesticus*)

History:
Seven 6-month-old pigs were shipped to a research facility and all animals developed a high-grade fever and high respiratory rate one week after arrival. The animals were treated with antibiotics and nonsteroidal anti-inflammatories to reduce the fever. One died overnight and was submitted for necropsy.

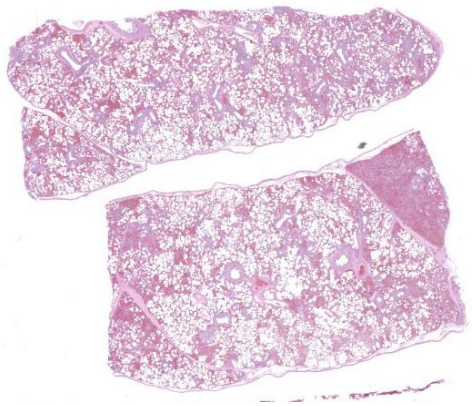

Figure 2-1. Lung, pig. Two sections of lung are submitted for examination. There is patchy to lobular inflammation scattered throughout the sections. (HE, 5X)

Gross Pathology:
The lungs were diffusely mottled red to dark red, with patchy areas of consolidation on the right side.

Laboratory Results:
PCR positive for Porcine Reproductive and Respiratory Syndrome Virus.

PCR negative for Porcine circovirus-2, PCV-3, and Influenza A.

Lung culture resulted in moderate amounts of mixed bacterial growth.

Microscopic Description:
In multifocal to coalescent foci affecting approximately 30% of the examined area of lung, alveolar spaces are filled with erythrocytes, fibrin, large numbers of macrophages, fewer multinucleated giant cells, and scattered eosinophils and neutrophils. Adjacent alveolar septa are moderately to markedly widened by fibrin and similar inflammatory infiltrates, and occasionally form confluent ruptured spaces (emphysema). Multifocally,

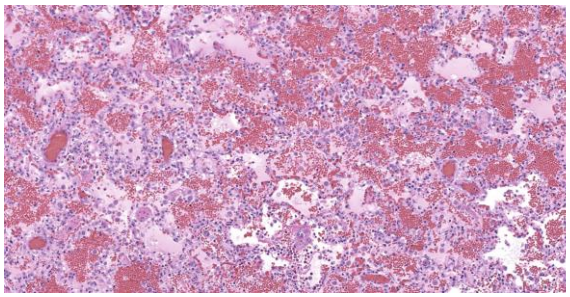

Figure 2-2. Lung, pig. In inflamed areas, septa are markedly expanded and alveoli are hypercellular with abundant hemorrhage, edema, and occasionally, aggregates of polymerized fibrin. (HE, 152X)

alveolar macrophages are hypereosinophilic and contain pyknotic nuclei (necrosis). The inflammatory infiltrate often extends into and fills terminal bronchioles, with expansion and disruption of the epithelium by inflammation. Affected bronchioles are lined incompletely by attenuated epithelium. Multifocally throughout affected and unaffected regions of lung are numerous nematode larvae within both alveoli and bronchioles. Nematode larvae are 40-60 µm in diameter, with a 3 µm thick smooth cuticle, prominent lateral alae, large lateral chords, and coelomyarian-polymyarian musculature. The pseudocoelom contains a polycytous intestine lined by uninucleate epithelial cells. Some bronchioles that contain nematodes are lined by variably hyperplastic to eroded epithelium infiltrated by increased numbers of eosinophils. Interlobular septa are expanded by edema.

Contributor's Morphologic Diagnosis:
Lung: Interstitial pneumonia, histiocytic and eosinophilic, acute, multifocal to coalescing, moderate, with intra-alveolar macrophage necrosis, and intra-alveolar and intra-bronchiolar ascarid larvae consistent with *Ascaris suum*.

Contributor's Comment:
While the patchy inflammatory infiltrate is occasionally centered on nematode larva in this case, interstitial pneumonia in pigs has several viral and bacterial differential diagnoses. The presence of necrotic alveolar macrophages increased the suspicion for Porcine Reproductive and Respiratory Syndrome (PRRS) virus, and the virus was detected in the lung by PCR.

PRRS virus is a porcine arterivirus with a wide variety of clinical manifestations in pig herds depending on the endemic nature of the virus in the herd, age, immune status, and presence of coinfecting pathogens.[2] Most notably, the virus causes reproductive and respiratory disease. The virus infects macrophages at the point of entry and disseminates to local lymphoid tissue, resulting in viremia and systemic infection.[7] Pulmonary lesions are characterized by interstitial pneumonia with expansion of the alveolar septa by increased numbers of mononuclear leukocytes.

Necrotic macrophages and smudged chromatin within alveoli are consistent findings in PRRS infection.[2]

PRRS virus infection has been reported to have immunosuppressive effects that enable secondary viral and bacterial infections.[7] Multiple mechanisms of immunosuppression have been described, including reduction in NK cell cytotoxic activity, promotion of immunosuppressive cytokines IL-10 and TGF-B, and impairment of pulmonary macrophage functional activity.[2,5,7] *Streptococcus suis*, *Glaesserella parasuis*, and *Salmonella* spp. are common co-infecting pathogens, but an association with pulmonary parasitism or parasite migration has not been described.[2]

The intrapulmonary helminths in this case are morphologically consistent with ascarid nematodes. In combination with the signalment, the histologic features of the ascarid nematode (diameter, presence of prominent lateral alae, and appearance of the hypodermis, musculature, and intestinal tract) are compatible with larval *Ascaris suum*.[4]

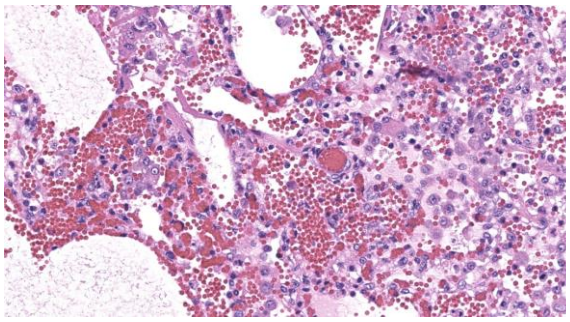

Figure 2-3. Lung, pig. Two sections of lung are submitted for examination. In inflamed areas, septa are expanded by macrophages, neutrophils, fibrin, and type II pneumocytes, and similar inflammatory cells are present within alveoli where they are admixed with abundant hemorrhage, fibrin, and edema. (HE, 381X)

Ascaris suum is ubiquitous in swine populations and infection results in production losses and potentially severe pathologic consequences.[1] The life cycle, as with most ascarids, involves ingestion of the ascarid egg which hatches in the gastrointestinal tract. The larvae gain access to the portal vasculature, leading to larval migration through the hepatic parenchyma. From there, larvae access the pulmonary vasculature and enter alveoli. Eventually larvae ascend the bronchiolar tree and are coughed up and swallowed back into the gastrointestinal tract where they develop into sexually mature adults. Mechanical damage by the migrating larvae in the lung results in hemorrhage, edema, and eosinophil infiltration. As the larvae mature, an eosinophilic bronchiolitis ensues, with reactive hyperplasia or denuding of bronchiolar epithelium and invasion of eosinophils into bronchiolar walls.[1,2]

While an immunologic association between the PRRS infection and the ascarid infection could not be determined, this case highlights the importance of ruling out primary viral causes of pneumonia in pigs with pulmonary ascariasis.

Contributing Institution:
Washington State University
Department of Veterinary Microbiology and Pathology and the Washington Animal Disease Diagnostic Laboratory
https://waddl.vetmed.wsu.edu/, and https://vmp.vetmed.wsu.edu/

JPC Diagnoses:

1. Lung: Pneumonia, interstitial, lymphohistiocytic, multifocal, marked, with type II pneumocyte hyperplasia and peribronchiolar and perivascular lymphoid hyperplasia.

2. Lung: Pneumonia, interstitial, histiocytic and eosinophilic, multifocal, mild, with eosinophilic bronchiolitis and ascarid larvae.

JPC Comment:
Ascarids are nematodes of extremes. They are among the largest of the worms found in domestic animals, with members of the order Ascaridida ranging from several inches up to 2 feet in length.[1] Ascarid eggs are also remarkably resistant to chemical and physical insults in the environment and can remain infective in soil for years.[1]

The life cycle of the terrestrial ascarids tend to be direct, and larvae undergo two molts within their hardy eggshell, emerging within the host as infective L3 larvae.[1] Ascarids also tend to be relatively host specific, and most domestic species have at least one ascarid to call their very own; *Parascaris equorum* infects horses, *Toxocara vitulorum* infects cattle, *Taxocara canis* infects dogs, *Toxocara cati* infects cats, and, of course, *Ascaris suum* infects swine.[1]

There are exceptions to this "one ascarid, one host" rule. Historically, *Ascaris suum* was thought to be identical to *Ascaris lumbricoides* in humans, though these two

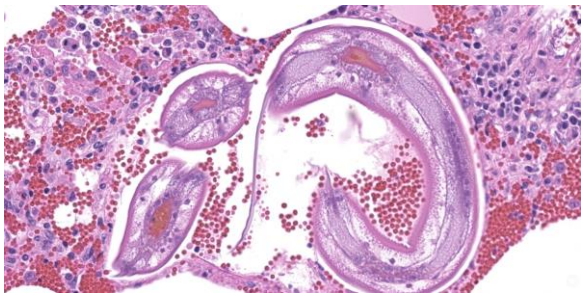

Figure 2-4. Lung, pig. Cross and tangential sections of ascarid larvae are present within the parenchyma. The larvae (which at this stage possess neither gonads nor eggs) have lateral alae, polymyarian-coelomyarian musculature, prominent lateral chords, and a uninucleate intestine. (HE, 450X)

organisms are now considered distinct species. Nevertheless, *A. lumbricoides* can mature in swine and *A. suum* can mature in humans, as evidenced by one recent study where 50 *A. suum* eggs were fed to healthy, human research subjects.[1,3] Once they emerged from the required regulatory paperwork, researchers found that experimental infection produced clinical symptoms identical to *A. lumbricoides* infection, including respiratory discomfort and radiographic evidence of pulmonary larval migration, and *A. suum* eggs were recovered from the feces of the intrepid volunteers.[3] *A. suum* may also infect sheep, causing mild respiratory disturbances in young lambs. Calves exposed to yards contaminated with infective pig feces may develop severe acute interstitial pneumonia with millions of *A. suum* larvae present in the lungs.[6]

The contributor provides an excellent summary of the winding walkabout taken by the typical *A. suum* larva after emerging from its egg in the small intestine of its porcine host. In young pigs, extensive pulmonary damage can lead to severe respiratory disease, with rapid, shallow breaths and audible expiratory efforts ("thumps") that may lead to death.[1] As larvae wander through the liver, the mechanical damage and ensuing inflammation heal by fibrosis, producing "milk spots" that cause condemnation of the liver at slaughter.[1] While less pathogenic, infection by adult worms may cause diarrhea, impaired nutritional uptake and growth, and rare disorders such as perforated bowels or bile duct occlusion.[1] Taken together, these effects make *Ascaris suum* the most economically important nematode of swine.

Dr. Gardiner reminded conference participants that nematode larvae are typically coiled; thus, when assessing parasite load on histology, it is helpful to remember that a close grouping of cross sections typically represents only one larva, not multiple. Dr. Gardiner also noted that conference participants failed to describe the nematode excretory cells, visible as eosinophilic material within the larval lateral cords.

Dr. Williams noted that you rarely find only one process in pig lungs; they tend to reward careful evaluation with additional revelations. In this case, while the nematode larvae may initially hog the spotlight, careful examination reveals multiple areas within the lungs that are devoid of nematodes but rich in macrophages, fibrin, hemorrhage, edema, and multinucleated cells. These lesions are not entirely attributable to nematode migration, and a young pig with many macrophages and multinucleated cells in the lungs should raise suspicion for PRRSV and PCV-

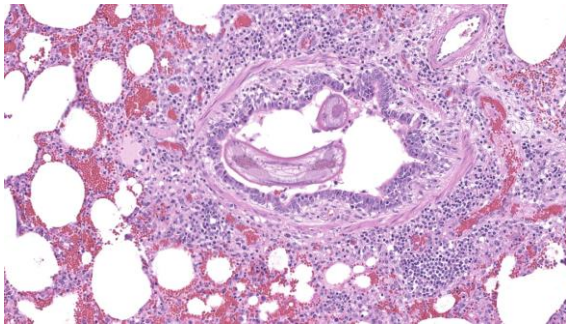

Figure 2-5. Lung, pig. Ascarid larvae are also present in airways. (HE, 175X)

2. Differentiating the two can be difficult, though large numbers of necrotic macrophages, while not apparent in the section examined at conference, are characteristic of PRRSV infection.

There was spirited discussion about whether to combine the nematode and PRRSV lesions into one morphologic diagnosis, particularly since assigning histologic effects to one etiology or another is somewhat artificial in this case. The separatists carried the day, however, as the majority of participants felt the etiologic agents were unrelated, each notable, and each deserving of their due.

References:

1. Bowman DD. *Georgis' Parasitology for Veterinarians*. 10th ed. Elsevier;2014: 191-192.
2. Caswell JL, Williams KJ. The respiratory system. In: Maxie MG, ed. *Jubb, Kennedy, and Palmer's Pathology of Domestic Animals*. 6th ed. Vol 2. Elsevier Saunders;2016:523-526.
3. da Silva TE, Barbosa FS, Magalhaes LMD, et al. Unraveling Ascaris suum experimental infection in humans. *Microbes Infect*. 2021;23(8):104836.
4. Gardiner CH, Poynton SL. *An Atlas of Metazoan Parasites in Animal Tissues*. Armed Forces Institute of Pathology/ American Registry of Pathology; 2006:2-29.
5. Toman M, Celer V, Kavanova L, et al. Dynamics and differences in systemic and local immune responses after vaccination with inactivated and live commercial vaccines and subsequent subclinical infection with PRRS virus. *Front Immunol* 2019;10:1689.
6. Uzal FA, Plattner BL, Hostetter JM. Alimentary System. In: Maxie MG, ed. *Jubb, Kennedy, and Palmer's Pathology of Domestic Animals*. 6th ed. Vol 2. Elsevier Saunders;2016:218-219.
7. Zimmerman JJ, Benfield DA, Dee SA, et al. Porcine reproductive and respiratory syndrome (porcine arterivirus). In: Zimmerman JJ, Karriker LA, Ramirez A, Schwartz KJ, Stevenson GW, eds. *Diseases of Swine*. 10th ed. Blackwell Publishing;2012:52,461-480.

CASE III:

Signalment:
Age unknown, adult male octopus (*Octopus vulgaris*)

History:
An experimentally naïve octopus was found dead in the morning. The animal was caught from the shores of the Florida Keys and had been doing well for up to a month when it started displaying periods of lethargy and decreased appetite. One night, the animal went into one of its tunnels and never re-emerged. Water quality parameters were within normal limits during this period.

Gross Pathology:
A dead, frozen male octopus with mottled pale brown to gray skin was received for examination in severely autolyzed post-mortem condition. The skin had numerous foci of subtle white discoloration.

Figure 3-1. Esophagus and digestive gland, octopus. One section of the esophagus (above) and digestive gland (below) are submitted for examination. (HE, 5X)

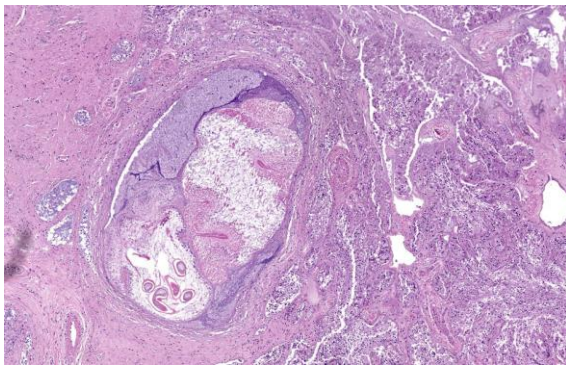

Figure 3-2. Digestive gland, octopus. A larval cestode (left) is embedded within an area of fibrosis within the digestive gland. (HE, 52X)

Microscopic Description:
Digestive gland: Approximately 20% of the digestive gland mucosa is effaced by multifocal to coalescing nodules of fibrosis, necrosis, and inflammation centered around cestode larvae of up to 650 µm in diameter, with a 4-6 µm thick, homogeneous, eosinophilic tegument, spongy parenchyma, numerous peripheral calcareous corpuscles, suckers, and bilaterally symmetrical bothria with multiple tentacles that were anchored by prominent bulbs encircled by striated retractor muscles that attached to everted or invaginated hooks. Confident assessment of mucosal and cellular details is hampered by a high degree of postmortem autolysis and freeze-thaw artifacts.

Esophagus: Occasionally within the lumen or embedded in the esophageal wall are cestode larvae with similar features as previously described.

Contributor's Morphologic Diagnosis:
Digestive gland and esophagus: Moderate, multifocal to coalescing, chronic cestodiasis, with hemocytic infiltrates, necrosis, and fibrosis.

Contributor's Comment:
Despite the severe degree of postmortem autolytic and freeze-thaw artifacts, this octopus had unequivocal cestodiasis in the digestive tract, widespread coccidiosis in all examined skin tissues (including arms, funnel, and dorsal mantle), eyes, and gills, consistent with *Aggregata* spp. infection, and varying degrees of systemic hemocyte infiltration throughout the body.

Cestodiasis in cephalopods is common, and many cephalopod species serve as intermediate or paratenic hosts and act as vectors for other intermediate or definitive hosts. Adult cestodes are not frequently reported, but the diversity of larval and post-larval stages found in cephalopods suggests that they are important intermediate hosts for the development of adult stages that parasitize cartilaginous and bony fish. In cephalopods, larval cestodes most often infect the digestive tract, but may be found free in the mantle cavity or encysted within the mantle musculature. The most commonly reported cestode to infect cephalopods is *Phyllobothrium* spp, but cestodes from other genera have also been identified in the common octopus (*Octopus vulgaris*) and include the onchoproteocephalidean *Acanthobothrium* spp, the tetraphyllidean *Anthobothrium* spp, and the trypanorhynch *Nybelinia* spp. Adult stages of Tetraphyllidea and Trypanorhynchea are found within the gastrointestinal tract of sharks, skates, and rays, and their larval forms are some of the most commonly identified cestodes in cephalopods.[3]

Coccidiosis is a common, chronic disease in cephalopods, caused by an obligate, intracellular protozoa in the phylum Apicomplexa, family Aggregatidae. To date, 10 species have been described worldwide in octopus, squid, and cuttlefish. All 10 species are considered pathogenic. This disease primarily affects the digestive tract of cephalopods, but extraintestinal coccidiosis, as seen in this case, have been reported when it harbors an intense infection. Damage to the host includes mechanical, biochemical, and molecular effects, and infection severely weakens

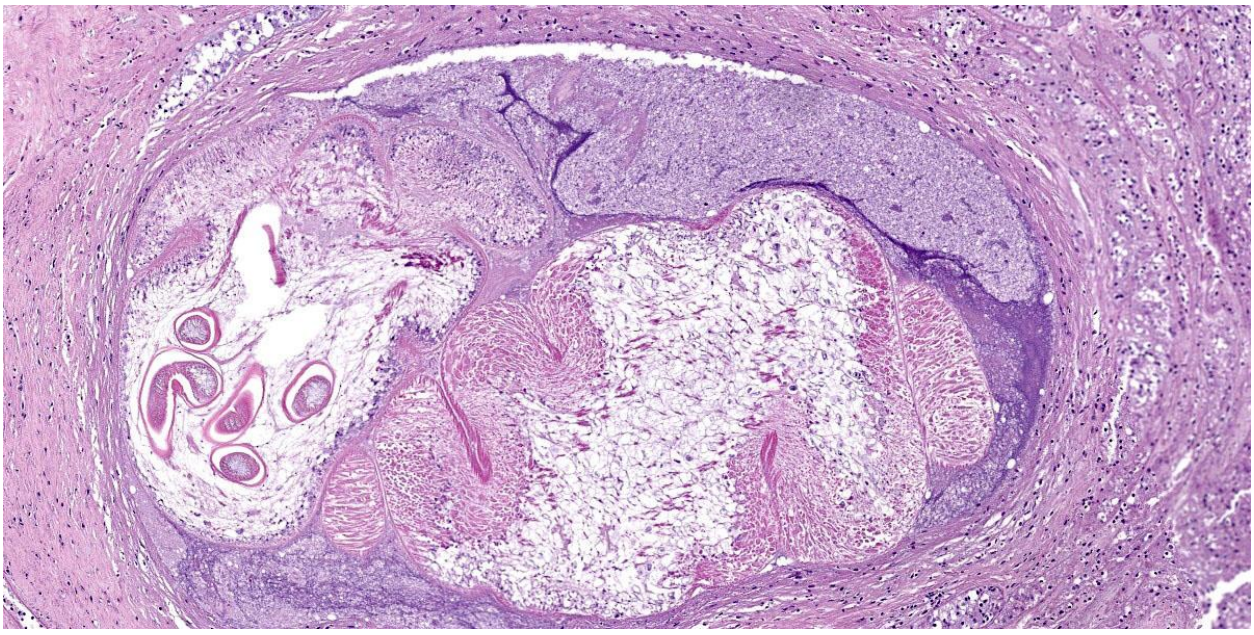

Figure 3-3. Digestive gland, octopus. The cestode has an armed rostellum (suckers with birefingent hooklets), a spongy parenchyma, and numerous calcareous corpuscles. (HE, 106X)

the host's innate immunity making it vulnerable to secondary infections. Notable signs of disease include malabsorption syndrome, decrease in the number of hemocytes, plasmatic protein, and iron in hemolymph, as well as up- regulation of immune genes.[1]

Senescence can also cause immunosuppression and make the octopus more susceptible to secondary diseases. This octopus also had evidence of cataract in one eye, similar to what has been described in the literature, in which possible underlying causes for the intraocular lesions included water quality, ocular manifestation of a systemic disease, intraocular infection, or natural senescence. Senescence is a natural pre-death process in octopuses and other species. While senescence is not a disease or a result of illness, diseases can be a symptom of senescence. Clinical signs of senescence in octopuses are observed over a couple of months and are reported to include loss of appetite, weight loss, retraction of skin around the eyes, uncoordinated movements, and increased undirected activity level. In octopuses, senescence-like symptoms can also be triggered by collection stress, systemic diseases, and improper water temperature or water quality.

Octopuses lack a humoral immune system, and their innate immune system with cellular factors is their primary mechanism of defense against disease. The octopus' hemocytes respond to infection with phagocyntesis, encapsulation, infiltration or cytotoxicity, aiming to destroy or isolate pathogens.[2] In summary, senescence and/or stress may have facilitated parasitic burden, inflammation, other infectious processes, and potential sepsis as contributory factors to the demise of this octopus.

Contributing Institution:
Laboratory of Comparative Pathology
(Memorial Sloan Kettering Cancer Center, The Rockefeller University, and Weill Cornell Medicine)
http://www.mskcc.org/research/comparative-medicine-pathology-0

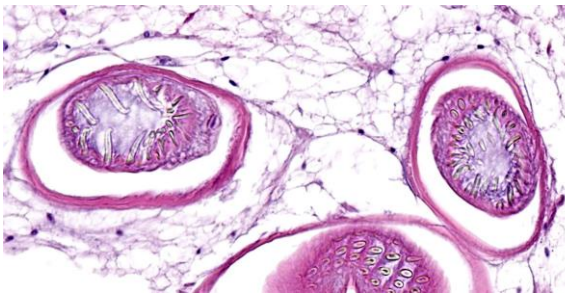

Figure 3-4. Digestive gland, octopus. High magnification of the hooked tentacles of the cestode. (HE, 660X)

JPC Diagnoses:

1. Digestive gland and esophagus: Larval cestodes, multiple, with fibrosis and hemocytic inflammation.
2. Digestive gland: Atrophy, diffuse, moderate.

JPC Comment:

This case provides an excellent example of cestodiasis in an unusual species, and the contributor provides a good summary of the histologic lesions that typify cestode infections in cephalopods.

An additional finding in this case was atrophy of the digestive gland, the histologic correlate for which is loss of eosinophilic cytoplasmic globules. Although this is a common lesion in senescence, it can be observed in any animal with negative energy balance.

In this case, the reported severe coccidiosis and resultant malabsorption likely led to negative energy balance and digestive gland atrophy. While infections are reportedly more common and more abundant in senescent animals, the primary lesion of senescence is gonadal atrophy.[4]

Coccidia were not observed in the examined slide, which included esophagus and digestive gland. While the gills and the intestines are commonly infected, esophagus and digestive gland can be infected with coccidia in severe cases. Of all cephalopod species, common octopuses are one of the most commonly infected with *Aggregata* spp.

Conference discussion was facilitated by JPC's very own Dr. Elise LaDouceur, who discussed cephalopod anatomy generally, before diving into the histologic lesions. The digestive gland is analogous to the mammalian liver and the normally abundant eosinophilic globules within the digestive gland are typically packed with storage products such as glycogen and lipid. Dr. LaDouceur noted that the digestive gland was extremely autolyzed, but despite the autolysis, the lack of eosinophilic globules within the digestive gland was notable. This led to a discussion of senescence, a feature of many invertebrates' life history, where metabolism is shut down after release of gonads.

Conference participants discussed the large cestode larvae within the digestive gland and the accompanying multifocal areas of necrosis in the adjacent parenchyma, interpreted as migration tracts. Dr. Gardiner believed the organism to be an encysted cestode, which would typically grow in place without mov-

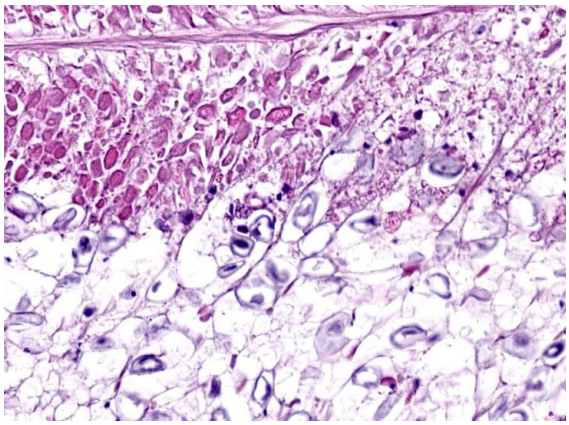

Figure 3-5. Digestive gland, octopus. There are oval amphophilic calcareous corpuscles within the spongy body parenchyma. (HE, 570X)

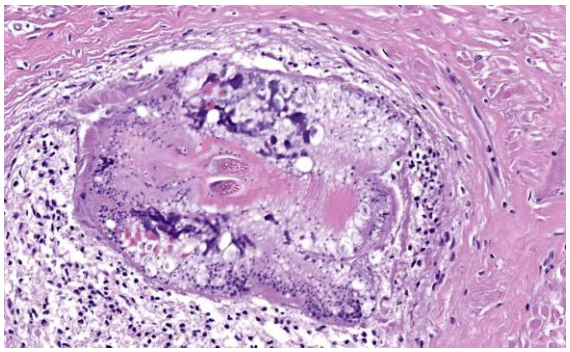

Figure 3-6. Esophagus, octopus. A similar larval cestode is present within the muscular wall. Nuclei of hemocytes are present adjacent to the cestode. (HE, 315X)

ing through the tissue and questioned whether the histologic features represented true migration tracts. These histologic features do, however, align with recent published reports in cephalopods that feature cestodes invading tissues of organs with non-chitinized epithelium, leaving behind trailing necrotic foci.

Finally, Dr. LaDouceur pointed conference participants to an excellent, open-source resource by Gestal, *et al* (see reference below), which provides excellent gross and histologic images of common cephalopod pathogens, along with discussion of the unique biology of these interesting Molluscans.

References:

1. Castellanos-Martínez S, Gestal C, Pascual S, Mladineo I, Azevedo C. Protist (Coccidia) and related diseases. In: Gestal C, Pascual S, Guerra Á, Fiorito G, Vieites J, eds. *Handbook of pathogens and diseases in Cephalopods*. Springer; 2019:143-152.
2. de Linde Henriksen M, Ofri R, Shomrat T, et al. Ocular anatomy and correlation with histopathologic findings in two common octopuses (Octopus vulgaris) and one giant Pacific octopus (Enteroctopus dofleini) diagnosed with inflammatory phakitis and retinitis. *Vet Ophthalmol*. 2021;24(3):218-228.
3. Finnegan DK, Murray MJ, Young S, Garner MM, LaDouceur EEB. Histologic lesions of cestodiasis in octopuses. *Vet Pathol*. 2023;60(5):599-604.
4. Gestal C, Pascual S, Guerra Á, Fiorito G, Vieites J, eds. *Handbook of Pathogens and Diseases in Cephalopods*. Springer; 2019. Available at: https://link.springer.com/book/ 10.1007/ 978-3-030-11330-8.
5. Rich AF, Denk D, Sangster CR, Stidworthy MF. A retrospective study of pathologic findings in cephalopods (extant subclasses: Coleoidea and Nautiloidea) under laboratory and aquarium management. *Vet Pathol*. 2023;60(5):578-598.

CASE IV:

Signalment:
1-year-old, Gypsy Vanner colt (*Equus caballus*)

History:
The patient presented for acute recumbency and was treated in the field with antimicrobials, plasma, and IV fluids. He was unable to rise but would sit in sternal recumbency and would eat when offered hay. On presentation, he was in lateral recumbency on the trailer, but was able to stand when assisted with the sling. He was severely underweight with muscle wasting. His heart rate was 80 bpm with a systolic murmur, his respiratory rate was 40 bpm, and his rectal temperature was 98.5 ºF. Mucous membranes were pale with a capillary refill time of 2 seconds.

Thoracic ultrasound revealed mild pneumonia (comet tailing cranioventrally) with a small amount of pleural fluid. Abdominal ultrasound revealed edema in the wall of the colon, small intestine, and cecum along with a moderate amount of fluid within the

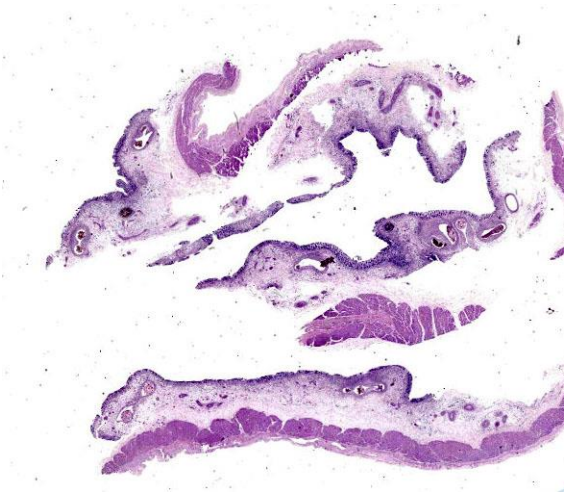

Figure 4-1. Colon, horse. Marked edema is evident in the submucosa and, to a lesser extent, the mucosa of the submitted sections. (HE, 5X)

cecum and colon. A small amount of peritoneal fluid was present.

Medical therapy consisted of IV fluids, ceftiofur, flunixin, vitamin E, and supportive care. Two days after presentation, the patient was found colicking and abdominal radiographs at that time revealed a large amount of intestinal sand. He began passing large amounts of diarrhea but continued to have a good appetite and remained standing (assisted with sling). A plasma transfusion was given, but the patient continued to have profuse watery diarrhea and began to slowly decline over the next 36 hours. Two days later he became increasingly dull and spontaneously died.

Gross Pathology:
The cecal and ventral colonic mucosa contains numerous widespread multifocal, brown to red, 1-2 mm diameter circular nematodes. In the region of the diaphragmatic flexure, the right dorsal colon contains a moderate amount of wet, packed, tan, granular material (sand) admixed with numerous 8-5 x 1 mm red round nematodes and a small amount of green fibrous ingesta. The wall of the cecum and ventral colon is mildly to moderately expanded by clear gelatinous material. Numerous pinpoint red foci are present within the mucosa of the dorsal colon.

Laboratory Results:
Complete blood count:
WBC = 12,700/µL
Fibrinogen = 600 mg/dL

Serum chemistry:
Total protein = 5.6 g/dL (6.1-8.4)
Albumin = 2.2 g/dL (2.7-4.5)
Potassium = 5.6 mEq/L (2.2-5.3)
Sodium = 130 mEq/L (136-144)
Chloride = 94 mEq/L (96-105)

Fecal float: Negative.

Microscopic Description:
Randomly distributed throughout the large intestinal submucosa and rarely within the mucosa, there are encapsulated 20-400 µm diameter larval nematodes. The nematodes have a ridged eosinophilic cuticle, platymyarian-meromyarian musculature, vacuolated lateral cords, and an intestine that is lined by few multinucleated cells and contains red to brown granular material. Occasional nematodes are mineralized. The nematodes are often surrounded by a moderate number of macrophages and few fibroblasts. The submucosa is markedly edematous and

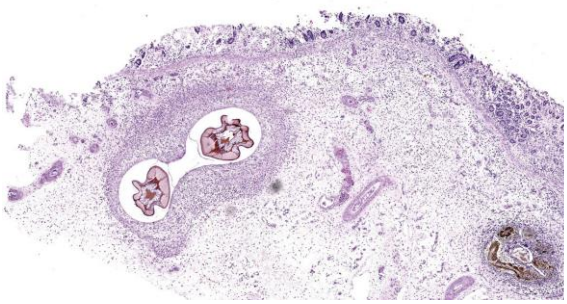

Figure 4-2. Colon, horse. Large larval nematodes are surrounded by poorly formed granulomas within the submucosa. (HE, 47X)

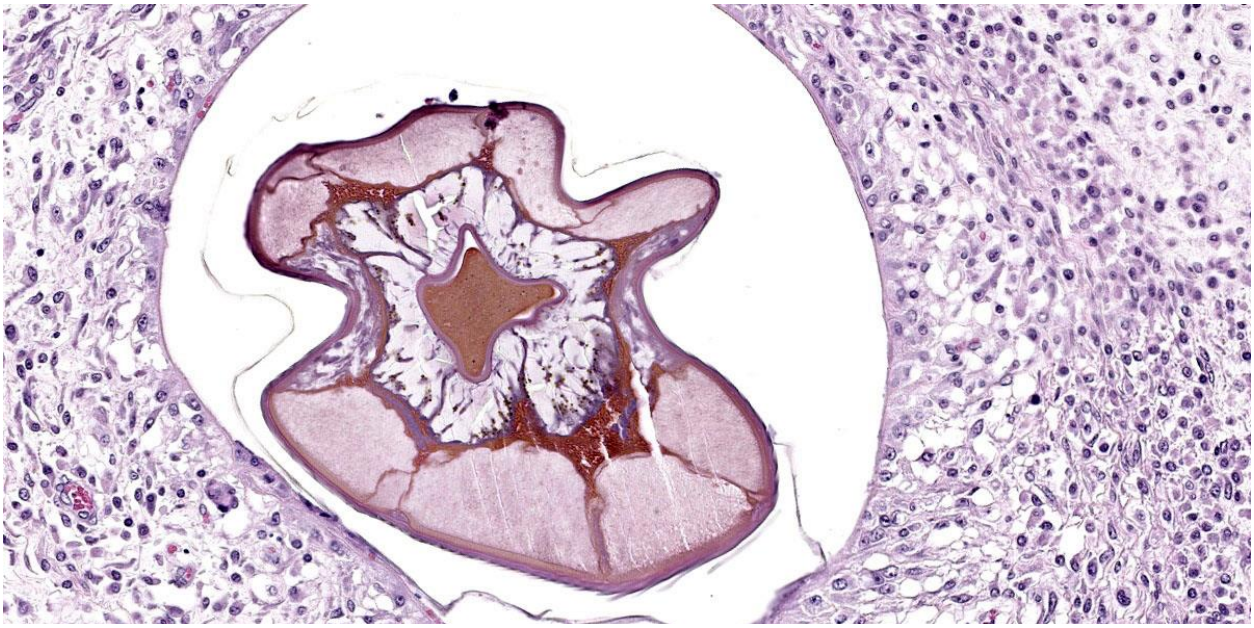

Figure 4-3. Colon, horse. Embedded nematodes have a thin cuticle, pseudocoelom, platymyarian-meromyarian musculature, large lateral chords, and a central large intestine with uninucleated, tall columnar cells which contains luminal blood pigment. (HE, 278X)

contains a low number of lymphocytes and fewer plasma cells. The lamina propria contains a low to moderate number of plasma cells, including occasional Mott cells, fewer lymphocytes and occasional macrophages and neutrophils. There are rare small superficial mucosal erosions.

Contributor's Morphologic Diagnosis:
Colon: Colitis, granulomatous, chronic, with edema and intralesional encapsulated nematodes consistent with small strongyles.

Contributor's Comment:
Referred to as small strongyles or red worms, the more than 50 species of cyathostomins can infect horses of any age, but more severe clinical disease is typically noted in young horses.[2] Cyathostomins have a direct life cycle and horses become infected with cyathostomins by ingestion of the early L3 stage, which burrows into the mucosa of the hindgut and forms a fibrous capsule within two weeks, cloaking it from the host's immune system.[2,4] Development can arrest for as long as 2 years in the early L3 stage.[2]

Late fourth stage larvae exit the mucosa to mature to the adult stage in the intestinal lumen.[4] The emergence of a large number of L4 larvae from the hindgut, in late winter and early spring in temperate regions and late summer and early fall in tropical regions, triggers the syndrome of larval cyathostomiasis.[3] Clinically, horses present with rapid weight loss, colic, leukocytosis, hyperglobulinemia, hypoproteinemia, rough hair coat, and severe diarrhea containing a large number of larval cyathostomins detectable by dilution of feces with water and viewing under a microscope.[3,4] Edema of the limbs and ventrum can also be seen.[3]

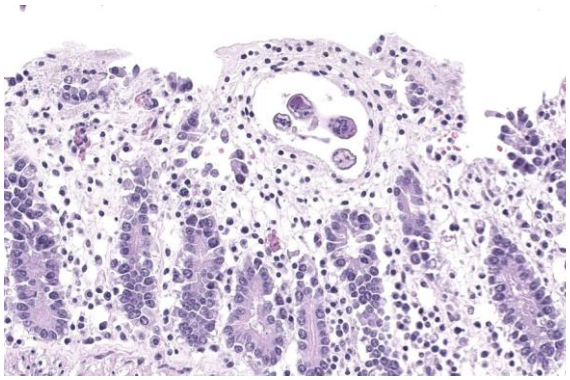

Figure 4-4. Colon, horse. The overlying edematous mucosa contains 3rd stage larvae. Colonic glands are separated by edema and moderate numbers of lymphocytes and plasma cells. (HE, 166X)

Contributing Institution:
University of Florida
College of Veterinary Medicine
Department of Infectious Diseases and Pathology
Gainesville, FL 32611-0880
http://idp.vetmed.ufl.edu/

JPC Diagnosis:
Colon: Colitis, granulomatous, multifocal, mild to moderate, with marked submucosal edema and small strongyle larvae.

JPC Comment:
As the contributor notes, there are approximately 40-50 species of cyathostomins that parasitize the cecum and colon of horses, and as many as 15 to 20 of these species commonly colonize the same host at the same time.[1] Luckily, cyathostomin larvae do not migrate far beyond the mucous membranes of the cecum and colon and feed mainly on intestinal contents, so their pathogenic effect can be minimal.[1,5] However, infection by large numbers of arrested cyathostomin larvae and their simultaneous emergence from the gut wall can cause the clinical disease of larval cyathostominosis described by the contributor.

Larval cyathostominosis is a significant cause of morbidity and mortality in horses and can affect horses of any age.[5] Grossly, the colonic mucosa is studded with 2-5 mm diameter nodules that are slightly raised, red or black, and contain encysted third or fourth stage hypobiotic (developmentally arrested) larval nematodes.[5] Histologically, the mucosa and submucosa are edematous, as in this case, and may contain a mixed inflammatory response either centered on encysted larvae in the submucosa or more diffusely throughout the lamina propria.[5]

Cyathostomins are widespread throughout the world, and even apparently healthy horses may be infected with tens to hundreds of thousands of their larvae. As anthelmintic resistance of cyathostomins is a large and growing problem, many current preventive measures are focused on pasture and herd management solutions.[1] It has been said (by a parasitologist, naturally) that "the king's horses probably had fewer worms" owing to the immediate removal of fecal material after deposition, and this concept has inspired the development of pasture vacuums and pasture sweepers.[1] Other suggested preventive measures include rotation of administered anthelmintics, orchestrating field plowing to reduce the spreading of infective fecal material, and the composting of horse manure.[1]

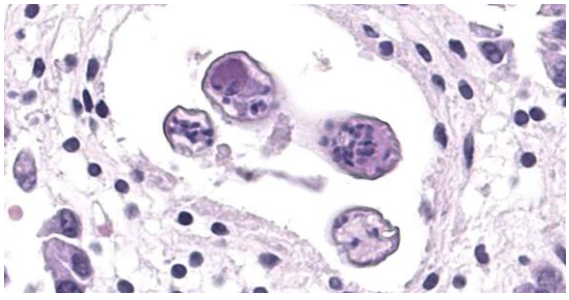

Figure 4-5. Colon, horse. 3rd stage larvae do not have numerous nuclei lining developing internal organs. (HE, 576X)

Conference discussion focused initially on tissue identification. The significant amount of autolysis in section complicated the issue, but the lack of identifiable villi placed this solidly in the colon. The examined section was notable for the lack of fibrosis around the larvae, leading conference participants to speculate that this tissue section was procured early in infection or that the horse's immune response to the larvae might have been impaired. Participants also discussed how simultaneous eruption of myriad larvae can cause loss of the enteric mucosal barrier, providing fertile soil for the development of a potentially profound enterotoxemia.

References:

1. Bowman, DD. Helminths. In: Bowman DD, ed. *Georgis' Parasitology for Veterinarians*. 9th ed. Elsevier;2009:92-94.
2. Corning S. Equine Cyathostomins: A review of biology, clinical significant and therapy. *Parasites and Vectors*. 2009*;* 2(S2): S1.
3. Peregrine AS, McEwen B, Bienzle D, Koch TG, Weese JS. Larval cyathostominosis in horses in Ontario: an emerging disease? *Can Vet J*. 2006;47(1):80-82.
4. Sellon DC, Long MT. Strongylosis. In: Sellon DC, Long MT, eds. *Equine Infectious Diseases*. Saunders; 2007:480-486.
5. Uzal FA, Plattner BL, Hostetter JM. Alimentary System. In: Maxie MG, ed. *Jubb, Kennedy, and Palmer's Pathology of Domestic Animals*. 6th ed. Vol 2. Elsevier;2016:216.

WSC 2023-2024
Conference 8 Self-Assessment

1. Which of the following life stages has not been identified in *Eimeria leukarti* in horses*?*
    a. Oocysts
    b. Schizont
    c. Microgamete
    d. Macrogamete

2. True or false: *Eimeria leuckarti* is the only known coccidian in horses.
    a. True
    b. False

3. Necrotic forms of which of the following are consistent findings in the lungs PRRSV in pigs?
    a. Eosinophils
    b. Macrophages
    c. Type II pneumocytes
    d. Viral syncytia

4. Migration of Ascaris suum occurs in which of the following immediately prior to return to the intestine to mature?
    a. Pulmonary alveoli
    b. Pulmonary airways
    c. Liver
    d. Gastric wall

5. True or false. Horses are infected with small strongyles by ingesting infective larvae rather than eggs.
    a. True
    b. False

Joint Pathology Center
Veterinary Pathology Services

WEDNESDAY SLIDE CONFERENCE 2023-2024

Conference #9 **18 October 2023**

CASE I:

Signalment:
8-year-old, male neutered Pembroke Welsh corgi, canine (*Canis lupus familiaris*)

History:
This dog developed labored breathing. An echocardiogram showed pulmonary hypertension and degenerative valve disease of the mitral, tricuspid, and pulmonic valves. The dog was started on sildenafil and pimobendan therapy and improved; however, approximately 1.5 months after the initial diagnosis the dog went into decompensated congestive heart failure and was humanely euthanized.

Gross Pathology:
The lungs were soft, wet, and mottled pink and reddish brown. The right ventricle of the heart was moderately dilated with a thickened wall. Both atrioventricular valves had moderate endocardiosis. The liver had evidence of chronic passive congestion (moderate enlargement, rounded lobar margins, meaty texture, roughened surface, and small amounts of fibrin on the capsular surface). The dog had mild ascites.

Microscopic Description:
Lung: Throughout all sections there are multiple variably sized, poorly demarcated areas within which there is increased cellularity of alveolar septa and lumina. Within these areas, alveolar septa are mildly to moderately

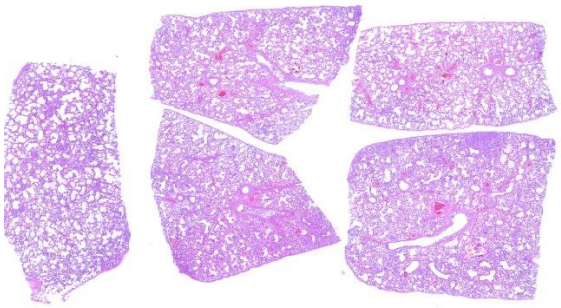

Figure 1-1. Lung, dog. Five sections of lung are submitted for examination. (HE, 5X)

expanded by variable numbers of mesenchymal cells and rare small amounts of collagen. In a few small areas, the expansion of this mesenchymal population results in markedly thickened and tortuous alveolar septa which obscure the adjacent alveolar lumina. There is frequent, regionally variable, type II pneumocyte hyperplasia with a few small areas containing markedly hypertrophied, vacuolated, and/or misshapen type II pneumocytes with up to 3 nuclei. Alveolar spaces contain large numbers of macrophages which infrequently contain finely granular, golden-brown, intracytoplasmic pigment (hemosiderin) as well as small numbers of neutrophils and lymphocytes. Infrequently, alveolar spaces contain variable amounts of fibrillar to beaded, eosinophilic material (fibrin) which often lines the alveolar septa with or without admixed cellular debris (hyaline membranes). Alveolar spaces also frequently contain finely granular, eosinophilic material (proteinaceous fluid). Within these areas as well as unaffected areas, pulmonary veins

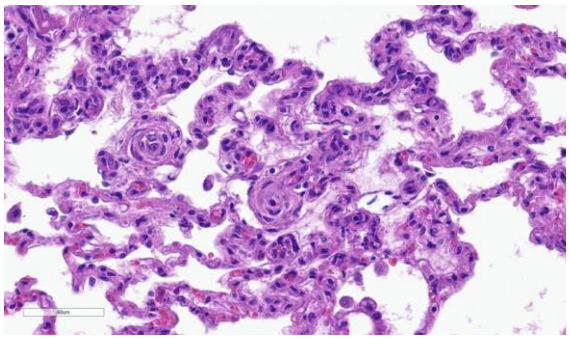

Figure 1-2. Lung, dog. There is concentric hypertrophy of the walls of tortuous pulmonary veins. Adjacent septa are hypercellular with prominent endothelial cell nuclei. (HE, 400X)

(distinguished by their location within the alveolar parenchyma) frequently exhibit remodeling, with expansion of the tunica media by plump spindle cells resulting in partial to complete occlusion of the lumen. Often associated with these remodeled veins are variably sized networks of alveolar capillaries which are moderately to markedly congested. The wall of one large pulmonary artery exhibits segmental fibrinoid necrosis.

A large number of thickened vessels within the alveolar parenchyma have external, dark purple to black elastic laminae only (as seen on Verhoeff-van Gieson stain), distinguishing them as veins, in comparison to arteries which have internal and external elastic laminae. Immunohistochemical stains for smooth muscle actin (SMA) revealed SMA immopositive mesenchymal cells expanding vein walls, consistent with smooth muscle hypertrophy/hyperplasia. The cells lining the variably congested alveolar capillaries exhibit strong immunoreactive for CD31, confirming endothelial origin.

Contributor's Morphologic Diagnoses:

1. Lung: Venous medial hypertrophy, multifocal, marked, chronic, with moderate perivenous capillary congestion.
2. Lung: Capillary hemangiomatosis, multifocal, marked, chronic, with minimal alveolar septal fibrosis.
3. Lung: Alveolar histiocytosis, multifocal, marked, chronic, with hyaline membrane formation and moderate to marked type II pneumocyte hyperplasia.

Contributor's Comment:

The combination of the findings of venous medial hypertrophy and alveolar capillary proliferation are consistent with pulmonary veno-occlusive disease (PVOD) and capillary hemangiomatosis (PCH). PVOD and PCH are rare forms of pulmonary hypertension (PH) which result from progressive remodeling and obstruction of pulmonary veins, and proliferation of thin-walled microvessels within alveolar septa, respectively.[2,6] As the two lesions often occur concurrently, the World Health Organization (WHO) recognizes that they may belong to a spectrum of the same pulmonary vascular disease.[7] In humans, the WHO recognizes five clinical groups of PH: group 1, which was recently updated to include PVOD and PCH, comprises diseases involving pulmonary arterial hypertension (PAH); group 2 represents diseases caused by left-sided heart disease; group 3 causes of PH relate to lung disease and/or hypoxia; group 4 is PH caused by pulmonary artery obstruction; and group 5 is composed of various disease with unclear and/or multifactorial mechanisms.

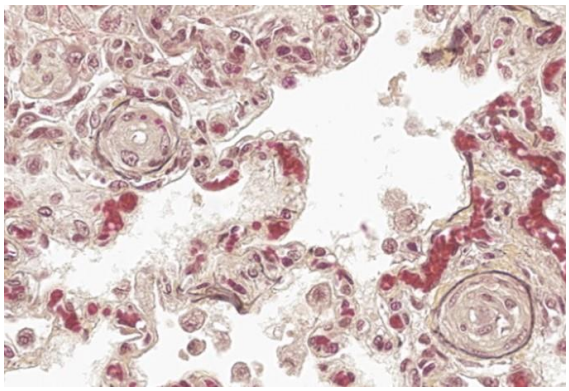

Figure 1-3. Lung, dog. An elastin stain demonstrates the lack of internal elastic lamina, establishing the primary affected vessels as veins. (Elastin, 400X)

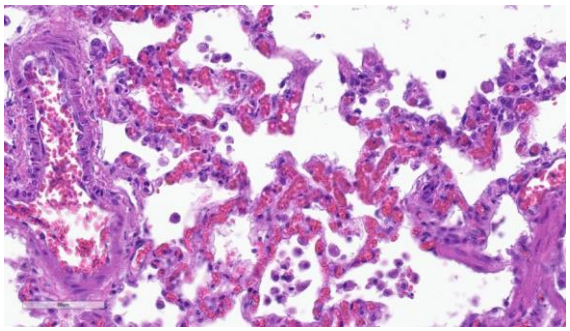

Figure 1-4. Lung, dog. There is marked segmental septal congestion due to increased capillary pressure. (HE, 400X)

In a recent retrospective study of 15 dogs with PVOD and PCH, all dogs were older than 8 years of age (median 11 years).[4] There was no clear sex or breed predilection, although the sample sizes were small. The underlying causes of these diseases in dogs remain unknown. In humans, patients with PVOD are predominantly young to middle-aged, and both genetic and non-genetic risk factors have been identified. Genetically, one study found that 13/13 familial and 5/20 sporadic cases of PVOD had a loss of function mutation of EIF2AK4; however, the link between this mutation and PVOD remains unclear.[1] Other risk factors for PVOD in humans include chemotherapeutics, exposure to organic solvents, bone marrow or stem cell transplants, neoplasia, connective tissue disorders, autoimmune diseases, sarcoidosis, HIV infection, and pulmonary Langerhans cell histiocytosis.[4] Only genetic factors have been implicated for PCH in humans.

In dogs, clinical signs involve rapidly progressive respiratory signs that include coughing, tachypnea, dyspnea, hypoxia, epistaxis, and hemoptysis.[3] Diagnostically, thoracic radiographs should demonstrate an interstitial or alveolar pattern with enlargement of the pulmonary arteries, without evidence of cardiomegaly.[4]

Gross lesions in dogs with PVOD typically involve diffusely edematous and firm to 'meaty' lungs with widespread areas of hemorrhage or congestion.[3] In a study of 11 dogs, there was no gross evidence of underlying cardiac disease and 2 dogs demonstrated compensatory hypertrophy of the right ventricle.[8]

Histologically, the hallmark feature of PVOD is extensive, patchy remodeling of small- to medium-sized pulmonary veins. This remodeling involves expansion of the vessel wall with plump spindle cells and collagen, resulting in narrowed or occluded venous lumina. As a result of this luminal occlusion, there is upstream congestion of adjacent alveolar capillaries and in some cases pulmonary arterial remodeling. PCH, which in humans is concomitantly present in 75% of PVOD cases, is characterized by proliferation of alveolar capillaries, which can extend into pulmonary arteries and veins. Additionally, there are increased numbers of alveolar macrophages which frequently contain cytoplasmic hemosiderin. In some dogs there may be small accumulations of fibrin as well as hyaline membrane formation.

Contributing Institution:
Veterinary Diagnostic Laboratory
University of Minnesota
St. Paul, MN.
https://vdl.umn.edu/

JPC Diagnosis:
Lung: Venous intimal fibrosis and smooth muscle hyperplasia and stenosis, multifocal to coalescing, severe, with septal endothelial hypertrophy (capillary hemangiomatosis), segmental alveolar capillary engorgement, alveolar histiocytosis and siderosis, and arterial medial hypertrophy.

JPC Comment:
As the contributor notes, PVOD and PCH are rare causes of pulmonary hypertension in humans and are exceedingly rare and only recently described in dogs. This case provides

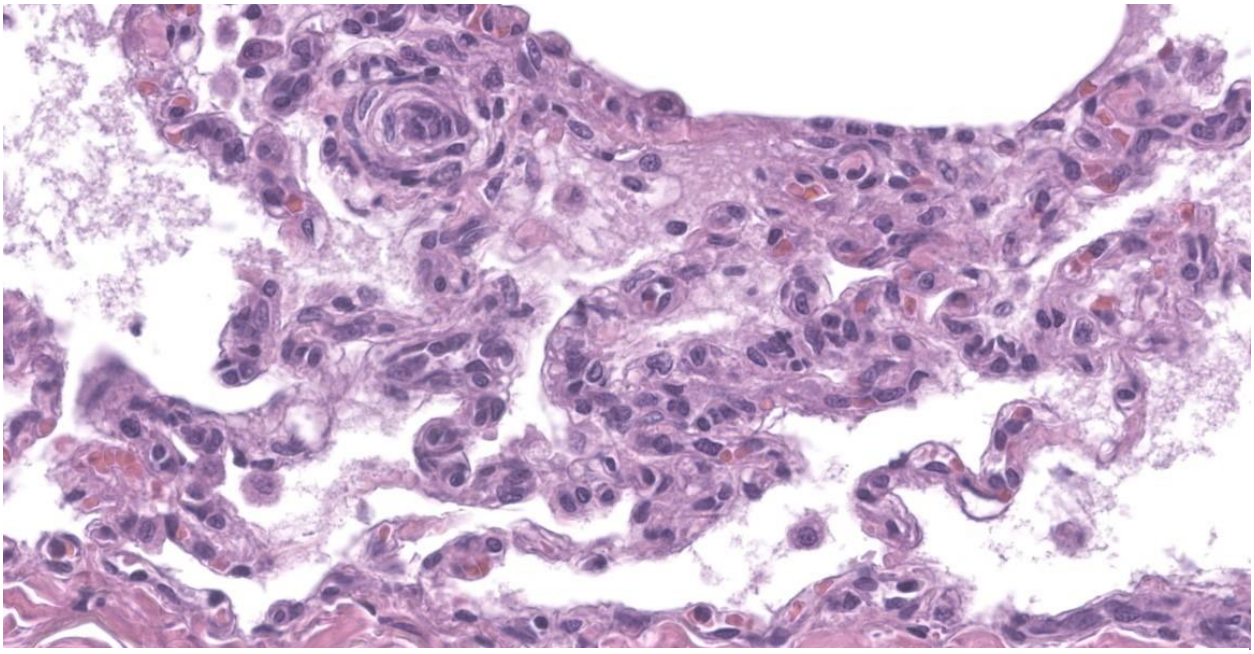

Figure 1-5. Lung, dog. Due to increased capillary pressure, there is proliferation of the capillary endothelium (capillary hemangiomatosis) (HE, 400X)

an excellent example of the characteristic histologic features of these conditions and the contributor provides an excellent summary of the current state of knowledge surrounding this unusual entity.

Pulmonary hypertension can be caused by four broad mechanisms: increased pulmonary blood flow, increased pulmonary vascular resistance, increased pulmonary venous pressure, or some combination of these factors.[5] The American College of Veterinary Internal Medicine has recently published a proposed classification scheme that categorizes pulmonary hypertension based roughly on these broad casual mechanisms.[5] The classification scheme includes many well-known causes of pulmonary hypertension including left-sided heart disease, pulmonary disease, hypoxia, congenital left-to-right cardiovascular shunts, and *Dirofilaria immitis* or *Angiostrongylus vasorum* infection.[5] Under this rubric, PVOD and PCH are nested in their own subcategory under the pulmonary arterial hypertensive diseases, a categorization that may be initially confusing since the vascular lesions of PVOD preferentially affect the pulmonary veins; however, PVOD is classified as a distinct cause of pulmonary *venous* hypertension whose clinical expression is severe pulmonary *arterial* hypertension.[8]

The placement of PVOD and PCH in their own subcategory within the proposed classification scheme is neither merely descriptive nor academic, but instead highlights a key difference in the response of PVOD and PCH patients to typical pulmonary arterial hypertension treatments. The treatment mainstays for these conditions include the use of type-5 phosphodiesterase (PDE5) inhibitors, the most well-known of which are sildenafil and tadalafil. Human PVOD and PCH patients treated with PDE5 inhibitors can develop acute, massive, and fatal pulmonary edema due to the inability of occluded vasculature to accomodate the increased blood flow caused by these potent vasodilators.[2] Though this effect has not been definitely proven in dogs, the consensus statement extrapolates from human literature and recommends administering PDE5 inhibitors only in hospital where

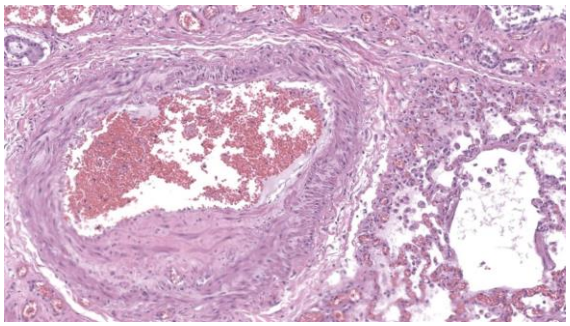

Figure 1-6. Lung, dog. Multifocally, pulmonary arterioles demonstrate asymmetric myointimal hyperplasia. (HE, 400X)

patients can be carefully monitored for the development of pulmonary edema.[5]

This week's conference moderator was Dr. Kurt Williams, Director of the Oregon Veterinary Diagnostic Laboratory and pulmonary system enthusiast. Dr. Williams waxed poetic at the start of the conference about the ability of a slide to tell a story about pathogenesis. He encouraged conference participants to spend time understanding that story and then to structure slide descriptions and interpretations to convey it accurately to others.

In this case, the story being told centers on the vasculature, so an accurate description should describe the vessels in full, to include which branches of the vascular tree and what caliber of vessels are being affected. In cases such as PVOD, where occlusive changes can make it difficult to distinguish vein from artery, a Verhoeff-van Gieson stain, which highlights vascular elastic lamina, can be helpful in characterizing the vessels; veins will have only an external elastic lamina, while arteries will have both internal and external elastic laminae. In the absence of special stains, anatomy can be useful, as arteries are typically adjacent to airways, while veins tend to branch out more diffusely into the parenchyma.

Dr. Williams noted that the hemosiderin-laden macrophages, or "heart failure cells," associated with PVOD typically have an abundance of hemosiderin far in excess of that normally found in garden-variety heart failure. Conference participants remarked on the generally unimpressive nature of these cells in this case, while Dr. Bruce Williams cautioned against the use of this term in communications meant for clinicians, as the term could cause the inappropriate administration of positive ionotropes which are contraindicated and potentially fatal in PVOD patients.

As the contributor notes (and this case exemplifies), capillary hemangiomatosis typically accompanies PVOD. Dr. Williams noted that the capillaries in capillary hemangiomatosis are not simply congested but also larger than normal. For this reason, Dr. Williams prefers the more dramatic term, "capillary engorgement" to "capillary congestion." Finally, Dr. Williams noted several vessels that contained foci of intimal thickening with longitudinally-oriented blood vessels embedded within. This change is characteristic of hypoxic injury in the lung and can be seen in other contexts, such as in high mountain/brisket disease in cattle.

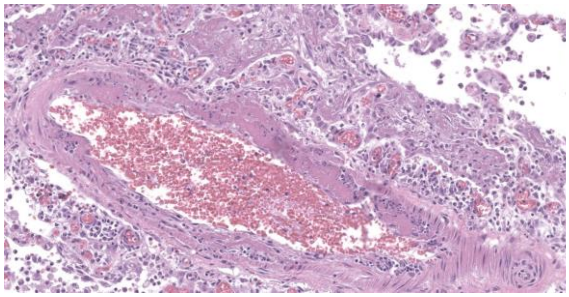

Figure 1-7. Lung, dog. Occasional pulmonary arterioles demonstrate extrusion of protein and fibrin into their walls. (HE, 200X)

References:

1. Eyries M, Montani D, Girerd B, et al. EIF2AK4 mutations cause pulmonary veno-occlusive disease, a recessive form of pulmonary hypertension. *Nat Genet*. 2014;46(1):65-9.
2. Guzman S, Khan, MS, Chodakiewitz, et al. Pulmonary capillary hemangiomatosis: a lesson learned. *Autops Case Rep*. 2019;9(3):e2019111.
3. Maxie MG, Jubb KVF, Kennedy PC, Palmer N. *Jubb, Kennedy, and Palmer's Pathology of Domestic Animals*. Elsevier Saunders; 2007.
4. Reinero CR, Jutkowitz LA, Nelson N, et al. Clinical features of canine pulmonary veno-occlusive disease and pulmonary capillary hemangiomatosis. *J Vet Intern Med*. 2019;33(1):114 –123.
5. Reinero C, Visser LC, Kellihan HB, et al. ACVIM consensus statement guidelines for the diagnosis, classification, treatment, and monitoring of pulmonary hypertension in dogs. *J Vet Intern Med*. 2020;34(2);549-573.
6. Siddiqui NA, Charoenpong P. *Pulmonary Veno-Occlusive Disease*. StatPearls Publishing; 2023.
7. Simonneau G, Montani D, Celermajer DS, et al. Haemodynamic definitions and updated clinical classification of pulmonary hypertension. *Eur Respir J*. 2019;53 (1):1801913.
8. Williams K, Andrie K, Cartoceti A, et al. Pulmonary veno-occlusive disease: a newly recognized cause of severe pulmonary hypertension in dogs. *Vet Pathol*. 2016;53(4):813-22.

CASE II:

Signalment:
10-year-old, female spayed mixed breed, canine (*Canis lupus familiaris*)

History:
This dog presented with an approximately 3-month history of chronic coughing. Thoracic radiographs revealed a multifocal alveolar pattern extending to the caudodorsal lung fields. The alterations appeared to have progressed compared to a radiograph taken 7 weeks prior. The tracheobronchial lymph nodes were enlarged but appeared to be of similar size as noted in the previous radiograph. Due to poor prognosis, humane euthanasia was elected.

Gross Pathology:
The lungs were diffusely mottled red to dark red with numerous coalescing firm, tan nodules embedded in the pulmonary parenchyma of all lobes. Representative tissue samples floated in 10% neutral buffered formalin. The tracheobronchial lymph nodes were enlarged, ranging in size from 1x2x1 cm to 1.7x4.0x1.5 cm. On the cut surface of these nodes, there were multiple variably sized, random, light to dark brown areas. The liver had several pinpoint to 0.3 cm diameter tan foci throughout.

Laboratory Results:

Bacteriology (Aerobic culture), lung: No bacteria isolated.

Mycology (Fungal culture), lung: No fungi isolated.

Microscopic Description:
Lung: Corresponding to the coalescing firm tan nodules noted grossly, there is multifocal to coalescing infiltration of the pulmonary parenchyma by large number of mixed inflammatory cells consisting predominantly of macrophages and eosinophils, fewer

Figure 2-1. Lung, dog. The lungs were diffusely mottled red to dark red with numerous coalescing, firm tan nodules embedded in the pulmonary parenchyma of all lobes. (*Photo courtesy of:* Louisiana Animal Disease Diagnostic Laboratory (LADDL), School of Veterinary Medicine, Louisiana State University, http://www1.vetmed.lsu.edu/laddl/index.html)

neutrophils, lymphocytes, and plasma cells, and occasional multinucleated giant cells, amidst a background of multifocal polymerized fibrin deposits, occasional mild hemorrhage, multiple plump type II pneumocytes, and spindle cells. In some areas, the inflammation concentrates in the bronchiolar and perivascular interstitium, variably extending into the airways (often as epithelium-lined fibrous polypoid structures) and the vascular wall. No microorganisms are apparent, and Gomori's methenamine silver (GMS) staining is negative. Within the remaining areas of the pulmonary parenchyma, the alveoli often contain moderately increased numbers of alveolar macrophages and fibrin strands. In addition, in some sections the pleural surface is multifocally expanded by villous fibrous proliferation with a mixed, predominantly eosinophilic inflammatory infiltrate.

Additional histologic findings (sections not submitted) include marked eosinophilic and granulomatous lymphadenitis of the tracheobronchial lymph nodes, mild eosinophilic and granulomatous portal hepatitis, and mild to moderate extramedullary hematopoiesis in the spleen.

Contributor's Morphologic Diagnosis:
Lung: Pneumonia, eosinophilic and granulomatous, multifocal to coalescing, marked, chronic (consistent with eosinophilic pulmonary granulomatosis).

Contributor's Comment:
Eosinophilic pulmonary granulomatosis (EPG) is an uncommon, idiopathic disease of dogs with clinical signs of progressive coughing, exercise intolerance, variable dyspnea, and eosinophilia.[2,3,6,8,13] EPG is differentiated from the other eosinophil-rich conditions, such as eosinophilic pneumonia and eosinophilic bronchopneumopathy (EBP), by the formation of nodules and masses composed of eosinophils, macrophages, and various combinations of other leukocytes within fibrous tissue.[1] Some authors have speculated that EPG might represent a progressed form of EBP, which is a more commonly diagnosed idiopathic condition in young dogs.[1,2,6,7,9,12] Although eosinophilic airway inflammation and peripheral eosinophilia may be seen in both conditions, EBP is microscopically characterized by airway and pulmonary involvement without granuloma formation or lymph node involve-

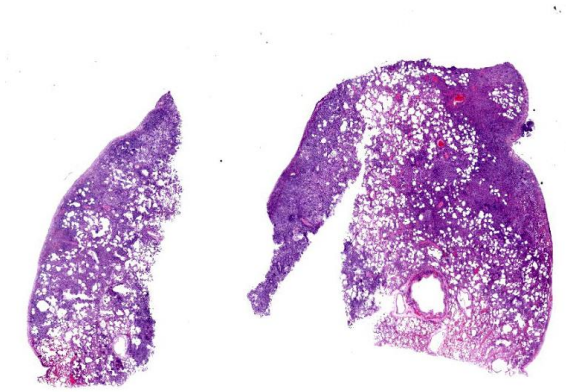

Figure 2-2. Lung, dog. Two sections of lung are submitted for examination. There are multifocal to coalescing areas of consolidation, particularly in subpleural areas. (HE, 5X)

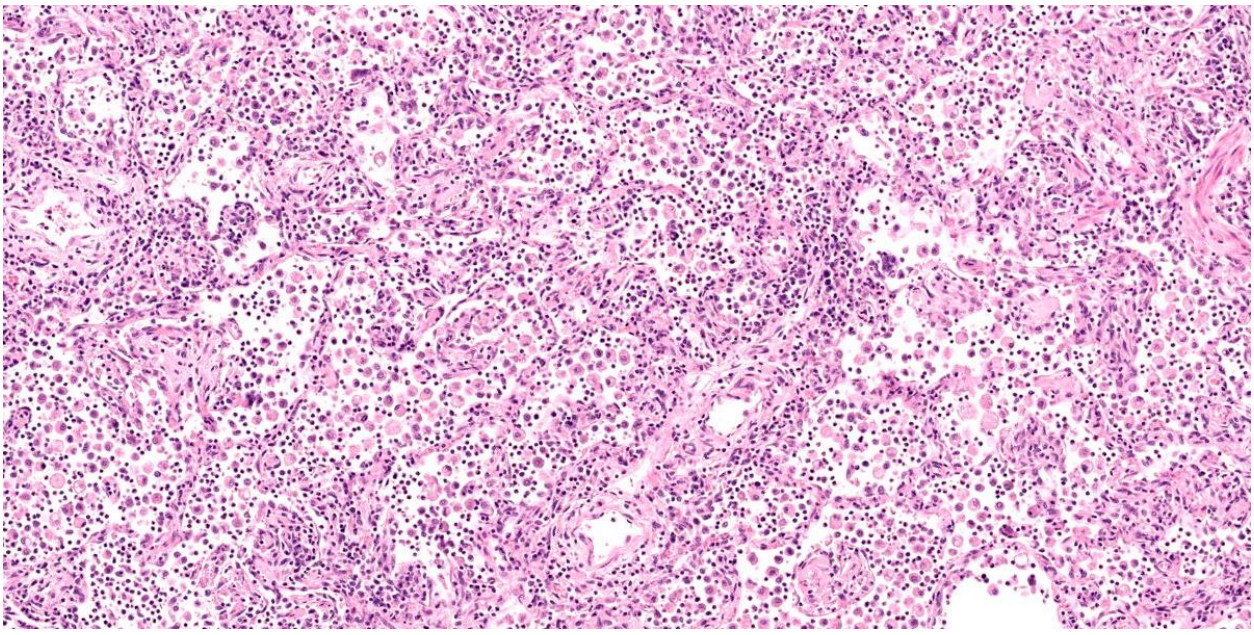

Figure 2-3. Lung, dog. In consolidated areas, alveoli are filled with a markedly cellular exudate, and septa are fibrotic. (HE, 81X)

ment.[2,8] Clinically, EBP responds to immunosuppressive treatment far better than EPG.[2,6,8]

The cause and pathogenesis of EPG have yet to be determined.[4,8] Multiple reports in the veterinary literature have discussed an association between *Dirofilaria immitis* infection and EPG.[1,2,4-6] However, affected dogs do not always have gross, microscopic, or serologic evidence of dirofilariasis.[1,2,6,8,10,13] In this case, there was no gross or microscopic evidence of concurrent or previous *D. immitis* parasitism. In addition, bacterial and fungal cultures of the lung were negative.

Typical gross findings of EPG include firm, consolidated pulmonary parenchyma with multifocal to regionally extensive discrete nodules.[2,5,6,10] Similar nodules may be found in the regional lymph nodes, heart, liver, and spleen.[1,2,5] Microscopically, the nodules are predominantly composed of eosinophils, macrophages, epithelioid macrophages, and small numbers of neutrophils, lymphocytes, and plasma cells, and are separated and surrounded by variably thick fibrous connective tissue.[1,2,5,6,10] In some cases, eosinophilic and/or granulomatous inflammation is also described in the trachea, kidney, stomach, and small intestine.[1] In this case, the tracheobronchial lymph nodes and the liver had similar but milder inflammation as that in the lung, likely all part of the same disease process.

The diversity of the reported affected canine breeds does not suggest a breed predisposition. Although 6 of the 26 dogs with EPG included in a literature review were German Shepherd or German Shepherd crossbred dogs, the authors speculated that this might simply represent the popularity of the breed.[1] There does not appear to be sex predilection for EPG in dogs.[1]

Brown Norway rats, which have been used to study the pathogenesis of asthma, may also develop a spontaneous eosinophil-rich granulomatous pneumonia in the absence of any experimental procedure. While lesions have been observed in rats of various ages, they

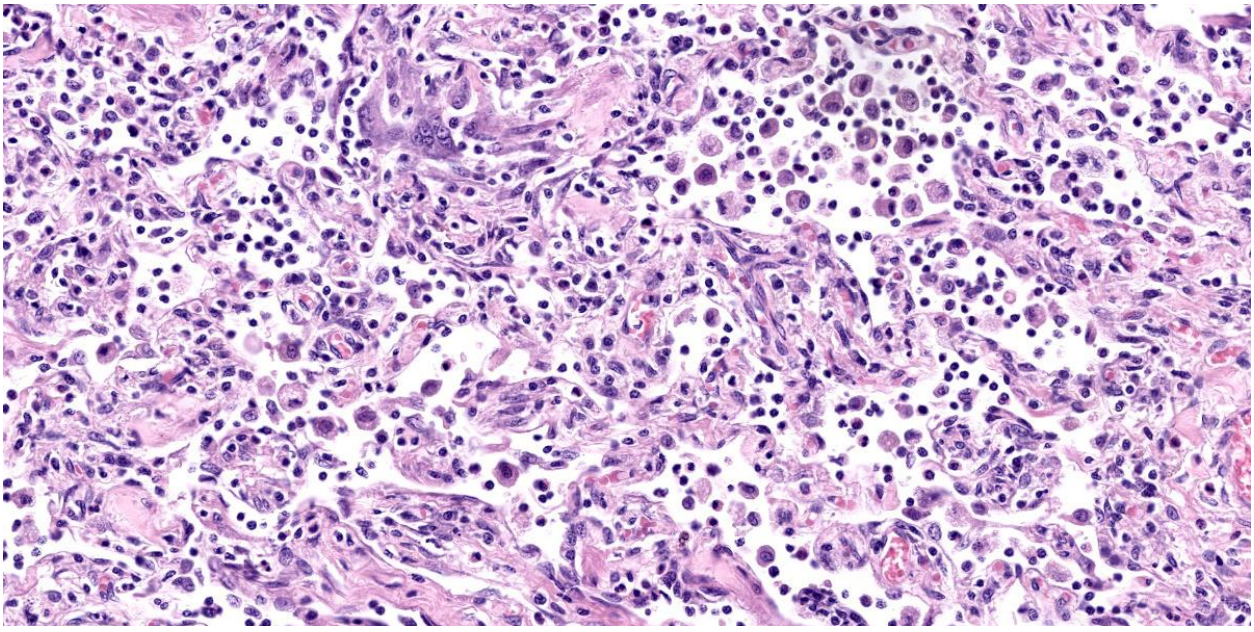

Figure 2-4. Lung, dog. Higher magnification of pulmonary parenchyma. There is an organizing chronic pneumonia with an infiltrate large numbers of macrophages and eosinophils with occasional multinucleated giant cell macrophages. Alveolar septa are expanded by protein yet to be resorbed (covered by proliferating epithelium and abundant collagen and fibroblasts. (HE, 381X)

seem to affect particularly young adult animals. Both sexes are susceptible. Typical gross findings are multiple 1-3 mm diameter, pale tan to gray to red foci scattered throughout the pulmonary parenchyma. Microscopic findings are characterized by multifocal to diffuse granulomatous pneumonia composed of epithelioid cells with or without prominent multinucleated giant cells. There may be marked perivascular and peribronchiolar edema with mixed leukocytic infiltrates rich in eosinophils. Detection of possible infectious agents by serology, bacterial culture, and special stains on affected lungs have all been negative.[11]

Treatment of EPG includes administration of immunosuppressive and cytotoxic drugs, based on a presumed immune-mediated pathogenesis.[6,7] Immunosuppressive doses of prednisone, azathioprine, and cyclophosphamide are among the documented treatments; the efficiency of other immunosuppressive drugs (e.g., cyclosporine) is not known.[2,6-8,10] The prognosis is poor due either to partial response to treatment or rapid recurrence of respiratory clinical signs after cessation of treatment.[2,6,10]

Contributing Institution:
Louisiana Animal Disease Diagnostic Laboratory (LADDL)
School of Veterinary Medicine
Louisiana State University
http://www1.vetmed.lsu.edu/laddl/index.html

JPC Diagnosis:
Lung: Pneumonia, eosinophilic, organizing, chronic, multifocal to coalescing, severe.

JPC Comment:
As the contributor notes, there is a long-standing debate, referenced in every review of EPG, of a potential association between *D. immitis* infection infection and the development of the eosinophilic granulomas that characterize the disease. In the earliest cases, reported in the 1980's, *D. immitis* infection

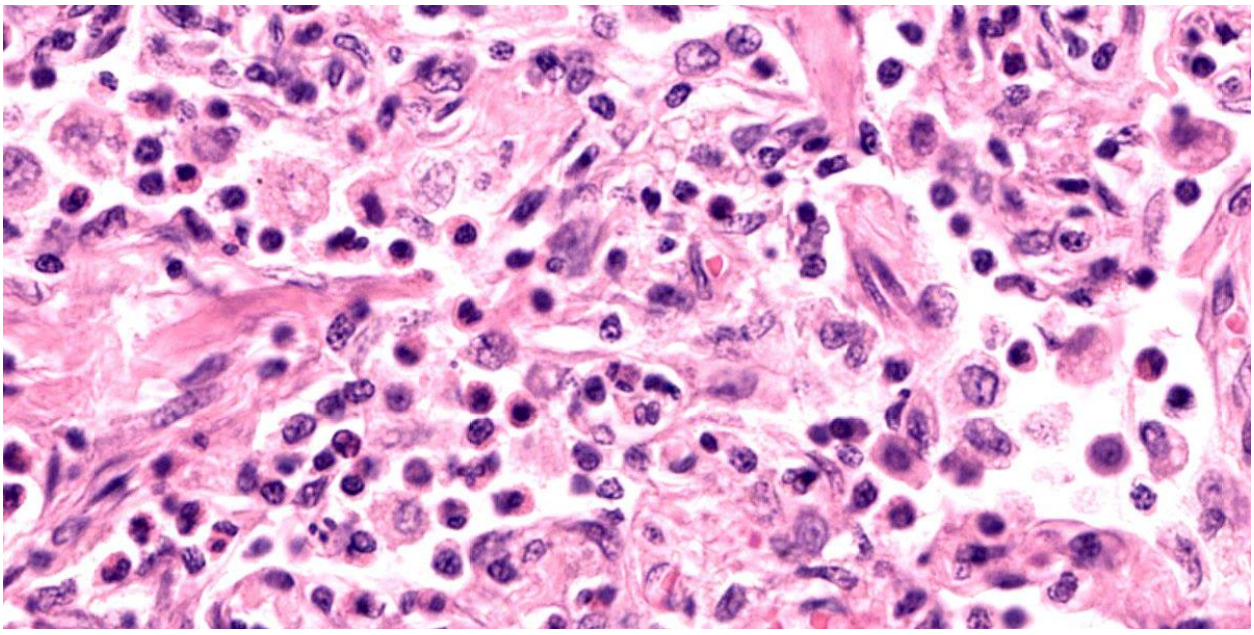

Figure 2-5. Lung, dog. The inflammatory infiltrate is composed primarily of eosinophils and macrophages. (HE, 850X)

was common.[2,5,10] Since that time, however, *D. immitis* infection has become uncommon in reported cases, perhaps indicating the development and widespread adoption of heartworm prophylaxis in the intervening years.[1] In fact, a recent study notes that, of the 19 cases of EPG reported before 1988, 8 were infected with *D. immitis*; of the 7 cases reported since, none had evidence of *D. immitis* disease.[1]

Many cases of EPG present with concurrent peripheral eosinophilia and basophilia. The presence of basophilia is a particularly uncommon clinical pathology finding that tends to narrow a differential list significantly. Among the causes for peripheral basophilia are allergic diseases, including eosinophilic granulomas; neoplastic diseases such as mast cell tumors, thymomas, and lymphomatoid granulomatosis; drug reactions; stress (in birds); and parasitism, including *Dirofilaria immitis*.[14] The fact that EPG and *D. immitis* infection both provoke this uncommon clinical pathology further stokes suspicion that a casual link underlies this association.

Whether the eosinophilia and basophilia is useful diagnostically and whether there is a causal link between *D. immitis* infection and EPG are currently both open questions that require further investigation.[1]

There is speculation that EPG might be a more progressed form of eosinophilic bronchopneumopathy (EBP), an uncommon, typically steroid responsive condition of young dogs.[3] The eosinophilic bronchitis with epithelial hyperplasia, ulceration, and/or squamous metaplasia that characterize this condition tends to destroy airway walls and leads to bronchiectasis in 25% of cases.[3] EBP is currently thought to be immune-mediated, but a diagnosis of EBP requires that more specific conditions be ruled out. These include the tracheobronchial parasites *Crenosoma vulpis, Eucoleus aerophilus,* and *Oslerus osleri*; the lung worms *Angiostrongylus vasorum* and *Filaroides hirthi*; *Dirifilaria immitis* infection; and neoplasia, including pulmonary carcinoma, histiocytic sarcoma, lymphoma, and lymphomatoid granulomatosis.[3]

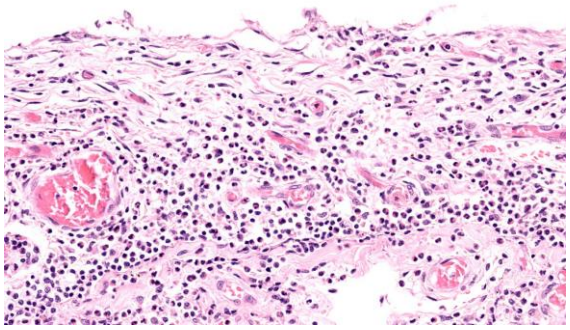

Figure 2-6. Lung, dog. The inflammatory infiltrate extends into the pleura. (HE, 318X)

Conference discussion initially focused on the lesion distribution, which is predominantly parenchymal and is curiously concentrated subjacent to the pleura. Dr. Williams prefers to describe this distribution, which most closely resembles an interstitial pattern but isn't an exact fit to any of the establish patterns, as simply pneumonia. Conference participants also remarked on the lack of a clear nodular pattern that is typical of EPG.

A particular striking histologic feature in this slide is the irregular, eosinophilic, densely cellular material found protruding into airways and multifocally adhered to alveolar walls. Though most conference participants interpreted this as alveolar fibrosis, Dr. Williams interpreted these areas as ancient remnants of previously suffered bouts with an extremely exudative inflammatory process. The fibrous tissue left behind represents attempts by the lung to repair the damage, referred to as organizing pneumonia. In less affected areas of lung, alveoli are multifocally mineralized, a lesion that likely represents a more recent stage of injury, providing multiple temporal stages in the disease process in one slide.

Participants also discussed the nature of the inflammatory infiltrate at length. While eosinophils are clearly the main driver of disease in this case, the remainder of the inflammation was characterized by the conference participants as mixed, with large numbers of plasma cells, lymphocytes, and histiocytes.

Based on these discussions, the JPC morphologic diagnosis highlights the eosinophilic nature of the inflammation and eschews the reference to granulomatous due to the heterogenous nature of the infiltrate. Conference participants also felt that the multifocal foci of organizing pneumonia was an important histologic feature to highlight as it provides a window into pathogenesis and an indicator of chronicity.

References:

1. Abbott DEE, Allen AL. Canine eosinophilic pulmonary granulomatosis: case report and literature review. *J Vet Diagn Invest*. 2020;32(2):329-335.
2. Calvert CA, Mahaffey MB, Lappin MR, Farrell RL. Pulmonary and disseminated eosinophilic granulomatosis in dogs. *J Am Anim Hosp Assoc.* 1988;24:311–320.
3. Caswell JL, Williams KJ. Respiratory system. In: Maxie MG, ed. *Jubb, Kennedy and Palmer's Pathology of Domestic Animals*. 6th ed., vol. 2. Saunders Elsevier; 2016:501-502,513.
4. Clercx C, Peeters D. Canine eosinophilic bronchopneumopathy. *Vet Clin North Am Small Anim Pract.* 2007;37:917–935.
5. Confer AW, Qualls Jr CW, MacWilliams PS, Root CR. Four cases of pulmonary nodular eosinophilic granulomatosis in dogs. *Cornell Vet.* 1983;73:41–51.
6. Dehghanpir SD, Leissinger MK, Jambhekar A, et al. Pathology in Practice: Eosinophilic pulmonary granulomatosis (EPG) with extension into the mediastinal and tracheobronchial lymph nodes in a dog. *J Am Vet Med Assoc*. 2019;254(4):479-482.
7. Hawkins EC. Chapter 22: Disorders of the pulmonary parenchyma and vasculature. In: Nelson RW, Couto CG, eds.

Small Animal Internal Medicine. 6th ed. Elsevier;2019:348–349.
8. Katajavuori P, Melamies M, Rajamäki MM. Eosinophilic pulmonary granulomatosis in a young dog with prolonged remission after treatment. *J Small Anim Pract.*2013;54(1):40-43.
9. Marolf AJ, Blaik MA. Bronchiectasis. *Compend Contin Educ Pract Vet.* 2006;28:766–775.
10. Neer TM, Waldron DR, Miller RI. Eosinophilic pulmonary granulomatosis in two dogs and literature review. *J Am Anim Hosp Assoc.* 1986;22:593–599.
11. Percy DH, Barthold SW, Griffey SM. *Pathology of Laboratory Rodents and Rabbits*. 4th ed. Blackwell Publishing;2016: 160.
12. Reinero C. Interstitial lung diseases in dogs and cats, part II: known cause and other discrete forms. *Vet J*. 2019;243:55–64.
13. Von Rotz A, Suter MM, Mettler F, Suter PF. Eosinophilic granulomatous pneumonia in a dog. *Vet Rec*. 1986;118:631-632.
14. Webb JL, Latimer KS. Leukocytes. In: Latimer KS, ed. *Duncan & Prasse's Veterinary Laboratory Medicine Clinical Pathology*. 5th ed. Wiley-Blackwell;2011:76.

CASE III:

Signalment:
4-year-old, Angus cow, bovine *(Bos taurus*)

History:
Four adult Angus cows and an adult Hereford bull died suddenly a few days after being moved to lush pasture.

Gross Pathology:
The lungs did not collapse when the thorax was opened. The majority of the lung parenchyma was red, heavy, wet and meaty with emphysema and edema in the interlobular septa and moderate numbers of petechiae on the surface. Approximately 10-30% of the lung parenchyma in the cranioventral lung fields was dark red to plum colored, firm and consolidated.

Figure 3-1. Lung, ox. The lungs failed to collapse when the thorax was opened. They are reddened, and interlobular septal expansion is prominent with interlobular emphysema in the caudal lobes. (Photo courtesy of: New Mexico Department of Agriculture Veterinary Diagnostic Services, www.nmda.nmsu.edu/vds)

Laboratory Results:
Pasteurella multocida was isolated on bacterial culture of the consolidated lung.

PCR testing of the lung was negative for bovine viral diarrhea (BVD) virus, bovine herpesvirus-1 (IBR), bovine respiratory syncytial virus (BRSV), *Mycoplasma bovis*, bovine respiratory coronavirus, and bovine influenza virus (BIV).

Microscopic Description:
The lung is diffusely congested. In the majority of the lung, the alveoli are filled with edema and fibrin mixed with variable numbers of macrophages, small numbers of neutrophils and rare multinucleated giant cells. The fibrin occasionally forms hyaline membranes that are associated with the alveolar wall. The alveolar septa are thickened by

Figure 3-2. Lung, ox. When removed from the thorax, the lungs fail to collapse, there is extensive consolidation of all lobes, and leaked fluid pools beneath them. (Photo courtesy of: New Mexico Department of Agriculture Veterinary Diagnostic Services)

fibrin, edema, macrophages, lymphocytes and swollen type II pneumocytes that epithelialize the alveolar wall. The interlobular septa and pleura are thickened by edema and emphysema.

Contributor's Morphologic Diagnosis:
Lung: Interstitial pneumonia, acute, diffuse, severe, with hyaline membrane formation, type II pneumocyte hyperplasia, edema, and emphysema (acute bovine pulmonary edema and emphysema)

Contributor's Comment:
The clinical history and the gross and microscopic lesions are consistent with the respiratory disease known as acute bovine pulmonary edema and emphysema (ABPEE). ABPEE is a toxic interstitial pneumonia of cattle.[3,5] The disease most commonly occurs in adult cattle.

Calves appear to be resistant to the disease. ABPEE typically occurs in the fall 4-10 days after cattle are moved from summer pastures to lusher fall pastures, but it can occur any time of the year when cattle are moved to lush pastures.

ABPEE is caused by L-tryptophan within plants being converted to 3-methylindole by rumen microbes.[1,2,3,5,6,7] The 3-methylindole formed in the rumen is absorbed into the bloodstream, eventually making it to the lungs.[3,5] There is evidence that suggests 3-methylindole preferentially binds in the lung of susceptible species compared to other organs such as the liver.[7] Within the lung, 3-methylindole is converted to unknown toxic metabolites by mixed function oxidases, mainly cytochrome p450 in the nonciliated bronchiolar epithelial cells.[3,5] The toxic metabolite of 3-methylindole causes necrosis of bronchial epithelium and type I pneumocytes, endothelial cell swelling, and increased vascular permeability. The increase in vascular permeability leads to edema and thickening of the alveolar wall. Type II pneumocyte hyperplasia occurs in response to necrosis of type I pneumocytes.

Typical gross lesions of ABPEE in cattle include pale to red, edematous, meaty and rubbery lungs that fail to collapse when the thorax is opened.[3,5] The lungs are often emphysematous. Microscopically, there is interstitial and alveolar edema with hyaline membrane formation in alveoli. There is often in-

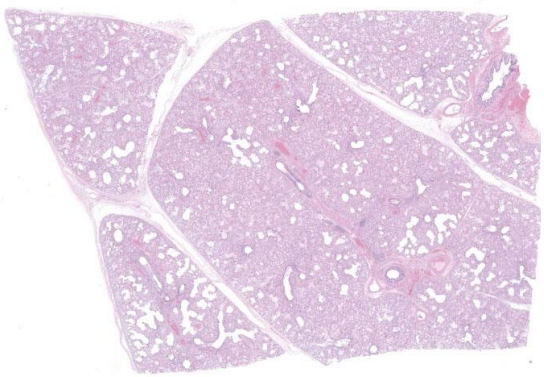

Figure 3-3. Lung, ox. At subgross magnification, there is diffuse lobular consolidation and marked expansion of interlobular septa. (HE, 5X)

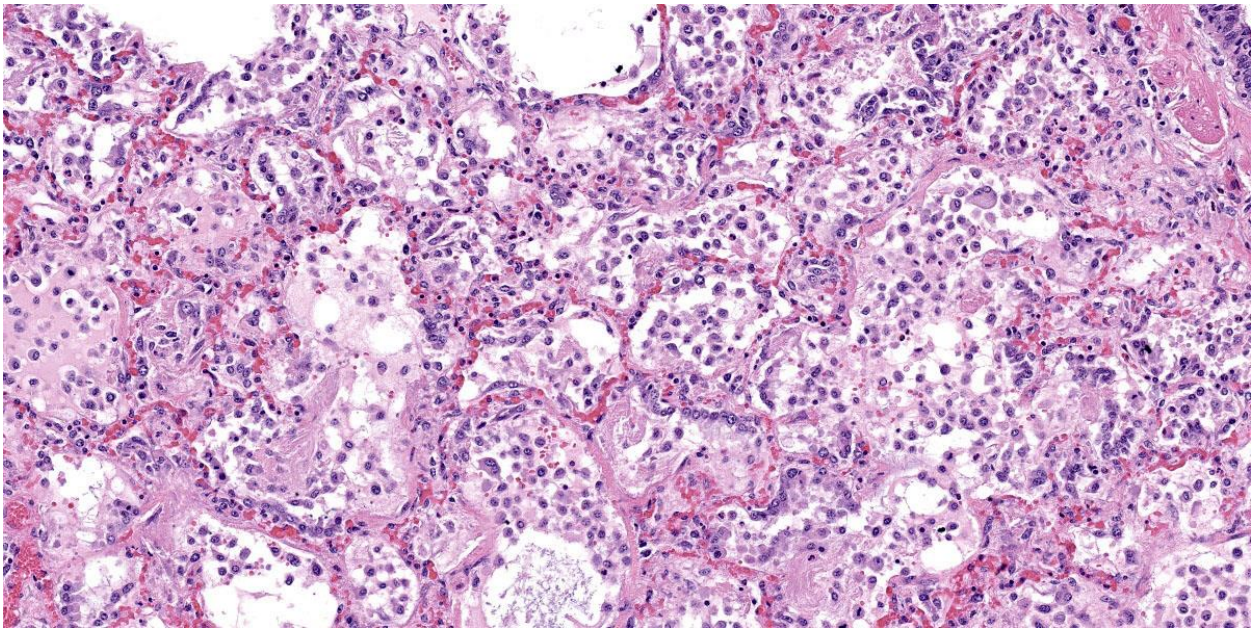

Figure 3-4. Lung, ox. Diffusely, alveoli are filled with edema and numerous alveolar macrophages. Alveolar septa are expanded by edema and multifocally lined by type II pneumocytes. (175X)

terstitial emphysema. Eosinophils and neutrophils may be present within alveolar septa. In more chronic cases, there is diffuse type II pneumocyte hyperplasia and alveolar fibrosis. Secondary suppurative bronchopneumonia can occur. Differential diagnoses include 4-ipomeanol from ingestion of *Fusarium solani*-contaminated sweet potatoes, ingestion of purple mint (*Perilla frutescens*), ingestion of rapeseed and kale (*Brassica* species), ingestion of stinkwood (*Zieria arborescens*), extrinsic allergic alveolitis, hypersensitivity to *Dictyocaulus* larvae, and viral pneumonia, particularly that caused by BRSV.

Contributing Institution:
New Mexico Department of Agriculture
Veterinary Diagnostic Services
www.nmda.nmsu.edu/vds

JPC Diagnosis:
Lung: Pneumonia, interstitial, diffuse, severe, with septal necrosis, marked alveolar and interlobular edema, hyaline membranes, and type II pneumocyte hyperplasia.

JPC Comment:
3-methylindole (3-MI) toxicity is a prime example of biotransformation gone bad. Biotransformation refers to metabolic reactions that generally serve to increase the water solubility of compounds and thus enhance their excretion.[4] These reactions transform toxic compounds into benign metabolites and are also critical to the metabolism of endogenous compounds such as cholesterol, steroids, vitamin D, bile acids, and fatty acids.[4] In some instance, however, biotransformation may form reactive intermediates, such as electrophiles and free radicals, that are directly toxic or mutagenic.[4]
Biotransformation is typically described as a phased process, with Phase I reactions consisting primarily of oxidation, reduction, and hydrolytic reactions that cause small changes in the water solubility of the compound.[4] It is the subsequent Phase II reactions where large changes in water solubility are effected, typically via conjugation reactions where a variety of hydrophilic moieties are added to the subject compound.[4] Phase III, the final phase

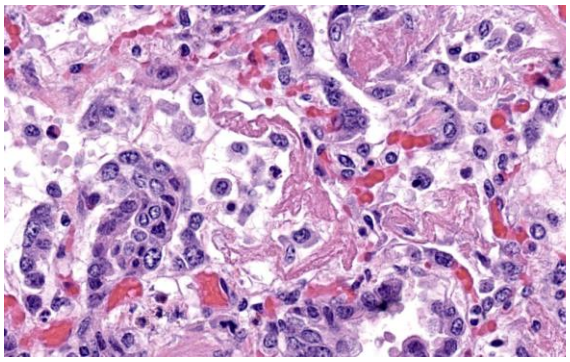

Figure 3-5. Lung, ox. Multifocally, alveoli are filled with polymerized fibrin which occasionally compacts and lines the damaged alveolar septa (hyaline membranes). (HE, 575X)

of biotransformation, refers to the transporter-mediated efflux of the metabolite for excretion.

Phase I metabolism is carried out largely through a family of heme-containing enzymes referred to as cytochrome P450s (CYPs). Given its major role in detoxification, the liver expresses high levels of a variety of CYPs located in the smooth endoplasmic reticulum of hepatocytes.[4] In all species, CYPs are more highly expressed in centrilobular zone hepatocytes, leading to centrilobular necrosis when biotransformation creates toxic intermediates. CYPs are not restricted to the liver but are found in a variety of tissues throughout the body. In the lung, CYP2F enzymes are abundant, particularly in the club cells, the nonciliated bronchiolar epithelial cells formerly called Clara cells.[4]

Phase II biotransformation reactions are primarily conjugation reactions that occur in the cytosol. These reactions include glucuronidation, sulfation, and glutathione conjugation, along with less common reactions such as methylation, acetylation, and amino acid conjugation.[4] There are significant species differences in which reactions predominant, particularly with glucuronidation and sulfation reactions. Glucuronidation is the major Phase II metabolic pathway in all mammalian species except for cats, who assert their feline singularity by preferentially using sulfation reactions.[4]

As the contributor notes, the critical step in the pathogenesis of ABPEE is the biotransformation of 3-MI, a relatively inert compound, to a toxic electrophilic intermediate by CYPs in the lung. The resulting toxic intermediate alkylates cellular macromolecules, resulting in lipid peroxidation, membrane damage, and the subsequent necrosis of bronchiolar epithelial cells and type I pneumnocytes.[3] Type II pneumocytes are relatively unaffected despite their high CYP activity due to their high levels of glutathione and phase II enzymes which are thought to protect them from injury.[3] In fact, type II pneumocyte hyperplasia, not necrosis, is a characteristic histologic change of ABPEE as type II pneumocytes proliferate to repair the extensively damage alveolar epithelium.

Dr. Williams felt that this case was a great, straightforward example of atypical interstitial pneumonia in cattle. He noted areas within the lung where the alveolar type I pneumocytes appeared to be replaced with bronchiolar epithelium, a metaplastic change referred to as bronchiolarization or Lambertosis. This change occurs when bronchiolar epithelium attempts to repair alveolar damage by growing out from the bronchioles and into the alveolar sacs and occurs with severe diffuse alveolar damage.

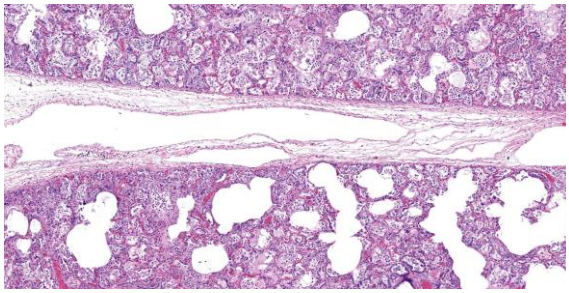

Figure 3-6. Lung, ox. Interlobular septa are markedly expanded by edema. (HE, 47X)

Dr. Williams also noted what appear as undulating nodules of smooth muscle in the wall of the pulmonary vein. This represents a normal spiral of smooth muscle present normally in the pulmonary veins of bovids and should not be confused with hypertensive or neoplastic change. Finally, Dr. Williams noted that edema fluid can drain through lymphatic slits present around the bronchovascular bundle, making this a good location to find siderophages if you suspect heart failure.

Dr. Williams discussed the edema and emphysema noted by the contributor. While the interlobular septa are markedly expanded by clear space, on the examined slide, these spaces appeared largely to be lymphatic channels filled with edema fluid. Dr.Williams interpreted the remaining clear spaces within the pulmonary parenchyma to be alveolar ducts rather than discontinuous alveolar septa. The JPC morphologic diagnosis reflects these interpretations, arrived at after much discussion.

References:

1. Bray TM, Emmerson KS. Putative mechanisms of toxicity of 3-methylindole: from free radical to pneumotoxicosis. *Annu Rev Pharmacol Toxicol*. 1994;34: 91-115.
2. Carlson JR, Yokoyama MT, Dickinson EO. Induction of pulmonary edema and emphysema in cattle and goats with 3-methylindole. *Science*. 1972; 176(4032): 298-299.
3. Caswell JL, Williams KJ. Respiratory system. In: Maxie G, ed. *Jubb, Kennedy, and Palmer's Pathology of Domestic Animals*. 6th ed. Vol 2. Elsevier;2016:465-591.
4. Lehman-McKeeman LD, Armstrong LE. Biochemical and molecular basis of toxicity. In: Haschek WM, Rousseaux CG, Wallig MA, et al., eds. *Haschek and Rousseaux's Handbook of Toxicologic Pathology*. Academic Press;2022: 24-30.
5. Lopez A, Martinson SA. Respiratory system, mediastinum, and pleura. In: Zachary JF, ed. *Pathologic Basis of Veterinary Disease*. 6th ed. Elsevier;2017:471-560.
6. Schiefer B, Jayasekara MU, Mills JHL. Comparison of naturally occurring and tryptophan-induced bovine atypical interstitial pneumonia. *Vet Pathol*. 1974; 11 (4):327-339.
7. Yost GS. Mechanisms of 3-methylindole pneumotoxicity. *Chem Res Toxicol*.1989; 2(5):273-279.

CASE IV:

Signalment:
10-month-old, male Dorper sheep, ovine (*Ovis aries*)

History:
The farm has a Dorper sheep herd comprising 1500 animals. Four sheep showed clinical respiratory signs characterized by cough and tachypnea. They were administered antibiotics and nonsteroidal anti-inflammatory drugs, but no clinical improvement was noted. Fifteen animals died within 10 days. One sheep was euthanized owing to poor quality of life and underwent necropsy.

Gross Pathology:
Lung: Gross examination revealed bilaterally consolidated areas that were focally extensive, dark red, and firm on palpation, affecting the cranioventral region of the right (40%) and left (10%) lobes. On cut surface, the parenchyma was light brown to dark red and consolidated. A large amount of translucent seromucous fluid was seen at the opening of the bronchi.

Figure 4-1. Lung, sheep. There is marked consolidation and atelectasis of the ventral aspects of the right cranial, middle and caudal lung lobes. (*Photo courtesy of:* Laboratório de Patologia Veterinária, Universidade Federal de Mato Grosso, Brazil)

Laboratory Results:
Bacteriology: *Pasteurella multocida* and *Mannheimia haemolytica* PCR were negative (lung).

Virology: PCR of the lung tissue was positive for *Mycoplasma* spp. and lentivirus of small ruminants, which were confirmed as *Mycoplasma ovipneumoniae* and Maedi visna using genetic sequencing.

Microscopic Description:
Lung: Alveolar lumina are variably filled by large numbers of neutrophils and macrophages admixed with mild edema affecting 30-40% of the parenchyma within submitted sections. Multifocally, moderate numbers of affected alveoli are lined with plump and cuboidal epithelial cells (type II pneumocyte hyperplasia). Multifocally, the lumens of the bronchi and bronchioles are also filled with variable numbers of neutrophils admixed with fewer macrophages. The submucosa of the bronchi and bronchioles, as well as the adventitia of the blood vessels, are frequently expanded by cuffs of lymphocytes and plasma cells arranged in follicular aggregates.

Contributor's Morphologic Diagnosis:
Lung: Bronchopneumonia, suppurative and histiocytic, chronic-active, diffuse, severe, with bronchial epithelial and type II pneumocyte hyperplasia and peribronchiolar lymphofollicular proliferation.

Contributor's Comment:
Maedi-visna (MV), also known as ovine progressive pneumonia (OPP), is an incurable viral disease in sheep with a prolonged incubation period that develops into a life-long infection.[3] This disease is caused by non-oncogenic exogenous retroviruses, namely maedi-visna virus (MVV) and caprine arthritis-encephalitis virus (CAEV), both of which belong to a subgroup of viruses known as small ruminant lentiviruses (SRLVs).[10] For years, lentiviruses isolated in ovines were considered MVV and ones in caprines were considered CAEV, and the two were considered to be species-specific; however, phylogenetic analyses and findings of cross-infection have demonstrated differences in genotypes and lentiviral subtypes that can infect both goats and sheep.[1,5-7,12,14,16,17]

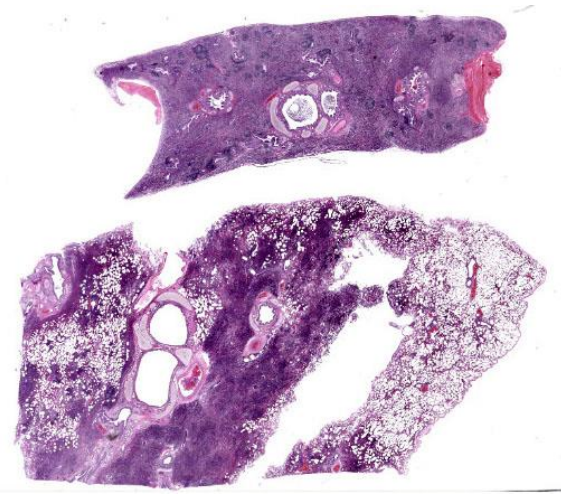

Figure 4-2. Lung, sheep. Two sections of lung are submitted for examination. One section exhibits total consolidation. A second section demonstrates profound peribronchiolar and peribronchial lymphoid hyperplasia. (HE. 6X)

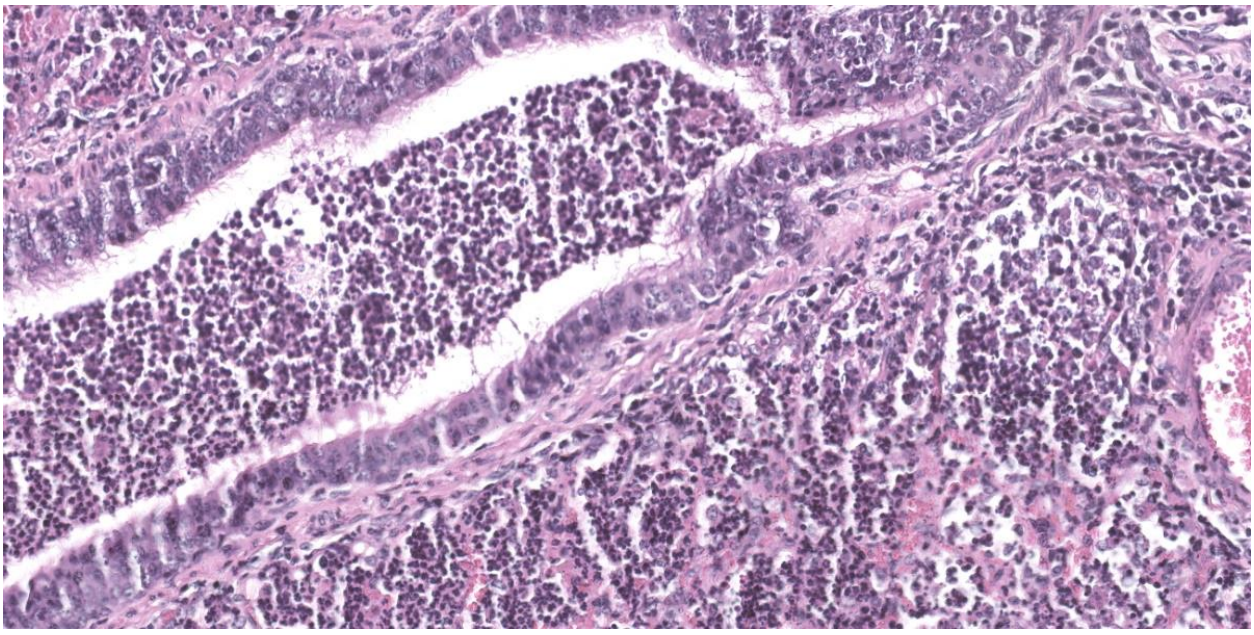

Figure 4-3. Lung, sheep. Airways and surrounding alveoli contain innumerable neutrophils. (HE, 166X)

SRLVs exhibit tropism for the mononuclear-phagocyte system and induce slow, chronic, and persistent inflammation mainly in four target organs (the lung, joints, nervous system, and mammary gland), resulting in different clinical phenotypes (i.e., pulmonary, articular, nervous, and mammary, respectively). Interestingly, the occurrence of each clinical form and lesion severity depends on viral factors, as well as the host immune response.[2,4,9,11] In the present case, the lung lesions were typical of SRLVs, characterized by lymphoplasmacytic infiltration in septa with type II pneumocyte hyperplasia and infiltration of lymphocytes in the bronchi and bronchioles, and eosinophilic exudates in alveoli.[3,17]

The farm where the outbreak occurred had a system of extensive breeding without control measures. Ewes and breeding males were acquired from another Brazilian state, Bahia, where seroprevalence studies have demonstrated the presence of SRLV.[15] Thus, it is probable that the purchase of these animals introduced the disease into the herd via asymptomatic animals.

In the present case, *M. ovipneumoniae* was detected by PCR from pulmonary tissue. *M. pneumoniae* is a respiratory bacterium commonly detected in both healthy and diseased lambs.[8] Although speculation, it is possible that Maedi, a retrovirus, may cause immunosuppression, thereby contributing to the establishment of subsequent *ovipneumoniae* colonization.

A definitive diagnosis of maedi was made based on the characteristic lesions identified grossly and histopathologically, along with a supportive clinical history of the disease. The diagnosis was confirmed by molecular techniques.

Contributing Institution:
Laboratório de Patologia Veterinária
Faculdade de Medicina Veterinária
Universidade Federal de Mato Grosso
Brazil.

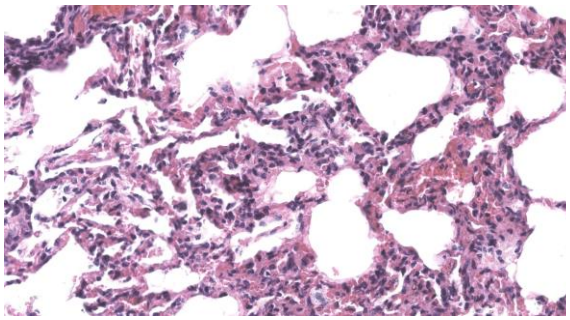

Figure 4-4. Lung, sheep. In areas not totally overrun by the suppurative bronchopneumonia, alveolar septa are expanded by lymphocytes and macrophages. (HE, 166X).

JPC Diagnosis:

1. Lung: Bronchopneumonia, neutrophilic, diffuse, moderate, with bronchiolar epithelial hyperplasia, alveolar collapse, and peribronchiolar and perivascular lymphoid hyperplasia.
2. Lung: Pneumonia, interstitial, lymphohistiocytic, multifocal, mild.

JPC Comment:

Maedi-Visna virus (MVV) was first described in Iceland in 1954 by Bjorn Sigurdsson, who made history three years later by isolating MVV and thereby becoming the first scientist to isolate a lentivirus. Maedi-visna and Iceland have history that began in 1933 when the country imported several Karakul sheep tasked with improving the native Icelandic sheep breed. Unfortunately, Icelanders had the wool pulled over their eyes as the apparently healthy Karakul managed to introduce ovine pulmonary adenomatosis, pseudotuberculosis, and MVV to the native herds.[18] The long incubation period characteristic of MVV delayed the first clinically apparent epidemic until six years after importation of the sheep, allowing the virus to spread throughout the country undetected and unimpeded for years.[18]

What followed the discovery of MVV was a concerted effort to understand, contain, and eradicate the disease. The disease name originates in the Icelandic words for dyspnea (maedi) and wasting (visna), and the virus was officially designated Maedi-Visna Virus to honor the outstanding efforts of Icelandic scientists.[18] Though it persists throughout most countries in the world today, the disease was eradicated from the Icelandic islands during the 1960s through mass slaughter of sheep on affected farms.

MVV is, in many ways, a typical lentivirus, though it differs from its genus-mates in that it typically does not cause immunosuppression. Lentiviruses are a genus of retroviruses characterized by causing slowly progressing disease. Members of the Retroviridae family are unique in possessing a reverse transcriptase that transcribes the linear, positive-sense single stranded RNA genome into double stranded DNA.[13] This reverse transcriptase is transcribed by one of the three genes that make up the minimum armamentarium of any self-respecting retrovirus: gag, pol, and env. The gag (group-specific antigen) gene encodes structural proteins, the pol (polymerase) gene encodes the reverse transcriptase and integrase enzymes, and env (envelope) encodes the major envelope glycoprotein.[13]

Retroviruses gain entry to host cells through interactions with the envelope glycoprotein and a specific cell receptor that varies depending on the individual virus. Once inside the cell, reverse transcriptase synthesizes double stranded DNA copies of the viral genome in the host which move to the nucleus and are integrated randomly into the host genome via viral integrase.[13] Viral DNA is then transcribed using host cell replication machinery, and mature virions are assembled in the host cytoplasm and acquire an envelope as they bud from the host cell membrane.

Infection with MVV is frequently subclinical, and although virus is widely distributed throughout affected animals, MVV is

transmitted mainly in pulmonary exudates, colostrum, and milk.[13] The wide distribution of affected tissues is due to a unique "Trojan horse" pathogenic mechanism where provirus integrated into the genome of monocytes and their precursors is activated only when monocytes develop into macrophages.[13] This restricted viral replication in monocytes permits MVV to transit surreptitiously through the body with minimal immune stimulation.

In conference, Dr. Williams emphasized how much information can be gleaned from subgross examination of this particular slide. The most striking feature is the complete lack of air in the majority of the submitted sections. The affected area is sharply demarcated on the gross aspect (Fig. 4-1) and represents complete alveolar collapse, and Dr. Williams emphasized that these changes should prompt participants to consider small airway disease. Subsequent examination of the bronchioles and surrounding vessels revealed bronchial epithelial hyperplasia and robust smooth muscle within arteriole walls. The arteriolar medial hypertrophy is likely due to the lung's paradoxical response to hypoxia; if the alveoli are not being properly ventilated, endothelin-mediated vasoconstriction attempts to match perfusion with ventilation and shunts the blood away from the ineffectual alveoli. With chronicity, this can result in the arteriolar medial hypertrophy seen throughout this section.

There was robust discussion about ascribing particular histologic lesions to either MVV or *Mycoplasma ovipneumonia* in these particular sections. Generally, MVV should cause BALT hyperplasia and lymphohistiocytic interstitial pneumonia, while *M. ovipneumonia* should cause airway epithelial hypertrophy and an exudative neutrophilic bronchitis and bronchiolitis. Participants believed that the majority of the histologic lesions were likely attributable to *Mycoplasma ovipneumonia*, as the section was dominated by airway disease and BALT hyperplasia. In less affected areas of the lung, where alveoli were inflated and septa could be properly evaluated, a mild interstitial lymphohistiocytic pneumonia was present, though this was deemed a minor lesion in the evaluated section.

Participants also noted the history, which describes a quickly moving epidemic, and the young age of the animal. Both factors are more consistent with *Mycoplasma ovipneumonia* disease since MVV typically only causes clinical signs in animals many years post-infection. Participants vigorously discussed combining all histologic changes into a single morph; however, a reluctant, sheepish consensus was eventually reached to split the lesions into multiple morphologic diagnoses. The first diagnosis emphasizes participants' assessment that the major histologic lesions were attributable to *Mycoplasma ovipneumonia*, while the second diagnosis emphasizes the mild interstitial disease that is potentially attributable to MVV.

References:

1. Angelopoulou K, Karanikolaou K, Papan-astasopoulou M. First partial characterization of small ruminant lentiviruses from Greece. *Vet Microbiol.* 2005; 109(1-2):1-9.
2. Blacklaws BA. Small ruminant lentiviruses: Immunopathogenesis of visna-maedi and caprine arthritis and encephalitis virus. *Comp Immunol Microbiol Infect Dis*. 2012;35(3):259-269.
3. De Boer GF. Zwoegerziekte virus, the causative agent for progressive interstitial pneumonia (maedi) and meningo-leucoencephalitis (visna) in sheep. *Res VetSci*. 1975;18:15–25.
4. Gayo E, Polledo L, Balseiro A, et al. Inflammatory Lesion Patterns in Target Organs of Visna/Maedi in Sheep and their

Significance in the Pathogenesis and Diagnosis of the Infection. *J Comp Pathol*. 2018;159:49-56.
5. Gjerset B, Rimstad E, Teige J, et al. Impact of natural sheep-goat transmission on detection and control of small ruminant lentivirus group C infections. *Vet Microbiol*. 2009;135(3-4):231-238.
6. Kuhar U, Barlic-Maganja D, Grom J. Phylogenetic analysis of small ruminant lentiviruses detected in Slovenia.*Vet Microbiol*. 2003;162(1):201-206.
7. Leroux C, Cruz JCM, Mornex JF. SRLVs: A genetic continuum of lentiviral species in sheep and goats with cumula-tive evidence of cross species transmission. *Curr HIV Res*. 2010;8(1):94-100.
8. Manlove K, Branan M, Baker K, et al. Risk Factors and Productivity Losses Associated with Mycoplasma Ovipneumoniae Infection in United States Domestic Sheep Operations. *Prev Vet Med*. 2019;168:30-38.
9. Minguijón E, Reina R, Pérez M, et al. Small ruminant lentivirus infections and diseases. *Vet Microbiol.* 2015;181(1-2):75-89.
10. Pálsson PA. Maedi-Visna. History and Clinical Description. In: Pétursson G, Hoff-Jørgensen R, eds. *Maedi-Visna and Related Diseases: Developments in Veterinary Virology*. Kluwer Academic Publishers;1990:3-74.
11. Pinczowski P, Sanjosé L, Gimeno M, et al. Small Ruminant Lentiviruses in Sheep: Pathology and Tropism of 2 Strains Using the Bone Marrow Route. *Vet Pathol*. 2017;54(3):4131424.
12. Pisoni G, Bertoni G, Manarolla G, et al. Genetic analysis of small ruminant lentiviruses following lactogenic transmission. *Virology*. 2010;407(1):91-99.
13. Quinn PJ, Markey BK, Leonard FC, et al. *Veterinary Microbiology and Microbial Disease*. 2nd ed. Wiley-Blackwell;2011:619-633.
14. Reina R, Mora MI, Glaria I, et al. Molecular characterization and phylogenetic study of Maedi Visna and Caprine Arthritis Encephalitis viral sequences in sheep and goats from Spain. *Virus Res*. 2006;121(2):189-198.
15. Sampaio TS, Costa JN, Martinez PM, et al. Estudo sorológico da Maedi-Visna pelo método da imunodifusão em gel de ágar em rebanhos ovinos de Juazeiro, Bahia, Brasil. Rev *Bras Saúde Prod. An*. 2007;8:276-282.
16. Shah CA, Böni J, Huder JB, et al. Phylogenetic analysis and reclassification of caprine and ovine lentiviruses based on 104 new isolates: evidence for regular sheep-to-goat transmission and worldwide propagation through livestock trade. *Virology*. 2004;319(1):12-26.
17. Shah C, Huder JB, Böni J et al. Direct evidence for natural transmission of small- ruminant Lentiviruses of subtype A4 from goat to sheep and vice versa. *J Virol*. 2004;78(14):7518-7522.
18. Staub, OC. Maedi-visna infection in sheep. History and present knowledge. *Comp Immunol Microbiol Dis*. 2004;27(1):1-5.

WSC 2023-2024
Conference 9 Self-Assessment

1. True or false? In pulmonary veno-occlusive disease in dogs, arteriolar remodeling is consistently seen.
    a. True
    b. False

2. True or false? The veterinary literature has suggested a link between ascarid larval migration and eosinophilic pulmonary granulomatosis.
    a. True
    b. False

3. True or false? Eosinophilic pulmonary granulomatosis has a strong breed predilection for French bulldogs
    a. True
    b. False

4. 3-methylindole is converted to toxic metabolites in which of the following?
    a. Centrilobular hepatocytes
    b. Type I pneumocytes
    c. Non-ciliated respiratory epithelium
    d. Ciliated respiratory epithelium

5. True or false. The Maedi-Visna virus can infect both sheep and goats.
    a. True
    b. False

Joint Pathology Center
Veterinary Pathology Services

WEDNESDAY SLIDE CONFERENCE 2023-2024

Conference #10 **15 November 2023**

CASE I:

Signalment:
Adult female betta fish, piscine (*Betta splendens*)

History:
This adult, female betta fish exhibited erratic and abnormal swimming behavior for 17.5 days. The owner described the fish as happy-go-lucky since being purchased at the local fish store. The fish even swam up to be caressed on the head at times. One day, after 2 years, the owner noted the fish had difficulty swimming. The owner also noticed that the fish had a greatly distended coelomic cavity. The fish was subsequently euthanized.

Gross Pathology:
There was an approximately 1 cm diameter distension of the coelomic cavity. On cut section, the mass was tan and solid.

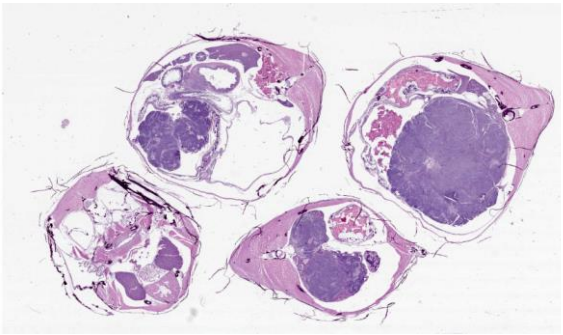

Figure 1-1. Transverse sections, betta. Subgross magnification demonstrates a large basophilic neoplasm occupying a large portion of the coelom. (HE, 5X)

Microscopic Description:
Kidney: Expanding and occupying greater than 90% of the coelomic cavity, compressing and displacing adjacent organs, and arising from the kidney, is a well-demarcated, unencapsulated, densely cellular, 0.75 cm diameter neoplasm composed of three distinct cell populations supported on a variably fine fibrovascular stroma. The first cell population is composed of polygonal cells (blastemal cells) which irregularly merge into two other populations. An epithelial cell population is arranged in palisading, branching, and tubule-like formations that often resemble lumens.

The third population resembles small, compact tufts of cells (glomeruloid structures). Spindle to stellate cells are scattered throughout the neoplasm (embryonal mesenchyme). Polygonal blastemal cells have indistinct cell borders, a high nuclear to cytoplasmic ratio, a scant amount of eosinophilic cytoplasm, round to oval nuclei, and dense chromatin with indistinct nucleoli. Epithelial cells are cuboidal to columnar with variably distinct cell borders, a moderate amount of eosinophilic cytoplasm, round to oval nuclei with stippled chromatin and variably distinct nucleoli. Embryonal mesenchymal cells are spindle to stellate and loosely arranged, with indistinct cell borders, scant eosinophilic cytoplasm with elongate to oval nuclei and indistinct nucleoli. Mitotic figures are not present in the neoplasm. Peripherally, ova are

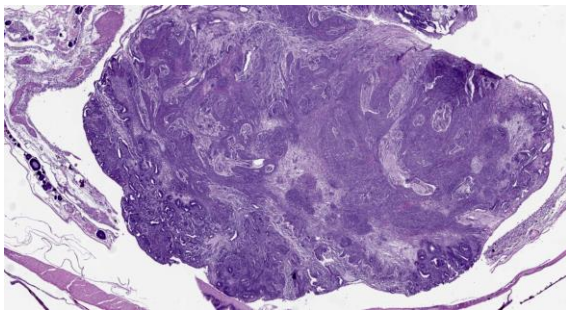

Figure 1-2. Coelom, betta. A large neoplasm is composed of multiple patterns including broad streams, bundles, and tubules. (HE, 36X)

multifocally degenerate and are atrophied with variably sized, irregularly shaped oocyte borders.

Transmurally and multifocally expanding the stomach wall are variably dense aggregates of macrophages interspersed with areas of spindle cells and fibrous connective tissue. Multifocally throughout the stomach wall and extending into the coelomic cavity are 40-100um diameter granulomas characterized by a core of brightly eosinophilic necrotic debris, foamy macrophages, degenerate inflammatory cells, and mineral which are surrounded by variably dense concentric lamellations of spindle cells and macrophages. Multifocally, there are less developed granulomas that contain foamy macrophages with a light yellow-brown hemosiderin-like pigment. Scattered throughout the ovaries are multiple granulomas as previously described.

Contributor's Morphologic Diagnoses:

1. Betta fish, kidney: Nephroblastoma.
2. Betta fish, ovaries, stomach and coelomic cavity: Granulomas, multiple, most likely *Mycobacteria* spp.

Contributor's Comment:

Nephroblastoma is considered a common primary tumor of pigs, chicken, and fish with varying reports in dogs, cats, and cattle.[7] In this case, spontaneous nephroblastoma in *Betta splendens* ("Siamese fighting fish") has been reported with other fish species, to include Japanese eels (*Anguilla japonica*), koi (*Cyprinus carpio*), and striped bass (*Morone saxatilis*).[2,4,6,12] Nephroblastomas arise from neoplastic transformation of nephrogenic stem cells, which give rise to the characteristic blend of three cell populations that attempt to parallel the histo-anatomic components of the kidney through epithelial, blastemal, and mesenchymal cells. The cause of these tumors in fish is considered spontaneous, but has also been attributed to carcinogens.[5] Other than coelomic enlargement, the clinical presentation of nephroblastoma in fish varies.

Mycobacteriosis affects wild and cultured freshwater, marine, and brackish fish worldwide, and frequently manifests as a chronic, progressive, and systemic disease.[10] Transmission routes vary but may include cannibalism of infected fish, consumption of contaminated feed and/or detritus, or shedding from other aquatic vertebrates.

Although many *Mycobacteria* species have been isolated from fish, the most frequent and significant fish mycobacterioses include *M. chelonae*, *M. fortuitum*, and *M. marinum*.[1] Granuloma formation due to *Mycobacteria* infection in fish can be identified grossly (grayish-white, miliary nodules) and histologically in a variety of organs to include, but

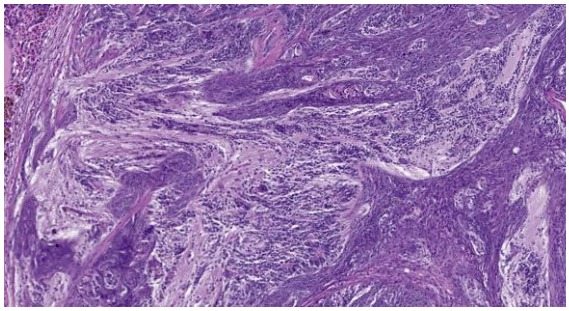

Figure 1-3. Coelomic mass, betta. The predominant cells are neuroectodermal and are occasionally embedded in neuropil. (HE, 183X)

not limited to, the spleen, kidney, liver, and coelomic cavity. The histologic appearance of granulomas in most fish species is characterized by an outer wall of concentrically layered epithelioid macrophages, necrotic centers, and variable numbers of acid-fast bacilli within the core. The epithelial cell characteristics of these epithelioid macrophages is demonstrated by positive immunoreactivity for cytokeratin.[8,9]

The cause of death in this fish is most likely multi-factorial and attributed to pathophysiologic changes associated with tumor compression of vital organs and granuloma formation in multiple organs.

JPC Diagnosis:

1. Ovaries, posterior kidney, and coelom: Teratoma.
2. Ovaries: Follicular degeneration and necrosis, multifocal, chronic, moderate (follicular stasis/egg binding).
3. Stomach and coelom: Granulomatous and fibrosing gastritis, transmural, regionally extensive, severe, with regional coelomitis and intralesional birefringent debris (foreign body).

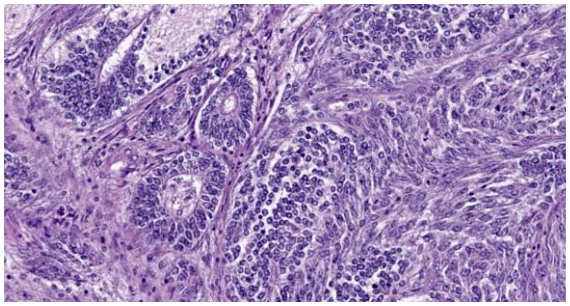

Figure 1-4. Neoplasm, betta. Rosettes are commonly seen in the neuroectomal tissue. (HE, 613X)

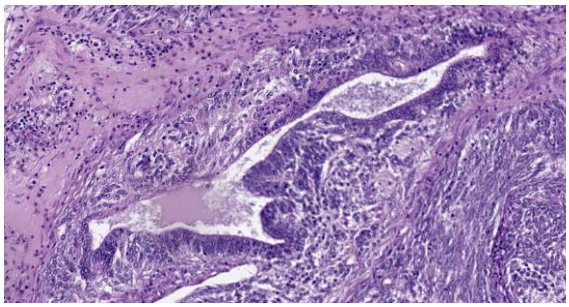

Figure 1-5. Neoplasm, betta. Columnar epithelium forms torturous single-layered structures resembling gastrointestinal tissue. (HE, 363X)

JPC Comment:

We agree with the contributor that there are three populations of cells within the examined section; however, we interpret these populations to originate from the three primordial germ layers, and thus prefer a diagnosis of teratoma. The examined section contains multiple large areas of neural differentiation (ectoderm), sheets of primitive mesenchymal tissue (mesoderm), and numerous tubular structures (endoderm). The teratoma is adhered to and infiltrates both the posterior kidney and the ovary. Intracoelomic teratomas usually originate from the ovary in female fish, making ovarian origin most likely for this tumor.[11] As in this case, teratomas in fish often present as large coelomic masses causing coelomic distention.[2,11]

While most cases of granulomatous inflammation in fish should be stained with acid fast stains to rule out mycobacteriosis, the distribution of granulomas in this case would be an unusual presentation. Mycobacteriosis in fish typically causes discrete granulomas or sheets of macrophages in the liver, spleen, kidney, skin, and coelom. In this case, infection and fibrosis track through the gastric wall in a manner most consistent with trauma (foreign body). The H&E slide was examined under polarized light and birefringent material was noted in the granulomas in the coelomic cavity adjacent to the gastric lesion,

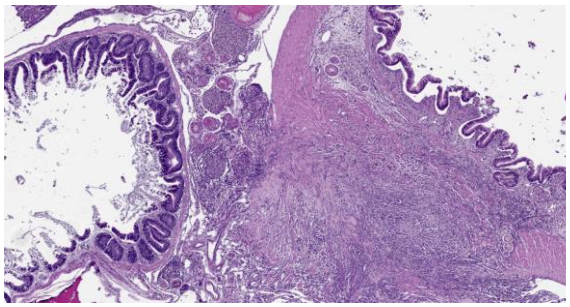

Figure 1-6. Stomach, betta. There is a focal fibrous adhesion between the stomach and a loop of bowel with embedded granulomas. (HE, 69X)

further supporting foreign body trauma. Acid fast stains were applied to the lesions and were negative.

We note the contributor's reference to granulomas in the ovaries; however, in our examined sections, these structures consist mostly of shrunken and necrotic ovarian follicles being engulfed by macrophages. This is a common lesion of follicular degeneration/egg binding and was likely caused by the mass effect of the teratoma preventing normal follicular release.

This week's conference was moderated by Dr. Elise LaDouceur, Chief of Extramural Projects and Research at the Joint Pathology Center. Conference participants were of two

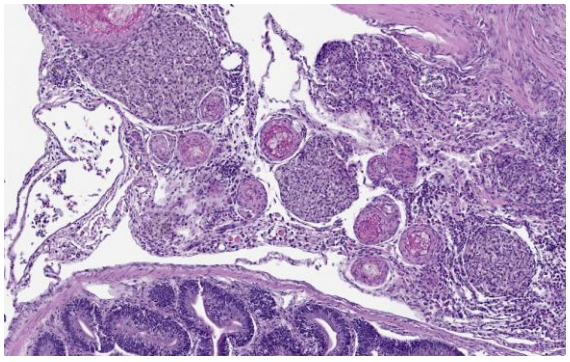

Figure 1-7. Omentum, betta. There are numerous well-formed granulomas within the omental adhesion. (HE, 186X)

schools, with all participants diagnosing either nephroblastoma or teratoma. All participants were eventually convinced of teratoma by the large areas of neural differentiation and ciliated epithelium.

Discussion also centered on whether the tumor was arising from or invading into the posterior kidney and ovary. While this was impossible to determine from the examined sections, in all species, teratomas most commonly arise in the gonads, making ovarian origin mostly likely.

Participants discussed egg binding, also known as follicular stasis. This condition in teleost fish has many causes, including mass effect, inflammation, or lack of access to nesting areas.

References:

1. Decostere A, Hermans K, Haesebrouck F. Piscine mycobacteriosis: a literature review covering the agent and the disease it causes in fish and humans. *Vet Microbiol*. 2004;99(3-4):159-166.
2. Groff JM. Neoplasia in fishes. *Vet Clin North Am Exot Anim Pract*. 2004;7(3): 705-706.
3. Helmboldt CF, Wyand DC. Nephroblastoma in a striped bass. *J Wildl Dis*. 1971; 7:162–165.
4. Lombardini ED, Law M, Lewis BS. Nephroblastoma in two Siamese fighting fish (*Betta splendens*). *Fish Pathol*. 2010;45:137–139.
5. Lombardini ED, Hard GC, Harshbarger JC. Neoplasms of the urinary tract in fish. *Vet Pathol*. 2014;51(5):1000-1012.
6. Masahito P, Ishikawa T, Okamoto N, et al. Nephroblastomas in the Japanese eel, Anguilla japonica Temminck et Schlegel. *Cancer Res*. 1992;52:2575–2579.
7. Meuten DJ, Everitt J, Inskeep W, et al. *Histological classification of tumors of the urinary system of domestic animals*.

Armed Forces Institute of Pathology; 2004.
8. Noga EJ, Dykstra MJ, Wright JF. Chronic inflammatory cells with epithelial cell characteristics in teleost fishes. *Vet Pathol*. 1989;26(5):429-437.
9. Polinas M, Padrós F, Merella P, et al. Stages of granulomatous response against histozoic metazoan parasites in mullets (Osteichthyes: Mugilidae). *Animals (Basel)*. 2021;11(6):1501
10. Puk K, Guz L. Occurrence of *Mycobacterium* spp. in ornamental fish. *Ann Agric Environ Med*. 2020;27(4):535-539.
11. Romanucci M, Arbuatti A, Massimini M, Defourny SP, Della Salda L. Ovarian teratoma in an adult female *Zoogoneticus tequila* (Webb & Miller 1998): histological and immunohistochemical features. *J Fish Dis*. 2017;40(6):859-862.
12. Stegeman N, Heatley JJ, Rodrigues A, et al. Nephroblastoma in a koi (*Cyprinus carpio*). *J Exotic Pet Med*. 2010;19:29803.

CASE II:

Signalment:
1-year-old, female red abalone (*Haliotis rufescens*)

History:
Four red abalone were acquired from California for placement in an aquarium. Receding tissues were noted in one of the animals. The co-housed animal was apparently healthy.

Laboratory Results:
PCR for *Xenohaliotis californiensis* was positive.

Microscopic Description:
Posterior esophagus**:** Moderate numbers of epithelial cells lining the posterior esophagus contain large (15-20 µm in diameter) basophilic cytoplasmic inclusions. The inclusions range from palely basophilic and homogeneous to moderately basophilic and punctate to deeply basophilic and granular. The majority of inclusions are located in the

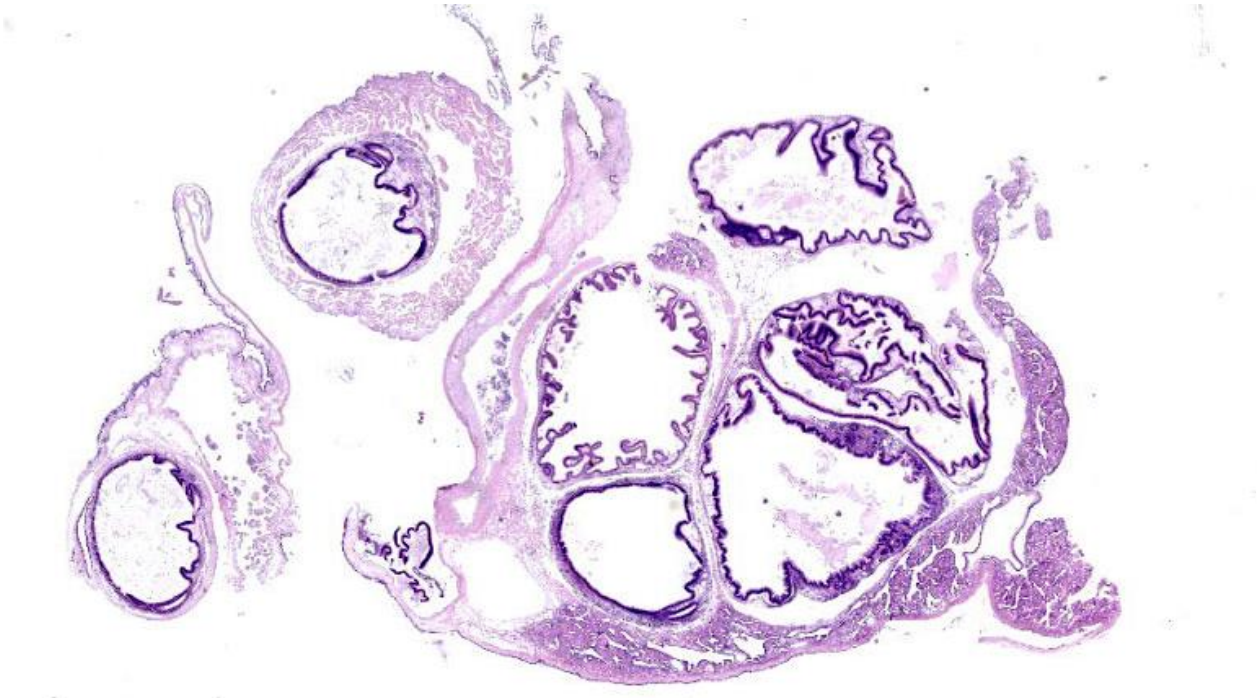

Figure 2-1. Transverse section, abalone. A transverse section of the body of an abalone (and two additional sections of gut) is submitted for examination with no lesions visible at this magnification. (HE, 5X)

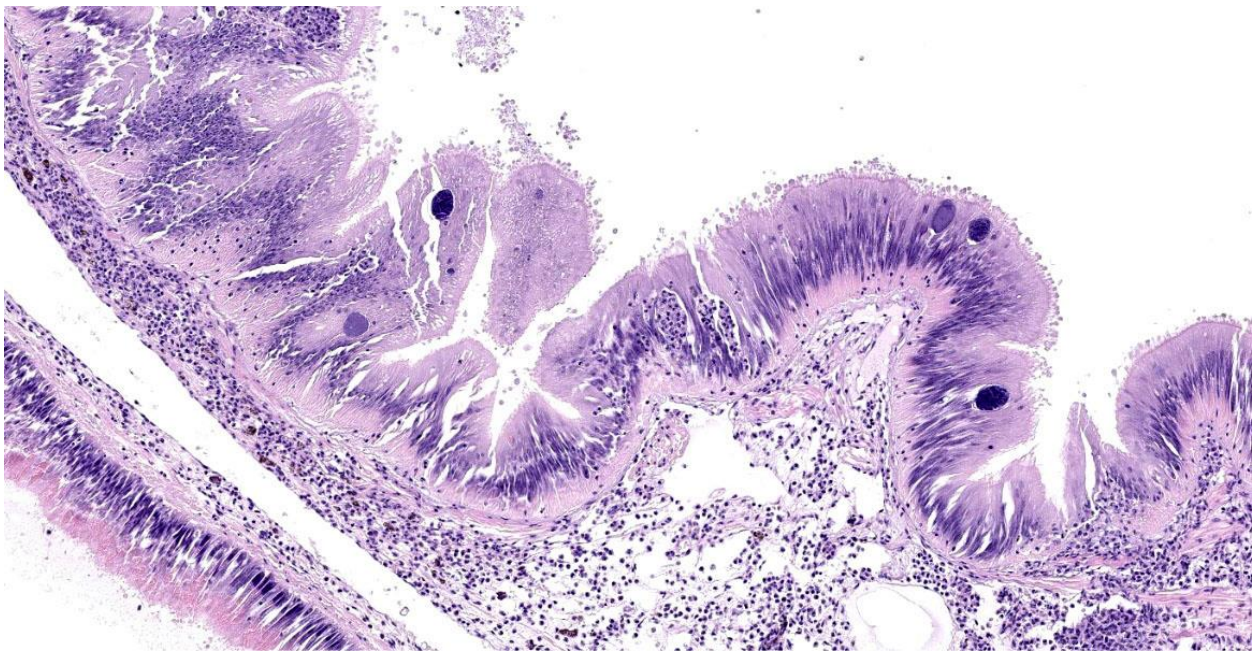

Figure 2-2. Gut, abalone. There are scattered epithelial cells which are markedly distended by a cytoplasmic vacuole containing numerous punctate bacilli. (HE, 137X)

apical aspect of the epithelial cells. Rarely, there are similar inclusions in the intestinal epithelium. Hucker-Twort gram stain shows the organisms within the inclusions to be gram negative.

Contributor's Morphologic Diagnosis:
Posterior esophagus: Moderate numbers of intracytoplasmic epithelial inclusions consistent with rickettsiae (abalone rickettsiosis).

Contributor's Comment:
Inclusions within the digestive tract of this animal are consistent with infection with the rickettsial organism *Xenohaliotis californiensis*, the agent associated with abalone withering syndrome. As this disease is reportable to the OIE, samples were submitted to the NVSL for confirmatory histopathology and PCR testing. A PCR product generated with PCR primers proscribed by the OIE was sequenced and showed 99.37% identity with *X. californiensis* sequences in Gen Bank.[4]

Abalone withering syndrome affects multiple species within the *Haliotis* genus in both wild and farmed animals. The causative agent, *Xenohaliotis californiensis*, primarily infects the posterior esophagus and the digestive gland, but can also be seen to a lesser extent in the intestine.[5] Some of the slides submitted here have rare cytoplasmic inclusions present in intestinal epithelial cells. Sections of the digestive gland from this animal are not present on the submitted slides; additional sections containing the digestive gland examined by the submitter did not exhibit inclusions within digestive gland cells. Infection of the digestive gland leads to degeneration/metaplasia of the digestive tubules which leads to anorexia, depletion of glycogen reserves, and subsequent use of the foot muscle as an energy source.[5] Atrophy of the foot muscle is the characteristic gross change that gives the syndrome its name.

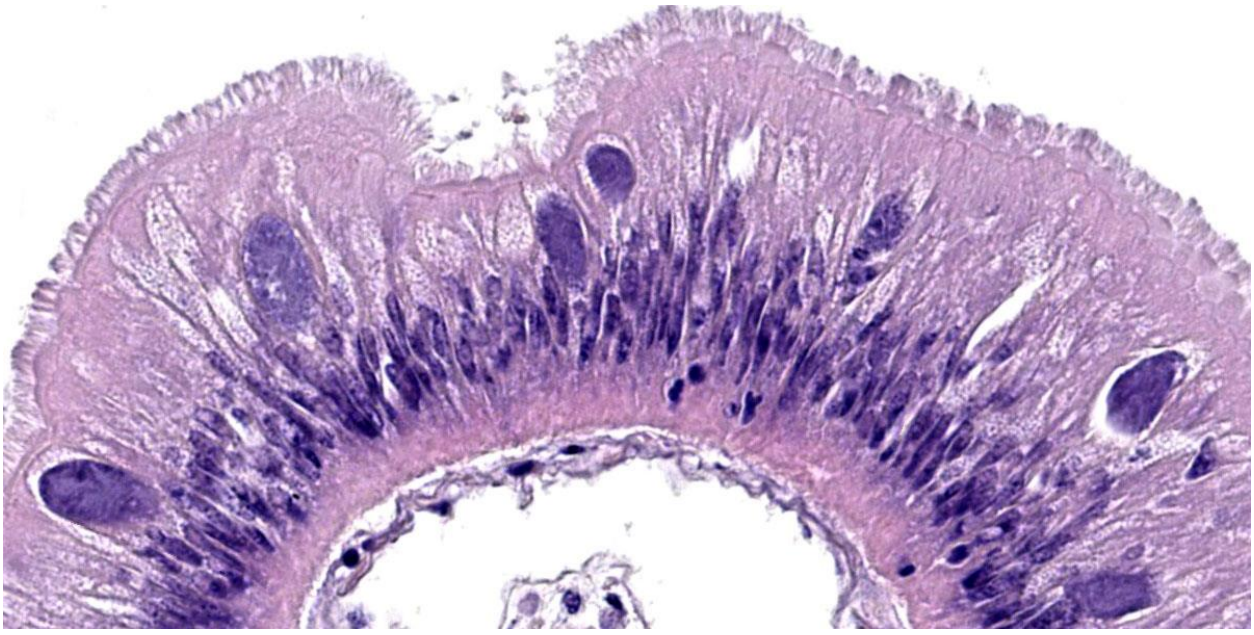

Figure 2-3. Gut, abalone. This field contains several infected intestinal epithelial cells with rickettsial inclusions at varying stages of maturity. (HE, 381X)

Contributing Institution:
USDA/APHIS
NVSL Pathology Laboratory
https://www.aphis.usda.gov/aphis/ourfocus/animalhealth/lab-info-services/sa_about_ nvsl/ct_about_nvsl

JPC Diagnosis:
1. Gut: Epithelial necrosis, single cell, multifocal, moderate, with hemocytic inflammation and intracytoplasmic bacterial inclusions.
2. Kidney: Coccidiosis, intraepithelial, multifocal, moderate with mild epithelial degeneration.

JPC Comment:
Withering syndrome (WS) is a bacterial disease characterized by a severely shrunken body and infection by the organism *Xenohaliotis californiensis*. The organism is an obligate intracellular bacterium that infects the abalone digestive epithelia, causing the morphologic abnormalities detailed by the contributor and resulting in physiologic starvation.[1] The organism is likely spread via direct fecal-oral transmission, with initial infection in the post-esophagus, followed by the intestine, and finally and most devastatingly, the digestive gland.[1]

WS affects all members of the *Haliotis* genus with varying degrees of severity, depending on species and environmental conditions. The disease was first observed in black abalone populations on the California coast in 1985 after a particularly strong El Niño event caused sustained, increased water temperatures off the western US.[1] This pattern has held in subsequent years, with the geographic range of clinical WS moving steadily ever northward with increasing coastal water temperatures and episodic high-mortality events associated with El Niño years.

Temperature is the central factor in the ecology of WS with transmission and disease nearly eradicated at water temperatures of 12.3^{o}C, but high transmission and extreme clinical signs evident at 18.7^{o}C.[1] The susceptibility of *Haliotis* species also varies widely, with green and pink abalone exhibiting no

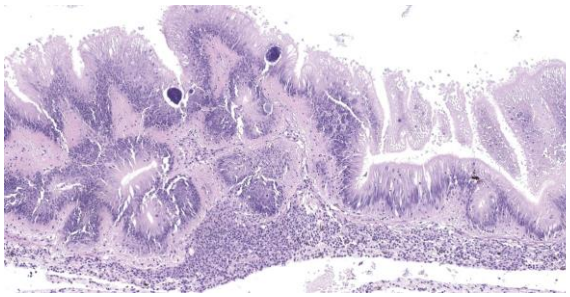

Figure 2-4. Gut, abalone. There are numerous hemocytes infiltrating the spongy connective tissue adjacent to the affected sections of gut. (HE, 317X)

clinical effects of infection and no mortality, red abalone exhibiting moderate mortality, and black abalone exhibiting catastrophic mortality rates of up to 99%.[1]

Diagnosis of WS requires both identification of the pathogen, either by *in situ* hybridization or by PCR and sequence analysis, and observation of the characteristic histologic changes of pedal and digestive gland atrophy and digestive gland metaplasia. PCR may also be used to detect *Xenohaliotis californiensis* prior to the movement of animals as part of infectious disease prevention protocols.[1] Scrupulous husbandry practices, such as reduced stocking densities, maintaining cool water temperatures, disinfection of hands and equipment when moving among groups or tanks of animals, and isolation or culling of infected animals are the mainstays

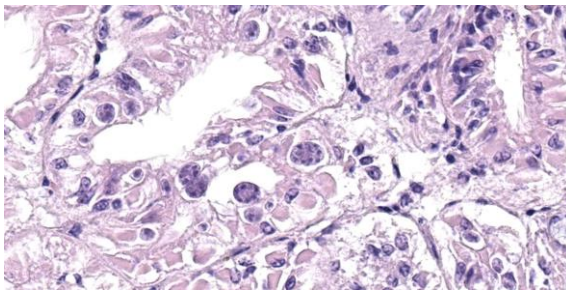

Figure 2-5. Renal papilla, abalone. There are numerous apicomplexan meronts and shizonts within the epithelium of the renal papilla. (HE, 391X)

of WS prevention in *Haliotis* species under human care.

Despite the dramatic mass mortality events associated with WS, certain black abalone populations appear to have developed some resistance to the disease, with progeny of mass mortality event survivors experiencing longer survival times upon infection.[2] In a second optimistic development, a bacteriophage has been identified within *Xenohaliotis californiensis* in WS-affected farmed abalone. The presence of this bacteriophage effectively eliminates the ability of *Xenohaliotis californiensis* to cause disease in farmed abalone, though the extent to which the phage is present in the wild is currently unknown.[2] More research is currently needed to understand the complex interactions of climate change, water temperatures, natural selection pressures, and host-agent-parasite relationships and what these interactions portend for the future of *Haliotis* species.

Conference participants briefly discussed the anatomy and ecology of the red abalone, which, due to their endangered status, can only be harvested via recreational free diving. Participants also discussed the coccidial organisms noted throughout the kidney. These are most consistent with *Margolisiella haliotis* (formerly called *Pseudoklossia haliotis*; also called, rather pointedly, abalone kidney coccidia) which infects multiple species of abalone and targets renal epithelial cells. Lesions reportedly associated with this infection include renal epithelial cell hypertrophy and inflammation.[3]

Participants discussed lesion localization within the abalone digestive tract. The moderator felt it unnecessary to parse the different gastrointestinal segments present on the examined slide, particularly since the term "gut" is used extensively in invertebrate pathology to refer to the entire invertebrate

tubular alimentary tract. Discussion ended with a quick review of rickettsia-like bacterial diseases of veterinary note, including *Epitheliocystis, Rickettsiella scorpionisepticum, Neorickettsia risticii,* and *Neorickettsia helmintheca*.

References:

1. Crosson LM, Wight N, VanBlaricom GR, Kiryu I, Moore JD, Friedman CS. Abalone withering syndrome: distribution, impacts, current diagnostic methods and new findings. *Dis Aquat Org*. 2014;108:261-270.
2. Friedman CS, Wight N, Crosson LM, VanBlaricom GR, Lafferty KD. Reduced disease in black abalone following mass mortality: phage therapy and natural selection. *Front Microbiol*. 2014;5:1-10.
3. Friedmann CS, Gardner GR, Hedrick RP, Stephenson MD, Cawthorn RJ, Upton SJ. *Pseudoklossia haliotis* sp. n. (Apicomplexa) from the kidney of California abalone, *Haliotis*spp. (Mollusca). *J. Invertebr. Pathol*. 1995;66:33-38.
4. World Health Organization. Chapter 2.4.8 *Infection with* Xenohaliotis californiensis In: Aquatic Animal Health Code. 2019:8-9.
5. World Health Organization. Chapter 2.4.8 *Infection with* Xenohaliotis californiensis In: Aquatic Animal Health Code. 2019:2-3.

CASE III:

Signalment:
Juvenile, male Harbour porpoise, cetacean (*Phocoena phocoena*)

History:
This animal was found dead on the beach.

Gross Pathology:
There was white frothy material in the trachea which extended to just proximal to the tracheal bifurcation (mild to moderate pulmonary oedema). There was a moderate amount of white frothy material in the primary bronchi (pulmonary oedema). There were myriad, large (approx. 6 cm long and 1 mm diameter) nematodes within the primary, secondary and tertiary bronchi.

In the smaller bronchi the lumens were frequently filled with nematodes. The right lung was diffusely slightly darker red than the left (hypostasis). The left lung exhibited several parallel dark and light red stripes (rib imprints). Throughout the lung parenchyma, bilaterally, there were multiple firm foci ranging from 5 to 15 mm diameter, which were red to cream on cut surface, and sometimes contained nematodes (severe verminous pneumonia). Other lesions included: gastritis, multifocal, subacute, moderate, with intralesional nematodes and mucosal ulceration; inner ear, nematodiasis, bilateral, subacute, moderate to severe; abdominal cavity, haemoperitoneum, acute, diffuse, mild to moderate; mesenteric lymph nodes, lymphadenomegaly, diffuse, subacute, moderate; skin, abrasion, multifocal, acute, mild to moderate; liver, scar, multifocal, chronic, minimal.

Figure 3-1. Lung, porpoise. Secondary bronchi contain numerous nematodes. (Photo courtesy of: The University of Liverpool, https://www.liverpool.ac.uk/veterinary-science/)

Figure 3-2. Lung, porpoise. Pulmonary froth has washed several nematodes up into the proximal trachea. (Photo courtesy of: The University of Liverpool)

Laboratory Results:
Lung: Light growth of *Salmonella* spp. obtained from cultures.

Microscopic Description:
Two sections of lung: Multiple secondary and tertiary bronchi contain multiple intraluminal 1 mm diameter nematodes characterised by the presence of a 15 µm thick cuticle, coelomyarian musculature, and lateral cords. Bronchi also contain immature individuals and embryonated eggs, as well as degenerated sloughed epithelial cells and extravasated erythrocytes (haemorrhage). There is moderate diffuse infiltration of eosinophils and fewer lymphocytes, plasma cells and macrophages in the epithelium and lamina propria of the affected bronchi.

Approximately 50% of the section examined is effaced by multifocal to coalescing accumulations of a dense light eosinophilic material surrounded by elongated cells (fibroblasts), foreign body type multinucleated giant cells (up to 20 nuclei) and epithelioid macrophages (granulomas). These areas occasionally contain a moderate to large amount of eosinophilic to basophilic angular to crystalline material (mineralization).

Multifocally, bronchioles and alveoli are filled with a moderate to large amount of necrotic cellular debris, a moderate number of eosinophils, macrophages with foamy cytoplasm, lymphocytes, light eosinophilic amorphous material (oedema), light eosinophilic fibrillary material (fibrin) and, occasionally, 0.5 um maximum length extracellular basophilic coccobacilli. These areas are often associated with the presence of thin-walled cysts (up to 1.5 mm diameter) within the parenchyma, which contain multiple small (200 µm diameter) nematodes in both transverse and longitudinal section. These nematodes have a 5-10 µm cuticle with coelomyarian musculature, and lateral cords. The coelom contains an intestinal tract and reproductive tract with larvae. There is also a mixed inflammatory infiltration on the alveolar wall, composed of eosinophils, lymphocytes and plasma cells and multifocal areas of dark basophilic angular to crystalline material (mineralisation).

Pulmonary arteries show marked smooth muscle hyperplasia with reduction of the arterial lumen. Alveolar capillaries show proliferation and congestion. There are also areas of atelectasis and alveolar distension with rupture of alveolar wall (emphysema).

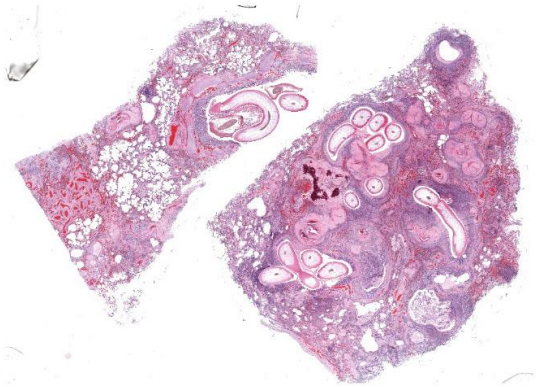

Figure 3-3. Lung, porpoise. At subgross magnification, numerous nematodes can be seen within airways. The alveolar parenchyma is largely effaced by fibrosis and inflammation. (HE, 5X)

Contributor's Morphologic Diagnosis:
Lung: Bronchopneumonia, granulomatous and eosinophilic, multifocal, chronic, severe, with intralesional nematodes, fibrosis and mineralisation.

Contributor's Comment:
The histological features represent a case of granulomatous and eosinophilic bronchopneumonia associated with lungworms in a harbor porpoise. In the present case, *Salmonella enterica* Group B has also been isolated from the pulmonary lesions and is likely to be a clinically significant finding.

Lungworms are a common finding in wild cetaceans, with species of nematodes reported in up to 69% of stranded Harbour porpoises (*Phocoena phocoena*), all from the family *Pseudaliidae*.[6,7] *Pseudalius inflexus* and *Torynurus convolutus* are found in the bronchi, bronchioles and blood vessels, whereas *Halocercus invaginatus* inhabits the pulmonary parenchyma.[2,9]

Verminous pneumonia is a common finding although is not frequently thought to be the primary cause of death. However, there can be severe changes, resulting in extensive fibrosis and mineralisation, as seen in this case. There is evidence that increased parasitic burden is associated with high levels of pollutants (polychlorinated biphenyls) which are associated with immunosuppression.[3] In addition, some studies suggest that lungworms may act as a potential means of transfer of bacterial infections in harbour porpoise, with *Salmonella enterica* Group B, as cultured in the current case, identified as potentially spread in this way.[4-6] The case presented here reinforces the theory that parasites should be considered as potential vectors of zoonotic bacterial infections in marine mammals.

Contributing Institution:
The University of Liverpool
https://www.liverpool.ac.uk/veterinary-science/

JPC Diagnosis:
1. Lung: Bronchopneumonia, eosinophilic, multifocal, with intrabronchial metastrongyle nematodes.
2. Lung: Pneumonia, interstitial, eosinophilic, multifocal, chronic, severe, with intraparenchymal adult metastrongyle nematodes.
3. Lung: Pneumonia, interstitial, eosinophilic, multifocal severe, with intraparenchymal nematodes.

JPC Comment:
This case provides an excellent example of lungworm parasitism in a harbour porpoise, a marine species found in the North Atlantic Ocean that typically bears a heavy pulmonary parasite burden.[3] Studies of the harbour porpoise have found that parasites are most common in the respiratory system, and lungworms have been found in virtually all harbour porpoises older than 1 year, most often in the bronchial tree and the pulmonary blood vessels.[9] As in this case, parasites within the pulmonary parenchyma typically incite an eosinophilic and granulomatous bronchointerstitial pneumonia. When found in the pulmonary blood vessels, nematodes can cause chronic thrombosis and vasculitis, often with calcification of thrombotic material.[9]

In general, far less is known about the biology of pulmonary parasites of marine mammals compared to their terrestrial counterparts; however, two of the nematodes examined here belong to the metastrongyle family which, collectively, are far less mysterious. Metastrongyles, or "lungworms," have coelomyarian musculature, an external cuticle that is typically smooth, an intestine lined by few multinucleated cells, and accessory hypodermal cords. Mature females can produce either eggs or fully developed embryos;

species that produce eggs deposit them into host tissues where they embryonate.[10] Other notable metastrongyles of veterinary importance include *Angiostrongylus cantonensis* (rat), *Dictyocaulus viviparus* (ruminants), *Muellerius capillaris* (small ruminants), *Metastrongylus apri* (pigs), *Aelurostrongylus abstrusus* (cats), and *Filaroides hirthi* (dogs).

This case incited robust discussion among conference participants. Participants identified three different nematode species in section: the large nematodes within the airways and two, much smaller nematode species within the parenchyma. Some participants remarked that many areas identified initially as granulomas could represent foci of severe vasculitis, possibly secondary to intravascular lungworms. Of the three nematodes identified in section, participants felt that the smallest of the three, which were approximately 60um in diameter, had features consistent with filarid parasites, which could account for the possible vasculitis. Post-conference consultation with Dr. Christopher Gardiner confirmed that these nematodes are consistent with filarid nematodes, though we were unable to speciate them with the minimal features present in section.

The two largest nematodes in section are metastronglyes and contain very nice examples of the classic metastrongyle morphologic features described above. The largest nematodes are over 1mm in diameter and are morphologically consistent with *Pseudalius inflexus*; however, the lack of gonads within the examined section did not allow for definitive speciation. Interestingly, there are reports of *Pseudalius inflexus* causing similar lesions in Burmeister's porpoises; those cases were accompanied by vasculitis and thrombosed arteries with a morphologic appearance similar to many of the presumptive occlusive vascular changes in this section.[1]

Finally, the mid-sized nematode population, with a diameter of approximately 225um, contain classic metastrongyle features and female gonads contain developing larvae (see Figure 3-8). Similar to the previously discussed nematodes, we were unable to speciate these metastrongyles, though the species discussed by the contributor appear to be the most common causes of marine mammal pulmonary nematodiasis.

Conference participants debated combining the morphologic diagnoses or creating separate diagnoses based on etiology. As the three different nematodes each had different pathologic effects, participants preferred separate morphologic diagnoses. And while participants felt strongly that a significant vasculitis was evident in the examined section, vasculitis was not included in the diagnosis due to the inability to confirm vasculitis with immunohistochemical stains on this entirely digital submission.

References:

1. Alvarado-Rybak M, Toro F, Abarca P, Paredes E, Espanol-Jimenez S, Seguel M. Pathological findings in cetaceans sporadically stranded along the Chilean coast. *Front Mar Sci*. 2020;7.
2. Balbuena JA, Aspholm PE, Andersen KI, Bjorge A. Lung-worms (Nematoda: Pseudaliidae) of harbour porpoises (Phocoena phocoena) in Norwegian waters: patterns of colonization. *Parasitology*. 1994;108:343-349.
3. Bull JC, Jepson PD, Sauna RK, et al. The relationship between polychlorinated biphenyls in blubber and levels of nematode infestations in harbour porpoises, Phocoena phocoena. *Parasitology*. 2006; 132**:**565-573.
4. Davison N, Barnett J, Rule B, Chappell S, Wise G. Group B *Salmonella* in lungworms from a harbour porpoise (Phocoena phocoena). *Vet Rec*. 2010; 167**:**351-352.

5. Davison NJ, Simpson VR, Chappell S, et al. Prevalence of a host-adapted group B Salmonella enterica in harbour porpoises (Phocoena phocoena) from the south-west coast of England. *Vet Rec*. 2010; 167**:** 173-176.
6. Foster G, Patterson IA, Munro DS. Monophasic group B Salmonella species infecting harbour porpoises (Phocoena phocoena) inhabiting Scottish coastal waters. *Vet Microbiol*. 1999;65**:** 227-231.
7. Jepson PD, Baker JR, Kuiken T, Simpson VR, Kennedy S, Bennett PM. Pulmonary pathology of harbour porpoises (Phocoena phocoena) stranded in England and Wales between 1990 and 1996. *Vet Rec*. 2000;146**:**721-728.
8. Reckendorf A, Everaarts E, Bunskoek P, et al. Lungworm infections in harbour porpoises (Phocoena phocoena) in the German Wadden Sea between 2006 and 2018, and serodiagnostic tests. *Int J Parasitol Parasites Wildl*. 2021;14**:** 53-61.
9. Siebert U, Wunschmann A, Weiss R, Frank H, Benke H, Frese K. Post-mortem findings in harbour porpoises (Phocoena phocoena) from the German North and Baltic Seas. *J Comp Pathol*. 2001;124**:** 102-114.
10. Gardiner CH, Poynton SL. *An Atlas of Metozoan Parasites in Animal Tissues*. Armed Forces Institute of Patholoy;2006.

Figure 4-1. Liver, bald eagle. The liver was markedly enlarged (weighing 149g) and discolored brown to green with numerous pinpoint, beige, poorly-defined foci. (*Photo courtesy of:* Veterinary Diagnostic Laboratory, University of Minnesota, St Paul, MN. https://vdl.umn.edu/)

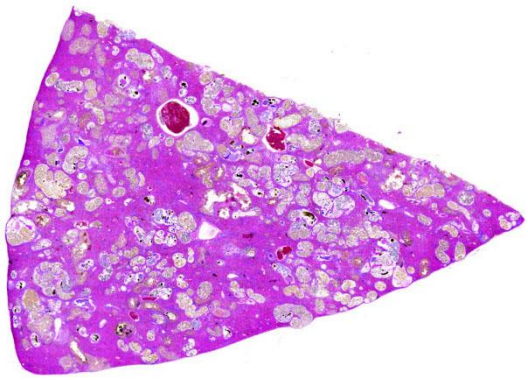

Figure 4-2. Liver, bald eagle. One section of liver is submitted for examination. At subgross magnification, numerous areas of pallor are scattered throughout the section. (HE, 6X)

CASE IV:

Signalment:
Hatch-year, female bald eagle, avian (*Haliaeetus leucocephalus)*

History:
The animal was emaciated. It was euthanized at admission to the wildlife clinic with suspected West Nile disease (neurologic signs and eye lesions consistent with chorioretinitis) and liver enlargement.

Gross Pathology:
The liver was markedly enlarged (weighing 149g) and discolored brown to green with numerous pinpoint, beige, poorly defined foci. Numerous fragile thin-walled parasites (flukes) less than 5.0 mm long were embedded in the liver.

Laboratory Results:
A liver sample tested positive for *Erschoviorchis* sp. by PCR and sequencing.

Microscopic Description:
Approximately 75% of the liver section is infiltrated by myriad metazoan parasites that have a thin, smooth tegument, a variably discernible ventral sucker, and numerous

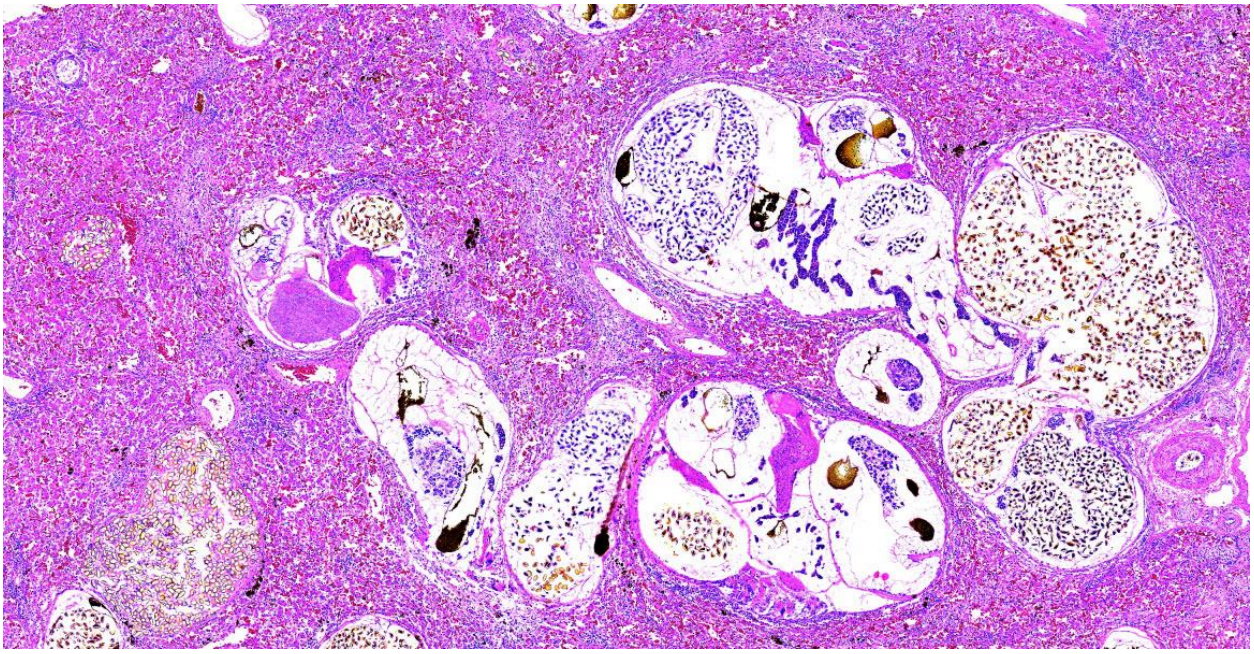

Figure 4-3. Liver, bald eagle. Numerous flukes are embedded within the hepatic parenchyma. (HE, 46X)

intraparenchymal, golden, operculated eggs that are approximately 25.0 x 12.0 µm (morphologically consistent with adult trematodes).

Hepatic cords are often dissociated, and sinusoids are frequently expanded by either brown to black fluke pigment, ova, fibrin, and/or numerous lymphocytes, heterophils, and macrophages, including multinucleated cells. Small numbers of lymphocytes, macrophages, and heterophils frequently surround trematodes and occasionally form small granulomas that are centered on areas of lytic necrosis.

Contributor's Morphologic Diagnosis:
Liver: Granulomatous hepatitis, multifocal to coalescing, moderate, chronic with numerous intraparenchymal adult trematodes.

Contributor's Comment:
Hepatic trematodosis is a sporadically reported disease in raptors, with a predominance for species in the *Opisthorchiidae* family. *Opisthorchis* sp., *Metorchis bilis*, and *Amphimerus elongatus* are all members of the *Opisthorchiidae* family and have been implicated in the previous cases of hepatic trematodosis of eagles. However, recently, a fluke of the genus *Erschoviorchis* has been reported to cause severe liver infections in bald eagles in the upper Midwest of the United States.[3,5] Until recently, the only species within this genus was *E. lintoni*, which infects the pancreas of the common loon (*Gavia immer*) in North America.[1] *E. anuiensis*, the other species within this genus, was described from experimental infections of Muscovy ducks using metacercaria recovered from fish from the Amur River basin in the Russian Far East.[4] Whether the *Erschoviorchis* sp. affecting the bald eagles was newly introduced to the United States or has long been established in North America and possibly confused with *Amphimerus elongatus* remains unknown.

Erschoviorchis flukes are notoriously difficult to tease out from the affected tissue due to their fragile nature. As a result, the parasitological features described in this case are

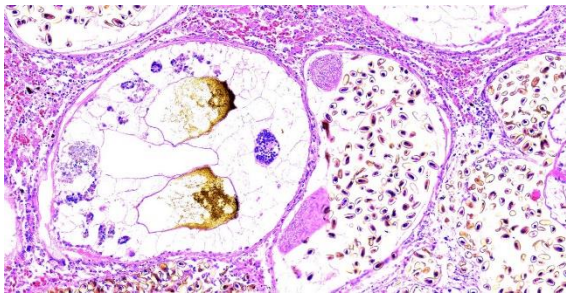

Figure 4-4. Liver, bald eagle. Cross sections of multiple trematodes demonstrate key characteristic diagnostic features for trematodes (it is difficult to find a single trematode that has all of them in section). Key characteristic features are a spongy body cavity, paired ceca (brown due to the presence of hematin), scattered vitellarian glands (on fluke at left), two cross sections of one or more suckers, and cross sections of a uterus with eggs. (HE, 46)

based on fluke fragments. Recovering complete flukes would be necessary to assign a new species denomination.

The life cycle of opisthorchiid flukes includes two intermediate hosts, typically a snail and a fish as the first and second host, respectively. Adult trematodes release eggs that are passed in the feces. The first intermediate host, a gastropod snail, ingests the eggs, which then release miracidia. These miracidia undergo several stages of development within the snail: sporocyst→rediae→cercariae. Cercariae are released from the snail and encyst in the skin or muscle of freshwater fish, the second intermediate host, to become metacercariae. The definitive host becomes infected by ingesting the raw, metacercariae-laden fish. Metacercariae generally excyst within the upper gastrointestinal tract of the definitive host and ascend to the biliary ducts where they develop into adults.[2] The exact life cycle of this *Erschoviorchis* sp. is uncertain, but likely is similar to that of other opisthorchiid flukes.

Although *E. anuiensis* appears to be highly pathogenic based on experimental infections, the clinical significance of massive hepatic trematodosis in this case remains uncertain since West Nile virus infection was considered to be the more important disease problem. Co-infections of bald eagles with *Erschoviorchis* sp. liver flukes with West Nile virus appear to be common.[3]

Contributing Institution:
Veterinary Diagnostic Laboratory
University of Minnesota, St Paul, MN
https://vdl.umn.edu/

JPC Diagnosis:
Liver: "Extrematodiasis". 😊

JPC Comment:
The contributor provides an excellent summary of *Erschioviorchis* sp. parasitism and the discovery of a potentially new pathogen of bald eagles in the upper Midwest of the United States.

In general, trematodes can be identified histologically by the following key histologic features: an oral sucker, paired ceca, no body cavity, spongy parenchyma, vitelline (yolk-forming) glands, hermaphroditism, and, with few exceptions, the presence of operculated eggs. Some common trematodes of veterinary importance include *Fasciola hepatica* in

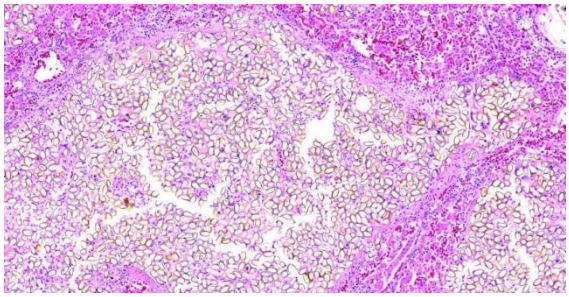

Figure 4-5. Liver, bald eagle. Aggregates of free eggs are present in the hepatic parenchyma. (HE, 137X)

the bile ducts and gallbladder of ruminants, *Fascioloides magna* in the liver of certain wild ruminants, *Paragonimus kellicotti* in the lungs of dogs and cats, and *Heterobilharzia americanum* in dogs and some wildlife.

Conference discussion focused largely on the stunning appearance of the examined section, with eggs and adult trematodes in seemingly every micrometer of the tissue. Participants struggled to characterize the severity of the parasitism in this section, with "massive" and "extreme" being popular modifiers. Participants settled on a morph of "Liver: Trematodiasis, multifocal, extreme, with moderate, multifocal necrosis and granulomatous inflammation." Disappointment was palpable in the room, however, as many felt that this rather quotidian diagnosis failed to capture the full glory of this gorgeous histologic specimen. Our cheeky JPC diagnosis was suggested by an eagle-eyed resident with a love of puns, and, once suggested, "Extrematodiasis" quickly soared to the top. We shall return to normal professional standards next week (perhaps); in the meanwhile, the contributor provides an excellent morphologic diagnosis, as do we, buried midway through the paragraph above.

References:

1. Gower WC. A new trematode from the loon, *Gavia immer*, and its relationship to *Haematotrephus fodiens* Linton, 1928. *Proc US National Museum* 1939;87:139–143.
2. King S, Scholz T. Trematodes of the family *Opisthorchiidae*: a minireview. *Korean J Parasitol* 2001;39:209–221.
3. McDermott KA, Greenwood SJ, Conboy GA, Franzen-Klein DM, Wünschmann A. Massive hepatic trematodosis in 5 juvenile bald eagles. *J Vet Diagn Invest*. 2023;35(4):409-412.
4. Tatonova YV, Besprozvannykh VV, Katugina LO, Solodovnik DA, Nguyen HM. Morphological and molecular data for highly pathogenic avian parasite *Erschoviorchis anuiensis* sp. n. and phylogenetic relationships within the *Opisthorchiidae* (*Trematoda*). *Parasitol Int* 2020; 75:102055.
5. Wünschmann A, Armien AG, Hoefle U, Kinne J, Lowenstine LJ, Shivaprasad HL. Birds of Prey. In: Terio KA, McAloose D, St. Leger J, eds. *Pathology of Wildlife and Zoo Animals*. Elsevier;2018:738.

WSC 2023-2024
Conference 10 Self-Assessment

1. Which of the following is NOT a common mycobacterial species seen in fish?
    a. M. cheloniae
    b. M. fortuitum
    c. M. piscihominis
    d. M. marinum

2. “Abalone withering syndrome” is which type of infection?
    a. Fungal
    b. Bacterial
    c. Protozoal
    d. Viral

3. True or false? Lungworm infections are a common cause of mortality of cetaceans.
    a. True
    b. False

4. The first intermediate of opisthorchiid flukes is a?
    a. Copepod
    b. Fish
    c. Snail
    d. Beetle

5. The first intermediate of opisthorchiid flukes is a?
    a. Copepod
    b. Fish
    c. Snail
    d. Beetle

WEDNESDAY SLIDE CONFERENCE 2023-2024

Conference #11 **29 November 2023**

CASE I:

Signalment:
20-month-old female spayed Domestic Shorthair cat, feline (*Felis catus*)

History:
Sudden death with no previously identified clinical signs. The submitting veterinarian suggested congestive heart failure, feline infectious peritonitis, or toxin exposure as possible differentials.

Gross Pathology:
The subcutaneous and internal fat stores were mildly icteric. The liver was small and diffusely orange to brown with multifocal, slightly raised yellow nodules on the hepatic surface and throughout the parenchyma on cut section. An impression smear of the liver showed frequent spindle cells suggestive of fibroblasts or oval cells, and cells with multiple small, clear cytoplasmic vacuoles suggestive of hepatic lipidosis.

Laboratory Results:
A sample of fresh liver was submitted for mass spectrometry. A copper level of 611.2 ppm on a wet matter basis was found (normal <45ppm), which is equivalent to 2139.2 ppm on a dry matter basis.

Microscopic Description:
Liver: There are large coalescing areas of degeneration and necrosis of hepatocytes affecting all zones (massive pattern)

Figure 1-1. Liver, cat. The liver was small and diffusely orange to brown with multifocal, slightly raised yellow nodules on the hepatic surface. (*Photo courtesy of:* Western College of Veterinary Medicine, University of Saskatchewan, 52 Campus Dr, Saskatoon, SK, Canada, S7N 5B4, https://wcvm.usask.ca/departments/vet-pathology.php)

interspersed with randomly distributed, well-delimited nodules of viable hepatocytes. Portal areas and periacinar regions are close to each other (parenchymal collapse, loss of hepatocytes). Hepatocytes show marked distension of cytoplasm by small to large vacuoles (microvesicular to macrovesicular steatosis, positive Oil-red-O staining), ill-defined borders, granular eosinophilic cytoplasm, a prominent nucleus characterized by pyknosis, karyorrhexis or karyolysis. Endothelial cells are often plump (reactive) and there are reactive spindle cells (perisinusoidal cells), free pyknotic debris, and ill-defined ducts (oval cell hyperplasia). Large numbers of Kupffer cells with pale brown granules and

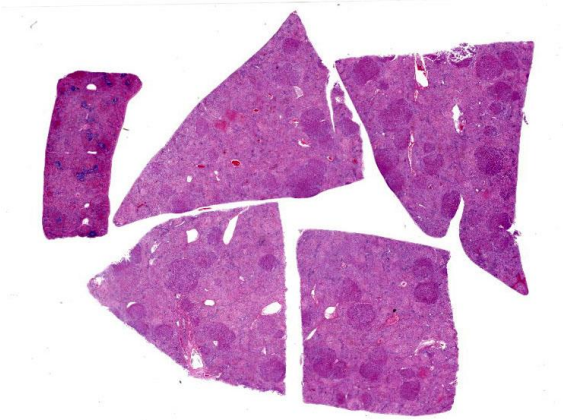

Figure 1-2. Liver, cat. Four sections of liver and one section of spleen are submitted. At subgross magnification, areas of pallor and few regenerative nodules are evident. (HE, 5X)

rare red blood cells are present and similar pigment is seen in few hepatocytes.

The nodules consist of thick, disorganized hepatic plates, large hepatocytes with fine cytoplasmic vacuolation (fat, positive Oil-red-O staining), and one to two prominent nuclei. Bile canaliculi are distended by bile plugs and Kupffer cells contain large amounts of pale brown pigment (nodular regeneration). Portal areas are infiltrated by small numbers of plasma cells and lymphocytes, small amounts of collagen, and there is bile duct and oval cell hyperplasia with extension and destruction of the limiting plate. There is multifocal bridging portal-to-portal fibrosis. Terminal hepatic venules are difficult to discern. Sublobular veins are often infiltrated by small numbers of plasma cells and fat-laden macrophages. There are few foci of extramedullary hematopoiesis.

Special stains: There are large numbers of copper granules with rhodanine stain in macrophages and to a lesser degree in hepatocytes in areas of necrosis. There is a very small amount of copper in areas of regeneration. This is accompanied by large number of positive granules on Schmorl's stain (lipofuscin) and there is a moderate amount of hemosiderin in macrophages on Perl's stain. There is mild collapse and mild to moderate thickening of reticulin fibers in periacinar regions. These areas correspond to deposition of collagen with Masson's trichrome stain. There is a small amount of collagen in periportal parenchyma.

Contributor's Morphologic Diagnoses:
Liver: Hepatic fatty degeneration and necrosis, acute to subacute, with bile duct hyperplasia, fibrosis, nodular regeneration.

Contributor's Comment:
Primary copper toxicity has been well-described in dogs and humans; however, it is poorly described in cats.[3] The most well-known primary copper toxicity of animals occurs in Bedlington terriers, which has an autosomal recessive inheritance pattern that may be linked to a deletion in the *COMMD1* genes.[1] Similarly, Wilson's disease in humans is an autosomal recessive disorder that affects the *ATP7B* gene, which affects secretion of copper.[1] Both genes are used in copper secretion into the blood and bile.[2] Without proper copper secretion, copper accumulates in hepatocytes, leading to increased cellular oxidative stress that quickly uses up intracellular glutathione.[2] Ultimately, oxidative stress leads to hepatocyte necrosis.[2]

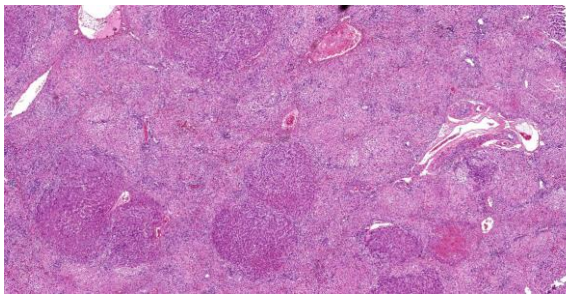

Figure 1-3. Liver, cat. Regenerative nodules are evident in areas of hepatocellular degeneration and necrosis. (HE, 30X)

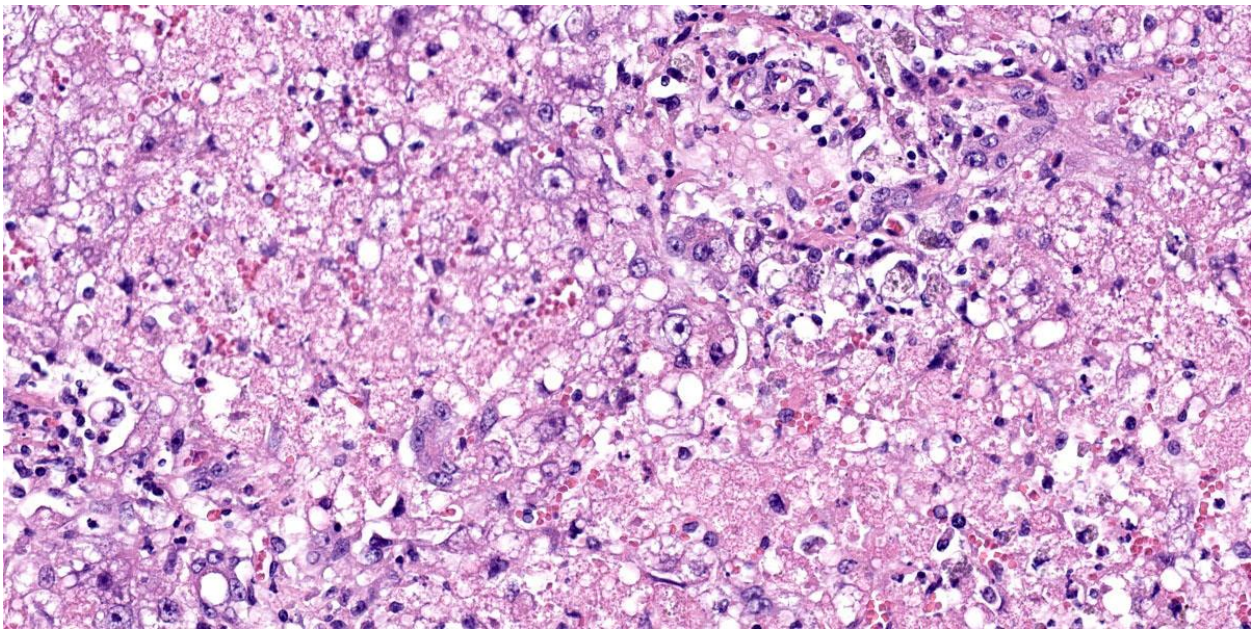

Figure 1-4. Liver, cat. There are large areas of hepatocellular degeneration and necrosis with infiltration of small numbers of neutrophils. (HE, 340X)

Previous reports in cats have been infrequent, but are often diagnosed based on being young, having histological findings consistent with copper toxicity, and no history of excessive copper intake.[1,4,5] Reported histological findings in these reports include regenerative nodules, hepatic fibrosis, and hepatocytes containing brown granules that stain positively on rhodanine stain.[1,5] These hepatocytes were most frequently found in the centrilobular areas.[1,5] Similar rhodanine-positive granules were identified in the kidney and lung.[4] These findings are similar to copper toxicity in dogs.[1,5] In a study examining 104 feline liver biopsies, only 5 cases were identified with centrilobular copper.[7] A similar study examining liver samples from 100 cases of hepatic disease in cats found 11 presumed cases of primary copper toxicity.[5] Both of these studies suggest that primary copper toxicity is very rare.[5,7]

To date, the causative gene and potential inheritance pattern of primary copper toxicity in cats is unknown. One reported case of two sibling cats with primary copper toxicity showed two single-nucleotide variations in the *ATP7B* gene, the same gene affected in humans.[1] A subsequent study identified single-nucleotide variations in *ATP7B* in three of four cats examined, suggesting this is the most likely cause of primary copper toxicity in cats.[2]

Contributing Institution:
Western College of Veterinary Medicine
University of Saskatchewan
Saskatoon, SK Canada S7N 5B4
https://wcvm.usask.ca/departments/vet-pathology.php

JPC Diagnosis:
1. Liver: Hepatocellular degeneration and necrosis, massive, with marked hepatocellular lipidosis.
2. Liver: Nodular hepatocellular regeneration, multifocal, moderate with mild biliary hyperplasia.

JPC Comment:
Copper is an essential heavy metal that is required for the proper function of a wide variety of enzymes, including the cytochrome

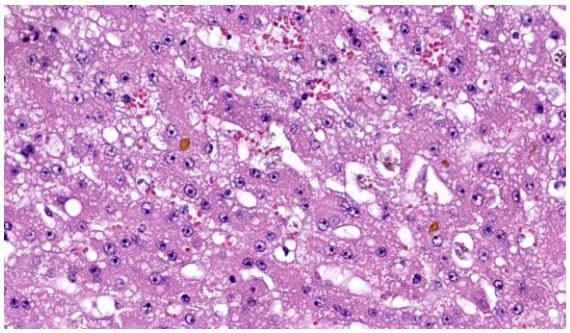

Figure 1-5. Liver, cat. Remaining hepatocytes contain abundant lipid vacuoles and there is cholestasis. (HE, 340X)

oxidases (mitochondrial respiration), lysyl oxidase (collagen synthesis), tyrosinase (melanin synthesis), ceruloplasmin (iron synthesis), and antioxidant defense (superoxide dismutase).[3] In excess, the multiple redox states of copper can lead to free radical production and oxidative damage to cellular components, and animals have responded to this threat by developing regulatory mechanisms to ensure excess copper is rendered inert and excreted.

Copper metabolism begins in the gut, where dietary copper is actively transported across the mucosal surface of small intestinal enterocytes. This function is performed by a specific copper transporter, Ctr1, and by the nonspecific transporter, divalent metal transporter (DMT1), which also transports several trace elements (e.g., iron and zinc) with which copper competes for transport. Once in the enterocyte, copper is incorporated into enzymes or, if in excess, bound to metallothionein and stored in lysosomes to protect the cell from free copper.[6] Once metallothionein is saturated, copper is excreted into the blood, where it is bound to the carrier proteins ceruloplasmin and transcuprein, or to albumin, and transported to the liver via the portal blood.[6]

Copper enters the hepatocyte via the same Ctr1 transporter found in the enterocytes. Once in the hepatocyte cytoplasm, chaperone proteins send copper to mitochondria and to the Golgi body, where copper is transported into the Golgi by the transporter ATP7B. ATP7B directs the incorporation of copper into ceruloplasmin for return to the systemic circulation and distribution to other tissues.[6] If the ceruloplasmin/copper complex returns to the liver, it is taken up into hepatocytes and secreted into bile for excretion. If copper accumulates in excess of metabolic requirements within the hepatocytes, it is complexed with metallothionein or glutathione and stored within lysosomes as in enterocytes.[6]

Perturbations in any of the above processes, such as a primary metabolic defects in hepatic copper metabolism, altered hepatic biliary excretion of copper, or excess dietary copper intake, can result in hepatic copper toxicosis.[3] Species susceptibility to copper toxicosis varies widely, with sheep being most prone to copper poisoning due to a lack of sufficient capacity to excrete copper into the bile and to a very small copper metallothionein binding capacity.[3] When faced with a sudden dietary excess, biliary excretion can't keep up with the influx of copper, leading to very high levels of copper deposition within the liver. When the binding capacity of metallothionein is exceeded, a sudden, generally fatal intravascular hemolytic crises can occur.[3,6]

The contributor provides an excellent survey of the few cases of feline copper toxicity reported in the veterinary literature which, for all their rarity, present with familiar histologic features: severe fibrosis, regenerative nodules, and excessive intracytoplasmic copper as evidenced by rhodanine staining. Copper toxicity does not, however, typically present with abundant hepatic necrosis, and the significant necrosis in the examined section provoked robust discussion before, during, and after this week's conference.

The moderator of today's conference was Dr. Anna Travis, Chief of Education Operations at the Joint Pathology Center, who began discussion of this case with a review of copper metabolism, as summarized above, and a review of the typical histologic changes associated with copper toxicity. Conference participants noted the small amount of fibrosis evident on Masson trichrome stain, which was surprising given the significant number of regenerative nodules.

Conference participants also noted the abundant, multifocal to coalescing hepatic necrosis, which for many was the predominate histologic feature of this case. The abundant necrosis also hampered qualitative evaluation of the rhodanine staining, which, in the remaining intact hepatocytes, appeared sparse in relation to the incredibly high copper levels measured in this patient. While participants agreed that the amount of rhodanine staining was abnormal, many felt that the amount of staining was not consistent with the dry weight of copper value obtained in the lab results. Finally, the participants felt that a second, acute insult resulted in widespread necrosis which may have obscured a more traditional pattern of feline copper toxicity.

This case was sent for post-conference consult with Dr. John Cullen, Distinguished Professor at the North Carolina State University College of Veterinary Medicine. Dr. Cullen agreed that the histologic picture in this case is not a perfect match for copper toxicity as a sole insult. Copper accumulation in reported feline cases is typically centrilobular and has a substantial inflammatory component, neither of which is apparent in this case.

Though a tidy resolution for this case remains elusive based on a complex interplay of acute and chronic pathogeneses, conference participants continue to believe that the primary

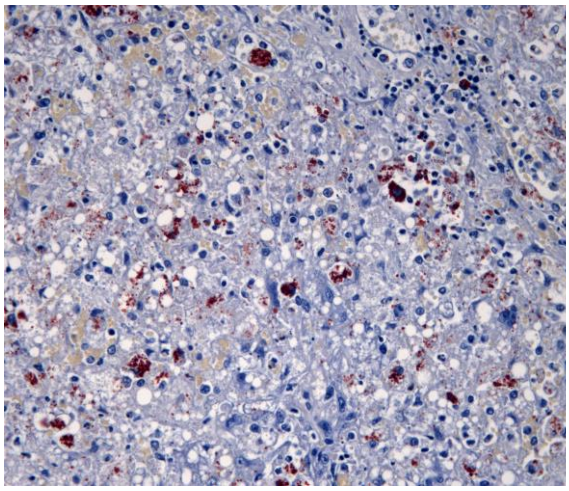

Figure 1-6. Liver, cat. There are small to moderate amounts of copper, but only in macrophages. (Rhodanine, 200X)

lesion in this case is an acute, necrotizing insult, the cause of which is not apparent. The excessively high copper dry weight almost certainly contributed to the observed pathology in this case; however, the substantial acute necrosis is confounding, and participants preferred to separate the morphologic diagnoses into acute and chronic effects to emphasize the presumed dual pathologic processes in this fascinating case.

Getting short shrift this week was the forlorn section of spleen, located literally and figuratively on the periphery and characterized by mild to moderate chronic diffuse congestion with hemosiderin-laden macrophages.

References:

1. Asada H, Kojima M, Nagahara T, et al. Hepatic copper accumulation in a young cat with familial variations in the *ATP7B* gene. *J Vet Intern Med*. 2019;33:874–878.
2. Asada H, Chambers JK, Kojima M, et al. Variations in ATP7B in cats with primary copper-associated hepatopathy. *J Feline Med Surg*. 2020;22:753-759.
3. Cullen JM, Stalker MJ. Liver and Biliary System. In: Maxie GM, ed. Vol. 2, *Jubb*,

Kennedy, and Palmer's Pathology of Domestic Animals. Elsevier, Inc;2016: 302, 342-343.
4. Haynes JS, Wade PR. Hepatopathy associated with excessive hepatic copper in a Siamese cat. *Vet Pathol*. 1995; 32:427–429.
5. Hurwitz BM, Center SA, Randolph JF, et al. Presumed primary and secondary hepatic copper accumulation in cats. *J Am Vet Med Assoc*. 2014;244:68–77.
6. Lopez-Alonso M, Miranda M. Copper supplementation in cattle: a challenge. *Animals (Basel)*. 2020;10(10):1890.
7. Whittemore JC, Newkirk KM, Reel DM, et al. Hepatic copper and iron accumulation and histologic findings in 104 feline liver biopsies. *J Vet Diagn Invest*. 2012; 24:656–661.

CASE II:

Signalment:
17-year-old, male, intact, Pacific pond turtle (*Actinemys marmorata pallida*)

History:
A wild-hatched turtle housed at the zoological institution had a history of severe chronic pitting and ulcerated lesions on the shell for over a year. Recently, it had a rapid clinical decline with anorexia and obtunded mentation. Given the poor prognosis, humane euthanasia was elected.

Laboratory Results:
Panfungal (ITS3-ITS-4) PCR assay on frozen shell yielded a 203 base pair fragment with 100% identity and 100% query cover age to MG780506, *Emydomyces* sp. isolate 13-1796.

Microscopic Description:
Head, dorsal: Extending from a focal ulcer on the skin surface and through the dermis to efface 60% of the dorsal calvarium, expand the meninges, and invade into the brain, as well as extending ventrally along the lateral aspect of the skull, are numerous coalescing epithelial inclusion cysts containing fungal hyphae. The epithelial inclusion cysts are lined by keratinized squamous epithelium and contain lamellated keratin, necrotic debris, entrapped necrotic bony fragments, fungal hyphae, and mixed bacteria. The fungal hyphae are 1 to 4 µm in diameter, regularly septated, and have acute to right-angle branching. The effaced bone has empty lacunae with loss of osteocytes (osteonecrosis), with moth-eaten margins and osteoclasts in Howship's lacunae (osteolysis).

Figure 2-1. Presentation, Pacific pond turtle: Multifocal coalescing ulcers and depressions are present along the midline of the carapace, as well as on the plastron, where there is occasional bone exposure. (*Photo courtesy of:* Disease Investigations, Institute for Conservation Research, San Diego Zoo Wildlife Alliance, http://institute.sandiegozoo.org/disease-investigations)

Figure 2-2. Dorsal aspect of the head, Pacific pond turtle. The skin has a focal brown crusty depression on the dorsal aspect (arrowhead). (*Photo courtesy of:* Disease Investigations, Institute for Conservation Research, San Diego Zoo Wildlife Alliance)

The affected meninges are also expanded by increased fibrous tissue. In this area, the epithelial inclusion cysts penetrate into the brain parenchyma and are associated with moderate heterophilic and histiocytic inflammation, necrotic debris, and rarefaction of the neuropil. In other sections, fungal invasion disrupts the ependymal lining of the ventricle. Variable numbers of heterophils, histiocytes, and lymphocytes are associated with the cysts and fungi throughout the section, but inflammation is most prominent in the skeletal muscle along the lateral aspect of the skull, where there are numerous, coalescing fungal heterophilic granulomas.

Contributor's Morphologic Diagnosis:
Multiple tissues, dorsal head: Severe, regionally extensive, chronic-active, necro-ulcerative heterophilic and granulomatous dermatitis, myositis, osteomyelitis, and meningoencephalitis with epithelial inclusion cysts, osteonecrosis and osteolysis, and intralesional fungal hyphae (consistent with *Emydomyces* sp., presumably *E. testavorans*).

Contributor's Comment:
Emydomyces testavorans, a newly described fungus, is strongly associated with 'ulcerative shell disease' or 'pond turtle shell disease' in free-ranging and captive aquatic turtles in North America.[2,4,5] The classical shell lesions associated with emydomycosis are ulcerations in the carapace and/or plastron with increased pliability. In some cases, the turtles have expansile nodular masses within the shell, displacing the coelomic membrane, distorting the shell contour, and compressing internal viscera.[4] The present case has an unusual presentation, in which the fungal infection affected the tissues of the head, in addition to the shell, and invades deeply into the brain causing meningoencephalitis with antemortem neurological signs.

Histologic features associated with *E. testavorans* infection include multilocular intradermal and intraosseous epithelial inclusion cysts, which are lined by keratinized stratified squamous epithelium and contain keratin debris and necrotic bone.[2,4] The cysts are also associated with squamous metaplasia, hyperkeratosis, osteonecrosis, and inflammation, all of which are consistent with the present case of the Pacific pond turtle in our collection.[4] Although *E. testavorans* is strongly as-

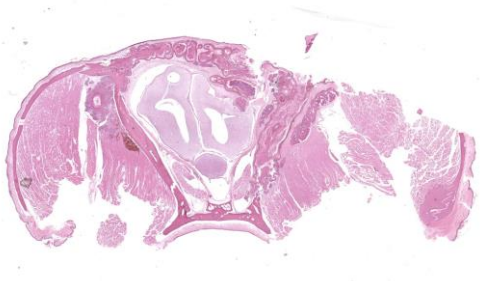

Figure 2-3. Head, Pacific pond turtle. A cross section of the head through the olfactory lobes of the brain is submitted for examination. There are numerous epithelial inclusion cysts within the dermis that extend downward to replace the bone of the calvarium and compress the underlying cerebrum. (HE, 5X)

Figure 2-4. Head, Pacific pond turtle. Epithelial inclusion cysts measure 2mm in diameter, often coalesce, and are lined by 4-5 layers of basally pigmented epithelium which undergoes gradual keratinization. The cyst lumina contain abundant lamellated keratin, fragments of necrotic bone, and brightly eosinophilic cellular debris. (HE, 69X)

sociated with ulcerative shell disease in freshwater aquatic chelonians, causation has not been proven through experimental infections.

Very little is known about the pathogenesis and lesion progression of emydomycosis, and it is unclear if it is a primary pathogen or if a combination of factors is required to elicit disease. Reported histologic features do not appear to be consistently pathognomonic for *E. testavorans* infection. Instead, they could be non-specific and indicative of a chronic healing process with cysts representing walling off of the damaged tissue or dyskeratosis.[4] Other differential diagnoses for ulcerative shell lesions in aquatic turtles include septicemic cutaneous ulcerative disease (SCUD), which is caused by a combination of trauma, bacterial infection, and poor water quality. Epithelial inclusion cysts have also been reported in one case of mycobacteriosis, with no evidence of concurrent fungal infection.[4]

Emydomyces testavorans is in the order Onygenales, along with other emerging pathogenic reptile keratinophilic fungi, such as *Ophidiomyces ophiodicola* and *Nannizziopsis guarroi*.[5] Presumably, like many fungi in this order, *E. testavorans* is also an environmental saprophyte.[5] *Emydomyces testavorans* was first reported in free-living turtles in California in 2020, but has been isolated from turtles in Illinois and Washington in samples from as early as 2016, suggesting a potentially broad geographic distribution.[2,5] As Pacific pond turtles are listed as a vulnerable species, there is some concern that this recently described and likely underdiagnosed disease could pose a significant threat to already at-risk populations.[1]

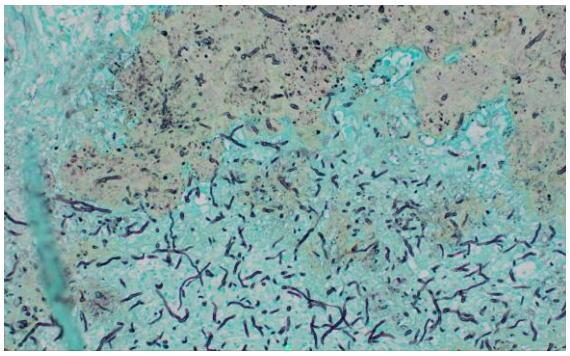

Figure 2-5. Head, Pacific pond turtle. A GMS stain on the inclusion cysts demonstrates numerous 2-4µm diameter, parallel-walled, dichotomously branching, septate fungal hyphae. (GMS, 200X)

Contributing Institution:
Disease Investigations
Institute for Conservation Research
San Diego Zoo Wildlife Alliance
PO Box 120551
San Diego, CA 92112
http://institute.sandiegozoo.org/disease-investigations

JPC Diagnosis:
Head: Epithelial inclusion cysts with osteonecrosis, granulomatous dermatitis, cellulitis, myositis, and meningitis, and fungal hyphae.

JPC Comment:
As the contributor notes, the key histologic features of emydomycosis are ulcerative dermatitis, necrotizing osteomyelitis, and inclusion cysts lined by keratinized stratified squamous epithelium containing keratin debris. Fungal hyphae that are thin-walled, regularly septate, and occasionally branched can be demonstrated with GMS or PAS staining, making for a relatively straightforward histologic diagnosis.[5] Grossly, however, the lesions of emydomycosis may be difficult to identify as they can be highly localized lesions and may lurk under the shell surface after the initial shell defect has healed over.[2] The contributor describes typical gross lesions in the excellent summary above, but gross lesions may also be rather subtle, and consist only of carapace flaking or bleaching.[2] In a recent study of affected pond turtles in Washington state, emydomycosis was diagnosed based on external exam in 25-50% of wild caught animals, but in greater than 80% of animals based on CT scans, which revealed the inclusion cysts and osteolytic lesions that characterize the disease.[2]

Emydomycosis presents similarly to its main differential diagnosis, septicemic cutaneous ulcerative disease (SCUD), which can cause ulcerated lesions on the plastron and carapace, petechial hemorrhage, emaciation, lethargy, and death.[3] SCUD is currently considered a multifactorial disease caused by poor water conditions and environmental stressors which predispose the animal to bacterial infection. SCUD was originally associated with *Citrobacter freundii* infection, but it is now understood that a variety of gram-negative organisms can cause the syndrome.

Conference discussion focused on reptilian dermatomycoses generally and on specific dermatologic disease of chelonids. In addition to SCUD and mycotic shell disease

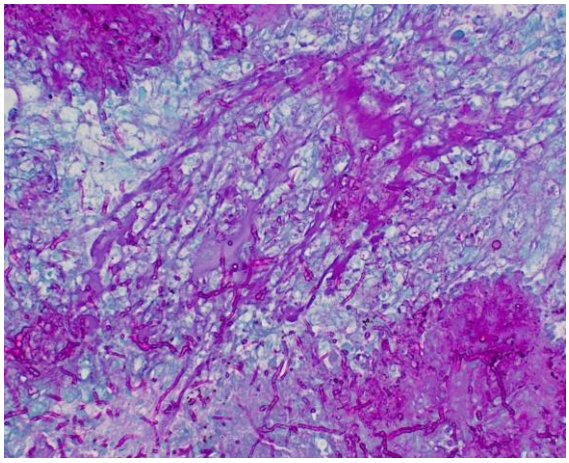

Figure 2-6. Head, Pacific pond turtle. Morphology of the fungal hyphae are better observed with a PAS stain (with malachite green).

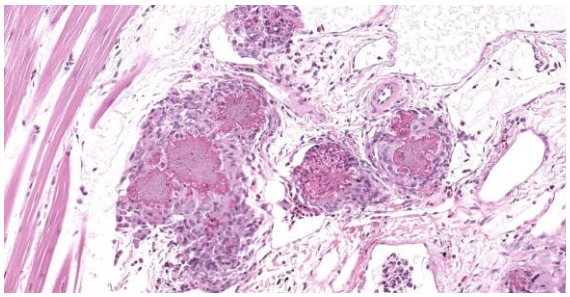

Figure 2-7. Head, Pacific pond turtle. In some areas, such as infiltrated skeletal muscle, there are fungal granulomas without inclusion cyst formation. (HE, 200X)

caused by *E. testavorans*, participants also discussed fibropapillomatosis in sea turtles, caused by chelonid herpesvirus-5, which are characteristic tumors of the skin around the eyes, mouth, limbs, shell, and cornea. These tumors can vary in appearance from flat, plaque-like lesions to exophytic or verrucous masses. They may also form on internal organs and grow large enough to impair buoyancy, leading to death.

Discussion of the morphologic diagnosis centered on whether the rather exuberant epithelial inclusion cysts were invading or merely compressing the brain. Participants felt the brain was only being compressed and thus preferred a diagnosis of meningitis rather than meningoencephalitis.

References:

1. Adamovicz L, Allender MC, Gibbons PM. Emerging infectious diseases of chelonians: an update. *Vet Clin North Am Exot Anim Pract.* 2020;23(2):263-283.
2. Lambert MR, Hernandez-Gomez O, Krohn AR, et al. Turtle shell disease fungus (*Emydomyces testavorans*): first documented occurrence in California and prevaelence in free-living turtles. *Ichthyology & Herpetology*. 2021;109 (4):958-962.
3. Mitchell MA, Tully TN. *Current therapy in exotic pet practice*. Elsevier;2016.
4. Woodburn DB, Kinsel MJ, Poll CP, et al. Shell lesions associated with *Emydomyces testavorans* infections in freshwater aquatic turtles. *Vet Pathol*. 2021;58(3):578-586.
5. Woodburn DB, Miller AN, Allender MC, Maddox CW, Terio KA. *Emydomyces testavorans*, a new genus and species of Onygenalean fungus isolated from shell lesions of freshwater aquatic turtles. *J Clin Microbiol*. 2019;57(2).

CASE III:

Signalment:
Fetus aborted at approximately 120 days of gestation, ovine, (*Ovis aries*)

History:
In July 2015, two of approximately 200 pastured sheep in a family farm in Colonia, Uruguay, aborted three fetuses at approximately 4 months of gestation.

Gross Pathology:
The fetus was a female, with a crown-to-rump length of 32 cm (estimated gestational age: 120 days) with a complete wool/hair coat, in a moderate state of post-mortem decomposition (moderate autolysis). The fetus was fully formed, with a complete wool/hair coat and no external abnormalities. The liver was moderately enlarged, with rounded edges, and there were numerous, discrete, white to yellowish, pinpoint to ≤2 mm foci throughout the hepatic parenchyma with a multifocal widespread (disseminated) distribution (necrotizing hepatitis). There were fibrin strands in the abdominal and pericardial cavities (moderate fibrinous peritonitis and pericarditis). No other gross lesions were noted. The lungs were unventilated/unexpanded, and there were no colostrum/milk curds in the lumen of the abomasum.

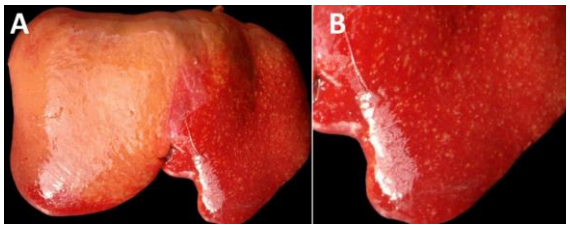

Figure 3-1. Liver, ovine abortus. The liver contains numerous miliary foci of necrosis. (Photo courtesy of: The University of Liverpool (Reprinted from: Giannitti F, Dorsch MA, Schild CO, Caffarena RD, Sverlow K, Armién AG, Riet-Correa F. Pathologic and immunohistochemical evidence of possible Francisellaceae among aborted ovine fetuses, Uruguay. Emerg Infect Dis. 2023 Jan;29(1):141-144.)

Laboratory Results:
IHC using a monoclonal primary antibody against *Francisella tularensis* lipopolysaccharide (LPS) revealed abundant and strong immunoreactivity colocalizing extracellularly with the hepatic lesions and intracellularly in infiltrating inflammatory cells.

Microscopic Description:
Liver: Randomly throughout the parenchyma, there are multiple foci of necrosis and inflammation. These foci are characterized by disruption and effacement of the hepatic cord architecture and replacement by necrotic cell debris; the hepatocytes have angular cell borders, hypereosinophilic cytoplasm, and either nuclear pyknosis or karyorrhexis (necrosis). Within these foci, there is an accumulation of eosinophilic fibrillar material (fibrin), and inflammatory cell infiltrates, mostly neutrophils and macrophages. There is an increased number of neutrophils in the sinusoids (circulating neutrophilia).

Contributor's Morphologic Diagnosis:
Liver: Hepatitis, necrotizing and fibrinosuppurative, multifocal widespread, random, severe.

Contributor's Comment:
The hepatic lesions in this fetus were suggestive of an infectious etiology. In addition, the microscopic examination of other fetal tissues revealed multifocal neutrophilic myocarditis, multifocal neutrophilic bronchiolitis and alveolitis, and fibrinous splenic capsulitis (peritonitis). Altogether, these lesions were suggestive of a bacterial cause.

Ancillary testing to assess for possible abortifacients of sheep, in this case, included immunohistochemistry (IHC) for *Chlamydia* spp., *Listeria monocytogenes*, *Coxiella burnetii*, *Salmonella enterica*, and *Toxoplasma gondii*, all of which yielded negative results. Additionally, no curved bacilli (i.e., *Campylobacter*), spirochetes (i.e., *Leptospira*, *Flexispira*) or fungi were identified in sections of liver stained with Steiner silver stain and Gomori´s methenamine silver stain, and no intralesional bacteria were visualized with tissue Gram stain. However, IHC using a monoclonal primary antibody against *Francisella tularensis* lipopolysaccharide (LPS) revealed abundant and strong immunoreactivity colocalizing extracellularly with the hepatic lesions and intracellularly in infiltrating inflammatory cells. Finally, transmission electron microscopy on formalin-fixed paraffin-embedded liver revealed intraphagocytic (intrahistiocytic) and extracellular ~0.7–1.7 µm coccobacilli (expected size for *Francisella* spp.) in the foci of necrotizing hepatitis. Details of the diagnostic investigation conducted in this case were recently published.[5]

The *Francisellaceae* family comprises gram-negative coccobacilli and four genera are currently recognized: *Francisella*, *Allofrancisella*, *Pseudofrancisella*, and *Cysteiniphilum*, of which only *Francisella* is currently considered of clinical relevance. *Francisella tularensis* is the most studied species because it causes tularemia, a highly transmissible,

Figure 3-2. Liver, ovine abortus. One section of liver is submitted for examination. (HE, 5X)

potentially life-threatening, zoonotic disease, also considered a potential bioterrorism agent.[8] Tularemia occurs over almost the entire Northern Hemisphere but is rarely reported in the Southern Hemisphere, where the only published cases have occurred in Australia.[4]

Although *F. tularensis* has a broad host range, sheep have been considered the only livestock species affected by epizootics of tularemia and have been implicated in disease transmission to sheep industry workers.[7,10] The abortifacient effects of *F. tularensis* in sheep have been described in the United States, and tularemia has been regarded as an overlooked syndrome in sheep.[10]

From a pathologic viewpoint, necrotic foci in the liver, spleen, or lungs in late term aborted ovine fetuses are characteristic of tularemia and should raise suspicion, although gross lesions can be absent even in cases with typical histologic inflammatory and necrotizing lesions.[10] Contrary to most bacterial abortifacients of sheep, *F. tularensis* is not visible upon histopathologic examination of tissues stained with hematoxylin and eosin, Steiner silver stain or Gram stain, even in tissues that have a high bacterial burden demonstrated by IHC.[3,10] The diagnostic investigation of any case of ovine abortion with fetal lesions indicating a bacterial etiology should include ancillary testing to identify *F. tularensis* and rule out other abortigenic pathogens.[3]

The etiologic diagnosis in our case was reached by the immunohistochemical demonstration of abundant intralesional antigen by a specific monoclonal antibody raised against *F. tularensis* LPS. IHC has proven useful for identifying *F. tularensis* in diagnostic settings.[6,10] *F. tularensis* LPS is a main specific antigen and virulence factor and differs from the LPS of other gram-negative bacteria.[9] According to the manufacturer, the primary antibody used in this case for the IHC does not cross-react with *Francisella novicida*, *Yersinia pestis*, *Y. pseudotuberculosis*, *Y. enterocolitica*, *Vibrio cholerae*, *Escherichia coli*, *Salmonella enterica* serovar Typhimurium, *Brucella abortus*, *B. suis*, *B. ovis*, *B. melitensis*, or *B. neotomae*. We tested the IHC in cases of ovine abortion caused by *Campylobacter jejuni* and *C. fetus* but observed no cross-reactivity with these pathogens. Although cross-reaction with other members of *Francisellaceae* cannot be completely ruled out, *F. tularensis* is currently the only species of this family recognized as an ovine abortifacient. Definite species and sub-species identification requires bacterial isolation and DNA analysis, which we were unable to perform in this case. The ultrastructural demonstration of intracellular gram-negative coccobacilli of the expected size in phagocytic and inflammatory cells in tissues with lesions, as in our case, aids in the diagnosis, but is by no means confirmatory.

The lack of historical reports of tularemia outside endemic areas of North America and Eurasia has been puzzling.[4] Recently, tularemia emerged in Australia and reemerged in the Northern Hemisphere.[8,15] South America has been considered free of tularemia, which seems to be based solely on the lack of disease reporting.[15] However, tularemia might have been undiagnosed because of limitations in disease surveillance systems in the region. No clinical disease caused

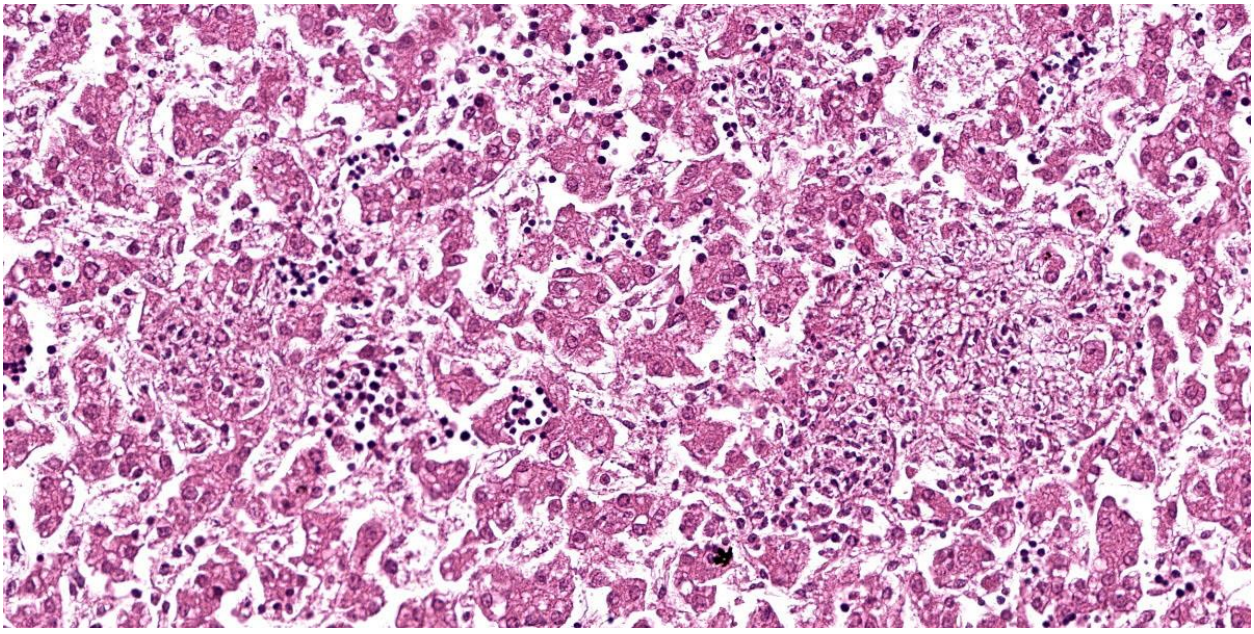

Figure 3-3. Liver, ovine abortus. Hepatocellular plates are disassociated. There are randomly scattered areas of lytic necrosis within the parenchyma which exhibit hepatocellular loss and stromal collapse, with few infiltrating neutrophils. Surrounding hepatocytes contain cytoplasmic lipid vacuoles. (HE, 314X)

by *Francisella* spp. in mammals in the Americas south of Mexico has been described. This case raised concerns about the possible occurrence of tularemia in South America.[5]

The source of infection in this sheep remains unknown; however, *F.tularensis* has a broad range of animal reservoirs, including arthropods, rodents, lagomorphs, and marsupials.[4,12] Brown hares (*Lepus europaeus*), a species that plays a primary role in the ecology of tularemia in Europe, have been introduced to Uruguay and are frequently seen around the affected farm.[6] In addition, *F. tularensis* can be transmitted by ticks, including *Amblyomma* spp., *Haemophysalis* spp., and *Ixodes* spp. ticks, which are endemic in Uruguay. Of note, a gamma-proteobacterium related to *Francisella*-like organisms, but different from *F. tularensis*, was identified in Uruguay in *Amblyomma triste* ticks, the most prevalent tick species reported in human tick bites in the country.[14]

Contributing Institution:
Plataforma de Investigación
en Salud Animal,
Instituto Nacional de Investigación
Agropecuaria (INIA),
La Estanzuela, Uruguay
http://www.inia.uy

JPC Diagnosis:

1. Liver: Hepatitis, necrotizing, multifocal and random, moderate.
2. Liver: Extramedullary hematopoiesis, diffuse, moderate.

JPC Comment:

Francisella tularensis is poorly staining gram-negative coccobacillus that is non-motile, aerobic, and is a facultative intracellular pathogen. There are three subspecies that vary in their geographic distribution and virulence. *F. tularensis* subsp. *tularensis* accounts for the majority of clinical infections in domestic animals, is highly pathogenic, and is found in North America and Europe.[11]

Two less virulent strains, *F. tularensis* subsp. *holartica* and *F. tularensis* subsp. *mediasiatica* occur in Europe/North America and Asia, respectively. Interestingly, subsp. *holartica* is frequently linked to aquatic mammals such as beavers and muskrats, and its reservoir is considered to be a protozoal organism rather than a mammal.[11]

In vivo, the organism enters host macrophages, where it arrests the maturation and acidification of the phagolysosome.[11] The organism then escapes the phagosome and replicates freely in the cytoplasm, where it can trigger either caspase 3-mediated apoptosis or an inflammatory form of host cell death called pyroptosis, resulting in release of bacteria that can initiate another round of host cell infection.[2,11] The ability of *F. tularensis* to survive the phagosome is dependent on the gene products of a 30kb stretch of bacterial DNA, known as the Francisella Pathogenicity Island (FPI), that encodes 18 genes, 14 of which are required for growth within and escape from macrophages.[2] Among the virulence factors encoded on the FPI is a recently discovered Type VI secretion system which is required for macrophage escape and intracytoplasmic replication.[1] *F. tularensis* organisms that are deficient in key pieces of this secretion nanomachine are rendered essentially avirulent in mouse models.[1]

If all is working well, however, *F. tularensis* can cause fulminating, fatal disease in wildlife species, domestic animals, and humans. In most species, the disease is characterized by fever, depression, inappetence, and manifestations of septicemia. Outbreaks have been reported in sheep, horses, and young pigs, while adult pigs, cattle, and dogs appear to be relatively resistant to infection.[11]

Cats are the domestic animal most associated with disease, with clinical forms (typhoidal, respiratory, ulceroglandular, and

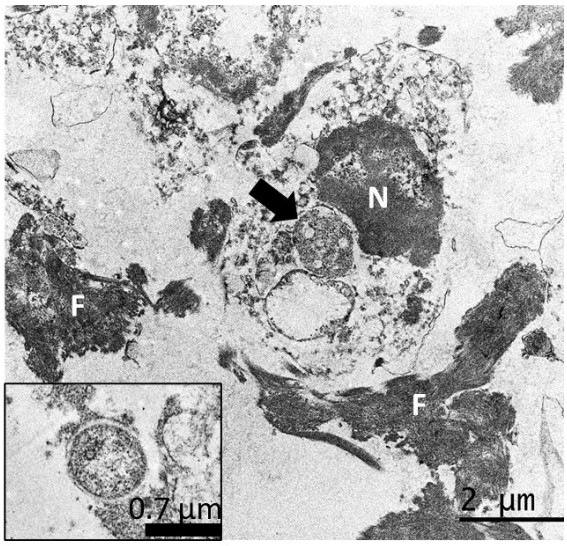

Figure 3-4. Liver, ovine abortus. An infiltrating phagocyte (center), presumably a macrophage, contains intracytoplasmic debris, including debris of a gram-negative bacterium within a phagolysosome (arrow) and is surrounded by extravasated fibrin (F). N: phagocyte nucleus, bar = 2 µm. Inset: A preserved gram-negative bacterium of the expected size for *Francisella* spp. is seen in an adjacent extracellular location, bar = 0.7 µm. Photos courtesy of Dr. Aníbal G. Armién (California Animal Health and Food Safety Laboratory, University of California, Davis, CA, USA).

oropharyngeal) mirroring those described in humans.[11] Grossly, tularemia in cats is characterized by sizeable (2mm diameter or more), miliary white foci in the liver, spleen, and lymph nodes.[13] Histologically, lesions are identical to those presented here, with focal areas of severe necrosis with bacteria that are difficult to visualize on H&E section.[13]

Conference discussion focused largely on the typical presentations and pathogenesis of tularemia in various species. From a diagnostic standpoint, it is important to remember that, unlike most infectious differentials for hepatic necrosis, *F. tularensis* is, rather unhelpfully, not visible on H&E, Steiner, or Gram stains, even in tissues with high bacterial burdens demonstrated with

immunohistochemical staining. Dr. Travis also discussed documented human cases of tularemia contracted from "face snuggling" domestic dogs ("if we die, we die") and from aerosolized infective material liberated from wildlife carcasses during yard work.

Despite the absence of demonstrable organisms, this case provides an excellent example of the hepatic manifestation of gram-negative sepsis. Participants noted multifocal areas of extramedullary hematopoiesis within sinusoids, which was felt substantial enough to include in the morphologic diagnoses.

References:

1. Brodmann M, Dreier RF, Broz P, Basler M. *Francisella* requires dynamic type VI secretion system and ClpB to deliver effectors for phagosomal escape. *Nat Commun*. 2017;8:15853.
2. Clemens DL, Lee BY, Horwitz MA. The *Francisella* type VI secretion system. *Front Cell Infect Microbiol*. 2018;8: 00121.
3. Dorsch MA, Cantón GJ, Driemeier D, Anderson ML, Moeller RB, Giannitti F. Bacterial, protozoal and viral abortions in sheep and goats in South America: a review. *Small Rumin Res*. 2021;205 :106547.
4. Eden JS, Rose K, Ng J, et al. *Francisella tularensis* ssp.*holarctica* in Ringtail Possums, Australia. *Emerg Infect Dis*. 2017; 23:1198-1201.
5. Giannitti F, Dorsch MA, Schild CO, et al. Pathologic and immunohistochemical evidence of possible Francisellaceae among aborted ovine fetuses, Uruguay. *Emerg Infect Dis*. 2023;29:141-144.
6. Gyuranecz M, Szeredi L, Makrai L, et al. Tularemia of European Brown Hare (*Lepus europaeus*): a pathological, histopathological,and immunohistochemical study. *Vet Pathol*. 2010;47:958-63.
7. Jellison WL, Kohl GM. Tularemia in sheep and in sheep industry workers in western United States. *Public Health Monogr*. 1955;28:1-19.
8. Maurin M. *Francisella tularensis* as a potential agent of bioterrorism? *Expert Rev Anti Infect Ther*. 2015;13:141-144.
9. Okan NA, Kasper DL. The atypical lipopolysaccharide of *Francisella*. *Carbohydr Res*. 2013; 378:79-83.
10. O'Toole D, Williams ES, Woods LW, et al. Tularemia in range sheep: an overlooked syndrome? *J Vet Diag Invest*. 2008;20:508-513.
11. Quinn PJ, Markey BK, Leonard FC, Fitz-Patrick ES, Fanning S, Hartigan PJ. *Veterinary Microbiology and Microbial Disease*. 2nd ed. Blackwell;2011.
12. Sjöstedt A. Tularemia: history, epidemiology, pathogen physiology, and clinical manifestations. *Ann N Y Acad Sci*. 2007; 1105:1-29.
13. Valli VEO, Kiupel M, Bienzle D. Hematopoietic System. In: Maxie GM, ed. Vol. 3, *Jubb, Kennedy, and Palmer's Pathology of Domestic Animals.* Elsevier, Inc;2016:184-186.
14. Venzal JM, Estrada-Peña A, Portillo A, et al. Detection of Alpha and Gamma-Proteobacteria in *Amblyomma triste* (Acari: Ixodidae) from Uruguay. *Exp Appl Acarol*. 2008;44:49-56.
15. Yeni DK, Büyük F, Ashraf A, Shah MSUD. Tularemia: a re-emerging tick-borne infectious diseas. *Folia Microbiol (Praha)*. 2021;66:1-14.

CASE IV:

Signalment:
Adult female Zebrafish (*Danio rerio*)

History:
The animal presented with an ulceration on the right caudal abdomen, but appeared otherwise bright, alert, and responsive and was in good body condition.

Figure 4-1. Presentation, zebrafish. There are ulcers on the right abdominal wall and gill plate. (*Photo courtesy of:* Laboratory of Comparative Pathology, Memorial Sloan Kettering Cancer Center, The Rockefeller University, Weill Cornell Medicine, http://www.mskcc.org /research/comparative-medicine-pathology-0)

Gross Pathology:
The skin of the right caudal abdomen contains a single approximately 1.5-2 mm diameter circular pale tan ulceration. Fin clip and gill clip wet mounts are unremarkable.

Laboratory Results:
Aerobic culture of ulcerated region: Mixed bacterial flora including *Plesiomonas shigelloides* and *Pseudomonas putida.*

Aerobic and anaerobic culture of kidney: Negative

Microscopic Description:
Markedly expanding the coelomic cavity and separating and surrounding viable and degenerate developing eggs within the ovary is a large inflammatory population composed of numerous epithelioid macrophages, granulocytes, and rare multinucleated giant cells. This inflammatory population is admixed with small amounts of necrotic cellular debris, moderate hemorrhage, and fibrin. This inflammatory process extrudes through the extensively ulcerated overlying body wall with loss of all layers including the skin, muscle, and coelomic cavity lining. Few small basophilic rod-shaped bacterial colonies are present near the surface of the ulceration within the degenerate egg material. The myocytes adjacent to this body wall ulceration are multifocally degenerate, with swollen vacuolated sarcoplasm, or necrotic with shrunken, hypereosinophilic, fragmented sarcoplasm. Several macrophages infiltrate between and surround damaged myocytes.

Contributor's Morphologic Diagnosis:
Ovary and coelom: Severe, multifocal to coalescing, chronic granulomatous and granulocytic oophoritis and coelomitis with hemorrhage, degenerating eggs, myocyte loss, degeneration, and necrosis, and severe full thickness body wall, dermal, and epidermal ulceration with multifocal intralesional rod-shaped bacterial colonies.

Contributor's Comment:
Chronic ovarian and coelomic inflammation in zebrafish associated with degenerating eggs is a common condition observed in laboratory facilities and is referred to as Egg Associated Inflammation (EAI). The cause of this condition is uncertain with some individuals describing this as a syndrome of egg retention.[6] A potential link to Mycobacterial infection has been suggested though no causative agents have been identified currently and

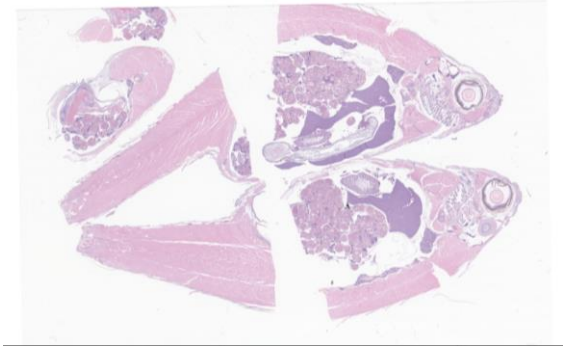

Figure 4-2. Whole body, zebrafish. Two longitudinal and two cross sections are presented for examination. At subgross magnification, there is a hole in the body wall on one transverse section and internal pathology is evident. (HE, 6X)

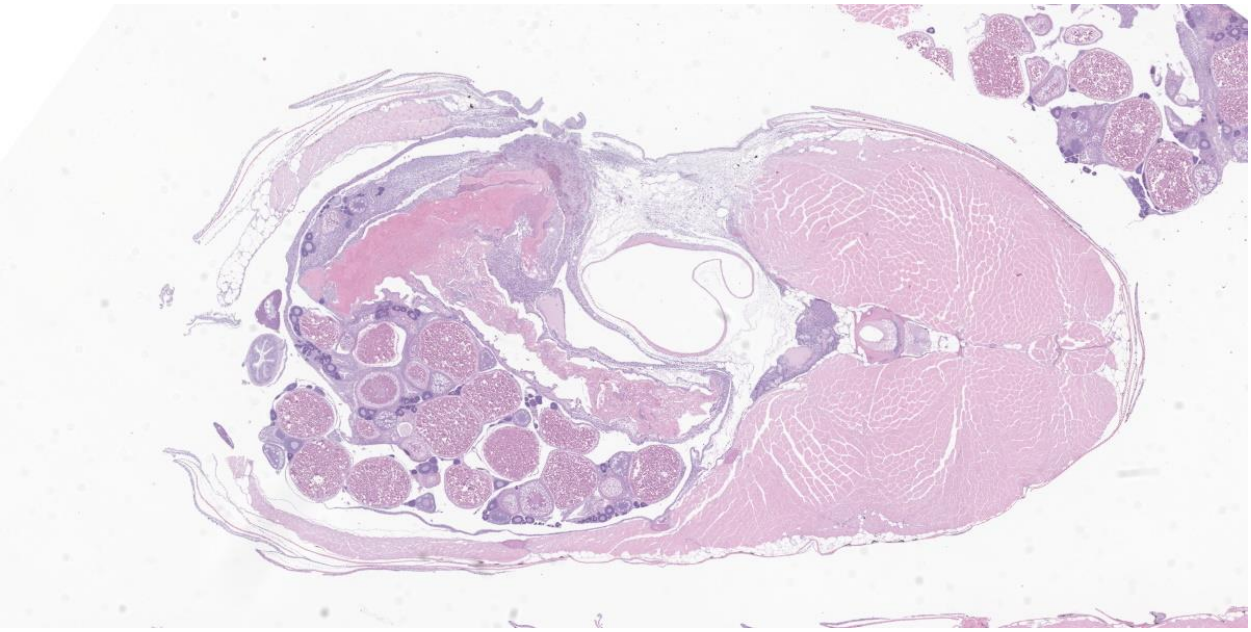

Figure 4-3. Cross section, zebrafish. This one cross section has all the goodies. There is full-thickness necrosis of the body wall which extends into the coelom. There is marked histiocytic inflammation within the ovary centered on degenerating ova and a large mass of brightly eosinophilic protein. (HE, 16X)

it is uncertain that Mycobacterium is a primary pathogen in this disease.[2] Acid fast staining of our case was undertaken to rule out Mycobacterial infection and was negative.

Gross examination of these fish reveals a large abdomen that when opened may contain a mass of tissue, possibly adhered to the overlying coelomic cavity lining and body wall. Occasionally, as in our case, a full thickness ulceration may be visible externally, covered or surrounded by a rim of pale tan to white tissue. This ulceration is secondary to the extrusion of tissue through the body wall from the point of underlying coelomic adhesion.

Microscopically, the observed inflammation is often granulomatous with varying numbers of granulocytes and is always associated with various stages of degenerating eggs within the coelom. The inflammatory population may be surrounded and infiltrated by abundant fibroplasia and rarely this may promote the formation of fibromas and fibrosarcomas.[6]

The rod-shaped bacterial colonies noted on H&E-stained sections highlight as gram negative with gram staining. Aerobic culture of the ulcerated region grew *Plesiomonas shigelloides* and *Pseudomonas putida*, both gram negative rod-shaped bacteria. *Plesiomonas shigelloides* is found commonly within the environment and gut of laboratory and wild zebrafish but has been identified in few cases to be pathogenic to zebrafish.[5] *Pseudomonas putida* is another bacterium widely distributed in soil, water, and on the skin of animals.[3] The skin ulceration secondary to EAI likely lead to an optimal situation for these environmental organisms to grow within the damaged tissue.

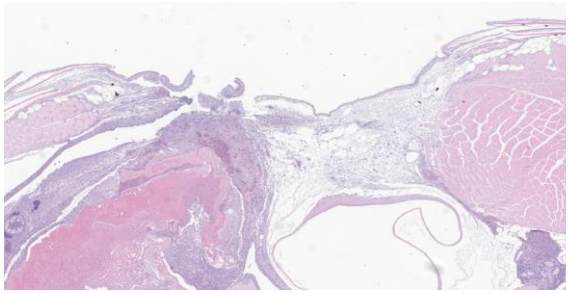

Figure 4-4. Abdominal wall, zebrafish. Higher magnification of the full thickness necrosis of the body wall. (HE, 37X)

Contributing Institution:
Laboratory of Comparative Pathology
Memorial Sloan Kettering Cancer Center
The Rockefeller University
Weill Cornell Medicine
http://www.mskcc.org/research/comparative-medicine-pathology

JPC Diagnosis:
Body wall, ovary, coelom: Granulomatous inflammation with ovarian follicular degeneration, extracellular bacteria, and body wall perforation.

JPC Comment:
As the contributor notes, egg associated inflammation (EAI), also referred to as Egg Associated Inflammation and Fibroplasia (EAIF) is thought to be associated with egg retention in fish that have not had proper opportunity to spawn.[1] While mild forms of the condition may be clinically inapparent, in many cases female zebrafish present with an enlarged, ulcerated abdomens and superimposed bacterial infections within the fertile, yolky soil of the affected ovary.[6]

The histologic features of this case are typical of the condition. The eosinophilic coaglum represents yolk from atretic follicles and the periphery of this material is often characterized by finely granular basophilic material consisting of lysed inflammatory cells, necrotic cellular debris, and visible bacterial colonies.[1] This material is usually rimmed by an intense granulomatous reaction with epithelioid macrophages and multinucleated giant cells.[1]

EAI is currently considered a non-infectious condition, though that assertion is typically heavy with caveats. As the contributor notes, some cases have been associated with mycobacteriosis; however, infectious agents are not usually found in cases of EAI in the absence of body wall defects, and the granulomatous and inflammatory changes seen in zebrafish with mycobacteriosis are typically found in organs other than ovaries, whereas EAI arises, as the name implies, from the ovaries.[4]

In addition to the detrimental effects of EAI on the individual animal, the condition raises confounding concerns due to the use of zebrafish in experimental interrogations of developmental genetics. Zebrafish are used extensively to investigate the effects of exogenous chemicals, particularly endocrine disrupting compounds, on the vertebrate reproductive system.[1] Follicular atresia is a common non-specific effect of several classes of these compounds and research results may be confounded by the chronic oophoritis that is characteristic of EAI.[1] In females with subclinical EAI, egg production may be

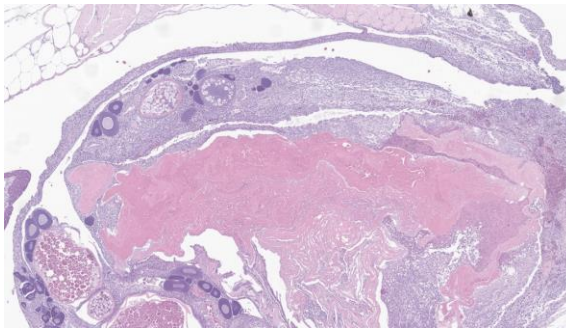

Figure 4-5. Ovary, zebrafish. Profound histiocytic inflammation within the ovary is centered on extruded protein from degenerate eggs. (HE, 50X)

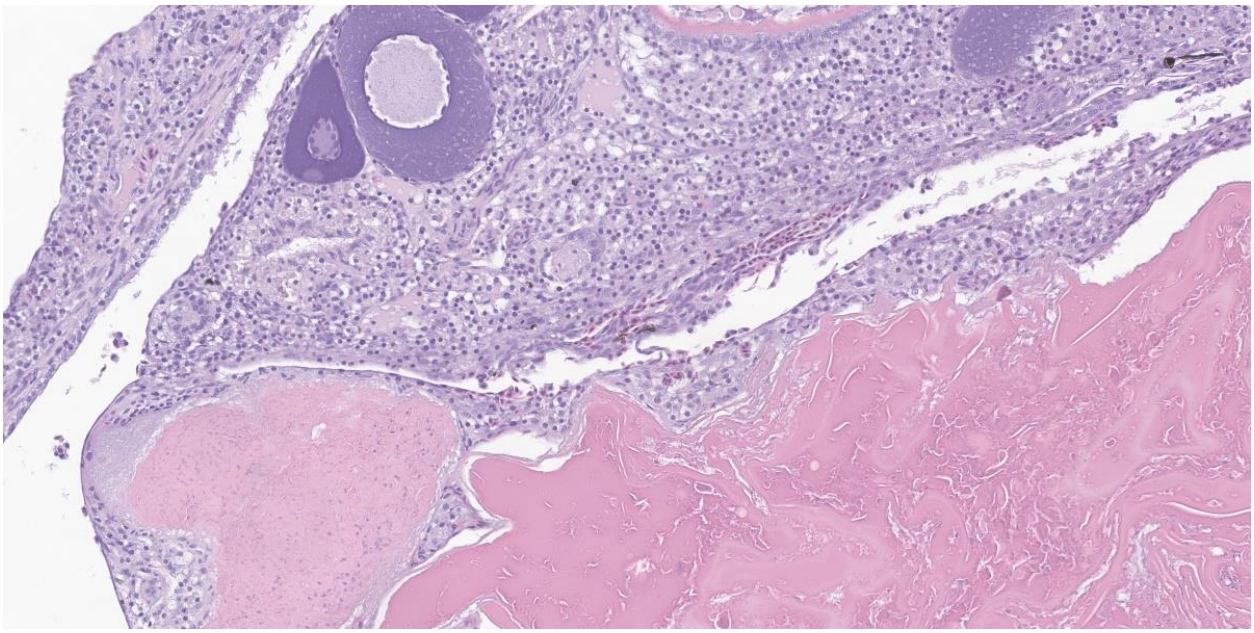

Figure 4-6. Ovary, zebrafish. Higher magnification of the histiocytic inflammation within the ovary. (HE, 60X)

reduced, leading to skewed research results in studies that use fecundity endpoints.[1]

The appearance of these apparently spontaneous degenerative and inflammatory changes in the ovaries of zebrafish highlight the importance of recognizing baseline variations in the histologic morphology of target organs in research animals.[4]

The specifics of this condition are largely unknown, leaving scant fodder for conference discussion. Dr. Travis discussed several factors that have been associated with EAI, including small body size, obesity, overcrowding, water quality issues, sex ratio imbalances, stress, and lack of proper environmental cues (e.g., photoperiod, temperature) in cultured fish. Conference participants also considered sequelae of the profound abdominal distention characteristic of the disease, including organ compression and malfunction, prolapse of the ovary through the genital pore, and dystocia.

References:

1. Kent ML, Harper C, Wolf JC. Documented and potential research impacts of subclinical diseases in zebrafish. *ILAR J*. 2012;53(2):126-134.
2. Kent ML, Watral VG, Kirchoff NS, Spagnoli ST, Sharpton TJ. Effects of subclinical mycobacterium chelonae infections on fecundity and embryo survival in zebrafish. *Zebrafish*. 2016;13(S1):S88-95.
3. Oh WT, Kim JH, Jun JW, Giri SS, Yun S, Kim HY. Genetic characterization and pathological analysis of a novel bacterial pathogen, *Pseudomonas tructae*, in rainbow trout (Oncorhynchus mykiss). *Microorganisms*. 2019;7(10):432.
4. Rossteuscher S, Schmidt-Posthaus H, Schafers C, Teigler M, Segner H. Background pathology of the ovary in a laboratory population of zebrafish *Danio rerio*. *Dis Acquat Org*. 2008;79:169-172.
5. VanderHoek ZK, Browning AM, Washburn Q, Kent ML, Sharpton T, Gaulke CA. Draft genome sequence of Plesiomonas shigelloides Strain zfcc0051

(Phylum *Proteobacteria*). *Microbiol Resour Announc*. 2022; 11(7):e0007422.
6. Zebrafish International Resource Center. Non-Infectious and Idiopathic Diseases. April 6, 2016. Accessed November 17, 2023. https://zebrafish.org/wiki/health/disease_manual/noninfectious_and_idiopathic.

WSC 2023-2024
Conference 11 Self-Assessment

1. Which of the following genes has been incriminated in cats with copper toxicosis?
    a. ABCDA1
    b. COMMD1
    c. ATP7B
    d. 1ADAM12
2. The typical histologic lesion associated with *Emydomyces testivorans* is a?
    a. Granuloma
    b. Epithelial inclusion cyst
    c. Abscess
    d. Draining tracts from adjacent bone
3. *Emydomyces testavorans* is a?
    a. Gram-positive bacillus
    b. Gram-negative bacillus
    c. Protozoan
    d. Fungus
4. Tularemia is most likely transmitted by?
    a. Ticks
    b. Mosquitoes
    c. Biting flies
    d. Fleas
5. A syndrome associated with chronic ovarian and coelomic inflammation in zebrafish associated with degenerating eggs is known as…?
    a. “Tank layers”
    b. “Egg-associated inflammation”
    c. “Ovopositional derangement syndrome”
    d. “Roe Roe Roe Your butt”

Joint Pathology Center
Veterinary Pathology Services

WEDNESDAY SLIDE CONFERENCE 2023-2024

Conference #12 06 December 2023

CASE I:

Signalment:
12-year-old male neutered domestic shorthair cat (*Felis catus*)

History:
The cat was rescued from a hoarding situation in the year prior to euthanasia. The cat was evaluated for weight loss, hyporexia, icterus, diarrhea, polyuria, polydipsia, hypertension, neurologic signs (circling, head tilt, nystagmus, dullness), eyelid and ear canal masses, retinal detachment, anterior uveitis, and blindness. Lymphoma was suspected and the cat was euthanized.

Gross Pathology:
At necropsy the cat was icteric and the liver, spleen, intestinal walls, and mesenteric lymph nodes were enlarged. The capsular surface of the kidneys was pitted (chronic interstitial nephritis). As noted clinically, there were 4-8 mm raised cutaneous, variably ulcerated or alopecic nodules primarily concentrated around the face, paws and pinnae. There was bilateral axial corneal opacity and roughening (ulceration and edema). In the left eye, the anterior chamber contained flocculent white to yellow material (fibrin) and the iris was diffusely expanded by tan material. In both eyes, the retina and choroid were variably expanded by tan material.

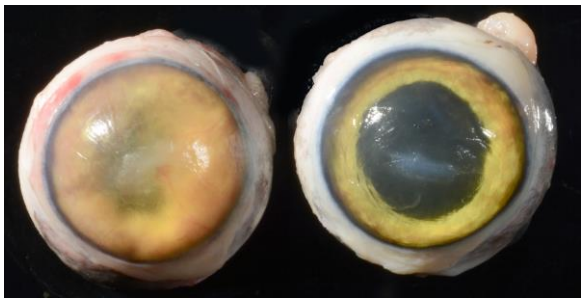

Figure 1-1. Eye, cat. There was bilateral axial corneal opacity and roughening (ulceration and edema). (*Photo courtesy of:* University of Tennessee, College of Veterinary Medicine, Department of Biomedical and Diagnostic Sciences, http://www.vet.utk.edu/departments/path/index.php)

Microscopic Description:
The left eye was more severely affected, but the following lesions are apparent in both eyes. The iris, ciliary body, trabecular meshwork, choroid and retina are variably expanded by sheets of large foamy macrophages that contain myriad, round to oval, 2-4 µm, basophilic yeast surrounded by a clear halo. There are associated lymphocytes and plasma cells. The retina is detached and there is loss of photoreceptor outer segments. There is thinning and mixing of all retinal layers (atrophy). Retinal blood vessels are often cuffed by lymphocytes (retinitis). In some sections, the subretinal space contains abundant fibrin with fewer lymphocytes and yeast-laden macrophages. The lens or lens capsule is present in some sections and exhibits mild peripheral lens fiber swelling and

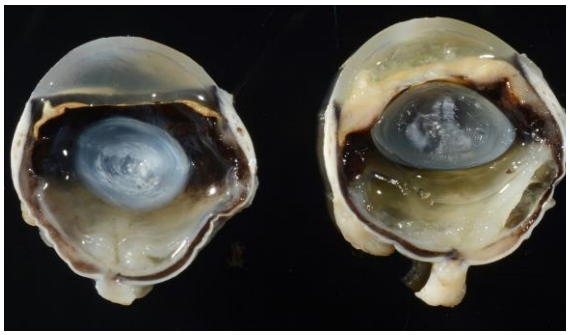

Figure 1-2. Eye, cat. In the left eye, the anterior chamber contained flocculent white to yellow material (fibrin) and the iris was diffusely expanded by tan material (*Photo courtesy of:* University of Tennessee, College of Veterinary Medicine, Department of Biomedical and Diagnostic Sciences)

posterior migration of lens epithelial cells (cataract). There is mid-stromal and deep corneal vascularization. In some sections, there is axial corneal ulceration with associated bacterial colonies, fibrin and neutrophils; the adjacent intact corneal epithelium is attenuated.

Contributor's Morphologic Diagnosis:
Eye: Severe diffuse granulomatous endophthalmitis with intrahistiocytic yeasts, retinal detachment, cataract and corneal ulceration.

Contributor's Comment:
The morphology of the yeasts is most consistent with *Histoplasma* spp. At necropsy, gross lesions were also identified in the skin, liver, spleen, intestines and lymph nodes, and microscopic examination identified similar lesions and yeast in those tissues as well as in the kidneys and lungs.

In the United States, histoplasmosis is usually due to *Histoplasma capsulatum* and cases occur most commonly in midwestern and southern states. Bird and bat feces are a common source of infection. *Histoplasma* spp. are dimorphic fungi and infection is usually acquired by inhalation of microconidia. In the lungs, the microconidia take on the yeast form. The yeast are phagocytized and proliferate by budding intracellularly. The yeast can then spread via the blood and lymphatics to distant sites resulting in systemic infection. Although the lungs are usually the primary site of infection, the skin and gastrointestinal tracts may also be primary sites of infection.

As with many fungal infections, immunocompromised individuals are more susceptible to infection and dissemination. In some immunocompetent hosts, *Histoplasma* spp. can be dormant until reactivation during times of immunosuppression.[1]

Clinical signs and lesions depend on the organs affected. As in this case, the lungs, liver, spleen and lymph nodes are commonly affected in systemic histoplasmosis.[1]

Ocular involvement may be present in about 24% of cats and may include blepharitis, conjunctivitis, chorioretinitis, panuveitis, panophthalmitis, retinal detachment, and optic neuritis.[1,2]

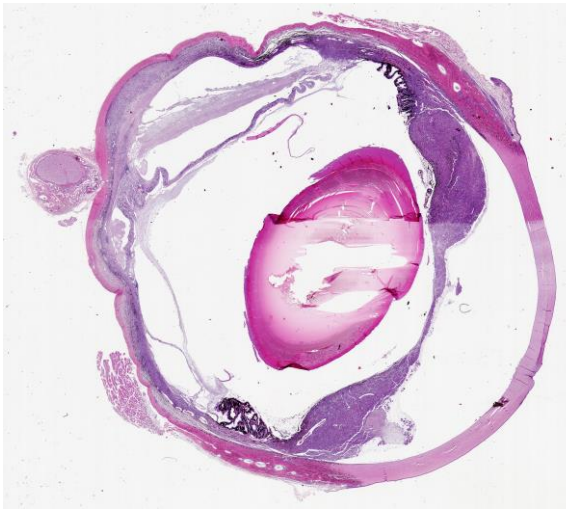

Figure 1-3. Eye, cat. The uvea and choroid are diffusely and markedly expanded by a cellular exudate which extends into the anterior and posterior chambers. There is retinal detachment and atrophy with subretinal exudate. (HE, 5X) (*Photo courtesy of:* University of Tennessee, College of Veterinary Medicine, Department of Biomedical and Diagnostic Sciences)

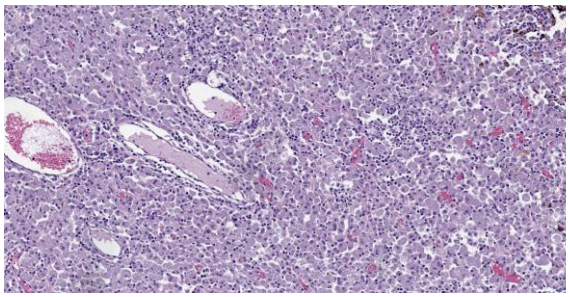

Figure 1-4. Iris, cat. The iris is expanded by sheets of large macrophages with fewer lymphocytes. (HE, 5X)

Contributing Institution:
University of Tennessee
College of Veterinary Medicine
Department of Biomedical and Diagnostic Sciences, http://www.vet.utk.edu/departments/path/index.php

JPC Diagnosis:
Eye: Endophthalmitis, granulomatous, diffuse, severe, with retinal detachment and atrophy, and numerous intrahistiocytic yeasts.

JPC Comment:
Histoplasma capsulatum is found primarily in soils enriched in bird and bat guano where it exists as a conidia-forming mold. Once inhaled, the pleasant 37°C temperature of the host converts the organism to a yeast phase composed of 2 to 4µm oval budding yeasts that can be found both extracellularly and within macrophages.[3] There are three varieties of *Histoplasma capsulatum* of veterinary importance: *Histoplasma capsulatum* var. *capsulatum*, the most common variant and the subject of this comment; *Histoplasma capsulatum* var. *duboisii*, which primarily causes cutaneous disease in humans and baboons in Africa; and *Histoplasma capsulatum* var. *farciminosum*, which causes epizootic lymphangitis, or "pseudoglanders," in equids.

Exposure to *Histoplasma* spp. in endemic areas is common, but disease is rare. As the contributor notes, disease, when present, primarily affects the lungs; systemic disease typically results only when the exposed host lacks sufficient cell-mediated immunity to arrest the macrophage-associated spread of yeast throughout the body. Localized, pulmonary, and disseminated histoplasmosis have been described in both domestic and wild felids, and histoplasmosis is reported to be the second most common systemic fungal infection in cats (second only to cryptococcosis).[5] The most common body systems affected are the respiratory tract, eyes, musculoskeletal system, hemolymphatic organs, and the skin.[5]

It is unclear how commonly feline histoplasmosis affects the eyes. In one case series, all cats with confirmed disseminated histoplasmosis had ocular lesions discovered on ophthalmic evaluation, while more recent reports place this number at 24%.[2,5] Typical ocular signs include optic neuritis, anterior uveitis, panuveitis, endophthalmitis, choroiditis/chorioretinitis, often with retinal detachment, and secondary glaucoma.[5]

Research in humans and in animal models has shown that *H. capsulatum* organisms can persist in tissues in a dormant state for many years.[5] In immune-competent animals, the immune system retards or eliminates the organisms' ability to replicate but does not kill them, leading to the granulomatous lesions that are characteristic of the disease.[5] Reactivation of disease may occur with immune suppression, with disseminated disease occurring many years after the host has been removed from exposure to the organism.[5] This has implications for ocular histoplasmosis as the eye is an immunologically sequestered tissue that is separated from the rest of the body by the blood-aqueous and blood-retinal barriers.[5] While sequestration of *H. capsulatum* in the eye and subsequent systemic dissemination after discontinuation of antifungal therapy has not been

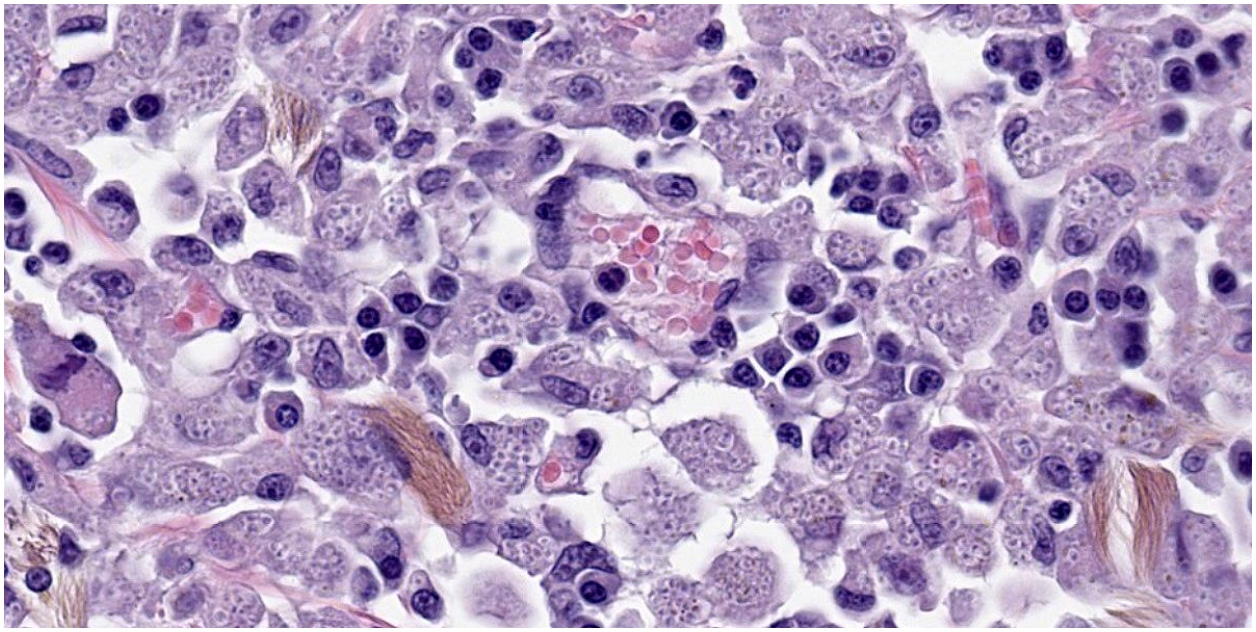

Figure 1-5. Eye, cat. Macrophages contain numerous intracytoplasmic 2-4um round to elliptical yeasts. Interspersed melanocytes contain golden brown filamentous pigment characteristic of the feline eye. (HE, 783X)

definitively proven, studies of ocular *Blastomyces* spp. infections suggest that fungal persistence in the eye can delay clearance of the organism and perhaps serve as a reservoir for recrudescent infection.[5] The ability to effectively treat ocular histoplasmosis is further complicated by the poor sensitivity of current laboratory tests, such as serial urine and serum antigen assays, at detecting histoplasmosis that is restricted to ocular tissues.[5]

Detecting the organism was not a particular challenge in this case, however, which delighted conference participants with its somewhat ostentatious display of yeast-laden macrophages. The florid nature of the infection frustrated resident attempts to pinpoint exactly which ocular structures were involved. Our moderator for the week, Dr. Rachel Neto, Assistant Clinical Professor at Auburn University College of Veterinary Medicine and ocular pathology enthusiast, allowed that there might be scattered inflammation within the sclera, but felt that this was primarily a uveocentric disease process and preferred to describe the lesion as an endophthalmitis rather than a panophthalmitis.

A considerable amount of discussion centered on the need to read through processing and sectioning artifacts. Dr. Neto particularly noted that she would be cautious in interpreting changes to the drainage angle based on the examined section alone as the section did not include the pupil and was likely a parasagittal cut.Neoplasia should be included on any differential list that is based solely on gross appearance. As this is a cat (evidenced here by the many melanocytes containing filamentous, golden pheomelanin), feline diffuse iris melanoma, lymphoma, and post-traumatic sarcoma should be on the list. Infectious differentials include FIP, *Toxoplasma,* and the dimorphic fungi. On histologic exam, however, the size, morphology, and intrahistiocytic location of the organism narrows the list considerably to *Histoplasma* and *Leishmania.* Dr. Neto also discussed a dimorphic fungus, *Blastomyces helicus,* that

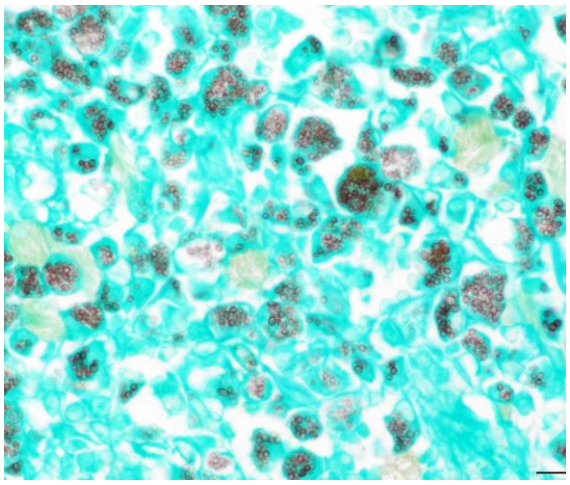

Figure 1-6. Eye, cat. A GMS stain demonstrates the yeasts. (GMS, 400X) (*Photo courtesy of:* University of Tennessee, College of Veterinary Medicine, Department of Biomedical and Diagnostic Sciences)

looks virtually identical to *Histoplasma capsulatum*, is a recently-described cause of feline pneumonitis, and should be considered when confronted with *Histoplasma*-like organisms in cats.[4]

References:

1. Bromel C, Greene CE. Chapter 58: Histoplasmosis. In: Green CE, ed. *Infectious Diseases of the Dog and Cat.* 4th ed. Elsevier; 2012.
2. Ewald MM, Rankin AJ, Meekins JM, McCool ES. Disseminated histoplasmosis with ocular adnexal involvement in seven cats. *Vet Ophthalmol.* 2020;23: 905-912.
3. Kauffman CA. Histoplasmosis: a clinical and laboratory update. *Clin Microbiol Rev*. 2007;20(1):115-132.
4. Martinez CR, Jensen TD, Bradley AM, Bohn AA. Pathology in Practice. *JAVMA*. 202;256(8):1895-1897.
5. Smith KM, Strom AR, Gilmour MA, et al. Utility of antigen testing for the diagnosis of ocular histoplasmosis in four cats: a case series and literature review. *J Feline Med Surg*. 2017;19(10)1110-1118.

CASE II:

Signalment:

3-day-old male White Shorthorn calf *(Bos taurus).*

History:

A male, White Shorthorn calf was delivered with assistance and born blind. This was the third calf to be born blind in the last two calving seasons. All blind calves were sired by the same White Shorthorn bull and offspring from other sires were unaffected.

Initially, the submitting veterinary surgeon suspected Vitamin A deficiency during gestation. However, a bolus strategy containing Vitamin A had no effect. Also, cohort sampling of 10 cows revealed unremarkable vitamin A levels in 9/10 cows and, therefore, the herd relevance of Vitamin A deficiency was unclear. The herd is vaccinated against BVD and all animals have tested negative for BVD.

Figure 2-1. Eyes, right and left, calf. Both globes are smaller than normal, with the right globe (on the left in this image) being considerably smaller than the contralateral eye. (*Photo courtesy of:* Department of Pathobiology and Population Sciences (PPS), Royal Veterinary College, Hawkshead Lane, Brookmans Park, Hatfield, Hertfordshire, AL9 7TA. www.rvc.ac.uk)

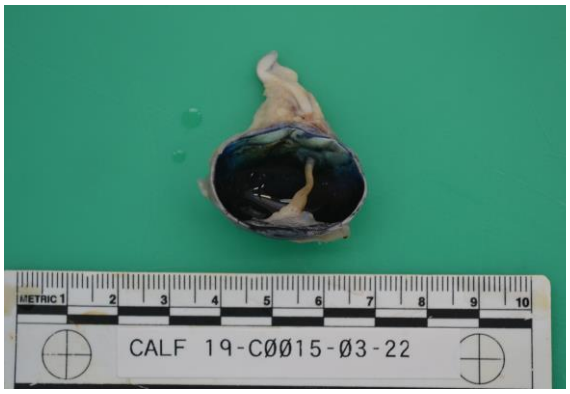

Figure 2-2. Eye, right. The retina is not anchored and attaches to th posterior asprect of a hypoplastic lens. (*Photo courtesy of:* Department of Pathobiology and Population Sciences (PPS), Royal Veterinary College, Hawkshead Lane, Brookmans Park, Hatfield, Hertfordshire, AL9 7TA.)

Clinical examination of the blind calf by veterinary ophthalmologists revealed bilaterally microphthalmic globes, a wandering nystagmus, and a tendency for ventral rotation. Both pupils were small and the pupillary light reflexes and dazzle reflexes were absent. Close examination of both eyes revealed anterior segment dysgenesis with microcornea, shallow anterior chambers and small pupils. Detailed assessment of the lenses was not feasible due to small pupil size. The calf was euthanized by barbiturate injection.

Gross Pathology:
The ocular globes are mildly sunken into the orbits. Both globes are reduced in diameter, measuring 2.7 x 2.5 cm on the right (OD) and 3.1 x 2.7 cm on the left (OS), respectively. Bilaterally, there are multifocal scleral haemorrhages. Examination of the cut-sections post-fixation reveals both eyes have little obvious lens remaining. The left eye shows collapse of the anterior chamber and there are presumptive lens remnants. These are connected by a cream colored, soft membrane to the posterior pole of the eye. The other organs, including the cerebrum, cerebellum and brainstem were grossly unremarkable.

Laboratory Results:
BVDV PCR (spleen): Negative.

Microscopic Description:
As both eyes showed similar macroscopic and histopathological changes, only the left globe is described below.

Eye (OS): Compressing against the posterior aspect of the ciliary body and the posterior pole of the lens and displacing these structures anteriorly, there is a diffusely detached, disorganized and folded retina, which crosses the posterior chamber and joins with the optic nerve head. The underlying retinal pigmented epithelium is multifocally rounded and hypertrophied (tombstoning).

The dysplastic retina is characterized by the following histological features: multifocally the outer nuclear layer forms numerous tubular structures and rosettes surrounding a central space containing eosinophilic fibrils (presumptive necrotic rods and cones) admixed with scattered degenerate neutrophils. The outer plexiform layer surrounding these rosettes and tubules is diffusely thinned and the inner and outer nuclear layers frequently co-

Figure 2-3. Eye, right. A cross section of the globe demonstrates the lack of retinal anchoring, marked disorganization of retinal layers, and attachment to the posterior surface of a lens that is flattened craniocaudally, and collapse of the anterior chamber. (HE, 5X)

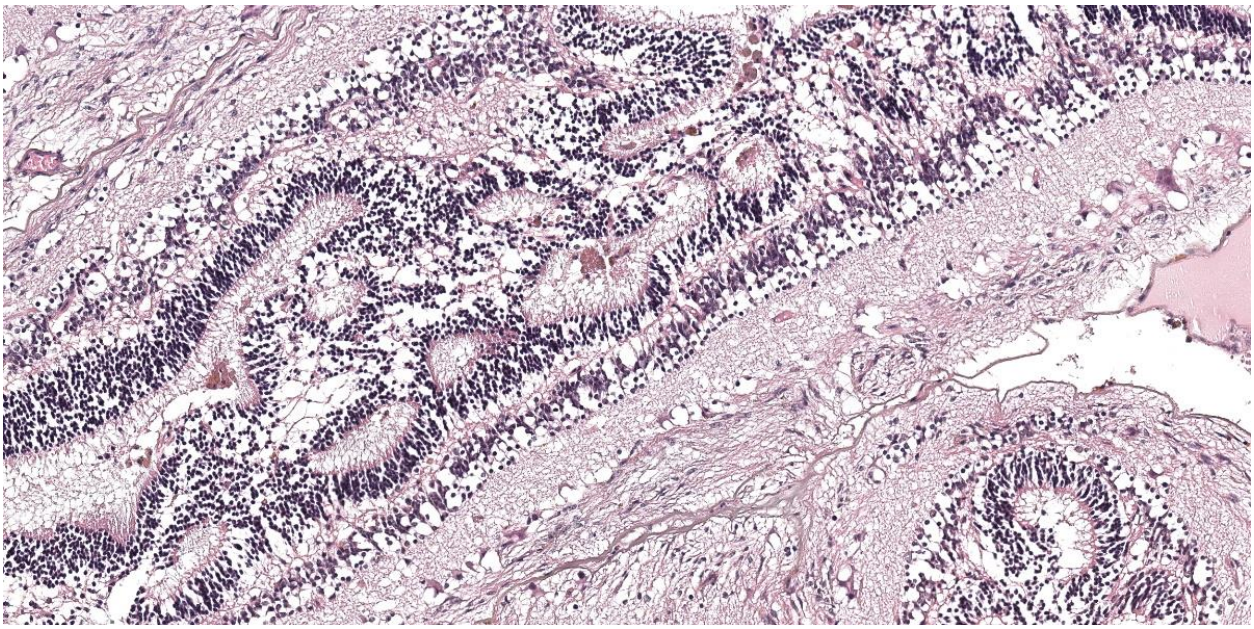

Figure 2-4. Right eye, retina. There is marked disorganization of the retina with folding upon itself. There is blending of the inner and outer nuclear layers. Rosettes formed from these combined layers, with photoreceptors projecting into the lumens of the rosettes, are common. (HE, 159X)

alesce. The inner plexiform layer, ganglion cell layer, nerve fiber layer and internal limiting membrane multifocally frequently blend together and are not readily distinguishable. However, the ganglion cell layer can be occasionally distinguished in areas of retinal folding. Multifocally, randomly distributed throughout the dysplastic retina there are large lakes of amorphous eosinophilic material admixed with melanocytes and karyorrhectic cellular debris (lytic necrosis). The nerve fibers within the adjacent optic nerve head are mildly vacuolated and there is a diffusely, mildly increased cellularity (likely oligodendrocytes) within the endoneurium of the optic nerve. As a result of the aforementioned changes, the anterior chamber is markedly collapsed, and the iris and ciliary body attach to the anterior pole of the lens (posterior synechiae).

The lens shows one or more of the following histological features: markedly reduced size, liquefaction of the cortical and nuclear fibers and moderate numbers of swollen cells with scattered retained nuclei (bladder cells). The posterior contour of the lens is uneven and there is rupture of the posterior capsule with formation of multifocal Morgagnian globules (cataract). Fragments of ruptured lens stroma are frequently surrounded by the previously described dysplastic retina. The corneal stroma is multifocally mildly edematous.

Contributor's Morphologic Diagnosis:
Globe (OS): Severe retinal dysplasia with posterior synechiae and secondary cataract.

Contributor's Comment:
Retinal dysplasia is an anomaly of the neuroectoderm that can be defined as abnormal differentiation of the retina characterized by glial proliferation and disorganization of the retinal layers.[11] As ruminants are born with mature retinas, unlike dogs and cats which continue to have post-partum retinal development, the underlying etiological cause for the retinal dysplasia in ruminants occurs in utero. In cattle and ruminants, common etiological causes include: viral infection (e.g., BVDV or bluetongue virus), hypovitaminosis A, and

Species	Cause
Sheep	Bluetongue virus
Dogs	Adenovirus, herpesvirus, genetically inherited breed-related dysplasia (English Springer Spaniel, Collies, Miniature Schnauzers, Labrador Retrievers, Samoyeds, Dobermans, Akitas, Chow Chows, Australian Shepherd dogs).[7]
Cats	Feline leukemia virus, feline panleukopenia virus, genetically inherited breed-related dysplasia (Abyssinian).
Chickens	A genetic retinal dysplasia linked to a mutation in the *MPDZ* gene has been identified.[4]

Table 1-1: Selected causes of retinal dysplasia.

genetic causes such as those documented in Shorthorn calves.[1,3,6,10,11]

In cattle, post-necrotic retinal scarring of the developing retina associated with infection by BVDV between 79 and 150 days of gestation is the most frequently studied retinal dysplasia of viral aetiology.[11] The most significant findings suggesting a viral versus a genetic cause are the presence of inflammatory infiltrates, post-necrotic retinal scarring, and scarring within the optic nerve and the choroid. BVDV has an affinity for neural tissues and, therefore, all calves with retinal dysplasia induced by the virus should also have cerebellar hypoplasia with or without hydrocephalus or hydranencephaly. While areas of necrosis are seen within the retina in this case, there was no evidence of retinal scarring or cerebellar hypoplasia, hydrocephalus, hydranencephaly or inflammation and the calf had a negative result from a BVDV PCR, making this differential less likely.

Bluetongue virus has only been described in the literature as causing retinal dysplasia in sheep, and the United Kingdom is currently free from the disease, with the last outbreak occurring in 2007.[1]

Retinal dysplasia has been described in some cases of hypovitaminosis A. This deficiency has been linked to feeding of brewer's grain, sorghum, or wheat straw which all contain low β-carotene activity and low potential vitamin A activity.[10] However, in cases of hypovitaminosis A there are usually additional changes, including a reduction in the size of the optic nerve, which were not observed in this case. Furthermore, the clinical history in this case of incidences being limited to calves from one sire and the non-responsiveness to Vitamin A supplementation the following calving season make involvement of hypovitaminosis A very unlikely.

To conclude, the most likely cause of the retinal dysplasia in this calf is a 'true' retinal dysplasia with an underlying genetic etiology, especially as in this case only calves from the same sire showed similar ocular changes. The previously documented cases of retinal dysplasia in Shorthorn cattle demonstrated a concurrent hereditary internal hydrocephalus which was not grossly observed in the submitted case. A recessive or incompletely penetrant dominant mode of inheritance was suggested, but the exact genetic mutation in Shorthorn cattle has not been identified.[3] Similarly, a genetic retinal dysplasia in Hereford calves has been described with a proposed dominant inheritance of varied expressivity although again, the underlying genetic mutation has not been defined.[5] Finally, other breeds of cattle that have suspected congenital retinal dysplasias documented in the literature include Simmentals and Japanese Black Cattle.[8,9]

The pathogenesis of retinal dysplasia in cattle is not as well characterized as in other

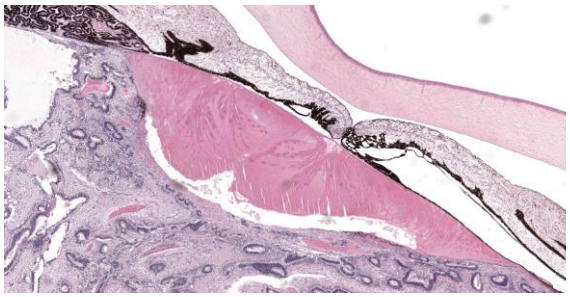

Figure 2-5. Right eye, retina and lens. The dysplastic retina is attached to the posterior aspect of the lens (there is artifactual separation due to processing). There is no capsule at the area of attachment. The lens is flattened in a craniocaudal direction. There is collapse of the anterior chamber. (HE, 32X)

domestic species, such as dogs, but is expected to follow similar mechanisms which are described below.[11]

Primary (type 1) or true retinal dysplasia is rare. It occurs due to failure of maturation by an inherently defective retinal pigmented epithelium (RPE) or failure of apposition of the two layers of the optic cup. The condition is histologically characterized by retinal rosettes, retinal folds, blending of the nuclear layers, glial scars, loss of retinal cells and retinal detachment. Rosettes should be composed of a central lumen encompassed by 1-3 layers of neuroblasts.

Secondary (type 2), or post-necrotic retinal dysplasia, is common in cattle. Secondary retinal dysplasia occurs when an infectious cause (most likely viral-induced) triggers an initial nonsuppurative panuveitis and retinitis with an associated multifocal retinal and choroidal necrosis. Over several weeks the inflammation reduces and there are scant remnants of inflammatory cells remaining microscopically and only post-necrotic scarring. The condition is characterized histologically by the presence of residual inflammation and post-necrotic retinal scarring, optic nerve scarring, and choroidal scarring. The RPE undergoes reactive hyperplasia, migration into the scarred retina or forms metaplastic, multilayered fibroglial plaques to replace the simple cuboidal epithelium. The nuclear layers are disorganized and there is rosette formation. Lesions are more common bilaterally in the non-tapetal retina and are often asymmetrical.

Retinal folding is a type of retinal dysplasia that is common in dogs and is caused by an unbalanced growth rate between the retina and the outer layers of the optic cup (choroid and sclera) or defective RPE signaling. Histologic examination reveals infolding of the neuroblastic layer away from the RPE. The folds may be transient and disappear with continued choroidal and scleral growth.

Contributing Institution:
Department of Pathobiology and Population Sciences (PPS)
Royal Veterinary College
Brookmans Park, Hatfield, Hertfordshire
www.rvc.ac.uk

JPC Diagnosis:
Eye: Ocular dysgenesis with retinal dysplasia, retinolenticular adhesion, and cataract.

JPC Comment:
The contributor gives an excellent overview of the pathogenesis, classification, and histopathologic lesions of retinal dysplasia. The various manifestations of retinal dysplasia can best be understood in the context of ocular organogenesis, which begins with bilateral evaginations of the forebrain that become separated from the developing diencephalon by the optic stalks.[11] These evaginations, called optic vesicles, grow outward toward the surface ectoderm, where signaling from a thickened area of surface ectoderm called the lens placode causes the distal optic vesicles to evaginate. These evaginations form the bilayered optic cups, and signaling from and to the lens placode causes its

evagination and separation from the ectoderm to form the developing lens.[12] The inner layer of the optic cup proliferates and becomes the retinal neuroepithelium, while the outer layer of the optic cup, via interactions with the surrounding mesenchyme, becomes the retinal pigmented epithelium (RPE). The surrounding mesenchyme subsequently develops into the vascular and fibrous tunics of the eye.[11,12]

The RPE is distinguished from the neural retina by the presence of pigment and by a monolayer epithelial arrangement as opposed to the pseudostratified epithelial arrangement of the neural retina. If these features are not present, this is considered a failure of RPE differentiation, which has implications for further ocular development as the RPE is required for subsequent retinal and ocular morphogenesis.[13] In early development, the neural retina and the RPE depend on intercellular cross-talk for normal development, and hyperplasia of one layer can occur at the expense of the other if this complex signaling is perturbed.[13]

As noted by the contributor, true retinal dysplasia is caused either by improper apposition of the two layers of the optic cup, leading to improper cell-cell signaling interactions during development, or to an improperly formed or defective RPE.[11] The histologic hallmark of true retinal dysplasia is the rosette, several most excellent examples of which are present in the examined slide, composed of a central lumen surrounded by 1-3 layers of neuroblasts with varying amounts of retinal differentiation and pink fibrils, representing photoreceptors, projecting into the lumen.[11]

In dogs, true retinal dysplasia occurs in combination with chondrodysplasia in several dog breeds, including the Labrador Retriever and Samoyeds, and retinal dysplasia may be

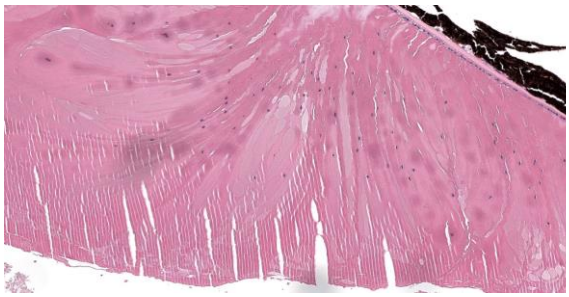

Figure 2-6. Right eye, lens. Lenticular changes include disorganization of posterior lens epithelium and cataract.

accompanied by persistent hyaloid membranes and cataracts in these breeds.[11]

Conference participants quickly found themselves engaged in discussions at once semantic and existential. Several participants interpreted the lenticular changes and the attendant inflammation as phacoclastic uveitis; however, Dr. Neto felt the term inappapropriate given that it implies a lens capsule rupture. In this case, the lens, including the lens capsule, likely formed neither correctly nor completely. Can that which was never formed be ruptured? Similarly, the term "retinal detachment" implies that the retina was once attached to the RPE, perhaps an erroneous assumption in the context of retinal dysplasia, where the layers of the optic cup were likely never properly opposed. Can that which was never together be separated?

More practically, Dr. Neto noted that this case is a great example of why one should always evaluate the slide grossly prior to histologic examination. Doing so in this case reveals an entire calf eye that fits on a standard slide – a likely indication that the eye is too small. Dr. Neto then discussed the difference between nanophthalmos, where the eye is smaller than the control eye, but is anatomically intact, and microphthalmos. Microphthalmos comes in two varieties. In simple microphthalmos, the eye is small due to a developmental problem with the optic vesicle or due to difficulty maintaining intraocular

pressures, but the eye is anatomically intact. Some consider simple microphthalmos and nanophthalmos to be equivalent conditions. Complex microphthalmos occurs when, as in this case, the eye is small but is anatomically abnormal, often with disorganized tunics. Microphthalmos can encompass anterior segment abnormalities such as cataract, as well as posterior segment abnormalities such as chorioretinal coloboma and retinal dysplasia.

Discussion of the morphologic diagnosis reflected the philosophical discussion noted above, with participants choosing to describe the retinal changes as simple dysplasia versus detachment and dysplasia. Some participants felt strongly that the chronic inflammation surrounding the lens should be included in the diagnosis, but the majority felt the inflammation was mild and relatively insignificant compared to the severe anatomic disorder present in this remarkable eye.

References:

1. Coetzee P, Vuuren MV, Venter EH, Stokstad M. A review of experimental infections with bluetongue virus in the mammalian host. *Virus Res*. 2014; 182; 21-34.
2. Gladden N, Rodriguez VG, Marchesi F, Orr J, Murdoch F. Multiple congenital ocular abnormalities including microphthalmia, microphakia and aphakia in a Simmental cross bull. *Vet Record Case Reports*. 2019; 7:e000702.
3. Greene HJ, Leipold HW. Hereditary internal hydrocephalus and retinal dysplasia in Shorthorn Calves. *Cornell Vet*; 1974; 64; 367-375.
4. Hocking PM, Guggenheim JA. The chick as an animal model of eye disease. *Drug Discovery Today: Disease Models*. 2013; 10(4); 225-230.
5. Kaswan RL, Collins LG, Blue JL, Martin CL. Multiple hereditary ocular anomalies in a herd of cattle. *J Am Vet Med Assoc*. 1987; 191(1); 97-9.
6. Leipold HW, Gelatt KN, Huston K. Multiple ocular anomalies and hydrocephalus in grade beef Shorthorn cattle. *Am J Vet Res*. 1971; 32; 1019-1026.
7. Online Medelian Inheritance in Animals (OMIA). Accessed June 23, 2023. https://omia.org/home/.
8. Siepker CL, Zimmer JL, Bedard KM, Hart KA, Czerwinski SL, Carmichael KP. Congenital cataracts and microphakia with retinal dysplasia and optic nerve hypoplasia in a calf. *Case Rep Vet Med*. 2021;2064103.
9. Uchida K, Kunieda T, Abbasi AR, Ogawa H, Murakami T, Tateyama S. Congenital multiple ocular defects with falciform retinal folds among Japanese Black Cattle. *Veterinary Pathology*. 2006; 43(6); 1017-1021.
10. Van der Lugt JJ, Prozesky L. The pathology of blindness in new-born calves caused by hypovitaminosis A. *Onderstepoort J. Vet Res*. 1989; 56; 99-109.
11. Wilcock BP, Njaa BL. Special Senses. In: *Maxie MG, ed. Jubb, Kennedy, and Palmer's Pathology of Domestic Animals*. Vol 1. 6th St. Louis, MO: Elsevier; 2016: 419-420, 469-470.
12. Vielle A, Park YK, Secora C, Vergara MN. Organoids for the study of retinal development and developmental abnormalities. *Front Cell Neurosci*. 2021;15:1-7.
13. Fuhrmann S, Zou CJ, Levine EM. Retinal pigmented epithelium development, plasiticity, and tissue homeostasis. *Exp Eye Res*. 2014;141-150.

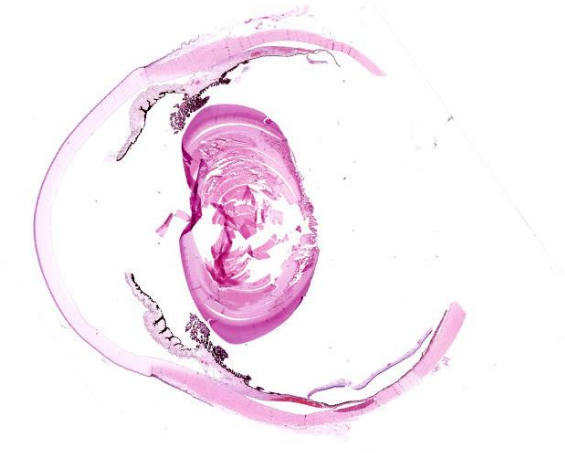

Figure 3-1. Eye, calf. A hemisection of the globe is submitted for examination. The caudal aspect of the globe, including the optic nerve, is not evident. (HE, 5X)

CASE III:

Signalment:
Juvenile intact female Black Angus calf (*Bos taurus*)

History:
Seven weaned calves had a history of rapidly progressive neurologic signs, blindness, recumbency, and death. No obvious ocular lesions were appreciated clinically, and animals were unresponsive to dexamethasone and thiamine administration.

Gross Pathology:
A 200 kg calf had mild postmortem autolysis. The anterior chambers of the right and left eyes contained a moderate amount of fibrin and opaque fluid (hypopyon). Within the cerebral white matter, there was a focally extensive area characterized by numerous, up to 2 mm diameter, dark red to brown foci (infarcts). Additional gross lesions included a severe mural and valvular endocarditis of the right atrium and ventricle, fibrinosuppurative polyarthritis, suppurative bronchopneumonia, and fibrinosuppurative bilateral otitis media.

Laboratory Results:
Aerobic culture of synovial fluid, brain, and meningeal swab: No growth detected.
Mycoplasma bovis PCR, lung: Positive.
Mycoplasma bovis PCR, synovial fluid: Negative.
Histophilus somni PCR, brain: Positive.
Histophilus somni PCR, lung: Positive.

Microscopic Description:
Right eye: Frequently, small and medium-caliber blood vessels within the retina, choroid, anterior uvea, and optic nerve (not present in the section) are expanded with partial to complete occlusion of vascular lumina by fibrin thrombi containing small numbers of degenerate neutrophils and small numbers of gram-negative coccobacilli. The walls of affected blood vessels are transmurally infiltrated and effaced by moderate numbers of viable and degenerate neutrophils and small amounts of fragmented cellular and nuclear debris (necrotizing vasculitis). Frequently, retinal tissue surrounding the most severely affected vessels is edematous and contains infiltrates of small to large numbers of degenerate neutrophils admixed with hemorrhage, necrotic cellular debris, and fibrin (ischemic necrosis). The subretinal space and vitreous contain small numbers of neutrophils admixed with hemorrhage and large amounts of loose fibrin. Free floating within the anterior chamber and disrupting and infiltrating the ciliary body at the iridocorneal angle are small to moderate amounts of fibrin admixed with small numbers of viable and degenerate neutrophils.

Contributor's Morphologic Diagnoses:
1. Right eye: Severe, multifocal to coalescing, acute necrohemorrhagic chorioretinitis and anterior uveitis with necrotizing fibrinoid vasculitis, fibrin thrombi, and intralesional gram-negative coccobacilli.
2. Right eye: Moderate, multifocal to locally extensive, acute to subacute hypopyon.

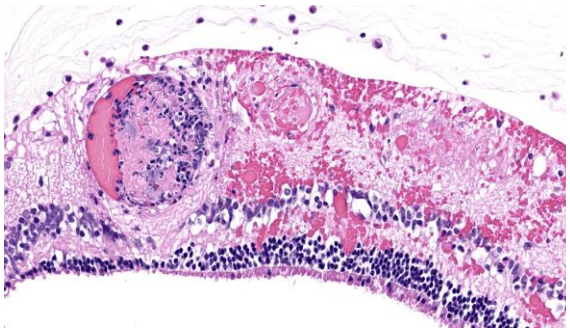

Figure 3-2. Retina, calf. There is vasculitis of small and medium-caliber vessels within the retina. Hemorrhage and edema distort the normal layered retinal architecture and result in a generalized spongiosis of the nerve fiber layers. (HE, 391X)

Contributor's Comment:
Histophilus somni (formerly *Haemophilus somnus*) is an economically significant disease of cattle and, to a lesser extent, sheep. Part of the Bovine Respiratory Disease Complex, it is associated with acute, fulminant shipping fever pneumonia primarily characterized by a fibrinous and suppurative bronchopneumonia with leukocyte necrosis, bronchiolar epithelial attenuation, and intravascular thrombi. While more commonly associated with pneumonia caused by *Mannheimia haemolytica*, oat cells are a commonly appreciated histologic feature.[4,9]

H. somni bacteremia, often a sequela to pneumonia, is reported to cause numerous and often severe changes in several tissues across multiple organ systems – termed the *H. somni* disease complex.[5,8,12,13] The most well-known manifestation of this syndrome is thrombotic meningoencephalitis (TME) characterized grossly by multiple foci of hemorrhage and necrosis throughout the brain and spinal cord, and histologically by necrotizing vasculitis with intravascular thrombosis and ischemic necrosis of dependent tissues.[2,10] Other common disease entities secondary to bacteremia include otitis externa, laryngitis/tracheitis, myocarditis, metritis causing abortion or infertility, polyarthritis, mastitis, epididymitis, ampullitis, orchitis, and conjunctivitis.[2] The hallmark histologic lesion is vasculitis with secondary thrombosis, and colonies of gram-negative coccobacilli are commonly observed within vascular thrombi, affected blood vessels, and infarcted tissues most commonly affecting the central nervous system and retina, as observed in this case.[2]

Considered part of the normal flora of the male and female genital tracts and the nasal cavity, several mechanisms of transmission have been proposed.[5,8,12,13] Calves are suspected to become infected within the first few months of life via aerosolized urine and genital discharges. As with other pathogens of the bovine respiratory disease complex, infection is usually preceded by stressful events such as weaning, routine cattle processing, or shipping.[3,4,8,9,13] Synergism with concurrent viral infections, particularly Bovine Respira-

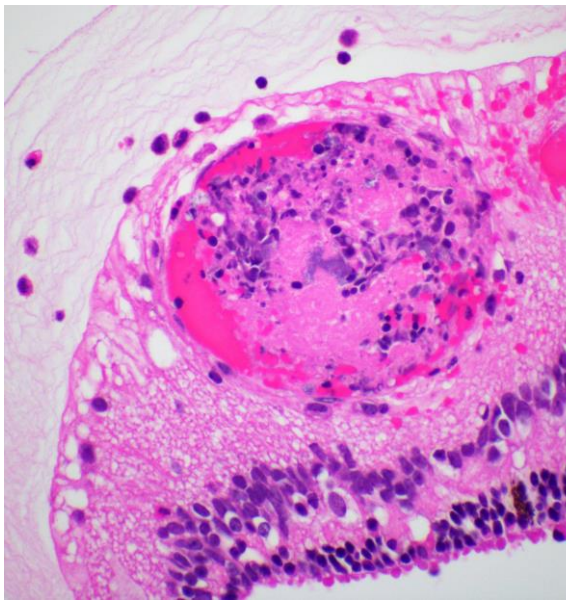

Figure 3-3. Retina, calf. Occasionally, colonies of coccobacilli are present within the thrombi (HE, 600X). (*Photo courtesy of:* Department of Veterinary Pathobiology, Oklahoma State University, Stillwater, OK 74078 USA. https://vetmed.okstate.edu/veterinary-pathobiology/index.html)

tory Syncytial Virus, in further facilitating lung damage, pneumonia, and bacteremia has been documented.[1,3] In cases of pneumonia, several virulence factors facilitating disease have been proposed including immunoglobulin Fc binding proteins (IgBPs) to resist serum and complement mediated killing; transferrin-binding proteins used in iron acquisition; biofilm formation; free oxygen-radical inhibition; and various other mechanisms of intracellular survival and immune evasion.[2,4,5,8,9,12,13] While evasion of bovine neutrophils and macrophages has been inconsistently reported as a potential virulence factor, the innate immune system (primarily via extracellular traps produced by neutrophils, macrophages, mast cells, and eosinophils) has been observed to successfully restrict the growth of *H. somni* in several anatomic locations, including the respiratory system.[8]

In cases of vasculocentric pneumonia or vasculitis secondary to bacteremia, surface lipooligosaccharide (LOS) has been proposed as a significant virulence factor. LOS has been demonstrated *in vitro* to induce endothelial cell apoptosis via activation of caspase 3, triggering the production of reactive oxygen species and nitrogen intermediates.[2,5,12,13] Another pathway suggests LOS triggers platelet activation leading to endothelial apoptosis via caspases 8 and 9, endothelial cell cytokine production and adhesion molecule expansion, and promotion of endothelial cell production of reactive oxygen species which further enhances endothelial apoptosis.[2] LOS has been demonstrated to undergo phase and antigenic variation and sialylation contributing to immune resistance.[5,13] It has been proposed that predisposed sites of infarctive lesions and vasculitis include those in which there are dramatic changes in blood vessel diameter or flow patterns that increase the likelihood of endothelial or platelet activation.[10]

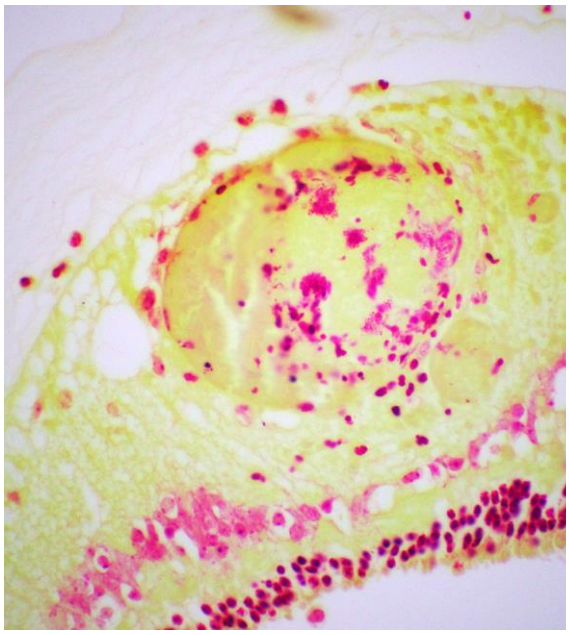

Figure 3-4. Retina, calf. A Gram stain demonstrates gram-negative coccobacilli. (Gram, 500X) (*Photo courtesy of:* Department of Veterinary Pathobiology, Oklahoma State University, Stillwater, OK 74078 USA. https://vetmed.okstate.edu/veterinary-pathobiology/index.html)

In the present case, necrotizing and fibrinoid vasculitis with thrombosis and tissue infarction was observed within the cerebrum, cerebellum, brainstem, right eye, and left ventricle and papillary muscle of the heart. In addition, there was a severe fibrinosuppurative bronchopneumonia, right ventricular endocarditis, fibrinosuppurative otitis media, and multifocal fibrinosuppurative polyarthritis. Samples of lung and brain were positive for *H. somni* on PCR. *Mycoplasma bovis* was an important differential diagnosis in this case, and PCR testing was positive for *M. bovis* in the lung but negative in the synovial fluid of the joints.

Contributing Institution:
Department of Veterinary Pathobiology
Oklahoma State University
Stillwater, OK 74078 USA
https://vetmed.okstate.edu/veterinary-pathobiology/index.html

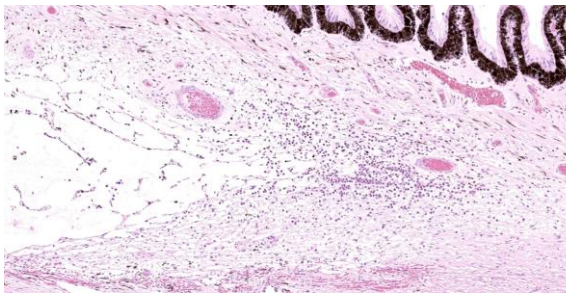

Figure 3-5. Drainage angle, calf. There is an accumulation of neutrophils and small amounts of fibrin in the drainage angle, likely the result of accumulation from low-grade anterior uveitis. (HE, 400X)

JPC Diagnosis:
Eye, retina and uvea: Vasculitis, necrotizing, multifocal, with fibrin thrombi, coccobacilli, and mild neutrophilic endophthalmitis.

JPC Comment:
Ocular histophilosis is a less common presentation of thrombotic meningoencephalitis (TME) in cattle; when present, however, the lesions are identical to the common, well-described lesions found in the brain of affected animals.[15] Ocular histophilosis commonly presents with suppurative thrombotic lesions in the choroid and the retina, often with intravascular bacterial colonies visible on H&E.[6,15] Ocular histophilosis can also present with retinitis as the sole ocular lesion, a histologic presentation shared with toxoplasmosis and infections with neurotropic viruses.[15] The presence of ocular lesions is useful as an aid in clinical diagnosis of TME and is estimated to occur in 30-50% of animals with the septicemic form of the disease.[15]

The contributor provides an excellent overview of the typical disease syndromes of histophilosis and of the virulence factors which cause its characteristic lesions. In addition to LOS, the key virulence factor discussed above, *H. somni* appears able to form biofilms on the endothelial surfaces of the microvasculature, particularly in the heart and the brain.[11] Biofilms are collections of bacteria enclosed in a matrix composed of extracellular polysaccharides, proteins, and nuclei acids. The matrix allows cells to adhere to each other and/or other surfaces and allows for metabolic cooperation among the colony.[11] The matrix also provides protection from antibacterial agents, with bacteria within biofilms being less susceptible to antimicrobial therapy.[11] It is unknown whether biofilm formation occurs within ocular histophilosis, but biofilm formation and the subsequent concentration of endotheliotoxic virulence factors appears to be a significant contributor to pathogenesis in cardiac histophilosis and TME.[11]

Conference discussion initially revolved around differential diagnoses, with the moderator gently prodding residents to recall *Chlamydia pecorum*, which can cause many of the same clinical signs and histologic lesions as *H. somni*. *Chlamydia pecorum* can be cound in aborted fetuses, calves, and cows, and can cause meningoencephalitis, thrombosis, vasculitis, pericarditis, and polyserositis, with intracytoplasmic bacteria in endothelial and mononuclear cells visible on histology.[14]

Dr. Neto discussed the various manifestations of histophilosis and noted that a negative culture does not necessarily rule out histophilosis. A recent study found that culture of *Histophilus somni* from infection-confirmed tissue is often unsuccessful, making PCR the preferred diagnostic modality.[7] Finally, Dr. Neto discussed the very nature of the thrombus itself, providing examples of fibrin-rich thombi, with the expected PTAH stain positivity, and platelet-rich thrombi, which did not stain with PTAH. Immunohistochemical staining with CD61, which forms part of the platelet fibrinogen receptor glycoprotein IIb/IIIa, can be used to identify these platelet rich, PTAH-negative thrombi in formalin-fixed tissues.

References:
1. Agnes JT, Zekarias B, Shao M, Anderson ML, Gershwin LJ, Corbeil LB. Bovine respiratory syncytial virus and *Histophilus somni* interaction at the alveolar barrier. *Infect Immun.* 2013; 81:2592-2597.
2. Cantile C, Youssef S. Nervous System. In: Maxie MG, ed. *Jubb, Kennedy, and Palmer's Pathology of Domestic Animals.* 6th ed., vol 1. Saunders Elsevier; 2016:364-365.
3. Caswell JL. Failure of respiratory defenses in the pathogenesis of bacterial pneumonia of cattle. *Vet Pathol.* 2014;51: 393-409.
4. Caswell JL, Williams KJ. Respiratory System. In: Maxie MG, ed. *Jubb, Kennedy, and Palmer's Pathology of Domestic Animals.* 6th ed., vol 2. Saunders Elsevier;2016:494, 544-546.
5. Corbeil LB. *Histophilus somni* host-parasite relationship. *Anim Health Res Rev.* 2007;8:151-160.
6. Dukes TW. The ocular lesions of thromboembolic meningoencephalitis (TEME) in cattle. *Can Vet Jour*. 1971; 12(9):180-182.
7. Headley SA, Pereira AHT, Balbo LC, et al. *Histophilus somni*-associated syndromes in sheep from Southern Brazil. *Braz J Microbiol*. 2018;49(3):591-600.
8. Hellenbrand KM, Forsythe KM, Rivera-Rivas JJ, Czuprynski CJ, Aulik NA. *Histophilus somni* causes extracellular trap formation by bovine neutrophils and macrophages. *Microb Pathog*. 2012; 54: 67-75.
9. Lopez A, Martinson SA. Respiratory System, Mediastinum, and Pleurae. In: Zachary JF, ed. *Pathologic Basis of Veterinary Diseases*. 6th ed. Elsevier; 2017:530-531.
10. Miller AD, Zachary JF. Nervous System. In: Zachary JF, ed. *Pathologic Basis of Veterinary Diseases*. 6th ed. Elsevier; 2017:882.
11. O'Toole D, Hunter R, Zekarias B, et al. Effect of *Histophilus somni* on heart and brain microvascular endothelial cells. *Vet Pathol.* 2017;54(4):629-639.
12. Sandal I, Inzana TJ. A genomic window into the virulence of *Histophilus somni*. *Trends Microbiol*. 2010; 18:90-99.
13. Siddaramppa S, Inzana TJ. *Haemophilus somnus* virulence factors and resistance to host immunity. *Anim Health Res Rev*. 2004; 5:79-93.
14. Struthers JD, Lim A, Ferguson S, et al. Meningoencephalitis, vasculitis, and abortions caused by *Chlamydia pecorum* in a herd of cattle. *Vet Pathol*. 2021;58(3):549-557.
15. Wilcock BP, Njaa BL. Special Senses. In: Maxie MG, ed. *Jubb, Kennedy, and Palmer's Pathology of Domestic Animals.* 6th ed., vol 1. Saunders Elsevier;2016:474.
16. Zachary JF. Mechanisms of Microbial Infections. In: Zachary JF, ed. *Pathologic Basis of Veterinary Diseases*. 6th ed. Elsevier;2017:189.

CASE IV:

Signalment:
11-year-old spayed female Maine Coon cat (*Felis catus)*

History:
This animal had access to the external environment and exhibited a recognized propensity for predation. No other cats shared the same household. The cat presented with multiple indolent nodular skin lesions ranging from 5 to 20 mm in diameter around both eyes, on the right ear-base region, and on the ventral aspect of the tongue, as well as an ulcerated skin nodule on the tail. The cat was referred to a veterinary ophthalmologist. A cutaneous mycobacteriosis was diagnosed through cytological and histological examination. Surgical excision accompanied by a

Figure 4-1. Eye, cat. There are multiple inflammatory nodules extending from the cornea, limbal conjunctiva, and one nodule (lower left) infiltrates the sclera. (HE, 5X).

4-week course of antimicrobial therapy (rifampicin combined with clarithromycin) was implemented. A culture followed by the molecular characterization of the isolate identified *Mycobacterium lepraemurium* in the resected periocular nodule.

The animal remained free from recurrences for at least one year following the surgical intervention; however, the cat subsequently experienced a relapse and was euthanized. The case was referred to the Institute of Veterinary Pathology of Zurich (IVPZ) for necropsy.

Gross Pathology:
The skin and subcutis, particularly on the head, dorsal region, distal limb area, and the periocular region, conjunctiva, and cornea, presented numerous randomly distributed, well-circumscribed, alopecic, beige, soft, elevated nodules with sizes varying between 0.2 and 1.5 cm in diameter. The nodules in the rostral facial region were infiltrating and destroying the osseous structures (os nasale, os incisivum, nasal conchae).

Microscopic Description:
Right eye: Within the cornea and sclera, infiltrating and expanding the ciliary body and the iris and obliterating the irido-corneal angle with focal disintegration of Descemet's membrane are multiple, well-circumscribed, coalescing granulomas ranging up to 1.2 cm in diameter. The granulomas contain numerous epithelioid macrophages, occasional multinucleate giant cells (foreign body type), scattered small lymphocytes, plasma cells, fibroblasts, fibrous connective tissue, and neutrophils. Occasionally, nodules contain a central area of necrosis characterized by abundant eosinophilic cellular and karyorrhectic debris. The cytoplasm of macrophages contains numerous negative staining rod-shaped structures. The corneal epithelium, which lines the distended corneal stroma affected by granulomas, exhibits multifocal areas of ulcerations characterized by loss of epithelial lining cells. Numerous smaller granulomas are present interspersed among the connective tissue of the eyelid and conjunctiva.
A Ziehl-Neelsen acid fast stain revealed myriad intrahistiocytic and free, 0.5 x 2 µm, acid-fast filamentous bacilli.

Contributor's Morphologic Diagnosis:
Globe: Severe, multifocal to coalescing, chronic granulomatous keratoconjunctivitis and anterior uveitis with numerous intrahistiocytic and extracellular acid-fast bacilli.

Contributor's Comment:
Mycobacteria in cats can have different clinical presentations, ranging from localized cutaneous lesions to generalized, systemic infections. Mycobacteria are categorized into three main groups.

The ***Mycobacterium tuberculosis*** **complex (MTBC)** contains 9 closely-related host adapted species with varying ability to cross species barriers. Among cats, the most prevalent species from this group (in the UK) are the rodent-adapted *Mycobacterium microti* and the cattle-adapted *Mycobacterium bovis.*[6] The lesions caused by MTBC are usually present in skin and lymph nodes as an effect of

bite and fighting wounds, but may also be present in the lungs, gastrointestinal tract, and rarely, joints.[8]

Non-tuberculosis mycobacteria (NTM) include mainly opportunistic organisms that may be found in the environment, including water, soil, aerosols, and vegetation. In cats, the species of main concern are *Mycobacterium malmoense*, *Mycobacterium branderi/ shimoidei*, and *Mycobacterium avium.* The infections caused by pathogens from this group are usually systemic and have a high shedding potential given the fact that extracellular bacilli are found in respiratory and intestinal epithelium as well as in glomerular tufts.[7]

The ***Mycobacterium leprae*** **complex (MLC)** causes "feline leprosy syndrome" (FLS) and includes *M. lepraemurium, M. visibile,* and *Mycobacterium* sp. strain Tarwin. The standard microbiological methods are not effective for the culture of these species. Clinical presentation of the infection is usually limited to skin, and the dermal lesions are nodular, often ulcerated, and present predominantly on the head and the forelimbs. The generalized nodular skin disease consists of numerous disseminated skin nodules and is a rarely observed pattern of infection. Despite the predisposition of *M. lepraemurium* to cause damage in the head area, it does not tend to involve the eyes. In contrast, *Mycobacterium* sp. strain Tarwin can cause feline leprosy with a particular propensity to produce lesions on the head, particularly involving the eyes and periocular skin.[5]

Histologically, the lesions seen in cats affected by feline leprosy syndrome can be divided into two categories. Lepromatous leprosy is thought to be the malignant form and is accompanied by numerous, typically intracellular acid-fast bacilli (multibacillary), whereas the tuberculoid leprosy is frequently

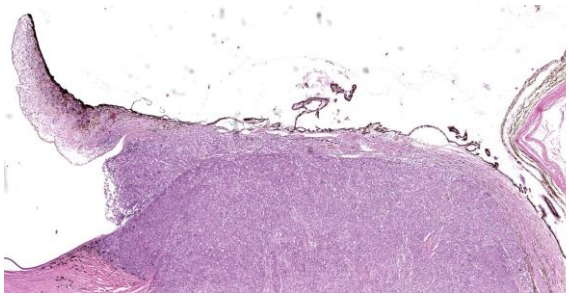

Figure 4-2. Eye, cat. The inflammatory nodule infiltrating the sclera extends into the drainage angle, uvea, and choroid. (HE, 60X)

recognized as the benign form of the disease and is defined by the presence of relatively small numbers of intrahistiocytic acid-fast bacilli (paucibacillary).[2]

The most likely method of transmission for *M. lepraemurium*, which causes leprosy in cats and rodents, is through the bites of infected prey during hunting. It has not yet been established whether there is a niche in the environment where the pathogen can survive without its host; however, the clinical and histological findings in wild rodents, where the pathogen is well adapted, and cats serving as incidental hosts seem to support this hypothesis.[1]

Contributing Institution:
Institut für Veterinärpathologie
Vetsuisse-Fakultät, Universität Zürich
https://www.vetpathology.uzh.ch

JPC Diagnosis:
Eye: Keratoconjunctivitis, scleritis, and uveitis, pyogranulomatous, multifocal to coalescing, severe.

JPC Comment:
As the contributor notes, *Mycobacterium lepraemurium* does not typically involve the ocular tissues; in fact, this is the only case of ocular mycobacteriosis due to *M. lepraemurium* reported in Europe to date.[1,3] In a recent study of ocular mycobacteriosis in cats, tuberculosis (infection with *Mycobacterium*

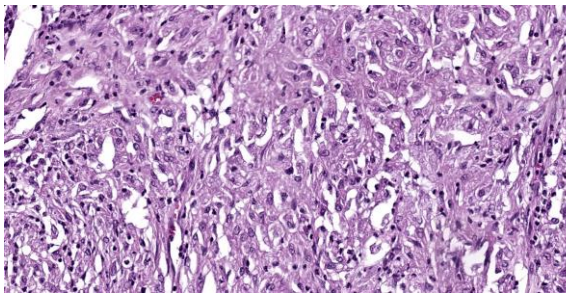

Figure 4-3. Eye, cat. The inflammatory nodules are composed of innumerable epithelioid macrophages with fewer lymphocytes, plasma cells, and neutrophils. (HE, 311X)

bovis, Mycobacterium microti, or a nonspeciated *Mycobacterium tuberculosis* complex pathogen) was diagnosed in 91% of cats, while *Mycobacterium lepraemurium* was identified in only 9% of cats, providing further evidence for the relative rarity of this pathogen in ocular tissues.[3] The study found that the choroid, retina, ciliary body, and sclera were the tissues most affected in ocular disease caused by mycobacterial organisms other than *M. lepraemurium*, with inflammation being most florid within the choroid.[3] By contrast, the two ocular cases of *M. lepraemurium* infection contained lesions restricted to the cornea, sclera, and conjunctiva.[3] Infection restricted to the external tunic of the eye is typical of this infection and may be due to the inability of *M. lepraemurium* to replicate well at higher body temperatures.[3]

The division of feline leprosy syndrome into lepromatous or tuberculoid forms is based on the differential elaboration of canonical cytokines by CD4+ T lymphocytes. In the tuberculoid form, Th1 lymphocytes produce large amounts of IL-2 and interferon gamma, resulting in a cell-mediated immune response rich in activated macrophages and T-cells which, in a virtuous immune feedback loop, stimulate mutual proliferation and activation and the subsequent containment of infection.[4] Lesions of this type are paucibacillary due to the low numbers of surviving infectious organisms.

By contrast, lepromatous disease produces multibacillary lesions that are driven by a Th2 lymphocyte response. In these cases, the Th2 lymphocytes produce a cytokine milieu rich in IL-4, IL-10, and IL-13, all of which suppress macrophages and stimulate B lymphocytes, and IL-5, which recruits eosinophils. The resulting humoral response stifles cell-mediated immunity and allows infections to progress, resulting in more diffuse, multibacillary infections such as that present in this case.[4] In vivo, these responses do not exist as discrete entities, but rather occur on a continuum with the relative contribution of Th1 and Th2 responses driving disease progression and clinical outcomes. In fact, the recent study discussed above found that high bacterial loads were found with infections with *M. bovis, M. microti* and *M. lepraemurium*, indicating that the presence of multibacillary lesions is not necessarily restricted to infections with non-tuberculosis mycobacteria and *Mycobacterium leprae* complex pathogens.[4]

Conference participants discussed the origin of these stiking lesions and debated whether the infection was of hematogenous or external, "outside-in" origin. Given the gross appearance and the nodules arising from the conjunctiva and cornea, participants decided that an external origin was most likely. Participants also discussed whether the discontinuity in Descemet's membrane was real or artifactual, before deciding that the lesion is real due to the highly reactive underlying stroma. Elsewhere in the cornea, some loss of stromal clefting was noted, but Dr. Neto cautioned resident against overinterpreting corneal edema in a necropsied animal as some post-mortem corneal aqueous absorption is common.

Dr. Neto also discussed the choice of carbolfuchsin stains for acid-fast organisms. In general, she finds Ziehl-Neelsen to be less

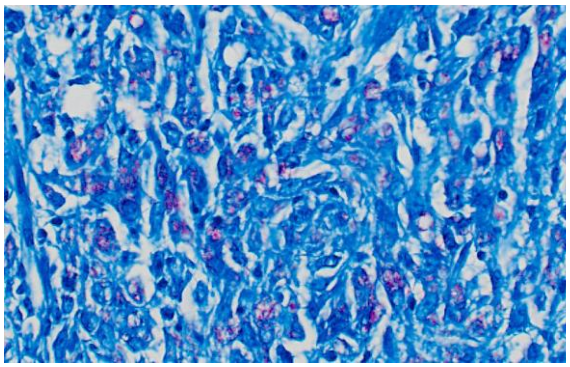

Figure 4-4. Eye, cat. An acid-fast stain demonstrates acid-fast bacilli in numerous macrophages within the inflammatory infiltrate. The inflammatory nodules are composed of innumerable epithelioid macrophages with fewer lymphocytes, plasma cells, and neutrophils. (Fite-Faraco, 400X)

effective for non-tuberculous *Mycobacterium* as the solvent used may rapidly remove dye from the organisms' thinner walls; however, Fite-Faraco has can cause indiscriminate staining of necrotic material, making Ziehl-Neelsen the stain of choice in the face of abundant necrosis.

References:

1. Ghielmetti G, Schmitt S, Friedel U, Guscetti F, Walser-Reinhardt L. Unusual presentation of feline leprosy caused by *Mycobacterium lepraemurium* in the alpine region. *Pathogens*. 2021;10(6):687.
2. Juarez-Ortega M, Hernandez, VG., Arce-Paredes P, Villanueva EB, Aguilar-Santelises M, Rojas-Espinosa O. Induction and treatment of anergy in murine leprosy. *Int. J. Exp. Pathol*. 2014;96:31-41.
3. Mitchell JL, MacDougall L, Dobromylskj MJ, et al. Ocular mycobacterial lesions in cats. *Vet Pathol*. 2022; 59(5):792-805.
4. Modlin RL. Th1-Th2 paradigm: insights from leprosy. *J Invest Dermatol*. 1994;102(6):828-832.
5. O'Brien CR, Malik R, Globan M, Reppas G, McCowan C, Fyfe JA. Feline leprosy due to Candidatus 'Mycobacterium tarwinense': Further clinical and molecular characterisation of 15 previously reported cases and an additional 27 cases. *J Feline Med Surg*. 2017;19(5):498-512.
6. O'Halloran C, Gunn-Moore D. Mycobacteria in cats: an update. *Practice*. 2017 Oct;39(9):399-406.
7. Pekkarinen H, Airas N, Savolainen L.E, et al. Non-tuberculous mycobacteria can cause disseminated mycobacteriosis in cats. *J Comp Pathol*. 2018 Apr;160:1-9.
8. Peterhans S, Landolt P, Friedel U, et al. *Mycobacterium microti*: not just a coincidental pathogen for cats. *Front Vet Sci*. 2020;7:590037.
9. World Organisation for Animal Health (OIE). Bovine tuberculosis. In: *OIE Terrestrial manual*. 8th ed. OIE;2018;1058-1074.

WSC 2023-2024
Conference 12 Self-Assessment

1. Which of the following is inhaled in animals infected with *Histoplasma capsulatum*?
    a. Yeasts
    b. Arthrospores
    c. Macroconidia
    d. Microconidia

2. Which of the following has not been identified as a cause of retinal dysplasia in cattle?
    a. Bovine pestivirus
    b. Hypovitaminosis A
    c. Bovine orbivirus (BT virus)
    d. Bovine herpesvirus-1

3. True or false: Hemophilus somnus is part of the normal flora of cattle.
    a. True
    b. False

4. In cases of vasculocentric Hemophius somni infection, which of the following has been proposed as a significant virulens factore?
    a. Lipo-oligopolysaccharide
    b. Trnasferrin-binding proteins
    c. Biofilm formation
    d. Free oxygen-radical inhibition

5. True or false: The sole cause of feline leprosy in M. lepraemurium?
    a. True
    b. False

Joint Pathology Center
Veterinary Pathology Services

WEDNESDAY SLIDE CONFERENCE 2023-2024

Conference #13 **13 December 2023**

CASE I:

Signalment:
3-year-old intact male, Chinese-origin cynomolgus macaque (*Macaca fascicularis*)

History:
This cynomolgus macaque from a maintenance colony at a contract research organization presented for ptosis of the left eye (OS). Physical exam additionally identified mydriasis, exophthalmos, abnormal retropulsion, and ophthalmoplegia OS. Direct pupillary light reflex (PLR) was absent OS, and consensual PLR was normal in the right eye (OD); direct PLR was normal OD, and consensual PLR was absent OS. The diagnosed ophthalmoplegia OS was refractive to medical treatment, and euthanasia was elected.

Gross Pathology:
The left orbit was pale yellow. There was a firm, yellow-tan mass filling the left caudal sinuses and displacing the nasal turbinates and adjacent bone, including the orbit and ventral cranium. The ventral cranial vault was focally displaced ventrally, and there was malacia of the adjacent left temporal brain.

Microscopic Description:
Arising from the nasal turbinates and infiltrating the nasal turbinates, skeletal muscle, and surrounding bone is a densely cellular, poorly circumscribed proliferation of neoplastic cells. Neoplastic cells are arranged in nests and packets that are supported by fine fibrovascular stroma. These cells are polygonal to spindloid, have variably distinct cell borders, and contain a moderate amount of eosinophilic cytoplasm. Nuclei are ovoid to reniform, have coarsely stippled chromatin, and frequently contain 1-2 prominent nucleoli. Anisokaryosis is moderate and there are 1-3 mitoses per high power field. In areas where the neoplasm extends to the overlying squamous epithelium, there is erosion and ulceration with associated hemorrhage,

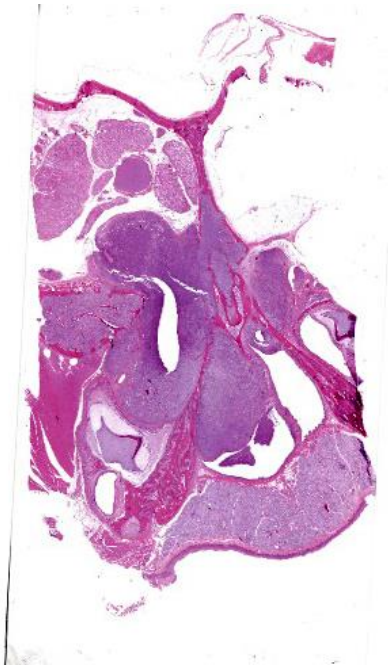

Figure 1-1. Nasal cavity, cynomolgus macaque. A densely cellular neoplasm infiltrates and effaces the bone of the nasal turbinate and maxilla and extends into the surrounding skeletal muscle. (HE, 5X)

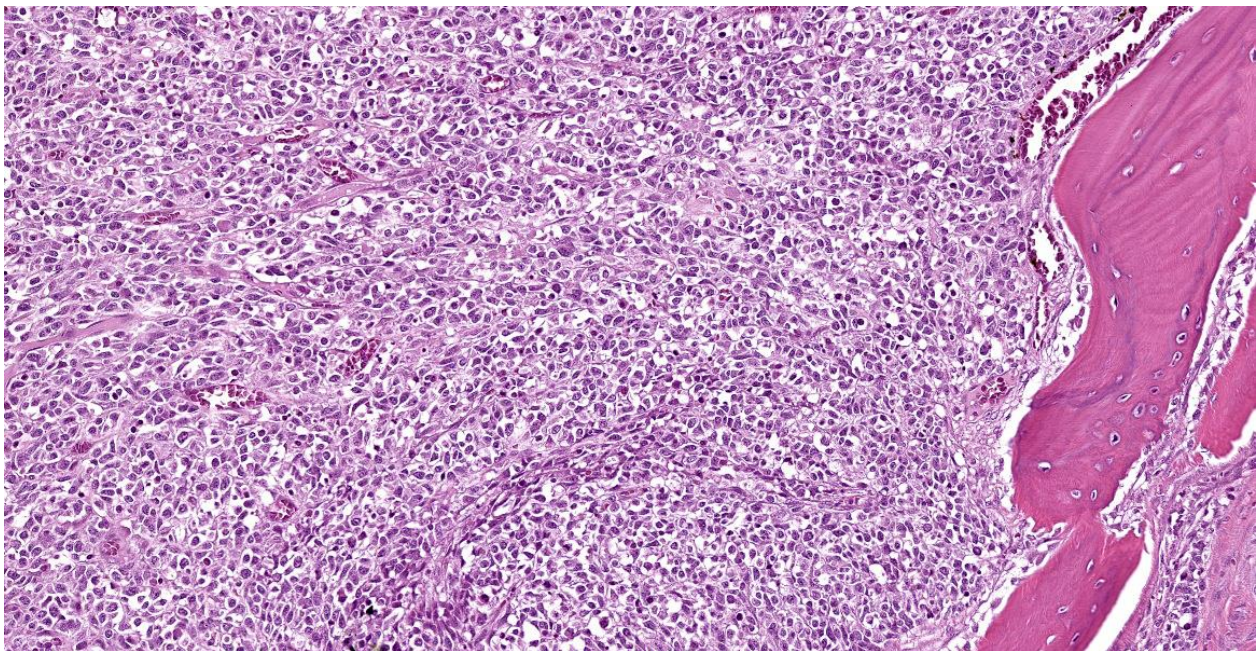

Figure 1-2. Nasal cavity, cynomolgus macaque. Neoplastic cells are arranged in nests and packets and efface the surrounding bone. (HE, 183X)

inflammatory infiltrates of lymphocytes, plasma cells, and neutrophils, and abundant coccoid bacteria. Neoplastic cells were not present in sections of ocular or periocular tissue, although there was degeneration and regeneration of the extraocular skeletal muscle. There is destruction of cortical and woven bone, with replacement by neoplastic cells.

Contributor's Morphologic Diagnosis:
Nasal turbinates: Esthesioneuroblastoma (Olfactory neuroblastoma).

Contributor's Comment:
Esthesioneuroblastomas are malignant neoplasms that appear histologically similar to neuroendocrine tumors. They arise from the neuroectoderm of the olfactory mucosa along the superior nasal vault. Esthesioneuroblastomas have been reported in humans, dogs, cats, horses, cows, mice, axolotls, and fish; however, they are rarely reported in cynomolgus macaques. To the authors' knowledge, this is the second report of an esthesioneuroblastoma in a cynomolgus macaque.

In the horse, literature describes neoplastic cells labelling for antibodies against neurofilament protein, synaptophysin, glial fibrillary acidic protein, neuron-specific enolase, microtube-associated protein, and S-100 protein. Microtubule-associated protein (MAP-2) has been reported to label positively in the dog, cat, and horse; however, due to the lack of specificity of immunohistochemical markers, definitive diagnosis is made by visualizing cell processes that contain microtubule neurofilaments on transmission electron microscopy. Dense core neurosecretory granules are also visualized on TEM. These neoplasms are locally aggressive and often invade through the cribriform plate and into the sinuses and brain.

Contributing Institution:
Pathology Department
Charles River Laboratories – Mattawan
www.crl.com

JPC Diagnosis:
Nasal cavity and maxilla: Malignant neoplasm.

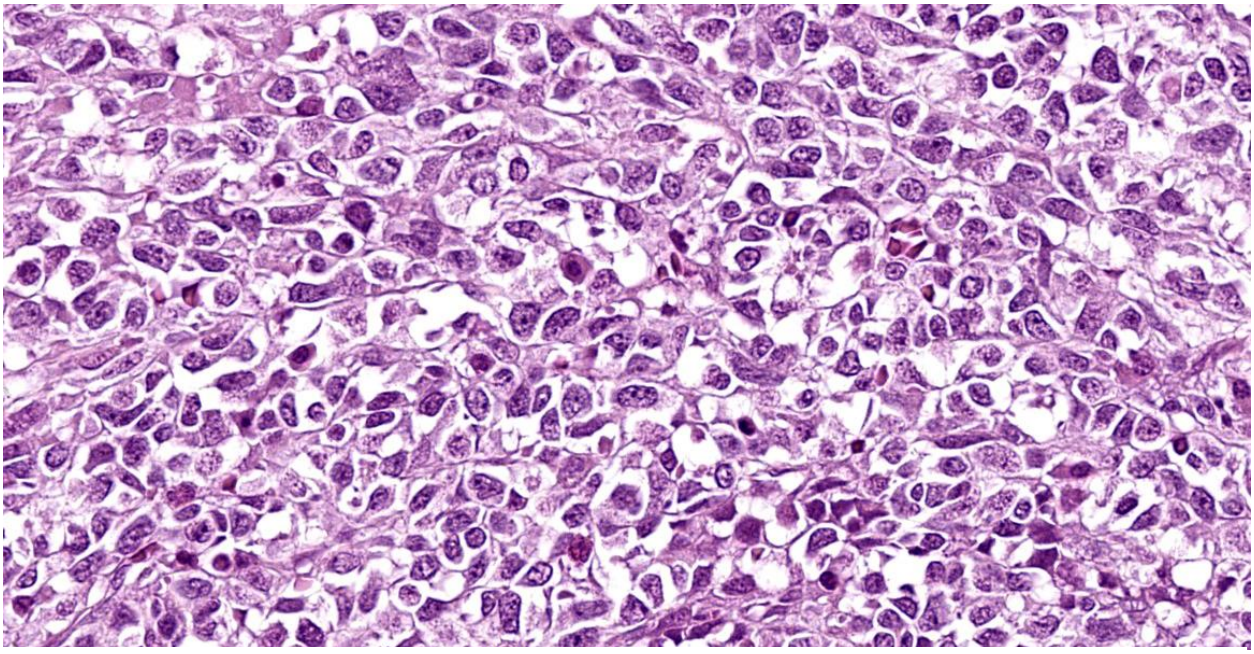

Figure 1-3. Nasal cavity, cynomolgus macaque. High magnification of neoplastic cells. (HE, 597X)

JPC Comment:
Esthesioneuroblastomas, also known as olfactory neuroblastomas (ONBs), are characterized histologically by epithelioid neoplastic cells with indistinct borders and scant cytoplasm that are often separated by neurofibrillary material. Rosette formation is a characteristic feature.[2] ONBs are presumed to originate from olfactory epithelium and most tumors are located in the caudal nasal cavity in close proximity to the cribriform-plate.[5] ONBs are typically invasive, leading to osteolysis of facial structures, deformation of the ethmoturbinates, and invasion into the cerebral cortex.[2,5]

Human ONBs are evaluated using a four-tiered grading scheme and case reports in veterinary medicine tend to apply this scheme to animal ONBs, though it isn't clear that this grading predicts biologic behavior in animals.[1,5] Under this rubric, grade I ONBs exhibit lobular architecture, minimal nuclear pleomorphism, prominent neurofibrillary matrix, rosette formation, no mitotic figures or necrosis, and variable amount of calcification. By contrast, grade IV ONBs have variable amounts of lobular architecture, marked nuclear pleomorphism, absent neurofibrillary matrix, occasional rosette formation, marked mitoses, prominent necrosis, and no calcification.[1]

This week's conference was moderated by Dr. Derron Alves, Chief of the Infectious Disease Pathogensis Section at the National Institute of Allergy and Infectious Diseases. Conference discussion began with a review of the microscopic anatomy of the nasal cavity and surrounding structures and the types of epithelium present in the nasal cavity.

Conference discussion focused on the seeming mismatch between the histologic appearance of ONB described in the literature and the appearance of the neoplasm on the examined slide. Participants noted the complete lack of rosette formation, the lack of neurofibrillary matrix, and the presence of respiratory epithelium with no identifiable olfactory epithelium within the examined section. An attempt was made to match the tumor to the described Grade IV ONB histomorphology, but the lack of necrosis and rosette formation

did not pass the smell test. Immunohistochemical results were similarly vexing, with neoplastic cells negative, or the stains non-contributory, for the following immunohistochemical markers: NSE, NeuN, synaptophysin, chromogranin, CD3, CD20, CD138, pancytokeratin, and vimentin.

Participants had a wide range of differential diagnoses for this enigmantic tumor, including lymphoma, plasma cell tumor, round cell tumor, ONB, adenocarcinoma, and non-productive osteosarcoma. While most partipants agreed that the tumor was malignant based on the significant invasion and bony remodeling, participants felt that the histomorphology present in this section made ONB unlikely. The moderator proposed a differential diagnosis of "undifferentiated tumor, high grade," which was as specific as participants were willing to get without further investigation.

This case was referred for post-conference consultation to the soft tissue and oral and maxillofacial MD pathologists at the Joint Pathology Center, who agreed that the morphologic characteristics of the tumor were inconsistent with human ONB. They proposed an additional battery of immunohistochemical stains, to include CD45rb, desmin, ERG, MUC-1, S-100, and smooth muscle actin, to sniff out the cell of origin. These stains were performed; however the vast majority of immunohistochemical stains performed on this neoplasm were non-contributory due to inappropriate behavior of internal controls, making our immunohistochemical results, in the main, unreliable.

After multiple external consultations and a plethora of unhelpful immunohistochemistry, conference participants remained unable to ascribe a cell of origin to this inscrutable neoplasm and preferred a somewhat on-the-nose morphologic diagnosis of "malignant neoplasm."

References:

1. Brosinski K, Janik D, Polkinghorne A, von Bomhard W, Schmahl W. Olfactory neuroblastoma in dogs and cats – a histological and immunohistochemical analysis. *J Comp Path*. 2012;146:152-159.
2. Caswell JL, Williams KJ. Respiratory System. In: Maxie MG, ed. *Jubb, Kennedy, and Palmer's Pathology of Domestic Animals*. 6th ed. Vol 2. Elsevier;2016:479.
3. Lubojemska A, Borejko M, Czapiewski P, et al. Of mice and men: olfactory neuroblastoma among animals and humans. *Vet Comp Oncol*. 2014,13:70-82.
4. Meuten, DJ. *Tumors in Domestic Animals*. 5th ed. Iowa State Press;2016:473-474.
5. Siudak K, Klingler M, Schmidt MJ, Herden C. Metastasizing Esthesioneuroblastoma in a Dog. Veterinary Pathology. 2015;52(4):692-695.

CASE II:

Signalment:
4-year-old, intact male rhesus monkey (*Macaca mulatta*)

History:
The animal was experimentally infected with Simian-Human Immunodeficiency Virus (SHIV) and had a two-month history of nasal discharge and coughing and intermittent diarrhea for over a year.

Gross Pathology:
The animal is in lean body condition. Upon opening the carcass, scant adipose stores are observed. Upon opening the peritoneal cavity, the gallbladder and common bile ducts are moderately thickened. The liver is diffusely slightly pale and on cut surface the bile

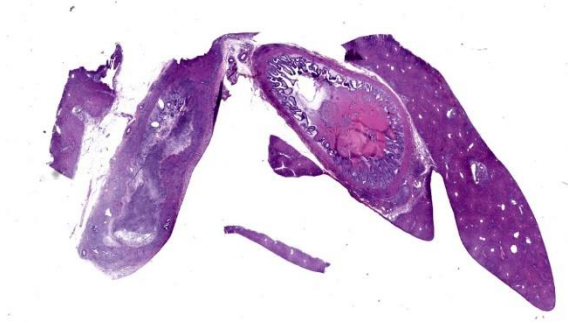

Figure 2-1. Liver, gallbladder, common bile duct, rhesus macaque. Subgross magnification of submitted tissue with (L-R): liver, common bile duct, and a second larger section of liver with gallbladder. There is partial effacement of the mucosa of the common bile duct with abundant inflammation. (HE, 5X)

ducts are prominent throughout. Upon opening the pleural cavity, the lungs are mottled a pink, pale tan with a speckling of red and purple. Upon cutting through the nasal cavity, the nasal turbinates on the right side appear somewhat thickened or inflamed. Lesions are not observed in the brain, heart, kidneys, spleen, pancreas, the entire male reproductive tract, and the entire gastrointestinal tract.

Laboratory Results:
Nasal cavity swabs: *Staphylococcus aureus* (MRSA positive).
PCR on lungs: Positive for *Pneumocystis carinii.*

PCR on common bile duct: Negative for *Enterocytozoon bieneusi*; positive for *Cryptosporidium parvum*.

Microscopic Description:
Common bile duct: There is a large area of mucosal and submucosal necrosis with abun dant degenerate neutrophils and lesser macrophages. The remaining superficial mucosa is attenuated and the submucosa is edematous with abundant neutrophils, eosinophils, macrophages, and plasma cells. A few small areas of hemorrhage are observed. Areas of mucosal herniation through the muscle layers are observed. The smooth muscle has areas of atrophy and fibrosis with a mild eosinophilic and neutrophilic infiltrate. Numerous cells (smooth muscle, fibroblasts, epithelial cells) contain large basophilic intranuclear viral inclusion bodies. The mucosa has multifocal areas of 3-5 µm round protozoal organisms.

Liver: The portal areas have a mild interstitial fibrosis, mild to moderate biliary hyperplasia, a mild mixed inflammatory infiltrate, a few small areas of hepatocellular necrosis, and occasional biliary mucosal protozoal organisms.

Gallbladder: The lumen contains what appears to be a thick eosinophilic secretion admixed with mineralized and cellular debris. There are multifocal areas of submucosal edema. The mucosa has multifocal areas of protozoal organisms. The serosa has dense areas of plump fibroblastic proliferation admixed with numerous eosinophils.

Contributor's Morphologic Diagnoses:
1. Common bile duct: Cholangitis, necrotizing, severe, with intranuclear inclusion bodies consistent with cytomegalovirus and protozoal organisms consistent with *Cryptosporidium*.
2. Liver: Hepatitis, portal, with biliary hyperplasia and *Cryptosporidium*.
3. Gallbladder: Cholecystitis, with *Cryptosporidium*.

Contributor's Comment:
This is a classic example of opportunistic infections in an immunocompromised rhesus macaque. The monkey was experimentally infected with Simian-Human Immunodeficiency Virus (SHIV). SHIV is a chimeric virus that contains HIV-1 viral envelope protein (Env) with a SIV backbone. The macaque adapted SIV (SIVmac) mirrors many of the key components of HIV-1 infection;

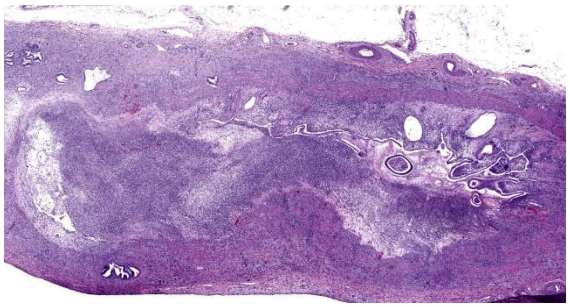

Figure 2-2. Common bile duct, rhesus macaque. There is segmental necrosis and suppurative inflammation of the wall of the common bile duct. Suppurative inflammation is present in the lumen of the duct. (HE, 19X)

however, there are differences between their Envs and the creation of a SIV virus with a HIV Env allows animal models to be used.[2] SHIV leads to a severe decrease in CD4 lymphocyte populations allowing opportunistic bacteria, fungi, viruses, and protozoa to cause disease.

Cytomegalovirus (CMV) is a betaherpesvirus.[1] CMV is ubiquitous in non-human primate populations. It has been identified in rhesus macaques (*Macaca mulatta*), Japanese macaques (*Macaca fuscata*), african green monkeys (*Cercopithecine aethiops*), drill monkeys (*Mandrillus leucophaeus*), squirrel monkeys (*Saimiri sciureus*), baboons (*Papio* sp.), marmosets (*Saquinus fuscicollis*, *Callithrix jacchus*), and chimpanzees (*Pan troglodytes*).[1]

In breeding colonies of rhesus macaques, 50% of infants are seropositive for CMV by 6 months of age and almost 100% are seropositive by 1 year of age. Horizontal transmission is believed to be from mother to infant through breast milk and saliva.[1] Virus is also secreted in urine, semen, and cervical secretions. In immunocompetent animals, the virus has a predilection for salivary glands.[1] In immunodeficient animals, as in human CMV, simian CMV can produce end-organ disease in the central and peripheral nervous system, lungs, lymph nodes, hepatobiliary system, gastrointestinal tract and arteries.[3] CMV can be detected within multiple tissues or may be limited to a single site.[1,3]

The virus produces intranuclear (owl's eye appearance) and intracytoplasmic inclusion bodies and induces tissue necrosis and neutrophilic infiltrate in immunosuppressed animals similar to that seen in human CMV. Cells most commonly infected include fibroblasts, epithelial cells, endothelial cells, smooth muscle cells, and macrophages.[9]

Cryptosporidium is a parasitic protozoa belonging to the phylum Apicomplexa.[10] It is associated with enteric disease (diarrhea) in numerous species.[5] Animals can be infected with multiple species of *Cryptosporidium*.[10] Transmission is through the fecal-oral route and contact with animals, manure, or contaminated food and water.[5] Transmission occurs through ingestion of oocysts which release sporozoites that infect intestinal epithelial cells. The parasite then replicates asexually in an intracellular but extracytoplasmic niche present at the luminal surface of intestinal epithelial cells. Lysis of the host cell releases merozoites that reinvade other epithelial cells. After three rounds of asexual replica-

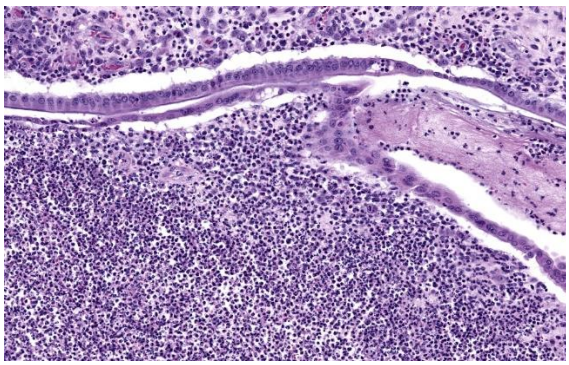

Figure 2-3. Common bile duct, rhesus macaque. There is segmental loss of the mucosal epithelium and profound suppurative and lymphocytic inflammation of the edematous lamina propria. (HE, 190X)

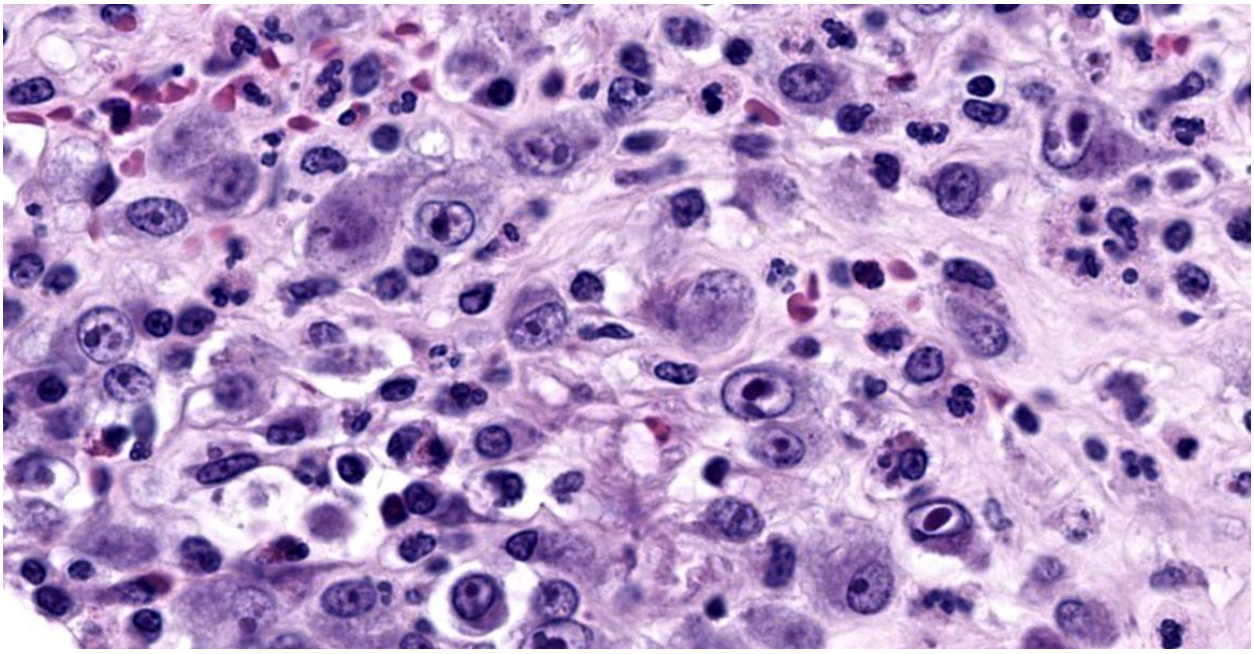

Figure 2-4. Common bile duct, rhesus macaque. Mesenchymal and inflammatory cells within the inflamed lamina propria contain karyomegalic cytomegalovirus inclusions. (HE, 881X)

tion, obligate sexual reproduction leads to generation of more oocysts which can hatch and reinfect within the same host or be shed into feces for transmission.[4,5] In immunodeficient human hosts, infection leads to chronic disease, which can manifest as biliary involvement and sclerosing cholangitis. Cryptosporidium can also infect the respiratory tree, stomach, and pancreas.[7,11] In human AIDS, cryptosporidiosis infection increases as CD4+ T-cell numbers decrease. Restoration of these cell numbers are associated with clearance of the parasite.[4]

Hepatobiliary dysfunction is common in HIV/AIDS. AIDS cholangiopathy (AC) is a well-documented biliary syndrome in severely immunocompromised AIDS patients. AC is a syndrome of biliary obstruction and liver damage due to infection-related strictures of the biliary tract. AC is highly associated with opportunistic infections. These infections, in decreasing prevalence, are *Cryptosporidium*, cytomegalovirus, and *Enterocytozoon bieneusi*.[6]

Contributing Institution:
National Institutes of Health
Division of Veterinary Resources
Bethesda, MD

JPC Diagnoses:

1. Common bile duct: Choledochitis, necrotizing, circumferential, chronic, diffuse, marked, with intranuclear karyomegalic viral inclusions and apicomplexan schizonts.
2. Liver, bile ducts: Cholangiohepatitis, lymphoplasmacytic and eosinophilic, chronic, multifocal, mild, with biliary hyperplasia and apicomplexan schizonts.
3. Gallbladder: Cholecystitis, lymphocytic and eosinophilic, diffuse, mild, with apicomplexan schizonts.

JPC Comment:
As the contributor notes, the pathology in this case is due to opportunistic pathogens emboldened by immunosuppression secondary to experimental SHIV infection. SHIV is a chimeric retrovirus consisting of an HIV

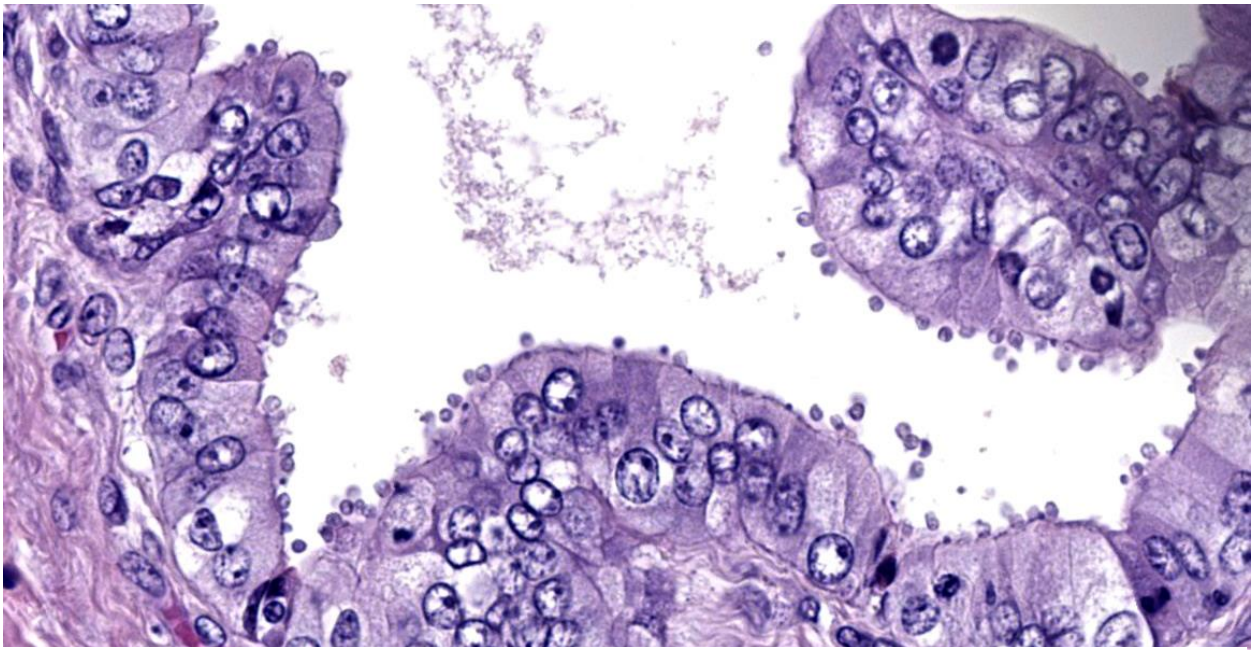

Figure 2-5. Liver, rhesus macaque. Schizonts of *Cryptosporidium* sp. Are intimately attached to the epithelium lining the sublobular bile ducts. (HE, 775X)

envelope protein produced within an SIV carrier that is used for research into HIV-1 antibody-based vaccines, neutralizing antibodies, and other envelope protein-targeting strategies.

Retroviruses such as SHIV, SIV, and HIV take their family name from the presence of a reverse transcriptase within the virion that is encoded in the viral genome.[7] Reverse transcriptase is an RNA-dependent DNA polymerase that transcribes in a "reverse" fashion from RNA to DNA. All replication-competent members of the retrovirus family contain a minimum armamentarium of three major genes: *gag*, *pol*, and *env*. Reverse transcriptase is encoded by *pol* (polymerase), which also encodes the key enzyme integrase.[7] The *gag* (group-specific antigen) gene encodes structural proteins and the *env* (envelope) gene encodes an envelope transmembrane glycoprotein that is broken down into a surface protein subunit (SU) and a transmembrane subunit (TM), is displayed on the virion surface, and is responsible for entry into host cells.[7] A fourth essential gene, *pro*, encodes a protease that cleaves viral precursor proteins and is expressed differently in various retroviruses.[7]

A mature retroviral virion includes a nucleocapsid containing the RNA genome and the enzymes reverse transcriptase, protease, and integrase, all of which are surrounded by an envelope studded with many SU and TM proteins. Upon encountering a host cell, the SU envelope glycoprotein makes first contact and initiates conformational changes within the TM subunit that leads to fusion of the viral and host cellular membranes and the extrusion of the nucleocapsid into the host cytoplasm. Once in the cytoplasm, reverse transcriptase co-opts the host cell replicative machinery and produces double-stranded DNA copies of the viral genome which are then integrated into random sites within the host's chromosomal DNA by the viral enzyme integrase.[7] Release of virions from the host cell typically occurs via budding from the plasma membrane.

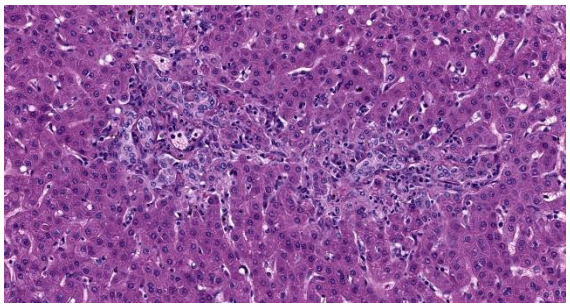

Figure 2-6. Liver, rhesus macaque. There is moderate biliary hyperplasia and mild lymphoplasmacytic pericholangitis. (HE, 250X)

Several retroviruses can induce oncogenesis via several mechanisms. Malignant transformation can occur when proviral DNA randomly inserts near host genes that regulate the cell cycle (proto-oncogenes). The promoter and enhancer DNA that is part of the viral insertion may result in dysregulation of the cell cycle and promote tumorigenesis.[7] It should be noted that this is a relatively rare occurrence as most viral genome integrations are innocuous. A second method of oncogenic transformation occurs when retroviruses contain viral oncogenes. It is thought that viruses acquire these viral oncogenes from host genomes during viral recombination events; typical viral oncogenes include tyrosine kinases, growth factors, growth factor receptors, transcription factors (*v-myc*) and G proteins (*v-ras*).[7] These oncogenes are integrated into the host genome and exert strong effects on endogenous mitogenic signalling pathways, often resulting in oncogenesis. Bovine leukemia virus exemplifies a third method of oncogenesis that relies on a viral oncogene, *tax*, which upregulates both viral and host promoter sequences, no matter where on the genome *tax* is integrated (a mechanism termed trans-activation).[7]

SIV is one of many retroviruses of veterinary importance, many of which are well-studied and well-characterized. Examples include avian leukosis virus and retriculoendotheliosis virus, the oncogenic retroviruses of poultry; Jaagsiekte sheep retrovirus, enzootic nasal tumor virus, maedi-visna virus, and caprine arthritis-encephalitis virus of small ruminants; feline leukemia virus and feline immunodeficiency virus; bovine leukemia virus and bovine immunodeficiency virus; and equine infectious anemia virus.[7]

Conference discussion reviewed the SHIV animal model of HIV infection and the pathogenesis of HIV infection generally. The moderator admonished residents to remember that, while HIV famously infects and destroys CD4+ T lymphocytes, it also affects members of the monocyte-macrophage system, including microglia. Once infected, these cells secrete cytokines that ramp up the immune system, resulting in giant cell encephalitis, giant cell interstitial pneumonia, and granulmomatous lymphadenitis.

Dr. Alves drew participants' attention to the expansion of the tunica intima that was a repeatable finding throughout the vasculature in section. Arteriopathy has long been associated with SIV and HIV infection, and there have been reports of cytomegalovirus infections that manifest with intimal thickening and fibrosis with varying degrees of vasculitis. Dr. Alves could not say with certainty which, if either, of CMV or SHIV was the source of the vascular changes, but reminded conference participants not to neglect the vasculature when evaluating lesions.

References:

1. Barry PA, Chang WLW. Primate betaherpesviruses. In:Arvin A, Campadelli-Fiume G, Mocarski E, et al., eds. *Human Herpeviruses: Biology, Therapy, and Immunoprophylaxis*. Cambridge University Press; 2007:1-71.
2. Bauer AM, Bar KJ. Advances in simian-human immunodeficiency viruses for non-human primate studies of HIV

prevention and cure. *Curr Opin HIV AIDS*. 2020;15(5):275-281.
3. Berg MR, Owston MA, Gauduin MC, et al. Cytomegalovirus hypophysitis in a simian immunodeficiency virus infected rhesus macaque (Macaca mulatta). *J Med Primatol*. 2017;46(6):364-367.
4. Cohn IS, Henrickson SE, Striepen B, Hunter CA. Immunity to *Cryptosporidium*; lessons from acquired and primary immunodeficiencies. *J Immunol*. 2022; 209:2261-2268.
5. Khan SM, Witola WH. Past, current, and potential treatments for cryptosporidiosis in humans and farm animals: A comprehensive review. *Front Cell Infect Microbiol*. 2023; 13:1115522.
6. Naseer M, Dailey F, Al Juboori, et al. Epidemiology, determinants, and management of AIDS cholangiopathy: a review. *World J Gastroenterol*. 2018;24(7):767-774.
7. Quinn PJ, Markey BK, Leonard FC, Fitz-Patrick ES, Fanning S, Hartigan PJ. *Veterinary Microbiology and Microbial Disease*. 2nd ed. Blackwell Publishing, Ltd.; 2011:618-634.
8. Reina FTR, Ribeiro CA, de Araujo RS, et al. Intestinal and pulmonary infection by Cryptosporidium parvum in two patients with HIV/AIDS. *Rev. Inst Med Trop Sao Paulo*. 2016;58:21-24.
9. Sinzger C, Grefte A, Platcher B, et al. Fibroblasts, epithelial cells, endothelial cells and smooth muscle cells are major target organs of human cytomegalovirus infection in lung and gastrointestinal tissue. *J Gen Virol*. 1995; 76(4):741-750.
10. Widmer G, Koster PC, Carmena D. *Cryptosporidium hominis* infections in non-human species: revisiting the concept of host specificity. *Int J Parasitol*. 2020; 50:253-262.
11. Yanai T, Chalifoux LV, Mansfield KG, et al. Pulmonary cryptosporidiosis in Simian Immunodeficiency Virus-infected rhesus macacques. *Vet Pathol*. 2000;37 (5):472-475.

CASE III:

Signalment:
14-week-old female Sprague Dawley rat (*Rattus norvegicus*)

History:
This animal gave birth with no apparent complications. At seven days post-partum, she developed paraparesis of both hind limbs. No history of trauma or mishandling was noted by the laboratory.

On physical exam, the rat was bright, alert, and responsive, euhydrated, and nursing her pups. Neurologic exam revealed absent conscious proprioception of both hind limbs, but motor reflex was intact when stimulated with a toe pinch. There was no overt pain on spinal palpation, and urination and defecation were reported to be normal. Over 48 hours, paraparesis progressed, and she lost ~7% of body weight. Euthanasia was elected due to poor prognosis.

Figure 3-1. Heart and lung, rat. One section of heart and three sections of lung are submitted. At subgross magnification, a large thrombus occupies the right heart and several sections contain occlusive thrombi in the pulmonary arteries. (HE, 5X)

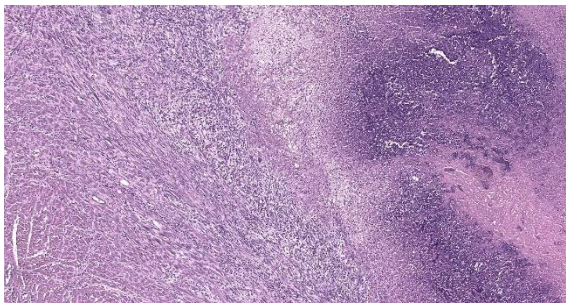

Figure 3-2. Heart, rat. The luminal thrombus is at right. The endocardium is effaced by large numbers of neutrophils, plump fibroblasts, and collagen, which extends into the adjacent myocardium (left). (HE, 125X)

Gross Pathology:
On necropsy, the lungs were diffusely pink with multifocal dark pink depressions and all sections floated in formalin. The heart was diffusely dark red. On cut section, a 2x5x2 mm thrombus was adhered to the right atrioventricular valve. Both kidneys were diffusely dark red and unremarkable on cut section. The spine/spinal cord appeared grossly unremarkable.

Laboratory Results:
PCR results on formalin-fixed cardiac tissue:
Corynebacterium kutscheri: Negative.
Staphylococcus aureus: Negative.
Streptococcus pneumoniae: Negative.
Group B *Streptococcus* (GBS): Positive.

Microscopic Description:

Lung: Approximately 50% of small, medium, and large-caliber pulmonary vessels are distended and occluded by intralumenal abundant degenerate neutrophils, karyorrhectic debris, eosinophilic fibrillar material (fibrin), and large basophilic bacterial colonies (thrombi/thromboemboli). The elastic laminae are frequently indistinguishable, and the tunica intima, media, and adventitia are replaced by abundant degenerate neutrophils and karyorrhectic debris (necrosis). There is moderate perivascular edema and perivascular inflammation comprised of moderate numbers of neutrophils, macrophages, and lymphocytes. Occasionally, alveolar septa are expanded up to 5 times normal width by variable numbers of neutrophils, lymphocytes, and histiocytes. Bronchi/bronchioles are unremarkable.

Heart: The endocardium and right atrioventricular valve are expanded and replaced by large numbers of plump spindled cells (fibroblasts) associated with parallel capillaries within a lightly eosinophilic, fibrillar (collagenous) matrix (granulation tissue). Attached to the endocardium is a thick layer of degenerative neutrophils and karyorrhectic debris with a central area of brightly eosinophilic amorphous to laminated material (thrombus) and coalescing large basophilic bacterial colonies. Infiltrating the myocardium and dissecting around myofibers are proliferating fibroblasts and multifocal mixed inflammation consisting of neutrophils, macrophages, and lymphocytes. There is mild myofiber degeneration characterized by cytoplasmic hypereosinophilia, swelling, loss of striations, and pyknotic nuclei. The epicardium is focally expanded by mild mixed mononuclear infiltrates at the apex of the heart.

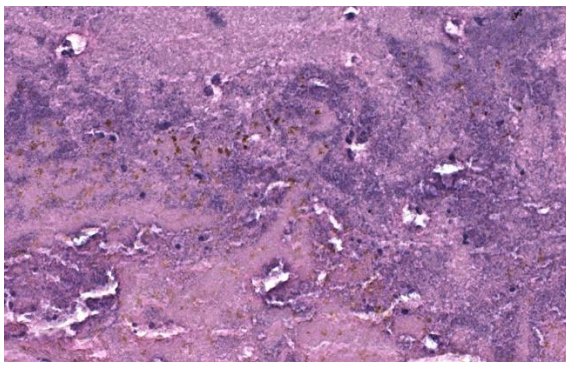

Figure 3-3. Heart, rat. There are numerous colonies of cocci within the thrombus. (HE, 580X)

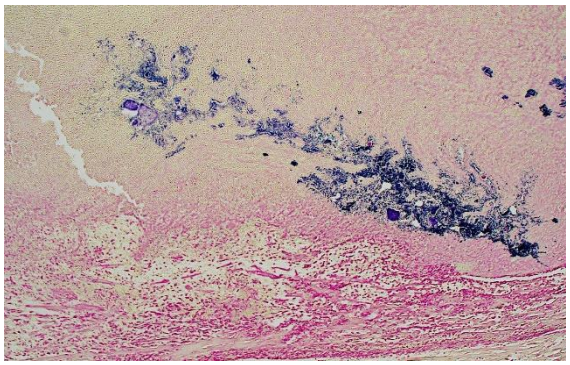

Figure 3-4. Heart, rat. Colonies of cocci within the thrombus are gram-positive. (Brown-Hopps, 100X)

Gram staining of the lung revealed abundant intravascular Gram-positive bacterial diplococci. Gram staining of the heart revealed abundant Gram-positive bacterial cocci within an atrial thrombus.

Contributor's Morphologic Diagnoses:

1. Lung: Obstructive thromboemboli, chronic, severe with necrosuppurative vasculitis/perivasculitis, and intravascular large bacterial colonies (cocci).
2. Lung: Interstitial pneumonia, chronic, multifocal to coalescing, severe, neutrophilic and lymphohistiocytic, with intralesional large bacterial colonies (cocci).
3. Heart, right atrium and AV valve: Endocarditis and myocarditis, fibrinosuppurative, chronic, regionally-extensive, severe with intralumenal thrombus, large colonies of bacterial cocci, and granulation tissue formation.

Contributor's Comment:

In addition to the right atrial thrombus and embolic bacterial pneumonia, significant microscopic findings include severe suppurative inflammation in the bladder, kidneys, and right stifle joint. Clinically noted 'paraparesis' is attributed to septic arthritis in the right stifle, though thromboemboli affecting the spinal cord or other sites is also possible.

In laboratory rodents, expected causes of prominent intralesional bacterial colonies associated with pneumonia can include *Corynebacterium*, *Streptococcus*, and *Staphylococcus* sp. Other bacterial causes of pneumonia in rats include *Pseudomonas aeruginosa* (gram-negative), *Mycoplasma pulmonis* (gram-negative), and *Filobacterium rodentium* (gram-negative).[2,3,8]

Important features of this case include a prominent embolic pattern without significant involvement of the large and small airways. A major differential for bacteremia and embolic lesions in rats is *Corynebacterium kutscheri* (pseudotuberculosis), a gram-positive short rod that can cause similar changes to this case.[3,4,8]

Gram stain of the heart and lungs revealed intravascular gram-positive pairs and chains of cocci in thrombi, consistent with streptococcal infection. Consistent with non-aerogenous extra-pulmonary bacterial etiology, bacteria were not evident in airways. PCR on formalin-fixed tissues was positive for Group B *Streptococci* (GBS).

GBS are commensal bacteria residing in the urogenital, respiratory, and intestinal tract and can be associated with opportunistic infections, particularly in neonates and immunosuppressed individuals.[6] Most notably, maternal colonization of GBS in humans is a risk factor for neonatal meningitis, septicemia, pneumonia, and death. However, GBS infection in gravid rats is reported to cause multi-systemic lesions (suppurative pan-carditis, splenitis, pancreatitis, interstitial pneumonia, metritis, and bacterial thromboemboli) in the dam, with suppurative urocystitis as the possible source.[3] Uterovaginal origin also seems likely post-partum, however these tissues were unremarkable in our case.

GBS were among the most commonly identified bacteria in rat specimens (2016-2020

PCR results) in a recent report, with approximately 20% prevalence.[1] FELASA 2014 recommends quarterly monitoring for GBS in rats.[7] GBS is frequently excluded from routine health monitoring in laboratory rodents.[5] This case highlights a potentially important cause of morbidity in breeding colonies.

Contributing Institution:
Johns Hopkins University
School of Medicine
Department of Molecular & Comparative Pathobiology
https://mcp.bs.jhmi.edu/

JPC Diagnoses:
1. Heart: Endocarditis, myocarditis, and valvulitis, chronic-active, suppurative, diffuse, with septic thrombus, granulation tissue, and numerous cocci.
2. Lung, pulmonary arteries: Arteritis, necrotizing, multifocal, severe, with septic thrombi and numerous cocci.

JPC Comment:
Group B *Streptococci*, also known as *Streptococcus agalactiae*, are opportunistic bacteria that are estimated to colonize the gastrointestinal and urogenital tracts of 1 in 4 humans.[3] GBS are divided into 10 different serotypes based on the composition of their polysaccharide capsules, with different serotypes causing more or less virulent disease with implications for patient prognosis. Invasive GBS infection is causing growing levels of mortality and morbidity among neonates, pregnant women, the elderly, and those with underlying health conditions. Invasive GBS infections have also been reported in primates, dogs, fish, and cattle, and rodents and primates have been used as experimental models of infection both neonatal and adult GBS infection.[3]

In laboratory rats, case reports of spontaneously occurring GBS infections often

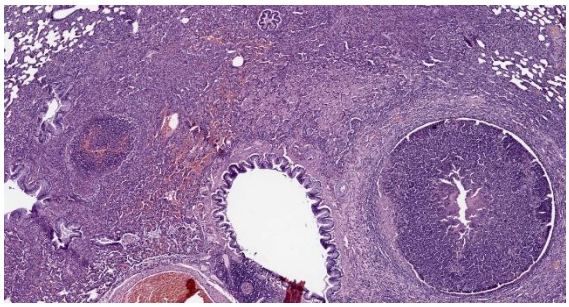

Figure 3-5. Lung, rat. Septic thrombi are also present within pulmonary arteries. The adjacent alveoli are atelectatic, and some contain various combinations and concentrations of neutrophils, cellular debris, and polymerized fibrin. (HE, 155X)

recapitulate late-onset GBS infections in humans, with infections characterized by myocarditis, metritis, meningitis, and septicemia.[3] Comparative phylogenetic analyses from animals as diverse as tilapia, cattle, and humans show that GBS strains are extremely closely related, and thus could represent an anthropozoonotic risk. Whether such transspecies transmission actually occurs is an active area of research; in the meanwhile, personal protective equipment and training on preventive measures for laboratory animal handlers is recommended.[3]

Discussion of this case centered initially on cardiac anatomy, with conference participants divided on whether the cardiac thrombus was located in the right or the left side of the heart. Dr. Alves noted that sequelae of a left-sided thrombus would be widely dissementated thrombus formation, while right sided thrombi might be expected to propagage clots within the pulmonary vasculature, as seen in this case. Duly convinced that the thrombus likely began in the heart, partipants noted the multiple small caliber blood vessels in the myocardium, particularly at the apex of the heart, and agreed with the contributor that, while a surprising location, these likely represented granulation tissue subjacent to the completely denuded endocardium.

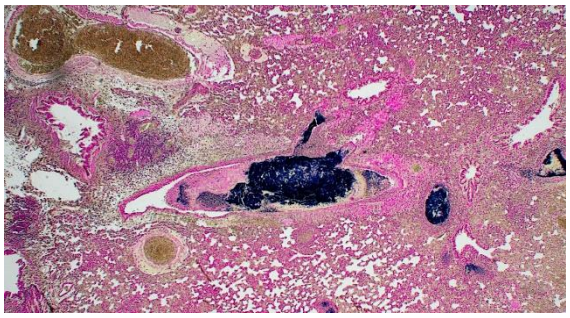

Figure 3-6. Lung, rat. Colonies of cocci within the pulmonary arteriolar thrombi are gram-positive. (Brown-Hopps, 100X)

Gram staining highlighted the embolic nature of this disease process, with large colonies of gram-positive bacteria throughout the pulmonary vasculature. The moderator also noted the substantial interstitial pneumonia present in the lungs and characterized the infiltrate as primarily lymphoplasmacytic with fewer neutrophils using immunohistochemical staining, including a stain for myeloperoxidase (MPO), which helpfully highlighted neutrophils.

Dr. Alves discussed coagulation more broadly, revisiting Virchow's triad of turbidity, endothelial damage, and hypercoagulability. In this case, the animal had recently given birth, and the hormonal changes associated with pregnancy and periparturition are known risk factors for hypercoagulability. The inflammatory conditions created by the massive bacterial infection could also cause vascular changes leading to slowing of blood flow and endothelial damage which could contribute to turbidity and exposure of tissue factor, all of which increase the risk of thrombus formation.

Conference participants preferred not to include the notable interstitial pneumonia in the morphologic diagnoses as it was likely secondary to the main process; however, the interstitial pneumonia was seen, acknowledged, and appreciated. Conference participants discussed the thrombus location within the heart at length, particularly whether it was located in the atrium or the ventricle. Participants noted the contributor's location of right atrium, which is undoubtedly correct; however, based on the slide evaluated at conference, participants could not definitively localize the thrombus and hedged with a generally correct location of "heart."

References:

1. Albers TM, Henderson KS, Mulder GB, Shek WR. Pathogen prevalence estimates and diagnostic methodology trends in laboratory mice and rats from 2003 to 2020. *JAALAS*. 2023;62(3):229-242.
2. Barthold SW, Griffey SM, Percy DH. *Pathology of Laboratory Rodents and Rabbits.* 4th ed. Blackwell Publishing; 2016.
3. Bodi Winn C, Bakthavatchalu V, Esmail MY, et al. Isolation and molecular characterization of group B *Streptococcus* from laboratory Long-Evans rats (*Rattus norvegicus*) with and without invasive group B streptococcal disease. *J Med Microbiol*. 2018;67(1):97-109.
4. Cooper TK, Meyerholz DK, Beck AP, et al. Research-relevant conditions and pathology of laboratory mice, rats, gerbils, guinea pigs, hamsters, naked mole rats, and rabbits. *ILAR J.* 2021;62(1-2):77-132.
5. Hansen AK, Nielsen DS, Krych L, Hansen CHF. Bacterial species to be considered in quality assurance of mice and rats. *Lab Anim*. 2019;53(3):281-291.
6. Mähler C, Berard M, Feinstein R, et al. FELASA recommendations for the health monitoring of mouse, rat, hamster, guinea pig and rabbit colonies in breeding and experimental units. *Lab Anim.* 2014; 48(3):178-192.
7. Otto GM. Chapter 4 - Biology and Diseases of Rats. In: *Laboratory Animal Medicine.* 3rd ed. Boston Academic Press; 2015.

8. Shuster KA, Hish GA, Selles LA, et al. Naturally occurring disseminated group B streptococcus infections in postnatal rats. *Comp Med*. 2013 Feb;63(1):55-61.

CASE IV:

Signalment:
Age and gender unknown, Sprague Dawley rat (*Rattus norvegicus*)

History:
The patient was enrolled in an IACUC protocol. Following surgery, the rat was not grooming, was urinating on itself, was very lethargic, and lost more than 15% of its body weight. There was no sign that it was eating food or gel packs. Euthanasia was performed and a necropsy was performed by the research technician.

Gross Pathology:
The bladder was distended and discolored. Urine collected aseptically was purulent and bloody. The stomach was full, but the rest of the gastrointestinal tract was empty. Both kidneys had multifocal white spots on the cortex. The remaining organs appeared normal. Gross dissection of the bladder revealed numerous uroliths.

Laboratory Results:
Proteus mirabilis was cultured from the urinary bladder. Stone analysis was not performed.

Microscopic Description:
Affecting 40% of primarily the renal cortex, but extending into the medulla, tubules are necrotic and degenerate, lost and replaced, or expanded and widely separated by viable and degenerate neutrophils, necrotic cellular debris (lytic necrosis) and large colonies of basophilic bacterial rods. Tubules are degenerate or regenerating. Multifocally tubules have retention of cellular architecture and loss of

Figure 4-1. Kidney, rat. Uroliths collected from the bladder. There was blood in the urine and culture of the urine yielded *Proteus mirabilis. (Photo courtesy of* Tri Service Research Laboratory, http://www.wpafb.af.mil /afrl/711HPW/)

differential staining (coagulative necrosis). Within tubules there is a homogenous eosinophilic material (proteinosis) or sloughed epithelium admixed with neutrophils and cellular debris (cellular cast) and rarely deeply basophilic crystalline material (mineral). The interstitium is expanded by the same cellular debris and fibrin, hemorrhage and edema. Glomerular changes include synechia, parietal cell hypertrophy, necrosis of mesangial cells and protein in Bowman's space.

The renal surface is undulant with a mildly thickened capsule expanded by adherent fibrin and inflammatory cells. The renal pelvis is dilated (hydronephrosis) and contains previously described lytic necrosis and inflammatory cells which transmigrate the multifocally lost and necrotic (ulcerated) urothelium.

Contributor's Morphologic Diagnosis:
Kidney: Pyelonephritis, suppurative, multifocal, severe, chronic, with large colonies of bacteria, tubular degeneration, regeneration and necrosis, protein and cellular casts, intratubular bacteria, hydronephrosis, and urethritis.

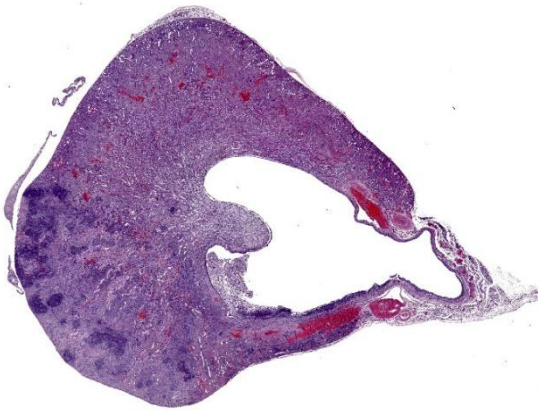

Figure 4-2. Kidney, rat. At subgross magnification, the renal pelvis is markedly dilated and irregular in shape. There is exudate in the lumen and foci of inflammation extending up to the undulant capsular surface. (HE, 6X)

Contributor's Comment:
Proteus mirabilis is a gram-negative, flagellated, swarming, commensal inhabitant of the intestinal tract in humans and the respiratory and digestive tract of mice.[5] This bacteria may affect multiple organs by gaining access to the systemic circulation, inducing bacteremia, or can infect the urinary system through an ascending infection. In people, this is a common nosocomial cause of catheter associated urinary tract infections. In the dog and cat, *Escherichia coli* followed by *Proteus mirabilis* are the two most frequently isolated gram negative bacteria in urinary tract infections.[3] On a more historic note, *P. mirabilis* has been a source of surgical infection via contaminated instrumentation and has rarely been implicated in cases of meningitis and cerebral abscesses in neonates.[8]

The pathogenesis of *P. mirabilis* involves its unique ability to differentiate from a swimmer cell to a swarmer cell depending on the environment. In a liquid environment, the bacteria swim, (called swimmers) while on a solid surface, such as a urinary catheter, they differentiate into swarmers forming rapidly moving rafts of bacteria.[2] *P. mirabilis* has several virulence factors, including flagella for increased motility, adhesion factors for binding to epithelium in the urinary tract, and the ability to utilize host iron.[1,2] This infection also creates an overwhelming neutrophilic response and damages host tissue via hemolysin, which is cytotoxic to epithelial cells, and urease. Urease breaks down urea to ammonia, raising the pH of the urine and precipitating the formation of stones which are often struvite or carbonate hydroxyapatite, thus causing additional mechanical epithelial damage.[1,2]

One current area of research has been the investigation of *P. mirabilis* and its potential to alter tumor hypoxia thereby inhibiting tumor growth.[9] Through various mechanisms, such as gene delivery and immunomodulator delivery, *Salmonella typhimurium*, *E. coli* and *Clostridium* sp. have also been investigated for their potential roll in treating cancer.[7] One particular study found that *P. mirabilis* may be a potential method for suppressing growth of primary breast cancer in murine models.[9]

Although not a common pathologic entity in veterinary medicine, this bacteria should be considered as a differential for cases of suppuarative pyelonephritis in rodents.

Contributing Institution:
Tri Service Research Laboratory
Fort Sam Houston, TX
http://www.wpafb.af.mil/afrl/

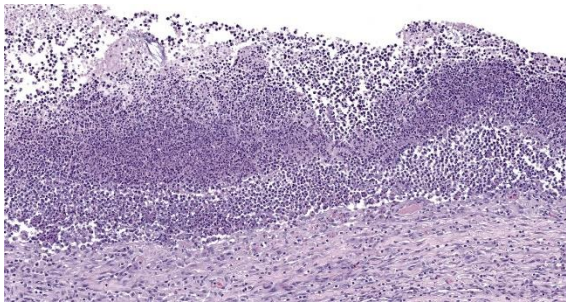

Figure 4-3. Kidney, rat. There is intense suppurative inflammation adjacent to ulcerated areas of the dilated pelvis. (HE,170X)

JPC Diagnoses:

1. Kidney: Pyelonephritis, chronic-active, suppurative, severe, multifocal to coalescing, with cellular and protein casts and moderate hydronephrosis.
2. Kidney: Interstitial nephritis, lymphoplasmacytic, mild, with tubular atrophy.

JPC Comment:

The contributor provides an excellent overview of *Proteus mirabilis*, a bacterium blessed with many gifts, the most spectacular of which may be its remarkable and pleasingly alliterative swimmer-swarmer motility. This unique feature inspired the name of the *Proteus* genus upon its discovery in 1885 by the German pathologist Gustav Hauser.[7]

Hauser, a Greek mythology enthusiast, named the genus based on Proteus, the prophetic sea god, who appears in, among other writings, Homer's *Odyssey*. In addition to herding seals for Poseidon – a fine enough avocation in itself – Proteus was omniscient, knowing all things past, present, and future. Proteus was loathe, however, to share his knowledge with others, and those who sought his counsel could only bide their time and attempt to capture Proteus during his midday nap and demand prophetic answers. Proteus, however, was not just your run-of-the-mill omniscient seal-herding deity; he could also change shape into lions, serpents, or even water in order to avoid capture.

The name Proteus also appeared in the 15th century Shakespeare play, *The Two Gentlemen of Verona*, where one of the main characters is so named because of his capricious, frequently-changing affections. The modern word "protean" also shares this derivation, and is defined by Merriam-Webster to mean "of or resembling Proteus in having a varied nature or ability to assume different forms; displaying great diversity or variety; versatile."[9] It was this culture context that led

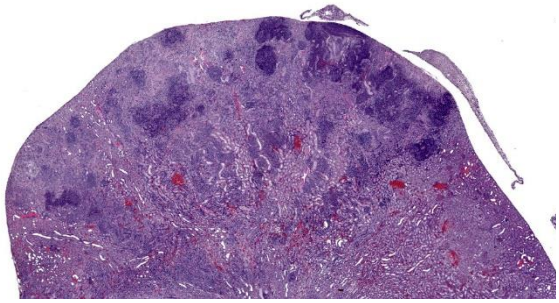

Figure 4-4. Kidney, rat. Rays of inflammation extend upward into the superficial cortex. (HE,17X)

Hauser, who recognized the ability of *Proteus mirabilis* to differentiate from a short vegetative swimmer cell to an elongated, highly flagellated swarmer cell, to name the bacterium after Proteus, mythology's famous shape-shifter.[8]

What Hauser couldn't have know at the time, however, is that *P. mirabilis* can perform even more feats of molecular chicanery that allow it to evade the host immune system. *P. mirabilis* produces an IgA-degrading protease, named ZapA metalloprotease, that is able to completely degrade IgA.[1] The bacterium produces ZapA during its transition from swimmer to swarmer, enabling it to neutralize the host's mucosal immunity during a critical time in pathogenesis. One of the key characteristics of the swarmer cell is the exuberant expression of flagella of many different types. These flagella are encoded by three different flagellin genes which, via homologous recombination, allow individual bacteria to produce antigenically novel flagella capable of evading host immune defenses.[1] Finally, the production of urease leads to the production of struvite and carbonate hydroxyapatite stones. Stone formation is typical of *P. mirabilis* infection and allows the bacterium to sequester itself and replicate within the stones, protected from the antibodies and antibiotics that mean it harm.[1] Conference participants found this slide a feast for the eyes and, as in all cases this

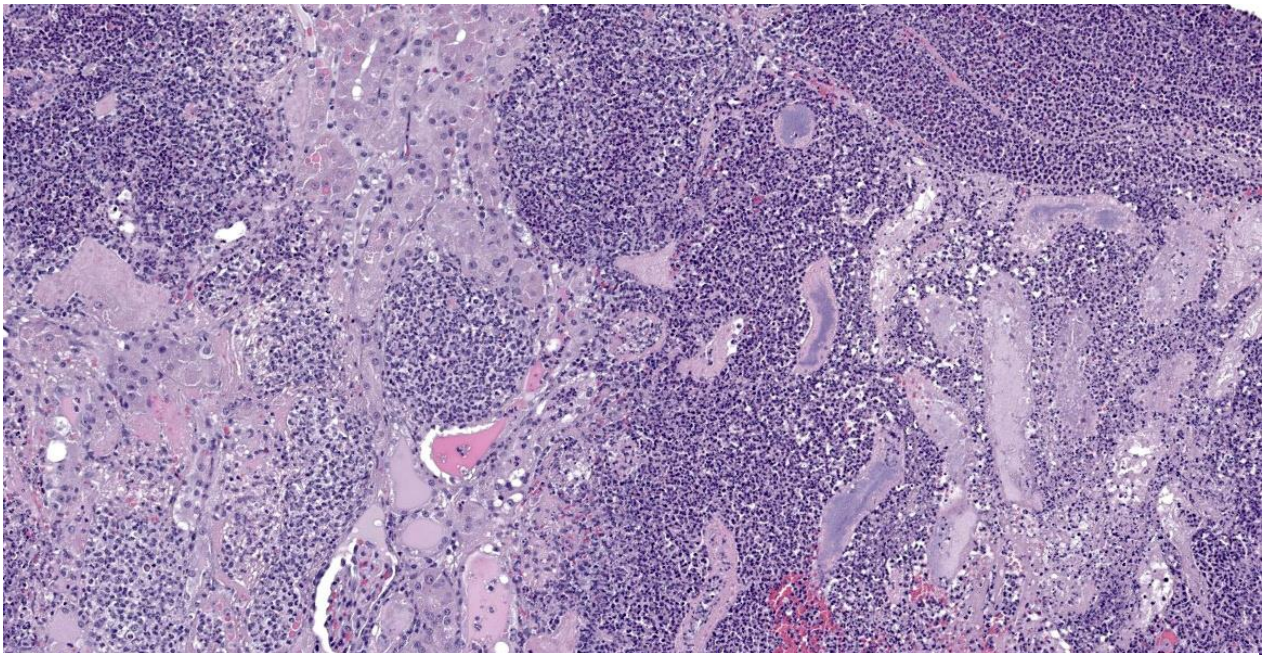

Figure 4-5. Kidney, rat. Tubules are expanded and effaced by suppurative inflammation which extends into the surrounding interstitium. Some tubules contain protein casts filled with apparent bacterial colonies. (HE,144X)

week, full of description-rich details. Dr. Alves advised conference participants to structure slide descriptions by starting with the most severe lesion; if severity doesn't provide an obvious starting point, one might structure the description around the presumed pathogenesis. In this case, the most severe pathology was in cortical tubules, which were characterized by large areas of both coagulative and lytic necrosis. Dr. Alves noted that many seemingly destroyed tubules retained their basement mebranes in a remarkable display of renal resilience. He also noted that many tubular lumina contain blue-gray, finely granular material that appear to be bacteria, but that did not show up on gram stain. Gram staining was repeated post-conference and the intratubular material again resisted gram staining. Despite the presence or absence of organisms on gram stain, this section provides an excellent example of a "gram-negative kidney," with lesions similar to what would be expected with *E. coli*, *Proteus mirabilis*, *Klebsiella*, and other less-common gram negative organisms.

Dr. Alves also noted eosinophilic round inclusions within many renal tubular epithelial cells, interpreted as hyaline droplets. These well-documented droplets are produced by one of three distinct processes: 1) by sequestration of alpha2U-globulin in the lysosomes of male rats, 2) by histiocytic sarcoma, which produces excessive lysozyme that spills into the renal tubules and is resorbed, or 3) by overproduction of high molecular weight proteins. These three etiologies can only be differentiated with special stains.

Finally, Dr. Alves noted an area near the renal pelvis that, in contrast to the vast majority of the kidney which is awash in neutrophils, contains an interstitial inflammatory infiltrate composed largely of lymphocytes and plasma cells. These chronic inflammatory cells separate and surround small renal tubules with attenuated epithelium, interpreted as tubular atrophy. Dr. Alves believes this area represents a second pathologic process distinct from the obvious bacterial infection. Though the age of the animal is not provided, chronic

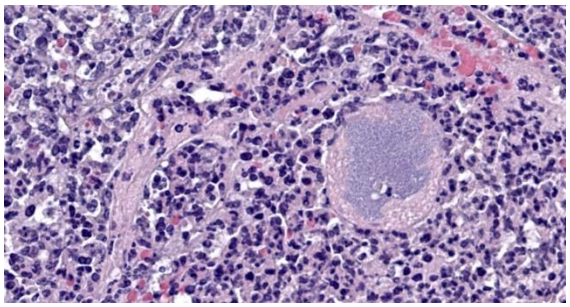

Figure 4-6. Kidney rat. High magnification of the granular material within the lumen of a dilated tubule in the superficial cortex. (HE, 914X)

progressive nephropathy is a common lesion in older rats and could account for this focus of chronic inflammation. Conference participants felt this was a significant lesion and warranted capture in a second morphologic diagnosis.

References:

1. Coker C, Poore CA, Li X, Mobley HLT. Pathogenesis of *Proteus mirabilis* urinary ratct infection. *Microbes Infect.* 2000; 2(12):1497-1505.
2. Jones B, Young R, Mahenthiralingam E, Stickler D. Ultrastructure of *Proteus mirabilis* swarmer cell rafts and role of swarming in catheter-associated urinary tract infection. *Infect Immun.* 2004; 72 (7):3491-3950.
3. Marques C, Belas A, Franco A, Aboim C, Gama LT, Pomba C. Increase in antimicrobial resistance and emergence of major international high-risk clonal lineages in dogs and cats with urinary tract infection: 16 year retrospective study. *J Antimicrob Chemother*. 2018;73(2):377-384.
4. Mobley HLT. Virulence of *Proteus mirabilis*. In: Mobley H, Warren J, eds. *Urinary Tract Infections: Molecular Pathogenesis and Clinical Management.* ASM Press;1996:245-269.
5. Percy DH, Barthold SW, eds. *Pathology of Laboratory Rodents and Rabbits.* 4th ed. Blackwell Publishing; 2016:66.
6. Protean. 2023. In:*Merriam-Webster.com.* Retrieved December 9, 2023, from https://www.merriam-webster.com/dictionary.
7. Sellaturay SV, Nair R, Dickinson IK, Sriprasad S. Proteus: mythology to modern times. *Indian J Urol*. 2012;28(4):388-391.
8. Smith ML, Mellor D. *Proteus mirabilis* meningitis and cerebral abscess in the newborn period. *Arch Dis Child.* 1980; 55(4):308-310.
9. Zhang H, Diao H, Jia L, Yuan Y, Thamm D et al. Proteus mirabilis inhibits cancer growth and pulmonary metastasis in a mouse breast cancer model. *PLoS One.* 2017;12(12):e0188960.

WSC 2023-2024
Conference 13 Self-Assessment

1. Esthesioneuroblastomas arise from?
    a. Nerve sheath of the olfactory nerve
    b. Neuroectodem of the superior nasal cavity
    c. Neuroectoderm of the anterior olfactory lobe
    d. Distributed neuroendocrine tissue of the nasal cavity

2. Which of the following is incorporated into the SIV virus to create SHIV?
    a. HIV gag gene
    b. HIV pol gene
    c. HIV env gene
    d. A piece of ham

3. Schizonts of *Cryptospordium* are traditionally located:
    a. Intracellular, extracytoplasmic
    b. Extracellular, intracytoplasmic
    c. Intracellular, intracytoplasmic
    d. Extracellular, extracytoplasmic

4. In humans, Group B streptococcus is also known as *Streptococcus*?
    a. *Meningitidis*
    b. *Uberis*
    c. *Agalactiae*
    d. *Jirovecii*

5. True or false: Proteus mirabilis is the4 second most common cause of pyelonephritis in dogs and cats.
    a. True
    b. False

Joint Pathology Center
Veterinary Pathology Services

WEDNESDAY SLIDE CONFERENCE 2023-2024

Conference #14 3 January 2024

CASE I:

Signalment:
Adult female Norwegian Fjord horse (*Equus caballus*)

History:
This horse was born near Hanover, Germany. It was kept solely in northern Germany and has never been abroad. It was presented to the local veterinarian due to lameness. During the clinical examination, the veterinarian detected multiple cutaneous nodules. Two representative samples (elbow and periorbital skin) were surgically excised, fixed in 10% formalin, and submitted for histological examination.

Gross Pathology:
In both samples, the haired skin showed focal alopecia, focal ulceration, and poorly demarcated lumps with a size of up to 1.2 cm in diameter.

Laboratory Results:
Genome fragments of *Leishmania* sp. were detected in the cytoplasm of multinucleated giant cells and macrophages using *in situ* hybridization.

Microscopic Description:
Haired skin: The superficial and deep dermis shows a multifocal to coalescing periadnexal and a multinodular to coalescing severe inflammatory cell infiltrate consisting of myriad macrophages admixed with low to moderate numbers of plasma cells and lymphocytes, as well as single eosinophilic granulocytes. Randomly distributed throughout the whole lesion, there are multinucleated giant cells with a size of up to 50 µm in diameter, containing up to 10 predominantly peripherally located nuclei (Langhans type). Occasionally in the extracellular space, but predominantly and frequently within the cytoplasm of macrophages, there are multiple protozoal structures (amastigotes) with a diameter of 2 to 3 µm often surrounded by a clear halo suggestive of a clear parasitophorous vacuole. The round organisms are characterized by a clear cytoplasm and a single eccentric nucleus of approximately 1-2 µm diameter. Furthermore, in the superficial dermis, fibroblastic connective tissue is moderately hyperplastic. In addition, low numbers of macrophages with brown-black intracytoplasmic pigment are present in the subepidermal tissue (pigmentary incontinence). Occasionally, hair shafts and sebaceous glands are missing.

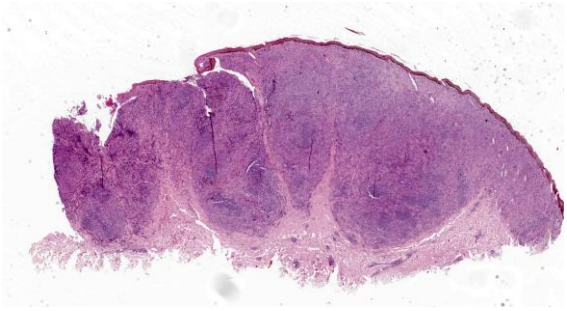

Figure 1-1. Haired skin, horse. A submitted section of skin contains coalescing inflammatory nodules within the dermis. (HE, 5X)

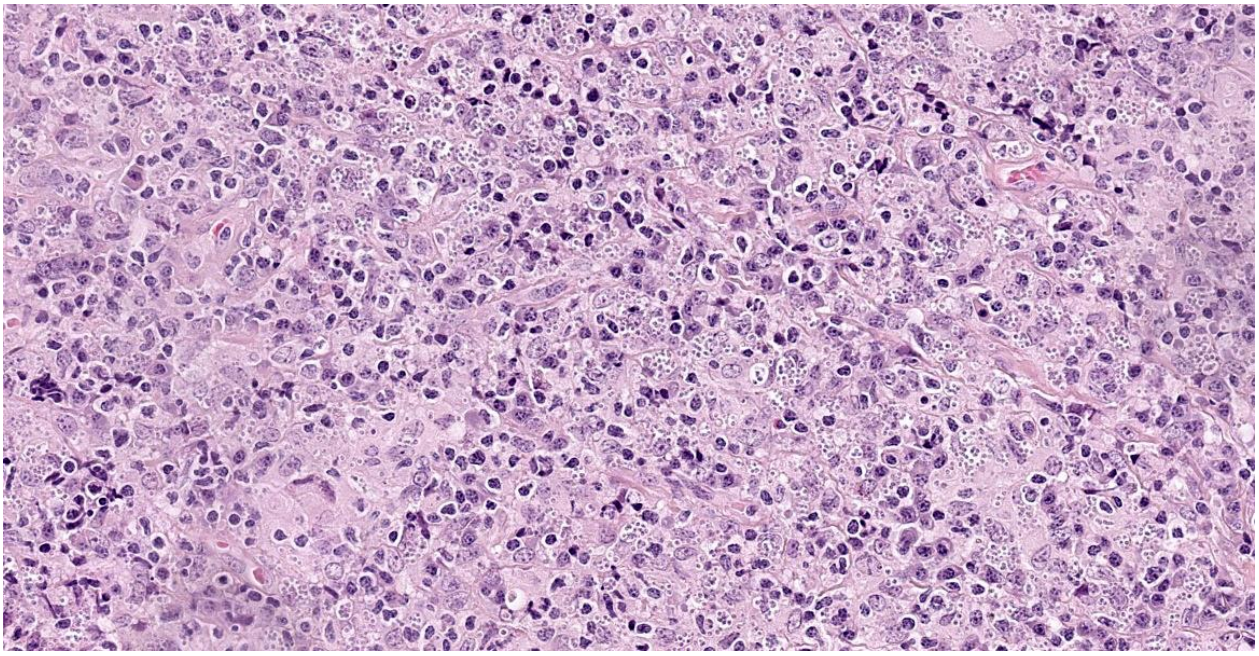

Figure 1-2. Haired skin, horse. Inflammatory nodules are composed primarily of histiocytes with large numbers of lymphocytes scattered throughout, often in aggregates. Macrophages contain multiple round protozoal amastigotes within their cytoplasm. (HE, 381X)

Contributor's Morphologic Diagnosis:
Haired skin: Dermatitis, chronic, severe, focally extensive, periadnexal to diffuse, granulomatous, with multinucleated giant cells (Langhans type) and intrahistiocytic protozoal amastigotes, equine.

Contributor's Comment:
Leishmaniasis is a globally occurring infectious disease in humans and animals caused by obligate intracellular protozoan parasites of the genus *Leishmania*. The disease is endemic in Southern Europe, North Africa, South and Central America, and Asia.[13] In Europe, it occurs mainly in the Mediterranean region. Due to increased travel activities with companion animals, the number of animals infected with *Leishmania* sp. in Northern Europe has increased. Additionally, since the 1980s, the sandflies that transmit leishmaniasis have increasingly appeared in Northern Europe, especially in Germany, possibly due to climate change.[1,8] This has initiated the discussion about the occurrence of autochthonous cases of leishmaniasis in Europe north of the Alps.[7]

Leishmania sp. require both arthropods and vertebrates for their development. Sandflies such as *Phlebotomus* sp. and *Lutzomyia* sp. play an important role as vectors of *Leishmania* sp. in Europe and South and Central America.[1] The amastigote form of *Leishmania* sp. is found in the cells of the mononuclear phagocyte system of vertebrates, predominantly in liver, spleen, bone marrow, and lymph nodes. Occasionally, the organisms are detected in other leukocytes, endothelial cells, fibroblasts, and neoplastic cells.[2,10] After ingestion of macrophages containing *Leishmania* amas-tigotes by a female arthropod during a blood meal, the amastigotes are transformed into promastigotes in the intestine and subsequently enter the biting mouthparts of the arthropod.[13,18] Transmission of the pathogen through either mechanical vectors such as bloodsucking insects and ticks or a direct and vertical transmission has also been reported.[6,11,18]

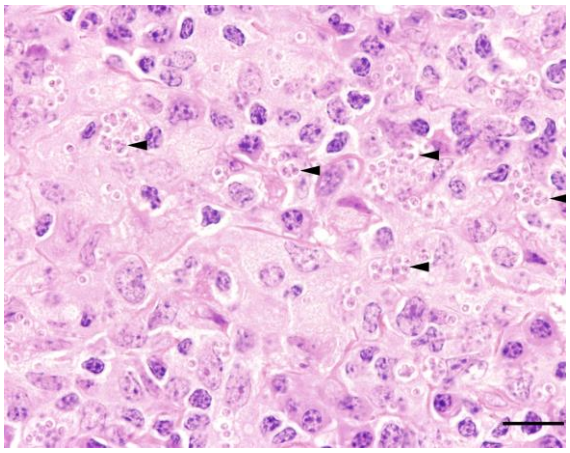

Figure 1-3. Haired skin, horse. Amastigotes are characterized by a clear cytoplasm and a single eccentric nucleus of approximately 1-2 µm diameter. (*Photo courtesy of:* Department of Pathology, University of Veterinary Medicine, Hannover, Buenteweg 17, 30559 Hannover, Germany. http://www.tiho-hannover.de/ klin iken-institute/institute/institut-fuer-pathologie). (HE, 600X)

There are more than 50 species of *Leishmania* based on a complex classification scheme. The species of *Leishmania* vary by region, and different species are thought to cause different disease manifestations.[1] Currently,three different *Leishmania* sp. have been confirmed to cause cutaneous leishmaniasis in horses in Europe: *Leishmania braziliensis, Leishmania siamenis*, and *Leishmania infantum*.[14]

In animals and humans, leishmaniasis can cause three different disease patterns: cutaneous leishmaniasis, mucocutaneous leishmaniasis, and visceral leishmaniasis.[13] Clinical signs of equine cutaneous leishmaniasis are usually less severe than in other host species and the disease in equids is typically not life-threatening. The most common lesions are single or multiple papules or nodules characterized by hyperkeratosis with prominent scaling, alopecia, depigmentation, and ulceration in the areas where sand flies commonly feed, including periorbital skin, muzzle, neck, pinnae, scrotum, and legs.[13,14]

Histologically, a nodular to diffuse lymphohistiocytic dermatitis is a consistent feature of cutaneous leishmaniasis.[14] The inflammation mainlyvoccurs in one of the following three patterns: granulomatous perifolliculitis, super-ficial and deep perivascular dermatitis, or interstitial dermatitis.[13] However, the burden of the protozoa may vary. This reflects the dynamics of the interaction between the host and the pathogen. Moreover, the incubation time of cutaneous leishmaniasis varies from several months up to seven years.[13] Spontaneous regression and recurrence of cutaneous leishmaniasis have been reported in cats and horses.[15]

Not all infected animals become ill. In infected animals, leishmania-specific and non-specific polyclonal B-cell activation may occur, which can lead to deposition of immune complexes and formation of autoantibodies against erythrocytes, platelets, and nuclear antigens. In diseased animals, a Th2-immune response predominates. In contrast, a type IV hypersensitivity reaction and a Th1-immune response are found in asymptomatic carriers or in animals after successful chemotherapy.[13]

Due to the variety of possible lesions and the various infectious and noninfectious differential diagnoses, the diagnosis of leishmaniasis requires direct cytologic or histological identification of amastigotes in the cytoplasm of macrophages, best visible by Giemsa staining.[13] Furthermore, pathogen detection is possible by immunohistological, culture, and molecular (PCR and *in situ*-hybridization) detection methods.[3,12] A positive serological test indicates that an infection has occurred, but does not imply

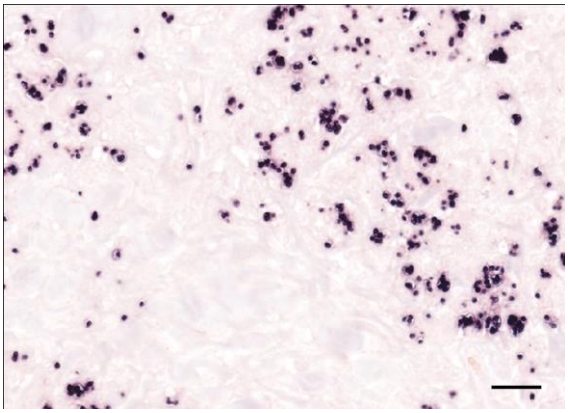

Figure 1-4. Haired skin, horse. In-situ hybridization against *Leishmania* sp. (*Photo courtesy of:* Department of Pathology, University of Veterinary Medicine, Hannover, Buenteweg 17, 30559 Hannover, Germany.) (anti-*Leishmania* ISH.)

that the parasite is still present in the infected host.[3]

Contributing Institution:
Department of Pathology
University of Veterinary Medicine, Hannover
Buenteweg 17, 30559
Hannover, Germany.

JPC Diagnosis:
Haired skin: Dermatitis, granulomatous, multifocal to coalescing, severe, with numerous intrahistiocytic amastigotes.

JPC Comment:
The contributor provides an excellent overview of leishmaniasis, a zoonotic disease most consistently found in humans and dogs and which has not historically been considered endemic in the United States. In recent decades, cutaneous and visceral leishmaniasis has been reported among certain canine breeds in the United States and Canada, and cases of cutaneous leishmaniasis have been reported in U.S. horses without a history of travel to endemic areas.[16,17]

The first documented report of a domestically acquired case of equine leishmaniasis occured in a Morgan horse mare in Florida in 2011.[4,16] As noted by the contributor, the canonical mode of transmission of *Leishmania* sp. is via the bite of sandflies from the genera *Phlebotomus* and *Lutzomyia*, and Florida is host to two possible sand fly vectors, *Lutzomyia shannoni* and *Lutzomyia vexator*.[17] *Lutzomyia shannoni* is known to feed on both humans and other mammals, and it has been experimentally shown capable of infection with *Leishmania infantum* when fed on infected dogs; however, it is not known if the infective amastigote forms develop within *Lutzomyia shannoni*.[17] The search for a competent sandfly vector may be superfluous, however, as recent research has demonstrated that the species of *Leishmania* isolated from infected Florida horses, *Leishmania martiniquensis*, is likely transmitted by *Culicoides* spp. biting midges.[5,9,17] Due to the presence of competent vectors in the United States and a small but growing number of confirmed cases of domestically-acquired equine leishmaniasis, the American Association of Equine Practitioners recently released guidelines on the diagnosis and treatment of the disease.[4]

Equine cutaneous leishmaniasis commonly presents as solitary or multiple ulcerated nodules on the head, pinnae, scrotum, legs, and neck.[17] To date, equine leishmaniasis has been confined to the skin and the more serious and potentially fatal visceral form of the disease seen in dogs and humans has not been reported in horses; most clinical equine cases spontaneously resolve in 3-6 months and the prognosis is therefore generally good.[4,17]

This week's conference was moderated by Joint Pathology Center Director and equestrian enthusiast LTC(P) Sherri Daye. LTC(P) Daye led conference participants in a discussion of the differences among molecular

diagnostic techniques such as *in situ* hybridization and immunohistochemistry before moving to differential diagnoses. Participants were even-ly split between *Histoplasma capsulatum* and *Leishmania* spp. as the likely etiologic agent of this lesion, and significant conference discussion focused on how to differentiate between the two organisms when presented with only an H&E section. Participants noted that leishmaniasis typically presents with abundant plasmacytic inflammation, which is absent in this case. In addition, the clear capsule-like rings surrounding the organisms are unusual in leishmaniasis and further contributed to the diagnostic confusion.

Though cutaneous leishmaniasis has not historically been top of mind in the United States and Northern Europe, the incidence of this disease is likely to increase as competent vectors, driven by migratory movements of people and animals and climate change, move into newly favorable geographic niches.

References:

1. Akhoundi M, Kuhls K, Cannet A, et al. A historical overview of the classification, evolution, and dispersion of *Leishmania* parasites and sandflies. *PLOS Negl Trop Dis*. 2016;10**:**e0004349.
2. Albanese F, Poli A, Millanta F, et al. Primary cutaneous extragenital canine transmissible venereal tumour with *Leish-mania*-laden neoplastic cells: a further suggestion of histiocytic origin? *Vet Dermatol.* 2002;13**:**243–246.
3. Albuquerque A, Campino L, Cardoso L, et al. Evaluation of four molecular methods to detect *Leishmania* infection in dogs. *Parasit Vectors*. 2017;10**:**57.
4. American Association of Equine Practitioners. *AAEP Infectious Disease Guidelines:Equine Cutaneous Leishmaniasis.* 2022. Available at https://aaep.org/document/equine-cutaneous-leishmaniasis.
5. Becvar T, Vojtkova B, Siriyasatien, et. al. Experimental transmission of *Leishmania* (*Mundia*) parasites by biting midges (Diptera: Ceratopogonidae). *PLos Pathog*. 2021;17(6):e1009654.
6. Bogdan C, Schönian G, Bañuls AL, et al. Visceral leishmaniasis in a German child who had never entered a known endemic area: case report and review of the literature. *Clin Infect Dis*. 2001;32**:**302-306.
7. Dujardin JC, Campino L, Canavate C, et al. Spread of vector-borne diseases and neglect of leishmaniasis, Europe. *Emerg Infect Dis*. 2008;14**:**1013–1018.
8. Harms G, Schönian G, Feldmeier H. Leishmaniasis in Germany. *Emerg Infect Dis*. 2003;9:872-875.
9. Kaewmee S, Mano C, Phanitchakun T, et al. Natural infection with *Leishmania (Mundia) martiniquensis* supports *Culicoides peregrinus* (Diptera: Ceratopogonidae) as a potential vector of leishmaniasis and characterization of a *Crithidia* sp. isolated from the midges. *Front Microbiol*. 2023;14:1-17.
10. Kegler K, Habierski, A, Hahn, H, et al. Vaginal canine transmissible venereal tumour associated with intra-tumoural *Leishmania* spp. amastigotes in an asymptomatic female dog. *J Comp Pathol.* 2013;149:156-161.
11. Koehler K, Stechele M, Hetzel U, et al. Cutaneous leishmaniosis in a horse in southern Germany caused by *Leishmania infantum*. *Vet Parasitol*. 2002;109:9-17.
12. Maia C, Campino L. Methods for diagnosis of canine leishmaniasis and immune response to infection. *Vet Parasitol*. 2008;158:274–287.
13. Mauldin EA, Peters-Kennedy J. Integumentary System. In: Maxie G, ed. *Jubb, Kennedy and Palmer`s Pathology of*

Dom-estic Animals. 6th ed. Vol 1. Elsevier; 2016:240.
14. Mhadhbi M, Sassi A. Infection of the equine population by Leishmania parasites. *Equine Vet J*. 2020;52:28-33.
15. Müller N, Welle M, Lobsiger L, et al. Occurrence of *Leishmania* sp. in cutaneous lesions of horses in Central Europe. *Vet Parasitol*. 2009;166:346-351.
16. Petersen CA, Barr SC. Canine leishmaniasis in North America: emerging or newly recognized? *Vet Clin North Am Small Anim Pract*. 2009;39(6):1065-1074.
17. Reuss SM. Review of equine cutaneous leishmaniasis: not just a foreign animal disease. *AAEP Proceedings*. 2013;59:256-260.
18. Serafim TD, Coutinho-Abreu IV, Dey R, et al. Leishmaniasis: the act of transmission. *Trends Parasitol*. 2021;37: 976-987.

CASE II:

Signalment:
10-year-old, intact female Tennessee Walking Horse (*Equus caballus)*

History:
The patient had a history of a mass in the nose and troubled breathing. A mass was confirmed on radiographs and via endoscopic examination.

Gross Pathology:
The carcass was in adequate body condition (5.5/9). A mild creamy yellow viscous mucus-like nasal discharge was present. Saggital sectioning of the head revealed multiple firm to hard cream-colored masses. In the ventral nasal concha there was an oval 7 cm x 4 cm x 2 cm mass with a linear cobblestone appearance in the rostral aspect of the mass.

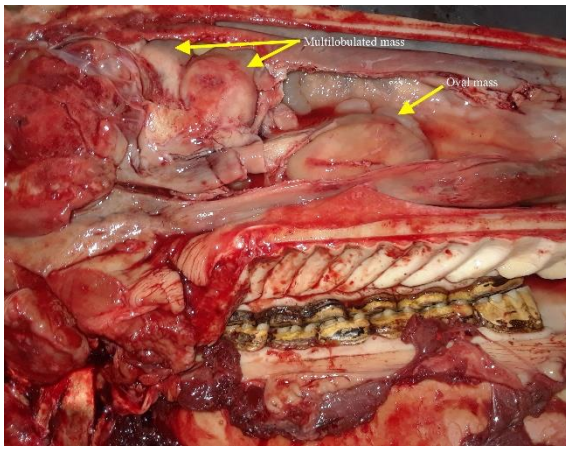

Figure 2-1. Nasal turbinates, horse. There are multiple firm to hard, cream-colored masses. in the ventral nasal concha there was an oval 7cm x 4 cm x 2 cm mass with a linear cobblestone appearance in the rostral aspect of the mass (*Photo courtesy of:* Tuskegee University, College of Veterinary Medicine, Department of Pathobiology, https://www.tuskegee.edu/programs-courses/colleges-schools/cvm)

Invading the dorsal concha was another irregular multilobulated mass, measuring 5.5 cm x 4 cm x 5 cm, which contained several tan to gray soft, rounded cyst-like fluid-filled structures. The left ethmoid turbinates contained a similar 5 cm x 5 cm mass.

On the surface of the right caudal lung lobe at the caudal border, there was a 6.5 cm x 7 cm, slightly elevated, cream-colored, gelatinous, irregular, focally extensive area with short thick projections. The surface of these projections had multifocal to coalescing pinpoint to 2 cm red foci, and cut section of this area revealed two round, semi-firm, opaque yellow nodules that extended 1 cm into the lung parenchyma. Twelve centimeters cranially to the aforementioned lesion there was another similar (cream colored, gelatinous with pinpoint red discolorations) area measuring 1 cm x 0.5 cm.

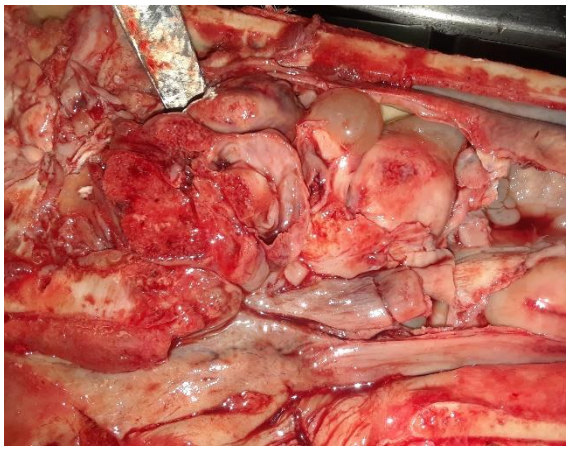

Figure 2-2. Nasal turbinates, horse. The sample is from an oval 7 cm x 4 cm x 2 cm mass with a linear cobblestone appearance. (*Photo courtesy of:* Tuskegee University, College of Veterinary Medicine, Department of Pathobiology)

Microscopic Description:
Nasal turbinates: Infiltrating and effacing >90% of the nasal turbinates are multifocal to coalescing nodular foci of inflammation centered on myriad dematiaceous mycotic agents. The inflammation consists of numerous macrophages with Langhans and foreign body type macrophages, numerous plasma cells, fewer lymphocytes, and random aggregates of neutrophils, which are surrounding numerous round to oval, 30-60 µm spherules with a 2-3 µm clear to brown stained capsule. These structures are frequently filled with several 3-6 µm clear to lightly basophilic rounded structures that are clustered together. The mycotic agents are frequently within multinucleated giant cells. Rarely, the organisms form 5-6 µm septate hyphae which were observed with Periodic Acid-Schiff (PAS) stain.

Contributor's Morphologic Diagnosis:
Nasal cavity: Severe multifocal granulomatous rhinitis with intralesional dematiaceous fungi (Phaeohyphomycosis).

Contributor's Comment:
On macroscopic examination it was thought that the lesion in the nose was a neoplastic process; however, histologic examination revealed the presence of dematiaceous (pigmented) mycotic agents associated with a granulomatous inflammatory process.

Dematiaceous fungi are naturally pigmented molds whose hyphae and conidia contain melanin.[2] They are ubiquitous and can be found in soil, plants, and organic debris.[2]

Melanin is what gives the dematiaceous fungi their pigmentation and it is believed to contribute to the organism's ability to elude the host immune response.[5,6] Melanin contributes to the evasion of the immune response by blocking the effects of hydrolytic enzymes on the cell wall and scavenging free radicals released by phagocytic cells during the oxidative burst.[6] There are several clinical presentations of dematiaceous molds, including eumy-cetoma, chromoblastomycosis,and phaeohyphomycosis. Our case is an example of phaeohyphomycosis.

Phaeohyphomycosis is an infection caused by dematiaceous (pigmented) fungi which typically affects immunocompromised individuals, but can also affect those that are immunocompetent.[2,5] Clinically, infections range from superficial colonization to systemic abscess formation and dissemination.[6]

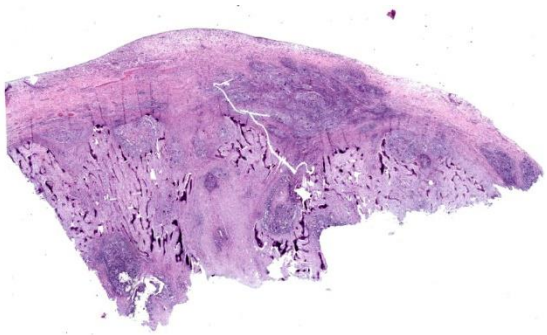

Figure 2-3. Nasal turbinate, horse. There is loss of normal turbinate architecture. The submucosa is expanded and the lytic turbinate bone is largely effaced by large areas of inflammation. (HE, 9X)

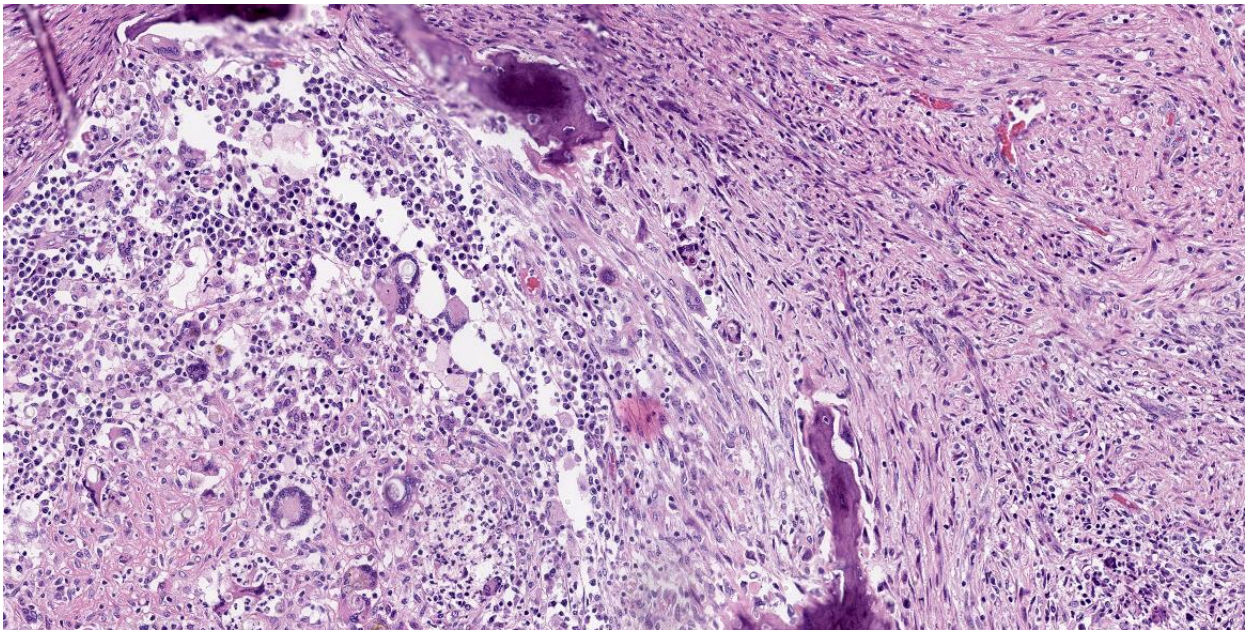

Figure 2-4. Nasal turbinate, horse. There is marked granulomatous inflammation with multinucleated foreign body macrophages against a background of fibrosis and lytic turbinate bone. (HE, 190X)

The fungi can be unicellular as well as yeast-like, but the key feature is the melanin pigment which distinguishes them from other fungi that may have similar morphology.[6] There are many causes of phaeohyphomycosis; the ones most commonly reported in equines are *Alternaria* sp., *Dreschslera* sp., and *Curvularia* sp.[1]

The presence of pigmentation on histopathology warrants a diagnosis of phaeohyphomycosis. In cases with dematiaceous fungi that are poorly pigmented, Fontana-Masson can be used to accentuate the melanin.[5] As with other mycotic agents, Periodic Acid-Schiff (PAS) and Grocott-Gomori methenamine silver (GMS) are common stains used to visualize the agents. Culture as well as molecular analysis can also be used to further narrow the identification down to the species level.[6]

Contributing Institution:
Tuskegee University
College of Veterinary Medicine
Department of Pathobiology,
https://www.tuskegee.edu/programs-courses/colleges-schools/cvm

JPC Diagnosis:
Nasal mucosa: Rhinitis, granulomatous, multifocal to coalescing, severe, with turbinate bone lysis and numerous pigmented fungal yeast-like cells and hyphae.

JPC Comment:
This case provides both an excellent example of dematiaceous fungi and a reason to revisit the various classifications of cutaneous fungal infections, particularly in light of an excellent, recently published review article on the subject.[3]

In general, cutaneous infection with opportunistic fungi presents as nodules or masses in the dermis and/or subcutis which may become ulcerated and develop draining tracts.[3]

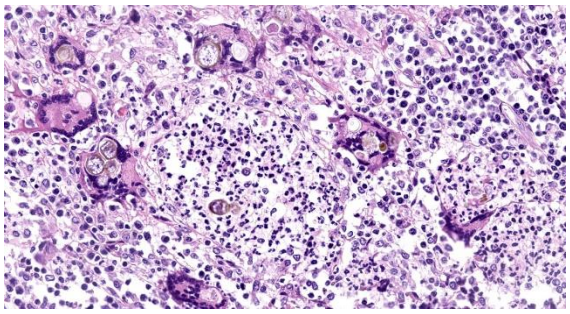

Figure 2-5. Nasal turbinate, horse. Pigmented hyphae and large round "yeast-like cells" are phagocytized by macrophages and multinucleated foreign body macrophages. (HE, 381X)

Histologically, fungal lesions are typically characterized by pyogranulomatous or granulomatous inflammation; some fungal infections may have a significant eosinophilic component, depending on species.[3] Fungi generally grow as hyphae in tissue and can be demonstrated by PAS and GMS stains to highlight histomorphologic features useful in narrowing differential diagnoses.[3]

Infection with non-dermatophytic, non-dimorphic, nonpigmented saprophytic fungi that grow as hyphae in tissue is referred to broadly as hyalohyphomycosis. Note that *Aspergillus* sp., fungi of the order *Mucorales*, and *Conidiobolus* spp and *Basidiobolus* spp, the agents of entomophthoromycosis, while all nonpigmented hyphae-forming fungi, are typically categorized separately from general hyalohyphomycosis.[3]

Phaeohyphomycosis refers to infection with *pigmented* saprophytic fungi that grow as hyphae and yeast-like cells in tissue. The term chromoblastomycosis is used for infection with a subset of pigmented fungi that predominately form large, round, thick-walled cells with prominent septations, called sclerotic bodies or Medlar bodies.[3] While small numbers of hyphae may be observed in chromoblastomycosis, sclerotic bodies are the predominant fungal form in the lesion.[3] Note that, as in this case, phaeohymphocosis may contain yeast-like cells; these may be differentiated from the sclerotic bodies of chrombolastomycosis by their thinner walls, septations in a single plane, and typical arrangement in chains.[3]

Agent Category	Description	Representative Species
White-grain eumycotic mycetoma	• Septate, nonpigmented hyphae • Infrequent dichotomous branching • Frequent terminal cystic dilations	• *Pseudallescheria boydii* • *Pencillium dupontii*
Black-grain eumycotic mycetoma	• Septate, pigmented hyphae • Infrequent dichotomous branching • Frequent terminal cystic dilations	• *Curvularia* spp. • *Cladophialophora bantiana*
Hyalohyphomycosis	• Septate hyphae with parallel walls and occasional acute-angle branching	• *Fusarium* spp. • *Scedosporium* spp.
Phaeohyphomycosis	• Pigmented hyphae, +/- branching • Yeast-like cells • Fontana-Masson may highlight melanin	• *Alternaria* spp. • *Curvularia* spp. • *Bipolaris* spp.
Chromoblastomycosis	• Pigmented sclerotic bodies with transverse and longitudinal septation	• *Cladophialophora bantiana* • *Curvularia* spp.
Entomophthoromycosis	• Sparsely septate hyphae • Nonparallel walls, rare irregular branching, terminal bulbous dilations • Eosinophilic sleeve around hyphae	• *Conidiobolus* spp. • *Basidiobolus* spp.

Table 2-1. Selected organisms causing dermal to subcutaneous fungal infections in animals. Adapted from Hoffman, et al. *Vet Pathol*. 2023;60(6):814.[3]

It is unknown what factors cause a particular fungus to cause phaeohyphomycosis versus chromoblastomycosis, though most cases of chromoblastomycosis in veterinary medicine have been described in amphibians and horses.[3]

Separate from the categorization of pigmented vs. non-pigmented fungi is the clinical presentation referred to as mycetoma. A mycetoma is a dermal and/or subcutaneous nodule with three typical features: swelling, an exudate containing *grossly apparent grains* or *granules* that represent large aggregates of the infectious agent, and a draining tract.[3] Mycetomas are divided into those caused by bacteria (termed actinomycotic mycetomas) or fungi (eumycotic mycetomas). Eumycotic mycetomas may be further subdivided into black-grain eumycotic mycetomas and white-grain eumycotic mycetoma, depending on whether they are caused by pigmented or non-pigmented fungi, respectively.[3] Confusingly, eumycotic mycetoma is a morphologic classification that is not based on the inciting organism, so the same fungal species that may cause hyalohyphomycosis or phaeohyphomycosis may alternatively cause eumycotic mycetomas if tissue grains are present.[3] Common representative species of each of the categories discussed above are presented in Table 2-1.

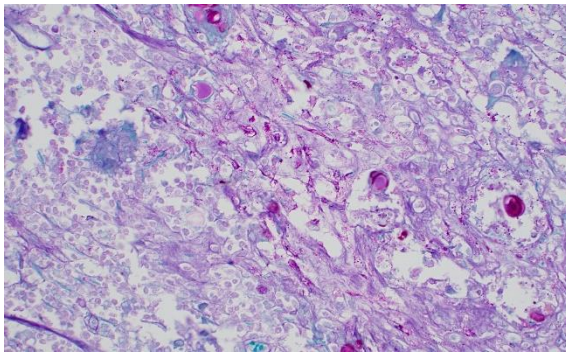

Figure 2-6. Nasal turbinate, horse. A PAS stain demonstrates the fungal hyphae and yeast-like cells within macrophages and multinucleated foreign body macrophages. (PAS, 400X)

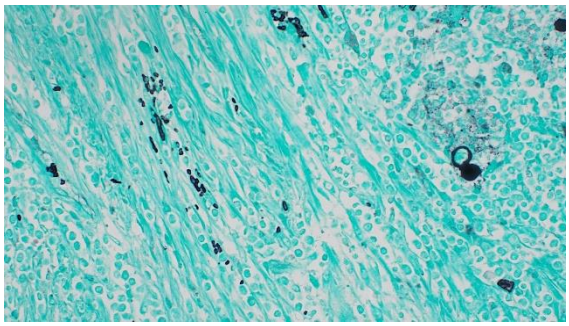

Figure 2-7. Nasal turbinate, horse. A silver stain demonstrates the fungal hyphae and yeast-like cells within macrophages and multinucleated foreign body macrophages. (Grocott's methenamine silver, 400X)

Participants discussed the yeast-like cells present throughout the section and considered a diagnosis of chromoblastomycosis given the prominence of the yeast-like cells on H&E section; however, PAS staining revealed numerous hyphae and participants noted that the yeast-like cells are frequently arranged in chains, making phaeohyphomycosis the appropriate diagnosis. Participants also discussed the arrangement and character of the bone present in section, particularly the arrangement of the bone fragments perpendicular to the nasal mucosa. Participants felt that the bony fragments represent periosteal new bone growth rather than lysed turbinates, which be oriented parallel to the mucosal surface. Participants felt that the turbinates have been destroyed completely by this inflammatory process, leaving behind only remodeling woven bone. The morphologic diagnosis retains the emphasis on bony lysis, though, in the examined section, we are left with only its aftermath to appreciate.

References:

1. Cafarchia C, Figueredo LA, Otranto D. Fungal diseases of horses.*Veterinary Microbiology*. 2013:215-234.
2. Guarner J, Brandt ME Brandt. Histopathologic diagnosis of fungal infections in the 21st century. *Clinical Microbiology Reviews*. 2011:247-280.

3. Hoffman AR, Ramos MG, Walker RT, Stranahan LW. Hyphae, pseudohyphae, yeasts, spherules, spores, and more: A review on the morphology and pathology of fungal and oomycete infections in the skin of domestic animals. *Vet Pathol*. 2023;60(6):812-828.
4. Mauldin EA, Peters-Kennedy J. Integumentary System. In: Maxie G, ed. *Jubb, Kennedy and Palmer`s Pathology of Domestic Animals*. 6th ed. Vol 1. Elsevier; 2016.
5. Pumlee Q, Meason-Smith C, Dieterly A, et al. Chaetomiaceae fungi, novel pathogens of equine neurotropic phaeohyphomycosis. *Vet Pathol*. 2017;54(5):813-819.
6. Seyedmousavi S, Guillot J, de Hoog GS. Phaeohyphomycoses, emerging opportunistic diseases in animals. *Clin Microbiol Rev*. 2013;26(1):19-35.

CASE III:

Signalment:
19-year-old, Polo mare (*Equus caballus*)

History:
This 19-year-old Polo mare presented with a recent history of coughing and exercise intolerance.

Gross Pathology:
On endoscopy, several irregular, broad, pedunculated, polypoid lesions were detected at the laryngeal aditus and aryepiglottic folds. The masses were mottled cream to red-brown and slightly granular.

Microscopic Description:
At low magnification, raised polypoid proliferations of loose fibrovascular tissue covered by an intact, mildly hyperplastic, non-keratinizing stratified squamous epithelium

Figure 3-1. Larynx, horse. Endoscopy of the polypoid masses at the laryngeal aditus and aryepiglottic folds. (*Photo courtesy of:* Henry Tremaine, B&W Equine Vets, https://www.bwequinevets.co.uk/183/henry-tremaine-eq-uine-vet-glouces-ter/)

expand the mucosa and submucosa. Numerous spherical structures of varying size are randomly distributed throughout the lamina propria and submucosa, and are occasionally present within the laryngeal epithelium. These spherical structures represent sporangia in different stages of development. Sporangia are also present within submucosal glands that are dilated and are sometimes surrounded by deposits of amorphous eosinophilic material.

Small juvenile, immature sporangia (trophocytes) measure 10-100 μm, have a thick unilamellar, eosinophilic wall, and a single central round nucleus surrounded by granular amphophilic cytoplasm. Intermediate sporangia are characterized by the loss of the central single nucleus, a size of up to 300 μm, and the presence of numerous punctate eosinophilic granules. With progressing maturation, nuclei become more discrete 1-4 μm ovoid structures (prophase nuclei) and intermediate sporangia exhibit a mixture of punctate granules and small eosinophilic ovoid structures.[4]

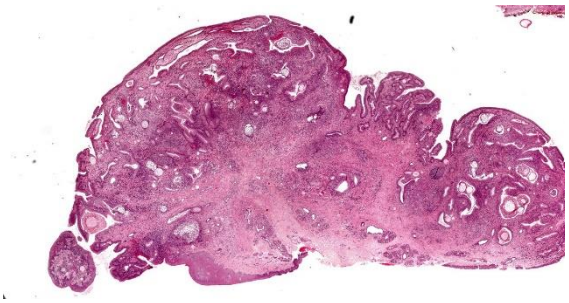

Figure 3-2. Larynx, horse. The laryngeal mucosa is markedly hyperplastic and thrown into numerous and deep folds. (HE, 12X)

Mature sporangia are spherical and 100-400 µm in diameter with a bilamellar, outer eosinophilic and inner amphophilic wall. The mature endospores are 10 µm, eosinophilic to basophilic, ovoid to round structures with a cell wall and single nucleus. Often a centripetal or centrifugal zone of small round eosinophilic structures (germinative zone) and mature endospores is present within the mature sporangia. Multifocally, the mature sporangia are ruptured or release endospores through their operculum (pore). Rupture of sporangia is accompanied by infiltration of large numbers of neutrophils and fewer macrophages.

Moderate numbers of lymphocytes and plasma cells and fewer neutrophils are multifocally present within the stroma of the lamina propria and the submucosa. Multifocally, small numbers of neutrophils migrate into the overlying mucosal epithelium (exocytosis).

A thin layer of coagulative necrosis (cautery artefact) is present around the margins and is often associated with mild multifocal oedema and haemorrhage. In some of the sections examined, sporangia are detected very close to the areas of cautery.

Contributor's Morphologic Diagnosis:
Laryngitis, proliferative, lymphocytic, plasmacytic, neutrophilic, and histiocytic, multifocal to coalescing, moderate, chronic, with intralesional juvenile and mature sporangia consistent with *Rhinosporidium seeberi*.

Contributor's Comment:
Rhinosporidium seeberi is a eukaryotic, hydrophilic organism from the Mesomycetozoa clade (DRIP clade) that also includes several fish pathogens such as *Dermocystidium* spp.[11,18] Its exact phylogenetic classification is unclear, with some discussion as to whether it should be grouped differently. The organism is generally found in stagnant waters and is the causative agent of rhinosporidiosis in humans.[11,17] In addition, rhinosporidiosis has been described in multiple other species, including cats, horses, cattle, buffaloes, dogs, mules, swans, and wild fowls.[3,14,17] Rhinosporidiosis is endemic in India, Sri-Lanka, in parts of the Americas, and Africa.[12,14,17] In horses, in addition to endemic areas, cases have also been recorded in countries traditionally free of rhinosporidiosis. Those cases have mostly been restricted to imported ani-

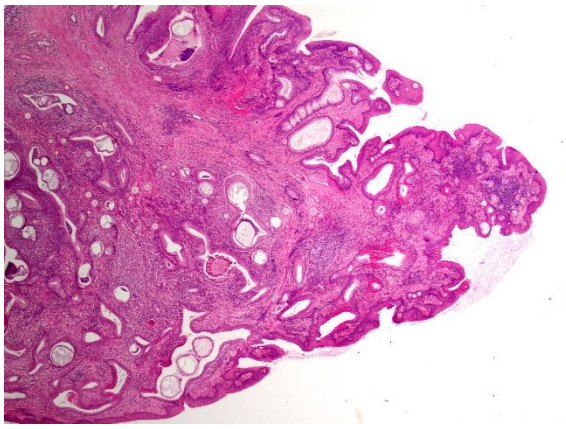

Figure 3-3. Larynx, horse. The polypoid proliferation of loose connective tissue of the laryngeal mucosa on subgross magnification. Multiple sporangia at different stages of development are present within the submucosa. The mass is covered by a hyperplastic epithelium (HE, 20X)(*Photo courtesy of:* Department of Veterinary Medicine, The Queen's Veterinary School Hospital, University of Cambridge, Cambridge CB3 0ES, UK. https://www.vet. cam.ac.uk)

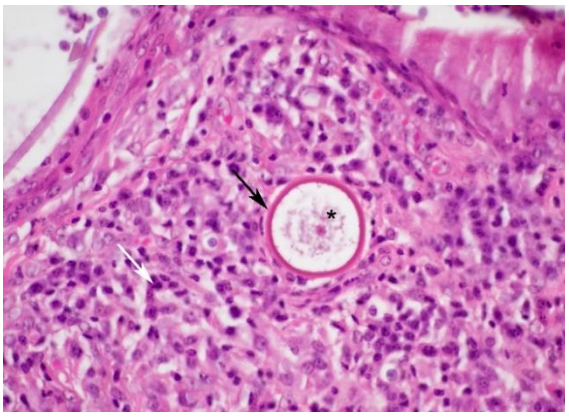

Figure 3-4. Larynx, horse. Juvenile sporangia (trophocytes) measuring ~50 µm, with a thick unilamellar, eosinophilic wall (black arrow), a single central round nucleus surrounded by amphophilic granular material (cytoplasm, asterisk). Lymphocytes and plasma cells infiltrate the connective tissue (white arrow) (HE, 400X)(*Photo courtesy of:* Department of Veterinary Medicine, The Queen's Veterinary School Hospital, University of Cambridge. Cambridge CB3 0ES, UK)

mals, such as four polo ponies that were imported from Argentina to the United Kingdom.[4,12,17] However, the potential for the disease to inhabit traditionally non-endemic areas was highlighted by a recent report from Europe. In that case, a Belgian warmblood horse, born in Belgium, that had never left the country, was diagnosed with rhinosporidiosis.[15] The source of infection remained unclear; however, as this organism is not contagious, the case suggests that the organism was present in the environment in Belgium.[16]

Due to difficulties with *in vitro* culturing of this organism, the life cycle of *Rhinosporidium seeberi* is still not fully understood.[18] It is believed that the infective stage is the mature endospore which enters the host through damaged epithelium of mucous membranes, mostly of the nose.[10,18] In the host tissue the endospore develops into a juvenile sporangium (trophocyte) with a single central nucleus. Subsequent reproduction takes place in intermediate sporangia via sole synchronized nuclear division. Cytokinesis occurs only once shortly before the formation of the mature sporangium. [9,13] Furthermore, it is suggested that mature sporangia are capable of additional "de novo" production of mature, cell-walled endospores.[9]

Based on the finding that only a few humans out of the many bathing in contaminated water become infected with *Rhinosporidium seeberi*, an individual host susceptibility has been suggested. The susceptibility is assumed to correlated to the presence of certain blood groups, but this relation has not be confirmed.[2]

Rhinosporidiosis most often localises in mucous membranes of the head region, with the nostrils and conjunctivae most commonly affected.[1,10] In humans, infection of the throat, eye, ear, oropharynx, larynx, trachea, bronchi, and genitourinary tract are also described.[7,16] Infected tissues develop single to multiple, pink, multilobular, broad-based, granulomatous, pedunculated, non-infiltrative masses. The affected mucosa is often red with stippled, pinpoint white granules (mature sporangia) that give the mass a mulberry-like or strawberry-like appearance.[5] The masses are slow growing and generally painless; however, irritation due to the presence of the masses can lead to sneezing, discharge, and when obstructing airways, may result in respiratory distress.[5,8]

In this horse, multiple polypoid masses were detected around the laryngeal aditus and at the aryepiglottic folds, resulting in coughing and exercise intolerance. The localisation in the laryngeal mucosa is rather unusual in horses. To our knowledge, two cases of equine laryngeal rhinosporidiosis have been described so far. In both of these cases, the masses were centred around the larynx, were surgical excised, and recurred.[4,15] So far, half

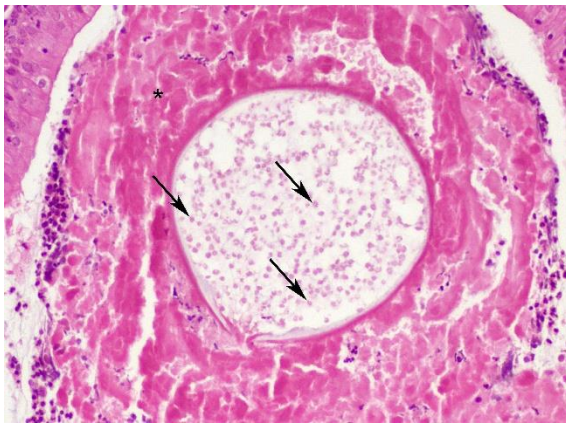

Figure 3-5. Larynx, horse. Intermediate sporangia in the lumen of a submucosal gland surrounded by eosinophilic material. At this stage of development sporangia measure up to 300 µm and contain numerous punctate eosinophilic granules or discrete 1-4 µm ovoid structures (prophase nuclei, black arrows). (HE, 200X)(*Photo courtesy of:* Department of Veterinary Medicine, The Queen's Veterinary School Hospital, University of Cambridge. Cambridge CB3 0ES, UK)

a year after surgical excision, no recurrence was observed in this horse.

Rhinosporidiosis remains an uncommon infection that can be diagnostically challenging. The diagnosis of equine rhinosporidiosis is based on clinical history, characteristic macroscopic and histopathologic appearance, and potentially, confirmatory polymerase chain reaction.[4,12,15] Treatment of choice is surgical excision with broad, clear margins and electrocauterization or cryotherapy of adjacent tissues[4,5,15] In humans, additional administration of dapsone is used to prevent maturation.[10] Recurrence was reported to occur in 11% of human cases and is due to spreading of mature endospores.[10,12] In addition, due to a long incubation period reported to be at least 10 months in one pony, clinically inapparent animals may be transported from endemic areas and might shed the organism.[12] Given the long incubation period, increased international movement of animals, and climate change, rhinosporidiosis has the potential to be an emerging disease and to become endemic in areas that have traditionally been free of rhinosporidiosis.

Contributing Institution:
Department of Veterinary Medicine
The Queen's Veterinary School Hospital
University of Cambridge.
Cambridge CB3 0ES, UK.
https://www.vet.cam.ac.uk

JPC Diagnosis:
Larynx: Laryngitis, proliferative, chronic-active, diffuse, moderate, with numerous juvenile and mature sporangia and endospores.

JPC Comment:
The contributor provides an excellent, thorough summary of *Rhinosporidium seeberi* infection, a classic disease with a classic, virtually unmistakable histological appearance. As the contributor notes, the laryngeal location is uncommon; the more typical presentation of rhinosporidiosis is a soft, pink unilateral fleshy polyp, usually in the nose of a dog.[6]

While the gross appearance of *R. seeberi* may be confused for a variety of inflammatory or neoplastic conditions, particularly when found in an unusual location, once under the microscope, *R. seeberi* sporangia are not histologic wallflowers, but are large, striking, and distinctive. The juvenile sporangia are 15-75µm in diameter, have a unilamellar, PAS-positive wall, and a single nucleus.[6] The real stars, however, are the mature sporangia, which can grow to an astonishing 100-400 µm, have a PAS-positive bilamellar wall, and contain myriad 5-10 µm endospores. The presence of these eye-catching sporangia in the histologic section of a nasal polyp is essentially pathognomonic for rhinosporidiosis.

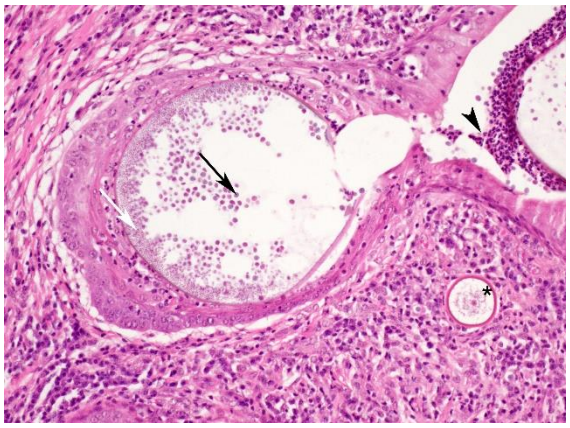

Figure 3-6. Larynx, horse. Mature sporangia have a bilamellar wall, are 100-400 µm in diameter. A zone of small round eosinophilic structures (germinative zone, white arrow) and mature endospores (black arrow) is present within the mature sporangia. The mature sporangia release endospores through their pore. The rupture of sporangia causes infiltration of large numbers of neutrophils (arrowhead). A juvenile sporangium is present in the connective tissue. (asterisk, HE, 200X)

R. seeberi belongs to a class of organisms aptly termed endosporulators. Other endosporulators of veterinary importance include *Coccidioides immitis*, *Coccidioides posadasii*, *Prototheca* sp., *Chlorella* sp., and *Batrachochytrium dendrobatidis*. Of these, only *Coccidioides* is of a size and morphology that could be confused with *R. seeberi*. Immature *Coccidioides* spherules, the analogue to the *R. seeberi* sporangia, are approximately 10-20 µm in diameter and grow into mature spherules of up to 200 µm in diameter filled with numerous 2-5µm endospores.[6]

Participants struggled with tissue identification with this slide, with most defaulting to nasal mucosa based on the typical location. Conference discussion focused largely on the morphologic diagnosis and how to capture the significant, mixed inflammatory component of the lesion. Some participant felt strongly that the morphologic diagnosis should emphasize the extensive lymphohistiocytic and plasma-cytic character of the lesion, while others argued that the significant neutrophilic infiltrate should also be included. In the end, participants decided that "chronic-active" implied the existnence of both a neutrophilic (active) component and a lymphohistiocytic component with marked hyperplasia of the mucosa (a chronic change) and preferred the pared down diagnosis given above.

References:

1. Allison RW, Ramachandran A. What is your diagnosis? Ulcerative nasal lesion in a Quarter Horse. *Vet Clin Path*. 2015; 44: 455-456.
2. Arseculeratne SN. Recent advances in rhinosporidiosis and *Rhinosporidium seeberi*. *Indian J Med Microbiol*. 2002;20: 119-131.
3. Berrocal A, López A. Nasal rhinosporidiosis in a mule. *Can Vet J*. 2007;48: 305-306.
4. Burgess HJ, Lockerbie BP, Czerwinski S, Scott M. Equine laryngeal rhinosporidiosis in western Canada. *J Vet Diagn Invest*. 2012;24(4):77-780.
5. Caniatti M, Roccabianca P, Scanziani E, et al. Nasal rhinosporidiosis in dogs: four cases from Europe and a review of the literature. *Vet Rec*. 1998;142:334-338.
6. Caswell JL, Williams K. Respiratory System. In: Maxie MG, ed. *Jubb, Kennedy, and Palmer's Pathology of Domestic Animals*. 6th ed. Vol 2. 2016; Elsevier:579-584.
7. Costa EF, Pinto LM, Campos MAG, Gomes TM, et al. Partial regression of large anterior scleral staphyloma secondary to rhinosporidiosis after corneoscleral graft - a case report. *BMC Ophthalmology*. 2018;18:61.
8. Das S, Kashyap B, Barua M, et al. Nasal rhinosporidiosis in humans: new interpretations and a review of the literature of

this enigmatic disease. *Medical Mycol*. 2011;49:311-315.
9. Delfino D, Mendoza L, Vilela R. *Rhinosporidium seeberi* nuclear cycle activities using confocal microscopy. *J Parasitol*. 2016;102(1):60-68.
10. Harissi-Dagher M, Robillard N, Corriveau C, Mabon M, et al. Histopathologically confirmed ocular rhinosporidiosis in two Canadians. *Can J Ophthalmol*. 2006;41: 226-229.
11. Herr RA, Ajello L, Taylor JW, Arseculeratne SN, Mendoza L. Phylogenetic analysis of *Rhinosporidium seeberi*'s 18S small-subunit ribosomal DNA groups this pathogen among mem-bers of the Protoctistan Mesomycetozoa Clade. *J Clin Microbiol*. 1999;37(9):2750-2754.
12. Leeming G, Smith KC, Bestbier ME, Barrelet A, Kipar A. Equine rhinosporidiosis in United Kingdom. *Emerg Infect Dis*. 2007;13(9):1377-1379.
13. Mendoza L, Vilela R. Presumptive synch-ronized nuclear divisions without cyto-kinesis in the *Rhinosporidium seeberi* parasitic life cycle. *Microbiology*. 2013; 159:1545-1551.
14. Moses JS, Balachandran C. Rhinosporidiosis in bovines of Kanyakumari district, Tamil Nadu, India. *Mycopathologia*. 1987;100:23-26.
15. Nollet H, Vercauteren G, Martens A, et al. Laryngeal rhinosporidiosis in a Belgian warmblood horse. *Zoonoses Public Health*. 2008;55:274-278.
16. Putthia H, Manjunatha BS, Astekar M, Taufiq S. Palatal rhinosporidiosis: an unusual case report and review of the literature. *J Korean Assoc Oral Maxillofac Surg*. 2018;44:293-297.
17. Sudasinghe T, Rajapakse RPVJ, Perera NAND, et al. The regional sero-epidemiology of rhinosporidiosis in Sri Lankan humans and animals. *Acta Tropica*. 2011;120:72-81.
18. Vilela R, Mendoza L. The taxonomy and phylogenetics of the human and animal pathogen *Rhinosporidium seeberi*: A critical review. *Rev Iberoam Micol*. 2012;29(4):185-199.

CASE IV:

Signalment:
3-year-old, Thoroughbred filly (*Equus caballus*)

History:
Found dead in stall.

Gross Pathology:
Both kidneys have numerous pinpoint raised, tan foci with a red halo scattered throughout the renal cortices.

Laboratory Results:
Aerobic culture, kidney: *Actinobacillus* sp., mixed flora (*Actinobacillus* sp. were also isolated from the liver and lung).

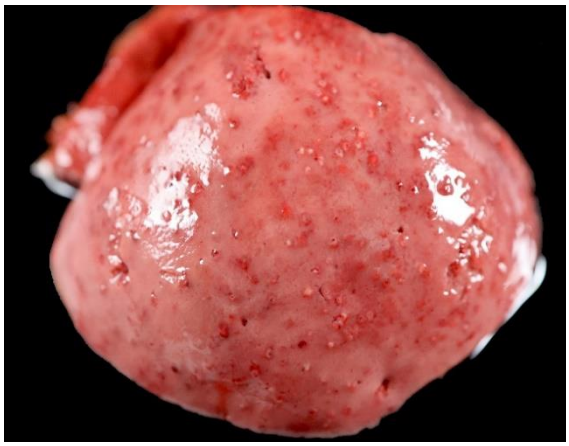

Figure 4-1. Kidney, horse. The kidney has raised white foci of inflammation on the capsular surface surrounded by red halos. *(Photo courtesy of* California Animal Health and Food Safety Laboratory San Bernardino Branch, https://cahfs.vetmed.ucdavis.edu/)

Figure 4-2. Kidney, horse. On cut section, the cortex has focal randomly scattered areas of suppurative inflammation surrounded by hemorrhage. *(Photo courtesy of* California Animal Health and Food Safety Laboratory San Bernardino Branch)

DNA sequence analysis: DNA sequencing of a ~600 bp region of the 16S rRNA gene identified the isolate as most closely related to *Actinobacillus equuli* ssp. *Equuli*.

Microscopic Description:
Within the renal cortical interstitium, there are randomly scattered, unencapsulated aggregates of neutrophils (measuring up to 3 mm in diameter), often with a central region of necrosis or hemorrhage, that efface the tubular and glomerular architecture. In some areas, these aggregates of neutrophils appear to be centered on glomeruli or blood vessels. There are aggregates of intra- and extravascular coccobacilli associated with these neutrophilic infiltrates. Glomeruli have similar bacteria and fibrin in the capillaries. There is also mild tubular degeneration. Coccobacilli are gram-negative.

Contributor's Morphologic Diagnosis:
Kidney: Nephritis, embolic-suppurative, multifocal, with intra- and extravascular Gram-negative coccobacilli.

Contributor's Comment:
Actinobacillus spp. (Family: *Pasteurellaceae*) are pleomorphic, non-motile, non-spore forming, gram-negative, rod-shaped bacteria characterized by their ability to grow on MacConkey agar, produce β-galactosidase, and ferment carbohydrates without the production of gas.[8] There are a number of *Actinobacillus* species of significance within veterinary medicine, including *A. lignieresii* (causative agent of wooden tongue in cattle), *A. pleuropneumoniae* (causative agent of porcine contagious pleuropneumonia in pigs), *A. suis* (cause of septicemia in pigs), *A. capsulatus* (cause of joint disease in rabbits), and *A. seminis* (cause of epididymitis in rams).[8] As with many pathogenic bacteria within the family *Pasteurellaceae*, Actinobacillus often produce repeats-in-toxin (RTX) toxins, which are typically hemolytic and cytotoxic.[3]

In horses, *Actinobacillus* are common commensals and can be isolated from the gastrointestinal, respiratory, and urogenital tracts of healthy animals.[4] *Actinobacillus* spp. isolated from horses include: *A. equuli* ssp. *equuli*, *A. equuli* ssp. *haemolyticus*, *A. arthritidis*, *A. lignieresii*, *A. suis*, and *A. pleuropneumoniae*. Of these, *A. equuli* ssp. *equuli* and *A. equuli* ssp. *haemolyticus* are isolated most frequently from horses. These subspecies are differentiated based on the presence or absence of an RTX toxin, *A. equuli* toxin (or Aqx), encoded on the *aqx gene*.[3,8]

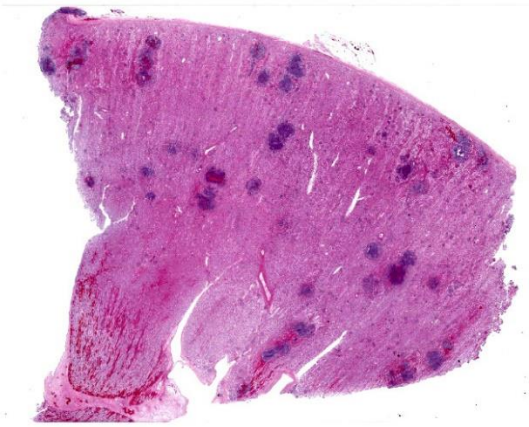

Figure 4-3. Kidney, horse. There are randomly scattered foci of inflammation within the cortex and medulla. (HE, 6X)

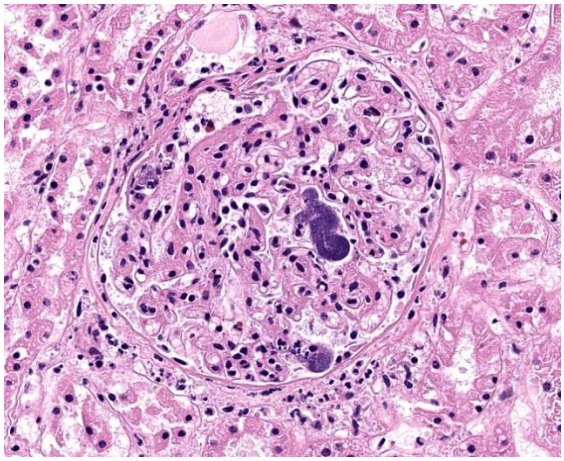

Figure 4-4. Kidney, horse. Glomerular capillaries contain colonies of coccobacilli. (HE, 317X)

Actinobacillus equuli ssp. *equuli* is typically carried in the oral cavity and alimentary tract of juvenile and adult horses and is primarily associated with septicemia in neonatal foals (often referred to as "sleepy foal disease").[4,8] There are also reports of *A. equuli*-associated peritonitis and septicemia in adult horses, with gross and microscopic lesions similar to those described in foals.[4-7,9] Predisposing factors for "sleepy foal disease" include failure of passive transfer and concurrent bacterial/viral infections.[4]

Similarly, actinobacillosis in adult horses can be associated with stress (such as shipping) and concurrent bacterial/viral infections; there is, however, evidence that *A. equuli* can act as a primary pathogen in horses in the absence of stress/concurrent disease.[4]

Typical light microscopic findings of *A. equuli* infection include: suppurative embolic nephritis, suppurative embolic pneumonia, multifocal suppurative hepatitis, lymphoid necrosis, suppurative oomphalitis, and suppurative meningoencephalitis. *A. equuli* is zoonotic with sporadic reports of disease in people.[1]

Contributing Institution:
California Animal Health and Food Safety Laboratory (San Bernardino Branch)
https://cahfs.vetmed.ucdavis.edu/

JPC Diagnoses:
Kidney: Nephritis, suppurative, embolic, with numerous large colonies of bacilli.

JPC Comment:
This case is an excellent example of suppurative embolic nephritis, in which septic emboli lodge in glomerular and peritubular capillaries and produce variably sized abscesses, primarily in the renal cortex.[2] In horses, *Actinbacillus equuli* is the most common cause of embolic suppurative nephritis, generally seen in neonatal foals after acquiring the infection in uetero, during parturition, or shortly after birth via the umbilicus.[2]

As the contributor notes, there are two subspecies of *A. equuli* that differ based on the presence of absence of an RTX toxin. *A. equuli* subspecies *haemolyticus* produces Aqx, an RTX toxin similar to the leukotoxins and hemolysins produced by related *Pasteurellaceae* such as *Mannheimia haemolytica, A. pleuropneumonia, A. suis*, and hemolytic *E. coli*.[4] The Aqx toxin is highly cyto

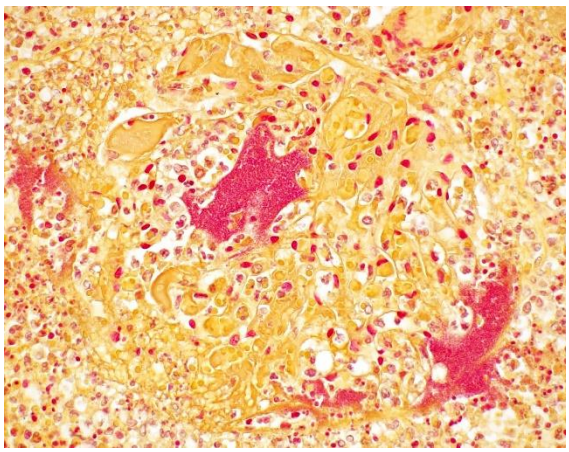

Figure 4-5. Kidney, horse. Coccobacilli within glomerular capillaries are gram-negative. (Gram, 400X)

lytic to equine erythrocytes and lymphocytes, and has less virulent lytic activity against the same cells in pigs.

The vast majority of *A. equuli* septicemia cases are cause by *A. equuli* subspecies *equuli*, which does not produce the Aqx toxin, indicating that other virulence factors likely play the key roles in neonatal septicemic actinobacillosis.[4]

Like any self-respecting gram-negative bacterium, *A. equuli* subspecies *equuli* is armed with endotoxin which, upon the destruction of the bacterium, damages endothelium and causes the vasculitis and bacterial emboli that are characteristic of septicemic actinobacillosis.[4] As illustrated in this case, a particular quirk of equine actinbacillosis is the presence of large bacterial colonies present in affected vessels, unlike other gram-negative bacteria which do not form such obvious intravascular aggregates.[4] This has led to speculation that *A. equuli* subspecies *equuli* may express an adhesion for endothelium. Unfortunately, other than the well-characterized Aqx toxin present in *A. equuli* subspecies *haemolyticus*, little is definitively known about the virulence factors that enable the spectacular lesions of equine actinobacillosis.[4]

Conference discussion focused initially on the age of the animal since, as noted above, *A. equuli* embolic nephritis is typically a disease of neonatal foals. The moderator noted reports of this presentation in non-stressed, non-immunocompromised adult animals and reminded residents to think broadly about differential diagnoses, even when the signalment isn't a perfect fit. The moderator led conference participants in a discussion other famous *Actinobacillus* species of veterinary importance, including the species noted above by the contributor. Finally, participants discussed the presence of bacterial colonies within glomeruli and whether this would constitute glomerulonephritis. Participants felt

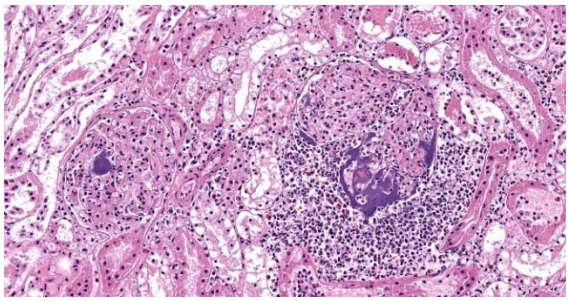

Figure 4-6. Kidney, horse. Glomerular capillaries contain colonies of coccobacilli. (HE, 317X)

that, since the pathogeneses behind the established categories of glomerulonephritis (membranoproliferative, membranous, etc.) did not pertain to a suppurative embolic nephritis, the term glomerulonephritis was inappropriate. Glomerulitis would be a more appropriate term; however, since suppurative inflammation was present within the glomeruli, tubules, and interstitium, the preferred morphologic diagnosis is the all-inclusive term "nephritis."

References:

1. Ashhurst-Smith C, Norton R, Thoreau W, Peel MM. *Actinobacillus equuli* septicemia: an unusual zoonotic infection. *J Clin Microbiol*. 1998;36(9):2789-90.
2. Cianciolo RE, Mohr FC. Urinary System. In: Maxie MG, ed. *Jubb, Kennedy, and Palmer's Pathology of Domestic Animals*. 6th ed. Vol 2. Elsevier;206:433.
3. Frey J, Kuhnert P. RTX toxins in *Pasteurellaceae*. *Int J Med Microbiol*. 2002;292(3-4):149-58.
4. Layman QD, Rezabek GB, Ramachandran A, Love BC, Confer AW. A retrospective study of equine actinobacillosis cases: 1999-2011. *J Vet Diagn Invest*. 2014; 26(3):365-75.
5. Matthews S, Dart AJ, Dowling BA, Hodgson JL, Hodgson DR. Peritonitis associated with *Actinobacillus equuli* in horses: 51 cases. *Aust Vet J*. 2001;79(8):536-9.

6. Means K, Townsend K, Johnson P. Multicavitary septic effusions associated with actinobacillosis in an adult Tennessee Walking Horse with weight loss. *Equine Vet Educ*. 2022;34(1):e60-6.
7. Patterson-Kane JC, Donahue JM, Harrison LR. Septicemia and peritonitis due to *Actinobacillus equuli* infection in an adult horse. *Vet Pathol*. 2001;38(2):230-2.
8. Rycroft AN, Garside H. *Actinobacillus* species and their role in animal disease. *Vet J*. 2000;159(1):18-36.
9. Uchida-Fujii E, Niwa H, Kinoshita Y, Nukada T. *Actinobacillus* species isolated from Japanese Thoroughbred racehorses in the last two decades. *J Vet Med Sci*. 2019;81(9):1234-7.

WSC 2023-2024
Conference 14 Self-Assessment

1. Which of the following is NOT a disease pattern of leishmaniasis?
    a. Mucocutaneous leishmaniasis
    b. Hematopoietic leishmaniasis
    c. Visceral leishmaniasis
    d. Cutaneous leishmaniasis

2. Which of the following stains is best to visualize *Leishmania* amastigotes?
    a. Giemsa
    b. Grocott
    c. Toluidine blue
    d. Gram

3. Which of the following is a virulence factor in dematiaceous fungi?
    a. Lysozyme
    b. Melanin
    c. Phospholipase A
    d. Ferrochelatase

4. *Rhinosporidium seeberi* is most closely related to which of the following fish pathogens?

    a. Epitheliocystis
    b. Ichthyophonus
    c. Icthyophthirius multifillis
    d. Dermocystidium

5. True or false: *Actinobacillus equuli* subsp. is a normal inhabitant of the gastrointestinal tract of horses.
    a. True
    b. False

Joint Pathology Center
Veterinary Pathology Services

WEDNESDAY SLIDE CONFERENCE 2023-2024

Conference #15 10 January 2024

CASE I:

Signalment:
Four-year-old, male neutered Pygmy goat (*Capra aegagrus hircus*)

History:
This pygmy goat was presented to the Royal Veterinary College Farm Animal Hospital for further evaluation and possible treatment of an oral mass. Computed tomography (CT) of the head identified severe bony enlargement of the rostral aspect of both mandibles with destructive and lytic bony changes from the rostral margins of the mandible up to the first premolar bilaterally. Moderate soft tissue swelling surrounded the misshaped mandibles. The 402, 403, and 404 teeth were missing and the remaining incisors were displaced laterally. Surgical options were discussed with the owner but due to the extent of the lesion and the complexity of the surgical approach, the owner elected to euthanise the animal.

Gross Pathology:
Arising from the rostral mandible predominantly to the right of midline is a proliferative, dark red, moderately soft mass measuring 8x3x2.5cm with a bleeding surface. On sectioning, the mass is grey and solid. The mass displaces the five remaining incisors over to the left side and all the incisors are loose.

Figure 1-1. Mandible, goat. Arising from the rostral mandible, predominantly to the right of midline, is a dark, red mass measuring 8x3x2.5 cm. (*Photo courtesy of:* Dept of Pathobiology & Population Sciences, The Royal Veterinary College, https://www.rvc.ac.uk/pathology-and-diagnostic-laboratories)

Microscopic Description:
Rostral mandibular mass: Arising within the mandibular bone is an unencapsulated, moderately well demarcated, expansile, multinodular neoplasm which raises the contour of the gingival epithelium. The mass is composed of abundant multinucleated giant cells interspersed with a dense population of spindle shaped cells in a fibrovascular stroma. Each cell type represents approximately 50% of the cellular population in the section. The giant cells have well demarcated borders with abundant eosinophilic cytoplasm that contains varying numbers of microvacuoles, and between two and ten nuclei which are randomly distributed in the centre of the cell and

Figure 1-2. Mandible, goat. The mass displaces the five remaining incisors over to the left side and all incisors are loose. (Photo courtesy of: Pathobiology & Population Sciences, The Royal Veterinary College)

have finely stippled chromatin. The spindle-shaped cells are poorly defined with a moderate amount of eosinophilic fibrillar cytoplasm, elongate nuclei, and finely clumped chromatin. There is mild anisokaryosis and anisocytosis of both cellular populations. There are four mitoses detected in 10 HPF's (x400), three of which are bizarre mitoses. At the periphery of the neoplasm, there is fragmentation and necrosis of the mandibular bone and hyperplasia of osteoblasts. Occasional giant cells contain multiple pyknotic nuclei (apoptosis or individual cell necrosis). Multifocally, macrophages contain yellow to brown, globular pigment (haemosiderophages). The overlying gingival epithelium exhibits mild hyperplasia.

Contributor's Morphologic Diagnosis:
Mandible: Central giant cell granuloma (aggressive form).

Contributor's Comment:
Differential diagnoses for masses arising in the jaw which contain numerous giant cells include giant cell granulomas of the jaws, osteosarcoma (giant cell variant), osseous fibroma, or low grade spindle cell sarcoma with giant cells. The density of the giant cell population and the lack of osteoid or mineralized matrix is not consistent with the latter three differentials in this case.

Giant cell granulomas of the jaws are currently differentiated based on location into peripheral or central giant cell granulomas.[10] Peripheral giant cell granuloma (PGCG, previously known as giant cell epulis, peripheral giant cell tumor, osteoclastoma, reparatory giant cell granuloma, and giant cell hyperplasia of the oral mucosa) is a reactive and non-neoplastic gingival lesion that clinically presents as a soft to firm, polypoid or nodular lesion on the gingiva and alveolar ridge and is believed to originate from the periosteum or periodontal ligament.[1,5,6, 9, 10] There is minimal bone lysis associated with PGCG. These lesions, along with pyogenic granuloma and fibrous hyperplasia, are the most common reactive hyperplastic lesions in the oral cavity and have been described in humans, dogs, and cats.[1-3,6,11]

Central giant cell granuloma (CGCG), on the other hand, is a rare benign, non-metastatic, intraosseous lesion which is further subdivided into non-aggressive and aggressive forms based on its biological behavior. The

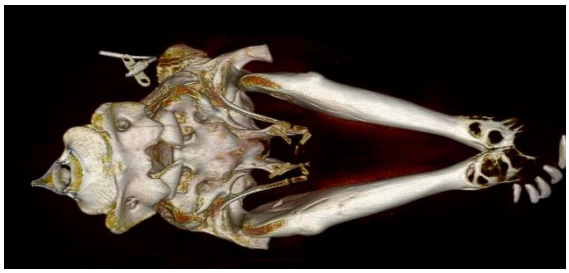

Figure 1-3. Mandible, goat. Computed tomography (CT) of the head identified severe bony enlargement of the rostral aspect of both mandibles with destructive and lytic bony changes from the rostral margins of the mandible up to the first premolar bilaterally (*Photo courtesy of:* Pathobiology & Population Sciences, The Royal Veterinary College)

former is associated with asymptomatic swelling and the latter associated with pain, cortical bone destruction, tooth root resorption, displacement of teeth, and a high recurrence rate.[7] Histologically, peripheral and central giant cell granulomas are characterized by variable numbers of multinucleated giant cells intermixed with a dense population of mononuclear spindle-shaped cells and variable amounts of collagenous matrix; however, CGCG may exhibit more foci of haemorrhage and occasional trabeculae of woven bone compared to PGCG.[7] Some investigators consider CGCG to be a variant of giant cell tumor of bone, which arise in the ends of long bones, and prefer the term 'giant cell lesion' with no distinction of granuloma.[6,11] One report in the literature describes a case of 'giant cell tumour' within the caudal mandible of a goat which also involved the temporomandibular joint.[4] CGCG in humans shows a female predilection (2:1) and is more common in the mandible than maxilla.[1] CGCG can also affect extragnathic bones, mainly in the craniofacial region.[10]

In this case, given the intraosseous location of the mass, the presence of osteolysis, displacement of the incisor teeth, and the lack of mineralized and osteoid matrix, a diagnosis of aggressive central giant cell granuloma was made.

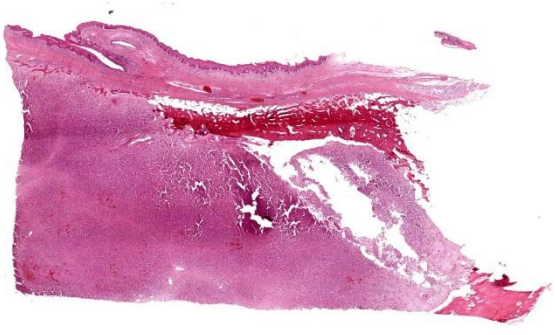

Figure 1-4. Mandible, goat. One section of a mass effacing the normal architecture of the mandible is submitted for examination. The mass is covered by an intact and slightly hyperplastic mucosa. (HE, 5X)

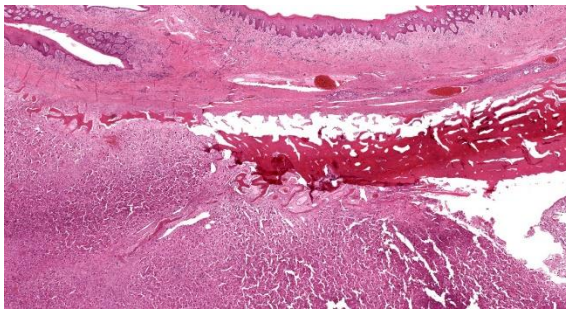

Figure 1-5. Mandible, goat. Higher magnification of the effacement of cortical bone by the mass. (HE, 18X)

The pathogenesis of CGCG is poorly understood and there is still dispute over whether this is a neoplastic or reactive lesion.[7] Giant cells within giant cell granulomas are thought to arise from osteoclasts and positive histochemical staining for tartrate-resistant acid phosphatase (TRAP), which is an enzyme unique to osteoclasts, and receptor activator of nuclear factor kappa B (RANK), which regulates osteoclast differentiation and activation, supports an osteoclastic origin for these masses.[2,3]

Contributing Institution:
Pathobiology & Population Sciences
The Royal Veterinary College
Hawkshead Lane, North Mymms
Hertfordshire, UK
https://www.rvc.ac.uk/

JPC Diagnosis:
Jaw: Giant cell tumor of bone.

JPC Comment:
The contributor provides an excellent overview of central giant cell granuloma (CGCG), an entity that is well-described in human literature. The World Health Organization defines CGCG in humans as "an intraosseous lesion consisting of cellular fibrous tissue containing multiple foci of

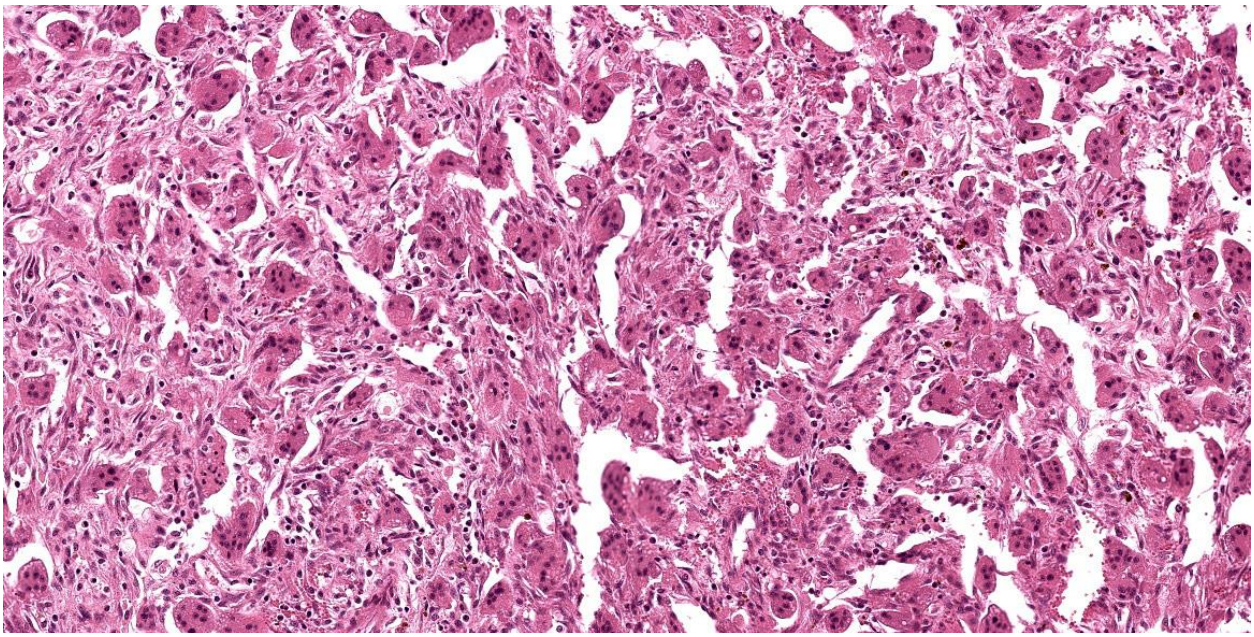

Figure 1-6. Mandible, goat. High magnification of the neoplastic cells composing the mass. Multinucleated cells are common. (HE, 147X)

hemorrhage, aggregations of multinucleated giant cells, and, occasionally, trabeculae of woven bone."[7] While this is an apt description of the examined sections in this case, it could well describe several other types of bone tumors with a giant cell component, and differentiating among these entities remains challenging.

Given the paucity of reported veterinary cases, much of what is "known" about this tumor in veterinary species is extrapolated from human literature. Even within the human literature, CGCG remains a contentious entity as the pathogenesis is unknown and experts disagree on fundamental issues, such as whether CGCG is neoplastic or reactive, or whether the lesion is a single neoplastic lesion or a mix of neoplastic and reparative processes.[7] Many researchers also believe this entity is simply a giant cell tumor of bone in an uncommon location. What is fairly clear, however, is that the term "granuloma" is a misnomer, as the multinucleated giant cells are osteoclastic rather than macrophagic, as would be expected in a true granuloma.

The biologic behavoir of CGCG is difficult to predict. When surgical resection is elected, reported recurrence rates in humans vary between 11 and 49%.[7] The most consistent gross lesion present in aggressive CGCG is perforation of cortical bone; however, despite investigating myriad histologic parameters, no studies have identified reliable histologic features that can predict the course of disease.[7]

As an interesting side note, a key differential for CGCG in human medicine is cherubism, an autosomal dominant disorder characterized by bilateral expansion of the mandible and/or the maxilla which appears in the first few years of life.[7] The dysplastic fibrous tissue of the mandible and/or maxilla can extend into the orbital floor and is often accompanied by swelling of the submandibular lymph nodes. These changes cause a characteristic upward tilting of the eyes and fullness of the face, resulting in the cherubic expression that gives the condition its name.[12] Cherubism is yet another non-neplastic fibrotic lesion confined to the jaws that cannot

be distinguished from other giant cell lesions of bone by histology alone.[12]

This week's conference was moderated by Dr. Linden Craig, Professor of Anatomic Pathology at the University of Tennessee College of Veterinary Medicine. Conference discussion began with a discussion of the bony features present in the examined section, followed by a discussion of basic definitional terms. Mature bone is divided into compact (also called cortical) and cancellous (also called spongy) varieties. The collagen in compact bone is typically oriented into a strong parallel, lamellar arrangement that is organized into osteons, and this dense, compact bone is typically present on the peripheral or exterior portion of the bone. The collagen in cancellous bone is less dense than compact bone, with collagen organized into trabeculae which create cavities that may contain bone marrow. Bone can also be categorized as lamellar or woven, with the former being characterized by mature, organized collagen and the later characterized by more immature, haphazardly arranged collagen fibers. Woven bone represent early osteogenesis and will typically be remodeled and replaced by lamellar bone as it matures. Woven bone can be easily distinguished from lamellar bone by the use of polarized light, which highlights the degree of collagen organization present in the tissue.

Dr. Craig discussed other entities characterized by giant cells, including giant cell tumor of soft parts, giant cell osteosarcoma, peripheral giant cell granuloma, and ethmoid hematomas. Participants discussed the differences between these entities and how the line between reactive and neoplastic seems particularly porous with these entities. Participants noted that "central giant cell granuloma" appears to be a human entity that is rarely diagnosed in veterinary medicine. Though typically occurring in the long bones and digits, participants favored a diagnosis of giant cell tumor of bone, a well-described veterinary entity with a histologic appearance identical to the examined tissue.

References:

1. Chandna P, Srivastava N, Bansal V, Wadhwan V, Dubey P. Peripheral and central giant cell lesions in children: institutional experience at Subharti Dental College and Hospital. *Indian J Med Paediatr Oncol.* 2017;38(4):440.
2. De Bruijn ND, Kirpensteijn J, Neyens IJS, Van den Brand JMA, Van den Ingh TSGAM. A clinicopathological study of 52 feline epulides. *Vet Pathol*. 2007; 44(2):161-169.
3. Desoutter AV, Goldschmidt MH, Sánchez MD. Clinical and histologic features of 26 canine peripheral giant cell granulomas (formerly giant cell epulis). *Vet Pathol*. 2012;49(6):1018-1023.
4. Dixon J, Weller R, Jeckel S, Pool R, Mcsloy A. Imaging diagnosis—the computed tomographic appearance of a giant cell tumor affecting the mandible in a pygmy goat. *Vet Radiol Ultrasound*. 2016; 57(5):1-3.
5. Gandara-Rey JM, Pacheco JMC, Gandara-Vila P, et al. Peripheral giant-cell granuloma. Review of 13 cases. *Med Oral.* 2002;7(4):254-259.
6. Hiscox LA, Dumais Y. Peripheral Giant Cell Granuloma in a Dog. *J Vet Dent.* 2015;32(2):103-110.
7. Kruse-Lösler B, Diallo R, Gaertner C, Mischke KL, Joos U, Kleinheinz J. Central giant cell granuloma of the jaws: a clinical, radiologic, and histopathologic study of 26 cases. *Oral Surg Oral Med Oral Pathol Oral Radiol Endod.* 2006;101(3):346-354.
8. Jané-Salas E, Albuquerque R, Font-Muñoz A, González-Navarro B, Estrugo Devesa A, López-López J. Pyogenic granuloma/peripheral giant-cell

granuloma associated with implants. *Int J Dent.* 2015; 2015:839032.
9. Lester SR, Cordell KG, Rosebush MS, Palaiologou AA, Maney P. Peripheral giant cell granulomas: a series of 279 cases. *Oral Surg Oral Med Oral Pathol Oral Radiol.* 2014;118(4):475-482.
10. Motamedi MHK, Eshghyar N, Jafari SM, et al. Peripheral and central giant cell granulomas of the jaws: a demographic study. *Oral Surg Oral Med Oral Pathol Oral Radiol.* 2007;103(6);e39-e43.
11. Uzal FA, Plattner BL, Hostetter JM. Alimentary System. In: Maxie MG, ed. *Jubb, Kennedy, and Palmer's Pathology of Domestic Animals*. 6th ed. Vol 2. Elsevier; 2016:20-22.
12. Papdaki ME, Lietman SA, Levine MA, Olsen BR, Kaban LB, Reichenberger EJ. Cherubism: best clinical practice. *Orphanet J Rare Dis*. 2012;24(Suppl 1):S6.

CASE II:

Signalment:
40-day-old male Cobb broilers (*Gallus gallus domesticus*)

History:
Two male 40-day-old Cobb broilers from a commercial farm in Victoria were submitted for necropsy and diagnostic work up following euthanasia by cervical dislocation. The farm was culling 200 birds per shed (approximately 0.5% of birds) at the time. The submitting veterinarian reported that the birds have normal mentation but have paresis or paralysis and a characteristic posture, sitting back on their hocks with legs extended in front of them and wing walking. Post mortem examination of one bird by the submitting veterinarian showed a small bursa and femoral head necrosis.

Figure 2-1. Vertebral column, chicken. At T4-T5, there is an abscess, pathologic fracture of the vertebral body, and compression of the spinal cord. (*Photo courtesy of:* Department of Veterinary Biosciences and Australian Pacific Centre for Animal Health, Melbourne Veterinary School, The University of Mel-bourne, Werribee, Victoria, Australia; and Inghams Enterprises, Victoria, Australia, unimelb.edu.au)

Gross Pathology:
Both birds examined were well-preserved and in good body condition. The free thoracic vertebra was expanded and effaced by a yellow-tan multinodular mass that appeared to be inflammatory, associated with a presumably pathologic fracture, and to focally and severely compress the spinal cord. The bisected T4-T5 vertebral sections of both subjects revealed focal red discolouration of the hypaxial muscles surrounding the cord compression focus. The left femoral head was diffusely, markedly red on the articular surface and appeared enlarged compared to the right in both birds. There was some soiling (brown, soft material) of the vent of one bird. The bursa and other organs, including other vertebrae examined, showed no noteworthy changes grossly.

Laboratory Results:
Aerobic culture (vertebral abscess swabs) yielded a lightly contaminated growth, with *Enterococcus cecorum* isolated as the predominant organism.

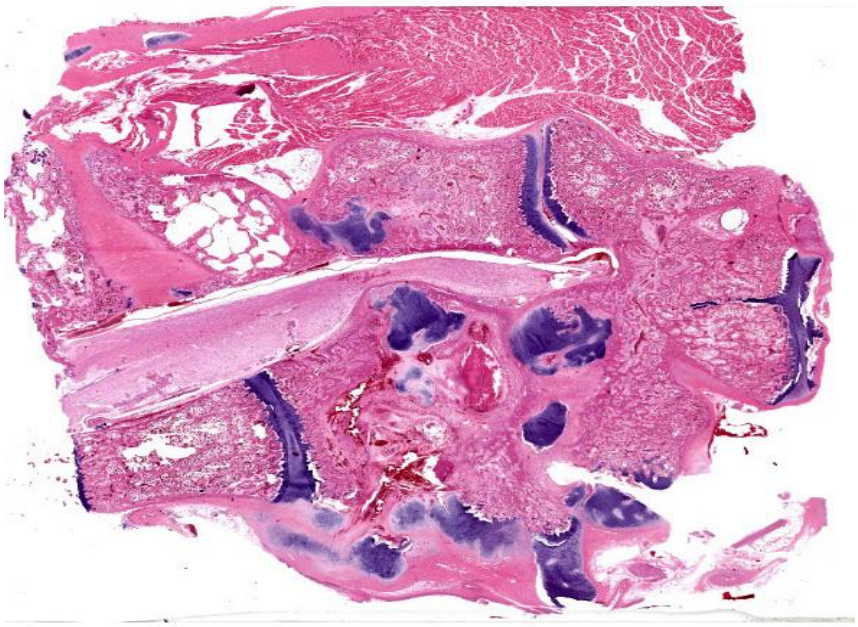

Figure 2-2. T4-T5 vertebrae, chicken. There is fracture of the vertebral body with a focal heterophilic granuloma, compression of the spinal cord, and callus formation with abundant production of cartilaginous matrix. (HE, 5X)

Microscopic Description:
Histologically, the femur, bursa, and other organs apart from the free thoracic vertebra (FTV) showed no noteworthy changes. In both birds, covering over 70% of the sagittal plane examined, the architecture of the vertebral bodies of T4/T5 was largely obliterated and replaced by extensive multinodular callus formation. The spinal cord was severely compressed at this level by the callus. There was mild to moderate Wallerian degeneration characterised by vacuolation of the adjacent white matter, with spheroids, degenerate macrophages, or axonal debris noted in some vacuoles, these changes interpreted as confirming that the compression was real, as opposed to a plane of section artifact. Within the vertebra, there was extensive necrosis, osteolysis, oedema, fibrin deposition, haemorrhage and moderate infiltration by heterophils, histiocytes, lymphocytes, and plasma cells. Multifocally within these areas of necrosis and remodelling there were large numbers of small monomorphic bacterial aggregates (mainly cocci). On Gram stained sections, these were shown to be gram positive cocci.

Contributor's Morphologic Diagnosis:
T4/T5 vertebrae: Spondylitis, severe, heterophilic, lymphoplasmacytic, haemorrhagic, necrotising with extensive remodelling, pathologic fracture, callus formation and focal spinal cord compression.

Contributor's Comment:
The colloquial term "kinky back" is occasionally used in practice to refer to Enterococcal spondylitis of the T4/T5 vertebrae. *Enterococcus cecorum* is a gram-positive enteric commensal of poultry; however, strains of *E. cecorum* causing outbreaks have significantly smaller genomes than commensal *E. cecorum*.[1] Pathogenic *E. cecorum* has also been reported to cause disease in Pekin

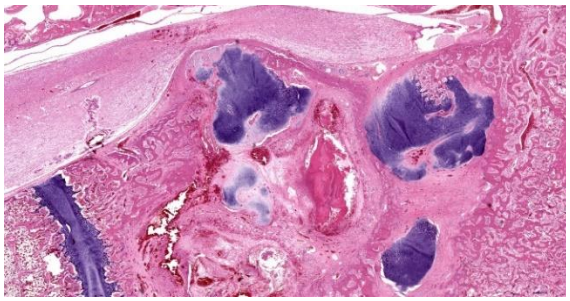

Figure 2-3. T4-T5 vertebrae, chicken. Higher magnification of the heterophilic granuloma and callus causing spinal cord compression. (HE, 13X)

ducklings and pigeons. The posture of the broilers (sitting back on their hocks) is characteristic, although not pathognomonic of this condition. Wing walking is used for locomotion, and this also limits their access to food. An interesting feature of this condition is the characteristic lesion localisation at the free thoracic vertebra (FTV). The FTV has greater weight-bearing articulations compared to the adjacent notarium and synsacrum, potentially predisposing it to infection with pathogenic *E. cecorum*.

Another condition that is also referred to as "kinky back" is spondylolisthesis caused by subluxation of the fourth thoracic vertebra (T4). Ventral displacement of the cranial end of T4 also results in compression of the spinal cord via narrowing of the vertebral canal (dorsal projection of its posterior extremity). The aetiology of spondylolisthesis is primarily genetic, as opposed to bacterial as is the case for enterococcal spondylitis, but the occurrence is influenced by increased growth rate.

Contributing Institution:
Department of Veterinary Biosciences and
Australian Pacific Centre for Animal Health
Melbourne Veterinary School
The University of Melbourne
Werribee, Victoria, Australia
unimelb.edu.au

JPC Diagnosis:
Vertebrae: Spondylitis, necrotizing, focally extensive, severe, with pathologic fracture, callus, and focal spinal cord compression.

JPC Comment:
This case provides an excellent example of a classic entity of poultry. As the contributor notes, one of the curiosities of Enterococcal spondylitis (ES) is its tropism for the free thoracic vertebra (FTV). Cranial to the FTV, the thoracic vertebrae are fused into the notarium via synchondrosis rather than with synovial articulations and intervertebral discs, as in mammals.[1] Caudal to the FTV, the caudal thoracic vertebrae, lumbosacral vertebrae, and the pelvic bones are similary fused into the synsacrum, leaving the FTV as the only vertebra in the thoracolumbar column to have weight bearing articulations.[1] This anatomic oddity places substantial mechanical stress on the FTV as it transfers body weight to the hips and hind limb, perhaps predisposing the FTV to injury and to subsequent infection with pathogenic *Enterococcus cecorum*.[1]

By the time clinical signs are evident, typically in weeks 4-6 of life, spinal lesions are already well developed, with histologic evidence of chronic infection.[1] A recent study evaluated lesion development in ES during

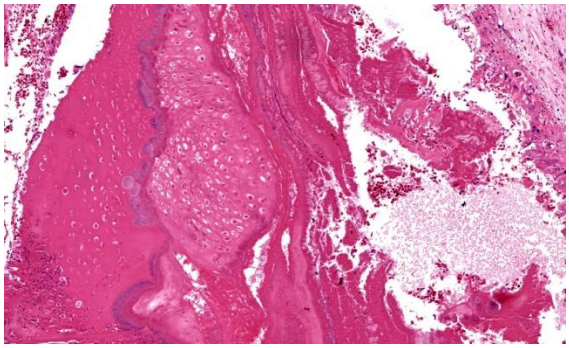

Figure 2-4. T4-T5 vertebrae, chicken. High magnification of the heterophilic granuloma with incorporated necrotic bone. (HE, 13X)

the first four weeks of life, when affected chickens are incubating subclinical disease. The study found that the first step in the development of ES is the colonization of the gut by pathogenic *E. cecorum* species within the first week of life. This is in contrast to commensal *E. cecorum*, which arrives in the chicken gut around 3 weeks of age. The authors speculate that the ability to colonize the gut early in life may be a key virulence event, conveying a competitive advantage that allows pathogenic bacteria to disseminate throughout a flock.[1]

A second likely step in ES pathogenesis is the development of osteochondrosis dissecans (OCD) lesions in the FTV.[1] OCD lesions progress through a stereotypical sequence, thought to be initiated and driven by vascular disturbances or increased type II collagen production.[2] The earliest changes observable in the cartilage consist of a poorly defined focus of eosinophilia and hypocellularity in the articular cartilage, termed osteochondrosis latens, which may extend to the subchondral bone.[1,2] These areas may remain stable, or may progress to osteochondrosis manifesta, characterized by areas of cartilage retention in the ossification zone.[1] Finally, fully-fledged OCD lesions are characterized by clefts in the hyaline cartilage which may communicate with the joint space or extend into subchondral bone.[1,2]

Large cartilaginous clefts are the hallmark lesion of OCD and are readily identifiable in affected birds as early as 1 week of age; these clefts are variably filled with fibrin, erythrocytes, and, in some birds, bacterial cocci consistent with *E. cecorum*.[1] These lesions progress over the next two weeks with an influx of heterophilic and histiocytic inflammation targeting these cocci-filled cartilaginous clefts.[1] Continued progression leads to the bone remodeling and spinal cord

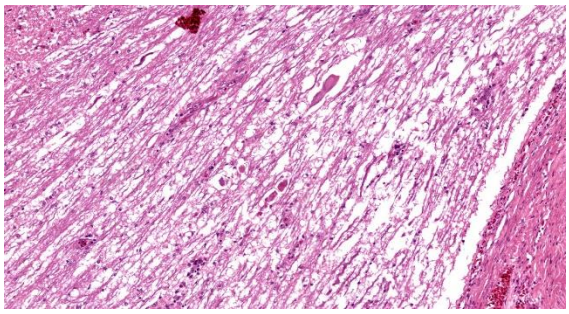

Figure 2-5. Thoracic spinal cord, chicken. There is Wallerian degeneration of the spinal cord at the area of compression with edema, dilation of myelin sheaths, and spheroid formation. (HE, 189X)

compression that comprise the stereotypical ES lesion.[1]

It remains unclear why cartilage clefting predisposes chickens to ES lesions. One theory is that hemorrhage into the cartilage clefts introduces bacteremic, pathogenic *E. cecorum* to the site of injury and, once there, the devitalized cartilage provides a favorable niche for bacterial persistence and proliferation. Whatever the reason, the unique anatomic features of the weight-bearing FTV, which articulates through epiphyseal cartilage without the benefit of joint capsules or intervertebral discs, makes it uniquely susceptible to trauma, and the FTV is the only location within the vertebral column where OCD lesions and subsequent *E. cecorum* colonization occur.[1]

Dr. Craig discussed the alternating layers of bacteria and cartilage within the lesion. These layers provide histologic support for the tidy pathogenic narrative discussed above. Without engaging in excessive flights of fancy, it is easy to imagine the successive rounds of cartilage clefting and bacterial colonization that result in this spectacular ES lesion. Dr. Craig also noted several basophilic, circular areas within the tissue that represent residual mineral left over from the decalcification process. These artifacts can be misinterpreted as mast cells, macrophages, or other

histologic features, and can be avoided by copious rinsing of tissue after decalcification and prior to further processing.

Discussion of the morphologic diagnosis focused initially on whether to include the various inflammatory cells present in the lesion. Conference participants felt that the chronic nature of the lesion, evidenced by callous formation, implied the existence of a chronic inflammatory infiltrate and made the inclusion of this histologic feature superfluous. Partipants also decided to omit the bacterial cocci which, while confirmed with Gram stain, were not convincingly evident to all participants based on H&E evaluation alone.

References:

1. Borst LB, Suyemoto MM, Sarsour AH, et al. Pathogenesis of enterococcal spondylitis caused by *Enterococcus cecorum* in broiler chickens. *Vet Pathol*. 2017;54:61-73.
2. Olstad K, Ekman S, Carlson CS. An update on the pathogenesis of osteochondrosis. *Vet Pathol*. 2015;52(5):785-802.

Figure 3-1. Tibia and tarsus, dog. A hard mass surrounds the hock joint and involves the tarsal and metatarsal bones. (*Photo courtesy of*: the Department of Pathology, University of Guelph).

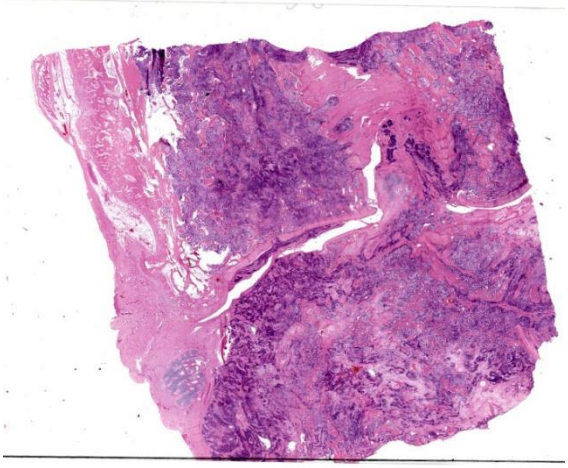

Figure 3-2. Long bone, dog. The cortical and medullary architecture is effaced by a large infiltrative mass. (HE, 6X)

CASE III:

Signalment:
4-year-old, female spayed Standard poodle dog (*Canis familiaris*)

History:
A pilomatrixoma was excised from this animal's tail base two years prior to presentation for non-weight bearing lameness on the right pelvic limb. Polyostotic aggressive bone lesions were seen on survey radiography. Staging identified pulmonary nodules.

Gross Pathology:
The right hock is circumferentially expanded by a hard, round mass. There is a mass involving the tarsal bones and the metatarsals. There is marked periosteal new bone formation of the distal tibia. There are multiple 1-5 cm nodules throughout the lungs.

Microscopic Description:
This sample has remnants of normal bone and bony trabeculae of the subchondral/epiphyseal regions. There is a small amount of articular cartilage, some joint space and joint capsule, and opposing bone across and around the joint space. Much of the cortical and trabecular bone is missing and the

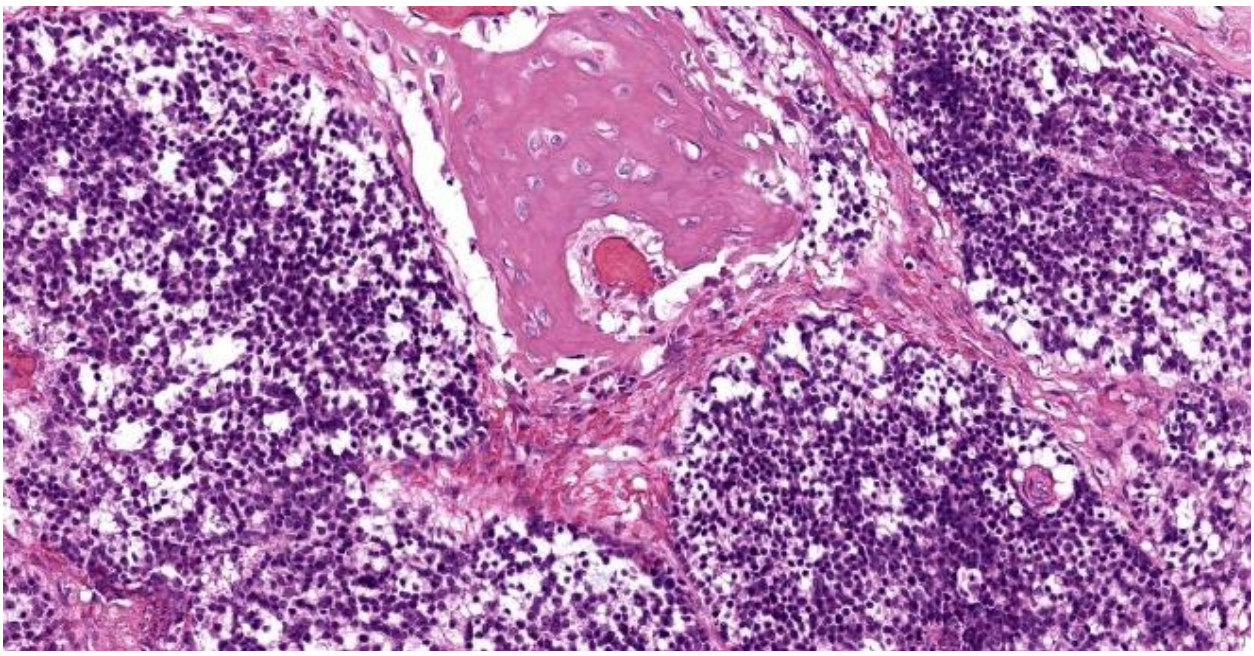

Figure 3-3. Long bone, dog. The neoplasm is composed of small polygonal densely-packed epithelial cells arranged in nests and packets. Remodeling periosteal bone is at center, top. (HE, 177X)

intertrabecular spaces are filled with sheets of hyperchromatic cells with focal areas of keratin formation. There is some periosteal new bone formation at the edge of the cortical bone and some endosteal new bone formation, but about 90% of this sample is neoplastic tissue. Neoplastic cells form nodules, clusters, and streams of cells that completely fill the intertrabecular spaces. There are some bands of fibrous tissue throughout the lesion. In the centre of nodules and clusters are small hyperchromatic cells similar to those on the periphery and in some, the central cells have more cytoplasm. In many, the cytoplasm is vacuolated. In occasional focal areas there is keratinization with dense keratin and the ghostlike nuclear outline of matricial keratinization. About 10% of this mass is necrotic.

Contributor's Morphologic Diagnoses:
Metastatic pilomatrixoma to bone with extensive bony lysis and periosteal and endosteal new bone formation.

Contributor's Comment:
The appearance of the cells within the bone and similar appearing cells in the lung (not provided) with keratinization of the matricial type is typical of metastasis of pilomatrixoma. It is rare for pilomatrixoma to metastasize, but when they do, previous reports indicate metastasis to the bone is common.

Contributing Institution:
Department of Pathobiology
Ontario Veterinary College
University of Guelph
Guelph, Ontario,Canada

JPC Diagnosis:
Bone: Metastatic pilomatricoma.

JPC Comment:
Pilomatricoma (also known as pilomatrixoma) is an adnexal neoplasm that arises from the germinative cells of the follicular matrix, or hair bulb, and is reported mainly in dogs and humans.[1,8] Pilomatricomas are diagnosed most commonly in 4-8 year-old dogs, and

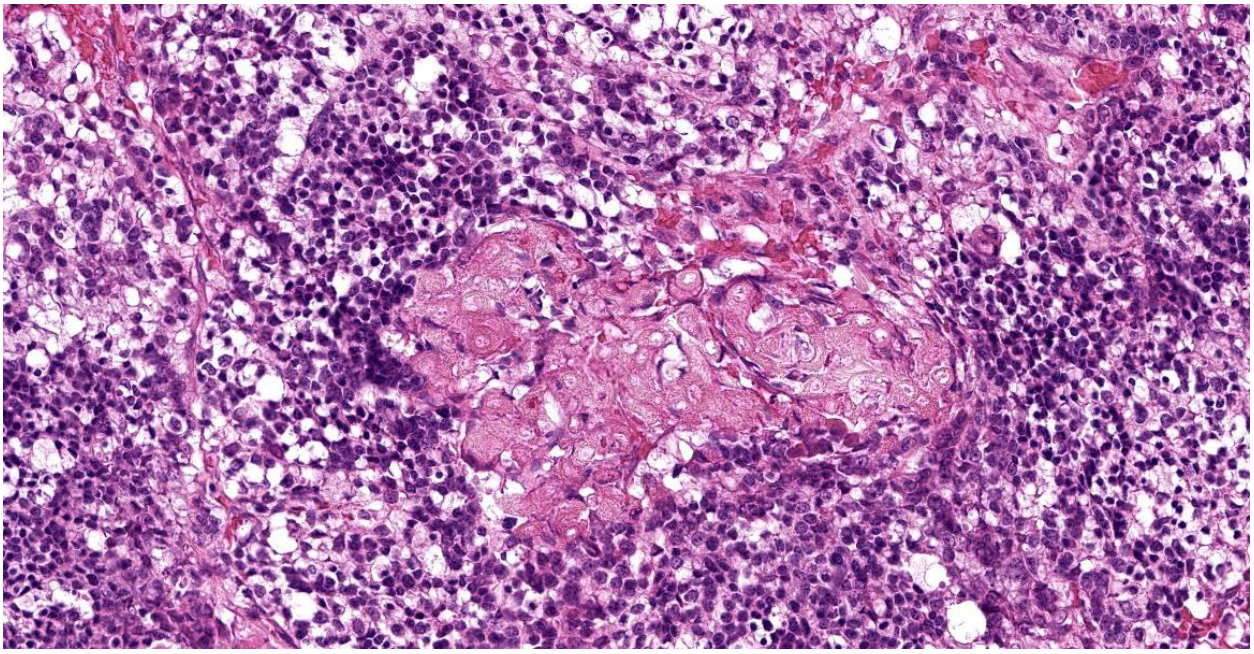

Figure 3-4. Long bone, dog. There are numerous foci of abrupt keratinization of neoplastic cells. (HE, 314X)

Kerry Blue Terriers, Soft Coated Wheaten Terriers, Standard Poodles, and other breeds with continuously growing hair coats are overrepresented in the patient pool, likely because the high number of anagen hair follicles, and their attendant replicating cells, provide fertile soil for neoplastic transformation.[1]

Consistent with their follicular origin, pilomatricomas typically present as intradermal or subcutaneous masses composed of one or more lobules separated by collagenous stroma.[3] The lobules contain a peripheral zone of basophilic cells with hyperchromatic nuclei, a high N:C ratio, and a moderate to high number of mitotic figures.[3] The neoplastic cells exhibit an abrupt transition to a central zone of ghost cells which often contain significant accumulations of melanin.[3]

As the contributor notes, most pilomatricomas exhibit benign, non-metastatic biologic behavior and excision with wide surgical margins is typically curative.[3] Malignant pilomatricoma is typically differentiated from its bengin counterpart by being poorly circumscribed, less differentiated, anaplastic, infiltrative, rapidly or erratically growing, and, definitially, metastatic.[1,3] Metastatic pilomatricoma has been reported in various organs, including lymph nodes, lungs, bone, and skin; metastasis to the liver and spleen is less common.[1,8] Despite the variety of reported metastatic sites, malignant pilomatricoma seems predisposed to metastasize to bone, with metastasis reported in vertebrae, ribs, the mandible, maxilla, and femur.[1]

The primary differential for primary or metastatic malignant pilomatricoma is malignant trichoepithelioma, a follicular neoplasm with differentiation to all three segments of the hair follicle.[3] Differentiating between these two neoplasms can be difficult, but malignant trichoepitheliomas have tricohyaline granules and prominent inner and outer root sheath differentiation, along with smaller epithelial aggregates, fewer matrical cells, and fewer ghost cells.[1,3]

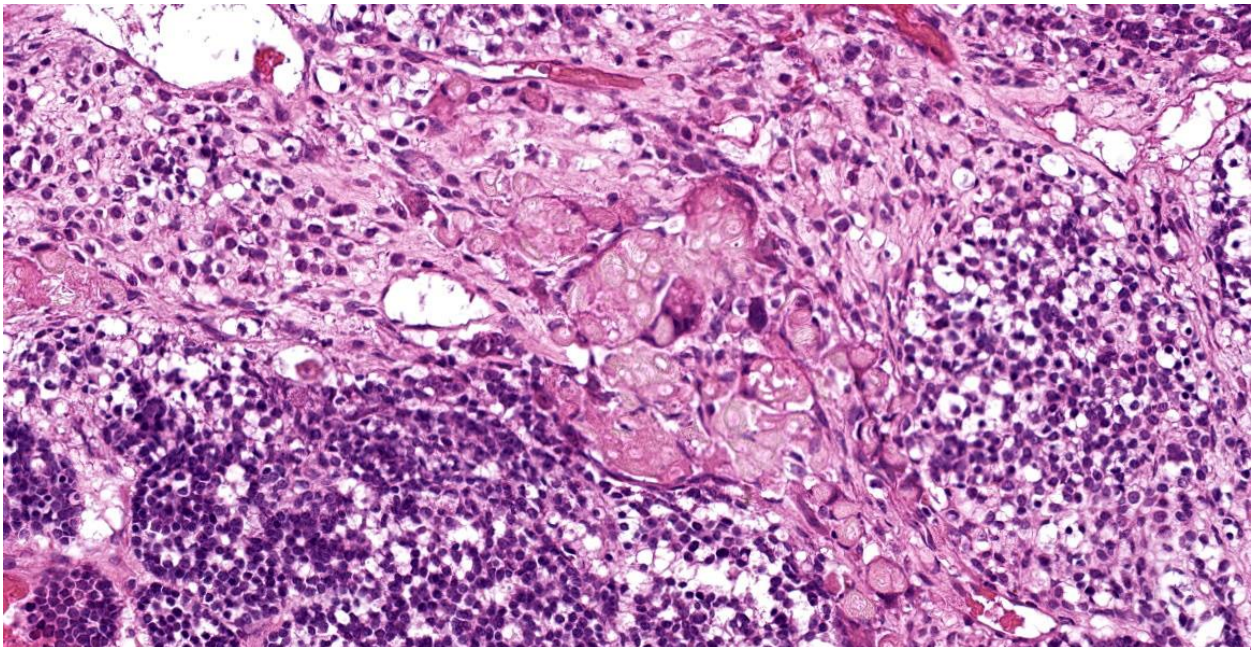

Figure 3-5. Long bone, dog. In some foci, abrupt keratinization has resulted in the formation of "ghost cells" which are characteristic of follicular tumors, particular pilomatricoma. (HE, 314X)

The moderator began discussion by noting the palisading layer of cells around the periphery of the neoplastic trabeculae, the first clue that this neoplasm is of epithelial origin. Dr. Craig also noted that the islands of ghost cells can be easily mistaken for necrotic bone with empty lacunae without careful examination. Dr. Craig, a self-described breed predisposition enthusiast, noted that Bassett Hounds are predisposed to pilomatricomas generally and since pilomatricomas often metastasize to bone, metastatic pilomatricoma should be on the differential list for lameness in this breed. As an additional breed-related curiosity, Dr. Craig noted that large breed black dogs, such as the Standard Poodle, Giant Schnauzer, Bouvier des Flanders, and others, unrelated except for size and color, are predisposed to multiple digital squamous cell carcinomas.

The moderator lead a more general discussion of carcinomas within bone, noting that metastatic carcinoma is more common than primary bone tumors in many species. In dogs, metastasis to bone is most frequent in the ribs, vertebrae, and proximal long bones. Dr. Craig noted that most textbooks state that metastasis of carcinomas to bone is uncommon in sites distal to the elbow or stifle; however, there are many examples, including this case, in which metastatic carcinoma is found in more distally, making location an unreliable diagnostic criterion for metastatic carcinoma.

References:

1. Carroll EE, Fossey SL, Mangus LM, et al. Malignant pilomatricoma in 3 dogs. *Vet Pathol*. 2010;47(5):937-43.
2. da Silva EO, Green KT, Wasques DG, Chaves RO, dos Reis AC, Bracarense AP. Malignant pilomatricoma in a dog. *J Comp Pathol*. 2012;147(2-3):214-217.
3. Goldschmidt MH, Minday JS, Scruggs JL, Klopfleisch R, Kiupel M. *Surgical Pathology of Tumors of Domestic Animals*. Vol 1: Epithelial Tumors of Skin. The Davis-Thompson Foundation; 3rd ed:112-114.

4. Huzella L, Ide A, Steinbach TJ, Blanchard TW, Lipscomb TP, Schulman FY. Osteosarcoma in malignant pilomatricoma. *Vet Pathol* 2005;42:700.
5. Jackson K, Boger L, Goldschmidt M, Walton RM. Malignant pilomatricoma in a soft-coated Wheaten Terrier. *Vet Clin Pathol*. 2010;39(2):236-40.
6. Johnson RP, Johnson JA, Groom SC, Burgess L. Malignant pilomatrixoma in an old english sheepdog. *Can Vet J*. 1983;24: 392-394.
7. Martano M, Navas L, Meomartino L, et al. Malignant pilomatricoma with multiple bone metastases in a dog: histological and immunohistochemical study. *Exp Ther Med*. 2013;5(4):1005-1008.
8. Treggiari E, Elliott JW. Malignant pilomatricoma in a dog with local and distant metastases treated with chemotherapy and bisphosphonates. *Open Vet J*. 2017; 7(3):208-213

CASE IV:

Signalment:
3-year-old, male intact budgerigar *(Melopsittacus undulatus)*

History:
This animal was a member of a zoological collection and was found dead in its enclosure.

Gross Pathology:
This blue, 39.3g male budgerigar had a dark blue cere. Both testes were enlarged (left was bilobed and 8x5x5mm, right was spherical and 5x5x5mm in diameter).

Microscopic Description:
Both testes (slide not provided) contained a neoplasm composed of polygonal cells in packets separated by a dense fibrous stroma. Neoplastic cells had distinct borders, eosinophilic cytoplasm, and round nuclei. Foci of a similar neoplastic population were within the marrow of both femurs. Both femurs and humeri had basophilic, non-birefringent bone lining the medullary trabeculae (medullary bone) that was most pronounced near the metastatic foci.

Figure 4-1. Presentation, parakeet. This male parakeet had a dark blue cere. (*Photo courtesy of:* University of Tennessee College of Veterinary Medicine, Department of Biomedical and Diagnostic Sciences, 2407 River Drive, Room A201, Knoxville, TN 37996, https://vetmed.tennessee.edu/academics/biomedical-and-diagnostic-sciences/)

Contributor's Morphologic Diagnosis:
Femur: Metastatic Sertoli cell tumor with associated medullary bone.

Contributor's Comment:
Medullary bone (also known as laying bone) is formed and removed along the endosteal surfaces of bones in female birds during the egg-laying cycle as a source of calcium for eggshells. In females, it typically spares the pneumatic bones, mostly forming in the hematopoietic bones such as the femur and tibiotarsus, but this varies with species.

This femur is from one of 7 male budgerigars in a publication that described medullary bone as a feature of paraneoplastic feminization. The medullary bone deposition was diffuse in 4 cases and multifocal in 3 (including this one) and affected both pneumatic (humeri) and hematopoietic (femurs) bones.[2] This was the only case in which bony metastases were detected. Interestingly, the medullary bone in this case is most pronounced near the metastatic foci.

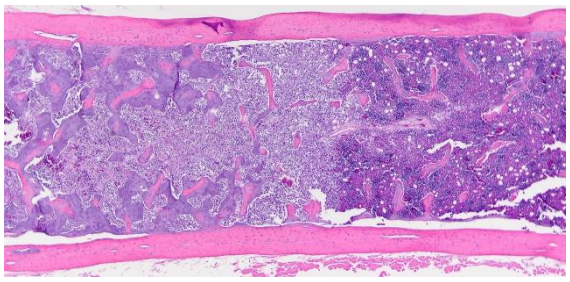

Figure 4-2. Femur, parakeet. The medullary cavity has a focus of metastatic neoplasia. (HE, 40X)(*Photo courtesy of*: University of Tennessee College of Veterinary Medicine, Department of Biomedical and Diagnostic Sciences, 2407 River Drive, Room A201, Knoxville, TN 37996)

The testicular tumors associated with medullary bone included Sertoli (sustentacular) cell tumors, seminomas, and one mixed (Sertoli-interstitial cell) tumor.[2] Although estrogen production is characteristic of Sertoli cells tumors, estrogen production and feminization have been reported in humans and dogs with seminomas.[1,3]

Female budgerigars normally have a bright pink cere, while males have a light blue cere. Cere color change is another feature of paraneoplastic feminization reported in budgerigars.[4] In the published study of 7 budgerigars with testicular tumors and medullary bone, 4 had a blue-brown or red-brown cere, 2 had a light blue cere, and one (this bird, case 3 in reference 2) had a dark blue cere.[2]

Contributing Institution:
University of Tennessee
College of Veterinary Medicine
Biomedical and Diagnostic Sciences
2407 River Drive, Room A201
Knoxville, TN 37996
https://vetmed.tennessee.edu/academics/biomedical-and-diagnostic-sciences/

JPC Diagnosis:
Long bone: Metastatic sustentacular cell tumor with associated medullary bone.

JPC Comment:
This fascinating case provides an excellent example of medullary bone, a new concept for many conference participants this week. As noted by the contributor, medullary bone is normally produced in the hematopoietic bones of female birds to serve as calcium stores for the arduous task of mineralizing eggs. This sex-specific tissue is produced by female birds from approximately 10 days pre-ovulation until the completely mineralized egg is laid.[2] Medullary bone can be distinguished from woven bone by its increased basophilia, due to an increased proteoglycan content compared to woven bone, and by the absence of birefringence under polarized light.[2]

The formation of medullary bone occurs simultaneously with the maturation of ovarian follicles, and is believed to be due to incompletely understood interactions among the hypothalamus, pituitary gland, and ovaries.[2] The ovum produces estrogens upon the binding of luteinizing hormone produced by the pituitary gland, and these estrogens bind estrogen receptors on osteoblasts, leading to the

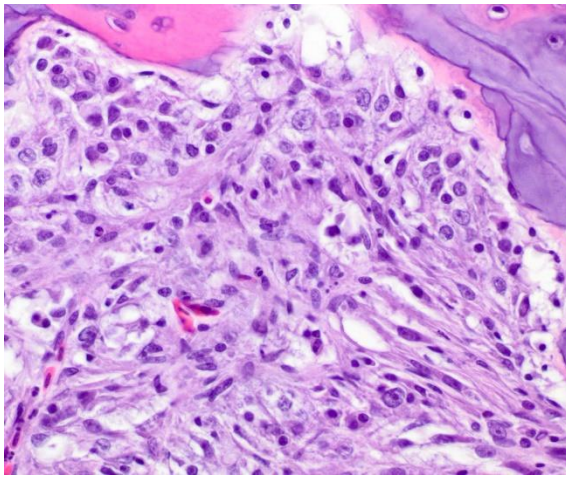

Figure 4-3. Femur, parakeet. High magnification of neoplastic cells. (HE 400X)(*Photo courtesy of*: University of Tennessee College of Veterinary Medicine, Department of Biomedical and Diagnostic Sciences, 2407 River Drive, Room A201, Knoxville, TN 37996)

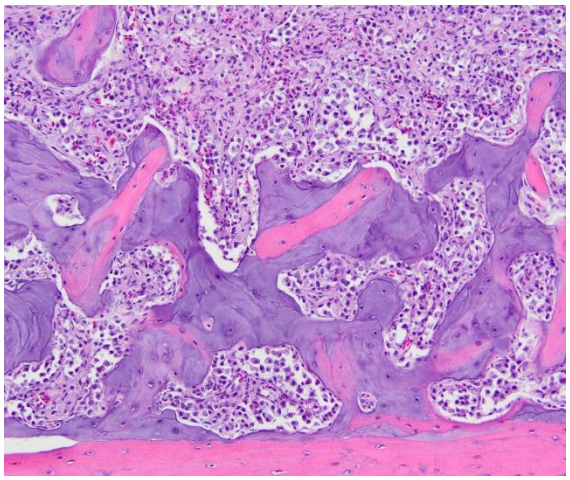

Figure 4-4. Femur, parakeet. The bone adjacent to the neoplasm has a densely basophilic matrix covering the endosteum, which is called "medullary" or "laying" bone. (*Photo courtesy of*: University of Tennessee College of Veterinary Medicine, Department of Biomedical and Diagnostic Sciences, 2407 River Drive, Room A201, Knoxville, TN 37996)

deposition of type I collagen on the endosteal surfaces of hematopoietic bones of female birds.[2] Once the egg is ovulated and reaches the shell gland, mineralization-induced hypocalcemia induces parathyroid hormone secretion, which in turn stimulates osteoclasts to resorb medullary bone, releasing calcium stores into the bloodstream for use in egg mineralization.[2]

The contributor provides an excellent overview of the concept of paraneoplastic feminization, defined as "the acquisition of feminine characteristics as an indirect consequence of a neoplasm, usually due to production of chemical signalling molecules such as hormones."[2]

In veterinary medicine, this condition is well-described in male dogs with sustentacular (Sertoli) cell tumors, in which estrogen production by neoplastic cells produces female behavior and other characteristic changes such as gynecomastia, alopecia, prostatic squamous metaplasia, and myelosuppression.[2] Removal of the neoplastic tissue typical results in normalization of serum estrogen and reversion to more gender-stereotypic behavior and physiology. In male budgerigars with testicular neoplasia, paraneoplastic feminization is typically described as involving medullary bone formation, cere color change, widening of the pelvic inlet, and protrusion of the cloaca.[2] The production of medullary bone can be diagnostically useful, as the resulting increase in bone density can be identified radiographically and can serve as an early indication of testicular neoplasia.[2]

Conference discussion focused on the histologic appearance of medullary bone, including the basophilia and lack of birefringence, as noted above. Conference participants also examined Masson and Movat pentachrome stains, in which the medullary bone stained blue and green, respectively. The moderator noted that medullary bone in male budgerigars can be present with all three testicular tumors though not all produce the estrogen

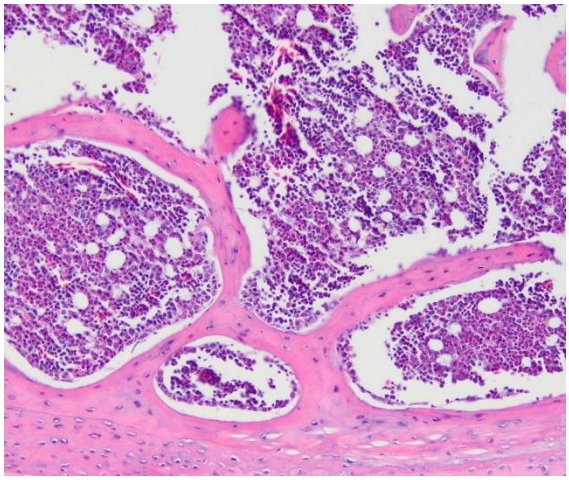

Figure 4-5. Femur, parakeet. For comparison, in areas of marrow devoid of neoplastic cells, the bone is of normal morphology. (*Photo courtesy of:* University of Tennessee College of Veterinary Medicine, Department of Biomedical and Diagnostic Sciences, 2407 River Drive, Room A201, Knoxville, TN 37996)

throught responsible for the formation of medullary bone. This curiosity highlights the fact that the physiologic basis for medullary bone deposition remains incompletely understood and is likely multifactorial.

References:

1. Duparc C, Boissiere-Veverka G, Lefebvre H, et al. An oestrogen-producing seminoma responsible for gynaecomastia. *Horm Metab Res*. 2003;35(5):324-329.
2. Hoggard NK, Craig LE. Medullary bone in male budgerigars (*Melopsittacus undulatus*) with testicular neoplasms. *Vet Pathol.* 2022;59(2):333-339.
3. Kim O, Kim KS. Seminoma with hyperesterogenemia in a Yorkshire terrier. *J Vet Med Sci*. 2005;67(1):121-123.
4. Mans C, Pilny A. Use of GnRH-agonists for medical management of reproductive disorders in birds. *Vet Clin North Am Exot Anim Pract*. 2014;17(1):23–33.

WSC 2023-2024
Conference 15 Self-Assessment

1. True or false: Central giant cell granulomas are labeled “central” due to their propensity to arise in intraosseous locations.
    a. True
    b. False

2. Which of the following vertebral bodies is most often affected in spondylolisthesis of poultry
    a. T2
    b. T4
    c. L1
    d. L2

3. In addition to poultry, *Enterococcus cecorum* causes disease in which of the following?
    a. Emus
    b. Pelicans
    c. Pigeons
    d. Crows

4. Which of the following is a common spot for metastasis of pilomatricoma?
    a. Bone
    b. Brain
    c. Eye
    d. Kidney

5. “Metabolic” bone is a common source of what in birds?
    a. Phosphorus
    b. Calcium
    c. Glycogen
    d. Vitamin D

Joint Pathology Center
Veterinary Pathology Services

WEDNESDAY SLIDE CONFERENCE 2023-2024

Conference #16 17 January 2024

CASE I:

Signalment:
Three-year-old male intact Lop rabbit (*Oryctolagus cuniculus*)

History:
The rabbit presented with soft stools and decreased activity. No abnormalities were found on physical examination, except for the presence of loose stools in the perianal area. Treatment with probiotics was initiated. Over the subsequent two days, the rabbit stopped producing fecal pellets and eating. It presented on the third day with no menace response, no gut sounds, and the inability to use the hind limbs. On radiographs, kidneys appeared enlarged. The rabbit died during blood sampling. CPR was attempted but was unsuccessful.

Gross Pathology:
Across all hepatic lobes there were multiple, well demarcated, white foci ranging from <1 to 1 mm in diameter. Affecting approximately 50-60% of the spleen, there were large multifocal to coalescing, circular, poorly delineated, well demarcated firm, cream to white nodules, which extended into the parenchyma and measured up to 9 mm in diameter, and bulged up to 3 mm from the splenic surface. The apical 10 cm of the cecal mucosa and serosa also showed numerous, multifocal to coalescing, white foci, measuring 2-3 mm in diameter, and the cecal wall was moderately thickened.

Figure 1-1. Cecum, rabbit. The cecum is distended and numerous foci of necrosis are visible through the serosa. (*Photo courtesy of:* Veterinary Pathology Service, School of Veterinary Medicine and Science, University of Nottingham, https://www.nottingham.ac.uk/vet /service-for-business/veterinary-pathology-service/companion-and-equine-pathology/index.aspx)

Laboratory Results:
Microbiological culture of spleen: Moderate growth of *Yersinia pseudotuberculosis*.

Microscopic Description:
Spleen: Affecting approximately 80% of the examined sections and effacing white and red pulp are large multifocal to coalescing foci of necrosuppurative inflammation characterized by a central, hypereosinophilic area of cellular and karyorrhectic debris (lytic necrosis) admixed with viable and degenerate neutrophils surrounded by numerous macrophages, lymphocytes, and fewer plasma cells. There

Figure 1-2. Spleen, rabbit. There are numerous foci of necrosis which are randomly scattered throughout the splenic parenchyma. (*Photo courtesy of:* Veterinary Pathology Service, School of Veterinary Medicine and Science, University of Nottingham)

is an outer layer of fibrous tissue which is infiltrated by lymphocytes, plasma cells, and eosinophils, and often contains scattered to extensive areas of extravasated erythrocytes (hemorrhage) and eosinophilic, fibrillar material (fibrin). Multifocally within and often at the periphery of the areas of necrosis there are colonies, up to 100 µm in diameter, of 1-2 µm amphophilic, gram negative coccobacilli. Scattered throughout the affected and non-affected parenchyma are moderate numbers of macrophages containing intracytoplasmic, golden brown, granular pigment (hemosiderin).

*Cecum***:** In approximately 90-95% of the examined section, the submucosa is markedly effaced and expanded by the presence of multifocal large foci of necrosuppurative inflammation which often extend into the lamina propria. These foci are characterized by a central, area of hypereosinophilic cellular and karyorrhectic debris (lytic necrosis) admixed with mostly degenerate and fewer viable neutrophils, surrounded by numerous macrophages, lymphocytes and fewer plasma cells, multifocal eosinophilic, fibrillar material (fibrin), and by an outer layer of fibrous tissue which is infiltrated by fewer numbers of lymphocytes, plasma cells, and eosinophils. Multifocally within areas of necrosis there are small numbers of scattered, 1-2 µm amphophilic, gram negative coccobacilli. The adjacent mucosal associated lymphoid tissue is multifocally compressed and the remaining submucosa is heavily infiltrated by mostly lymphocytes and fewer plasma cells and macrophages, which occasionally contain black and green, granular intracytoplasmic material. Multifocally within the lamina propria there are mildly to moderately increased numbers of lymphocytes and plasma cells.

*Liver***:** Multifocally, adjacent to portal spaces, there are a few smaller foci of necrosuppurative inflammation with extensive lytic necrosis similar to those described in the spleen and caecum. The portal spaces are often mildly to markedly infiltrated by lymphocytes and plasma cells, which occasionally mildly extend through the limiting plate to the adjacent parenchyma. Small numbers of lymphocytes are often infiltrating the biliary epithelium. Across all examined sections, there are numerous multifocal to coalescing, midzonal to centrilobular areas where hepatocytes are markedly swollen, exhibiting a pale staining cytoplasm arranged in thin strands, or vacuolar change of the cytoplasm (hepatocellular degeneration). Rarely, there is variable occlusion of the lumen of blood vessels by fibrin thrombi with few enmeshed neutrophils and lymphocytes.

Contributor's Morphologic Diagnoses:

1. Spleen**:** Splenitis, necrosuppurative, subacute, multifocal to coalescing, severe, with intralesional colonies of coccobacilli and microabscesses
2. Cecum: Typhlitis, necrosuppurative, subacute, multifocal to coalescing, severe, with intralesional coccobacilli and microabscesses
3. Liver: Hepatitis, necrosuppurative, subacute, multifocal to coalescing, mild,

with multifocal microabscesses and marked hepatocellular degeneration.

Contributor's Comment:
Yersiniosis (or pseudotuberculosis) is a disease caused by infection with gram-negative bacteria *Yersinia pseudotuberculosis* or *Yersinia enterocolitica*.[1,3,14] While susceptible, domestic rabbits are not commonly affected.[1] This infection is, however, commonly seen in rodents, birds, non-human primates, ruminants, and other zoo species.[2,3,7,11,14]

Transmission is thought to occur via the fecal-oral route through ingestion of contaminated food and/or water.[1,14] Infection may result either in acute death or development of clinical signs and lesions, as is the case with ruminants and pigs.[3,14] In this case, the clinical history and length of duration of clinical signs was unknown; however, the morphology of the lesions identified would suggest a more subacute timeline of infection.

After ingestion, the bacteria colonize the intestinal epithelium M cells, resulting in the destruction of Peyer's patches and epithelium and the formation of suppurative inflammation and microabscessation in the lamina propria.[14] *Yersinia* spp. virulence requires the presence of a 70-kb virulence plasmid.[9,14] This plasmid encodes the production of Yops proteins which inhibit phagocytosis, aiding the bacterial spread to mesenteric lymph nodes and other organs.[9,14,15] The bacteria may then disseminate to the liver or systemically through the venous drainage and lymphatic system.[14] Typical post-mortem findings include necrotizing hepatitis and splenitis, fibrinonecrotizing enterocolitis, and lymphadenitis.[2,3,9,14] On histology, there may be microcolonies of gram-negative coccobacilli and formation of microabscesses.[14] It is not possible to differentiate between *Y. pseudotuberculosis* and *Y. enterocolitica* based on macroscopic and histological lesions alone.[14]

As zoonotic agents, *Y. pseudotuberculosis* and *Y. enterocolitis* can cause acute gastroenteritis and mesenteric lymphadenitis in humans.[8] In Europe, multiple strains of *Y. pseudotuberculosis* of varying pathogenicity have been identified in wild boars, and pathogenic strains of *Y. enterocolitis* have been associated with wildlife, suggesting that wildlife species may play an important role as a reservoir for human infections.[6,13] While hospitalizations and deaths secondary to these infections have been reported, it is important to differentiate yersiniosis from plague, which is caused by *Yersinia pestis* and is a World Health Organization-reportable disease with much higher fatality rates.[3,8,17]

In veterinary medicine, macroscopic findings in *Y. pestis* infections may include pulmonary, lymph node, and cutaneous/subcutaneous hemorrhages, as well as necrosuppurative lymphadenitis, necrotizing pneumonia, and multifocal abscessation with intralesional gram-negative coccobacilli with a characteristic bipolar, safety-pin-like morphology.[3] Geographic location may help include or exclude *Y. pestis* as a likely/unlikely differential.

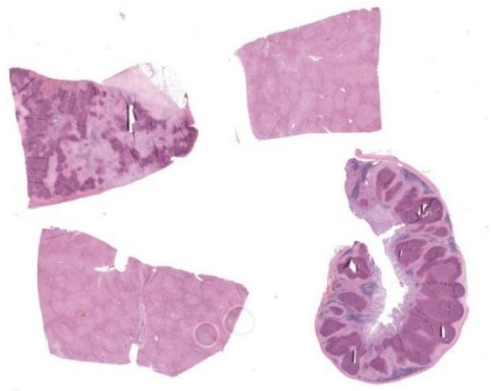

Figure 1-3. Cecum, spleen, liver, rabbit. Two sections of liver and one each of cecum and spleen are submitted for examination. (HE, 5X)

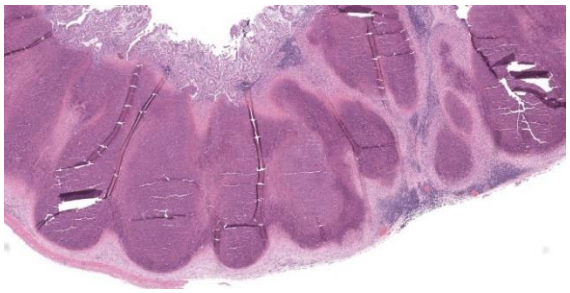

Figure 1-4. Cecum, rabbit. There is diffuse necrosis of Peyer's patches and replacement by numerous necrotic heterophils and cellular debris. (HE, 25X)

The diagnosis of yersiniosis is typically made through identification of microabscesses with microcolonies of coccobacilli on histology and subsequent confirmation with bacterial culture.[14] *Francisella tularensis* infection – tularemia - can cause small foci of caseous granulomas in the liver, spleen and lymph nodes, and could therefore be a potential differential diagnosis for the gross lesions.[4] Amongst other lesions, systemic listeriosis, caused by *Listeria monocytogenes*, can also present with hepatic necrotic foci, and could potentially be a less likely differential; however, gram-positive staining would differentiate this condition from yersiniosis.[4]

Contributing Institution:
Veterinary Pathology Service
School of Veterinary Medicine and Science
University of Nottingham
https://www.nottingham.ac.uk/vet/

JPC Diagnoses:
1. Cecum: Peyer's patch necrosis, diffuse, with mild, chronic typhlitis.
2. Spleen: Splenitis, necrotizing and heterophilic, chronic, diffuse, severe, with coccobacilli.
3. Liver: Vacuolar change, centrilobular and midzonal, diffuse.

JPC Comment:
The contributor provides an excellent overview of the typical course of disease in yersiniosis caused by *Y. pseudotuberculosis* and *Y. enterocolitica*. These two species are typically associated with a relatively benign gastrointestinal disease rather than the well-described, fulminant syndromes associated with *Y. pestis*, but the pathogenetic mechanisms of the enteric disease caused these species remain incompletely understood.

As the contributor notes, *Y. pseudotuberculosis* and *Y. enterocolitica* cross the mucosa through the M cells of Peyer's patches; once in the mucosa, they are engulfed by macrophages, where they survive and are trafficked to the lymph nodes and beyond.[12] A key virulence factor, shared by all three pathogenic *Yersinia* species, is a type 3 secretion system, similar to that found in *Salmonella* species, that allows the organism to inject effector proteins into the host cell cytoplasm.[12] In *Yersinia* species, these effector proteins are termed *Yersinia* outer proteins ("Yops"). Yops are injected into macrophages and neutrophils and interfere with phagocytosis and the production of reactive oxygen species, ensuring bacterial survival and dissemination.[12] Yops come in at least six different varieties – YopE, YopM, YopO, YopT, YopP, and YopH – each with its own pernicious bag of tricks aimed at frustrating the host's immune system.[5] For instance, YopP blocks pro-inflammatory NF-kappaB and MAPK-signaling pathways, and YopM is thought to block the inflammasome by binding caspase-1.[5] The end result of all of this molecular subterfuge is bacterial persistence and disease.

Birds and rodents are throught to be the principal reservoirs of *Yersinia pseudotuberculosis*, which causes enteric, often subclinical infection in many wild and domestic animals.[12,16] Enteric yersiniosis is relatively common in young deer and lambs, where disease is characterized by profuse watery diarrhea which can be rapidly fatal if untreated; clinically similar but less severe disease can

be seen in young ruminants.[12] The septicemic form of the disease, often called pseudotuberculosis, occurs most commonly in laboratory rodents and aviary birds.[12] Finally, sporadic abortion caused by *Y. pseudotuberculosis* has been reported in cattle, sheep, and goats.[12]

Despite the canonical association of *Y. pseudotuberculosis* with enteritis, a recently reported outbreak in African lions was notable for its presentation, which was characterized by respiratory distress and pulmonary bacterial colonization without gastrointestinal lesions.[16] Also notable was the unusual pleomorphic, filamentous morphology of the bacteria, confirmed to be *Y. pseudotuberculosis* via culture.[16] This filamentous morphology has been previously described in *Y. pseudotuberculosis* infections in squirrel monkeys and is thought to be a bacterial adaptation to the use of antibiotics.[16]

Our moderator this week was Dr. Patti Pesavento, Department Chair and Professor of Pathology, Microbiology, and Immunology at the University of California Davis College of Veterinary Medicine. Dr. Pesavento began discussion of this case by noting that low-magnification evaluation is invaluable in this slide, which contains four tissues, some of which contain flashy lesions with remarkable distributions and tinctorial differences. Dr. Pesavento cautioned against getting bogged down looking at every micrometer of tissue and exhorted residents to use low magnification to spot areas of interest, take closer looks at those particular areas, and then hop back to subgross magnification for further investigation.

Conference participants found tissue identification on the section of alimentary tract to be somewhat difficult and discussed possible locations, including the vermiform appendix, the cecal tonsil, the ilem, or the sacculus rotundus. Participants felt they could not be

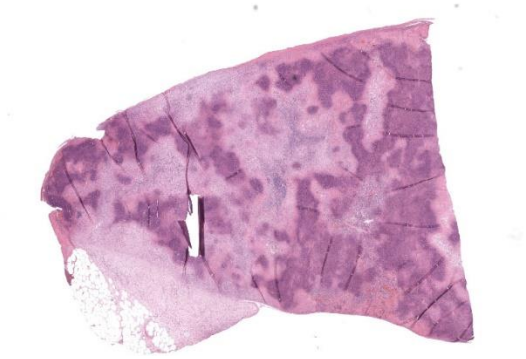

Figure 1-5. Spleen, rabbit. There is diffuse loss of the splenic architecture with multifocal to coalescing areas of lytic necrosis. There is rupture of the capsule (lower left) (HE, 25X)

definitive based on the examined section alone due to the complete obliteration of tissue architecture both in this tissue and in the spleen. Participants also noted the presence of substantial fibrosis indicating that, despite the apparent fulminant nature of the lesions in the spleen and gastrointestinal tract, the process was likely chronic. Chronicity could also explain the lack of large cloud-like bacterial colonies which would be expected of *Yersinia* spp., the "Y" in the "STACY" mnemonic used to denote large colony-forming bacteria (the others being ***S****taphylococcus*, ***S****treptococcus* ***A****ctinomyes*, ***A****ctinobacillus*, ***C****orynebacterium*, ***C****lostridium, and* ***T****rueperella*).

Participants marveled at the liver, which had no right to look as great as it did. Given that *Y. pseudotuberculosis* enters from the gut, the liver receives the brunt of the bacterial onslaught. Dr. Pesavento noted that the liver does an admirable and largely unsung job of clearing bacteria from the portal blood and, considering the destruction noted in the spleen and gut, the relatively normal looking liver is a testament to the its effective immunologic vigilance. Some participants noted the mild periportal lymphoplasmacytic hepatitis, which is a fairly typical finding in rabbits, and thought it unrelated to the bacterial infection. Participants did appreciate a mild

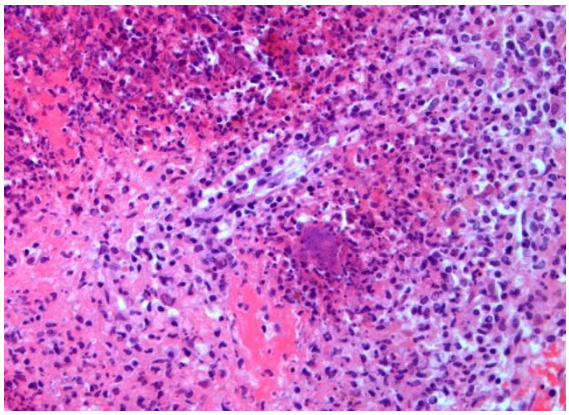

Figure 1-6. Spleen, rabbit. There are rare large colonies of coccobacilli within the spleen. (*Photo courtesy of:* Veterinary Pathology Service, School of Veterinary Medicine and Science, University of Nottingham) (HE 400X)

lipid vacuolation that seemed concentrated in the centrilobular and midzonal areas, and felt that this was the most believable lesion present in the liver.

Once participants were thoroughly unimpressed with the histologic appearance of the liver, Dr. Pesavento pulled a proverbial rabbit out of the hat, wowing the crowd with a reticulin stain. Reticulin, a connective tissue composed of type III collagen, lines the spaces of Disse. When visualized with a reticulin silver stain, the patency of these fibers can be assessed to determine the integrity of the hepatic cord and sinusoidal architecture. In this case, the seemingly bland appearance of the liver belied the fact that the entire reticulin network was completely destroyed.

Participants felt that the cecal tissue should get pride of place in the morphologic diagnosis given the striking necrosis. Participants could not convincingly identify coccobacilli in the examined cecal section, but were convinced of their presence in the spleen. The remarkable liver, despite its lack of underlying reticulin network, was felt to be largely normal in the examined section, with no areas of necrosis or identifiable bacteria. Participants felt, however, that the zonal distribution of the vacuolar change was a believable, perhaps sentinel lesion, and deserved to be included in the diagnosis.

References:

1. Barthold SW, Griffey SM, Percy DH. Rabbit. In: *Pathology of Laboratory Rodents and Rabbits*. John Wiley & Sons; 2016:253-324.
2. Ceccolini ME, Macgregor SK, Spiro S, Irving J, Hedley J, Guthrie A. Yersinia pseudotuberculosis infections in primates, artiodactyls, and birds within a zoological facility in the United Kingdom. *J Zoo Wildl Med*. 2020;51(3):527-538.
3. Delaney MA, Treuting PM, Rothenburger JL. Rodentia. In: *Pathology of Wildlife and Zoo Animals*. Elsevier 2018:499-515.
4. Delaney MA, Treuting PM, Rothenburger JL. Lagomorpha. In: *Pathology of Wildlife and Zoo Animals*. Elsevier 2018:481-498.
5. Grabowski B, Schmidt MA, Ruter C. Immunomodulatory Yersinia outer proteins (Yops) – useful tools for bacteria and humans alike. *Virulence.* 2017;8(7): 1124-1147.
6. Le Guern AS, Martin L, Savin C, Carniel E. Yersiniosis in France: Overview and potential sources of infection. *Int J Infect Dis*. 2016;46:1-7.
7. Hammerl JA, Barac A, Bienert A, et al. Birds kept in the German zoo "Tierpark Berlin" are a common source for polyvalent *Yersinia pseudotuberculosis* phages. *Front Microbiol*. 2022;12: 634289.
8. Long C, Jones TF, Vugia DJ, et al. *Yersinia pseudotuberculosis* and *Y. enterocolitica* Infections, FoodNet, 1996–2007. *J Infect Dis*. 2010;16(3):566-567.
9. Najdenski H, Vesselinova A, Golkocheva E, Garbom S, Wolf-Watz H.

Experimental infections with wild and mutant *Yersinia pseudotuberculosis* strains in rabbits. *J Vet Med Ser B*. 2003;50(6):280-288.
10. Nakamura S, et al. Aberrant form of *Yersinia pseudotuberculosis* as spheroplasts and filaments in yersiniosis in squirrel monkeys. *Vet Pathol*. 2012;52: 393-396.
11. Pereira M, Stidworthy MF, Denk D, Spiro S, Guthrie A, Patterson S. A retrospective study of morbidity and mortality identified at postmortem examination of captive langurs (*Trachypithecus* spp) from six United Kingdom zoological institutions: A 19-year review. *J Zoo Wildl Med*. 2021;52 (4):1123-1134.
12. Quinn PJ, Markey BK, Leonard FC, FitzPatrick ES, Fanning, S, Hartigan PJ. *Veterinary Microbiology and Microbial Disease*. Wiley-Blackwell;2011:280-282.
13. Reinhardt M, Hammerl JA, Kunz K, Barac A, Nöckler K, Hertwig S. *Yersinia pseudo-tuberculosis* prevalence and diversity in wild boars in northeast Germany. *Appl Environ Microbiol*. 2018;84(18):1-10.
14. Uzal FA, Plattner BL, Hostetter JM. Alimentary system. In: Maxie MG, ed. *Jubb, Kennedy & Palmer's Pathology of Domestic Animals*. 6th ed. Vol 2. Elsevier 2016.
15. Visser LG, Annema A, Van Furth R. Role of Yops in inhibition of phagocytosis and killing of opsonized *Yersinia enterocolitica* by human granulocytes. *Infect Immun*. 1995;63(7):2570-2575.
16. Womble M, Cabot ML, HarrisonT, Terumi Negrao Watanabe T. Outbreak in African lions of *Yersinia pseudo tuberculosis* infection, with aberrant bacterial morphology. *J Vet Diag Invest*. 2022; 34(2):334-338.
17. World Health Organization. Plague. 2022:1-5. Available at https://www.who.int/news-room/fact-sheets/detail/plague; accessed on 05/23/23.

CASE II:

Signalment:
2-month-old male rose-ringed parakeet (*Psittacula krameri*)

History:
Sudden death without any clinical signs of disease.

Gross Pathology:
Necropsy revealed sparse feathers in the abdomen and back areas, multifocal subcutaneous hemorrhage and hemorrhage in pectoral muscles and muscles of extremities and extensive hepatic necrosis and hemorrhage.

Laboratory Results:
PCR testing for avian polyomavirus was positive; PCR testing for psittacine beak and feather disease, avian bornavirus, herpesvirus, and *Chlamydia* was negative.

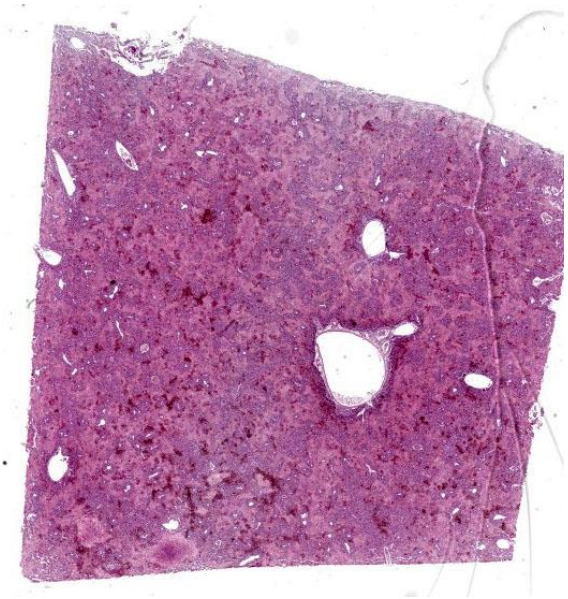

Figure 2-1. Liver, parakeet fledgling. One section of liver is submitted for examination. (HE, 5X)

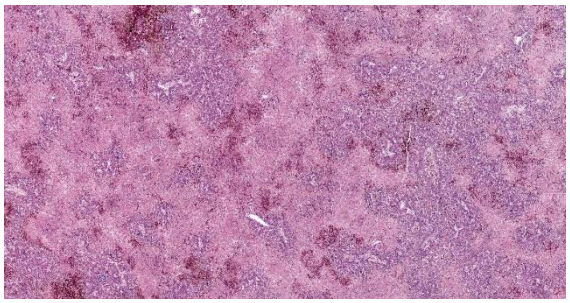

Figure 2-2. Liver, parakeet fledgling. There is a retiform pattern of pallor representing centrilobular and midzonal necrosis. (HE, 41X)

Microscopic Description:
Liver: Affecting up to 70% (this percentage somewhat varies between the slides) of the liver parenchyma there is disruption and loss of the hepatic architecture evident by either of the following: loss of differential staining and paleness of hepatocytes with karyolysis (lytic necrosis), eosinophilic cellular and karyorrhectic debris with hypereosinophilic cytoplasm and pyknosis (coagulative necrosis), and moderate numbers of extravasated erythrocytes (hemorrhage). Such changes affect mostly centrilobular and midzonal portions of the lobules and frequently coalesce (centrilobular and midzonal necrosis). Adjacent hepatocytes are frequently swollen with pale vacuolated cytoplasm (hepatocellular degeneration). Rarely such hepatocytes have mildly enlarged nuclei that contain large amphophilic to lightly eosinophilic, irregularly round inculsion bodies that completely efface the nuclear chromatin and peripheralize the nuceloli. Multifocally within the portal areas there is an increase in the number of bile duct profiles (ductular reaction). Scattered throughout the sinusoids are uncommon aggregates of hematopoietic cells with erythroid and fewer myeloid precursors (extramedullary hematopoiesis).

Contributor's Morphologic Diagnosis:
Liver: Hepatocellular necrosis and degeneration, acute, multifocal to coalescing, submassive, severe, with rare large intranuclear amphophilic viral inclusion bodies.

Contributor's Comment:
Avian polyoma virus (APV) is one of the most significant viral pathogens of caged birds. It results in substantial economic losses for aviculturalists and pet store owners each year. APV is included in the genus *Polyomavirus*, family *Papovaviridae*. Its ability to infect and cause disease in birds is dependent on the age of the bird, the species, the immune status of the bird, and other poorly understood factors.[6]

APV was first characterized as a pathogen in young budgerigars in 1981 and was designated budgerigar fledgling disease virus.[1] Now it is called avian polyomavirus because it affects many different species of psittacine birds. To date, four polyomaviruses in birds are known, namely avian polyomavirus, goose hemorrhagic polyomavirus (GHPV), finch polyomavirus (FPyV) and crow polyomavirus (CPyV).

In fledgling and young budgerigars, APV causes acute death, abdominal distention and feather abnormalities known as "French molt." It also causes a loss of down feathers on the back and abdomen, filoplumes on the head and neck, and subcutaneous hemorrhage of nesting budgerigars. In other avian orders, including psittacine species, APV causes clinical signs similar to those observed in budgerigars, but the severity of the disease seems to be dependent on the species infected.[4] Other species of psittacine birds can be very ill at weaning with nonspecific weight loss, anorexia, partial paralysis of the gut, polyuria, and watery droppings. They have a tendency to haemorrhage easily, and may have CNS signs. Not all the birds get the disease and not all of those affected die; some (especially the

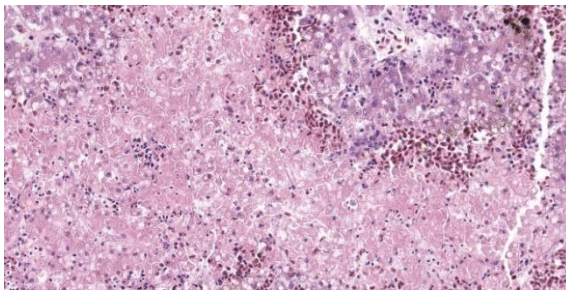

Figure 2-3. Liver, parakeet fledgling. Higher magnification of the relatively sudden transition from areas of coagulative necrosis to viable hepatocytes which are often bordered by a line of hemorrhage. (HE, 317X)

older birds) recover to become asymptomatic carriers.[2]

Typical pathologic changes in psittacine birds include hydropericardium, enlarged heart, swollen liver, congested kidneys, and hemorrhage within the body cavities. Histopathology typically reveals large and slightly basophilic intranuclear inclusion bodies in various tissues, especially in the spleen, liver, and kidneys.[4]

Recent references about APV are mainly related to monitoring of free-ranging and captive birds for polyomavirus and other avian viruses. Kessler et al., 2020, demonstrated that the prevalence of polyomavirus in free-ranging *Psittacula* populations in Europe is low despite the general susceptibility of these species to this virus.[5] Rahaus and Wolff, 2005, conducted a survey to detect subclinical poly-omavirus infections in captive psittacine birds in Germany and they did not detect APV in any samples.[8] However, surveys in Australia and Poland detected significant rates of infection in captive parrot populations with APV.[3,7] All of this emphasizes the need to adhere to strict biosecurity measures and regular testing for common psittacine pathogens especially in rehabilitation centers and breeding units.

Contributing Institution:
Department of Veterinary Pathology
Faculty of Veterinary Medicine
University of Zagreb
Heinzelova 55
10000 Zagreb, Croatia
http://www.vef.unizg.hr/

JPC Diagnosis:
Liver: Necrosis, coagulative, multifocal to coalescing, severe, with mild to moderate hepatocellular lipidosis.

JPC Comment:
The contributor provdes an excellent overview of avian polyomavirus, an important avian disease that exhibits a wide variety of case presentations ranging from subclinical disease tosudden death, depending on species susceptibility. Conference participants found this case particularly rewarding as it provide ample fodder for discussion of foundational issues in liver pathology, such as lesion distribution and the association between lesion distribution and possible etiologies.

In this liver, the distribution of the main lesion - striking, large areas of necrosis – was the main point of discussion. Dr. Pesavento began with a subgross evaluation of the distribution, which many participants felt was zonal, while others felt that the distribution, while geographic and incorporating wide swaths of tissue, was essentially random. Dr. Pesavento noted that every lobule of the liver appears to be affected, which argues against a random distribution, but agreed that the distribution of hepatic lesions in birds can generally be difficult to determine, as this case demonstrates.

The majority of participants agreed that the lesion appeared concentrated in the centrilobular and midzonal areas. Due to this zonality and the diffuse necrosis throughout all liver lobules in section, participants felt that insults expected to have a zonal distribution,

such as hypoxia and toxin exposure, should be included in the differential diagnosis list. Other differentials suggested by participants included viral causes, such as psittacid herpesvirus 1, and avian polyomavirus.

Dr. Pesavento discussed the reticulin-staining in this liver, contrasting it with the rabbit liver in the previous case. In this bird, the reticulin framework appeared intact, indicating a more acute process. The intact reticulin network also suggests that the observed necrosis is affecting hepatocytes, not endothelial cells. This suggestion is bolstered by the reduced distance between the intact peri-sinusoidal reticulin networks, which is an indicator of hepatocellular loss.

Returning to the H&E slide and the proposed polyomaviral etiology, participants noted the lack of convincing polyomaviral inclusions, which are typically large, intranuclear, basophilic to amphophilic features which can substantially obscure the nucleus. Polyomaviral infections typically generate many of these dramatic inclusions and participants found their absence surprising. Participants were also perplexed by the zonal, non-random lesion distribution, which is unusual for a viral infection. The moderator noted that subclinical polyomaviral infections are relatively common, raising the possibility that this animal's lesions were not caused by polyomavirus, despite being PCR-positive for the agent.

Conference participants discussed what additional diagnostics could be used to investigate possible etiologic agents. Participants felt that Giemsa or Gram staining would be helpful to rule out septicemia, and that in situ hybridization (ISH) would be helpful to confirm the presence of polyomavirus in the liver and to determine if the virus is co-localized with areas of necrosis. Finally, participants noted that avian polyomavirus inclusions are most reliably found in the spleen, adding an H&E section of splenic tissue to the diagnostic wish list.

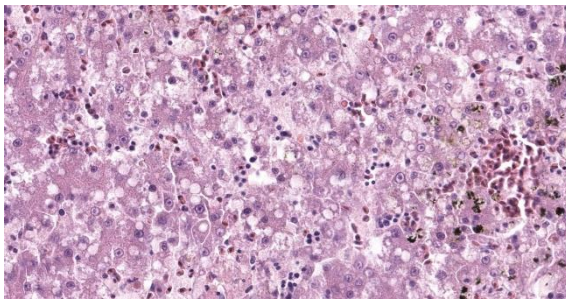

Figure 2-4. Liver, parakeet fledgling. Viable, largely periportal hepatocytes often contain cytoplasmic lipid droplets. There are hemosiderin-laden macrophages in areas of hemorrhage. (HE, 458X)

Despite being open to alterate etiologies for the observed lesions, conference participants largely agreed with the contributor's morphologic diagnosis. No lesion distribution was included in the JPC diagnosis as participants remained equivocal as to whether the lesions were random or zonal, and despite intense searching, no intranuclear inclusions were observed in the section examined in conference.

References:

1. Davis RB, Bozeman LH, Gaudry D, Fletcher OJ, Lukert PD, Dykstra MJ. A viral disease of fledgling Budgerigars. *Avian Dis.* 1981;25(1):179-183.
2. Harcoutt-Brown NH. Psittacine birds. In: Tully TN, Dorrestein GM, Jones AK, eds. *Handbook of Avian Medicine*. 2nd ed. Saunders Elsevier; 2000:138.
3. Hulbert CL, Chamings A, Hewson KA, Steer PA, Gosbell M, Noormohammadi AH. Survey of captive parrot populations around Port Phillip Bay, Victoria, Australia, for psittacine beak and feather disease virus, avian polyomavirus and psittacine adenovirus. *Aust Vet J*. 2015;93 (8):287-292.

4. Katoh H, Ogawa H, Ohya K, Fukushi H. A Review of DNA Viral Infections in Psittacine Birds. *J Vet Med Sci*. 2010;72(9):1099-1106.
5. Kessler S, Heenemann K, Krause T, et al. Monitoring of free-ranging and captive *Psittacula* populations in Western Europe for avian bornaviruses, circoviruses and polyomaviruses. *Avian Pathol*. 2020;49 (2):119-130.
6. Phalen DN. Avian Polyomavirus: My Thoughts. *Alfa Watchbirb*. 1998;25(5):28-39.
7. Piasecki T, Wieliczko A. Detection of beak and feather disease virus and avian polyomavirus DNA in Psittacine birds in Poland. *Bull Vet Inst Pulawy*. 2010;54: 141-146.
8. Rahaus M, Wolff MH. A survey to detect subclinical polyomavirus infections of captive psittacine birds in Germany. *Vet Microbiol.* 2005;105:73-76.

CASE III:

Signalment:
13-year-old Appaloosa-cross mare (*Equus caballus*)

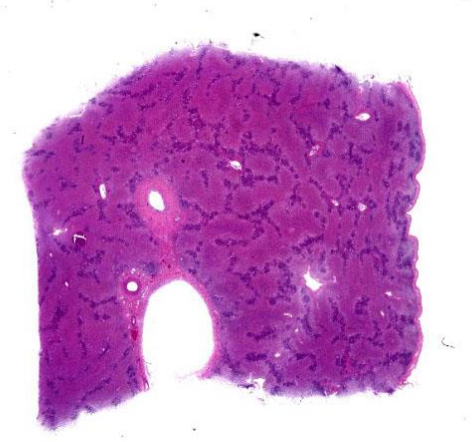

Figure 3-1. Liver, horse. A single section of liver is submitted for examination. A retiform pattern of necrosis is visible at subgross magnification. (HE, 5X)

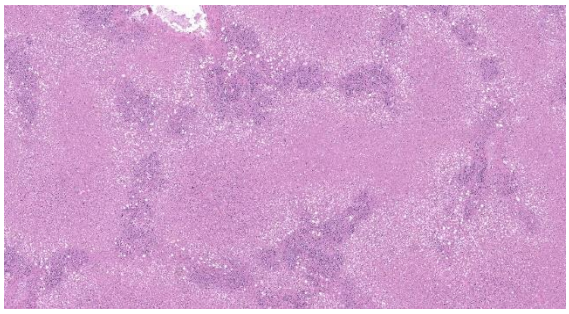

Figure 3-2. Liver, horse. There is diffuse, massive necrosis with the most profound changes in the centrilobular and midzonal areas. (HE, 41X)

History:
The horse presented with petechiae and edema of the upper lip and appeared to be rubbing the area. The animal was treated but did not improve. The horse was found down two days later with icterus and died shortly afterwards.

Gross Pathology:
The horse was icteric. The liver was small and collapsed or flattened.

Microscopic Description:
The tissue submitted is liver. There is centrilobular to massive hepatocellular necrosis. Portal triads have bile duct hyperplasia, mild lymphoplasmacytic inflammation, and fibrosis with partial bridging between portal triads.

Contributor's Morphologic Diagnoses:
1. Massive hepatocellular necrosis
2. Mild, chronic lymphoplasmacytic hepatitis

Contributor's Comment:
This is a case of equine serum hepatitis, also known as Theiler's disease. The histologic features of this disease are unique and diagnostic. There is an acute centrilobular to massive hepatocellular necrosis and a chronic portal hepatitis. Grossly, the liver is small and collapsed and sometimes flabby or flaccid.

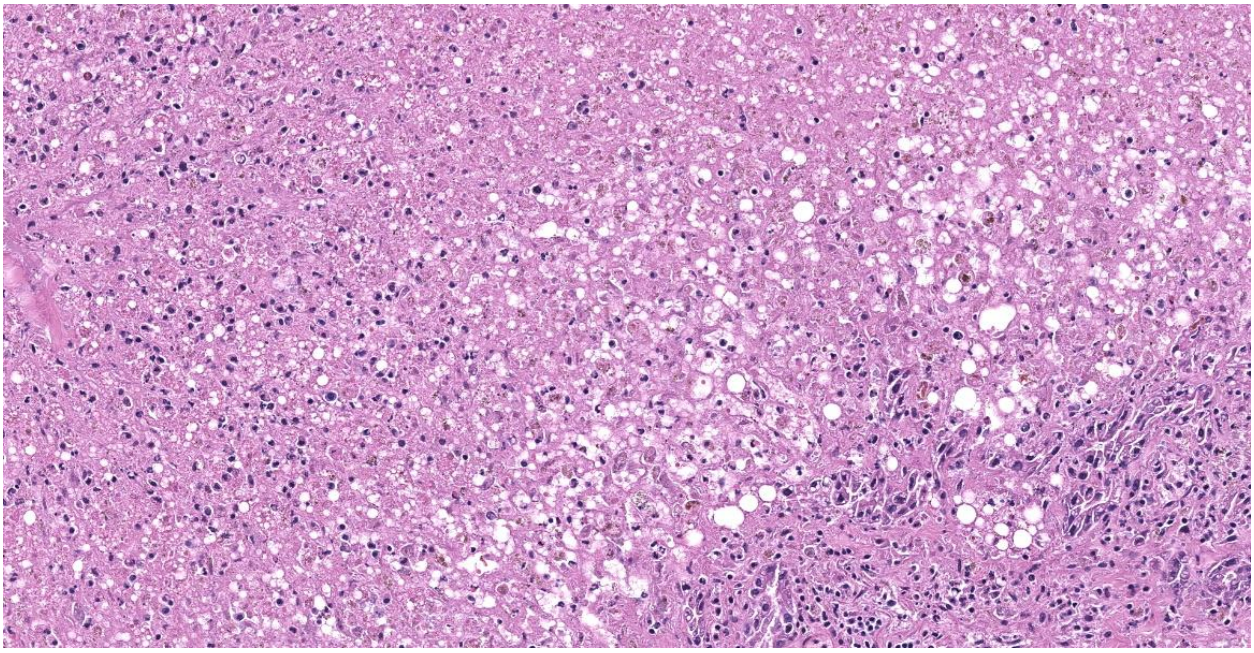

Figure 3-3. Liver, horse. There is total hepatocellular necrosis in the centrilobular and midzonal area. A portal area is present at lower right. (HE, 192X)

Equine serum hepatitis was first described by Theiler early in the 20th century. The disease was associated with the use of various biologics containing equine serum, usually vaccines, and occurred 1-3 months following the use of these products.[1,3] However, many cases occurred that had not received equine serum. The cause of the disease is now thought to be viral.[2]

Contributing Institution:
College of Veterinary Medicine
Virginia Tech
www.vetmed.vt.edu

JPC Diagnosis:
Liver: Necrosis, massive, diffuse, with stromal collapse and hepatocellular lipidosis.

JPC Comment:
Theiler's disease was first described in 1919 by South African veterinarian Sir Arnold Theiler after hundreds of horses acutely died of hepatitis after being vaccinated against African Horse Sickness.[2] Since first described, Theiler's disease has been documented worldwide in horses treated with a variety of biologics, including tetanus antitoxin, botulinum antitoxin, antiserum against *Streptococcus equi*, and equine plasma, though for the past 50 years, disease has been most commonly associated with administration of tetanus antitoxin.[2] A variety of potential causes have been investigated and proposed as the etiologic agent of Theiler's disease, most notably a pegivirus named Theiler's Disease-Associated Virus (TDAV); however, the currently accepted etiologic agent is a parvovirus, named equine parvovirus hepatitis virus (EqPV-H), which was discovered, isolated, and characterized in 2018.[1,2]

A typical case presentation of Theiler's disease involves rapidly progressive symptoms of lethargy, anorexia, and jaundice 2-3 months following the administration of blood products; clinical pathology abnormalities include elevated serum levels of liver enzymes and bilirubin.[1] Some horses may have fever and central nervous system signs such as cortical blindness, ataxia, behavior changes, or

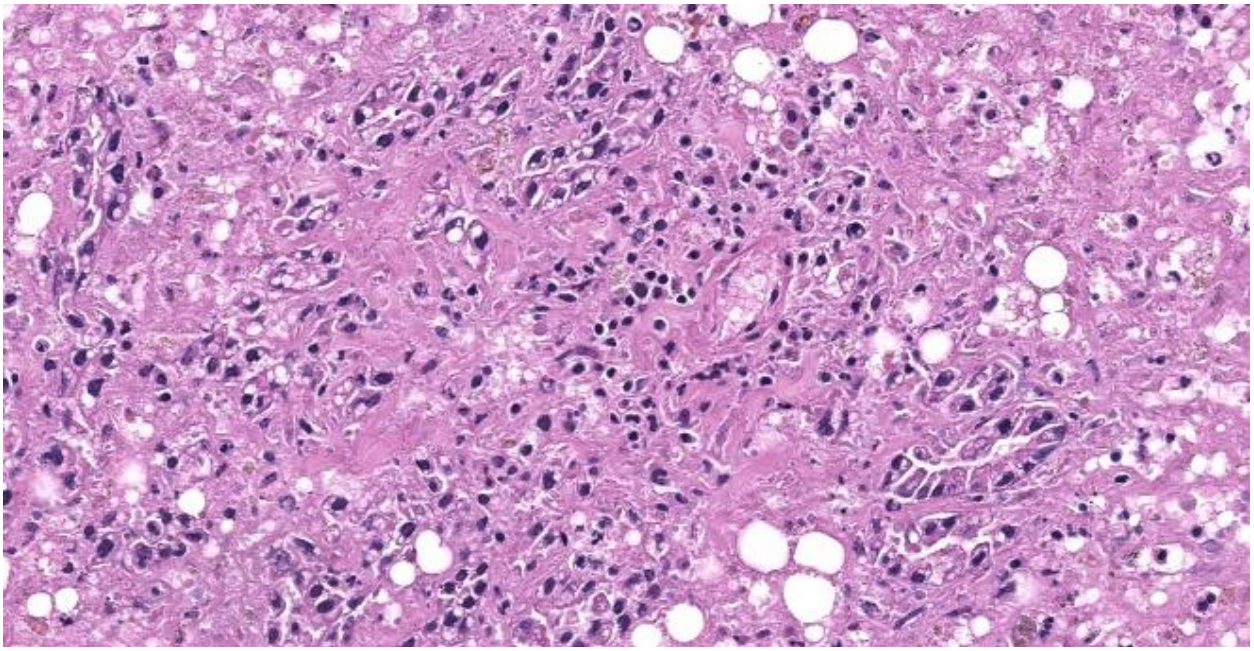

Figure 3-4. Liver, horse. Due to the massive necrosis, even normal structures in portal areas are difficult to discern. Few irregular shunken hepatocytes remain and a bile duct is evident at lower right. (HE, 397X)

coma.[1] Histologically, Theiler's disease is characterized by massive hepatocellular necrosis, as illustrated nicely by this case. Mortality rates between 50% and 90% are reported.[1] Experimental studies of EqPV-H have revealed the virus to be endemic in the United States, parts of Europe, and China, with estimated prevalence of 2.9-17%, with up to 54% prevalence on farms with recent outbreaks of Theiler's disease.[2] The virus has been shown to be transmitted via stem cell therapy for orthopedic injuries and by oral inoculation with viremic serum; vertical transmission appears to be minimal.[2] EqPV-H is shed in oral and nasal secretion and in feces, leading to potential environmental accumulation of this hearty virus.[2] Research into effective biosecurity measures to minimize EqPV-H transmission is ongoing.

Participants felt that slide description in this case was a challenge as virtually nothing was left to describe! On subgross evaluation, however, participants noted the wrinkling of the liver capsule and the irregular distances between central veins and portal triads throughout the section, both indicators of microhepatica due to massive necrosis/stromal collapse. Dr. Pesavento contrasted this presentation with liver shunting, which typically presents with capsule wrinkling but relatively constant central vein to portal triad distances.

Even without the subgross suggestion of microhepatica, however, the massive hepatocellular necrosis evident on histological examination is characteristic of Theiler's disease, which should be included in every differential list for massive hepatic necrosis in a horse. Evaluation of a Masson trichrome illustrated some fibrosis, but participants felt that the amount of fibrosis was likely normal for a 13-year-old horse. Fibrosis is generally not a histologic feature of Theiler's disease as animals typically do not live long enough to develop it.

Participants were surprised by the reticulin stain in this case, which looked relatively

normal. Similar to the previous case, the reticulin framework remained intact despite the massive necrosis, once again highlighting the hepatocellular-centric nature of this disease.
Dr. Pesavento discussed the current understanding of Theiler's disease which, in a testament to the rapid advancement of scientific knowledge, has changed and solidified since this case was originally submitted to the Wednesday Slide Conference. At that time, the current theory was that a pegivirus, termed Theiler's disease-associated virus (TDAV) was responsible for the disease; however, researchers were skeptical of this claim from the outset as pasteurization of the serum products implicated in the transmission of Theiler's disease should have incapacitated TDAV. Further research lead to the discovery EqPV-H, a parvovirus that can withstand typical pasteurization temperatures, and subsequent studies have established a strong correlation between EqPV-H and Theiler's disease.

Discussion of the morphologic diagnosis was relatively short as the hepatocellular necrosis was glaring and all-encompassing. Participants noted the periportal lymphoplasmacytic hepatitis described by the contributor, but chose to omit it from the JPC diagnosis to emphasize the necrosis-driven pathogenesis.

References:

1. Chandriani S, Skewes-Cox P, Zhong W, et al. Identification of a previously undescribed divergent virus from the Flaviviridae family in an outbreak of equine serum hepatitis. *Proc Nat Acad Sci*. 2013; 10(15):E1407-E1415.
2. Divers TJ, Tennant BC, Kumar A, et. al. New parvovirus associated with serum hepatitis in horses after inoculation of common biologic product. *Emerg Infect Dis.* 2018;24(2):303-310.
3. Stalker MJ, Hayes MA. Liver and biliary system. In: Maxie MG, ed. *Pathology of Domestic Animals*. 5th ed, vol 2. Elsevier-Saunders;2007:343-344.

CASE IV:

Signalment:
9-year-old, male castrated domestic shorthair cat (*Felis catus*)

History:
The cat presented for a 12-hour history of lethargy and inappetence. Complete blood chemistry revealed severe normocytic normochromic anemia and severe thrombocytopenia. Serum chemistry showed moderate elevation in ALT and mild azotemia. Abdominal radiographs revealed a moderate peritoneal effusion, a suspected small intestinal linear foreign body-associated mechanical obstruction, and generalized hepatomegaly. AFAST and abdominal fluid sampling and cytology confirmed a hemoabdomen of unknown origin. The patient was taken to surgery for an exploratory laparotomy.

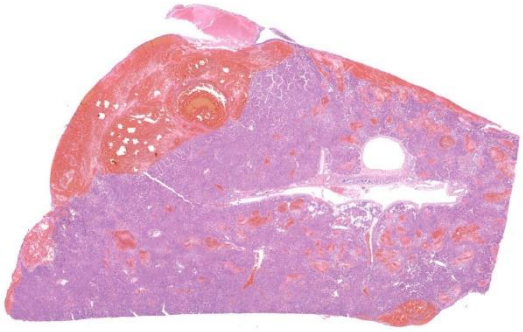

Figure 4-1. Liver, cat. The section of liver has a area of subcapsular acute hemorrhage surrounding a large dilated vessel, as well as smaller areas of dissecting hemorrhage throughout the parenchyma. (HE, 5X)

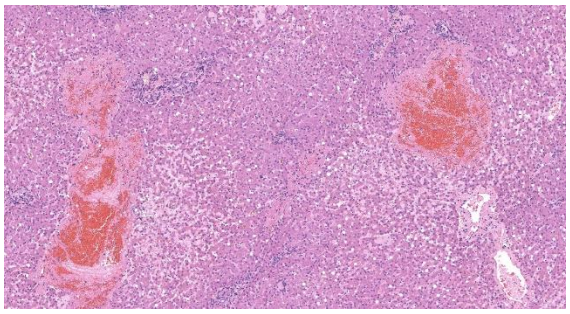

Figure 4-2. Liver, cat. Smaller areas of dissecting hemorrhage are scattered throughout the parenchyma. There is pink matrix (amyloid) within the surrounding sinusoids. (HE, 81X)

Gross Pathology:
A hepatic mass involving the left and quadrate lobes was observed during exploratory laparotomy. laparotomy. The remainder of the liver parenchyma was mildly friable. No other gross abnormalities were noted during the surgical procedure. The mass was excised and submitted for histopathology.

Laboratory Results:

	Result	Reference	Units
WBC	12.19	5.5-19.5	x10^3/ul
Neutrophil	7.07	2.5-12.5	x10^3/ul
Band Neutrophil	0.00	0.0-0.3	x10^3/ul
Lymphocyte	5.12	1.5-7.0	x10^3/ul
Monocyte	0.00	0.0-0.85	x10^3/ul
Eosinophil	0.00	0.0-0.75	x10^3/ul
Basophils	0.00	0.0-0.1	
RBC	3.84	4.6-10.2	x10^6/ul
Hemoglobin	5.5	8.5-15.3	gm/dl
Hematocrit	16.5	26.0 - 47 .0	%
MCV	43.0	38.0 – 54.0	fl
MCH	14.4	11.8-18.0	pg
MCHC	33.5	29.0-36.0	gm/dl
RDW	19.5	16.0-23.0	%
Nucleated RBC	0.00		
Platelet-Auto	52	100-518	x10^3/ul
MPV	11.8	9.9-16.3	fl

	Result	Reference	Units
Albumin	3.8	2.2-4.4	gm/dl
Alk Phos	12	10-90	IU/L
ALT	465	20-100	IU/L
Amylase	1124	300-1100	
T. bilirubin	0.3	0.1-0.6	mg/dl
BUN	46	10-30	mg/dl
Calcium	10.9	8.0-11.8	mg/dl
Phosphorus	3.2	3.0-6.9	mg/dl
Creatinine	2.6	0.8-2.1	mg/dl
Glucose	87	70-150	mg/dl
Sodium	159	142-164	mEq/L
Potassium	4.3	3.7-5.8	mEq/L
T. Protein	7.5	5.4-8.5	gm/dl
PTT	239	80-119	sec

Microscopic Description:
Left lateral liver lobe: Multifocally, portal tracts contain profiles of small arterioles, several of which lack portal venules. Several small arterioles extend into adjacent hepatic parenchyma, and these typically are in a bizarre orientation and have hypertrophied endothelium. Central veins are difficult to identify. The space of Disse in the centrilobular areas contains a substantial amount of eosinophilic, homogeneous, hyaline-like material. Also, there are aggregates of hyaline-like material associated with clusters of cells within

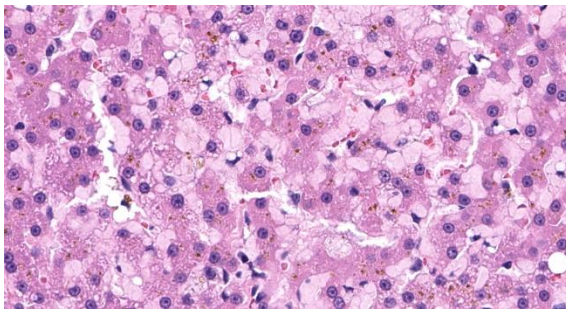

Figure 4-3. Liver, cat. Hepatic sinusoids are expanded by amyloid. There is abundant brown pigment within hepatocytes and Kupffer cells (likely hemosiderin). (HE, 605X)

the sinusoids. Often, the portal tracts are moderately expanded by infiltration of lymphocytes, plasma cells, and a few eosinophils. There are large foci of disrupted hepatic cords with sinusoids expanded by hemorrhage (telangiectasia), aforementioned hyaline-like material, and fibrin thrombi throughout the parenchyma.

Contributor's Morphologic Diagnosis:
Left lateral liver lobe:

1. Hepatic microvascular dysplasia with portal venule hypoplasia
2. Hepatic amyloidosis, with telangiectasia, hemorrhage, and thrombosis

Contributor's Comment:
This case had morphological findings consistent with hepatic microvascular dysplasia and portal venule hypoplasia as well as amyloidosis that was confirmed by Congo Red staining. The coexistence of these two findings in this patient is considered to be unique.

Hepatic microvascular dysplasia (HMD) is an intrahepatic shunting of blood through microscopic vessels within the liver.[3] Clinical signs described in canine patients include inhibited growth, ammonium biurate crystalluria, hepatic encephalopathy, vomiting, and diarrhea.[3,7] HMD may occur as an isolated congenital malformation or may be present with a concurrent macroscopic portosystemic shunt vessel.[7] Some dogs lacking other hepatic abnormalities, such as a macroscopic congenital portosystemic shunt, may be asymptomatic.[7] Rarely, multiple acquired portosystemic shunts may arise secondary to HMD and subsequent portal hypertension.[7,12]

HMD is fairly frequently reported in small-breed dogs, particularly the Cairn Terrier and Yorkshire Terrier.[14] In Cairn Terriers an autosomal recessive pattern of inheritance has been described.[11] Cases of HMD and/or portal vein hypoplasia in the cat are infrequently reported in the literature.[12] Recently, a case of multiple acquired portosystemic shunts secondary to portal vein hypoplasia was reported in a cat.[12,14]

Histologic lesions consistent with HMD include increased arterioles in portal triad regions, ectatic pericentral vascular spaces, and mural hypertrophy of central veins.[4,7] HMD and portal vein hypoplasia are both congenital defects in the development of intrahepatic portal veins and may occur concurrently.[14] Histologically, portal vein hypoplasia is characterized by decreased numbers of portal vein branches within small portal triads.[14] If histology reveals evidence of HMD or portal vein hypoplasia, a macroscopic congenital portosystemic shunt must be ruled out by advanced imaging techniques as this abnormality results in similar histologic lesions.[7,14]

Hepatic amyloidosis is commonly found in association with generalized amyloidosis in the majority of species. Generalized, or systemic, amyloidosis is frequently associated with an overproduction of an amino-terminal fragment of the inducible acute-phase protein serum amyloid A, simply termed "amyloid A."[4] This disease occasionally occurs in a variety of species including horses, cattle, dogs, and cats, and is often a subsequent response to chronic tissue destruction or disease.[1,2,4,6,9]

Familial amyloid A amyloidosis is another potential underlying etiology of systemic amyloidosis. This disease is recognized in Chinese Shar-Pei dogs and Abyssinian and Siamese cats.[8,10] The condition bears a resemblance to familial amyloidosis in humans (familial Mediterranean fever), and affected animals exhibit episodic pyrexia, swollen hocks, renal amyloidosis, and occasional concurrent hepatic amyloidosis. [8,10]

Systemic amyloidosis in horses is most often secondary to chronic inflammation and is observed with increased frequency in horses used for the production of hyperimmunized serum.[1] Affected horses may develop icterus and other signs of hepatic dysfunction.[1] In contrast, cattle, dogs, and cats generally first exhibit clinical signs of renal dysfunction from concurrent renal amyloid deposition.[6] It is reported that cattle may rather die of the underlying primary disease.[6] Though infrequent, cats have been reported to present with spontaneous hepatic rupture, as in this case.[2,6]

Contributing Institution:
Iowa State University
College of Veterinary Medicine
Department of Veterinary Pathology
Ames, IA 50010-1250
https://vetmed.iastate.edu/vpath

JPC Diagnoses:
1. Liver: Amyloidosis, intrasinusoidal, multifocal, marked, with parenchymal rupture and acute hemorrhage.
2. Liver: Primary portal vein hypoplasia with numerous portal arteriolar profiles.

JPC Comment:
This beautiful slide, striking at subgross, reveals even more delights upon closer examination. As the contributor nicely describes, the liver is characterized by three major pathologic processes: large accumulations of blood throughout the hepatic parenchyma,

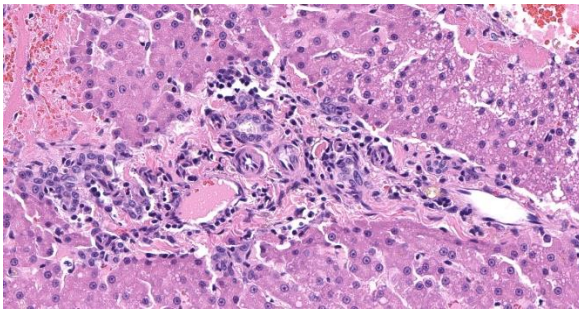

Figure 4-4. Liver, cat. There are numerous cross-section of tortuous arterioles within portal areas, including two venous profiles in this portal area. (HE, 395X)

multifocal accumulations of eosinophilic hyaline material, and portal areas comprised of increased numbers of arterioles, bile ductules, and portal veins.

On subgross evaluation, the large lakes of hemorrhage are most eye-catching, and conference discussion focused initially on the character of these lesions. Participants wondered if these could represent peliosis hepatis, defined as randomly distributed, cystic blood-filled spaces in the liver.[5] This is well-reported in cats and can result either from obstruction of the portal vasculature with subsequent hepatic atrophy and dilation of the sinuisoids (referred to as telangiectasis) or from hepatocyte necrosis.[5] Telangiectasis is distinguished from hemorrhage by the presence of an endothelial lining, and participants discussed which process was predominant in this lesion, decided that the lakes of blood represented hemorrhage as they were not lined by discernable endothelium.

Discussion then turned to the eosinophilic deposits, interpreted by the contributor and conference participants as amyloid.

A Congo Red performed at JPC in preparation for the conference was negative, prompting considerations of other differentials for the the eosinophilic material; however, in cats, amyloid is often best illustrated using

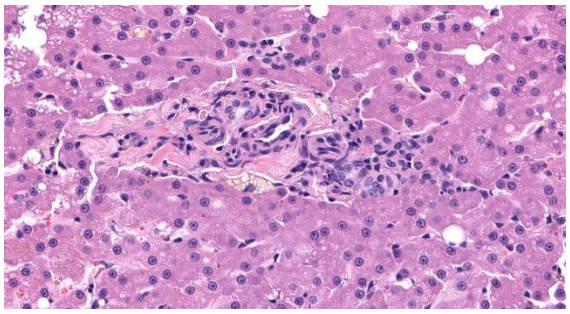

Figure 4-5. Liver, cat. Other portal areas contain numerous arteriolar profiles but are lacking venous profiles. (HE, 395X)

thioflavin T staining and a post-conference thioflavin T staining performed at the University of California, Davis, was weakly positive, confirming the material as amyloid.

Discussion of the portal abnormalities quickly turned semantic, with participants discussing the terms "microvascular dysplasia" versus "portal vein hypoplasia." This distinction is challenging and likely artificial due to the stereotypical histologic response of the liver to inadequate portal vein flow.[5] With decreased portal blood flow, the portal vein and its tributaries become reduced and hepatic arteries respond to this hypoperfusion by increasing their blood flow, in the processes becoming more tortuous, proliferative, and hypertrophic.[5] Histologically, as seen in this case, this is evidenced by an increased number of arteriolar profiles in the portal tracts, sometimes with an accompanying increase in the number of biliary ductular profiles along with slight fibrosis.[5] The increased arterial hepatic flow may result in increased sinusoidal pressure and subsequent sinusoidal dilation.[5]

Primary portal vein hypoplasia is a congenital disorder of dogs and, rarely, of cats, which is characterized by the histologic findings typical of portal vein hypoperfusion discussed above.[5] The World Small Animal Veterinary Association's standardization board for canine and feline liver circulatory disorders has stated that there have been "no clinical or biochemical findings to suggest that [microvascular dysplasia] is different from primary portal vein hypoplasia" and that the authors "have decided to abandon the name microvascular dysplasia" and prefer to call this condition "primary portal vein hypoplasia," which the authors find more descriptive.[5]

Primary portal vein hypoplasia varies widely in clinical severity and morphology and overlaps histologically with other causes of hypoperfusion, including congenital portosystemic shunts, intrahepatic arterioportal fistulas, and portal vein obstruction.[5] In 30% of dogs, the vascular changes are mild with no evidence of portal fibrosis; others have moderate to marked fibrosis in the portal tracts, hypoplasia or absence of the portal veins, and a proliferation of arterioles and bile ductules, as seen in this case.[5] Importantly, this diagnosis is based on histologic examination of a liver biopsy in combination with ultrasonographic findings which exclude the presence of congenital portosystemic shunt, arteriovenous fistula, or portal vein thrombosis.[5] In this case, the portal areas contain all the classic hallmarks of hypoperfusion; however, the case history contains no record of ultrasonographic findings to exclude the other causes of hypoperfusion.

Examination of a reticulin stain illustrated complete destruction of the reticulin framwork in this case. Dr. Pesavento noted that no research currently exists on whether this is a feature of microvascular dysplasia or amyloid deposition, but the reticulin destruction in this case was striking, with small remnant fragments of reticulin extending only a short distance from central veins. The lack of a reticulin framework and the hemorrhagic presentation in this case is reminiscent of fatty liver hemorhagic syndrome in poultry, in which vacuolar swelling of hepatocytes

disrupts the reticulin structure of the hepatic cords, leading to hemorrhage from the sinusoids.[13]

Given that the principal cause of death was hemorrhage, presumably due to hepatic fracture secondary to amyloidosis, participants favored placing amyloidosis front and center in the morphologic diagnosis. Despite the persistence of the term "microvascular dysplasia" in the literature, participants preferred to use the WSAVA-recommended term "primary portal vein hypoplasia" to capture the full complement of architectural derangements present in the examined portal areas.

References:

1. Abdelkader SV, Gudding R, Nordstoga K. Clinical chemical constituents in relation to liver amyloidosis in serum-producing horses. *J Comp Pathol*. 1991;105(2):201-211.
2. Blunden AS, Smith KC. Generalised amyloidosis and acute liver haemorrhage in four cats. Vol 5. *J Small Anim Pract*. 1992;33(12):566-570.
3. Christiansen JS, Hottinger HA, Allen L, Phillips L, Aronson LR. Hepatic microvascular dysplasia in dogs: a retrospective study of 24 cases (1987-1995). *J Am Anim Hosp Assoc*. 2000;36(5):385-389.
4. Cullen J, Stalker M. Liver and Biliary System. In: Maxie MG, ed. *Jubb, Kennedy, and Palmer's Pathology of Domestic Animals*. 6th ed. Vol 2. Elsevier 2016:278-279.
5. Cullen MJ, van den Ingh TSGAM, Bunch WE, Rothuizen J, Washabau RJ, Desmet VJ. Morphological classification of circulatory disorders of the canine and feline liver. In: Rothuizen J, ed. *WSAVA Standards for Clinical and Histological Diagnosis of Canine and Feline Liver Disease*. Elsevier;2006:41-59.
6. Elitok OM, Elitok B, Unver O. Renal amyloidosis in cattle with inflammatory diseases. *J Vet Intern Med*. 2008;22(2):450-455.
7. Hwang T, An S, Kim A, Han C, Huh C, Lee HC. Acquired portosystemic shunts secondary to hepatic microvascular dysplasia in a young dog. *J Vet Clin.* 2020; 37(2):88-90.
8. van der Linde-Sipman JS, Niewold TA, Tooten PC, de Neijs-Backer M, Gruys E. Generalized AA-amyloidosis in Siamese and Oriental cats. *Vet Immunol and Immunopathol*. 1997;56(1-2):1-10.
9. Neo-suzuki S, Mineshige T, Kamiie J, et al. Hepatic AA amyloidosis in a cat: cytologic and histologic identification of AA amyloid in macrophages. 2017;46(2):331-336.
10. Olsson M, Meadows JRS, Truvé K, et al. A novel unstable duplication upstream of HAS2 predisposes to a breed-defining skin phenotype and a periodic fever syndrome in Chinese Shar-Pei dogs. 2011; 7(3):e1001332.
11. Schermerhorn T, Center SA, Dykes NL, et al. Characterization of hepatoportal microvascular dysplasia in a kindred of cairn terriers. *J Vet Intern Med.* 1996;10(4):219-230.
12. Sugimoto S, Maeda S, Tsuboi M, et al. Multiple acquired portosystemic shunts secondary to primary hypoplasia of the portal vein in a cat. Vol. 80, *J Vet Med Sci*. 2018:874-877.
13. Trott KA, Giannitti F, Rimoldi G, et al. Fatty liver hemorrhagic syndrome in the backyard chicken: a retrospective histopathologic case series. *Vet Pathol*. 2015; 51(4):787-795.
14. Watson P. Canine breed-specific hepatopathies. *Vet Clin North Am Small Anim Pract*. 2017;47(3):665-682.

WSC 2023-2024
Conference 16 Self-Assessment

1. After ingestion, Yersinia sp. colonize which of the following?.
    a. Lymphocytes in Peyer's patches
    b. Macrophages
    c. Intestinal M cells
    d. Neutrophils

2. Which of the following species of bird does not have a species-specific polyomavirus?
    a. Swan
    b. Goose
    c. Crow
    d. Finch

3. Equine serum hepatitis results from infection with which of the following?
    a. Flavivirus
    b. Hepacivirus
    c. Parvovirus
    d. Pegivirus

4. True or false: Generalized amyloidosis in animal species is most commonly AA type

    a. True
    b. False

5. Which of the following clinical signs has not been described in dogs with hepatic microvascular dysplasia
    a. Hepatoencephalopathy
    b. Pulmonary minderalization
    c. Ammonium biurate crystalluria
    d. Diminished growth

Joint Pathology Center
Veterinary Pathology Services

WEDNESDAY SLIDE CONFERENCE 2023-2024

Conference #17 24 January 2024

CASE I:

Signalment:
1-year-old, male neutered mixed-breed dog (*Canis familiaris*)

History:
This dog presented for severe cervical pain progressing to C6-T1 myelopathy with paraplegia. An MRI of the cervical region and a CSF analysis were within normal limits. The patient was not responsive to antibiotics, prednisone, or cytarabine treatment. The owner elected euthanasia, and the body was submitted for necropsy.

Gross Pathology:
The gross examination was unremarkable except for a 12 x 6 x 6 cm, firm, tan, multilobulated mass in the posterior mediastinum adjacent to the bodies of vertebrae T5-T7. The mass extended through the intervertebral foramen into the vertebral canal, compressed the spinal cord at the level of T6, and infiltrated the adjacent epaxial skeletal muscle.

Microscopic Description:
The mass is composed of lobules of round to polygonal neoplastic cells separated by thick bands of connective tissue. The cells show considerable variation in size, ranging from 15µm to over 100µm in diameter. The small cells are round with scant eosinophilic cytoplasm and round nuclei with coarsely clumped chromatin and indistinct nucleoli (neuroblasts). The larger cells have abundant granular cytoplasm which is eosinophilic around the nucleus and basophilic at the periphery. Nuclei in these cells are round and usually eccentric with vesicular chromatin and single, large, central nucleoli (ganglion cells). The larger cells are often dissected by streams of spindle cells and wavy fibrillar to vacuolated eosinophilic material (Schwannian stroma). Anisocytosis and anisokaryosis are marked and the mitotic rate is higher in the smaller cells (15 in 2.37 mm^2) than in the larger cells (2 in 2.37 mm^2). In approximately 25% of the mass, the cells are hypereosinophilic with loss of cellular detail (coagulation necrosis), and a focal area is replaced by granular basophilic material (mineralization). At the periphery of the mass, the neoplastic cells infiltrate the adjacent adipose tissue.

Figure 1-1. Posterior mediastinum, dog. There is a 12 x 6 x 6 cm, firm, tan, multilobulated mass in the posterior mediastinum adjacent to the bodies of vertebrae T5-T7. (*Photo courtesy of:* Virginia Tech College of Veterinary Medicine, https://vetmed.vt.edu/)

Figure 1-2. Posterior mediastinum, dog. The mass extends through the intervertebral foramen into the vertebral canal, compresses the spinal cord at the level of T6, and infiltrates the adjacent epaxial skeletal muscle. (*Photo courtesy of:* Virginia Tech College of Veterinary Medicine)

Contributor's Morphologic Diagnosis:
Posterior mediastinal mass: Ganglioneuroblastoma.

Contributor's Comment:
Peripheral neuroblastic tumors arise from immature cells in the ganglia of the cranial and spinal nerves and the sympathetic nervous system. Locations include the adrenal gland, neck, mediastinum, retroperitoneal space, and pelvis. These tumors are classified based on the degree of differentiation: neuroblastomas are composed of small, undifferentiated cells (neuroblasts); ganglioneuroblastomas also contain neuroblasts, along with maturing and mature ganglion cells, nerve fibers, Schwann cells and stroma (Schwannian stroma); and ganglioneuromas, the most differentiated of the three, are composed of mature ganglion cells, nerve fibers, Schwann cells, and Sch-wannian stroma. Ganglioneuroblastomas are further classified, based on the amount of Schwannian stroma, into intermixed (Sch-wannian stroma-rich) and nodular (Schwannian-stroma rich and Schwannian stroma-poor areas) subtypes. The presence of neuroblasts, gangliocytes, nerve fibers and Schwannian stroma in this case is consistent with a gangiolneuroblastoma.[20] Based on the human classification system, this tumor could be further characterized as a nodular subtype.

Neuroblastomas, ganglioneuroblastomas, and ganglioneuromas can also arise from neuronal progenitors in the central nervous system (central neuroblastic tumors) and the olfactory epithelium (olfactory neuroblastic tumors). Olfactory neuroblastomas are also known as esthesioneuroblastomas. Ganglioneuromatosis is a condition characterized by nodular proliferation of neural tissue in the intestine with a segmental or diffuse distribution.

Ganglioneuromatosis is classified as a hamart-omatous rather than neoplastic process and is associated with genetic syndromes, such as phosphatase and tensin homolog hamartoma (PTEN) syndrome, neurofibromatosis type 1 or 2, and multiple endocrine neoplasia type IIb.[9] By immunohistochemistry, neuroblasts are positive for synaptophysin, neuron specific enolase (NSE), and chromogranin A, although immunoreactivity in this population may be weak or variable; ganglion cells and neural processes are posi-

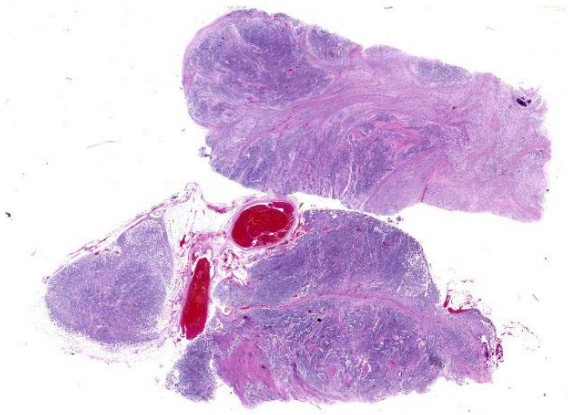

Figure 1-3. Posterior mediastinum, dog. Two sections of a multilobulated mass infiltrating the mediastinal fat are submitted for examination. (HE, 5X)

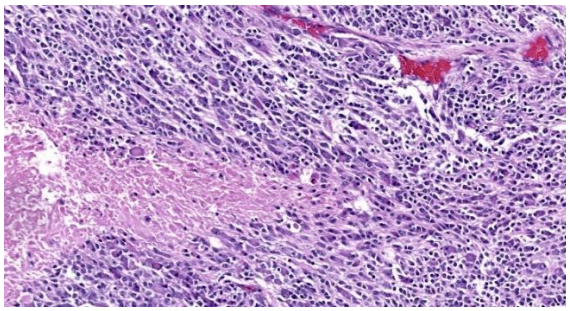

Figure 1-4. Posterior mediastinum, dog. The neoplasm is composed of two cell types arranged in poorly defined streams and areas of coagulative necrosis. (HE, 230X)

tive for neurofilament and NSE; and Schwann cells are positive for S100, NSE, and GFAP.[3,7,10] In humans, neuroblastic tumors comprise 80% of neoplasms in children under 5 years old and are rare after the age of 10.[1] Prognosis depends on tumor type, and cellular features (degree of differentiation, mitotic rate, karyorrhexis).[19]

In general, ganglioneuromas develop in older children and adults and are considered benign with a favorable prognosis. The prognosis for neuroblastomas depends on the age of the patient, the degree of differentiation of the neuroblasts, and the mitosis-karyorrhexis index. Intermixed ganglioneuroblastomas are associated with a favorable prognosis while the prognosis of the nodular subtype depends of the degree of differentiation of the neuroblastic component.

Peripheral neuroblastomas have been documented in dogs[3] and cattle[11,22] and peripheral ganglioneuromas are described in dogs,[5] horses,[2] cats,[8] and pigs.[7] Ganglioneuromatosis has also been reported in a horse,[16] dogs,[12] and cattle.[4] Previous reports of veterinary ganglioneuroblastomas are listed in Table 1.

Contributing Institution:
Virginia-Maryland
College of Veterinary Medicine
205 Duck Pond Dr.
Blacksburg VA 24061
https://vetmed.vt.edu/

JPC Diagnosis:
Fibroadipose tissue: Ganglioneuroblastoma.

JPC Comment:
As the contributor notes, peripheral neuroblastic tumors arise from sympathetic nervous system progenitor cells. These progenitor cells migrate from the neural crest to form, among other tissues, sympathetic ganglia and the chromaffin cells of the adrenal medulla.[3]

The factors that lead to the persistence and subsequent neoplastic transformation of these progenitor cells are incompletely understood in both human and veterinary medicine.

In humans, most neuroblastic tumors carry an excellent prognosis if detected early in life; however, an unpredictable subset of human neuroblastic tumors carries increased risk and a poorer prognosis. The most well-characterized marker of these high-risk tumors is increased expression of MYCN, a transcription factor in the MYC family, which occurs in approximately 25% of pediatric neuroblasto-

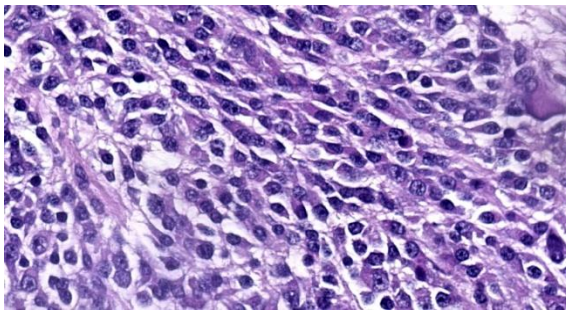

Figure 1-5. Posterior mediastinum, dog. The primary cell type is a small polygonal cell (neuroblast). (HE, 808X)

Species (breed)	Age/Sex	Location	Clinical Outcome
Dog (Bichon-frise)[10]	13 years/MN	Oral cavity	Died of heart failure 2 months after surgery
Dog (Lab)[18]	18 months/M	Cranial mediastinum	Euthanized 1 week after diagnosis
Dog (German Shepherd)[17]	8 years/M	Footpad	Amputation with no recurrence for over 1 year
Cat (mixed)[15]	11 month/MN	Facial nerve	Died 30 days after onset of neurologic signs
Cat (DSH)[21]	8 years/MN	Footpad	Treated with electrochemotherapy; remission for more than 1 year
Sheep (Akkaraman)[23]	18 months/not specified	Retroperitoneum	Diagnosed at slaughter
Calf (Japanese Black)[13]	Newborn/M	Cervical	Euthanized

Table 1. Reported peripheral ganglioneuroblastomas in veterinary species.

mas.[6] Rodent studies have determined that MYCN, like MYC, can induce cellular proliferation and cell cycle progression in quiescent cells; however, there is a spatiotemporal difference between the two transcription factors. MYC is expressed in a broad spectrum of tissues and gradually subsides over time in adult mice.[6] By contrast, MYCN is found only during early developmental stages and is expressed most substantially in the forebrain, hindbrain, and kidneys of newborn mice.[6]

Given its role in early development, it is perhaps unsurprising that the degree of differentiation in neuroblastoma cells is negatively correlated with MYCN expression, with more differentiated tumors characterized by lower levels of MYCN than less differentiated tumors.[6] MYCN is also involved in maintaining the multipotency and capacity for self-renewal characteristic of the neural crest cells from which neuroblastic tumors arise, and mouse models have induced neuroblastomas by targeted overexpression of MYCN in migrating neural crest cells.[6]

MYCN's contribution to the stem cell-like state of neural crest and neoplastic cells is multifactorial. MYCN increases expression of proliferation-permissive proteins such as CDK1 and CDK4, promotes angiogenesis by stimulating VEGF production, and facilitates cell survival through the p53-blocking protein MDM2.[6] MYCN also inhibits the production of cell cycle arrest proteins and transcription factors that promote differentiation, down regulates immune surveillance by MCP-1, and creates a pro-metastasis environment through, among other actions, blocking production of E-cadherin and certain integrins.[6]

In dogs and humans, clinical signs vary widely depending on tumor localization and extent, and on the presence or absence of any paraneoplastic syndromes.[3,14] In humans, 65% of peripheral neuroblastic tumors arise in the abdomen, with half of these originating

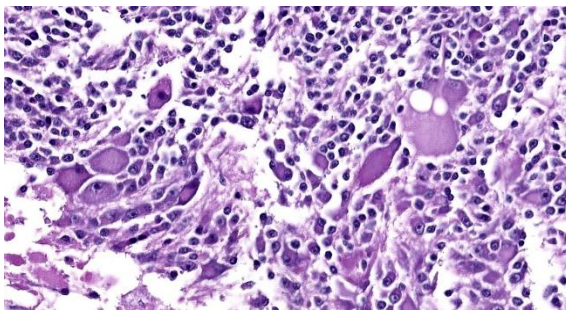

Figure 1-6. Posterior mediastinum, dog. The second cell type strongly resembles a ganglion cell. (HE, 483X)

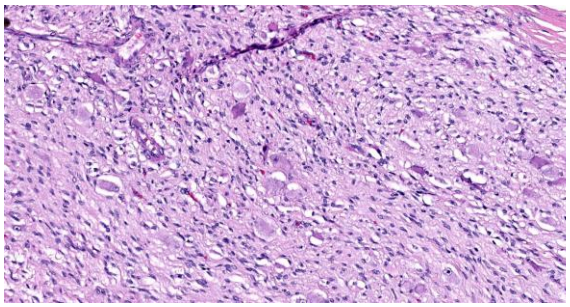

Figure 1-7. Posterior mediastinum, dog. Neoplastic cells are embedded in stroma that strongly resembles a peripheral nerve ("Schwannian stroma"). (HE, 250X)

in the adrenal medulla.[14] With local or regional disease, patients may be asymptomatic, while more extensive disease may cause abdominal distention and pain, Horner's syndrome (for cervical tumors), and episodic secretory diarrhea due to tumor production of vasoactive intestinal peptides.[3,14]

Due to the paucity of published case reports, the prognoses and biologic behaviors of canine peripheral neuroblastic tumors are hard to predict. In a recent case study of canine

neuroblastomas, the majority of the dogs were either euthanized at the time of diagnosis or lost to follow up; of those submitted for necropsy, metastatic disease was discovered in 4/9 dogs, most commonly in the liver.[3]

This week's moderator, Dr. Andrew Miller, Associate Professor and Section Chief of the Department of Population Medicine and Diagnostic Sciences at the Cornell University College of Veterinary Medicine, began discussion by reviewing the characteristics of various embryonal tumors. This heterogenous group of tumors includes central and peripheral neuroblastoma, ganglioneuroblastoma, medulloblastoma, and primitive neuroectodermal tumors, all of which can occur as paraspinal masses that compress the spinal cord. As a definitional matter, Dr. Miller noted that the term "primitive neuroectodermal tumor," or PNET, is no longer used in human neuropathology due to the World Health Organization's reclassification of nervous system tumors based on genetic and molecular markers. In veterinary medicine, the umbrella term "PNET" persists as the genetic mutations underlying nervous system tumors and the molecular methods used to diagnose them are less fully developed.

Ganglioneuroblastomas are generally rare in veterinary medicine, and diagnosis requires clear, obvious ganglion cell differentiation, neuroblasts, and some amount of Schwann cells and Schwannian stroma. Dr. Miller noted these elements in the examined slide and called attention to the large areas of confluent necrosis, an indication that the neoplasm was aggressive and rapidly growing.

Discussion of the morphologic diagnosis was blissfully straightforward, with only momentary debate about tissue localization. Conference participants were not able to detect the tissue's mediastinal origin from the H&E section alone and thus chose to omit any reference to a specific anatomic location.

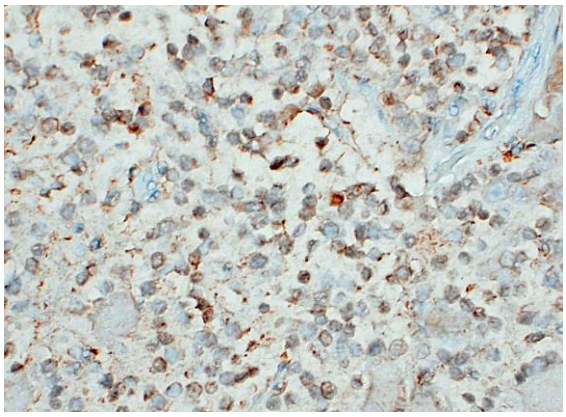

Figure 1-8. Posterior mediastinum, dog. Neuroblasts demonstrate strong nuclear immunopositivity for synaptophysin. (Anti-synaptophysin, 250X)

References:

1. Alessi S, Grignani M, Carone L. Ganglioneuroblastoma: Case report and review of the literature. *J Ultrasound*. 2011; 14(2):84-88.
2. Allen D, Swayne D, Belknap JK. Ganglioneuroma as a cause of small intestinal obstruction in the horse: a case report. *Cornell Vet*. 1989;79(2):133-141.
3. Arenas-Gamboa AM, Tanabe M, Edwards J, Storts R. Peripheral neuroblastomas in dogs: a case series. *J Comp Pathol*. 2014; 150(4):361-365.
4. Cole DE, Migaki G, Leipold HW. Colonic Ganglioneuromatosis in a Steer. *Vet Path- ol*. 1990;27(6):461-462.
5. Goto M, Yonemaru K, Hirata A, Furuhashi H, Yanai T, Sakai H. Lingual ganglioneuroma in a dog. *J Vet Med Sci*. 2018; 80(3):488-491.
6. Huang M, Weiss WA. Neuroblastoma and MYCN. *Cold Spring Harbor Perspect Med*. 2013;3(10):a014415.
7. Inoue R, et al. Cardiac ganglioneuroma in a juvenile pig. *J Vet Med Sci*. 2016;78(1): 117-119.
8. Kobayashi R, Ohsaki Y, Yasuno K, et al. A malignant and metastasizing feline cardiac ganglioneuroma. *J Vet Diagn Invest*. 2012;24(2):412-417.
9. Koullouros M, Candler S, Smith C, Olakkengil S. Appendicitis and ganglioneuroma-an unusual co-existence. *J Surg Case Rep*. 2022;2022(1):rjab632.
10. Nakamura K, Ochiai K, Kadosawa T, Kimura T, Umemura T. Canine ganglioneuroblastoma in the oral mucosa. *J Comp Pathol*. 2004;130(2):205-208.
11. Omi K, Kitano Y, Agawa H, Kadota K. An immunohistochemical study of peripheral neuroblastoma, ganglioneuroblastoma, anaplastic ganglioglioma, schwannoma and neurofibroma in cattle. *J Comp Pathol*. 1994;111(1):1-14.
12. Paris JK, McCandlish IAP, Schwarz T, Simpson JW, Smith SH. Small intestinal ganglioneuromatosis in a dog. *J Comp Pathol*. 2013;148(4):323–328.
13. Park CH, Shiwa N, Kimitsuki K, Kakizaki T, Watanabe D. Cervical ganglioneuroblastoma in a new born Japanese Black calf. *J Vet Med Sci*. 2018;80(5):755-759.
14. Park JR, Eggert A, Caron H. Neuroblastoma: biology, prognosis, and treatment. *Pediatr Clin North Am*. 2008;55(1):97-120.
15. Pereira PR, Tagliari NJ, Leite-Filho RV, Schaefer G da C, Costa FVA da, Pavarini SP. Facial nerve ganglioneuroblastoma in a feline leukemia virus-positive cat. *Ciênc Rural*. 2017;47(5)1-5.
16. Porter BF, Storts RW, Payne HR, Edwards JF. Colonic ganglioneuromatosis in a horse. *Vet Pathol*. 2007;44(2):207–210.
17. Salvadori C, Cantile C, Massari F, Chiti L, Colombo S, Abramo F. Footpad peripheral ganglioneuroblastoma in a dog. *Vet Dermatol*. 2019;30(4):346-e100.
18. Schulz KS, Steele KE, Saunders GK, Smith MM, Moon ML. Thoracic ganglioneuroblastoma in a dog. *Vet Pathol*. 1994;31(6):716–718.
19. Shimada H, Chatten J, Newton WA, et al. Histopathologic prognostic factors in neuroblastic tumors: definition of subtypes of ganglioneuroblastoma and an age-linked classification of neuroblastomas. *J Natl Cancer Inst*. 1984;73(2):405-416.
20. Shimada H, Umehara S, Monobe Y, et al. International neuroblastoma pathology classification for prognostic evaluation of patients with peripheral neuroblastic tumors. *Cancer*. 2001;92(9):2451-2461.
21. Spugnini EP, Citro G, Dotsinsky I, Mudrov N, Mellone P, Baldi A. Ganglioneuroblastoma in a cat: a rare neoplasm treated with electrochemotherapy. *Vet J Lond Engl 1997*. 2008;178(2):291-293.

22. Uchida K, Murakami T, Tometsuka T, Iwakiri A, Yamaguchi R, Tateyama S. Peripheral neuroblastoma and primitive neuroectodermal tumor in Japanese black cattle. *J Vet Med Sci*. 1998;60(7):871–875.
23. Yener Z, Kiran MM. Undifferentiated Ganglioneuroblastoma in a Sheep. *J Comp Pathol*. 2002;126(2):216-219.

CASE II:

Signalment:
13-year old, intact female Indian origin Rhesus macaque (*Macaca mulatta*)

History:
This female Rhesus macaque presented with progressive weight loss, vision loss, and wide circling to the right over the course of one year. She also exhibited galactorrhea for approximately 4 years, despite not having given birth in over two years. Ophthalmologic exam revealed inability to fix or follow an object, searching behavior, and subjective bilateral optic nerve pallor on fundic exam. Subsequent MRI revealed a large (3.2 x 2.9 x 2.5 cm) contrast-enhancing hypophyseal mass protruding from the pituitary fossa with associated mar-ked compression of the adjacent brain parechyma. Due to poor prognosis, humane euthanasia was elected.

Figure 2-1. Pituitary gland, rhesus macaque. MRI examination revealed a large (3.2 x 2.9 x 2.5 cm) contrast-enhancing hypophyseal mass protruding from the pituitary fossa with associated marked compression of the adjacent brain parenchyma. (*Photo courtesy of:* Johns Hopkins University School of Medicine, Department of Molecular and Comparative Pathobiology, http://www.hopkinsmedicine .org/mcp)

Figure 2-2. Pituitary gland, rhesus macaque. There is a 2.4 x 2.0 x 1.4 cm, well-circumscribed, tan, firm mass attached to the mid-ventral aspect of the brain at the level of the pituitary gland dorsal to the sella turcica. (*Photo courtesy of:* Johns Hopkins University School of Medicine, Department of Molecular and Comparative Pathobiology)

Gross Pathology:
Gross necropsy revealed a 2.4 x 2.0 x 1.4 cm, well-circumscribed, tan, firm mass attached to the mid-ventral aspect of the brain at the level of the pituitary gland dorsal to the sella turcica. The mass compressed adjacent neural tissue and the optic nerve at the level of the optic chiasm. On cut section, the mass extended as far rostrally as the basal ganglia and as far caudally as the pons. The mass also asymmetrically compressed the lateral

Figure 2-3. Pituitary gland, rhesus macaque: The mass extended as far rostrally as the basal ganglia and as far caudally as the pons. The mass also asymmetrically compressed the lateral ventricles. (*Photo courtesy of:* Johns Hopkins University School of Medicine, Department of Molecular and Comparative Pathobiology)

ventricles, causing mild to moderate hydrocephalus.

Laboratory Results:
Significant clinical pathology results are listed below:

- Complete blood count (CBC): Stress leukogram
- Chemistry panel: Mild hypokalemia
- Thiamine: WNL
- Estrogen (E2): WNL (<5 pg/ml)
- Progesterone (P4): WNL (0.10 ng/ml)
- Prolactin: Elevated (147.6 ng/ml - expected value 20-50 ng/ml)

Immunohistochemistry:

- Synaptophysin (+)
- ACTH (-)
- FSH (-)
- Growth hormone (-)
- MSH (-)
- Prolactin (-)

Microscopic Description:
Cerebrum: Expanding and compressing surrounding neuroparenchyma is a densely cellular, well-demarcated, nodular, unencapsulated neoplasm. Neoplastic cells are closely packed and are arranged in nests/packets supported on a fine fibrovascular stroma. Neoplastic cells frequently palisade around blood vessels (pseudorosettes) or a central area of fiber-rich neuropil (Homer-Wright rosettes). Cells are columnar to polygonal with indistinct cell borders and a scant to moderate amount of eosinophilic granular cytoplasm. Nuclei are round and centrally located with coarsely stippled chromatin and 1-2 variably prominent nucleoli. Anisocytosis and anisokaryosis are mild. Mitoses are rare (avg <1 per 10 high powered fields). There are multifocal areas of necrosis within the center of the neoplasm consisting of pyknotic and karyorrhectic cellular debris admixed with concretions of mineral, fibrosis, and rare cholesterol clefts. There is no evidence of vascular or lymphatic invasion. There is diffuse compression and variable rarefaction of the adjacent neuropil. Within the normal adjacent section of brain, there are numerous mineralized blood vessels.

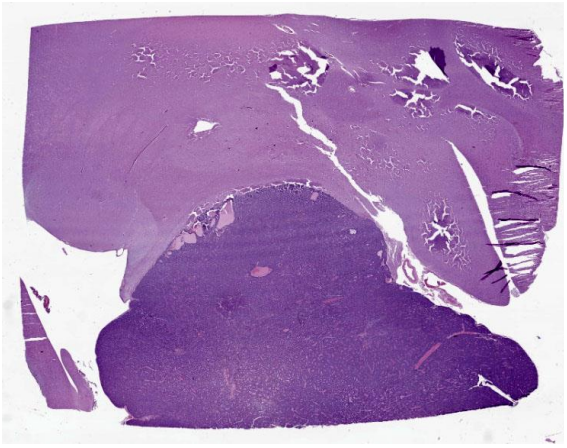

Figure 2-4. Pituitary gland, rhesus macaque. A pituitary neoplasm effaces the normal glandular architecture and compresses the overlying hypothalamic neuropil. (HE, 5X)

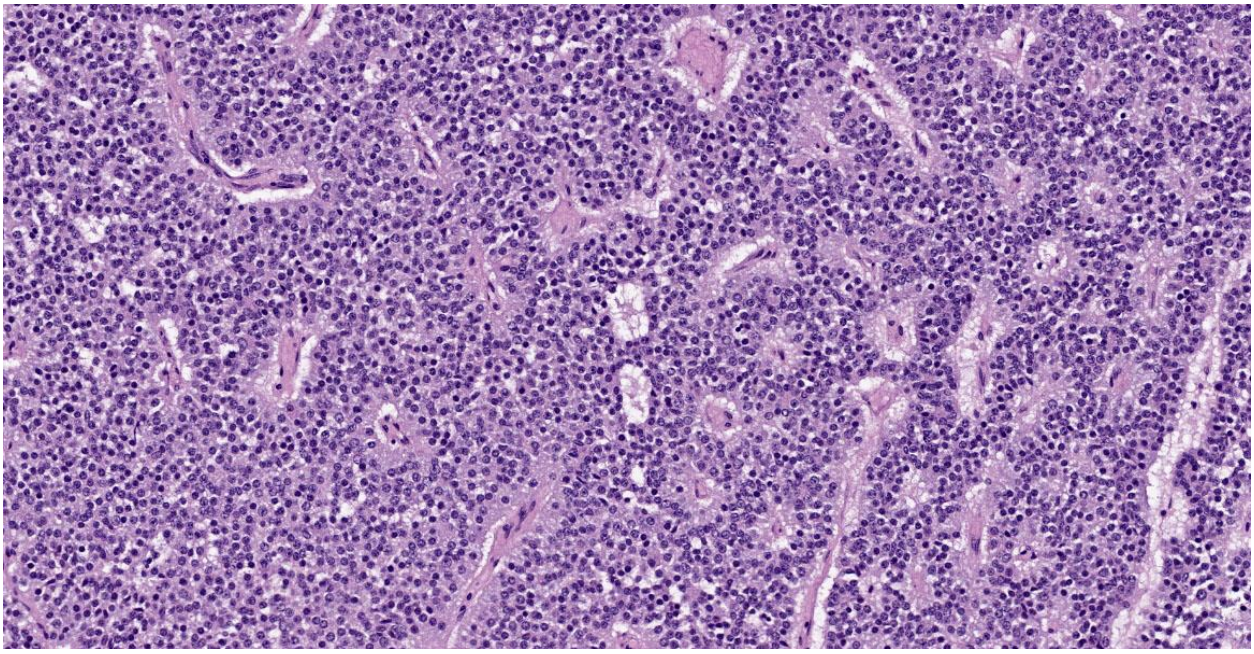

Figure 2-5. Pituitary gland, rhesus macaque. Neoplastic cells are arranged in nests and packets with frequent pseudorosette and rosette formation. (HE, 199X)

Transmission electron microscopy: Neoplastic cells have indistinct borders. Within the cytoplasm are multiple, approximately 100 nm, electron dense, spherical granules. The Golgi apparatus and endoplasmic reticulum are indistinct and often poorly formed.

Contributor's Morphologic Diagnosis:
Cerebrum: Pituitary null-cell adenoma.

Contributor's Comment:
This aged female rhesus macaque presented with progressive weight loss, hyperprolactinemia and galactorrhea without recent pregnancy, and neurologic signs including vision loss and circling. The most significant lesion on necropsy was a large, compressive pituitary adenoma, which is believed to be the main contributing factor for all clinical findings. Immunohistochemistry of the tumor is diffusely negative for hormone production and electron microscopy revealed multiple small, approximately 100 nm granules. Combined, these results highly suggest that this tumor is an endocrinologically inactive (aka, non-functional or null) adenoma.

In veterinary species, non-functional pituitary adenomas occur most commonly in dogs, cats, and parakeets, with the most common type being chromophobe adenomas arising from the pars distalis.[12,13] Reports of pituitary adenomas in non-human primates are scattered, but have been noted in both Old World and New World primates.[4,5,11] The majority of these tumors are described as lactotroph or corticotroph adenomas.[5,11] However, there is one case report of a suspected non-functional adenoma with galactorrhea in a male Rhesus macaque, which describes a similar entity to the present case, both clinically and histologically.[4]

As these tumors are often behaviorally benign, clinical signs of nonfunctional adenomas are typically due to expansion of the tumor into the unaffected pituitary and adjacent CNS, leading to decreased secretion of pituitary hormones and/or CNS dysfunction.[12,13] For instance, progressive weight loss and muscle atrophy occurs due to decreased growth hormone; gonadal atrophy due to decreased gonadotropic hormones;

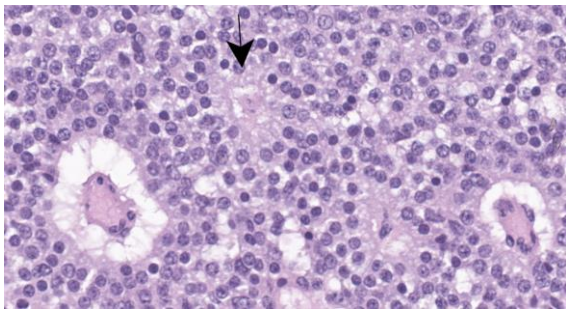

Figure 2-6. Pituitary gland, rhesus macaque. High magnification of neoplastic glands with two pseudorosettes and one rosette (arrow) in this field. (HE, 689X)

and dilute urine with low specific gravity in the face of dehydration due to decreased antidiuretic hormone. Thus, panhypopituitarism caused by endocrinologically inactive pituitary adenomas should be a differential in older animals with incoordination, depression, polyuria, blindness, and sudden behavioral changes. Additionally, as in this case, animals may develop blindness with fixed, dilated pupils due to dorsal extension of the tumor and compression of the optic nerves. Ophthalmic exam is typically otherwise unremarkable because dysfunction is originating from the CNS.

Typical gross lesions of null cell pituitary adenomas can include the following:

- Large tumor (>1cm) with compression or replacement of the remaining adenohypophysis, infundibular stalk, and hypothalamus;
- Small thyroid glands;
- Small adrenal glands due to cortical atrophy;
- Small gonads due to atrophic seminiferous tubules with little active spermatogenesis; and
- Atrophy of skin and muscle.[12,13]

Histopathologic and electron microscopic features characteristic of null cell adenomas in humans are elongated small cells forming pseudorosettes around dilated capillaries; modest cytoplasm; poorly developed rough endoplasmic reticulum and Golgi apparatus; and rare, round, small secretory granules (up to 250 nm).[7,9,10]

Ancillary diagnostics, including immunohistochemistry (IHC) and electron microscopy, are key to diagnosing null cell adenomas. The pituitary gland is made up of at least six different cell types that can give rise to tumors that are clinically functioning or silent. Each of these cell types produce one or more specific hormones that can be targeted via immunohistochemistry (See Table 2).[9,10] Moreover, plurihormonal adenomas can also occur. Furthermore, neuroendocrine tumors from other regions of the body may metastasize to the pituitary and thus can be positive for both synaptophysin and chromogranin; therefore, other markers may be necessary for differentiation.[2]

Electron microscopy can provide important information regarding the intracellular structure and hormonal activity of the cells.[9] The

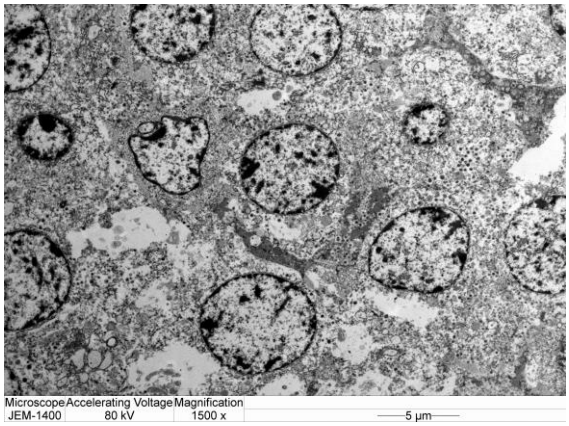

Figure 2-7. Pituitary gland, rhesus macaque. Neoplastic cells have indistinct borders. The Golgi apparatus and endoplasmic reticulum are indistinct. (*Photo courtesy of:* Johns Hopkins University School of Medicine, Department of Molecular and Comparative Pathobiology)

Marker	Tumor Type
GH	Somatotroph adenomas Mammosomatotroph adenomas
PRL	Lactotroph adenomas Lactotroph ademonas with GH reactivity
TSH	Thyrotroph adenomas
ACTH	Corticotroph ademonas
FSH	Gonadotroph adenomas
MSH	Melanotroph adenomas

Table 2. IHC hormone markers for pituitary adenomas.
GH: Growth Hormone; PRL: Prolactin; TSH: Thyroid Stimulating Hormone; ACTH: Adrenocorticotropin Hormone; FSH: Follicle Stimulating Hormone; MSH: Melanocyte Stimulating Hormone

size and number of secretory granules as well as the degree of development of organelles such as rough endoplalsmic reticulum (RER) and Golgi apparatus can help indicate the secretory status of tumor cells.[8,9] In the present case, the poorly-formed RER and Golgi as well as scant, small granules suggest a non-functional secretory status.[8,10]

Interestingly, this animal was galactorrheac with elevated serum prolactin levels despite diffuse negative immunoreactivity for prolactin in the tumor. We propose that hyperprolactinemia in this case is due to "stalk syndrome" or "pituitary stalk compression syndrome," a phenomenon in which non-secretory suprasellar tumors induce hyperprolactinemia by inhibiting dopamine delivery to lactotrophs.[1-3] Since dopamine is a prolactin-inhibiting factor, reduction of dopamine levels leads to increased prolactin output. It is hypothesized that dopamine levels are reduced by one of two mechanisms: 1) physical compression of the dopaminergic neurons of the infundibular stalk or 2) disruption of hypophyseal portal blood flow delivering dopamine to lactotrophs.[3,7] However, increased compression caused by continued growth of the tumor may eventually lead to lactotroph insufficiency and failure.[3]

In humans, the degree of prolactinemia can provide some clues to help differentiate a prolactinoma from a large tumor with "stalk syndrome." Serum prolactinemia over 200 ng/mL in humans is almost always due to a hormone-producing prolactinoma, while less than 200 ng/mL can be associated with stalk effect.[6] In the present case, serum prolactin levels measured at 147.6 ng/ml (expected value 20-50 ng/ml). Unfortunately, normal ranges are less established in rhesus macaques, and the relationship of degree of elevation to tumor type remains unclear.

Contributing Institution:
Johns Hopkins University School of Medicine
Department of Molecular and Comparative Pathobiology
http://www.hopkinsmedicine.org/mcp

JPC Diagnosis:
Pituitary gland: Pituitary adenoma.

JPC Comment:
As noted by the contributor, the pituitary gland is classically described as having six different cell types, each of which can become neoplastic. The clinical and biochemical signatures of pituitary adenomas differ depending on the cell or cells of origin and on whether these cells produce their native hormone products.

Hormone production is rarely an all-or-nothing affair in pituitary tumors, and clinical signs referable to these neoplasms therefore exist on a continuum.[6] In humans, a large number of pituitary adenomas, 22% - 54% depending on the study, present with signs related to the mass effect of the tumor rather than excess hormone secretion; these tumors are referred to as "clinically nonfunctioning pituitary adenomas," or NFPAs.[6] A related term, the "silent pituitary adenoma," or SPA, refers to tumors that express transcription factors or their hormone products at a level detectable by immunohistochemistry, but not at a level detected clinically.[6] A NFPA can be converted to an SPA if a a clinically silent pituitary adenoma nonetheless, on investigation, shows positive IHC immunoreactivity to relevant hormones or transcription factors. In between these lie the "whispering adenomas," characterized by elevated serum hormone levels, but borderline, often overlooked clinical symptoms.[6]

At the extreme end of this secretory spectrum is the rarest pituitary tumor type of them all, the null cell adenoma. Null cell adenoma is a diagnosis of exclusion and requires immunonegativity of all adenohypophyseal hormones and, in humans, a lack of cell lineage-specific transcription factors.[6] The distinction is important in humans as null cell adenomas generally have a more aggressive course and more unfavorable outcomes compared with SPAs, including those who produce no hormones, but still express lineage-specific transcription factors.[6]

Conference discussion of this deceptively complex case began with a review of the anatomy and histology of the pituitary gland and its consistuent parts—the pars distalis, pars intermedia, and pars nervosa—along with an overview of pituitary neoplasia generally. Dr. Miller noted that several pituitary neoplasias have species predilections,

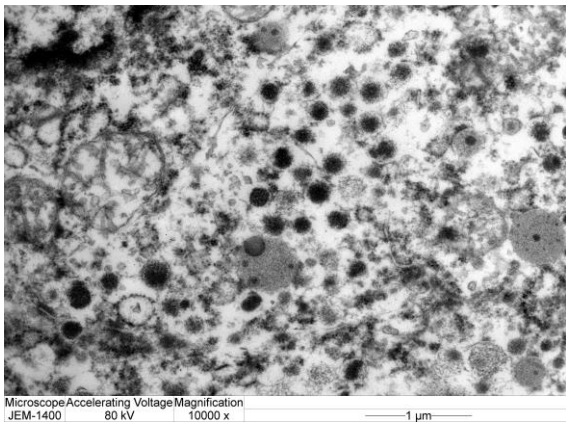

Figure 2-8. Pituitary gland, rhesus macaque. Within the cytoplasm are multiple, approximately 100 nm, electron dense, spherical granules. (*Photo courtesy of:* Johns Hopkins University School of Medicine, Department of Molecular and Comparative Pathobiology)

including corticotroph adenoma/carcinoma (most common in dogs); pars intermedia adenoma (most common in horses and associated with pituitary pars intermedia dysfunction, or PPID); somatotroph adenoma (most common in cats and budgerigars); and lactotroph adenomas (most common in macaques, rats, and rabbits). Particular attention was given to the equine pars intermedia adenoma as its pathogenesis is unique and results from loss of dopaminergic inhibitory innervation from the hypothalamus, leading to unchecked proliferation of the pars intermedia.

With this background knowledge firmly in hand, conference participants moved to the first hurdle: tissue identification. While most conference participants were able to identify the tissue confidently, a significant minority initially identified this tumor as an embryonal tumor such as medulloblastoma. Dr. Miller noted that a firm grasp of neuroanatomy is key to tissue identification in this slide. Evaluation of the adjacent neuroparenchyma contains a haphazard arrangement of scattered neuronal cell bodies that is characteristic of the thalamus. This location, along with the rich vascularization of and the multifocal

aggregates of eosinophilic fluid within the tumor, all suggest pituitary origin.

With the neoplasm localized to the pituitary, Dr. Miller emphasized its well-demarcated, expansile, non-invasive nature, which is apparent on subgross examination. As invasion is the most important histologic feature that differentiates pituitary adenoma from carcinoma, the lack of invasion gives this tumor a fairly classic pituitary adenoma appearance. Finally, Dr. Miller noted the multifocal mineralization in vascular walls throughout the neuroparenchyma in the examined section. This is a common age-related lesion in many animals and, in aged macaques, the thalamus is a common location to find this incidental change.

References:

1. Al-Brahim NYY, Asa SL. My approach to pathology of the pituitary gland. *J Clin Pathol*. 2006;59:1245-1253.
2. Asa SL. Practical pituitary pathology: what does the pathologist need to know? *Arch Path Lab Med*. 2008;132(8):1231-1240.
3. Bergsneider M, et al. The pituitary stalk effect: is it a passing phenomenon? *J Neurooncol*. 2014;117(3):477-84.
4. Chalifoux LV, MacKey JJ, King NW. A sparsely granulated, nonsecreting adenoma of the pars intermedia associated with galactorrhea in a male Rhesus Monkey (Macaca mulatta). *Vet Pathol*. 1983; 20:541-547.
5. Daviau JS, Trupkiewicz JG. Pituitary adenoma with galactorrhea in an adult male Cynomologus Macaque (Macaca fascicularis). *JAALAS*. 2001;40(5):57-59.
6. Drummond J, Roncaroli F, Grossman AB, Korbonits M. Clinical and pathological aspects of silent pituitary adenomas. *J Clin Endocrinol Metab*. 2019;104(7):2473-2489.
7. Dulai M, Vogel H. Pituitary adenomas. In: *Nervous System*. New York, NY: Cambridge University Press; 2009:262-284.
8. Horvath E, Kovacs K. Fine structural cytology of the adenohypophysis in rat and man. *J Electron Microsc Tech*. 1998;8(4): 401-432.
9. Kovacs K, Horvath E, Vidal S. Classification of pituitary adenomas. *J Neurooncol*. 2001;54:121-127.
10. Osamura RY, et al. Pathology of the human pituitary adenomas. *Histochem Cell Biol*. 2008;130:495-507.
11. Remick AK, et al. Histologic and immunohistochemical characterization of spontaneous pituitary adenomas in fourteen Cynomolgus Macaques (Macaca fascicularis). *Vet Pathol*. 2006;43:484-493.
12. Rosol TJ, Grone A. Pituitary gland. In: Maxie MG, ed. *Jubb, Kennedy, and Palmer's Pathology of Domestic Animals*. 6th ed. Volume 3. Elsevier;2016:276-291.
13. Rosol TJ, Meuten DJ. Tumors of the pituitary gland. In: *Tumors in Domestic Animals*. 5th ed. Wiley-Blackwell;2017:768-782.

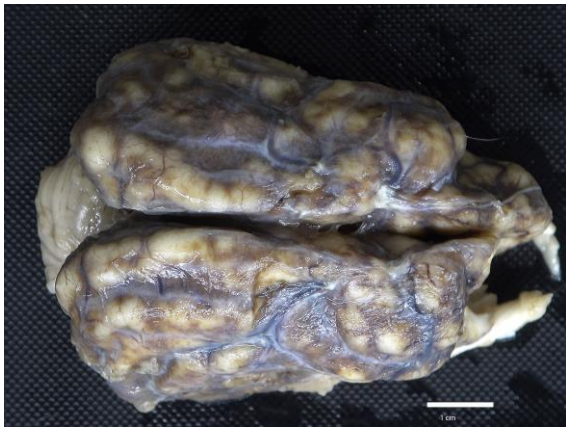

Figure 3-1. Cerebrum, dog. The cerebrum was hardened, lacked distinct sulci, and meninges were diffusely expanded by tan to dark brown exudate. (*Photo courtesy of* Michigan State University Veterinary Diagnostic Laboratory, 4125 Beaumont Rd, Lansing, MI 48910 https://cvm.msu.edu/vdl).

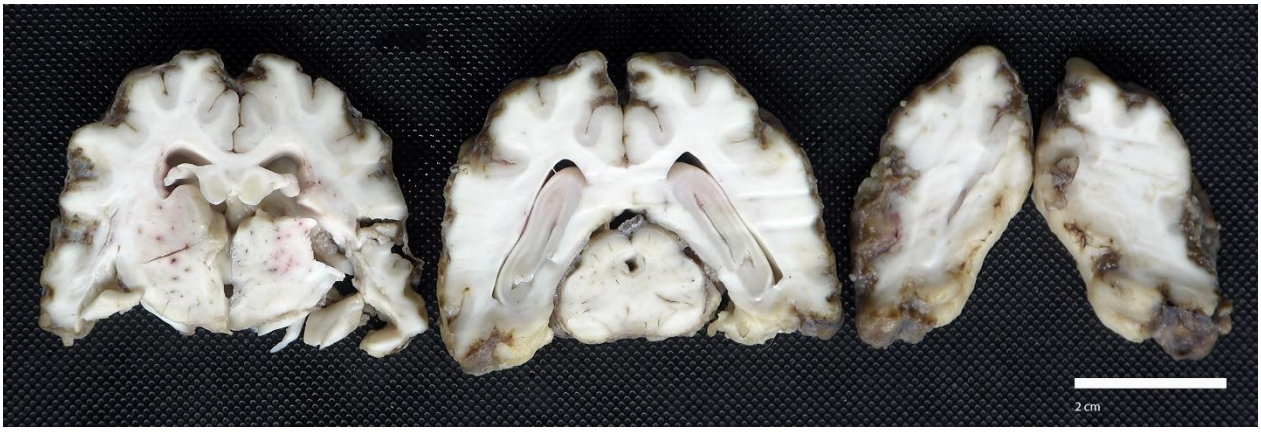

Figure 3-2. Cerebrum, dog. On cut surface, the exudate extended into and replaced the outer layers of the cerebral cortex. (*Photo courtesy of:* Michigan State University Veterinary Diagnostic Laboratory, 4125 Beaumont Rd, Lansing, MI 48910, https://cvm.msu.edu/vdl).

CASE III:

Signalment:
3-year-old, male castrated mixed breed dog (*Canis lupus familiaris*)

History:
This dog initially presented to the submitting veterinarian for significant anxiety and urinating and defecating in the home.

Bloodwork was performed and revealed a marked eosinophilia (4,341 cells/µL, RR: 70-1,490 cells/ µL). Idexx SNAP test was negative for heartworm antigen, *Borrelia burgdorferi*, *Anaplasma* spp., and *Ehrlichia* spp. No additional diagnostics were pursued. At that time, the animal was started on Prozac for generalized anxiety; however, his condition continued to progress, and the owner began noticing additional sensory deficits (sight and smell) and incoordination. Approximately six months later, humane euthanasia was elected due to poor quality of life and increasing aggression toward the owner. The owner was bitten by the dog, resulting in rabies testing and a full necropsy.

Gross Pathology:
The cerebrum was semi-firm, lacked distinct sulci, and meninges were diffusely expanded by tan to dark brown exudate. On cut surface, the exudate extended into and replaced the outer layers of the cerebral cortex.

Laboratory Results:
Direct fluorescent antibody for rabies virus, brain: Negative
Neospora caninum PCR, brain: Not detected
Toxoplasma gondii PCR, brain: Not detected
Qualitative fecal analysis: Negative

Microscopic Description:
Brain: Meninges were markedly expanded by numerous eosinophils, hemosiderin-laden macrophages, fewer plasma cells, and rare multinucleated giant cells. This infiltrate extended into the cerebral gray matter and surrounded large regions of necrosis and rarefaction. The adjacent white matter contained low numbers of scattered spheroids and Virchow-Robin spaces were expanded by low numbers of lymphocytes and plasma cells. No infectious agents, infarction, or neoplastic cells were observed on hematoxylin and eosin, periodic acid-Schiff reaction, or Gram-stained sections.

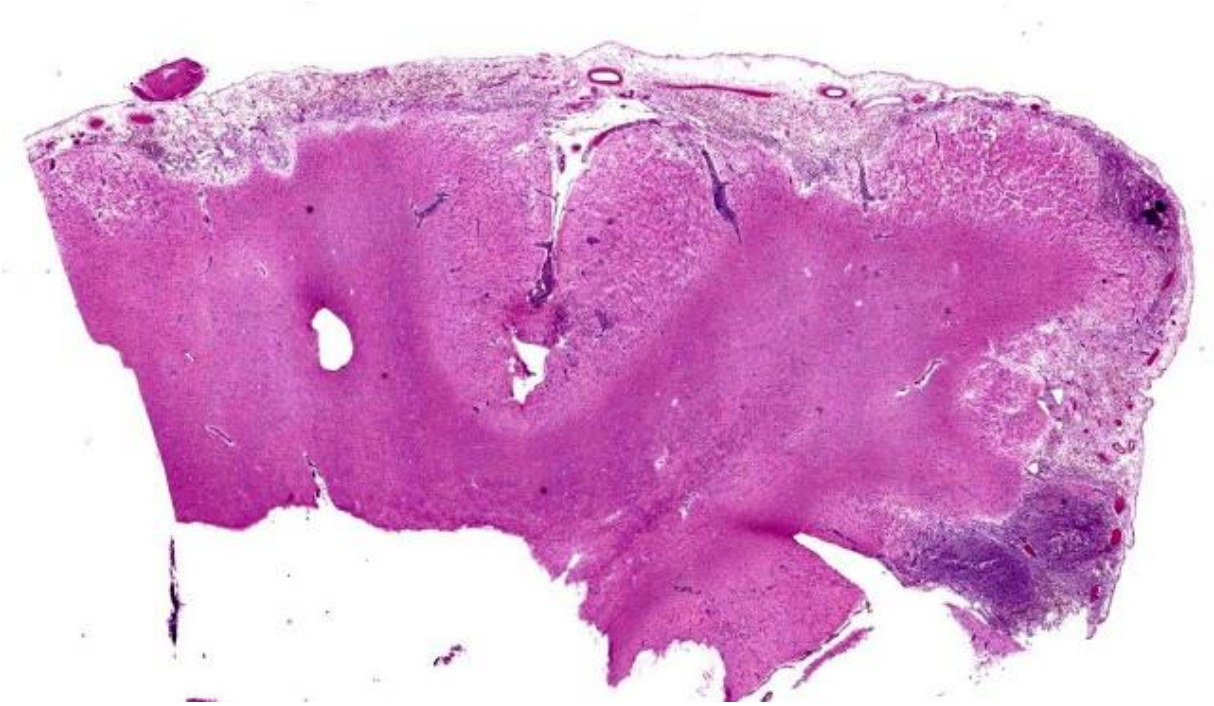

Figure 3-3. Cerebrum, dog. There is marked expansion, hypercellularity, and edema of the meninges with a loss of demarcation with the underlying submeningeal neuropil. (HE, 9X)

Contributor's Morphologic Diagnosis:
Brain: Severe, chronic, diffuse, eosinophilic and granulomatous to necrotizing meningoencephalitis with perivascular cuffing.

Contributor's Comment:
This case is consistent with eosinophilic meningoencephalitis (EME), which is an uncommon to rare neurologic disease in humans and animals.[2,3,8,12] In humans, EME is often associated with parasitic infections (such as *Angiostrongylus cantonensis*, *Gnanthostoma spinigerum*, cysticercosis (*Taenia* spp.), schistosomiasis, paragonimiasis, fascioliasis, and *Toxocara canis*) and occasionally tuberculosis, syphilis, coccidiodomycosis, and meningeal lymphoma.[8,9,12]

In veterinary medicine, EME is most often reported in dogs and has been associated with the following etiologies: *Toxoplasma gondii*, *Neospora caninum*, *Cryptococcus* spp., *Prototheca* spp., canine distemper virus, rabies virus, bacterial encephalitis, and aberrant migration of parasites (including *Angiostrongylus* spp. and *Cuterebra* spp).[3,6,8,9,12,13] Other non-infectious causes of EME include infarction, trauma, or neoplasia.[8,12] Additionally, if an underlying disease process cannot be identified, it is classified as idiopathic EME.[3,12] Within the literature, idiopathic EME is predominantly noted in dogs, but has rarely been reported in cats, cattle, and sheep.[2,3,6-13] Clinically, these dogs often present with mentation or behavioral changes, seizures, ataxia, blindness, and pain.[3,6,8-10,12,13] On a routine diagnostic work-up, the only major abnormality may be peripheral eosinophilia, as seen in this case. Only about half of these cases have peripheral eosinophilia; therefore, cerebrospinal fluid analysis is considered more sensitive.[3,12,13] On MRI, these cases have variable findings but often have bilateral, symmetrical lesions limited to the cerebral cortex that are associated with diffuse meningeal contrast uptake.[3,13] In the reported

case, neither CSF evaluation nor MRI was performed.

On postmortem examination, the meninges are often reported to appear thickened and green.[12] However, this was not observed in our case, likely due to the abundant amount of hemosiderin within the macrophages. Microscopically, the leptomeninges of the brain and spinal cord in cases of EME are frequently infiltrated by eosinophils, macrophages, and other mononuclear cells, and there is a variable amount of parenchymal loss, degeneration, and necrosis within the underlying cortical grey matter with multifocal regions of perivascular cuffing.[8-10,12]

The CNS, particularly neurons and myelinated axons, are highly susceptible to eosinophilic-induced neurotoxicity.[8,12] Eosinophils are often activated in association with chronic inflammatory conditions (asthma, chronic allergen, etc.) by helper T (Th2) cells releasing IL-4, IL-5, IL-3, and granulocyte-macrophage colony-stimulating factor (GM-CSF).[5,6,8,12] Once activated, eosinophils release major basic protein, eosinophil cationic protein, eosinophil peroxidase, and oxygen free radicals which aid in killing parasites.[2,5,6,10,12] However, they are also neurotoxic and can cause severe tissue damage within the CNS.[12] In the reported case, the absence of overt infectious agents, parasites, infarction, trauma, or neoplasia, combined with the ancillary testing, make a diagnosis of idiopathic EME most likely.

The exact pathogenesis of idiopathic EME is unknown. Idiopathic EME is reported more often in young to middle-aged, large breed dogs.[2,8,10,12,13] Additionally, rottweilers and golden retrievers appear to be over-represented in the population of reported cases, suggesting a possible breed predisposition.[2,6,9,10,12,13]

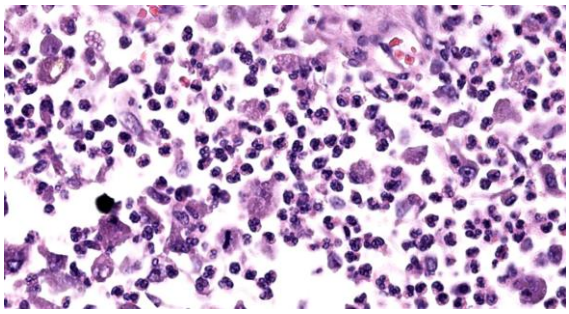

Figure 3-4. Cerebrum, dog. The meninges are infiltrated by large numbers of eosinophils, debris-laden macrophages and fewer lympho-cytes and plasma cells. (HE, 736X)

Many of the reported cases of idiopathic EME had minor to drastic improvement in the patient's condition when treated with corticosteroids, which has led to the hypothesis that there is an underlying immune-mediated or hypersensitivity process.[2,3,6-9,12] It is important to note that this improvement could be due to the normal pathophysiological interactions of steroids in the body rather than treating a specific underlying disease process, as steroids can induce eosinophil apoptosis and reduce the number within the blood.[5] Mayhew IG, et al. discussed a case of EME in a dog with suspected underlying hypersensitivity or drug-induced (firocoxib) reaction.[7] Additional cases with extensive clinical and pathological evaluation are necessary to further understand the underlying etiology and prognosis of idiopathic EME.

Contributing Institution:
Michigan State University
Veterinary Diagnostic Laboratory
4125 Beaumont Rd, Lansing, MI 48910
https://cvm.msu.edu/vdl

JPC Diagnosis:
Cerebrum: Meningoencephalitis, eosinophilic, superficial, marked, with cortical necrosis.

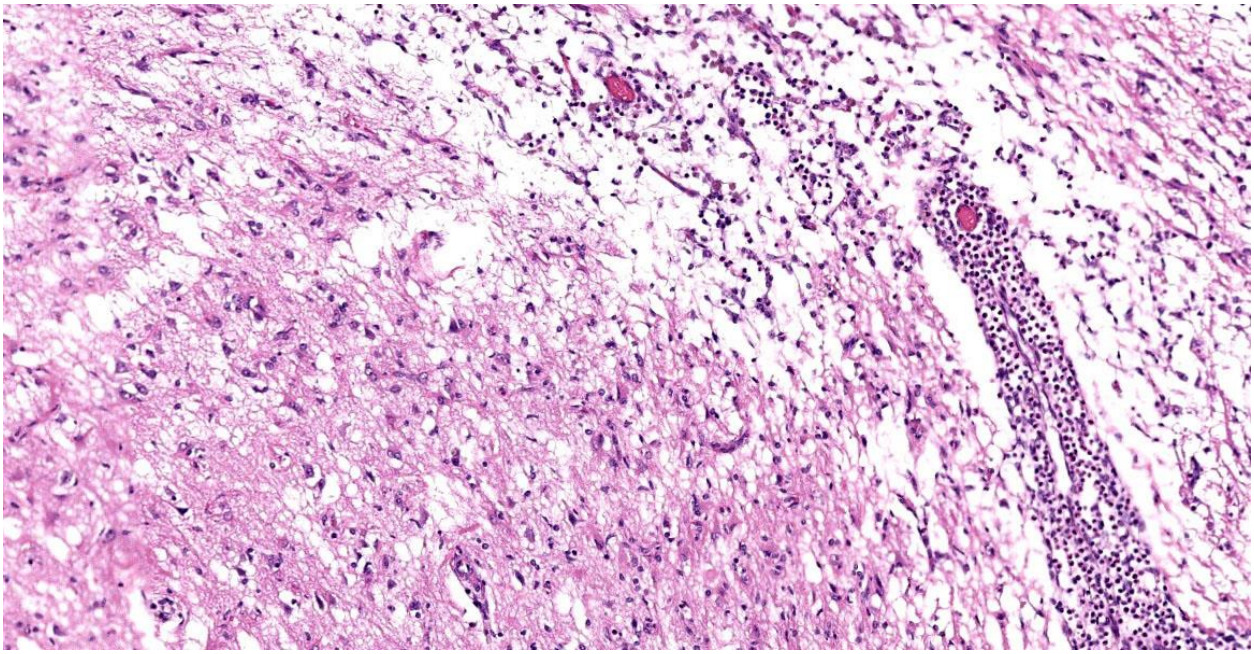

Figure 3-5. Cerebrum, dog. There is marked rarefaction of the neuropil of the submeningeal cortex and expansion of Virchow Robin spaces by numerous inflammatory cells. (HE, 149X)

JPC Comment:

Dogs play host to a wide range of diseases, including EME, for which the contributor provides an excellent summary, that are characterized histologically by the accumulation of eosinophils. Canine eosinophilic pulmonary granulomatosis and eosinophilic bronchopneumopathy were discussed earlier this conference year, and insights on these conditions can be found in WSC #9, case 2. Other canine eosinophilic diseases include eosinophilic granuloma; eosinophilic furunculosis; eosinophilic esophagitis, gastritis, and gastroenteritis; eosinophilic cystitis; and hypereosinophilic syndrome.

Canine eosinophilic granuloma is an uncommon skin disease that frequently presents as papules, nodules, or plaques, most frequently in the oral cavity.[4] Canine eosinophilic granuloma is attributed to hypersensitivity reactions to insect bites or environmental and food allergens, though some bacterial and fungal agents have been implicated.[4] There is a pronounced breed predilection in Siberian husky dogs and Cavalier King Charles Spaniels, suggesting a genetic basis in at least some cases.[4]

Eosinophilic gastrointestinal disease (EGID) is an umbrella terms encompassing a spectrum of disorders characterized by eosinophilic inflammation in one or more sites such as the esophagus, stomach, intestine, and colon.[1] Diagnosis of EGID requires abnormal numbers and distributions of eosinophils in the gastrointestinal tract in the absence of other underlying etiologies such as parasitism.[1] Some studies have noted that the number of identifiable eosinophils in tissue section is likely an undercount, as degranulated eosinophils are easily overlooked or confused with other granulocytes. Immunohistochemical staining for eosinophil peroxidase, which highlights both viable and degranulated eosinophils, have revealed a four to 40-fold increase in eosinophil number over H&E evaluation alone, depending on the examined tissue.[1] As in the

rest of the eosinophilic entities, EGID is thought to be a Th-2 driven hypersensitivity reaction likely, in the case of EGID, due to food allergens.[1]

The moderator began discussion with a broad overview of possible causes for eosinophilic encephalitis and meningoencephalitis, including parasitic involvement, protozoal infection, hypersensitivity reactions, and the breed specific presentations noted by the contributor. Dr. Miller noted the striking subgross histologic appearance of this slide, with the eosinophil-induced neuroparenchymal necrosis giving the cerebral profile an unusual, scalloped appearance. Dr. Miller noted that the tissue loss focally extends into the white matter in the examined section and, as such, the term neuropil, which refers exclusively to gray matter, would be an inappropriate descriptor here; neuroparenchyma, encompassing both gray and white matter, would be the correct term to refer to the extent of the tissue loss.

The neuroparenchymal loss and eosinophilic inflammation present in section are both more extensive than typically seen with EME and more closely resemble lesions associated with parasitism. Dr. Miller noted that *Cuterebra* larval migration, relatively common in cats and occasionally occurring in dogs, has a very similar histologic presentation. Neuroparenchymal loss caused by *Cuterebra* is due to an exotoxin secreted by the larvae that leads to necrosis of adjacent neuroparenchyma. The lesion is both necrotizing and eosinophil-rich, often with concurrent vasculitis, and larvae are frequently not identified in histologic section. Dr. Miller provided examples of the gross and histologic appearance of feline ischemic encaphlopathy caused by *Cutererba* larval migration and reminded participants to keep this differential in mind when presented with this histologic picture.

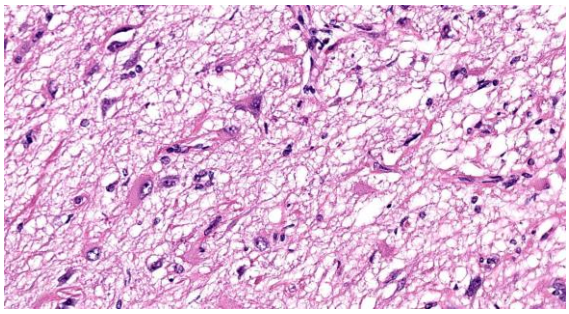

Figure 3-6. Cerebrum, dog. There are numerous gemistocytic astrocytes within rarefied areas of neuropil. (HE, 381X)

Consideration of the morphologic diagnosis for this case sparked robust discussion. Participants noted the numerous histiocytes within the examined section and considered whether to include "granulomatous" or "histiocytic" to characterize the inflammation. Participants decided to omit the histiocytic component as the pathogenesis here is likely eosinophil-driven, with histiocytes called in secondarily to repair the damage. Participants also struggled to capture the extent and distribution of the striking lesions. After much discussion, participants felt that "superficial" best conveyed the location of the inflammation within the meninges and in the outermost portion of the cortex. A few participants doggedly argued for the term "cortical loss" to capture the unique appearance of the cerebral contour; however, as the loss was caused by necrosis, participants felt that "cortical necrosis," while perhaps not as punchy, was most appropriate.

References:

1. Bastan I, Rendahl AK, Seelig D, et al. Assessment of eosinophils in gastrointestinal inflammatory disease in dogs. *J Vet Intern Med*.
2. Bennett PF, Allan FJ, Guilford WG, et al. Idiopathic eosinophilic meningoencephalitis in Rottweiler dogs: three cases (1992-1997). *Aust Vet J*. 1997;75:786-789.

3. Cardy TJA, Cornelis I. Clinical presentation and magnetic resonance imagining findings in 11 dogs with eosinophilic meningoencephalitis of unknown aetiology. *J Small Anim Pract*. 2018;59(7):422-431.
4. Knight EV, Shipstone MA. Canine eosinophilic granuloma of the digits treated with prednisolone and chlorambucil. *Vet Dermatol*. 2016;27(5):446-e119.
5. Kumar V, Abbas AK, Aster JC. *Robbins & Cotran Pathologic Basis of Disease*. 10th ed. Elsevier;2020.
6. Lillihook I, Gunnarsson L, Zakrisson G, Tvedten H. Disease associated with pronounced eosinophilia: a study of 105 dogs in Sweden. *J Small Anim Pract*. 2000; 41:248-253.
7. Mayhew IG, Hill KE, Ahn Y, Jones BR. Can drug-induced aseptic meningitis account for some cases of eosinophilic meningitis/meningoencephalitis in dogs? *N Z Vet J*. 2022;70(3):184-185.
8. Olivier AK, Parkes JD, Flaherty HA, Kline KL, Haynes JS. Idiopathic eosinophilic meningoencephalomyelitis in a Rottweiler dog. *J Vet Diagn Invest*. 2010; 22(4):646-648.
9. Smith-Maxie LL, Parent JP, Rand J, et al. Cerebrospinal fluid analysis and clinical outcome of eight dogs with eosinophilic meningoencephalomyelitis. *J Vet Intern Med*. 1989;3:167-174.
10. Sykes JE, Weiss DJ, Buoen LC, et al. Idiopathic hypereosinophilic syndrome in 3 Rottweilers. *J Vet Intern Med*. 2001;15: 162-166.
11. Vidana B, Floyd T, Brena C, et al. First case of idiopathic eosinophilic meningoencephalitis in a sheep. *J Comp Pathol*. 2020;174:58-62
12. Williams JH, Koster LS, Naidoo V, et al. Review of idiopathic eosinophilic meningitis in dogs and cats, with a detailed description of two recent cases in dogs. *J S Afr Vet Assoc*. 2008;79(4):194-204.
13. Windsor RC, Sturges BK, Veranu KM, Vernau W. Cerebrospinal fluid eosinophilia in dogs. *J Vet Intern Med*. 2009;23: 275-281.

CASE IV:

Signalment:
5-month-old, intact male Siberian Husky (*Canis lupis familiaris)*

History:
The dog had a history of progressive tetraparesis. Magnetic resonance imaging demonstrated bilaterally symmetric white matter hyperintensities in the corpus callosum, cerebrum, and thalamus. An analysis of the cerebrospinal fluid was normal. Given the breed and signalment, GM1 gangliosidosis was suspected and the dog was euthanized.

Gross Pathology:
There was subtle flattening of the cervical spinal cord.

Laboratory Results:
DNA testing did not identify the gene mutation associated with GM1 gangliosidosis in Huskies.

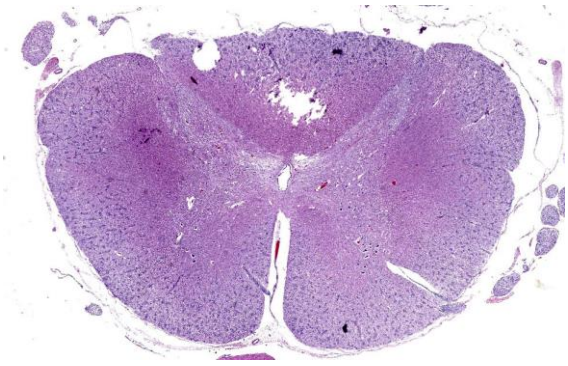

Figure 4-1. Spinal cord, dog. There is diffuse pallor of all funiculi. (HE, 15X)

Microscopic Description:
Cervical spinal cord: Within the white matter are aggregates of large round to polygonal cells with finely granular, lightly basophilic cytoplasm and eccentric nuclei (globoid cells). These cells occasionally surround blood vessels. The globoid cells contain faintly magenta material with a periodic acid-Schiff stain. There is marked loss of myelin and axons highlighted by Luxol fast blue and Sevier-Munger stains, respectively. The white matter in other portions of the brain and spinal cord were similarly affected.

Contributor's Morphologic Diagnosis:
Marked widespread axonal degeneration with marked histiocytosis.

Contributor's Comment:
The clinical signs, gross, and microscopic findings are attributed to axonal degeneration in the brain and spinal cord as a result of globoid cell leukodystrophy. Globoid cell leukodystrophy occurs due to deficient activity of the lysosomal enzyme galactocerebrosidase. Globoid cell leukodystrophy is a genetic condition reported in many pure breed dogs (Cairn Terriers, West Highland White Terriers, Miniature Poodles, Bluetick Hounds, Basset Hounds, Beagles, Irish Setters and the Australian Kelpie).[1] It has not been reported in Siberian Huskies. Additionally, sheep, cats and primates may be affected.[3]

The pathophysiology of globoid cell leukodystrophy is complicated and not fully understood. Galactocerebrosidase normally breaks down galactocerebroside and galactosylsphingosine (psychosine).[1] Interestingly, at the time of diagnosis, many individuals have decreased amounts of galactocerebroside; this paradox may reflect the decreased amounts of myelin remaining late in the disease course.[2] There is, however, accumulation of psychosine in the oligodendroglia and

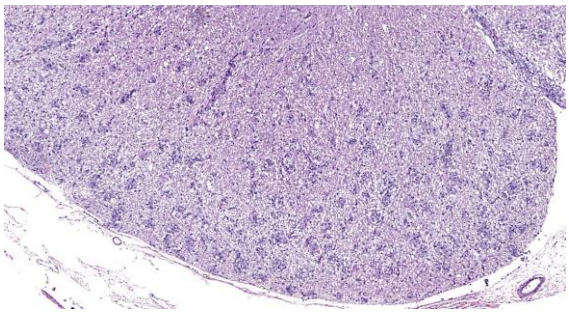

Figure 4-2. Spinal cord, dog. Diffusely, myelin sheaths are dilated. Blood vessels are outlined by a cellular infiltrate. (HE, 16X)

Schwann cells. The psychosine is extremely toxic to these cells and results in their death. The loss of oligodendroglial cells and Schwann cells results in decreased myelination of axons and ultimately, axonal degeneration. Macrophages attempt to clear remaining myelin and galactocerebrosides, but without the enzyme they are also unable to break down galactocerebrosides. As a result, the macrophages become swollen with PAS-positive debris and are termed "globoid cells."[1] The globoid cells often accumulate around blood vessels, as in this case. Although a biopsy of peripheral nerves can be useful to make an antemortem diagnosis, in this case, the sciatic nerve was not clearly affected.[1]

Contributing Institution:
University of Tennessee
College of Veterinary Medicine
Department of Biomedical and Diagnostic Sciences
http://www.vet.utk.edu/departments/path/index.php

JPC Diagnosis:
Spinal cord, white matter: Histiocytosis, perivascular, diffuse, marked, with abundant intracellular myelin.

JPC Comment:
Globoid cell leukodystrophy (GLD), also known as Krabbe disease, is an autosomal

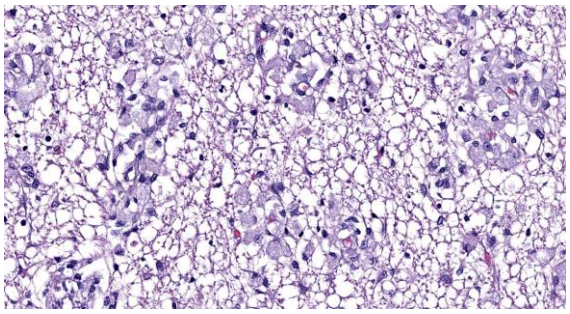

Figure 4-3. Spinal cord, dog. The rarefied white matter is infiltrated by large amphophilic macrophages with abundant vacuolated cytoplasm (Gitter cells or "globoid cells"). (HE, 381X)

recessive, fatal lysosomal storage disease caused by mutations in galactoceramide beta-galactosidase (also known as galactosylceramidase, galactocerebrosidase, or GALC). GLD develops early in life and, as noted by the contributor, is characterized by impaired aberrant myelin metabolism and the subsequent accumulation of galactosylceramide (GalCer) and psychosine, the major substrates of GALC.[3]

Compared with normal cellular membranes, myelin has a very high lipid content and is enriched in GalCer.[2] Myelin is remarkably stable, but is contininously remodeled at a basal rate and at a faster rate in response to injury or disease. The complex myelin degradation process relies on a number of enzymes, including GALC, to break down its consitutent parts, including GalCer.[2] GALC is expressed ubiquitously in the lysosomes of all cell types in the nervous system, and is particularly enriched in oligodendrocytes.[2] In health, once GalCer is processed in the lysosome, its consitutent molecular parts are recycled and become building blocks in the constitutively active myelin remodeling/remyelination pathway.[3]

In GLD, mutations diminish GALC enzyme activity, resulting in impaired degradation of GalCer during myelin remodeling. The resulting lack of sufficient building blocks for remyelination leads to myelin loss.[3] Concurrently, toxic pysochosine, normally produced by oligodendrocytes and also degraded by GALC, begins to accumulate, leading to extensive oligodendrocyte degeneration and death with consequent degeneration of existing myelin and impairment of remyelination.[1]

As the contributor notes, macrophages arrive to clean up the degenerating myelin, but they are also GALC-deficient and cannot metabolize GalCer. The accumulation of the undigested substrate leads to the "globoid cells" for which the condition is named.[1]

The globoid cells appear in perivascular cuffs in the white matter of the CNS, in the leptomeninges, and in the endoneurium of peripheral nerves.[1]

This case is an excellent example of the pathognomonic histology of GLD, characterized by marked myelin loss, markedly reduced numbers of oligodendrocytes, and, most dramatically, the infiltration of numerous large, round macrophages filled with PAS-positive storage material, most abundant in areas of

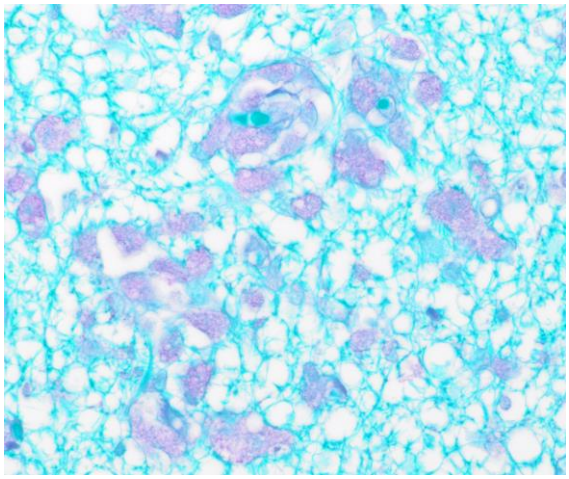

Figure 4-4. Spinal cord, dog. Globoid cells contain PAS-positive material within their cytoplasm. (PAS, 400X)

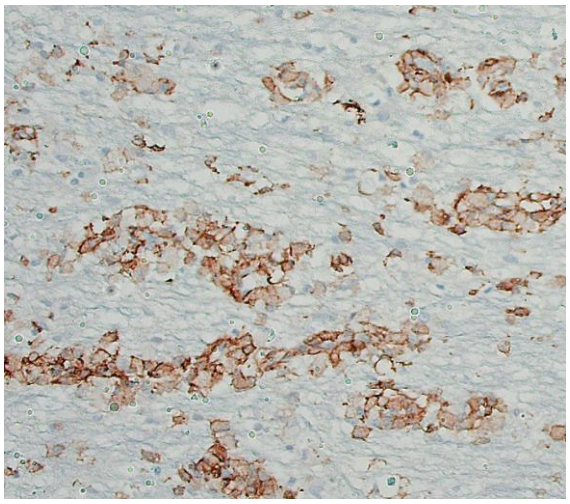

Figure 4-5. Spinal cord, dog. Globoid cells are strongly positive for IBA-1. (HE, 395X)

active demyelination.[3] The presenting clinical signs in this case–ataxia and limb weakness and tremors that progress to paralysis and muscular atrophy–are also typical.[4] Some animals may also develop blindness. Typical gross lesions include slight gray discolorations of the white matter, particularly in the centrum semiovale of the cerebrum and in the spinal cord.[4]

Conference participants enjoyed the photogenic and straightforward nature of this case. Dr. Miller cautioned residents not to overinterpte the gray matter vacuolation present in some sections of the spinal cord since, as in so many neuroparenchymal lesions, this likely represents autolysis artifact. Dr. Miller discussed leukodystrophies in general, noting that the various diseases have in common a failure of myelinating cells to maintain their myelin sheaths. Such diseases are typically early onset, symmetrical, and typically unaccompanied by significant inflammation.

Dr. Miller briefly reviewed the biology and function of the lysosome as well as sphingolipid metabolism and the diseases that result from associated enzyme deficiencies. Dr. Miller discussed the histochemical staining characteristics of globoid cells and noted that IBA1, an immunohistochemical stain for macrophages; PAS, which stains the material accumulated in globoid cells; and Olig2, an immunohistochemical stain for oligodendrocytes, can be used in concert to demonstrate that the accumulation in GLD is occurring in within histiocytes and not oligodendrocytes.

References:

1. Cantile C and Youssef S. Chapter 4: Nervous System. In: Maxie MG ed. *Jubb, Kennedy and Palmer's Pathology of Domestic Animals*. 6th ed. vol. 1. Elsevier; 2016.
2. Feltri ML, Weeinstock NI, Favret J, Dhimal N, Wrabetz L, Shin D. Mechanisms of demyelination and neurodegeneration in globoid cell leukodystrophy. *Glia.* 2021. 69:2309-2331.
3. Lee E, Fuller M, Carr M, Manavis J, Finnie J. Globoid cell leukodystrophy (Krabbe's disease) in a Merino sheep. *J Vet Diagn Invest.* 2019;31:118-121.
4. Miller AD, Porter BF. Nervous System. In: Zachary JF, ed. *Pathologic Basis of Veterinary Disease*. 7th ed. Elsevier; 2022:945-946.

WSC 2023-2024
Conference 17 Self-Assessment

1. Which of the following cell types in a ganglioneuroblastoma will demonstrate immunopositivity for synaptophysin?
    a. Ganglion cells
    b. Neuroblasts
    c. Schwann cells
    d. None of these

2. Which of the following species of is NOT a characteristic of a null cell pituitary adenoma?
    a. Small thyroid glands
    b. Adrenocortical atrophy
    c. Atrophic seminiferous tubules
    d. Skeletal muscle hypertrophy

3. True or false? Null cell pituitary adenomas are usually non-functional.
    a. True
    b. False

4. In which of the following species is idiopathic eosinophilic meningoencephalitis most commonly seen?

    a. Dogs
    b. Cats
    c. Sheep
    d. Cattle

5. Which of the following clinical signs has not been described in dogs with hepatic microvascular dysplasia?
    a. Hepatoencephalopathy
    b. Pulmonary mineralization
    c. Ammonium biurate crystalluria
    d. Diminished growth

Joint Pathology Center
Veterinary Pathology Services

WEDNESDAY SLIDE CONFERENCE 2023-2024

Conference #18 **31 January 2024**

CASE I:

Signalment:
Adult female American bison (*Bison bison*)

History:
Owner reports weight loss and sporadic loss of animals of all ages for the past year.

Gross Pathology:
The pleural surface is covered in a thick mat of fibrin. On cut section, there are multifocal 0.1-1.0 cm diameter abscesses containing caseonecrotic exudate.

Laboratory Results:
Aerobic culture: No growth.
PCR for BHV-1, BRSV, BVDV, PI3: Undetected.
PCR for *Histophilus somni*: Undetected.
PCR for *Mycoplasma bovis*: Undetected.

Microscopic Description:
Throughout the section there is multifocal to coalescing necrosis affecting >50% of the lung tissue. Necrotic foci efface bronchioles and are characterized by a hypereosinophilic core surrounded by a peripheral rim of degenerate neutrophils admixed with pyknotic to karyorrhectic debris. There is central mineralization in some necrotic foci. In the adjacent alveoli, there is frequent necrosis of septa with abundant hyalinized material and/or flooding of remnant alveolar spaces by edema, fibrin, hemorrhage, and many

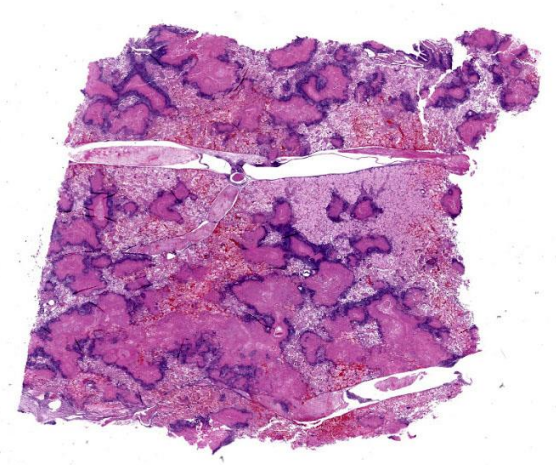

Figure 1-1. Lung, bison. At subgross magnification, there are well-delineated areas of lytic necrosis which correspond to airways. (HE, 5X)

foamy macrophages. Large bronchi have mildly hyperplastic epithelium. Some vessels are occluded by hyalinized fibrin thrombi.

Immunohistochemistry: There is positive immunoreactivity for *Mycoplasma bovis* in the previously described lesions, particularly at the edges of necrotic foci. The lung is diffusely negative for *Histophilus somni* immunoreactivity.

Special stains: No organisms were detected with acid-fast and modified acid-fast stains.

Contributor's Morphologic Diagnosis:
Bronchopneumonia, severe, diffuse, subacute to chronic, necrosuppurative, with caseonecrotic abscesses and fibrinous pleuritis.

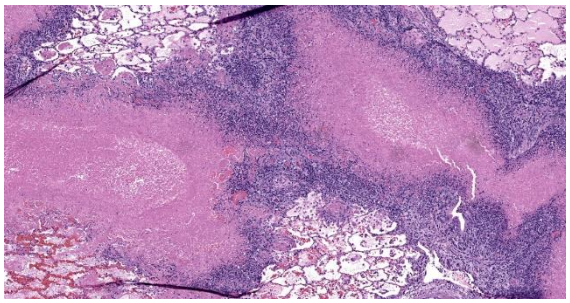

Figure 1-2. Lung, bison. Airway outlines are visible within areas of lytic necrosis. All layers of the airway walls are replaced by cellular debris and neutrophils and bounded by epithelioid macrophages. (HE, 61X)

Contributor's Comment:
Mycoplasma is a genus of ubiquitous bacteria that consists of over 100 described species. The organisms are anaerobic, self-replicating, and lack a cell wall. Tissue tropism and host specificity vary between Mycoplasma species, and the manner in which infection leads to disease is not well understood.

Mycoplasma bovis is a globally distributed, economically important bacterial pathogen that contributes to the bovine respiratory disease complex.[4] In addition to pneumonia, *M. bovis* can cause mastitis, polyarthritis, otitis media, keratoconjuncitivitis, and reproductive losses in cattle.[11] Historically, *M. bovis* was rarely detected in other species. In the early 2000's, however, *M. bovis* was documented as the cause of several high morbidity and mortality disease outbreaks in American bison.[19] The emergence of mycoplasmosis in bison has resulted in devastating economic loss to the commercial bison industry and continues to threaten bison production operations throughout North America.[1,5,6,9,18]
Since the initial emergence, numerous clinical manifestations of mycoplasmosis have been dscribed in bison. These include pneumonia, necrotic pharyngitis, polyarthritis, reproductive disorders, and systemic disease.[5,6,9,18] In contrast to cattle in which co-infecting pathogens are common, there is evidence that *M. bovis* acts as a primary pathogen in bison with increased virulence and higher case fatality rates.[9,11,15,19]

Control of *M. bovis* has been challenging.[3] Efforts to protect bison via autogenous vaccines have been met with difficulty due to the remarkable evolutionary capacity of the bacterium.[1,8,12] Treatment is limited due to the absence of a cell wall and associated resistance to many commonly used antibiotics.[4,11] Further, a recent study documented that approximately 3% of bison are asymptomatic carriers of *M. bovis*.[14] Chronic carriers can be difficult to identify and detect, complicating herd assessment and management strategies.[16,17]

Recently, *M. bovis* was detected as the cause of a high mortality outbreak in free-ranging pronghorn (*Antilocapra americana*) in Wyoming.[10] Mule deer and white-tailed deer are also susceptible to *M. bovis*, meriting concern for impacts to wildlife, including non-commercial bison.[7,13]

Contributing Institution:
University of Wyoming
Wyoming State Veterinary Laboratory
Department of Veterinary Sciences
https://www.uwyo.edu/vetsci/

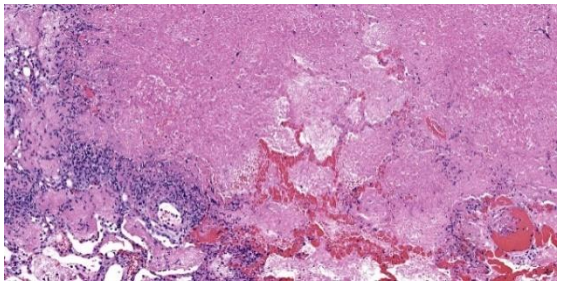

Figure 1-3. Lung, bison. Necrosis extends into the adjacent alveolar parenchyma resulting in septal necrosis and abundant hemorrhage and polymerized fibrin. (HE, 61X)

JPC Diagnosis:
Lung: Bronchopneumonia, necrotizing and fibrinosuppurative, diffuse, severe, with fibrinous pleuritis and bronchiectasis.

JPC Comment:
The rugged American bison is emblematic of the untamed American West and, as of 2016, serves as the national mammal of the United States. Once hunted to near extinction, decades of conservation efforts have restored buffalo numbers to healthy levels in the Western United States and Canada. The emergence of *Mycoplasma bovis* in American bison herds in the last few decades has therefore been met with alarm, particularly due to the severity of disease in this species compared to cattle, and, as the contributor notes, the lack of effective vaccines against or treatments for this wily bacterium.

Despite being a well-documented member of the bovine respiratory disease complex, the molecular mechanisms that underly the virulence and pathogenicity of *M. bovis* remain incompletely understood.[2] A key contributor to the bacterium's host immune system evasion is a fairly complex system of antigenic variation. This variation is accomplished via several prominent, interchangeable transmembrane proteins that act as major immunogens and are switched out when effective host antibodies are encountered.[2] These proteins belong to a family of 13 variable membrane surface lipoproteins (Vsps), encoded by 13 corresponding genes, only two of which are expressed at any one time.[2] These Vsps can be expressed in different combinations, and their co-expression creates "*M. bovis* surface mosaics" that each have different antigenic properties.[2] Additional antigenic variability can be introduced through insertions and deletions in sequence repeats within these genes, resulting in the production of differently sized protein variants, presumably with different antigenic properties, from a

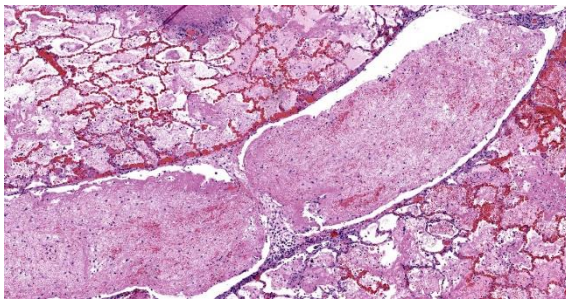

Figure 1-4. Lung, bison. Interlobular lymphatics contain large fibrin thrombi. (HE, 61X)

limited number of Vsp genes. Variation in Vsp expression and size has been demonstrated among individual bacterial subpopulations in affected animals, and this subpopulation diversity thwarts the host's immune system and contributes to the chronic, intractable nature of disease caused by *M. bovis*.[2]

M. bovis, like all mycoplasma species, is a streamlined organism with a small genome, no cell wall, and a lifestyle that depends heavily on host cells for life-sustaining nutrients and cellular processes. This co-dependence requires close association between the bacterium and host cells; however, little is definitively known about how *M. bovis* adheres to and survives inside host cells. The previously discussed Vsps are thought to also facilitate host cell adhesion, though the variability in surface antigens, so useful in immune system evasion, can lead to more or less successful adhesion depending on the efficacy of the expressed bacterial ligands.[2] A bacterial subpopulation's particular Vsp complement can also enhance or degrade its ability to form biofilms, likely a critical component of bacterial persisteance. *M. bovis* is also able to survive intracellulary within phagosomes and to modulate host immune responses by inducing apoptosis of host T lymphocytes, among other immunomodulatory actions; however, the mechanisms behind these antics have not been fully elucidated. The end result of all of this bacterial subterfuge is chronic infection, and the

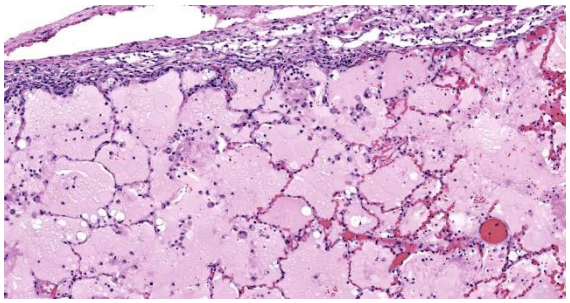

Figure 1-5. Lung, bison. Alveoli throughout the lung have hypercellular septa and are filled with edema. (HE, 128X)

hallmark of *M. bovis* disease in bison is an initially promising response to antibiotic therapy followed by repeated relapses, wasting, and eventual death or human euthanasia.[19]

This week's conference was moderated by LTC Chris Schellhase, Chief of Diagnostic Services at the Joint Pathology Center, who began discussion by noting the massive amount of fibrin, edema, and necrosis appreciable on subgross evaluation. Some participants were intrigued by the multifocal vasculitis present throughout the section and wondered if the vasculitis was a primary lesion, which would be unusual with *M. bovis* infection, or if the vessels were simply bystanders being taken along for a very inflammatory ride. Conference participants also discussed whether some of the large fibrin aggregates, such as those within the interlobular septa, were present within blood or lymphatic vessels. Participants noted the large, dilated bronchi which were multifocally effaced by inflammatory cells, fibrin, and edema and felt that these changes likely represent bronchiectasis, a common finding in *Mycoplasma* pneumonias generally. Finally, participants reviewed special stains, including a Fite-Faraco, which unexpectedly contained many acid fast bacteria. The significance of this finding is unclear.

Discussion of the morphologic diagnosis revisited the vasculitis debate. Participants felt that the vasculitis was likely a bystander rather than a primary process and it was, for this reason, omitted from the final diagnosis.

References:

1. Bras AL, Barkema HW, Woodbury MR, Ribble CS, Perez-Casal J, Windeyer MC. Clinical presentation, prevalence, and risk factors associated with Mycoplasma bovis-associated disease in farmed bison (Bison bison) herds in western Canada. *J Am Vet Med Assoc*. 2017;250(10):1167-1175.
2. Burki S, Frey J, Pilo P. Virulence, persistence and dissemination of *Mycoplasma bovis*. *Vet Microbiol*. 2015;179(1-2):15-22.
3. Calcutt MJ, Lysnyansky I, Sachse K, Fox LK, Nicholas RAJ, Ayling RD. Gap analysis of Mycoplasma bovis disease, diagnosis and control: An aid to identify future development requirements. *Transbound Emerg Dis*. 2018;65 Suppl 1:91-109.
4. Caswell JL, Archambault M. Mycoplasma bovis pneumonia in cattle. *Anim Health Res Rev*. 2007;8(2):161-186.
5. Dyer N, Hansen-Lardy L, Krogh D, Schaan L, Schamber E. An outbreak of chronic pneumonia and polyarthritis syndrome caused by Mycoplasma bovis in feedlot bison (Bison bison). *J Vet Diagn Invest*. 2008;20(3):369-371.
6. Dyer N, Register KB, Miskimins D, Newell T. Necrotic pharyngitis associated with Mycoplasma bovis infections in American bison (Bison bison). *J Vet Diagn Invest*. 2013;25(2):301-303.
7. Dyer NW, Krogh DF, Schaan LP. Pulmonary mycoplasmosis in farmed white-tailed deer (Odocoileus virginianus). *J Wildl Dis*. 2004;40(2):366-370.
8. Kumar R, Register K, Christopher-Hennings J, et al. Population genomic

analysis of Mycoplasma bovis elucidates geographical variations and genes associated with host-types. *Microorganisms*. 2020;8 (10):1561.
9. Kyathanahalli S. Janardhan MH, Neil Dyer, Richard D. Oberst, Brad M. DeBey. Mycoplasma bovis outbreak in a herd of North American bison (Bison bison). *J Vet*
10. Malmberg JL, O'Toole D, Creekmore T, et al. Mycoplasma bovis Infections in Free-Ranging Pronghorn, Wyoming, USA. *Emerg Infect Dis*. 2020;26(10): 2807-2814.
11. Maunsell FP, Woolums AR, Francoz D, et al. Mycoplasma bovis infections in cattle. *J Vet Intern Med*. 2011;25: 772-783.
12. Perez-Casal J, Prysliak T, Maina T, Suleman M, Jimbo S. Status of the development of a vaccine against Mycoplasma bovis. *Vaccine*. 2017;35(22):2902-2907.
13. Register KB, Jelinski MD, Waldner M, et al. Comparison of multilocus sequence types found among North American isolates of Mycoplasma bovis from cattle, bison, and deer, 2007-2017. *J Vet Diagn Invest*. 2019;31(6):899-904.
14. Register KB, Jones LC, Boatwright WD, et al. Prevalence of Mycoplasma spp. in the Respiratory Tract of Healthy North American Bison (Bison bison) and Comparison with Serum Antibody Status. *J Wildlife Dis*. 2021;57(3):683-688.
15. Register KB, Olsen SC, Sacco RE, et al. Relative virulence in bison and cattle of bison-associated genotypes of Mycoplasma bovis. *Vet Microbiol*. 2018;222:55-63.
16. Register KB, Parker M, Patyk KA, et al. Serological evidence for historical and present-day exposure of North American bison to Mycoplasma bovis. *BMC Vet Res*. 2021;17(1):1-10.
17. Register KB, Sacco RE, Olsen SC. Evaluation of enzyme-linked immunosorbent assays for detection of Mycoplasma bovis-specific antibody in bison sera. *Clin Vaccine Immunol*. 2013;20(9):1405-1409.
18. Register KB, Woodbury MR, Davies JL, et al. Systemic mycoplasmosis with dystocia and abortion in a North American bison (Bison bison) herd. *J Vet Diagn Invest*. 2013;25(4):541-545.
19. Sweeney S, Jones R, Patyk K, LoSapio C. Mycoplasma bovis-an emerging pathogen in ranched bison. 2013. Available at https://www.aphis.usda.gov/animal_health/nahms/bison/downloads/bison14/

CASE II:

Signalment:
Adult male striped skunk (*Mephitis mephitis*)

History:
This striped skunk was found alive but twitching in a residential area of Charlottetown, Prince Edward Island. The skunk was euthanized and submitted for post mortem examination.

Gross Pathology:
The skunk was in good body condition. The caudodorsal lung lobes were bright red and slightly firm with numerous flat, white, 2 mm in greatest diameter, white foci randomly scattered throughout all lung lobes. The tra-

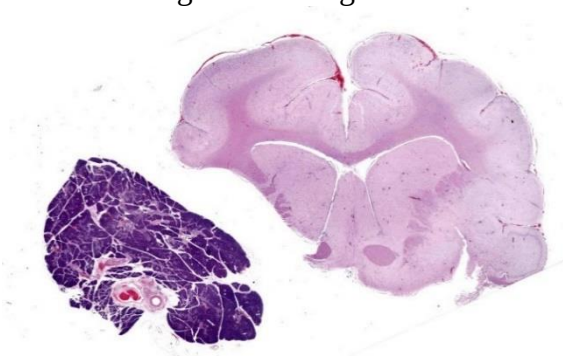

Figure 2-1. Pancreas and cerebrum, skunk. Aside from a small amount of meningeal hemorrhage, no lesions are visible at subgross magnification. (HE, 5X)

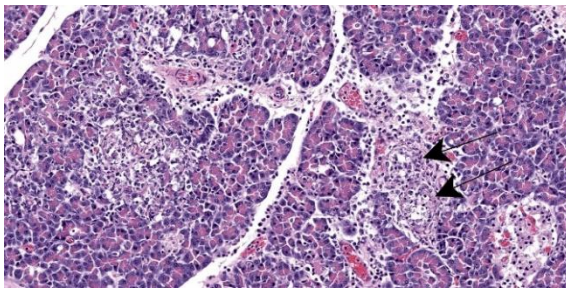

Figure 2-2. Pancreas, skunk. There are randomly scattered areas of necrosis affecting both acinar tissue (left) and ducts (right, arrows). (HE, 61X)

chea and mainstem bronchi contained pink-tinged froth. The liver was diffusely and mildly enlarged, dark red and friable and all liver lobes contained numerous pinpoint, white, flat, round foci. There were multiple skull fractures with clotted blood multifocally within the temporal muscles and meninges.

Laboratory Results:
Real-time RT-PCR for Influenza A matrix gene on oropharyngeal swab: Positive.

Real-time RT-PCR for Avian Influenza Virus H5 subtype on oropharyngeal swab: Positive.

Microscopic Description:
Brain: Surrounding numerous blood vessels in the cerebral grey matter and meninges are small numbers of degenerate neutrophils, lymphocytes, plasma cells, microglial cells and pyknotic cellular debris. Adjacent to these areas in the cerebral cortex, neurons are occasionally hypereosinophilic and shrunken with pyknotic nuclei (acute degeneration/necrosis) and are surrounded by small numbers of microglial cells. The Virchow Robin space is diffusely expanded by small to moderate numbers of lymphocytes and plasma cells. The grey matter neuropil is moderately hypercellular with an increased number of microglial and glial cells. Meningeal blood vessels are diffusely cuffed by lymphocytes and plasma cells and there are multiple areas where the meninges contain moderate numbers of erythrocytes (hemorrhage).

Pancreas: Randomly scattered throughout the exocrine pancreas, replacing pancreatic acini and occasionally surrounding blood vessels are numerous, variably-sized nodular aggregates that are composed of moderate numbers of degenerate neutrophils, macrophages, eosinophilic granular material, and pyknotic cellular debris . These areas often contain moderate amounts of pale eosinophilic, amorphous, fibrillar to flocculent, extracellular matrix (amyloid). Pancreatic acini in the periphery of these areas are often fragmented with singular acinar cells remaining. The interstitium contains moderate numbers of neutrophils, macrophages, eosinophilic fluid, and fewer lymphocytes and plasma cells and pyknotic cellular debris. The lumen of pancreatic ducts often contains small numbers of neutrophils

Contributor's Morphologic Diagnosis:
1. Brain: Necrotizing meningoencephalitis, multifocal, acute, severe, with multifocal acute neuronal necrosis, gliosis and satellitosis
2. Brain: Multifocal, acute, severe, meningeal hemorrhage
3. Pancreas: Necrotizing pancreatitis, multifocal, subacute, severe with multifocal acinar loss

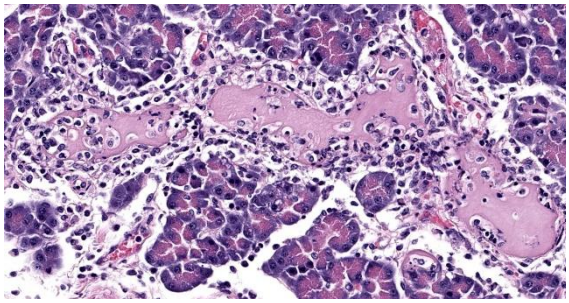

Figure 2-3. Pancreas, skunk. Numerous vessel contain inflammatory cells within their walls where they are admixed with cellular debris (vasculitis). (HE, 387)

Figure 2-4. Cerebrum, skunk. The meninges and Virchow Robins spaces are expanded by a moderate mixed cell infiltrate. (HE, 89X)

Contributor's Comment:
Influenza viruses are enveloped RNA viruses that have the potential to undergo gene reassortment in a host when they are infected with multiple viruses.[1,3] Gene reassortment can lead to the development of highly pathogenic strains that infect multiple species and can result in pandemics.[3]

The A/Goose/Guangdong/1/96 lineage of H5 highly pathogenic avian influenza virus (HPAI), which first emerged in Southeast Asia in 1996, was detected in wild and domestic birds in Atlantic Canada in late 2021.[2] H5N1 viruses in Newfoundland, Canada, in late 2021 were most closely related to HPAI viruses circulating in northwestern Europe in spring 2021, and were most likely carried across the Atlantic via migratory birds.[2] Since that time, H5N1 viruses have spread throughout North America, resulting in neurologic signs and widespread mortality in a wide variety of wild birds and mammals, as well as significant impacts on the poultry industry.[1] In early 2023, fully Eurasian H5N5 viruses began to be detected in wild birds in Atlantic Canada, presumably representing a new incursion to the region via migratory birds. Genetic analysis of samples from the skunk in this submission revealed H5N5 subtype of the 2.3.4.4b Eurasian lineage of HPAI.

In Atlantic Canada, H5N1 HPAI has been detected in red foxes (*Vulpes vulpes*), striped skunks (*Mephitis mephitis*), and raccoons (*Procyon lotor*), with additional diagnoses in these species and other mammals throughout North America.[1] H5N5 HPAI has been detected in raccoons, one striped skunk, and multiple American crows in the region. Mammals infected with H5N1 HPAI typically show neurologic signs, including seizures, twitching, foaming at the mouth, circling, or are found dead.[1] Gross post mortem lesions include pulmonary edema, bronchointerstitial pneumonia, nasal turbinate edema, multifocal (2 to 3 mm in greatest diameter) areas of necrosis throughout the pulmonary and hepatic parenchyma, and meningeal congestion. The most common microscopic lesions include meningoencephalitis, gliosis, bronchointerstitial pneumonia, pulmonary edema and congestion, necrotizing hepatitis and cerebral and brainstem neuronal necrosis.[1] Although the lesions in H5N5 HPAI positive cases are not yet described, the gross and microscopic lesions in this case are consistent with those described in H5N1 HPAI positive skunks and other North American mammals in the current outbreak.

Contributing Institution:
Atlantic Veterinary College, University of Prince Edward Island
Department of Pathology and Microbiology
https://www.upei.ca/avc/pathology-and-microbiology

JPC Diagnosis:
1. Cerebrum: Meningoencephalitis, necrotizing and lymphohistiocytic, diffuse, mild to moderate.
2. Pancreas: Pancreatitis, necrotizing and lymphoplasmacytic, diffuse, moderate.
3. Pancreas: Amyloidosis, multifocal, mild.

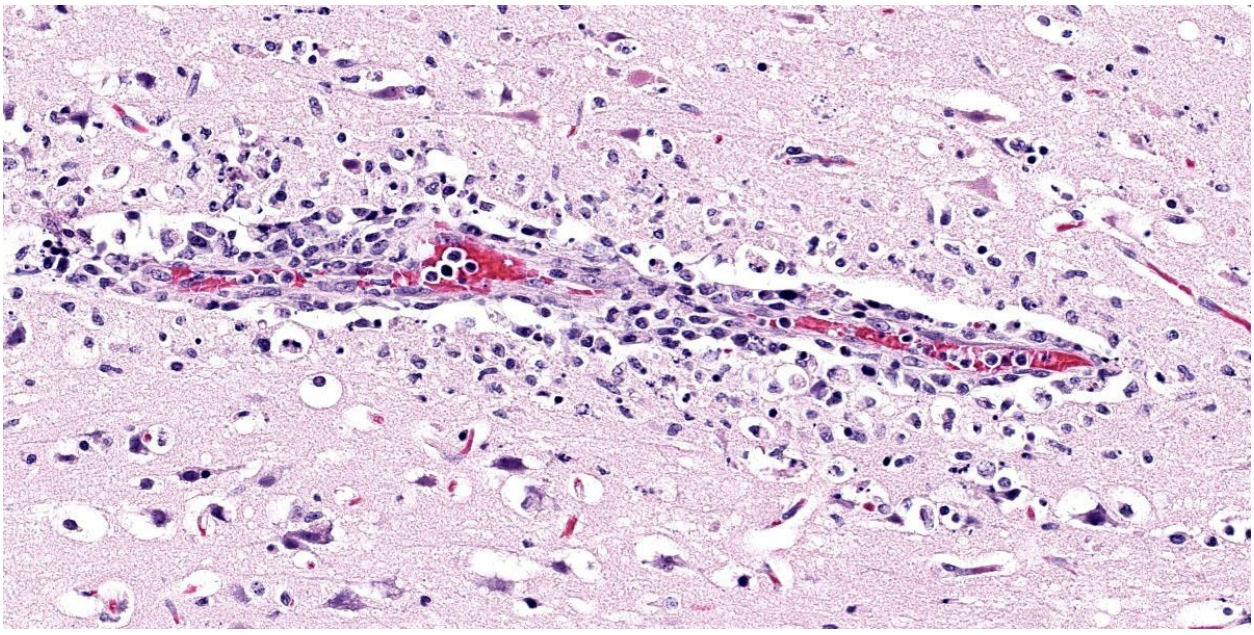

Figure 2-5. Cerebrum, skunk. Inflammatory cells emigrate into the surrounding neuropil, resulting in necrosis. (HE, 314X)

JPC Comment:

As noted by the contributor, Influenza A viruses exchange genetic information through reassortment of their segmented RNA genomes. Reassortment, a method to supercharge viral evolution, is a strategy available only to RNA viruses with segemented genomes and requires concurrent co-infection with more than one Influenza A strain. Reassortment occurs when RNA segments from different influenza viruses are intermixed during the virion assembly process, resulting in a large genomic change and the development of a new virus subtype, a process known as genetic shift. This is in contrast to the emergence of new virus types due to random point mutations, a slower, more conservative change known as antigenic drift.

Influenza A viruses have a broad host range, with established lineages circulating in poultry, pigs, humans, and other mammals, and a particularly rich tapestry of viral diversity circulating in wild birds.[3] Particular influenza viral lineages tend to be restricted to their preferred mammalian hosts; however, reassortment occasionally produces novel influenza viruses that are able to cross species barriers and cause viral pandemics.[3] Research has shown that such reassortment occurs frequently in vivo, leading to viral genotypic diversity both between animals and among the various levels of the respiratory tract in individual animals.[3]

Pigs are of particular interest in influenza ecology as they are susceptible to swine, human, and avian influenzas, and thus provide an accommodating microbial mixing vessel that can give rise to recombinant viruses.[3] These novel viral subtypes have been behind most major historical influenza pandemics to date, and the emergence of a new viral influenza subtype with pandemic potential is an ever-present threat.[4]

This case generated robust discussion, particulary around changes within the neuroparenchyma. Multiple conference participants were convinced that many neurons contained intranuclear eosinophilic viral inclusions, which would not be expected with influenza

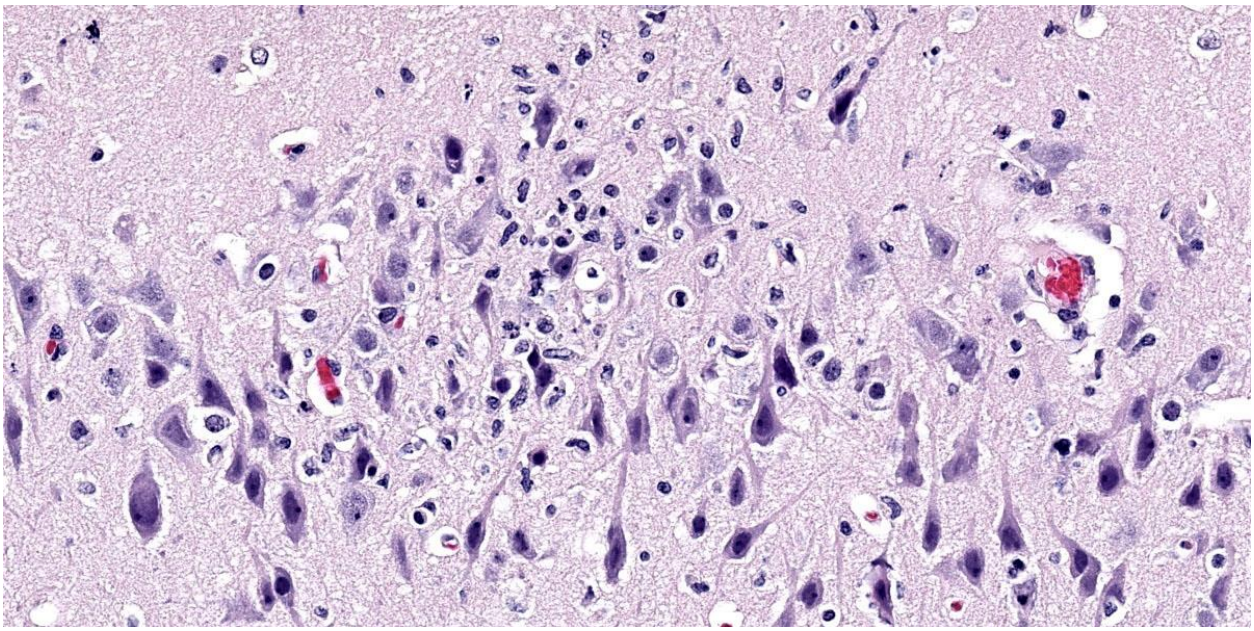

Figure 2-6. Cerebrum, skunk. There is scattered neuronal necrosis adjacent to areas of meningeal inflammation within the submeningeal cortex. (HE, 381X)

infection. The discussion quickly turned to the age-old "inclusion body or nucleoli" debate without satisfactory resolution. Several participants also believed there to be neuronal loss, though while neuronal necrosis was evident, most participants felt that the substantial gliosis made the neuroparenchyma appeared hypercellular, not hypocellular.

Despite the nuances in the neuroparenchymal pathology, the moderator emphasized that the nature and distribution of the inflammation in section are highly suggestive of a viral etiology. Participants discussed various differential diagnoses before noting that the presence of necrotizing pancreatitis considerably narrowed the differential list. Differentials for pancreatic necrosis in a bird include West Nile Virus, Avian Adenovirus, HPAI, *Sarcocystis* sp., and zinc toxicity; however, the most likely cause of necrotizing pancreatitis and meningoencephalitis in a bird is HPAI.

The ensuring morphologic diagnosis discussion was scentillating. Participants were skeptical that the meningeal hemorrhage was replated to the HPAI and wondered if this could be euthanasia artifact. Participants were similarly unconvinced that the amyloid noted in the pancreatic acini and islets was due to HPAI infection. The agreed-upon morphologic diagnosis highlights the necrosis that characterizes the disease and separates out the amyloidosis as a discrete disease process.

References:

1. Alkie TN, Cox, S, Embury-Hyatt C, et al. Characteriziation of neurotropic HPAI H5N1 viruses with novel genome constellations and mammalian adaptive mutations in free-living mesocarnivores in Canada. *Emerg Microbes Infect*. 2023;12(1):2186608.
2. Caliendo V, Lewis NS, Pohlmann A, et al. Transatlantic spread of highly pathogenic avian influenza H5N1 by wild birds

from Europe to North America in 2021. *Sci Rep*. 2022;12(1):1-18.
3. Ganti K, Bagga A, Caranccini S, et al. Influenza A virus reassortment in mammals gives rise to genetically distinct within-host subpopulations. *Nat Commun*. 2022;13(1): 6846.
4. Quinn PJ, Markey BK, Leonard FC, Fitz-Patrick ES, Fanning S, Hartigan PJ. *Veterinary Microbiology and Microbial Diseases*. Blackwell Publishing Ltd;2011: 647-659.

CASE III:

Signalment:
Adult male black-tailed jackrabbit (*Lepus californicus*)

History:
A dead black-tailed jackrabbit without signs of predation was found by a private citizen that was falcon hunting in southern California.

Gross Pathology:
The carcass was in a mild to moderate state of postmortem decomposition and poor nutritional condition. There was a moderate amount of serosanguineous fluid in the thorax. The lungs were pink to red, swollen, and wet. The liver was dark-red, congested, and oozed dark-red fluid on cut surface.

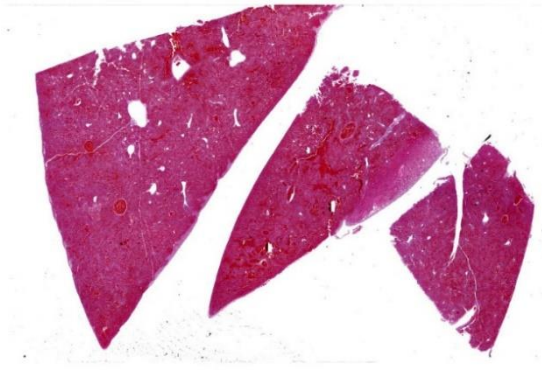

Figure 3-1. Liver, jackrabbit. Three sections of liver are presented for examination. (HE, 3X)

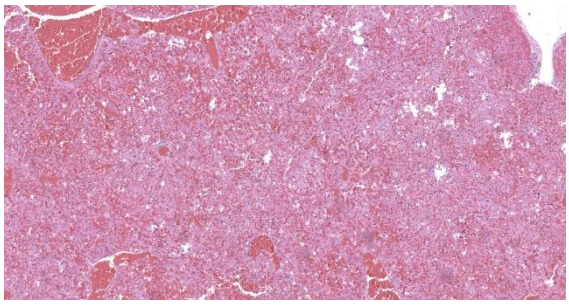

Figure 3-2. Liver, jackrabbit. There is diffuse loss of sinusoidal architecture with numerous areas of hemorrhage. (HE, 60X)

Laboratory Results:
RHDV2 RT-qPCR: Positive (Ct 11.8).
Pan-lagovirus IHC in liver (antibodies provided by Drs. Lavazza and Capucci, IZSLER, Italy): Positive.

Microscopic Description:
Liver: There is diffuse, periportal to panlobular hyperosinophilia with disorganization of hepatic cords (necrosis) and abundant hemorrhage and congestion. Hepatocytes show one or more of the following changes: membrane and cytoplasmic fragmentation, pyknosis, karyorrhexis, and occasional individual mineralization. There are rare, scattered heteorophils, and mild infiltrates of lymphocytes, histiocytes, and plasma cells in the portal spaces, as well as some subscapular follicular aggregates of lymphocytes.

Contributor's Morphologic Diagnosis:
Liver, necrosis, panlobular, severe, acute with hemorrhage

Contributor's Comment:
Rabbit hemorrhagic disease virus type 2 (RHDV2 or GI.2) belongs to the genus *Lagovirus*, a group of viruses within the family *Caliciviridae* that affects species in the order Lagomorpha.[5] This virus was detected for the first time in France in 2010 and has been spreading among domestic and wild leporid species in North America since 2020.[7,11] A distinctive feature of RHDV2 is its host range, which is wider than that of its close

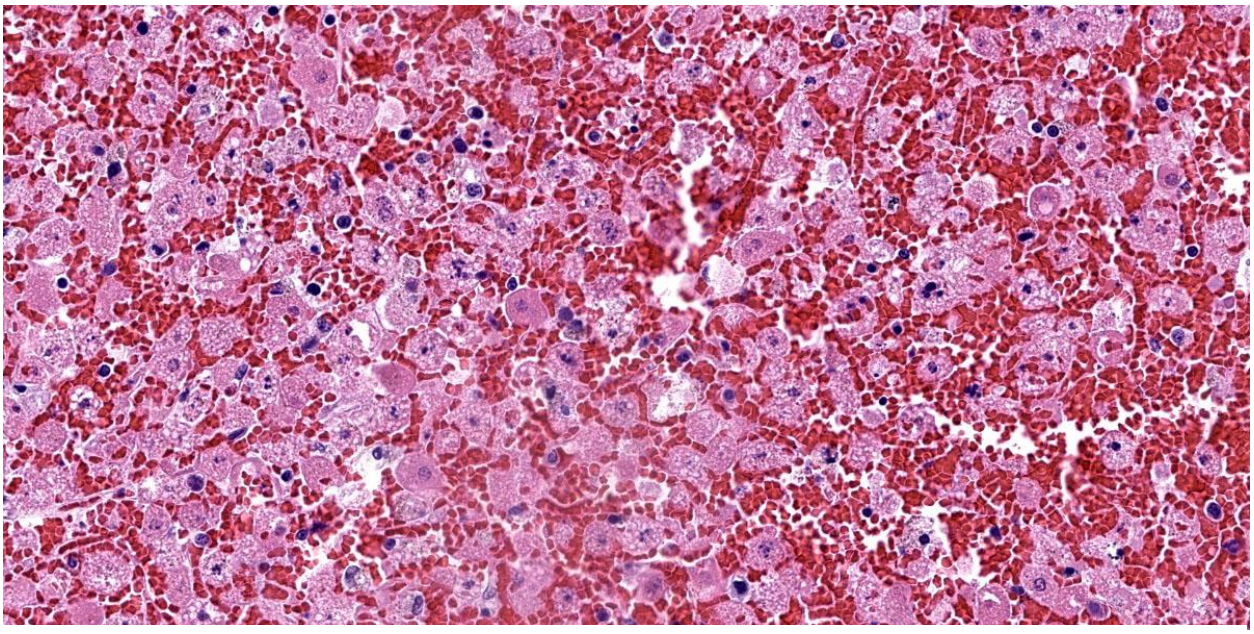

Figure 3-3. Liver, jackrabbit. Hepatocytes are disassociated and necrotic throughout the entire lobule. (HE, 381X)

relative, classic RHDV (or GI.1); the latter affects principally domestic and wild European rabbits (*Oryctolagus cuniculus*), whereas RHDV2 affects also several hare and jackrabbit species (*Lepus* spp.), as well as cottontails and other wild rabbits native to the American continent (*Sylvilagus* spp.).[11] RHDV2 is broadening its host range as it spreads and new leporid species are exposed to it for the first time.

In domestic rabbits, classic RHD is associated with high mortality; animals generally succumb after a short period of fever, lethargy, seizures and bleeding through body orifices.[1] Hepatomegaly with pallor and reticular pattern, pulmonary congestion with hemorrhages, splenomegaly, hemorrhages in multiple tissues, and icterus are the most common gross findings. Histologically, there is periportal to panlobular hepatic necrosis, splenic red pulp necrosis and lymphoid depletion, and systemic thrombosis in small capillaries (e.g., in renal glomeruli and pulmonary septae).

RHDV2 seems to cause similar clinical signs and lesions, although possibly with more variable mortality according to some reports.[7,10] Specifically in hares (*Lepus* spp.), RHDV2 causes a disease process similar to RHD in rabbits or to the European brown hare syndrome (caused by another *Lagovirus*, EBHSV or GII) in several hare species from Europe.[4] Clinicopathologic data of RHDV2 infection in hares is limited to just a few studies that would suggest that mortality is lower and more variable than in rabbits.[4,12]

Data on the pathology of RHDV2 on North American leporid species is very limited. An experimental study confirmed for the first time that that the eastern cottontail (*Sylvilagus floridanus*) was susceptible to RHDV2 and developed a similar disease process as observed in New Zealand white rabbits (*Oryctolagus cuniculus*).[9] According to one of the first reports of natural disease in cases from early 2020 in the USA, the pathology of RHDV2 in desert cottontails (*Sylvilagus audubonii*) and black-tailed jackrabbits (*Lepus californicus*) is similar to

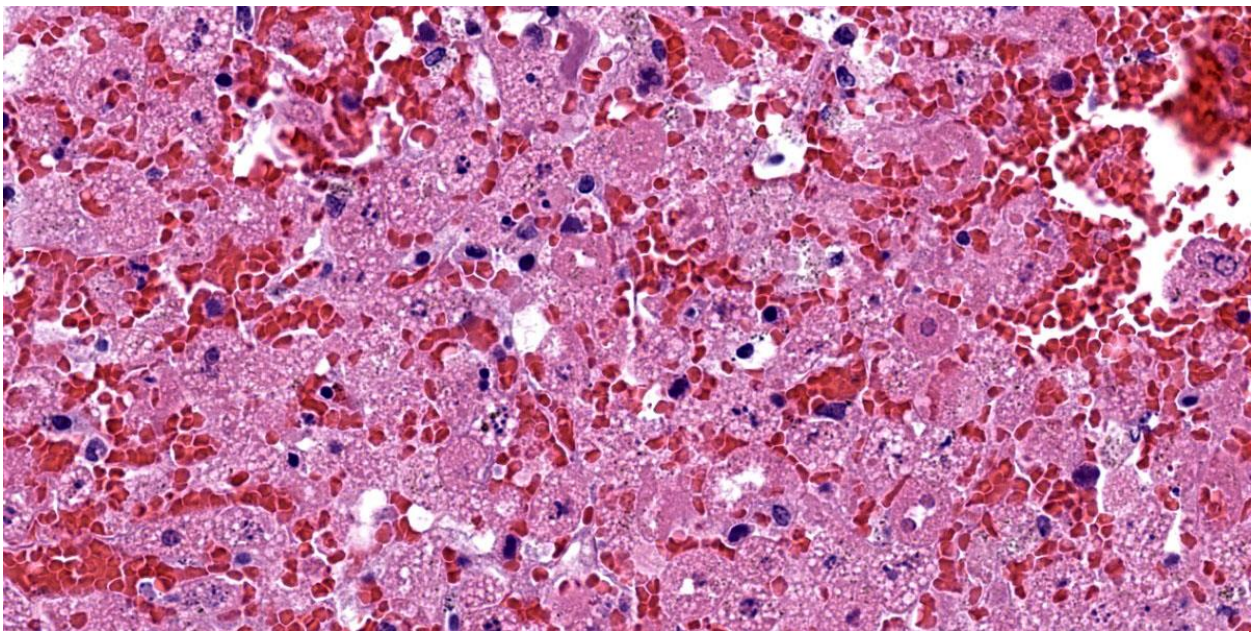

Figure 3-4. Liver, jackrabbit. Degenerating and necrotic hepatocytes contain numerous cytoplasmic vacuoles which may be the result of apoptosis or dilation of smooth endoplasmic reticulum. (HE, 578X)

previous descriptions in wild and domestic European rabbits and other hare species, with hepatic necrosis as the most diagnostically relevant finding; however, glomerular or pulmonary fibrin thrombi and splenic necrosis were not identified in the animals of the mentioned report, which differs with previous descriptions of RHDV2 in rabbits of European origin.[6]

In California, RHDV2 was confirmed for the first time in a black-tailed jackrabbit on May 2020 as part of an outbreak that was spreading throughout the southwest at that time.[2] The disease spread quickly among multiple southern counties of the state between 2020 and 2021, and was later detected in northern areas as well. Domestic rabbits (including pets, backyard rabbitries, and a few commercial farms), black-tailed jackrabbits, desert cottontails, Western brush rabbits (*Sylvilagus bachmani*) and its endangered subspecies, the Riparian brush rabbit (*Sylvilagus bachmani riparius*), have been affected by RHDV2 in California. Some of the early circulating viruses in the south of the state were phylogenetically similar to other detections in Arizona, Texas, and New Mexico earlier in 2020. Among all the detections of RHVD2 in North America since the first cases in Quebec, Canada, in 2016, the early California sequences were more similar to a virus collected in British Columbia, Canada, in 2018.[3]

Contributing Institution:
California Animal Health and Food Safety Laboratory System (CAHFS)
University of California-Davis
San Bernardino, California
https://cahfs.vetmed.ucdavis.edu/locations/san-bernardino-lab

JPC Diagnosis:
Liver: Hepatitis, necrotizing, acute, massive, diffuse, severe, with hemorrhage.

JPC Comment:
The contributor provides an excellent overview of the biology, natural history, and unfortunate spread of RHDV2. The spread of

RHDV2 is concerning not only for native susceptible lagomorph species, but also for the predators which depend on them for a food source. RHDV2 can profoundly alter the ecosystems in which it is introduced as evidenced by the emergence of RHDV2 on the Iberian Peninsula in 2013. In that outbreak, the wild rabbit population of northern Spain declined precipitously; unfortunately, population numbers for the Iberian lynx and the Spanish eagle, both endanged species that rely heavily on rabbit-based diets, declined in tandem.[3] This scenario has repeated with each introduction of RHDV2 into a new ecosystem and is particularly instructive for the current outbreak in California, as the state has established populations of mountain lions, bobcats, coyotes, and golden eagles that also make rabbit a staple of their diets.[3]

Until recently, prevention measures have been confined to biosecurity and husbandry practices such as handwashing, quarantining animals, disinfectants, and limiting contact with animals. These efforts have been generally unsuccessful in slowing the unrelenting spread of the virus due to RHDV's multiple routes of transmission; the virus can be spread mechanically by flies and other vectors, by fomites, and by infected carcasses which can harbor communicable virus for up to three months.[4] The primary route of transmission is oral, though nasal, subcutaneous, intravenous, and intramuscular transmission has been identified.[4] Wildlife researchers and rabbit hobbyists alike were cheered in 2021, when the USDA gave Emergency Use Authorization to a US-based RHDV2 vaccine; the vaccine was given a Conditional Use license in November 2023, providing a new weapon in the fight against this fatal, emerging disease.[8]

The hallmark of RHDV2 is massive hepatocellular necrosis as abundantly illustrated by this case. Conference participants remarked on the incredible degree of hepatocellular

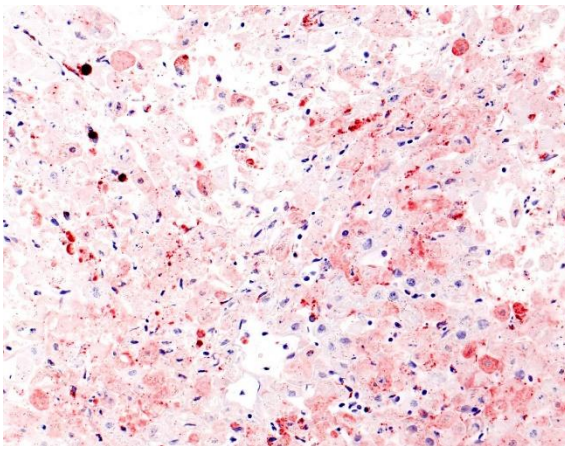

Figure 3-5. Liver, jackrabbit. A pan-fungal RHDV IHC demonstrates abundant antigen within degenerating hepatocytes. (*Photo courtesy of:* California Animal Health and Food Safety, San Bernardino Branch).

destruction, the abundant hemorrhage that separated and surrounded the remnant hepatocytes, and the general lack of associated inflammation. Conference participants also considered a reticulin stain which showed complete loss of sinusoidal architecture, confirming the tissue destruction evident on H&E. The moderator noted that it would be easy to focus on the astonishing amount of hemorrhage and destruction and overlook the finer descriptive points of nuclear features (karyorrhexis, karyolysis), type and extent of necrosis, and the mineralization noted occasionally throughout the section.

Conference participants noted the vacuolar changes in the hepatocytes and debated whether these were lipid-type or glycogen-type changes. Participants decided that the vacuoles were likely neither, but instead represented swelling of the endoplasmic reticulum during cellular necrosis. The moderator called attention to the eosinophilic globules present throughout the section, called acidophilic or "Councilman bodies." Councilman bodies are aggregated apoptotic hepatocyte fragments that are observed in viral hepatitides and are named after American pathologist William Thomas Councilman who

discovered them during his work on yellow fever. Finally, participants discussed lung lobe torsion, a differential common in rabbits, which would appear as a whole-lobe coagulative necrosis with retention of hepatocellular architecture, quite different from the impressive lytic necrosis present in this slide.

Discussion of the morphologic diagnosis was fairly straightforward in this case, though not without minor drama. One particularly insistent conference participant argued for the inclusion of hemorrhage in the morphologic diagnosis due to the prominence of this feature in the disease itself and on the examined slide. Dissenting voices argued that necrosis implies hemorrhage, making its inclusion redudant; however, persistence carried the day and hemorrhage won by a hare.

References:

1. Abrantes J, van der Loo W, Le Pendu J, et al. Rabbit haemorrhagic disease (RHD) and rabbit haemorrhagic disease virus (RHDV): a review. *Vet Res*. 2012;43(1): 12.
2. Asin J, Nyaoke AC, Moore JD, et al. Outbreak of rabbit hemorrhagic disease virus 2 in the southwestern United States: first detections in southern California. *J Vet Diagn Invest*. 2021;33(4):728-731.
3. Asin J, Rejmanek D, Clifford DL, et al. Early circulation of rabbit haemorrhagic disease virus type 2 in domestic and wild lagomorphs in southern California, USA (2020-2021). *Transbound Emerg Dis*. 2022;69(4):e394-e405.
4. Byrne AW, Marnell F, Barrett D, et al. Rabbit Haemorrhagic Disease Virus 2 (RHDV2; GI.2) in Ireland Focusing on Wild Irish Hares (Lepus timidus hibernicus): An Overview of the First Outbreaks and Contextual Review. *Pathogens*. 2022; 11(3):288.
5. Capucci L, Cavadini P, Lavazza A. Rabbit hemorrhagic disease virus and European brown hare syndrome virus. In: Bamford DH, Zuckerman M, eds. *Encyclopedia of Virology*. 4th ed. Vol. 2. pp. Academic Press, Elsevier; 2021:724-729.
6. Lankton JS, Knowles S, Keller S, Shearn-Bochsler VI, Ip HS. Pathology of Lagovirus europaeus GI.2/RHDV2/b (Rabbit Hemorrhagic Disease Virus 2) in Native North American Lagomorphs. *J Wildl Dis*. 2021;57(3):694-700.
7. Le Gall-Reculé G, Lavazza A, Marchandeau S, et al. Emergence of a new lagovirus related to Rabbit Haemorrhagic Disease Virus. *Vet Res*. 2013;44(1):81.
8. "Medgene's RHDV2 vaccine granted critical license of USDA's center for veterinary biologics." Nov 2, 2023. Available at: https://www.prnewswire.com/news-releases/medgenes-rhdv2-vaccine-granted-critical-license-by-usdas-center-for-veterinary-biologics-301974936.html.
9. Mohamed F, Gidlewski T, Berninger ML, et al. Comparative susceptibility of eastern cottontails and New Zealand white rabbits to classical rabbit haemorrhagic disease virus (RHDV) and RHDV2. *Transbound Emerg Dis*. 2022;69(4):e968-978.
10. Neimanis A, Larsson Pettersson U, Huang N, et al. Elucidation of the pathology and tissue distribution of Lagovirus europaeus GI.2/RHDV2 (rabbit haemorrhagic disease virus 2) in young and adult rabbits (Oryctolagus cuniculus). *Vet Res*. 2018;49(1):46.
11. Shapiro HG, Pienaar EF, Kohl MT. Barriers to management of a foreign animal disease at the wildlife-domestic animal interface: the case of rabbit hemorrhagic disease in the United States. *Front Conserv Sci*. 2022;3:857678.
12. Velarde R, Cavadini P, Neimanis A, et al. Spillover events of infection of brown hares (Lepus europaeus) with Rabbit Haemorrhagic Disease Type 2 Virus

(RHDV2) caused sporadic cases of an European brown hare syndrome-like disease in Italy and Spain. *Transbound Emerg Dis*. 2017;64(6):1750-1761.

CASE IV:

Signalment:
Immature (presumed yearling) female white-tailed deer (*Odocolieus virginianus*)

History:
In the Canadian province of Nova Scotia, Department of Natural Resources officers were called by a concerned citizen because a young deer was acting strangely in a residential area. The deer would walk in tight circles, had a prominent head tilt, lacked fear of people and appeared to be blind as it would walk into obstacles, fall down, and struggle back to its feet. The deer appeared to be breathing heavily and was drooling excessively. The officer euthanized the deer by shooting her in the head several times with a 22 caliber gun. The head, lungs, heart, gastrointestinal tract, liver, and kidneys were harvested, frozen, and submitted to the Canadian Wildlife Health Cooperative, Atlantic Region, for examination.

Gross Pathology:
Abundant fat stores were noted in the epicardial groove, in the connective tissue surrounding the kidneys, and within the mesentery indicating that this animal appeared to be in good body condition. There were several skin abrasions on the head (attributed to trauma associated with falling) and traumatic lesions due to mode of euthanasia (i.e., gunshot to the head) were noted.

An approximately 4.5 cm x 3.5 cm x 3.5 cm, round, expansile, pale tan mass focally replaced the parenchyma in the left cranioventral lung. This mass was soft and when sectioned, was white-tan with fine fibrous septa dissecting through it. Multiple similar,

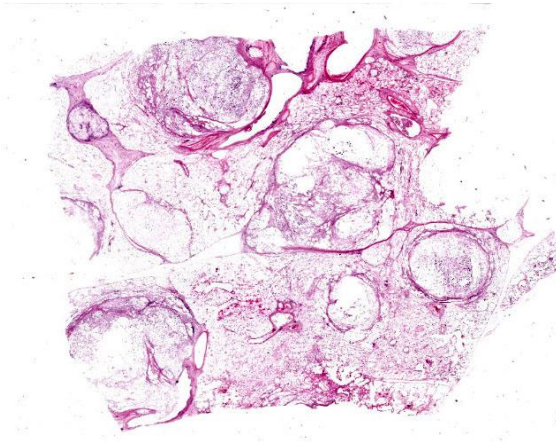

Figure 4-1. Lung, deer. A section of lung with multiple expansile, poorly cellular nodules is submitted. (HE, 5X)

smaller masses, ranging from 0.5 cm - 1.0 cm in greatest diameter, were randomly scattered throu-ghout the remaining left lung. The right lung was enlarged and largely effaced by multifocal to coalescing similar soft masses, the largest of which measured approximately 8 cm in greatest diameter. The tracheobronchial lymph nodes were moderately to severely enlarged; the largest was approximately 10 cm in greatest diameter and had a necrotic center filled with viscous yellow material. When sectioned, these lymph nodes were otherwise similar in appearance to the grossly affected lung.

Prominent cerebellar coning was noted when the calvarium was removed. When the brain was sectioned sagitally along the midline, several, small, 1-2 mm in greatest diameter, pitted lesions with dark rims were noted in the neuropil of the thalamus and superior colliculus. Following fixation, similar tiny lesions were also noted in the caudal nasal cavity. This exudate largely replaced the right ethmoturbinates and disrupted the adjacent cribiform plate. The inner and middle ears were grossly unremarkable. No significant abnormalities were noted in the liver, kidney, or gastrointestinal tract.

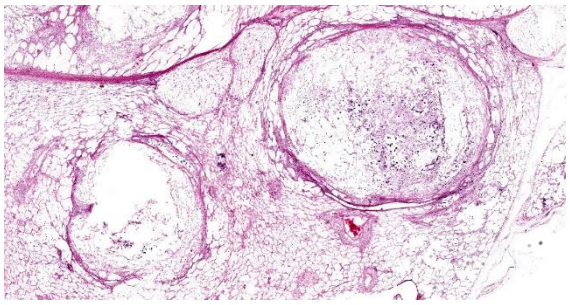

Figure 4-2. Lung, deer. Higher magnification of several of the pulmonary nodules. (HE, 16X)

Laboratory Results:
Light growth of *Cryptococcus* sp. was identified from lymph node culture swabs.

Multilocus sequence typing identified this fungus as *Cryptococcus gattii* (type VGII).

Microscopic Description:
Tissues exhibit moderate autolysis. Sections of the mass-like lesions in the lung are all similar. These masses are poorly defined and are composed of areas where alveoli are markedly expanded and are often ruptured forming variably sized spaces filled with myriads of yeast. Small to moderate infiltrates of large, pale macrophages are also present within these air spaces and the interstitium. A mild increase fine fibrous stroma multifocally expands the interstitium forming thin septa and sometimes thicker fibrous bands. Yeast are round to ovoid, 10-20 microns in diameter, and have a very pale pink, often faintly visible, thick capsule that is highlighted with mucicarmine staining. In some areas, the capsule appears basophilic. Rarely, very narrow based budding is noted. Many scattered yeasts contain coarse black melanin pigment which is highlighted with Fontana-Masson staining. Large bronchioles are sometimes partially distended with basophilic debris. Occasional dense clusters of bacilli are scattered within the tissue (interpreted as postmortem bacterial overgrowth).

Sections of the ethmoturbinates, brain, and tracheobronchial lymph nodes contain similar lesions, which often appear cystic, and consist of myriads of the described yeast associated with mild to moderate granulomatous inflammation.

Contributor's Morphologic Diagnosis:
Lung: Pneumonia, granulomatous, multifocal, mild to moderate, chronic, with myriads of intralesional yeast (compatible with *Cryptococcus* sp.).

Contributor's Comment:
The neurologic and respiratory clinical signs reported in this young deer are attributed to severe, systemic infection due to *Cryptococcus* sp. Multilocus sequence typing identified this fungus as *Cryptococcus gattii* type VGII. To our knowledge, this is the first laboratory confirmed case of *C. gattii* infection in the Atlantic provinces in eastern Canada, and the first confirmed case in a deer.

Disease in humans and susceptible animals due to cryptococcosis is generally restricted to several species, grouped into the *C. neoformans-C. gattii* complex, which include *C. neoformans* var. *neoformans*, *C. neoformans* var. *grubii* and *C. gattii*.[1,2] *C. gattii* is further classified via genotyping into 4 groups: VGI, VGII, VGIII, and VGIV.

Until the 1990's, *C. gattii* was generally considered restricted to several tropical and subtropical regions of the world, including Australia, South America, southeast Asia, parts of Africa, and an area of California. Since 1999, human hospitals on Vancouver Island, Canada, have reported a marked increase in laboratory confirmed cases of *C. gatii* (mainly types VGI and VGII) infection and the Pacific Northwest is now considered an endemic area.[1] In this same time period, laboratory confirmed cases of *C. gattii* infections (again, mainly type VGI and VGII) in

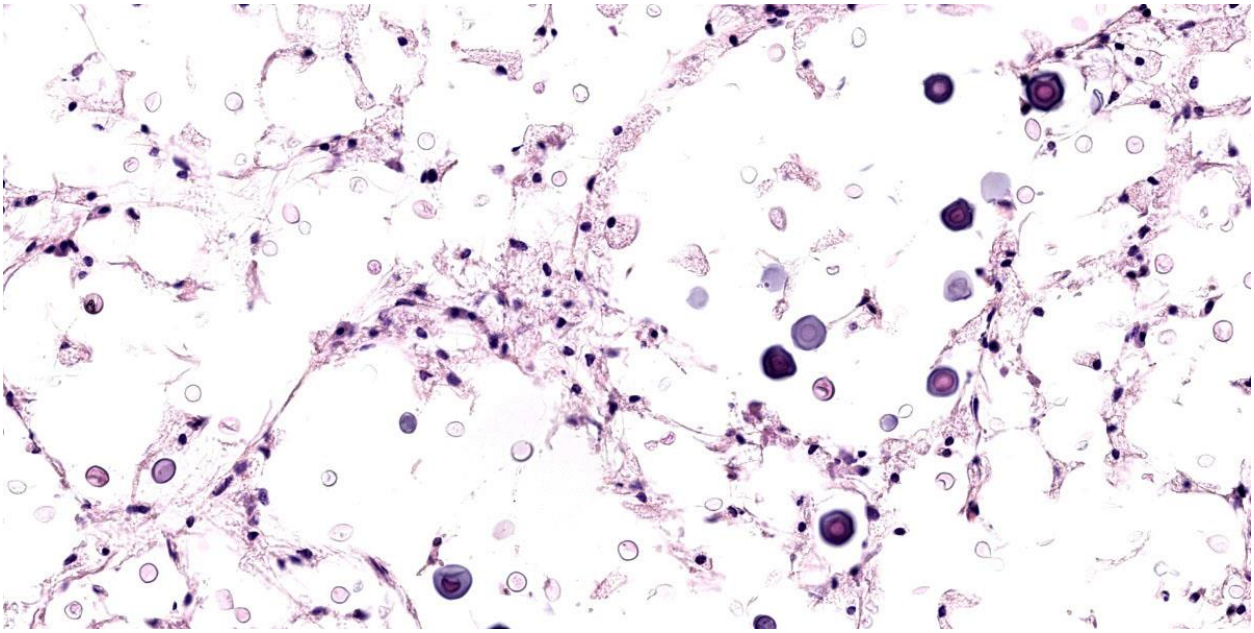

Figure 4-3. Lung, deer. Alveolar nodules contain low numbers of widely spaced, occasionally concave yeasts consistent with *Cryptococcus* sp. (HE, 379X)

pet dogs and cats from the area were also common.[5] In general, veterinary cases were diagnosed 2-3 times more frequently than human cases.[5]

C. gattii is considered an emerging pathogen in a broad range of animals and infection has been reported in domestic cats, dogs, horses, sheep, cattle, koalas, dolphins, gray squirrels, ferrets, birds, and marsupials.[1] The organism lives in the environment and can be isolated from the soil, bark from a wide variety of trees, and decaying organic material. In endemic areas, the fungus has also been isolated from the air, freshwater, and sea water, and has been recovered from car wheel wells and on footwear from high traffic areas.[2] Because of some of the latter findings, disruptive environmental activities (like logging and construction), traffic from endemic areas, and movement of bark mulch have all been implicated in the gradual spread of this organism to new areas.[5]

Infection is typically via inhalation of small basidiospores or desiccated yeast forms present in the environment. Rarely direct infections through skin wounds have been reported, most frequently in cats. A variety of virulence factors have been identified. The fungus can multiply at body temperatures. The large gelatinous capsule, which gradually enlarges in chronic infections, serves to prevent phagocytosis by macrophages and neutrophils. The capsule traps and depletes complement and circulating capsular antigens aid in the removal of selectins from endothelial surfaces, thus inhibiting migration of neutrophils into tissues. Melanin production helps to protect the yeast from host-induced oxidative injury and when present, appears to assist the organism in invading the central nervous system.[7] It is interesting that although *C. neoformans* and *C. gattii* share many of the same virulence factors, *C. gattii* (especially types VGI, VGII, and possibly VGIII) most commonly causes infection in non-immunocompromised people and animals while *C. neoformans* primarily infects immune-compromised individuals.[2] *C. gattii* is considered a primary pathogen, while *C. neoformans* is generally an opportunistic

infection. The cause of this observation is unknown. It may be related to the level of environmental exposure, that is, immunocompromised individuals may have more exposure to *C. neoformans* than *C. gattii*. Host genetic factors and inherent resistances or susceptibility to cryptococcal infection may also play a role.[2]

Given that infection is typically via inhalation, in animals, clinical disease due to *C. gattii* infection most commonly presents as chronic rhinitis and pneumonia. Encephalitis, via direct invasion from the nasal cavity, or sometimes via hematogenous routes, may result in a wide range of neurologic clinical signs. Widespread systemic infection has been reported in affected animals. As mentioned, cutaneous granulomatous lesions typically resulting from wound contamination may also occur, most commonly in cats.

In other areas, wild and domestic animals have acted as sentinels in the early detection of *C. gattii* infection and clinical disease is often detected first in animals before human cases are identified. Because of this finding, Nova Scotia public health officials have been notified to include *C. gattii* infection on their list of differential diagnoses, and testing protocols for suspect cases have been established.

Contributing Institution:
Department of Pathology/Microbiology
Atlantic Veterinary College
University of Prince Edward Island
www.avc.upei.ca

JPC Diagnosis:
Lung: Pneumonia, granulomatous, multifocal to coalescing, mild, with numerous yeast consistent with *Cryptococcus* sp.

JPC Comment:
Cryptococcus neoformans and *C. gattii* are both stunners, notable among the dimorphic fungi for their arresting, large capsule. While *C. neoformans* has been known and admired since it was first isolated from fermented peach juice in the 1890s, *C. gattii*, perhaps a bit more shy, waited until 1970 to be discovered in a leukemic patient and has, until its recent incursion in to the Northwest of Canada and the United States, stayed respectfully confined to a fairly narrow subtropical niche.[3]

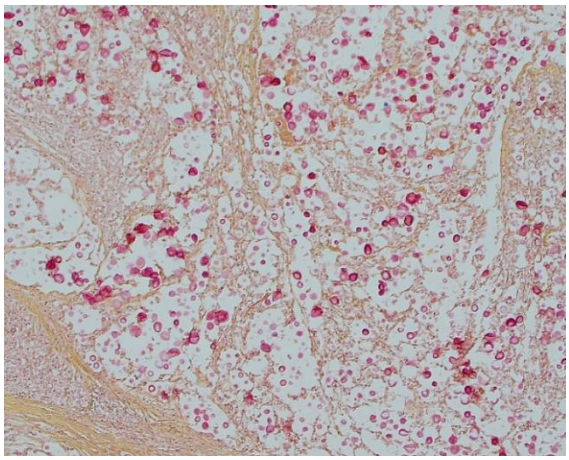

Figure 4-4. Lung, deer. Yeasts are strongly positive for mucicarmine. (Mucicarmine, 400X)

Despite their differences in temperament, however, they both share, as a primary virulence factor, a carbohydrate-rich outer capsule composed primarily of glucuronoxylomannan with lesser amounts of galactoxylomannan.[3] Far from being just a pretty adornment, the capsule is a dynamic and defensive structure. It can suppress the host immune response by downregulating cytokine and chemokine secretion in dendritic cells, inhibiting binding of complement component C3, frustrating phagocytosis, and preventing dessication in the environment.[3,8]

One of the more interesting attributes of the *Cryptococcus* capsule is its ability to switch phenotypes. Phenotype switching is an adaptive mechanism characterized by structural modifications to the capsule and the cell

wall.[3] Phenotype switching in *C. gattii* is a reversible change between two forms – a mucoid form and a smooth form – that occurs infrequently in vitro and in chronic infections.[3] Typically, infection begins with mucoid form, but subsequent phenotype switching to the smooth form, which is characterized by reduced capsular polysaccharide, allows for penetration of the blood-brain barrier and dissemination to the brain; consequently, while both smooth and mucoid forms are found in pulmonary infection, only smooth variants are typically found in the brain.[3]

The importance of the capsule to *Cryptococcus* pathogenicity is best illustrated by the effects of its absence. Acapsular *C. gattii* strains are far less virulent, and are quickly recognized and killed by macrophages and dendritic cells.[6] If, however, these acapsular strains have *C. gattii* capsular polysaccharide deposited on their surface, phagocytosis is hindered, the secretion of pro-inflammatory cytokines is not triggered, and the fungi are not cleared, confirming the key role that the capsule plays in immune evasion.[8]

Conference participants appreciated the straight-forward nature of this slide, which provides an embarrassment of visual fungal riches. Participants noted the minimal amount of granulomatous inflammation in section, which is much less than would be expected with other dimorphic fungal infections of this severity. Partipants hypothesized that this rather languid inflammatory response might be due to the cloaking of the *Cryptococcus* capsule. Participants also admired a mucicarmine stain which, while beautiful, also provoked some discussion on whether mucicarine was staining the capsule, the organism, or both. Participants noted that mucicarmine stains the capsule, while silver stains such as GMS can be used to highlight the organism and to evaluate the broad or narrow-based nature of the budding.

Participants discussed the size of the yeast which, in some cases, appeared to exceed the standard 5-10 um expected size for *Cryptococcus gattii*. This lead to a discussion of Titan cells, which are a unique adaptation of *Cryptococcus* species where they grow to unusually large size as another mechanism to evade phagocytosis. Finally, the efforts of some industrious participants were rewarded by the discovery of several unheralded nematode larvae within the examined section.

Discussion of the morphologic diagnosis centered around whether the diagnosis should refer to fungal organisms generally or *Cryptococcus* sp. specifically. The majority of participants felt strongly that, given the unique morphology, budding, and staining characteristics exhibited in section, this was a diagnosis that could confidently be made on H&E examination alone.

References:

1. Chen S, Meyer W, Sorrell T. *Cryptococcus gattii* infections. *Clin Microbiol Rev*. 2014;27(4):980-1024.
2. Diti A, Carroll SF, Qureshi ST. *Cryptococcus gattii*: an emerging cause of fungal disease in North America. *Interdiscip Perspect Infect Dis.* 2009;840452.
3. Dixit A, Carroll SF, Qureshi ST. *Cryptococcus gattii*: an emerging cause of fungal disease in North America. *Interdiscip Perspect Infect Dis*. 2009;840452.
4. Dylag M, Colon-Reyes RJ, Kozubowski L. Titan cell formation is unique to *Cryptococcus* species complex. *Virulence*. 2020;11(1):719-729.
5. Epsinel-Ingroff A, Kidd SE. Current trends in the prevalence of *Cryptococcus gattii* in the United States and Canada. *Infect Drug Resist*. 2015;8:89-97.

6. Frietas GJC, Santos DA. *Cryptococcus gattii* polysaccharide capsule: an insight on fungal-host interactions and vaccine studies. *Eur J Immunol*. 2021;51(9):2206-2209.
7. Lester SJ, Malik R, Bartlett KH, Duncan CG. Cryptococcosis: update and emergence of *Cryptococcus gattii*. *Vet Clin Pathol*. 2011;40(1):4-17.
8. Saidykhan L, Onyishi CU, May RC. The *Cryptococcus gattii* species complex: unique pathogenic yeasts with understudied virulence mechanisms. *PLoS Negl Trop Dis*. 2022;16(12):e0010916.

WSC 2023-2024
Conference 18 Self-Assessment

1. True or false? In bison, *Mycoplasma bovis* requires a co-pathogen to manifest disease.
    a. True
    b. False

2. True or false? There is no chronic carrier state of *Mycoplasma bovis* in bison.
    a. True
    b. False
    2

3. True or false? Mammals infected with the H5N1 strain of highly pathogenic avian influenza raely demonstrate neurologic signs.
    a. True
    b. False

4. Which of the following is not a common histologic finding in rabbit hemorrhagic disease?

    a. Hepatocellular necrosis
    b. Splenic red pulp necrosis
    c. Lymphohistiocytic meningitis
    d. Systemic thrombosis

5. True or false? Cryptococcus can be transmitted by cutaneous wounds.
    a. True
    b. False

Joint Pathology Center
Veterinary Pathology Services

WEDNESDAY SLIDE CONFERENCE 2023-2024

Conference #19 7 February 2024

CASE I:

Signalment:
Adult female corn snake (*Pantherophis guttatus*)

History:
An adult corn snake housed as part of a teaching colony presented for a two week history of regurgitation. During physical examination, a coelomic mass-effect was palpated as well as scale changes that prompted a scrape. Mites were identified and confirmed as *Ophyionissus natricis*. Supportive care was initiated. The snake was found dead in its enclosure several days after initial examination.

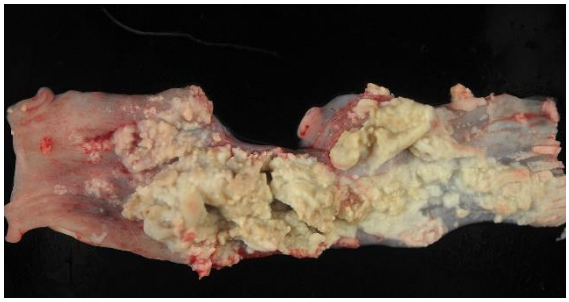

Figure 1-1. Stomach and intestine, cornsnake. The mucosa is multifocally ulcerated with dense adherent fibrinonecrotic material extending deep into the tissue. (*Photo courtesy of:* Department of Population Health and Pathobiology, North Carolina State University College of Veterinary Medicine, Raleigh, NC. https://php.cvm.ncsu.edu/)

Gross Pathology:
The pleural surface is covered in a thick mat of fibrin. On cut section, there are multifocal 0.1-1.0 cm diameter abscesses containing caseonecrotic exudate.

Laboratory Results:
PCR on fresh gastrointestinal tissue was positive for *Salmonella* sp. and subsequent culture/genotyping identified *S. enterica ssp. enterica* serogroup C.

PCR on formalin-fixed paraffin embedded gastrointestinal tissue was positive for *Entamoeba invadens*.

Microscopic Description:
Stomach, ileum and colon: Multifocally the mucosa is eroded to ulcerated and overlain by thick mats of abundant fibrin mixed with cellular and karyorrhectic debris, numerous bacterial colonies, and marked histiocytic and heterophilic inflammation (diphtheritic membrane). In areas of ulceration where the membrane has been lifted, the exposed submucosa is often lined by numerous round protozoal organisms measuring 7-10 µm in diameter with a thin basophilic wall filled with fibrillar to granular basophilic cytoplasm and a single, often eccentrically placed, round basophilic nucleus 2-3 µm in diameter (ameboid trophozoites). Affected submucosa is sometimes expanded by granulation tissue and fibrin Thrombi are frequently present within submucosal capillaries. Rarely, necrosis and inflammation extend into the tunica muscularis but does not breach the serosal membrane.

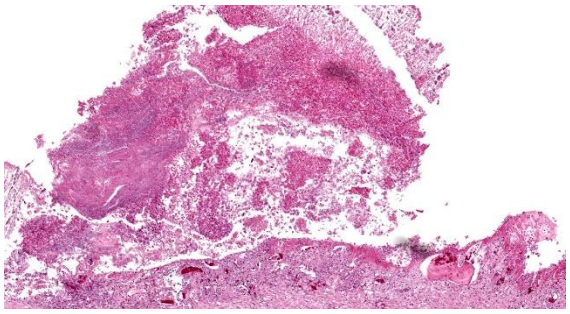

Figure 1-2. Intestine, cornsnake. There is extensive necrosis of the mucosa with abundant adherent necrotic debris. (HE, 61X)

Special stains: Periodic acid-Schiff (PAS) stain applied to sections of gastrointestinal tract highlights the cell wall of amoebic trophozoites.

Contributor's Morphologic Diagnosis:
Gastrointestinal tract: Severe multifocal, segmentalfibrinonecrotic and histiocytic enteritis with intralesional amoebic trophozoites, diphtheritic membranes and fibrin thrombi.

Contributor's Comment:
Of amoebic infections in reptiles, *Entamoeba invadens* is one of the more significant pathogenic species.[4,7] Turtles and crocodiles are considered host reservoirs for the organism and transmission follows the fecal-oral route.[4,7] Infective cysts are shed in feces and can persist in the environment for prolonged periods.[4] Ingestion of cysts by susceptible species results in enteritis, as seen in this case, with some cases extending to the liver as well.[4,7] Rare systemic infections have been reported.[4] The pathogenesis of *Entamoeba invadens* is similar to *Entamoeba histolytica*, a pathogenic amoeba that causes dysentery in humans and nonhuman primates.[9,14] *E. invadens* is often used as a laboratory model for *E. histolytica* due to its ability to undergo encystation in vitro, which *E. histiolytica* lacks.[7,9]

The life stages of *Entamoeba* species include the transmissible cyst and the infective trophozoite.[10] Hosts ingest cysts from contaminated environments and the cyst hatches into a trophozoite via "excystation" within the intestinal lumen.[10] Trophozoites then attach to epithelial cells inducing cell injury and death through a variety of mechanisms.[2] Attachment of trophozoites to mucins coating the intestinal mucosa and enterocytes occurs via the amebic Gal/GalNAc lectin.[2,10] Trophozoites then induce cell death by releasing pore-forming polypeptides called amoebapores and by biting off portions of viable cells, a phenomenon referred to as trogocytosis.[2] Both result in increased intracellular calcium, culminating in cell death.

Amoeba-induced enterocyte death results in ulcerative lesions of the gastrointestinal tract and exposes the underlying stroma into which trophozoites can invade by releasing proteases that break down the extracellular matrix.[2] This invasion allows for passage of trophozoites into the blood vessels where they can colonize extraintestinal sites in an embolic fashion. In particular, the liver is thought to be infected through a hematogenous route from the portal vein, resulting in liver abscesses.[12] Some trophozoites transform back into cysts via "encystation" which are passed into the feces to perpetuate the life cycle.[10]

Severity of disease may be affected by the environment (namely temperature), host immune status, and protozoal virulence factors.[4,7] Additional host factors may include diet. Typically, carnivorous lizards and snakes develop disease with *E. invadens* infection while herbivorous turtles infrequently develop lesions.[7] This may be due in part to the protective gut microenvironment that an herbivorous diet imparts. Virulence of *E. invadens*, namely encystation and invasion into tissues, decreases in environments rich in glucose and gram-negative bacteria.[7,9,14] When comparing the diets of studied reptiles

and chelonids, the majority of animals on a carnivorous diet developed *E. invadens*-induced lesions while those on omnivorous and herbivorous diets had intermediate and low rates of lesion development.[7]

Aside from *E. invadens*, snakes can develop disease from *E. ranarum* infection.[8,11] Both can present as a necrotizing gastroenteritis, though extra-intestinal lesions have not been reported with *E. ranarum*.[4,8,11] For cases of *E. invadens* that only manifest as intestinal disease, as was seen in this case, ancillary testing is needed to definitively determine the species present. Moreover, it is difficult to distinguish between amoebic species on routine histologic examination and so molecular testing, namely polymerase chain reaction assays, have been developed to distinguish between species.[1,4] Special stains can be performed to highlight certain features of the organisms. PAS will stain the walls of cysts and trophozoites while trichrome stain can identify certain cellular features such as the dark pink chromatoid bodies.[4] The latter is best visualized in fecal preparations.[4]

Differential diagnoses for gastroenterocolitis in snakes include salmonellosis and coccidiosis.[4] While *Salmonella* spp. PCR and cultures were positive in this case, the yielded bacterium, *Salmonella enterica* ssp. *Enterica*, is considered a commensal in reptiles.[4] It's possible dysbiosis secondary to intestinal amebiasis led to overgrowth of *S. enterica* ssp. *enteric*a and contributed to morbidity in this case. Coccidiosis was also considered based on routine histologic evaluation due to the relatively smaller size of the organisms than is previously reported in cases of *E. invadens*;[4] however, fecal analysis of cohabitants of this snake did not find coccidian organisms and PCR detected *E. invadens* in this case.

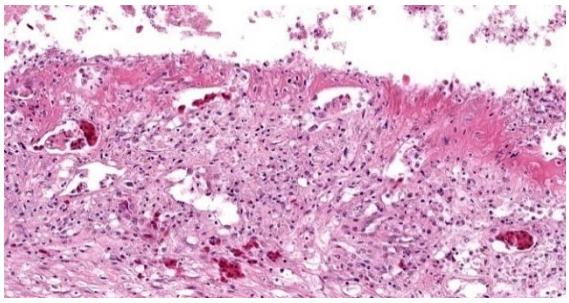

Figure 1-3. Intestine, cornsnake. Higher magnification of the necrotic mucosa. There are numerous flagellates infiltrating the mucosa. (HE, 381X)

Contributing Institution:
Department of Population Health
and Pathobiology
North Carolina State University
College of Veterinary Medicine
https://php.cvm.ncsu.edu/

JPC Diagnoses:
1. Gastrointestinal tract: Gastroenterocolitis, necrotizing, multifocal, moderate, with numerous flagellates and superficial bacteria.
2. Kidney: Urate stasis with rare gouty tophi.
3. Presumed ovary: Granulomas, multiple.

JPC Comment:
The contributor provides an excellent overview of enteric disease caused by *Entamoeba invadens* and the virulence factors that make *Entamoeba* spp. in general so damaging. As the contributor notes, the organisms in this case are smaller (approximately 4 µm in diameter) than reported for *E. invadens*, which drew additional, careful scrutiny during conference discussion.

In additional to their small size, the examined protozoa are also irregularly shaped and have eccentric, small, darkly basophilic, nuclei measuring approximately 1 µm in diameter. The cytoplasm is occasionally tapered at one end into a thin filament, which is interpreted

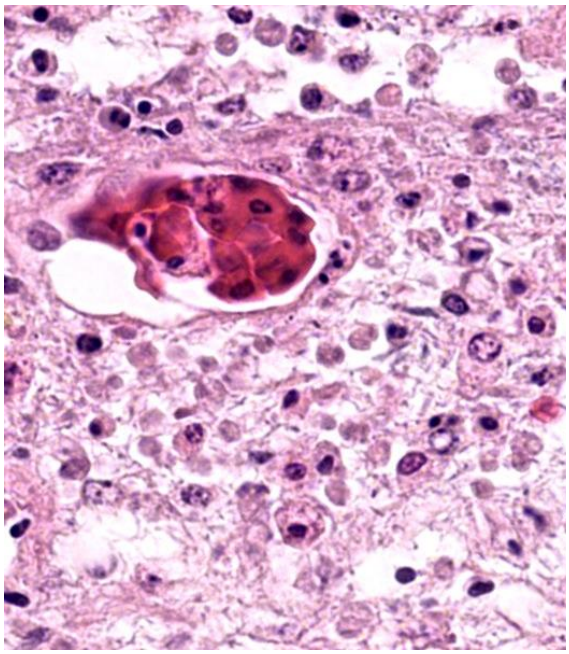

Figure 1-4. Intestine, cornsnake. Numerous flagellates infiltrate the necrotic mucosa and submucosa. (HE, 892X)

as a flagellum. The protozoa are often present in large clusters of dozens of organisms and are overlying ulcerated epithelium.

These characteristics are most consistent with infection with flagellates, which commonly infect the intestines of snakes and are associated with ulceration and secondary bacterial infections.[13] Flagellates infect similar anatomic regions as *Entamoeba* sp., which can make differentiation of these protozoa challenging. *Entamoeba invadens* are larger (10-15 µm in diameter) than flagellates and have discrete round nuclei *Entamoeba invadens* typically occur individually (rather than in clusters of dozens of organisms) and are more invasive with more necrosis, hemorrhage, and inflammation than the flagellates seen in this case.[13]

Interestingly, a previous publication investigated 51 snakes with histologically suspected *Entamoeba invadens* infection. The authors used immunohistochemistry to confirm or rule out *Entamoeba* infection. Only 22 cases were confirmed as *Entamoeba invadens*; all other cases were intestinal flagellate infections with histological feature similar to the present case.

Histologic lesions secondary to flagellate infection included inflammation and ulceration of the intestines with a fibrinonecrotizing membrane, and flagellates were reported on the surface of ulcerated mucosa, as seen in this case.[5] This work underscores the histologic similarity between *Entamoeba invadens* and flagellate infections in snakes, and the present case serves as an excellent example of the difficulty in differentiating these infections.

Flagellates that cause enteritis in snakes are not well characterized. Most cases are assumed to represent *Monocercomonas* spp. based on the few reports of this flagellate in snake enteritis lesions; however, confirmation of the genus of infective flagellates is rarely performed in cases of snake enteritis.[15] Flagellates can infect other organs in reptiles. Recent reptile work has described renal flagellates, suspected of finding their way to the kidney via reflux into the urinary system from the cloaca; flagellate-associated gastroenteritis was also commonly reported in that case series.[6] Conference participants did find rare amoebas of the appropriate size within the luminal contents, consistent with the contributor's PCR results; however, snakes can be asymptomatic but PCR positive for *Entamoeba invadens*, which is suspected in this case.[3]

This week's conference was moderated by Dr. David Needle, Associate Professor at the University of New Hampshire and Senior Veterinary Pathologist and Pathology Section Chief at the New Hampshire Veterinary Diagnostic Laboratory. Dr. Needle led participant discussion of this description-rich slide, which, after much discussion of the etiologic agent as previously detailed, moved to more

ancillary lesions, including the gouty tophus within the kidney. Participants noted the abundant pigment within the renal tubules, which is a normal finding in reptiles and is of unknown origin. Participants also noted the unidentified tissue surrounded by macrophages with intracytoplasmic yellow pigment, which participants thought might represent degenerative changes within aged ovaries, though mycobacterial granulomas could not be ruled out in the absence of acid-fast staining.

Consideration of the morphologic diagnosis recapitulated much of the previous conference discussion, with participants convinced that the gastrointerstinal pathology was caused by the flagellates aggregated within areas of tissue necrosis rather than by the occasional amoeba found within the lumen of the gastrointestinal tract.

References:

1. Bradford CM, Denver M, Cranfield MR. Development of a polymerase chain reaction test for *Entamoeba invadens*. *J Zoo Wildl Med*. 2008;39(2):201-207.
2. Espinosa-Cantellano M, Martínez-Palomo A. Pathogenesis of intestinal amebiasis: from molecules to disease. *Clin Microbiol Rev*. 2000;13(2):318-31.
3. Heng Y, Hsu CD, Mathew A, Oh PY, Li WT, Xie S. Management of *Entamoeba invadens* in the herpetological collection at the Singapore zoo. *J Wildl Med*. 2023 Jul;54(2):272-281.
4. Jacobson ER, Garner MM. *Infectious Diseases and Pathology of Reptiles: Color Atlas and Text*. 2nd ed. CRC/Press; 2021:860-862, 904-905.
5. Jakob W, Wesemeier HH. Intestinal inflammation associated with flagellates in snakes. *J Comp Pathol*. 1995;112 (4):417-21.
6. Juan-Sallés C, Garner MM, Nordhausen RW, Valls X, Gallego M, Soto S. Renal flagellate infections in reptiles: 29 cases. *J Zoo Wildl Med*. 2014 Mar;45(1):100-9.
7. McFarland A, Conley KJ, Seimon TA, Sykes JM. A retrospective analysis of amoebiasis in reptiles in a zoological institution. *J Zoo Wildl Med*. 2021;52(1): 232-240.
8. Michaely LM, von Dornberg K, Molnar V. Entamoeba ranarum infection in a ball python (*Python regius*). *J Comp Path*. 2020;179:74-78.
9. Mi-Ichi F, Yoshida H, Hamano S. Entamoeba encystation: new targets to prevent the transmission of amebiasis. *PLoS Pathog*. 2016;12(10):e1005845.
10. Ralston KS, Solga MD, Mackey-Lawrence NM, Somlata, Bhattacharya A, Petri Jr.WA. Trogocytosis by *Entamoeba histolytica* contributes to cell killing and tissue invasion. *Nature*. 2014;508(7497): 526-530.
11. Richter B., Kübber-Heiss A., Weissenböck H. Diphtheroid colitis in a Boa constrictor infected with amphibian Entamoeba sp. *Vet Parasitol*. 2008;153(1-2):164-167.
12. Usuda D, Tsuge S, Sakurai R, et al. Amebic liver abscess by Entamoeba histolytica. *World J Clin Cases*. 2022;10(36): 13157-13166.
13. Walden HDS, Greiner EC, Jacobson ER. Parasites and parasitic diseases of reptiles. In: Jacobson ER, Garner MM, eds. *Infectious Diseases and Pathology of Reptiles*. 2nd ed. CRC Press;2020.
14. Watanabe K, Petri WA. Learning from the research on amebiasis and gut microbiome: is stimulation by gut flora essential for effective neutrophil mediated protection from external pathogens? *Gut Microbes*. 2019;10(1):100-104.
15. Zwart, Peernel and SFM, Teunis. Monocercomoniasis in reptiles. September 1982. Conference: First International colloquiem on pathology of reptiles and amphibians. At: Angers (France). 73-76.

CASE II:

Signalment:
Adult male white-eared opossum (*Didelphis albiventris*)

History:
The animal was found dead in an urban park in the city of Belo Horizonte, Brazil, and was immediately submitted to necropsy.

Gross Pathology:
There was an extensive area of skin laceration with exposure of bone and muscle in the dorsal proximal portion of the tail. Lungs were pale pink with diffuse decreased crepitation. The myocardium had multifocal to coalescing 0.2 to 0.4 cm white areas. The liver was diffusely yellow and friable. The spleen was markedly enlarged with multifocal to coalescent white-red areas. The kidneys were diffusely yellow with pinpoint multifocal white areas. The pelvis of the right kidney was moderately dilated, as was the right ureter, which was partially obstructed by a white friable plug. The gastric and duodenal lumens had
multiple cylindrical white worms which were 3 cm long and 0.3 cm in diameter (morphologically compatible with nematodes).

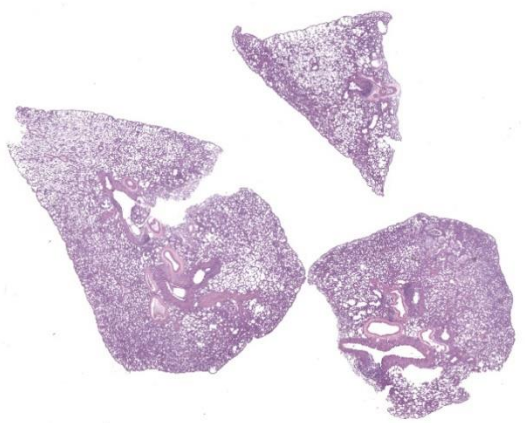

Figure 2-1. Lung, opossum. Three sections of lung are submitted for examination. (HE, 5X)

Laboratory Results:
Samples of liver, spleen and kidney were submitted for bacterial culture. *Streptococcus didelphis* was isolated from all samples.

The nematodes found in the stomach and duodenum were identified as *Turgida turgida*.

Microscopic Description:
Lung: Bronchi and bronchioles are expanded by moderate amount of mucus, intact and degenerate neutrophils, and some macrophages. Interspersed with the mucus, there was a moderate number of nematode larvae approximately 50 µm in length x 7 µm in diameter. Alveolar septa were diffusely and moderately thick and filled by neutrophils and histiocytes. Multifocally, in the alveolar lumena and terminal bronchioles there are multiple adult metastrongyles approximately 260 µm in diameter. The parasites have a small and ornamented cuticle, a pseudocoelom, an intestine with cuboidal cells full of brown intracytoplasmic granules, a uterus with numerous larvae in females and testes with globose spermatozoa in males. There are mild multifocal areas of rupture and coalescence of alveolar septa (emphysema). Additionally, multifocally there are foamy macrophages in the alveolar septa and lumena adjacent to the adult parasites. Blood vessels are filled with leukocytes.

Contributor's Morphologic Diagnoses:
1. Lung: Bronchitis and bronchiolitis, catarrhal, neutrophilic and histiocytic, multifocal, moderate, with intraluminal nematode larvae.
2. Lung: Interstitial pneumonia, neutrophilic and histiocytic, diffuse, moderate, with nematodes morphologically compatible with *Didelphostrongylus hayesi* in the lumen of alveoli and terminal bronchioles, and mild multifocal emphysema.

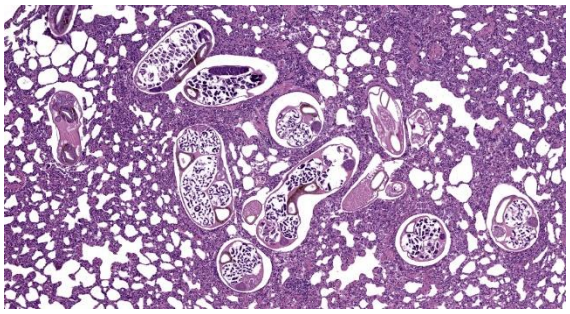

Figure 2-2. Lung, opossum. Bronchioles contain multiple cross and tangential sections of adult male and female metastrongylid nematodes. (HE, 35X)

Contributor's Comment:

White-eared opossums (*Didelphis albiventris*) are marsupial mammals that inhabit forests and peri-urban areas in Brazil, Bolivia, Argentina, Paraguay, and Uruguay, and, according to the IUCN red list, the species is considered of Least Concern for the risk of extinction.[3] Parasitic infections are frequently reported in these opossums, often by parasites that also can affect domestic animals and humans, such as ectoparasites, protozoans (*Leishmania* spp., *Toxoplasma gondii*, and *Trypanosoma cruzi*), and helminths (*Toxocara* sp., *Ancylostoma caninum*, and *Schistosoma* spp.).[1]

Didelphostrongylus hayesi is a nematode of the Order *Strongylida* and superfamily *Metastrongyloidea* that infects the lungs of opossums. Infection occurs by ingestion of snails (*Mesodon perigraptus* and *Triodopsis albolabris*) which are the intermediate hosts.[9] The infection can be mild to severe, and the animals may be asymptomatic or symptomatic, with dyspnea, fever and apathy. Radiographically, the lungs may have a bronchial pattern and fecal examination may support the *in vivo* diagnosis by visualizing larval stages.[7] At necropsy, the lungs may be hyperemic with a cranioventral pattern. Lungs do not collapse when the thoracic cavity is opened, and they are firm, with disseminated micronodules and adult parasites of approximately 1.5 to 2.0 mm may be seen in the bronchi. In cases of mild to moderate infection, as in this case, gross changes may be mild or absent. Histologically, there are larvae and adult parasites in the lumen of bronchi, bronchioles and alveoli, with mucus and an inflammatory infiltrate that can be neutrophilic, eosinophilic, or histiocytic. The infiltrate associated with the adult parasites is mild or absent, whereas larvae and eggs induce a more exacerbated inflammatory response, with granulomatous or pyogranulomatous inflammation.[7,8] There is also hyperplasia of the smooth muscle of the bronchi and bronchioles, hyperplasia of the respiratory epithelium, and emphysema.[4, 8] Worm infections of the lower airways (trachea, bronchi, bronchioles, and alveoli) are important causes of morbidity and mortality in domestic and wild animals. Histological lung lesions by helminthic infections can range from mild, such as bronchitis and bronchiolitis in cases of mild infections by *Dictyocaulus viviparus*, to granulomatous, necrotizing, hyperplastic and emphysematous lesions. The intensity of the lesions will depend on the immune status of the host, as well as the parasite load and reproductive stages of the parasites.[2]

Traumatic injuries frequently occur in opossums due to their synanthropic habits, whether due to car accidents, or attacks by dogs or people. In this case, the animal presented with areas of skin laceration and systemic involvement by *Streptococcus didelphis*. Neutrophilic and histiocytic interstitial pneumonia, in addition to being associated with the parasites, may result from the systemic bacterial process. *Streptococcus didelphis* is a poorly known bacterium that is associated with cutaneous lesions in opossums.[10] A study identified the bacteria in nine opossums that had skin lesions. It is believed that skin lesions may have been the entry

point for this agent in this case and the cause of the subsequent development of systemic lesions.[10]

Contributing Institution:
Departamento de Clínica e Cirurgia Veterinária
Escola de Veterinária
Universidade Federal de Minas Gerais
Av. Presidente Antônio Carlos,
Belo Horizonte, MG, Brazil.
www.vet.ufmg.br

JPC Diagnoses:
1. Lung: Bronchopneumonia, catarrhal and lymphohistiocytic, multifocal, mild to moderate, with metastrongyle adults, larvae, and eggs.
2. Lung: Pneumonia, interstitial, lymphohistiocytic and neutrophilic, diffuse, moderate.

JPC Comment:
Didelphostrongylus hayesi is an opossum lungworm with a wide distribution and high prevalence, above 70% in some studies, in opossums in the Americas.[8] Oppossums become infected after ingesting intermediate hosts which, as the contributor notes, are terrestrial snails. The migratory path of the nematode larvae from the gut to the lung is unknown, but once in the lung, third-stage larvae mature into adults in the airways, particularly the intrapulmonary bronchi.[8] Unlike other lungworms, which produce eggs that are deposited in host tissues or feces for futher development, *D. hayesi* produces eggs which hatch within their uteri.[6] The hatched stage one larvae migrate up the trachea, are coughed up, swallowed, and then passed in the feces where they contaminate the environment and are ingested by their intermediate gastropod hosts.[6]

Typical gross lesions include lungs that do not collapse, focal to coalescing areas of

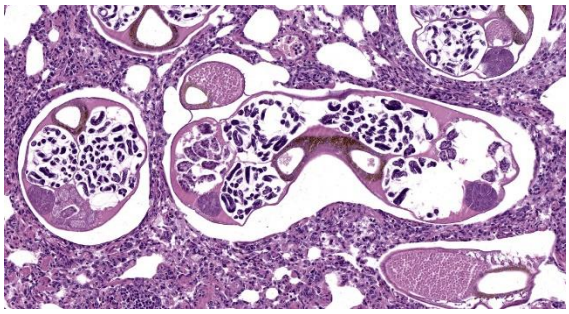

Figure 2-3. Lung, opossum. Higher magnification of adult nematodes. The larger female has multiple cross sections of a uterus containing larvated eggs and an intestine lined by few epithelial cells which contains hemosiderin. The males (arrows) have a smaller diameter and a single cross section of a testis. (HE, 164X)

emphysema, white to tan raised nodules on the pleural surface that roughly track the branching of intrapulmonary airways, and visible adult forms of *D. hayesi* on the visceral pleura.[8] Histologically, *D. hayesi* shares many common characteristics with its metastrongyle brothers and sisters, to include a smooth cuticle, a pseudocoelom, an intestine composed of few multinucleated cells with an indistinct brush border, and coelomyarian musculature. In the United States, opossum lungs are frequently co-infected with *D. hayesi* and the capillarid nematode *Eucoleus aerophilus*.[8]

Discussion of this case centered initially on the histologic appearance of the lungworm itself, with some participants noting an apparent eosinophilic fluid within the pseudocoelom, typically a feature of spirurids. The moderator noted that this is commonly seen in wildlife nematode infections and speculated that this could be a degenerative change. Other participants noted that spirurids typically have, among other distinguishing features, prominent lateral cords, which are not present in the examined section.

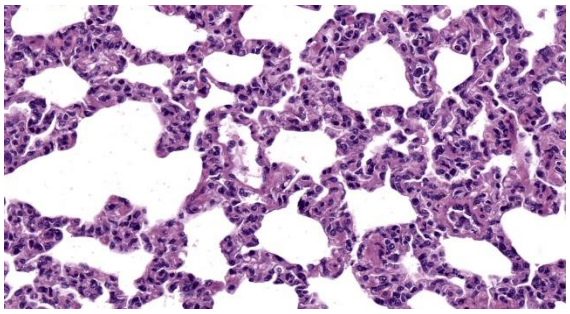

Figure 2-4. Lung, opossum. Alveolar septa are hypercellular with hyperplasia of intraseptal macrophages, lymphocytes, and neutrophils. (HE, 380X)

Participants noted the rather dramatic smooth muscle hyperplasia within vascular walls throughought the section, the extent of which seems inconsistent with the small number of organisms in section. Other participants noted that a prominent smooth muscle layer is normal in the vasculature of some species, such as the cat, and that opossum control tissue would be helpful in determining if the vascular "lesions" are, in fact, pathologic.

Finally, participants discussed the thickened alveolar septa and prominent diffuse interstitial pneumonia, lesions which are not typically associated with lungworm infection. Participants reviewed the clinical history and speculated that the interstitial pneumonia was likely due to bacterial sepsis. This separate pathogenesis warranted two separate differential diagnosis, with the bronchopneumonia attributed to the metastrongyles and the interstitial pneumonia attributed to sepsis.

References:

1. Bezerra-Santos MA, Ramos RAN, Campos AK, Dantas-Torres F, Otranto D. *Didelphis* spp. opossums and their parasites in the Americas: A One Health perspective. *Parasitol Res*. 2021; 120:4091-4111.
2. Caswell JL, Willians K. Respiratory system. In: Maxie MG, ed. *Jubb, Kennedy and Palmer's Pathology of Domestic Animals*. 6th ed. Vol 2. 2016;536-590.
3. Costa LP, Astúa D, Brito D, Soriano P, Lew D. *Didelphis albiventris* (amended version of 2015 assessment). The IUCN Red List of Threatened Species 2021.
4. Duncan RBJ, Reinemeyer CR, Funk RS. Fatal lungworm infection in a opossum. *J Wildl Dis*. 1989;25(2):266-269.
5. Gardiner CH, Poynton SL. *An Atlas of Metazoan Parasites in Animal Tissues*. American Registry of Pathology. Washington, DC;1999:27-29.
6. Jones KD. Oppossum nematodiasis: diagnosis and treatment of stomach, intestine, and lung nematodes in the Virginia opossum (*Didelphis virginiana*). *J Exot Pet Med*. 2013;22(4):375-382.
7. Lamberski N, Reader JR, Cook LF, Johnson EM, Baker DG, Lowenstine LJ. A retrospective study of 11 cases of lungworm (*Didelphostrongylus hayesi*) infection in opossums (*Didelphis virginiana*). *J Zoo Wildl Med*. 2002;33(2):151-156.
8. López-Crespo RA, López-Mayagoitia A, Ramírez-Romero R, Martinez-Burnes J, Prado-Rebolledo OF, Garcia-Marquez LJ. Pulmonary lesions caused by the lungworm (*Didelphostrongylus hayesi*) in the opossum (*Didelphis virginiana*) in Colima, Mexico. *J Zoo Wildl Med.* 2017;48(2):404-412.
9. Prestwood AK. *Didelphostrongylus hayesi* gen. et sp. n. (*Metastrongyloidea*: *filaroididae*) from the opossum, *Didelphis marsupialis*. *J Parasitol*. 1976;62 (2):272-275.
10. Rurangirwa FR, Teitzel CA, Cui J, et al. *Streptococcus didelphis* sp. nov., a *streptococcus* with marked catalase activity isolated from opossums (*Didelphis virginiana*) with suppurative dermatitis and liver fibrosis. *Int J Syst Evol Microbiol*. 2000;50:759-765.

CASE III:

Signalment:
5-year-old male porcupine (*Erethizon dorsatum*)

History:
This porcupine was born in captivity and transferred to another zoo one year later. The animal showed the following clinical signs: apathy, shortness of breath, and ataxia. The

clinical examination revealed a body temperature of 33.2°C. The animal died shortly after the onset of symptoms.

Gross Pathology:
Liver: On gross examination, the liver was predominantly wine-red, with some black-red areas. The liver margins were partly blunt-edged. The cut surface was demarcated, wine-red and firm. Furthermore, there were several to abundant beige-coloured, soft, sharply demarcated foci with a diameter of 1 to 5 mm.

Microscopic Description:
Liver: There are multifocal, randomly distributed hypercellular foci affecting 30% of the liver parenchyma. The foci consist of many macrophages, lymphocytes, and few neutrophils. Scattered hepatocytes display cytoplasmic swelling, pallor, membranous rupture, nuclear pyknosis and karyorrhexis (lytic necrosis). Within the inflammatory foci there are rare intrahepatocytic, intracytoplasmic, 15-20 µm in diameter, oval apicomplexan cysts with a thin capsule and more than 20, 1-2 µm, basophilic, banana-shaped bradyzoites, and rare extracellular, 1-2 µm, basophilic, oval tachyzoites. Portal areas are expanded by 2-5 layers of lymphocytes, macrophages, and plasma cells. There is minor

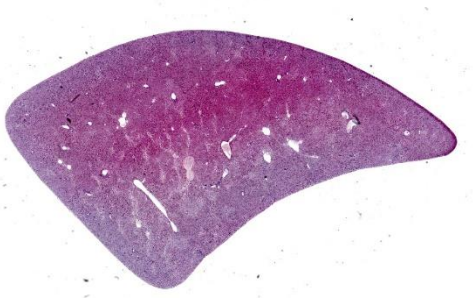

Figure 3-1. Liver, porcupine. The submitted section of liver does not show any lesion (except subjective rounding of edges) at subgross magnification. (HE, 5X)

and variably distributed bile duct hyperplasia and portal fibrosis.

Inflammatory changes with variable severity were found in the heart, lungs, intestines, spleen, urinary bladder, and brain (not on submitted slide).

Contributor's Morphologic Diagnosis:
Liver: Hepatitis, lymphohistioplasmacytic and necrotizing, multifocal, random, subacute, moderate with intralesional apicomplexan cysts.

Contributor's Comment:
Due to the typical histomorphological findings, an infection with *Toxoplasma gondii (T. gondii)* was suspected as the cause of the lesions in the present case. Immunohistochemistry was performed and *T. gondii* was verified as the causative agent.

Toxoplasmosis is one of the most common and widespread diseases in humans and warm-blooded animals worldwide.[10] In 1908, the parasitic pathogen was first isolated from a gundi (*Ctenodactylus gundi*) in Tunis and a rabbit from South America.[1] The genus toxoplasma contains *T. gondii* as the only species, which can be divided into 189 different genotypes.[1,3] The epidemiological and pathogenetic significance depends on the respective genotypes. In the northern hemisphere,

especially in Europe, the most common genotypes are 1 and 3. Genotypes 2 and 5 are mainly isolated in North America and genotypes 2 and 3 in Africa. In China, genotypes 9 and 10 represent the majority of isolates.[1] *T. gondii* has a very broad host spectrum; thus, numerous warm-blooded animals as well as humans are susceptible as intermediate host. Cats and wild felids serve as final hosts.

Epidemiology: Approximately one third of the world's human population is infected with *T. gondii*, although prevalence varies from region to region. In the USA and the United Kingdom, about 16 to 40% of people are infected.[7,9] In contrast, the infection rate in Central and South Africa and continental Europe is 50 to 80%.[9] Evidence of infection was found in 31 of the world's 39 felid species.[10] Prevalence in wildlife animals depends on various physical, biological, and ecological factors as well as climatic conditions and the susceptibility of host species.[10] The prevalence in marine mammals (e.g., seals, sea otters and dolphins) is particularly interesting, as it ranges from 47 to 100%. There have been some reports of toxoplasmosis in New World porcupines emphasizing this species as susceptible to the disease. Numerous comparable cases of toxoplasmosis have been described in various animals in zoologic gardens, including New World primates, Australian marsupials, and Pallas' cats.[2] Toxoplasmosis is an important cause of sporadic and epizootic mortality in zoo populations. In most cases, the affected animals are over 12 months old. Old world monkeys, rats, cattle, and horses seem highly resistant to infection.[1,2]

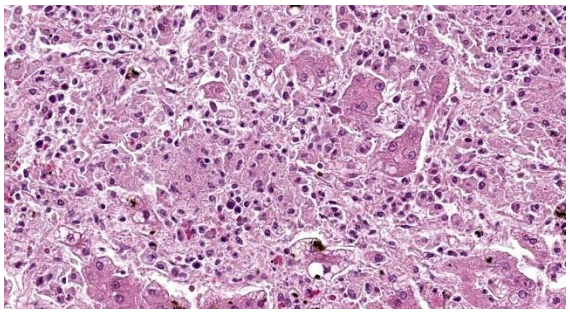

Figure 3-2. Liver, porcupine. There are areas of hepatocellular necrosis and loss with infiltration of macrophages and neutrophils randomly scattered throughout the section. (HE, 480X)

Pathogenesis/development cycle: *T. gondii* exhibits facultative heteroxenic development.[3,12] Depending on the position in the developmental cycle, different morphological stages of *T. gondii* occur.[8] Tachyzoites represent slightly curved, crescent-shaped cells with an apical complex at the anterior pole and a nucleus in the posterior half of the cell. The cell contains one chromosomal and one mitochondrial genome as well as a genome of circular DNA. Outside the host cell, the tachyzoites are only viable for a short period of time and are destroyed during gastric passage. During endodyogeny, bradyzoites are formed within the cyst lumina. The cysts, which are up to 150 µm in size, develop intracellularly in various tissues and, due to their resistant wall, have a relatively long life span in the host. A cyst can carry up to several thousand bradyzoites. The oocyst contains two sporocysts with four sporozoites each. Overall, development in the final and intermediate host proceeds along different paths, whereby only nucleated cells are infected. Both intermediate and definitive hosts can become infected under natural conditions mainly via three infectious routes: oral ingestion of oocysts from the environment (horizontal); oral ingestion of cysts within the tissues of intermediate hosts (horizontal); and diaplacental or galactogenic transmission of tachyzoites (vertical).

A particular key role in transmission or spread is played by cats, which are the only domestic animals that serve as a final host. In cats that are primarily infected by cysts, a massive excretion of oocysts, which can last

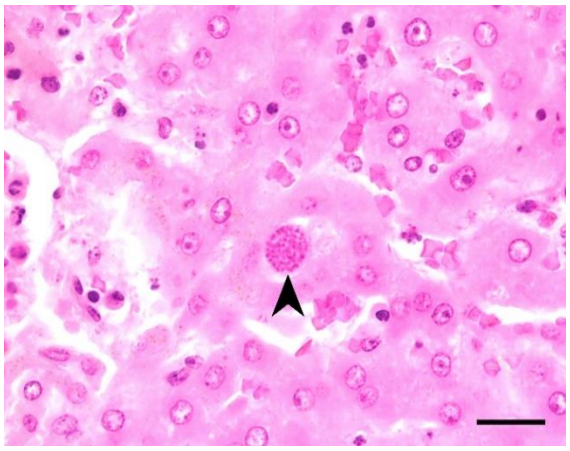

Figure 3-3. Liver, porcupine. Cytoplasmic cyst of *Toxoplasma gondii* within a hepatocyte. (*Photo courtesy of:* Institute of Veterinary Pathology, Faculty of Veterinary Medicine, Leipzig University; An den Tierkliniken 33, 04103 Leipzig, Germany; https://www.vetmed.uni-leipzig.de/institut-fuer-veterinaer-pathologie) (HE, 400X)

up to 20 days, occurs after a prepatency period of 3 to 10 days. The majority of bradyzoites released from ingested cysts usually remain in the small intestine. They initiate merogony and gametogeny in the intestinal epithelium, giving rise to the unsporulated oocysts. The remaining bradyzoites immediately penetrate the intestinal wall and reach the other internal organs via the lymphatic and blood pathways, resulting in extraintestinal development of the parasite. In contrast, when the cat is infected with oocysts, asexual reproduction must immediately take place in the extraintestinal organs. Some of the tachyzoites subsequently migrate into the intestinal wall and initiate development in epithelial cells until oocysts are formed. After a prepatency of 18 to 36 days, about 50 % of the cats excrete oocysts with the faeces.

The oocysts excreted by the cat are initially unsporulated and non-infectious. The generation of the infectious sporulated oocysts takes 1 to 5 days under conditions of sufficient oxygen supply, moisture, and temperature. Due to their very high resistance to environmental destruction, the sporulated oocysts pose a high risk of infection for humans and other animals. Once the intermediate host is infected, the bradyzoites or sporozoites immediately penetrate the intestinal wall after oral ingestion of the oocysts or cysts. This is followed by lymphohaematogenous spread into various organ systems, including mesenteric lymph nodes, liver, lungs and striated muscles. Two asexual multiplication phases are carried out in the organs. Intestinal development is absent.

Macroscopic and microscopic findings: Depending on the localization of the parasitic structures, macroscopic and histologic lesions can be found in several organs. The lungs, brain, and liver are most commonly affected by the changes.[4] The lungs show interstitial pneumonia, type II pneumocyte hyperplasia, and a necrotizing component associated with edema and hemorrhage. The liver shows mild hepatomegaly and clearly visible grey, white, or yellow foci. In histopathology of the liver, as in the other affected organs, necrosis is dominant. In the brain, *T. gondii* is found in most cases as a tachyzoite form in macrophages, glial cells, or neurons. Furthermore, it is possible to detect tissue cysts. In all affected organs, macrophages, lymphocytes and plasma cells are the dominant cell population of the inflammatory component. The formation of granulomas can occur. There may be a minor and variable neutrophilic component.
In a previously published case report of toxoplasmosis in a porcupine, microscopic changes were found in the liver, lungs, heart, and spleen, in agreement with the present case.[6] Reported histopathologic findings in porcupines include necrotizing hepatitis, lymphohistiocytic and necrotizing myocarditis, lymphohistiocytic encephalitis, and lymphohistiocytic interstitial nephritis.[6] Thin-walled tissue cysts with numerous bradyzoites, as well as tachyzoites, have been

described within alveolar macrophages, free in the alveoli, between myocardial fibers, and within glomeruli and tubular epithelial cells.[6]

Diagnosis: *T. gondii* infection can be diagnosed by many different methods. For the selection of the most suitable diagnostic procedure, the immune status of the patient, the clinical signs, and the severity of the symptoms should be considered. The detection can be done indirectly using serology or by direct detection of the parasite antigen or DNA.[10] The following techniques can be used: polymerase chain reaction (PCR; parasite detection), enzyme-linked immunosorbent assays (ELISAs; IgG/IgM/IgA detection; serology), indirect fluorescence antibody tests (IFATs; serology), comparative Western blotting (serology), Sabin-Feldman dye test (serology), and mouse bioassay. In veterinary medicine, histopathology and immunohistochemistry are of primary diagnostic importance. Furthermore, the diagnosis can be confirmed by electron microscopy.

Differential diagnosis: The genera *Hammondia*, *Neospora* and *Besnoitia* should be considered as etiologic differential diagnoses.[3] Like the genus *Toxoplasma*, these belong to the family Toxoplasmatidae. A reliable differentiation of the oocysts of the named genera is not possible by means of histological examination alone.

Contributing Institution:
Institute of Veterinary Pathology
Faculty of Veterinary Medicine
Leipzig University
Leipzig, Germany
https://www.vetmed.uni-leipzig.de/institut-fuer-veterinaer-patholgie/

JPC Diagnosis:
Liver: Hepatitis, necrotizing, subacute, multifocal, random, mild to moderate, with intracytoplasmic apicomplexan zoites.

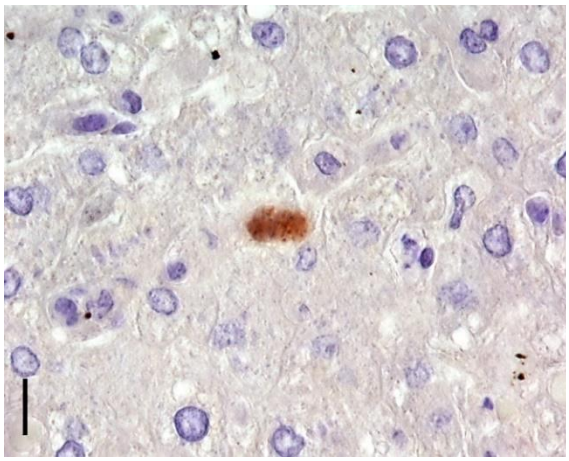

Figure 3-4. Liver, porcupine. Apicomplexan cysts are strongly immuopositive for antibodies against *Toxoplasm gondii*. (*Photo courtesy of:* Institute of Veterinary Pathology, Faculty of Veterinary Medicine, Leipzig University; An den Tierkliniken 33, 04103 Leipzig, Germany) (anti-*T. gondii*, 400X)

JPC Comment:
The contributor provides an excellent, thorough overview of toxoplasmosis, and rightly notes that *Toxoplasma gondii* infection has been documented in a wide range of mammalian hosts. Prevalence rates vary, but are throught to surpass 50% in dogs, rabbits, and sea otters; 60% in rats, mice, and birds; and 70% in humans, cats, bears, and deer.[13]

T. gondii has been extraordinarily successful by protozoal standards, and its successful transmission to many species worldwide is due, in part, to its ability to modify its hosts' behavior for its own benefit.[13] This "manipulation hypothesis" explains how parasites that are immature in the intermediate host ensure that they are eaten by the appropriate definitive host so the parasite can mature and complete its life cycle.[13] The classic toxoplasmosis pairing is the cat, which serves as the definitive host in which gamteogeny occurs, and the mouse, in which shizogeny occurs, and this classic pair provides an illustrative example of the manipulation hypothesis. Infective oocysts, which develop in the feline

host, are ingested by the wild rodent, where the parasites
undergo asexual reproduction followed by encystation in multiple tissues, including the brain.[13] Because sexual maturation can be accomplished only in felines, there is strong evolutionary pressure for the parasite to develop mechanisms to ensure transmission from the mouse to the cat through predation.[13]

Researchers investigating the behaviors of *T. gondii*-infected mice found that the infected mice showed decreased learning capacity and memory compared to their uninfected counterparts. Because cats are more attracted to moving, exposed prey, investigators conducted a series of studies to determine if *T. gondii* infection increased activity levels. Researchers determined that infected mice were more active than their uninfected counterparts and spent more time in exposed or novel environments than control mice.[13]

Subsequent mouse and rat studies evaluated whether *T. gondii* infection affected rodents' perception of cat predation risk as measured by their response to cat odor.[13] Cat odor is well-known to elicit aversion behavior in laboratory rodents, even after hundreds of generations have been raised in the laboratory environment with no lived experience with feline predation.[13] Results show that, while uninfected rodents show the expected aversive behaviors toward cat-treated areas, infected rodents exhibited not only a reduction in this aversive behavior, but also exhibited a significant, potentially suicidal preference for cat-treated areas.[13]

Convinced that *T. gondii* has behavior-modifying effects, researchers investigated whether treatment with antipsychotic drugs, many of which were known to inhibit *T. gondii* replication in cell cultures, could ameliorate the behavioral effects of *T. gondii* in rodents.[13] Infected but untreated rodents demonstrated the same attraction to feline odors as seen previously; however, following treatment with schizophrenia drugs such as haloperiodol and valproic acid, such cat-seeking behaviors, as well as the numbers of neurons and glial cells immunohistochemically positive for *T. gondii*, were significantly reduced.[13]

The mechanisms by which *T. gondii* modifies rodent behavior are currently unknown, though neuromodulation has been suggested as the dominant mechanism. Studies attempting to determine the neurologic basis of anxiety often use the reaction of rodents to cats as a research model, and such studies have found that blocking certain receptors in the amygdala or providing serotonin antagonists causes rodents to display the same lack of aversion to cats that *T. gondii*-infected rodents display.[13] Additional research has shown substantial differences in certain neurotransmitter levels in infected versus uninfected rodents, suggesting additional mechanisms by which *T. gondii* may be achieving its behavior modulatory effects.[13] Additional research is needed to further elucidate the protozoal magic that causes normally avoidant rodents to run headlong into the jaws of a primary predator. Though interesting in its own right, understanding these mechanisms could have profound implications for human behavior given the high levels of suspected *T. gondii* infection in the human population.

The moderator emphasized the need for molecular diagnostics when attempting to differentiate among the various apicomplexans, many of which look identical on H&E examination. Participants appreciated this straightforward example of hepatic toxoplasmosis, which sparked a discussion of how an organism such as *T. gondii*, which has no known

virulence factors, can cause such significant necrosis.

References:

1. Aguirre AA, Longcore T, Barbieri M, et al. The One Health approach to toxoplasmosis: epidemiology, control, and prevention strategies. *EcoHealth*. 2019;16(2):378-90.
2. Denk D, Neck S de, Khaliq S, Stidworthy MF. Toxoplasmosis in zoo animals: A retrospective pathology review of 126 cases. *Animals*. 2022;12(5).
3. Deplazes P, Eckert J, Samson-Himmelstjerna G von, Zahner H. *Lehrbuch der Parasitologie für die Tiermedizin.* 3. Auflage. Stuttgart: Enke Verlag; 2013; 87-94.
4. Dubey JP, Carpenter JL. Histologically confirmed clinical toxoplasmosis in cats: 100 cases (1952-1990). *J Am Vet Med Assoc.* 1993;203(11):1556-1566.
5. Control of intestinal protozoa in dogs and cats. ESCCAP Recommendation No. 6. https://www.esccap.de/empfehlung/protozoen/. Updated May 30, 2022. Accessed May 30, 2022.
6. Fayyad A, Kummerfeld M, Davina I, et al. Fatal systemic Toxoplasma gondii infection in a red squirrel (Sciurus vulgaris), a swinhoe's striped squirrel (Tamiops swinhoei) and a New World porcupine (Erethizontidae sp.). *J Comp Pathol.* 2016;154 (2-3):263-267.
7. Fuglewicz AJ, Piotrowski P, Stodolak A. Relationship between toxoplasmosis and schizophrenia: A review. *Adv Clin Exp Med.* 2017;26(6):1031-1036.
8. Halonen SK, Weiss LM. Toxoplasmosis. *Handb Clin Neurol.* 2013;114:125-145.
9. Hill D, Dubey JP. Toxoplasma gondii: transmission, diagnosis and prevention. *Clin Microbiol Infect.* 2002;8(10):634-40.
10. Robert-Gangneux F, Dardé M-L. Epidemiology of and diagnostic strategies for toxoplasmosis. *Clin Microbiol Rev*. 2012; 25(2):264-296.
11. Schnieder T, Boch J, eds. *Veterinärmedizinische Parasitologie.* 6. Aufl. Stuttgart: Parey; 2006; 144-148, 298, 366-367, 428-432.
12. Tenter AM, Heckeroth AR, Weiss LM. Toxoplasma gondii: from animals to humans. *Int J Parasitol.* 2000;30(12-13): 1217-1258.
13. Webster JP. The effect of *Toxoplasma gondii* on animal behavior; playing cat and mouse. *Schizophr Bull*. 2007;33(3):752-756.

CASE IV:

Signalment:
1-year-old male Visayan hornbill (*Penelopides panini*)

History:
The animal was found dead from suspected hypothermia following an enclosure heating malfunction. The animal was submitted for necropsy. No other birds were affected.

Gross Pathology:
The bird weighed 0.5 kg (slightly underweight) and was in lean body condition with ample skeletal muscle bulk and minimal body fat. The ventriculus contained a moderate amount of yellow, soft, diphtheritic material replacing the koilin layer centered on a central, ovoid, 14 x 18 mm mucosal ulcer. The adjacent duodenum was diffusely and transmurally reddened and contained moderate volumes of red-tinged mucoid fluid overlying eroded intestinal mucosa. Concurrent macroscopic findings included moderate diffuse splenomegaly and marked diffuse pulmonary edema.

Laboratory Results:
Microbiology: Anaerobic cultures of the ventriculus and small intestine isolated a moderate growth of *Clostridium perfringens*.

Figure 4-1. Ventriculus, hornbill. There is a thick fibrinonecrotic membrane adherent to the mucosa of the ventriculus. (*Photo courtesy of:* International Zoo Veterinary Group Pathology, https://www.izvg.co.uk/pathology/ about.htm)

Aerobic cultures produced mixed scant growth of *Proteus* spp., *Escherichia coli*, and *Enterococcus* spp. Selective cultures for *Salmonella, Campylobacter, Shigella,* and *Yersinia* were sterile.

PCR: The bacterial isolate was identified as *Clostridium perfringens* by matrix-assisted laser desorption/ionization time of flight (MALDI-TOF) analysis.

A PCR toxin profile identified alpha toxin; beta, epsilon, iota, beta-2, and enterotoxin were all absent.

Microscopic Description:
Ventriculus-duodenal junction: Overall affecting approximately 70-80% of the examined ventriculus, there is widespread multifocal-to-coalescing erosion and degeneration of the koilin layer, characterized by superficial erosive scalloping and variable separation of the superficial horizontal koilin matrix layers due to fibrillary to finely globular protein degeneration with numerous intralesional small interspersing colonies of gram-positive rod-like bacteria that range in size from 1-2 x 3-6 µm. Multifocal areas of more extensive koilin necrosis are seen, characterised by complete loss of horizontal koilin matrix architecture and replacement by hypereosinophilic amorphous koilin protein debris. Where extensive, koilin necrosis is confluent with regions of ventricular mucosal ulceration, with tissue replaced by hypereosinophilic lytic cytonuclear debris admixed with abundant fibrin, moderate heterophilic and histiocytic inflammation, and numerous small (approx. 50-micron diameter) to medium-sized (approx. 400-micron diameter) colonies of dense rod-like bacteria, together forming a fibrinonecrotising (diphtheritic) membrane. Remnant epithelial mucosa exhibits variable features of crypt dilatation (containing either fine fibrillary hypoeosinophilic proteinaceous content or hypereosinophilic koilin matrix) and epithelial cell degeneration (including cell swelling, loss of apical cilia, loss of cytoplasmic detail, karyorrhexis and nuclear pyknosis), the latter multifocally leading to lytic necrosis (cytoplasmic rupture, exudation of degenerate cytoplasm and karyolitic nuclei). Mild to moderate mixed inflammatory infiltrates (mostly degenerate heterophils, lymphocytes, and plasma cells with occasional macrophages) are seen throughout the lamina propria. Ventricular smooth muscle layers are multifocally disrupted by infiltrating heterophils with variable degrees of myofibrillar swelling, fiber splitting, striation loss, and nuclear pyknosis and karyorrhexis. Mild heterophilic infiltrates occasionally infiltrate through the subserosal layers, and are mostly associated with variably degenerate adipose tissue. Myenteric plexi are unaffected. Ventricular blood vessels exhibit relative increases in circulating heterophils (granulocytosis). Small sections of duodenum are also present in the examined section, which exhibit mild to moderate superficial autolytic mucosal exfoliation. Where better preserved, mild multifocal areas of lytic mucosal necrosis are

observed with associated loss of villi and crypts, plus blunting and fusion of remaining adjacent villi. Prominent lymphoplasmacytic infiltrates are seen within the lamina propria, with occasional heterophils scattered throughout. The submucosa, muscle layers, and serosa appear generally unremarkable. Gram stain confirms the prescence of numerous gram-positive, rod-like bacteria, consistent with *Clostridium perfringens*. Ziehl-Neelsen stain for acid-fast organisms is negative. PAS stains were negative for fungal organisms.

Pancreas: Histologically unremarkable.

Contributor's Morphologic Diagnosis:
Severe, subacute, multifocal-to-coalescing, fibrinonecrotising and ulcerative ventriculitis with koilin necrosis and intralesional gram-positive rod-like bacteria consistent with *Clostridium perfringens*, gizzard.

Contributor's Comment:
The gram-positive anaerobic spore-forming bacteria *Clostridium perfringens* is a major enteric pathogen in animals, represented by 7 distinct toxinotypes (A to G) based on the detection of 6 toxin genes: alpha (cpa gene), beta (cpb), epsilon (etx), iota (itx), enterotoxin (cpe), and necrotic enteric B-like toxin (netb).[1,2] Whilst typically found in intestinal flora of healthy birds, physiologic stress may promote *C. perfringens*-associated necrotic enteritis (NE), a significant disease caused by types A (cpa only), C (cpa and cpb), and G (cpa and netb-toxin).[3,5] Necropsy findings in this case include distended and friable small intestines with multifocal-to-coalescing fibrinonecrotising mucosal ulcers covered by "Turkish-towel"-like diphtheritic pseudomembranes.[2] *C. perfringens* may subsequently invade the portal system and biliary tract, causing cholangiohepatitis.[2] Histologically, gram-positive rod-like bacteria may be seen initially adhered to villous tips and later

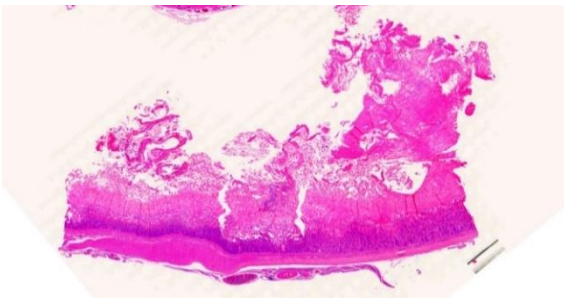

Figure 4-2. Ventriculus, hornbill. There is extensive loss of koilin and partial-thickness mucosal necrosis. A large fibrinonecrotic membrane extends into the lumen. (HE, 9X)

embedded within foci of mucosal to transmural intestinal necrosis.[2]

Outbreaks in avian collections occur infrequently, with clinical infection characterized by sudden onset of high mortality and small intestinal mucosal necrosis. NE typically affects domestic poultry but has also been described in more wild and exotic avian species such as lorikeets, macaws, toucans, and crows.[1-3,5,9] *C. perfringens* can be ubiquitous in the environment, particularly if soil-based substrate is used in the enclosure, therefore review of enclosure hygiene protocols is usually recommended in zoological collections when cases occur.

This case was particularly unusual in that the ventriculus was the primary organ affected, rather than the small intestine, which is more typical in other avian species. The most immediate cause of death was attributed to bacteraemic sepsis, based on the observation of heterophilic infiltrates within other viscera (i.e., liver, lung, and spleen) plus necrotizing hepatitis associated with similar intralesional gram-positive rod-like bacteria. To the contributor's knowledge, this is the first reported case of *C. perfringens*-associated ventriculitis in a hornbill, and in the Order Bucerotiformes.

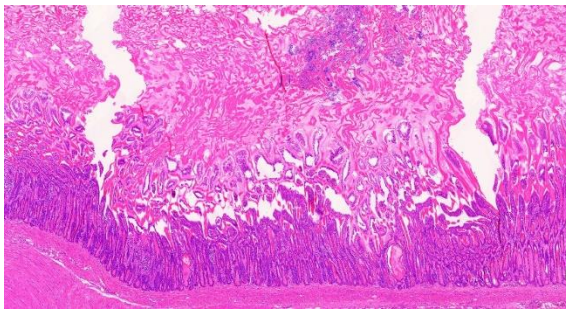

Figure 4-3. Ventriculus, hornbill. Higher magnification of the mucosal necrosis with numerous bacterial colonies. (HE, 48X)

Contributing Institution:
International Zoo Veterinary Group
Station House, Parkwood Street
Keighley, West Yorkshire
United Kingdom
http://www.izvg.co.uk/pathology/pabout.htm

JPC Diagnoses:
1. Ventriculus: Koilin erosion and ulceration, multifocal, subacute, moderate, with glandular hyperplasia and numerous extracellular bacteria.
2. Ventriculus: Vasculitis, fibrinoid and heterophilic, multifocal, moderate.
3. Adipose: Atrophy, diffuse, moderate.

JPC Comment:
Clostridium perfringens and its various subtypes and toxins are well-known to veterinary students, residents, and practitioners, who have developed all manner of mnemonics dedicated to classifying *C. perfringens* types based on toxin production. This pathogen is so well-known because it is so ubiquitous in the environment and is the cause of many distinct enteric diseases in humans and in a wide variety of animal species, particularly among herbivores.[8]

The currently classification scheme classifies *C. perfringens* types based on the production of particular "typing toxins," but all isolates produce numerous other toxins and hydrolytic
enzymes that contribute to virulence.[8] In addition, genes encoding beta, epsilon, and iota toxins are encoded on plasmids which also contain conjugation loci, and transfer of epsilon toxin plasmids from type D strains to type A strains, with subsequent production of epsilon toxin, which effectively turns type A into type D, has been observed, meaning that the beloved classification scheme is essentially based on the plasmid complement carried by an individual organism.[8]

The only clostridial toxin isolated in this case, alpha toxin (CPA), is a chromosomally-encoded toxin that is produced by all strains of *C. perfringens*.[8,10] CPA is a phospholipase that compromises cellular function by degrading phosphatidylcholine and sphingomyelin, both of which are components of eukaryotic cell membranes.[10] Release of CPA causes damage to erythrocyte and other cell membranes, resulting in cell lysis via phospholipid degradation and the activation of other cellular mechanisms that culminate in lysis. CPA also activates the arachidonic acid metabolic pathways, resulting in the production of thromboxanes, leukotrienes, and prostaglandins, resulting in inflammation and vasoconstriction.[10] In small amounts, CPA impaires leukocyte migration and causes their intravascular aggregation at the periphery of lesions, leading to a reduction in blood flow, subsequent hypoxia and necrosis, and the creation of an anaerobic niche for the proliferation of *C. perfrigens*.[10]

The role of CPA in mammalian intestinal disease is controversial. *C. perfringens* type A causes yellow lamb disease, a rare form of enterotoxemia in lambs that is characterized by depression, anemia, icterus and hemoglobinuria.[10] It is generally assumed that these clinical signs and the associated gross and microscopic lesions are caused by the action

of CPA, but no definitive proof is available.[10] Similarly, *C. perfrigens* type A is blamed for enteritis, abomasitis, and enterotoxemia in cattle, horses, goats, and pigs, though no definitive evidence for CPA's role in the pathogenesis of these diseases has been discovered.[10] The picture is further muddied by the detection of CPA in the intestinal contents of clinically healthy animals, making the presence of CPA diagnostically irrelevant for type A diseases in many species.[10] *C. perfringens* type A is known to produce gas gangrene (also known as malignant edema) in many domestic animals and in humans and CPA has long been assumed to be the causative agent; however, in a recurring theme, there is no concrete evidence that the disease produced by the bacterium is the result of CPA.[10]

The controversy surrounding CPA extends to avian diseases. While *Clostridium perfrigens* type A is frequently found as the sole agent in a variety of enteric avian diseases, it is unclear if CPA is responsible for the observed lesions.[3,5,8] In fact, CPA was long considered the key virulence factor for necrotizing enteritis in broiler chickens until recent research demonstrated that NetB, not CPA, is the main lesion-causing virulence factor produced by the newly-described *C. perfringens* type G strain.[5,7]

This case prompted robust discussion from conference participants, who noted, as did the contributor, how the ventriculus is an unusual and surprising location for *C. perfringens*-associated disease. Participants were surprised at the extent of the koilin destruction and ulceration, which would be an unusual manifestation of clostridial disease and is more intense than would be expected from stress induced from a relatively short period of cold exposure.

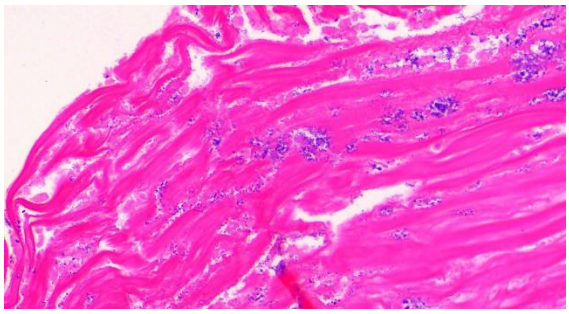

Figure 4-4. Ventriculus, hornbill. There are numerous bacterial colonies within the degenerate koilin in the ventricular lumen. (HE, 48X)

In general, koilin erosion and ulceration in the ventriculus of birds has many associated conditions, and is likely a multifactorial disease. In chickens, koilin erosion and ulceration is considered a syndrome and termed "gizzard erosion and ulceration," or GEU. Numerous causes for GEU have been proposed, including starvation, genetic factors, inappropriate feed, toxins, nutritional deficiencies, and infections. *C. perfringens* is one infection agent that has been putatively associated with this condition and may have caused the koilin erosion and ulceration in this case.[4]

Also of particular interest was the multifocal heterophilic vasculitis present through the ventriculus. The cause of this vasculitis is not apparent in the examined section and vasculitis is not a lesion commonly associated with clostridial infection in birds, leading participants to believe that this likely represents a separate pathologic process. As heterophilic vasculitis and koilin ulceration can be caused by fungal infections in birds,[6] participants scrutinized the section for fungal hyphae, but no fungal elements were observed. Other possible causes of vasculitis include bacterial sepsis, viral disease, and immune-mediated vasculitis. In this case, the cause of the vasculitis is ultimately unknown.

Participants also noted fat atrophy in the examined section, corresponding to the clinical history that the bird was underweight. The fat atrophy, vasculitis, and severe koilin layer ulceration and erosion comprise an unusual constellation of lesions which prompted an array of hypothetical pathogeneses, none of which could be definitely confirmed by the examined section alone. In the end, participants chose to separate each lesion into separate morphs due to the uncertain relationships between them.

References:

1. Asaoka Y, Yanai T, Hirayama H, et al. Fatal necrotic enteritis associated with *Clostridium perfringens* in wild crows (*Corvus macrorhynchos*). *Avian Pathol*. 2004;33 (1):19-24.
2. Boulianne M. Clostridial Diseases. In: Swayne DE, Boulianne M, Logue CM, et al., eds. *Diseases of Poultry*. 14th ed. Wiley-Blackwell; 2020.
3. De Santi M, Schocken-Iturrino RP, Casagrande MF, et al. Necrotic enteritis caused by *Clostridium perfringens* in blue and gold macaws (*Ara ararauna*). *J Avian Med Surg*. 2020;34(1):65-69.
4. Gjerve AG, Kaldhusdal M, Eriksen GS. Gizzard erosion and ulceration syndrome in chickens and turkeys: a review of causal or predisposing factors. *Avian Pathol*. 2013;42(4):297-303.
5. Grau-Roma L, Navarro M, Blatter S, et al. *Clostridium perfringens*-associated necrotic enteritis-like disease in coconut lorikeets (*Trichoglossus haematodus*). *Vet Pathol*. 2021;58(2):423-427.
6. Jeffrey JS, Chin RP, Shivaprasad HL, Meteyer CU, Droual R. Proventriculitis and ventriculitis associated with zygomycosis in ostrich chicks. *Avian Dis*. 1994;38(3):630-4.
7. Lee KW, Lillehoj HS. Role of *Clostridium perfringens* necrotic enteritis B-like toxin in disease pathogenesis. *Vaccines (Basel)*. 2022;10(1):61.
8. Rood JI, Adams V, Lacey J, et al. Expansion of *Clostridium perfringens* toxin-based typic scheme. *Anaerobe*. 2018;53:5-10.
9. Trupkiewicz J, Garner MM, Juan-Salles C. Passeriformes, Caprimulgiformes, Coraciiformes, Picipformes, Bucerotiformes and Podiformes. In: Terio K, Mcaloose D, St. Leger J, eds. *Pathology of Wildlife and Zoo Animals*, 1st ed. Academic Press;2018.
10. Uzal FA, Vidal JE, McClane BA, Gurjar AA. *Clostridium perfringens* toxins involved in mammalian veterinary disease. *Open Toxinology J*. 2010;2:24-42.

WSC 2023-2024
Conference 19 Self-Assessment

1. Which of the following is least likely to develop lesions associated with *Entamoeba invadens*?
    a. Snake
    b. Herbivorous turtles
    c. Lizard
    d. Crocodilians

2. *Entamoeba invadens* kills cells by which of the following?
    a. Oncosis
    b. Necrosis
    c. Trogocytosis
    d. Apoptosis

3. Which of the following is the intermediate host of the metastrongyle parasite *Didelphstrongylus hayesi*?
    a. Cockroaches
    b. Oligochaete worms
    c. Snails
    d. Copepods

4. How many species are in the genus *Toxoplasma*?
    a. 1
    b. 2
    c. 3
    d. 4

5. Necrotic enteritis caused by Clostridium perfringens is most commonly seen in which of the following?
    a. Corvid birds
    b. Chickens
    c. Waterfowl
    d. Zoo birds

Joint Pathology Center
Veterinary Pathology Services

WEDNESDAY SLIDE CONFERENCE 2023-2024

Conference #20 **14 February 2024**

CASE I:

Signalment:
12-year-old, female spayed Schipperke dog (*Canis familiaris*)

History:
A 12-year-old, female spayed Schipperke dog presented with multisystemic disease including severe enteropathy, hepatopathy, pneumonia, and dermatitis. The patient had been on long-term budesonide, prednisone, and dexamethasone for inflammatory bowel disease.

Gross Pathology:
Gross examination revealed severe ulceration of the mucosal surface of the colon, with abundant necrotic and fibrinous debris overlying the sites of mucosal injury. The medial/internal aspect of the right ear pinna was crusted with regionally extensive ulceration and mild hemorrhage. The skin, sclera, gingiva, and subcutaneous fat were mildly icteric. The liver was friable and homogenously pale tan and moderately enlarged, with slightly rounded margins. All liver lobes had disseminated pale tan foci ranging from 3-5 mm in diameter. The spleen was mildly enlarged with a meaty consistency. The lungs were diffusely mottled pink to purple, with similar disseminated pale tan foci as the liver. The bone marrow (left femur) was diffusely reddened.

Figure 1-1. Colon, dog. There is diffuse ulceration of the colonic mucosa with abundant adherent necrotic debris. (*Photo courtesy of:* Veterinary Diagnostic Laboratories, Colorado State University, Fort Collins, CO, http://csu-cvmbs.colostate.edu/vdl/Pages/default.aspx)

Laboratory Results:
Neospora caninum PCR: DNA detected in colon samples.
Toxoplasma gondii PCR: DNA not detected in colon.
Leishmania spp. PCR: DNA not detected in liver samples.

Microscopic Description:
Colon: There is marked multifocal to coalescing ulceration of the colonic mucosa. Overlying the injury are thick mats of necrotic cellular debris, fibrin, large numbers of histiocytes and degenerate neutrophils, entrapped mixed bacteria, and low amounts of hemorrhage. Inflammation, necrosis, and edema extend deep throughout the submucosa and muscularis, disrupting the mural architecture. Throughout areas of inflammation and within muscle fibers of the muscularis are myriads of unicellular tachyzoite parasitic organisms. Tachyzoites are 2-3 µm long by

Figure 1-2. Colon, dog. There is diffuse ulceration of the mucosa and multifocal transmural necrosis of the wall. (HE, 5X)

1-2 µm wide, almond shaped, with a round basophilic nucleus, and perinuclear clearing extending to both tapered ends. Rarely there are encapsulated clustered of tachyzoites (cysts). These organisms are also present within epithelial cells and endothelial cells.

Protozoal tachyzoites and cysts stain positive for Giemsa and negative for GMS and Gram stain.

Contributor's Morphologic Diagnosis:
Colon: Severe, multifocal to coalescing, necroulcerative colitis with myriad intralesional protozoa.

Contributor's Comment:
In addition to the lesions in the colon, tachyzoites were identified in the liver, spleen, and skin, and fewer numbers were identified in the bone marrow and lungs. There was variable necrotizing to histiocytic inflammation in each affected tissue. The morphology of the tachyzoites, along with the detection of *Neospora caninum* by PCR, are diagnostic of an unusual case of disseminated neosporosis. Differentials considered included *Toxoplasma gondii* and *Leishmania* spp. Toxoplasmosis cannot be distinguished from neosporosis histologically. Molecular diagnostics such as PCR have been instrumental in the diagnosis and differentiation of the two diseases. Leishmaniasis typically can be distinguished from the apicomplexan parasites due to the presence of the kinetoplast within amastigotes, but this is not always readily identifiable in standard H&E preparations.

Neospora caninum is an apicomplexan parasitic organism with a heteroxenous life cycle, for which canids are the definitive host.[4,7,8] In canids, disease is uncommon but typically presents as neuromuscular disease.[8,12,13] In puppies (<6 months) the typical clinical presentation is an ascending, progressive paralysis with rigidity and muscle atrophy, mostly of the pelvic limbs.[3,4,5,12] Adult dogs may experience recrudescence of latent infections, with multifocal CNS signs and polymyositis. The gross findings may include embolic foci of necrosis and hemorrhage in the brain and spinal cord and white streaking, corresponding to necrosis, in the muscles. Tachyzoites can be found free in the tissues or within histiocytes, endothelial cells, neurons, and epithelial cells, and are usually accompanied by marked necrosis and granulomatous inflammation.[1,2,5,6,12]

Cases of myocarditis, pneumonia, dermatitis, and dissemination are less common and have typically been associated with immunosuppression including steroid or chemotherapeutic administration.[4,9,10,11] In this case, the pa

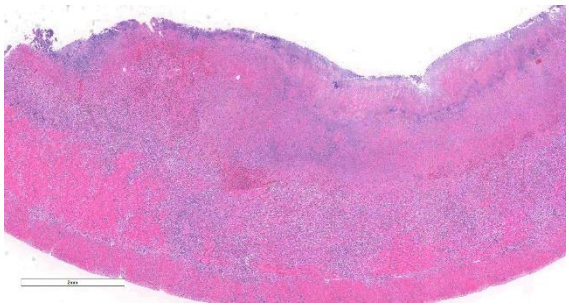

Figure 1-3. Colon, dog. There is transmural necrosis of the wall. (HE, 15X)

tient was on immunosuppressive doses of budesonide, prednisone, and dexamethasone for presumptive inflammatory bowel disease. Additionally, the patient had a history of coprophagia as well as regular exposure to cattle. Cattle are the most common intermediate host, for which mid-term abortion (at about 5-6 months gestation) is the most common clinical presentation.[3,4,5,7,8,] The absence of gross lesions is common in cattle; however, if present, the pathognomonic lesion in aborted fetuses is multifocal foci of necrosis in brain tissue.[5,6,14]

Contributing Institution:
Veterinary Diagnostic Laboratories
Colorado State University
Fort Collins, CO
http://csu-cvmbs.colostate.edu/vdl/Pages/default.aspx

JPC Diagnosis:
Colon: Colitis, necrotizing, multifocal to coalescing, transmural, with vasculitis, thrombosis, and numerous intramyocytic, intraendothelial, and free zoites.

JPC Comment:
Neospora caninum shares many histologic and biologic features with the closely related apicomplexan parasite *Toxoplasma gondii*; however, there are key differences between the two related to host range, virulence factors, and pathogenesis.[4] *N. caninum* follows a life cycle in which canids, including domestic and wild dogs, coyotes, wolves, and dingoes, serve as definitive hosts where sexual replication occurs, and a variety of intermediate hosts provide the ecological niche for asexual replication. As the contributor notes, the most common intermediate host is cattle, and it appears that the *N. caninum* life cycle is maintained globally through the close association between domestic dogs and cattle farms.[4] Evidence also exists for a sylvatic cycle, involving wild canids and ruminant species in North

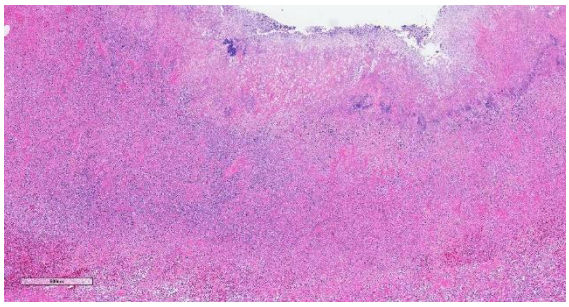

Figure 1-4. Colon, dog. Higher magnification of the transmural necrosis. (HE, 25X)

America, with a particular high seroprevalence noted among North American white-tailed deer.[4]

The *N. caninum* life cycle involves three main life stages: sporozoites within sporulated oocysts, rapidly dividing tachyzoites, and slowly dividing bradyzoites that are sequestered from the host immune system within tissue cysts.[4] The oocyst is the environmentally hearty form of the parasite and is formed by sexual replication in the intestinal epithelial cells of canids and subsequently expelled in their feces. The oocysts then sporulate within 24-72 hours in the environment and develop two sporocysts, each of which contains four sporozoites.[4] Intermediate hosts become infected by ingesting sporulated oocysts, which then release their sporozoites in the gastrointestinal tract. Sporozoites then infect intestinal epithelial cells, where they transform into tachyzoites that infect a variety of nucleated cells, including mononuclear cells that can traffic them throughout the body, and then replicate within parasitophorous vacuoles within the host cell cytoplasm.[4]

During acute infection, tachyzoites may be found in almost all tissues of the body and repeated cycles of replication, host cell lysis, tachyzoite release, and infection of surrounding cells produce characteristic lesions and clinical signs. After approximately 20 cycles of replication, tachyzoites differentiate into

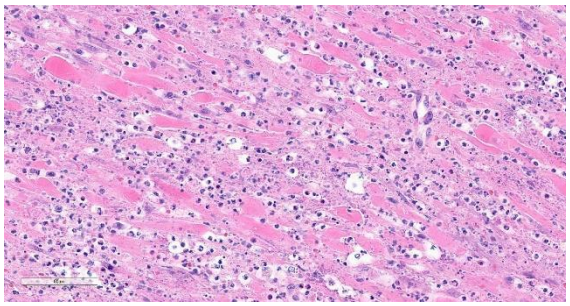

Figure 1-5. Colon, dog. There is extensive necrosis within the smooth muscle of the inner longitudinal layer. Some fibers are shrunken and hypereosinophilic (atrophy) (HE, 300X)

bradyzoites within tissue cysts under pressure from the host immune response, and a quiescent, asymptomatic infection develops that can last for the life of the host.[4] This long-term persistent infection may recrudesce with changes in the host's immune status, such as pregnancy, immunodeficiency, or, as in this case, immunosuppressive therapy.[4]

Transmission of *N. caninum*, which can be vertical or horizontal, has been extensively studied due to the economic losses caused by abortions in infected cattle herds.[3,4] Vertical transmission is the predominant form of transmission in cattle, and can occur following ingestion of sporulated oocysts from the environment (exogenous transplacental transmission) or following recrudescence of infection of a persistently infected cow during pregnancy (endogenous transplacental transmission).[4] Endogenous transplacental transmission is the main mechanism by which *N. caninum* is maintained in the domestic cattle population, with fetal transmission rates as high as 95%.[4] Persistently infected cattle have an abortion risk between 1.7-7.4 times the risk of a naïve cow, though the risk diminishes with successive pregnancies, suggesting that some degree of host immunity sufficient to frustrate endogenous transplacental transmission develops over time.[4]

As illustrated by this case, a robust host immune response is critical to controlling *N. caninum* infection. Studies in cattle demonstrate that a Th1-type response is essential for restricting parasite replication and the conversion of tachyzoites to bradyzoites in tissue cysts.[4] Conversely, host immunosuppressiontips the scales toward a Th2-type response, causing recrudescence characterized by the conversion of bradyzoites to tachyzoites and uncontrolled tachyzoite proliferation.[4]

The role of humoral immunity is less clear, but it likely controls *N. caninum* infection by antibody neutralization of extracellular tachyzoites.[4]

This week's moderator was Dr. Francisco Uzal, Professor in the Department of Pathology, Microbiology and Immunology at the University of California Davis School of Veterinary Medicine and the California Animal Health and Food Safety Laboratory. Discussion of this case initially centered on the terms "ulceration" and "erosion," and whether either was appropriate to describe the mucosa in this case. Conference partici

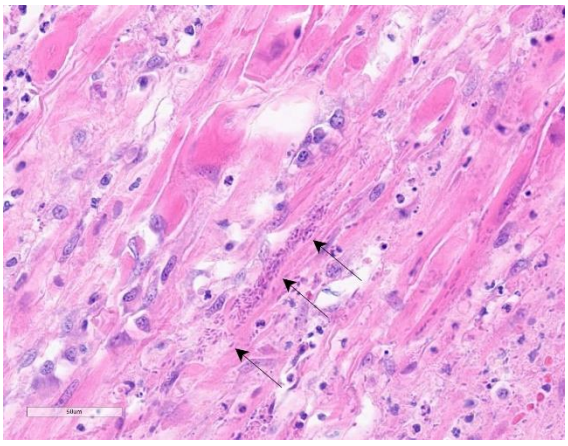

Figure 1-6. Colon, dog. Attempts at regeneration of damaged smooth muscle are evidenced by large, often pleomorphic nuclei within smooth muscle cells. Leiomyocytes occasionally contain a cytoplasmic cyst containing numerous zoites (arrows). (HE, 400X)

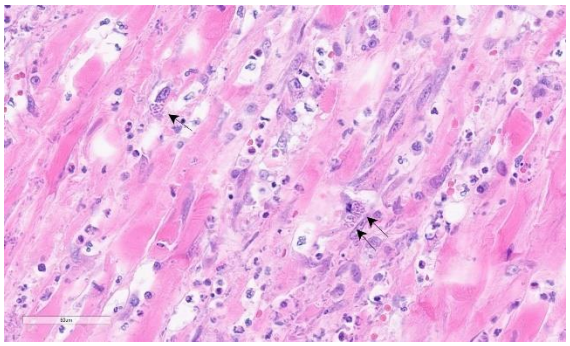

Figure 1-7. Colon, dog. Another field in which smooth muscle cells contain cytoplasmic apicomplexan cysts. (HE, 400X)

pants opined that the difference between the two was a matter of depth, with some participants using "ulceration" to indicate that the mucosal epithelium is lost, whereas others define the term to mean a lesion that extends deep to the muscularis mucosa. The term "erosion," for both camps, is reserved for more superficial mucosal loss, especially in areas in which the mucosa is composed of multiple layers of cells, such as the esophagus.

Participants next discussed the significant vasculitis observed throughout the section and whether the vasculitis was the cause or an effect of the massive, transmural necrosis present throughout the section. Participants felt that, while organisms were found in many endothelial cells, the vasculature was largely caught up in the inflammatory and necrotic milieu produced by *N. caninum*. Participants also noted the clinical history of inflammatory bowel disease and wondered if pathology associated with that condition was confounding histologic interpretation.

Discussion of the morphologic diagnosis was relatively straightforward in this case, though participants felt they would not have been able to determine whether the section was from the large or small intestine without the contributor's tissue identification. Participants also felt that the vasculitis and the tissue distribution of the organisms were notable histologic features and were thus included in the morphologic diagnosis.

References:

1. Barber JS, Trees AJ. Clinical aspects of 27 cases of neosporosis in dogs. *Vet Rec*. 1996;139(18):439-443.
2. Brown CB, Baker DC, Barker IK, 2007. The alimentary system. In: Maxie MG, ed. *Jubb, Kennedy, and Palmer's Pathology of Domestic Animals*. 5th ed. Vol 2. 2007; Elsevier Saunders: 272-273.
3. Buxton D, McAllister MM, Dubey JP. The comparative pathogenesis of neosporosis. *Trends Parasitol*. 2002;18(12):546-552.
4. Donahoe SL, Lindsay SA, Krockenberger M, Phalen D, Slapeta J. A review of neosporosis and pathologic findings of Neospora caninum infection in wildlife. *Int J Parasitol Parasites Wildl*. 2015; 4(2):216-238.
5. Dubey JP. Review of Neospora caninum and neosporosis in animals. *Korean J Parasitol*. 2003;41(1):1-16.
6. Dubey JP, Schares G. Diagnosis of bovine neosporosis. *Vet Parasitol*. 2006;140(1-2):1-34.
7. Dubey JP, Schares G, Ortega-Mora LM, Epidemiology and control of neosporosis and Neospora caninum. *Clin Microbiol Rev*. 2007;20(2):323-367.
8. Dubey JP, Jenkins MC, Rajendran C, Miska K, Ferreira LR, Martins J, et al. Gray wolf (Canis lupus) is a natural definitive host for Neospora caninum. *Vet Parasitol*. 2011;181(2-4):382-387.
9. Hoon-Hanks LL, Regan D, Dubey JP, Porter MC, Duncan CG. Hepatic neosporosis in a dog treated for pemphigus foliaceus. *J Vet Diagn Invest*. 2013;25(6):807-810.
10. La Perle, KM, Del Piero F, Carr RF, Harris C, Stromberg PC. Cutaneous neosporosis in two adult dogs on chronic

immunosuppressive therapy. *J Vet Diagn Invest*. 2001; 13(3):252-255.
11. Magaña A, Sánchez F, Villa K, Rivera L, Morales E. Systemic neosporosis in a dog treated for immune-mediated thrombocytopenia and hemolytic anemia. *Vet Clin Pathol*. 2015;44(4):592-596.
12. Reichel MP, Ellis JT, Dubey JP. Neosporosis and hammondiosis in dogs. *J Small Anim Pract*. 2007;48(6):308-312.
13. Ruehlmann D, Podell M, Oglesbee M, Dubey JP. Canine neosporosis: a case report and literature review. *J Am Anim Hosp Assoc*. 1995;31(2):174-183.
14. Schlafer DH, Miller RB. Female genital system. In: Maxie MG, ed. *Jubb, Kennedy, and Palmer's Pathology of Domestic Animals*. 5th ed. Vol 3. 2007; Elsevier Saunders:514–516.

CASE II:

Signalment:
Three month old female Quarter Horse (*Equus caballus*)

History:
A 3-month-old Quarter Horse filly presented to the Iowa State University Equine Internal Medicine Service for diarrhea of two weeks duration. The foal had been treated with omeprazole and sucralfate and several courses of trimethoprim sulfa and ceftiofur with no resolution of clinical signs.

Gross Pathology:
There were severe multifocal to coalescing, 0.1 cm to 5 cm pale nodules in all lung lobes. Some nodules were cream-colored with a friable consistency and were surrounded by a firm, white capsule. Others had a pale yellow liquid exudate exuding from the center of the nodule. The jejunum had multifocal, up to 0.5 cm in diameter ulcerations. Throughout the large colon and cecum, there were multifocal to coalescing ulcerations of the mucosa, which were covered by thick, yellow to dark

Figure 2-1. Colon, horse. Throughout the large colon and cecum, there are multifocal to coalescing ulcerations of the mucosa. On the serosal surface, mostly along the mesentery, there are numerous multifocal to coalescing nodules containing caseous yellow material. (*Photo courtesy of*: Department of Veterinary Pathology, College of Veterinary Medicine, Iowa State University, https://vetmed.iastate .edu/vpath)

green, friable material. On the serosal surface, mostly along the mesentery, there were numerous multifocal to coalescing nodules containing caseous yellow exudate. These nodules had a thick white capsule and ranged in size from 1 mm to 5 cm. The peritoneal cavity contained yellow, cloudy fluid.

Laboratory Results:
A fecal sample was submitted to UC Davis for foal gastrointestinal and diarrhea panel testing (*Clostridium difficile* toxins A and B, Equine coronavirus, *Lawsonia intracellularis*, *Salmonella* spp, *Cryptosporidium* spp, equine rotavirus, *Rhodococcus equi*, *Clostridium perfringens* antigen and toxins CPA, CPB, CPB2, netF, and CPE). The sample was positive for *Rhodococcus equi* and *Rhodococcus* VapA gene was confirmed by PCR.

Microscopic Description:
Colon, cecum, and mesenteric lymph node: Elevating the ulcerated mucosa, expanding

the submucosa and muscularis with extension to the serosa and the nearby lymph node are multifocal to coalescing aggregates of hypereosinophilic coagulum surrounded by numerous degenerate neutrophils admixed with plump foamy macrophages, epithelioid macrophages and multinucleated giant cells that frequently contain clusters of basophilic 1 to 3 um coccobacilli (pyogranulomatous inflammation with liquefactive necrosis). The mucosa is partially or completely devoid of epithelium and is replaced by fibrinonecrotic debris and similar inflammatory cells surrounded by proliferated fibrous connective tissue. Multifocally, blood vessels are occluded by numerous degenerate inflammatory cells, foamy macrophages with intracytoplasmic coccobacilli, and hyalinized fibrinous meshes. Within the mesenteric lymph node, there is a complete loss of nodal architecture and the cortex and medulla are replaced by pyogranulomas.

Histochemical staining: The intrahistiocytic coccobacilli are highlighted by Gram stain (in blue color) and Fite's stain.

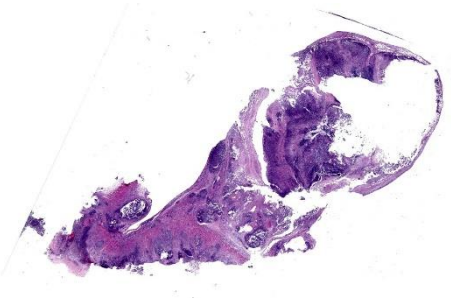

Figure 2-2. Colon and lymph node, horse. A section of colon and adjacent lymph node is submitted. The mucosa and submucosa are effaced by abundant pyogranulomatous inflammation that multifocally extends into the underlying muscularis and serosa. The lymph node is effaced by the same inflammatory infiltrate. (HE, 5X)

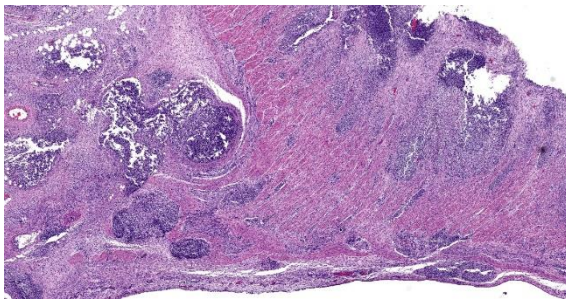

Figure 2-3. Colon, horse. Higher magnification of pyogranulomatous inflammation within the colonic wall. (HE, 20X)

Contributor's Morphologic Diagnoses:

1. Colon and cecum: Severe, multifocal to coalescing, chronic, pyogranulomatous, fibrinonecrotic typhlocolitis, with numerous intrahistiocytic coccobacilli.
2. Lymph nodes: Severe, multifocal to coalescing, chronic, pyogranulomatous lymphadenitis with numerous intrahistiocytic coccobacilli.

Contributor's Comment:

Rhodococcus equi is a gram-positive, facultative intracellular bacterium commonly found in soil and the gastrointestinal tract of herbivores.[6] The pathogen primarily causes diseases in foals and also affects cattle, sheep and goats, pigs, dogs, llamas, and immunocompromised humans.[1,3,6] Infections of *Rhodococcus equi* usually occur in foals between 1 and 6 months of age and usually present as pyogranulomatous bronchopneumonia and ulcerative enterocolitis.[6]

In horses, inhalation of the bacterium from the environment and swallowing of mucus-containing *Rhodococcus equi* from the airway are the major routes of infection.[3,6] *R. equi* is phagocytosed by macrophages and dendritic cells through the mannose-binding receptor, and the uptake of the bacteria is enhanced by complement and complement receptor 3.[9] With plasmid pathogenicity island (PAI)-encoded virulence-associated protein A (VapA) gene and positive regulators (orf4 and orf8), *Rhodococcus equi* can survive and

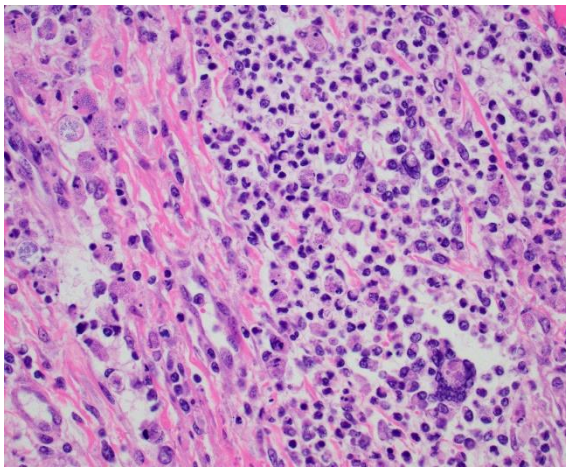

Figure 2-4. Colon, horse. Pyogranulomas are composed of numerous variably degenerate neutrophils admixed with plump foamy macrophages, epithelioid macrophages, and multinucleated giant cells that frequently contain clusters of basophilic, 1 to 3 um coccobacilli. (HE, 400X) (*Photo courtesy of*: Department of Veterinary Pathology, College of Veterinary Medicine, Iowa State University)

replicate in macrophage phagosomes through inhibition of phagosome acidification and phagosome-lysosome fusion.[6,7,9] Hematogenous dissemination within macrophages to other sites in the body then occurs. Horizontally-acquired chromosomal virulence factors, such as a polysaccharide capsule, mycolic acid, lecithinase, phospholipase C, and cholesterol oxidase also play key roles in the development of systemic pyogranulomatous inflammation.[6,7,9] In goats and pigs, *R. equi* with VapN and VapB plasmids, respectively, are considered the virulent strains that cause systemic pyogranulomatous inflammation.[7] *R. equi* without the aforementioned Vap genes are classified as avirulent.[4]

In foals, multifocal to coalescing nodules with caseous centers usually develop in the cranioventral lung, but all lung lobes may be affected in severe cases.[6] Volcano ulcers covered by necrotic debris are seen over Peyer's patches in the small intestine, cecum, and large colon.[6] The nearby lymph nodes are enlarged with variably-sized abscesses. The histologic features of *R. equi* infection include suppurative to pyogranulomatous bronchopneumonia with numerous neutrophils, macrophages, and multinucleated giant cells. In the intestine, infiltration of macrophages and neutrophils in the lymphoid follicles and caseous necrosis that extends to the covering epithelium are characteristic features. With time, the mucosa is covered with thick fibrinonecrotic debris. Some foals can also develop polyarthritis, osteomyelitis, and abscessation in multiple internal organs.[6,7] Infrequently, abortion caused by *R. equi* has been described in horses, with fetal lesions comparable to those in foals.[5] With special histochemical stains, *R. equi* is gram-positive and weakly acid-fast.

Differential diagnoses for systemic pyogranulomatous inflammation in horses include fungal and mycobacterial infections; however, concurrent pyogranulomatous pneumonia and ulcerative enterotyphlocolitis are characteristic of *R. equi*. Bacterial culture with positive detection of the VapA gene in isolated *R. equi* can confirm the diagnosis.

Contributing Institution:
Department of Veterinary Pathology
College of Veterinary Medicine
Iowa State University
https://vetmed.iastate.edu/vpath

JPC Diagnoses:
1. Colon: Colitis, pyogranulomatous and necrotizing, chronic, multifocal to coalescing, severe, with pyogranulomatous lymphangitis and edema, and numerous intrahistiocytic and free coccobacilli.
2. Lymph node: Lymphadenitis, pyogranulomatous and necrotizing, chronic, multifocal to coalescing, severe, with numerous intrahistiocytic and free coccobacilli.

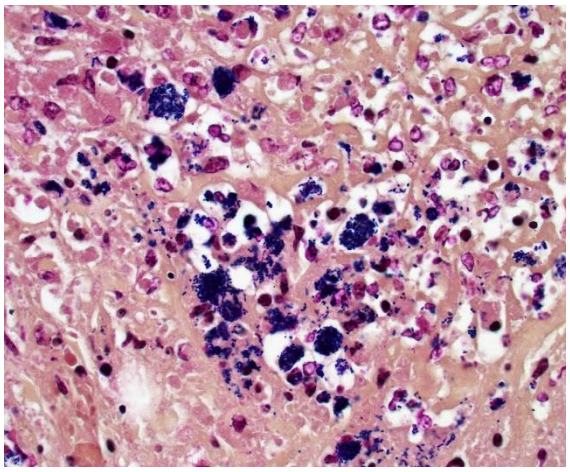

Figure 2-5. Colon, horse. A Gram stain highlights bacteria within macrophages. (Gram, 400X) (*Photo courtesy of*: Department of Veterinary Pathology, College of Veterinary Medicine, Iowa State University)

JPC Comment:

As the contributor notes, pathogenic *Rhodococcus equi* strains have the ability to replicate unimpeded within equine macrophage vacuoles.[2] The ability to persist inside these vacuoles is dependent on the rapid and abundant production of virulence-associated protein A (VapA), which is triggered primarily by temperatures above 33ºC, as occurs in mammalian hosts, and secondarily by low environmental pH.[2] Once expressed, VapA localizes to the bacterial membrane where it interacts with or is released into the vacuolar environment.[2,8]

VapA promotes the intracellular survival of *R. equi* by increasing phagosome and lysosome pH. Reserachers were initially surprised to find lysosomal acidification affected by VapA since *R. equi* multiply, and VapA is produced, within special phagocytic vacuoles that are distinct from host cell lysosomes; however, further research demonstrated that VapA is transferred from the phagocytic vacuole to lysosomes early in infection, possibly by vesicular transport.[8] In both the phagocytic vacuole and the lysosome, secreted VapA raises the pH of the compartment, leading to increased proliferation of *R. equi* and inactivation of acid hydrolases that would normally kill and digest the organisms.[2]

VapA raises the pH of intracellular compartments via two main mechanisms, the first of which is the exclusion of the proton-pumping ATPase (vATPase) from the phagosome membrane.[8] In normal cellular metabolism, lysosomal and phagosomal membranes are enriched with hundreds of vATPase complexes which acidify the lysosome by pumping hydrogen ions from the cytosol into the lysosome. In phagosomes and lysosome containing VapA, however, the plasma membranes have minimal, background levels of vATPase complexes, and this vATPase exclusion continues with prolonged infection times, preventing rapid acidification of lysosomes.[8] The exact mechanism of the vATPase exclusion remains unknown.

VapA also raises the pH of lysosomes and phagosomes by permeabilizing their lipid membranes, further dissipating the acidic proton gradient.[2,8] Studies have demonstrated that this permeabilization *in vivo* is sufficient to allow the release of protons or protonated water, but not complete enough to lead to lysis of the phagosomal or lysosomal membranes.[2] The end result of these two mechanisms is to create "leaky," semipermeable intracytoplasmic niches of relatively neutral pH where *R. equi* can thrive.

The intracellular thriving of *R. equi* is well illustrated in this slide, with scores of coccobacilli packed within macrophages and free throughout the examined tissue. The tremendous tissue damage wrought by *R. equi* once again made tissue identification difficult for conference participants, though most were able to narrow the tissue to either cecum or colon. Some participants remarked on prominent smooth muscle in the wall of many

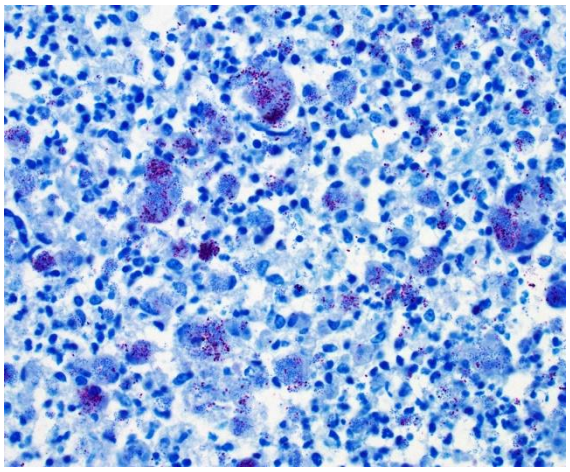

Figure 2-6. Colon, horse. Coccobacilli are acid-fast, as demonstrated by a Fite-Faraco stain. (Fite-Faraco, 400X)(*Photo courtesy of*: Department of Veterinary Pathology, College of Veterinary Medicine, Iowa State University)

vessels in section; however, the moderator noted that this, along with occasional mineralization, is a common, incidental feature of equine vasculature.

The moderator noted that VapA production is necessary for pathogenesis and that *R. equi* strains without the plasmid-encoded gene are clinically inert. While an etiologic diagnosis of *R. equi* infection may technically require PCR for the VapA gene, the moderator noted that *R. equi* has a distinctive look (pyogranulomas, volcano ulcers) and distribution (lungs and colon) that make the diagnosis fairly straightforward if you have good old-fashioned horse sense. This is particularly true when, as in this case, the tremendous tissue destruction provides strong gross and histologic circumstantial evidence of pathogenicity.

References:

1. Bryan LK, Clark SD, Díaz-Delgado J, et al. Rhodococcus equi infections in dogs. *Vet Pathol*. 2017;54(1):159-163.
2. Hansen P, Haubenthal T, Reiter C, et al. Differential effects of *Rhodococcus equi* virulence-associated proteins on macrophages and artificial lipid membranes. *Microbiol Spect.* 2023;11(2):e0341722.
3. Löhr CV, O'Neill TW, Daw DN, Pitel MO, Schlipf JW. Pyogranulomatous enteritis and mesenteric lymphadenitis in an adult llama caused by *Rhodococcus equi* carrying virulence-associated protein A gene. *J Vet Diagn Invest*. 2019;31(5):747-751.
4. Stranahan LW, Plumlee QD, Lawhon SD, Cohen ND, Bryan LK. Rhodococcus equi infections in goats: characterization of virulence plasmids. *Vet Pathol*. 2017;55(2): 273-276.
5. Szeredi L, Molnár T, Glávits R, et al. Two cases of equine abortion caused by Rhodococcus equi. *Vet Pathol*. 2006;43(2):208-211.
6. Uzal FA, Plattner BL, Hostetter JM. Alimentary system. In: Maxie MG, ed. *Jubb, Kennedy, and Palmer's Pathology of Domestic Animals*. Vol 2. 6th ed. Elsevier; 2016:197-198.
7. Vázquez-Boland JA, Giguère S, Hapeshi A, MacArthur I, Anastasi E, Valero-Rello A. Rhodococcus equi: the many facets of a pathogenic actinomycete. *Vet Microbiol*. 2013;167(1-2):9-33.
8. von Bargen K, Scraba M, Kramer I, et al. Virulence-associated protein A from *Rhodococcus equi* is an intercompartmental pH-neutralising virulence factor. *Cell Microbiol*. 2019;21(1):e12958.
9. Zachary JF. Mechanisms of microbial infections. In: Zachary JF, ed. *Pathologic Basis of Veterinary Disease*. 6th ed. Elsevier Mosby; 2017:168-169.

CASE III:

Signalment:
5-year-old female Holstein (*Bos taurus*)

History:
This adult cow was admitted to the clinic with sudden onset of weakness, abdominal pain,

and bloody feces. In the preliminary report, an embryo wash was performed three weeks prior to submission. A suspected diagnosis of hemorrhagic bowel syndrome was made. The animal underwent abdominal surgery (manual blood clot dissolution) and symptomatic treatment; however, the cow spontaneously died the following night.

Gross Pathology:
The distal jejunum was distended and filled with coagulated blood. Multifocal intramural hematomas (approximately 3 x 2 x 1 cm) as well as blood coagula adherent to the intestinal mucosa (approximately 40 cm length, on average) were present in the affected segment.

Orally to the described lesion, the jejunal mucosa was diffusely bright red with multifocal dark red areas and multiple, up to 1 mm in diameter large, submucosal hematomas. Intestinal contents in the cecum and colon were dark-red, viscous, and admixed with large amounts of coagulated blood, whereas the rectum was empty. Additionally, there were multifocal petechial hemorrhages on the serosal surfaces of internal organs. A small amount of serous, red fluid was found in the greater omentum. Moderate pharyngeal edema was present. Additionally, the liver was diffusely soft and beige-yellow with mildly rounded edges. Moreover, the nose and lungs showed diffuse, moderate hyperemia and the lung also a mild, diffuse, alveolar edema.

Laboratory Results:
Salmonella spp. were not isolated from a small intestine sample. Bovine viral diarrhea virus and bovine herpesvirus-1 were not isolated in cell culture. PCR for Bluetongue virus and bovine herpesvirus-1 were negative as well. The test for the proteinase K-resistant prion protein was negative.
Immunohistochemistry on smooth muscle actin using the avidin-biotin peroxidase

Figure 3-1. Jejunum, ox. The distal jejunum is filled with clotted blood. (*Photo courtesy of:* Department of Pathology, University of Veterinary Medicine, Hannover, Buenteweg 17, 30559 Hannover, Germany, http://www.tiho-hannover.de/kliniken-institute/institute/institut-fuer-pathologie)

technique revealed a splitting of the lamina muscularis mucosae with accumulation of blood between the muscle layers.

Microscopic Description:
Approximately 90% of the tissue section shows a separation of the mucosa from the submucosa due to extensive submucosal hematoma formation. The overlying mucosal layer displays moderate necrosis but also autolysis with bright eosinophilic cellular debris and multifocal dilated villus lacteals. Furthermore, the mucosal layer is focally eroded. Also moderate numbers of rod-shaped bacteria can be observed on the luminal surface as well as mild fibrin formation in between the separated muscle layers.

Contributor's Morphologic Diagnosis:
Jejunum: Segmental mucosal necrosis and intramural hematoma formation, bovine.

Contributor's Comment:
Hemorrhagic bowel syndrome (HBS), first described in the early 90s, is a sporadic, often fatal disorder characterized by acute extensive segmental jejunal hemorrhage and intramural hematoma formation predominantly

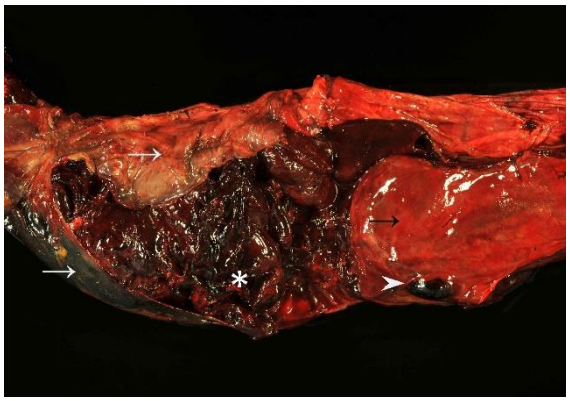

Figure 3-2. Jejunum, ox. Multifocal intramural hematomas, as well as blood coagula adherent to the intestinal mucosa, are present in the affected segment. (*Photo courtesy of:* Department of Pathology, University of Veterinary Medicine, Hannover, Buenteweg 17, 30559 Hannover, Germany)

affecting adult dairy cattle.[2,3] A significant proportion of the affected animals are of Brown Swiss breed.[2]

Among other clinical symptoms, notable blackberry jelly-like blood clots within feces, decreased milk production, tachycardia and/or palor of mucous membranes are commonly reported.[3] Post-mortem findings usually include one or more short jejunal segments with severe intramural hemorrhage/hematoma formation, which may completely or partially obstruct the intestinal lumen.[5] These findings were also observed in this case. Intraluminal blood clots were mostly observed at the areas of ruptured mucosa. The histologic findings in this case are consistent with previously described lesions.[1,2] A mild to moderate vasculitis, which has been described in some cases, was not observed in the presented case.[1,2,5]

The etiology and pathogenesis of this disorder is currently unknown. Several infectious factors, including the contribution of *Clostridium perfringens* or *Aspergillus fumigatus*, have been suspected, but no statistically significant relations have been detected so far.[5] Thus, the observed bacteria are more likely secondary to the progressing disease and autolysis.[5] Due to dilated villus lacteals and the moderate to severe submucosal vasculitis observed in other reported cases, it has been hypothesized that an initial vasculopathy or abnormal lymphatic function may be responsible for the prominent dissecting hemorrhages, but these theories have not been confirmed.[1]

Recent findings indicate that hemorrhages appear to originate within the lamina muscularis mucosa (Lmm) and lead to the eruption of the mucosa with severe intraluminal bleeding and blood clot formation within the jejunum.[2] The splitting of the Lmm potentially leads to the rupture of the many arterioles that course through the Lmm and supply blood from the submucosa to the subepithelial capillary beds.[2] This process is further accelerated by the arterial blood pressure, which results in a "zipper-mechanism" characterized by expanding, dissecting hemorrhages.[2]

In the present case, an immunohistochemical stain for α-smooth muscle actin (SMA) was performed which identified SMA-positive fragments of Lmm beneath the mucosa adjacent to the hemorrhage as well as on the contralateral side framing the tunica muscularis. Furthermore, immunohistochemical cytokeratin staining visualized the intestinal epithelium. Overall, the described findings correspond to previously reported cases and support the assumption that the fragmentation of the Lmm, which surrounds the hematoma, is a consequence of the intramuscular hematoma formation.[2] The cause of the spontaneous detachment of the Lmm layers remains unclear. Mucosal necrosis is considered as a change secondary to the resulting ischemia rather than a primary inflammatory entity such as described in hemorrhagic enteritis.[2]

Shock gut syndrome and hemorrhagic enteritis should be considered as differential

Figure 3-3. Jejunum, ox. There is dissecting hemorrhage within the wall of the jejunum. (HE, 4X)(*Photo courtesy of:* Department of Pathology, University of Veterinary Medicine, Hannover, Buenteweg 17, 30559 Hannover, Germany)

diagnoses. The "shock gut" syndrome is most common in dogs and results in decreased perfusion of the intestine. It is morphologically characterized by congestion of intestinal mucosa, as well as reddish intestinal content.[5] Hemorrhagic enteritis in adult cattle can be caused by infectious (*Salmonella* spp., coronaviruses) and non-infectious factors (arsenic, oak, oleander poisoning) and manifests as reddish intestinal content, congested mucosa and diarrhea.[5]

Cattle affected by HBS often show acute onset of poor general condition, clotted blood in the feces, and sudden death.[1] The treatment can be symptomatic or surgical; however, in either case the prognosis is rather poor with most animals dying or being euthanised.[5]

Contributing Institution:
Department of Pathology
University of Veterinary Medicine
Hannover, Germany
http://www.tiho-hannover.de/kliniken-institute/institute/institut-fuer-pathologie/

JPC Diagnosis:
Small intestine: Mural hemorrhage, segmental, acute, diffuse, severe.

JPC Comment:
The typical gross and histologic lesions of hemorrhagic bowel syndrome (HBS), also known as jejunal hemorrhage syndrome, have been well described in the veterinary literature and are nicely summarized by the contributor.[1-3] Other common causes of intraluminal intestinal hemorrhage include intussusception, volvulus, salmonellosis, bovine viral diarrhea virus infection, coccidioisis, coagulopathies, and intestinal foreign bodies; however, HBS differs from these differentials by the presence of large intraluminal or intramural blood clots that result in small intestinal obstruction, most commonly in the jejunum.[2,3]

Hematologic parameters of HBS-affected cattle largely reflect the acute, hemorrhagic nature of the disease. There is usually a neutrophilia and hyperglycemia, both attributable to the release of inflammatory cytokines and endogenous, stress-related steroid release.[3] The physical obstruction of the proximal intestine results in sequestration of abomasal secretions, leading to electrolyte abnormalities, most commonly hypochloremia and hypokalemia.[3] Liver enzymes, such as sorbitol dehydrogenase and gamma-glutamyltransferase may be elevated due to gastrointestinal obstruction or stasis and subsequent absorption of bacteria and toxins from the affected area of intestine.[3] Other abnormalities include increased blood urea nitrogen, attributed to intraluminal digestion of blood, hyperlactatemia, and acidemia; inconsistent calcium and magnesium derangements have been reported.[3,4]

The acute nature of the disease and the poor prognosis despite treatment make HBS a source of high economic losses, and efforts are underway to determine the cause of the disease, the existence of any ante-mortem biomarkers, and the most promising treatments for acutely affected animals. Recent efforts

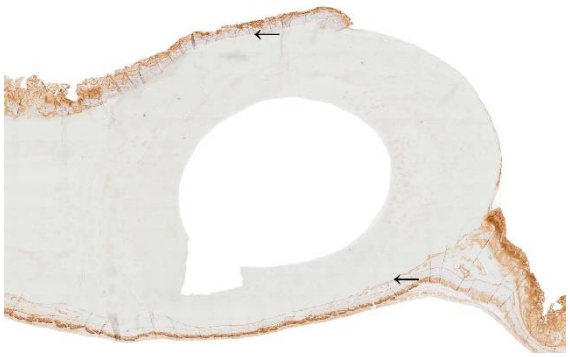

Figure 3-4. Jejunum, ox. A smooth muscle actin stain demonstrates the elevation of the mucosa off of the underlying submucosa and smooth muscle layers. (anti-SMA, 4X)(*Photo courtesy of:* Department of Pathology, University of Veterinary Medicine, Hannover, Buenteweg 17, 30559 Hannover, Germany)

have begun mining biosensor data, routinely collected from dairy cows to monitor estrus and milk yields, to determine if any clinically silent premonitory signs can be identified. The first such report on these efforts found that decreases in rumination time and activity, rumen mobility, rumen temperature, and milk yields preceeded clinically evident signs, offering a potential early alert mechanism to identify and treat dairy cows early in the course of disease.[4]

Conference participants appreciated the unique, striking subgross histologic appearance of this case and discussion focused largely on whether the mucosal changes represent necrosis or autolysis. Participants believed that the changes were largely autolytic due to the lack of visible thrombi in section and the fact that tissue in less-affected, normal areas of the section had a similar histologic appearance. Participants also reviewed a smooth muscle actin immunohistochemical stain which illustrated the dramatically thin rim of muscularis mucosae lining the hematoma and nicely illustrated the splitting of this histologic layer as described in a recently published article characterizing this entity.[2]

The moderator noted that, though HBS cases have become rare recently, his diagnostic lab has historically seen multiple cases of HBS per week. The moderator shared a wealth of gross and histologic HBS images from this historic caseload that delighted conference participants. The moderator challenged the textbook clinical presentation of blood clots in the feces. In his experience, most animals die of intestinal obstruction caused by the intramural hematoma; it is only if the animal survives the acute period that the hematoma ruptures the mucosa and blood appears in the manure.

References:

1. Adaska JM, Aly SS, Moeller RB, et al. Jejunal hematoma in cattle: a retrospective case analysis. *J Vet Diagn Inv*. 2014; 26 (1):96 -103.
2. De Jonge B, Pardon B, Goossens E, et al. Hemorrhagic bowel syndrome in dairy cattle: Gross, histological, and microbiological characterization. *Vet Pathol*. 2023;60(2):235–244.
3. Dennison AC, VanMetre DC, Callan RJ, et al. Hemorrhagic bowel syndrome in dairy cattle: 22 cases (1997-2000). *J Am Vet Med Assoc*. 2002;221(5):686-689.
4. Ha SM, Kang SG, Jung MY, et al. Retrospective study using biosensor data of a milking Holstein cow with jejunal haemorrhage syndrome. *Vet Med (Praha)*. 2023; 68(9):375-383.
5. Uzal FA, Plattner BL, Hostetter JM. Alimentary system. In: Maxie MG, ed. *Jubb, Kennedy & Palmer's Pathology of Domestic Animal*. 6th ed. Vol. 2. Elsevier; 2016:1-257.

CASE IV:

Signalment:
3-week-old female suckling domestic piglet (*Sus scrofa domesticus)*

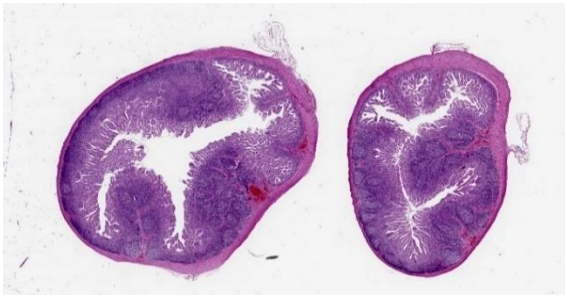

Figure 4-1. Ileum. Two sections of ileum are submitted for examination. (HE, 5X)

History:
The farm noticed increased morbidity and mortality of approximately 20-30% during the last three weeks. The piglets showed clinical signs of diarrhea, fever, lameness, tremor, and anemia. This animal was euthanized for diagnostic proposes shortly before necropsy.

Gross Pathology:
The animal was in poor nutritional condition. There was a small amount of milk in the stomach. The contents of all intestinal segments were yellow and watery. A high amount of turbid synovial fluid was found in all examined joints. The meninges were diffusely cloudy.

Laboratory Results:
Adenoviral particles were detected by transmission electron microscopic examination of the ileal mucosa.

In the bacteriological examination of an elbow joint (synovia) and of the brain meninges a small amount of *Streptococcus suis* was isolated. PCR serotyping identified *S. suis* Serotype 1.

No parasites were identified on fecal flotation.

Microscopic Description:
Multifocally, ileal villi are mildly to moderately fused and blunted with maintenance of normal enterocyte architecture. Enterocytes occasionally contain a single intranuclear inclusion body that leads to margination of the chromatin. These inclusion bodies are amphophilic, round to oval shaped, and 5-15 µm in diameter. In the lamina propria, a mild diffuse infiltration with lymphocytes, eosinophils, plasma cells, and granular lymphocytes is present. The vessels show an increased number of erythrocytes (congestion).

Contributor's Morphologic Diagnosis:
Mild, subacute, diffuse, lymphoplasmatic and eosinophilic enteritis (ileitis) and mild, multifocal, atrophic enteritis with villus fusion and intranuclear viral inclusion bodies (Adenovirus).

Contributor's Comment:
Adenoviruses are non-enveloped, double-stranded DNA viruses with icosahedral symmetry. Adenovirus infections occur in a wide variety of animals inducing clinical signs ranging from subclinical to enteric or respiratory. Three species of Porcine adenoviruses (PAdVs), Porcine mastadenovirus A, Porcine mastadenovirus B, and Porcine mastadenovirus C, and five serotypes have been identified by virus neutralization assays.[1,3,7] Adenoviruses are considered host-specific and the pig is the only known species that is susceptible to PAdVs.[1]

Watery to pasty diarrhea, dehydration, and decreased weight gain are the most commonly observed clinical signs in pigs.[1] Cases of diarrhea caused by PAdVs are mostly seen in suckling pigs (1–4 weeks of age), but weaned and fattening pigs can also be affected.[1] Furthermore, PAdVs have been isolated from pigs with respiratory signs, encephalitis, nephritis, and abortions; they have also been isolated from animals without evident clinical history.[1,3-5] Transmission occurs mostly via the fecal-oral route or possibly by aerosol exposure. Mechanical vectors (tools,

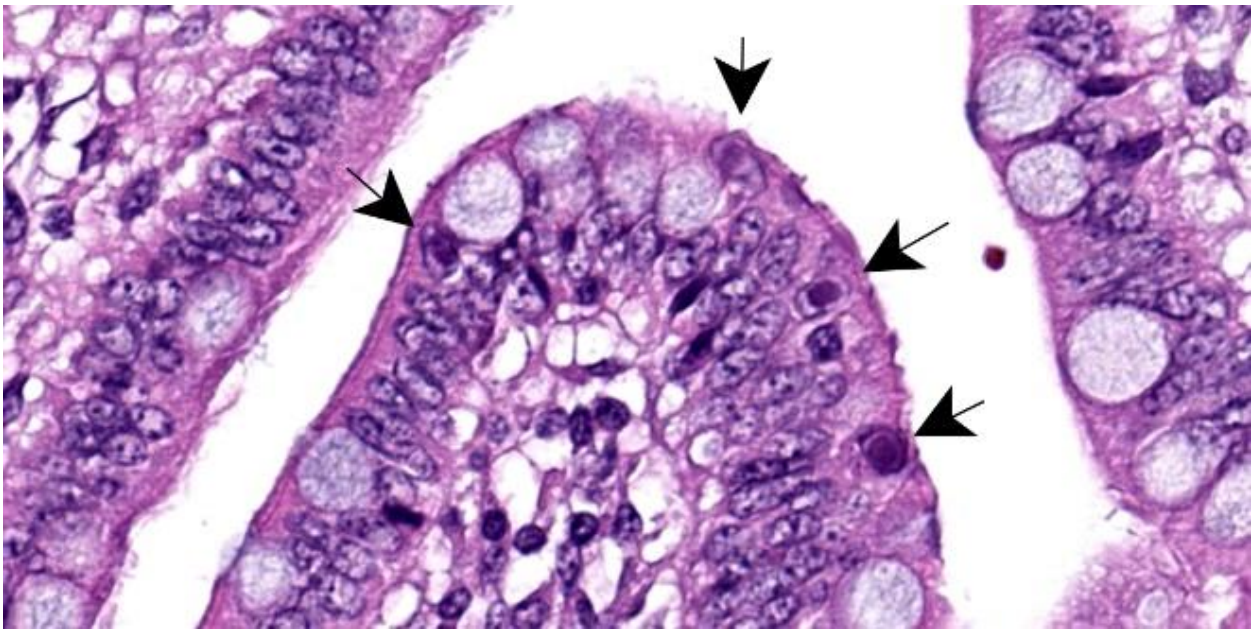

Figure 4-2. Ileum, piglet. Scattered villar enterocytes have large intranuclear viral inclusions. (HE, 750X)

boots, vehicles, etc.) might have a possible role considering the high stability of the virus in the environment.[1]

Similar to this case, typical histological lesions include villous fusion, blunting, and shortening with intranuclear basophilic inclusion bodies in enterocytes of the distal jejunum and ileum.[1,8] To confirm an infection with PAdVs, the virus can be detected by electron microscopy, cytology from mucosal smears, or by the detection of viral antigens in tissues by immunofluorescence or immunohistochemistry.[1,6] In general, PAdVs mostly lead to subclinical infections and are not known to have public health significance. Adenoviruses should nevertheless be considered as a differential diagnosis for gastrointestinal and possibly respiratory diseases in pigs.[1]

Contributing Institution:
Institute of Veterinary Pathology Zurich
www.vetpathology.uzh.ch

JPC Diagnosis:
Small intestine: Enteritis, lymphoplasmacytic, diffuse, mild, with few epithelial intranuclear viral inclusions.

JPC Comment:
Adenoviruses, so named due to their discovery in cultures of human adenoids, are notable histologically for their large, often basophilic intranuclear inclusion bodies. These inclusions represent newly assembled virions that form crystalline aggregates within the nucleus.[9] As flashy as these inclusions may be, as the contributor notes, adenoviral infection in pigs is typically asymptomatic, with the main presenting signs being yellow, watery diarrhea of three to four days' duration in 1-4 week old piglets.[2]

Once ingested, porcine adenovirus undergoes intranuclear replication, primarily in the enterocytes and lymphoid tissue located in the distal jejunum and ileum.[2] Viral antigen may be found 24 hours after infection and for up to 45 days post-infection, and infected enterocytes may be destroyed or may lose their

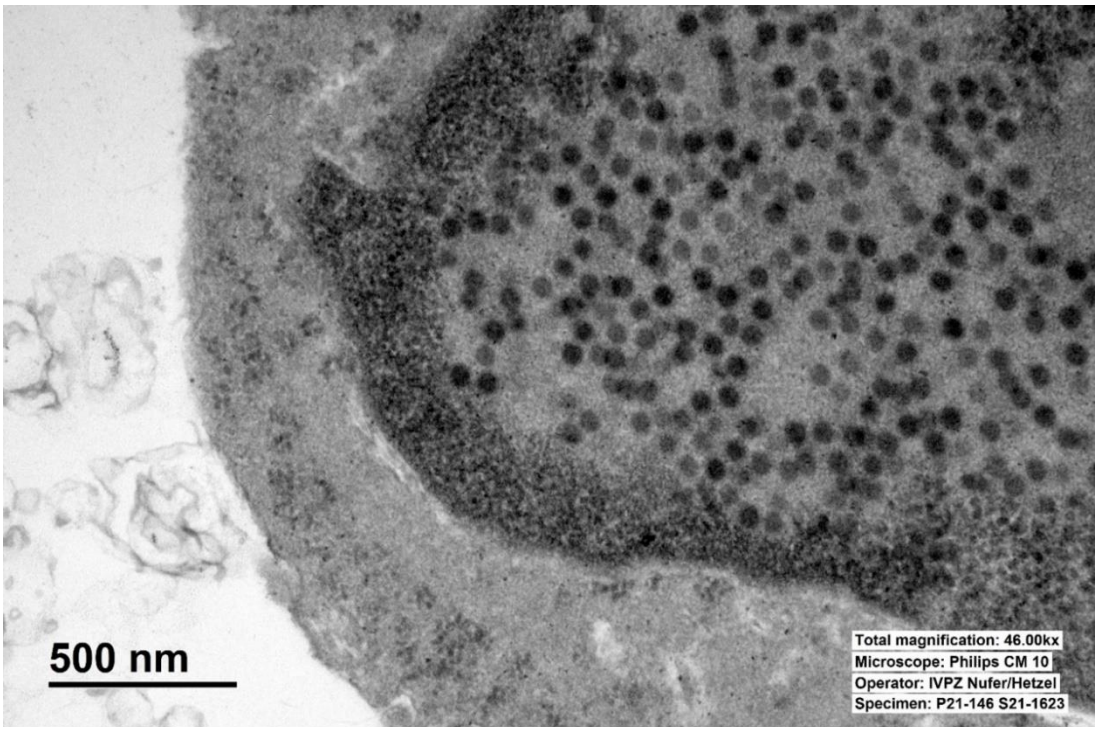

Figure 4-3. Ileum, piglet. Electron microscopy reveals adenoviral particles in the nucleus of an enterocyte. The particles measure 75–80 nm in diameter. (*Photo courtesy of:* Institute of Veterinary Pathology Zurich (IVPZ), www.vetpathology.uzh.ch)

villi during the acute phase of infection.[2] Interestingly, virus has been found in the tonsils after infection of enterocytes, raising the possibility of clinically silent viremia with certain isolates.[2] Porcine adenovirus has also rarely been associated with nephritis, raising the possibility of urinary-oral and urinary-nasal transmission.[2]

Gross lesions in cases of adenovirus-induced diarrhea include thinning of the wall of the distal small intestine, enlargement of the mesenteric lymph nodes, and the presence of yellow, watery contents in the small and large intestines.[2] In additional to the histologic features described by the contributor, the lamina propria is often infiltrated by histiocytes, plasma cells, and lymphocytes, as illustrated by this case. In cases of porcine adenovirus nephritis, the renal interstitium contains multifocal accumulations of lymphocytes and plasma cells, and renal tubules contain sloughed, necrotic tubular epithelial cells, some of which may contain characteristic intranuclear inclusion bodies.[9]

Aside from the eye-catching inclusion bodies, histologic lesions in the examined section were subtle, leaving participants rooting around for descriptive points. Conference participants discussed the length of the villi and, while the contributor described fused and blunted villi, these changes were not appreciated in the examined section. Participants also noted multifocal areas where crypt and villar epithelium appeared hyperplastic and piled up, though most felt these apparent lesions were simply function of cut. Similarly, the occasional lymphocytolysis observed in Peyer's patches were thought to be within normal limits as some lymphocytolysis is expected during normal lymphocyte turnover.

Discussion turned to the quantity and character of the inflammatory cells, which left some participants unimpressed; however, the majority felt that the number of lymphocytes and plasma cells was mildly elevated and likely responsive to the obvious viral infection being telegraphed by the inclusion bodies.

The moderator noted that, while diarrhea can be experimentally induced by PAdVs, current veterinary literature is divided on whether these viruses cause porcine diarrhea in natural infections. While direct causation is not definitively established, PAdVs should be on differential lists of porcine diarrhea, particularly in the absence of other common etiologic agents, such as rotavirus or coronavirus, which can cause subtle histologic lesions similar to the examined case while causing significant to profound clinical diarrhea.

References:

1. Benfield DA, Hesse RA. Adenoviruses. In: Zimmerman JJ, Karriker LA, Ramirez A, et al., eds. *Diseases of Swine*. 11th ed. Wiley & Sons;2019:438-441.
2. Center for Food Security and Public Health. Porcine Adenovirus. Iowa State University;2015. Available at: cfsph.iastate.edu/pdf/which-factsheet-porcine-adenovirus.
3. Clarke MC, Sharpe HBA, Debryshire JB. Some characteristics of three porcine adenoviruses. Agricultural Research Council, Institute for Research on Animal Diseases, Berkshire England;1967:91-97.
4. Ducatelle R, Coussement W, Hoorens J. Sequential pathological study of experimental porcine adenovirus enteritis. *Vet Pathol*. 1982;19:179-182.
5. Haig DA, Clarke MC. Isolation of an adenovirus from a pig. *J Comp Pathol*. 1964;74:81-84.
6. Nietfeld JC, Leslie-Steen P. Interstitial nephritis in pigs with adenovirus infection. *J Vet Diagn Invest*. 1993;5:269-273.
7. Sanford SE, Hoover DM. Enteric adenovirus infection in pigs. *Can J Comp Med*. 1983;47:396-400.
8. Sharpe HBA, Jessett DM. Experimental infection of pigs with 2 strains of porcine adenovirus. *J Comp Pathol.* 1967;77:45-50.
9. Quinn PJ, Markey BK, Leonard FC, Fitz-Patrick ES, Fanning S, and Hartigan PJ. *Veterinary Microbiology and Microbial Disease*. 2nd ed. Blackwell;2011:588-592.

WSC 2023-2024
Conference 20 Self-Assessment

1. Which of the following is least likely to develop lesions associated with *Entamoeba invadensis the most common intermediate host for Neospora caninum*?
    a. Opossum
    b. Ox
    c. Sheep
    d. Slug

2. In puppies less than six months old, the primay manifestation of *Neospora caninum* infection is?
    a. Colitis
    b. Myelitis
    c. Myocarditis
    d. Encephalitis

3. Which of the following is not a virulence factor (other than Vaps) in *Rhodococcus equi*?
    a. Phospholipase A
    b. Lecithinase
    c. Polysaccharide capsule
    d. Cholesterol oxidase

4. The hematoma in hemorrhagic bowel syndrome dissects through which of the following layers of the intestine?

    a. Mucosa
    b. Lamine muscularis mucosae
    c. Submucosa
    d. Inner circumferential layer

5. Porcine adenoviruses have NOT been associated with which of the following syndromes in pigs?.
    a. Enteritis
    b. Abortion
    c. Myocarditis
    d. Encephalitis

Joint Pathology Center
Veterinary Pathology Services

WEDNESDAY SLIDE CONFERENCE 2023-2024

Conference #21 **03 April 2024**

CASE I:

Signalment:
11-year-old, intact male German Shepherd Dog (*Canis familiaris*)

History:
This patient presented to the Emergency Service for evaluation of a cough of 1-week duration that was unresponsive to Baytril and Torbutrol. His cough became acutely worse, at which time he regurgitated and became dyspneic. Over the next 24 hours the patient became lethargic, weakly ambulatory, and febrile (104ºF). Pertinent previous history included chronic intermittent coughing followed by vomiting/regurgitation. Three-view thoracic radiographs showed a bilateral interstitial to alveolar pattern in the cranioventral lung lobes, marked distention of the thoracic esophagus, and a homogenous oblong soft tissue mass in the cranial mediastinum. An inflammatory leukogram was identified on CBC. While hospitalized he became progressively weaker with marked reduction in pelvic limb reflexes, requiring a sling to walk. Euthanasia was elected.

Gross Pathology:
The thoracic cavity contained approximately 2 ml of a non-viscous, translucent, dark red (serosanguinous) fluid. The thoracic esophagus was diffusely distended and was 3.5 cm at its widest dimension. The cranial mediastinum was focally expanded by a poorly demarcated, 14.4 cm x 3.6 cm x 4.5 cm,

Figure 1-1. Mediastinum, dog. The cranial mediastinum is expanded by a poorly demarcated, 14.4 cm x 3.6 cm x 4.5 cm, multilobulated, firm to friable, tan to dark red mass (*Photo courtesy of:* Schwarzman Animal Medical Center, Department of Anatomic Pathology. www.amcny.org)

multilobulated, firm to friable, tan to dark red mass. The cut surfaces of this mass comprised anastomosing, firm, tan trabeculae separated by a soft to friable, dark red tissue.

The right middle lung lobe was diffusely red and firm. Sections from the right middle lung lobe sank in 10% buffered formalin. The right cranial, right caudal, accessory, and left cranial lung lobes were diffusely red and contained multifocal to coalescing, mildly to moderately firm regions. Sections from these lung lobes inconsistently floated, floated low, or sank in 10% buffered formalin. The left caudal lung lobe was diffusely red and rubbery. Sections from the left caudal lung lobe floated in 10% buffered formalin. From the cut surfaces of all lung lobes oozed a

moderate amount of non-viscous, translucent, dark red (serosanguinous) fluid.

Laboratory Results:

Parameter	Value	Reference Range
WBC	25.8 K/µL	4.9-17.6 K/µL
Neutrophils	23.33 K/µL	2.94-12.67 K/µL
Bands	258 /µL	0-170 /µL
Lymphocytes	0.52 K/µL	1.06-4.95 K/µL
Monocytes	1.806 K/µL	0.13-1.15 K/µL
Eosinophils	0 K/µL	0.07-1.49 K/µL
Basophils	0 K/µL	0.0-0.1 K/µL
Platelets	345 K/µL	143-448 K/µL

Microscopic Description:

Mediastinal mass cytology: Touch imprints of the cranial mediastinal mass comprise large numbers of streaming, mildly pleocellular spindle cells mixed with small numbers of mast cells, few small to intermediate size lymphocytes, and few macrophages containing variable amounts of hemosiderin on a background of peripheral blood. There are scattered mesothelial cells.

Lung cytology: Touch imprints of the right middle lung lobe comprise abundant degenerate and viable neutrophils and macrophages mixed with small numbers of respiratory epithelial cells on a hemodiluted background with abundant extracellular bacteria. Macrophages infrequently contain hemosiderin. Intracellular bacteria are not identified.

Mediastinal mass histology: Expanding the fibrofatty stroma is a poorly demarcated, unencapsulated neoplasm consisting of mildly pleomorphic oval to spindle to polygonal cells arranged in fascicles, short and long streams, small bundles, and solid regions supported by a fine fibrovascular stroma with congested blood vessels and traversed by dense connective tissue trabeculae. Neoplastic cells are oval to spindle to polygonal with indistinct cell borders and small to

Figure 1-2. Mediastinum, dog. Dissected mediastinal mass. (*Photo courtesy of:* Schwarzman Animal Medical Center, Department of Anatomic Pathology)

moderate amounts of eosinophilic cytoplasm with inconsistent cytoplasmic vacuolization. Nuclei are round to oval with evenly distributed, finely stippled chromatin and up to one prominent nucleolus. No mitotic figures are identified in ten HPF (40x x FN22; 2.37mm^2). Scattered within the neoplastic population are a small number of individualized macrophages and small lymphocytes, as well as rare plasma cells. Macrophages infrequently contain intracytoplasmic, deep to golden brown pigment (hemosiderin and lipofuscin). The neoplastic population is multifocally separated by areas of hemorrhage that occasionally form large cavitated regions bordered by neoplastic cells. Rare mineral is present. Hassall's corpuscles and protein-filled perivascular spaces are not identified.

Immunohistochemistry: Approximately 90% of the neoplastic population display moderate to strong, cytoplasmic to membranous immunoreactivity for cytokeratin AE1/3 and are diffusely immunonegative for vimentin. Individualized CD3 immunopositive round cells are scattered throughout the mass and comprise less than 5% of the total cell mass.

Contributor's Morphologic Diagnosis:

Mediastinal mass: Thymoma, epithelial-rich (prominent spindle cell morphology) with multifocal to coalescing, moderate to severe

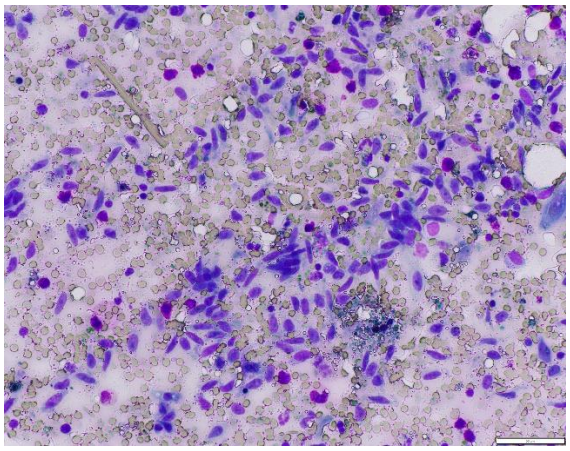

Figure 1-3. Mediastinum, dog. Touch imprints demonstrate numerous pleocellular spindle cells against a background of peripheral blood. (Wright-Giemsa, 400X) (*Photo courtesy of:* Schwarzman Animal Medical Center, Department of Anatomic Pathology)

hemorrhages and few intratumoral small lymphocytes.

Contributor's Comment:

Based on the clinical presentation, identification of a cranial mediastinal mass with thoracic radiographs, megaesophagus, and an interstitial to alveolar pulmonary pattern in the cranioventral lung lobes, the working clinical diagnosis was thymoma-associated myasthenia gravis with secondary aspiration pneumonia. Gross exam confirmed a multilobular mass in the cranial mediastinum, megaesophagus, pleural effusion, and aspiration pneumonia. Differentials for a cranial mediastinal mass include neoplasia (i.e., thymic epithelial tumor, lymphoma, thymic germ cell tumor, stromal sarcoma, tumors of ectopic thyroid and parathyroid tissues, chemodectoma, lipoma, schwannoma, metastatic disease), thymic cyst, brachial cyst, abscess, and granuloma.[14,15,17,23,26] In this case, histopathology supported a diagnosis of an epithelial-rich thymoma with prominent spindle morphology.

The distinction between WHO classified type A and type AB thymomas is difficult, as both share a predominance of bland spindle cells and are distinguished by the percentage of immature T cells (few in type A and high numbers in type AB).[9,10] In this case, three representative sections were evaluated as part of the postmortem examination, and all contained a paucity of lymphocytes. These findings would be most consistent with a type A thymoma.

However, as type AB thymomas can have lymphocyte-poor and lymphocyte-rich regions, it is possible that lymphocyte-rich regions were not represented in the examined sections and thus a type AB thymoma could not be entirely ruled out.[9,10] As euthanasia was elected before confirmatory AChR antibody titers could be submitted, myasthenia gravis could not be confirmed but was suspected.

As a lymphoepithelial organ, the thymus is formed by a combination of epithelial and lymphoid tissues (differentiating and proliferating T lymphocytes).[5,21] In addition, a small population of myoid cells that resemble striated muscle fibers are of unclear origin and thought to play a key role in the development of thymoma-associated myasthenia gravis.[21] During development, the thymic epithelium forms from the 3rd pharyngeal pouch's endoderm that subsequently becomes invaded by blood vessels and connective tissue trabeculae from the adjacent mesoderm and infiltrated by bone marrow derived lymphocyte progenitors.[5,8,21] Grossly, the thymus is separated into distinct lobes (paired cervical lobes, an intermediate lobe at the thoracic inlet, and a thoracic lobe), but the arrangement and prominence of each lobe varies among species.[5,21] In both ruminants and pigs, the cervical lobes are large.[5,6,21] Further, in ruminants the thoracic lobe is in the dorsal part of the cranial mediastinum.[5] In

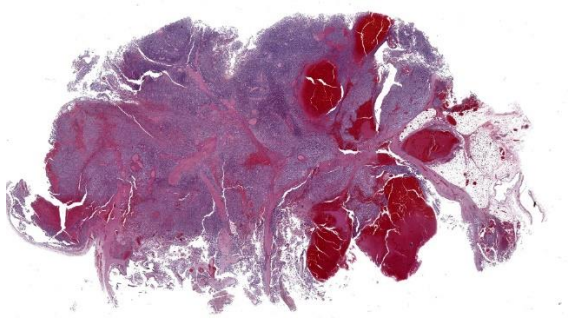

Figure 1-4. Mediastinum, dog. One section of a moderately cellular, cystic neoplasm with multifocal areas of hemorrhage is submitted for examination. (HE, 5X)

horses, the cervical lobes are small with a large thoracic lobe.[5,21] In domestic small animals, the cervical lobes are small (cats) to absent (dogs).[5,21] In both cats and dogs, the thoracic lobe is in the ventral cranial mediastinum and extends to the pericardium where in cats it can mold to the pericardial surface.[5] The thymus is partially separated into lobules by connective tissue septa that extend from the capsule so that each lobule comprises a central medulla and surrounding cortex.[5,21] The cortex is created by epithelial reticular cells and densely packed differentiating precursor T lymphocytes.[5,21] Meanwhile, the medulla contains epithelial reticular cells (relatively larger and more prominent when compared to the cortex), Hassall's corpuscles, interdigitating dendritic cells, and relatively fewer, less densely packed lymphocytes.[5,21] The thymus reaches its maximum size at birth and involutes after sexual maturity, although remnants may be retained through adulthood.[5,21] Differentiation between normal age-associated involution and disease-associated thymic atrophy requires interpretation of thymic features considering the patient's age, clinical presentation, and nutritional state.[5,21]

Thymic disorders include thymic hyperplasia, congenital thymic cysts, inflammatory diseases, hemorrhages and hematomas, neoplasia (i.e., thymic lymphoma and thymic epithelial tumors), and congenital immunodeficiency disorders.[5,21] The most common reaction pattern in the thymus is lymphoid atrophy, which can occur secondary to a multitude of underlying diseases processes including physical and physiologic stresses, cachectic states, toxins (lead, mercury, halogenated aromatic hydrocarbons, mycotoxins (i.e., fumonisin B1 & B2 and aflatoxin)), drugs, radiation, neoplasia, and viral infections.[5,21] True thymitis is rare but can be seen with certain infectious etiologies (i.e., *Neorickettsia helminthoeca* [salmon poisoning], *Neorickettsia elokominicas* [Elokomin fluke fever], epizootic bovine abortion, and porcine circovirus 2).[5,21] Thymic hemorrhage and hematomas are more frequently reported in young dogs, for which reported causes include anticoagulant rodenticides, dissecting aneurysm, trauma, and idiopathic/spontaneous.[5,21]

Tumors primary to the thymus are uncommon and include thymic lymphoma, thymic epithelial tumors, and thymic germ cell tumors.[5,7,9,10,20,21] Thymic epithelial tumors (TET) are uncommon cranial mediastinal neoplasms originating from the thymic epithelium and include thymoma, thymic carcinoma, and thymic neuroendocrine tumors.[1,5-7,14,15,18,20-26] Thymomas have been reported in numerous species, including dogs, cats, small and large ruminants, horses, pigs, rabbits, ferrets, birds, non-human primates, rodents, a polar bear, and an otter, and are most typically identified in adult to aged animals, without a sex predilection.[2,3,5,6,8,14,15,17,18,20-24,26] They are reportedly more common in goats with a 25% incidence reported in a single closed herd of Saanen dairy goats.[3,5,6,14,15,17,20,21,24,26] Generally, thymomas are not associated with a specific breed predisposition in domestic small animals but medium to large breed dogs are often affected.[15,20] In one retrospective case

series, Labrador retrievers and German shepherd dogs were overrepresented.[15,20]

Thymomas can be incidental but, when present, clinical signs are non-specific and include weight loss, vomiting/regurgitation, respiratory distress, dyspnea, cough, lethargy, exercise intolerance, and edema of the ventral head, neck, and forelimbs.[6,15-17,18,20,21,23,24] In cases of cervical thymoma, a visible or palpable subcutaneous mass may be present.[6] Associated imaging findings include a soft tissue opacity in the cranial mediastinum, dorsal displacement of the cardiac silhouette and/or trachea, and/or pleural effusion.[6,15,26] Advanced imaging (CT or MRI) is the most reliable method to assess tumor invasiveness.[6,15,17] Additional clinical signs, gross examination findings, and imaging findings associated with paraneoplastic syndrome(s) may be present.

The most common location of thymoma is the cranial mediastinum, but thymomas have been reported in the neck, thoracic inlet, and rarely in ectopic thymic tissues.[6,8,17,20,21,23] Cytologic features indicative of thymoma include lymphocytes (predominantly small T lymphocytes), thymic epithelial cells, and few mast cells, eosinophils, and/or macrophages.[15,17,26] As the non-neoplastic lymphoid component exfoliates readily, neoplastic epithelial cells are variably present in cytologic preparations.[15,20,24,26] In this case, the predominant cell population on cytology was mildly pleocellular spindle cells mixed with few mast cells, lymphocytes, and hemosiderin-laden macrophages. Initially, these spindle cells were of unclear etiology (neoplastic versus reactive population), but when evaluated along with the histology, they represented neoplastic epithelial cells displaying a spindle morphology.

The histologic appearance of thymomas is diverse due to the range of neoplastic cell

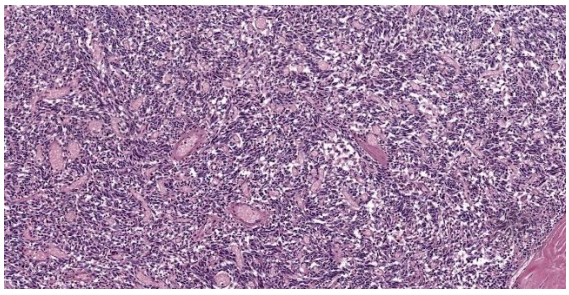

Figure 1-5. Mediastinum, dog. Spindled epithelial cells are arranged in short streams and bundles. There are numerous congested blood vessels. (HE, 128X)

morphologies and degree of benign lymphocyte infiltration.[1,5,6,14,17,20,23] Additional features inconsistently seen in thymomas include loss of normal thymic architecture, loss of corticomedullary junction distinction, protein-filled cysts, necrosis, and hemorrhages.[6,8,20,21,26] Neoplastic thymic epithelial cells can display spindle, oval, and round to polygonal morphologies and exhibit various growth patterns.[3,14,17,20,23,26] Typically, neoplastic cells have ill-defined cell margins and single nuclei with vesicular chromatin and up to one prominent nucleolus.[3,15,17,20,23,26] An uncommon clear cell variant comprised of large round cells with abundant amounts of clear cytoplasm and prominent cell margins has been described.[15,20] In one study, 30.6% of canine cases were inconclusive on cytology and 66.7% of cases had diagnoses with histology alone.[24] Thus a small percentage of tumors will require immunohistochemistry for final diagnosis. [24, 26]

Thymomas have historically been categorized based on their cellular composition, defined as epithelial-rich, lymphocyte-rich, and mixed/ intermediate types with clear cell, spindle cell, and pigmented variants.[8,14,15,17,20,21,23,24] It is rare for thymic epithelial tumors to consist purely of epithelial cells.[21] Tumors can be further differentiated as to whether they are encapsulated /non-invasive or invasive.[3,15,17,21] Recently, the human WHO classification has been shown to

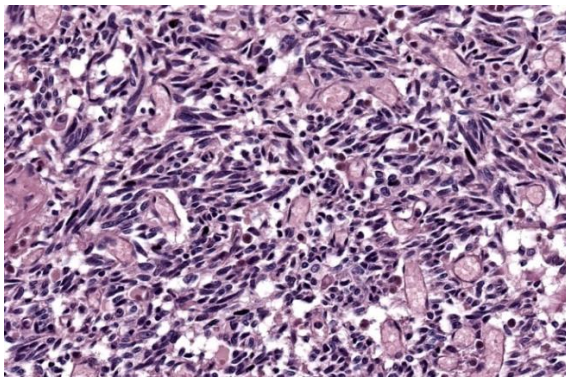

Figure 1-6. Mediastinum, dog. High magnification of neoplastic cells. (HE, 384X)

be applicable in canines.[21,24] In people the histologic subtype carries prognostic significance, but prognostic significance between subtypes has not been established in veterinary medicine.[9,10,20,21,24]

The WHO classification is based on epithelium morphology, severity of cellular pleomorphism, and degree of proliferating non-neoplastic lymphocyte; under this scheme, thymomas are classified into A, AB, B1, B2, and B3 type, micronodular, and metaplastic thymomas.[2,7,9,10,21,24,25] Type A thymomas contain bland oval to spindle-shaped neoplastic epithelial cells arranged in streaming, storiform, fascicular, pericytomatous, or pseudorosettes with a paucity of T-lymphocytes.[7,9,10,21,24,25] Micronodular thymomas likely represent a subvariant of type A tumors where spindle shaped neoplastic epithelial cells are separated by large aggregates of lymphocytes.[7,9,10,21] Type A thymomas with atypia exist and represent a separate histologic variant.[7,9,10,21] Type AB thymomas comprise similar oval to spindle shaped neoplastic cells but are mixed with a focal to diffuse abundance of non-neoplastic lymphocytes.[7,9,10,21,24,25] Polygonal epithelial cells can be present in both type A and AB thymomas.[9,10] Type B thymomas contain oval to polygonal neoplastic cells with varying numbers of non-neoplastic lymphocytes, as well as variably present perivascular spaces and Hassall's corpuscles and are further divided into B1, B2, and B3 types.[7,9,10,21,24,25] Type B1 tumors maintain a thymus-like microarchitecture and comprise non-clustered neoplastic cells that lack atypia and are mixed with small numbers of lymphocytes.[7,9,10,21,24,25] In Type B2 tumors individualized or clustered oval polygonal neoplastic cells lack atypia and are mixed with large numbers of lymphocytes.[7,9,10,21,24,25] Lastly, Type B3 thymomas comprise mild to moderately atypical polygonal neoplastic cells arranged in sheets and contain a paucity of small lymphocytes.[7,9,10,21,24,25] Metaplastic thymomas are characterized by islands of polygonal neoplastic cells displaying variable atypia on a background of bland spindle cells.[7,9,10,21,24,25] Thymic carcinomas comprise neoplastic thymic epithelial cells that display overt features of malignancy and an invasive growth pattern.[7,9,10,20,21,24,25]

Molecular profiling in humans shows mirroring of the WHO histological classifications and molecular subgrouping, including A-like and AB-like clusters with frequent GFT2I and HRAS mutations, an intermediate B-like cluster with T-cell signaling profile, and a carcinoma-like cluster with high tumor molecular burden and frequent CDKN2A and TP53 alterations.[7] Further, thymic carcinomas and B2 and B3 thymomas showed a higher frequency of large copy number variation involving entire chromosomes.[7] The GTF2I gene encodes for the TFII-I protein involved in transcription regulation and, in people, GTF2I mutations appear to play a pivotal role in thymic epithelial tumors and may represent a thymoma-specific oncogene.[7,25]

Typically, thymomas have a benign biologic behavior and the vast majority are slow growing and heavily encapsulated.[3,5,6,14,15,17,18,20,21,23,26] However, all thymoma subtypes have the potential to behave aggressively with infrequent local tissue invasion and rare

metastasis.[24] When metastases occur, they most commonly occur to the lungs and regional lymph nodes.[17] With surgical excision, most thymomas have a favorable long-term prognosis.[1,6,15,17,21,23,24,26] The results of one case series in goats suggests that anatomic location may be a key factor in influencing survival where the prognosis for cervical thymomas with surgical excision were favorable, while excision of mediastinal thymomas more likely carried a guarded prognosis.[6] In small animals, there is limited information regarding radiation as a treatment modality in thymomas with reports suggesting a high overall response rate (50-75%) with radiation therapy alone; however, complete response is reportedly rare.[15,17,24] In people, the main prognostic factors described with thymomas are tumor size, tumor spread, resection status, histologic subtype, patient characteristics (i.e., age and comorbidities), and response to treatment.[7] Prognostic factors in veterinary medicine vary and can be contradictory between studies, but reported factors associated with increased survival times are surgical excision and absence of megaesophagus; those associated with decreased survival times include presence of a paraneoplastic syndrome, myasthenia gravis (as a single variant), metastases, moderate to marked neoplastic cellular pleomorphism, percentage lymphocyte composition, presence of another concurrent tumor, and higher pathologic stage (based on the Masaoka-Koga Staging Systems).[15,17,20,24,26] The Masaoka-Koga Staging System evaluates tumor encapsulation, invasion location, and metastases.[3,7,24,26] In humans, the Masaoka-Koga Staging System is significantly associated with survival and decreased survival rates are seen with increasing stage regardless of histologic subtype.[7,15,24] In one report in dogs, patients with lower staging (stages I, IIa, and IIb) had significantly longer survival times than those with higher staging (stages III, IVa, and IVb);however, a contradictory study did not find a prognostic significance of between stages in dogs.[15,24]

Paraneoplastic syndromes are complications of malignancy distant from the primary tumor that in some instances can be more harmful than the direct effects of the neoplasm.[4,15,24] These syndromes can aid in tumor identification, as well as function as markers of response to treatment.[4] The high rate of paraneoplastic syndromes associated with thymic disorders is related to the crucial function of the thymus in immune tolerance through differentiation, selection, and maturation of T lymphocytes from progenitors.[1,5,8,11,20,21,24,26] Naïve, CD34+ and CD7+ T lymphocytes are pluripotent and lack helper, suppressor, and killer functions; these progenitors undergo a sequential pattern of antigen expression as a function of orderly gene rearrangements encoding the T cell receptor (TCR).[21] While T lymphocytes traverse from the cortex to the medulla, they undergo differentiation and selection via both positive and negative selection, after which only a small percentage of progenitor T lymphocytes survive.[5,21] Positive selection occurs in the cortex, where only lymphocytes that recognize MHC molecules, but not self-antigens, are allowed to mature.[5,21] Meanwhile, negative selection occurs at the corticomedullary junction, where lymphocytes that recognize both MHC and self-antigen are removed.[5,21] Thymic "nurse cells" produce IL-1 which drives lymphoproliferation.[21] Once mature, T lymphocytes leave the thymus, enter the bloodstream, and circulate through secondary lymphoid organs.[5,21] Thymomas have been associated with a vast array of paraneoplastic processes with related clinical signs; these include myasthenia gravis, hypercalcemia of malignancy, immune-mediated polymyositis, keratoconjunctivitis sicca (KCS), immune-mediated thrombocytopenia, immune-mediated anemia, granulocytopenia, hypergammaglobulinemia,

cardiac myositis with arrhythmias, feline exfoliative dermatitis, erythema multiforme, and T lymphocytosis.[2-4,11,13-15,17-21,23,24,26]

Disruption of central tolerance has been proposed as one of the mechanisms leading to autoimmunity associated with thymoma.[11] Thymic epithelial cells express elevated levels of MHC I and II molecules.[20] Aberrant expression of autoantigens and decreased expression of MHC molecules and autoimmune regulator (AIRE) on neoplastic epithelial cells result in defective thymic selection and survival of autoreactive lymphocytes.[20] Clinical signs associated with paraneoplastic syndromes may resolve after surgical excision of the mass, but sometimes clinical features of paraneoplastic syndromes can develop after mass removal.[2-4,11,13-15,17-21,23,24,26]

Myasthenia gravis and hypercalcemia related to parathyroid hormone-related peptide (PTHrP) are the most frequently reported thymoma-associated paraneoplastic syndromes in dogs with reported prevalence of 10-45% (myasthenia gravis) and 30% (hypercalcemia).[2,6,14,15,20,26] In this case, myasthenia gravis was suspected based on the clinical presentation but was not confirmed with ancillary testing. The syndrome is classically categorized as either acquired or congenital myasthenia gravis; however, recently alternative terminology has been suggested where myasthenia gravis exclusively refers to acquired forms and the term congenital myasthenia syndromes is proposed for congenital forms.[12,18,19,21] Acquired myasthenia gravis can occur with or without thymoma, and is associated with thiourylene medication administration in cats.[12]

Immune-mediated myasthenia gravis is most commonly due to the production of autoantibodies towards acetylcholine receptors (AChR) leading to destruction of the postsynaptic membrane and reduction of available functional AChR at the neuromuscular junction.[2,5,12-14,18-21] Less frequently, autoantibodies targeted against other muscle specific proteins (muscle specific kinase [MUSK], titan, and ryanodine proteins) have been reported. The pathogenesis of autoantibody production with thymoma is not entirely known but thymic myoid cells and dysregulation of T lymphocyte selection is thought to play a role.[2,13-15,18-21] Differentiating T lymphocytes recognize autoantigens to AChR or other skeletal muscle specific protein subunits and, due to a defective selection process, they survive and in turn stimulate proliferation and differentiation of B lymphocytes with subsequent autoantibody production.[12,18,20,21] At the neuromuscular junction, proposed mechanisms for receptor damage/inactivation include direct damage or formation of cross-linked antibodies leading to receptor internalization.[19]

The clinical manifestations of myasthenia gravis are divided into focal, generalized, or acute fulminating forms.[12,21] Focal manifestations affect an isolated skeletal muscle group outside the appendicular skeletal muscles (i.e., facial, esophageal, pharyngeal, and laryngeal skeletal muscles).[12,21] Generalized manifestations are defined as appendicular skeletal muscle weakness with or without facial, esophageal, pharyngeal, or laryngeal skeletal muscle involvement.[12] In fulminant forms patients present with an acute, rapidly progressive, and severe form of generalized myasthenia gravis that can progress to respiratory collapse requiring intubation and mechanical ventilation.[12]

Clinical signs vary between patients and include exercise intolerance, decreased or absent peripheral reflexes, cervical weakness, muscle weakness, flaccid paralysis, episodic collapse, hypersalivation, dysphonia, dysphagia, and regurgitation.[2,12,13,18-21,26] Initially enough functional AChRs are present to allow for normal transmission, but with

sustained muscle activity the number of available receptors decreases, leading to progressive or episodic weakness and collapse.[19] Megaesophagus is a common sequela that predisposes patients to aspiration pneumonia.[5,21,26] Diagnosis of myasthenia gravis requires detection of circulating antibodies to AChR, however a subset of dogs with generalized disease will be seronegative.[12,13,15,18,20] There is a correlation between fluctuations in autoantibodies and clinical course of disease.[18] Clinical responses to administration of an anticholinesterase drug (edrophonium chloride; Tensilon) can be helpful but are not absolutely specific.[12,13,15,19,20] Therefore, ancillary testing results should be evaluated in concert with thoracic imaging and clinical signs.[12] Complete excision may lead to normalization of neuromuscular junction activity and resolution of clinical signs, but signs of myasthenia gravis can also develop after thymectomy.[12,15,18-21]

Contributing Institution:
Schwarzman Animal Medical Center
Department of Anatomic Pathology
www.amcny.org

JPC Diagnosis:
Mediastinal mass: Thymoma, type A.

JPC Comment:
The contributor provides an excellent, thorough overview of thymoma, the various applicable classification schemes, and associated paraneoplastic syndromes; it is an enjoyable, informative read and a lily that requires no gilding.

This week's conference was moderated by Dr. Amy Durham, Professor of Anatomic Pathology at the University of Pennsylvania School of Veterinary Medicine, who opened discussion of this case by noting that the basics of this neoplasm, including tissue identification and cell of origin, are not particularly

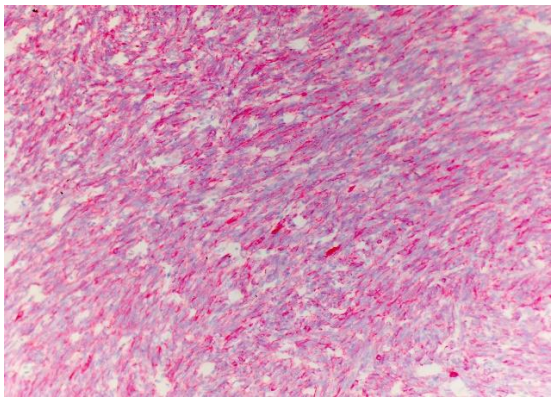

Figure 1-7. Mediastinum, dog. Neoplastic cells demonstrate moderate cytoplasmic immunopositivity for cytokeratin. (anti-AE1/AE3, 400X). *Photo courtesy of:* Schwarzman Animal Medical Center, Department of Anatomic Pathology)

obvious without the clinical history and diagnostic results provided by the contributor. Conference participants seemed to agree, as, in addition to thymoma, a wide range of differentials were presented, including various sarcomas and vascular entities. The moderator noted that a well-curated immunohistochemistry plan, including vimentin, cytokeratin, and lymphocyte markers, makes the diagnosis. Vimentin is particularly helpful in this case given the spindle-cell morphology of the epithelial cells, which is uncommon in dogs and can easily cause the neoplasm to be misidentified as mesenchymal without immunohistochemistry.

A particularly astute conference participant noted the presence of multifocal pockets of ciliated epithelium within the thymic parenchyma and suggested that these might represente branchial cysts. The moderator noted that branchial cysts, which are persistent remnants of the embryonic pharyngeal pouches, are commonly encountered in the mediastinal tissues and, while interesting, are typically of no moment.

Conference participants discussed the value of the various classification schemes which,

as noted by both the contributor and the moderator, currently have no prognostic value. The moderator noted that she typically prefers to diagnose these simply as thymomas, without subclassification, unless the specifics of a particular case warrant emphasizing the tumor's morphology. Other conference participants shared this approach, but all remained ready to adopt any classification scheme that becomes clinically useful in the future. During discussion of the morphologic diagnosis, however, a resident noted that the WHO classification scheme is exhaustively detailed in the primary veterinary pathology textbooks; therefore, for educational purposes, this delightful and slightly enigmatic neoplasm's WHO Type A classification was retained in the morphologic diagnosis.

References:

1. Agrafiotis AC, Siozopoulou V, Hendricks JNH, et al. Tumor microenvironment in thymic epithelial tumors: A narrative review. *Cancers*. 2022;14:6082-6093.
2. Akiyama T, Morita T, Takimoto Y, et al. Lymphoepithelial thymoma characterized by proliferation of spindle cells in a Samoyed dog. *J Vet Med Sci*. 2009;71(9): 1265-1267.
3. Cavalcanti JV, Maura MP, Montiera FO. Thymoma associated with exfoliative dermatitis in a cat. *J Feline Med Surg*. 2014;16(12):1020-1023.
4. Cullen JM, Breen M. An overview of molecular cancer pathogenesis, prognosis, and diagnosis. In: Meuten DJ, ed. *Tumors in Domestic Animals*. 5th ed. Ames, IA: Wiley Blackwell;2017:15-16.
5. Durham AC, Boes KM. Bone Marrow, Blood Cells, and the Lymphoid/Lymphatic System. In: Zachary JF, ed. *Pathologic Basis of Veterinary Disease*. 7th ed. Elsevier:2022;856,862-864,878-880, 888.
6. Hill JA, Fubini SL, Hackett RP. Clinical features and outcome in goats with thymoma: 13 cases (1990-2014). *J Am Vet Med Assoc*. 2017;251:829-834.
7. Kuhn E, Pescia C, Mendogni P, et al. Thymic epithelial tumors: an evolving field. *Life*. 2023;13:314-335.
8. Li WT, Chang HW, Jeng CR, et al. Concurrent spindle-cell thymoma and thymic cysts in a Barbary sheep (*Ammotragus lervia*): case report and review of the literature. *J Vet Diagn Invest*. 2016;28(6):744-749.
9. Marx A, Chan JKC, Chalabreysse L, et al. The 2021 WHO classification of tumors of the thymus and mediastinum: what is new in thymic epithelial, germ cell, and mesenchymal tumors? *J Thorac Oncol.* 2021;17(2):200-213.
10. Marx A, Chan JKC, Coindre JM, et al. The 2015 World Health Organization classification of tumors of the thymus: continuity and changes. *J Thorac Oncol*. 2015;10: 1383-1395.
11. Mendoza-Kuznetsova E, Piedra-Mora C, Bizikova P. Comorbidity of ectopic thymoma-associated exfoliative dermatitis and pemphigus foliaceus in a cat. *Can Vet J*. 2021;62:1067-1070.
12. Mignan T, Targett M, Lowrie M. Classification of myasthenia gravis and congenital myasthenia syndromes in dogs and cats. *J Vet Intern Med*. 2020;34:1707-1717.
13. Miller AD, Porter BF. Nervous System. In: Zachary JF, ed. *Pathologic Basis of Veterinary Disease*. 7th ed. Elsevier: 2022;987.
14. Moller CA, Bender H. Pathology in Practice. *J Am Vet Med Assoc*. 2017;250(4): 387-390.
15. Robert CS, Casario L, Gaeta CL, et al. Clinical features, treatment options, and outcome in dogs with thymoma: 116 cases (1999-2010). *J Am Vet Med Assoc*. 2013; 243:1448-1454.

16. Rottenberg S, von Tscharner C, Roosja PJ. Thymoma-associated exfoliative dermatitis in cat. *Vet Pathol*. 2004;41:429-433.
17. Serfilippi LM, Quance JL. Pathology in Practice. *J Am Vet Med Assoc*. 2018;253 (2):173-176.
18. Singh A, Boston SE, Poma R. Thymoma-associated exfoliative dermatitis with post-thymectomy myasthenia gravis in a cat. *Can Vet J*. 2010;51:757-760.
19. Valentine BA. Skeletal Muscle. In: Zachary JF, ed. *Pathologic Basis of Veterinary Disease*. 7th ed. Elsevier; 2022: 1013-1014, 1033.
20. Valli VE, Bienzle D, Neuten DJ, Linder KE. Tumors of the Hemolymphatic System. In: Meuten DJ, ed. *Tumors in Domestic Animals*. 5th ed. Wiley Blackwell; 2017:305-308.
21. Valli VEO, Kiipel M, Bienzle D. Hematopoietic System. In: Maxie MG, ed. *Jubb, Kennedy and Palmer's Pathology of Domestic Animals*. Vol 3. 6th ed. Elsevier Saunders;2016:141-158.
22. Welle MM, Linder KE. The Integument. In: Zachary JF, ed. *Pathologic Basis of Veterinary Disease*. 7th ed. Elsevier: 2022;1209,1261.
23. Wernick MB, Hilbe M, Kaufmann-Bart M, et al. Pathology in Practice. *J Am Vet Med Assoc*. 2013;243(8):1117-1119.
24. Yale AD, Priestnall SL, Pittaway R, et al. Thymic epithelial tumors in 51 dogs: histopathologic and clinicopathologic findings. *Vet Comp* Oncol. 2022;20:50-58.
25. Yang J, Zhang B, Guah W, et al. Molecular genetic characteristics of thymic epithelial tumors with distinct histological subtypes. *Cancer Med*. 2023;12: 10575-10586.
26. Zitz JC, Birchard SJ, Couto GC, et al. Results of excision of thymoma in cats and dogs: 20 cases (1984-2005). *J Am Vet Med Assoc*. 2008;232(8):1186-1192.

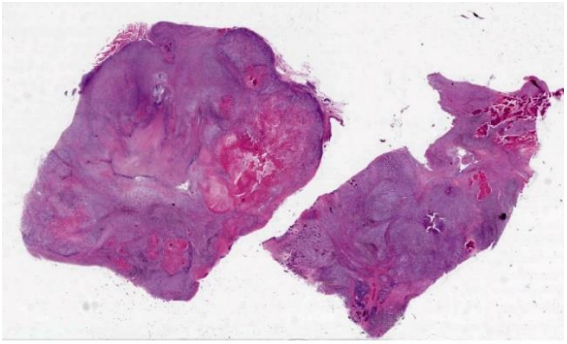

Figure 2-1. Oral mucosa, dog. Two sections of oral mucosa are submitted for examination. Multiple area of bone are visible at subgross magnification in both sections. (HE, 5X)

CASE II:

Signalment:
13-year-old, female spayed Yorkshire terrier (*Canis familiaris*)

History:
A 13-year-old Yorkshire terrier presented with a previously debulked oral mass associated with the caudal hard palate and soft palate. After 3 months of palliative treatment, the dog presented with inappetence, weight loss, and increased respiratory effort. Physical examination showed rapid growth of the mass since the most recent checkup, with partial upper airway obstruction. Euthanasia was elected given the rapid clinical decline.

Gross Pathology:
Within the caudal oral cavity and oropharynx, there is an irregularly shaped, 5 x 3 x 1.5 cm, firm, pale tan to dark gray mass extending ventrally from the hard and soft palate. The submandibular lymph nodes are enlarged, firm, and gray on cut section with loss of corticomedullary architecture. There are dozens of, firm, pale tan to gray, round to multinodular masses ranging from 2-10 mm in diameter within the lungs, mediastinum, spleen, liver, and right adrenal gland.

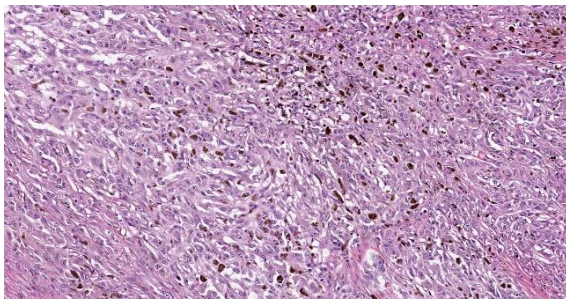

Figure 2-2. Oral mucosa, dog. The neoplasm is composed of pleomorphic cells which range from polygonal to spindle, and approximately 20% of the cells contain cytoplasmic melanin. (HE, 178X)

Microscopic Description:
Oral mucosa: Expanding the lamina propria is an unencapsulated, highly cellular mass composed of a pleomorphic population of neoplastic cells supported by sparse fibrovascular stroma. Neoplastic cells range from polygonal and arranged in sheets or thin cords, to spindle-shaped and arranged in streams and bundles. The neoplastic cells have variably distinct borders, abundant eosinophilic cytoplasm, round to ovoid nuclei, finely stippled chromatin, and 1-2 prominent nucleoli. Anisocytosis is marked and anisokaryosis is moderate. There are 24 mitotic figures in 10 examined 400X fields. Rarely, neoplastic cells contain scant black, fine, granular intracytoplasmic material (melanin). Sporadically throughout the mass, there are numerous round cells with abundant black, granular intracytoplasmic material (melanomacrophages). Within the neoplasm are several foci of homogenous, eosinophilic, extracellular matrix (osteoid) that is frequently associated with individual or thin aggregates of neoplastic cells, and rarely mineralized. Adjacent to and entrapped within the neoplasm are occasional islands of salivary gland tissue and salivary ducts. Centrally within the mass, there are large foci of coagulation necrosis with loss of differential staining, pyknotic and karyorrhectic debris, and occasional pockets of neutrophils. The overlying mucosa is multifocally ulcerated and replaced by a mat of fibrin and necrotic cellular debris with abundant bacteria of mixed morphology.

Immunohistochemistry for SOX10, PNL2, Melan-A, and S100 was performed. >80% of neoplastic cells exhibit strong, nuclear labeling for SOX10 and cytoplasmic labeling for S100. Approximately 50% of neoplastic cells exhibit cytoplasmic labeling for PNL2 with regional variability throughout the tissue. Only sparse neoplastic cells exhibit strong cytoplasmic labeling for Melan-A (<10%).

The same neoplastic population with variable deposition of osteoid comprises all masses in other examined tissues (metastatic sites).

Contributor's Morphologic Diagnosis:
Oral mucosa: Malignant melanoma, osteogenic.

Contributor's Comment:
Malignant melanoma, composed of neoplastic melanocytes of neural crest ectoderm origin, is one of the most common oral tumors in dogs.[16] Canine oral melanomas have been associated with worse clinical outcomes than those arising at other sites. Most canine oral melanomas have metastasized by time of diagnosis, and the median survival time with treatment is under 3 years.[7,9,16] However, a subset of oral melanocytic tumors in dogs exhibits a less aggressive biological behavior despite being characterized histologically as malignant.[5] Mitotic index, nuclear atypia, and Ki67 positivity are reported as relevant prognostic features.[14] Oral melanomas frequently contain a significant amelanotic component, as in this case, but this does not correlate well with biological behavior.

Melanomas can vary widely in their histologic appearance. Cellular morphology can range from round to polygonal to spindle-

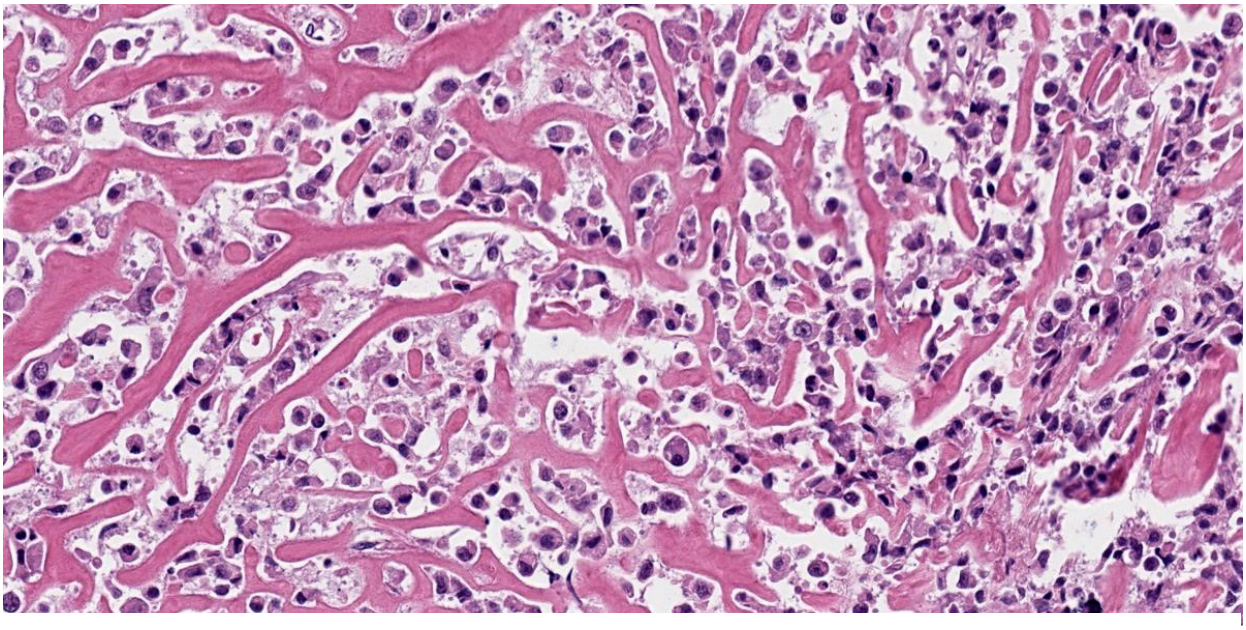

Figure 2-3. Oral mucosa, dog. Neoplastic cells are surrounded by thin anastomosing trabeculae of osteoid. (HE, 381X)

shaped, often within the same anaplastic tumor, likely reflecting their neural crest origin drawing from both neural and epithelial roots. Junctional activity (subepithelial proliferation of neoplastic cells) is considered a characteristic feature that should increase suspicion for melanoma, even when pigmentation is sparse or absent.

The presence of osteoid in the stroma of this melanoma is a rare concurrent finding in canine melanomas, with only a few case reports in the literature.[3,4,8,11] While this osteogenic variant of melanoma is rare, it is important to recognize since osteosarcoma and malignant melanoma differ in prognosis and treatment. Human cases of melanoma with stromal osteoid and/or bone are also rare.[12] Heterologous differentiation in human melanoma is well-recognized and characterized, although these patterns are not widely used in veterinary species and prognostic significance has not been established. Such differentiation patterns include osteocartilaginous, fibroblastic, rhabdomyoblastic, Schwannian, and ganglionic.[1] Cases with osteoid and bone formation are classified as "osteosarcomatous" or "osteocartilaginous" which, as implied by the names, frequently also contain cartilage.[2,6,10]

The mechanism for osteoid and bone formation with canine or human melanoma is unresolved, but multiple hypotheses have been proposed.[1] Because some cranial skeletal elements are derived from neural crest, some postulate that metaplasia of pluripotent precursors results in production of osteoid and bone by the tumor cells. Others have speculated that it represents a stromal response to local trauma, although this does not explain production at sites of metastasis. Alternatively, osteoid and bone could be produced by the tumor stroma in response to release of factors by the neoplastic cells. Such factors have not been characterized in cases of osteogenic melanoma, but could include bone morphogenetic proteins, as an example. Of these possible sources, direct production by metaplastic tumor cells is favored in this case since the matrix is directly surrounded by cells that are

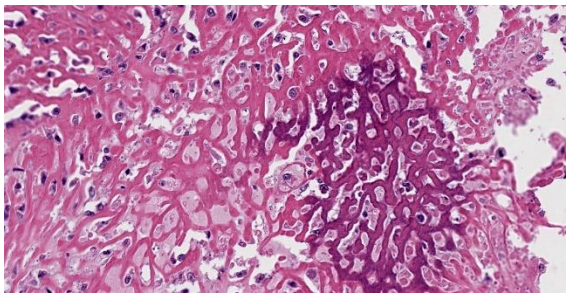

Figure 2-4. Oral mucosa, dog. Multifocally, osteoid is mineralized. (HE, 381X)

morphologically consistent with the neoplastic population; however, immunohistochemistry may contradict this interpretation since most of these "osteogenic" cells are negative for our melanocytic markers.

Because anaplastic melanomas can pose a diagnostic challenge, particularly with poor pigmentation and divergent differentiation, immunohistochemical evaluation is a useful tool. Markers for which melanocytic tumors are typically positive include Melan-A, PNL2, S100, SOX10, TRP-1, and TRP-2.[13,15] Over-reliance on a single immunohistochemical marker can result in false negatives. This occurred in the present case, as the top clinical differential was a poorly-differentiated sarcoma based on a reported negative result for Melan-A on the initial mass debulk.

Contributing Institution:
The Ohio State University
College of Veterinary Medicine
Department of Veterinary Biosciences
https://vet.osu.edu/biosciences

JPC Diagnosis:
Oral mucosa: Osteogenic melanoma.

JPC Comment:
As noted by the contributor, osteogenic melanoma is rare in both human and veterinary medicine. Due to the paucity of reported cases, it is unclear if cartilaginous or osteogenic differentiation is of prognostic significance; therefore, current prognoses and treatment plans for these neoplasms are the same as for conventional, non-productive melanomas.[4]

Most reported cases of osteogenic melanoma have occured primarily in older, small breed dogs, are typically oral, and arise primarily in the gingiva.[4] As noted above, the biological behavior of these tumors is, in the small number of reported cases, similar to oral melanoma.[4] Features common to reported cases of osteogenic melanoma are the absence of primary bony involvement, the presence of junctional activity, and neoplastic cells with distinct melanin granules or Melan-A and S-100 positive cells adjacent to and/or embedded in tumor osteoid.[4]

While the molecular basis for the osteogenic part of osteogenic melanoma remains unclear, melanomas are known to express "runt-related transcription factor 2," or RUNX2, an osteogenic master regulator typically only expressed in osteoblasts and in mesenchymal stem cells during osteogenic commitment.[2,17] In vitro studies have shown that melanoma

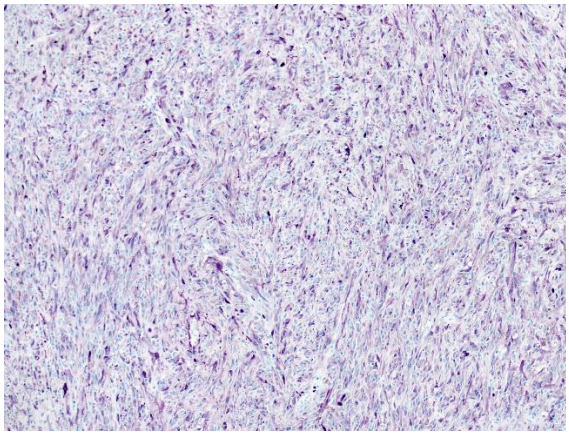

Figure 2-5. Oral mucosa, canine. >80% of neoplastic cells exhibit cytoplasmic labeling for S100. (*Photo courtesy of*: The Ohio State University College of Veterinary Medicine, Department of Veterinary Biosciences, https://vet.osu.edu/biosciences) (anti-S100, 100X)

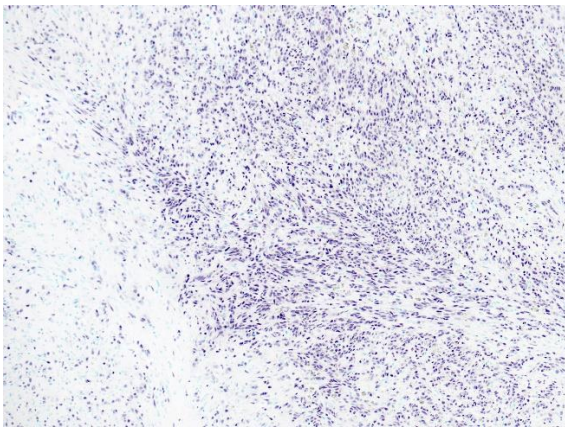

Figure 2-6. Oral mucosa, canine. >80% of neoplastic cells exhibit nuclear labeling for SOX10, with some regional variability. (*Photo courtesy of*: The Ohio State University College of Veterinary Medicine, Department of Veterinary Biosciences) (anti-SOX10, 100X)

cells can be induced to form bone directly by expression of both bone sialoprotein and RUNX2.[4] Increased RUNX2 expression also induces the expression of specific metalloproteinases and collagenases that potentiate matrix degradation and tumor invasion. Because of this, it has been suggested that the presence of neoplastic bone in malignant melanoma suggests that mesenchymal conversion has occurred and that osteogenic melanoma may, therefore, have a greater metastatic potential when compared to its non-osteogenic counterpart.[4]

The presence of osteoid, multinucleated cells, and suspected melanin-containing cells initially stymied diagnostic progress among conference participants, and discussion quickly narrowed to the two main differentials of melanoma and osteosarcoma. Further frustrating efforts was the paucity of oral mucosa in the examined section, making it difficult to assess junctional activity, the presence of which would have helped convince a skeptical audience of the melanocytic origin of this neoplasm. Conference participants discussed and reviewed melanocytic immunohistochemical marker PLN2, which was convincingly positive in approximately 30-40% of neoplastic cells. Participants remarked on the quantitative and qualitative variability in staining among the neoplastic cells, causing the moderator to speculate that not all neoplastic cells are perfectly clonal, and this variability in gene expression, coupled with genetic variability induced by the tumor microenvironment could account for the pleomorphic quality often seen with immunohistochemical staining.

Conference participants discussed whether the prominent bone within section was produced by the neoplasm, or part of normal anatomic structures. The moderator noted that the section was not decalcified, which would normally be required for section through the mandible or maxilla, suggesting that all the bone in section was produced by the tumor.

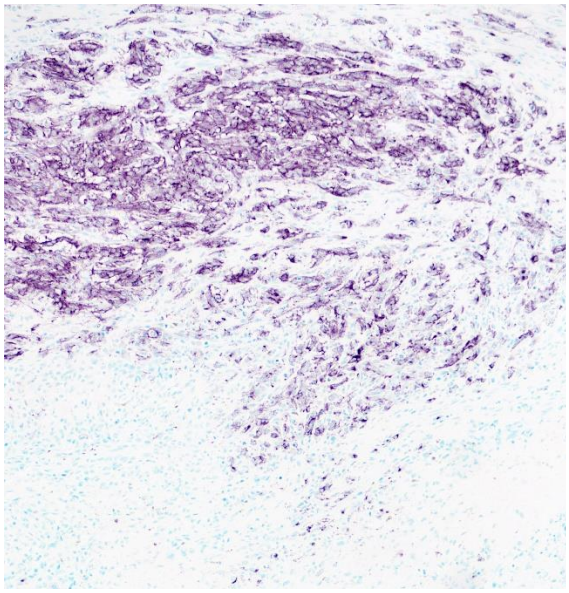

Figure 2-7. Oral mucosa, canine. Approximately 50% of neoplastic cells exhibit cytoplasmic labeling for PNL2 with significant regional variability. (*Photo courtesy of*: The Ohio State University College of Veterinary Medicine, Department of Veterinary Biosciences) (anti-PNL2, 100X)

The moderator cautioned participants to maintain an index of suspicion for osteogenic melanoma, particularly in the oral cavity where neoplasms such as ossifying fibroma and osteosarcoma or lesions producing cemento-osseous matrix are more apt to come to mind when presented with spindle cells producing an osteoid-like matrix.

References:

1. Banerjee SS, Eyden B. Divergent differen-tiation in malignant melanomas: a review. *Histopathology*. 2008;52(2):119-129.
2. Barroso de Carvalho B, Batista Dos Santos Medeiros D. Melanoma with osteo-cartilaginous differentiation. *An Bras Dermatol*. 2023;98(2):266-269.
3. Chénier S, Doré M. Oral malignant melanoma with osteoid formation in a dog. *Vet Pathol*. 1999;36(1):74-76.
4. Ellis AE, Harmon BG, Miller DL, Northrup NC, Latimer KS, Uhl EW. Gingival osteogenic melanoma in two dogs. *J Vet Diagn Invest.* 2010;22(1):147-151.
5. Esplin DG. Survival of dogs following surgical excision of histologically well-differentiated melanocytic neoplasms of the mucous membranes of the lips and oral cavity. *Vet Pathol*. 2008;45(6):889-896.
6. Lucas DR, Tazelaar HD, Unni KK, et al. Osteogenic melanoma. A rare variant of malignant melanoma. *Am J Surg Pathol*. 1993;17(4):400-409.
7. Nishiya AT, Massoco CO, Felizzola CR, et al. Comparative aspects of canine melanoma. *Vet Sci*. 2016;3(1):7.
8. Oyamada T, Tanaka H, Park C-H, Ueki H, Komiya T, Arai S. Pathology of canine oral malignant melanoma with cartilage and/or osteoid formation. *J Vet Med Sci*. 2007;69(11):1155-1161.
9. Pazzi P, Steenkamp G, Rixon AJ. Treatment of canine oral melanomas: a critical review of the literature. *Vet Sci*. 2022;9(5):196.
10. Saleh J, Wang ML, Harms PW, Patel RM, Fullen DR. Malignant melanoma with osteosarcomatous differentiation in a lymph node metastasis. *J Cutan Pathol*. 2018;45(9):701-704.
11. Sánchez J, Ramirez GA, Buendia AJ, et al. Immunohistochemical characterization and evaluation of prognostic factors in canine oral melanomas with osteo-cartilaginous differentiation. *Vet Pathol*. 2007;44(5):676-682.
12. Savant D, Kenan S, Kenan S, Kahn L. Osteogenic melanoma: report of a case mimicking osteosarcoma and review of the literature. *Skeletal Radiol*. 2018;47(5): 711-716.
13. Smedley RC, Lamoureux J, Sledge DG, Kiupel M. Immunohistochemical diagnosis of canine oral amelanotic melanocytic neoplasms. *Vet Pathol*. 2011;48(1): 32-40.
14. Smedley RC, Spangler WL, Esplin DG, et al. Prognostic markers for canine melan-ocytic neoplasms: a comparative review of the literature and goals for future inves-tigation. *Vet Pathol*. 2011;48 (1):54-72.
15. Tsoi MF, Thaiwong T, Smedley RC, Noland E, Kiupel M. Quantitative expression of TYR, CD34, and CALD1 discriminates between canine oral malignant melanomas and soft tissue sarcomas. *Front Vet Sci*. 2021;8:701457.
16. Uzal FA, Plattner BL, Hostetter JM. Alimentary System. In: Maxie MG, ed. *Jubb, Kennedy, and Palmer's Pathology of Domestic Animals*. 6th ed. Vol 2. Saunders;2016:1-257.e2.
17. Valenti MT, Carbonare LD, Mottes M. Ectopic expression of the osteogenic master gene RUNX2 in melanoma. *World J Stem Cells*. 2018;10(7):78-81.

Figure 3-1. Eye, dog. A section of the globe is submitted for examination. At subgross magnification, the uvea is markedly expnded by a neaoplastic round cell tumor. The lens is pushed artifactually into the vitreous in this section. (HE, 5X)

CASE III:

Signalment:
7-year-old, female spayed Bassett hound (*Canis familiaris*)

History:
The patient initially presented to a veterinary clinic with a two-day history of inappetence and lethargy. Blood work performed in-house at that time revealed elevated liver enzyme activities. Splenomegaly was detected by ultrasound, and the spleen was consequently removed surgically. Three months later, the dog re-presented with exophthalmos of the left eye. The clinician diagnosed a luxated lens and glaucoma. The eye was enucleated and submitted for histology. The clinical concern was metastasis to the eye from the previously diagnosed splenic mass.

Gross Pathology:
The submitted trimmed globe was 24 x 24 x 27 mm.

Microscopic Description:
Globe: There is severe multifocal infiltration of the uveal tract by unencapsulated sheets of moderately pleomorphic round cells, resulting in thickening of the choroid (to 600 µm) and iris (to 2.5 mm). Neoplastic cells have scant, lightly eosinophilic cytoplasm and irregularly round to elliptical nuclei with 1-2 atypically large nucleoli. The mitotic rate averages 2-4 per HPF. There is moderate anisokaryosis. Similar cells are present in the lumina of choroidal vessels, as well as in ciliary process epithelium and in the anterior chamber. The neoplastic round cells form sheets adherent to the anterior aspect of the iris. They are also present between the sensory and non-sensory retina, admixed with melanin-containing macrophages of presumptive retinal pigmented epithelium (RPE) origin. Modest numbers of small lymphocytes, interpreted as an inflammatory response, are present at the margins of the intra-uveal neoplastic infiltrates. Other changes include retinal detachment with tombstone hypertrophy of the RPE, deep neovascularization of the corneal substantia propria, hemorrhage with fibrin exudation in the anterior chamber, and hemorrhage in the posterior chamber and in the vitreous. There is posterior luxation of the lens, edema of ciliary processes, mild vacuolation of lens fibers at the lenticular bow, cytoplasmic vacuolation with partial loss of corneal endothelium, and partial occlusion of the drainage angle.

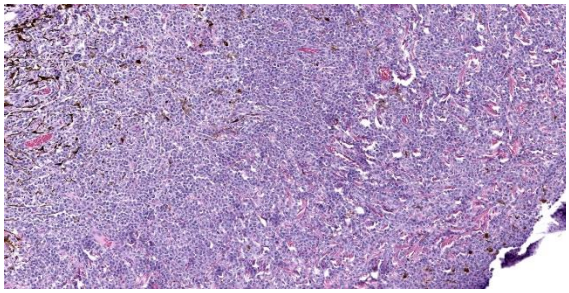

Figure 3-2. Eye, dog. The iris is markedly expanded by sheets of neoplastic lymphocytes. (HE, 102X)

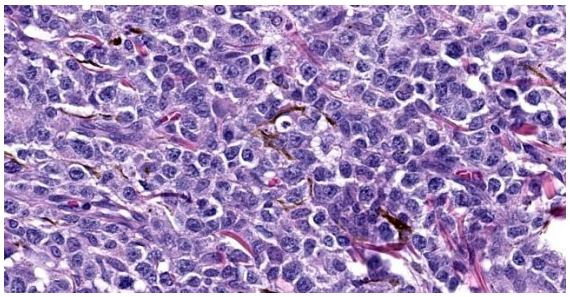

Figure 3-3. Eye, dog. High magnification of neoplastic lymphocytes within the iris.

Contributor's Morphologic Diagnosis:
Eye, uvea: Lymphoma, metastatic, with secondary retinal detachment, intraocular hemorrhage, uveitis and glaucoma, Basset hound, canine.

Contributor's Comment:
The dog was diagnosed three months earlier with intrasplenic T cell lymphoma. This was based on positive staining for CD3 and negative staining for CD79a. A comparable staining pattern was evident in the intraocular mass. The clinician's concern about intraocular metastasis, resulting in lens luxation and glaucoma, was warranted.

Lymphoma is the most common metastatic intraocular tumor of dogs.[1] It may occur in as many as one third of canine lymphosarcoma cases.[8,11] Primary intraocular lymphomas (presumed solitary ocular lymphoma [PSOL], corresponding to the primary intraocular lymphoma [PIOL] of human patients) can also occur. Such tumors are considered rare in dogs.[5,7,11]

The clinical presentation in this case (i.e., glaucoma and lens luxation) is fairly typical for dogs with lymphoma metastatic to the eye. Clinical features may also include uveitis, retinal hemorrhage, retinal detachment, hyphema, and conjunctivitis.[1,5] Most of these features were found histologically in this dog. Ocular signs may represent the initial finding in dogs with generalized lymphoma, prompting owners to take the animal to a clinician. This salmagundi of intraocular changes can mimic other primary intraocular conditions and mislead clinicians, analogous to the masquerade syndrome in people.[2]

Confirmation of metastasis of lymphoma to the eye(s) can be of prognostic value for dogs undergoing standard chemotherapeutic regimens. Such dogs have a lifespan only 60 – 70% as long as those without ocular metastasis. Intraocular metastasis of lymphoma to one or both globes is therefore an ominous development.[1] Neoplastic lymphocytes are thought to localize initially in the anterior ciliary body and/or iris root.[5] When the intraocular lymphoma is at a more advanced stage, as in this case, the anterior uvea tends to be the most severely infiltrated component, followed by the choroid.[1] Median survival time in one study of 100 dogs with intraocular lymphoma was 104 days. There was no statistical difference in survival time between animals with lymphoma of T versus B cell derivation.[5] Survival times in dogs with true primary intraocular lymphoma are longer (MST: 769 days) and some appear to have been cured by surgical enucleation alone.[5] Survival times in dogs undergoing chemotherapy for intraocular lymphoma can be as long as one year, compared to 2-4 weeks for untreated dogs.[5]

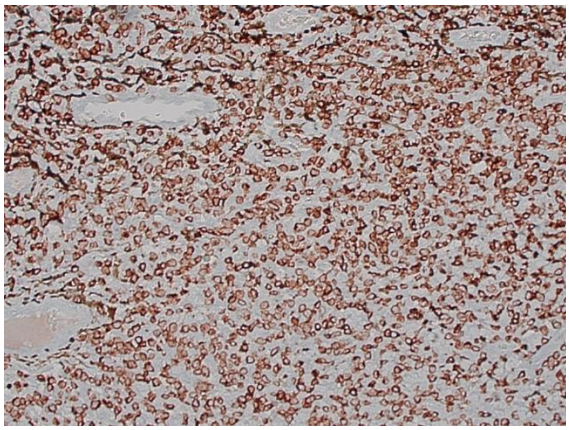

Figure 3-4. Eye, dog. Neoplastic lymphocytes stain strongly immunopositive for CD3 (a T-cell marker). (anti-CD3, 400X)

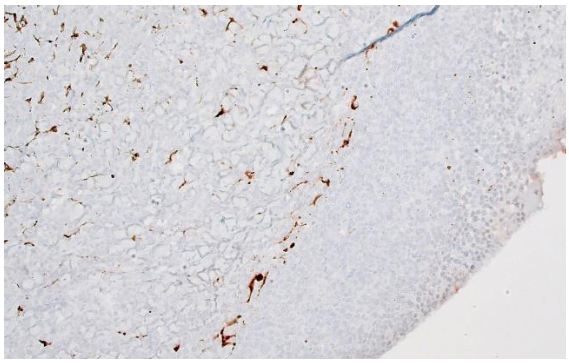

Figure 3-5. Eye, dog. Neoplastic cells are immunonegative for CD20 (a B-cell marker). (anti-CD20, 400X)

There is an interesting disparity between intraocular lymphoma in dogs with multicentric T cell lymphoma relative to human patients. People with generalized T cell lymphoma rarely develop intraocular metastases.[5] By contrast, a voluminous literature now exists about primary intraocular lymphoma in people, generally of B lymphocyte origin, which may also involve brain, spinal cord and/or meninges.[2] These are thought to arise in a multicentric fashion in the CNS and in the retina-vitreous.

In our experience, clinicians prefer to enucleate eyes in which they suspect intraocular neoplasia rather than use cytology first to establish the identity of the tumor. Some current cytology texts provide guidelines for interpretation so that cytology and/or antigen receptor rearrangement (PARR) testing may be used more in the future following anterior chamber paracentesis.[9,10] For understandable reasons, cytology is more commonly used in human ophthalmology for intraocular masses, relative to dogs or cats. It is likely in this case that cytological sampling of anterior chamber could have generated a diagnosis of lymphoma.

Contributing Institution:
Wyoming State Veterinary Laboratory
1174 Snowy Range Road
Laramie, WY 82070.
http://www.uwyo.edu/wyovet/

JPC Diagnosis:
Eye, uvea: Lymphoma, intermediate cell, mid-grade.

JPC Comment:
This case provides an excellent, classic example of the ocular manifestation of canine multicentric lymphoma. As the contributor notes, ocular involvement is seen in over one-third of dogs with multicentric lymphoma and is second only to enlarged lymph nodes as the most common clinical finding in canine lymphoma. Due to hematogenous spread, the uveal tract, most commonly the choroid, is affected in the vast majority of cases (97% in one large retrospective study), followed by the retina (46%), the cornea (32%), and the sclera (43%).[5] As in this case, peripheral T-cell lymphoma is the most common histologic subtype encountered in the eye, followed closely by diffuse large B-cell lymphoma (DLBCL).[5]

While lymphoma is the most common metastatic intraocular tumor, it is, of course, not the only one. A recent large retrospective study of 173 canine intraocular tumors found that the median age of diagnosis was 10 years, and the most commonly represented breeds included neoplasia stalwarts Labrador Retrievers and Golden Retrievers as well as mixed breed dogs.[4] In this patient population, the primary multicentric malignancies were lymphoma and histiocytic sarcoma, consistent with previous reports.[4] Intraocular histiocytic sarcoma is associated with a particularly short post-diagnosis survival time lending support to the view that intraocular histiocytic sarcoma is most commonly manifestation of disseminated, multicentric disease.[4]

Excluding the hematopoietic/multicentric tumors, hemangiosarcoma was found to be the most common metastatic intraocular tumor. Metastatic epithelial neoplasms represented in the study included mammary, pancreatic, and urothelial carcinomas.[4]

The moderator began discussion of this case by noting the mild edema and multifocal vascularization of the cornea, which had been overlooked in initial descriptions of the slide. The moderator cautioned participants to examine all tissues present, particularly when, as in this case, the slide is dominated by one major, attenting-grabbing lesion. And while a dramatic lesion, conference participants made relatively short diagnostic work of this neoplasm. Participants briefly discussed the possibility of melanoma, which the moderator noted would, in dogs, typically be nodular rather than the diffusely thickend iris examined in section. The common top differential was lymphoma, confirmed by the diffuse positive cytoplasmic immunoreactivity of neoplastic cells for CD3.

Conference discussion moved to the clinical diagnosis of glaucoma and the lack of convinving evidence of glaucoma on histologic examination. The moderator noted that degeneration of the retinal ganglion cell layer is a key histologic hallmark of glaucoma that was absent in the examined section. Participants remarked on the tombstoning and hypertrophy of the retinal pigmented epithelium which suggests that the observed retinal detachment is unlikely artifact, though a cause for the detachment was not apparent histologically.

The moderator noted that presence of intraocular lymphoma automatically makes for stage V disease under the WHO lymphoma guidelines. This is a codification of the lymphoma dogma of "if it's in the eye, it's everywhere." The moderator noted that this view

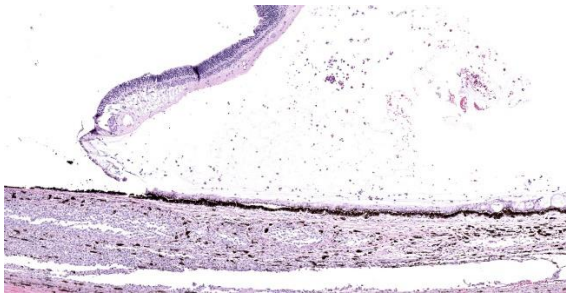

Figure 3-6. Eye, dog. Neoplastic cells expand the choroid beneath the detached, mildly atrophic retina. (HE, 66X).

is changing, pointing to the presence of presumed solitary ocular lympoma [PSOL] which can often be successfully treated by enucleation.

Discussion ended with a brief survey of unique feline ocular neoplasias, including feline diffuse iris melanoma. The moderator noted that the examined section would be suspicious for this entity if the patient were a cat as the histological appearance is similar. Conference participants also discussed feline post-traumatic ocular sarcoma, an aggressive neoplasm that is locally invasive with metastatic potential. The sarcoma arises from metaplastic lens epithelium and can invade extraorbital tissues, typically via the limbus or the optic nerve.

References:

1. Carlton WC, Hutchinson AK, Grossniklaus HE. Ocular lymphoid proliferations. In: Peiffer RL, KB Simons KB, eds. *Ocular Tumors in Animals and Humans*. Iowa State Press;2002:379-413.
2. Coupland SE, Chan CC, Smith J. Pathophysiology of retinal lymphoma. *Ocul Immunol Inflamm*. 2009;17:227-237.
3. Coupland SE, Damato B. Understanding intraocular lymphomas. *Clin Experiment Ophthalmol*. 2008;36:564-578.
4. Krieger EM, Pumphrey SA, Wood CA, Mouser PJ, Robinson NA, Maggio F. Retrospective evaluation of canine primary, multicentric, and metastatic

intraocular neoplasia. *Vet Ophthalmol*. 2022;25(5): 343-349.
5. Lanza MR, Musciano AR, Dubielzig RD, Durham AC. Clinical and pathological classification of canine intraocular lymphoma. *Vet Ophthalmol*. 2018;21:167-173.
6. Levy-Clarke GA, Greenman D, Sieving PC, et al. Ophthalmic manifestations, cytology, immunohistochemistry, and molecular analysis of intraocular metastatic T-cell lymphoma: report of a case and review of the literature. *Surv Ophthalmol*. 2008;53:285-295.
7. Malmberg JL, Garcia T, Dubielzig RR, Ehrhart EJ. Canine and feline retinal lymphoma: a retrospective review of 12 cases. *Vet Ophthalmol*. 2017;20:73-78.
8. Miller PE, Dubielzig RR. Ocular tumors. In: Withrow SJ, Vail DM, Page RL, eds. *Small Animal Clinical Oncology*. 5th ed. Elsevier;2013:597-607.
9. Pate DO, Gilger BC, Suter SE, Clode AB. Diagnosis of intraocular lymphosarcoma in a dog by use of a polymerase chain reaction assay for antigen receptor rearrangement. *JAVMA*. 2011;238:625-630.
10. Raskin RE. Eyes and adnexa. In: Raskin RE, Meyer DJ, eds. *Canine and Feline Cytology. A Color Atlas and Interpretation Guide*. 3rd ed. Elsevier;2016;408-429.
11. Wiggans KT, Skorupski KA, Reilly CM, Frazier SA, Dubielzig RR, Maggs DJ. Presumed solitary intraocular or conjunctival lymphoma in dogs and cats: 9 cases (1985–2013). *JAVMA*. 2014;244:460-470.
12. Krieger EM, Pumphrey SA, Wood CA, Mouser PJ, Robinson NA, Maggio F. Retrospective evaluation of canine primary, multicentric, and metastatic intraocular neoplasia. *Vet Ophthalmol*. 2022;25(5): 343-349.

Figure 4-1. Pancreas, dog. A 15 x 3 x 3 cm segment of the left limb and body of the pancreas was submitted for histologic evaluation. (*Photo courtesy of:* Department of Population Health and Pathobiology, North Carolina State University College of Veterinary Medicine, Raleigh, NC 27607 https://php.cvm.ncsu.edu/)

CASE IV:

Signalment:
11-year-old, female spayed German shorthaired pointer (*Canis familiaris)*

History:
This patient initially presented for bilious vomiting and a pancreatic mass was subsequently identified on abdominal ultrasound and confirmed with computed tomography (CT). Partial pancreatectomy to excise a 15 mm diameter mass from the right distal limb of the pancreas was performed. The patient presented 6 weeks later for a recheck CT at which time an additional pancreatic mass was identified. Another partial pancreatectomy, this time of the left limb and body of the pancreas, was performed.

Gross Pathology:
A formalin-fixed, 15 x 3 x 3 cm segment of the left limb and body of the pancreas was submitted for histologic evaluation. Near the

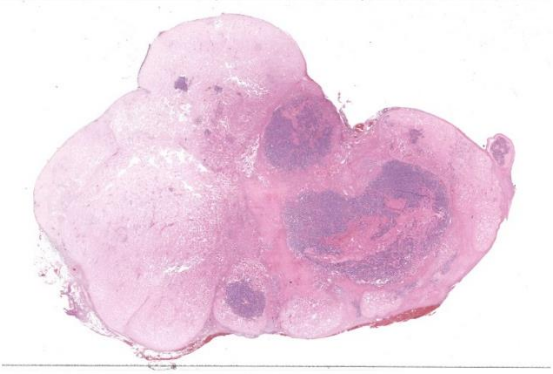

Figure 4-2. Pancreas, dog. A nodule of neoplastic acinar tissue is largely replaced by eosinophilic hyaline material. (HE, 4X)

proximal aspect was a rounded, 4 x 3 x 2.5 cm, light brown mass. The cut section revealed multifocal to coalescing rounded, smooth, firm, light brown, waxy nodular material (up to 1.4 x 1.2 x 1.2 cm diameter) with embedded and semi-firm brown tissue.

Microscopic Description:
Pancreas: Markedly expanding, replacing, and effacing the pancreatic architecture and compressing resident pancreatic tissue, is a poorly-demarcated multilobular mass of neoplastic polygonal cells and extracellular matrix. Neoplastic cells form irregular acini and ducts and are embedded within and adjacent to an abundant, acellular, eosinophilic, hyalinized matrix that comprises approximately 30-70% of the mass (varied in different sections). Neoplastic epithelial cells have variably distinct cell borders, moderate to abundant brightly eosinophilic granular cytoplasm, and a large vesicular nucleus often with central single prominent nucleolus, but occasionally up to three nucleoli. Anisocytosis and anisokaryosis are moderate with frequent karyomegaly and 14 mitotic figures in 10 hpfs (2.37 mm^2). Multifocally, ducts have lost cellular detail and contain eosinophilic cellular debris. Cellular debris and few macrophages with intracellular pyknotic debris are scattered throughout the neoplasm. Differentiation between overtly neoplastic cells and resident cells is limited in marginal areas where more normal tubules and acini are also in close proximity to the hyalinized matrix.

Contributor's Morphologic Diagnosis:
Pancreas: Exocrine pancreatic adenocarcinoma, hyalinizing type.

Contributor's Comment:
This pancreatic mass is consistent with a hyalinizing type of exocrine pancreatic carcinoma. A recent review of pancreatic carcinomas in the dog reports these tumors are rare with no clear sex-predilection and a potential breed predisposition in Airedale terriers.[1] Clinical signs are typically non-specific and can include vomiting, inappetence, diarrhea, polyuria/polydipsia, and a palpable abdominal mass.[1] The hyalinizing variant has only been reported in dogs, with most occurring in the right limb of the pancreas.[3]

The composition of the hyalinized matrix has not been fully characterized, though application of special and immunohistochemical stains to masses of this type have not been consistent with amyloid A, laminin, collagen, immunoglobulin, or alpha-1 antitrypsin.[3]

Types of recognized and reported variants of exocrine pancreatic carcinomas in the dog include acinar, ductal, hyalinizing, and mixed endocrine-exocrine.[1,2] Growth patterns are described including acinar, solid, rosette, clear, mucinous, and tubulopapillary with variable differentiation.[1,4] Acinar is most commonly reported in dogs, as compared to humans, in which exocrine pancreatic carcinomas are more often ductal, though differentiation can overlap within the same tumor.[1] Exocrine pancreatic carcinomas have the potential for metastasis, especially to the liver and local lymph nodes.[3] Evidence of metastasis was not identified in additional tissues submitted for this patient.

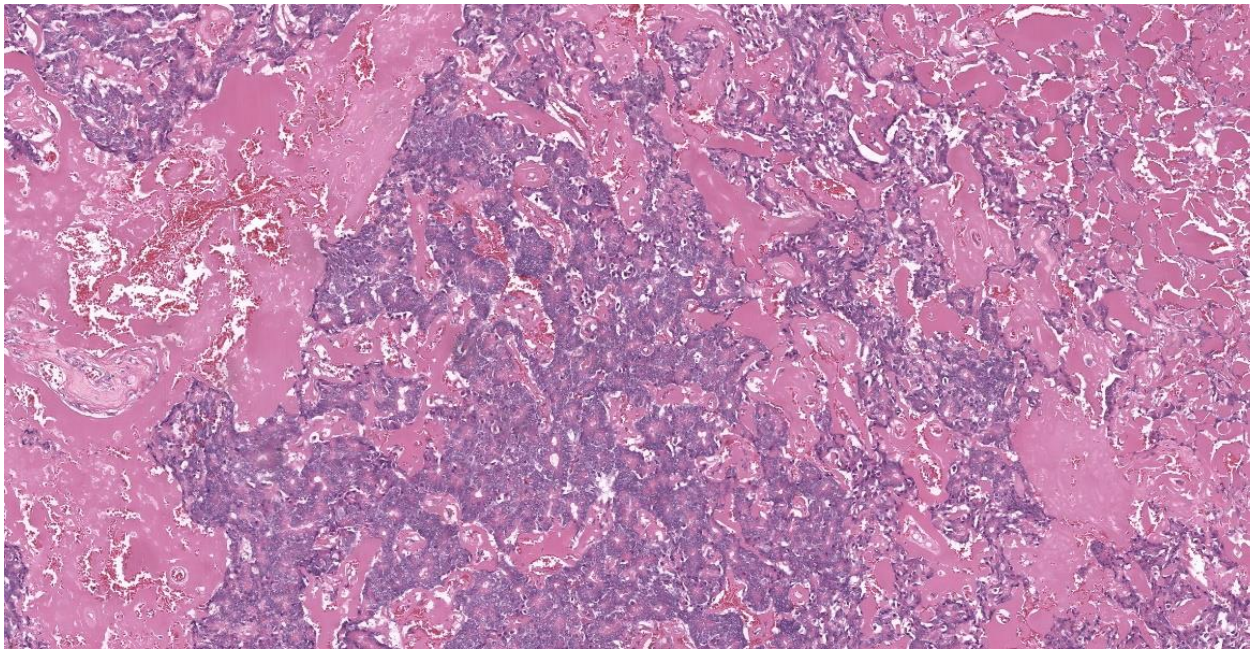

Figure 4-3. Pancreas, dog. Foci of neoplastic acinar tissue are embedded in abundant eosinophilic hyaline material. (HE, 80X)

As cases are rare, no particular set of prognostic features has been established, though the hyalinizing variant may have better post-diagnosis survival times, especially if the patient survives the acute-post surgical interval.[3] The patient in this case was alive at time of submission, nearly seven months after initial diagnosis.

Contributing Institution:
Department of Population Health
and Pathobiology
North Carolina State University
College of Veterinary Medicine
Raleigh, NC 27607
https://php.cvm.ncsu.edu/

JPC Diagnosis:
Pancreas: Exocrine adenocarcinoma, hyalinizing type.

JPC Comment:
As the contributor notes, pancreatic neoplasia in dogs is rare, and the hyalinzing variant, so beautifully demonstrated by this case, is rarer still. Most canine pancreatic neoplasms are derived from the exocrine epithelium and are usually malignant, with clinical signs appreciated only after extensive local growth or metastasis to the liver, lymph nodes, or lymph nodes has occurred.[3]

Canine exocrine pancreatic carcinomas come in many varieties, with cuboidal, polygonal, or columnar cells of varying polarities and degrees of granulation forming tubules, acinar structures, or solid sheets of cells on stromal elements raning from delicate and fibrovascular to scirrhous. Histologic subcategories based on morphology are described for canine pancreatic neoplasias, though these subcategories currently have no confirmed prognostic significance or ability to predict biologic behavior.[3]

The hyalinizing variant of exocrine pancreatic carcinoma was first and most extensively described in a case series of six older mid-sized dogs; in most of these patients, the mass was present grossly as a single solitary mass, and most were discovered incidentally.[3] As

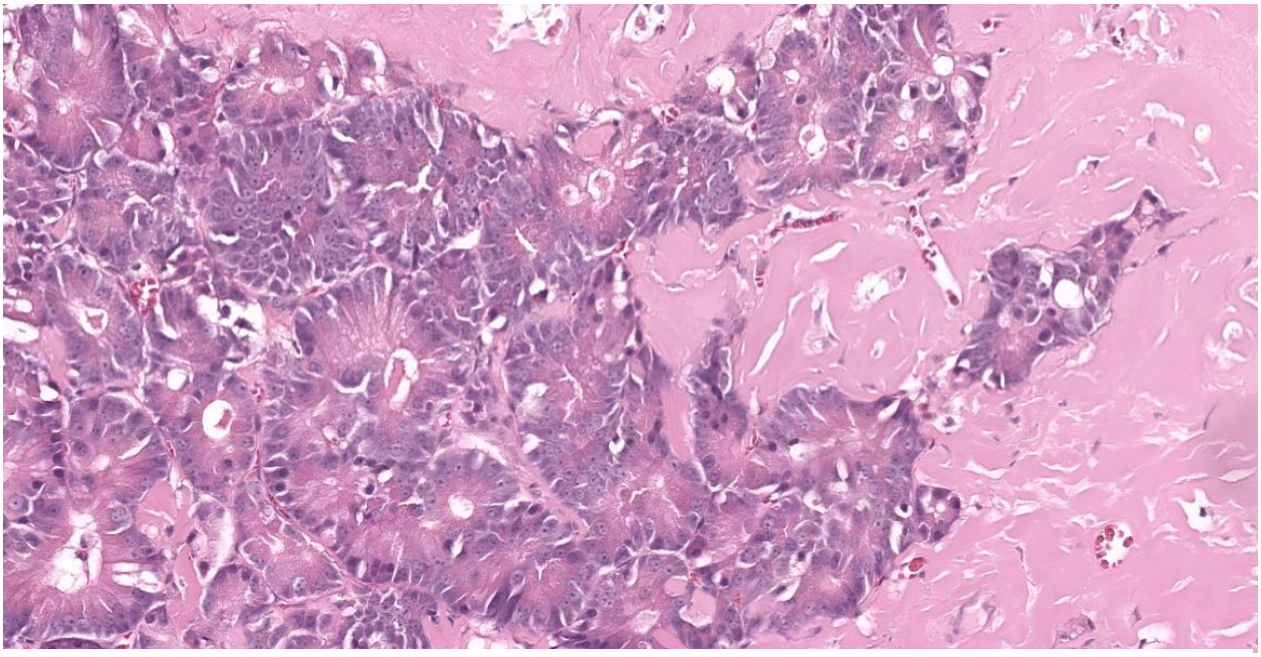

Figure 4-4. Pancreas dog. High magnification of neoplastic acinar cells embedded in hyaline material. (HE, 237X)

nicely demonstrated by this case, the feature that distinguishes the hyalinzing variant from a traditional exocrine pancreatic carcinoma is the presence of large contiguous areas of accumulated extracellular hyaline material that has the appearance, though not the staining or immunohistochemical properties, of amyloid.[3] Neoplastic cells typically form tubules and are well-differentiated, with recognizable zymogen granules within the cytoplasm.[3] In the initial case study, these histological features suggested a low-grade malignancy in all six cases, though some features of malignancy were noted, such as mild cellular atypia, frequent mitotic figures, and stromal invasion.[3]

As the contributor notes, based on the few reported cases of hyalinizing exocrine pancreatic adenocarcinoma, it is possible that this variant has a less aggressive course than its conventional counterpart. In contrast to conventional exocrine pancreatic adenocarcinomas, which have often metastasized or invaded at the time of diagnosis, in the initial descriptive case study of 6 dogs, metastatic disease was present in only 1 dog, and this dog lived for 16 months post-diagnosis.[3] Speculating on the possible causes for this relatively indolent behavior, researchers posited that perhaps the unique accumulations of hyalinized matix within the tumor provided mechanical or biochemical impediments to the cell-matrix interactions required for tumor growth, invasion, and metastasis.[3]

Conference participants were struck by the abundant matrix that is the main histologic feature of this neoplasm. This matrix, together with the relatively differentiated neoplastic cells, made for an easy, though unfamiliar diagnosis. Discussion focused predominately on the nature of the matrix itself which, as noted, is of unknown composition. Participants evaluated a Masson trichrome, which stained the matrix an unusual gray-blue which was quite distinct from the vibrant blue staining of normal mature collagen. Evaluation of a Movat pentachrome stain revealed a deep yellow-orange color, most consistent with, but not specific for, collagen. While a tumor of first instance for most

conference participants, the moderator noted that these tumors do occasionally appear in her diagnostic workload, including, an as-yet unpublished case in a cat.

References:

1. Aupperle-Lellbach H, Törner K, Staudacher M, Müller E, Steiger K, Klopfleisch R. Characterization of 22 canine pancreatic carcinomas and review of literature. *J Comp Pathol*. 2019;173:71-82.
2. Belshaw Z, Bacon NJ, Foale RD, Mannion PM, Reuter R. Pancreatic mixed acinar-endocrine carcinoma in a dog. *Vet Comp Oncol*. 2005;3(3):145-148.
3. Dennis MM, O'Brien TD, Wayne T, Kiupel M, Williams M, Powers BE. Hyalinizing pancreatic adenocarcinoma in six dogs. *Vet Pathol*. 2008;45(4):475-483.
4. Pavone S, Manuali E, Eleni C, Ferrari A, Bonanno E, Ciorba A. Canine pancreatic clear acinar cell carcinoma showing an unusual mucinous differentiation. *J Comp Pathol*. 2011;145(4):355-358.

WSC 2023-2024
Conference 21 Self-Assessment

1. Which of the following thymoma variants are characterized by spindle epithelial cells?
    a. Type A
    b. Type AB
    c. Type B
    d. Types A and AB

2. Which of the following is not a documented form of heterologous differentiation in melanomas?
    a. Lipomatous
    b. Osteosarcomatous
    c. Fibroblastic
    d. Encephalitis

3. Which of the following is true?
    a. There was no statistical difference in survival time between animals with ocular lymphoma of T versus B cell derivation.
    b. Primary intraocular has a shorter mean survival time than metastatic ocular lymhoma.
    c. The choroid is primarily involved in advanced intraocular lymphoma

4. The composition of the matrix in hyalinizing pancreatic adenocarcinoma is composed of:
    a. AA amyloid
    b. AL amyloid
    c. LPH-1-antitrypsin
    d. It’s yet unknown.

5. Which of the following is not a recognized fom of pancreatic exocrine adenocarcinoma?.
    a. Hyalinizing
    b. Solid
    c. Clear cell
    d. Rosette

Joint Pathology Center
Veterinary Pathology Services

WEDNESDAY SLIDE CONFERENCE 2023-2024

Conference #22 12 April 2024

CASE I:

Signalment:
18-month-old Angus heifer, *Bos taurus*, bovine.

History:
Two out of a herd of one hundred heifers had a history of progressive wasting and diarrhea. One of the heifers had a body condition score of 1/5 and was euthanised.

Gross Pathology:
A field post-mortem was performed and over 10 adult liver flukes were observed in the liver parenchyma, as well as occasional multifocal areas of chronic pulmonary consolidation and suspected ileum thickening.

Laboratory Results:
Serum liver fluke ELISA S/P % - 158 (strong positive).

Serum pestivirus antigen capture ELISA - negative.

Bovine Johne's disease liquid culture and PCR - negative.

Microscopic Description:
Portal areas are markedly expanded by proliferative fibroblasts, mature connective tissue, markedly increased numbers of small caliber bile ducts (biliary hyperplasia) replacing periportal hepatocytes and frequently joining between adjacent portal areas and

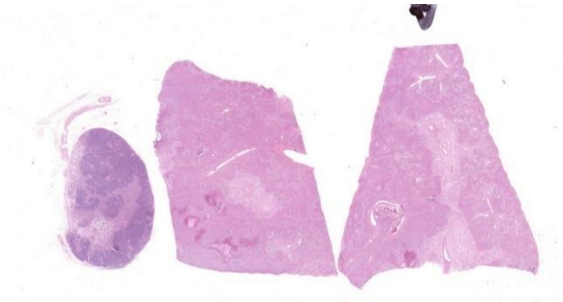

Figure 1-1. Liver, ox. One section of reactive lymph node (left) and two section liver are submitted for examination . At subgross magnification, there is bridging fibrosis between portal areas, and on the section at right, a cross section of a fluke is present in a bile duct. (HE, 4X)

isolating hepatic lobules (bridging fibrosis), and numerous eosinophils and lymphocytes. Macrophages scattered in portal areas and sinusoids often contain yellow-brown pigment (likely bile). Multifocally replacing parenchyma, there are several irregular, well demarcated areas of homogenous eosinophilic material (proteinaceous oedema) with extravasated erythrocytes (haemorrhage) and frequent intact and degenerate eosinophils and macrophages, surrounded by fibrillar eosinophilic material (fibrin) (liver fluke migration tract). Focally replacing the parenchyma, there is a longitudinal section of a 3.1 x 0.9 mm metazoan parasite which features a prominent outer tegument with spines on the anterior two thirds, muscular anterior (oral) and ventral suckers, with a digestive tract which includes a caecum containing yellow-brown pigment, surrounded by parenchyma,

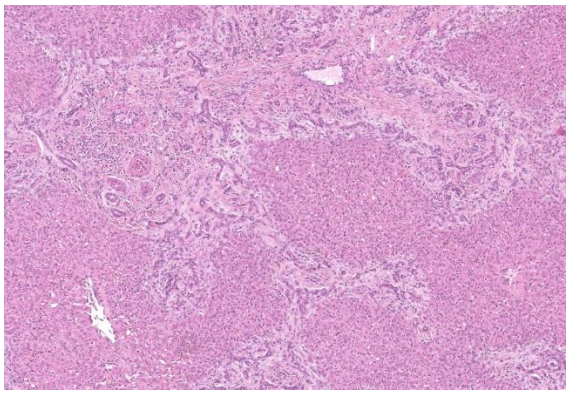

Figure 1-2. Liver, ox. There is bridging fibrosis of portal areas and marked biliary hyperplasia. (HE, 82X)

and no evidence of a uterus, vitellarian glands, or eggs (morphology consistent with juvenile *Fasciola hepatica*).

Contributor's Morphologic Diagnosis:
Liver: Fibrosis, periportal and bridging, marked, diffuse, chronic, with marked biliary hyperplasia, eosinophilic and lymphocytic portal hepatitis, parasitic migration tracts and intralesional juvenile trematode, morphology consistent with *Fasciola hepatica, Bos taurus.*

Contributor's Comment:
Liver fluke (*Fasciola hepatica*) is a common endoparasite of cattle and sheep which is endemic to Eastern Australia and poses a major economic threat to producers.[1] The life cycle of the liver fluke in the animal begins with excystment of metacercariae in the small intestine where newly emerged juvenile flukes migrate to the liver and then over 8-10 weeks migrate through the hepatic parenchyma to the bile ducts. Here, they mature into adult flukes and produce eggs in the bile and feces 8-10 weeks post infection.[2] In the acute phase, the migration through the liver causes extensive inflammation and hepatocellular damage, which induces an antibody response.[2]

There are several different methods used to diagnose liver fluke, including fecal sedimentation examination, necropsy, histopathology, and immunological based tests which include an antibody ELISA, or a commercial fecal copro-antigen ELISA (cELISA; Bio X diagnostics, Belgium). Each method has advantages and disadvantages, and test results should be interpreted in light of the tests' shortcomings.

Fecal sedimentation results in cattle have variable sensitivity (30-60%) due to the intermittent shedding of the fluke eggs, volume of the feces produced, and the relatively long prepatent period.[14] The specificity is high at 99%.[7] This test will only detect the presence of female adult fluke.

Liver fluke antibody ELISA may be performed on serum and milk and will detect IgG antibodies for *F. hepatica* excretory- secretory (E/S) antigen from 2-4 weeks post infection.[13] The sensitivity and specificity for the serum antibody ELISA varies depending on the season and ranges from 72-94% and 76-89%, respectively.[7] Another advantage of the antibody ELISA is that it can be used for surveillance and herd level diagnosis in bulk milk samples with ranges of sensitivity and specificity being 81.3-95% and 98.2-100%, respectively.[11] The antibody ELISA can only detect exposure and may remain positive for at least 4 weeks post flukicide treatment; therefore, veterinarians should take caution interpreting these results as cattle may not be currently infected.[2]

The cELISA detects *F. hepatica* E/S antigen in the feces 6-8 weeks post-infection and can detect low liver fluke burdens.[6] The cELISA was designed for and is commercialized for the use of detecting liver fluke in sheep. Many studies have reviewed the use of the fecal copro-antigen ELISA in cattle. Palmer et

al. (2014) illustrated that the specificity of the cELISA was 100% in cattle.[9]

When following the recommended cut off for the commercial kit the sensitivity was 80% in comparison to 87% when using a lower custom cut off for liver fluke detection in Australian cattle.[9] Multiple studies have used a modified cut off when using the commercial cELISA in cattle and therefore there is no consensus on the method and hence sensitivity of the commercial kit.[2,3,9] Furthermore, the sensitivity of this test varies over time as the antigens are released intermittently.[5,7] An advantage of the method over the antibody ELISA is that worm burden can be differentiated pre- and post- anthelmintic treatment.[2] Unfortunately, a fecal sample was not submitted for testing in this case.

Finding *F. hepatica* on liver necropsy is considered gold-standard however this method is not available for living animals. Estimated sensitivity and specificity are 99% and 98%, respectively.[7] These values are much higher compared to liver inspections at abattoirs which were estimated to have a sensitivity and specificity of 68% and 88%, respectively.[7] Liver histopathology can support a diagnosis of liver fluke, although sections often do not contain trematodes themselves. In this case, the size of the fluke and lack of gonad fits with the life cycle as juvenile flukes migrate through the liver parenchyma to the bile ducts where they become sexually mature.

Typical hepatic lesions in acute infection are characterized by hemorrhagic tortuous tracts with an element of coagulative necrosis and occasional inclusion of young flukes. As the disease progresses, these lesions are infiltrated by eosinophils followed by macrophages and giant cells which clear away the debris before healing occurs by formation of granulation tissue and fibrosis. Studies have shown that immature *F. hepatica* enters the liver parenchyma at 0.2 mm long and in cattle are approximately 1.5-3 mm long 21 days post-infection.[8,12] Most juvenile flukes migrate to the bile ducts; however, some encyst in a fibrous capsule within the parenchyma.[8] Mature flukes grow to approximately 2.5 cm long and reside in the large bile ducts and cause cholangitis. Biliary hyperplasia is a result of irritation by the flukes and biliary stasis. In this case, there is evidence of both acute and chronic fluke infection, with the presence of immature *F. hepatica* and migration tracts, and biliary hyperplasia and portal fibrosis, respectively. This suggests that this animal has been previously infected, with current reinfection.

Test	Sensitivity (%)	Specificity (%)
Fecal sedimentation	30-60[12]	99[12]
Liver fluke serum antibody ELISA	72-94[6]	76-89[6]
Liver fluke milk antibody ELISA	81-95[9]	98-100[9]
Commercial fecal copro-antigen ELISA	80-87[8]	100[8]
Liver necropsy	99[6]	98[6]
Abattoir liver inspections	68[6]	88[6]

Table 1: Summary of sensitivity and specificity for different diagnostic tests for *F. hepatica* detection.[7]

Contributing Institution:

Elizabeth Macarthur Agricultural Institute
Woodbridge Rd
Menangle, NSW, Australia
www.regional.nsw.gov.au

JPC Diagnosis:

Liver: Fibrosis, portal, bridging, diffuse, moderate to severe, with biliary hyperplasia, parasite migration tracts, and larval trematode.

Figure 1-3. Liver, ox. Within a bile duct, there is a sagittal section of a larval trematode. The larva has a ridged tegument, a spongy body cavity with numerous subtegumental somatic cell nuclei, and numerous cross sections of intestine. (HE, 87X)

JPC Comment:
Fasciola hepatica has a broad geographic range and causes estimated annual losses of US $3.5 billion in the global livestock industry; beyond livestock, many species of mammals are affected with approximately 170 million humans worldwide at risk of infection.[4] Many mammals serve as definitive hosts for the fluke, including cattle, sheep, buffalo, and humans.

F. hepatica has a rather complicated life cycle which begins when non-embryonated eggs are shed in the feces of an infected definitive host.[1,10] Eggs become embryonated and hatch in water, followed by release of miracidia which then penetrate an aquatic snail which serves as the intermediate host.[1,10] Development continues within the intermediate host until the free-swimming cercarial form is released into the environment.[1,10] Cercariae encyst on plants and form metacercariae which are then ingested by a human or animal host.[1,10] As noted by the contributor, once inside the host the metacercariae migrate through the duodenal wall, the peritoneal cavity, and then through the parenchyma of the liver for six to seven weeks until they reach the bile duct, where they mature into adults.[1,10] Once a patent infection is established, flukes are prodigious egg layers, with a single adult fluke contaminating the environment with 20,000-50,000 eggs per day over a long time period.[1] In cattle, egg production eventually begins to decline as the animal develops resistance to chronic infection.

Acute fascioliasis may occur following heavy intake of metacercariae, typically when livestock are grazed on heavily contaminated, wet ground.[1] Clinical signs may be absent, or may include abdominal pain and/or jaundice. Death is usually the result of liver hemorrhage secondary to the immature fluke's migration through the hepatic parenchyma.[1] Subacute disease is heralded by jaundice, ill thrift, and anemia secondary to extensive migration-related liver damage which results in death in 8-10 weeks.[1]

Chronic fascioliasis is the most common form of the disease in cattle, sheep, goats, horses, and pigs, and develops when the flukes reach the bile ducts, begin ingesting blood, and cause anemia, chronic inflammation, and enlargement of the bile ducts.[1] The disease is insidious, with increasing severity of anemia, decreasing appetite, reluctance to move, and, in some animals, submandibular edema ("bottle jaw").[1]

A complication of fluke infection is Black disease, an acute and fatal liver disease that develops in fluke-infested sheep and cattle. Black disease is caused when fluke migration-induce liver damage provides a suitably anaerobic environment for the germination of *Clostridium novyi* type B spores within the liver. *C. novyi* multiplies in areas of hepatic necrosis and elaborates a necrotizing alpha toxin which causes more tissue damage, leading to a vicious cycle of bacterial proliferation and toxin elaboration. The disease, also called infectious necrotic hepatitis, causes acute death primarily in sheep, sometimes in cattle, and rarely in pigs and horses.[1] Control is largely through reduction of fluke or

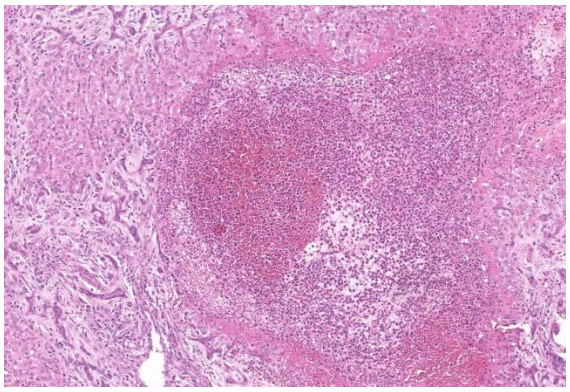

Figure 1-4. Liver, ox. Scattered randomly throughout the parenchyma, there are foci of necrosis (migration tracts) in which hepatocytes are replaced by various combinations and concentrations of neutrophils, macrophages, eosinophilis, lymphocytes, fibroblasts, and collagen. (HE, 116X)

intermediate host (snail) numbers, though a *C. novyi* toxoid is available for use to control outbreaks.

This week's conference was a double-feature, with Dr. Paul Stromberg, Professor Emeritus at The Ohio State University College of Veterinary Medicine, and Dr. Don Meuten, Professor Emeritus at North Carolina State University College of Veterinary Medicine, sharing moderator duties. Dr. Stromberg began discussion of this case by noting the loss of tissue architecture, the "alarmed" hepatocytes, and the abundant inflammation and necrosis present within the liver. These acute changes are present against a background of severe fibrosis and chronic inflammation.

The moderator noted that the histologic features of the trematode, particularly the lack of a reproductive tract, the trematode as a juvenile and this, along with the gross findings of adult trematodes in the biliary tree, indicate that this animal is likely living in a contaminated environment and subject to recurrent bouts of infection, explaining the acute-on-chronic nature of the observed lesions. The moderator noted the dilated sinusoids and attenuated hepatocytes and speculated that these changes result from impeded hepatic circulation due to the massive hepatic fibrosis appreciated in section.

References:

1. Boray JC, Love S. Liver fluke disease in sheep and cattle. *NSW Department of Primary Industries*. 2017.
2. Brockwell YM, Spithill TW, Anderson GR, Grillo V, Sangster NC. Comparative kinetics of serological and coproantigen ELISA and faecal egg count in cattle experimentally infected with Fasciola hepatica and following treatment with triclabendazole. *Vet Parasitol*. 2013;196 (3-4):417-426.
3. Charlier J, De Meulemeester L, Claerebout E, Williams D, Vercruysse J. Qualitative and quantitative evaluation of coprological and serological techniques for the diagnosis of fasciolosis in cattle. *Vet Parasitol*. 2008;153(1-2):44-51.
4. Garza-Cuartero L, Garcia-Campos A, Zintl A, et. al. The worm turns: trematodes steering the course of co-infections. *Vet Pathol*. 2014;51(2):385-392.
5. George SD, George AJ, Rolfe PF, Emery DL. Comparative assessment of faecal diagnostics for detection and predictive modelling of endemic Fasciola hepatica infection in sheep and cattle on Australian farms. *Vet Parasitol*. 2019;276:S100001.
6. Martínez-Sernández V, Orbegozo-Medina RA, González-Warleta M, Mezo M, Ubeira FM. Rapid enhanced MM3-COPRO ELISA for detection of Fasciola coproantigens. *PLoS Negl Trop Dis*. 2016;10(7):e0004872.
7. Mazeri S, Sargison N, Kelly RF, Bronsvoort BM deC., Handel I. Evaluation of the performance of five diagnostic tests for Fasciola hepatica infection in naturally infected cattle using a bayesian

no gold standard approach. Yu X, ed. *PLoS One*. 2016;11(8):e0161621.
8. Moazeni M, Ahmadi A. Controversial aspects of the life cycle of Fasciola hepatica. *Exp Parasitol*. 2016;169:81-89.
9. Palmer D, Lyon J, Palmer M, Forshaw D. Evaluation of a copro-antigen ELISA to detect *Fasciola hepatica* infection in sheep, cattle and horses. *Aust Vet J*. 2014; 92(9):357-361.
10. Pecararo HL, Stenger BLS, Rice LE, Webb BT. Gross and histologic description of trematodiasis in fetal and neonatal beef calves in North Dakota and Minnesota. *J Vet Diagn Invest*. 2022;34(5):870-873.
11. Reichel MP, Vanhoff K, Baxter B. Performance characteristics of an enzyme-linked immunosorbent assay performed in milk for the detection of liver fluke (Fasciola hepatica) infection in cattle. *Vet Parasitol*. 2005;129(1-2):61-66.
12. Ross JG, Todd JR, Dow C. Single experimental infections of calves with the liver fluke, Fasciola hepatica (Linnaeus 1758). *J Comp Pathol*. 1966;76(1):67-81.
13. Salimi-Bejestani MR, McGarry JW, Felstead S, Ortiz P, Akca A, Williams DJL. Development of an antibody-detection ELISA for Fasciola hepatica and its evaluation against a commercially available test. *Res Vet Sci*. 2005;78(2):177-181.
14. Statham JME. Control of liver fluke: an emerging issue in terms of veterinary residues. *Vet Rec*. 2015;177(20):519-521.

CASE II:

Signalment:
9-year-old female Tinker horse (*Equus caballus*)

History:
A mature female horse was admitted to the vet with hematuria. Bloodwork showed a

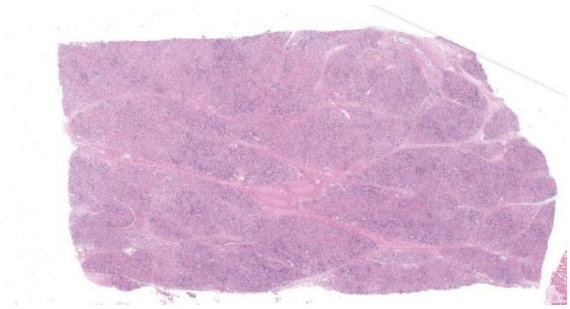

Figure 2-1. Mammary gland, horse. A section of mammary gland is submitted; the normal architecture is distorted and inflammation is evident at subgross. (HE, 4X)

hypoalbuminemia. The clinical signs improved after treatment with antibiotics and anti-helminthics. 3 weeks later, the horse developed a fever and ataxia. Treatment with doxycycline and NSAIDs was started, but one day later the horse was in lateral recumbency and had a vertical nystagmus. It was humanely euthanized.

Gross Pathology:
The horse was in a good body condition with normal musculature and normal fat reserves. Both kidneys contained multifocal, pale, firm, well-circumscribed masses varying in size from 1 to 10 cm in diameter. The mammary glands contained a moderate amount of watery, yellow fluid and were diffusely light pink on cut surface. Multifocally, the back muscles and gluteal muscles were diffusely pale compared to the other muscles.

Microscopic Description:
Mammary gland: Multifocally to coalescing, the original tissue architecture is extensively disrupted by foci of granulomatous inflammation, characterized by large numbers of epithelioid macrophages and few multinucleated giant cells (Langhans-type), admixed with large numbers of lymphocytes, plasma cells and eosinophils. The inflammation is centered around sections of nematode adults, larvae, and eggs, which are randomly spread throughout the tissue. The adult nematodes

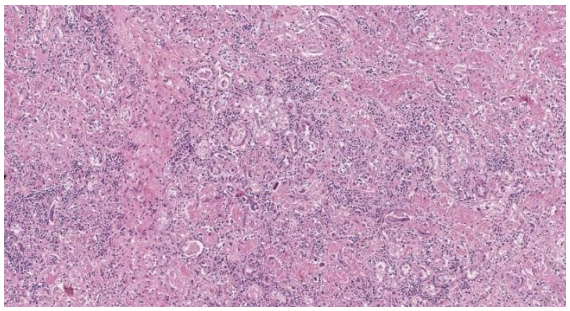

Figure 2-2. Mammary gland, horse. At higher magnification, the normal acinar architecture is effaced by fibrosis and granulatomous inflammation. Acinar epithelium is necrotic and acini are often lined by thin attenuated epithelium. Larval nematodes are scattered throughout the field. (HE, 91X)

are approximately 15-20 microns in diameter and up to 300-400 microns in length, and have a thin cuticle, platymyarian-meromyarian musculature, intestinal tract, and characteristic rhabditiform esophagus with a corpus, isthmus and terminal bulb. The nematode larvae measure 10-15 microns in diameter and 150-250 microns in length and have a rhabditiform esophagus. Nematode eggs are ovoid, both embryonated and larvated, and measure approximately 10 x 50 microns. Incidentally, parasites are surrounded by karyorrhexis and karyolysis, with loss of cell detail (lytic necrosis).

Contributor's Morphologic Diagnosis:
Mammary gland: Severe, chronic, multifocal to coalescing, granulomatous, eosinophilic and lymphoplasmacytic mastitis with myriad intralesional rhabditoid nematode adults, larvae, and eggs, etiology presumptive *Halicephalobus gingivalis.*

Contributor's Comment:
The parasite with its accompanying inflammation was also extensively present in the cerebrum, cerebellum, kidneys and some skeletal muscles.

Halicephalobus gingivalis is a facultative, opportunistic nematode of the order *Rhabditidia*, family *Panagrolaimidae,* and causes a rare form of meningoencephalomyelitis in equids, humans, and ruminants.[4,5] The life cycle and pathogenesis of this opportunistic pathogen is still poorly understood. *Halicephalobus* nematodes are found free-living in association with water, soil, and decaying organic matter and it is thought that transmission occurs primarily via wounds in the skin or mucous membranes.[3] Rarely, other routes of infection have been suggested, including transmammary.

Upon infection, dissemination of the infection is then thought to occur hematogenously.[2] Sexual reproduction is believed to occur during the free-living part of the life cycle and although both males and females exist in the environment, only female nematodes have been observed within microscopic lesions. This suggests that within a host, reproduction occurs asexually via parthenogenesis.[1]

Histologic identification of consistent lesions and morphologically compatible rhabditoid nematodes found postmortem are an indication for diagnosis, although the nematodes can be extracted from fresh tissue or the parasite can be shed in the urine if there is renal involvement.

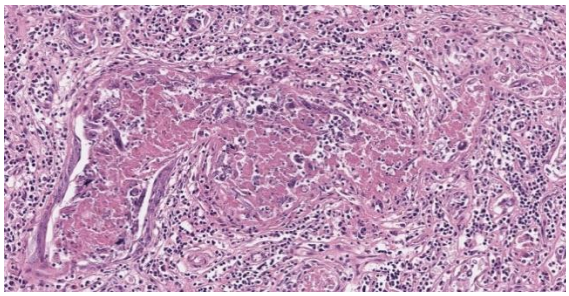

Figure 2-3. Mammary gland, horse. Lactiferous ducts are filled with cellular debris and intrepid rhabditid larvae. (HE, 209X)

Contributing Institution:
Veterinair Pathologisch Diagnostisch Centrum
University of Utrecht
https://www.uu.nl/onderzoek/veterinair-pathologisch-diagnostisch-centrum

JPC Diagnosis:
1. Mammary gland: Mastitis, granulomatous and eosinophilic, chronic, diffuse, marked, with numerous adult and larval rhabditid nematodes.
2. Lymph node: Reactive hyperplasia, diffuse, moderate.

JPC Comment:
Halicephalobiasis is an infection characterized by localized or disseminated granulomatous lesions that has been sporadically reported in horses and zebras and less commonly in cows and humans.[6] As the contributor notes, surprisingly little is known about the pathogenesis of the disease and the biology of the causative agent, *Halicephalobus gingivalis*. The nematode was first described in 1954 after the worms were discovered within a gingival granuloma in a horse, providing the species name for this enigmatic pathogen.[5] *H. gingivalis* has since been described in, among other tissues, the central nervous system, kidneys, oral cavity, eyes, lungs, adrenal glands, spleen, liver, heart, and, with this case, the mammary gland.[5,6]

Due to the variety of tissues that can be affected, the clinical presentations and signs of halicephalobiasis are highly variable; however neurologic and renal lesions, and their attendant clinical signs, appear to be overrepresented in published case reports.[6] The nematode itself has a distinctive morphology, which is nicely demonstrated in the abundant longitudinal and cross sections present in the examined slide. Adult *H. gingivalis* nematodes are cylindrical with

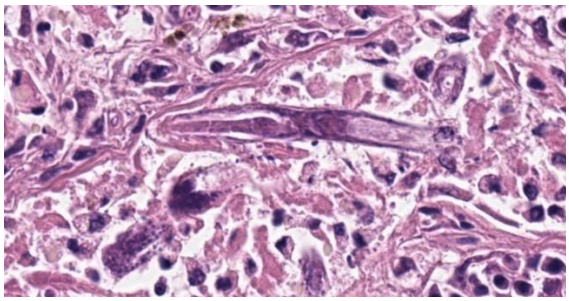

Figure 2-4. Mammary gland, horse. Larva have a rhabditoid esophagus with a corpus, isthmus, and bulb. (Obligatory picture.) (HE, 1025X)

tapered anterior ends and pointed tails, and possess a classic rhabditiform esophagus composed of the canonical corpus, isthmus, and bulb.[6]

The central nervous system is most commonly affected in horses, with massive intracranial invasion often causing an acute disease with a short course.[1] Gross lesions include focal arachnoid hemorrhages and multifocal thickening of the meninges. Histologically, female nematodes and larvae are found within lesions, particularly in perivascular spaces, and lesions are characterized by granulomatous and eosinophilic meningoencephalitis, myelitis, or polyradiculitis; parasitic granulomas in the kidneys and gingiva often accompany, and are perhaps antecedent to, central nervous system invasion.[1] Treatment of *H. gingivalis* infection is typically ineffective, most likely due to the inability of drugs such as ivermectin to penetrate the robust granulomatous lesions or to cross the blood-brain barrier; thus, these infections typically have a poor prognosis and a short course.[6] Other rhabditid nematodes that can infect horses include *Strongyloides westeri*, *Pelodera strongyloides* (more commonly associated with cutaneous lesions in dogs), and *Cephalobus* spp.; however, the size and distinct morphology of *H. gingivalis* allow for a presumptive diagnosis.[6]

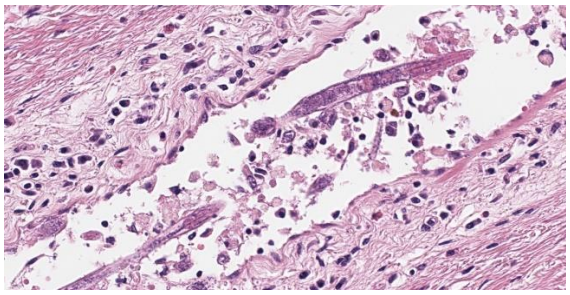

Figure 2-5. Mammary gland, horse. There goes a female *Halicephalobus* sailing away down the vessel (she's got to get away from the kids!). (HE, 500X)

Dr. Stromberg challenged conference participants, who all agreed with the contributor's identification of *Halicephalobus gingivalis*, to consider their level of confidence in their parasite identification. Considering the large number of rhabditid nematodes that exist in the environment, how does one know definitively that this nematode is *H. gingivalis*, particularly given the unusual anatomic location in which this nematode is found? Additionally, the extremely small size of the parasite makes evaluation of fine anatomic features, such as the type of musculature present, particularly challenging. The moderator, while agreeing with the etiology and diagnosis, urged conference participants to at least acknowledge when a diagnosis is based on probability; while, by definition, a probability-based identification is often correct, it behooves the diagnostic pathologist to realize that these diagnoses deserve extra scrutiny.

Dr. Stromberg noted that the intensity of the inflammatory response evoked by a particular parasite can give insight into the evolutionary history of the parasite/host relationship. In this case, the typically robust inflammatory response suggests that the evolutionary history of *H. gingivalis* and the horse is short and still being written. The raging chronic mastitis is evidenced by a range of fibrosis throughout the mammary gland, which conference participants appreciated by examination of a Masson trichrome stain. Dr. Stromberg noted the correlation between the degree of damage and fibrosis and the number of adult and larval nematodes in a particular area, with fibrosis ranging from barely perceptible to obliterative in the most severely affected sections.

The JPC morphologic diagnosis omits a specific etiology, preferring, based on Dr. Stomberg's discussion of uncertainty, to describe the parasite simply as a rhaditid nematode. Participants also felt that the changes observed in the accompanying lymph node were severe enough to warrant their own mention.

References:

1. Cantile C, Youssef S. Nervous system. In*:* Maxie MG, ed. *Jubb, Kennedy, and Palmer's Pathology of Domestic Animals*. Vol 1. 6th ed. Elsevier; 2016:390.
2. Henneke C, Jespersen A, Jacobsen S. The distribution pattern of *Halicephalobus gingivalis* in a horse is suggestive of a haemotogenous spread of the nematode. *Acta Vet Scand*. 2014;56:1-4.
3. Hermosilla C, Coumbe KM, Habershon-Butcher J, Schöniger S. Fatal equine meningoencephalitis in the United Kingdom caused by the panagrolaimid nematode *Halicephalobus gingivalis*: case report and review of the literature. *Equine Vet J*. 2011;43:759-763.
4. Lim CK, Crawford A, Moore CV, et al. First human case of fatal *Halicephalobus gingivalis* meningoencephalitis in Australia. *J Clin Microb.* 2015;53(5):1768-1774.
5. Onyiche TE, Okute TO, Oseni OS, et al. Parasitic and zoonotic meningoencephalitis in humans and equids: Current knowledge and the role of *Halicephalobus gingivalis*. *Parasite Epidemiol Control*. 2018;3(1):36-42.

6. Pillai VV, Mudd LJ, Sola MF. Disseminated *Halicephalobus gingivalis* infection in a horse. *J Vet Diagn Invest*. 2023;35(2):173-177.

CASE III:

Signalment:
10-year-old male neutered dog (*Canis familiaris*).

History:
Left hind leg/distal femur mass. Radiographs showed bone lysis and periosteal reaction. An amputated hind leg was received at the diagnostic laboratory for diagnosis.

Gross Pathology:
Left hind leg mass involving the bone and associated soft tissues (skin/muscle/subcutis).

Microscopic Description:
Multiple tissues from the amputated left hind leg received were examined. Sections of bone were examined after decalcification. The examined tissues contained a non-demarcated, non-encapsulated neoplasm composed of variably loose to solid sheets of spindle to polygonal cells supported on

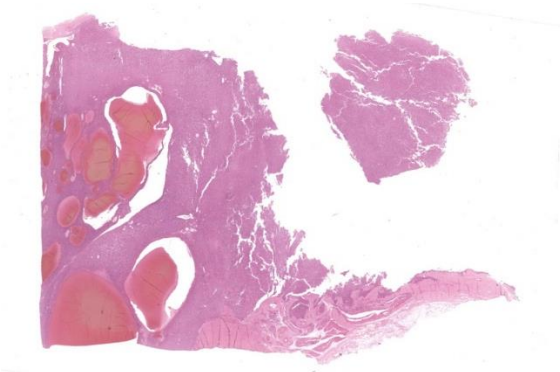

Figure 3-1. Skeletal muscle, quadriceps, dog. A neoplasm extends into and effaces the skeletal muscle. (HE, 5X)

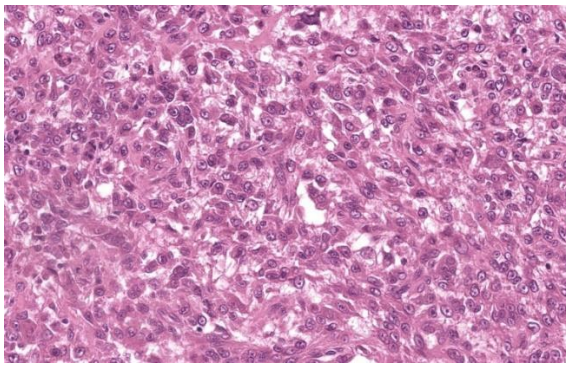

Figure 3-2. Skeletal muscle, quadriceps, dog. Neoplastic cells are arranged in short streams and bundles. (HE, 160X)

ample fibrovascular stroma. The cells had indistinct to variably distinct cell borders, ample eosinophilic cytoplasm, round to oval vesicular nuclei and distinct nucleoli. Six mitotic cells were observed in 2.4 mm2/equivalent to 10 N22/40x high power fields. Anisocytosis and anisokaryosis were moderate and there were multifocal multinucleated giant cells consistent with osteoclasts in the mass. The neoplastic cells multifocally surrounded eosinophilic fibrillar material (osteoid) and osseous trabeculae.

Contributor's Morphologic Diagnosis:
Osteosarcoma, Metastatic.

Contributor's Comment:
Osteosarcoma (OSA) is the most common primary bone tumor in dogs. In general, the risk of developing osteosarcoma appears to be amplified under conditions that drive excess osteoblast activation. OSA most commonly develops at or near growth plates, where cell turnover is highest, and represents up to 85% of all primary malignant bone tumors in the dog.[4,5,7] Appendicular OSA is diagnosed most frequently in middle-aged to older, large and giant breed dogs, and affects the forelimb, particularly the humerus, more frequently than the hindlimb.

Significant differences in distribution patterns are reported between age, tumor

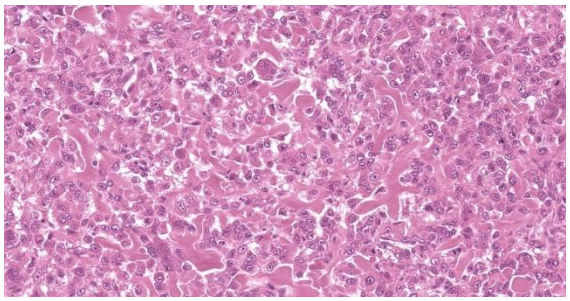

Figure 3-3. Skeletal muscle, quadriceps, dog. Neoplastic cells regionally produce and are entrapped in osteoid matrix. (HE, 350X)

location, and phylogenetic clusters. There are also significant variations in distribution patterns between neuter status, age, and dog sizes.[7] High risk of appendicular osteosarcoma in large and giant breed dogs may often be the result of replicative mutations caused by normal processes of cell division required to create longer bones, with only modest contributions from heritable or environmental factors.[4]

Some studies identify breed associations with osteosarcoma risk in terms of both predisposition and protection. These results can inform breed health reforms, especially in breeds such as the Rottweiler, Rhodesian Ridgeback and the Great Dane which have been shown to be highly at risk.[3] The skin or subcutaneous tissue is often the first osteosarcoma metastatic site detected as was observed in this case. After cutaneous and subcutaneous metastasis, the prognosis is grave with a median survival time of less than 2 months.[5] Treatment with surgery and chemotherapy is suggested to improve outcome and was reported to be significantly associated with survival time after the diagnosis. The median cutaneous/subcutaneous metastasis-survival time for dogs treated with surgery and chemotherapy or chemotherapy alone was significantly longer than in the untreated ones, although the prognosis for dogs with metastatic tumors much poorer than for individuals with only primary tumors.[6]

Contributing Institution:
Tifton Veterinary Diagnostic and Investigational Laboratory
College of Veterinary Medicine
Department of Veterinary Pathology
University of Georgia.
https://vet.uga.edu/diagnostic-service-labs/veterinary-diagnostic-laboratory/.

JPC Diagnosis:
Skeletal muscle and tendon: Osteosarcoma.

JPC Comment:
Osteosarcoma is well-known and well-studied in veterinary medicine; however, despite the familiarity of this tumor, it remains difficult to differentiate OSA from other primary bone neoplasms, which often present with similar clinical signs and radiographic appearances.[1] The issue is clinically urgent as OSA has a high risk of metastasis and an aggressive clinical course, yet histopathologic diagnosis of bone neoplasms was found to be only 72% accurate in one study, with only 13 of 18 malignant tumors accurately diagnosed.[1] Of the misdiagnosed tumors, 3 were initially diagnosed as less aggressive tumors, but were ultimately proved to be OSA.[1]

Histologic differentiation of bone tumors is difficult primarily because of their morphologic similarities and the small tissue samples typically provided for examination. Because of this, various immunohistochemical (IHC)

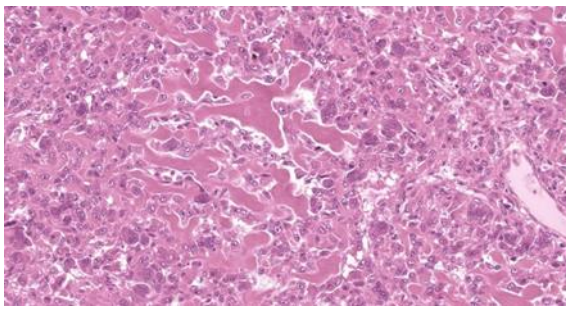

Figure 3-4. Skeletal muscle, quadriceps, dog. Neoplastic cells regionally produce and are entrapped in osteoid matrix. (HE, 350X)

markers have been evaluated for their potential to increase the sensitivity and specificity of an OSA diagnosis; however, a single sensitive and specific marker to differentiate ostoblastic cells in formalin-fixed tissue has yet to be identified.[1] A recent study in *Veterinary Pathology* characterized the expression patterns of four osteoblast-associated markers—Alkaline phosphatase (ALP), runx2, osteonectin, and osteopontin—to determine if the expression patterns of these proteins would be useful in differentiating OSA from other bone tumors.[1]

ALP is already used for this purpose in cytology, where staining for ALP enzyme activity on cytologic samples can increase the sensitity and specificity of an OSA diagnosis to 100% and 87%, respectively.[1] In contrast, ALP IHC staining identifies the protein rather than its enzymatic activity, and, on formalin-fixed tissue, has an excellent sensitivity (100%) but only a limited specificity (30%), making it unreliable for diagnosing OSA as a sole marker.[1] Runx2 is a transcription factor that is essential for osteogenesis, skeletal development, and osteoblastic differentiation. Its expression is consistently elevated in both human and canine OSA, and runx2 IHC staining was found to be 87% sensitive and 78% specific in the diagnosis of canine OSA.[1]

Based on the sensitivity and specificity profiles of the four examined markers, the authors found the greatest diagnostic benefit from running ALP and runx2 in series.[1] The diagnostic algorithm requires running the ALP IHC first. Due to the high sensitity of ALP, if the sample is negative, the tumor is likely not an OSA and no further testing is necessary. If the tumor expressed ALP, however, runx2 should be interrogated to further characterize the tumor. When performed in series in this order, ALP and runx2 have a combined sensitivity of 87% and a specificity of 85% providing a useful set of diagnostic OSA markers.[1]

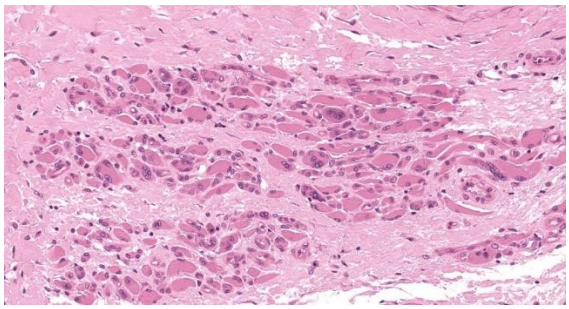

Figure 3-5. Skeletal muscle, quadriceps, dog. There is marked fibrosis for the skeletal muscle and atrophy of individual myofibers. (HE, 400X)

The moderator for this half of the conference, Dr. Meuten, used this classic entity to compare and contrast the traditional narrative, descriptive reports produced by most veterinary pathology diagnostic institutions, including this one, with the more streamlined, data point-driven process of synoptic reporting. After noting that synoptic reporting has become the standard in human pathology practice, Dr. Meuten led a robust discussion centered on the practical challenges associated with and the institutional and individual resistance to the transition.

Synoptic reporting dispenses with narrative descriptions and pares down diagnostic deliverables to discrete pieces of data reported in defined formats in a checklist-style report.[2] As extensively discussed in conference, the challenge with synoptic reporting is choosing what data gets collected, what data gets reported, and to whom the data is disseminated. While it is facile to state that only data which has proven diagnostic, prognostic, and predictive value should be reported, in practice, this becomes complicated by practical considerations related to the need for future data mining, the different needs of different audiences, and what is considered diagnostic or

prognostic enough to merit inclusion in the report.

In the context of this particular tumor, discussion focused on whether histologic subtype, which does not currently have clear predictive value, should be included on a hypothetical synoptic report template for OSA. Some residents thought that the examined OSA might be a telangiectatic subtype and felt that this information should be collected. The moderator countered that the potential oncologist reading the report would likely treat the animal the same, regardless of histologic subtype, so should the synoptic report include only the diagnosis?

The interesting, rhetorical discussion raged on for some time with the moderator passionately exploring the concept of synoptic reporting to an engaged but admittedly skeptical audience. An excellent discussion of the considerations involved in synoptic reporting can be found at the Veterinary Cancer Guidelines and Protocols website.[2]

References:

13. Barger A, Baker K, Driskell E, et al. The use of alkaline phosphatase and runx2 to distinguish osteosarcoma from other common malignant primary bone tumors in dogs. *Vet Pathol*. 2022;59(3):427-432.
14. Dark MJ, Bertram CA, Donovan TA, Meuten DJ, Miller AD, Moore FM. Synoptic Reporting Guideline, version 1.0. *Veterinary Cancer Guidelines and Protocols*. 2021. Available at: http://vetcancerprotocols.org. Accessed on 15 April 2024.
15. Edmunds GL, Smalley MJ, Beck S, et al. Dog breeds and body conformations with predisposition to osteosarcoma in the UK: a case-control study. *Canine Med Genet*. 2021;8(1):2.
16. Makielski KM, Mills LJ, Sarver AL, et al. Risk factors for development of canine and human osteosarcoma: a comparative review. *Vet Sci*. 2019;6(2):48.
17. Parachini-Winter C, Curran KM, Pellin M, et al. Cutaneous and subcutaneous metastasis of appendicular osteosarcoma in dogs: 20 cases. *J Vet Intern Med*. 2019;33:2200-2208.
18. Simpson S, Dunning MD, Simone de Brot, et al. Comparative review of human and canine osteosarcoma: morphology, epidemiology, prognosis, treatment and genetics. *Acta Vet Scand.* 2017;59(1):71.
19. Tuohy JL, Shaevitz MH, Garrett LD, Ruple A, Selmic LE. Demographic characteristics, site and phylogenetic distribution of dogs with appendicular osteosarcoma: 744 dogs (2000-2015). *PLoS One*. 2019;14 (12):e0223243.

CASE IV:

Signalment:
8-year-old female intact American Staffordshire terrier (*Canis familiaris).*

History:
The dog presented to the small animal hospital with acute onset of tachypnea, abdominal breathing, tachycardia, and bright red mucous membranes. The dog had been coughing for a month, had been inappetent, exercise intolerant, and had been losing weight for 1-2 weeks. Two weeks prior, the dog was diagnosed with a urinary tract infection. The dog was euthanized without further diagnostics and subsequently submitted for necropsy.

Gross Pathology:
The dog was in good body condition. Originating from the mucosa of the trigone area of the urinary bladder was an irregularly and indistinctly outlined mass, approximately 6 cm in diameter, with homogenous white to yellow colour, firm consistency, and a smooth, solid white cut surface. The mass extended into and infiltrated nearly the full length of the urethra. The inguinal lymph nodes were

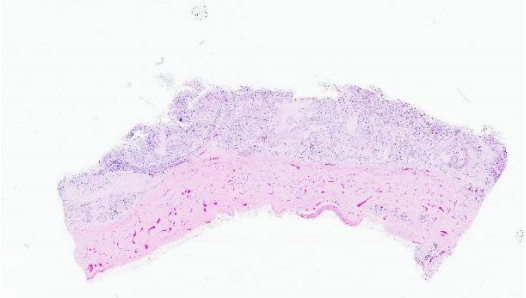

Figure 4-1. Urinary bladder, dog. One section of urinary bladder is submitted for examination. There is transmural infiltration of the bladder wall (predominantly at lower right). (HE, 5X).

severely enlarged with a homogenous light colour, firm consistency, and a smooth, solid cut surface. Bilaterally in the adrenal medulla, 0.5 cm diameter, well-demarcated masses of similar appearance were found. Multifocally within all lobes of the lungs were abundant nodular, well demarcated masses of light colour, firm consistency, and smooth, solid cut surface, ranging from 0.3-2.0 cm in diameter. The tracheobronchial and mediastinal lymph nodes displayed a similar appearance as the inguinal lymph nodes.

Microscopic Description:
Urinary bladder: Diffusely obliterating and irregularly thickening the mucosa and extending into the submucosa is a plaque-like, poorly demarcated and unencapsulated, infiltrative, densely cellular epithelial neoplasm, extending to cut borders. A few scattered neoplastic cells are also seen within the muscular layer. Neoplastic cells are polygonal, markedly pleomorphic, and grow in cords, tubules, and poorly defined aggregates in a scant to moderate fibrovascular stroma. Nuclei are large, round to oval with vesicular chromatin and 1-2 central, prominent nucleoli. Multiple multinucleated cells and cells with bizarre, giant nuclei are seen. The cytoplasm is moderate, eosinophilic, and homogenous to vacuolated, and cell borders are mostly distinct. The N:C ratio is increased. Multifocally, neoplastic cells exhibit large intracytoplasmic vacuoles with eccentric peripherally located nuclei (signet ring formation) or large intracytoplasmic vacuoles containing homogenous or granular eosinophilic, PAS-positive material (Melamed-Wolinska bodies). The mitotic activity is high (25 mitoses per 10 HPF) and atypical mitoses are present. Multifocally, neoplastic cells display pyknotic or karryorhectic nuclei (single cell necrosis) and there are multifocal larger, confluent areas of necrosis. In the *muscularis* layer are multiple tumoral emboli within thin-walled vessels (lymphovascular invasion).

Contributor's Morphologic Diagnosis:
Urinary bladder: Urothelial carcinoma, non-papillary and infiltrative, high grade.

Contributor's Comment:
Tumors of the urinary bladder are uncommon in dogs, accounting for ≤1% of all canine neoplasms and 2% of all malignant canine neoplasms.[3,7] Lower urinary tract carcinomas have four histological types: (1) urothelial, (2) squamous, (3) adenocarcinoma, or (4) undifferentiated carcinoma.[3] Of these, the urothelial carcinoma (UC), previously called transitional cell carcinoma (TCC), is the most common bladder neoplasm in all species including dogs.[7] UC is derived from the transitional epithelium of the urinary tract (urothelium).[7] UC also occurs in cats and cattle, and may develop in cattle as a sequela to ingestion of bracken fern (enzootic hematuria).[3] Bladder neoplasms of any type are rare in other species.[7]

Urothelial carcinoma occurs primarily in older dogs (average age 9-11 years), and females seem to be more often affected than males, however a statistically significant gender difference is lacking.[7] Neutered dogs seem to be predisposed to bladder neoplasms.[7] Scottish terriers have an 18 to 20-

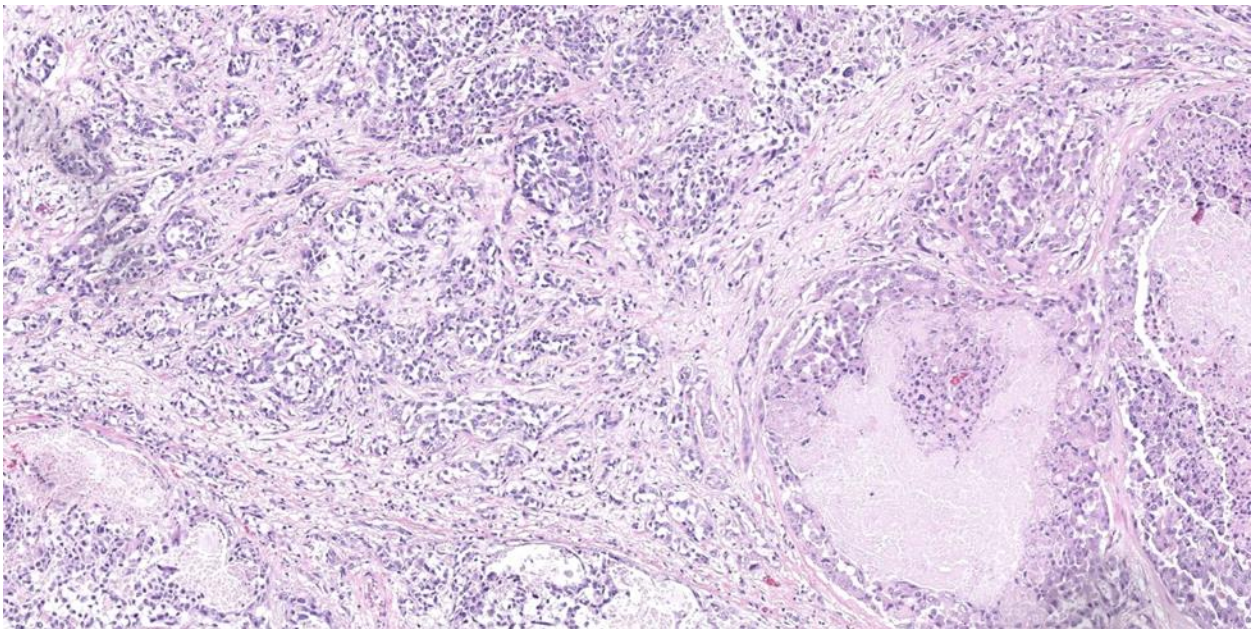

Figure 4-2. Urinary bladder, dog. Neoplastic cells form tubules, trabeculae, and occasionally solid nests on a dense fibrous stroma. There is scattered lytic necrosis within the center of large nests. (HE, 111X)

fold higher risk for UC than other dogs. Other breeds at higher risk are Airedale terriers, Shetland sheepdogs, West Highland white terriers, fox terriers and beagles.[7]

Most of the UC neoplasms in dogs occur in the trigone area of the bladder, possibly because of a prolonged contact time of urine and potential carcinogens with the urothelium in this area.[7] In 30-55% of bladder UCs there will be concurrent neoplastic lesions in the prostate and/or urethra.[7] Grossly, most tumors are solitary, but they can be multiple and cover nearly the entire urinary bladder mucosa.[7] They may form either papillary growths projecting into the lumen of the bladder or non-papillary, flat plaques or masses that bulge from the mucosa into the bladder lumen.[7] Most are infiltrative into the muscle layers, producing a thickened bladder wall.[7]

A histological grading scheme is available for histological diagnosis of canine UC. The grading scheme has been based largely on the World Health Organization (WHO) histological criteria for human UCs, and was last modified in 2012.[1,7] In the classification scheme for dogs, UC is divided into low and high-grade variants.[1,7] The most aggressive region of the tumor should be used to assign a grade.[7] High-grade UCs are defined by features of malignancy such as disorganized growth and loss of cell polarity, cellular atypia, nuclear pleomorphism, mitotic activity, deep invasion and invasion into lymphatics or blood vessels.[1,7] Low-grade UCs display no invasion and are confined to the mucosa, exhibit mild pleomorphism, and contain no or only a few mitoses.[7] The great majority of UC/TCC are high-grade and invasion is present in the majority of canine UCs (>90%).[7] However, studies assessing the prognostic relevance of the grading scheme are lacking, and some studies have shown no correlation between histologic variables and prognosis.[1,11] Prospective studies determining the relationship between low- and high-grade features are needed to know if the grading scheme for UC accurately predicts clinical outcomes in dogs.[1,7]

Canine UCs can also be divided based on morphological pattern of growth, namely papillary (projecting into the lumen, around 50% of cases) or non-papillary (sessile or flat, 50%), and infiltrating (90%) or non-infiltrating (10%). This designation should be based on the dominant gross and microscopic features.[7] In a case series of 3 canine UCs, unique additional cellular morphologies were revealed, resembling human plasmacytoid and rhabdoid variants of UC.[5] Reduced E-cadherin expression was shown by immunohistochemistry (IHC) in 2 of the cases, possibly representing increased invasiveness and epithelial-mesenchymal transition (EMT).[5]

Keys to the histological diagnosis of UC are location in the urinary bladder, presence of large epithelial cells with multiple cellular and nuclear features of atypia, invasion below the mucosa or into lymphatics or blood vessels, and the presence of so-called Melamed-Wolinska bodies.[7] Melamed-Wolinska bodies are large cytoplasmic vacuoles that may be empty or contain homogenous or stippled periodic acid Schiff (PAS) positive eosinophilic material, as was confirmed in this case. The Melamed-Wolinska bodies are also uroplakin positive and are so characteristic of UC that if seen in preparations from other locations such as lymph node, skin, or abdominal or pleural fluid, UC should be listed as the most likely differential diagnosis.[7] Urothelial tumor cells typically exhibit eosinophilic cytoplasm, large and vesicular nuclei, and numerous mitoses, some of which are bizarre. Multinucleated cells are common. Regions of squamous and/or glandular metaplasia and signet ring cell formation may occur, as well as desmoplasmic reactions.[7]

High-grade, invasive UCs are one of the most aggressive neoplasms in veterinary medicine and the prognosis is poor.[4,7] Survival times are short for almost all UCs in dogs, and most dogs (>80%) die within the first year of treatment.[4,7] Metastases occur most commonly to the lungs and regional lymph nodes, but may also occur to bones and skin.[7] Additional metastases may be found in almost any organ examined.[7] In a retrospective study, 17 of 188 canine UC cases (9%) had histologically confirmed skeletal metastasis, mainly affecting vertebrae.[2] Possible routes of metastases of canine UCs include vascular dissemination with tumor emboli, direct extension (peritoneal implantation) from transmural bladder infiltration, or iatrogenic seeding through diagnostic sampling by fine needle aspirate or surgery.[7]

Implantation of tumor along surgical excision paths is well documented with UC.[7] In one study, skin metastases were seen near the vulva or prepuce, possibly because of urine scalding of the skin and subsequent transepidermal spread.[10] Clinically, bladder carcinomas in dogs are staged with the Tumor Nodes Metastasis (TNM) system.[7] At the time of clinical diagnosis, 20% of dogs will have radiographically detectable metastases, and metastases are present in a majority of dogs (50-90%) at autopsy.[4,7]

Special genetic profiles seem to be associated with the development of canine UC.[7] Studies of canine UC biopsies have revealed aberrant chromosomal numbers (aneuploidy) of *Canis familiaris* (CFA) chromosome 13, 19, and 36, with gain of CFA13 and 36 and loss of CFA19.[13] Aberrant copy number variations in the same chromosomes were detected also by droplet digital polymerase chain reaction (ddPCR).[8] In addition, a digital PCR assay has been used to detect copy number aberrations (CNAs) in the ErbB2 (HER2) oncogene, whose product, the cell surface receptor tyrosine kinase ErbB2, is overexpressed in a variety of human malignancies.[12] In the study, ErbB2 copy number aberrations were detected in 33% of UC bladder tissue, and in 35% of UC urinary sediment, meanwhile no ErbB2 CNAs were detected in normal controls.[12] In a immunohistochemical study

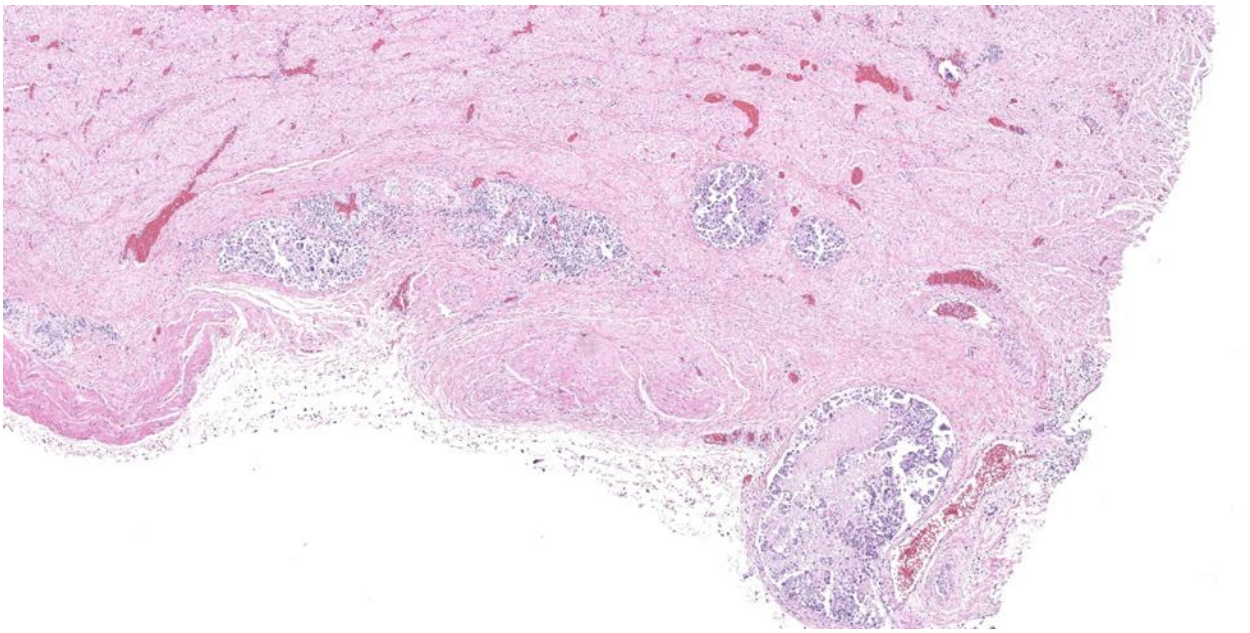

Figure 4-3. Urinary bladder, dog. Neoplastic cells are present in lymphatics within the mural smooth muscle and serosa. (HE, 46X)

performed on 23 samples of canine UCs, intense membranous ErbB2 (HER2) immunoreactivity was frequently observed in neoplastic cells.[16] In another study, 36 of 47 dogs (76.6% with UCs) had a mutation in proto-oncogene B-raf ($BRAF^{V595E}$ mutation).[6] The mutation was associated with tumor-produced chemokine CCL17 and infiltration regulatory T-cells, which may act as immune suppressors but also are thought to play a role in tumor progression.[6]

Immunohistochemistry is rarely needed to diagnose primary UC unless the tumor is anaplastic.[7] If needed, uroplakin III (UPIII) is considered the best IHC marker to recognize urothelium, and is a useful primary biomarker to identify tumors of suspected urothelial origin.[7] Uroplakin consists of four proteins located in a specialized plasma membrane (asymmetrical unit membrane, AUM) that connects the surface of urothelial cells with cytoplasmic filaments.[7] UPIII is specific to terminally differentiated superficial urothelial cells (umbrella cells) and exhibits discrete membranous immunoreactivity, primarily at the surface of cell membranes.[7] UPCIII cannot be used to differentiate neoplastic from non-neoplastic lesions, but it is highly specific for urothelial tumors, and may be helpful to rule in or out UC origin in metastases or cancer of unknown primary site.[7] Due to its high specificity in canine urothelial neoplasm, UPIII expression in less than 5% of neoplastic cells is considered diagnostic.[7] UPIII labeling may however be lost in some high-grade, anaplastic UCs, possibly due to loss of cell adhesion molecules, enhancing the ability to metastasize.[7] Lack of immunoreactivity may therefore indicate a more aggressive tumor.[7]

Antibodies to uroplakin II have been evaluated in human pathology and have been shown to outperform UPIII.[15] Urothelium (transitional epithelial cells) also contain cytokeratins associated with simple-type epithelium (CK7, CK20, CK8, CK18, CK19) and stratified-type epithelium (CK13, CK17).

CK7 and CK20 have been used in UC diagnosis in humans.[7] In a canine study, CK7 and UPIII outperformed CK20 in the diagnosis of UC.[9] CK7 staining was diffusely cytoplasmic and stained over 98% of primary UCs, whereas UPIII labeled 91% of primary UCs.[9] Another potential immunohistochemical marker for canine UC is cyclooxygenase-2 (COX-2). COX-2 and associated production of prostaglandin E_2 have been ascribed several roles in carcinogenesis, including immunosuppression, increased metastatic potential of neoplastic epithelial cells, and stimulation of angiogenesis.[14] Immunoreactivity for COX-2 has been detected in UCs of dogs, but also in non-neoplastic proliferative bladder lesions.[14]

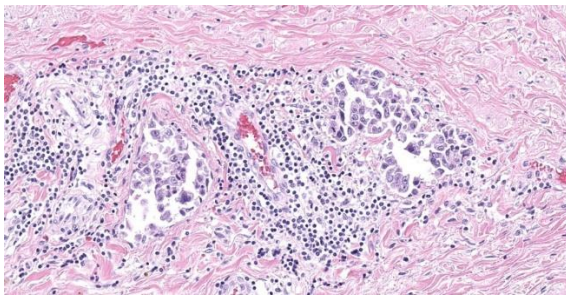

Figure 4-4. Urinary bladder, dog. High magnification of lymphovascular invasion of neoplastic urothelium. There are lymphocytes and fewer plasma cells surrounding ectatic lymphatics containing neoplastic cells. (HE, 237X)

Contributing Institution:
Swedish University of Agricultural Sciences
Department of Biomedical Sciences and
Veterinary Public Health
Pathology Section
Uppsala, Sweden
https://www.slu.se/en/departments/biomedical-sciences-veterinary-public-health/

JPC Diagnosis:
Urinary bladder: Urothelial carcinoma, papillary and infiltrative.

JPC Comment:
The contributor provides an excellent overview of the extensively researched and described canine urothelial carcinoma. Interestingly, despite UC also being the most common bladder tumor in cats, far less has been published about feline UC. Feline UC comprises only about 0.5% of all feline malignancies, compared with around 2% of all canine malignancies, and this difference has been speculatively explained by, among other variables, the lower quantities of tryptophan metabolites excreted in feline urine, differences in the chemical composition of feline flea and tick preventatives, and potential masking by concurrent disease in aged cats.[17]

A recent descriptive study of feline UC in 38 cats found that the typical histologic presentation is of an unencapsulated, densely cellular neoplastic mass, often with ulceration or erosion of the bladder mucosa.[17] As in canine UC, the two main histologic patterns reported are papillary, exophytic growths extending into the bladder lumen (21%) or the formation of non-papillary sessile growths (79%).[17] The case series found evidence of Melamed-Wolinska bodies or signet ring formation in only 3 of 38 cases, perhaps indicating that this histologic finding is less frequent in feline cases compared with canine UC. Mitotic rate was variable with occasional bizarre mitotic figures.[17]

Neoplastic cells are typically arranged in similar patterns, such as trabeculae, cords, and islands, as their canine UC counterparts; however, feline UCs frequently (9/38) contain a glandular histomorphology that appears similar to a histologic variant seen in humans, but not dogs, and researchers suggest that this unique morphology should be described in pathologic reports of feline UC to aid in identifying metastatic disease that may show this unexpected pattern.[17] Feline UC neoplastic cells are present on variable

stroma that ranges in quantity and morphology; stroma may be sparse or abundant, and may be characterized as mucinous, myxomatous, or scirrhous. Inflammatory infiltrates, when present, are primarily composed of lymphocytes with fewer plasma cells and neutrophils.[17]

There are some reported associations between feline UC and urinary tract infection, with concurrent infections reported in up to 70% of feline UC patients.[7,17] In the most recent case series, approximately 28% of patients for whom clinical history was available had cystitis, stones or bladder crystals at the time of diagnosis.[17]

Though data is sparse, feline UC is thought to be highly recurrent, and metastasis at the time of diagnosis, typically to the regional lymph nodes or lungs, has been reported in 12-50% of cases. As the contributor notes, the prognosis for canine UC is strongly associated with the TNM staging system; however, TNM staging is typically not performed with feline UCs and prognostic information has therefore not been established.[17]

As in the previous case, Dr. Meuten chose to discuss this classic neoplasm in the context of synoptic reporting. Participants discussed whether infiltration, grade, or both should be reported. Dr. Meuten noted, as does the contributor, that there is no veterinary research that ascribes prognostic or clinical meaning to UC grading, and he would therefore be inclined to omit this data. This lead to a broader discussion of how synoptic reporting could potentially be tailored to meet the needs of the intended recipient, as information considered useful by a general practitioner is likely different than what would be useful for a veterinary oncologist. Conversation broadened to discuss which stakeholders are best positioned to generate synoptic reporting templates. Should it be the pathologists, who are not necessarily up to date on the latest prognostic, therapy-determinative factors for all tumors in veterinary oncology, or should it be the oncologist, who are more knowledgeable on those points and who are, after all, the end users. Dr. Meuten felt strongly that collaborative effort was needed between veterinary oncologists and pathologists to ensure that any synoptic report templates are targeted, useful, and relevant to the widest audience possible.

As discussed above, the authors of the most recent descriptive feline UC study noted that a particular histomorphologic feature (glandular morphology) should be reported in veterinary reports, not because it had prognostic value, but because it had potential utility in identifying metastatic disease with an unexpected histomorphology. This data point, not prognostic and not backed up by extensive research yet nonetheless useful, gets at the heart of many conference participants' concerns over the trend toward synoptic reporting. A checklist, "just the facts" style of report, while perhaps efficient, easy to read, streamlined, and standardized, feels as if it strips the profession of something fundamental: the ability to communicate impressions and findings, born not solely from metrics, but from experience, that others may find useful when practicing the art of medicine. As synoptic reporting continues to gain popularity, discussions such as these should continue to ensure that nuanced evaluation and communication are not sacrified on in the interest of data-driven efficiency.

On a more prosaic note, conference participants preferred to omit grading from the diagnosis as, per conference discussion, the histologic grade currently has no prognostic significance. Conference participants noted the contributor's classification of the UC as non-papillary; however, in the section examined at conference, participants felt that the

dominant pattern was papillary, and this view is reflected in the morphologic diagnosis.

References:

1. Avallone G, Rasotto R, Chambers JK, et al. Review of histological grading systems in veterinary medicine. *Vet Pathol*. 2021;58(5):809-828.
2. Charney VA, Miller MA, Heng HG, Weng HY, Knapp DW. Skeletal metastasis of canine urothelial carcinoma: pathologic and computed tomographic features. *Vet Pathol*. 2017;54(3):380-386.
3. Cianciolo RE, Mohr FC. Urinary system. In: Maxie MG, ed. *Jubb, Kennedy, and Palmers Pathology of Domesticated Animals.* 6th ed. Elsevier;2016:461-463.
4. Cullen JM, Breen, M. An overview of molecular cancer pathogenesis, prognosis and diagnosis. In: Meuten DJ, ed. *Tumors in Domestic Animals*. Wiley-Blackwell;2017 :1-26.
5. Je-Han Lin, Kao CF, Wang FI, et al. Urothelial carcinomas of the urinary bladder with plasmacytoid or rhabdoid features and tendency of epithelial-mesenchymal transition in 3 dogs. *Vet Pathol.* 2018;55(5):673-677.
6. Maeda S, Yoshitake R, Chambers JK, et al. $BRAF^{V595E}$ mutation associates CCL17 expression and regulatory T cell recruitment in urothelial carcinoma of dogs. *Vet Pathol*. 2021;58(5):971-980.
7. Meuten DJ, Meuten TLK. Tumors of the urinary system. In: Meuten DJ, ed. *Tumors in Domestic Animals.* Wiley-Blackwell; 2017:632-688.
8. Mochizuki H, Shapiro SG, Breen M. Detection of copy number imbalance in canine urothelial carcinoma with droplet digital polymerase chain reaction. *Vet Pathol.* 2016;53(4):764-772.
9. Ramos-Vara JA, Miller MA, Boucher M, Roudabush A, Johnson GC. Immunohistochemical detection of uroplakin III, cytokeratin 7 and cytokeratin 20 in canine urothelial tumors. *Vet Pathol.* 2003;40:55-62.
10. Reed LT, Knapp DW, Miller MA. Cutaneous metastasis of transitional cell carcinoma in 12 dogs. *Vet Pathol*. 2012;50(4): 676-681.
11. Rocha TA, Mauldin GN, Patnaik AK, Bergman PJ. Prognostic factors in dogs with urinary bladder carcinoma. *J Vet Intern Med.* 2000;14:486-490.
12. Sakai K, Maeda S, Saeki K, et al. ErbB2 copy number aberration in canine urothelial carcinoma detected by a digital polymerase chain reaction assay. *Vet Pathol.* 2020;57(1):56-65.
13. Shapiro SG, Raghunath S, Williams C, et al. Canine urothelial carcinoma: genomically aberrant and comparatively relevant. *Chromosome Res*. 2015; 23:311-331.
14. Sledge DG, Patrick DJ, Fitzgerald SD, Xie Y, Kiupel M. Differences in expression of uroplakin III, cytokeratin 7 and cyclooxygenase-2 in canine proliferative urothelial lesions of the urinary bladder. *Vet Pathol*. 2015;52(1):74-82.
15. Smith SC, Mohanty SK, Kunju LP, et al. Uroplakin II outperforms uroplakin III in diagnostically challenging settings. Histopathology. 2014;65:132-138.
16. Tsuboi M, Sakai K, Maeda S, et al. Assessment of HER2 expression in canine urothelial carcinoma of the urinary bladder. *Vet Pathol*. 2019;56(3):369-376.
17. van der Weyden L, O'Donnell M, Plog S. Histological characterization of feline bladder urothelial carcinoma. *J Comp Pathol.* 2021;182:9-14.

WSC 2023-2024
Conference 22 Self-Assessment

1. Adult *Foasciola hepatica* are found where?
    a. Liver parenchyma
    b. Cecum and colon
    c. Bile ducts
    d. Small intestine

2. Which of the following test is considered the most sensitive for detection of Fasicola hepatica?
    a. Necropsy
    b. cELISA
    c. Serology for antibody
    d. Fecal sedimentation

3. Halicephalobus gingivalis is a member of which family of nematodes?
    a. Strongyles
    b. Spirurids
    c. Ascardis
    d. Rhabditids

4. Which of the following breeds has an increased incidence of urothelial carcinoma?
    a. Labrador retrievers
    b. Bedlington terrier
    c. Scottish terriers
    d. Russian wolfhounds

5. Which of the following breeds has an increased incidence of osteosarcoma?
    a. Rottweilers
    b. Labrador retrievers
    c. Greyhounds
    d. Cane Corso

Joint Pathology Center
Veterinary Pathology Services

WEDNESDAY SLIDE CONFERENCE 2023-2024

Conference #23 17 April 2024

CASE I:

Signalment:
1.5 year-old neutered male domestic short-hair cat (*Felis catus*).

History:
The cat presented for signs of pain evolving over the last month. Palpation during the clinical examination localized the pain to the cervical vertebral spine. Cervical radiographs revealed a moth-eaten lesion involving the left part of C3. A CT scan identified a monostotic osteoproliferative lesion centered on the left pedicle of C3 and causing stenosis of the spinal canal. A benign primitive bone neoplasia was suspected. Decompressive hemilaminectomy was performed one month later. Post-operative CT scan showed residual compressive bone material at the surgical site. The animal's condition rapidly declined after surgery (stage IV cranial cervical myelopathy). Unfortunately, the cat became comatose and was maintained under artificial ventilation for a few hours before owners elected euthanasia.

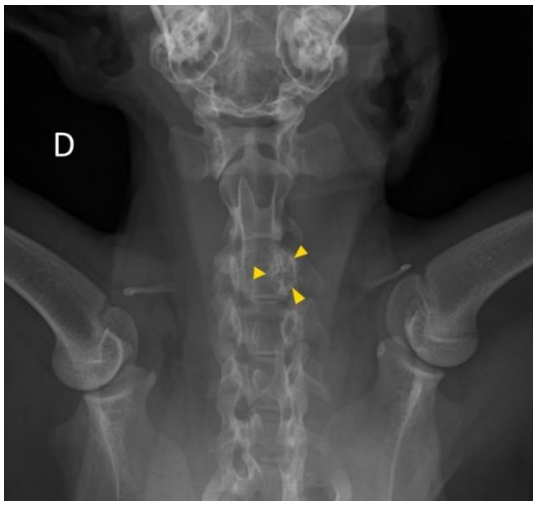

Figure 1-1. Vertebra, cat. Cervical radiographs revealed a moth-eaten lesion involving the left part of C3. (*Photo courtesy of:* Unité d'Histologie et d'Anatomie pathologique, BioPôle Alfort, Département des Sciences Biologiques et Pharmaceutiques, Ecole Nationale vétérinaire d'Alfort (EnvA). https://www.vet-alfort.fr/).

Gross Pathology:
The left lamina of C3 was fractured and an entire fragment of bone was missing due to the hemilaminectomy procedure. The left pedicle of C3 showed a focal and poorly demarcated 1-1.5 cm osteoproliferative lesion with irregularly branching bone trabeculae giving a spongy appearance. The spinal cord was dorsally displaced in the vertebral canal and a central focus of hemorrhagic myelomalacia was identified. The other organs were grossly unremarkable.

Microscopic Description:
Arising from the left pedicle of the C3 vertebra and protruding into the spinal canal and replacing the bone marrow is proliferative fibrovascular tissue that is poorly demarcated, moderately cellular and infiltrative. The tissue is composed of capillary and arteriole-type vessels, and less often venule-like

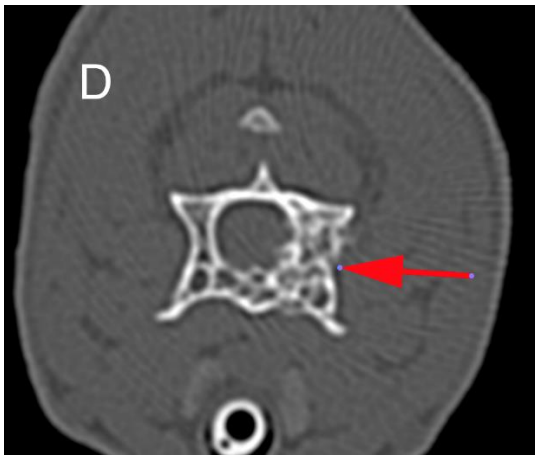

Figure 1-2. Vertebra, cat. CT scan identified a monostotic osteo-proliferative lesion centered on the left pedicle of C3 and causing a stenosis of the spinal canal.

vessels, that irregular branch and grow within a loose, edematous and myxoid stroma. These vessels are lined by squamous and bland endothelial cells surrounded by pericytes (capillary-like vessels) or by a layer of smooth muscle cells (arteriole-like vessels). Atypias are minimal and no mitoses are observed. Some vessels are associated with small acute hemorrhages, fibrin exudation, or microthrombi. The surrounding trabecular bone shows bone remodeling characterized by irregular and scalloped outlines lined by plump osteoblasts and osteoclastic activity within Howship's lacunae.

The cervical spinal cord shows a dorso-lateral rotation around its longitudinal axis. Multiple foci of acute hemorrhagic necrosis/myelomalacia are seen within the grey and white matter, most likely secondary to the surgery. Some perivascular cuffs of neutrophils, macrophages and lymphocytes are identified nearby. Multifocally in the white matter, myelin sheaths are irregularly dilated and sometimes contain vacuolated macrophages indicative of Wallerian-like degeneration. Some axons are also severely dilated and form spheroids. These changes are most likely secondary to the spinal cord compression.

Contributor's Morphologic Diagnoses:

1. Cervical vertebra C3 (left pedicle): Vertebral angiomatosis (vascular vertebral malformation/hamartoma)
2. Cervical spinal cord: Myelomalacia, multifocal, acute, marked, with hemorrhages, axonal degeneration and spheroids.

Contributor's Comment:

Feline vertebral angiomatosis was first described in 1987 by Wells and Weisbrode in a case series of three cats. In this paper, the lesions were restricted to the thoracic vertebrae and diagnosed as an intraosseous vascular malformation.[16]

This entity is characterized by a focal proliferation of non-neoplastic blood vessels, hence the more recent denomination of vertebral angiomatosis.[4,5,7,10,11,13-16] Similar histological lesions are recognized in human medicine with other names including skeletal angiomatosis, vertebral hemangioma, lymphangiomatosis, and hamartoma.[7,16] This condition is not recognized as a true neoplasm because the vascular walls are well differentiated and are composed of multiple cell types, including pericytes, smooth muscle cells, and fibroblasts.[7,10]

Figure 1-3. Vertebra, cat. The left lamina of C3 was fractured and an entire fragment of bone was missing (consequence of the hemilaminectomy). The left pedicle of C3 showed a focal and poorly demarcated osteoproliferative lesion.

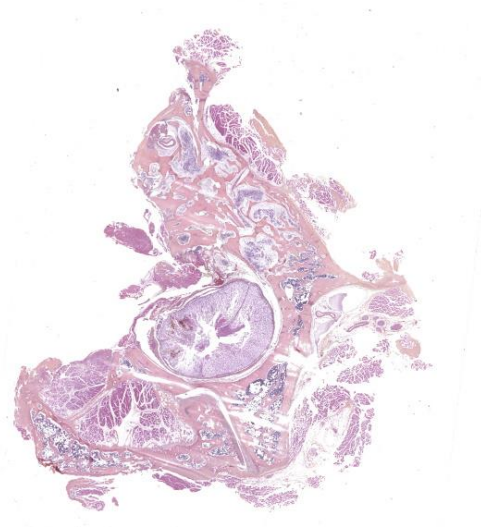

Figure 1-4. Vertebra, cat. One section of vertebra and spinal cord are submitted for examination. Part of the vertebral arch is missing as a result of hemilaminectory. There is loss of marrow within the remaining vertebral arch. (HE, 3X)

This condition is rare but is well described in the literature with 12 documented cases.[4,5,7,10,11,13-16] Affected cats are typically young and less than 2 years old except for a 3.5 years old cat.[4,5,7,10,11,13-16] No sex or breed predisposition have been reported. Animals present with a history, usually over 1 month, of chronic pain, lethargy, reluctance to walk, or progressive paraparesis.[4,5,7,10,11,13-16] Most lesions are localized to the thoracic vertebrae but lumbar lesions have been described.[4,5,7,10,11,14-16] They tend to originate from the vertebral arch, pedicle, or body and seem to spare the spinous process.[7] Occasionally, they can involve multiple vertebrae, but no associated systemic vascular lesion has been observed.[5,13] It is considered benign but can be locally aggressive.[4,7,10,15] Our case is original because it is the first report to our knowledge of cervical involvement. The clinical signs are likely caused by the spinal cord compression resulting from the expansion of angiomatosis into the spinal canal.

The diagnosis is first approached by imaging, mostly post-myelographic CT scan or MRI, in order to localize the lesion and evaluate the associated spinal cord compression.[4,5,7,10,11,13-16] The differential diagnoses include vertebral new bone formation due to an old trauma, disc extrusion, bone abscess, granuloma, ancient hematoma or migrating foreign body.[15] Neoplasia is less likely considering the young age of the affected animals, but lymphoma (especially in FeLV positive cats) or osteosarcoma should be considered.[7,15]

The therapeutic approach is always surgical with a dual goal: 1) removing the spinal cord compression and 2) making biopsies for histopathological diagnosis.[4,5,7,10,11,13-16] Cytologic imprints can be done during the surgery but are of poor diagnostical value.[13,15] Adjuvant radiotherapy can be considered because of the potentially locally aggressive nature of the lesion and also because of the difficulty of complete resection in this area.[7,11] Outcomes are variable. Some animals receiving surgery with or without radiotherapy are reported as free of disease over the following months or years.[5,7,10] However, the surgery is not without risk, and relapse is also reported.[4,15]

The pathogenesis of feline vertebral angiomatosis is still unclear. Because of the occurrence in young cats and the absence of an associated inflammatory or infectious process, developmental anomaly is currently considered most likely.[7,10,11,16]

Histopathological features are consistent among all cases and are characterized by a proliferation of rather well-differentiated capillaries, arterioles, and occasionally venules, into a loose and myxoid connective tissue with invasion of the spinal canal and the bone marrow, as well as bone remodeling and new bone formation.[4,5,7,10,11,13-16]

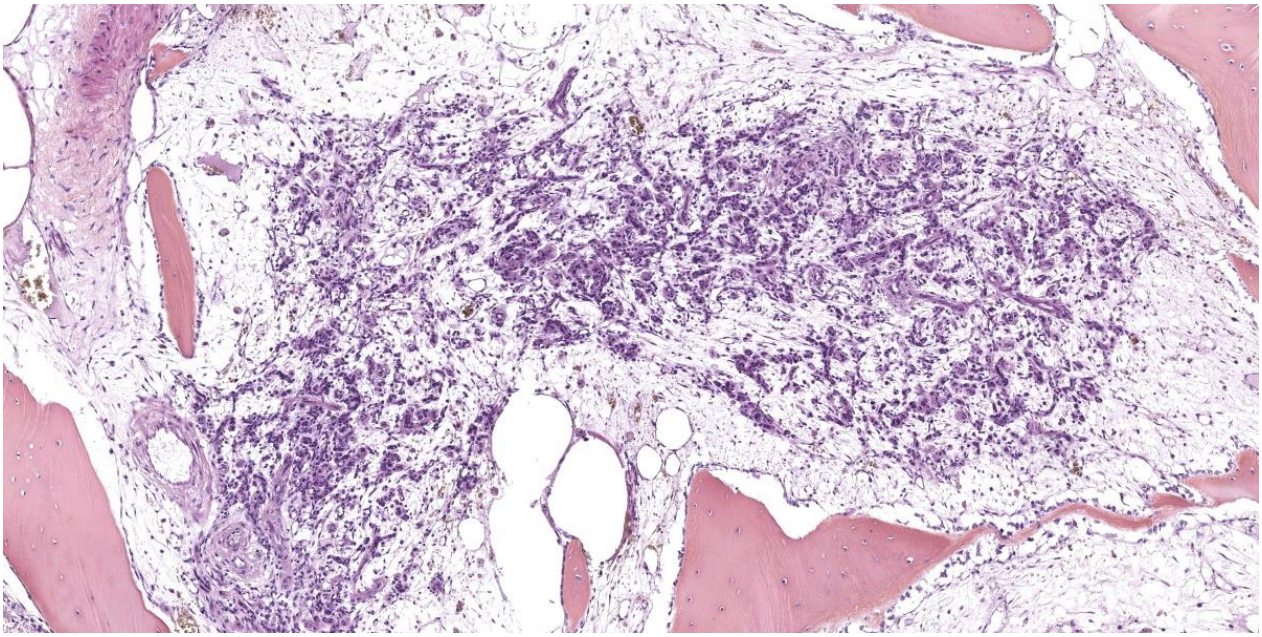

Figure 1-5. Vertebra, cat. Marrow speces are devoid of marrow and contain plexiform proliferations of tortuous capillaries. (HE, 90X)

Other type of angiomatosis have been reported in the cat, affecting the skin,cerebrum, meninges, and lungs.[1-3,8,9]

Contributing Institution:
Unité d'Histologie et d'Anatomie pathologique
BioPôle Alfort, Département des Sciences Biologiques et Pharmaceutiques
Ecole Nationale vétérinaire d'Alfort (EnvA)
https://www.vet-alfort.fr/

JPC Diagnoses:
1. Vertebra, pedicle and body, hemi-laminectomy site: Angiomatosis, focally extensive, marked, with reactive osteolysis and osteoproliferation (bone modeling).
2. Cervical spinal cord, gray and white matter: Myelomalacia, diffuse, severe, with hemorrhage and axonal degeneration.

JPC Comment:
The contributor provides an excellent overview of this enigmatic condition that, until recently, had only been reported in young cats. Earlier this year, however, vertebral angiomatosis was reported in a three year old female intact Cavalier King Charles Spaniel who presented for ataxia and paraparesis.[6] CT revealed osteolysis of the vertebral body and pedicles of T5 with compressive extradural material within the spinal canal.The dog was treated surgically with a dorsal hemilaminectomy and histopathologic samples collected intraoperatively were consistent with vertebral angiomatosis.[6]

Vertebral angiomatosis is one member of a cohort of non-neoplastic vascular malformations beset by confusing terminology, overlapping histologic features, and uncertain pathogeneses. Angiomatosis (also known as hemangiomatosis) has two microscopic patterns: either a mixture of blood vessel types, some of which can be cavernous, or a predominance of capillaries. Lobules of mature adipose tissue characteristically accompany the vascular elements.[12]

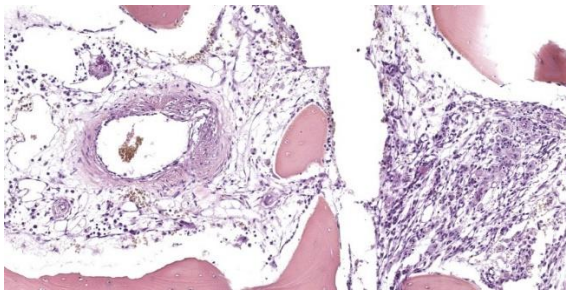

Figure 1-6. Vertebra, cat. Arterioles (left) within areas of vascular proliferation have asymmetric fibrosis of the smooth muscle wall and adventitia. (HE, 90x)

In addition to the vertebral angiomatosis so nicely discussed by the contributor, angiomatosis has been identified within the skin and subcutis of cats and dogs and in the skin of cattle. Calves have a reported generalized pattern of angiomatosis in which the heart, lungs, kidneys, and an assortment of other organs are involved.[12] There is a single case report of cerebral angiomatosis in a young cat presenting with generalized seizures, the clinical manifestation of bilateral nests of differentiated capillaries within the cerebral gray matter.[12]

Human and veterinary medicine is rich with various other hamartomatous vascular conditions, including meningoangiomatosis, angioma, and arteriovenous malformations, the parsing of which requires equal measures of stamina and will. An excellent 2021 comparative review of proliferative vascular disorders in the central nervous system is a helpful reference for those attempting to understand the nuances of these difficult diagnoses.[12]

Our moderator this week was Dr. Julie Engiles, Professor of Pathology at the University of Pennsylvania School of Veterinary Medicine. Dr. Engiles began discussion of this case with a review of vertebral anatomy and by noting the important structures, such as the vertebral artery, that can be used as orientation landmarks on this challenging slide. Dr. Engiles also stressed the importance of a collaborative approach among pathologists, radiologists, and clinicians in cases like this, where locating and appropriately sampling the lesion would be difficult without the insight provided by other members of the medical team. In this case, the lesions presented radiographically with an aggressive, moth-eaten appearance which provides helpful context for the relatively bland histologic appearance of the proliferative cells.

Immunohistochemically, the vascular markers Factor VIII and ERG helped to visualize the disorganized proliferation of vascular elements, while smooth muscle actin highlighted the smooth muscle in the proliferating vessel walls. Dr. Engiles noted that the proliferation of multiple cell types, including endothelial smooth muscle myocytes, and pericytes, supports the nonneoplastic classification of this entity, as neoplasia is typically characterized by the aberrant proliferation of a single cell type. The moderator noted that this lesion is sometimes called a hamartoma, which seems to connote an indolent, static process at odds with the typically proliferative and infiltrative behavior of these lesions. For this reason, the moderator prefers the more dynamic term angiomatosis.

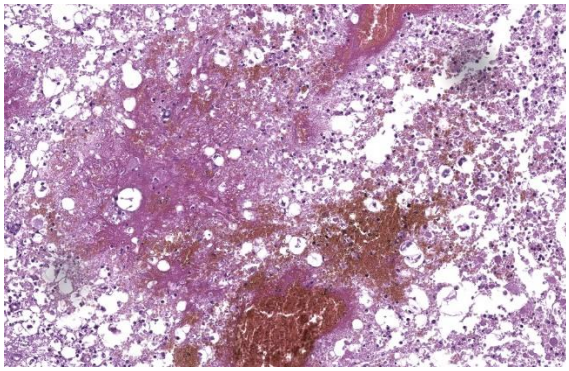

Figure 1-7. Spinal cord, cat. There is marked congestion and hemorrhage of vessels within the spinal cord. There is diffuse malacia of the gray and white matter with numerous spheroids. (HE, 169X)

Conference participants discussed the abundant ancillary changes in section, such as the polyphasic atrophy, degeneration, and regeneration present in the surrounding skeletal muscle. The history of hemilaminectomy at the site complicated analysis of these changes, making it difficult to determine which changes were due to surgical manipulation and which were caused by the pressure of the expansile vertebral angiomatosis.

Participants felt that the bone changes caused by the vertebral angiomatosis were significant and should be mentioned in the morphologic diagnosis. Participants also felt the morphologic diagnosis should acknowledge the hemilaminectomy that is an obvious feature of the section. Both were ultimately included in the morphologic diagnosis for this fascinating entity.

References:

1. Baron CP, Puntel FC, Fukushima FB, da Cunha O. Progressive cutaneous angiomatosis in the metatarsal region of a cat. *J Am Vet Med Assoc*. 2020;256(2):226-229.
2. Bulman-Felming J, Gibson T, Kruth S. Invasive cutaneous angiomatosis and thrombocytopenia in a cat. *J Am Vet Med Assoc.* 2009;234(3):381-384.
3. Corbett M, Kopec B, Kent M, Rissi DR. Encephalic meningioangiomatosis in a cat. *J Vet Diagn Invest*. 2022;34(5): 889-893.
4. Belluzzi E, Caraty J, Vincken G, Esmens MC, Bongartz A. Vertebral angiomatosis recurrence in a 14-month-old Maine Coon cat. *Vet Rec Case Rep*. 2018;6(4):11-13.
5. Frizzi M, Ottolini N, Spigolon C, Bertolini G. Feline vertebral angiomatosis: two cases. *J Feline Med Surg Open Rep*. 2017;3(2): 205511691774412.
6. Gagliardo T, Pagano TB, Lo Piparo S, et al. Vertebral angiomatosis in a dog. *J Am Anim Hosp Assoc*. 2024;60(1):36-39.
7. Hans E, Dudley R, Watson A, et al. Long-term outcome following surgical and radiation treatment of vertebral angiomatosis in a cat. *J Am Vet Med Assoc.* 2018;253 (12):1604-1609.
8. Jenkins T, Jennings R. Pulmonary capillary hemangiomatosis and hypertrophic cardiomyopathy in a Persian cat. *J Vet Diagn Invest*. 2017;29(6): 900-903.
9. Kipar A, Hetzel U, Armien A, Baumgartner W. Bilateral focal cerebral angiomatosis associated with nervous signs in a cat. *Vet Pathol.* 2001;38(3):350-353.
10. Kloc PA, Scrivani PV, Barr SC, et al. Vertebral angiomatosis in a cat. *Vet Radiol Ultrasound.* 2001;42(1):42-45.
11. Leonardi H, Poirier V, Iverson M, Samarani F. Successful long-term outcome with radiation and prednisolone following a postoperative feline vertebral angiomatosis relapse. *JFMS Open Rep*. 2023;9(1): 205511692311550.
12. Marr J, Miranda IC, Millder AD, Summers BA. A review of proliferative vascular disorders of the central nervous system of animals. *Vet Pathol*. 2021;58(5):864-880.
13. Meléndez-Lazo A, Ros C, de la Fuente C, Anor S, Fernandez-Flores F, Pastor F. What is your diagnosis? Vertebral mass in a cat. *Vet Clin Pathol.* 2017;46(1):185-186.
14. Ricco C, Bouvy B, Gomes E, Cauzinille L. Lumbar vertebral angiomatosis in a cat: a clinical case. *Revue Med Vet*. 2015;166 (11): 332-335.
15. Schur D, Rademacher N, Vasanjee S, McLaughlin L, Gaschen L. Spinal cord compression in a cat due to vertebral angiomatosis. *J Feline Med Surg*. 2010;12(2): 179-182.
16. Wells M, Weisbrode S. Vascular Malformations in the Thoracic Vertebrae of

Three Cats. *Vet Pathol.* 1987;24(4): 360-361.

CASE II:

Signalment:
Juvenile female sandhill crane (*Antigone canadensis)*.

History:
The animal was presented to a local wildlife center with a cup attached to its beak. On initial exam, the submitting veterinarian noted emaciation, dehydration, and indentation on the beak as well as swelling of the right hock and left tibiotarsus, with no obvious abnormalities on radiographs. The bird was moved to an outside rehabilitation space 1 day after presentation and was eating and gaining weight reliably. The animal was found deceased a few weeks later.

Gross Pathology:
The animal weighs 2.2 kg and is in thin physical condition as evidenced by atrophied pectoral musculature and adipose tissue. There is a concentric deep indentation midway along the length of the beak. Overlying the right ankle are multiple firm, occasionally ulcerated nodules that are 2 to 5 mm in diameter. When sectioned the nodules are pale blue or tan, firm, and translucent with a botryoid appearance. Dissection of the joint shows many similar nodules firmly attached to the dermis, soft tissues, ligaments, and tendons. The condyle of the tibiotarsus has a fracture with pitting and marked proliferation of white firm nodules in the defect and epicondyle.

There is a focal, firm, nodular swelling overlying the distal left tibiotarsus that measures 1.8 cm x 0.8 cm. When sectioned, the nodule is tan and translucent. Relative to the right pectoral muscle, there is moderate wasting of the left pectoral musculature.

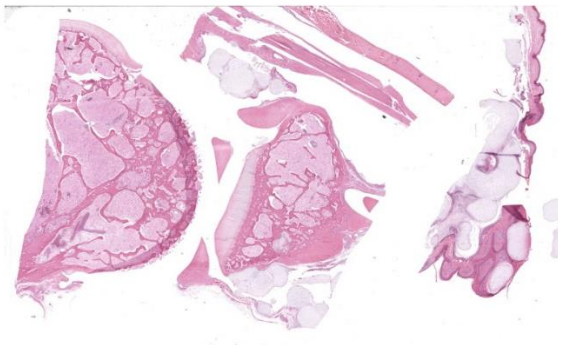

Figure 2-1. Tibiotarsal joint, sandhill crane. The joint is dissected. At lower left is the tibiotarsal joint, at top is the gastrocnemius tendon and sheath, and at right is the overlying skin. At subgross magnification, there are nodules of proliferating cartilage within the joint space, tendon sheath, and overlying dermis. (HE, 4X)

Within the mid-trachea at the level of the reflexive curvature are multiple intraluminal trematodes. The organisms are 1.4 cm long, flat and fusiform with a bulbous anterior end; they are white with bilateral dark brown linear striations. Within the affected area, the tracheal mucosa is red and slightly thickened.

There are no significant gross abnormalities in the tongue, esophagus, lungs, heart, liver, spleen, pancreas, kidneys, proventriculus, ventriculus, small intestine, large intestine, or brain. The spinal cord is not examined in this case.

Microscopic Description:
Ankle joint: The bone profile is irregular due to many cartilage nodules that arise from the synovium of the joint spaces (synovium) and tendon sheaths (tenosynovium). Nodules contain many evenly spaced chondrocytes in hyaline pale blue matrix; they have moderate finely vacuolated pale purple cytoplasm and large round nuclei with peripheralized chromatin and 1-3 nucleoli. Anisocytosis and anisokaryosis are marked. Mitoses are not evident. Binucleate cells are occasionally evident, and a trinucleate cell was seen. Many of

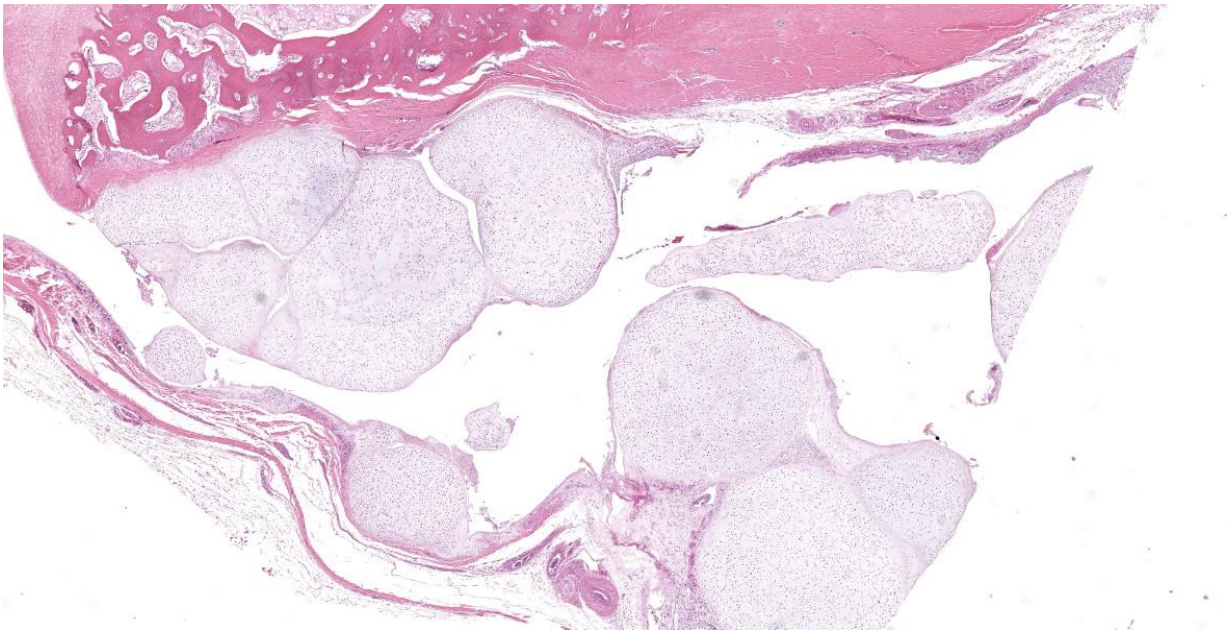

Figure 2-2. Tibiotarsal joint, sandhill crane. Arising from the joint capsule and lining the proximal tibia are nodules of cartilage measuring about 8mm in diameter. (HE, 23X)

the chondrocytes are pyknotic or karyolytic with pink cytoplasm (necrosis); such cells are dispersed between viable cells or predominate in the center of nodules where there is fragmentation of matrix and rarefaction of tissue. In larger nodules, the central chondrocytes cluster with intervening areas of acellular matrix. The synovium is thin and often necrotic when stretched over the nodules, with small thrombi in the associated vessels. In other areas the subintima is thickened by large mesenchymal cells embedded in mucinous matrix and variable numbers of lymphocytes, plasma cells, and heterophils. Scant fibrin and karyorrhectic cells are present in the joint spaces. The bone surfaces have mild remodeling, there is marked serous atrophy of marrow fat, and skeletal myocytes are atrophied.

The skin bulges and is ulcerated due to several cartilage nodules in the subcutis, dermis, and epidermis. Synovium surrounds the intradermal nodules and merges with the inflamed and fibrotic dermis. Intraepidermal nodules are demarcated from the dermis by many heterophils; their cartilage matrix is pale blue to pink, and cells are pyknotic along the subcorneal surface. The epidermis overlying the intraepidermal nodules is necrotic and the surrounding epidermis is hyperplastic (acanthosis, increased mitoses). The stroma around and deep to the intraepidermal nodules is expanded by many red cells, heterophils, and compact collagen that has many fine karyorrhectic fragments, as well as small thrombosed vessels.

Contributor's Morphologic Diagnoses:

1. Tibiotarsus: Moderate chronic heterophilic synovitis with synovial and tenosynovial chondromatosis
2. Skin: Multifocal chondromatosis with epidermal hyperplasia and necrosis, heterophilic dermatitis, and transepithelial elimination

Contributor's Comment:

Synovial chondromatosis (also known as synovial chondrometaplasia) is an uncommon non-neoplastic process characterized by the formation of multiple cartilage nodules in synovial tissues of a joint, tendon sheath, or

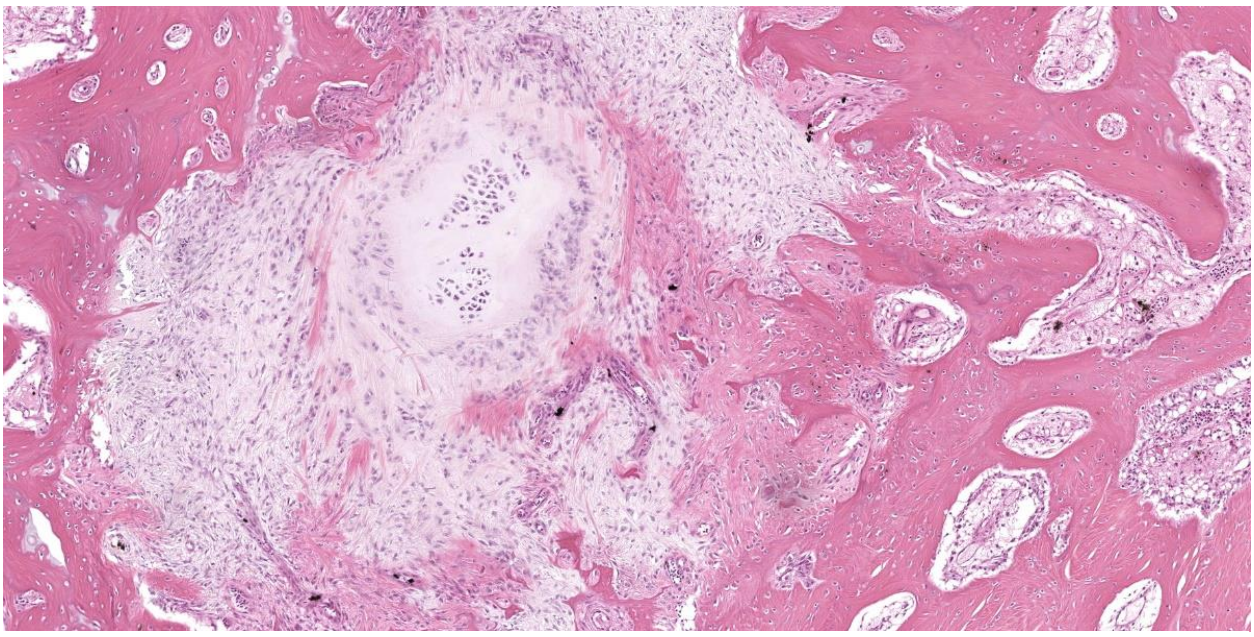

Figure 2-3. Tibiotarsal joint, sandhill crane. Proliferating mesenchymal cells within the tibial marrow space are giving rise to cartilage. (HE, 91X)

bursa. When the majority of these nodules undergo endochondral ossification, the term osteochondromatosis is used.[2,3,7] Reports in animals have mostly been in dogs[1,7,8,10,14] and raptors[11,15,18] but horses and pigs can also be affected.[6,13] It should be noted that osteochondromatosis of cats is different in its biological behavior, distribution, and possible etiology, and thus should not be combined when discussing the disease entity in other species.[3]

Males predominate in reports from both dogs and humans, while the few reports in raptors have increased numbers of females.[3,11,15,18] In dogs most reports are from large and giant purebreds from 7 months to 11 years old. The shoulder joint is most often affected, although cases have also been observed in the stifle, elbow, hock, and digits.[2,3] Clinical signs include chronic progressive lameness with swelling of the joint.[1,7,8,10]

In raptors, the majority of cases are reported bilaterally in the scapulohumeral joints of great horned owls (*Bubo virginianus*), with or without osteoarthritic change. Fewer cases of chondromatosis in the stifle joints have been reported.[11,15,18] Birds often present in poor nutritional condition due to severe mobility restriction. This case is the first report of chondromatosis in the *Gruiformes* group and affecting the ankle joints.

Two forms of synovial chondromatosis (primary and secondary) have been described. Primary (idiopathic) chondromatosis occurs spontaneously within the synovium of a single, otherwise unremarkable joint; it is rare in humans and animals. Grossly, primary synovial chondromatosis presents with more nodules than secondary chondromatosis.[3] The pathogenesis of primary synovial chondromatosis is unknown, and it is thought to be an idiopathic nodular cartilaginous metaplasia of the synovium. Secondary chondromatosis is thought to be a reaction to a traumatic, degenerative, or inflammatory joint disease. Speculatively, the etiology in raptors is thought to be a chronic inflammatory process due to joint strain.[15] In older horses and dogs,

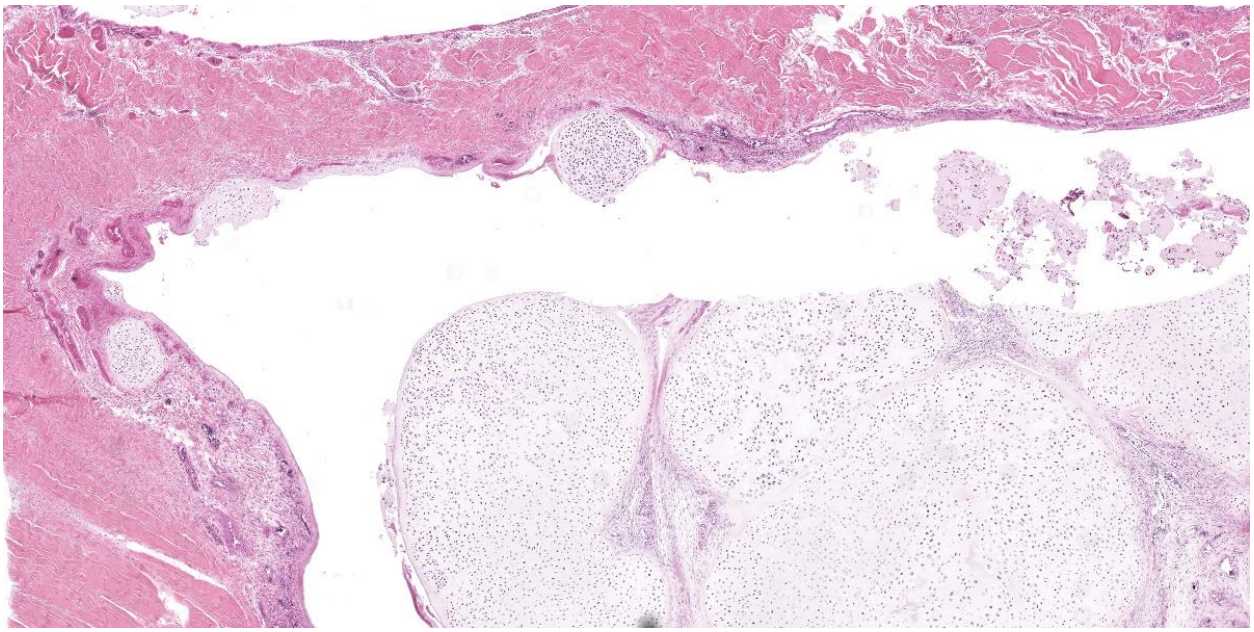

Figure 2-4. Tibiotarsal joint, sandhill crane. Nodules of cartilage arise within the tendon sheath (at left) and extend into the tendon sheath lumen (center). (HE, 39X)

it is usually an incidental finding at necropsy, while in raptors it is often associated with the demise of the individual due to an inability to fly.[3,15] Nodules are reported to be less numerous and mixed with other forms of synovial proliferation and metaplasia. Erosive changes in the articular cartilage are often more marked than the degree of synovial proliferation.[3] In this case, the bilateral occurrence in the ankles, presence of synovitis, and fracture of the tibiotarsus indicates secondary synovial chondromatosis.

Classically, gross lesions are described as multiple firm or hard white nodules embedded in the synovium and periarticular connective tissues, with variably intact articular cartilage.[2,3,14] The nodules consist of islands of highly cellular hyaline cartilage covered by a layer of synoviocytes or fibrous tissue attached to or continuous with the synovial lining of joints or bursae. Chondrocytes may be haphazardly clustered, large, and sometimes binucleate. In this case, trinucleate chondrocytes were rarely evident. Areas of fibrocartilage, central necrosis, or endochondral ossification with medullary hematopoiesis may also be present. In some cases proliferative plasmacytic synovitis is reported.[3,17] Nodules may detach from the synovium and float freely in the joint. In these cases, they are termed "loose bodies" and may undergo ischemic necrosis.[2,12] Extra-articular chondromatosis has been rarely reported; in this case chondrometaplasia was evident in a tendon sheath.[7]

Under certain circumstances, nondermal elements enter the epidermis and are eliminated to the outside, a process termed 'transepithelial elimination' (TE).[12] Four subdivisions of TE are described, two of which involve large portions of tissue, as in our case (subdivisions 3 and 4). As migrating tissues compress the epidermis from below, epithelial damage occurs with necrosis and ulceration, and possible sloughing.[12] Transepithelial elimination, to the authors' knowledge, has not been reported in association with synovial chondromatosis or in the class *Aves*. In this case, TE probably occurs as a result of the pressures exerted on the nodules by the relatively

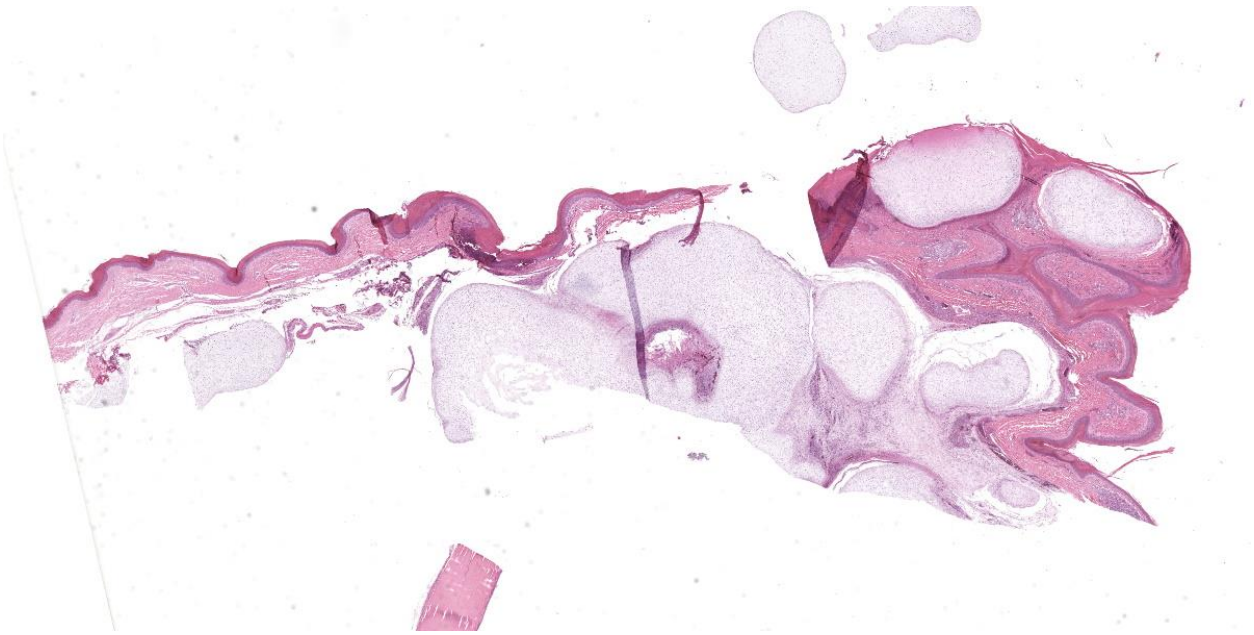

Figure 2-5. Tibiotarsal joint, sandhill crane. Nodules of cartilage are present within the dermis and extend to the epidermis (transepidermal elimination). (HE, 39X)

immobile and non-distensible skin of the ankle in birds. This area may also have increased susceptibility to ulceration versus a more protected scapulohumeral lesion, which is more often seen in birds with chondromatosis.

Differential diagnoses for synovial chondromatosis include chondroma and chondrosarcoma. Chondroma is a benign neoplasm of cartilage that has been occasionally reported in multiple veterinary species. Histologically, chondromas may have similar irregular lobules of hyaline cartilage, which may also have foci of endochondral ossification and mineralization. In fact, some report that primary chondromatosis may be a multifocal form of a chondroma.[5,6] An important differential diagnosis is synovial chondrosarcoma. Malignant transformation of synovial chondromatosis to chondrosarcoma is rarely reported in dogs.[1,7] Features that suggest chondrosarcoma are bone invasion and replacement of the chondrocyte cluster pattern with a more random distribution of cells.[1,3,7]

Contributing Institution:
Veterinary Diagnostic Laboratory
University of Illinois at Urbana-Champaign
Urbana, IL
https://vdl.vetmed.illinois.edu/

JPC Diagnosis:
Joint capsule, tendon sheath, and overlying skin: Chondromatosis, nodular, multifocal, severe, with intra-osseous extension, transepidermal elimination, and chronic tenosynovitis and dermatitis.

JPC Comment:
The contributor provides an excellent summary of synovial chondromatosis (SC) as this photogenic entity presents in dogs, birds, pigs, and horses. Cats, however, long known for their flair for the idiosyncratic, have a similar sounding but distinct condition, feline osteochondromatosis, which is distinct from the synovial chondromatosis discussed above and from osteochondromatosis in other animals.[16] In horses, dogs, pigs, and humans, osteochondromatosis demonstrates an autosomal dominant inheritance pattern and

typically occurs in young animals only during the period of active bone growth.[16] The cartilage-capped tumors that arise from bone surfaces give the condition its name and tumor growth arrests once growth plates close.[16]

In contrast, feline osteochondromatosis usually presents in adult cats (most commonly 2-4 years old) long after skeletal maturity is achieved. The condition presents with no breed or sex predisposition and does not appear to be inherited. The disease affects the axial skeleton and, in a sad departure from the tumor arrest seen in other animals, tumors show progressive growth and can undergo malignant transformation to osteosarcoma or chondrosarcoma.[16]

Interestingly, feline osteochondromatosis is usually diagnosed in cats concurrently infected with feline leukemia virus (FeLV), leading to speculation that FeLV infected fibroblasts account for the special pathogenesis and distinct clinical behavior of osteochondromatosis in cats relative to other species.[9,16] FeLV particles have been visualized within feline osteochondromatous tissue via electron microscopy and via in situ hybridization; however, a direct pathogenetic link between FeLV infection and the condition has not been conclusively established, and osteochondromatosis has been reported in FeLV-negative cats.[9,16]

In humans, dogs, and a few cats, osteochondromatosis has been associated with premature stop codon-producing frameshift mutations in the exostosin glycosyltransferase 1 and 2 genes (EXT1 and EXT2, respectively), whose protein products form an enzyme complex that modifies heparan sulfate chains.[4] It is thought that heparan sulfate chain dysfunction can scramble chondrocyte differentiation or proliferation pathways, fibroblastic growth factors, bone morphogenic proteins, and Wnt signalling pathways, all of which could account for the lesions of osteochondromatosis.[4] These theoretical pathogeneses have not been proven in human or in veterinary medicine, and in all species tested, EXT1 and EXT2 mutations are absent in an significant subset of osteochonromatosis cases.[4]

One such recent case report detailed the radiographic and pathologic findings of feline osteochondromatosis in an aged, 12-year-old Russian Blue, FeLV-negative cat with a years-long history of progressive forelimb lameness.[9] Radiographs revealed bilateral, calcified proliferative lesions of the elbow joints and multiple vertebral bodies and ribs. Grossly, the elbow joints were completely ankylosed by large, round masses containing white material that replaced normal tissue architecture; the affected vertebrae and ribs contained similar lesions.[9] Testing for EXT1 and EXT2 mutations and FeLV infection were all negative, confirming that this condition can arise spontaneously in aged cats.[9]

Back in the joints of the sandhill crane, the moderator noted that this, along with vertebral angiomatosis, was yet another entity with bland looking cells that nevertheless have no business being where they are. Conference participants noted the lack of anisocytosis, anisokaryosis, and mitotic figures, all of which point toward a benign process; however, the intra-osseous nodule of cartilage, which should not be present in a pure case of synovial chondromatosis, raised the spectre of chondrosarcoma for some participants. Participants ultimately decided that the bland histologic appearance of the cells likely a precluded chondromsarcoma diagnosis, but the phrase “with intra-osseous extension” was added to the morphologic diagnosis to capture this unusual feature.

References:

1. Aeffner F, Weeren R, Morrison S, Grundmann INM, Weisbrode SE. Synovial osteochondromatosis with malignant transformation to chondrosarcoma in a dog. *Vet Pathol*. 2012;49(6):1036-1039.
2. Craig LE, Dittmer KE, Thompson KG. Bones and Joints. In: Maxie MG, ed. *Jubb, Kennedy, and Palmer's Pathology of Domestic Animals*. 6th ed. Vol 1. 2016;Elsevier:161-163.
3. Craig LE, Thompson KG. Tumors of Joints. In: Meuten DJ, ed. *Tumors in domestic animals*. 5th ed. John Wiley & Sons Inc;2016:337-355.
4. D'Arienzo A, Andreani L, Sacchetti F, Colangeli S, Capanna R. Hereditary multiple exostoses: current insights. *Ortho Res Rev*. 2019;11:199-211.
5. Davis RI, Foster H, Arthur K, Trewin S, Hamilton PW, Biggart DJ. Cell proliferation studies in primary synovial chondromatosis. *J Pathol*. 1998;184(1):18-23.
6. de Brot S, Grau-Roma L, Vidal E, Segalés J. Occurrence of osteochondromatosis (multiple cartilaginous exostoses) in a domestic pig (Sus scrofa domesticus). *J Vet Diagn Invest*. 2013;25(5):599-602.
7. Díaz-Bertrana C, Durall I, Rial JM, Franch J, Fontecha P, Ramis A. Extra- and intra-articular synovial chondromatosis and malignant transformation to chondrosarcoma. *Vet Comp Orthop Traumatol*. 2010;23(4): 277-283.
8. Edinger DT, Manley PA. Arthrodesis of the shoulder for synovial osteochondromatosis. *J Small Anim Pract*. 1998;39(8): 397-400.
9. Gomez A, Rodriguez-Largo A, Perez E, et al. Feline osteochondromatosis in a 12-year-old feline leukaemia virus-negative cat. *J Comp Pathol.* 2003;25:24-26.
10. Gregory SP, Pearson GR. Synovial osteochondromatosis in a labrador retriever bitch. *J Small Anim Pract*. 1990;31(11): 580-583.
11. Howard MO, Nieves MA, Miles KG. Synovial chondromatosis in a great horned owl (Bubo virginianus). *J Wildl Dis*. 1996;32(2):370-372.
12. Mehregan AH, Hashimoto, K. General Pathology: Terminology. In *Pinkus' Guide to Dermatohistopathology* Appleton & Lan-ge;1995:83-100.
13. Smith RK, Coumbe A, Schramme MC. Bilateral synovial chondromatosis of the metatarsophalangeal joints in a pony. *Equine Vet J*. 1995;27(3):234-238.
14. Smith TJ, Baltzer WI, Löhr C, Stieger-Vanegas SM. Primary synovial osteochondromatosis of the stifle in an English Mastiff. *Vet Comp Orthop Traumatol*. 2012;25(2):160-166.
15. Stone EG, Walser MM, Redig PT, Rings B, Howard DJ. Synovial chondromatosis in raptors. *J Wildl Dis*. 1999;35(1):137-140.
16. Szilasi A, Koltai Z, Denes L, Balka G, Mandoki M. In situ hybridization of feline leukemia virus in a case of osteochondromatosis. *Vet Sci*. 2022;9(2):59.
17. Villacin AB, Brigham LN, Bullough PG. Primary and secondary synovial chondrometaplasia: histopathologic and clinicoradiologic differences. *Hum Pathol*. 1979;10(4):439-451.
18. Xie S, Nevis J, Lezmi S. Pathology in practice. Chondro-osseous metaplasia consistent with synovial chondromatosis in a great horned owl. *J Am Vet Med Assoc*. 2014;245(7):767-769.

CASE III:

Signalment:
4-year-old male African pygmy hedgehog (*Atelerix albiventris*).

History:
This hedgehog presented to the teaching hospital for severe dental disease. A

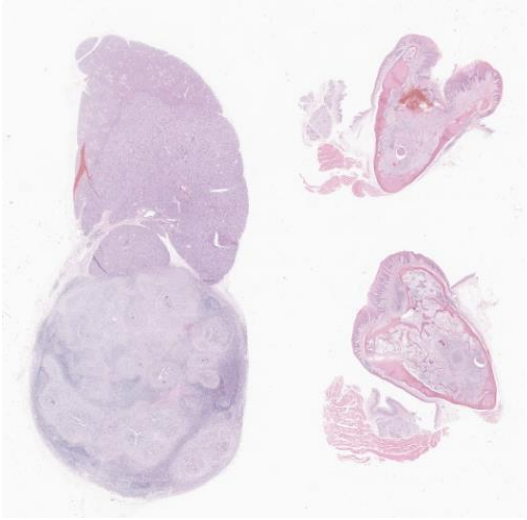

Figure 3-1. Lymph node and jaw, hedgehog. One section of mandibular lymph node and two sections of jaw are submitted for examination. At this magnification, 75% of the nodal architecture is effaced by an inflammatory infiltrate. (HE, 5X)

submandibular mass was noted during examination. Under anesthesia for a dental procedure, the animal decompensated, developing cyanosis. The patient showed clinical improvement when naloxone was administered and had a prolonged recovery from anesthesia. The patient was mobile and eating following recovery, but acutely decompensated 1.5 hours later. Resuscitation was attempted but was unsuccessful.

Gross Pathology:

The hedgehog was in good body condition. There was slight deviation of the muzzle to the right. Only one tooth (the lower right first incisor) remained in the dental arcade and was easily removed with traction. Both mandibles were mildly thickened and slightly irregular with smooth undulations noted in the gingiva.

Mild hemorrhage was present near the right submandibular salivary gland and a 0.5 cm pale nodule (presumed enlarged lymph node) was associated with the gland. Dark pink discoloration and consolidation of the lung was present bilaterally and scattered, small (1 mm) white foci were noted in the affected regions. The heart weighed 1.8 g (0.56% of the total body weight).

Laboratory Results:

Light growth of *Neisseria animaloris* was isolated from the right submandibular lymph node (aerobic culture; species identified using MALDI-TOF). No microbial growth was isolated from this organ on anaerobic culture.

Microscopic Description:

Submandibular lymph node: Large coalescing regions of pallor obscure the normal architecture of the enlarged lymph node. Areas of pallor consist of multifocal to coalescing nodular aggregates of mostly neutrophils with fewer epithelioid macrophages, lymphocytes, plasma cells, eosinophils, and multinucleated giant cells. At the center of the infiltrates are frequent deposits of basophilic bodies occasionally with peripheralized eosinophilic acellular material (Splendore-Hoeppli reaction). Small, non-filamentous, coccoid Gram-negative bacteria are identified at the center of these deposits using a Gram stain. At the periphery of the cell aggregates, there are thin concentric bands of connective tissue and moderate eosinophilic infiltrates. A few small scattered secondary lymphoid follicles are separated by sheet like infiltrates of plasma cells.

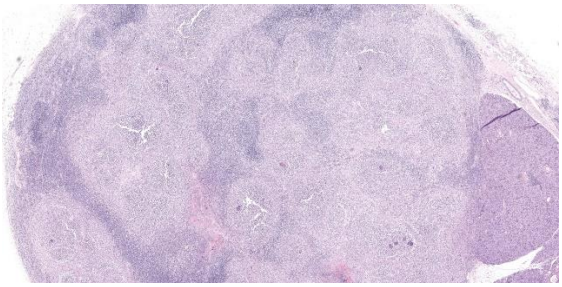

Figure 3-2. Lymph node, hedgehog. Nodal architecture is effaced by numerous poorly demarcated pyogranulomas. (HE, 111X)

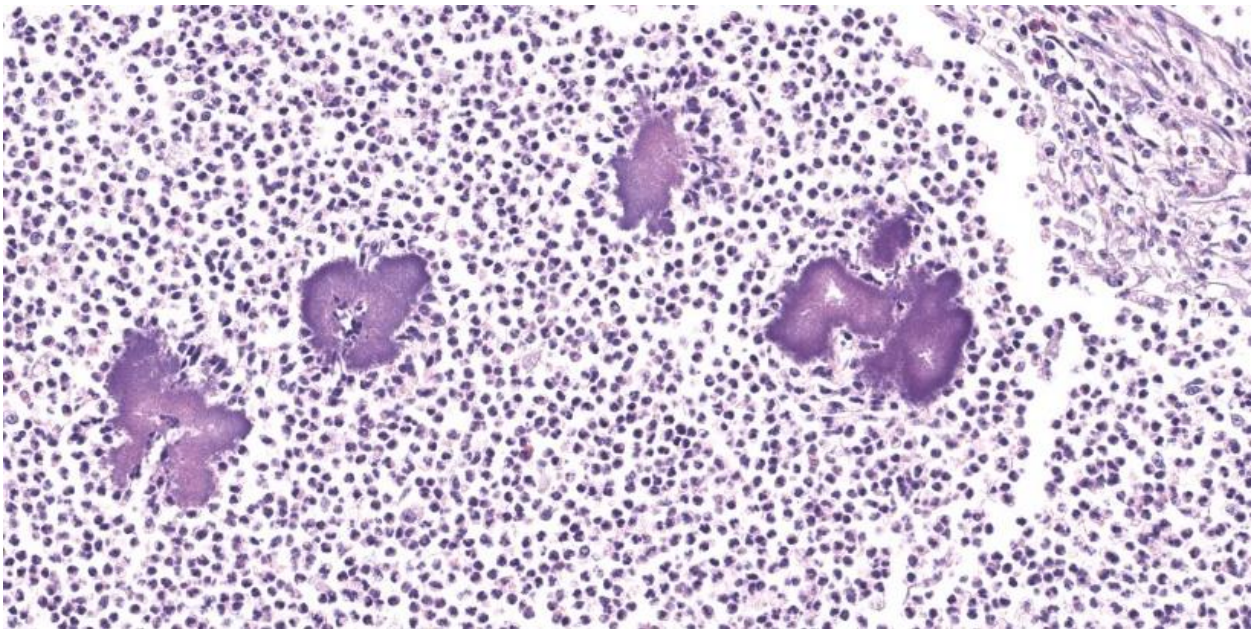

Figure 3-3. Lymph node, hedgehog. Pyogranulomas are centered on colonies of cocci enmeshed in Splendore-Hoeppli material. (HE, 337X)

Jaw: There are multifocal to coalescing regions of increased cellularity and loss of trabecular bone within the mandible. Cellular infiltrates consist of nodular aggregates of mostly neutrophils with fewer epithelioid macrophages, lymphocytes, plasma cells, and rare eosinophils and multinucleated giant cells. At the center of the infiltrates are rare radiating deposits of basophilic material with peripheralized eosinophilic acellular material (Splendore-Hoeppli reaction). At the periphery of the cell aggregates, there are thin concentric bands of connective tissue, plasma cell infiltrates, and focal hemorrhage. Remodeling of the surrounding bone with new woven bone formation is evident. The gingival mucosal epithelium is hyperplastic, eroded, and infiltrated by neutrophils and fewer eosinophils.

Contributor's Morphologic Diagnoses:

1. Submandibular lymph node: Lymphadenitis, pyogranulomatous, multifocal to coalescing, chronic, severe, with intralesional Gram-negative bacteria and Splendore-Hoeppli reaction.
2. Jaw: Osteomyelitis, pyogranulomatous, multifocal to coalescing, chronic, severe, with intralesional bacteria and Splendore-Hoeppli reaction.

Contributor's Comment:

This hedgehog had a history of significant dental disease resulting in loss/removal of most of the teeth. Dental diseases, including gingivitis, periodontitis, tooth fracture, tooth loss, excess dental wear, dental abscesses, and even oral osteomyelitis are common in this species.[1,6] Mandibular osteomyelitis was marked and was accompanied by a similar reaction in the draining lymph node and in the lung (not included in the submission). Splendore-Hoeppli phenomenon was evident within the lesions. This nonspecific reaction is thought to reflect the deposition of antigen-antibody complexes and inflammatory cell products/debris, and occurs around clusters of microorganisms, such as bacteria and fungi, or biologically inert substances.[5] Genera of bacteria that are commonly associated with this reaction include *Actinomyces*,

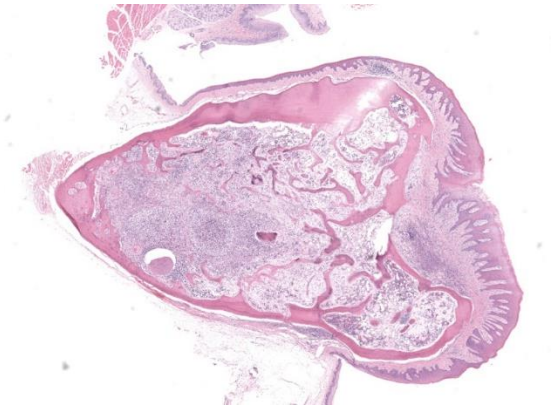

Figure 3-4. Mandible, hedgehog. There are similar pyogranulomas within the medullary cavity of the mandible. (HE, 18X)

Nocardia, *Staphylococcus*, *Streptococcus*, *Proteus*, *Pseudomonas*, and *Escherichia coli*.[5]

Mandibular osteomyelitis is not uncommon as a cause of morbidity in pet and wild hedgehogs and may occur secondary to periodontitis, but there are few studies confirming the etiology of these lesions.[6,7,10] In mortality studies on European hedgehogs (*Erinaceus europaeus*), mandibular abscesses and botryomycosis were detected in 23% of evaluated animals but these lesions were reportedly confined to the submandibular soft tissues, and they were not evaluated microbiologically.[10]

The lesion in this hedgehog has a similar appearance to "lumpy jaw" resulting from *Actinomyces bovis* infections in cattle, and a similar lesion has been described in a captive African pygmy hedgehog infected with *Actinomyces naeslundii*.[7,8] Like the reported case, there was involvement of the draining lymph node and the lung in this hedgehog. However, the bacterium in the submitted case was Gram-negative and pure growth of *Neisseria animaloris* was isolated from the lesion.

Neisseria animaloris is a common inhabitant of the oral cavity of animals (particularly cats and dogs) and may cause systemic infections in humans and animals, often as a result of a bite wound.[2,3,4] These infections can result in localized or systemic pyogranulomatous lesions which exhibit Splendore-Hoeppli reaction around the Gram-negative diplococci.[2,3] Given the zoonotic potential of this bacterium, it would be interesting to know if this organism is part of the normal oral microbiome of the African pygmy hedgehog.[3,4] If so, this may add to the growing list of known zoonotic bacterial pathogens potentially carried by captive and wild hedgehogs, which already includes *Leptospira* spp., *Salmonella* spp., *Mycobacterium* spp, methicillin-resistant *Staphylococcus aureus*, and *Streptococcus* spp.[9]

While the oral lesions in this case were considered significant, cyanosis during anesthesia and the subsequent death of this patient was most likely due to heart failure resulting from cardiomyopathy.

Contributing Institution:
Atlantic Veterinary College
University of Prince Edward Island
Department of Pathology and Microbiology
https://www.upei.ca/avc/pathology-and-microbiology

JPC Diagnoses:
1. Lymph node: Lymphadenitis, pyogranulomatous, diffuse, marked, with Splendore-Hoeppli material and colonies of cocci.
2. Mandible: Osteomyelitis, pyogranulomatous, diffuse, marked, with pathologic fracture, ulcerative and lymphoplasmacytic gingivitis, Splendore-Hoeppli material, and colonies of cocci.

JPC Comment:
The contributor provides an excellent case of mandibular osteomyelitis in an African hedgehog which highlights to tendency of

this species to develop pathology in the oral cavity. African hedgehogs are short-lived exotic pets with a life expectancy of 4 to 6 years and are considered geriatric at 3-5 years of age.[6] They are particularly prone to neoplasia, even in early age, and are susceptible to age-related cardiovascular, renal, and periodontal disease.[6]

Hedghogs are particularly prone to dental disease, including gingivitis, dental calculus, periodontitis, and tooth loss.[6] Periodontal disease may be preventable with proper diet, with dry kibble and raw fruits and vegetables thought to promote periodontal health versus moist or canned foods.[6] Hedgehog oral disease of any variety may be accompanied by florid gingival hyperplasia that can be difficult to distinguish from neoplasia grossly. Clinical signs include reduced food intake or changes in food preferences, anorexia, weight loss, dysphagia, drooling, hemorrhage, and halitosis.[6] Gross findings may include gingival swelling and inflammation, loose or missing teeth, swelling of the face, and abnormal facial bone positioning.[6]

Oral squamous cell carcinoma (SCC) is the most common tumor of the African hedgehog digestive system and is reported to be the most common overall hedgehog neoplasia.[6] Oral SCC has been reported in hedgehogs as young as 1 year old and as old as 6 years. Diagnosis can be difficult without histology as the cytologic appearance of oral SCC needle aspirates can look very similar to early stage periodontal disease, and distinguishing the two conditions on cytology alone is often impossible.[6] Surgical excision of oral tumors, including SCC, is often incomplete and oral tumors frequently recur; prognosis is therefore poor for oral neoplasia, making differentiating between oral neoplasia and periodontal disease, which often responds well to targeted antimicrobial therapy, of prime prognostic importance.[6]

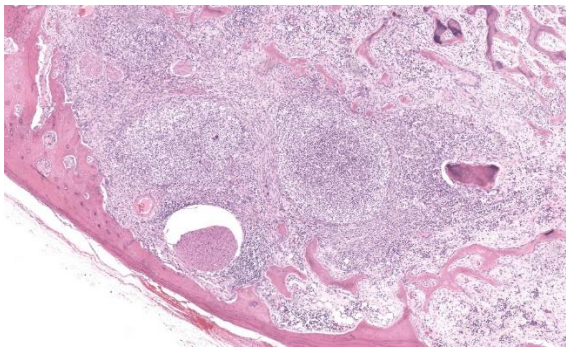

Figure 3-5. Mandible, hedgehog. There is marked resorption of medullary and, to a lesser extent, cortical bone with pyogranulomatous inflammation. (HE, 57X)

The aged hedgehog in this case read the textbook, with severe oral and cardiovascular disease at the time of death. Conference participants noted the large peripheral nerve surrounded by the intense inflammatory milieu and spared a thought for what must have been an extremely painful condition for this hedgie. The moderator encouraged participants to evaluate bone at the subgross level where symmetry is most easily assessed. Subgross evaluation in this case reveals an extremely unsymmetrical mandible, which is an initial indication of bone involvement. The moderator also noted that polarization at subgross magnification can reveal which bone is well-organized parent bone and which is reactive. Subgross evaluation also reveals impressive gingival ulceration, which presumably provided an excellent portal for *Neisseria animaloris* to enter the deeper tissue of the oral cavity and provoke the incredible inflammatory response captured on this delightful slide.

Conference participants noted the somewhat unexpected abundance of eosinophils in the inflammatory infiltrate, which some partipants noted was an occasional feature of inflammation in hedgehogs. This lead to a brief discussion of eosinophilic leukemia, a myelogenous leukemia of hedgehogs that appears in middle age and carries a grave prognosis.

Participants felt that the morphologic diagnosis should include elements critical to the pathogenesis, which in this case is presumed to begin with ulcerative gingivitis, bacterial invasion, and pyogranulomatous inflammation. Participants also interpreted the appearance of the submucosal bone fragments under polarized light as pathologic fracture, which all thought warranted mention in the morphologic diagnosis.

References:

1. Chaprazov T, Dimitrov R, Yovcheva KS, Uzunova K. Oral and dental disorders in pet hedgehogs. *Turk J Vet Anim Sci*. 2014; 38(1):1-6.
2. Foster G, Whatmore AM, Dagleish MP, et al. Forensic microbiology reveals that *Neisseria animaloris* infections in harbour porpoises follow traumatic injuries by grey seals. *Sci Rep* 2019;9(1):14338.
3. Helmig KC, Anderson MS, Byrd TF, Aubin-Lemay C, Moneim MS. A rare case of Neisseria animaloris hand infection and associated nonhealing wound. *J Hand Surg Glob Online* 2020;2(2):113-115.
4. Heydecke A, Andersson B, Holmdahl T, Melhus A. Human wound infections caused by Neisseria animaloris and Neisseria zoodegmatis, former CDC Group EF-4a and EF-4b. *Infect Ecol Epidemiol*. 2013;3:1-5.
5. Hussein MR. Mucocutaenous Splendore-Hoeppli phenomenon. *J Cutan Pathol* 2008;35(11):979-988.
6. Johnson DH. Geriatric Hedgehogs. *Vet Clin North Am Exot Anim Pract*. 2020; 23(3):615-637.
7. Martinez LS, Juan-Salles C, Cucchi-Stefanoni K, Garner MM. Actinomyces naeslundii infection in an African hedgehog (Atelerix albiventris) with mandibular osteomyelitis and cellulitis. *Vet Rec* 2005; 157(15):450-451.
8. Olson EJ, Dykstra JA, Armstrong AR, Carlson CS. Bones, joints, tendons and ligaments. In: Zachary JF, ed. *Pathologic Basis of Veterinary Disease*. 7th ed. Elsevier; 2022:1037-1490.
9. Ruszkowski JJ, Hetman M, Turlewicz-Podbielska H, Pomorska-Mól M. Hedgehogs as a potential source of zoonotic pathogens-a review and an update of knowledge. *Animals (Basel)* 2021;11(6): 1754.
10. Zacharopoulou M, Guillaume E, Coupez G, Bleuart C, Le Loc'h G, Gaide N. Causes of mortality and pathological findings in European hedgehogs (Erinaceus europaeus) admitted to a wildlife care centre in southwestern France from 2019 to 2020. *J Comp Pathol*. 2022;190:19-29.

CASE IV:

Signalment:
3-month old male Sprague Dawley rat (*Rattus norvegicus*).

History:
The mother of this rat was injected with valproic acid at 12 days gestation (animal model of autism). All of the pups in that litter had kinks in their tails.

Gross Pathology:
A 12 cm amputated tail was submitted in formalin. Three centimeters proximal to the tip, the tail is bent at an angle of approximately 270 degrees with a subtler bend 1 cm from the tip.

Microscopic Description:
Examined are three longitudinal sections of the tail (skin removed). One section is composed mostly of muscle. In the other sections, two normal caudal vertebrae flank a malformed vertebra. In the middle section, the linear arrangement of the caudal vertebra is

Figure 4-1. Tail, rat. This is a littermate of the rat submitted for examination. The tail has two angular deformities. (*Photo courtesy of*: Virginia-Maryland College of Veterinary Medicine, https://vetmed.vt.edu/)

distorted by a small, eccentric, round to wedge-shaped bone containing a curved physis with somewhat disordered maturation of chondrocytes. The direction of chondrocyte maturation is oriented away from the midline of the tail. Medial to the physis is a layer of woven bone that is thicker at the periphery and thinner in the middle (osseous endplate) which blends with a layer of cartilage (cartilaginous end plate). Connecting to the periphery of the osseous endplate are laminar bands of collagen and fibroblasts which also connect to the
adjacent vertebral body osseous endplates (annulus fibrosus). The annulus fibrosus also connects the osseous endplates of the cranial and caudal vertebrae and surrounds two foci of chondrocytes, amorphous amphophilic material (proteoglycans), and large vacuolated cells (nucleus pulposus cells). These two foci are separated by a band of the annulus fibrosus which connects to the center of the cartilaginous endplate of the abnormal vertebra. The changes in the other section are similar, except there are bilateral abnormal vertebral segments which are connected to one of the adjacent vertebrae by woven bone and separated from the other adjacent vertebra by a band of annulus fibrosus. The two bony segments are separated by a central pocket of nucleus pulposus cells and proteoglycans. The physis of one of the adjacent vertebrae blends with the central nucleus pulposus, bisecting the osseous and cartilaginous end plates.

Contributor's Morphologic Diagnosis:
Caudal vertebrae: Multifocal vertebral malformations (hemivertebra and butterfly vertebra).

Contributor's Comment:
The vertebrate tail is made up of between 2 (Manx cat) and 49 (long-tailed pangolin) caudal (or coccygeal) vertebrae. In tailless animals, the greatly reduced caudal vertebrae are fused to form the coccyx. The cranial-most caudal vertebrae have a well-developed vertebral arch with spinous and transverse processes. The vertebral canal contains the filium terminale and a variable number of caudal spinal nerve roots which exit the canal through the corresponding intervertebral foramina. The vertebrae toward the tip of the tail have a much simpler, cylindrical shape.

The intervertebral disc forms a fibrocartilaginous joint between adjacent caudal vertebrae. The intervertebral disc consists of a central nucleus pulposus surrounded by a tough annulus fibrosus. The nucleus pulposus is composed of water, type II collagen, proteoglycans, and nucleus pulposus cells. The large, vacuolated nucleus pulposus cells of young animals, similar to the notochordal cells (physaliferous cells) from which the disc is derived, are replaced by smaller, chondrocyte-like cells in adults.[2] The annulus fibrosus is composed of type I collagen and

fibrocartilage arranged in laminae that attach to the osseous endplates of two adjacent vertebral bodies and provide resistance to tensile forces on the spine. The osseous endplate has a strong, solid, peripheral epiphyseal rim and a central portion made of thin, porous bone.[11] The intervertebral disc is separated from the cortical bone of the vertebral endplate by a thin layer of hyaline cartilage, type II collagen, and proteoglycans called the cartilaginous endplate.[8] The dorsal and ventral boundaries of the intervertebral disc are the dorsal and ventral longitudinal ligaments.

Tail kinks can be caused by fracture with malunion or by congenital malformations. Congenital malformations can be further divided into genetic diseases and teratogenic effects during development of the vertebral column. Genetic tail kinks are common in dogs and cats, especially in dog breeds such as Bulldogs, Boston Terriers, and Pugs.[3] Embryologic development of the vertebral column begins with segmentation of the paraxial mesoderm on each side of the neural tube into somites. Next, each somite is divided into a ventral sclerotome, the precursor for the vertebrae, and a dorsal dermomyotome, which develops into the skeletal muscle and dermis of the back. The ventral sclerotome subunits fuse in cranial-caudal pairs as well as across the midline to form the vertebral body and the vertebral arch which encloses the developing spinal cord. Development and chondrification of the vertebrae precedes in an cranial to caudal direction, while the progression of ossification is less orderly.[1]

Congenital vertebral malformations have been classified into either failure of segmentation, where the mesoderm does not properly divide into somites, leading to the appearance of vertebral fusion, or failure of vertebral formation, where elements of an individual vertebra do not form, leading to abnormally shaped vertebrae (wedge, hemi-, or butterfly

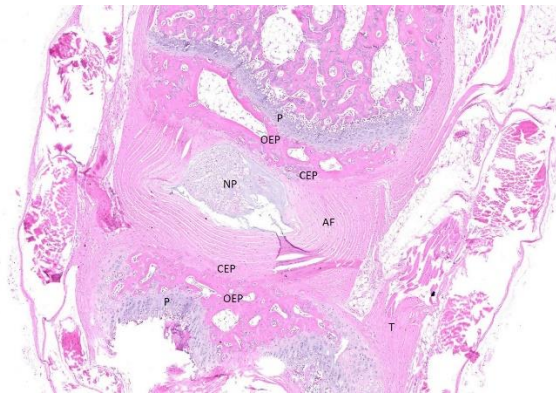

Figure 4-2. Tail, rat. Normal caudal vertebrae and intervertebral disc. (P = physis; OEP = osseous endplate; CEP = cartilaginous endplate; AF = annulus fibrosus; NP = nucleus pulposus; T = tendon.)

vertebrae). Either type of deformity can lead to scoliosis (lateral deviation of the vertebral column) or kyphosis (dorsoventral deviation of the vertebral column). These defects have been classified based on which part (dorsal, lateral, or median) of the developing vertebra is deficient and whether the deficiency is complete (aplasia; hemivertebra) or incomplete (hypoplasia; wedge vertebra).[3] A butterfly vertebra is caused by failure of the two lateral portions of the sclerotome to fuse across midline.[5] These malformations can be further classified as segmented (separated from the adjacent vertebrae by intervertebral discs), nonsegmented (attached to the adjacent vertebrae by bone), or semi-segmented (attached to one adjacent vertebra by bone and separated from the other by an intervertebral disc). A typical vertebra has three centers of ossification (one in the body and one on each side of the arch) and four physes (one at each endplate and one on each side where the vertebral arch joins the body).[1] Since most caudal vertebrae lack arches, they have just the caudal and cranial physes. Based on the single longitudinal sections of this rat's tail, the defects are consistent with a segmented hemivertebra and a butterfly vertebra; however, two view radiographs, MRI, or

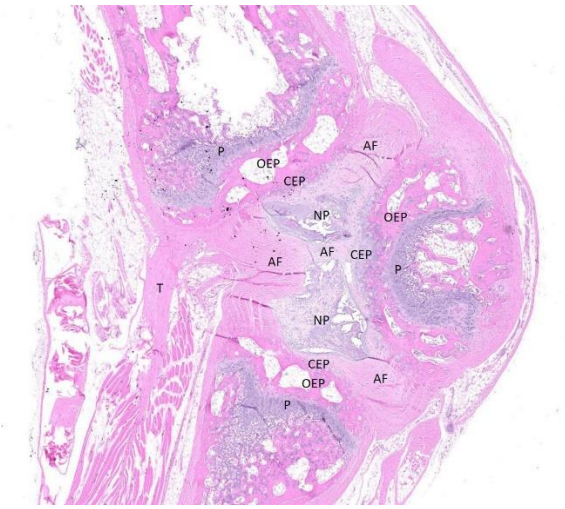

Figure 4-3. Tail, rat. Hemivertebra. (P = physis; OEP = osseous endplate; CEP = cartilaginous endplate; AF = annulus fibrosus; NP = nucleus pulposus; T = tendon.)

serial sections would be needed to confirm the diagnosis.

Valproic acid is a short chain fatty acid used to treat epilepsy, migraine, and bipolar disorder. Actions of the drug include modulation of neurotransmission and epigenetic regulation of gene expression. In humans, prenatal exposure to valproic acid has been associated with an increased risk of autism spectrum disorders, as well as a variety of congenital malformations.[9] Rodents exposed to valproic acid in utero are used as an animal model of autism.[6]

Although the exact pathogenesis is not known, proposed mechanisms of action for valproic acid-induced malformations include intracellular acidification, changes in lipid, zinc, folate, or retinoid metabolism, and alterations in developmental gene expression.[9]

Contributing Institution:
Virginia-Maryland College of Veterinary Medicine
Blacksburg, VA
https://vetmed.vt.edu/

JPC Diagnosis:
Tail: Vertebral malformation, multisegmental, with hemi- and butterfly vertebra formation.

JPC Comment:
As the contributor notes, the development of the vertebral column is complex, with the vertebral bodies forming from proliferating and migrating sclerotomes that surround the embryonic notochord.[4] This complex process is orchestrated via spatially and temporally discrete gene expression and cell signaling casacades that shape and position each vertebra in the proper cranial-caudal orientation.[4]

Even the most casual of anatomist will notice the segmental nature of the vertebrate spine and the different vertebral morphologies displayed at different levels of the spinal column. These patterning differences develop under the influence of *Hox* genes, which have been extensively studied in mice.[7] Researchers have painstakingly mapped the *Hox* genes to particular functions, finding, for instance, that *Hox10* expression deactivates the rib-forming program in non-thoracic ribs and, when expression is experimentally blocked, lumbar vertebrae grow ribs.[7] In snakes, *Hox10* genes have lost the ability to block rib formation, leading to rib growth down the entire length of the animal.[7]

Sonic hedgehog (Hh) signaling is another critical player in embryonic patterning and development. While Hh signaling is broadly important in the development of the face, skull, limbs, and axial skeleton, in the vertebral column, Hh signaling from the notochord is crucial in initial somite formation and the development and maintenance of intervertebral discs in development; in post-natal life, when the notochord becomes the nucleus pulposus, Hh signaling is key for the maintenance of intervertebral disc integrity.[4,10]

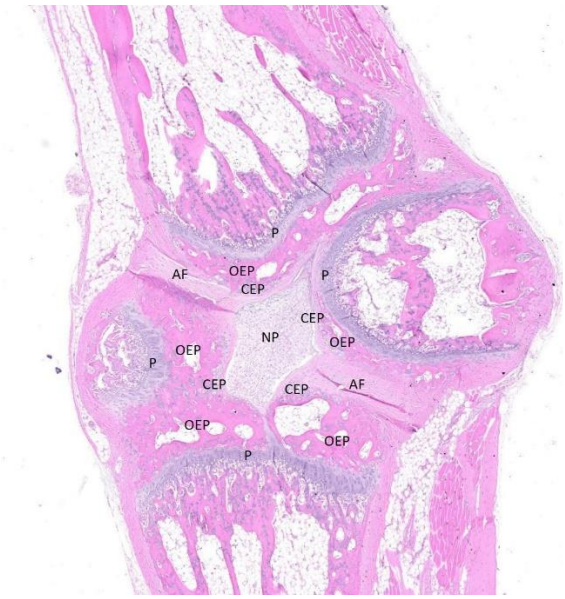

Figure 4-4. Tail, rat. Butterfly vertebra (C). (P = physis; OEP = osseous endplate; CEP = cartilaginous endplate; AF = annulus fibrosus; NP = nucleus pulposus; T = tendon.)

These two patterning pathways are just two among many, and any missteps in this complex developmental dance produce congenital defects in the formed vertebra. This case nicely demonstrates, and the contributor nicely describes, two such morphologic defects, but there are many others. In humans, aberrant expression of *Hox* and/or Hh signalling have been associated with a syndrome clunkily named VACTERL, for vertebral anomalies (V), anal atresia (A), cardiac malformation (C), tracheoesophageal fistula (TE), renal dysplasia (R), and limb abnormalities (L).[4] This clinical syndrome is diagnosed when a patient has three or more of the listed abnormalities, and among the listed defects, vertebral abnormalities are found in up to 95% of patients.[4] Perhaps a more familiar consequence of vertebral developmental defects is spina bifida, a congenital anomaly in which the vertebral arch fails to fuse. While the underlying pathogeneses have not been fully worked out, there is mounting evidence that abnormal *Hox* gene expression is the root cause of a number of neural tube defects, including anencephaly, spina bifida, hydrocephaly, and encephalocele.[12]

The complications of developmental anatomy were well illustrated on the histologic slide examined in conference. The moderator began by noting that the first location clue in this challenging slide is the prominent nucleus pulposus surrounded by the concentric rings of the annulus fibrosis. These features definitively localize the tissue to the vertebral column. In a rat, the nucleus pulposus should be a discoid shape and the affected vertebral joints in section feature very distorted architecture, indicating that the lesion is architectural and, therefore, likely developmental. The moderator agreed with the contributor that the exact nature of the vertebral malformations would be best assessed via advanced imaging, but that hemivertebra and butterfly butterfly formation were most likely based on the histologic features.

A common thread in this week's conference discussion was the perceived difficulty of evaluating bone pathology. In her closing thoughts, the moderator challenged that assertion with the view that bone responds to injury in a stereotypic manner. The key to understanding bone pathology, then, is understanding how bone behaves normally; once one understands how bone develops and how it undergoes modeling and remodling in response to injury, then the pathology that you see can be essentially reverse engineered to narrow down the universe of potential pathologic insults.

Discussion of the morphologic diagnosis was mercifully straightforward with this case. Participants preferred to call the distribution multisegmental to emphasize that multiple vertebrae were affected, but the contributor's diagnosis was otherwise adopted largely intact.

References:

1. Burbidge HM, Thompson KC, Hodge H. Post natal development of canine caudal cervical vertebrae. *Res Vet Sci*. 1995;59 (1):35-40.
2. Chen S, Fu P, Wu H, Pei M. Meniscus, articular cartilage and nucleus pulposus: a comparative review of cartilage-like tissues in anatomy, development, and function. *Cell Tissue Res*. 2017;370(1):53-70.
3. Gutierrez-Quintana R, Guevar J, Stalin C, Faller K, Yeamans C, Penderis J. A proposed radiographic classification scheme for congenital thoracic vertebral malformations in brachycephalic "screw-tailed" dog breeds. *Vet Radiol Ultrasound*. 2014; 55(6):585-591.
4. Kalamchi L, Valle C. Embryology, Vertebral Column Development. StatPearls Publishing; 2024. Available at https://www.ncbi.nlm.nih.gov/books/NBK549917.
5. Katsuura Y, Kim HJ. Butterfly vertebrae: a systematic review of the literature and analysis. *Glob Spine J*. 2019;9(6):666-679.
6. Mabunga DFN, Gonzales ELT, Kim J, Kim KC, Shin CY. Exploring the validity of valproic acid animal model of autism. *Exp Neurobiol*. 2015;24(4):285-300.
7. Mallo M, Wellik DM, Deschamps J. Hox genes and regional patterning of the vertebrate body plan. *Dev Biol* 2010;344(1): 7-15.
8. Moon SM, Yoder JH, Wright AC, Smith LJ, Vresilovic EJ, Elliott DM. Evaluation of intervertebral disc cartilaginous endplate structure using magnetic resonance imaging. *Eur Spine J*. 2013;22(8):1820-1828.
9. Padmanabhan R, Abdulrazzaq YM, Bastaki SMA. Valproic acid-induced congenital malformations: Clinical and experimental observations. *Congenit Anom*. 2000;40(4):259-268.
10. Rajesh D, Dahia CL. Role of sonic hedgehog signaling pathway in intervertebral disc formation and maintenance. *Curr Mol Biol Rep*. 2018;4(4):173-179.
11. Wang Y, Battié MC, Videman T. A morphological study of lumbar vertebral endplates: radiographic, visual and digital measurements. *Eur Spine J*. 2012;21(11): 2316-2323.
12. Yu J, Wang L, Pei P, et al. Reduced H2K27me3 leads to abrnomal *Hox* gene expression in neural tube defects. *Epigenetics Chromatin*. 2019;12:76.

WSC 2023-2024
Conference 23 Self-Assessment

1. Feline vertebral angiomatosis is considered to be a neoplasm. True or false?
    a. True
    b. False

2. Lesions of feline vertebral angiomatosis are most commonly seen in which of the following?
    a. Cervical vertebrae
    b. Thoracic vertebrae
    c. Lumbar vertebrae
    d. Caudal vertebrae

3. Synovial chondromatosis is most commonly seen in which of the following raptor species?
    a. Bald eagles
    b. Red-tailed hawks
    c. Great horned owls
    d. Peregrine falcons

4. True or false? Hemivertebrae arise as a lack of segmentation.
    a. True
    b. False

5. True or false? Neisseria animaloris is a common oral pathogen of the dog and cat.
    a. True
    b. False

Joint Pathology Center
Veterinary Pathology Services

WEDNESDAY SLIDE CONFERENCE 2023-2024

Conference #24 24 April 2024

CASE I:

Signalment:
28-year-old male American Flamingo (*Phoenicopterus ruber*).

History:
This flamingo had a 1-year history of progressive weight loss and a 10-year history of progressive bilateral pododermatitis. Two days prior to death, lethargy and separation from the flock were noted and the flamingo was treated with fluids, Excede, and meloxicam.

Gross Pathology:
On gross examination, the subcutaneous, coelomic, and pericardial fat stores were significantly reduced (BCS 2/5). Bilaterally, there were round, raised, proliferative nodules measuring 4 cm and 2.5 cm in diameter on the right and left metatarsal pads, respectively. There was a small amount of clear to white mucoid material in the lumen of the glottis. Multifocal, pale gray to brown, flat, circular regions measuring 1-5 mm in diameter were present on the tracheal mucosa. There were white to orange, speckled, granular deposits overlying the pericardium at the level of the right ventricle. Within the ventriculus, there was a 3 mm red, circular, area under the koilin membrane. Throughout all lobes of the liver, there were regions of mild pallor. Both kidneys were markedly enlarged, friable, and

Figure 1-1. Feet, flamingo. Flamingo feet, bilateral, January 2013. The plantar aspect of the metatarsal pad of each foot is focally expanded by round, firm tissue with central ulceration ("bumble"). (*Photo courtesy of:* The Ohio State University College of Veterinary Medicine, Department of Veterinary Biosciences, https://vet.osu.edu/biosciences)

mottled orange to yellow. Within the right stifle, there was a small amount of white, soft, chalky material.

Laboratory Results:
Severely elevated uric acid and heterophilia were present on serum biochemistry panel and complete blood count. Computed tomography revealed bilaterally enlarged kidneys.

Microscopic Description:
Kidney: Multifocally and randomly expanding and disrupting the interstitium and replacing tubules are foci of brightly eosinophilic cellular and karyorrhectic or pyknotic nuclear debris (necrosis) surrounded by a thin rim of

Figure 1-2. Flamingo feet, bilateral, April 2021. The plantar aspect of the metatarsal pad of each foot is focally expanded by a round to multilobular, firm, mass ("bumble") with central ulceration and accumulation of inspissated material in a central ulceration with formation of numerous exophytic projections of tissue with interspersed deep fissures. Compared to Figure 1-1, masses are approximately 2-3 times larger. (*Photo courtesy of:* The Ohio State University College of Veterinary Medicine, Department of Veterinary Biosciences, https://vet.osu.edu/biosciences)

lymphocytes, plasma cells, and histiocytes. These foci measure approximately 150-250 µm and occasionally contain clear clefts within central areas of necrosis (presumed washed-out uric acid crystals). Moderate numbers of red blood cells extend throughout the adjacent interstitium (hemorrhage). Diffusely and globally, glomerular tufts are expanded by variable amounts of acellular, homogenous, eosinophilic, glassy material (amyloid) that compresses capillaries and distorts glomerular architecture. Glomerular tufts are hypocellular with occasional karyorrhectic or pyknotic nuclear debris (necrosis) and frequently adhere to Bowman's capsule (synechiae). Tubules exhibit one or more of the following changes: swollen epithelium with microvacuolated cytoplasm and large, round vesiculated nuclei (degeneration); hypereosinophilia with pyknotic nuclei (necrosis); increased basophilia with crowded epithelial cells containing hyperchromatic nuclei (regeneration); round, crystalline, deeply basophilic deposits within tubular epithelium (mineral); marked ectasia with flattened, attenuated epithelium and intraluminal eosinophilic to amphophilic proteinaceous fluid or droplets. Multifocally, tubular lumina contain sloughed, necrotic epithelial cells admixed with cellular debris (cellular casts); the basement membranes of affected tubules are often disrupted (tubulorrhexis). Frequently, eosinophilic, homogenous, acellular material (amyloid) expands tubular basement membranes and forms broad cuffs around affected tubules. Multifocally, the tunica media of renal arteries and arterioles is expanded by lightly basophilic to amphophilic amorphous material (amyloid). Mild numbers of lymphocytes and plasma cells expand the renal interstitium.

Great vessels: There are no significant microscopic findings in the great vessels.

Congo Red and Von Kossa histochemical stains: Within glomeruli, tubular basement membranes, and walls of renal arteries and arterioles, there is congophilic pink-orange acellular material that exhibits strong apple-green birefringence when viewed under polarized light. Mineral deposits within renal tubules exhibit strong staining for calcium.

Contributor's Morphologic Diagnosis:

1. Kidney: Diffuse global glomerular amyloidosis with synechiae; moderate to marked renal tubular amyloidosis with degeneration, necrosis, loss, and regeneration with multifocal mineralization; and moderate, chronic, multifocal arteriolar amyloidosis.
2. Kidney: Multifocal urate tophi (presumed) with marked, chronic, multifocal

histiocytic and lymphoplasmacytic interstitial nephritis.
3. Kidney: Moderate to marked multifocal tubular ectasia with cellular casts.

Contributor's Comment:
This is a case of confirmed systemic amyloidosis and visceral gout in a flamingo. Amyloidosis in this case is presumably secondary to chronic pododermatitis, as this association has been well-documented in flamingos with this condition. Amyloidosis, pododermatitis, and gout are all reviewed below.

Amyloidosis: Systemic AA (reactive) amyloidosis is an important cause of death in domestic and captive wild birds. AA amyloid is derived from serum amyloid A (SAA), an acute phase lipoprotein produced by hepatocytes. Chronic inflammatory diseases or neoplastic conditions can lead to excessive synthesis of SAA and protein misfolding resulting in amyloidosis.[2,8,11] Several cytokines can induce hepatic synthesis of SAA including IL-1, IL-6, and TNF-α. SAA typically has an immuno-modulatory role in the inhibition of fever caused by IL-1β and TNF-α as well as the inhibition of platelet aggregation, suppression of thromboxane synthesis, and serotonin release from platelets.[8] While an increased pool of precursor protein is necessary for the development of amyloidosis, certain amino acid substitutions may favor amyloidogenicity and give rise to unstable intermediate proteins that can easily reshape into fibrils.[8]

Two types of amyloidosis have been identified in birds – AA amyloidosis and cerebral Aβ amyloidosis accompanied by cerebral amyloid angiopathy. Avian AA amyloidosis commonly affects waterfowl, small passerine birds, and chickens. Aβ amyloidosis has been reported in great spotted woodpeckers and eagles but not in flamingos.[11]

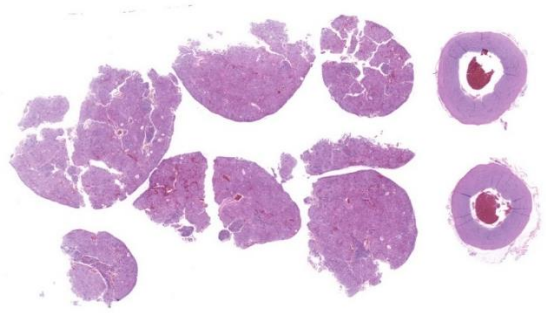

Figure 1-3. Kidney, flamingo. Multiple sections of kidney and sections of artery (right) are submitted for examination. (HE, 4X)

AA amyloid deposition occurs most frequently in the liver, spleen, kidneys, and small intestine with the proventriculus, large intestine, heart, gonads, and endocrine organs being less affected.[8] While lung, skin, and brain are rarely affected, vascular AA amyloid deposition has been reported in the central and peripheral nervous systems of flamingos.[11]

Grossly, affected organs are swollen, pale, and have a waxy consistency. The presence of amyloid can occasionally be demonstrated at the time of necropsy by applying Lugol's iodine to the cut surface and rinsing with sulfuric acid, rendering amyloid deposits dark brown or black. Amyloid accumulation results in organ dysfunction and may lead to organ rupture due to disruption of tissues by the abnormal protein. Affected tissues are typically friable, and hepatic fractures with subsequent exsanguination are a common cause of acute death.[1]

Histologically, amyloid is acellular, homogenous, eosinophilic material that commonly accumulates in hepatic sinusoids, renal glomeruli, perifollicular areas of the spleen, lamina propria of the intestines, and vascular walls.[1] The histologic diagnosis must be confirmed with Congo Red staining where amyloid stains peach or pink-orange and exhibits green birefringence under polarized light. AA amyloid can be confirmed via

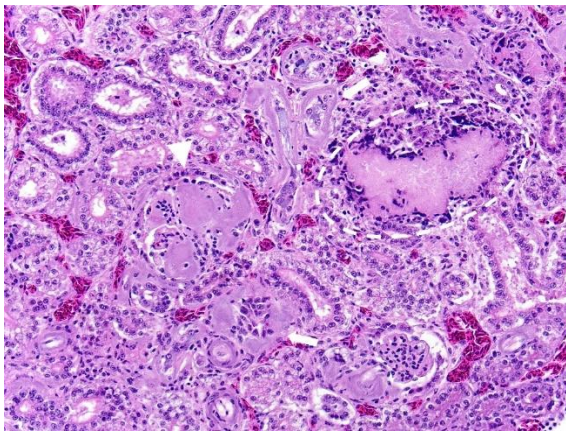

Figure 1-4. Kidney, flamingo. Diffusely and globally, glomerular tufts are expanded by homogenous, acellular, eosinophilic, glassy material (amyloid). (HE, 400X) (*Photo courtesy of:* The Ohio State University College of Veterinary Medicine, Department of Veterinary Biosciences, https://vet.osu.edu/biosciences)

elimination of Congo Red staining affinity by oxidation of tissue sections in potassium permanganate. After staining with thioflavine-T, amyloid exhibits bright yellow fluorescence.[2] Amino acid sequencing and immunohistochemical techniques utilizing monoclonal and polyclonal anti-AA antibodies directed against amyloid fibril proteins can aid in the identification of amyloid.[15] On electron microscopy, amyloid is characterized by nonbranching 7-10 nm-diameter fibrils. [2]

Experimentally, avian amyloidosis can be induced by repeated inflammatory stimuli, such as inoculation with bacterial extracts or vaccination with oil-emulsified bacterins. Thus, antigenic stimulation with bacteria is considered to promote the development of avian AA amyloidosis. In addition, recent studies have suggested that avian amyloidosis is transmissible. Horizontal transmission of amyloidosis via ingestion of amyloid-contaminated feed or feces is suspected to occur among avian species.[10]

Chronic inflammation associated with pododermatitis has been linked to systemic amyloidosis.[10] In this case, systemic amyloidosis is attributed to the patient's history of bilateral pododermatitis. Amyloid deposition was confirmed via Congo Red staining in the kidney, spleen, and pancreas. Arterial mineralization was confirmed in the spleen via Von Kossa staining. Despite the multifocal medial mineralization noted in small blood vessels, there was no evidence of atherosclerosis in the great vessels. It is possible that some of the gross lesions noted in the heart and GI tract at the time of postmortem exam represent foci of mineralization and/or amyloidosis. The grossly described white, chalky material in the stifle may be consistent with articular gout. However, no joint tissue was provided for confirmatory histopathological examination.

Pododermatitis: Pododermatitis (also known as bumblefoot) has only been documented in captive birds, and influencing factors include flooring in water ponds, prolonged periods indoors, environmental temperatures, age, weight, and potentially dietary zinc availability.[12,13,14] Foot lesions are classified as inflammatory or proliferative with inflammatory lesions being more common in younger birds and proliferative lesions more common in older birds.[1] Gross lesions include individual to coalescing nodules of thickened and hyperkeratotic epidermis with fissures, papillarybgrowths, erosions or ulcers overlying granulation tissue and inflammation. Early lesions include heterophilic dermatitis, hydropic epithelial degeneration, hyperplasia, serocellular crust formation, and pustules. Chronic lesions feature neovascularization, fibrosis, and infiltration by lymphocytes and macrophages.

Secondary bacterial infections with organisms, such as *Fusophorum* spp. and *Staphylococcus aureus* are common and can exacerbate tissue damage and inflammation.[4] Fungal and bacterial agents have not been consistently found and no virus has been isolated

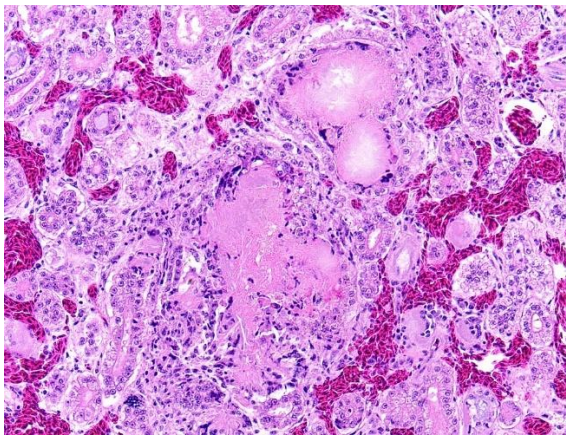

Figure 1-5. Kidney, flamingo. Multifocally, there is brightly eosinophilic cellular and karyorrhectic or pyknotic nuclear debris expanding and disrupting renal tubules and interstitium surrounded by mild to moderate numbers of histiocytes, lymphocytes, and plasma cells. These foci occasionally contain clear clefts (presumed washed-out uric acid crystals). (HE, 400X) (*Photo courtesy of:* The Ohio State University College of Veterinary Medicine, Department of Veterinary Biosciences, https://vet.osu.edu/biosciences)

in pododermatitis lesions.[12] Poxviral infection is the major differential for pododermatitis lesions.

Gout: Gout occurs in birds, reptiles, great apes, and humans due to the lack of the enzyme uricase, which oxidizes uric acid to allantoin. Uric acid in these species is normally eliminated through a combination of glomerular filtration, reabsorption, and secretion. Urate deposition (gout) usually occurs due to impaired excretion by the kidneys or overproduction of uric acid leading to hyperuricemia and precipitation of monosodium urate crystals (tophi) on visceral and articular surfaces. Comparatively, Dalmatian dogs also cannot oxidize uric acid to allantoin due to a defect in uricase, predisposing them to urate urolithiasis. This defect is an inherited autosomal recessive trait and linked to a mutation in *SLC2A9*, which encodes for a glucose transporter.[2,7]

Gout in birds occurs in acute (visceral) and chronic (articular) forms, which differ in frequency, age of onset, sex predilection, gross and microscopic lesions, pathogenesis and causes.[3] Lesions may appear grossly as white foci, streaks, or sheets on serosal surfaces and viscera. Articular forms of gout include chalky, white deposits in and around joints. Urate crystals are often leached out during tissue processing and may be detected as remnant, wispy, basophilic, "ghost" crystals. Thus, tissues fixed in alcohol rather than formalin may improve detection. Histologically, fine, radiating acicular clefts may be present in the absence of inflammation or associated with histiocytic, granulomatous, or mixed inflammation. Gout should be distinguished from pseudogout, which is composed of nonurate, calcium pyrophosphate crystals.[4]

In birds, acute (visceral) urate deposition is more common than chronic (articular) urate deposition. Acute urate deposition may occur at any age with renal lesions involving white, chalky precipitates. Visceral organs including liver, myocardium, spleen, and serosal surfaces are commonly affected, whereas soft tissues around the joints may or may not be involved. Microscopically, there is an inflammatory reaction around tophi in the kidney and viscera with usually no inflammation in the synovium. Acute urate deposition is typically due to renal failure with causes including dehydration, nephrotoxicity, nephrotropic infectious agents, vitamin A deficiency, urolithiasis, neoplasia, or immune-mediated glomerulonephritis.[3] Avian astroviruses have been identified as causes of visceral gout in the chicken, duckling, and gosling.[9]

In contrast, chronic urate deposition typically occurs in mature birds with the kidney being unaffected. Soft tissues other than synovium are rarely involved. Joints of the legs, wing, spine, and mandible may be affected. Microscopically, granulomatous inflammation is

present in the synovium. Chronic urate deposition is likely due to a metabolic defect in the secretion of urates by renal tubules. Causes include genetics and a high protein diet.[3]

In this case, it is difficult to determine the sequence of events. Presumably, the pododermatitis and chronic inflammation lead to systemic amyloidosis, which impaired renal function. Dehydration and/or impaired excretion of uric acid by the kidneys could have resulted in subsequent deposition of urates. The presumptive urate tophi in the kidney are correlated with the patient's hyperuricemia and bilaterally enlarged kidneys and consistent with acute (visceral) gout.

Contributing Institution:
The Ohio State University
College of Veterinary Medicine
Department of Veterinary Biosciences
https://vet.osu.edu/biosciences

JPC Diagnosis:
1. Kidney, glomeruli: Amyloidosis, segmental to global, diffuse, marked.
2. Kidney, arteries, and tubular basement membranes: Amyloidosis, diffuse, marked.
3. Kidney, tubules: Urate tophi, multiple.
4. Kidney: Nephritis, interstitial, chronic and lymphocytic, diffuse, mild to moderate.

JPC Comment:
Flamingos and amyloid are a classic combination, and the blessing continue in this case with the addition of visceral gout and a history of pododermatitis. The contributor does an admirable job of summarizing these three components of the flamingo party pack.

Pododermatitis, the presumed antigenic stimulus for the systemic amyloidosis in this case, has been reported in many birds, including raptors, water fowl, penguins, cocaktiels and, of course, flamingos.[12] Varying degrees of

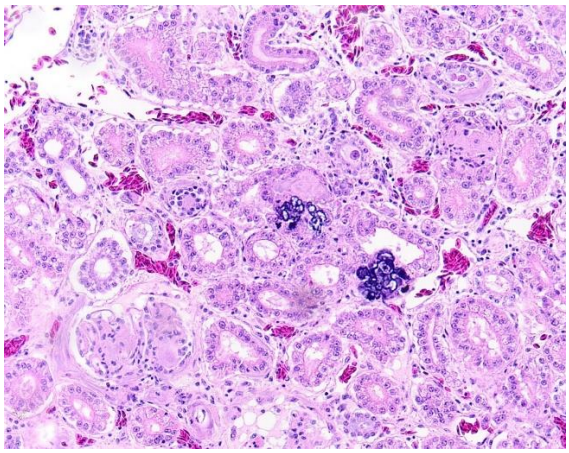

Figure 1-6. Kidney, flamingo. Renal tubules occasionally contain deeply basophilic, crystalline material (mineral). (HE, 400X) (*Photo courtesy of:* The Ohio State University College of Veterinary Medicine, Department of Veterinary Biosciences, https://vet.osu.edu/biosciences)

plantar lesions were found in up to 100% of captive flamingos in one study, and these lesions were the reason for euthanasia or a secondary finding in 95% of flamingos in another.[12] In contrast to classic bumblefoot lesions, which consist of nodules with central ulceration, flamingo pododermatitis often includes varying degrees of hyperkeratosis, fissues of varying depth, nodular lesions with or without ulceration, and papillomatous growths.[12]

A 2015 study attempted to characterized the pododermatitis lesions in a group of 19 flamingos from a zoological collection. Viral PCR assays for papillomaviruses and herpesviruses were performed and were all negative for papillomaviruses; unknown herpesviral DNA was detected in samples from three birds, but the inconsistent presence of the virus made this unlikely to be the sole etiologic agent.

An intriguing result of this study was the identification of *Micrococcus*-like bacteria invading the stratum corneum of juvenile flamingos. The bacteria had zoospores and

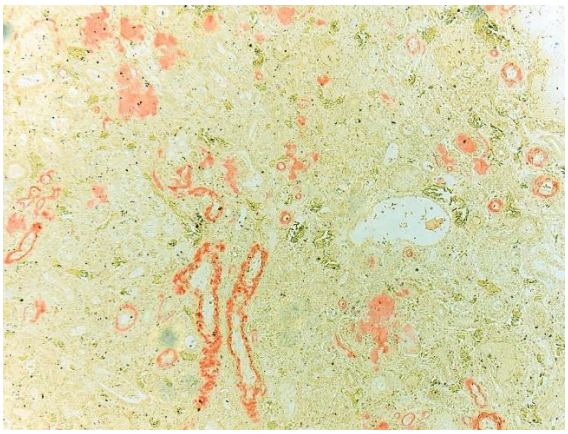

Figure 1-7. Kidney, flamingo. Congophilic, pink-orange, acellular material is present within glomeruli, tubular basement membranes, and the walls of renal arteries and arterioles. When viewed under polarized light (not shown), this material exhibits apple-green birefringence (consistent with amyloid). (*Photo courtesy of:* The Ohio State University College of Veterinary Medicine, Department of Veterinary Biosciences, https://vet.osu.edu/biosciences)

segmented, branching pseudohyphae that were PAS positive and Gram negative.[12] In addition to the invading bacteria, the epidermis was characterized by heterophilic exocytosis, serocellular crust formation, and hydropic degeneration of the keratinocytes, particularly within the stratum granulosum.[12] The subjacent dermis was characterized by accumulations of heterophis and lymphocytes, increased vascular profiles, and increased intercellular matrix. Invasion of *Micrococcus*-like bacteria was present in all examined juvenile flamingos (except two severely autolyzed carcasses), but the bacteria were rare in biopsies taken from adult animals.[12]

The bacteria found in the diseased plantar skin was isolated, subjected to 16S rRNA sequencing, and found to be a novel species within the genus *Arsenicicoccus*, which was subsequently named *A. dermatophilus*.[5] The *Arsenicoccus* genus comprises gram-positive, facultatively anaerobic, catalase-posivie, non-spore forming bacteria that have been isolated both from the environment and from animal sources.[6]

In the 2015 study, histologic lesions were detected in both non-lesional and lesional skin, and the authors suggest that the proliferative lesions of flamingo pododermatisis are a reaction to the inflammation caused by *A. dermatophius*, which is given a leg up by a skin barrier weaked by nutritional deficiencies and inappropriate husbandry practices.[12]

Conference participants were tickled pink with this visual feast of a slide. Leading discussion was this week's moderator, Dr. Neel Aziz, Supervisory Veterinary Medical Director and Head of the Diagnostic Pathology Unit at the Smithsonian National Zoological Park and Conservation Biology Institute. Dr. Aziz began by noting that diseases seen in zoological collections differ in kind and severity than thos seen in the wild, as this case illustrates. As noted by the contributor, pododermatisis is a disease of animal under human care; it is not seen in the wild. And this individual animal, at 28 years old, is an aged animal that has had time to collect more pathology than a typical wild flamingo.

Some conference participants were initially confused by the appearance of the amyloid on this slide which had a more basophilic hue than typica amyloid. Dr. Aziz noted that this amyloid can take on a variety of appearance, appearing more typically eosinophilic or more amphophilic, even within the same animal.

Dr. Aziz discussed the typical appearance of gout, which is characterized by the deposition of needle-like monosodium urate crystals that typically do not survive processing and leave behind only negative, ghost tophi shapes in histologic sections. By contrast, the gout

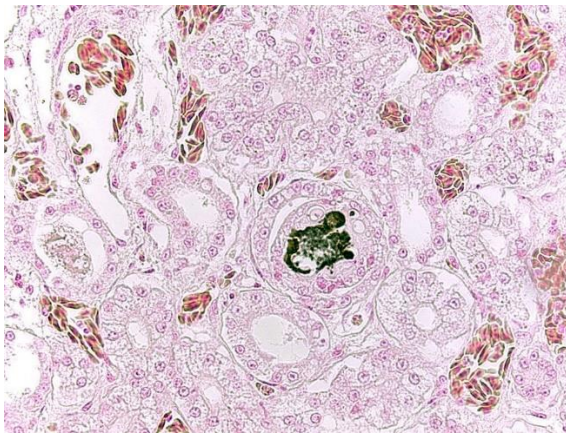

Figure 1-8. Kidney, flamingo. Brown to black granular deposits within renal tubules exhibit positive staining for calcium. (HE, Von Kossa)

appreciated in this case is consisted of amphophilic, amorphous material which the moderator speculated might represent an early stage lesion. Dr. Aziz noted that the terminology of "visceral" and "articular" should be reserved for the reptiles; in birds, "acute" versus "chronic" is the preferred terminology, with acute urate deposition occurring in the viscera of birds and chronic urate deposition occurring in the joints.

In an embarrassment of riches, Dr. Karen Terio, Clinical Professor in the Zoological Pathology Program at the University of Illinois, was also in attendance at conference this week. Dr. Terio noted that it can be overwhelming to describe a slide with this complexity. She recommended organizing such descriptions by pathogenesis and would start a description of this slide with glomerular changes, as the observed tubular changes are likely secondary to the glomerular amyloidosis.

Conference discussion produced a flock of morphologic diagnoses largely in agreement with the contributor. Participants discussed the interstitial nephritis at length and whether it was only in response to the urate deposition or if the inflammation also appeared in areas of the interstitium untouched by tophi. Participants thought it likely that the interstitial nephritis could not be completely explained by the urate deposition and thus preferred to describe it in a separate morphologic diagnosis.

References:

1. Buckles EL. Phoenicopteriformes. In: Terio KA, McAloose D, St. Leger J, eds. *Pathology of Zoo and Wildlife Animals*. Cambridge, MA, Academic Press; 2018: 687-688.
2. Cianciolo RE, Mohr FC. Urinary System. In: Maxie MG, ed. *Jubb, Kennedy, and Palmer's Pathology of Domestic Animals*. 6th ed. Vol 2. Elsevier; 2016:413-415,457.
3. Crespo R, França MS, Fenton H, Shivaprasad HL. Galliformes and Columbiformes. In: Terio KA, McAloose D, St. Leger J, eds. *Pathology of Zoo and Wildlife Animals*. Academic Press; 2018:743-744.
4. Fenton H, McManamon R, Howerth EW. Anseriformes, Ciconiiformes, Charadriiformes, and Gruiformes. In: Terio KA, McAloose D, St. Leger J, eds. *Pathology of Zoo and Wildlife Animals*. Academic Press; 2018:695-696,601-702.
5. Gobeli S, Thomann A, Wyss F, Kuehni-Boghenbor K, Brodard I, Perreten V. Arsenicicoccus dermatophilus sp. nov., a hypha-forming bacterium isolated form the skin of greater flamingos (Phoenicopterus roseus) with pododermatitis. *Int J Syst Evol Microbiol*. 2013;63(11):4046-4051.
6. Jeong JH, Kweon OJ, Kim HR, Kim TH, Ha SM, Lee MK. A novel species of genus *Arsenicoccus* isolated from human blood using whole-genome sequencing. *Ann Lab Med.* 2021;41(3):323-327.
7. Karmi N, Brown EA, Hughes SS, et al. Estimated frequency of the canine hyperuricosia mutation in different dog

breeds. *J Vet Intern Med*. 2010; 24(6):1337-1342.
8. Landman WJM, Gruys E, Gielkens ALJ. Avian amyloidosis. *Avian Pathol*. 1998; 27(5): 437-449.
9. Li L, Sun M, Zhang Y, Liao M. A review of the emerging poultry visceral gout disease linked to avian astrovirus infection. *Int J Mol Sci*. 2022; 23, 10429.
10. Murakami T, Ishiguro N, Higuchi K. Transmission of systemic AA amyloidosis in animals. *Vet Pathol*. 2014;51(2):363-371.
11. Ono A, Nakayama Y, Inoue M, Yanai T, Murakami T. AA amyloid deposition in the central and peripheral nervous systems in flamingos. *Vet Pathol*. 2020;57(5):700-705.
12. Wyss F, Schumacher V, Wenker C, et al. Pododermatitis in captive and free-ranging greater flamingos (Phoenicopterus ros-eus). *Vet Pathol*. 2015;52(6):1235-1242.
13. Wyss F, Wenker C, Hoby S, et al. Factors influencing the onset and progression of pododermatitis in captive flamingos (*Phoenicopteridae*). *Schweiz Arch Tierheilkd*. 2013;155:497-503.
14. Wyss F, Wolf P, Wenker C, et al. Comparison of plasma vitamin A and E, copper and zinc levels in free-ranging and captive greater flamingos (*Phoenicopterus ros-eus*) and their relation to pododermatitis. *J Anim Physiol and Anim Nutr*. (Berl) 2014; 98:1102-1109.
15. Zschiesche W, Linke RP. Immunohistochemical characterization of spontaneous amyloidosis in captive birds as AA-type, using monoclonal and polyclonal anti-AA antibodies against mammalian amyloid. *Acta Histochem*. 1989;86:45-50.

CASE II:

Signalment:
6-week-old male leopard tortoise (*Stigmochelys pardalis*).

History:
The animal presented with anorexia, lethargy, and yellow bumps along the skin. The animal was found deceased approximately 48 hours after onset of symptoms. There were 6 other clutch mates housed in the same enclosure with similar skin lesions, but without behavioral changes.

Gross Pathology:
The bilateral inguinal and gular skin is moderately thickened with fissures; ventrally and laterally, there are multifocal, pale tan-yellow, pinpoint, raised, nodular foci. No additional significant findings were observed.

Laboratory Results:
16S PCR and bidirectional Sanger sequencing identified the presence of *Austwickia chelonae* within the affected skin.

Microscopic Description:
The epidermis of the distal hind limb is multifocally overlain by lamellar, compact keratin admixed with dense mats of primarily filamentous but also fewer coccoid bacteria. The filamentous bacteria, along with fewer cocci, invade into the dermis and superficial skeletal muscle. Multifocally, the epidermis is eroded to ulcerated with sloughing and epidermal-dermal junctional clefting of the extant epidermis. The affected epidermis is often homogenously eosinophilic with pale cellular outlines (coagulative necrosis) and contains variably prominent intracellular and intercellular vacuolation (edema). Similar regions of coagulative necrosis are present within the dermis with low numbers of extravasated erythrocytes, scattered granulocytes, and occasional histiocytes. Venules

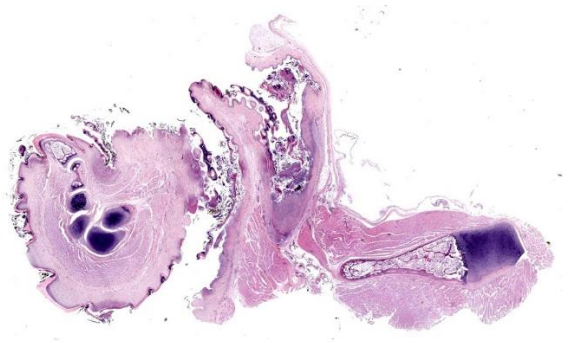

Figure 2-1. Leg, tortoise. There are areas of basophilic lamellar hyperkeratosis, with ulceration and accumulation of keratin debris within a fissure of the hyperplastic epithelium at top center. (HE, 4X)

and arterioles in these regions are often disrupted and necrotic with invasion of filamentous bacteria transmurally into the vascular lumen. Similar findings are seen within the pericloacal, gular, and cephalic skin.

Contributor's Morphologic Diagnosis:
Dermatitis, necrotizing, multifocal to coalescing, severe, chronic with abundant intralesional, gram-positive filamentous bacteria (morphology consistent with *Austwickia chelonae*) and fewer cocci.

Contributor's Comment:
Both the gross and histologic findings in this leopard tortoise are consistent with the PCR identification of *Austwickia chelonae*. *A. chelonae* is a gram-positive, filamentous, facultative anaerobic actinobacterium that can cause disease (austwickiosis) in both captive and free-ranging reptiles. Prior to 2010, this organism was categorized within the same genus as perhaps the best known member of the Dermatophilaceae, *Dermatophilus congolensis*.[3,5] First described in 1995 as *Dermatophilus chelonae*, the organism was later reassigned to the newly created genus, *Austwickia* (Family Dermatophilaceae).[3,8] As part of its initial characterization using samples collected from captive chelonians in a western Australian Zoo, *A. chelonae* showed many unique features in comparison to *D. congolensis.* These included different biochemical characteristics, distinct morphology, and specific culture requirements, including optimal growth occurring at 27° C compared to 37° C for *D. congolensis*.[8]
Most commonly, gross findings in chelonids consist of dermatitis with hyperkeratosis and progressive epidermal necrosis and ulceration often resulting in the formation of yellow to white nodules that can extend into the subcutis.[1,3] Although the extent of the potential host range of *A. chelonae* has not been fully determined, infections have been reported in numerous chelonian species, including captive desert (*Gopherus agassizii*), speckled cape (*Homopus signatus*), and sulcata (*Centrochelys sulcata*) tortoises.[3,7,9] Less frequently, *A. chelonae* has been implicated as a cause of septic arthritis and visceral granulomas in captive tortoises.[1,3] In captive, juvenile *C. sulcata*, *A. chelonae* infections were associated with extensive bone involvement with destruction of the nasal cavity and mandible.[9] In 2022, *A. chelonae* was documented for the first time in free-ranging chelonians in North America as a cause of cutaneous granulocytic granulomas in a wild gopher tortoise (*G. polyphemus*).[7]

Though the exact reservoir of *A. chelonae* has not been determined, the organism has been isolated from environmental soil and water sources.[4] It is suspected that initial local trauma to the skin, such as from tick bites or embedded foreign material, or inappropriate captive husbandry (high humidity or excessive soaking), are necessary to permit austwickiosis.[7,9] *A. chelonae* has recently been documented to encode a gene for a toxin similar to diphtheria toxin that had been previously only described within the genus *Corynebacterium*.[7] Diphtheria toxin terminates RNA synthesis and has been shown to notably interact with the host's immune system.[7] A presumptive diagnosis of

austwickiosis may be made based on the combination of signalment combined with gross and histologic features using routine and special histochemical (Gram, GMS) stains. A definitive diagnosis of *A. chelonae*, however, requires PCR, culture, or metagenomic next-generation sequencing (mNGS).[3,4]

Austwickiosis is not restricted to chelonians. Captive inland bearded dragons *(Pogona vitticeps*) coinfected with *A. chelonae* and ranavirus presented with multifocal superficial necrotizing dermatitis.[10] The reported histopathologic changes in the skin of the affected bearded dragon were similar to those reported in this case.[9] Recurrent granulomatous dermatitis associated with PCR confirmed *A. chelonae* (syn. *D. chelonae*), was described in a king cobra (*Ophiophagus hannah*) in 2004.[6,11] In 2019, a study of the endangered Chinese crocodile lizard (*Shinisaurus crocodilurus*) revealed cutaneous lesions associated with *A. chelonae*.[4] Interestingly, experimental inoculation of the bacteria resulted in austwickiosis not only in Chinese skinks (*Plestiodon chinensis*), but also in domestic sheep, rabbits, and guinea pigs.[4] This suggests that *A. chelonae* has the potential to infect a wider range of species, including mammals, though natural infections have not been reported.

Infections by other members of the family Dermatophilaceae have been reported in reptiles, mammals, birds, and humans.[4] In crocodiles, reports of ventrally located brown skin lesions, colloquially called "brown spot disease", has been reported in young captive crocodiles (*Crocodylus porosus and C. novaeguineae*) in Papua New Guinea, farmed saltwater crocodiles (*C. porosus*) in Australia, and farmed American alligators (*Alligator mississippiensis*) in the southeastern United States.[2,3] Of the saltwater crocodiles evaluated in Australia, approximately 30% of

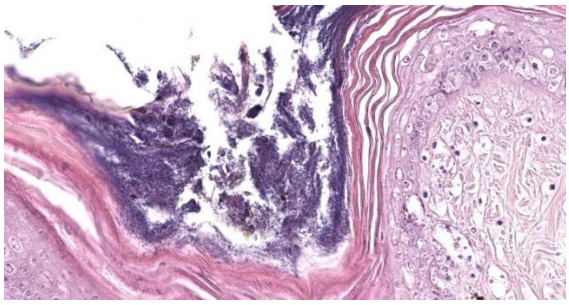

Figure 2-2. Skin of leg, tortoise. The most superficial layers of the dense lamellar keratin are replete with filamentous bacilli (and few cocci) that give it a dense blue color. (HE, 481X)

animals with clinical dermatitis contained intralesional filamentous, *Dermatophilus*-like bacteria.[2,3] In lizards, dermatophilosis has been reported in captive bearded dragons confirmed as *D. congolensis* on culture. Dermatophilus-like organisms have been observed by light microscopy in a number of other species, including bush anoles (*Polychrus marmoratus*), collared lizards (*Crotaphytus collaris*), green iguanas (*Iguana iguana*), Senegal chameleons (*Chamaeleo senegalensis*), savannah monitors (*Varanus exanthematicus*), and panther chameleons (*Furcifer pardalis*).[3]

Contributing Institution:
University of Florida
College of Veterinary Medicine
Department of Comparative, Diagnostic, and Population Medicine
Gainesville, Florida
https://cdpm.vetmed.ufl.edu/

JPC Diagnosis:
Skin: Dermatitis, necrotizing, multifocal to coalescing, with hyperkeratosis and numerous filamentous bacilli.

JPC Comment:
The contributor provides an excellent, thorough summary of austwickiosis in reptiles and

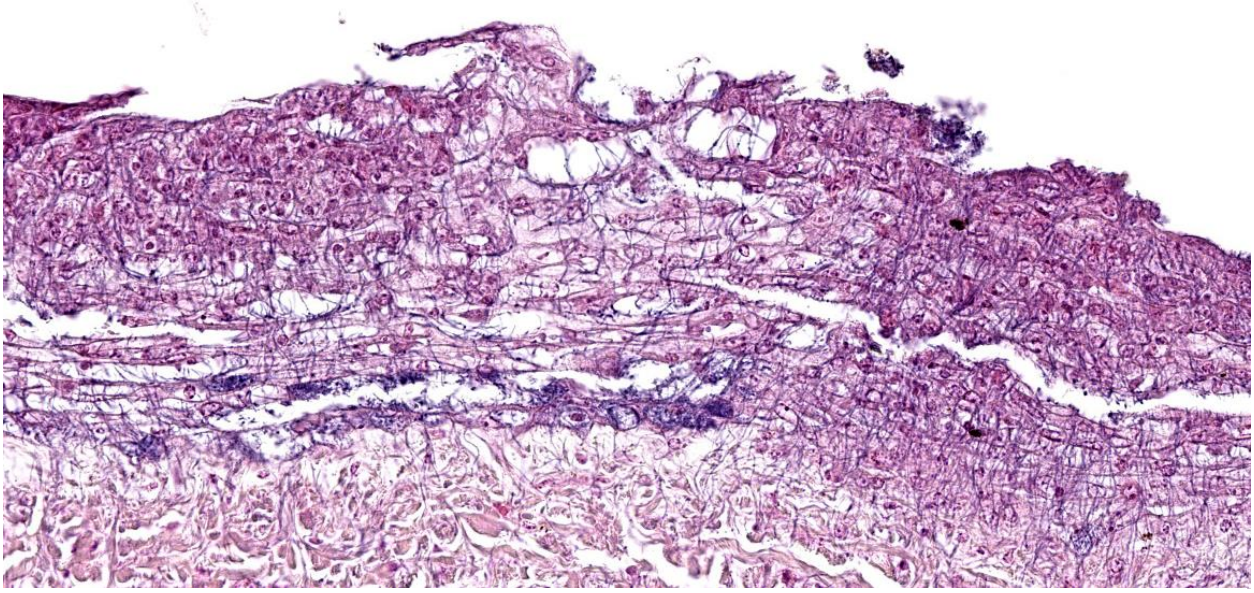

Figure 2-3. Skin, tortoise. There are areas of epidermal necrosis and ulceration with numerous filamentous bacilli penetrating into the underlying dermis. (HE, 91X)

notes an unusual feature of this organism: the presence of a toxin, similar to diptheria toxin, previously unknown outside of the *Corynebacterium* genus.

Diptheria toxin (DT), produced by specific species of *Corynebacterium*, is the main virulence factor responsible for the respiratory, neurologic, and cardiopulmonary symptoms that characterize diptheria in humans.[12] DT is encoded on a bacteriophage which is integrated into the bacterial genome at specific sites. Regulation of DT expression is reliant on bacterial chromosome encoded diptheria toxin repressor genes, whose products can bind bacterial DNA sequences and block transcription and expression of DT.[12]

DT is considered the first example of the A-B class of toxins, an evolutionarily conserved motif found in almost all intracellular toxins.[12] DT is produced as an inactive proenzyme that is cleaved to its active form on encountering a target cell. The two resulting peptides are DT-A, the catalytic portion of the toxin, and DT-B, which is required for receptor binding and subsequent translocation of the toxin into the target cell by receptor-mediated endocytosis.[12]

Once inside the cell, the acidic environment of the endosome causes a conformational change in DT, which causes the DT-A catalytic portion of the toxin to insert into the endosome membrane, exposing DT-A to the cytosol.[12] DT-A catalyzes the transfer of an ADP compound from NAD+ to a histidine residue on elongation factor-2 (EF-2). EF-2 catalyzes the movement of ribosomes along mRNA during translation, making it essential for protein synthesis. When EF-2 is modified by the action of DT-A, the ribosome is unable to move, translation is halted, and the cell ultimately dies.[12] DT-A disables EF-2 in all eukaryotic species except mice and rats, and one DT-A molecule exposed to the cytosol is enough to kill a cell.[12]

Diptheria-toxin like genes were identified in 2018 in several bacteria outside of the *Corynebacterium* genus, including *Austwickia* and *Streptomyces* spp.[13] The key

features of the toxin, including the catalytic and translocation domains, are conserved, but the receptor-binding domains are different, accounting for the different host ranges and cellular tropisms of the DT-like toxin in non-*Corynebacterium* organisms.[12] In addition, DT-like toxin is encoded in the bacterial genome of the new hosts rather than on bacteriophages, suggesting an alternate method of lateral gene transfer has occurred in these species.[12]

It is unclear if DT-like toxin has a role in the pathogenesis of *A. chelonae* infection; however, abundant necrosis is a hallmark of this disease in all species, raising the possibility that DT-like toxin causes the same cellular injury via the same mechanism as its DT ancestor.

Discussion of this case initially centered on the abundant autolysis which caused interpretive challenges for conference participants. Participants noted that the abundant filamentous bacteria were seemingly not accompanied by the a robust inflammatory reaction, prompting a lengthy discussion about whether the bacteria could represent postmortem bacterial overgrowth rather than true pathogenic bacteria. On closer inspection, however, participant believed that some of the ghost cells in the tissue are presumptive heterophils that have been rendered inapparent due to autolysis.

The organism itself cuts a striking filamentous figure in this slide. The moderator noted that this morphologic feature can be used to narrow the differential list considerably to the most commonly-encountered filamentous bacteria: *Actinomyces*, *Nocardia*, *Dermatophilus*, and *Streptobacillus*. The moderator also reminded participants not to neglect the bone marrow The bone marrow in this case appears mildly hypocellular, which comports with the observed mild inflammation. Dr. Terio noted that ambient temperature has a profound impact on the ability of poikilotherms to mount inflammatory responses and speculated that low body temperature might explain the disconnect between the level of inflammation and the extent of bacterial infection observed in this animal.

References:

1. Bemis DA, Patton CS, Ramsay EC. Dermatophilosis in captive tortoises. *J Vet Diagn Invest*. 1999;11(6):553-7.
2. Buenviaje GN, Ladds PW, Martin Y. Pathology of skin diseases in crocodiles. *Aust Vet J*. 1998;76(5):357-63.
3. Jacobson ER, Garner MM. Actinomycetales- Dermatophilus and Austwickia. In: Infectious diseases and pathology of reptiles-color atlas and text. 2nd ed. CRC Press; 2020.
4. Jiang H, Zhang X, Li L, et al. Identification of *Austwickia chelonae* as cause of cutaneous granuloma in endangered crocodile lizards using metataxonomics. *PeerJ*. 2019;7:e6574
5. Kagia K, Lieu WT. The Family Dermatophilaceae. In: Roseberg E, The Prokaryotes-Actinobacteria. 4th ed. Springer-Verlag Berlin Heidelberg; 2014
6. Latney LV, Wellehan JFX. Selected Emerging Infectious Diseases of Squamata: An Update. *Vet Clin North Am Exot Anim Pract*. 2020;23(2):353-371.
7. Liguori BL, Ossiboff RJ, Stacy NI, et al. Austwickia chelonae in a wild gopher tortoise (Gopherus Polyphemus) and evidence of positive selection on the diphtheria-like toxin gene. *J Wildl Dis*. 2022;58 (1):1-7.
8. Masters AM, Ellis TM, Carson JM, Sutherland SS, Gregory AR. Dermatophilus chelonae sp. nov., isolated from chelonids in Australia. *Int J Syst Bacteriol*. 1995;45: 50-56

9. Rostad SJ, Brandão J, Ramachandran A, Chien RC, Confer AW. Austwickiosis in captive African Spurred Tortoises (*Geochelone sulcata*) co-infected with *Cryptosporidium ducismarc*i. *J Comp Pathol*. 2019;173:1-7.
10. Tamukai K, Tokiwa T, Kobayashi H, Une Y. Ranavirus in an outbreak of dermatophilosis in captive inland bearded dragons (*Pogona vitticeps*). *Vet Dermatol*. 2016;27(2):99-105e28.
11. Wellehan JF, Turenne C, Heard DJ, Detrisac CJ, O'Kelley JJ. *Dermatophilus chelonae* in a king cobra (*Ophiophagus hannah*). *J Zoo Wildl Med*. 2004;35(4):553-6.
12. Young LS. New *Corynebacterium* species with the potential to produce diptheria toxin. *Pathogens*. 2022;11(11):1264.
13. Mansfield MJ, Sugiman-Marangos SN, Melnyk RA, Doxey AC. Identification of a diptheria toxin-like gene family beyond the Corynebacterium genus. *FEBS Lett*. 2018;592(16):2693-2705.

CASE III:

Signalment:
1-year-old, gender not specified Nile crocodile (*Crocodiles niloticus*).

History:
Biopsy from a farmed yearling Nile crocodile (*Crocodiles niloticus*) that presented with multifocal to coalescing 3-5 mm ovoid ulcerated lesions on the abdominal ventrum. There were no associated clinical abnormalities.

Gross Pathology:
Multifocal to coalescing 3-5 mm ovoid ulcerated lesions on the abdominal ventrum.

Laboratory Results:
Lesions were PCR positive for crocodile pox.

Microscopic Description:
Focal erosion, ulceration and hyperplasia of the epidermis with thick adherent serocellular crust. Ballooning degeneration of keratinocytes is a feature and numerous eosinophilic intracytoplasmic inclusions are observed.

There are marked perivascular to more widespread accumulations of admixed heterophils, lymphocytes, and macrophages within the subjacent superficial dermis.

Contributor's Morphologic Diagnosis:
Skin: Dermatitis, necrotizing and proliferative with ballooning degeneration and intra

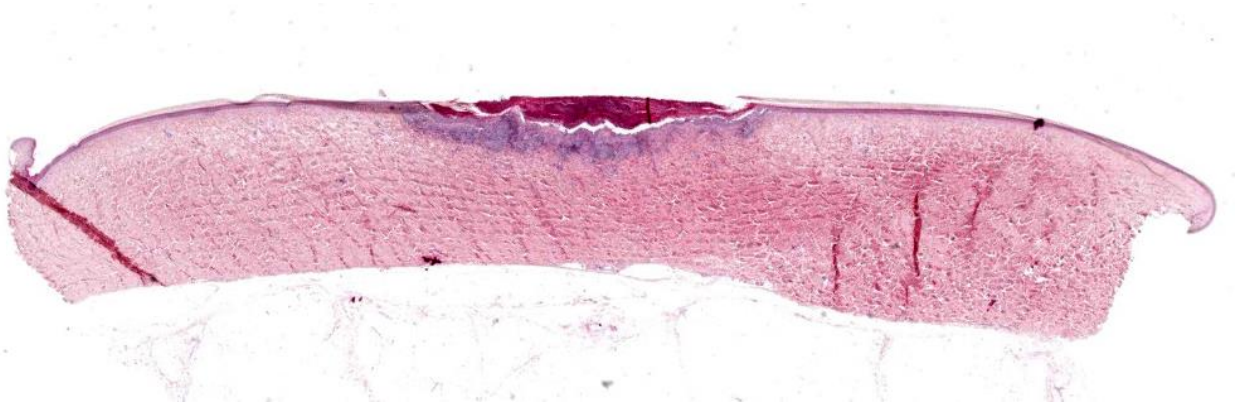

Figure 3-1. Skin, crocodile. A section of skin with a central area of necrosis is submitted for examination. (HE, 4X) (*Photo courtesy of*: Veterinary Sciences Centre, School of Veterinary Medicine, University College Dublin, Belfield, Dublin 4, Ireland, http://www.ucd.ie/vetmed/)

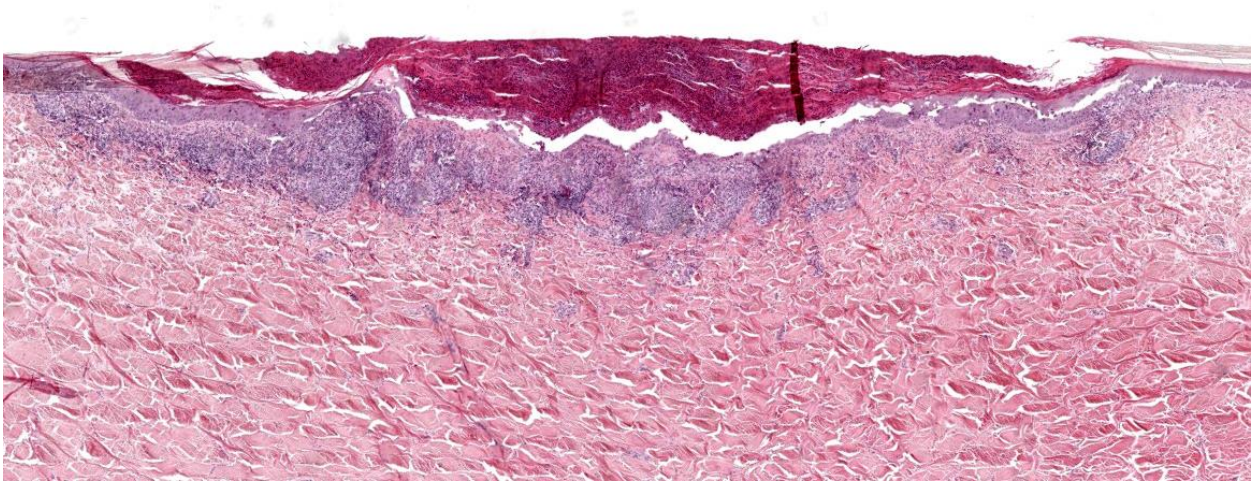

Figure 3-2. Skin, crocodile. There is full thickness necrosis of the epidermis in the center of the lesion. This area of necrosis is covered with a serocellular crust and there is a marked inflammatory infiltrate in the immediately subjacent superficial dermis. The crust extends over the periphery of the lesion. (HE, 33X)

cytoplasmic, eosinophilic inclusions consistent with poxvirus infection, Nile crocodile (*Crocodiles niloticus*), reptile.

Contributor's Comment:
The pathognomonic features of keratinocyte ballooning and eosinophilic intracytoplasmic inclusions, taken together with the clinical appearance and positive PCR result, are consistent with a diagnosis of crocodile poxvirus infection. Infection typically results in proliferative skin lesions approximately 1-3 mm diameter, grey to brown, and sessile or slightly depressed in contour. Lesions are variously encrusted, ulcerated or, less frequently, exophytic and wart-like and can occur over the entire body.[3, 4] Sequelae can include opportunistic infections by *Dermatophilus*-like bacteria or by fungi. The presence of pox virions can be confirmed by electron microscopy with visualization of characteristic 100 nm by 200 nm virions with a dumbbell-shape with cross striations.[2,4]

While some members of the poxvirus family are host specific, others can infect many species.[5] The *Poxviridae* family is subdivided into the *Entomopoxvirinae* and *Chordopoxvirinae* subfamilies and members of the latter subfamily cause disease where skin lesions are the predominant clinical sign. Currently, 29 members of this subfamily are known to infect mammals, 10 are found in birds and one species is associated with disease in reptiles including several crocodilian species.[5]

Poxvirus-associated disease in reptiles has been described in caimans (*Caiman crocodilus*), Nile crocodiles (*Crocodilus niloticus*), and in both saltwater (*Crocodylus porosus*) and freshwater (*Crocodilus johnstoni*) crocodiles.[2] Although found in crocodilians worldwide, only three crocodile poxvirus genomes have been published to date and the source of infection remains unclear, although mosquitos have been suggested as potential vectors following infection of saltwater crocodiles.[1,6]

Contributing Institution:
Veterinary Sciences Centre
School of Veterinary Medicine
University College Dublin
Belfield, Dublin 4, Ireland
http://www.ucd.ie/vetmed/

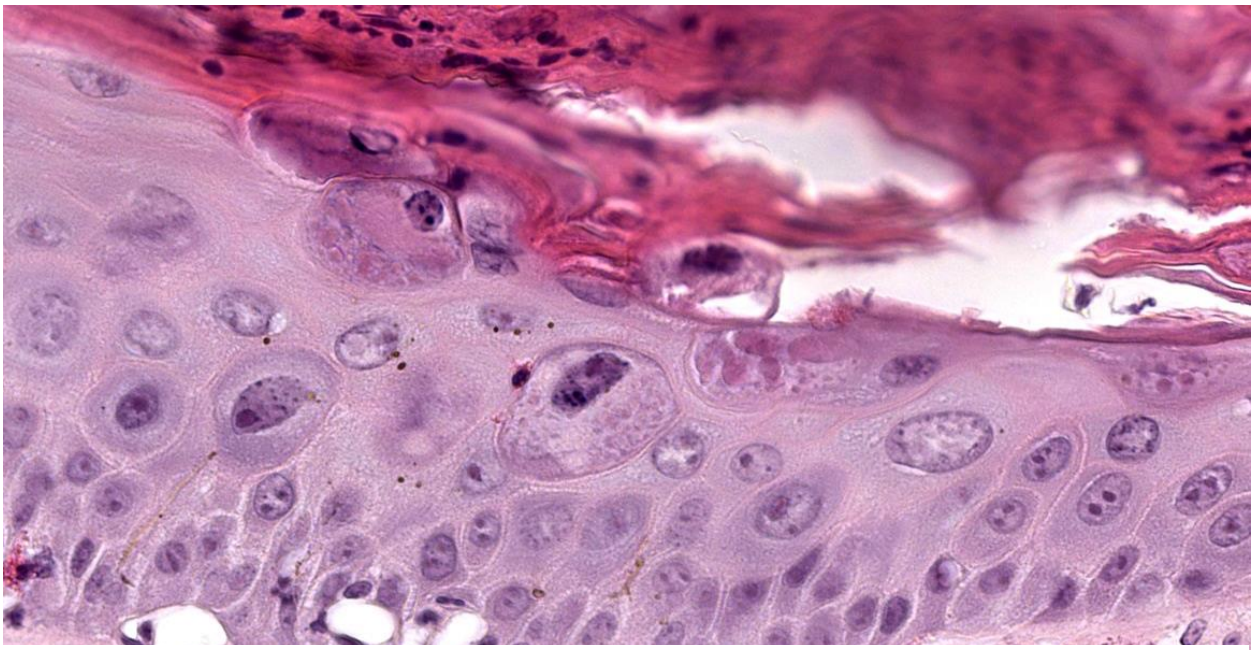

Figure 3-3. Skin, crocodile. Within the intact epithelium at the periphery of the lesion, keratinocytes within the stratum spongiosum are swollen with cytoplasmic clearing (ballooning degeneration), prominent nucleoli with prominent nucleoli, and several cells contain numerous pink cytoplasmic viral inclusions, consistent with poxvirus. (HE, 652X)

JPC Diagnosis:
Skin: Dermatitis, necrotizing and proliferative, focal, moderate with epidermal ballooning degeneration and intracytoplasmic viral inclusions.

JPC Comment:
This small piece of tissue packs a big punch, managing to illustrate both the characteristic histologic lesions of poxviral dermatitis and the wide variety of hosts in which the disease can occur. While the *Poxviridae* family is familiar to most, it likely comes a surprise to some that the family includes a small, evolutionarily divergent group of poxviruses in the genus *Crocodylidpoxvirus* that affects the order Crocodylia worldwide.[5] The currently-characterized members of this group include Nile crocodilepox virus-1 (CPV) and saltwater crocodilepox viruses 1 and 2.[6]

CPV most commonly causes a nonfatal dermatitis with complete recovery which is mostly of economic importance to the commercial crocodile leather farming industry. Occasionally, however, more severe disease can develop with clinical signs of ophthalmia, rhinitis resulting in asphyxia, and debilitating illness with stunting and high mortality.[1] Histopathologic features are characteristic of poxviral infection generally (necrosis, hyperkeratosis, ballooning degeneration, and intracytoplasmic inclusion bodies) as nicely illustrated by this histologic section.

The progression of poxviral dermatitis lesions has been detailed in the saltwater crocodile and classified into four stages: early active, active, expulsion, and healing.[4] Early active lesions are 1-3 mm in diameter, white to grey foci of pinpoint of keratin damage. Early active lesions are histologically characterized by epidermal hyperplasia and hypertrophy with visible intracytoplasmic inclusion bodies and in intact overlying kertain layer.[4] With progression to the active stage, affected surface area increases and lesions develop a distinct raised outer contour with a

depressed central core of abnormal keratin. The stage is characterized histologically by disruption of the superficial keratin layer and the development of a mild perivascular lymphocytic dermal infiltrate.[4]

In the expulsion stage, the central core of necrotic cells is released revealing a crust of necrotic inflammatory cells that given the gross lesion an orange/tan color; the underlying epidermis at this stage is of normal thickenss and cellular morphology.[4] In the final healing phase, the lesion surface area decreases, with the surface keratin appearing abnormal, though with the color of normal skin. The lesions slowly become less visible during this phase, eventually returning to an almost normal macroscopic appearance.[4]

CPV is most phylogenetically related to molluscum contagiosum virus, but is rather distinct from other *Chordopoxviruses*.[1] CPV lacks many recognizable virulcence genes common to other *Chrodopoxviruses*, including interferon responses, intracellular signaling, and host immune response modulation. The CPV genome contains many putative genes which are speculated to perform these functions in novel ways, though none have yet been characterized.[1] CPV remains a bit mysterious, with seemingly familiar gross and histomorphologic lesions that belie a unique, recently diverged, and largely unknown biological armamentarium.

Conference participants had no difficult identifying the poxviral etiology for these lesions, though there was some discussion about the size, quantity, and character of the intracytoplasmic viral inclusions, which participants felt looked slightly different from normal poxviral inclusions. The moderator, who has extensive experience with crocodile pathology and husbandry, noted that this histologic section is an excellent, quality example of crocodile skin. The moderator also directed participants to the lateral edges of the section to appreciate normal crocodile skin, which typically has a very thin epidermis. Comparing the normal skin to the lesional skin highlights the degree hyperkeratosis that is typical of poxviral dermatitis in any species.

References:

1. Afonso CL, Tulman ER, Delhon G, et al. Genome of crocodilepox virus. *J Virol.* 2006;80(10):4978–4991.
2. Buenviaje G, Ladds P, Melville L. Poxvirus infection in two crocodiles. *Aust Vet J*. 1992;69(1):15-16.
3. Buenviaje G, Ladds P, Martin Y. Pathology of skin diseases in crocodiles. *Aust Vet J*. 1998;76(5):357-363.
4. Moore RL, Isberg SR, Shilton CM, Milic NL. Impact of poxvirus lesions on saltwater crocodile (*Crocodylus porosus*) skins. *Vet Microbiol*. 2017; 211:29-35.
5. Oliveira G, Rodrigues R, Lima M, Drumond B, Abrahão J. Poxvirus host range genes and virus–host spectrum: a critical review. *Viruses.* 2017;9(11):331.
6. Sarker S, Isberg SR, Milic NL, Lock P, Helbig KJ. Molecular characterization of the first saltwater crocodilepox virus genome sequences from the world's largest living member of the Crocodylia. *Sci Rep-UK*. 2018;8(1):5623.

CASE IV:

Signalment:

Adult female koala **(***Phascolarctos cinereus)*.

History:

A free-ranging koala was found in poor body condition, surrendered to a wildlife hospital, and euthanised on welfare grounds.

Gross Pathology:

Consolidation of the left caudal lung lobe with pleural adhesions.

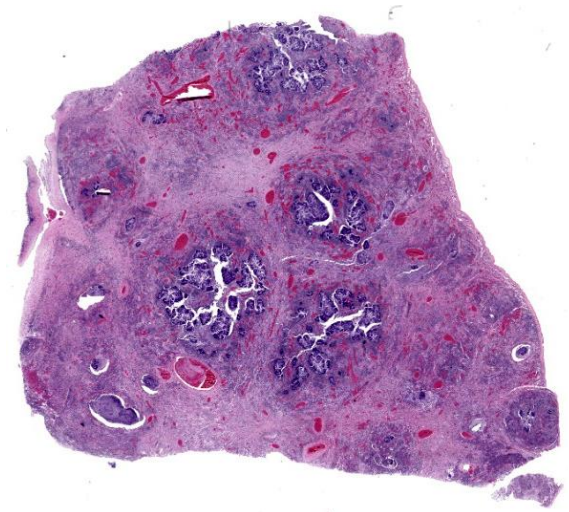

Figure 4-1. Lung, koala. One section of lung is submitted for examination. There are bacterial colonies and resulting inflammation within and effacing airways. (HE, 5X)

Laboratory Results:
Heavy growth of anaerobic bacteria from the left caudal lung lobe. Cultured bacteria were identified by bacterial 16S rRNA gene as a novel *Actinomyces* spp.

Microscopic Description:
Lung: The normal lung parenchyma is effaced and replaced by branching coarse fibrocollagenous connective tissue (fibrosis), which dissects between multifocal to coalescing densely cellular infiltrates of neutrophils, macrophages, and lymphocytes. Inflammatory infiltrates often cluster around lakes of amorphous necrotic debris and intensely eosinophilic radiating material which surround or are admixed with fine filamentous bacteria (pyogranulomas with central club colonies and Splendore-Hoeppli material). There is moderate to marked irregular expansion of the pleura by immature granulation tissue, haemorrhage, fibrin, and leukocytes.

Bacteria are gram-positive, Ziehl-Neelsen and modified Ziehl-Neelsen negative. No organisms are visualized with PAS or Alcian blue stains.

Contributor's Morphologic Diagnosis:
Lung: Severe chronic fibrosing pyogranulomatous pleuropneumonia with intralesional filamentous bacteria and Splendore-Hoeppli phenomenon.

Contributor's Comment:
In recent years, free-ranging and captive koalas (*Phascolarctos cinereus*) from the Mount Lofty Ranges of South Australia have been identified with chronic pyogranulomatous bronchopneumonia or lobar pneumonia, most frequently involving the left caudal lung lobe.[17] Within lesions, numerous gram-positive or gram-variable, non-acid-fast filamentous bacteria are observed in association with Splendore-Hoeppli phenomenon. Culture in this case yielded growth of anaerobic bacteria, subsequently identified by molecular techniques as a novel *Actinomyces* species (pulmonary actinomycosis).

Actinomyces is an anaerobic or facultative aerobic, gram-positive, filamentous bacteria, which is non-spore forming and non-motile.[14] *Actinomyces* species can be found in the normal healthy microbiota of the human oropharynx and gastrointestinal tract and on nasal, oral, or oropharyngeal mucosal surfaces of other animals and are most often associated with opportunistic infections.[4,14,18,20] Pulmonary actinomycosis is rare in animals but has been described in a small number of

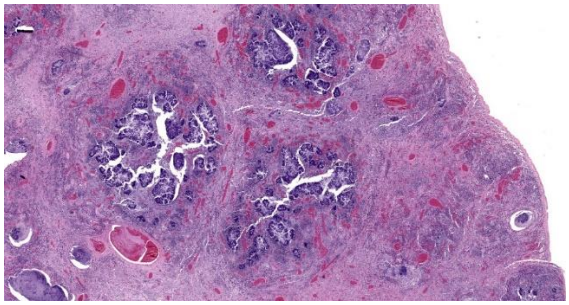

Figure 4-2. Lung, koala. Higher magnification of inflamed airways. (HE, 10X)

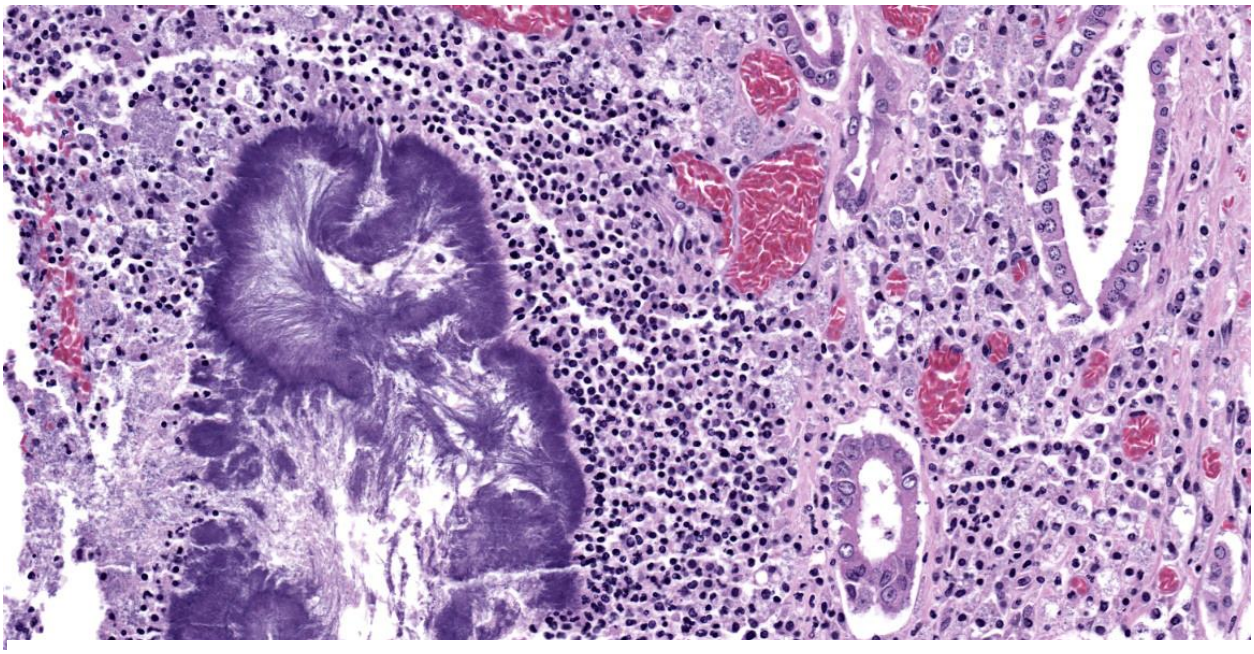

Figure 4-3. Lung, koala. High magnification of aggregates of filamentous bacteria surrounding by neutrophils and cellular debris. (HE, 252X)

free-ranging species including two chamois (*Rupicapra rupicapra*),[15] a black-tufted marmoset (*Cal-lithrix penicillata*),[16] and in a captive red kangaroo (*Osphranter rufus*).[8]

Actinomyces spp. have been reported as commensals of the oral microbiome and associated with similar pulmonary lesions in other species. Examination of resin lung casts from healthy koalas suggests greater laminar flow of air to the left caudal lung lobe in koalas.

Considering the predilection for involvement of the left caudal lung lobe observed in multiple in koalas with this condition, aspiration is suggested as the likely cause in at least some cases of pulmonary actinomycosis in koalas.

Other pathogens reported to cause pneumonia in koalas include *Bordetella bronchiseptica*,[3,11] *Chlamydia* spp.,[1,5,9] *Cryptococcus gattii* (previously *Cryptococcus neoformans* var. *gattii*),[3,7] *Pseudomonas aeruginosa*,[2,13] *Nocardia asteroides*,[19] *Staphylococcus epidermidis*,[19] *Mycobacterium ulcerans*,[12] and parasitic pneumonia associated with *Marsupiostrongylus* sp.[10]

Contributing Institution:
Veterinary Diagnostic Laboratory
School of Animal and Veterinary Sciences
University of Adelaide
Roseworthy, South Australia
https://sciences.adelaide.edu.au/animal-veterinary-sciences/

JPC Diagnosis:
Lung: Bronchopneumonia, pyogranulomatous, chronic, diffuse, severe, with colonies of filamentous bacilli and Splendore-Hoeppli material.

JPC Comment:
This stunning histologic slide is a remarkable example of bacterial pneumonia caused by *Actinomyces*, one of the members (along with *Yersinia*, *Actinobacillus*, *Corynebacterium*, *Streptococcus, and Staphylococcus* spp.) of the "YAACSS" large colony forming bacteria. As the contributor nicely describes, pulmonary actinomycosis is an increasingly

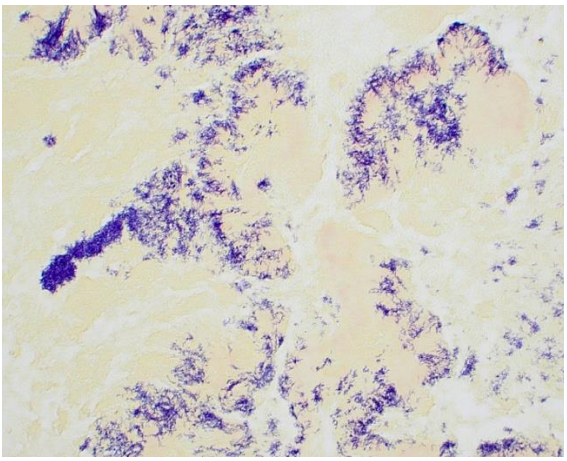

Figure 4-4. Lung, koala. Filamentous bacteria are gram-positive. (BB, 200X)

recognized disease of koalas, and the history and gross and histologic findings described in this case are characteristic.

The contributor provides an excellent summary here; a more fulsome discussion is provided in the published case series from which this case was taken.[17] Pulmonary actinomycosis in koalas affects the left caudal lung lobe in 82% of cases, and is the only affected lobe in 21% of cases.[17] In 43% of cases, both the left caudal and the right middle lung lobes are affected.[17] Resin cast studies provided a possible answer for this apparent site predilection as the left primary bronchus in the koala follows a relatively straight caudal path without branching into lobar bronchi until deep in the pulmonary parenchyma. In contrast, the right primary bronchus is less linear, branches from the trachea in a more lateral direction, and branches into lobar bronchi much earlier than the left primary bronchus.[17] Researchers speculate that the more linear bifurcation pattern creates greater laminar flow, essentially creating a more direct path for bacterial colonization of the left caudal lobe.[17]

Microbial culture and isolation were performed on five koalas from this case series and a variety of anaerobic agents were identified. PCR amplification and sequencing of the 16S rRNA gene matched most closely with *Actinomyces timonensis*, though due to only 95% sequence homology with the reference *A. timonensis* genome, researchers speculate that the etiologic agent could be a novel *Actinomyces* species.[17]

Pulmonary actinomycosis in South Australian koalas is occasionally accompanied by hypertrophic osteopathy.[6] In a recent case study describing this combination of lesions, imaging findings included periosteal reaction on multiple appendicular skeletal bones, including the scapula, humerus, ulna, radius, femur, tibia, fibula, and carpal bones. Gross findings included thick, roughened periosteum on the metaphyses and diaphysis of long bones, and histologic findings included proliferative trabecular bony spicules oriented perpendicular to the cortical bone.[6]

The moderator began discussion of this case by noting that tissue identification is difficult since the pulmonary architecture is almost entirely obliterated by the florid pyogranulomatous inflammation. The moderator noted that there are many clues to pathogen identity here, including the filamentous morphology of the bacteria, the pyogranulomatous nature of the inflammatory reaction, and the presence of Splendore-Hoeppli material.

As discussed in the previous case of *Austwickia chelonae* dermatitis, the most commonly encountered filamentous bacteria are *Actinomyces*, *Nocardia*, *Dermatophilus*, and *Streptobacillus*. The moderator also noted a variety of conditions that are typically associated with Splendore-Hoeppli reaction, including fungal infections (sporotrichosis, zygomycosis, candidiasis, aspergillosis, blastomycosis, orbital pythiosis, pityrosporum folliculitis), bacterial infections (botryomycosis, nocardiosis, and actinomycosis), and parasitic infections (strongyloidiasis,

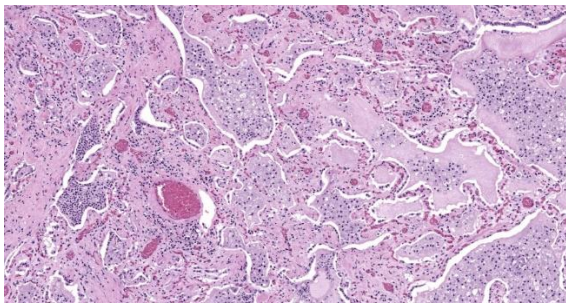

Figure 4-5. Lung, koala. The extensive fibrosis within the adjacent alveolar parenchyma has resulted in ectasia and an irregular shape to remaining alveoli ("traction emphysema") which are filled with alveolar macrophages and fewer neutrophils. (HE, 87X)

schistosomiasis, and cutaneous larval migrans). The intersection of these two differential lists raises a clinical suspicion of actinomycosis even before the inevitable google reveals the susceptibility of koalas to pulmonary actinomycosis. Nevertheless, the moderator noted that *Chlamydia* spp. is an important rule-out in this case, and participants reviewed a Giemsa stained section that was convincingly negative. Participants were amazed at the florid koality of the inflammation in this case which, even for a koala, is pretty severe, causing participants to speculate that the koala might be immunosuppressed.

Discussion of the morphologic diagnosis was straight-forward, with a short aside dedicated to whether the process could be described as necrotizing. In this case, the necrosis is due to inflammatory by-stander damage and not to virulence factors deployed by *Actinomyces*, so participants preferred a morphologic diagnosis of pyogranulomatous bronchopneumonia.

References:

1. Blanshard WH, Bodley K: Chapter 8: Koalas. In: Vogelnest L, Woods, R, eds. *Medicine of Australian Mammals*. CSIRO Publishing; 2008.
2. Canfield PJ. A mortality survey of free range koalas from the north coast of New South Wales. *Aust Vet J*. 1987:64(11): 325-328.
3. Canfield PJ, Oxenford CJ, Lomas GR, Dickens RK. A disease outbreak involving pneumonia in captive koalas. *Aust Vet J*. 1986:63(9):312-313.
4. Couto SS, Dickinson PJ, Jang S, Munson L. Pyogranulomatous meningoencephalitis due to *Actinomyces* sp. in a dog. *Vet Pathol*. 2000;37:650-652.
5. Gonzalez-Astudillo V, Allavena R, McKinnon A, Larkin R, Henning J. Decline causes of koalas in South East Queensland, Australia: a 17-year retrospective study of mortality and morbidity. *Sci Rep.* 2017;7:42587.
6. Griffith JE, Stephenson T, McLelland DJ, Woolford L. Hypertrophic osteopathy in South Australian koalas (*Phascolarctos cinereus*) with concurrent pulmonary actinomycosis. *Aus Vet J*. 2021;99(5):172-177.
7. Krockenberger MB, Canfield PJ, Malik R. *Cryptococcus neoformans* var. *gattii* in the koala (*Phascolarctos cinereus*): a review of 43 cases of cryptococcosis. *Med Mycol*. 2003;41(3):225-234.
8. Kunze PE, Sanchez CR, Pich A, Aronson S, Dennison S. Pulmonary actinomycosis and hypertrophic osteopathy in a red kangaroo (*Macropus rufus*). *Vet. Rec Case Rep.* 2018;6:e000666.
9. Mackie JT, Gillett AK, Palmieri C, Feng T, Higgins DP. Pneumonia due to *Chlamydia pecorum* in a Koala (*Phascolarctos cinereus*). *J Comp Pathol.* 2016;155(4):356-360.
10. McColl KA, Spratt DM. Parasitic pneumonia in a koala (Phascolarctos cinereus) from Victoria, Australia. *J Wildl Dis.* 1982;18(4):511-512.
11. McKenzie RA, Wood AD, Blackall PJ. Pneumonia associated with Bordetella bronchiseptica in captive koalas. *Aust Vet J*. 1979;55(9):427-430.

12. McOrist S, Jerrett IV, Anderson M, Hayman J. Cutaneous and respiratory tract infection with Mycobacterium ulcerans in two koalas (Phascolarctos cinereus). *J Wildl Dis.* 1985;21(2):171-173.
13. Oxenford CJ, Canfield PJ, Dickens RK. Cholecystitis and bronchopneumonia associated with *Pseudomonas aeruginosa* in a koala. *Aust Vet J*. 1986;63(10):338-339.
14. Quinn PJ, Markey BK, Leonard FC, FitzPatrick ES, Fanning S, Hartigan PJ. Chapter 16: Actinobacteria. In: Quinn PJ, Markey, B.K., Leonard, F.C., FitzPatrick, E.S., Fanning, S., Hartigan, P.J., ed. *Veterinary Microbiology and Microbial Disease*. 2 ed. Blackwell Publishing Ltd.; 2011.
15. Radaelli E, Andreoli E, Mattiello S, Scanziani E. Pulmonary actinomycosis in two chamois (*Rupicapra rupicapra*). *Eur J Wildl Res*. 2007;53(3):231-234.
16. Sousa DER, Wilson TM, Machado M, et al. Pulmonary actinomycosis in a free-living black-tufted marmoset (*Callithrix penicillata*). *Primates* 2019;60(2):119-123.
17. Stephenson T, Lee K, Griffith JE, et al. Pulmonary actinomycosis in South Australian koalas (Phascolarctos cinereus). *Vet Pathol*. 2021;58(2):416-422.
18. Valour F, Senechal A, Dupieux C, et al. Actinomycosis: etiology, clinical features, diagnosis, treatment, and management. *Infect Drug Resist*. 2014;7:183-197.
19. Wigney DI, Gee DR, Canfield PJ. Pyogranulomatous pneumonias due to Nocardia asteroides and Staphylococcus epidermidis in two koalas (Phascolarctos cinereus). *J Wildl Dis*. 1989;25(4):592-596.
20. Zhang M, Zhang XY, Chen YB. Primary pulmonary actinomycosis: a retrospective analysis of 145 cases in mainland China. *Int J Tuberc Lung Dis.* 2017;21(7):825-831.

WSC 2023-2024
Conference 24 Self-Assessment

1. Most amyloid in birds is of the AL-amyloid variety. True or false?
    a. True
    b. False

2. Which of the following viruses has been established as one of many causes of gout in chickens?
    a. Circovirus
    b. Polyomavirus
    c. Coronavirus
    d. Astrovirus

3. *Austwickia cheloniae* previously belonged to which of the following genera?
    a. Hemophilus
    b. Pasteurella
    c. Actinomyces
    d. Dermatophilus

4. True or false? Viruses in the *Chordopoxvirinae* subfamily normally cause extracutaneous lesions.
    a. True
    b. False

5. True or false? *Ntinomyces* are considered normal oropharyngeal flora.
    a. True
    b. False

Joint Pathology Center
Veterinary Pathology Services

WEDNESDAY SLIDE CONFERENCE 2023-2024

Conference #25 **01 May 2024**

CASE I:

Signalment:
Female goat (*Capra hircus*), age and breed unspecified.

History:
The owners had 3 goat does that aborted premature and full-term fetuses after being purchased 4 months prior. These goats were dewormed a week before sample submission. Submitted for necropsy evaluation are 2 fetuses and one placenta.

Gross Pathology:
No major gross lesions were observed in the placenta.

Laboratory Results:
Q-fever PCR at referral laboratory – Positive for *Coxiella burnetti*.

Microscopic Description:
Placenta (chorioallantois): In regionally extensive areas, numerous intracytoplasmic pleomorphic (cocci, coccobacillary, and bacillary morphologies), gram negative bacterial microorganisms are observed within hypertrophied syncytiotrophoblasts on the chorionic villi. The chorioallantois is severely expanded by edema and numerous inflammatory infiltrates, predominantly composed of plasma cells, lymphocytes and hofbauer cells (placental macrophages). Small caliber vessels in the chorionic stroma are moderately dilated by congestion.

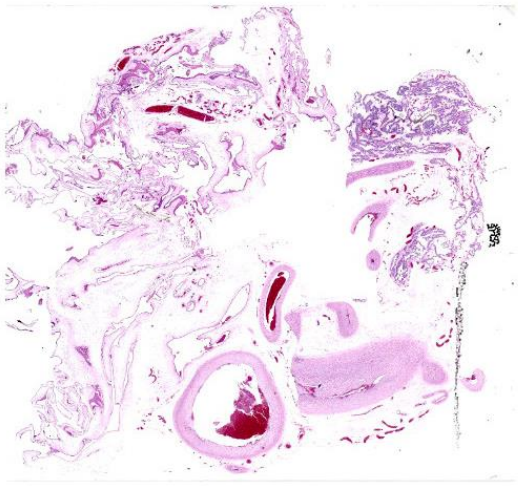

Figure 1-1. Placenta, goat. Sections of the cotyledonary (upper right) and inter-cotyledonary placenta (upper left) are submitted for examination. (HE, 5X)

Contributor's Morphologic Diagnosis:
Placenta: Placentitis, lymphoplasmacytic and histiocytic, acute to subacute, regionally extensive, severe with intratrophoblastic bacteria (*Coxiella burnetti*).

Contributor's Comment:
Q fever, the disease caused by the bacterial organism *Coxiella burnetti*, an obligate intracellular pleomorphic gram-negative bacterial microorganism, is considered a potential bioterrorism agent in many countries, including the United States. A worldwide presence has been reported, except in New Zealand.

The US Centers For Disease Control has classified *C. burnetti* as 'category B' – moderately easy to disseminate with moderate morbidity and mortality. Previous findings indicate that *C. burnetti* has a low infectious dose for initiating a disease process i.e., up to 90% probability for a single bacterium to initiate a disease process.[9]

Coxiella spp. belong to class Gammaproteobacteria, order Legionellales and family Coxiellaceae. *C. burnetti* has been identified in multiple species including domestic ruminants, birds, and some insects.[2,6,11,16] Domestic ruminants are frequently considered as reservoir hosts for *C. burnetti*.[7,13] This pathogen is zoonotic to humans, and can cause a wide array of clinical findings and lesions in different species, that includes abortions, stillbirths, hepatomegaly, splenomegaly, endocarditis, and encephalitis.[2]

C. burnetti has been identified in the gut cells of ticks (*Dermacentor* sp., *Haemaphysalis* sp., *Ixodes* sp., *Hyalomma* sp., *Ornithodoros* sp.,) implicating these ticks as one of the major modes of transmission for this pathogen.[3] Other recorded routes of transmission include aerosolization, ingestion of contaminated placenta (in dogs and cats), exposure to infected milk and other dairy products, horizontal (person-to-person), exposure to fomites, and contact with infected hide or wool from animals.[1] Transmission via fomites, reproductive tissues, and contaminated, unpasteurized dairy products are the most prominent causes for pathogen transmission across different species.

A biphasic growth pattern has been reported for this obligate intracellular gram-negative microorganism, characterized by two major cell types – a spore-like small cell variant (SCV) and an actively dividing large cell variant (LCV).[2,7,12,14] This spore-like SCV has a higher concentration of peptidoglycan, providing resistance to a wide array of

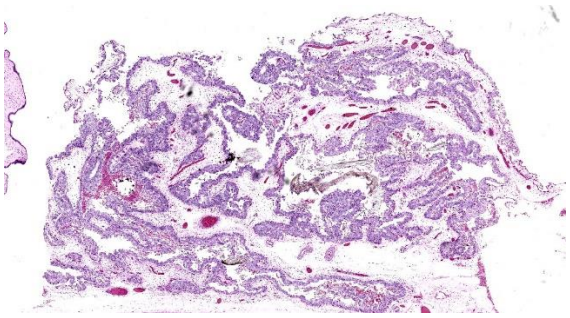

Figure 1-2. Placenta, goat. Cotyledonary epithelium (trophoblasts) are markedly and diffusely expanded. The chorioallantoic stroma is diffusely edematous. (HE, 23X)

physical and chemical stressors, thus permitting the pathogen to survive in the environment. SCVs are usually shed into the environment via placental fluids, mammary secretions, urine, feces, and fomites during the parturition process. By inhalation and close contact, these SCVs then spread to others in the immediate vicinity. Following inhalation, *C. burnetti* is commonly observed within macrophages in various organs including lungs, which leads to inhibition of cell death by impairing phagolysosome formation and macrophage function.[12,14] The exact mechanism for tropism towards trophoblasts is still definitively undetermined, although it is believed that mild immunosuppression during pregnancy may be one of the causes for pathogen localization in the placenta.[18] Maturation and development of SCV in the placenta following a biologically active LCV phase will lead to further spread of the pathogen through shedding into the environment.

In humans, *C. burnetti* can result in the following: self-limiting flu-like clinical signs, severe atypical pneumonia, hepatitis with severe hepatomegaly and icterus, maculopapular exanthema, pericarditis, myocarditis, aseptic meningitis, seizures, polyradiculoneuritis, optic neuritis, transient hypoplastic anemia, and/or lymphadenopathy, as well as other manifestations.[8] The chronic form of Qfever has been reported in 5% of all clinical

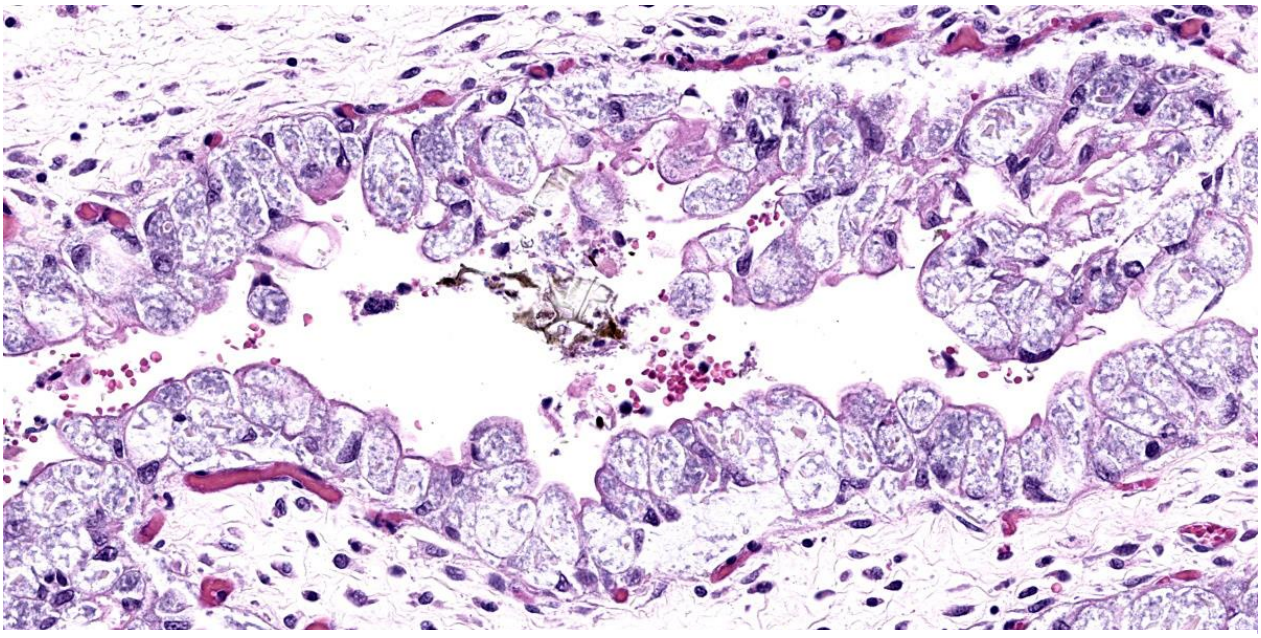

Figure 1-3. Placenta, goat. Higher magnification of trophoblasts. Almost every trophoblast contains numerous 1µm rickettsia within their cytoplasm. This foamy cytoplasmic appearance is characteristic of *Coxiella burnetti.* (HE, 381X)

reports and the most commonly reported lesions in chronic disease are endocarditis, hepatic fibrosis, osteoarthritis, osteomyelitis, as well as other manifestations.[8]

One previous study has reported strong placental tropism of *C. burnetti* at 2-4 weeks after inoculation in pregnant goats, and higher numbers of microorganisms isolated from these infected goats at the time of kidding.[15] In domestic ruminants, histological findings from reproductive tissues (such as the placenta) are a histiocytic and lymphoplasmacytic placentitis with numerous intrahistiocytic and intratrophoblastic bacterial microorganisms. Other commonly used diagnostic techniques includes immunoperoxidase staining for highlighting bacterial microorganisms, immunohistochemistry using monoclonal antibodies against *C. burnetti*, PCR amplification of different DNA targets including 16S and 23S, and serological techniques such as ELISA, complement fixation, western blotting, dot blotting, and microagglutination.[8]

Q-fever is still poorly understood and is zoonotically important due to its multiple attributes, including low infectious dose and environmental persistence. Subsequent screening of all abortions in domestic ruminants, decontamination, biosecurity and treatment are strongly recommended to curb the spread of this pathogen.

The main findings in this case are: 1) lymphoplasmacytic and histiocytic placentitis, 2) the presence of large numbers of intratrophoblastic gram negative bacterial organisms, and 3) PCR positive detection of *C. burnetti*. Altogether, these findings are consistent with *Coxiella burnetti* infection, resulting in abortion in this case.

Contributing Institution:
Oklahoma State University
Department of Veterinary Pathobiology
College of Veterinary Medicine
Stillwater, OK 74078 USA
www.vetmed.okstate.edu

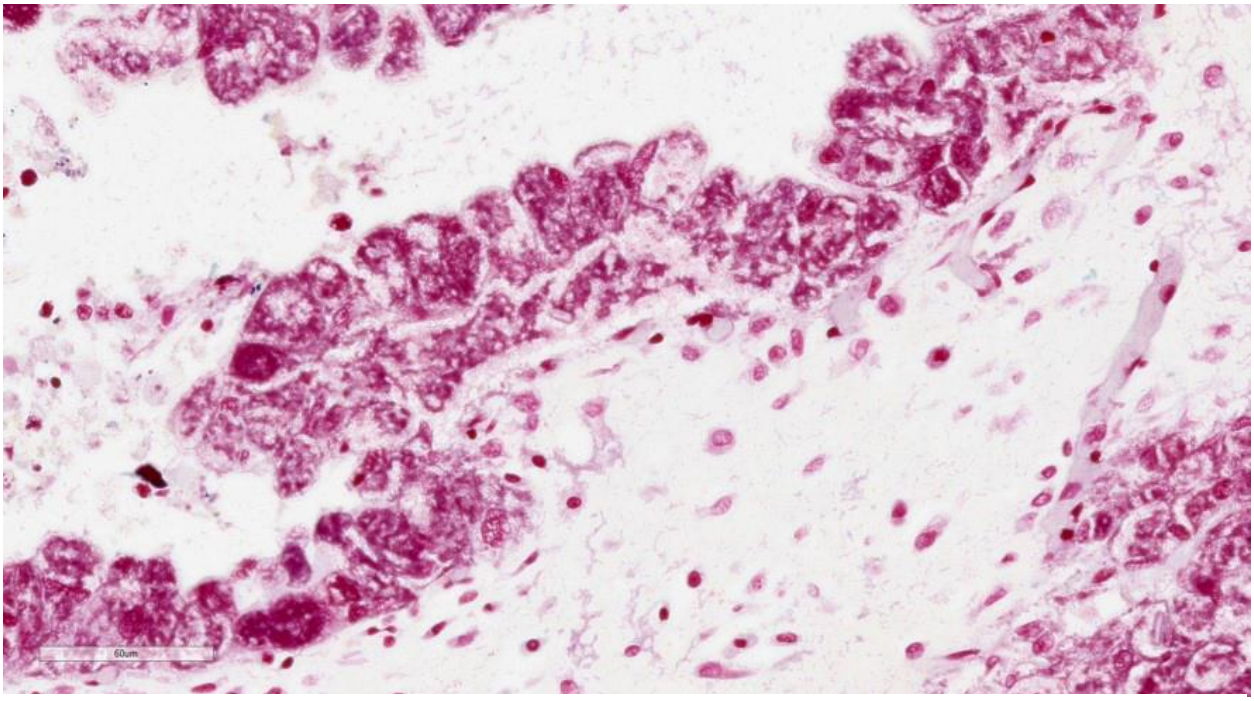

Figure 1-4. Placenta, goat. Gram-negative intratrophoblastic bacterial organisms, identified as *Coxiella burnetti* by PCR. (Gram, 400X) (*Photo courtesy of:* Oklahoma State University College of Veterinary Medicine, Stillwater, OK. https://www.vetmed.okstate.edu)

JPC Diagnosis:
Placenta: Placentitis, lymphohistiocytic, diffuse, mild, with innumerable intratrophoblastic coccobacilli.

JPC Comment:
Coxiella burnetii, like any self-respecting intracellular pathogen, must find a way to solve an existential problem: how to survive inside a cell that is trying to kill it. *C. burnetii* employs a variety of weapons to this end, some of which are well-characterized, and some of which remain poorly understood.

A key weapon in its arsenal is a Type IV secretion system (T4SS), one of several types of such systems used by microorganisms to transport macromolecules across cell membranes.[17] Once *C. burnetti* is phagocytosed by a macrophage, it uses its T4SS to modify host cellular processes to develop a *C. burnetti*-containing vacuole (CCV) in which it can thrive and replicate. The CCV is characterized by "promiscuous fusogenicity," prominent size, temporal stability, and the ability to promote *C. burnetti* replication, all of which distinguish the CCV from a typical lysosome.[10] The T4SS is critical to the formation and maintenance of this CCV intracellular niche and to thwarting the host cell death pathways which are typically arrayed against it.[4]

The *C. burnetii* T4SS transfers over 130 bacterial proteins, very few of which have been characterized, from the CCV into the macrophage cytoplasm.[4] Among those bacterial proteins with known functions, one, AnkG, binds mitochondrial p32 which inhibits the intrinsic apoptosis pathway. Another, inhibitor of caspase activation (IcaA), frustrates pyroptosis by inhibiting the NLRP3 inflammasome and caspase-1 activation.[4]

The effects of translocated bacterial proteins can be appreciated, even if the mechanism of action or the specific protein cannot be identified. One such example relates to the nutrient-sensing mammalian target of rapamycin complex 1 (mTORC1) which homeostatically inhibits autophagy but is itself inhibited in times of nutrient deprivation. Inhibition of mTORC1 typically leads to autophagy, the catabolism of cellular organelles and the repurposing of the liberated macromolecules as metabolic substrates. Inhibition of MTORC1 leads to the formation of large, fusogenic lysosomal organelles that anticipate the surge of incoming catabolic cargo.[10]

Research has demonstrated that *C. burnetti* inhibits mTORC1 by an unknown mechanism in the face of nutrient sufficiency, leading to the development of the large, fusogenic CCV that accommodates hundreds of replicative organisms.[10] The CCV fuses with autophagic vesicles and accumulates autophagy-related proteins such as beclin-1, LC3, and p62. The critical role of T4SS in this process, and by extension, the critical role of translocated bacterial proteins, is evidenced by experimental studies that disrupt T4SS function and inhibit nutrient-dependent autophagy and bacterial replication in *C. burnetti* infected cells.[10] Researchers have speculated that *C. burnetti* activates autophagic catabolism via mTORC1 inhibition to provide replication-supporting nutrients within the CCV.[10]

C. burnetti likely has many more undiscovered virulence factors which are the subject of active research due to its highly infectious nature and unique mechanisms of intracellular survival. A nice summary of the current understanding of *C. burnetti* virulence factors can be found in a 2020 review by Dragan and Voth.[5]

Our moderator this week was Dr. Susan Bender, Assistant Professor of Clinical Pathobiology ar the University of Pennsylvania School of Veterinary Medicine. Participants seemed to approach this slide with some trepidation and initial discussion focused on the basics of tissue identification and proper terminology. Dr. Bender noted that the challenge was made even more difficult by the tremendous distention of the trophoblasts by *Coxiella* organisms.

Participants also discussed an area of the tissue that appeared to contain squamous metaplasia, which provoked some discussion as this would be an unusual finding in the chorioallantois (though not unprecedented; this change can be observed in fungal abortions in goats). Dr. Bender noted that these most likely represent amniotic plaques, a normal finding in the amnion, a portion of which is likely in the slide along with the chorioallantois. A few participants also noted possible thrombi in a a few vessels; however, these are likely not significant without accompanying vascular injury, which is not seen in section and is not an expected finding for this disease entity.

The remarkable expansion of the trophoblasts in this case is a key histologic feature, which Dr. Bender noted should bring a differential list to mind. While the blue frothy material is a classic appearance for *Coxiella burnetii*, *Chlamydia abortus* should also be on the differential list. Other differentials include *Brucella* spp., *Listeria* spp., and *Campylobacter* spp., though those agents do not typically cause such massive trophoblast expansion. Dr. Bender ended discussion by reminding participants that Q fever is a reportable diseaes which, if encountered, should be promptly reported to state authorities with no bleating around the bush!

Participants noted the severe inflammation described by the contributor; however, in the section assessed in conference, participants felt the inflammation was rather mild and predominantly lymphohistiocytic, leading to some minor tinkering with the morphologic diagnosis.

References:

1. Angelakis E, Raoult D. Q fever. *Vet Microbiol*. 2010;140(3-4):297-309.
2. Van den Brom R, van Engelen E, Roest HIJ, van der Hoek W, Vellema P. Coxiella burnetii infections in sheep or goats: an opinionated review. *Vet Microbiol*. 2015; 181(1-2):119-129.
3. Celina SS, Cerný J. Coxiella burnetii in ticks, livestock, pets and wildlife: A mini-review. *Front Vet Sci*. 2022;9:1068129.
4. Delaney MA, den Hartigh A, Carpentier SJ, et al. Avoidance of the NLRP3 inflammasome by the stealth pathogen, *Coxiella burnetii*. *Vet Pathol*. 2020;58 (4):624-642.
5. Dragan AL, Voth DE. Coxiella burnetii: international pathogen of mystery. *Microbes Infect*. 2020;22(3):100-110.
6. Ebani VV, Mancianti F. Potential role of birds in the epidemiology of *Coxiella burnetii*, *Coxiella*-like agents and *Hepatozoon* spp. Pathogens. 2022;11(3):298.
7. Eldin C, Mélenotte C, Mediannikov O, et al. From Q fever to Coxiella burnetii infection: A paradigm change. *Clin Microbiol Rev*. 2017;30(1):115-190.
8. Fournier PE, Marrie TJ, Raoult D. Diagnosis of Q fever. *J Clin Microbiol*. 1998;36(7):1823-1834.
9. Jones RM, Nicas M, Hubbard AE, Reingold AL. The Infectious Dose of Coxiella Burnetii (Q Fever). *Appl Biosaf*. 2006;11(1):149-156.
10. Larson CL, Sandoz KM, Cockrell DC, Heinzen RA. Noncanonical inhibition of mTORC1 by Coxiella burnetii promotes replication within a phagolysosome-like vacuole. *mBio*. 2019;10(1):e02816-18.
11. Mccaughey C, Murray LJ, Mckenna JP, et al. Coxiella burnetii (Q fever) seroprevalence in cattle. *Epidemiol Infect*. 2010; 138(1):21-27.
12. McCaul TF, Williams JC. Developmental cycle of Coxiella burnetii: structure and morphogenesis of vegetative and sporogenic differentiations. *J Bacteriol*. 1981; 147(3):1063.
13. Miller JD, Shaw EI, Thompson HA. *Coxiella burnetii*, Q Fever, and Bioterrorism. In: Anderson B, Friedman H, Bendinelli M, eds. *Microorganisms and Bioterrorism*. Springer;2006:181-208.
14. Minnick MF, Raghavan R. Developmental biology of Coxiella burnetii. *Adv Exp Med Biol*. 2012;984:231-248.
15. Roest HJ, van Gelderen B, Dinkla A, et al. Q Fever in Pregnant Goats: Pathogenesis and Excretion of Coxiella burnetii. *PLoS One*. 2012;7(11):e48949.
16. Tokarevich NK, Panferova YA, Freylikhman OA, et al. Coxiella burnetii in ticks and wild birds. *Ticks Tick Borne Dis*. 2019;10(2):377-385.
17. Wallden K, Rivera-Calzada A, Waksman G. Type IV secretion systems: versatility and diversity in function. *Cell Microbiol*. 2010;12(9):1203-1212.
18. Zarza SM, Mezouar S, Mege JL. From Coxiella burnetii Infection to Pregnancy Complications: Key Role of the Immune Response of Placental Cells. Pathogens. 2021;10(5):627.

CASE II:

Signalment:

5-year-old female breed unspecified goat (*Capra aegagrus hircus*).

History:

Livestock farm with ecological and extensive goat production. After the introduction of

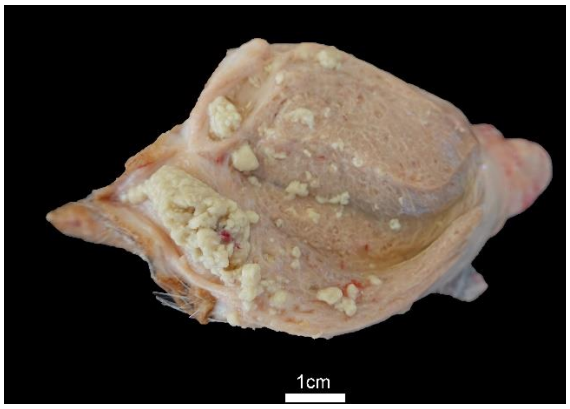

Figure 2-1. Mammary gland, goat. The mammary gland is firm with an abnormal turbid milky discharge admixed with fibrinous material. (*Photo courtesy of:* Department of Animal Pathology, Universidad de Zaragoza, Spain. http://patologiaanimal.unizar.es/)

new animals, blindness, polyarthritis, and chronic mastitis only affecting postpartum and lactating goats were observed. The process reached up to 20% mortality.

Gross Pathology:
Lesions were consistent with mastitis, characterized by a firm consistency of the mammary gland parenchyma and abnormal turbid milky discharge admixed with fibrinous material. Joints showed fibrino-purulent content in the joint space and significant thickening of the joint capsule, compatible with chronic polyarthritis. Unilateral keratitis with mild corneal opacity and bilateral blepharoconjunctivitis were also observed.

Laboratory Results:
Hematology and biochemical analysis revealed marked leukocytosis, neutrophilia, hyperglobulinemia, and increased gamma-glutamyl transferase (GGT) and aspartate aminotransferase (AST). *Mycoplasma agalactiae* was identified in mammary gland and synovial fluid swabs by Real Time Polymerase Chain Reaction (RT-PCR).

Microscopic Description:
Mammary gland: A severe, chronic active, multifocal inflammatory process comprising 70% of section appears to infiltrate and efface mammary gland lobules and acini. At higher magnification, inflammation is composed of abundant lymphocytes, macrophages, and plasma cells, admixed with fewer neutrophils and scattered eosinophils. Occasionally associated with mammary ducts and acini, lymphocytes and macrophages form round aggregates (tertiary lymphoid follicles). Epithelial ductal cells show one or more of the following changes: intracytoplasmic vacuoles and attenuation (degeneration), shrunken and hypereosinophilic cytoplasm with pyknotic to no nuclei (necrosis) or appear sloughing towards the ductal lumen. Ductal lumens are distended and partially or totally occluded by an abundant amorphous eosinophilic material (proteinaceous secretion), admixed with viable and degenerate neutrophils, macrophages, lymphocytes, and karyorrhectic and cellular debris. Within this secretion, there are occasionally amorphous basophilic granules (mineralization). Diffusely expanding the interlobular interstitium and mammary lobules, there is an increased number of mature collagen fibers (fibrosis).

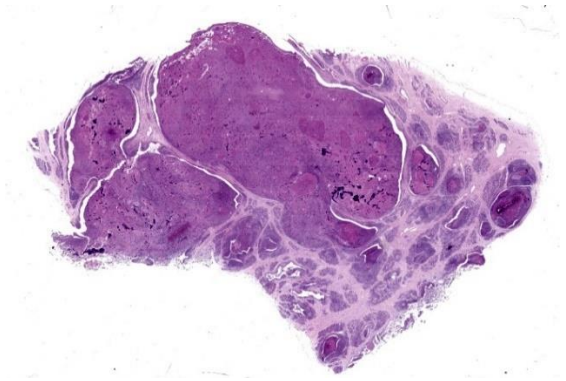

Figure 2-2. Mammary gland, goat. A section of mammary gland is submitted. Lactiferous ducts are markedly ectatic and filled with necrotic debris. (HE, 5X)

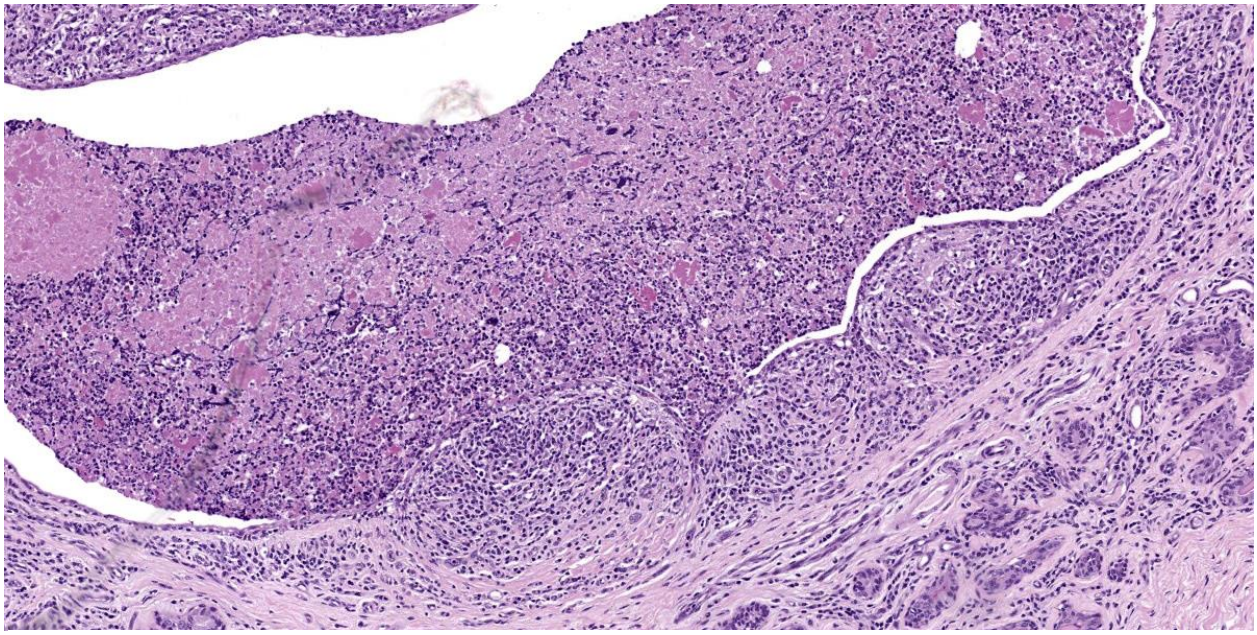

Figure 2-3. Mammary gland, goat. Macrophages and fewer lymphocytes and plasma cells accumulate beneath the segmentally ulcerated epithelium lining ectatic lactiferous ducts.

Contributor's Morphologic Diagnosis:
Mammary gland: Severe, chronic, multifocal to coalescing, lymphoplasmacytic and histiocytic mastitis with fibrosis and necrosis.

Contributor's Comment:
Contagious agalactia (CA) is a notifiable disease distributed worldwide that affects goats and sheep.[8] The etiological agent in sheep is *Mycoplasma agalactiae* (Ma), whereas in goats *M. mycoides subsp. capri* (Mmc), *M. capricolum subsp. capricolum* (Mcc), and *M. putrefaciens* (Mp) are also involved.[12] Oral, respiratory and mammary (milking parlor) are the main routes of transmission within the herd.[1,7,15] Clinical signs and lesions are highly variable and affect mainly postpartum and lactating adult females.[14] CA syndrome is characterized by mastitis, polyarthritis, keratoconjunctivitis, pneumonia, and septicemia,[6] all of which were observed in our case, with the exception of pneumonia.

Depending on the infection route, the primary site of colonization is the respiratory tract, small intestine, and/or alveoli of mammary glands.[1,7,15] Subsequently, Ma is disseminated through the circulation to different organs.[13] Microscopically, acute lesions are characterized by a neutrophilic infiltrate with foci of necrosis. Chronic stages develop into an inflammatory infiltrate composed mainly of macrophages, lymphocytes, and plasma cells, together with extensive fibrosis.[4]

In this case, chronic mastitis, polyarthritis, and keratoconjunctivitis, all characterized by a lymphoplasmacytic and histiocytic infiltrate and severe fibrosis, were observed. Other necropsied goats from the same farm showed acute lesions composed of a severe neutrophilic infiltrate and foci of necrosis in previously mentioned organs. This difference in lesion chronicity among different goats suggests that Ma was chronically present in the herd; however, the outbreak continued actively producing severe and acute cases.

In the typical acute forms, clinical signs and gross and microscopic lesions can facilitate the diagnosis of mycoplasmosis.[12] However, to confirm the etiological agent and

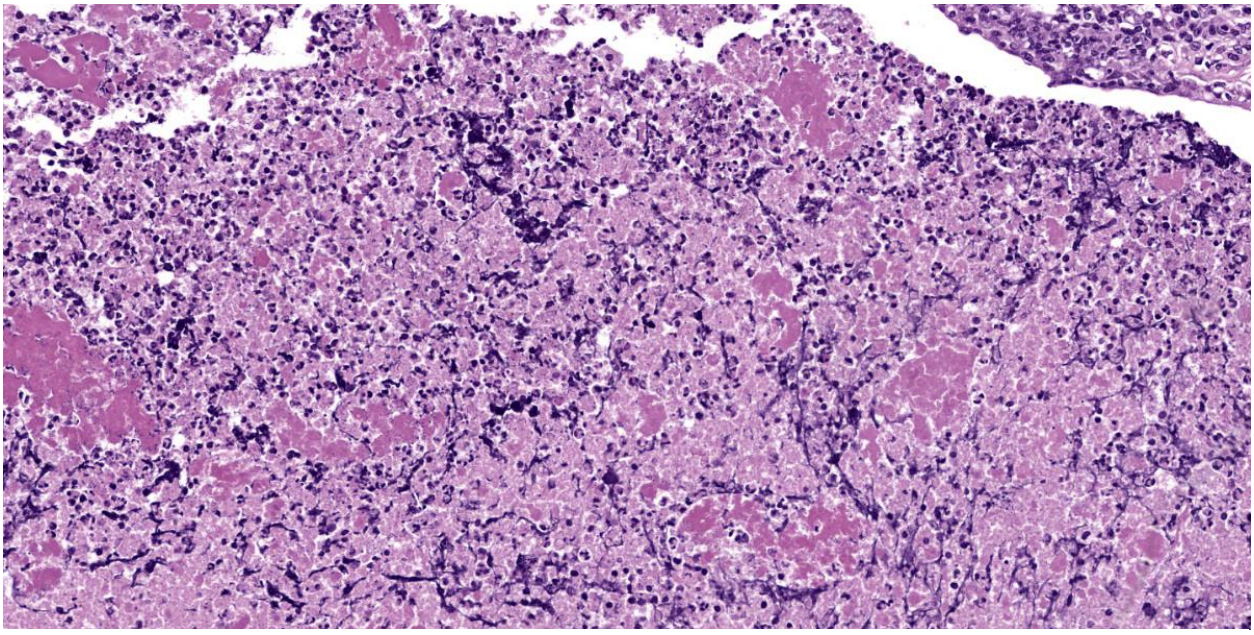

Figure 2-4. Mammary gland, goat. Lactiferous ducts contain a mix of viable and necrotic neutrophils, coagulated secretory product, basophilic homogenous aggregates of nuclear debris, and eosinophilic cell debris. (HE, 363X)

differentiate among *Mycoplasma* spp., it is necessary to perform molecular techniques such as PCR.[2,5,9,11] Relevant samples are joint fluid, eye swabs, or other affected organs seen at necropsy.[10] Bulk tank milk samples can increase the detection sensitivity on a farm.[12] Once the outbreak was detected, serology by indirect ELISA and PCRs of *Mycoplasma agalactiae* of all goats were performed and the positive ones were sacrificed.

Contributing Institution:
Department of Animal Pathology
Universidad de Zaragoza, Spain
http://patologiaanimal.unizar.es/

JPC Diagnosis:
Mammary gland: Mastitis, necrotizing and lymphohistiocytic, chronic, diffuse, marked, with acinar atrophy.

JPC Comment:
Contagious agalactia (CA) is among the most important diseases of small ruminants and is characterized primarily by mammary, joint, and ocular signs, with a drop in milk production followed by increased general morbidity and mortality.[3,8] The disease was first reported in Italy in 1816, where it was named "mal di sito," or "disease of the place," due to its ability to contaminate and persist in environments and then infect newly-introduced animals.[8]

Grossly, CA mammary disease may be unilateral or bilateral and is heralded by hot, swollen, and painful mammary glands and enlarged mammary lymph nodes. Infection spreads to the joints, with arthritis characterized by the accumulation of synovial fluid in the carpal or tarsal joints, frequently with concurrent keratoconjunctivitis.[3] Other clinical manifestations of CA exist, most notably pneumonia and occasionally abortion, and clinical syndromes may appear in isolation or in various combinations, making it difficult to differentiate CA from other infectious scourges of sheep and goats.

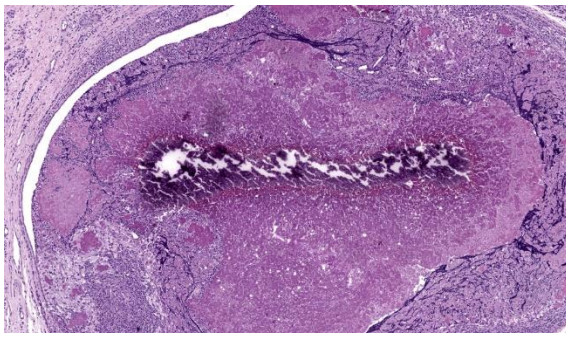

Figure 2-5. Mammary gland, goat. The debris within lactiferous ducts occasionally contains crystalline mineral. (HE, 363X)

The differential list for CA signs in sheep and goats is long. For mastitis, *Staphylococcus*, *Streptococcus*, and *Mannheimia* spp. should be ruled out, while caprine arthritis encephalitis virus is a prime differential for caprine arthritis.[3,8] The *Pasteurellacae*, along with visna-maedi and peste de petits ruminants viruses, as well as other *Mycoplasma* spp. such as *M. capricolum* subsp. *capripneumoniae* and *M. ovipneumoniae* should be excluded as causes for respiratory diseases.[8] Differentiating among these agents often requires extensive testing, and, as the contributor notes, milk, joint fluid, and eye swabs from several different animals in an infected herd are the recommended diagnostic samples.[8]

Histologically, CA mastitis is initially characterized by a mononuclear interstitial infiltrate composed primarily of macrophages, though with time, the prominent inflammatory cell becomes CD8+ T lymphocytes.[3] Lymphoid follicles are often present just beneath the epithelium, as nicely illustrated in this case.

All participants agreed that this mammary gland, even from subgross, looks "baaad". Participants appreciated the remarkable ductal ectasia that is a notable histologic feature of this slide. Participants also questioned that nature of the deep purple material present within the ducts, leading to a tangential but informative discussion of oat cells. Oat cells have a similar histologic appearance to the streaming purple material evident in section; however, oat cells are associated with agents that produce a leukotoxin that debilitates the affected cells. These cells remain intact, but their nuclear and cytoplasmic material stream out, particularly when sectioned, producing the characteristic histiologic oat cell appearance. The intraductal material observed here occurs with massive cell death and the resultant commingling of nuclear and cytoplasmic material that adheres together in the necrotic milieu.

Back on task, participants noted the lymphoid nodes which originally made them consider a viral etiology such as arthritis encephalitis virus as a possible cause. While these lymphoid nodules are a reported histologic feature of AC, the moderator noted that mixed mammary gland infections aren't particularly uncommon, and the presence of one agent doesn't necessarily preclude the presence of another. Dr. Bender concluded discussion of this case with a review of the various histologic changes associated with mammary development and lactation, noting that evaluating reproductive tissue is inherently challenging as the tissues dynamically respond to the ebb and flow of hormonal tides.

Conference participants felt that necrosis was a significant histologic feature of the examined slide and wanted to include it in the morphologic diagnosis. There was a brief discussion about including fibrosis, however most participants felt that chronicity implies fibrosis and it was omitted in the interest of brevity.

References:

1. Agnello S, Chetta DM, Vicari DD, et al. Severe outbreaks of polyarthritis in kids caused by Mycoplasma mycoides

subspecies capri in Sicily. *Vet Rec*. 2012;170 (16):416.
2. Amores J, Corrales JC, Martín AG, Sánchez A, Contreras A, de la Fe C. Comparison of culture and PCR to detect Mycoplasma agalactiae and Mycoplasma mycoides subsp. capri in ear swabs taken from goats. *Vet Microbiol*. 2010;140(1-2):105-108.
3. Arteche-Villasol N, Fernandez M, Gutierrez-Exposito D, Perez Valentin. Pathology of the mammary gland in sheep and goats. *J Comp Path.* 2022;193: 37-49.
4. de Azevedo EO, de Alcântara MDB, do Nascimento ER, et al. Contagious agalactia by Mycoplasma agalactiae in small ruminants in Brazil: first report. *Braz J Microbiol*. 2006;37(4):576-581.
5. Becker CAM, Ramos F, Sellal E, Moine S, Poumarat F, Tardy F. Development of a multiplex real-time PCR for contagious agalactia diagnosis in small ruminants. *J Microbiol Methods*. 2012;90(2):73-79.
6. Bergonier D, De Simone F, Russo P, Solsona M, Lambert M, Poumarat F. Variable expression and geographic distribution of Mycoplasma agalactiae surface epitopes demonstrated with monoclonal antibodies. *FEMS Microbiol Lett*. 1996; 143(2-3):159-165.
7. Bergonier D, Berthelot X, Poumarat F. Contagious agalactia of small ruminants: current knowledge concerning epidemiology, diagnosis and control. *Rev Sci Tech*. 1997;16(3):848-873.
8. Jay M, Tardy F. Contagious agalactia in sheep and goats: current perspectives. *Vet Med (Auckl)*. 2019;10:229-247.
9. Manso-Silván L, Perrier X, Thiaucourt F. Phylogeny of the Mycoplasma mycoides cluster based on analysis of five conserved protein-coding sequences and possible implications for the taxonomy of the group. *Int J Syst Evol Microbiol*. 2007; 57(10):2247-2258.
10. Marogna G, Rolesu S, Lollai S, Tola S, Leori G. Clinical findings in sheep farms affected by recurrent bacterial mastitis. *Small Rum Res*. 2010;88:119-125.
11. McAuliffe L, Ellis RJ, Lawes JR, Ayling RD, Nicholas RAJ. 16S rDNA PCR and denaturing gradient gel electrophoresis; a single generic test for detecting and differentiating Mycoplasma species. *J Med Microbiol*. 2005;54(8):731-739.
12. Nicholas R, Ayling R, McAuliffe L. *Mycoplasma diseases of ruminants*. CABI; 2008;76:92-98.
13. Razin S, Yogev D, Naot Y. Molecular ciology and pathogenicity of Mycoplasmas. *Microbiol Mol Biol* Rev. 1998;62 (4):1094-1156.
14. Szeredi L, Tenk M, Dán A. Infection of two goatherds with Mycoplasma mycoides subsp. capri in Hungary, evidence of a possible faecal excretion. *J Vet Med B Infect Dis Vet Public Health*. 2003;50 (4):172-177.
15. Todaro M, Puleio R, Sabelli C, Scatassa ML, Console A, Loria GR. Determination of milk production losses in Valle del Belice sheep following experimental infection of Mycoplasma agalactiae. *Small Rum Res*. 2015;123(1):167-172.

CASE III:

Signalment:
9-year-old female breed unspecified rabbit (*Oryctolagus cuniculus*).

History:
The owner noted bloody urine for a few weeks and hemorrhagic urine was found on urinalysis. The clinician suspected uterine adenocarcinoma based on clinical findings, so the patient was spayed.

Gross Pathology:
The uterus contained an 8cm mass.

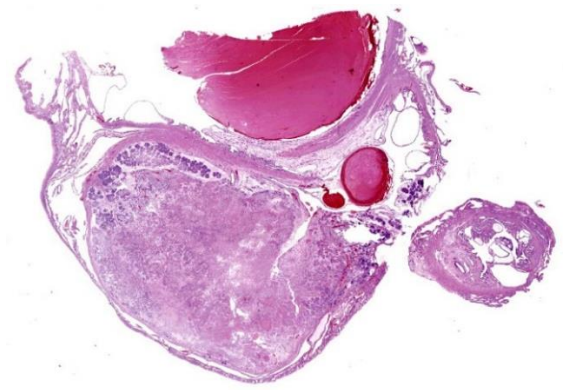

Figure 3-1. Uterus, rabbit. Multiple sections of uterus are submitted for examination. (HE, 4X)

Laboratory Results:
Hematuria, otherwise no significant findings.

Microscopic Description:
Uterus: Multifocally and transmurally infiltrating and effacing the uterine wall is an unencapsulated, densely cellular, poorly demarcated neoplasm composed of epithelial cells arranged in tubules, acini, and solidly cellular areas on a variably dense collagenous to myxomatous stroma. Neoplastic cells have indistinct cell borders, a small amount of eosinophilic cytoplasm, and a round to oval nucleus with finely stippled chromatin and indistinct nucleoli. Anisocytosis and anisokaryosis are mild, and there are less than 1 mitotic figures per 2.37mm.[2] Neoplastic tubules are ectatic with fronds of neoplastic epithelial cells bulging into the lumina, and lumina are often filled with eosinophilic proteinaceous and/or mucinous exudate admixed with variable amounts of necrotic cellular debris. There is abundant predominantly coagulative necrosis at the center of the neoplastic mass characterized by loss of differential staining with retention of architecture. The non-neoplastic uterine mucosal epithelium is multifocally hyperplastic, and uterine glands are multifocally dilated, forming ectatic cysts up to 2 mm in diameter lined by attenuated epithelium (cystic endometrial hyperplasia). Arising from the endometrium and projecting into the uterine lumen, there are several cross sections of markedly dilated, endothelial-lined veins (endometrial venous aneurysm) measuring up to 5 mm in diameter. These veins are subtotally occluded by large fibrin thrombi that often contain well-defined lines of Zahn, low numbers of enmeshed erythrocytes and leukocytes, and a rare dusting of mineral in areas of coagulative necrosis.

Contributor's Morphologic Diagnosis:
1. Uterus: Uterine adenocarcinoma with vascular invasion.
2. Uterus: Endometrial venous aneurysm with thrombosis and rare mixed bacteria.
3. Uterus: Cystic endometrial hyperplasia, multifocal, moderate.

Contributor's Comment:
Uterine adenocarcinoma is often considered the most common spontaneous neoplasm of domestic rabbits, although a recent large-scale study found that trichoblastomas and mammary tumors may surpass uterine adenocarcinomas in frequency of diagnosis.[1-3,6] The incidence of uterine adenocarcinoma increases with age, affecting approximately 80% of 5-6 year old does; most animals in research facilities and commercial rabbitries are relatively young, which explains why this tumor is infrequently seen in this in these facilities.[1,3] Uterine adenocarcinomas may be multicentric within the uterus, and may in

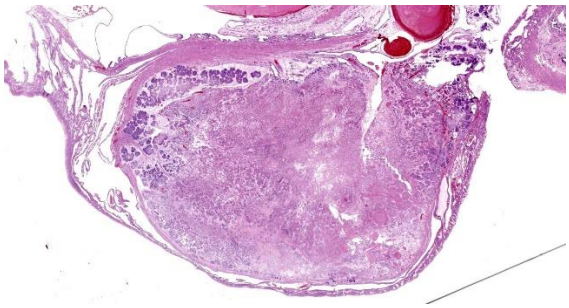

Figure 3-2. Uterus, rabbit. A polypoid neoplasm composed of glands on an edematous fibrous stroma arises from the endometrium and fills the uterine lumen. (HE, 4X)

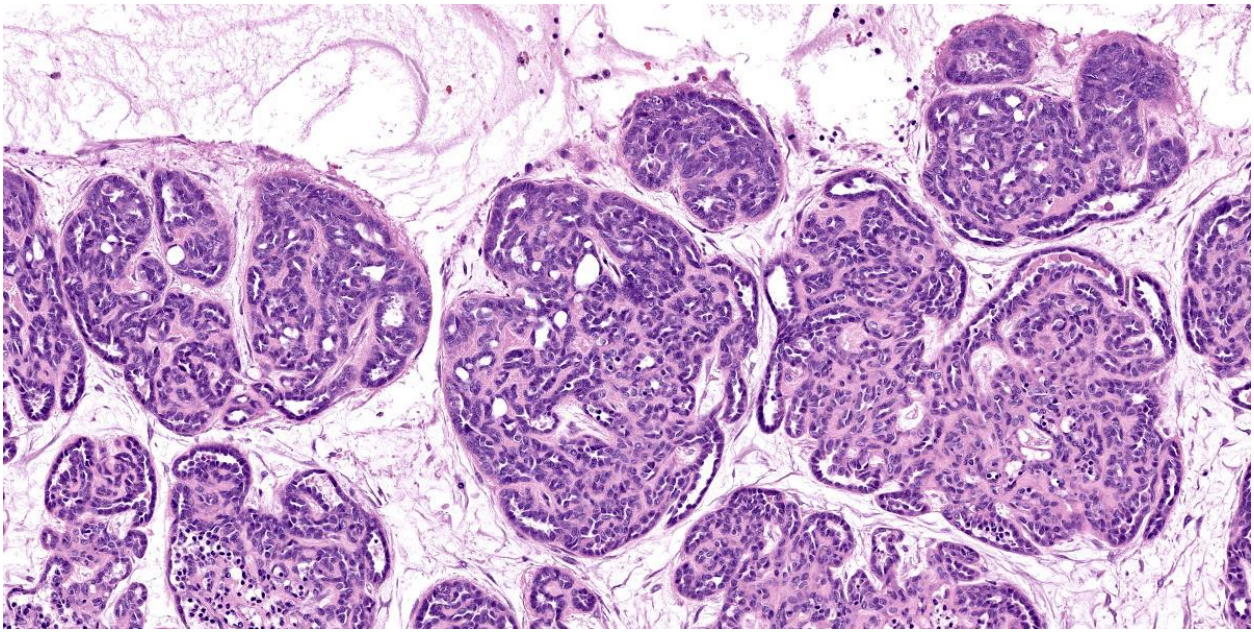

Figure 3-3. Uterus, rabbit. The neoplasm is composed of tortuous glands on an edematous stroma. (HE, 161X)

volve both uterine horns.[1,3] Metastasis to the lung is most common; metastasis to the liver and intra-abdominal carcinomatosis are also commonly reported.[1,3] Intratumoral necrosis is common.[1,3] Uterine adenocarcinomas are often concurrently diagnosed with endometrial hyperplasia.[2,3,6,10] Additionally, one study found that, of 84 uterine adenocarcinomas, 10 had concurrent uterine leiomyoma or leiomyosarcoma.[2]

Endometrial hyperplasia follows second to uterine adenocarcinoma in frequency of diagnosis in rabbit uteri and is the most commonly diagnosed non-neoplastic uterine lesion in rabbits.[1,3,6] The incidence increases with age, although it has been reported in rabbits less than 1 year of age.[3,6,10] It is often cystic and is often diffuse.[2,3] Endometrial hyperplasia is controversially considered to be a pre-neoplastic lesion by some, and is considered hormonally induced.[1,2,3]

Endometrial venous aneurysms were first reported in 1992 in rabbits and have yet to be reported in any species other than lagomorphs.[4] They have been reported in New Zealand White rabbits,[4] unspecified breeds of pet rabbits,[3,5] and a Holland lop rabbit.[7] They consist of venous varices that project from the endometrium into the uterine lumen. They have been reported in nongravid, multiparous does, but no predisposing factors have been identified.[1,3] They may cause uterine distension with subsequent abdominal enlargement.[1,4,7] The venous aneurysms may rupture, resulting in periodic bleeding into the uterine lumen (hemometra) with subsequent urogenital bleeding/hematuria, and clotted blood is often noted within the uterine lumen at necropsy.[1,2,4,7] In a recent large-scale study of genital tract pathology in female pet rabbits, Bertram and colleagues identified endometrial venous aneurysms in 1.6% (n=14) of all post-mortem examinations of entire female rabbits and in 3.3% (n=5) of all uterine biopsy samples, with a median age of 32 months.[3] In post-mortem examinations in this study, the endometrial venous aneurysms were considered incidental in 4 of the 14 rabbits with this diagnosis.[3] In another large-scale study of uterine

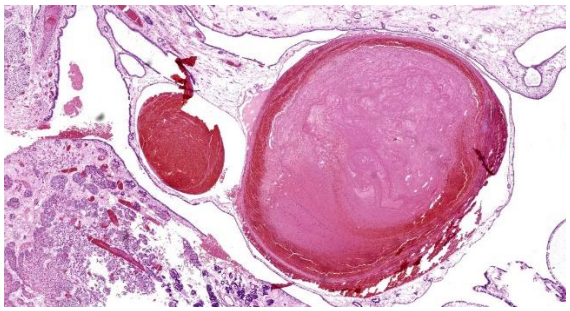

Figure 3-4. Uterus, rabbit. Multiple cross sections of a large thin-walled vein within the endometrium (endometrial venous aneurysm) protrude into the uterine lumen. (HE, 26X)

lesions in 1,928 rabbits, endometrial venous aneurysms were reported in 8 rabbits, none of which had clinical signs.[9] Ovariohysterectomy is considered curative and is recommended due to the risk of hemorrhage.[5,7]

All three of these uterine lesions (uterine adenocarcinoma, cystic endometrial hyperplasia, and endometrial venous aneurysm) can result in hematuria; all three of these lesions are present in this case, and hematuria was clinically noted and confirmed via urinalysis in this case.[1] Hematuria and/or serosanguinous vaginal discharge are clinical signs that should raise suspicion of uterine disease.[6] Other potential causes of hematuria in rabbits include uterine polyps, cystitis, urinary bladder polyps or tumors, pyelonephritis, and renal infarction.[1] Of note, differentials for hematuria in rabbits include pigmented urine due to crystals, porphyrin, or bilirubin; a urinalysis is required to differentiate between these causes.[1]

Contributing Institution:
Tri-Service Research Laboratory
https://www.afrl.af.mil/

JPC Diagnosis:
1. Uterus: Uterine adenocarcinoma.
2. Uterus: Endometrial venous aneurysm.
3. Uterus: Cystic endometrial hyperplasia, diffuse, severe.

JPC Comment:
This dazzling slide, a lagomorph uterine lesion party pack, delights from subgross and closer inspection in equal measure, and the contributor provides excellent summaries of the component lesions. The endometrial venous aneurysms are particularly striking and, of the trio of uterine conditions vying for attention, the most uncommon.

Aneurysms occur when the quality or quantity of the connective tissue within the vascular wall is compromised.[7] In humans, aneurysm formation has been associated with conditions such as defective synthesis of elastin or collagens I and III, vitamin C deficiency, atherosclerosis, systemic hypertension, pregnancy, or trauma.[7] In the few reported cases of endometrial venous aneurysm in rabbits, no predisposing factors have been identified, leading to the classification of this condition in rabbits, for now, as congenital.[7]

The primary clinical signs associated with endometrial venous aneurysms are a palpably enlarged uterus and, as the contributor notes, hematuria. These symptoms are not specific and further diagnostics are typically required. In reported cases, hematologic parameters have shown little diagnostic value, though the degree of anemia may provide clues to chronicity and the amount of blood loss suffered in cases of severe aneurysm rupture.[7] Plasma chemistry changes may include hyperglycemia and high creatine kinase, likely due to handling stress rather than any derangement caused by the endometrial aneurysm.[7]

Histologically, the weakened vessel wall can lead to massive dilation of the vein which, as

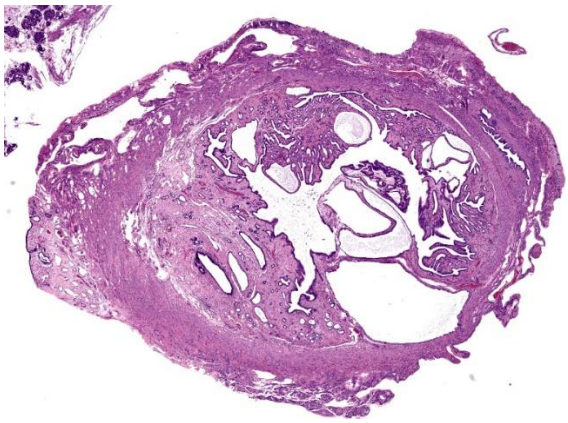

Figure 3-5. Uterus, rabbit. Another cross section of the uterine body demonstrates marked cystic endometrial hyperplasia of the endometrium, with glands occasionally deep in the smooth muscle wall (adenomyosis). (HE, 14X)

in this case, can be rather obtrusive and, if we're being honest, a little gaudy. The focally dilated vein maintains a complete endothelial lining of attenuated cells that expands the surrounding endometrial tissue. The attenuated wall may exhibit loss of smooth muscle cells and replacement with fibrous connective tissue components such as collagen or fibroblasts.[7] Within the vein, blood and thrombi are usually present, with thrombi characterized by varying amounts of organization, inflammatory cells, and hemosiderin resulting from erythrocyte degradation.[7]

Due to the risk of sudden, severe hemorrhage, venous aneurysms carry a poor to grave prognosis unless ovariohysterectomy is performed.[7] Additional sequelae include thromboembolism and recurrent bouts of excessive bleeding. Prognosis is good with ovariohysterectomy; however, it is still unknown whether this condition is truly congenital and, if so, whether endometrial venous aneurysm indicates a greater risk of aneurysm in other anatomic locations.[7] While there is currently no evidence of an association with a generally heightened risk of aneurysm, more research is needed to determine the prevalence and underlying pathogenesis of this uncommon, striking condition.

Discussion of this case focused generally around the difficult in distinguishing endometrial hyperplasia from neoplasm, and the general consensus was that these two entities likely exist on a neoplasm, though evidence is currently lacking. The moderator discussed a long list of causes for hematuria in rabbits before dropping the inconvenient fact that rabbit urine can normally be red under certain conditions, so be careful about hopping to conclusions. Physiologically normal, red urine should be relatively clear, while true hematuria will have the characteristic opacity of blood.

Discussion of the morphologic diagnosis was similarly straightforward; however, conference participants were unable to identify the vascular invasion or the bacteria noted by the contributor on the section examined at conference and these features were consequently omitted from the diagnoses.

References:

1. Barthold SW, Griffey SM, Percy DH. *Pathology of Laboratory Rodents and Rabbits.* 4th ed. John Wiley and Sons, Inc.;2016:256,310,320.
2. Baum B. Not just uterine adenocarcinoma – neoplastic and non-neoplastic masses in domestic pet rabbits (*Oryctolagus cuniculus*): a review. *Vet Pathol.* 2021;58(5): 890-900.
3. Bertram CA, Müller K, Klopfleisch R. Genital tract pathology in female pet rabbits (Oryctolagus cuniculus): a retrospective study of 854 necropsy examinations and 152 biopsy samples. *J Comp Pathol*. 2018;164:17-26.
4. Bray MV, Weir EC, Brownstein DG, Delano ML. Endometrial venous aneurysms in three New Zealand white rabbits. *Lab Anim Sci.* 1992;42(4):360-362.

5. Dettweiler A, Mundhenk L, Brunnberg L, Müller K. Fatal endometrial venous aneurysms in two pet rabbits (*Oryctolagus cuniculus*). *Kleintierpraxis*. 2012;57:69-75.
6. Kunzel F, Grinniger P, Shibly S, et al. Uterine disorders in 50 pet rabbits. *J Am Anim Hosp Assoc*. 2015;51(1):8-14.
7. Reimnitz L, Guzman DSM, Alex C, Summa N, Gleeson M, Cissel DD. Multiple endometrial venous aneurysms in a domestic rabbit (*Oryctolagus Cuniculus*). *J Exot Pet Med.* 2017;26:230-237.
8. Saito K, Nakanishi M, Hasegawa A. Uterine disorders diagnosed by ventrotomy in 47 Rabbits. *J Vet Med Sci.* 2002; 64(6):495-497.
9. Settai K, Kondo H, Shibuya H. Assessment of reported uterine lesions diagnosed histologically after ovariohysterectomy in 1,928 pet rabbits (*Oryctolagus cuniculus*). *J Am Vet Med Assoc.* 2020; 257(10):1045-1050.
10. Walter B, Poth T, Bohmer E, Braun J, Matis U. Uterine disorders in 59 rabbits. *Vet Rec*. 2010;166(8):230-233.

CASE IV:

Signalment:
Age and breed unspecified ram (*Ovis aries*).

History:
During mating, the animal would start shaking and mating could not continue. Since this happened several times, the animal was euthanized and submitted for necropsy.

Gross Pathology:
The subcutaneous tissue of the ventral part of the abdomen, preputium, and penis was affected by severe suppurative inflammation in the form of large encapsulated abscess.

Figure 4-1. Penis, sheep. One section of penis is submitted for examination. The mucosa is ulcerated and the lamina propria is markedly expanded. (HE, 5X).

Laboratory Results:
Bacteriological culture examination showed an increase in the mixed bacterial flora in which *Corynebacterium* spp. predominated. Species identification was done by the MALDI-TOF method which confirmed that the species belonged to *Corynebacterium xerosis*.

Microscopic Description:
Penis (glans): The most outer layer (penile mucosa) is replaced with amorphous eosinophilic material admixed with cellular debris mainly composed of degenerate neutrophils (necrosuppurative inflammation). There are multifocal colonies of coccobacillary bacteria on the surface. The lamina propria is diffusely infiltrated with larger numbers of lymphocytes, plasma cells, macrophages, and low numbers of neutrophils. The amount of inflammatory infiltrate decreases toward the internal parts of the penis (corpora cavernosa, corpus spongiosum, and urethra), which do not show pathological changes.

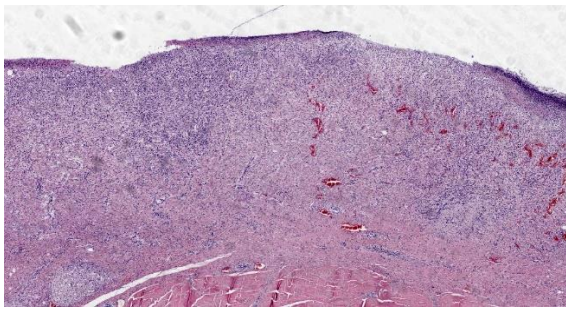

Figure 4-2. Penis, sheep. The submucosa and tunica dartos are effaced by densely cellular granulation tissue; the overlying mucosa is ulcerated. (HE, 30X)

Contributor's Morphologic Diagnosis:
Penis (glans): Balanitis, necrosuppurative, subacute to chronic, focally extensive, severe with intralesional coccobacillary bacteria.

Contributor's Comment:
Rams can develop a range of lesions of the penis and prepuce and inflammation is common pathology. Inflammation of the penis is *phallitis*, that of the head (glans) of the penis is *balanitis*, and inflammation of the prepuce is *posthitis*. It can be of viral and bacterial etiology, but foreign materials can also cause inflammation.[3] Although in our case the bacteriological examination showed an increase in mixed bacterial flora with a predominance of *Corynebacterium* spp., we believe that the isolated *Corynebacterium xerosis* (*C. xerosis*) played a role in the pathogenesis of this condition.

The genus *Corynebacterium*, which currently has more than 110 validated species, is highly diversified. It includes species that are of medical, veterinary, or biotechnological relevance.[1,7,9] The most common cause of cutaneous abscesses and caseous lymphadenitis (CLA) in sheep is *Corynebacterium pseudotuberculosis*. Caseous lymphadenitis in sheep almost always follows a wound infection, usually a shearing wound.[10] The sequence of events in progressive CLA is infection of a superficial wound, spread of infection to the local lymph nodes, which suppurate, and then lymphogenous and hematogenous extension to produce abscesses in internal organs. The progression is slow and may reach the bloodstream only in older animals, whereas in young animals the disease tends to be confined to the superficial lymph nodes, most commonly the precapsular and precrural.[10]

Corynebacterium xerosis is a commensal organism normally present in the skin and mucous membranes of humans.[2] It is considered an unusual pathogen, but it is able to cause endocarditis, skin infections, and other illnesess like maternal ventriculoperitoneal shunt infection, pneumonia, ear and brain abscess, and vertebral osteomyelitis.[1,2,5,12] *Corynebacterium xerosis* grows in colonies of 0.2–1.0 mm in diameter that are brown-yellowish in colour, slightly dry in appearance, and non-haemolytic when cultured in blood agar. Microscopically, *C. xerosis* appears as irregularly stained, pleomorphic gram-positive rods presenting club-like ends.[4]

Infections with *Corynebacterium xerosis* in animals are rarely described. It has been isolated in pure culture from normally sterile organs of animal clinical specimens. *C. xerosis* was isolated from the joint of a pig suffering from a subcutaneous abscess and from a goat liver suspected to have paratuberculosis.[11,12] The case for *C. xerosis* producing a clinical cutaneous abscess in sheep was reported in Mexico in 2016 and *C. xerosis* strain GS1 was isolated from a liver lesion with caseous nodules from a yak.[4,12]

Unlike *C. pseudotuberculosis* infection, the virulence factor that could contribute to the development of abscesses as a pathogenic toxin has not been reported in *C. xerosis*. The main factor of virulence and pathogenicity in *C. pseudotuberculosis* is the exotoxin phospholipase D, which is a permeability factor

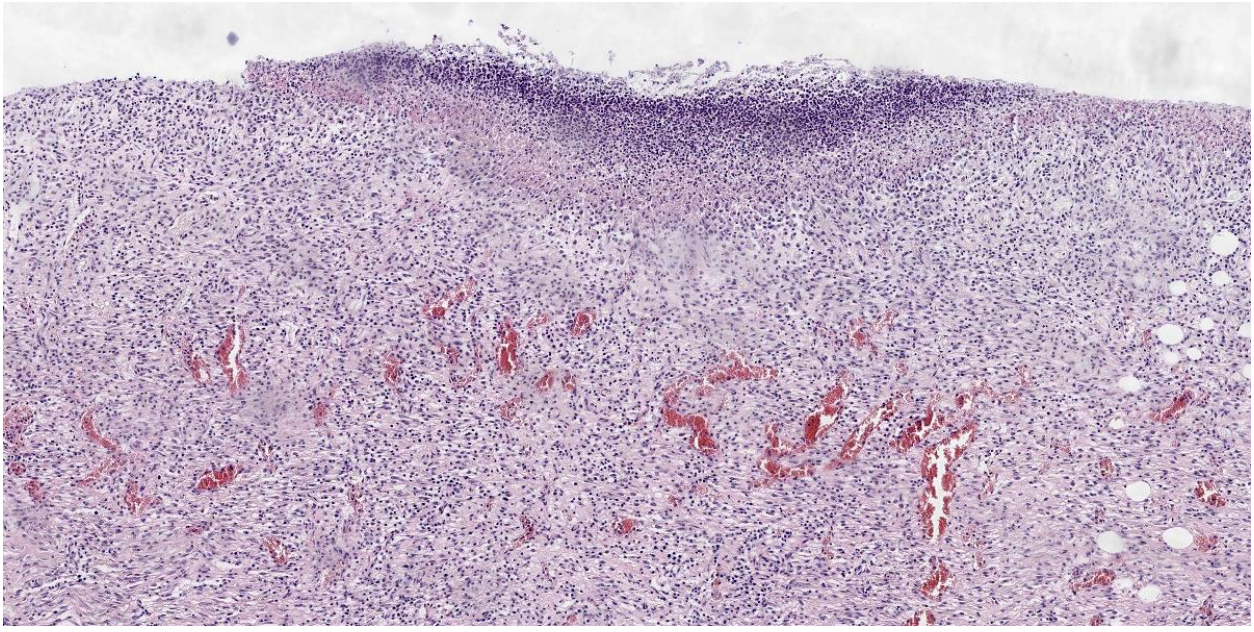

Figure 4-3. Penis, sheep. Higher magnification of the submucosal granulation tissue and ulcerated debris-laden surface. (HE, 38X)

that promotes hydrolysis of the ester bonds in sphingomyelin in mammalian cell membranes, possibly contributing to the spread of bacteria from the initial site of infection to secondary sites through the lymphatic system to regional ganglia.[6] This highlights the importance of carrying out further research regarding the mechanisms of infection present in this *Corynebacterium* species.[4]

In the presented case, the source of the infection remains unknown. Hernandez-Leon et al. discussed the possible epidemiology of *C. xerosis* in a sheep herd and hypothesized that a possible source of this bacterium could be pigs.[4] The ovine production system where the sample was obtained was previously used for swine, a species where *C. xerosis* has been reported as a common pathogen. Additionally, sharp objects were widespread all over the facilities, which increased the chance of injury to the animals, opening a portal for microorganisms including *C. xerosis*.[4,8,11] All these data indicate that *C. xerosis* has a certain clinical significance in veterinary medicine and that this bacterium should be considered as a possible cause of subcutaneous abscesses but also suppurative inflammation in other organs.

Contributing Institution:
Department of Veterinary Pathology
Faculty of Veterinary Medicine
University of Zagreb, Croatia
http://www.vef.unizg.hr/

JPC Diagnosis:
Penis: Balanitis, ulcerative, chronic, circumferential, severe, with granulation tissue and mixed colonies of bacteria.

JPC Comment:
As the contributor notes, *Cornynebacterium xerosis* is uncommonly isolated from veterinary patients and much of what is understood about this pathogen is extrapolated from human infections. Despite the novelty of the pathogen, however, this case presents a fairly straight-forward case of balanitis, which is typically accompanied by an inflammatory infiltrate composed of lymphocytes, plasma cells, and macrophages.[3] Lymphocytes and

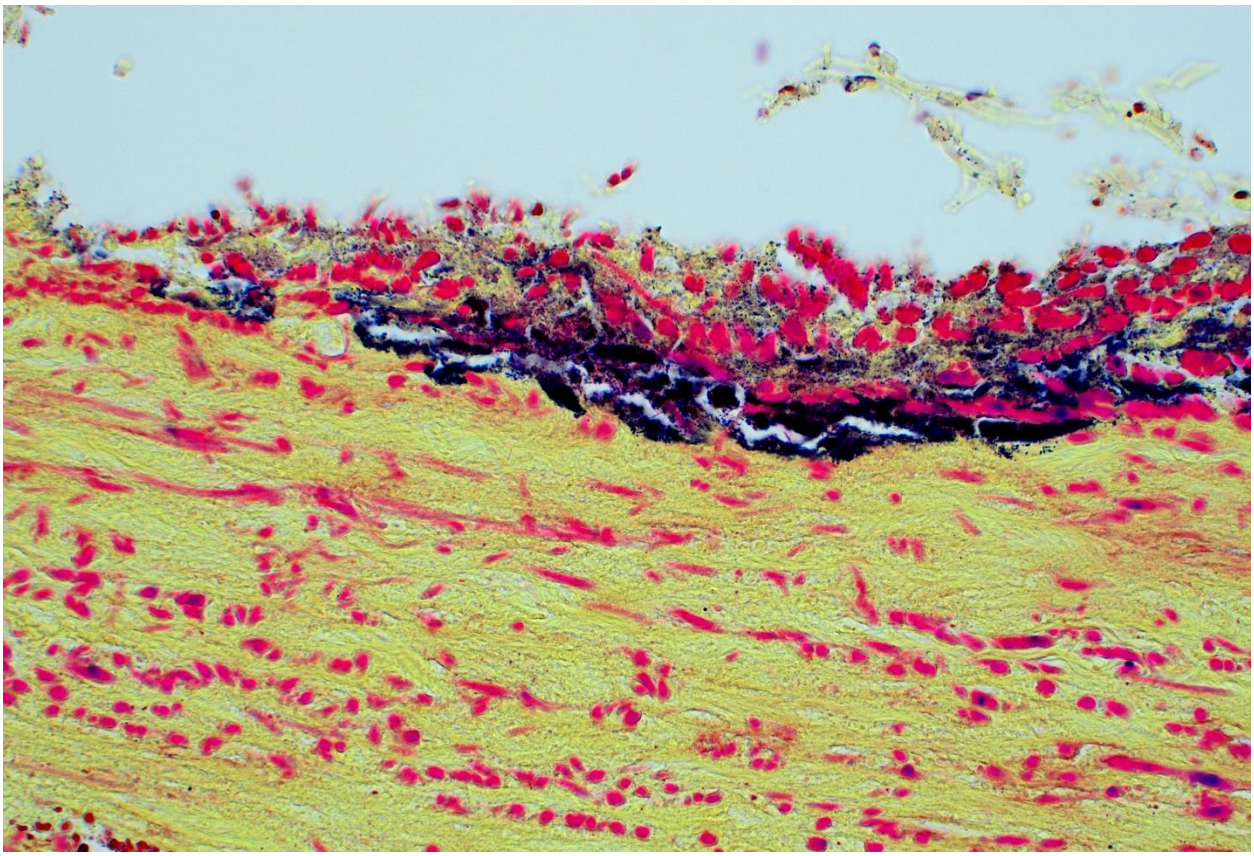

Figure 4-4. Penis, sheep. The necrotic coagulum contains mixed bacterial colonies. (Brown and Hopps, 400X).

plasma cells, and occasionally lymphoid follicles, are present within the normal preputial mucosa, and immunoglobulins derived from these plasma cells are present in preputial washes.[3]

In most cases of balanitis or balanoposthitis, ascribing pathogenicity to organisms isolated from a penile lesion is fraught with difficulty, as normal preputial bacterial flora may include a variety of nonpathogenic and potentially pathogenic bacteria such as *Corynebacterium renale*, fungi, mycoplasmas, ureaplasmas, chlamydial species, and a variety of protozoa.[3] Attempting to determine which, if any, of these resident organisms is responsible for particular lesions has lead to conflicting research and a morass of speculation in most cases.

Dorper sheep and Leicester rams have a distinct, severe form of ulcerative balanitis which can also cause vulvovaginitis in ewes with whom they are mated.[3] In the male, the condition is characterized by large, deep ulcers that occur on the ventral surface of the penis and typically progress to excessive granulation tissue and hemorrhage.[3] Chronically, adhesions form between the penis and the prepuce as a result of necrotic and purulent material covering the head of the penis. Mated ewes develop shallow ulcers on the labia and posterior vagina. The etiologic agent responsible for this condition remains unknown.[3]

Rams and wethers may also develop "ulcerative posthitis of wethers," commonly known as pizzle rot. The condition, which is unfortunately common, develops in the presence of

urea-hydrolyzing bacteria, such as *Corynebacterium renale*, in animals that excrete urea-rich urine.[3] Lesions progress from small areas of epithelial necrosis around the preputial orifice to more extensive geographic ulceration and granulation tissue that results in occlusion of the preputial orifice. The occlusion leads to the accumulation of urine and pus and, ultimately, to extensive internal ulceration of the prepuce, the urethral process, and the head of the penis.[3]

Balanitis occurs in all domestic species and is caused by a variety of familiar infectious agents, including bovine herpesvirus I in bulls; canid herpesvirus 1 and leishmaniasis in dogs; and Equid herpesvirus 1, *Trypanosoma equiperdum* (the causative agent of dourine), cutaneous habronemiasis, pythiosis, and cutaneous halicephalobiasis in horses.[3]

Conference participants began discussion of this case by noting the large colonies of bacteria, noting that these large colonies are a possible way to begin narrowing down the list of possible etiologic agents to one of the YAACSS agents (*Yersinia, Actinomyces, Actinobacillus, Corynebacterium, Streptococcus,* and *Staphylococcus*). The moderator cautioned participants not to read too much into the large colonies, as virtually any agent can form large colonies given enough time.

The agent isolated in this case is, of course, a member of YAACSS, albeit a somewhat enigmatic one, and discussion of this case largely centered on whether *C. xerosis* was the actual cause of the histologic lesions or just an opportunist. The question is largely rhetorical, and Dr. Bender used the discussion as a pivot to other *Corynebacterium* spp. of veterinary importance, including *Corynebacterium renale* and *Corynebacterium pseudotuberculosis*.

Discussion of the morphologic diagnosis centered largely on how to capture the unique appearance of this lesion and how to describe the bacteria. Participants felt the primary lesion was ulceration and that the granulation tissue was abundant enough to merit specific mention. Participants also felt that the bacterial population consisted of both cocci and bacilli and preferred to describe the bacterial population as mixed.

References:

1. Bernard K. The genus *Corynebacterium* and other medically relevant coryneform-like bacteria. *J Clin Microbiol*. 2012;50 (10):3152-3158.
2. Coyle BM, Lipsky BA. Coryneform bacteria in infectious diseases: clinical and laboratory aspects. *Clin Microbiol Rev*. 1990;3(3):227-246.
3. Foster RA. Male Reproductive System. In: Zachary JF, ed. *Pathologic Basis of Veterinary Disease*. 6th ed. Elsevier; 2016:1194-1222.
4. Hernandez-Leon F, Acosta-Dibarrat J, Vázquez-Chagoyán JC, Rosas PF, Oca-Jiménez RM. Identification and molecular characterization of *Corynebacterium xerosis* isolated from a sheep cutaneous abscess: first case report in Mexico. *BMC Res Notes*. 2016;9:358.
5. Krish G, Beaver W, Sarubbi F, Verghese A. *Corynebacterium xerosis* as a cause of vertebral osteomyelitis. *J Clin Microbiol*. 1989;27(12):2869-2870.
6. McKean SC, Davies JK, Moore RJ. Expression of phospholipase D, the major virulence factor of *Corynebacterium pseudotuberculosis*, is regulated by multiple environmental factors and plays a role in macrophage death. *Microbiology (Reading)*. 2007;153(7):2203-2211.
7. Oliveira A, Oliveira LC, Aburjaile F, et al. Insight of genus *Corynebacterium*: ascertaining the role of pathogenic and non-

pathogenic species. *Front Microbiol*. 2017;8:1937.
8. Palacios J, Vela AI, Molin K, et al. Characterization of some bacterial strains isolated from animal clinical materials and identified as *Corynebacterium xerosis* by molecular biological techniques. *J Clin Microbiol*. 2010;48(9):3138–3145.
9. Soares SC, Silva A, Trost E, et al. The pan-genome of the animal pathogen *Corynebacterium pseudotuberculosis* reveals differences in genome plasticity between the biovar ovis and equi strains. *PLos One*. 2013;8(1):e53818.
10. Valli T, Kiupel M, Bienzle D (with Wood RD). Hematopoietic System. In: Maxie MG, ed. *Jubb, Kenedy & Palmers Pathology of Domestic Animals*. 6th ed. Vol 2. Elsevier; 2016:103-267.
11. Vela AI, Gracıa E, Fernandez A, Dominguez L, Fernandez-Garayzabal JF. Isolation of Corynebacterium xerosis from animal clinical specimens. *J Clin Microbiol*. 2006;44(6):2242–2243.
12. Wen F, Xing X, Bao S, Hu Y, Hao B. Whole-genome sequence of Corynebacterium xerosis strain GS1, isolated from yak in Gansu Province, China. *Microbiol Resour Announc*. 2019;8(37): e00556-19.

WSC 2023-2024
Conference 25 Self-Assessment

1. Which of the following is spelled correctly?
    a. Coxiella burnetti
    b. Coviella burnetii

2. Which of the following is considered the reservoir host for the agent in the previous question?
    a. Ruminants
    b. Equids
    c. Poultry
    d. Rodents

3. Which of the following cause contagious agalactiae in sheep?
    a. *M. mycoides subsp. capri*
    b. *M. capricolum subsp. capricolum*
    c. *M. putrefaciens*
    d. *Mycoplasma agalactiae*

4. Which of the following is the most common site of metastasis of uterine adenocarcinoma in rabbits?
    a. Lung
    b. Lymph node
    c. Urinary bladder
    d. Kidney

5. Corynebacterium xerosis has completely been reported as a pathogen in which of the following?
    a. Cattle
    b. Chicken
    c. Swine
    d. Fish